Chemistry and Biology of Heparin and Heparan Sulfate

Editors: Hari G. Garg,
Robert J. Linhardt and Charles A. Hales

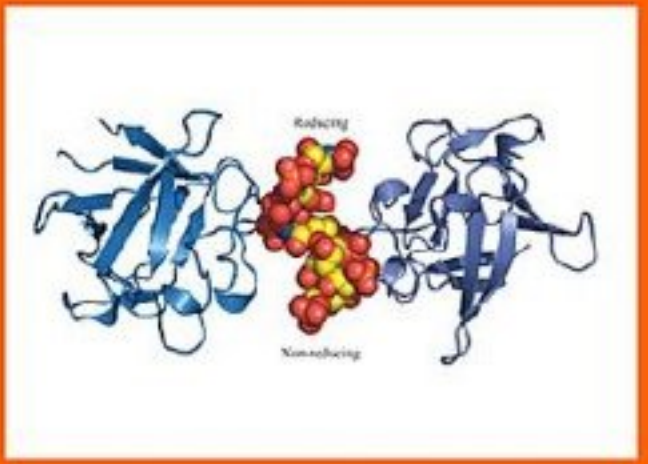

Preface

Heparin belongs to a class of linear, acidic polysaccharides known as glycosaminoglycans (GAGs). Nearly 90 years after its discovery by Howell, heparin and its derivatives remain important drugs in clinical practice. Among heparin's established uses are the prevention of postoperative thrombosis and the treatment of acute venous thrombosis. Little was known about the chemistry and the structure of heparin when the first clinical trials evaluating the use of heparin began in the mid-1930s. The definitive identification of its monosaccharide components began in 1936 and was not completed until 1964. Over the years, the development of chemical methods of degradation, and later, enzymatic depolymerization have played an important role in the elucidation of the structure of heparin. This development has led to an understanding of the detailed structural basis of heparin's anticoagulant activity in the early 1980s.

During the same time, there was a growing interest in the structure and function of heparan sulfate, a closely related GAG found in the body, which contains lower sulfation but greater structural heterogeneity than heparin. Investigation of the biosynthesis of heparin and heparan sulfate has significantly broadened our knowledge of the rules governing their biosynthesis and structure, leading to a deeper understanding of the relationship between heparin and heparan sulfate. The basic lesson was that GAG modifications did not go to completion. As a consequence of these incomplete biosynthetic modifications, GAGs are quite heterogeneous. This heterogeneity enables these molecules to play important roles in various processes in the body. Numerous studies over the last decade highlight heparin and heparan sulfate binding to many physiologically important proteins, thereby playing important roles in the regulation of physiological and pathophysiological processes. Thus, these macromolecules are currently at the forefront of the rapidly emerging field of glycobiology.

This book is designed to provide readers with a detailed panoramic review of the chemistry, structure, biological functions, and clinical applications of heparin and heparan sulfate.

The 27 chapters in this volume begin with the chemistry and biochemistry of heparin and heparan sulfate, followed by their function in various physiological and pathological conditions and finally their clinical applications.

The antithrombin activity of heparin results from a specific pentasaccharide sequence. Other minor sequences are responsible for additional biological activities. These sequences often comprise distinct domains associated with important activities. Chapter 1 is focused on the structure and active domains of heparin. Chapter 2 surveys the structure and function of cell associated and pericellular heparan sulfate proteoglycans.

The advent of more sophisticated instrumentation and techniques for data collection has resulted in rapid progress in heparin structural elucidation. Chapter 3 focuses on the methods used for the analysis of heparin and heparan sulfate.

Well-characterized heparin oligosaccharides are required to assess the many biological properties of heparin. Chapters 4–6 include the chemical synthesis, pharmacological rationale and strategies for sequencing heparin and heparan sulfate oligosaccharides.

The backbone of heparin and heparan sulfate is comprised of repeating glucuronic acid (GlcA) and *N*-acetylglucosamine (GlcNAc) residues, which undergo various modifications including *N*-acetylation, *N*-sulfonation of GlcNAc residues, C-5 epimerization of GlcA to iduronic acid (IdoA), and *O*-sulfonation at various positions of GlcA, IdoA, and GlcNAc residues. Chapter 7 presents an overview of the biosynthesis of heparin and heparan sulfate. Chapters 8–10 describe the remodeling and degradation of heparin and heparan sulfate by different enzymes.

Different biological activities of heparin and heparan sulfate are due to their interactions with biologically active proteins. Chapter 11 describes heparin regulation of the complement system and Chapter 12 discusses the surface-based studies of heparin/heparan sulfate–protein interactions, including considerations for surface immobilization of heparin/heparan sulfate and monitoring their interaction with binding proteins. Chapter 13 focuses on heparin activation of serine protease inhibitors.

Heparan sulfate required in signaling is mediated by fibroblast growth factors. Recent studies have shown that genetic defects can disturb growth factor signaling. Moreover, glycol-splitting chemistry has been used to modulate heparin and heparan sulfate based inhibition of growth factors and heparinase. Chapter 14 summarizes the role of heparan sulfate in fibroblast growth factor in signaling. Chapter 15 describes the role of heparan sulfate in mammalian reproduction. Chapter 16 describes glycol-splitting as an approach for modulating inhibition of growth factors and heparinase by heparin and heparin derivatives.

Chapters 17–19 incorporate different aspects of heparin and heparan sulfate. Chapter 17 includes the antithrombin activation and designing novel heparin mimics. Vascular changes after chronic hypoxia results in the migration of smooth muscle cells in the media of muscular and partially muscular pulmonary arteries. Chapter 18 discusses the influence of the chemical modification of heparin on its antiproliferative activity. Chapter 19 focuses on the mechanisms of cell growth regulation by heparin and heparan sulfate.

Chapters 20–27 detail the use of heparin and heparan sulfate in different pathological conditions. Chapter 20 discusses the emerging links between heparin and low molecular weight heparin in thrombosis and inflammation. Chapter 21 discusses basic and clinical differentiations of heparin and low molecular weight heparin. Chapter 22 focuses on the extracellular matrix heparan sulfate proteoglycan that regulates key events in vascular development and disease. Chapter 23 discusses heparin and low molecular weight heparins in clinical cardiology. Chapter 24 addresses heparin-induced thrombocytopenia. Chapter 25 discusses the role of heparan sulfate in cancer while Chapter 26 includes the use of heparin in older patients. Chapter 27 describes advances in low molecular weight heparin use in pregnancy.

Hari G. Garg
Robert J. Linhardt
Charles A. Hales

Contributors

Ariane I. de Agostini, Ph.D., Department of Gynaecology and Obstetrics, Unit of Medicine of Reproduction and Endocrinology, Geneva University Hospital, Geneva, Switzerland

Xingbin Ai, Ph.D., Instructor, Boston Biomedical Research Institute, Watertown, Massachusetts, U.S.A.

Karen J. Bame, Ph.D., Associate Professor, School of Biological Sciences, University of Missouri-Kansas City, Kansas City, Missouri, U.S.A.

Benito Casu, Ph.D., Lecturer on Biopolymers, Scientific Coordinator, G. Ronzoni Institute for Chemical and Biochemical Research, Milan, Italy

Ishan Capila, Ph.D., Senior Scientist, Momenta Pharmaceuticals Inc., Cambridge, Massachusetts, U.S.A.

William E. Dager, Pharm.D., FCSHP, Pharmacist Specialist, UC Davis Medical Center, Sacramento, California, U.S.A.

Umesh R. Desai, Ph.D., Associate Professor of Medicinal Chemistry, Institute for Structural Biology and Drug Discovery and Department of Medicinal Chemistry, Richmond, Virginia, U.S.A.

Matteo Nicola Dario Di Minno, M.D., Reference Center of Coagulation Disorders, Department of Clinical and Experimental Medicine, Naples, Italy

Ji-Cui Dong, Ph.D., Department of Gynaecology and Obstetrics, Unit of Medicine of Reproduction and Endocrinology, Geneva University Hospital, Geneva, Switzerland

Elazer R. Edelman, M.D., Ph.D., FACC., Thomas D. and Virginia W. Cabot Professor Health Sciences and Technology and Director, Harvard – Massachusetts Institute of Technology Biomedical Engineering Center, Cambridge, Massachusetts, U.S.A.

R. Erik Edens, M.D., Ph.D., Professor, Department of Pediatrics, College of Medicine, University of Arkansas Medical Sciences, Arkansas Children's Hospital, Little Rock, Arkansas, U.S.A.

Charles P. Emerson, Jr., Ph.D., Director and Senior Scientist, Boston Biomedical Research Institute, Watertown, Massachusetts, U.S.A.

Jawed Fareed, Ph.D., Professor, Pathology and Pharmacology, Director, Hemostasis Research Laboratories, Cardiovascular Institute, Loyola University Chicago, Maywood, Illinois, U.S.A.

Maria Fuller, Ph.D., Lysosomal Diseases Research Unit, Department of Genetic Medicine, Women's and Children's Hospital and Department of Pediatrics, University of Adelaide, Adelaide, Australia

Kimberly Forsten-Williams, Ph.D., Associate Professor of Chemical Engineering, Virginia Polytechnic Institute and State University, Blacksburg, Virginia, U.S.A.

Hari G. Garg, Ph.D., D.Sc., Associate Biochemist, Pulmonary and Critical Care Unit, Department of Medicine, Massachusetts General Hospital, and Principal Associate, Harvard Medical School, Boston, Massachusetts, U.S.A.

Ian A. Greer, M.D., Regius Professor of Obstetrics and Gynaecology, Reproductive and Mental Medicine, University of Glasgow, Scotland

Nur Sibel Gunay, Ph.D., Senior Scientist, Momenta Pharmaceuticals Inc., Cambridge, Massachusetts, U.S.A.

Charles A. Hales, M.D., Chief, Pulmonary and Critical Care Unit, Department of Medicine, Massachusetts General Hospital, and Professor, Harvard Medical School, Boston, Massachusetts, U.S.A.

Nicholas J. Harmer, Ph.D., Research Associate, Department of Biochemistry, University of Cambridge, Cambridge, UK

Debra A. Hoppensteadt, Ph.D., Associate Professor, Technical and Administrative Director, Hemostasis Research Laboratories, Cardiovascular Institute, Loyola University Chicago, Maywood, Illinois, U.S.A.

John J. Hopwood, Ph.D, Professor, Lysosomal Diseases Research Unit, Department of Genetic Medicine, Women's and Children's Hospital and Department of Pediatrics, University of Adelaide, Adelaide, Australia

Ghamartaj Hosseini, Ph.D., Department of Gynaecology and Obstetrics, Unit of Medicine of Reproduction and Endocrinology, Geneva University Hospital, Geneva, Switzerland.

James A. Huntington, Ph.D., Senior Non-Clinical Fellow, Scientific Director, Thrombosis Research Unit, University of Cambridge, Cambridge, UK

Omer Iqbal, M.D., Research Assistant Professor, Hemostasis Research Laboratories, Cardiovascular Institute, Loyola University Chicago, Maywood, Illinois, U.S.A.

Walter P. Jeske, Ph.D., Associate Professor, Thoracic-Cardiovascular Surgery and Pathology, Director, Platelet Research, Hemostasis Research Laboratories, Cardiovascular Institute, Loyola University Chicago, Maywood, Illinois, U.S.A.

Morris J. Karnovsky, M.B.B.Ch., D.Sc., Shattuck Professor of Pathological Anatomy, Emeritus, Harvard Medical School, Boston, Massachusetts, U.S.A.

Michael G. Kinsella, Ph.D., Research Associate Member, Hope Heart Program, Benaroya Research Institute at Virginia Mason, Seattle, Washington, U.S.A.

Hiroshi Kitagawa, Ph.D., Professor, Kobe Pharmaceutical University, Department of Biochemistry, Higashinada-Ku, Kobe, Japan

Mehmet E. Korkmaz, M.D., FECS, Professor of Cardiology, Head, Department of Cardiology, Guven Hospital, Kavaklidere, Ankara, Turkey

Marion Kusche-Gullberg, Ph.D., Department of Biomedicine, University of Bergen, Bergen, Norway

Ulf Lindahl, Ph.D., Uppsala University, IMBIM, Biomedical Center, Uppsala, Sweden

Robert J. Linhardt, Ph.D., Professor, Department of Chemistry and Chemical Biology, Biology and Chemical and Biological Engineering, Rensselaer Polytechnique Institute, Troy, New York, U.S.A.

Caini Liu, Ph.D., Ohio State university/OARDC, Department of Animal Sciences, Wooster, Ohio, U.S.A.

Dongfang Liu, M.D., Ph.D., Scientist, AstraZeneca Oncology Research and Development, Waltham, Massachusetts, U.S.A.

Peter J. Meikle, Ph.D., Lysosomal Diseases Research Unit, Department of Genetic Medicine, Women's and Children's Hospital and Department of Pediatrics, University of Adelaide, Adelaide, Australia

Shuji Mizumoto, M.S., Kobe Pharmaceutical University, Department of Biochemistry, Higashinada-Ku, Kobe, Japan

Shaker A. Mousa, Ph.D., M.B.A., F.A.C.C., F.A.C.B., Professor and Director, Pharmaceutical Research Institute at Albany College of Pharmacy, Albany, New York, U.S.A.

Eva M. Munoz, Ph.D., Department of Chemistry and Chemical Biology, Biology and Chemical and Biological Engineering, Rensselaer Polytechnique Institute, Troy, New York, U.S.A.

Annamaria Naggi, Ph.D., Vice Director, G. Ronzoni Institute for Chemical and Biochemical Research, Milan, Italy

Christian Noti, B.Sc., Laboratory for Organic Chemistry, ETH Honggerberg, Zurich, Switzerland

Matthew A. Nugent, Ph.D., Professor of Biochemistry and Ophthalmology, Boston University School of Medicine, Boston, Massachusetts, U.S.A.

Marc Princivalle, Ph.D., Department of Gynaecology and Obstetrics, Unit of Medicine of Reproduction and Endocrinology, Geneva University Hospital, Geneva, Switzerland

Tim Rudd, B.Sc., School of Biological Sciences, University of Liverpool, Liverpool, UK

Ram Sasisekharan, Ph.D., Professor of Biological Engineering, Massachusetts Institute of Technology, Cambridge, Massachusetts, U.S.A.

Peter H. Seeberger, Ph. D., Professor, Laboratory for Organic Chemistry, ETH Honggerberg, Zurich, Switzerland

Zachary Shriver, Ph.D., Associate Director, Momenta Pharmaceuticals Inc., Cambridge, Massachusetts, U.S.A.

Mark A. Skidmore, B.Sc., School of Biological Sciences, University of Liverpool, Liverpool, UK

Kazuyuki Sugahara, Ph.D., Professor and Chairman, Kobe Pharmaceutical University, Department of Biochemistry, Higashinada-Ku, Kobe, Japan

Andrew A. Thomson, M.D., Consultant in Obstetrics and Gynaecology, Royal Alexandria Hospital, Paisley, Scotland

Antonella Tufano, MD., Professor, Reference Center of Coagulation Disorders, Department of Clinical and Experimental Medicine, Naples, Italy

Jeremy E. Turnbull, Ph.D., Professor, School of Biological Sciences, University of Liverpool, Liverpool, UK

Sandra G. Velleman, Ph.D., Associate Professor, Ohio State University/OARDC, Department of Animal Sciences, Wooster, Ohio, U.S.A.

Ganesh Venkataraman, Ph.D., Senior Vice President, Momenta Pharmaceuticals Inc., Cambridge, Massachusetts, U.S.A.

Jeanine M. Walenga, Ph.D., Professor, Thoracic-Cardiovascular Surgery and Pathology, Co-Director, Hemostasis, Research Laboratories, Cardiovascular Institute, Loyola University Chicago, Maywood, Illinois, U.S.A.

Theodore E. Warkentin, M.D. Professor of Medicine, McMaster University, Hamilton, Ontario, Canada

Thomas N. Wight, Ph.D., Member, Hope Heart Program, Benaroya Research Institute at Virginia Mason, and Affilliate Professor of Pathology, University of Washington School of Medicine, Seattle, Washington, U.S.A.

Edwin A. Yates, Ph.D., Principal Experimental Officer, School of Biological Sciences, University of Liverpool, Liverpool, UK

Haining Yu, Ph.D., Division of Medicinal and Natural Products, University of Iowa, Iowa City, Iowa, U.S.A.

Chemistry and Biology of Heparin and Heparan Sulfate
H.G. Garg, R.J. Linhardt and C.A. Hales (Editors)

Chapter 1

Structure and Active Domains of Heparin

BENITO CASU

G. Ronzoni Institute for Chemical and Biochemical Research, G. Colombo, Milan, Italy

I. Introduction

Heparin is a sulfated polysaccharide belonging to the family of glycosaminoglycans (GAG) (1). The structure of heparin has been extensively investigated for more than 50 years, with the particular aim of unraveling the features associated with its potent anticoagulant activity (2). The emerging interest in nonanticoagulant properties of heparin (3) and their prospective therapeutic applications (4) has extended these studies in an attempt to gain an understanding of the molecular basis and possible interplay of different sequences. The present knowledge of structure and structure–activity relationships of heparin has emerged steadily over the years. The regular sequences in the prevalent product of heparin biosynthesis that constitute the majority of the sequences of beef lung heparins used in several structural studies has long been thought to be exclusively responsible for the anticoagulant activity. The discovery that this activity is mainly dependent on an antithrombin (AT)-binding domain that is present in only about one-third of the chains constituting heparins currently used in therapy, and that this domain is a specific pentasaccharide sequence, has led to the reappraisal of the role of minor sequences in determining specificities of biological interactions of heparin. Such a reappraisal has, in turn, been stimulated by an increasing interest in heparan sulfate (HS), a structural analog of heparin that plays important roles in a number of physiological and pathological processes. HS and heparin are biosynthesized from the common precursor *N*-acetyl heparosan and are constituted by the same disaccharidic building blocks, though in different proportions. HS is less sulfated and more heterogeneous than heparin, mainly as a result of more restricted action of the

enzymes that modify the common precursor (5). However, since HS is present on the surface of most cell types and in the extracellular matrix while heparin is usually sequestered in mast cells, HS is thought to exert physiologically some of the functions/activities pharmacologically exerted or counteracted by heparin (5). Heparin thus accompanied HS into the world of "new biology", with the perception that distinct domains of both GAGs preferentially bind proteins that modulate a number of physiological and pathological processes (6).

A deeper elucidation of the structure and information on biological interactions of both heparin and HS was made possible by the availability of structurally well-defined heparin oligosaccharides obtained by chemical synthesis (7) and by developments of methods for sequencing heparin/HS fragments (8). Developments in understanding the structure–activity relationships of heparin are covered in several reviews (5,9–13). The present knowledge is summarized in this chapter, with special emphasis on those structure–activity relationships that have been most extensively investigated. Different aspects of these and other activities are dealt with in more detail in other chapters of this book.

II. Heparin Components

A. Monosaccharide Residues

Like most of the GAGs, heparin is a linear polysaccharide constituted by alternating disaccharide sequences of a uronic acid and an aminosugar. The uronic acid residues of heparin are L-iduronic acid (IdoA) and D-glucuronic acid (GlcA), and its only aminosugar is D-glucosamine (GlcN). Indeed, IdoA, GlcA, and GlcN, together with the minor components D-galactose (Gal) and D-xylose (Xyl) belonging to the terminal of GAG chains linked to the peptide core of the original peptidoglycan are the only monosaccharide residues identified in purified heparins (2).

Whereas both IdoA and GlcN residues are linked α-1,4 to the next residue in the chain, GlcA is linked β-1,4. GlcN is prevalently *N*-sulfated in heparin and *N*-acetylated in minor sequences. Both the uronic acid (especially IdoA) and the aminosugar bear *O*-sulfate groups. The formulas of monosaccharide residues most represented in heparin are shown in Fig. 1. Heparin chains are made up of various combinations of these building blocks. As schematized in Fig. 2, different sulfation patterns are unevenly distributed along the heparin/HS chains, with less charged sequences mostly concentrated towards the reducing side of the chains (R) and the most charged ones towards the nonreducing side (NR), with mixed domains (NA/NS) between the two regions. The relative proportion of the different domains and the actual composition within the same domains of heparins vary depending on the animal and organ source and, to some extent, also on the purification procedures (14).

Some of the heparin chains terminate, at the R end, with the "linkage region" (LR) reminiscent of the attachment, through a serine (Ser) residue, to the peptide core of the original proteoglycan (2). As a result of the limited cleavage

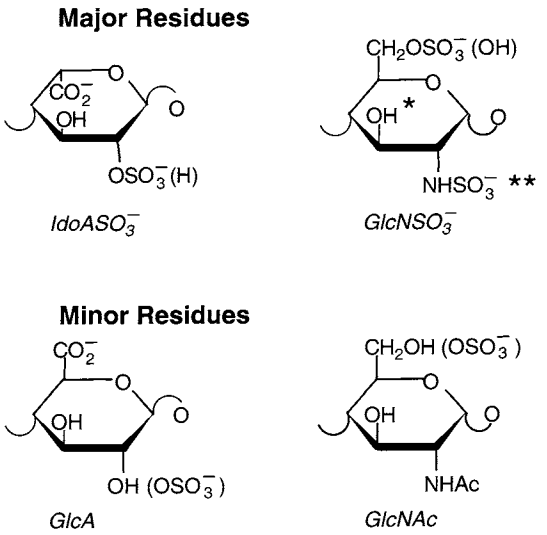

Figure 1 Monosaccharide components of heparin. Forms in parenthesis occur less frequently. Minor GlcN residues bear a SO_3^- substituent (*), or a free NH_2 group instead of a $NHSO_3^-$ group (**) (see text).

by β-D-glucuronidases of GlcA–GlcN linkages in the last step of biosynthetic modification of carbohydrate chains of the heparin proteoglycan, the terminal residue on the NR end of heparin chains is usually a GlcN (5). Depending on the extent of this latter modification and on its possible erosion during manufacturing/purification processes, heparins from different origins widely differ in their content in LR (see later).

B. Major Disaccharide Units

The composition of heparin is usually expressed in terms of their content in different disaccharide units. As illustrated in Fig. 2, the major disaccharide repeating sequences of heparin are those of the trisulfated disaccharide (TSD) IdoA2SO_3–GlcN$SO_3$6SO_3, which are concentrated in NS domains, where glucosamine residues are prevalently *N*-sulfated. TSD units represent up to 60–75% of heparins obtained from pig mucosa and up to 85% of heparins from beef lung (15,16). These relatively long segments of "fully sulfated" (i.e., *N*-, 2-*O*-, and 6-*O*-sulfated) disaccharide units along the heparin chains are often referred to as constituting "regular regions" and are the major contributors to the polyelectrolytic properties of heparin.

Also 2-*O*-sulfated GlcA residues have been identified in fully sulfated regions of heparin (17). Although minor components [less than 0.5% (w/w)], these residues may play important functions (10,17).

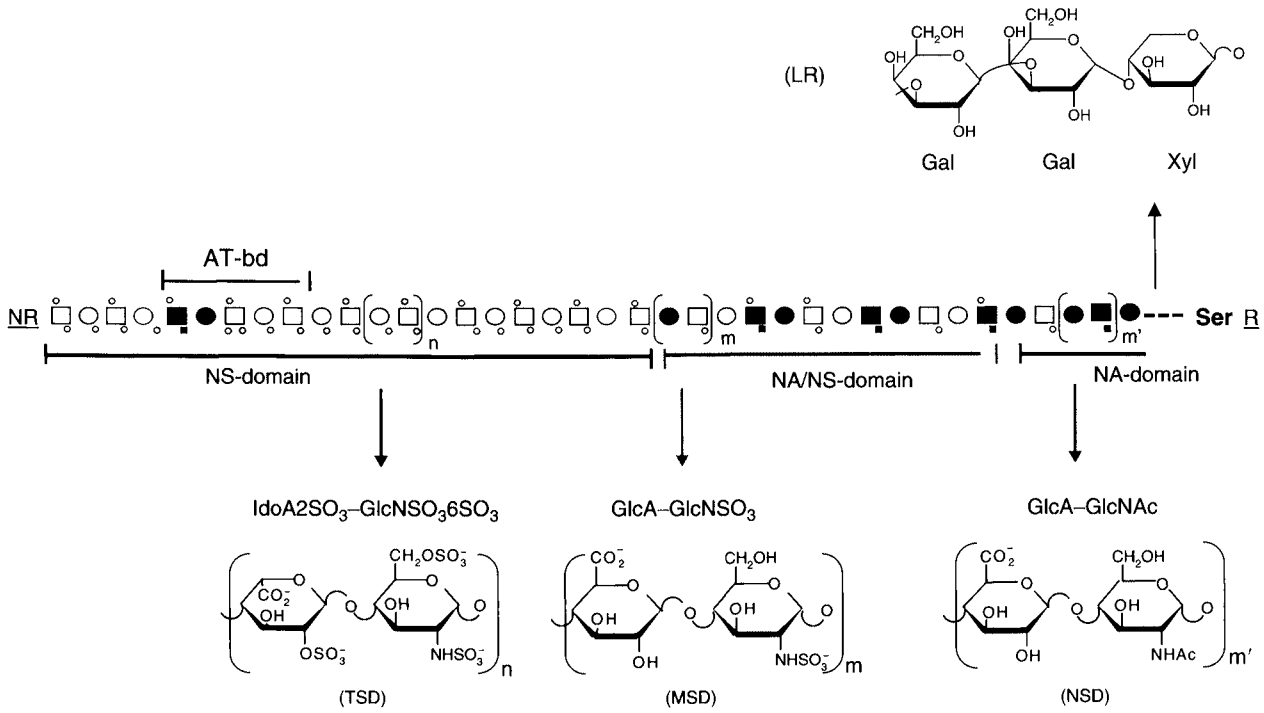

Figure 2 Idealized representation of a heparin chain constituted of *N*-acetylated (NA), *N*-sulfated (NS), and mixed NA/NS domains also containing an antithrombin-binding domain (AT-bd). The chain is conventionally represented as extending from its nonreducing (NR) to its "reducing" end. In fact, its biosynthesis starts from the "linkage region" (LR). Formulas of major disaccharidic sequences within NS, NA/NS and NA domains and of the "linkage region" (LR) originally linked (through Ser) to the Gly-Ser polypeptide core are shown. Symbols are as in Ref. 5.

As segments of a macromolecule, NS regions of heparin exclusively constituted by TSD sequences should not be defined as copolymers of repeating disaccharide units. In fact, the α-L configuration of IdoA residues involves a trans orientation of pairs of TSD units and heparin should thus be referred to as a copolymer of hexasulfated tetrasaccharide (HST) units, featuring arrays of three sulfate groups (NSO_3, 2-*O*-SO_3, and 6-*O*-SO_3) that alternate on both sides of the chains, as shown in Fig. 3. Such an arrangement of sulfate groups, confirmed by 3D structures (see Section III of this chapter), has an important bearing on protein-binding and related biological properties of heparin (see Section IV).

The length of repeating TSD units along the heparin chains has been assessed only in statistical terms and for a limited number of heparin types, mainly through size profiling of oligosaccharides generated by cleavage of heparins oxidized with periodate at the level of nonsulfated uronic acids (18,19). Without isolation and sequencing of individual oligosaccharides, this analytical approach quantificates only sequences made up of 2-*O*-sulfated disaccharide units and does not take into account occasional 6-*O*-desulfated glucosamine residues. The length of repeating "TSD" sequences in pig mucosal heparin corresponds to 4–12 disaccharide units (18), with an average size of eight disaccharide units (19). As illustrated in Fig. 4, the 2-*O*-sulfated sequences are separated from each other by GlcA-containing (less frequently by IdoA-containing) sequences (see later sections) (18).

C. Undersulfated Sequences

As schematically illustrated in Fig. 2, minor undersulfated repeating units (such as the monosulfated disaccharide (MSD) GlcA–$GlcNSO_3$) are part of mixed *N*-sulfated/*N*-acetylated, GlcA-containing NA/NS domains. The NA domain close to the linkage region LR is prevalently constituted of nonsulfated disaccharide (NSD) GlcA–GlcNAc repeating units. However, NA/NS regions may incorporate 2-*O*-sulfated IdoA and 6-*O*-sulfated $GlcNSO_3$/NAc residues, and some GlcN

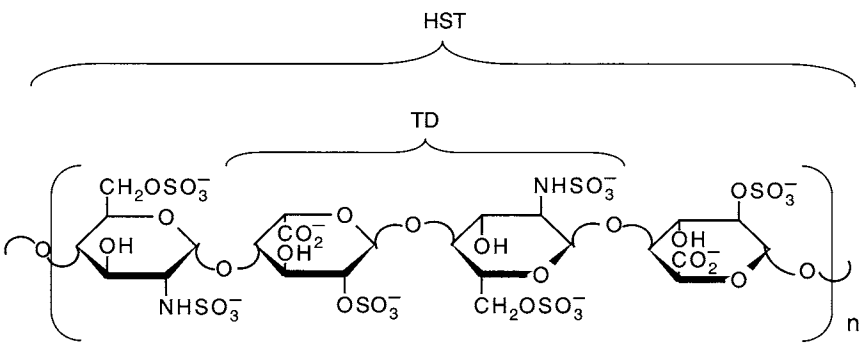

$[GlcNSO_36SO_3–IdoA2SO_3–GlcNSO_36SO_3–IdoA2OSO_3]_n$

Figure 3 Heparin (major sequences in the NS region) as a poly-tetrasaccharide.

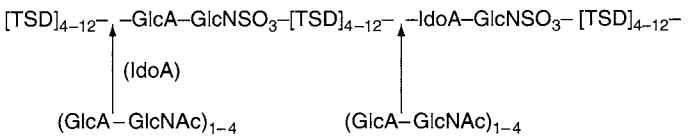

Figure 4 Proposed distribution of disaccharide units along an average heparin chain (18) TSD, trisulfated disaccharide. For simplicity, possible AT-binding and linkage regions are omitted. Arrows indicate possible insertion of GlcA-containing units.

residues in the NA domains are 6-*O*-sulfated. Heparins from different animal species and/or organs significantly differ from each other in their degrees of heterogeneity as revealed by a disaccharide analysis (14) or an NMR analysis of their sulfation patterns (20). As illustrated in Table 1, the relative contents of non-6-*O*-sulfated glucosamine and non-2-*O*-sulfated iduronic acid of pig mucosal heparins are consistently different from those of beef mucosal heparins (14,16,20). Also the extent of undersulfation associated with occurrence of nonsulfated GlcA residues widely varies among different types of heparin, ranging from a few percent of total uronic acids for beef lung heparins to up to 20% of pig mucosal heparins (16,20).

As illustrated in Fig. 2, nonsulfated GlcA (together with *N*-acetylated GlcN) residues are prevalently (though not exclusively) concentrated in NA and NA/NS regions. However, 2-*O*-desulfated iduronic acid residues and 6-*O*-desulfated glucosamine residues are spaced out along the heparin chains (21). Figure 5 schematically illustrates the concept that sulfation gaps associated with *O*-undersulfation in the NS/NA and NS regions of heparin separate fully sulfated sequences of different lengths. Due to the different requirements in terms of size of fully sulfated

Table 1 6-*O*- and 2-*O*-undersulfation of Different Heparin Preparations

	%A–6OH	%I–2OH		%A–6OH	%I–2OH
PM-1	18.0	12.9	BM-1	40.4	2.2
PM-2	19.0	13.5	BM-2	40.1	2.2
PM-3	21.7	nd	BM-3	38.6	2.3
PM-4	16.9	13.5	BM-4	39.1	nd
PM-5	18.6	nd	BM-5	40.7	2.3
PM-6	17.5	nd	BM-6	46.7	2.1
PM-7	nd	9.6	BM-7	36.7	2.7
PM-8	nd	12.9	BM-8	nd	2.2
PM-9	nd	12.8			
PM-10	nd	12.8			
PM-11	nd	12.6			
Average	18.6	12.7		40.3	2.3

PM, from pig intestinal mucosa; BM, from beef intestinal mucosa; A, aminosugar (GlcN); I, IdoA. (Source: Ref. 20).

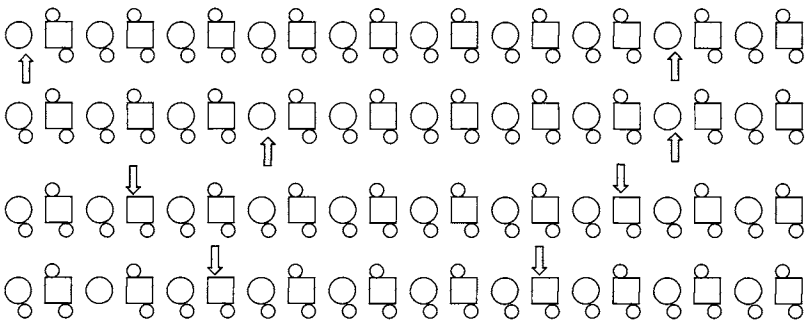

Figure 5 Idealized representation of heparin NS chains with 6-*O*- and 2-*O*-sulfation gaps (indicated by arrows) spaced out along the chains. For simplicity, AT-binding sequences are not shown. Sulfation gaps determine the length of "fully sulfated" segments made up of TDS sequences and modulate protein-binding and associated biological properties of heparin. Symbols as in Ref. 5.

sequences as effective ligands for most of the heparin-binding proteins (5,10,12), different frequencies of sulfation gaps conceivably modulate the protein-binding properties of heparins and heparin fractions.

A large number of heparin oligosaccharide fragments arising from the irregular regions of heparin are listed in Ref. 5. The number of identified heparin/HS oligosaccharides is steadily increasing (22–24). Recurrent patterns, such as the trisulfated hexasaccharide IdoA(GlcA)2SO_3–GlcNSO_3–IdoA–GlcNAc–GlcA–GlcNSO_3, have been identified in the low sulfated irregular region of pig mucosal heparin, the underlined trisaccharide sequence being shared by a number of the isolated oligosaccharides (25).

D. Specific Sequences

As illustrated in Fig. 2, some of the heparin chains contain a specific sequence constituting the antithrombin binding domain (AT-bd). This sequence is the pentasaccharide AGA*IA shown in Fig. 6, where the asterisk denotes a rare 3-*O*-sulfated GlcNSO_3 residue. The figure also indicates the three sulfate groups that are essential for high-affinity binding for AT, and underlines the fact that the GlcA residue is also essential. The IdoA residue preceding the pentasaccharide shown in the formula, though invariably present in natural AT binding domains, does not contribute to the affinity for AT. Some natural variants compatible with high affinity for AT (i.e., *N*-sulfation instead of *N*-acetylation of the first aminosugar residue and 6-*O*-sulfation of the 3-*O*-sulfated residue) are also shown (5).

The information summarized in Fig. 6 has been obtained since the unexpected finding (made independently by three research groups) that only about one-third of the chains constituting heparin currently used in therapy bind to AT and that most of the anticoagulant activity of heparin is attributable to species with high affinity

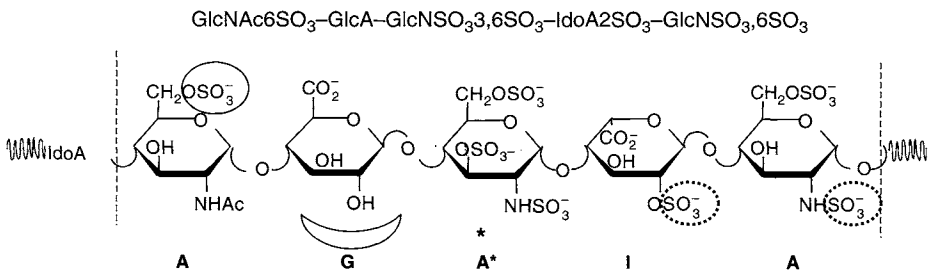

Figure 6 Pentasaccharidic antithrombin-binding sequence AGA*IA (where A is either $GlcNAc6SO_3$ or $GlcNSO_36SO_3$; A*, $GlcNSO_33,6SO_3$; G, GlcA; I, $IdoA2SO_3$). The asterisk marks the typical 3-*O*-sulfated glucosamine residue. Groups in parentheses are compatible with high affinity for AT. Circled sulfate groups are either essential (full circles) or marginally essential (dotted circles) for high affinity. The "half moon" below GlcA indicates that this residue is also essential. The IdoA residue preceding the pentasaccharide is not essential for AT binding, but invariably occurs in natural AT-binding domains of mucosal heparins.

(HA) for AT (26–28). The discovery that the rare 3-*O*-sulfated glucosamine residue is an essential component of the AT-bd (29) was followed by full elucidation of the structure of this active domain (30) and by chemical synthesis of heparin oligosaccharides, finally leading to a synthetic pentasaccharide exactly reproducing the structure of the natural one (7). The events leading to these developments are reviewed in Ref. 31. The involvement of the pentasaccharide in triggering AT-mediated biological activities is discussed in Section IVA and in other chapters of this book.

The location of the AT-bd along the heparin chain is still uncertain. Whereas an early study suggested that this domain was located prevalently towards the NR end of the molecule (32), another study suggested a more random distribution (33). On the other hand, the observation that the NMR signals typical for the "linkage region" concentrated exclusively in the heparin fraction with no affinity for AT (34) is in favor of the first hypothesis. Several oligosaccharides obtained by controlled depolymerization of heparin fractions with high affinity for AT contributed to defining structural features around the AT-bd (35–38).

As illustrated in Fig. 2, the linkage region is another well-characterized sequence common to heparin and HS, as well as to other GAGs (2,39). It consists of a trisaccharide β-1,3-linked to the last GlcA residue of the glycosaminoglycan chain and is constituted by three neutral residues: one D-galactose (Gal) residue β-1,3 linked to a second Gal, which is β-1,4-linked to a D-xylose (Xyl) residue β-linked to Ser (39). The content of LR in heparins varies widely depending on the origin of heparin [i.e., it is lower than 1% in beef lung heparins and up to 5% in pig mucosal heparins (39,40)]. Depending on treatments for purification and bleaching during the manufacturing process, heparin may lose the terminal Ser of the LR and most of the LR as well. Though potentially implicated in antiangiogenic properties of heparin/HS (41), the sequence of the LR is commonly regarded as a biologically inactive component of heparin.

III. Molecular Conformation of Heparin Residues and Sequences

The molecular conformation of GAGs, especially of those containing IdoA, such as heparin, HS and dermatan sulfate, has long been a matter of controversy (42). Modeling of 3D structures of polysaccharides in solution involves the assumption of the conformation of individual residues and building up the polymer chains with these residues in a way that minimizes the overall conformational energy. Molecular models must then be experimentally validated, usually by NMR spectroscopy. The assumption and experimental validation of the conformation of heparin components, such as GlcN and GlcA, are unproblematic. Whereas energy calculations and NMR parameters indicate a classic chair ($^4C_1$) conformation for both residues, apparently anomalous experimental data has long made the conformation of IdoA (and IdoA2SO$_3$) elusive (43).

The availability of a number of synthetic heparin oligosaccharides (7) has permitted extensive studies on the conformation of IdoA (and IdoA2SO$_3$) in different sequences, leading to the finding that IdoA pyranose rings may assume one of three equienergetic conformations (the chair $^4C_1$ and $^1C_4$, and the skew-boat $^2S_0$). In fact, the shape of the IdoA residues flips from one to at least one other of these conformations in rapid dynamic equilibrium (44). The relative population of two (or three) conformers depends on sulfation on the same residue (i.e., IdoA2SO$_3$ *vs* IdoA) and on adjacent GlcN residues (44, 45). Whereas IdoA2SO$_3$ residues in the NS domains of heparin are about 60% in the $^1C_4$ and 40% in the $^2S_0$ conformation, 3-*O*-sulfation of GlcNSO$_3$ as in the AT-binding domain reverses to 40:60 the population of these conformers (44,46). Such a proportion further varies in different heparin/HS oligosaccharides (45–49) as a function of sequence. Also, the $^1C_4$ form contributes to the conformational equilibrium of IdoA and IdoA2SO$_3$ residues in terminal positions (45). Conformer populations are also affected by extrinsic factors, such as the type of counter ions (45,47).

The capability of iduronate residues to assume more than one conformation confers on IdoA-containing chains a peculiar local flexibility ("plasticity"), with important bearing on binding and associated biological properties (50). This concept is illustrated in Fig. 7. Molecular modeling studies on heparin sequences in the regular region generated helices, as shown in A and B for chains build-up with IdoA2SO$_3$ residues in the $^1C_4$ and $^2S_0$ conformation, respectively (51). Both A and B helices feature arrays of three sulfate groups (ANS, I2S, and A6S) on alternate sides of the chain, as expected from configurational considerations on the primary structure (Fig. 3). However, the orientation in space of different substituent groups (including the anionic ones SO_3^- and COO^-) is widely different in the two helices and involves different spacings between the sulfate groups within each cluster. By contrast, the conformation of *N*-acetyl heparosan, taken as representative conformation in the NA domains of heparin/HS (Fig. 7C), is essentially invariant due to the stable $^4C_1$ conformation taken up by β-linked GlcA residues (43,52). Apart from affecting the relative conformer populations, sulfation gaps along the heparin chains do not involve substantial changes in the conformation of each type of helix (53). The foregoing concepts are discussed in critical reviews (5,50,54).

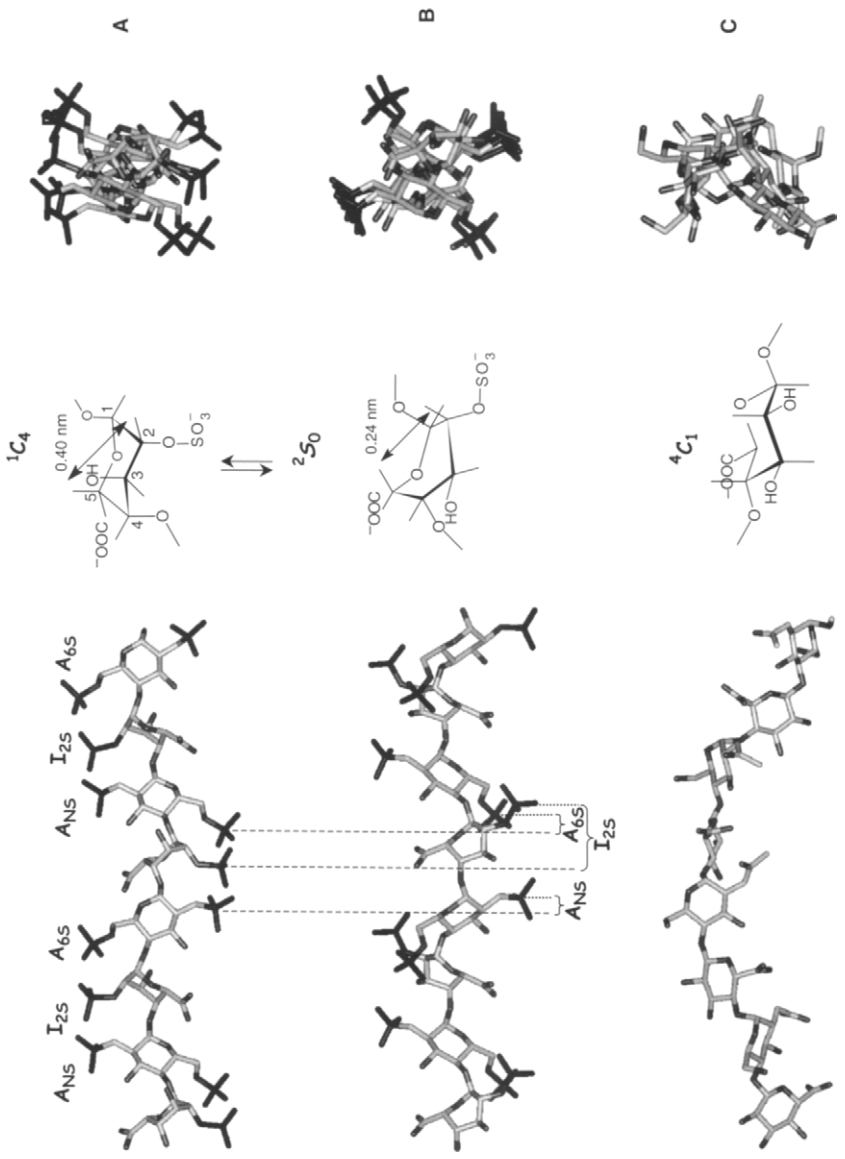
A
B
C
$^1C_4$
$^2S_0$
$^4C_1$
0.40 nm
0.24 nm
A_{NS}
I_{2S}
A_{6S}

IV. Heparin Domains Involved in Biological Interactions

A. Inhibition of Coagulation and Thrombosis

Heparin exerts its anticoagulant activity primarily by accelerating the rate of inhibition of the natural protease inhibitors antithrombin III (AT, which inhibits both Factor Xa and thrombin) and – to a minor extent – heparin cofactor II (HCII, which selectively inhibits thrombin). AT and HCII are structural homologues (55). However, AT binds only heparin, while HCII also binds dermatan sulfate, although involving different polypeptide sequences (56). Whereas the binding site of heparin for AT – the unique pentasaccharide sequence described in Section II.D – is contained in only about one-third of the chains of common heparins, HCII-binding sequences of heparin and dermatan sulfate are less specific and contained in practically all the GAG chains (56).

Extensive studies during the last 20 years have contributed to the elucidation of the molecular basis of the anticoagulant and antithrombotic activity of heparin, especially as regards their inhibition of Factor Xa and thrombin, the final two proteases of the coagulation cascade. Although Protein C-mediated interactions also play a role in preventing coagulation, major anticoagulant effects are mediated by AT and heparin HCII (for a review, see Ref. 57). Anticoagulant effects are also associated with GAG-induced release of tissue factor pathway inhibitor (TFPI) from vascular endothelium (58,59).

The activity of both AT and HCII is dramatically increased by binding with heparin. As mentioned in previous sections, the discovery of the active site for AT, and the finding that the anticoagulant properties of this GAG are largely concentrated in species containing a unique pentasaccharide sequence, represented a landmark in heparin research. Though occasionally found in non-AT-binding sequences (60), the 3-*O*-sulfate group of the central unit of the pentasaccharide is considered to be a marker of the active site.

Heparin sequences that specifically bind to HCII have not been identified. In fact, HCII seems to be bound by heparin rather nonspecifically (56,57,61). However, it is reasonable to assume that sequences of the trisulfated disaccharide (TSD, see Section II.B) are the major sites for HCII binding.

The present knowledge of the mechanism of the interaction between heparin, AT, and thrombin and related structural aspects is largely based on physicochem-

---

Figure 7 Molecular conformation of heparin NS chains (A, B) and NA chains (these latter represented by the biosynthetic precursor *N*-acetyl heparosan, C), illustrating the dramatic influence of changes (from $^1C_4$ to $^2S_0$) in the conformation of IdoA2SO$_3$ residues of heparin on spacing of sulfate groups along and across the chains (52). The rigid ($^4C_1$) conformation of GlcA residues in *N*-acetyl heparosan does not involve significant changes from the chain conformation shown in C, even when some of the OH groups are sulfated (M. Guerrini and M. Hricovini, unpublished). Structures A and B are redrawn from Ref. 51. The figure also shows that the three conformations of uronic acid residues are characterized by different dihedral angles between vicinal C–H bonds and distances between nonbonded atoms (i.e., between H5 and H2), typically measurable by NMR spectroscopy (44).

ical studies of these systems in solution (62,63) and on X-ray diffraction studies (64,65). Since these studies and their biological implications are covered in other chapters of this book, the present chapter briefly discusses only current information on heparin sequences involved in the above interactions and the dependence of these interactions on the size of GAG sequences and the location of active sites in these sequences.

The search for minimal sequences binding to AT and HCII and inducing inhibition of thrombin mediated by these cofactors has led to understanding the size-dependence of GAG activities associated with interaction with the two protease inhibitors. AT-, as well as HCII-mediated inhibition of thrombin need relatively long heparin chains as a requisite for binding to both the inhibitor and the enzyme in a ternary complex. Thrombin inhibition requires a minimum chain length of 14–16 monosaccharide residues (66). On the other hand, AT-mediated inhibition of Factor Xa requires only the pentasaccharide sequence of the active site for AT (reviewed in 5,7,57,67). This observation was at the basis of the introduction of low molecular weight heparins (LMWHs) as antithrombotic agents blocking the coagulation cascade at the level of Factor Xa. Being only marginally involved in the inhibition of thrombin and in side effects associated with full-length heparin, LMW heparin species were thought to reduce the hemorrhagic risks. However, as discussed in another chapter of this book, the major advantage of LMWHs over conventional heparin for certain therapeutic indications is their better bioavailability. Since, as observed upon partial digestion with heparinase 1 (68,69), depolymerization procedures used for obtaining LMWHs may occasionally cleave the AT-binding sequence, chains with high affinity for AT are usually less represented in LMWHs than in conventional heparins (70). On the other hand, a synthetic pentasaccharide closely reproducing the structure of the AT-bd (as a methyl glycoside, in a variant in which the first GlcN residue is *N*-sulfated instead of *N*-acetylated) and based on exclusive inhibition of Factor Xa was proved to be an effective antithrombotic agent (71).

Synthetic oligosaccharide chemistry has made an important contribution to establish the relationships between structure and AT-mediated activities (7,71,72). A pentasaccharide with an additional 3-*O*-sulfate group (on the fifth residue) with respect to AGA*IA was shown to be even more active than the natural pentasaccharide (7). Also, a systematic study of extension of the heparin chain on both sides of the pentasaccharide sequence has confirmed that the chain extension required to bind thrombin in the ternary complex with heparin and AT must be at least 14 monosaccharide residues long and definitely established that such an extension must be toward the nonreducing terminal of the heparin chain (73). The biological implications of the location of the AT-bd along heparin chains are illustrated in Fig. 8. The actual location of thrombin in the ternary complex was also confirmed by studies using neo-glycoconjugates (74) and conclusively by X-ray diffraction studies (65).

The minimum heparin size for significant HCII binding was a hexasaccharide corresponding to three TSD units; full affinity for HCII is practically reached at eight monosaccharide residues (56).

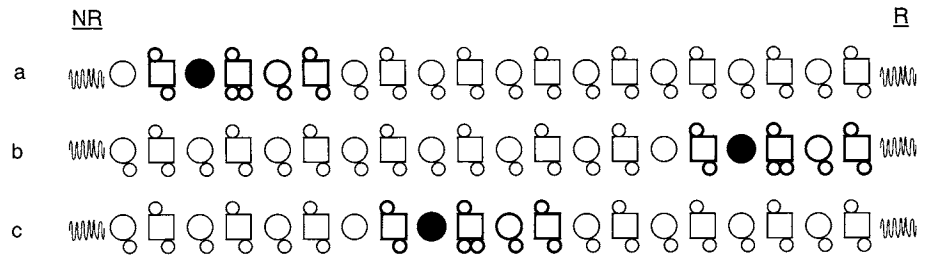

Figure 8 Heparin chains (arbitrary sequences) containing the pentasaccharidic antithrombin-binding domain (AT-bd) in different locations along the chains. Since inhibition of thrombin requires that the AT-bd is prolonged towards the nonreducing (NR) end by a decasaccharide (73), a-type chains are expected to exert substantial anticoagulant (anti-IIa, APTT) activity only when the AT-bd is located near the center of the chains. Symbols as in Ref. 5.

B. Inhibition of Release and Activation of Growth Factors

Accumulating evidence that HS sulfate chains of HSPGs interact with heparin-binding growth factors (GFs) and modulate their roles in cell growth, differentiation and, development (75–78) has stimulated extensive studies on these interactions (reviewed in Refs. 5, 9–12). GFs most widely studied for their implication in angiogenesis are the fibroblast growth factors (FGFs) and vascular endothelial growth factor (VEGF) (79,80). FGFs and VEGF are usually stored in inactive form by HS chains of HSPGs in the extracellular matrix and on the surface of endothelial cells. When released upon physiological or pathological breakdown of the HS chains, they can be activated by formation of complexes with HS fragments. These complexes are able to bind to tyrosine kinase cellular receptors (FGFRs, VEGFRs) and build up assemblies that trigger mitogenic signals (80,81). GFs can be displaced from HS chains also by the competitive action of exogeneous heparin (82). Some heparin/HS species as well as some heparin derivatives are good candidates as potential inhibitors of either release or activation of GFs, or both steps in growth signaling pathways (83–86). Binding to GFs is usually regarded as a prerequisite for inhibition of GF-induced angiogenesis and metastasis. Heparin sequences that bind individual GFs have been systematically searched, making use of heparin/HS fragments of different size and structure (87–91). Whereas significant binding to FGF-1 requires the three typical sulfate groups NSO_3, $2SO_3$, and $6SO_3$, 6-*O*-sulfation is not necessary for binding to FGF-2 (87–93). Figure 9 shows that different FGFs are bound to different extents by a heparin octasaccharide representative of the structure of heparin sequences in the NS regions. As shown in the same figure, the octasaccharide is a poor ligand for VEGF (91). As illustrated in Table 2, different GFs have been classified in terms of different sulfate groups in heparin octasaccharides needed for high-affinity binding (91).

As expected from the conformational flexibility of iduronic acid residues (50), comparison of synthetic pentasaccharides has demonstrated that IdoA-containing

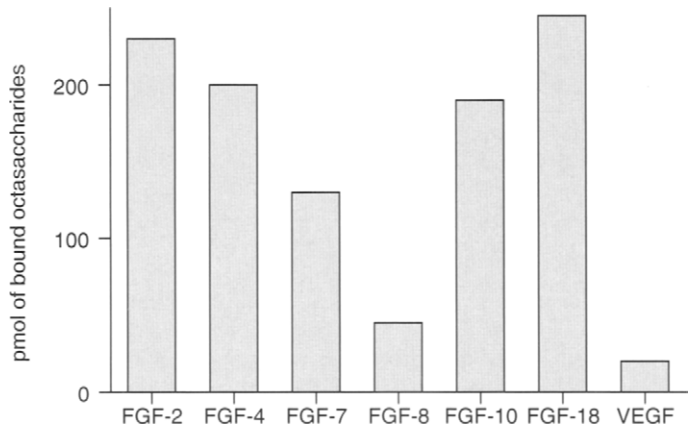

Figure 9 Different amounts of a heparin octasaccharide fraction with prevalent structure $(IdoA2SO_3-GlcNSO_36SO_3)_4$ bound to different growth factors (fibroblast growth factors FGF-2, -4, -7, -8, -10, -18, and to vascular growth factor VEGF). (Redrawn from Ref. 91).

sequences bind FGF-2 more efficiently than corresponding GlcA-containing sequences (94).

Activation of GFs through formation of ternary and larger assemblies also involving GF receptors requires heparin/HS sequences longer than octasaccharide (95). Such a concept has been strongly supported by X-diffraction and molecular modeling studies, clearly indicating that a minimum chain length is required for heparin chains to stabilize 2:2 complexes between GFs and their receptors by fitting in extended "basic canyons" generated by favored arrangements of the proteins (96–98).

The search for minimal GF-binding heparin/HS sequences is being facilitated by the use of oligosaccharide libraries obtained by systematic chemical or enzymatic modification of heparin/HS fragments or their biosynthetic precursors (92,93). Recurrent motifs required for high-affinity binding with certain growth factors have been identified. Thus, all heparin octasaccharides with a high affinity for FGF-1 contain the internal motif $IdoA2SO_3-GlcNSO_36SO_3-IdoA2SO_3$. However, a di-6-*O*-sulfated octasaccharide containing the $IdoA2SO_3-GlcNSO_3-IdoA2SO_3$ trisaccharide sequence binds to FGF-2 more strongly than the corresponding mono-6-*O*-sulfated octasaccharide, indicating that not only the number but also the

Table 2 *O*-Sulfate Groups Essential for Growth Factor Binding

Groups	GF	Necessary *O*-sulfate in octasaccharide
Group 1	FGF-2	2-*O*-SO_3
Group 2	FGF-10	6-*O*-SO_3
Group 3	FGF-18	2-*O*-SO_3 or 6-*O*-SO_3
Group 4	FGF-4; FGF-7; (FGF-1)	2-*O*- and 6-*O*-SO_3
Group 5	FGF-8; VEGF	

Source: Ref. 91.

position of sulfate groups determine the affinity for FGFs (92,93). Due to the variety of permutations within the heparin/HS structures, more than one sequence seems capable of strong binding with individual GFs, especially for sequences containing the conformationally flexible IdoA (or IdoA2SO_3) residues. On the other hand, the mitogeneity of GFs can be influenced by heparin-like GAGs, even without significant binding to GFs (99). As shown for FGFR4 (100), signaling may also be influenced by direct interactions with FGF receptors.

Besides the approaches of inhibiting GFs by inhibiting formation of ternary complexes with their receptors (85,86,101,102), GF-mediated signaling can be inhibited by inhibiting the enzyme heparanase (103–105). Heparanase is also involved in disruption of the extracellular matrix and its inhibition may impair cancer progression and metastasis (106,107). Heparanase is an endo-β-D-glucuronidase that cleaves HS chains at the level of GlcA residues (Fig. 10) (108). Minimal heparin/HS sequences that are efficiently cleaved by heparanase are shown in Table 3 (108–110). Although with somewhat reduced efficiency, GlcN residues bearing a 3-*O*-sulfate group – as in oligosaccharides with high affinity for antithrombin – are compatible with recognition and cleavage of the target GlcA residue (108–110). Heparanase is efficiently inhibited by heparin and some heparin derivatives (111). Heparin acts both as a substrate and an inhibitor of heparanase (108). Removal of 2-*O*-SO_3 or 6-*O*-SO_3 groups does not significantly impair the heparanase-inhibitory activity of heparin, provided that one of the two positions retains a high degree of sulfation (112,113). Removal of *N*-sulfate groups followed by *N*-acetylation involves a substantial decrease of the inhibitory activity, only however for degrees of *N*-acetylation higher than 50%, suggesting that only one NSO_3 group per tetrasaccharide unit is involved in binding with heparanase (113). The effects of some chemical modifications of heparin on the heparanase-inhibiting activity are illustrated in Fig. 11. Modification of the target GlcA residue as performed by glycol-splitting of all nonsulfated uronic acid residues causes complete loss of affinity for the enzyme while retaining heparanase-inhibition activity (113). Being endowed with potent heparanase-inhibiting and antimetastatic activity without significantly releasing GFs from endothelium, *N*-acetylated, glycol-split heparins are promising candidates for development as antiangiogenic and antimetastatic drugs (113).

C. Domains Involved in Other Interactions

Coverage of all reported interactions involving heparin and heparin oligosaccharides is beyond the scope of this chapter. Among these interactions, those with lipid- or

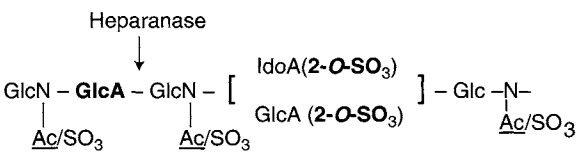

Figure 10 Heparin/HS linkages cleaved by heparanase (108). GlcA and sulfate groups in bold types are essential for recognition and cleavage by the enzyme.

Table 3 Heparin Oligosaccharides Cleaved by Heparanase

HA-Octa[a]

IdoA–GlcNAc6SO_3–GlcA↓–GlcN$SO_3$3,6SO_3–IdoA2SO_3–GlcNSO_3–IdoA2SO_3–AMol.6SO_3

Hexa-4[b]

ΔU2SO_3–GlcN$SO_3$6SO_3–IdoA–GlcNAc6SO_3–GlcA↓– GlcN$SO_3$6SO_3

Hexa-7[b]

ΔU2SO_3–GlcN$SO_3$6SO_3–GlcA↓–GlcN$SO_3$6SO_3–GlcA(↓)–GlcN$SO_3$6SO_3

Hexa-7S[b]

ΔU– GlcN$SO_3$6SO_3–GlcA(↓)–GlcN$SO_3$6SO_3–GlcA↓–GlcN$SO_3$6SO_3

HA-Penta[c]

GlcN$SO_3$6SO_3–GlcA↓–GlcN$SO_3$3,6SO3–IdoA2SO_3–GlcN$SO_3$6SO_3

Tetra-I[b]

U2SO_3–GlcN$SO_3$6SO_3–GlcA↓–GlcN$SO_3$6SO_3

[a]Data from Ref. 108.
[b]Data from Ref. 109.
[c]A. Bisio, J-P Li; and M. Petitou, personal communication.
HA, high affinity for AT; AMol, anhydromannitol; ΔU, unsaturated uronic acid.
Arrows indicate sites of cleavage by heparanase (in parentheses: secondary cleavage sites).

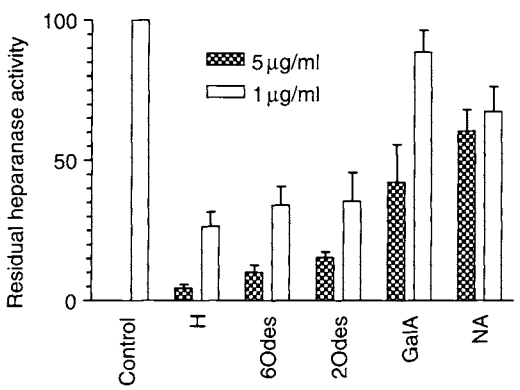

Figure 11 Heparanase-inhibiting activity of heparin (H) and heparin derivatives 100% desulfated at specific positions (6Odes, 6-*O*-desulfated; 2Odes, 2-*O*-desulfated, IdoA form; GalA, 2-*O*-desulfated, GalA form; *N*A, *N*-desulfated, *N*-acetylated) (113).

membrane-binding proteins, viruses, adhesion proteins, and chemokines are described and discussed in a comprehensive review (12). With the possible exception of those with the dengue virus envelope protein (114), structure–activity relationships have not yet been unraveled in such detail as those involving binding with antithrombin and growth factors. A number of heparin–protein interactions have also been studied from the protein side and have led to the identification of "consensus sequences," which permit, in favorable cases, the prediction and/or rationalization of heparin-binding properties of proteins (115–117). However, heparin-binding sites are seldom localized in short protein sequences and may involve (as in the case of antithrombin) sequences situated in different loops of the protein. A detailed study of these complex interactions requires structurally well-defined oligosaccharides longer than conveniently obtained at present both by fragmentation/fractionation of heparin and by chemical synthesis. Long oligosaccharides are most often required for studies of interactions involving more than one protein, as in the case of FGFs/FGFRs. As a first approach, heparin derivatives are used to assess whether all sulfate groups of the polysaccharide are involved in the interaction of interest. Heparin derivatization is indeed a strategy for obtaining general structure–activity relationships (118). The TSD sequences, representing the prevalent product of biosynthesis of mammalian heparins, are most often involved in the interactions with proteins inducing biological activities. However, as already indicated in some examples in Sections IVA and B of this chapter, use of selectively desulfated heparins has often shown that some of the sulfate groups are compatible, but not necessary, for high-affinity binding. In fact, heparin/HS sequences that specifically bind to a given protein site may be hidden within fully sulfated sequences, especially in the NS domains of the GAG chains (5). Whenever extra sulfate groups do not hinder active binding, oversulfation usually increases the strength of heparin–protein interactions, especially when these interactions are relatively nonspecific.

Rather unexpectedly, substituents other than sulfate groups were found to be required for important heparin/HS–protein interactions. As described in Section IVB, *N*-acetyl groups are compatible with recognition (108,109), as well as with inhibition of heparanase (113). More specifically, heparin/HS sequences containing *N*-acetylated GlcN residues are needed for interaction with endostatin (119) and with the BACE1 protein, a secretase involved in generation of β-amyloid (120). Also, free NH_2 groups, long thought to be just artifacts in the preparation of heparin and HS, were found to be natural constituents of HS and are involved in interactions with selectins (121,122).

V. Molecular Conformation of Active Domains

Although general structure–activity relationships may be obtained by considering primary structures, the effectiveness of biological interactions is largely determined by the shape taken up by heparin/HS sequences in their actual complexes with the relevant target proteins. The shape of heparin chains, especially in regions containing the conformationally flexible IdoA (or IdoA2SO_3), cannot be determined by

molecular modeling based only on theoretical calculations. X-ray diffraction studies of co-crystals of heparin oligosaccharides and antithrombin (64) and FGF-2 (123) have permitted us to determine "active" conformations of heparin sequences involved in these interactions and to emphasize the role of conformational plasticity of IdoA residues in determining the local and overall shape of the active domains. The conformation taken up in co-crystals by a heparin hexasaccharide complexed with antithrombin and FGF-2 is shown in Fig. 12. Of the two equienergetic conformations coexisting in the absence of the proteins (44,45), the IdoA2SO$_3$ residue of the hexasaccharide selects the chair $^1C_4$ in the actual FGF-2 binding site and the skew-boat $^2S_0$ outside the binding site (Fig. 12) (123), thus providing a proof-of-concept of the importance of conformational flexibility of IdoA residues in intermolecular interactions (50).

Active conformations of heparin oligosaccharides can also be determined in solution (124). NMR studies confirmed the findings from X-ray diffraction studies (64) that the conformational equilibrium of IdoA2SO$_3$ residue of the pentasaccharide AGA*IA is completely shifted to the $^2S_0$ form in the presence of antithrombin (125). This is illustrated in Fig. 13, which also shows that IdoA2SO$_3$ is not directly involved in interaction with the protein, its role apparently being only that of determining – by settling in the skew-boat form – the essential trisaccharide AGA* in the most favored conformation for binding to AT. Since the $^1C_4$ and $^2S_0$ conformations of IdoA2SO$_3$ residues are equienergetic (44), whether the system selects the form already prevalent in the free state remains an open question. Notably, as shown by data in Table 4, both the strength of the complex with AT and the corresponding inhibition of Factor Xa for three pentasaccharides increase with increasing proportion of the $^2S_0$ form already in the absence of AT (124). However, interaction of a heparin hexasaccharide with FGF-1 in solution involves IdoA2SO$_3$ residues in both $^1C_4$ and $^2S_0$ conformations.

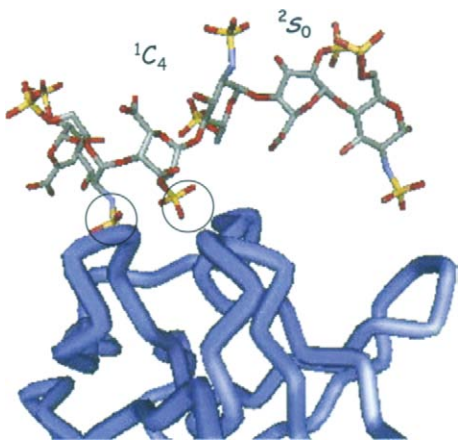

Figure 12 Details of the crystal structures of a 1:1 FGF-2 heparin hexasaccharide complex. (Redrawn from coordinates of Ref. 123; see Ref. 5), showing that the two 2-*O*-SO$_3$ residues select different conformations in binding to the growth factor.

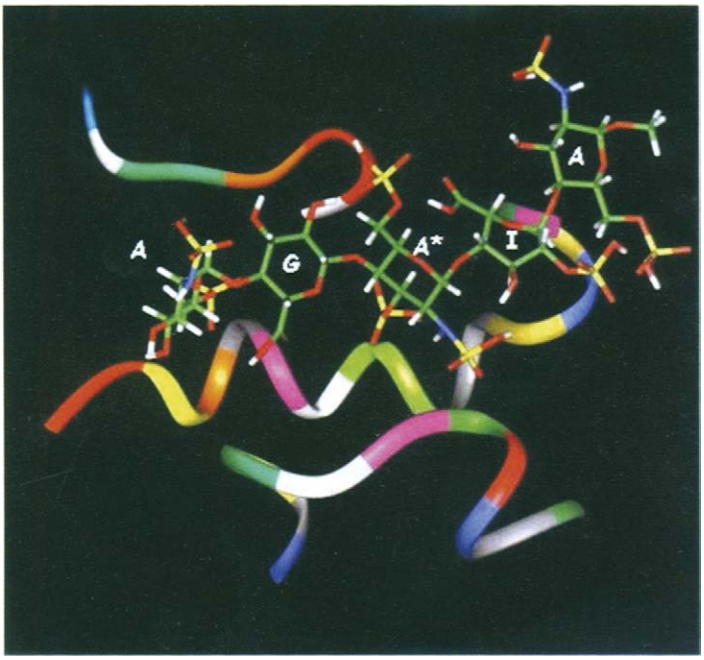

Figure 13 Solution conformation of pentasaccharide AGA*IA complexed with antithrombin, showing that residue I ($IdoA2SO_3$) is in the $^2S_0$ conformation and that the 2-*O*-SO_3 group is not directly involved in binding (125).

Molecular modeling studies on several heparin–protein systems for which crystal coordinates are available suggested that protein-binding domains along heparin chains are characterized by "kinks" associated with flexible IdoA ($IdoA2SO_3$) residues that adapt their shapes to that of the target protein (11, 127), a concept that could facilitate designing of heparin sequences that specifically bind to specific proteins.

VI. Conclusions and Perspectives

With a few exceptions, our knowledge of active domains in heparin are still incomplete and our view of the interplay of the corresponding sequences in determining actual biological activities are at best semiquantitative. Indeed, the wealth of information accumulated about structural requirements for biological interactions of heparin or heparin/HS oligosaccharides permits the prediction of the specificity and strength of some interactions. However, these conclusions can seldom be extended to more complex biological systems *in vivo*. In fact, bioavailability problems and the competition of several proteins for the same, or partially overlapping active domains greatly complicate the dissection of biological effects in terms of partial structures associated with different activities. The natural structural hetero-

Table 4 Conformational Equilibria Observed for the IdoA Residue in the Uncomplexed State and Biological Activity for Three Heparin Pentasaccharides[a]

Compound	$^1C_4/^2S_0$	KD for AT (nM)	Factor X_a inhibition (units mg/ml)
1. A G A* I (OH) A	75:25	380	350
2. A G A* I A	40:60	58	700
3. A G A* I A*[b]	10:90	1.3	1300

[a]Source: Ref. 124, and M. Petitou, personal communication.
[b]Compound 3 bears an extra 3-*O*-sulfate substituent at the terminal reducing A residue, a 2-*O*-sulfate substituent instead of a 2-*N*-sulfate substituent, and methyl substituents at all nonsulfated hydroxyl groups (7).

geneity of heparin further complicates such an interpretation. Also, although some of the activities of exogenously administered heparin can be reasonably associated with reinforcement of, or competition with, functions of the HS chains of HSPGs (no other biopolymer seems to have been so often defined as "ubiquitous"), comparison of heparin and HS structures is not always homogeneous. In fact, heparin contains a much lower variety of diverse structural features than HS. As noted (6), it should also be considered that heparin is a "purified" product, whereas HS is usually obtained in its natural heterogeneous form.

On the other hand, the current rapid developments of new tools for structural analysis (described in another chapter of this book), and new methodologies for chemical synthesis of heparin sequences (128,129), are expected to make a large number of heparin oligosaccharides available in sufficient purity and amounts for both biochemical/biological and pharmacological testing, as already achieved for novel antithrombotics (128). Heparin/HS oligosaccharide biosynthetic libraries (93) will also increasingly contribute to structure–activity studies and will soon be expanded with use of enzymatic (130) and chemo-enzymatic (131) modifications of the *Escherichia coli* K5 polysaccharide, which has the same structure as the heparin/HS precursor *N*-acetyl heparosan. Highly diversified sequences are also being generated by a combination of partial chemical modifications of heparin (132).

References

1. Fransson L-Å. Glycosaminoglycans. In: Aspinall GO, ed. The Polysaccharides. Orlando, FL: Academic Press, 1985; vol. 3:337–413.
2. Rodén L, Ananth S, Campbell P, Curenton T, Ekborg G, Manzella S, Pillion D, Meezan E. Heparin – an introduction. In: Lane DA, Björk I, Lindahl U, eds. Heparin and Related Polysaccharides. New York: Plenum Press, 1992; 1–20.
3. Lindahl U, Lidholt K, Spillmann D, Kjellén L. More to "heparin" than anticoagulation. Thromb Res 1994; 75:1–32.
4. Lever R, Page CP. Novel drug development opportunities for heparin. Nat Rev Drug Discov 2002; 1:140–148.
5. Casu B, Lindhal U. Structure and biological interactions of heparin and heparan sulfate. Adv Carbohydr Chem Biochem 2001; 57:159–206.

6. Lindahl U. Heparin – from anticoagulant drug into the new biology. Glycocon J 2000; 17:597–605.
7. Van Boeckel CAA, Petitou M. The unique antithrombin binding domain of heparin: a lead to new synthetic antithrombotics. Angew Chem Int Ed 1993; 32:1671–818.
8. Turnbull JE. Integral glycan sequencing of heparan sulfate and heparin saccharides. Methods Mol Biol 2001; 171:129–139.
9. Whitelock JM, Iozzo R. Heparan sulfate, a complex polymer charged with biological activity. Chem Rev 2005; 195:2745–2764.
10. Conrad HE. Heparin binding proteins. San Diego, CA: Academic Press, 1998.
11. Raman R, Sasisekharan V, Sasisekharan R. Structural insights into biological roles of protein-glycosaminoglycan interactions. Chemistry & Biology 2005; 12: 1–11.
12. Capila I, Linhardt RJ. Heparin–protein interactions. Angew Chem Int Ed 2002; 41:390–412.
13. Linhardt RJ. Heparin: structure and activity. J Med Chem 2003; 46:2551–2564.
14. Bianchini P, Liverani L, Mascellani G, Parma B. Heterogeneity of unfractionated heparins studied in connection with species, source, and production processes. Semin Thromb Hemost 1997; 23:3–10.
15. Guerrini M, Bisio A, Torri G. Combined quantitative ^{1}H and ^{13}C nuclear magnetic resonance spectroscopy for characterization of heparins. Semin Thromb Hemost 2001; 27:473–482.
16. Sudo M, Sato K, Chaidedgumjorm A, Toyoda H, Toida T, Imanari T. ^{1}H Nuclear magnetic resonance spectroscopic analysis for determination of glucuronic acid and iduronic acid in dermatan sulfate, heparin and heparan sulfate. Anal Biochem 2001; 297:42–51.
17. Yamada S, Murakami T, Tsuda H, Yoshida K, Sugahara K. Isolation of porcine heparin tetrasaccharides with glucuronate 2-*O*-sulfate. J Biol Chem 1995; 270:8695–8705.
18. Fransson L-Å, Malmström A, Sjöberg I, Huckerby TN. Periodate oxidation and alkaline degradation of heparin-related glycans. Carbohydr Res 1980; 80:131–145.
19. Islam T, Butler M, Sikkander SA, Toida T, Linhardt RJ. Further evidence that periodate cleavage of heparin occurs primarily through the antithrombin binding site. Carbohydr Res 2002; 337:2239–2243.
20. Casu B, Guerrini M, Naggi A, Torri G, De-Ambrosi L, Boveri G, Gonella S, Cedro A, Ferro L, Lanzarotti E, Paternò M, Attolini M, Valle MG. Characterization of sulfation patterns of beef and pig mucosal heparins by nuclear magnetic resonance spectroscopy. Arzneim-Forsh (Drug Res) 1996; 46:472–477.
21. Stringer SE, Kandola BS, Pye DA, Gallagher JT. Heparin sequencing. Glycobiology 2003; 13:97–107.
22. Krueger J, Salvimirta M, Sturiale L, Giménez-Gallego G, Lindahl U. Sequence analysis of heparan sulfate epitopes with graded affinities for fibroblast growth factors 1 and 2. J Biol Chem 2001; 276:30744–30752.
23. Thanawiroon C, Rice KG, Toida T, Linhardt RJ. Liquid chromatography/mass spectrometry sequencing approach for highly sulfated heparin-derived oligosaccharides. J Biol Chem 2004; 279:2608–2615.
24. Mourier AJ, Viskov C. Chromatographic analysis and sequencing approach of heparin oligosaccharides using cetyltrimethylammonium dynamically coated stationary phases. Anal Biochem 2004; 332:299–313

25. Yamada S, Yamane Y, Tsuda H, Yoshida K, Sugahara K. A major common trisulfated hexasaccharide core sequence, hexuronic acid (2 sulfate)-glucosamine (*N*-sulfate)–iduronic acid–*N*-acetylglucosamine–glucuronic acid–glucosamine (*N*-sulfate), isolated from the low sulfated irregular region of porcine intestinal heparin. J Biol Chem 1998; 273:1863–1871.
26. Lam LH, Silbert JE, Rosenberg RD. The separation of active and inactive forms of heparin. Biochem Biophys Res Comm 1976; 69:570–577.
27. Höök M, Björk I, Hopwood J, Lindahl U. Anticoagulant activity of heparin: separation of high-activity and low-activity heparin species by affinity chromatography on immobilized antithrombin. FEBS Lett 1976; 66:90–93.
28. Andersson LO, Barrowcliffe TW, Holmer E, Johnson EA, Sims GEC. Anticoagulant properties of heparin fractionated by affinity chromatography on matrix-bound antithrombin III and by gel filtration. Thromb Res 1976; 9:575–583.
29. Lindahl U, Bäckström G, Thunberg L, Leder IG. Evidence for a 3-*O*-sulfated D-glucosamine residue in the antithrombin-binding sequence of heparin. Proc Natl Acad Sci USA 1980; 77:6551–6555.
30. Thunberg L, Bäckström G, Lindahl U. Further characterization of the antithrombin-binding sequence in heparin. Carbohydr Res 1982; 100:393–410.
31. Petitou M, Casu B, Lindahl U. 1976–1983, a critical period in the history of heparin: the discovery of the antithrombin binding site. Biochimie 2003; 85:83–89.
32. Rosenfeld L, Danishefsky I. Location of specific oligosaccharides in heparin in terms of their distance from the protein linkage region in native proteoglycan. J Biol Chem 1988; 263:262–266.
33. Pejler G, Danielsson A, Björk I, Lindahl U, Nader HB, Dietrich, CP. Structure and antithrombin binding properties of heparin isolated from the clams *Anomalocardia brasiliana* and *Tivela macroides*. J Biol Chem 1987; 262:11413–11421.
34. Bisio A, Guerrini M, Yates EA, Torri G, Casu B. NMR identification of structural environment for 2,3- and 2,3,6-tri-sulfated glucosamine residues in heparin with high and no affinity for antithrombin. Glycoconj 1997; J14:89.
35. Toida T, Hileman RE, Smith AE, Petinka IV, Linhardt RJ. Enzymatic preparation of heparin oligosaccharides containing antithrombin III binding sites. J Biol Chem 1996; 271:32040–32047.
36. Shriver Z, Raman R, Venkataraman G, Drummond K, Turnbull J, Toida T, Linhardt R, Biemann K, Sasisekharan R. Sequencing of 3-*O*-sulfate containing heparin decasaccharides with a partial antithrombin III binding site. Proc Natl Acad Sci USA 2000; 97:10359–10364.
37. Guerrini M, Raman R, Venkataraman G, Torri G, Sasisekharan R, Casu B. A novel computational approach to integrate NMR spectroscopy and capillary electrophoresis for structure assignment of heparin and heparan sulfate oligosaccharides. Glycobiology 2002; 12:713–719.
38. Yamada S, Yoshida K, Sugiura M, Sugahara K, Khoo K-K, Morris HR, Dell A. Structural studies on the bacterial lyase-resistant tetrasaccharides derived from the antithrombin III-binding site of porcine intestinal heparin. J Biol Chem 1993; 268:4780–4787.
39. Lindahl U. Further characterization of the heparin–protein linkage region. Biochim Biophys Acta 1996; 130:368–382.

40. Iacomini M, Casu B, Guerrini M, Naggi A, Pirola A, Torri G. "Linkage region" sequences of heparins and heparan sulfates: detection and quantification by nuclear magnetic resonance spectroscopy. Anal Biochem 1999; 274: 50–58.
41. Hanhenberger R, Jakobson ÅM, Ansari A, Wehler T, Svahn CM, Lindahl U. Low-sulfated oligosaccharides derived from heparan sulfate inhibit normal angiogenesis. Glycobiology 1993; 3:567–573.
42. Casu B, Choay J, Ferro DR, Gatti G, Torri G, Petitou M, Sinaÿ P. Controversial glycosaminoglycan conformations. Nature 1986; 322:215–216.
43. Casu B. Conformation of individual residues and chain segments of glycosaminoglycans in solution by spectroscopic methods. In: Arnott F, Reeves DA, Morris, eds. Molecular Biophysics of the Extracellular Matrix. Clifton, NJ: Humana Press, 1983:69–93.
44. Ferro DR, Provasoli A, Ragazzi M, Torri G, Casu B, Petitou M, Sinaÿ P, Choay J. Evidence for conformational equilibrium of the sulfated L-iduronate residue in heparin and in synthetic mono- and oligosaccharides. J Am Chem Soc 1986; 108:6773–6778.
45. Ferro D, Ragazzi M, Provasoli A, Perly B, Torri G, Casu B, Petitou M, Sinaÿ P, Choay J. Conformers population of L-iduronic acid residues in glycosaminoglycan sequences. Carbohydr Research 1990; 195:157–167.
46. Ragazzi M, Ferro D, Perly B, Sinaÿ P, Petitou M, Choay J. Conformation of the pentasaccharide corresponding to the binding site of heparin for antithrombin III. Carbohydr Res 1990; 195:169–185.
47. Van Boeckel CAA, van Aelst SF, Wagenaars GN, Mellema J-R. Synthesis and conformational analysis of iduronic acid-containing heparin trisaccharides. Rec Trav Chim Pays Bas 1987; 106:19–29.
48. Mickailov D, Linhardt RJ, Mayo KH. NMR conformation of heparin-derived hexasaccharide. Biochem J 1997; 328:51–61.
49. Angulo J, Hricovini M, Gairi M, Guerrini M. de Paz JL, Ojeda R, Martin-Lomas M, Nieto PM. Dynamic properties of biologically active heparin-like hexasaccharides. Glycobiology 2005; 15:1008–1015.
50. Casu B, Petitou M, Provasoli M, Sinaÿ P. Conformational flexibility: a new concept for explaining binding and biological properties of iduronic acid-containing glycosaminoglycans. Trends Biochem Sci 1988; 13:221–225.
51. Mulloy B, Forster M, Jones C, Davies DB. NMR and molecular modeling studies in the solution conformation of heparin. Biochem J 1993; 293:849–858.
52. Casu B, Guerrini M, Torri G. Structural and conformational aspects of the anticoagulant and antithrombotic activity of heparin and dermatan sulfate. Current Pharmac Design 2004; 10:939–949.
53. Mulloy B, Forster MJ, Jones C, Drake AF, Johnson EA, Davies DB. The effect of variation of substitution on the solution conformation of heparin: a spectroscopic and molecular modelling study. Carbohydr Res 1994; 255:1–26.
54. Mulloy B, Forster MJ. Conformation and dynamics of heparin and heparan sulfate. Glycobiology 2000; 10:1147–1156.
55. Baglin TP, Carrell RW, Church FC, Esmon CT, Huntington JA. Crystal structures of native and thrombin-complexed heparin cofactor II reveal a multistep allosteric mechanism. Proc Natl Acad Sci USA 2002; 99:11079–11084.
56. Tollefsen DM. The interaction of glycosaminoglycans with Heparin Cofactor II: structure and activity of a high-affinity dermatan sulfate hexasaccharide.

In: Lane DA, Björk I, Lindahl, U, eds. Heparin and Related Polysaccharides. New York: Plenum Press, 1992; vol. 425:35–44, 167–176.
57. Bourin MC, Lindahl U. Glycosaminoglycans and the regulation of blood coagulation. Biochem J 1999; 289:313–330.
58. Brooze GI. Tissue factor pathway inhibitor. Thromb Haemost 1995; 74:90–93.
59. Hoppensteadt DA, Fareed J, Kaiser B. Tissue factor inhibitor: potential implications in the treatment of cardiovascular disorder. In: Sasahara AA, Loscalzo J, eds. New Therapeutic Agents in Thrombosis and Thrombolysis. New York: Marcel Dekker, 2003; 231–300.
60. Kusche M, Torri G, Casu B, Lindahl U. Biosynthesis of heparin: availability of glucuronosyl 3-*O*-sulfation sites. J Biol Chem 1990; 265:7292–7300.
61. Petitou M, Lormeau J-C, Perly B, Berthault P, Bonnesec , Sié P, Choay J. Is there a unique sequence in heparin for interaction with heparin cofactor II? Structural and biological studies of heparin-derived oligosaccharides. J Biol Chem 1988; 263:8685–8690.
62. Olson ST, Björk I. Role of protein conformational changes, surface approximation, and protein cofactors in heparin-accelerated antithrombin-proteinase reaction. In: Lane DA, Björk I, Lindahl U, eds. Heparin and Related Polysaccharides. New York: Plenum Press, 1992; 155–166.
63. Olson ST, Björk I, Sheffer R, Craig PA, Shore JD, Choay J. Role of antithrombin-binding pentasaccharide in heparin acceleration of antithrombin-proteinase reaction. Resolution of the antithrombin conformational change contribution to heparin rate enhancement. J Biol Chem 1992; 267: 12528–12538.
64. Jin L, Abrahams JP, Skinner R, Petitou M, Pike RN, Carrel RW. The anticoagulant activation of antithrombin by heparin. Proc Natl Acad Sci USA 1997; 94:14683–14688.
65. Li W, Johnson DJD, Esmon CT, Huntington JA. Structure of the antithrombin-thrombin-heparin ternary complex reveals the antithrombotic mechanism of heparin. Nature Str Mol Biol 2004; 11:857–862.
66. Laurent TC, Tengblad A, Thunberg L, Höök M, Lindahl U. The molecular-weight dependence of the anticoagulant activity of heparin. Biochem J 1978; 175:691–701.
67. Muñoz EM, Linhardt RJ. Heparin-binding domains in vascular biology. Arterioscler Thromb Vasc Biol 2004; 24:1549–1557.
68. Avci FY, Karst NA, Linhardt RJ. Synthetic oligosaccharides as heparin-mimetics displaying anticoagulant properties. Curr Pharmac Design 2003; 9:2323–2335.
69. Schriver Z, Sundaram M, Venkataraman G, Fareed F, Linhardt R, Biemann K, Sasisekharan R. Cleavage of the antithrombin III binding site in heparin by heparinases and its implication in the generation of low molecular weight heparin. Proc. Natl Acad Sci USA 2000; 12:71–77.
70. Fareed J, Haas S, Sahahara E. Differentiation of low molecular-weight heparins, applied and clinical considerations. Semin Thromb Hemost 1999; 3:1–147.
71. Petitou M, van Boeckel CAA. A synthetic antithrombin III binding pentasaccharide is now a drug! What comes next? Angew Chem Int Ed 2004; 43:3118–3133.

72. Bauer KA, Hawkins DV, Peters PC, Petitou M, Herbert J-M, van Boeckel CAA. Fondaparinux, a synthetic pentasaccharide: the first in a new class of antithrombotic agents-the selective factor Xa inhibitors. Cardiovascular Drug Reviews 2002; 20:37–52.
73. Petitou M, Herault JP, Bernat A, Driguez PA, Duchaussoy P, Lormeau JC, Herbert JM. Synthesis of thrombin-inhibiting heparin mimetics without side effects. Nature 1999; 398:417–422.
74. Rong J, Nordling K, Björk I and Lindahl U. A novel strategy to generate biologically active neo-glycosaminoglycan conjugates. Glycobiology 1999; 9:1331–1336.
75. Iozzo RV, San Antonio JD. Heparan sulfate proteoglycans: heavy hitters in the angiogenesis arena. 2001; 108:349–335.
76. Gallagher JT. Heparan sulfate: growth control with a restricted sequence menu. J Clin Inv 2001; 108:357–361.
77. Shriver Z, Liu D, Sasisekharan R. Emerging views of heparan sulfate glycosaminoglycan structure–activity relationships modulating dynamic biological functions. Trends Cardiovasc Med 2002; 12:71–77.
78. Lindahl U, Kusche-Gullberg M, Kjellén L. Regulated diversity of heparan sulfate. J Biol Chem 1998; 273:24979–24982.
79. Ornitz DM, Itoh N. Fibroblast growth factors. Genome Biol 2001; 2:R3005.
80. Cross MJ, Claesson-Welsh L. FGF and VEGF function in angiogenesis: signalling pathways, biological responses and therapeutic inhibition. Trends Pharmacol Sci 2001; 22:201–207.
81. Kato M, Wang H, Kainulainen V, Fitzgerald ML, Ledbetter S, Ornitz DM, Bernfield M. Physiological degradation converts the soluble syndecan-1 ectodomain from an inhibitor to a potent activator of FGF-2. Nat Med 1998; 4:691–697.
82. Gao G, Goldfarb M. Heparin can activate a receptor tyrosine kinase. EMBO J 1995; 108:357–361.
83. Ishai-Michaeli R, Svahn CM, Chajek-Shaul T, Korner G, Ekre HP, Vlodavsky I. Importance of size and sulfation of heparin in release of basic fibroblast growth factor from the vascular endothelium and extracellular matrix. Biochemistry 1992; 31:2080–2088.
84. Casu B, Naggi A. Antiangiogenic heparin-derived heparan sulfate mimics. Pure Appl Chem 2003; 75:155–164.
85. Lundin L, Larsson H, Kreuger J, Kanda S, Lindahl U, Salmivirta M, Claesson-Welsh L. Selectively desulfated heparin inhibits fibroblast growth factor-induced mitogenicity and angiogenesis. J Biol Chem 2000; 275:24653–24660.
86. Casu B, Guerrini M, Guglieri S, Naggi A, Perez M, Torri G, Cassinelli G, Ribatti D, Carminati P, Giannini G, Penco S, Pisano C, Belleri M, Rusnati M, Presta M. Undersulfated and glycol-split heparin derivatives endowed with antiangiogenic activity. J Med Chem 2004; 47:838–848.
87. Maccarana M, Casu B, Lindahl U. Minimal sequence in heparin/heparan sulfate required for binding of basic fibroblast growth factor. J Biol Chem 1993; 268:23898–23905.
88. Pye DA, Vives RR, Hyde P, Gallagher JT. Regulation of FGF-1 mitogenic activity by heparan sulfate oligosaccharides is dependent on specific structural features : differential requirements for the modulation of FGF-1 and FGF-2. Glycobiology 2000; 10:1183–1192.

89. Ishihara M. Structural requirements in heparin for binding and activation of FGF-1 and FGF-4 are different from that of FGF-2. Glycobiology 1994; 4:817–824.
90. Guerrini M, Agulles T, Bisio A, Hricovini M, Lay L, Naggi A, Poletti L, Sturiale L, Torri, G, Casu B. Minimal heparin/heparan sulfate sequences for binding to fibroblast growth factor-1. Biochem Biophys Res Comm 2002; 292:222–230.
91. Ashikari-Hada S, Habuchi H, Kariya Y, Itoh N, Reddi AH, Kimata K. Characterization of growth factor-binding structures in heparin/heparan sulfate using an octasaccharide library. J Biol Chem 2004; 279:12346–12354.
92. Kreuger J, Salmivirta M, Sturiale L, Giménez-Gallego G, Lindahl U. Sequence analysis of heparan sulfate epitopes with graded affinities for fibroblast growth factors 1 and 2. J Biol Chem 2001; 276:30744–39752.
93. Jemt P, Kreuger J, Kusche-Gulberg M, Sturiale L, Giménez-Gallego G, Lindahl U. Biosynthetic oligosaccharide libraries for identification of protein-binding heparan sulfate motifs. Exploring the structural diversity by screening for fibroblast growth factor FGF1 and FGF2 binding. J Biol Chem 2002; 277:30567–30573.
94. Kovensky J, Duchaussoy P, Bono F, Salmivirta M, Sizun P, Herbert J-M, Petitou M, Sinäy P. A synthetic heparan sulfate pentasaccharide, exclusively containing L-iduronic acid, displays higher affinity for FGF-2 than its D-glucuronic acid-containing isomers. Bioorg Med Chem 1999; 7:1567–1580.
95. Guimond S, Maccarana M, Olwin BB, Lindahl U, Rapraeger AC. Activating and inhibitory heparin sequences for FGF-2. Distinct requirements for FGF-1, FGF-2, and FGF-4. J Biol Chem 1993; 268:23906–23914.
96. Schlessinger J, Plotnikov AN, Ibrahimi OA, Eliseenkova AV, Yeh BK, Yayon A, Linhardt RJ, Muhammadi M. Crystal structure of a ternary FGF-FGRF-heparin complex reveals a dual role for heparin in FGFR binding and dimerization. Mol Cell 2000; 6:743–750.
97. Pellegrini L, Burke DF, von Delft F, Mulloy B, Blundell TL. Crystal structure of fibroblast growth factor receptor ectodomain bound to ligand and heparin. Nature 2000; 407:1029–1034.
98. Pellegrini I. Role of heparan sulfate in fibroblast growth factor signaling: a structural view. Curr Opin Struct Biol 2001; 11:629–634.
99. Wang H, Toida T, Kim YS, Capila I, Hileman RE, Bernfield M, Linhardt RJ. Glycosaminoglycans can influence fibroblast growth factor-2 mitogenicity without significant growth factor binding. Biochem Biophys Res Comm 1997; 235:369–373.
100. Loo B-M, Kreuger J, Jalkanen M, Lindahl U, Salmivirta M. Binding of heparin/heparan sulfate to fibroblast growth factor receptor 4. J Biol Chem 2002; 276:16868–16876.
101. Powell AK, Fernig DG, Turnbull JE. Fibroblast growth factor receptors 1 and 2 interact differently with heparin/heparan sulfate. Implication for a dynamic assembly of a ternary signaling complex. J Biol Chem 2002; 277:28544–28563.
102. Casu B, Guerrini M, Naggi A, Perez M, Torri G, Ribatti D, Carminati P, Giannini G, Penco S, Pisano C, Belleri M, Rusnati M, Presta M. Short heparin sequences spaced by glycol-split uronate residues are antagonists of

fibroblast growth factor 2 and angiogenesis inhibitors. Biochemistry 2002; 41:10519–10528.
103. Vlodavsky I, Friedman Y. Molecular properties and involvement of heparanase in cancer metastasis and angiogenesis. J Clin Inv 2001; 108:341–347.
104. Elkin M, Ilan N, Ishai-Michaeli R, Friedmann Y, Papo O, Pecker I, Vlodavsky I. Heparanase as mediator of angiogenesis: mode of action. FASEB J 2001; 15:1661–1663.
105. Parish CR, Freeman C, Hulett MD. Heparanase: a key enzyme involved in cell invasion. Biochim Biophys Acta 2001; 1471:M99–108.
106. Vlodavsky I, Zcharia E, Goldshmidt O, Eshel R, Katz BZ, Minucci S, Kovalchuk O, Penco S, Pisano C, Naggi A, Casu B. Involvement of heparanase in tumor progression and normal differentiation. Pathophysiol Haemost Thr 2003; 33:59–61.
107. Sanderson RD, Yang Y, Suva LJ, Kelly T. Heparan sulfate proteoglycans and heparanase-partners in osteolytic tumor growth and metastasis. Matrix Biol 2004; 23:341–352.
108. Sandbäck-Pikas D, Li J-P, Vlodavsky I, Lindahl, U. Substrate specificity of heparanases from human hepatoma and platelets. J Biol Chem 1998; 273:18770–18777.
109. Okada Y, Yamada S, Toyoshima M, Dong J, Nakajima M, Sugahara K. Structural recognition by recombinant human heparanase that plays critical roles in tumor metastasis. Hierarchical sulfate groups with different effects and the essential target disulfated trisaccharide sequence. J Biol Chem 2002; 277:42488–42495.
110. Gong F, Jemth P, Escobar Galvis ML, Vlodavsky I, Horner A, Lindahl U, Li J-P. Processing of macromolecular heparin by heparanase. J Biol Chem 2003; 278:35152–35158.
111. Vlodavsky I, Mohsen M, Lider O, Svahn CM, Ekre HP, Rigoda M, Peretz T. Inhibition of tumor metastasis by heparanase inhibiting species of heparin. Invasion Metastasis 1994; 14:290–302.
112. Lapierre F, Holme K, Lam L, Tressler RJ, Storm N, Wee I, Stack RJ, Castellot J, Tyrrell DJ. Chemical modification of heparin that diminish its anticoagulant but preserve its heparanase-inhibitory, angiostatic, antitumor and antimetastatic properties. Glycobiology 1996; 6:355–366.
113. Naggi M, Casu B, Perez M, Torri G, Cassinelli G, Penco S, Pisano C, Giannini G, Ishai-Michaeli R, Vlodavsky I. Modulation of heparanase-inhibiting activity of heparin through selective desulfation, graded *N*-acetylation, and glycol-splitting. J Biol Chem 2005; 280:12103–12113.
114. Marks RM, Lu H, Sundaresan R, Toida T, Suzuki A, Imanari T, Hernaiz MJ, Linhardt RJ. Probing the interaction of dengue virus envelope protein with heparin: assessment of glycosaminoglycan-derived inhibitors. J Med Chem 2001; 44:2178–2184.
115. Cardin AD, Weintraub HJ. Molecular modeling of protein-glycosaminoglycan interactions. Arteriosclerosis 1989; 9:21–32.
116. Fromm JR, Hileman RE, Caldwell EE, Weiler JM, Linhardt RJ. Pattern and spacing of basic aminoacids in heparin binding sites. Arch Biochem Biophys 1997; 343:92–100.
117. Mulloy B, Linhardt RJ. Order out of complexity – protein structures that interact with heparin. Curr Opin Struct Biol 2001; 11:623–628.

118. Casu B, Naggi A, Torri G. Chemical derivatization as a strategy to study structure-activity relationships of glycosaminoglycans. Semin Thromb Hemost 2002; 28:335–342.
119. Kreuger J, Spillmann D, Sasaki T, Timpl R, Lindahl U. Endostatin is recognized by heparan sulfate epitopes containing both sulfated and acetylated *N*-substituents. J Biol Chem 2001; 276:30744–30752.
120. Scholefield Z, Yates EA, Wayne G, Amour A, McDowell W, Turnbull JE. Heparan sulfate regulates amyloid precursor protein processing by BACE1, the Alzheimer β-secretase. J Cell Biol 2003; 163:97–107.
121. van der Born J, Gunnarsson K, Bakker MA, Kjellén L, Kusche-Gullberg M, Maccarana M, Berden JH, Lindahl U. Presence of *N*-unsubstituted units in native heparan sulfate revealed by a monoclonal antibody. J Biol Chem 1995; 270:31303–31309.
122. Norgrad-Sumnicht K, Varki A. Endothelial heparan sulfate proteoglycans that bind to L-selectins have glucosamine residues with unsubstituted amino groups. J Biol Chem 1995; 270:12012–12024.
123. Faham S, Hileman RE, Fromm JR, Linhardt RJ, Rees DC. Heparin structure and interactions with basic fibroblast growth factor. Science 1996; 271:116–120.
124. Hricovini M, Guerrini M, Bisio A, Torri G, Naggi A, Casu B. Active conformations of glycosaminoglycans. NMR determination of the conformation of heparin sequences complexed with antithrombin and with fibroblasts growth factors in solution. Semin Thromb Hemost 2002; 28:325–334.
125. Hricovini M, Guerrini M, Bisio A, Torri G, Petitou M, Casu B. Conformation of heparin pentasaccharide bound to antithrombin III. Biochem J 2001; 359:265–272.
126. Canales A, Angulo J, Ojeda R, Bruix M, Fayos R, Lozano R, Giménez-Gallego G, Martin-Lomas M, Nieto PM, Jiménez-Barbero J. Conformational flexibility of a synthetic glycosaminoglycan bound to a fibroblast growth factor. FGF-1 recognizes both the $^{1}C_{1}$ and $^{2}S_{0}$ conformations of a bioactive heparin-like hexasaccharide. J Am Chem Soc 2005; 127:5778–5779.
127. Raman R, Venkataraman G, Ernst S, Sasisekharan V, Sasisekharan R. Structural specificity of heparin binding in the fibroblast growth factor family of proteins. Proc Natl Acad Sci USA 2003; 100:2357–2362.
128. Petitou M, van Boeckel CAA. A synthetic antithrombin III binding pentasaccharide is now a drug! What comes next? Angew Chem Int Ed 2004; 43:3118–3133.
129. Seeberger PH. Solid phase oligosaccharide synthesis. Principles, synthesis, and applications. J Carbohydr Chem 2002; 21:613–643.
130. Kuberan B, Lech MZ, Beeler DL, Wu ZL, Rosenberg RD. Enzymatic synthesis of antithrombin III-binding heparan sulfate pentasaccharide. Nature Biotechnol 2003; 21:1343–1346.
131. Lindahl U, Li J-P, Kusche-Gullberg M, Salmivirta M, Alaranta S, Veromaa T, Emeis J, Roberts I, Taylor C, Oreste P, Zoppetti G, Naggi A, Torri G, Casu B. Generation of "Neoheparin" from *E. Coli* K5 capsular polysaccharide. J Med Chem 2005; 48:349–352.
132. Yates EA, Guimond SE, Turnbull JE. Highly diverse heparan sulfate analog libraries; a novel resource providing access to expanded areas of sequence space for bioactivity screening. J Med Chem 2004; 47: 277–280.

Chemistry and Biology of Heparin and Heparan Sulfate
H.G. Garg, R.J. Linhardt and C.A. Hales (Editors)

Chapter 2

Structure and Function of Cell Associated and Pericellular Heparan Sulfate Proteoglycans

SANDRA G. VELLEMAN and CAINI LIU

The Ohio State University/OARDC,
Department of Animal Sciences, Wooster, OH, USA

I. Introduction

The extracellular matrix is an organized structure located outside cells that is composed of proteins and polysaccharides locally produced by cells (1). Components of the extracellular matrix are directly involved in cell proliferation, adhesion, migration, and regulation of cell shape. The extracellular matrix macromolecules regulate cell behavior by binding to cell surface receptors which then transmit the signal intracellularly resulting in cellular changes. Proteoglycans are a class of molecules found both in the extracellular matrix and on the cell surface.

Proteoglycans are proteins that contain carbohydrates called glycosaminoglycans, which are covalently attached to a central core protein. The proteoglycan central core protein varies in size from approximately 40,000 to greater than 350,000 daltons (2). The glycosaminoglycans are polymers of disaccharide repeats that are highly sulfated and are, therefore, negative in charge. Many ionic interactions of the proteoglycan are due to the negative charge of the attached glycosaminoglycan chains. Typical glycosaminoglycans attached to the proteoglycan central core protein, include chondroitin/dermatan sulfate, heparan sulfate, and keratan sulfate. Chondroitin sulfate is composed of repeats of glucuronic acid and *N*-acetylgalactosamine with sulfate groups in the 4- or 6-position of the amino sugar. Heparan sulfate consists of repeats of glucuronic acid or iduronate and *N*-acetylglucosamine. Keratan sulfate contains disaccharide repeats of galactose and *N*-acetylglucosamine with the

sulfate at the 6-position of the amino sugar. The remainder of this chapter will focus on heparan sulfate and heparan sulfate containing cell surface and pericellular proteoglycans due to their role in key biological processes involved in the regulation of tissue growth and development.

During the formation of tissues, the regulation of cell migration, proliferation, and differentiation are central events. The signals governing these processes often involve the binding of ligands to heparan sulfate. A large portion of the ligand binding specificity to heparan sulfate is due to structural heterogeneity of the heparan sulfate chains attached to the proteoglycan core protein.

II. Heparan Sulfate Synthesis

Heparan sulfate biosynthesis requires the presence of a central core protein which will be modified by the addition of a linkage region to serine residues that are followed by a glycine (3, 4). Heparan sulfate is synthesized in the Golgi apparatus while attached to its core protein (5). The synthesis process consists of three major steps: chain initiation, chain polymerization, and chain modification (Fig. 1). The initiation of heparan sulfate synthesis is the formation of tetrasaccharide linkage region. Xylose (Xyl) is transferred by xylosyltransferase from UDP-Xyl to the hydroxyl group of specific serine residues on the core protein. Two galactose (Gal) residues are added by galactosyltransferases I and II, and glucuronic acid (GlcA) is added by glucuronosyltransferase I to complete the formation of the tetrasaccharide [–GlcA–Gal–Gal–Xyl–(Ser)] linkage region. A single *N*-acetylated glucosamine (GlcNAc) is then added to the linkage region by an unique transferase that can recognize the sites on core protein for heparan sulfate attachment. After the first GlcNAc residue is attached, GlcA and GlcNAc are alternatively added by a single heparan sulfate polymerase to form the repeating 1,4-linked disaccharide polymer. When the 1,4-linked-disaccharide polymer is formed (termed polymerization), the heparan sulfate chain is subjected to a series of sequential enzymatic modification reactions. The first modification reaction is the replacement of the *N*-acetyl group of GlcNAc residues with a sulfate by *N*-deacetylase/*N*-sulfotransferase. Then glucuronyl C-5 epimerase epimerizes D-GlcA residues to L–iduronic acid (IdoA). Following epimerization, the heparan sulfate chain undergoes extensive *O*-sulfations by uronosyl-2-*O*-sulfotransferase, 6-*O*-sulphotransferase, and 3-*O*-sulphotransferase. The uronic acids (GlcA or IdoA) can be sulfated at 2-*O* position, and the GlcNAc can be sulfated at the 3-*O* and 6-*O* positions.

III. Molecular Structure of Heparan Sulfate and Binding Ligands

The complicated biosynthetic scheme leads to enormous structural variability in heparan sulfate chains. Heparan sulfate chains have regions that remain unmodified (NA domain), segments with contiguous *N*-sulfated sequences (NS domain), and mixed sequences with alternating *N*-acetylated and *N*-sulfated disaccharide residues

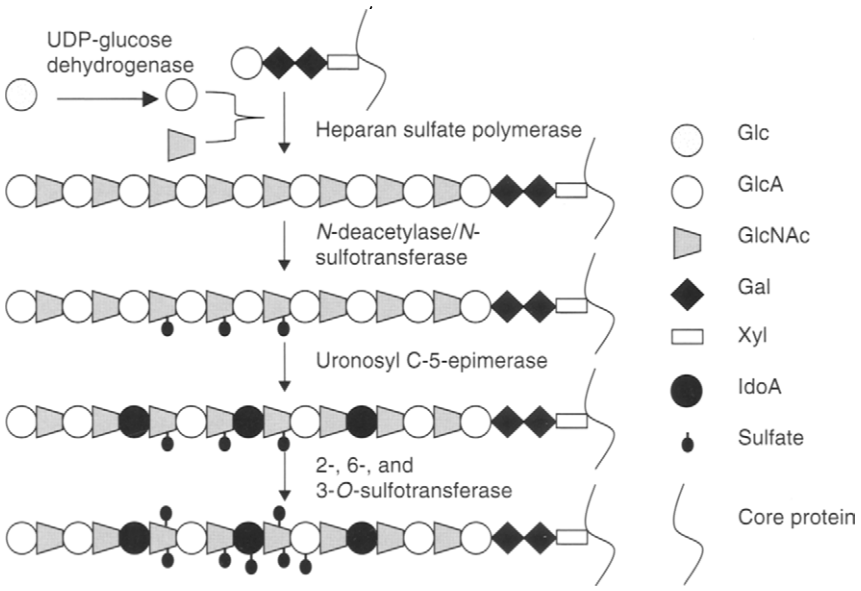

Figure 1 Scheme of heparan sulfate biosynthesis. Heparan sulfate (HS) synthesis is initiated by formation of a tetrasaccharide (core protein-Xyl-Gal-Gal-GlcA) linkage region. Then GlcA and GlcNAc are alternatively added to generate the disaccharide HS chain. As chain elongation proceeds, multiple enzymatic modifications take place sequentially, in which GlcNAc can be sulfated at *N*, 3-*O*, and 6-*O* positions, GlcA can be epimerized to IdoA, and IdoA can be sulfated at 2-*O* position. Glc, glucose; GlcA, glucuronic acid; GlcNAc, *N*-acetylated glucosamine; Gal, galactose; Xyl, xylose; IdoA, *L*–iduronic acid. (6).

(NA/NS domain). Most of the IdoA units are located within the NS domains and are 2-*O*-sulfated, whereas those located outside (mainly in NA/NS domains) are almost exclusively nonsulfated (7). The presence of the IdoA residues in the sulfated domains gives these regions considerable conformational versatility, which may be very important for the selective ligand-binding properties associated with heparan sulfate (8).

Heparan sulfate can interact with a variety of ligands and thus regulate their bioactivities. The identified binding ligands include extracellular matrix components, cell–cell adhesion molecules, growth factors, lipase, lipoproteins, and many other proteins (Table 1). Various ligands selectively bind specific heparan sulfate sequences, and the binding specificity is largely determined by unique modified residues or precise positioning of sugar units. One of the best characterized heparan sulfate–ligand interactions is the binding of antithrombin, which inhibits thrombin, a member of coagulation cascade. Antithrombin interacts with heparan sulfate through a pentasaccharide sequence in which a unique 3-*O*-sulfated Glc is essential for high-affinity binding (27). Another well-studied interaction is the modulation of

Table 1 Partial List of Ligands that Bind to Heparin or Heparan Sulfate

Factors	Reference
ECM components	
Collagen	9
Laminin	10
Fibronectin	11
Thrombospondin	12
Tenasin	13
Cell–cell adhesion molecules	
L-selectin	14
N-CAM	15
PECAM	16
Mac-1	17
Growth factors	
FGF	18
EGF	19
HGF	20
PDGF	21
TGF β	22
VEGF	23
Lipid metabolism proteins	
Lipoprotein lipase	24
ApoE	25
ApoB	26
Blood coagulation factor	
Antithrombin III	27
Protein C inhibitor	28
Chemokines and cytokines	
IL-2	29
IL-8	30
Microbial pathogens	
Herpes simplex viruses	31

Abbreviations: ApoB, apolipoprotein B; ApoE, apolipoprotein E; FGF, fibroblast growth factor; EGF, epidermal growth factor; HGF, hepatocyte growth factor; IL, interleukin; N-CAM, neural-cell adhesion molecule; PDGF, platelet-derived growth factor; PECAM, platelet-endothelial cell adhesion molecule; TGF, transforming growth factor; VEGF, vascular endothelial growth factor.

fibroblast growth factor-2 (FGF-2) interaction with its receptors by heparan sulfate. Heparan sulfate forms a low-affinity interaction with FGF-2 leading to the high-affinity binding of FGF-2 to its receptor forming a ternary signaling complex (32). The minimal binding structure for FGF-2 is a pentasaccharide with *N*-sulfated Glc (GlcNS) units and only one 2-*O*-sulfated IdoA residue is required for the binding (33). Herpes simplex virus type I binds cell surface heparan sulfate to gain entry into cells through viral glycoprotein gB and gC (34). The shortest glycoprotein C-binding heparan sulfate fragment has been described as 10 to 12 monosaccharide units containing at least one 2-*O*- and one 6-*O*-sulfate group that have to be localized in a sequence-specific way (35). Distinct heparan sulfate structures for binding have

also been characterized for other ligands (e.g., hepatocyte growth factor) (20), transforming growth factor (TGF;22), and fibronectin (36). In these interactions, various *N*- or *O*-sulfate groups have been implicated to play an important role.

IV. Types of Heparan Sulfate Proteoglycans

Heparan sulfate proteoglycans are located at both the cell surface and in the extracellular matrix, pericellular, surrounding many types of cells in vertebrates and invertebrates. Members of the cell surface heparan sulfate proteoglycans include the transmembrane syndecans, betaglycan, CD 44, and the glycosylphosphoinositol (GPI)-linked glypicans. The syndecan and glypican proteoglycan families are involved in the formation of receptor-signaling complexes, especially with FGF-2. Some of the cell surface proteoglycans like the syndecans are also shed into the extracellular matrix or serum and become soluble molecules interacting with other extracellular matrix macromolecules (37, 38). The pericellular heparan sulfate proteoglycans surround the cells and include perlecan, agrin, and collagen XVIII. These proteoglycans lack the ability to attach to or transverse the cell membrane. Perlecan is located in the basement membrane and, like agrin and collagen XVIII, is also located in the extracellular matrix.

V. Syndecans

The syndecans are type I transmembrane heparan sulfate proteoglycans that may also have attached chondroitin sulfate chains. To date there are four members of the syndecan family, 1–4; the numbering is based on the order of their cloning (39). Fig. 2 is a generalized schematic of the structure of the syndecans. The syndecans all have an N-terminal signal peptide, an extracellular or ectodomain that contains attachment sites for the glycosaminoglycans, a transmembrane domain, and a short C-terminal cytoplasmic domain containing conserved domain 1, variable domain, and conserved domain 2. The transmembrane and cytoplasmic domains are conserved across species and within the syndecan family. The ectodomain containing serine–glycine repeats for the attachment of glycosaminoglycans is less conserved. The syndecans are regulators of key cellular activities associated with both cell proliferation and differentiation. This modulation of cell behavior occurs due to the interaction of other ligands with the glycosaminoglycan chains, core protein, and cytoplasmic domain.

The glycosaminoglycan chains of syndecan bind a variety of ligands, most notably with FGF-2, which is a heparin-binding growth factor. It is thought that the binding of FGF-2 to the heparan sulfate chain leads to a dimerization of FGF-2 permitting high-affinity binding to its receptor. This is then followed by activation of intracellular tyrosine kinase signaling pathways. Modifications in the structure of the heparan sulfate chains, shedding, or degradation of these glycosaminoglycans will lead to changes in growth factor signal transduction. Salmivirta et al. (40) showed that heparan sulfate chains need to be attached to a proteoglycan core

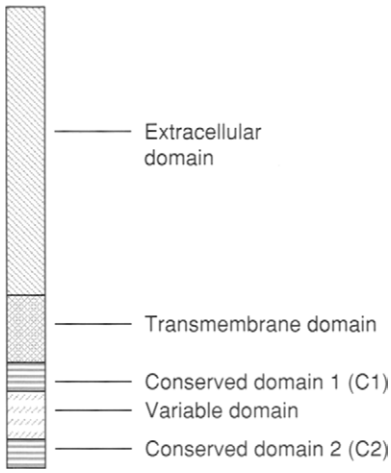

Figure 2 Schematic of the common structural features associated with the syndecans. The domain structure of the syndecans is illustrated showing the extracellular domain, transmembrane domain, conserved domain 1 (C1), variable domain, and conserved domain 2 (C2).

protein like syndecan to bind FGF-2 and extracellular matrix molecules. Chen et al. (41) have reported that syndecan-2 can function as a co-receptor for TGF-β permitting the interaction of TGF-β with its signaling receptor. Unlike FGF-2, TGF-β binds to syndecan-2 at its core protein in the extracellular region.

In addition to the attached heparan sulfate chains, in part, regulating the biological activity of the syndecans, the syndecan core protein plays a role in syndecan function. Cell adhesion, migration, and cytoskeletal signaling are some of the processes shown to be dependent upon the core protein. Although the syndecans share common structural features, there are differences in their functional properties as reflected by their different tissue distributions. Although primarily localized at the cell surface of epithelial cells (32), syndecan-1 has also been identified in tissues of mesodermal origin like skeletal muscle (42, 43). Syndecan-2 is expressed by mesenchymal cells, such as fibroblasts and hepatocytes (39, 44). Syndecan-3 is predominant in neural tissue but is also found in muscle tissue and myogenic satellite cells (39, 45, 46). Syndecan-4 is the most widely distributed of the syndecans and is expressed by epithelial and endothelial cells, fibroblasts, muscle cells, chondrocytes, and neural tissue (45–48).

Syndecan-1 was the first identified member of the syndecan proteoglycan family (48). Syndecan-1 has been shown to be involved in cell–cell adhesion (50), and growth factor binding (51, 52). The syndecan-1 cytoskeletal conserved domain (C2) at the C-terminus can bind proteins at the tetrapeptide sequence EFYA that contains a PSD-95, Discs-large, and Zonula occludens-1 (PDZ) region. This interaction is thought to link syndecan-1 to the cellular cytoskeleton resulting in reorganization of the actin containing filaments leading to changes in cell shape, which likely play a role in cell migration. Examples of PDZ containing proteins

affecting cell morphology and binding to the C2 domain of syndecan-1 include CASK (53) and syntenin (54).

Fibroblast growth factor-2 is a heparin-binding growth factor that stimulates cell proliferation and inhibits cell differentiation. Although FGF can bind to its tyrosine kinase receptor, the low-affinity interaction with heparan sulfate enables the formation of a high-affinity interaction with its receptor, resulting in growth factor mediated signaling at low growth factor concentrations. The interaction of syndecan-1 with FGF has been shown to play a role in skeletal muscle development (42), and wound repair (55). During wound repair, syndecan-1 expression is induced by FGF-2 (56). A 280 bp sequence located -10 kb from the syndecan-1 translation initiation site functions as a promoter element for the syndecan-1 response to FGF-2. This 280 bp domain is termed the fibroblast growth factor-inducible response element. To date, similar elements have not been reported for syndecans 2 through 4.

VI. Roles of Syndecan in Development

A. Cell Adhesion

For tissue development to proceed, cells must adhere to the extracellular matrix. After cell adhesion occurs, the processes of cell proliferation, migration, and differentiation can take place. The adhesion of cells to the extracellular matrix results in the formation of focal adhesions. Focal adhesion complexes are comprised of transmembrane integrin receptors which link the cell to the cell binding domain of the extracellular matrix macromolecule fibronectin, and intracellular proteins with both structural and signaling capabilities. The second component of the focal adhesion complex is the binding of a cell surface heparan sulfate proteoglycan to the heparin binding domain of fibronectin (57). Although all the syndecans are likely to play a role in the cell adhesion process, syndecan-4 appears to play a prominent role due to its binding to the heparin binding domain of fibronectin (58). The cytoplasmic domain of syndecan-4 binds at the variable region to phosphatidyl-inositol-4, 5-biphosphate, which enhances binding to activated protein kinase C (59). The localization of syndecan-4 in the focal adhesion is augmented by the protein syndesmos which binds to the syndecan-4 cytoplasmic domain (60). Once the focal adhesion complex is produced with both integrin and syndecan-4 interactions, cell spreading and cellular cytoskeleton actin stress fiber formation proceeds through a Rho-dependent signaling pathway. Thus, syndecan-4 provides a linkage between the extracellular and intracellular environments leading to the activation of signal transduction pathways.

Syndecans are also expressed at sites of cell to cell adhesion. Syndecan-1 is the earliest of the syndecans to be expressed at sites of cell to cell adhesion in the 16 through 32 cell stage mouse, and is subsequently expressed on all cells of the inner cell mass in the blastocyst (61). During tissue formation, syndecan-1 expression has been observed in the epidermis, the tooth, mammary epithelium, and other

epithelia-derived tissues (62). As development proceeds, syndecan-1 expression declines in the epithelia tissues and expression increases in the mesenchymal tissue (60). Throughout development, syndecan-1 is dynamically expressed to function at specific times.

B. Neuronal Development

Nervous system development occurs in three stages: with the formation of neurons from neural stem cells (neurogenesis), the guidance of axons to target cells, and the formation of synapses. Heparan sulfate proteoglycans have been shown to play a significant role in these stages of neural development due to their regulation of growth factor signaling, cell adhesion, and assembly of the extracellular matrix. Syndecan-2 has been shown to be involved in the morphogenesis of dendritic spines during synaptogenesis. Dendritic spines are small protusions on the surface of dendrites and are the sites of synapse formation, and receive the majority of excitatory synapse information. The lack of dendritic spine formation results in mental retardation as illustrated by fragile X syndrome (63).

The C2 domain EFYA tetrapeptide of syndecan-2 binds to the synaptic PDZ domain protein CASK. Ethell and Yamaguchi (64) showed that *in vitro* transfection of syndecan-2 in rhippocampal neurons results in early dendritic spine formation. Furthermore, deletion of the syndecan-2 EFYA C2 domain results in a lack of spine formation (65). In cultured hippocampal neurons, the protein synbindin colocalizes with syndecan-2 at the dendritic spines (66), with binding at the cytoplasmic EFYA region of the syndecan-2 cytoplasmic domain (64). Synbindin is a neuronal cytoplasmic protein that shares homology to yeast proteins involved in membrane trafficking and vesicle transport (66). Vesicle transport and trafficking likely play a role in the maturation of postsynaptic sites (67, 68). Based on the ligand interaction of synbindin with syndecan-2 and the proposed function of synbindin, syndecan-2 may function in the translocation of postsynaptic neurotransmitter vesicles, or the recruitment of calcium storing membrane compartments toward the synapses (66).

Syndecan-3 is localized predominantly in neural axons (69) and binds to heparin-binding growth associated molecule (HB-GAM). Heparin-binding growth associated molecule is a conserved extracellular matrix-associated growth factor (60) that is expressed in outgrowing axonal tracts in the developing brain (70). Syndecan-3 binds to HB-GAM at its attached heparan sulfate chains. Kinnunen et al. (71) showed that the binding of syndecan-3 to HB-GAM may activate a cortactin-Src kinase signaling pathway leading to neurite outgrowth. In this study, when Src kinase inhibitors were added to neuroblastoma cell cultures transfected with syndecan-3 and plated on HB-GAM, neurite outgrowth was inhibited.

C. Muscle Development

Skeletal muscle myogenesis is a complex process that involves muscle cell proliferation, migration, adhesion, fusion to form multinucleated myotubes, and further

differentiation to become mature muscle fibers (72). This process is under precise control through the interaction of muscle cells with the extracellular environment. Growth factors like FGF-2 and TGF-β are strong stimulators or inhibitors of muscle cell proliferation and differentiation, and interact with the cell by binding to proteoglycans. Syndecans-1 through -4 have been identified in skeletal muscle (42,73,74). *In vitro* studies with C_2C_{12} mouse skeletal muscle cells have shown that syndecan-1, syndecan-3, and syndecan-4 are down-regulated with muscle differentiation with expression being higher during the proliferation stage. Syndecan-2 expression remained constant during both *in vitro* muscle cell proliferation and differentiation. Larraín et al. (75) showed that C_2C_{12} cells overexpressing syndecan-1 had a 6- to 7-fold increase in fibroblast growth factor responsiveness and a corresponding decrease in the expression of, myogenin, creatine kinase, and myosin, key factors associated with muscle differentiation. Their results are suggestive of syndecan-1 playing a role in the terminal differentiation of muscle cells.

Postnatal muscle growth occurs through the activation of myogenic satellite cells. Satellite cells are located between the basement membrane and the sarcolemma of skeletal muscle fibers (76) and donate their nuclei to adjacent muscle fibers (77–79) leading to postnatal muscle growth through the process of hypertrophy. In the adult, satellite cells remain quiescent and are activated to repair and regenerate skeletal muscle. Therefore, understanding the role that syndecans may play in the regulation of FGF-2 signaling in *in vivo* muscle formation is of significance for both postnatal muscle formation and the regeneration of muscle in adults.

In studies by Cornelison et al. (46), the expression of syndecans-1 through -4 was studied in embryonic, fetal, postnatal, and adult muscle tissue, and primary adult muscle fiber cultures. They identified the expression of syndecans-1, -3, and -4 in developing muscle tissue, and syndecan -3 and -4 expression in adult muscle tissue was restricted to quiescent satellite cells. Upon satellite cell activation and subsequent fusion with existing myofibers, syndecan -3 and -4 expression was detected for at least 96 h. Disruption of heparan sulfate proteoglycan sulfation by the addition of chlorate delayed satellite cell proliferation. These data provide strong evidence that the heparan sulfate proteoglycans, syndecan-3 and -4, may be critical in maintaining satellite cell quiescence, activation, proliferation, and differentiation during the regeneration of skeletal muscle. Initial data reported by Casar et al. (80) provide the first *in vivo* evidence suggesting the requirement for syndecan-3 expression for successful skeletal muscle regeneration. In this study, inhibiting syndecan-3 expression resulted in normal muscle cell proliferation, but a decreased capacity of the cells to differentiate and form skeletal muscle fibers.

VII. Glypicans

Glypicans unlike the syndecans are not transmembrane heparan sulfate proteoglycans, but attached to the cell surface through a GPI lipid anchor. Fig. 3 presents a generalized schematic of the glypican structure. There have been six vertebrate glypicans identified: glypican-1 through -6, whose structure is conserved between

the different forms of glypican. The glypicans contain an N-terminus signal sequence, followed by a globular domain containing multiple cysteine residues, a glycosaminoglycan attachment domain, and a C-terminus that results in the formation of the GPI anchor to the cell surface. Glypicans tend to localize at membrane areas that are rich in cholesterol or lipids, and on the surface of polarized cells. To date, only heparan sulfate chains have been reported to be attached to the glypican core protein. The heparan sulfate chains show diversity in their structure due to modifications occurring after the attachment of the glycosaminoglycans to the core protein. Mertens et al. (81) showed that the amount of heparan sulfate determines where glypican will localize on the cell surface.

Similar to the syndecans, the glypican family binds to ligands including growth factors like FGF-2 that permit a high-affinity interaction with their respective receptors activating cell signaling pathways. Unlike the syndecans which can make direct contact with internal cytoskeletal components to activate signal transduction pathways, glypican activation of signaling pathways must be indirect and involve other transmembrane molecules, since glypican does not contain a transmembrane domain.

Although the function of each of the glypicans is not completely understood, each of the glypicans is differentially expressed during development. Glypican-1 is found in the brain, kidneys, skeletal muscle, and several other tissues (82–84). Glypican-2 is located in the developing nervous system (85); Glypican-3 in mesodermal tissue and during intestine development (86); Glypican-4 in the blood vessels, kidney, brain, and adrenal cortex (87); Glypican-5 in the kidney, limb, and brain (88, 89); and Glypican-6 expression is widespread with predominant expression in the human fetal kidney and adult ovary. Expression has also been

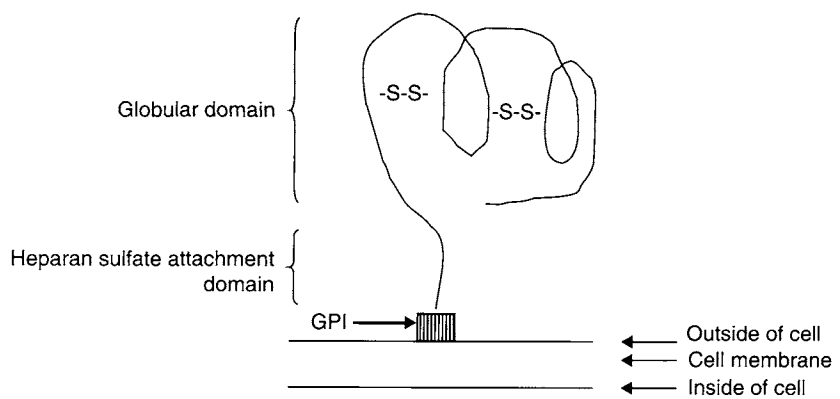

Figure 3 Schematic illustration of the structure of the glypicans. The complete structure of the glypicans is located extracellularly with the core protein attached to the cell surface through a glycosylphosphoinositol (GPI) anchor. The globular domain is composed of many disulfide bridges and the heparan sulfate chains are attached to the non-globular portion of the core protein.

detected in smooth muscle cells lining the aorta, mesenchymal cells of the intestine, kidney, lung, teeth, and gonads (90).

VIII. Roles of Glypican in Tissue Development

A. Cell Growth Control

Glypican-3 has been shown to play a role in the control of cell growth through the induction of apoptosis (91). Mutations in glypican-3 result in cell overgrowth. Control of cell growth is a function not usually attributed to cell surface heparan sulfate proteoglycans. Simpson-Golabi-Behmel syndrome (SGBS) is an X-linked disorder characterized by both pre- and postnatal overgrowth. A wide variety of clinical symptoms have been reported with this syndrome, which include heights over 6.5 ft in affected males, polydactyl, supernumerary nipples, cleft palate, congenital heart defects, higher risk for tumor development during early childhood, vertebrate and rib abnormalities, hernias, and altered facial appearance (92).

In cases of SGBS, a number of different small deletions or point mutations have been identified in glypican-3 (93–95). At this time, it is not possible to correlate glypican-3 gene mutations with the clinical phenotype, except to recognize the lack of a functional glypican protein. The mechanism for how glypican-3 regulates cell growth is not completely understood. However, one of the primary means in which glypican-3 may modulate cell growth is through glypican-3 acting as a regulator of insulin growth factor II (IGF-II) levels. Insulin growth factor II is a stimulator of both cell growth and differentiation. Beckwith-Wiedemann syndrome shares several clinical features with SGBS and results from an overexpression of IGF-II. Pilia et al. (92) hypothesized that glypican-3 functions as a negative regulator of IGF-II through the binding of IGF-II to the glypican-3 core protein. Studies addressing this hypothesis have not been conclusive, and it is likely that glypican-3 modulates other signaling pathways controlling cell growth. In glypican-3 knockout mice, developmental overgrowth of tissues occurs as in SGBS but circulating IGF-II levels do not differ from normal control mice.

B. Skeletal Muscle Development

Glypican-1 expression has been identified during skeletal muscle development (96). During skeletal muscle formation, syndecan-1 levels are high during the proliferation of muscle cells followed by an increase in glypican-1 expression during muscle cell differentiation (82). Both syndecan-1 and glypican-1 function in the signaling of FGF-2. Fibroblast growth factor 2 is a potent stimulator of muscle cell proliferation and a strong inhibitor of muscle cell differentiation. The differences in syndecan-1 and glypican-1 expression suggest that these proteoglycans function in a differential manner in the signaling of FGF-2. Brandan and Larraín (73) hypothesized, based on differences in their *in vitro* expression in myogenic cell cultures, that syndecan-1 may increase muscle cell proliferation by presenting FGF-2 to its receptor, and glypican may sequester FGF-2 to permit differentiation to proceed. Conclusive

evidence has not yet been obtained to support this hypothesis. Syndecans-2 through -4 are also expressed during skeletal muscle development, and their role in FGF-2 signaling is not well understood at this time. Therefore, it is likely that the hypothesis put forth by Brandan and Larraín (73) represents just one aspect of cell surface heparan sulfate proteoglycan regulation of skeletal muscle development.

C. Nervous System Development

The best characterized of the glypicans during development of the nervous system is glypican-4. Glypican-4 is expressed in the ventricular zone of the developing brain (97). Expression of glypican-4 is limited to only neuronal cells that express stem cell properties. Once the cells are committed, glypican-4 expression ceases (97). Neuronal stem cells are cells that can differentiate into neurons, astrocytes, and oligodendrocytes. Glypican-1 is also expressed in the ventricular zone, and is detected in postmitotic and differentiated neurons (98). Glypicans-2 and -5 are expressed in postmitotic neurons (88, 99).

Growth factor regulation is one of the critical elements during neurogenesis. It is likely that the different forms of glypican are involved in the regulation of FGF-2. Fibroblast growth factor 2 plays a role in the proliferation and differentiation of neural stem cells in the cerebral cortex. Levels of FGF-2 have been shown to influence the development of neural stem cells (100). High concentrations result in stems cells becoming glial cells, and low concentrations result in the generation of neurons. The mechanisms for how glypican regulates FGF-2 signaling and the specificity of the different forms of glypican in neuronal development are still an enigma.

IX. Betaglycan and CD44

A. Betaglycan

Betaglycan is a transmembrane heparan and chondroitin sulfate proteoglycan with an extracellular domain that functions as a coreceptor for TGF-β by binding it to the betaglycan core protein (101). Transforming growth factor-β exerts its biological effects through the activation of two high-affinity serine/threonine kinase receptors, type II (TβRII) and type I (TβRI) (102). Initial binding of TGF-β is to the TβRII receptor and is followed by the subsequent formation of a TβRII-TβRI complex. The complex formation results in TβRII phosphorylating TβRI and the phosphorylation of the receptor-associated molecules Smad2 and Smad3 by TβRI. Betaglycan binds to TGF-β through its core protein, not heparan or chondroitin sulfate chains. Betaglycan does not have any signaling activities on its own but affects the affinity of TβRI and TβRII for TGF-β. The transmembrane form of betaglycan, when bound to TGF-β, increases the affinity of TGF-β for TβRII (103). This upregulates cellular responsiveness to TGF-β, especially the TGF-β2 form of TGF-β (103).

A soluble or shed form of betaglycan exists and is found in serum, extracellular matrices, and conditioned medium during *in vitro* cell culturing. For shedding to occur the extracellular or ectodomain of betaglycan is enzymatically cleaved.

According to a recent study by Velasco-Loyden et al. (104), betaglycan shedding is regulated by matrix metalloproteases (MT-MMP), MT1-MMP and MT3-MMP. In contrast to the transmembrane form of betaglycan functioning as an enhancer to TGF-β mediated signaling, the soluble form inhibits TGF-β activities. Therefore, betaglycan may function as both an enhancer and inhibitor of TGF-β mediated signal transduction, and it is likely that the regulation of the expression of the betaglycan transmembrane form and cleavage to the soluble form are critical in the cellular response to TGF-β.

B. CD44

The CD44 is a cell surface glycoprotein with multiple forms generated from a single gene by alternative splicing of its mRNA. The functions of CD44 in cell-to-cell and cell–extracellular matrix interactions are largely influenced by the form of CD44 being expressed. The CD44 protein is composed of 19 exons with 12 exons containing variable splice sites (105). The different CD44 isoforms can be differentially modified with chondroitin sulfate, heparan sulfate, and keratan sulfate. Heparan sulfate is only added to exon V3 at the Ser-Gly-Ser-Gly site (106). This variant of CD44 can act as a low-affinity receptor for fibroblast growth factor.

X. Pericellular Heparan Sulfate Proteoglycans

In addition to the cell surface heparan sulfate proteoglycans, there is a group of heparan sulfate proteoglycans that do not contain the core protein motif to associate with the cell plasma membrane and are located in the extracellular matrix near, pericellular, the cells. Heparan sulfate proteoglycans belonging to the pericellular group include perlecan, agrin, and collagen XVIII.

A. Perlecan

Perlecan is a ubiquitous heparan sulfate proteoglycan found in all basement membranes (107). Perlecan was named for its appearance in rotary shadowing electron microscopy in that it looked like pearls on a string. Fig. 4 presents an illustration of the perlecan proteoglycan. The perlecan core protein is approximately 400 kDa with five unique domains. Domain I contains 3 heparan sulfate chains and a sperm protein enterokinase domain (110, 111). Domain II contains a low-density lipoprotein receptor and one Ig-like repeat; domain III is structurally similar to the short arm of the laminin A chain connected by laminin-1 epidermal growth factor-like repeats; domain IV contains neural cell adhesion molecule IgG-like repeats and binds to nidogens, laminin–nidogen, fibronectin, and heparin (112); and domain V has three laminin-1 globular homology domains connected by epidermal growth factor-like repeats and promotes beta 1 integrin-mediated cell adhesion, and binds to heparin, nidogen, and fibulin-2 (113).

Perlecan is essential for normal development to proceed. Results from perlecan gene knockout studies have shown that 40% of the mice die at embryonic day

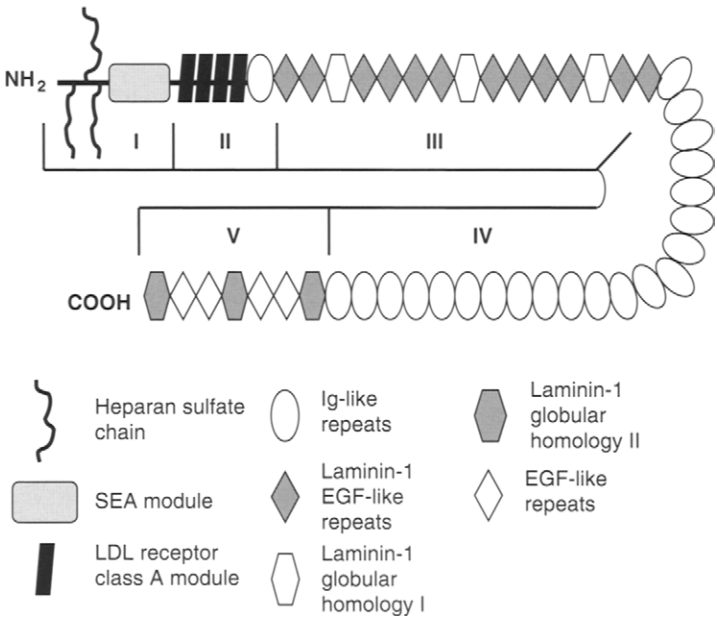

Figure 4 Schematic illustration of perlecan structure. Perlecan is comprised of five unique domains, each of which contains distinct protein modules. Domain I has three attachment sites for heparan sulfate chain attachment and a SEA module. Domain II has an LDL receptor class A module and one Ig-like repeat. Domain III has three laminin-1 globular homology domains (homologous to the short arm of laminin-1) connected by laminin-1 EGF-like repeats. Domain IV has multiple Ig-like repeats (21 repeats in human). Domain V has three laminin-1 globular homology domains (homologous to G domain of laminin-1) connected by EGF-like repeats. SEA, sperm protein, enterokinase, and agrin; LDL, low-density lipoprotein; EGF, epidermal growth factor. (108, 109).

10.5 with abnormal cephalic development and the remaining mice died shortly after birth with skeletal dysplasia (114). These results suggest that perlecan may play a structural role in the appropriate development of cartilage.

Perlecan null mice develop severe myocardial dysfunction between embryonic days 10 to 12 (115). The homozygous knock-outs died by cardiac arrest between embryonic days 10 to 12 with a loss of normal basement membrane structure surrounding the myocardial cells and the appearance of holes in the heart. Costell et al. (115) have hypothesized that the basement membrane structure without the expression of perlecan is functionally comprised and when the intraventricular blood pressure increases, the mice enter cardiac arrest.

Basement membranes located at neuromuscular junctions are enriched in perlecan (116). Acetylcholine, a neurotransmitter in skeletal muscle, binds to the acetylcholine receptor on the responding muscle cell surface and activates sodium channels inducing the contraction of muscle. Other macromolecular molecules localized in the neuromuscular junction include acetylcholinesterase, agrin, dystroglycan, rapsyn, and utrophin (117). Perlecan-null mice exhibit an absence of

acetylcholinesterase at the neuromuscular junction. Acetylcholinesterase synthesis is not affected by the absence of perlecan but the localization is modified, indicating that perlecan plays an essential role in the macromolecular organization of the neuromuscular junction (118).

B. Agrin

Agrin is a proteoglycan that contains both chondroitin and heparan sulfate attached glycosaminoglycan chains. Neurite outgrowth is inhibited by agrin in ciliary ganglia, dorsal root ganglia, retina, and hippocampus (119–123). The inhibitory function of agrin is limited to the N-terminus that contains heparan sulfate and chondroitin sulfate. A recent study by Baerwald-De La Torre (124) has reported that the agrin N-terminus inhibits neurite outgrowth by both glycosaminoglycan-dependent and -independent mechanisms. The N-terminal domain was divided into half. The more N-terminal fragment required the presence of the heparan sulfate chains to inhibit neurite outgrowth, whereas the more C-terminal portion of the N-terminus contains both heparan sulfate and chondroitin sulfate chains which contributed to inhibition of neurite outgrowth, but were not required for the inhibitory activity.

C. Collagen XVIII

Collagen XVIII is a heparan sulfate containing proteoglycan containing eight potential glycosaminoglycan glycosylation sites (125) localized in endothelial and epithelial basement membranes. A C-terminal peptide of collagen XVIII showed both anti-angiogenic and anti-tumor properties (126, 127). These discoveries have brought much research attention to collagen type XVIII. However, the angiogenic effects are limited to blood vessel development in only the eye, as shown through collagen XVIII null mice (128).

L-selectin functions as a lymphocyte receptor during lymphocyte migration to peripheral lymph nodes (129), and leukocyte migration into inflamed tissue (130, 131). Kidney L-selectin has been shown to bind both chondroitin and heparan sulfate proteoglycans (132). Purification of the L-selectin binding heparan sulfate proteoglycan has identified the proteoglycan as collagen type XVIII (133). In addition to interacting with L-selectin, collagen type XVIII in the kidney binds to monocyte chemoattractant protein-1 and induces integrin activation of monocytes. Based on these interactions, it is possible that kidney collagen type XVIII links L-selectin and integrin mediated cell adhesion during renal inflammation (133).

XI. Role in Disease Pathogenesis

A. Alzheimer's

Patients with Alzheimer's Disease have extensive neurofibrillary tangles, senile plaques, and vascular amyloid angiopathy in their brain tissue (134). The

senile plaques and cerebrovascular amyloid angiopathy contain amyloid β protein (135). The neurofibrillary tangles are composed of aggregates of hyperphosphorylated tau protein (136, 137). Heparan sulfate proteoglycans have been identified in senile plaques, tangles, and areas of cerebrovascular amyloid angiopathy (138, 139).

Heparan sulfate proteoglycans identified in Alzheimer's patients include perlecan, agrin, syndecan-1 through -3, and glypican-1. Perlecan expression is limited to senile plaques in the cortex but not cerebellum. The cortex is not the usual site for senile plaque formation (140). Based on the binding of perlecan to amyloid β protein and the amyloid precursor protein, it is possible that perlecan may play a role in amyloid fibril formation (141). Verbeek et al. (142) through immunohistochemical analysis showed that agrin is localized in senile plaques, neurofibrillary tangles, and cerebral blood vessels. Syndecan-1 through -3 and glypican-1 were also identified in the senile plaques and neurofibrillary tangles at a lower frequency than agrin. These results suggest that agrin, syndecans-1 through -3, and glypican-1 may play a role in senile plaque formation associated with Alzheimer's disease.

B. Cancer

Heparan sulfate proteoglycan expression has been shown to be associated with several types of cancer, including breast, pancreatic, and osteolytic myeloma tumor metastasis. Syndecan-1 is the predominant proteoglycan expressed on the cell surface of myeloma cells. In some patients, the myeloma syndecan-1 is shed at high levels into the serum (143). Patients with serum levels of syndecan-1 five times higher than normal have a poor prognosis (144), suggesting that syndecan-1 may be involved with the progression of osteolytic tumor growth. The soluble syndecan-1 contains the extracellular domain with the attached heparan sulfate chains. The presence of the heparan sulfate chains allows the soluble syndecan-1 to continue to interact with heparan sulfate binding ligands like FGF-2. Sanderson et al. (145) have found that soluble syndecan-1 transfected cells are hyperinvasive compared to control cells. Soluble syndecan-1 may, therefore, play a role in increasing the invasiveness of myeloma tumor cells by promoting tumor growth within the bone microenvironment.

Similar to myeloma tumors, metastatic breast carcinoma has the capability to grow in bone. Heparan sulfate proteoglycans may play a key role in the proliferation of breast tumors. Breast carcinoma cells have an enhanced ability to promote the formation of FGF-2 receptor complexes compared to normal breast epithelial cells (146). This increased interaction with FGF-2 likely stimulates carcinoma cell proliferation, as FGF-2 is a potent stimulator of cell growth. Barbareschi et al. (147) reported that high expression of syndecan-1 is associated with a poor prognosis and an aggressive phenotype.

One potential therapy for the treatment of cancer is the modification of heparan sulfate chains. Treatment of heparan sulfate with bacterial heparanase III inhibited both tumor cell proliferation and metastatis (148). In addition to enzymatic digestion of heparan sulfate, other possible approaches to modify the heparan sulfate chains to inhibit tumor cell growth include: antisense or siRNA technology to reduce the expression of heparan sulfate or heparan sulfate consensus peptides that will bind

to heparan sulfate ligand functional domains and block interactions with ligands, like FGF-2 that stimulate tumor cell growth and metastatis.

XII. Summary

The heparan sulfate proteoglycans represent a large family of both cell surface and pericellular macromolecules. Although not completely understood at this time, it is clear that subtle changes in heparan sulfate structure and macromolecular organization of the core protein can dramatically affect their function. The heparan sulfate proteoglycans are involved in both the development of tissue and organ systems, as well as disease pathogenesis. However, much still needs to be learned with regard to heparan sulfate proteoglycan function and structure. Some of the areas which require further investigation include: (1). how the fine structure of the heparan sulfate chains is regulated and what are the functional outcomes of structural modifications to the chains?, (2). what are the mechanisms that regulate the developmental and cell-specific expression of the different heparan sulfate proteoglycans?, (and 3). heparan sulfate proteoglycans within the same family as the syndecans or glypicans are structurally similar, what regulates their distinct functions? The answers to these questions and others will further our knowledge of the biology and functions of the heparan sulfate proteoglycans.

References

1. Scott JE. Extracellular matrix, supramolecular organization and shape. J Anat 1995; 187:259–269.
2. Iozzo RV, Murdoch AD. Proteoglycans of the extracellular environment: clues from the gene and protein side offer novel perspectives in molecular diversity and function. FASEB J 1996; 10:598–614.
3. Roden L, Koerner T, Olson C, Schwartz NB. Mechanisms of chain initiation in the biosynthesis of connective tissue polysaccharides. Federation Proceeding 1985; 44:373–380.
4. Bourdon MA, Krusuio T, Campbell S, Schwartz NB, Ruoslahti E. Identification and synthesis of a recognition signal for the attachment of glycosaminoglycans to proteins. Proc Natl Acad Sci USA 1987; 84:3194–3198.
5. Esko JD, Selleck SB. Order out of chaos: assembly of ligand binding sites in heparan sulfate. Annu Rev Biochem 2002; 71:435–471.
6. Perrimon N, Bernfield M. Specificities of heparan sulphate proteoglyycans in developmental processes. Nature 2000; 404:725–728.
7. Maccarana M, Sakura Y, Tawada A, Yoshida K, Lindahl U. Domain structure of heparan sulfates from bovine organs. J Biol Chem 1996; 271:17804–17810.
8. Casu B, Petitou M, Provasoli M, Sinay P. Conformational flexibility: a new concept for explaining binding and biological properties of iduronic acid-containing glycosaminoglycans. Trends Biochem Sci 1988; 13:221–225.

9. Koda JE, Bernfield M. Heparan sulfate proteoglycans from mouse mammary epithelial cells. Basal extracellular proteoglycan binds specifically to native type I collagen fibrils. J Biol Chem 1984; 259:11763–11770.
10. Skubitz AP, McCarthy JB, Charonis AS, Furcht LT. Localization of three distinct heparin-binding domains of laminin by monoclonal antibodies. J Biol Chem 1988; 263:4861–4868.
11. Saunders S, Bernfield M. Cell surface proteoglycan binds mouse mammary epithelial cells to fibronectin and behaves as a receptor for interstitial matrix. J Cell Biol 1988; 106:423–430.
12. Sun X, Mosher DF, Rapraeger A. Heparan sulfate-mediated binding of epithelial cell surface proteoglycan to thrombospondin. J Biol Chem 1989; 264:2885–2889.
13. Salmivirta M, Elenius K, Vainio S, Hofer U, Chiquet-Ehrismann R, Thesleff I, Jalkanen M. Syndecan from embryonic tooth mesenchyme binds tenascin. J Biol Chem 1991; 266:7733–7739.
14. Norgard-Sumnicht KE, Varki NM, Varki A. Calcium-dependent heparin-like ligands for L-selectin in nonlymphoid endothelial cells. Science 1993; 261:480–483.
15. Reyes AA, Akeson R, Brezina L, Cole GJ. Structural requirements for neural cell adhesion molecule-heparin interaction. Cell Regul 1990; 1:567–576.
16. DeLisser HM, Yan HC, Newman PJ, Muller WA, Buck CA, Albelda SM. Platelet/endothelial cell adhesion molecule-1 (CD31)-mediated cellular aggregation involves cell surface glycosaminoglycans. J Biol Chem 1993; 268:16037–16046.
17. Diamond MS, Alon R, Parkos CA, Quinn MT, Springer TA. Heparin is an adhesive ligand for the leukocyte integrin Mac-1 (CD11b/CD1). J Cell Biol 1995; 130:1473–1482.
18. Yayon A, Klagsbrun M, Esko JD, Leder P, Ornitz DM. Cell surface, heparin-like molecules are required for binding of basic fibroblast growth factor to its high affinity receptor. Cell 1991; 64:841–848.
19. Johnson GR, Wong L. Heparan sulfate is essential to amphiregulin-induced mitogenic signaling by the epidermal growth factor receptor. J Biol Chem 1994; 269:27149–27154.
20. Lyon M, Deakin JA, Mizuno K, Nakamura T, Gallagher JT. Interaction of hepatocyte growth factor with heparan sulfate. Elucidation of the major heparan sulfate structural determinants. J Biol Chem 1994; 269:11216–11223.
21. Feyzi E, Lustig F, Fager G, Spillmann D, Lindahl U, Salmivirta M. Characterization of heparin and heparan sulfate domains binding to the long splice variant of platelet-derived growth factor A chain. J Biol Chem 1997; 272:5518–5524.
22. Lyon M, Rushton G, Gallagher JT. The interaction of the transforming growth factor-betas with heparin/heparan sulfate is isoform-specific. J Biol Chem 1997; 272:18000–18006.
23. Gitay-Goren H, Soker S, Vlodavsky I, Neufeld G. The binding of vascular endothelial growth factor to its receptors is dependent on cell surface-associated heparin-like molecules. J Biol Chem 1992; 267:6093–6098.
24. Saxena U, Klein MG, Goldberg IJ. Metabolism of endothelial cell-bound lipoprotein lipase. Evidence for heparan sulfate proteoglycan-mediated internalization and recycling. J Biol Chem 1990; 265:12880–12886.

25. Ji ZS, Brecht WJ, Miranda RD, Hussain MM, Innerarity TL, Mahley RW. Role of heparan sulfate proteoglycans in the binding and uptake of apolipoprotein E-enriched remnant lipoproteins by cultured cells. J Biol Chem 1993; 268:10160–10167.
26. Weisgraber KH, Rall SC Jr. Human apolipoprotein B-100 heparin-binding sites. J Biol Chem 1987; 262:11097–11103.
27. Lindahl U, Thunberg L, Backstrom G, Riesenfeld J, Nordling K, Bjork I. Extension and structural variability of the antithrombin-binding sequence in heparin. J Biol Chem 1984; 259:12368–12376.
28. Pratt CW, Church FC. Heparin binding to protein C inhibitor. J Biol Chem 1992; 267:8789–8794.
29. Ramsden L, Rider CC. Selective and differential binding of interleukin (IL)-1 alpha, IL-1 beta, IL-2 and IL-6 to glycosaminoglycans. Eur J Immunol 1992; 22:3027–3031.
30. Webb LM, Ehrengruber MU, Clark-Lewis I, Baggiolini M, Rot A. Binding to heparan sulfate or heparin enhances neutrophil responses to interleukin 8. Proc Natl Acad Sci USA 1993; 90:7158–7162.
31. WuDunn D, Spear PG. Initial interaction of herpes simplex virus with cells is binding to heparan sulfate. J Virol 1989; 63:52–58.
32. Schlessinger J, Plotnikov AN, Ibrahimi OA, Eliseenkova AV, Yeh BK, Yayon A, Linhardt RJ, Mohammadi M. Crystal structure of a ternary FGF-FGFR-heparin complex reveals a dual role for heparin in FGFR binding and dimerization. Mol Cell 2000; 6:743–750.
33. Maccarana M, Casu B, Lindahl U. Minimal sequence in heparin/heparan sulfate required for binding of basic fibroblast growth factor. J Biol Chem 1993; 268:23898–23905.
34. Herold BC, Gerber SI, Polonsky T, Belval BJ, Shaklee PN, Holme K. Identification of structural features of heparin required for inhibition of herpes simplex virus type 1 binding. Virology 1995; 206:1108–1116.
35. Feyzi E, Trybala E, Bergstrom T, Lindahl U, Spillmann D. Structural requirement of heparan sulfate for interaction with herpes simplex virus type 1 virions and isolated glycoprotein C. J Biol Chem 1997; 272:24850–24857.
36. Walker A, Gallagher JT. Structural domains of heparan sulphate for specific recognition of the C-terminal heparin-binding domain of human plasma fibronectin (HEPII). Biochem J 1996; 317:871–877.
37. Bernfield M, Götte M, Park PW, Reizes O, Fitzgerald ML, Lincecum J, Zako M. Functions of cell surface heparan sulfate proteoglycans. Annu Rev Biochem 1999; 68:729–777.
38. Lander AD, Selleck SB. The elusive functions of proteoglycans: in vivo veritas. J Cell Biol 2000; 148:237–242.
39. Bernfield M, Kokenyesi R, Kato M, Hinkes MT, Spring J, Gallo RL, Lose EJ. Biology of the syndecans: a family of transmembrane heparan sulfate proteoglycans. Annu Rev Cell Bio 1992; 8:365–393.
40. Salmivirta M, Heino J, Jalkanen M. Basic fibroblast growth factor-syndecan complex at cell surface or immobilized to matrix promotes cell growth. J Biol Chem 1992; 267:17606–17610.
41. Chen L, Klass C, Woods A. Syndecan-2 regulates transforming growth factor-β signaling. J Biol Chem 2004; 279:15715–15718.

42. Larraín J, Cizmeci-Smith G, Troncoso V, Stahl RC, Carey DJ, Brandan E. Syndecan-1 expression is down-regulated during myoblast terminal differentiation. Modulation by growth factors and retinoic acid. J Biol Chem 1997; 272:18418–18424.
43. Liu X, McFarland DC, Nestor KE, Velleman SG. Developmental regulated expression of syndecan-1 and glypican in pectoralis major muscle in turkeys with different growth rates. Develop Growth Differ 2004; 46:37–51.
44. David G. Integral membrane heparan sulfate proteoglycans. FASEB J 1993; 7:1023–1030.
45. Kim CW, Goldberger OA, Gallo RL, Bernfield M. Members of the syndecan family of heparan sulfate proteoglycans are expressed in distinct cell-, tissue-, and development-specific patterns. Mol Biol Cell 1994; 5:797–805.
46. Cornelison DDW, Filla MS, Stanley HM, Rapraeger AC, Olwin BB. Syndecan-3 and syndecan-4 specifically mark skeletal muscle satellite cells and are implicated in satellite cell maintenance and muscle regeneration. Dev Bio 2001; 239:79–94.
47. Kojima T, Shworak NW, Rosenberg RD. Isolation and characterization of heparan sulfate proteoglycans produced by cloned rat microvascular endothelial cells. J Biol Chem 1992; 267:4859–4869.
48. Baciu PC, Acaster C, Goetinck PF. Molecular cloning and genomic organization of chicken syndecan-4. J Biol Chem 1994; 269:696–703.
49. Rapraeger AC, Bernfield M. Heparan sulfate proteoglycans from mouse mammary epithelial cells. A putative membrane proteoglycan associates quantitatively with lipid vesicles. J Biol Chem 1983; 258:3632–3636.
50. Hayashi K, Hayashi M, Jalkanen M, Firestone JH, Trelstad RL, Bernfield M. Isolation and characterization of fibronectin-binding proteoglycan carrying both heparan sulfate and dermatan sulfate chains from human placenta. J Biol Chem 1987; 262:8926–8933.
51. Mali M, Elenius K, Miettinen HM, Jalkanen M. Inhibition of basic fibroblast growth factor-induced growth promotion by overexpression of syndecan-1. J Biol Chem 1993; 268:24215–24222.
52. Kato M, Wang H, Kainulainen V, Fitzgerald ML, Ledbetter S, Ornitz DM, Bernfield M. Physiological degradation converts the soluble syndecan-1 ectodomain from an inhibitor to a potent activator of FGF-2. Nature Med 1998; 4:691–697.
53. Hsueh YP, Yang FC, Kharazia V, Naisbitt S, Cohen AR, Weinberg RJ, Sheng M. Direct interaction of CASK/LIN-2 and syndecan heparan sulfate proteoglycan and their overlapping distribution in neuronal synapses. J Cell Biol 1998; 142:139–151.
54. Grootjans JJ, Zimmermann P, Reekmans G, Smets A, Degeest G, Durr J, David G. Syntenin, a PDZ protein that binds syndecan cytoplasmic domains. Proc Natl Acad Sci USA 1997; 94:13683–13688.
55. Rautava J, Soukka T, Heikinheimo K, Miettinen PJ, Happonen R-P, Jaakola P. Different mechanisms of syndecan-1 activation through a fibroblast-growth-factor-inducible response element (FIRE) in mucosal and cutaneous wounds. J Dent Res 2003; 82:382–387.
56. Jaakkola P, Jalkanen M. Transcriptional regulation of syndecan-1 expression by growth factors. Prog Nuc Acid Res Mol Biol 2000; 63:109–138.

57. Woods A, Couchman JR. Syndecan 4 heparan sulfate proteoglycan is a selectively enriched and widespread focal adhesion component. Mol Biol Cell 1994; 5:183–192.
58. Baciu PC, Goetinck PF. Protein kinase C regulates the recruitment of syndecan-4 into focal contacts. Mol Biol Cell 1995; 6:1503–1513.
59. Oh ES, Woods A, Lim ST, Theibert AW, Couchman JR. Syndecan-4 proteoglycan cytoplasmic domain and phosphatidylinositol 4,5-biphosphate coordinately regulate protein kinase C acitivity J Biol Chem 1998; 273:10624–10629.
60. Rapraeger AC. Molecular interactions of syndecans during development. Cell Dev Biol 2001; 12:107–116.
61. Sutherland A E, Sanderson RD, Mayes M, Seibert M, Calarco PG, Bernfield M, Damsky CH. Expression of syndecan, a putative low affinity fibroblast growth factor receptor, in the early mouse embryo. Development 1991; 113:339–351.
62. Trautman MS, Kimelman J, Bernfield M. Developmental expression of syndecan, an integral membrane proteoglycan, correlates with cell differentiation. Development 119; 111:213–220.
63. Wisniewski KE, Segan SM, Miezejeski CM, Sersen EA, Rudelli RD. The Fra (X) syndrome: neurological, electrophysiological, and neuropathological abnormalities. Am J Med Genet 1991; 38:476–480.
64. Ethell IM, Yamaguchi Y. Cell surface heparan sulfate proteoglycan syndecan-2 induces the maturation of dendritic spines in rat hippocampal neurons. J Cell Biol 1999; 144:575–586.
65. Yamaguchi Y. Heparan sulfate proteoglycans in the nervous system: their diverse roles in neurogenesis, axon guidance, and synaptogenesis. Sem Cell Dev Biol 2001; 12:99–106.
66. Ethell IM, Hagihara K, Miura Y, Irie F, Yamaguchi Y. Synbindin, a novel syndecan-2-binding protein in neuronal dendritic spines. J Cell Biol 2000; 151:53–67.
67. Lledo P-M, Zhang X, Sudhof TC, Malenka RC Nicoll RA. Postsynaptic membrane fusion and long-term potentiation. Science 1998; 279:399–403.
68. Turner KM, Burgoyne RD, Morgan A. Protein phosphorylation and the regulation of synaptic membrane traffic. Trends Neurosci 1999; 22:459–464.
69. Hsueh YP, Sheng M. Regulated expression and subcellular localization of syndecan heparan sulfate proteoglycans and the syndecan-binding protein CASK/LIN-2 during rat brain development. J Neurosci 1999; 19:7415–7425.
70. Kinnunen A, Kinnunen T, Kaksonen M, Nolo R, Panula P, Rauvala H. N-syndecna and HB-GAM (heparain-binding growth-associated molecule) assoicated with early axonal tracts in the rat brain. Eur J Neurosci 1998; 10:635–648.
71. Kinnunen T, Kaksonen M, Saarinen J, Kalkkinen N, Peng HB, Rauvala H. Cortactin-Src kinase signaling pathway is involved in N-syndecan-dependent neurite outgrowth. J Biol Chem 1998; 273:10702–10708.
72. Swartz DR, Lim S-S, Fassel T, Greaser ML. Mechanisms of myofibril assembly. Proc Recip Meat Conf 1994; 47:141–153.
73. Brandan E, Larraín J. Heparan sulfate proteoglycans during terminal skeletal muscle cell proliferation: possible functions and regulation of their expression. Basic Appl Myol 1998; 8:107–114.

74. Fuentealba L, Carey DJ, Brandan E. Antisense inhibition of syndecan-3 expression during skeletal muscle differentiation accelerates myogenesis through a basic fibroblast growth factor-dependent mechanism. J Biol Chem 1999; 274:37876–37884.
75. Larraín J, Carey DJ, Brandan E. Syndecan-1 expression inhibits myoblast differentiation through a basic fibroblast growth factor-dependent mechanism. J Biol Chem 1998; 273:32288–32296.
76. Mauro A. Satellite cell of skeletal muscle fibers. Biophys Biochem Cytol 1961; 9:493–495.
77. Stockdale FE, Holtzer H. DNA synthesis and myogenesis. Exp Cell Res 1961; 24:508–520.
78. Moss FP, LeBlond CP. Satellite cells as the source of nuclei in muscles of growing rats. Anat Rec 1971; 170:421–462.
79. Schultz E, McCormick KM. Skeletal muscle satellite cells. Rev Physiol Biochem Parmacol 1994; 123:213–257.
80. Casar JC, Cabello-Verrugio C, Olguin H, Aldunate R, Inestrosa NC, Brandan E. Heparan sulfate proteoglycans are increased during skeletal muscle regeneration: requirement of syndecan-3 for successful fiber formation. J Cell Sci 2004; 117:73–84.
81. Mertens G, Van der Schueren B, Van den Berghe H, David G. Heparan sulphate expression in polarized epithelial cells: the apical sorting of glypican (GPI-anchored proteoglycan) is inversely related to its heparan sulphate content. J Cell Biol 1996; 132:487–497.
82. Liu X, McFarland DC, Nestor KE, Velleman SG. Developmental regulated expression of syndecan-1 and glypican in pectoralis major muscle in turekys with different growth rates. Develop Growth Differ 2004; 46:37–51.
83. Litwack ED, Ivins JK, Kumbasar A, Paine-Saunders S, Stipp CS, Lander AD. Expression of the heparan sulfate proteoglycan glypican-1 in the developing rodent. Dev Dyn 1998; 211:72–87.
84. David G, Lories V, Decock B, Marynen P, Cassiman J-J, Van den Berghe H. Molecular cloning of a phospatidylinositol anchored membrane heparan sulfate proteoglycan from human lung fibroblasts. J Cell Biol 1990; 124:149–160.
85. Stipp CS, Litwack ED, Lander AD. Cerebroglycan: an integral membrane heparan sulfate proteoglycan that is unique to the developing nervous system and expressed specifically during neuronal differentiation. J Cell Biol 1994; 124:149–160.
86. Pellegrini M, Pilia G, Pantano S, Lucchini F, Uda M, Fumi M, Cao A, Schlessinger D, Forabosco A. Gpc3 expression correlates with the phenotype of the Simpson-Golabi-Behmel syndrome. Dev Dyn 1998; 213:431–439.
87. Watanbe K, Yamada H, Yamaguchi Y. K-glypican: a novel GPI-anchored heparan sulfate proteoglycan that is highly expressed in developing brain and kidney. J Cell Biol 1995; 130:1207–1218.
88. Saunders S, Paine-Saunders S, Lander AD. Expression of the cell surface proteoglycan glypican-5 is developmentally regulated in kidney, limb, and brain. Dev Biol 1997; 190:78–93.
89. Veugelers M, Vermeesch J, Reekmans G, Steinfeld R, Marynen P, David G. Characterisation of glypican-5 and chromsomal localisation of human GPC5, a new member of the glypican gene family. Genomics 1997; 40:24–30.

90. Veugelers M, De Cat B, Ceulemans H, Bruystens AM, Coomans C, Durr J, Vermeesch Jm Marynen P, David G. Glypican-6, a new member of the glypican family of cell surface heparan sulfate proteoglycans. J Biol Chem 1999; 38:26968–26977.
91. Duenas Gonzalez A, Kaya M, Shi W, Song H, Testa JR, Penn LZ, Filmus J. OCI-5/GPC3, a glypican encoded by a gen that is mutated in the Simpson-Golabi-Behmel overgrowth syndrome, induces apoptosis in a cell line specific manner. J Cell Biol 1998; 141:1407–1414.
92. Pilia G, Huges-Benzie RM, MacKenzie A, Baybayan P, Chen EY, Huber R, Neri G, Cao A, Forabosco A, Schlessiinger D. Mutations in GPC3, a glypican gene, cause the Simpson-Golabi-Behmel overgrowth syndrome. Nat Genet 1996; 12:241–247.
93. Lindsay S, Ireland M, O'Brien O, Clayton-Smith J, Hurst JA, Mann J, Cole T, Sampson J, Slaney S, Schlessinger D, Burn J, Pilia G. Large scale deletions in the GPC3 gene may account for a minority of cases of Simpson-Golabi-Behmel syndrome. J Med Genet 1997; 34:480–483.
94. Xuan JY, Hughes-Benzie RM, MacKenzie AE. A small interstitial deletion in the GPC3 gene causes Simpson-Golabi-Behmel syndrome in a Dutch-Canadian family. J Med Genet 1999; 36:57–58.
95. Veugelers M, Cat BD, Muyldermans SY, Reekmans G, Delande N, Frints S, Legius E, Fryns JP, Schrander-Stumpel C, Weidle B, Magdalena N, David G. Mutational analysis of GPC3/GPC4 glypican gene cluster on Xq26 in patients with Simpson-Golabi-Behmel syndrome: identification of loss-of-function mutations in the GPC3 gene. Hum Mol Genet 2000; 9:1321–1328.
96. Brandan E, Carey DJ, Larraín J, Melo F, Campos A. Synthesis and processing of glypican during differentiation of skeletal muscle cells. Eur J Cell Biol 1996; 71:170–176.
97. Hagihara K, Watanabe K, Chun J, Yamaguchi Y. Glypican-4 is an FGF2-binding heparan sulfate proteoglycan expressed in neural precursor cells. Dev Dyn 2000; 219:353–367.
98. Litwack ED, Ivins JK, Kumbasar A, Paine-Saunders S, Stipp CS, Lander AD. Expression of the heparan sulfate proteoglycan glypican-1 in the developing rodent. Dev Dyn 1998; 211:72–87.
99. Stipp CS, Litwack ED, Lander AD. Cerebroglycan: an integral membrane heparan sulfate proteoglycan that is unique to the developing nervous system and expressed specifically during neuronal differentiation. Cell Biol 1994; 124:149–160.
100. Qian X, Davis AA, Goderie SK, Temple S. FGF2 concentration regulates the generation of neurons and glia from multipotent cortical stem cells. Neuron 1997; 18:81–93.
101. Cheifetz S, Bellon T, Cales C, Vera S, Bernabeu C, Massague J, Letarte M. Endoglin is a component of the transforming growth factor-beta receptor system in human endothelial cells. J Biol Chem 1992; 267:19027–19030.
102. Eickelberg O, Centrella M, Reiss M, Kashgarian M, Wells RG. Betaglycan inhbits TGF-β signaling by preventing type I-type II receptor complex formation. J Biol Chem 2002; 277:823–829.
103. Lopez-Casillas F, Wrana JL, Massague J. Betaglycan presents ligand to the TGF beta signaling receptor. Cell 1993; 73:1435–1444.

104. Velasco-Loyden G, Arribas J, Løpez-Casillas, F. The shedding of betaglycan is regulated by pervanadate and mediated by membrane type matrix metalloproease-1. J Biol Chem 2004; 279:7721–7733.
105. Screaton GR, Bell MV, Jackson DG, Cornelis FB, Gerth U, Bell J. Genomic structure of DNA encoding the lymphocyte homing receptor CD44 reveals at least 12 alternatively spliced exons. Proc Natl Acad Sci USA 1992; 89:12160–12164.
106. Tuhkanen AL, Tammi M, Tammi R. CD44 substituted with heparan sulfate and endo-beta-galactosidase-sensitive oligosaccharides: a major proteoglycan in adult human epidermis. J Invest Dermatol 1997; 109:213–218.
107. Hassell JR, Robey PG, Barrach HJ, Wilczek J, Rennard SI, Martin GR. Isolation of a heparan sulfate-containing proteoglycan from basement membrane. Proc Natl Acad Sci USA 1980; 77:4494–4498.
108. Iozzo RV. Matrix proteoglycyans: from molecular design to cellular function. Annu Rev Biochem 1998; 67:609–652.
109. Olsen BR. Life without perlecan has its problems. J Cell Biol 1999; 147: 909–911.
110. Ledbetter SR, Tyree B, Hassell JR, Horigan EA. Identification of the precursor protein to basement membrane heparan sulfate proteoglycans. J Biol Chem 1985; 260:8106–8113.
111. Ledbetter SR, Fisher LW, Hassell JR. Domain structure of the basement membrane heparan sulfate proteoglycan. Biochemistry 1987; 26:988–995.
112. Hopf M, Gohring W, Kohfeldt E, Yamada Y, Timpl R. Recombinant domain IV of perlecan binds to nidogens, laminin-nidogen complex, fibronectin, fibulin-2 and heparin. Eur J Biochem 1999; 259:917–925.
113. Brown JC, Sasaki T, Gohring W, Yamada Y, Timpl R. The C-terminal domain V of perlecan promotes beta1 integrin-mediated cell adhesion, binds heparin, nidogen and fibulin-2 and can be modified by glycosaminoglycans. Eur J Biochem 1997; 250:39–46.
114. Arikawa-Hirasawa E, Watanbe H, Takami H, Hassell JR, Yamada Y. Perlecan is essential for cartilage and cephalic development. Nat Genet 1999; 23:354–358.
115. Costell M, Gustafsson E, Aszódi A, Mörgelin M, Bloch W, Hunziker E, Addicks K, Timpl R, Fässler R. Perlecan maintains the integrity of cartilage and some basement membranes. J Cell Biol 1999; 147:1109–1122.
116. Bayne EK, Anderson MJ, Fambrough DM. Extracellular matrix organization in developing muscle: correlation with acetylcholine receptor aggregates. J Cell Biol 1984; 99:1486–1501.
117. Hassell J, Yamada Y, Arikawa-Hirasawa E. Role of perlecan in skeletal development and diseases. Glycoconjugate J 2003; 19:263–267.
118. Arikawa-Hirasawa E, Rossi SG, Rotundo RL, Yamada Y. Absence of acetylcholinesterase at the neuromuscular junctions of perlecan-null mice. Nat Neurosci 2002; 5:119–123.
119. Campagna JA, Rüegg MA, and Bixby JL. Agrin is a differentiation-inducing 'stop signal' for motoneurons in vitro. Neuron 1995; 15:1365–1374.
120. Chang D, Woo JS, Campanelli J, Scheller RH, Ignatius MJ. Agrin inhibits neurite outgrowth but promotes attachment of embryonic motor and sensory neurons. Dev Biol 1997; 181:21–35.

121. Halfter W, Schurer B, Yip J, Yip L, Tsen G, Lee JA, Cole GJ. Distribution and substrate properties of agrin, a heparan sulfate proteoglycan of developing axonal pathways. J Comp Neurol 1997; 383:1–17.
122. Mantych KB, Ferreira A. Agrin differentially regulates the rates of axonal and dendritic elongation in cultured hippocampal neurons. J Neurosci 2001; 21:6802–6809.
123. Bixby JL, Baerwald-De La Torre K, Wang C, Rathjen FG, Rüegg MA. A neuronal inhibitory domain in the N-terminal half of agrin. J Neurobiol 2002; 50:164–179.
124. Baerwald-De La Torre K, Winzen U, Halfter W, Bixby JL. Glycosaminoglycan-dependent and -independent inhibition of neurite outgrowth by agrin. J Neurochem 2004; 90:50–61.
125. Dong S, Cole GJ, Halfter W. Expression of collagen XVIII and localization of its glycosaminoglycan attachment sites. J Biol Chem 2003; 278: 1700–1707.
126. O'Reilly MS, Boehm T, Shing Y, Fukai N, Vasios G, Lane WS, Flynn E, Birkhead JR, Olsen BR, Folkman J. Endostatin: an endogenous inhibitor of angiogenesis and tumor growth. Cell 1997; 88:277–285.
127. Sasaki T, Fukai N, Mann K, Goering W, Olsen BA, Timpl R. Structure, function and tissue forms of the C-terminal globular domain of collagen XVIII containing the angiogenesis inhibitor endostatin. EMBO J 1998; 17:4249–4256.
128. Fukai N, Eklund L, Marneros AG, Oh S, Keene DR, Tamarkin L, Niemela M, Lives M, Li E, Philajaniemi M, Olsen B. Lack of collagen XVIII/endostatin results in eye abnormalities. EMBO J 2002; 21:1535–1544.
129. Gallatin WM, Weissman IL, Butcher EC. A cell-surface molecule involved in organ-specific homing of lymphocytes. Nature 1983; 304:30–34.
130. Ley K, Gaehtgens P, Fennie C, Singer MS, Lasky LA, Rosen SD. Lectin-like cell adhesion molecule 1 mediates leukocyte rolling in mesenteric venules in vivo. Blood 1991; 77:2553–2555.
131. von Andrian UH, Chambers JD, McEvoy LM, Bargatz RF, Arfors KE, Butcher EC. Two-step model of leukocyte-endothelial cell interaction in inflammation: distinct roles for LECAM-1 and the leukocyte beta 2 integrins in vivo. Proc Natl Acad Sci USA 1991; 88:7538–7542.
132. Li Y-F, Kawashima H, Watanbe N, Miyasaka M. Identification and characterization of ligands for L-selectin in the kidney. II. Expression of chondroitin sulfate and heparan sulfate proteoglycans reactive with L-selectin. FEBS Lett 1999; 444:201–205.
133. Kawashima H, Watanbe N, Hirose M, Sun X, Atarashi K, Kimura T, Shikata K, Matsuda M, Ogawa D, Heljasvaara R, Rehn M, Pihlajaniemi T, Miyasaka M. Collagen XVIII, a basement membrane heparan sulfate proteoglycan, interacts with L-selectin and monocyte chemoattractant protein-1. J Biol Chem 2003; 278:13069–13076.
134. Selkoe DJ. The molecular pathology of Alzheimer's disease. Neuron 1991; 6:487–498.
135. Glenner GG, Wong CW. Alzheimer's disease: initial report of the purification and characterization of a novel cerbrovascular amyloid protein. Biochem Biophys Res Commun 1984; 120:885–890.

136. Iqbal K, Grundke-Iqbal I, Wisniewski HM. Neuronal cytoskeleton in aging and dementia. Prog Brain Res 1986; 70:279–288.
137. Lee VM, Balin BJ, Otvos L, Trojanowski JQ. A68: a major subunit of paired helical filaments and derivatized forms of normal Tau. Science 1991; 251: 675–678.
138. Snow AD, Mar H, Nochlin D, Sekiguchi RT, Kimata K, Koike Y, Wight TN. Early accumulation of heparan sulfate in neurons and in the beta-amyloid protein–containing lesions of Alzheimer's disease and Down's syndrome. Am J Pathol 1990; 137:1253–1270.
139. Su JH, Cummings BJ, Cotman CW. Localization of heparan sulfate glycosaminoglycan and proteoglycan core protein in aged brain and Alzheimer's disease. Neuroscience 1992; 51:801–813.
140. Snow AD, Sekiguchi R, Nochlin D, Fraser P, Kimata K, Mizutani A, Schreier AM, Morgan DG. An important role of heparan sulfate proteoglycan (Perlecan) in a model system for the deposition and persistence of fibrillar A beta-amyloid in rat brain. Neuron 1994; 12:219–234.
141. Castillo GM, Lukito W, Wight TN, Snow AD. The sulfate moieties of glycosaminoglycans are critical for the enhnacement of β-amyloid protein fibril formation. J Neurochem 1999; 72:1681–1687.
142. Verbeek MM, Otte-Holler I, van den Born J, van den Heuvel LP, David G, Wesseling P, de Waal RM. Agrin is a major heparan sulfate proteoglycan accumulating in Alzheimer's disease brain. Am J Pathol 1999; 155: 2115–2125.
143. Dhodapkar MV, Kelly T, Theus A, Athota AB, Barlogie B, Sanderson RD. Elevated levels of shed syndecan-1 correlate with tumour mass and decreased matrix metalloproteinase-9 activity in the serum of patients with mutiple myeloma. Br J Haematol 1997; 99:368–371.
144. Seidel C, Sundan A, Hjorth M, Turesson I, Dahl IM, Abildgaard N, Waage A, Borset M. Serum syndecan-1: a new independent prognostic marker in multiple myeloma. Blood 2000; 95:388–392.
145. Sanderson RD, Yang Y, Suva LJ, Kelly T. Heparan sulfate proteoglycans and heparanase-partners in osteolytic tumor growth and metastasis. Matrix Biol 2004; 23:341–352.
146. Mundhenke C, Meyer K, Drew S, Friedl A. Heparan sulfate proteoglycans as regulators of fibroblast growth factor-2 receptor binding in breast carcinomas. Am J Pathol 2002; 160:185–194.
147. Barbareschi M, Maisonneuve P, Aldovini D, Cangi MG, Pecciarini L, Angelo Mauri F, Veronese S, Caffo O, Lucenti A, Palma PD, Galligioni E, Doglioni C. High syndecan-1 expression in breast carcinoma is related to an aggressive phenotype and to poorer prognosis. Cancer 2003; 98:474–483.
148. Liu D, Shriver Z, Venkataraman G, El Shabrawi Y, Sasisekharan R. Tumor cell surface heparan sulfate as cryptic promoters or inhibitors of tumor growth and metastasis. Proc Natl Acad Sci USA 2002; 99:568–573.

Chemistry and Biology of Heparin and Heparan Sulfate
H.G. Garg, R.J. Linhardt and C.A. Hales (Editors)

Chapter 3

Methods for Structural Analysis of Heparin and Heparan Sulfate

ISHAN CAPILA, NUR SIBEL GUNAY, ZACHARY SHRIVER and GANESH VENKATARAMAN

Momenta Pharmaceuticals, Inc., 675 West Kendall Street, Cambridge, MA, USA

I. Introduction

Heparin (HP) and heparan sulfate (HS) are complex, linear, acidic polysaccharides belonging to the glycosaminoglycan (GAG) family. In biological systems, they can be found on the cell surface, in the extracellular matrix, and intracellular granules. They can be either attached to a protein core (HS) or in a free form (HP). Heparin is a well-known anticoagulant drug and is extensively used in medical practice. It is widely used during heart surgery and in the prevention of postoperative thrombosis. The molecular basis for the anticoagulant function of heparin was elucidated in the early 1980s when a distinct pentasaccharide sequence within heparin chains was identified as being crucial for binding and activating antithrombin III, leading to accelerated inhibition of the coagulation cascade (1,2). Over the last 20 years, heparin and heparan sulfate have been shown to interact with a large number of important proteins thereby regulating a range of biological activities including cell proliferation, inflammation, angiogenesis, viral infectivity and development (3,4). Due to the structural diversity exhibited by these molecules, it is believed that possibly unique (in some cases) or most likely an ensemble of structural motifs might be responsible for different interactions. Therefore, it has become increasingly important to interpret the structural information represented in these complex molecules in order to enable a better understanding of their structure–function relationship. In this chapter we will discuss some of the established techniques, as well as emerging approaches, that are being used to probe the structure of heparin and heparan sulfate.

II. Structure of Heparin and Heparan Sulfate

Heparin and heparan sulfate are complex mixtures containing linear chains of repeating disaccharide units consisting of a glucosamine and uronic acid. The initial disaccharide unit that constitutes the growing chain during biosynthesis is a D-glucuronic acid β-1,4 linked to a D-*N*-acetylglucosamine. These units are linked to each other via an α-1,4 linkage. The subsequent biosynthetic modifications proceed in a sequential manner, beginning with the *N*-deacetylation and *N*-sulfonation of glucosamine residues within the chains. This is followed by epimerization of the glucuronic acid to iduronic acid and *O*-sulfonation at either the C-2 of the uronic acid or the C-6 of the glucosamine. The final modification step in this pathway is the *O*-sulfonation at the C-3 of the glucosamine. Each of these biosynthetic reactions is dependent on the previous modification to some extent, as products of one step can often act as substrates for the subsequent one. Another aspect of this pathway that has an important bearing on the final outcome is that each of these steps does not proceed to completion. Thus, the resulting chain can be differentially modified in various regions and this variability can extend between different chains as well. This accounts for the structural heterogeneity observed in these molecules. The structure of the predominant disaccharide sequence in heparin and heparan sulfate is shown in Fig. 1. The average heparin disaccharide contains ~2.7 sulfo groups whereas heparan sulfate contains ~1 sulfo group per disaccharide. Also, while L-iduronic acid predominates in heparin, the D-glucuronic acid epimer

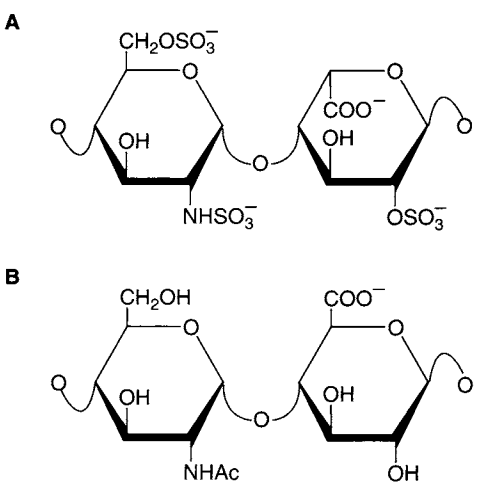

Figure 1 The major repeating disaccharide unit in (A) heparin and (B) heparan sulfate. Structural heterogeneity arises from the variable presence of either acetyl or sulfo groups at the *N*-position, sulfation at the 2-*O*-position on the uronic acid or 6-*O*- and 3-*O*-positions on the glucosamine, and epimerization at the C-5 of the uronic acid.

represents the majority of the uronic acid present in heparan sulfate. As such, heparin is often referred to as the more completely modified version of heparan sulfate and also possesses the highest negative charge density of any known biological macromolecule. While heparan sulfate contains all of the structural variations found in heparin, the frequency of occurrence of the minor sequence variations is greater than in heparin. Therefore, the extent of structural heterogeneity observed in heparan sulfate is usually greater. Both heparin and heparan sulfate chains are polydisperse, with a broad molecular weight distribution. Heparan sulfate chains are generally longer than heparin chains, and have an average molecular weight of ~30 kDa as compared to ~15 kDa for heparin. This structural variability at multiple levels makes heparin and heparan sulfate very challenging molecules to characterize.

III. Separation-Based Analysis of Heparin and Heparan Sulfate

While initial methods of analysis relied on chemical processes for specifically degrading these sugars, the isolation and characterization of the heparin lyase enzymes (5,6) expanded the analytical tool kit with which these molecules can be studied. These enzymes, based on their substrate specificity, enable breakdown of HP and HS into smaller units that can be analyzed by known separation techniques like high performance liquid chromatography (HPLC). Powerful separation technology is a key element for the analysis of these sugars as they are complex mixtures with many structurally variable components. The ability to detect these components effectively after separation is also another important issue that affects the ability to analyze them. Different separation approaches based upon HPLC, gel electrophoresis and capillary electrophoresis have been developed for the analysis of HP and HS. Various different modes of detection including ultraviolet (UV) absorbance and fluorescence have also been explored. These approaches are highlighted in this section.

A. High Performance Liquid Chromatography Analysis

A broad range of high-performance liquid chromatography (HPLC) techniques are available for the analysis of GAGs. The utility of HPLC for analysis of HP and HS includes identifying and purifying different types of GAGs, measuring the molecular weight, establishing their disaccharide building blocks and providing a complimentary tool for sequencing. A majority of the approaches used for heparin and heparan sulfate analysis are based upon either anion-exchange or reversed phase ion-pairing chromatography.

Among silica-based anion-exchangers there are two main groups; strong base anion-exchangers carrying quaternary ammonium groups and weak base anion-exchangers, carrying tertiary amine groups. Linhardt *et al.* developed quaternary amine based strong anion-exchange (SAX) technology for purification, oligosaccharide mapping, and characterization of heparin and heparan sulfate-derived

oligosaccharides from both commercial and biological sources (7,8). This technique involves separation of oligosaccharide species by their charge using salt gradient elution from 200 mM to 1–2 M sodium chloride. Karamanos *et al.* utilized reversed phase ion-pairing HPLC for the disaccharide composition analysis of dermatan sulfate (DS), chondroitin sulfate (CS), heparin (HP) and heparan sulfate (HS). In this procedure a binary acetonitrile gradient system with tetrabutylammonium as an ion-pairing reagent was used (9,10). More recently Chai *et al.* reported the use of a porous graphitized carbon (PGC) HPLC column run with an acetonitrile gradient for the analysis of oligosaccharides which are derived from partially *N*-deacetylated *Escherichia coli* K5 polysaccharide after heparin lyase III degradation (11). For most of these analyses, the oligosaccharides being analyzed are generated by action of heparin lyases that cleave the chain via a β-elimination mechanism. This generates an unsaturated uronic acid ($\Delta^{4,5}$-hexuronic acid) at the nonreducing end of each oligosaccharide, thereby enabling UV detection at 232 nm. In cases where the cleavage mechanism does not allow for the incorporation or generation of an easily detectable tag, other derivatization methods have been explored. Derivatization of glycosaminoglycans also represents a way to increase the sensitivity of the analysis, especially when dealing with small amounts of sample isolated from biological sources. Kinoshita and Sugahara developed a precolumn derivatization method for disaccharide composition analysis of CS, HP and HS and also for sequencing of CS-derived hexasaccharides (12). Disaccharides and oligosaccharides were derivatized at their reducing end with a fluorophore (2-aminobenzamide) and separation was conducted using an amine-bound silica column with a linear gradient of sodium monophosphate (NaH_2PO_4). Sensitivity of the disaccharide composition analysis was at the picomole level. Another study reported the analysis of GAG-derived disaccharides after their derivatization with dansylhydrazine (13). The separation was performed on μ-Bondapack NH_2 (aminopropylmethsilyl bonded amorphous silica) column with isocratic elution using acetonitrile/100 mM acetate buffer (90:10) pH 5.6 and monitored by fluorescence detection.

Sample preparation procedures for precolumn HPLC are usually tedious and time-consuming because removal of excess labeling reagent and interfering compounds is not straightforward. To address these issues, Toida and coworkers developed a fluorimetric postcolumn derivatization method for the disaccharide composition analysis of CS/DS and HP/HS from commercial and biological sources (14,15). The same research group also introduced a new, rapid reversed phase ion-pairing (RPIP)-HPLC method with postcolumn derivatization for the disaccharide composition analysis (16). The HPLC system includes: (1) a gradient pump; (2) a chromatointegrator; (3) fluorescence spectrophotometer; (4) a double plunger pump for the reaction solution; (5) dry reaction bath; (6) sample injector; and (7) a column heater. The eluents for the gradient include water, 200 mM sodium chloride, 10 mM tetra-*n*-butylammonium hydrogen sulfate, and 50% acetonitrile. To the effluent are added aqueous (0.5–1%) 2-cyanoacetamide solution and 0.25–1 M sodium hydroxide using a double plunger. The mixture passes through a reaction coil set in a dry temperature-controlled bath at 125°C, followed by a cooling coil. The effluent is monitored fluorimetrically. This methodology has broad

applicability and has been utilized for analyzing heparan sulfate from human liver tissue as well as capsular polysaccharides like K4 (17,18).

The recent availability of recombinant exolytic lysosomal enzymes that act on GAGs has allowed their exploitation for exosequence analysis of HP/HS derived oligosaccharides (19). In this method, a combined chemical and enzymatic scission protocol has been used for sequencing. Briefly, oligosaccharides were radiolabeled at their reducing end with ^{3}H (tritium), followed by partial deaminative cleavage with nitrous acid at low pH to yield ^{3}H-labeled intermediate fragments. The nitrous acid treatment not only reflects the position of *N*-sulfated glucosamine (GlcNS) but also makes the internal sequence amenable to the action of lysosomal exoenzymes. The nitrous acid fragments were incubated with enzymes such as iduronate 2-*O*-sulfatase (I2Sase); iduronidase (IdoAase); glucosamine 6-*O*-sulfatase (6Sase); α-*N*-acetylglucosaminidase singly or in combination, and digestion products were analyzed by SAX-HPLC. Sequence determination was achieved by enabling the positioning of GlcNS residues and a clear observation of shifts in elution positions of the fragments on SAX-HPLC after exoenzyme treatment. The regular disaccharide composition analysis by SAX-HPLC was used to confirm the structures of sequenced oligosaccharides. This technology has been applied for the sequencing of major oligosaccharides released from $^{35}SO_4$ metabolically radiolabeled mastocytoma heparin by partial nitrous acid degradation (20).

B. Gel Electrophoresis

Polyacrylamide gel electrophoresis (PAGE) has been widely used for the analysis of glycosaminoglycans and glycosaminoglycan-derived oligosaccharides prepared by enzymatic and chemical methods. Cowman *et al.* first described the separation of GAGs and their oligosaccharides in a 10% polyacrylamide gel matrix visualized by alcian blue staining (21). Rice *et al.* introduced the use of a discontinuous gradient PAGE system for high-resolution analysis of HP/HS oligosaccharides (Fig. 2) (22). Edens *et al.* demonstrated that PAGE analysis could be a useful method for determining the molecular weight (number-averaged M_N, weight-averaged M_W and polydispersity, P) of heparin and low molecular weight heparins (23). Gel electrophoresis based separation has also been used for development of a sequencing approach for heparin and heparan sulfate (24,25). In this methodology, the reducing end of the oligosaccharide was labeled with a sensitive fluorophore. This was followed by partial chemical degradation with nitrous acid at low pH and digestion of the fragments generated with a combination of exosulfatases and exoglycosidases. This method is in principle similar to the sequencing strategy described in the preceding section for HPLC separation.

Volpi *et al.* developed the application of agarose gel electrophoresis, coupled with a different staining procedure, for the analysis of GAGs. Using this procedure, nonlabeled GAGs could be resolved by agarose gel electrophoresis and visualized using staining with toluidine blue followed by Stains-All procedure (26). This method is applicable for analysis of all types of GAGs, nonsulfated polyanions, as well as identification and quantification of the contaminants of other polysaccharides

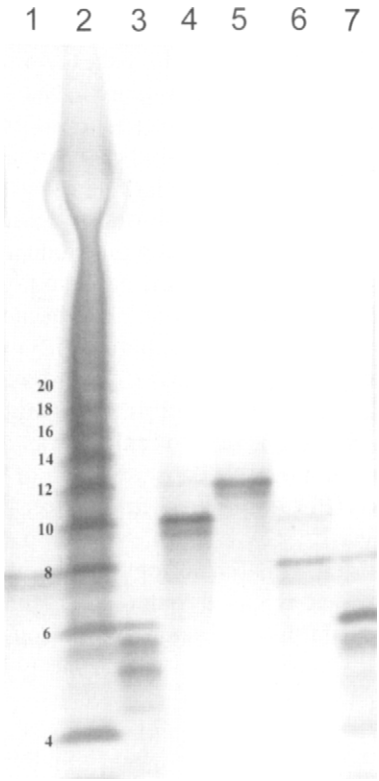

Figure 2 Gradient PAGE analysis of heparin-derived oligosaccharide mixtures. Lane 1: fully sulfated octasaccharide standard, lane 2: oligosaccharide mixture from bovine lung heparin with fully sulfated oligosaccharides from dp 4 to 20 labeled, lane 3: porcine intestinal heparin hexasaccharide (dp 6) mixture, lanes 4–7: bovine lung heparin size fractionated mixtures; dp 10, 12, 8 and 6 respectively. Reprinted from Gunay, NS, Linhardt RJ. J Chromatogr A 2003; 1014:225–233, with permission from publisher.

within GAG preparations. The same group also applied this method for blotting and immobilization of several nonsulfated and sulfated complex polysaccharides on nitrocellulose membranes (27). In this method, after the separation of polysaccharides on agarose gel, the species were transferred to nitrocellulose membranes derivatized with cationic detergent cetylpyridinium chloride. After reversible staining, single species were extracted from membrane for further characterization. It was reported that GAG recovery ranged between 70 and 100%. This technique was subsequently also adapted for the specific immunodetection of GAGs by antibodies (28).

C. Capillary Electrophoresis

Capillary electrophoresis (HPCE or CE) is a high-resolution (10^5–10^6 theoretical plates/m) separation technique that combines the characteristics of traditional PAGE and HPLC. CE seems to have an almost universal applicability and is used for peptides and proteins, oligonucleotides and nucleic acids, carbohydrates, different types of noncovalent complexes, and even small molecules (29–32). The wide applicability of CE is primarily because of the advantages of this technique, which include: (1) extremely high separation efficiency; (2) online detection; (3) short analysis time CE; (4) very low consumption of samples and buffers; and (5) automated and reproducible analysis.

Capillary electrophoresis was first applied to acidic oligosaccharides for the total compositional analysis of chondroitin sulfate-, dermatan sulfate-, and hyaluronan-derived disaccharides (33–35). The analysis of heparin and heparan sulfate-derived disaccharides has been developed under reversed polarity, using low pH buffer systems (36). All known 12 unsaturated disaccharides derived from heparin and heparan sulfate can be separated in a single run of 15 min with detection at 232 nm in a reversed polarity mode (Fig. 3) (37). Pervin *et al.* compared the CE resolution of 13 heparin-derived oligosaccharides of sizes ranging from disaccharide to tetradecasaccharide under either normal or reversed polarity (38). It was observed that oligosaccharides are less well resolved under acidic conditions using reversed polarity than normal polarity mode at alkaline conditions. The resolution of reversed-polarity separation decreases with increasing oligosaccharide size. It has also been reported that addition of electrolyte additives to the separation buffer enhances the resolution. Heparan sulfate-derived disaccharides were efficiently separated with alkaline borate containing triethylamine as an electrolyte additive under normal polarity mode (39). This approach was also successfully applied on the analysis of mixtures containing heparin and dermatan sulfate disaccharides.

Sensitivity and resolution of separation of carbohydrates can be improved by derivatization of these molecules. The most common method for the derivatization is reductive amination. The reductive amination reactions take place between the reducing end of the sugar and an amino group on the labeling reagent using sodium cyanoborohydride as a reducing agent. The most commonly used fluorophores include: 2-aminopyridine (2-AP) (40); 2-aminoacridone (AMAC) (41); 7-amino-1, 3-naphthalene disulfonic acid (42); p-aminobenzoic acid (43); 8-aminopyrene-1, 3, 6-trisulfonate (APTS) (44). Fluorescent labeling of saturated and unsaturated saccharides with 2-aminoacridone (AA) enabled the separation of chondroitin sulfate- and heparan sulfate-derived disaccharides, and oligosaccharides and subsequent detection using a laser-induced fluorescence (LIF) detector (41). Derivatization of all chondroitin and dermatan sulfate-derived unsaturated disaccharides with AA, followed by subsequent analysis under reversed polarity mode and detection using a LIF detector enhanced the sensitivity by approximately 100-fold when compared to UV detection at 232 nm (45).

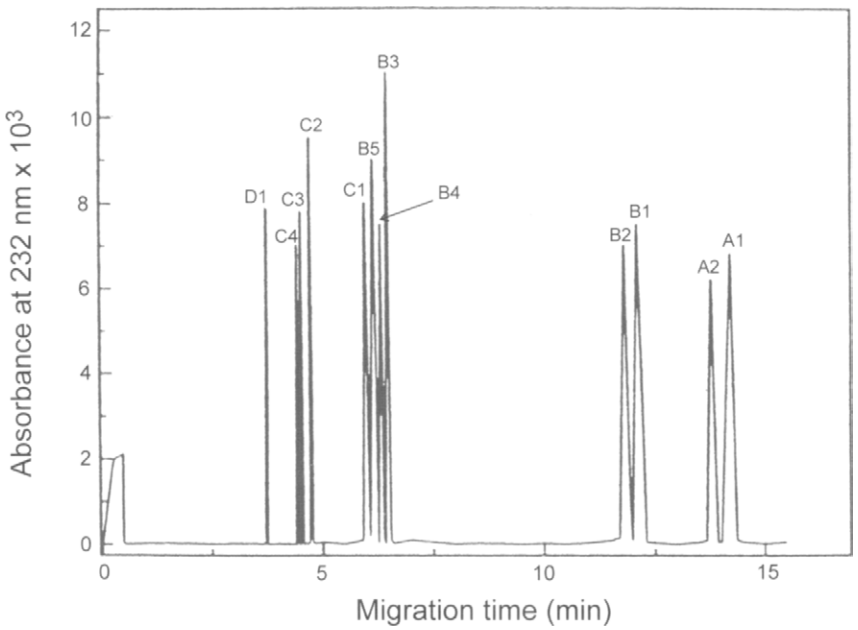

Figure 3 Electropherogram showing resolution of 12 heparin- and heparan sulfate-derived disaccharides. A1, A2, nonsulfated disaccharides; B1–B5, monosulfated disaccharides; C1–C4, disulfated disaccharides; and D1, trisulfated disaccharide. Adapted from reference (37), with permission from the publisher.

IV. Mass Spectrometric Analysis of Heparin and Heparan Sulfate

Perhaps no technique holds more promise for the structural determination of glycosaminoglycan oligosaccharides and glycosaminoglycan polysaccharides than mass spectrometry (MS) (46). The principle of all forms of MS is the same: compounds are discriminated from one another by separating molecular ions according to their mass-to-charge (m/z) ratio, allowing the determination of molecular mass provided their charge can be ascertained. To generate molecular ions, the analyte molecule is placed into an ionization source that induces the production of charged molecules. In addition, through high-energy collisions, molecular ions can be cleaved in highly specific ways to generate important information regarding saccharide structure.

Early efforts towards the mass spectrometric analysis of heparin species focused on the use of fast atom bombardment (FAB) as an ionization technique. While successful in the analysis and structural assignment of pure heparin fragments having a low degree of polymerization, the spectra resulting from FAB analysis are often complicated and confounding when considering analysis of a mixture. In lieu of FAB, two orthogonal strategies have been developed, and extensively used, for the analysis of heparin-like glycosaminoglycans: matrix-assisted laser desorption ionization

(MALDI) and electrospray ionization (ESI). Despite its current importance in HP and HS structural analysis, only recently have there been significant advances in the development of MS as an analytical tool for structural characterization of these complex polysaccharides. Whereas historically, MS procedures for biological samples have largely been investigated and optimized using peptides and proteins, recent efforts have been aimed at identifying experimental conditions amenable to the analysis of acidic GAGs. Such an endeavor has proven critical since early on it was discovered that application of traditional mass spectrometric approaches to the analysis of GAG structure were generally ineffective. GAGs are difficult to detect as molecular ions due to differential chelation of positively charged metal ions (such as sodium) and because they possess the tendency to fragment extensively due to the loss of sulfate prior to detection. A number of techniques have been developed to analyze GAGs via MS, including both ESI and MALDI techniques, which circumvent these shortcomings, thereby enabling the structural characterization of GAG oligosaccharides.

A. Electrospray Ionization Mass Spectrometry

In the past five years, a number of methodologies have been reported detailing the analysis of GAG oligosaccharides via ESI. Analysis of nonsulfated GAG oligosaccharides, such as those from hyaluronan, has proven to be much easier than the analysis of sulfated GAG oligosaccharides, such as chondroitin/dermatan sulfate and heparan sulfate fragments (47). For the analysis of heparin fragments, several distinct methodologies have been developed, including replacement of chelated monovalent and divalent ions, such as sodium or calcium, with ammonium ions or polycationic molecules, which serve to simplify the resulting mass spectrum (48,49). These techniques have been demonstrated to readily detect GAG oligosaccharides up to decasaccharide in length. In addition, nano-electrospray technologies have enabled the facile analysis of GAG samples to concentrations as low as 50 nM (50). Also, by placing a desalting system in-line, recent strategies have demonstrated the ability to determine masses for heparan fragments of up to octadecasaccharides. These techniques are especially exciting given the fact that they can be coupled to either HPLC (51,52) or CE (53) enabling in-line, high throughput separation and characterization of GAGs (see below for more discussion). Recent efforts have extended ESI to the analysis of complex mixtures, drawing a parallel to MS sequencing efforts for peptides isolated from unknown proteins.

Newly developed methodologies using selective metal chelation, specifically of divalent group IIa or transition metals, promise to enable MS^n analysis of short GAG oligosaccharides. In this case, it has been found that specific chelation stabilizes sulfates, preventing nonspecific cleavage and allowing for selective glycosidic bond cleavage. Accordingly, predictable fragmentation patterns can then be readily generated, yielding structural information for GAG oligosaccharides of unknown sequence (Fig. 4A). As such, these techniques raise the promise of *de novo* sequencing of GAG oligosaccharides completely within the mass spectrometer, similar to currently available techniques for peptides. Systematic rules for

the analysis of some GAG structures of disaccharide in length have been developed using an ion trap instrument and standards (54,55).

B. In-Line Techniques

Two major LC techniques have been coupled to ESI MS to enable in-line separation and quantification prior to MS analysis (Fig. 4). Gel permeation chromatography using MS compatible buffers, such as the volatile salts ammonium bicarbonate or

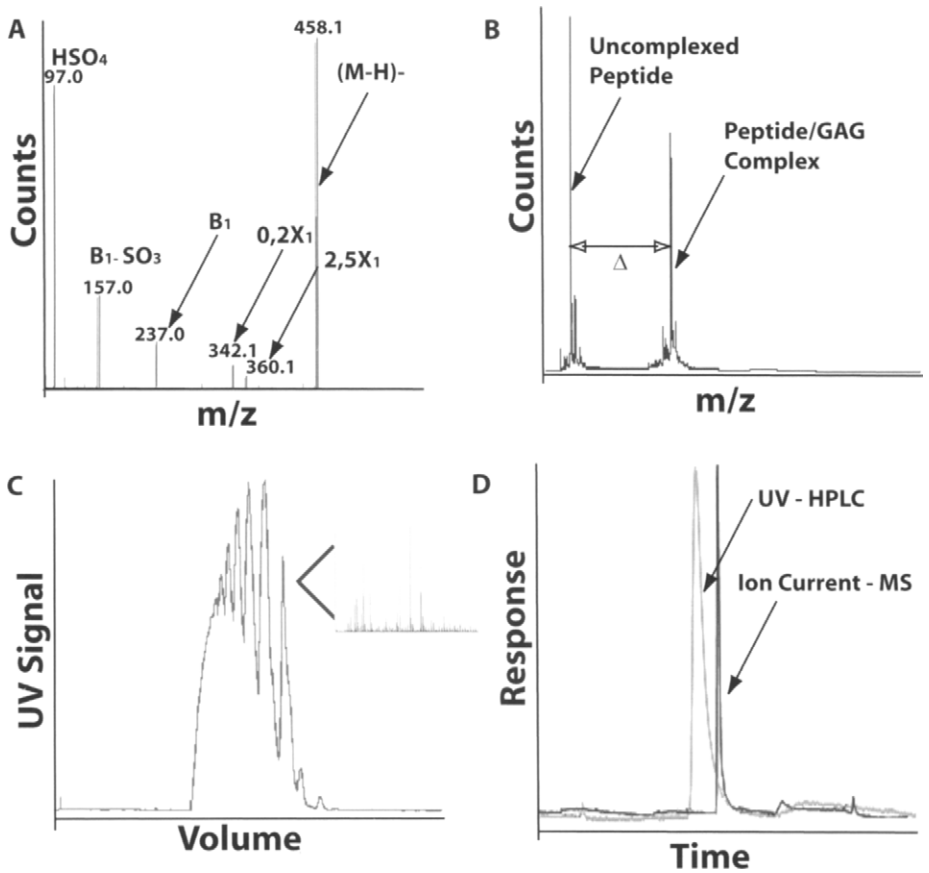

Figure 4 Different mass spectrometry techniques for the analysis of glycosaminoglycans. (A) ESI-MS/MS fragmentation pattern that enables identification of a disaccharide unit from heparin. (B) MALDI-TOF analysis of an oligosaccharide in a complex with a basic peptide. (C) GPC-MS of a low molecular weight heparin mixture. The UV trace shows the separation of the size-fractionated components in the mixture. The inset demonstrates the mass profile obtained from the in-line MS for a particular size fraction. (D) Capillary HPLC-MS of a disaccharide unit from heparin showing both the UV and ion-current peaks. The ion-current peak gives us the mass of the saccharide species contributing to the UV signal.

ammonium formate, has been used to separate heparin fragments on the basis of size, and these size separated mixtures have been analyzed by mass spectrometry. Such an approach has been used for the analysis of the low molecular weight heparin, tinzaparin (56). In addition to GPC, reversed phase ion-pairing HPLC has been used to separate small saccharide fragments prior to analysis. In this case, cationic surfactants chelate GAG oligosaccharides, masking their charge and adding significant hydrophobic character to the noncovalent complex, enabling the retention of GAG oligosaccharides on traditional reversed phase matrices which are then eluted using a gradient of organic solvent (i.e., acetonitrile or methanol). The key to successful in-line analysis after reverse phase is the use of volatile ion-pairing reagents, such as dibutylamine, that enable facile on-column separation, but enable identification of the molecular ion in the mass spectrometer.

This approach was first successfully used for analyzing heparosan oligosaccharides using a C_{18} column and methanol gradient in 5 mM dibutylammonium acetate. HS precursor oligosaccharides up to tetracontasaccharide (40-mer) were separated and detected by LC-MS (57). This methodology was also useful in characterizing the biologically important AT III binding pentasaccharide and its precursors. Subsequently, this methodology was also adapted for the separation and analysis of the higher sulfated heparin-derived oligosaccharides (58,59). In this separation system, an acetonitrile gradient from 20 to 65% with 15 mM tributylamine and 50 mM ammonium acetate were used (Fig. 5). It was reported that molecular ions could be assigned for oligosaccharides as large as tetradecasaccharide (14-mer) and mass detection was demonstrated up to 30-mer (58).

In-line CE-mass spectrometry (MS) technology for analysis of acidic carbohydrates has also recently been investigated. Duteil *et al.* (53) explored the direct coupling between CE and ESI-MS using both normal and reversed polarity modes. In their application on the analysis of enzymatically depolymerized porcine intestinal mucosa heparin, under positive polarity CE with negative MS ionization, composition of eight heparin-derived disaccharides and two heparin-derived tetrasaccharides could be established. Ruiz-Calero *et al.* also developed a CE method with reversed polarity mode for the analysis of heparin-derived disaccharides (60). The same research group in subsequent studies introduced a sheath-flow CE-ESI MS and MS/MS application for the disaccharide composition analysis of heparin (61). The CE-MS experiments were carried out in reversed polarity and negative ion mode ESI-MS detection.

C. Matrix Assisted Laser Desorption and Ionization Mass Spectrometry

Matrix assisted laser desorption and ionization mass spectrometry has been found to be an extremely flexible technology for the analysis of GAGs with the necessary sensitivity to analyze cell surface samples. Methodologies have been developed for the analysis of both intact proteoglycans, isolated from the cell surface, as well as GAG chains cleaved from them (62). In terms of detection of intact proteoglycans, matrices and instrument settings that were developed initially for the analysis of large proteins (>100 kDa) have enabled the rough analysis of proteoglycans, such

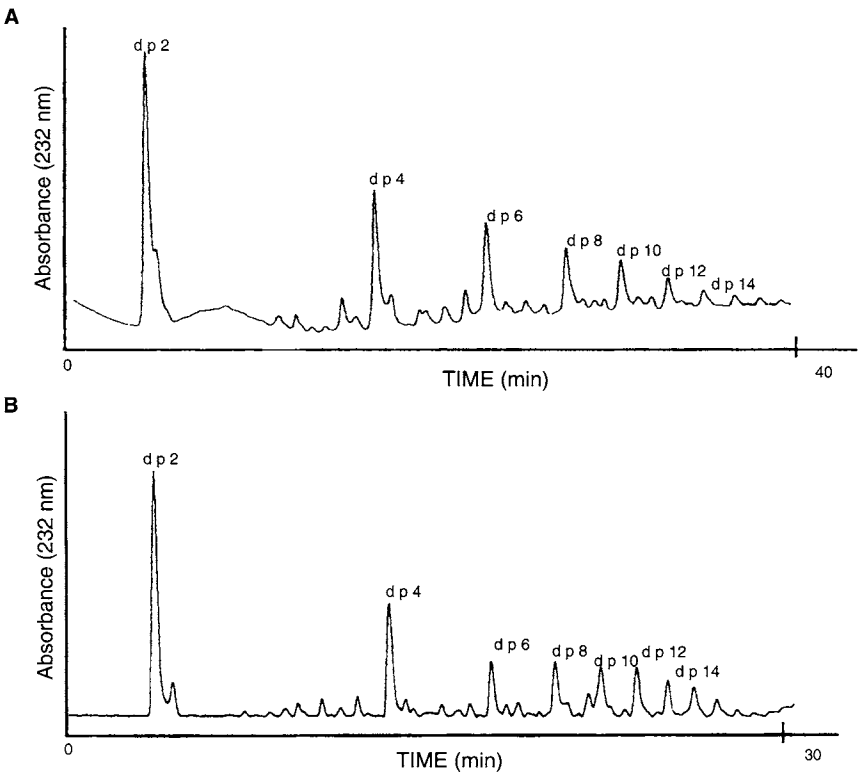

Figure 5 The reversed phase ion-pairing (RPIP) HPLC chromatogram showing separation of heparin-derived oligosaccharides using tributylammonium acetate (TrBA) as a volatile ion-pairing reagent. (A) An elution gradient of 0.2–2 M NaCl in 120 min was used keeping the percentage of acetonitrile (25%) and tributylammonium acetate concentration (15 mM) fixed at pH 7.0. (B) An elution gradient of 20–65% acetonitrile in 120 min was used while keeping the concentration of ammonium acetate (50 mM) and tributylammonium acetate (15 mM) fixed at pH 7.0. The replacement of sodium chloride with ammonium acetate in conjunction with the acetonitrile gradient makes this separation methodology amenable to in-line ESI-MS detection. Reproduced from reference (59) with permission from the publisher.

as syndecan, decorin and biglycan (62). However, due to the polydispersity of proteoglycans, the resolution in these cases is not sufficient to define the fine structure of proteoglycans. Traditional analysis of isolated glycans by MALDI primarily involves the use of 2,5-dihydroxybenzoic acid (46,47). In this case, matrix conditions and instrument parameters have been optimized for the analysis of neutral and slightly anionic glycans. It has been found that such analysis is readily extended to the analysis of oligosaccharides derived from unsulfated hyaluronic acid. In these studies, some differential chelation with metal ions is observed,

limiting to a certain extent, the sensitivity of this methodology. However, attempts to analyze other sulfated GAGs, including chondroitin/dermatan oligosaccharides, using DHB matrix have succeeded only in profiling the disaccharide composition of oligosaccharides (63).

Using MALDI MS, a highly reproducible, sensitive methodology has been developed for the analysis of sulfated HSGAG oligosaccharides that complements traditional MS approaches. This approach takes advantage of the fact that MALDI time-of-flight machines are optimized for the detection of peptides in the molecular mass range of 2000–10,000. In this case, anionic, sulfated GAG oligosaccharides are complexed with a basic peptide (of the form $(RG)_n$) and detected in the MS as 1:1 complexes (64,65). The uncomplexed peptide serves as an internal standard; the mass of the GAG oligosaccharide is derived by subtracting the signal of the uncomplexed peptide from the signal for the 1:1 complex (Fig. 4B). This technique has a number of distinct advantages that have made it one of the most popular methodologies available to structurally characterize GAGs. First, the technique results in a simple spectrum, typically involving only the molecular ion of the uncomplexed peptide as well as the ion arising from a 1:1 peptide:saccharide complex. As such, the spectrum is unfettered from metal adducts, allowing for a sensitivity of down to 50 fmol. In addition, the uncomplexed peptide acts as an internal calibration point, enabling rapid and accurate mass assignment of oligosaccharides with an unknown composition. Finally, the assay is widely applicable and has been used to assay the binding of GAGs to proteins, including gaining an understanding of stoichiometry and specificity (66,67). Importantly, however, unlike with ESI and MALDI analysis of uncomplexed GAGs, there is at present, no way to extend this analysis beyond mass detection of the intact parent ion (i.e., no post source dissociation or MS/MS is possible due to chelation of the GAG sample with the basic peptide.).

V. Nuclear Magnetic Resonance Analysis of Heparin and Heparan Sulfate

Nuclear magnetic resonance (NMR) spectroscopy represents an important technique in the structural analysis of glycosaminoglycans (GAGs). It is one of the few techniques that provide structural information on the intact polymer without resorting to chemical or enzymatic cleavage. This is advantageous as it avoids the possibility of loss or conversion of structural information as a result of breakdown of the polymer. The utility of NMR in understanding GAG structure and conformation has been established by numerous early studies (68–70). Over the years, improvements in the field strengths of magnets used for analysis have led to greater resolution of signals and enabled sequencing of heparin oligosaccharides by NMR. Depending on the level of analysis, NMR can provide information on the monosaccharide composition, presence of impurities, linkage and even sequence for these complex mixtures or purified oligosaccharides.

NMR spectroscopy has been successfully used for detecting and quantifying signals associated with major or minor structural features in heparins. One-dimensional (1D) proton and carbon NMR spectroscopy have been used to describe the prevalent patterns of sulfation and acetylation present in heparins isolated from different sources as well as chemically modified heparins (71,72). More recently, an approach involving the combined use of proton and carbon NMR spectroscopy has been developed to provide more quantitative information on the monosaccharide composition and sulfation pattern in different heparin preparations (73). In a regular 1D proton NMR spectrum of heparin there are few signals representative of a particular monosaccharide component that are unaffected by signal overlapping and can be directly used for quantification. In this study, two-dimensional (2D) proton–carbon correlation spectroscopy (HSQC) of heparin was used as a means of partially resolving and identifying signals with minimum overlap that represented a specific sulfation pattern (Fig. 6). Integration of these signals in a 1D spectrum of the polymer followed by simple calculations thereby facilitated a quantitative monosaccharide compositional analysis of different porcine mucosal heparin preparations (73). In a further refinement of these methods the same group has demonstrated the ability to extend this quantitative compositional analysis to standard 2D HSQC experiments (74). By taking into account the role of differences in the $^{1}J_{C-H}$ values of the integrated cross-peak signals, they have attempted to minimize these differences, thereby maximizing the volumes of the signals observed. This adjustment has made the comparison of integrated signals in the 2D HSQC spectrum more reliable and accurate. When coupled with the increased resolution gained by the 2D technique this represents an important methodology to not only quantify the basic monosaccharide constituents of the mixture but also assess their linkage environments in a quantitative manner (74).

High-field NMR analysis has also been used for probing the structure and sequence of purified oligosaccharides from heparin and heparan sulfate (75,76). In cases where the oligosaccharide structure has been characterized by NMR previously, a 1D proton NMR spectrum alone may be sufficient to assign structure, by comparison of the chemical shifts with previously reported values. However, it is best to do 2D NMR experiments (COSY, TOCSY and NOESY) to establish the through-bond and through-space relationships of the nuclei, thereby enabling a better understanding of the overall structure as well as sequence of the oligosaccharide. Another advantage of using NMR to study oligosaccharide structure is the ability to look at the ring conformations of carbohydrate units as defined by the *J*-coupling constants and inter-proton nuclear Overhauser effects (NOEs). This data in conjunction with molecular modeling studies, using restrained molecular dynamics and energy minimization, to refine structures has been used to study the conformation of residues in heparin, heparin sulfate and heparin oligosaccharides (77–79). Such analyses provide a better understanding of the conformations adopted by the oligosaccharide sugar units in solution, and enable the comparison with how these conformations vary when the oligosaccharides are bound to proteins (80).

NMR on heparin and heparan sulfate represents a very accurate method for direct quantification of the glucuronic and iduronic acid content in the polymer (81).

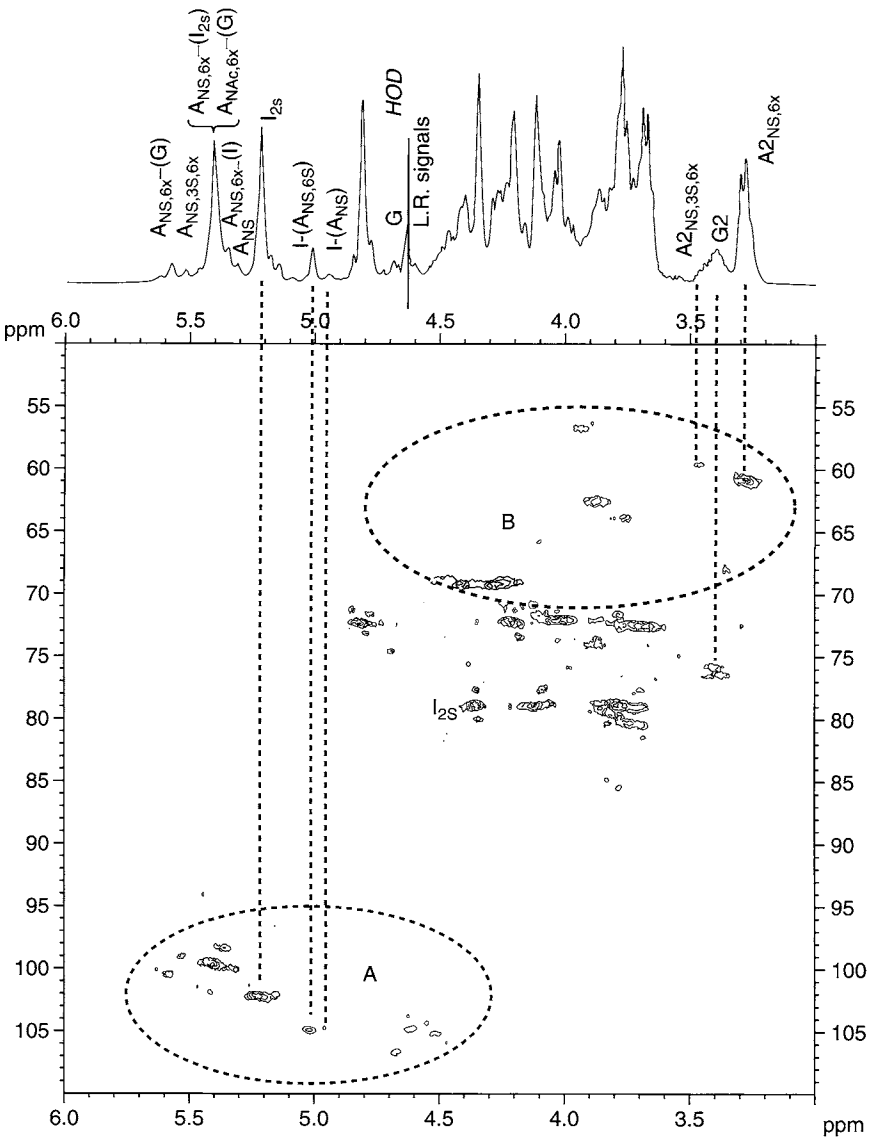

Figure 6 ^{1}H and HSQC spectra of pig mucosal heparin. Dashed circles A and B contain signals used for calculation of substituted monosaccharides by the HSQC method. Dashed lines indicate proton signals used for calculation of substituted monosaccharide components by the 1D method. Symbols $A_{NS,6X}$ and $A_{NS,3S,6X}$ indicate that position 6 may be sulfated or not. The signal of the *N*-acetyl group used for evaluation of *N*-acetyl glucosamine content is not shown. A, glucosamine; I, iduronic acid; G, glucuronic acid. Reproduced from reference (74), with permission from the publisher.

It also allows detection and quantification of minor sequences like the linkage region tetrasaccharide (82), as well the presence of dermatan sulfate impurities in industrial heparin samples (83). Structural differences in low molecular weight heparins arising from different chemical or enzymatic methods of depolymerization can also be assessed by NMR spectroscopy (84). Methods to obtain the molecular weights of low molecular weight heparins and heparin using ^{13}C NMR have also been reported (85). Thus it is clear that the versatility of NMR makes it an essential analytical tool for studying different aspects of glycosaminoglycan structure. However, it should be noted that one of the major limitations of the technique is the relatively large amount of sample required for NMR analysis when compared to other analytical techniques (MS and CE).

VI. New Methodologies for Structural Analysis of Heparin and Heparan Sulfate

Heparin and heparan sulfate represent the most information dense biopolymers in nature. Therefore one of the key issues in the analysis of structural information present in these complex mixtures is the ability to assimilate the generated experimental information in a bioinformatics framework that can encompass the vast structural diversity encoded by these molecules. Recently a property encoded nomenclature (PEN) computational platform for the structural analysis of heparin and heparan sulfate oligosaccharides was developed. The PEN framework represents a way to account for all the possible structural diversity present in a simple disaccharide unit (the basic building block of heparin and HS polymers) and assign it a one-letter code based on a hexadecimal notation system (64). It should also be noted that while each of the experimental methods described in this chapter represent a very essential tool in the structural analysis of GAGs, they are not without their limitations. It is therefore important to understand that different techniques provide complementary sets of information and an assimilation of these different data sets can help to provide a detailed characterization of these mixtures.

There have been a few recent studies that highlight the importance of this approach. In one report the combination of NMR and CE was used in conjunction with the property encoded nomenclature (PEN) platform (86). This approach utilized CE to provide information on the basic composition of the saccharide along with the uronic acid to glucosamine linkage information. However, the limitation of using just CE is that the lyase enzymes used to break down the oligosaccharide effectively destroy information about the epimerization state of the uronic acid, as well as the glucosamine to uronic acid linkage. However, using NMR, the anomeric proton signals of the glucosamines can be resolved to give linkage to the neighboring uronic acid and also the epimerization state of the uronic acid can be determined. Therefore, the data from these two complementary techniques were applied as constraints to a PEN computational framework, which

represented all the theoretically possible sequences for the oligosaccharides being analyzed. This facilitated the convergence to a unique sequence for the oligosaccharides (86). In another related study MALDI-MS and CE analysis were coupled with chemical and enzymatic digestion of HP oligosaccharides. The data generated from the different experiments carried out were applied as experimental constraints in the PEN framework. This enabled the determination of either a single unique sequence, in the case of a pure oligosaccharide, or complete structural characterization of components for a mixture of oligosaccharides (64,87). Such approaches have demonstrated tremendous potential for the analysis of heparin and heparan sulfate derived mixtures.

VII. Summary and Conclusions

Heparin and heparan sulfate are complex glycosaminoglycans that play multiple roles in the normal physiology and pathophysiology of the human body. The structural diversity displayed by these GAG chains makes them extremely challenging molecules to analyze. Also unlike DNA and proteins, it is not possible to amplify these structures, as their biosynthesis is not template driven. Therefore in cases where sample amounts are limited (e.g., isolated cell surface HS), it further magnifies the problem. Methodology for structural characterization of these molecules has primarily focused on: (1) chemical or enzymatic techniques for specifically degrading them to smaller oligosaccharides; (2) efficient means to separate them, coupled with sensitive detection procedures; and (3) the use of NMR and mass spectrometry. Together these techniques have provided a wealth of information for analyzing these complex mixtures as well as in determining sequences of isolated pure oligosaccharides. As analytical techniques get more sophisticated and are adapted to study sugar structure (e.g., MS/MS), they open more avenues to get structural insights into these complex mixtures. Having the PEN framework adds another layer of sophistication to the analysis of these mixtures as it enables the possible decoding of the structural information by taking into account multiple experimental data sets as constraints for sequence refinement.

Heparin and heparan sulfate have been implicated as playing crucial roles in many disease states by interacting with important proteins at key steps in different pathways. To better understand these interactions it is essential to know the key structural elements from both the sugar side as well as the protein side. While advances in protein technology have enabled a greater understanding from the protein side, understanding of complex sugar structure is lagging behind. Therefore, an understanding of the structure and sequence information displayed by the sugars that facilitate these interactions would possibly provide new targets for therapeutic intervention in different disease states. As the field of "glycomics" gains more importance, advances in analytical capabilities represent the cornerstone that will help shape the future.

References

1. Lindahl U, Backstrom G, Thunberg L, Leder IG. Evidence for a 3-*O*-sulfated D-glucosamine residue in the antithrombin-binding sequence of heparin. Proc Natl Acad Sci USA 1980; 77:6551–6555.
2. Petitou M, Casu B, Lindahl U. 1976–1983, a critical period in the history of heparin: the discovery of the antithrombin binding site. Biochimie 2003; 85: 83–89.
3. Capila I, Linhardt RJ. Heparin–protein interactions. Angew Chem Int Ed Engl 2002; 41:391–412.
4. Casu B, Lindahl U. Structure and biological interactions of heparin and heparan sulfate. Adv Carbohydr Chem Biochem 2001; 57:159–206.
5. Desai UR, Wang HM, Linhardt RJ. Substrate specificity of the heparin lyases from Flavobacterium heparinum. Arch Biochem Biophys 1993; 306:461–468.
6. Lohse DL, Linhardt RJ. Purification and characterization of heparin lyases from Flavobacterium heparinum. J Biol Chem 1992; 267:24347–24355.
7. Rice KG, Kim YS, Grant AC, Merchant ZM, Linhardt RJ. High-performance liquid chromatogarphic separation of heparin-derived oligosaccharides. Anal Biochem 1985; 150:325–331.
8. Linhardt RJ, Loganathan D, Al-Hakim A, Wang HM, Walenga JM, Hoppensteadt D, Fareed J. Oligosaccharide mapping of low molecular weight heparins: structure and activity differences. J Med Chem 1990; 33:1639–1645.
9. Karamanos NK, Vanky P, Tzanakakis GN, Tsegenidis T, Hjerpe A. Ion-pair high-performance liquid chromatography for determining disaccharide composition in heparin and heparan sulfate. J Chromatogr A 1997; 765:169–179.
10. Karamanos NK, Vanky P, Syrokou A, Hjerpe A. Identity of dermatan and chondroitin sequences in dermatan sulfate chains determined by using fragmentation with chondroitinases and ion-pair high-performance liquid chromatography. Anal Biochem 1995; 225:220–230.
11. Chai W, Leteux C, Westling C, Lindahl U, Feizi T. Relative susceptibilities of the glucosamine–glucuronic acid and *N*-acetylglucosamine–glucuronic acid linkages to heparin lyase III. Biochemistry 2004; 43:8590–8599.
12. Kinoshita A, Sugahara K. Microanalysis of glycosaminoglycan-derived oligosaccharides labeled with a fluorophore 2-aminobenzamide by high-performance liquid chromatography: application to disaccharide composition analysis and exosequencing of oligosaccharides. Anal Biochem 1999; 269:367–378.
13. Volpi N. Hyaluronic acid and chondroitin sulfate unsaturated disaccharides analysis by high-performance liquid chromatography and fluorimetric detection with dansylhydrazine. Anal Biochem 2000; 277:19–24.
14. Toyoda H, Motoki K, Tanikawa M, Shinomiya K, Akiyama H, Imanari T. Determination of human urinary hyaluronic acid, chondroitin sulphate and dermatan sulphate as their unsaturated disaccharides by high-performance liquid chromatography. J Chromatogr 1991; 565:141–148.
15. Toyoda H, Nagashima T, Hirata R, Toida T, Imanari T. Sensitive high-performance liquid chromatographic method with fluorometric detection for the determination of heparin and heparan sulfate in biological samples: application to human urinary heparan sulfate. J Chromatogr B 1997; 704:19–24.

16. Toyoda H, Yamamoto H, Ogino N, Toida T, Imanari T. Rapid and sensitive analysis of disaccharide composition in heparin and heparan sulfate by reversed-phase chromatography on a 2 μm porous silica gel column. J Chromatogr A 1999; 830:197–201.
17. Vogchan P, Warda M, Toyoda H, Toida T, Marks RM, Linhardt RJ. Structural characterization of human liver heparan sulfate. Biochim Biophys Acta 2005; 1721:1–8.
18. Volpi N. Separation of capsular polysaccharide-K4- and defructosylated-K4-derived disaccharides by high-performance liquid chromatography and postcolumn derivatization with 2-cyanoacetamide and fluorimetric detection. Anal Biochem 2004; 2004:359–361.
19. Vives RR, Pye DA, Salmivirta M, Hopwood JJ, Lindahl U, Gallagher JT. Sequence analysis of heparan sulphate and heparin oligosaccharides. Biochem J 1999; 339(Part 3):767–773.
20. Stringer SE, Kandola BS, Pye DA, Gallagher JT. Heparin sequencing. Glycobiology 2003; 13:97–107.
21. Cowman MK, Slahetka MF, Hittner DM, Kim J, Forino M, Gadelrab G. Polyacrylamide-gel electrophoresis and alcian blue staining of sulfated glycosaminoglycan oligosaccharides. Biochem J 1984; 221:707–716.
22. Rice KG, Rottink MK, Linhardt RJ. Fractionation of heparin-derived oligosaccharides by gradient polyacrylamide-gel electrophoresis. Biochem J 1987; 244:515–522.
23. Edens RE, Al-Hakim A, Weiler JM, Rethwisch DG, Fareed J, Linhardt RJ. Gradient polyacrylamide gel electrophoresis for determination of molecular weights of heparin preparations and low molecular weight heparin derivatives. J Pharm Sci 1992; 81:823–827.
24. Drummond KJ, Yates EA, Turnbull JE. Electrophoretic sequencing of heparin/heparan sulfate oligosaccharides using a highly sensitive fluorescent end label. Proteomics 2001; 2001:304–310.
25. Turnbull JE, Hopwood JJ, Gallagher JT. A strategy for rapid sequencing of heparan sulfate and heparin saccharides. Proc Natl Acad Sci 1999; 96:2698–2703.
26. Volpi N, Maccari F. Detection of submicrogram quantities of glycosaminoglycans on agarose gels by sequential staining with toluidine blue and stains-all. Electrophoresis 2002; 23:4060–4066.
27. Maccari F, Volpi N. Glycosaminoglycan blotting on nitrocellulose membranes treated with cetylpyridinium chloride after agarose-gel electrophoretic separation. Electrophoresis 2002; 23:3270–3277.
28. Maccari F, Volpi N. Direct and specific recognition of glycosaminoglycans by antibodies after their separation by agarose gel electrophoresis and blotting on cetylpyridinium chloride-treated nitrocellulose membranes. Electrophoresis 2003; 24:1347–1352.
29. Ramachandran A, Zhang M, Goad D, Olah G, Malayer JR, Rassi Z. Capillary electrophoresis and fluorescence studies on molecular beacon-based variable length oligonucleotide target discrimination. Electrophoresis 2003; 24:70–77.
30. Quang C, Malek A, Khaledi M. Separation of peptides and proteins by capillary electrophoresis using acidic buffers containing tetraalkylammonium cations and cyclodextrins. Electrophoresis 2003; 24:824–828.

31. Buchanan DD, Jameson EE, Perlette J, Malik A, Kennedy R. Effect of buffer, electric field, and separation time on detection of aptamer-ligand complexes for affinity probe capillary electrophoresis. Electrophoresis 2003; 24:1375–1382.
32. Peri-Okonny UL, Kenndler E, Stubbs EJ, Guzman N. Characterization of pharmaceutical drugs by a modified nonaqueous capillary electrophoresis-mass spectrometry method. Electrophoresis 2003; 24:139–150.
33. Al-Hakim A, Linhardt RJ. Capillary electrophoresis for the analysis of chondroitin sulfate- and dermatan sulfate-derived disaccharides. Anal Biochem 1991; 195:68–73.
34. Ampofo SA, Wang HM, Linhardt RJ. Disaccharide compositional analysis of heparin and heparan sulfate using capillary zone electrophoresis. Anal Biochem 1991; 199:249–255.
35. Carney SL, Osborne D. The separation of chondroitin sulfate disaccharides and hyaluronan oligosaccharides by capillary zone electrophoresis. Anal Biochem 1991; 195:132–140.
36. Damm JBL, Overklift GT, Vermeulen BWM, Fluitsma CF, Dedem G. Separation of natural and synthetic heparin fragments by high-performance capillary electrophoresis. J Chromatogr 1992; 608:297–309.
37. Karamanos NK, Vanky P, Tzanakakis GN, Hjerpe A. High performance capillary electrophoresis method to characterize heparin and heparan sulfate disaccharides. Electrophoresis 1996; 17:391–395.
38. Pervin A, Al-Hakim A, Linhardt RJ. Separation of glycosaminoglycan-derived oligosaccharides by capillary electrophoresis using reverse polarity. Anal Biochem 1994; 221:182–188.
39. Scapol L, Marchi E, Viscomi G. Capillary electrophoresis of heparin and dermatan sulfate unsaturated disaccharides with triethylamine and acetonitrile as electrolyte additives. J Chromatogr A 1996; 735:367–374.
40. Forsberg E, Pejler G, Ringvall M, Lunderius C, Tomasini-Johansson B, Bardosi A. Heparin binding lectin of human placenta as a tool for histochemical ligand localization and isolation. J Histochem Cytochem 1991; 39:1249–1256.
41. Kitagawa H, Kinoshita A, Sugahara K. Microanalysis of glycosaminoglycan-derived disaccharides labeled with a fluorophore 2-aminoacridone by capillary electrophoresis and high-performance liquid chromatography. Anal Biochem 1995; 232:114–121.
42. Park Y, Chao S, Linhardt RJ. Exploration of the action pattern of *Streptomyces* hyaluronate lyase using high-resolution capillary electrophoresis. Biochim Biophys Acta 1997; 1337:217–226.
43. Grill E, Huber C, Oefner PJ, Vorndran A, Bonn G. Capillary zone electrophoresis of p-aminobenzoic acid derivatives of aldoses, ketose and uronic acid. Electrophoresis 1993; 14:1004–1010.
44. Cheng MC, Lin SL, Wu SH, Inoue S, Inoue Y. High-performance capillary electrophoretic characterization of different types of oligo- and polysialic acid chains. Anal Chem 1998; 260:154–159.
45. Lamari F, Theocharis A, Hjerpe A, Karamanos N. Ultrasensitive capillary electrophoresis of sulfated disaccharides in chondroitin/dermatan sulfates by laser-induced fluorescence after derivatization with 2-aminoacridone. J Chromatogr B, Biomed Sci Appl 1999; 730:129–133.

46. Harvey DJ. Matrix-assisted laser desorption/ionization mass spectrometry of carbohydrates. Mass Spectrom Rev 1999; 18:349–450.
47. Yeung B, Marecak D. Molecular weight determination of hyaluronic acid by gel filtration chromatography coupled to matrix-assisted laser desorption ionization mass spectrometry. J Chromatogr A 1999; 852:573–581.
48. Siegel MM, Tabei K, Kagan MZ, Vlahov IR, Hileman RE, Linhardt RJ. Polysulfated carbohydrates analyzed as ion-paired complexes with basic peptides and proteins using electrospray negative ionization mass spectrometry. J Mass Spectrom 1997; 32:760–772.
49. Chai W, Luo J, Lim CK, Lawson AM. Characterization of heparin oligosaccharide mixtures as ammonium salts using electrospray mass spectrometry. Anal Chem 1998; 70:2060–2066.
50. Pope RM, Raska CS, Thorp SC, Liu J. Analysis of heparan sulfate oligosaccharides by nano-electrospray ionization mass spectrometry. Glycobiology 2001; 11:505–513.
51. Oguma T, Toyoda H, Toida T, Imanari T. Analytical method of heparan sulfates using high-performance liquid chromatography turbo-ionspray ionization tandem mass spectrometry. J Chromatogr B Biomed Sci Appl 2001; 754:153–159.
52. Oguma T, Toyoda H, Toida T, Imanari T. Analytical method of chondroitin/dermatan sulfates using high performance liquid chromatography/turbo ionspray ionization mass spectrometry: application to analyses of the tumor tissue sections on glass slides. Biomed Chromatogr 2001; 15:356–362.
53. Duteil S, Gareil P, Girault S, Mallet A, Feve C, Siret L. Identification of heparin oligosaccharides by direct coupling of capillary electrophoresis/ionspray-mass spectrometry. Rapid Commun Mass Spectrom 1999; 13:1889–1898.
54. Saad OM, Leary JA. Compositional analysis and quantification of heparin and heparan sulfate by electrospray ionization ion trap mass spectrometry. Anal Chem 2003; 75:2985–2995.
55. Saad OM, Leary JA. Delineating mechanisms of dissociation for isomeric heparin disaccharides using isotope labeling and ion trap tandem mass spectrometry. J Am Soc Mass Spectrom 2004; 15:1274–1286.
56. Henriksen J, Ringborg LH, Roepstorrf P. On-line size-exclusion chromatography/mass spectrometry of low molecular mass heparin. J Mass Spectrom 2004; 39:1305–1312.
57. Kuberan B, Lech M, Zhang L, Wu ZL, Beeler DL, Rosenberg RD. Analysis of heparan sulfate oligosaccharides with ion pair reverse phase capillary high performance liquid chromatography-microelectrospray ionization time-of-flight mass spectrometry. J Am Chem Soc 2002; 124:8707–8718.
58. Thanawiroon C, Rice KG, Toida T, Linhardt RJ. Liquid chromatography/mass spectrometry sequencing approach for highly sulfated heparin-derived oligosaccharides. J Biol Chem 2004; 279:2608–2615.
59. Thanawiroon C, Linhardt RJ. Separation of a complex mixture of heparin-derived oligosaccharides using reversed-phase liquid chromatography. J Chromatogr A 2003; 1014:215–223.
60. Ruiz-Calero V, Puignou L, Galceran M. Use of reversed polarity and a pressure gradient in the analysis of disaccharide composition of heparin by capillary electrophoresis. J Chromatogr A 1998; 828:497–508.

61. Ruiz-Calero V, Moyano E, Puignou L, Galceran M. Pressure-assisted capillary electrophoresis-electrospray ion trap mass spectrometry for the analysis of heparin depolymerised disaccharides. J Chromatogr A 2001; 914:277–291.
62. Zaia J, Liu B, Boynton R, Barry F. Structural analysis of cartilage proteoglycans and glycoproteins using matrix-assisted laser desorption/ionization time-of-flight mass spectrometry. Anal Biochem 2000; 277:94–103.
63. Schiller J, Arnhold J, Benard S, Reichl S, Arnold K. Cartilage degradation by hyaluronate lyase and chondroitin ABC lyase: a MALDI-TOF mass spectrometric study. Carbohydr Res 1999; 318:116–122.
64. Venkataraman G, Shriver Z, Raman R, Sasisekharan R. Sequencing complex polysaccharides. Science 1999; 286:537–542.
65. Juhasz P, Biemann K. Utility of non-covalent complexes in the matrix-assisted laser desorption ionization mass spectrometry of heparin-derived oligosaccharides. Carbohydr Res 1995; 270:131–147.
66. Venkataraman G, Shriver Z, Davis JC, Sasisekharan R. Fibroblast growth factors 1 and 2 are distinct in oligomerization in the presence of heparin-like glycosaminoglycans. Proc Natl Acad Sci USA 1999; 96:1892–1897.
67. Sturiale L, Naggi A, Torri G. MALDI mass spectrometry as a tool for characterizing glycosaminoglycan oligosaccharides and their interaction with proteins. Semin Thromb Hemost 2001; 27:465–472.
68. Dietrich CP, Nader HB, Perlin AS. The heterogeneity of heparan sulfate from beef-lung tissue: p.m.r.-spectral evidence. Carbohydr Res 1975; 41:334–338.
69. Gatti G, Casu B, Perlin AS. Conformations of the major residues in heparin. H-NMR spectroscopic studies. Biochem Biophys Res Commun 1978; 85: 14–20.
70. Jaques LB, Kavanagh LW, Mazurek M, Perlin AS. The structure of heparin. Proton magnetic resonance spectral observations. Biochem Biophys Res Commun 1966; 24:447–451.
71. Yates EA, Santini F, Guerrini M, Naggi A, Torri G, Casu B. 1H and 13C NMR spectral assignments of the major sequences of twelve systematically modified heparin derivatives. Carbohydr Res 1996; 294:15–27.
72. Casu B, Guerrini M, Naggi A, Torri G, De-Ambrosi L, Boveri G, Gonella S, Cedro A, Ferro L, Lanzarotti E, Paterno M, Attolini M, Valle MG. Characterization of sulfation patterns of beef and pig mucosal heparins by nuclear magnetic resonance spectroscopy. Arzneimittelforschung 1996; 46:472–477.
73. Guerrini M, Bisio A, Torri G. Combined quantitative (1)H and (13)C nuclear magnetic resonance spectroscopy for characterization of heparin preparations. Semin Thromb Hemost 2001; 27:473–482.
74. Guerrini M, Naggi A, Guglieri S, Santarsiero R, Torri G. Complex glycosaminoglycans: profiling substitution patterns by two-dimensional nuclear magnetic resonance spectroscopy. Anal Biochem 2005; 337:35–47.
75. Chai W, Hounsell EF, Bauer CJ, Lawson AM. Characterisation by LSI-MS and 1H NMR spectroscopy of tetra-, hexa-, and octa-saccharides of porcine intestinal heparin. Carbohydr Res 1995; 269:139–156.
76. Pervin A, Gallo C, Jandik KA, Han XJ, Linhardt RJ. Preparation and structural characterization of large heparin-derived oligosaccharides. Glycobiology 1995; 5:83–95.
77. Mikhailov D, Linhardt RJ, Mayo KH. NMR solution conformation of heparin-derived hexasaccharide. Biochem J 1997; 328 (Part 1):51–61.

78. Mulloy B, Forster MJ. Conformation and dynamics of heparin and heparan sulfate. Glycobiology 2000; 10:1147–1156.
79. Mulloy B, Forster MJ, Jones C, Davies DB. N.m.r and molecular-modelling studies of the solution conformation of heparin. Biochem J 1993; 293 (Part 3):849–858.
80. Mikhailov D, Mayo KH, Vlahov IR, Toida T, Pervin A, Linhardt RJ. NMR solution conformation of heparin-derived tetrasaccharide. Biochem J 1996; 318 (Part 1):93–102.
81. Sudo M, Sato K, Chaidedgumjorn A, Toyoda H, Toida T, Imanari T. (1)H nuclear magnetic resonance spectroscopic analysis for determination of glucuronic and iduronic acids in dermatan sulfate, heparin, and heparan sulfate. Anal Biochem 2001; 297:42–51.
82. Iacomini M, Casu B, Guerrini M, Naggi A, Pirola A, Torri G. "Linkage region" sequences of heparins and heparan sulfates: detection and quantification by nuclear magnetic resonance spectroscopy. Anal Biochem 1999; 274:50–58.
83. Ruiz-Calero V, Saurina J, Galceran MT, Hernandez-Cassou S, Puignou L. Potentiality of proton nuclear magnetic resonance and multivariate calibration methods for the determination of dermatan sulfate contamination in heparin samples. Analyst 2000; 125:933–938.
84. Casu B, Torri G. Structural characterization of low molecular weight heparins. Semin Thromb Hemost 1999; 25(Suppl3):17–25.
85. Desai UR, Linhardt RJ. Molecular weight of low molecular weight heparins by 13C nuclear magnetic resonance spectroscopy. Carbohydr Res 1994; 255:193–212.
86. Guerrini M, Raman R, Venkataraman G, Torri G, Sasisekharan R, Casu B. A novel computational approach to integrate NMR spectroscopy and capillary electrophoresis for structure assignment of heparin and heparan sulfate oligosaccharides. Glycobiology 2002; 12:713–719.
87. Shriver Z, Raman R, Venkataraman G, Drummond K, Turnbull J, Toida T, Linhardt R, Biemann K, Sasisekharan R. Sequencing of 3-*O*-sulfate containing heparin decasaccharides with a partial antithrombin III binding site. Proc Natl Acad Sci USA 2000; 97:10359–10364.

Chemistry and Biology of Heparin and Heparan Sulfate
H.G. Garg, R.J. Linhardt and C.A. Hales (Editors)

Chapter 4

Synthetic Approach to Define Structure–Activity Relationship of Heparin and Heparan Sulfate

CHRISTIAN NOTI and PETER H. SEEBERGER

Laboratorium für Organische Chemie, ETH Hönggerberg, Zürich, Switzerland

I. Introduction

Glycosaminoglycans (GAGs) are the most abundant heteropolysaccharides in the body. These molecules are highly functionalized, unbranched polysaccharides containing a disaccharide repeating unit. The disaccharide unit consists of a 2-amino-2-deoxy glycoside [either galactosamine (GalNAc) or glucosamine (GlcNAc)] and a uronic acid such as glucuronic acid (GlcA) or iduronic acid (IdoA). GAGs are major components of the extracellular matrix that surrounds all mammalian cells. Different core proteins anchor glycosaminoglycan polysaccharides in the outside of the lipid bilayer. The linkage of GAGs to the protein core involves a specific trisaccharide composed of two galactose residues and a xylose residue (GAG – Gal – Gal – Xyl – O – CH_2 – protein). The trisaccharide linker is coupled to the protein core through an *O*-glycosidic bond to a serine residue in the protein. The protein cores of proteoglycans are rich in serine and threonine residues, which allow multiple GAG attachments. Choindroitin sulfate, keratin sulfate, and dermatan sulfate belong to the family of GAGs as well as heparin and heparan sulfate, are the most complex glycosaminoglycans. GAGs have important biological functions by binding to different growth factors, enzymes, morphogens, cell adhesion molecules, and cytokines (1–5).

Heparin, found only in mastocytes, has served as an anticoagulant in heart disease for more than 60 years (6,7) and has a molecular weight ranging from 5 to 40 kDa, with an average molecular weight of about 15 kDa. These linear, unbranched, highly sulfated polysaccharides are composed of disaccharide units

consisting of an uronic acid 1,4-linked to a D-glucosamine unit (Fig. 2). The uronic acid residues are more often L-iduronic acid (90%) than its C-5 epimer D-glucuronic acid (10%). A prototypical heparin disaccharide contains three sulfate groups. These sulfate groups render heparin one of the most acidic macromolecule in nature. *O*-sulfation normally occurs at the 2-position of the uronic acids and the 3- and/or 6-position of the glucosamine. In addition, the glucosamine nitrogen may be sulfated, acetylated or, less frequently, may remain unmodified, thus resulting in 48 possible disaccharides that make up heparin (Fig. 1) (8).

Heparan sulfate is structurally related to heparin but is widely distributed in different cell types and tissues. At a molecular weight range of 5–50 kDa and an average molecular weight of 30 kDa, heparan sulfate chains are generally longer than those of heparin. Heparan sulfate, more heterogeneous than heparin, is richer in *N*-acetyl D-glucosamine (GlcNAc) and D-glucuronic acid (GlcA) units, and contains fewer *O*-sulfates (9).

Much research on the structure, function, and biological activity of heparin and heparan sulfate has been carried out. A more detailed structure–activity relationship for heparin oligosaccharides has evolved in recent years. This more detailed understanding of GAGs has been aided by the availability of synthetic, completely defined heparin oligosaccharides. Since many aspects of heparin chemistry (10–13) and biology (4,14,15) have been reviewed recently, we will focus, after a brief general introduction, on studies using synthetic heparin oligosaccharides to elucidate the structure–activity relationship of heparin and heparan sulfate.

II. Biosynthesis

To understand the way GAG sequences interact with particular proteins it is helpful to consider the mechanism by which nature synthesizes different heparins. Much progress in understanding GAG biosynthesis has been made in recent years (16). Heparin and heparan sulfate are assembled via a similar pathway (Fig. 3) (17). Chain initiation occurs in the Golgi apparatus. The transfer of xylose from UDP-xylose to the hydroxyl group of specific serine residues on the core protein is the initial step in the formation of the tetrasaccharide linkage region (–GlcA–Gal–Gal–Xyl–Ser). *N*-acetyl-D-glucosamine and glucuronic acid monosaccharide units are alternately incorporated from the nonreducing end of the nascent polymer using the corresponding sugar nucleotides. Glucuronic acid is attached by glucuronyltransferase followed by the addition of the first *N*-acetyl-glucosamine residue. Two glycosyl transferases (EXT1 and EXT2), which form a hetero-oligomeric complex in the Golgi, are responsible for the disaccharide addition (18). As the polysaccharide chain forms, it undergoes a series of modification reactions catalyzed by at least four families of sulfotransferases and one epimerase (19): *N*-deacetylation and *N*-sulfation is carried out by a *N*-deacetylase and a *N*-sulfotransferase, and the transformation of D-glucuronic units to L-iduronic units is catalyzed by a C-5 epimerase. Different *O*-sulfotransferases are responsible for *O*-sulfation of the iduronic acid residues. The action of these enzymes results in tremendous heterogeneity within modified

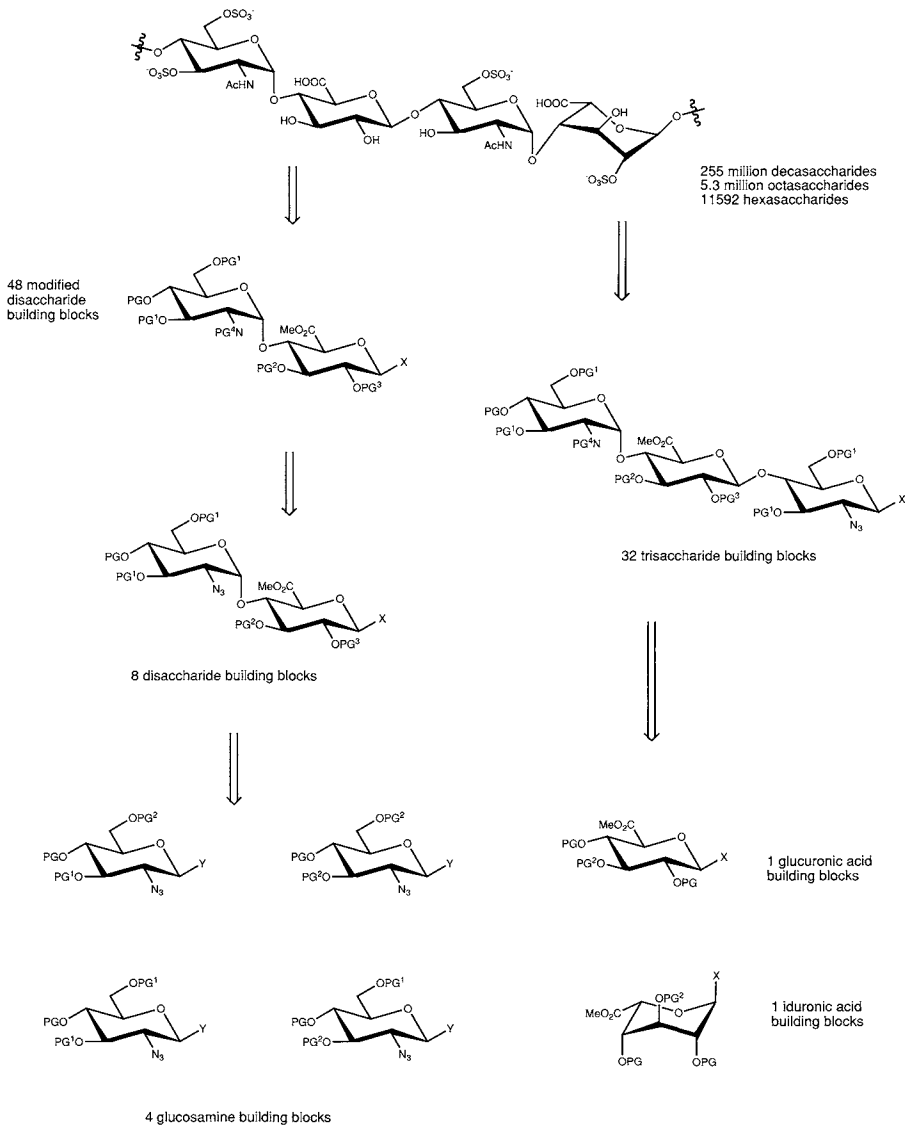

Figure 1 Retrosynthetic analysis of a general, modular approach to the preparation of heparin-like glycosaminoglycans (reprinted with permission, from *Chemistry, A European Journal*, Volume 9 © 2003 by Wiley-VCH, *www.wiley.com*).

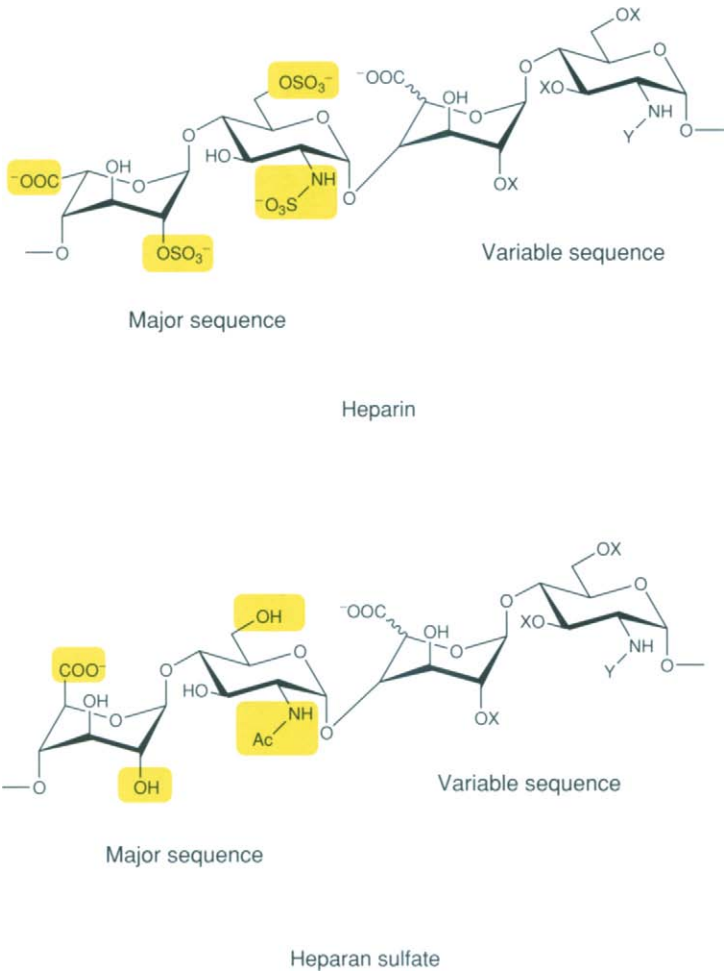

Figure 2 Major and minor disaccharide repeating units in heparin and heparan sulfate (X = H or SO_3^-; Y = Ac, SO_3^-, or H).

regions. Specific sulfation and uronic acid patterns give rise to particular binding sequences for the interaction with proteins.

III. Structure of Heparin/Heparan Sulfate

Heparin does not fold into tertiary structures like proteins, but exists primarily as a helical structure (20). The sulfate and carboxyl groups of heparin promote specific interactions with biologically important proteins (21). The pyranose rings of the monosaccharide residues within heparin oligosaccharides adopt the $^1C_4$ and $^4C_1$ chair conformation, as well as the $^2S_0$ skew-boat conformation (22–24). NMR

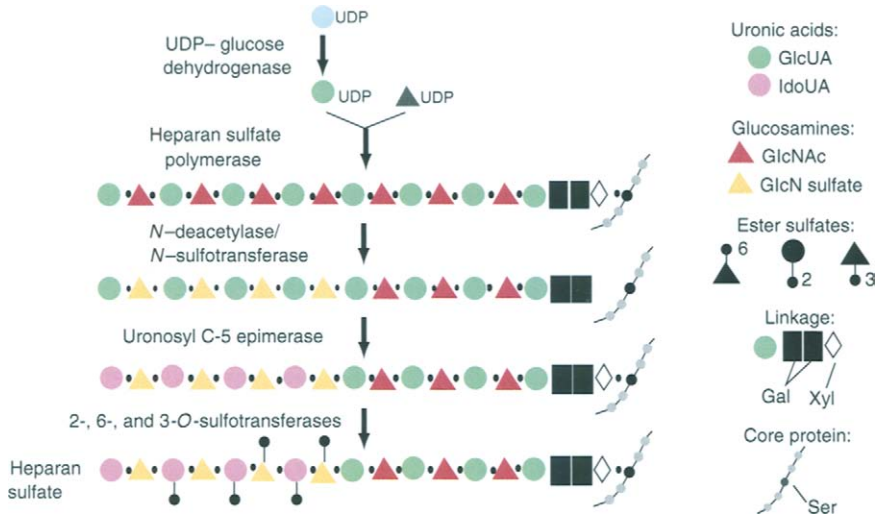

Figure 3 Scheme of heparan sulfate biosynthesis (reprinted with permission, from *Annual Review of Biochemistry*, Volume 68 © 1999 by Annual Reviews, *www.annualreviews.org*).

studies and X-ray structures show that the pyranose rings of glucuronic acid and glucosamine residues prefer the $^4C_1$ chair conformation whereby all non-hydrogen substituents, except the anomeric hydroxyl group of glucosamine, are equatorial (25,26). The iduronic acid pyranose is more flexible: bearing a sulfate group at C-2, the $^1C_4$ chair and $^2S_0$ the skew-boat conformation are preferred. Unsubstituted iduronic acid, however, resides predominantly in the $^1C_4$ form (Fig. 4) (25,27). The flexibility of the L-iduronic acid residues is important for specific heparin–protein interactions.

Different attractive forces are responsible for the heparin–protein interplay: ionic interactions are dominant as the negatively charged sulfate and carboxyl groups form ion pairs with positively charged amino acids. Nonionic interactions such as hydrogen bonding as well as hydrophobic forces also contribute to binding. The complexity of GAG polymers has greatly complicated the evolution of detailed

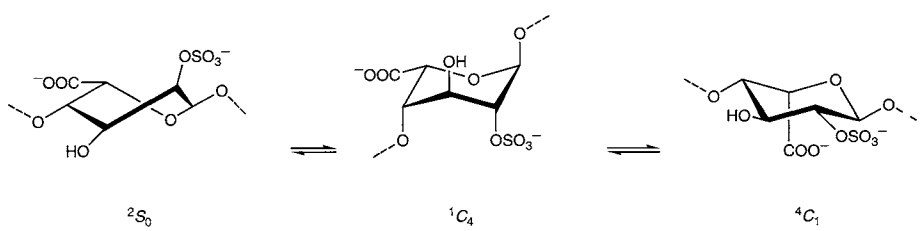

Figure 4 Conformational flexibility of L-iduronic acid.

structure–activity relationships. However, it has been shown that defined length and sequences of GAGs are responsible for the binding to and hence modulating the biological activity of particular proteins.

IV. Chemical Synthesis of Defined Heparin Oligosaccharides

To establish a detailed structure–activity relationship and correlate specific heparin sequences and sulfation patterns with protein binding and biological activity, access to defined heparin oligosaccharides is of the utmost importance. The purification of oligosaccharides following enzymatic digestion of GAG chains has provided access to usable quantities of oligomers up to hexasaccharides (28–30). Chemical synthesis, while challenging in the context of heparin oligosaccharides, has been used to procure defined sequences and analogs for biological studies and to define SAR (10–12). In this section, we first briefly summarize the preparation of building blocks used during heparin oligosaccharide assembly and then review the different general methods used to prepare oligosaccharides.

A. Synthesis of Building Blocks for Heparin Synthesis

The preparation of sufficient quantities of fully differentiated building blocks incorporating appropriate protecting groups is particularly important for the synthesis of complex oligosaccharides such as heparin. The placement of specific protecting groups is required at the 4-hydroxyl group of each building block to allow for ready deprotection in anticipation of chain elongation. Here, levulinoyl esters (31–33), Fmoc carbonates (34), silyl ethers (32,35,36) and PMB ethers (37–39) have found use. The hydroxyl groups to be *O*-sulfated at the end and those that should remain free have to be protected differentially. Commonly, acetate esters serve to mark the hydroxyl groups to be sulfated, while benzyl ethers mask hydroxyl groups that will not be modified. The amine group of D-glucosamine requires the placement of different protecting groups. Azides have been commonly used in this function (36, 39–41).

The choice of anomeric leaving groups presents another important consideration in oligosaccharide assembly. Increasingly efficient glycosylation reactions have been developed and glycosyl trichloroacetimidate and thioglycoside building blocks have replaced methods requiring the use of heavy metal activators.

Commonly used, commercially available, and inexpensive starting materials for the synthesis of differentially protected glucosamine and glucuronic acid building blocks are D-glucosamine **1** and diacetone glucose **2** (Fig. 5).

Since L-iduronic acid is not accessible from natural sources, many strategies have been developed to access this monosaccharide by manipulation of D-glucuronic acid derivatives (42–52). Recently, a host of methods have been reported, starting from D-glucuronolactone, D-diacetonglucose, and D-glucuronic acid glycals as starting materials (8,53–62). Nevertheless, the synthesis of iduronic acid building blocks remains a major challenge *en route* to the desired heparin oligosaccharides.

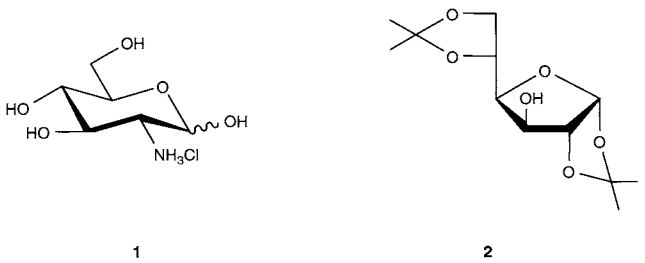

1 2

Figure 5 Common starting materials for the synthesis of heparin/heparan sulfate building blocks.

Initially, total synthesis efforts targeted a single heparin oligosaccharide and yielded many valuable insights. In recent years, modular approaches aimed at the synthesis of a broad range of heparin/heparan sulfate oligosaccharide fragments have been developed.

1. Modular Synthesis of Heparin Oligosaccharides

The first modular assembly approach targeted the common heparin repeat disaccharide **3** and its 6-*O*-unsulfated counterpart **4** (Scheme 1) (37). Disaccharide **3** was prepared in 5 steps from disaccharide **5** (29% overall yield) (42) while the assembly of **4** required 8 steps (30% yield).

Another modular approach relied on the late stage formation of uronic acids by selective oxidation of the C-6 hydroxyl groups of glucose and idose residues.

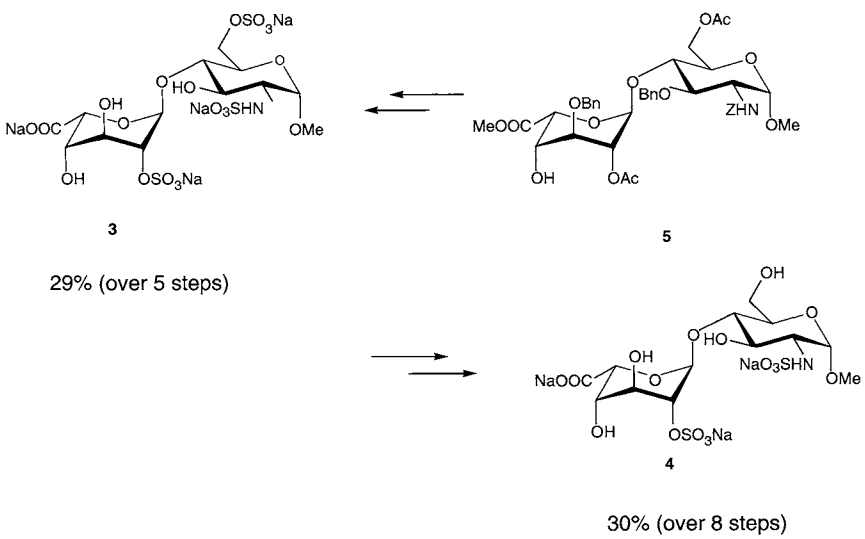

Scheme 1 Synthesis of the regular sequence disaccharides of heparin.

Thus, problems such as epimerization of the C-5 position of uronic acids and poor coupling efficiency of uronic acid-based glycosylating agents were circumvented (36). It was calculated that twenty disaccharide building blocks would be required to assemble all possible linear oligosaccharide chains. The synthetic strategy (Scheme 2) based on the assembly of a sulfated oligosaccharide containing glucose and idose units was synthesized before all protecting groups, except the TBDPS ethers that masked the C-6 hydroxyl groups of the D-glucosamine units, were removed. The primary C-6 hydroxyl groups of the glucoside and idoside units were then oxidized to the corresponding carboxylic acids. Finally, the primary hydroxyl groups of the D-glucosamine units were revealed.

Subsequently, hydroxyl groups to be sulfated were protected with levulinoyl esters, whereas acetyl esters were used for non-sulfated hydroxyl substituents (40).

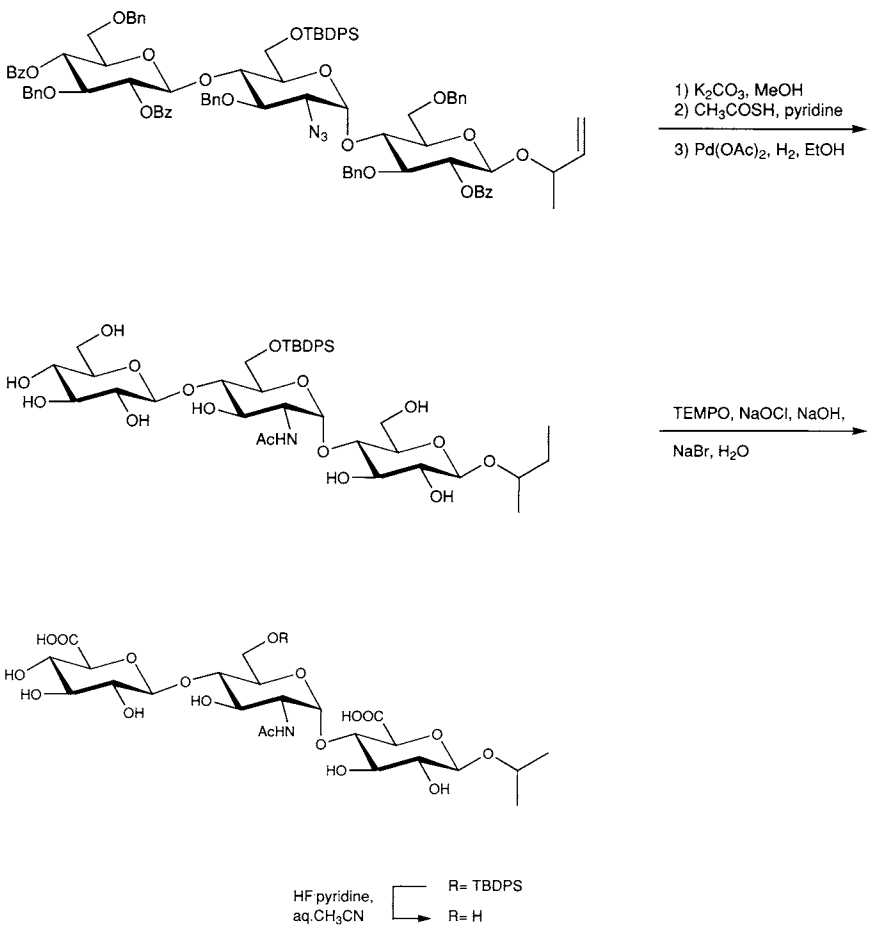

Scheme 2 New approach for heparin synthesis.

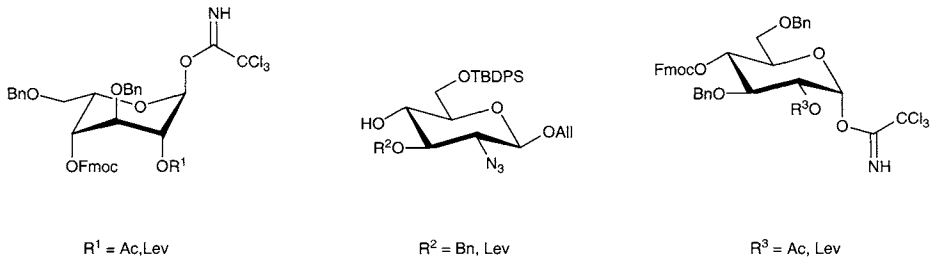

Figure 6 Building blocks for the synthesis of 20 different heparan sulfate disaccharide units.

Six different monosaccharide building blocks that can be combined to form the 20 disaccharides found in heparan sulfate were prepared (Fig. 6) (63). Four different protecting groups (Lev, Fmoc, TBDPS, and All) were employed in these syntheses. The Fmoc group was chosen to mark the C-4′ hydroxyls for chain extension, while the anomeric center of the disaccharide was protected in form of an allyl glycoside. Benzyl ethers masked primary hydroxyls that were subsequently oxidized to carboxylic acids and secondary hydroxyls that remain unsulfated. Levulinoyl esters were utilized to protect the C-2′ position and ensure the stereoselective formation of 1,2-*trans*-glycosidic linkages. Finally, the C-6 position of glucosamine was protected as a TBDPS ether.

Another path to disaccharide subunits starts from diacetone glucose **2**, which was converted via 1,2:3,5-di-*O*-isopropylidene-β-L-idofuranose **6** to the desired 1,6-anhydro-β-L-hexopyranose **7** (Scheme 3) (64,65). Union of **7** and **8** upon TMSOTf activation provided disaccharide **9**. The α-isomer was isolated, acetylated, and the 1,6-anhydro-β-L-idopyranosyl ring opened. Removal of the anomeric acetate afforded desired alcohol **10**, ready for the next glycosylation.

Two disaccharides (**11**,**12**) containing glucosamines at the nonreducing end allowed for a systematic approach to prepare inverse sequence (glucosamine–iduronic acid) oligosaccharides in contrast to the fragments obtained by chemical or enzymatic processing of polysaccharides (Fig. 7) (66).

The selective installation of the α-glucosamine glycosidic linkage found in this disaccharide by coupling glucosamine with an iduronic acid is the most challenging task in the synthesis of heparin oligosaccharides. A new approach to stereochemical control of glycosylation reactions by conformational control of the nucleophile was developed (67). Introduction of a cyclic protecting group (e.g., isopropylidene or cyclopentylidene) as conformational lock for the monosaccharide nucleophile **13** ensured the exclusive formation of the desired α-linked disaccharides (**19**,**20**) (Scheme 4) (61).

Preparation of disaccharide building blocks by regioselective and stereoselective glycosylation of an iduronic acid ester diol (**21**) with a 2-azido-2-deoxy-D-glucopyranosyl trichloroacetimidate (**22**) was also reported (68). Four different series of hexasaccharides and octasaccharides were synthesized using this disaccharide unit (Fig. 8).

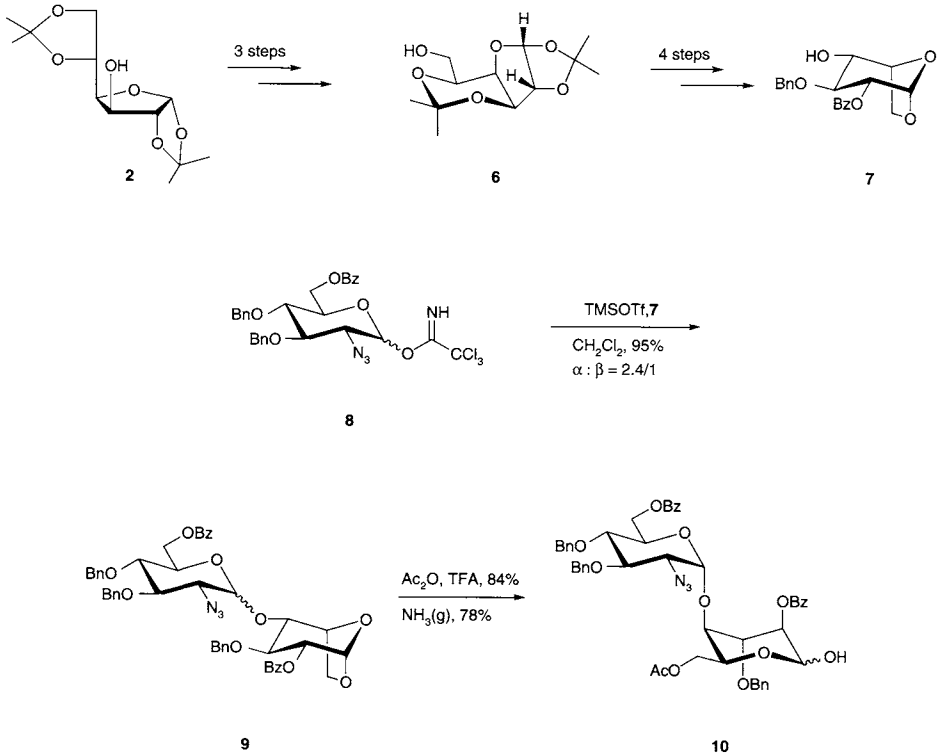

Scheme 3 Synthesis of the 1,6-anhydro-β- L-hexopyranose.

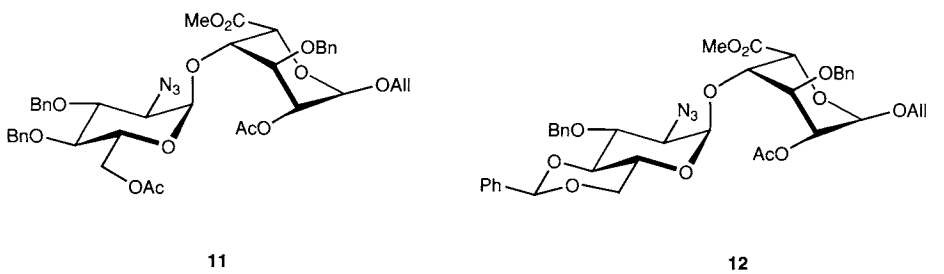

Figure 7 Disaccharide moieties with reversed sequences.

2. *Solid-Phase Synthesis of Heparin Oligosaccharides*

Ideally, defined heparin sequences could be prepared by automated solid phase synthesis using methods analogous to those that already exist for the assembly of oligonucleotides and peptides. While automated solid phase synthesis of oligosaccharides is now possible (69), only a few polymer-supported syntheses of heparin oligosaccharides have been disclosed (70–72). Soluble polyethylene glycol (PEG)

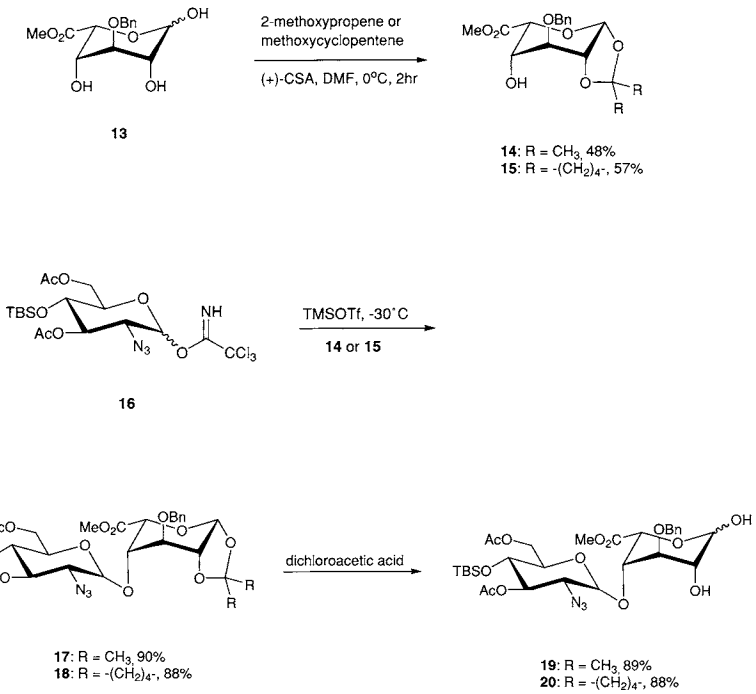

Scheme 4 Synthesis of a disaccharide using a locked iduronic acid acceptor.

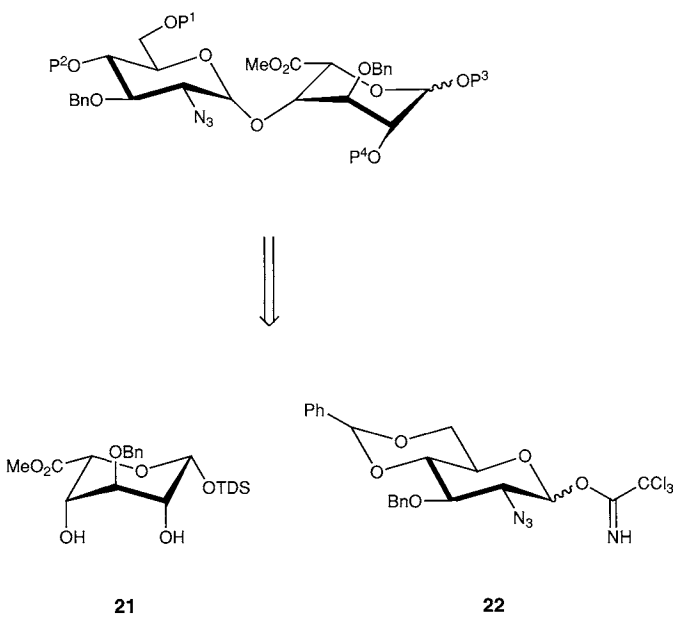

Figure 8 Disaccharide unit to prepare oligosaccharides.

polymers gave encouraging results for the synthesis of fully protected oligosaccharides **25** that were obtained by coupling the disaccharide **23** with the polymer-bound iduronic acid **24** (Scheme 5). Each elongation cycle incorporated levulinoate cleavage, coupling, and capping.

In a second approach, disaccharide **27** was coupled to polyethylene glycol monomethyl ether (MPEG)-bound disaccharide **26** to furnish MPEG-bound tetrasaccharide **28**. Reaction of **30** with disaccharide **31** afforded MPEG-bound hexasaccharide **32** that was cleaved from the solid support (Scheme 6).

This section has summarized different approaches for the modular synthesis of oligosaccharides. Future effort will focus on the synthesis of larger quantities of heparin and heparan sulfate using an automated oligosaccharide synthesizer to produce libraries of biologically significant heparin and heparan oligosaccharides.

B. Heparin Sequences of Biological Significance

Many aspects of heparin-binding proteins have been reviewed (4) and the best studied interactions are briefly summarized below.

1. *Chemokine Interactions*

Chemokines, a family of over 40 structurally related glycoproteins that facilitate leukocyte migration, angiogenesis, breast cancer metastasis (73), and leukocyte degranulation also interact with heparin. Platelet factor 4 (CXC chemokine ligand 4),

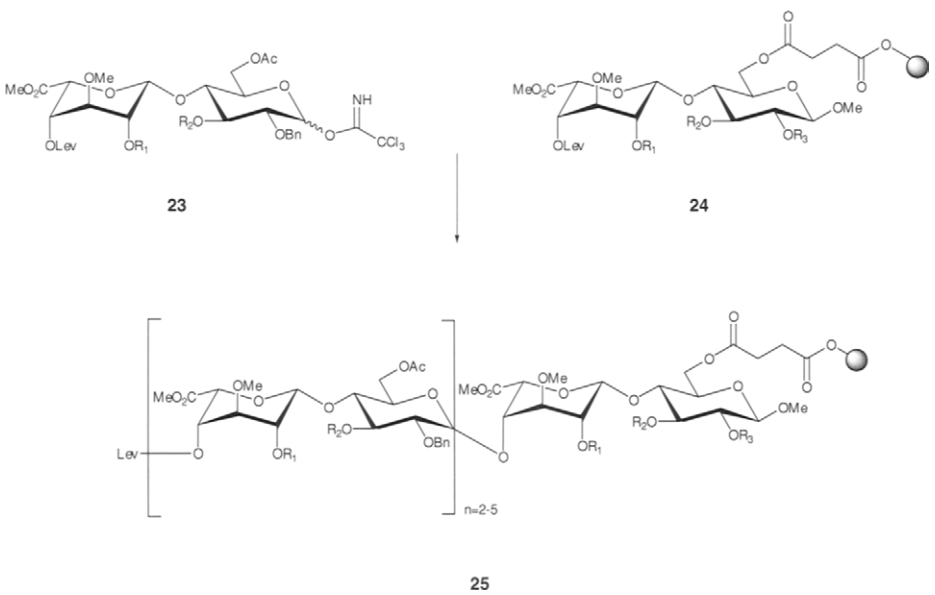

23 24 25

Scheme 5 Synthesis of a polymer-bound oligosaccharide.

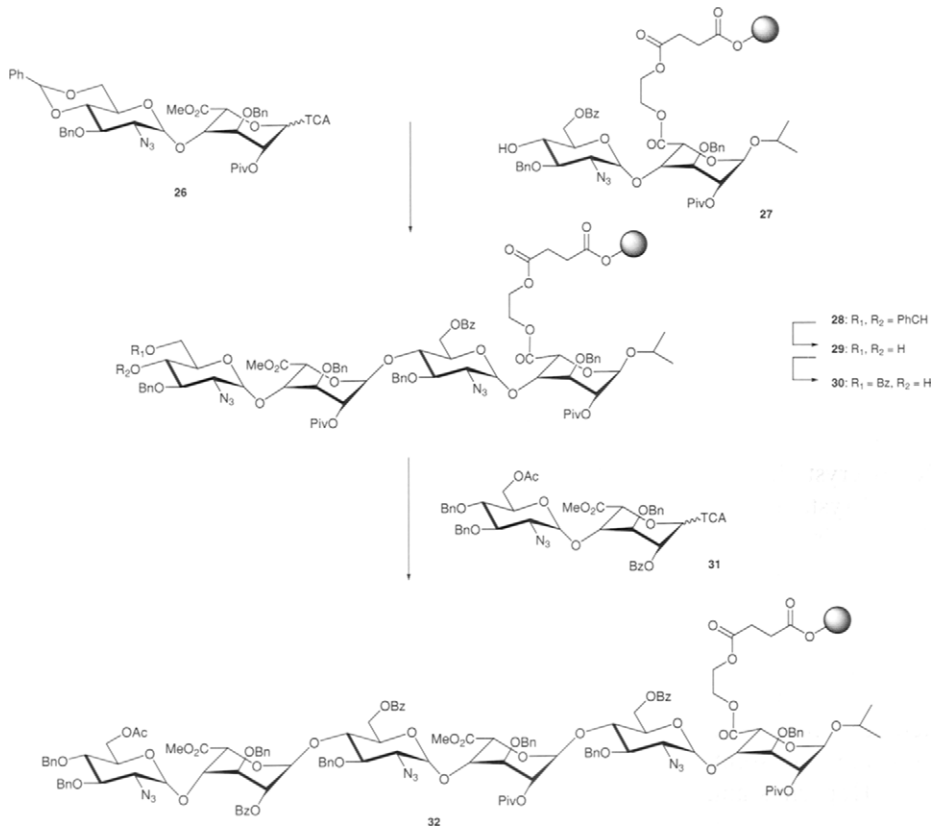

Scheme 6 Synthesis of the polymer-bound hexasaccharide.

a basic tetramer of identical subunits forms a very stable 1:1 complex with heparin (MW > 10,000) (74). Therapeutically administered heparin binds to PF-4, thus resulting in heparin-induced thrombocytopenia (HIT), a dangerous, immunologically induced loss of platelets.

Other chemokines that bind to heparin with varying affinity and specificity are the stromal cell derived factor-1α (SDF-1α), the monocyte chemoattractant protein-1 (MCP-1), and macrophage inflammatory peptide-1 (MIP-1).

2. *Annexin Interactions*

Annexins comprise a family of over 30 calcium- and phospholipid-binding proteins. At least one of the annexins is expressed in nearly every eukaryotic cell type, indicating the wide range of biological functions. The phospholipid/membrane-binding properties of the annexins are responsible for their anti-inflammatory activity, exhibiting anticoagulant and calcium channel activity (75,76). In addition, annexins are involved in membrane fusion, exocytosis, and endocytosis (77).

Annexin V is one of few proteins that bind heparin in a calcium-dependent manner (78) as verified by X-ray crystallography (79). The interaction of annexin V with heparin involves an oligosaccharide sequence of 6–8 residues (78) and sulfate groups on heparin are important. Annexins IV–VI were found to bind to heparin, heparan sulfate, and chondroitin sulfate (80).

3. *Interactions with Antithrombin III and Thrombin*

The most thoroughly studied heparin binding protein is the serine protease inhibitor antithrombin III (AT III), which interacts with thrombin and factor Xa in the blood-coagulation cascade (Fig. 9) (10). The heparin-AT III interaction is responsible for the anticoagulant activity of heparin. A characteristic heparin pentasaccharide sequence, termed DEFGH, is responsible for binding to AT III, a process that has been studied in great detail (81,82) including NMR spectroscopy (83) and X-ray crystallography (84,85).

Crystallographic studies of an AT III/pentasaccharide complex have identified the important functional groups within the pentasaccharide sequence: four charged sulfate groups and two carbonyl groups are responsible for the binding to AT III (86). The importance of the 3-*O*-sulfate group in unit F of the AT III binding site (87) was demonstrated by NMR. The 6-*O*-sulfate substituent of glucosamine D (88,89), the *N*-sulfate group of unit F (90) and the carboxylate group of the iduronic acid residue G are also required for binding to AT III and affect anticoagulant activity. The 2-*O*-sulfate group on iduronic acid G and the 6-*O*-sulfate group of unit H, while not essential for binding, contribute to the overall binding affinity (91).

Heparin's antithrombotic activity results from a ternary complex formed by heparin, AT III, and thrombin (92,93). The interaction of AT III with the pentasaccharide sequence DEFGH results in a conformational change of the protein (Fig. 10a) (4,94). AT III–pentasaccharide binding directly accelerates the inhibition of factor Xa, but not that of thrombin. The SAR of thrombin inhibition is much more complicated. In the case of thrombin, a conformational change is not sufficient to neutralize the enzyme. Although the pentasaccharide sequence is required

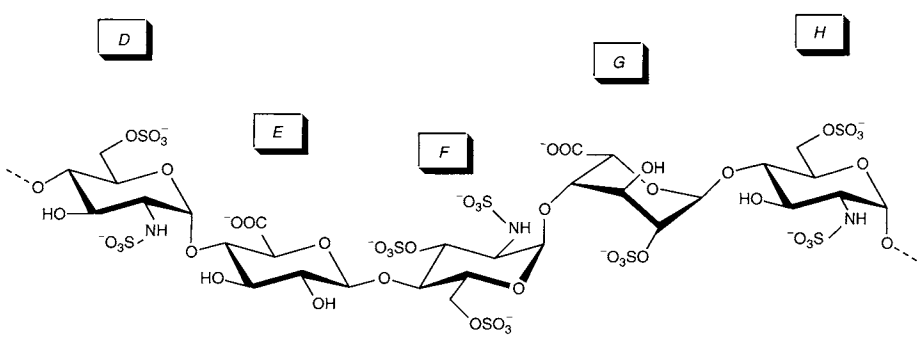

Figure 9 The AT III-binding domain.

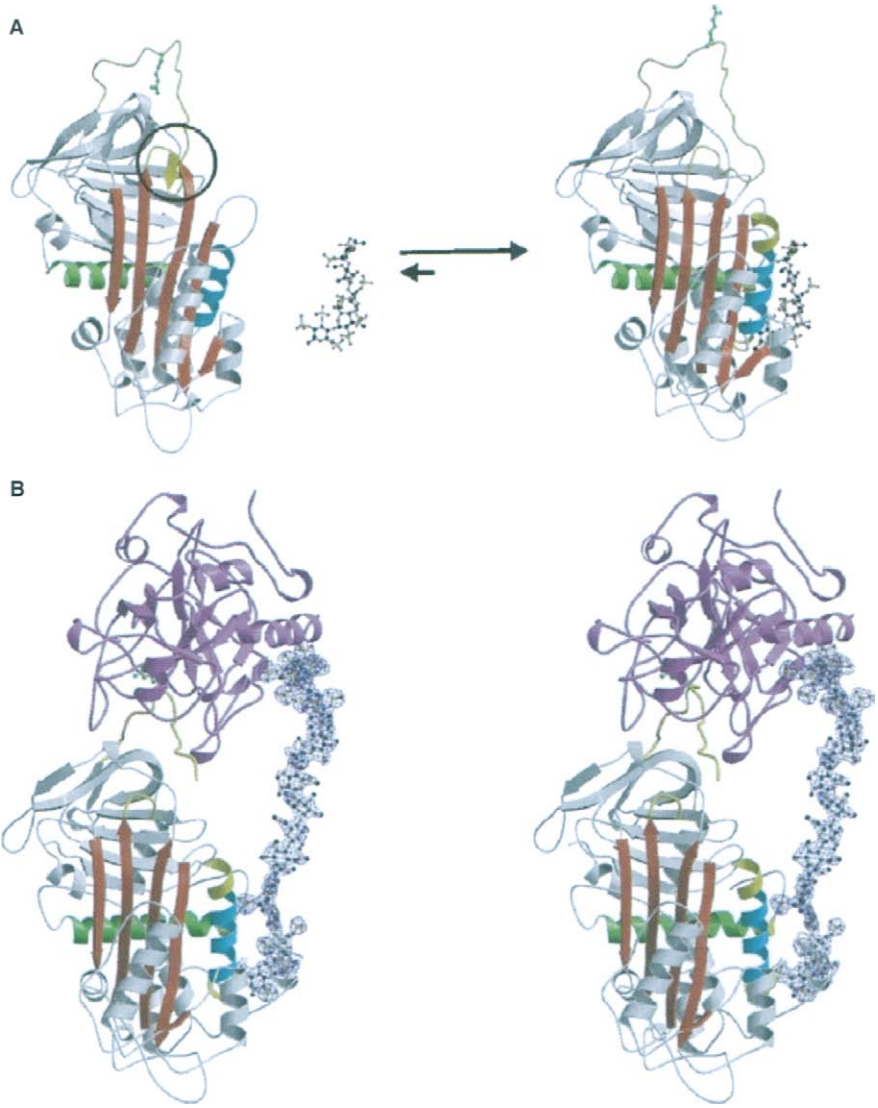

Figure 10 Heparin catalysis of thrombin inhibition by antithrombin. (A) The binding of the specific heparin pentasaccharide to antithrombin induces a global conformational change involving the expulsion of the hinge region (circled) of the reactive center loop (RCL, yellow) from the central β-sheet A (red), and extension (yellow) of the A and D helices (green and cyan, respectively). (B) Stereorepresentation of the crystal structure of the ternary complex between antithrombin (colored as above), thrombin (magenta) and heparin (balland-stick, with blue $2F_o–F_c$ electron density contoured at 1σ). Thrombin is docked toward the heparin-binding site of antithrombin, and makes several exosite interactions (reprinted with permission, from *Nature Structural & Molecular Biology*, Volume 11 © 2004 by Nature, *www.nature.com*).

for binding at AT III, a heparin chain containing 14–20 saccharide units is required to accelerate the AT III/thrombin interaction (Fig. 11). Heparin forms a bridge between AT III and thrombin in the ternary AT III/heparin/thrombin complex containing 6–8 sulfated monosaccharide units that do not interact with either protein. Although the thrombin inhibition is a desirable effect of heparin, nonspecific interactions with other proteins (e.g., platelet factor 4) result in life-threatening side effects (Fig. 10b) (95–97).

a. Synthesis of Heparin Oligosaccharides with Anti-Factor Xa Activity

The anticoagulant activity of pentasaccharide DEFGH (Fig. 9) prompted synthetic efforts aimed at the procurement of this structure as well as a host of related sequences (Fig. 12). The first synthetic heparin oligosaccharide **33**, with a high affinity for AT III, was synthesized in 1986 (98,99).

To simplify the chemical synthesis, α-methyl-glycoside **34**, displaying the same biological properties as **33**, was prepared (100,101). The synthesis of analogs of **33** has been reviewed in detail (10). Pentasaccharides **35–39** were synthesized to establish a detailed structure–activity relationship. Replacement of the reducing end glucosamine by a glucose residue indicated that *O*-sulfates can be effectively substituted for *N*-sulfates (101). The introduction of an extra 3-*O*-sulfate group at the reducing end of pentasaccharide **35** increased factor Xa affinity (102). Partial and complete *O*-methylation (**34–39**) did not significantly alter AT III affinity (Table 1) (103,104).

To assess the role of iduronic acid in the pentasaccharide with Xa affinity, this unit was replaced by an "opened carbohydrate" moiety to give **40** (Scheme 7). The "opened" fragments are readily accessible and offer the advantage that no α/β-mixture is formed during glycosylation. Coupling of **40** with glycosyl bromide **41**, followed by epimerization gave **42**. Union of **43** and **44** furnished trisaccharide **45**. Following deallylation, **46** was coupled with **43** to afford pentasaccharide **47**. The repetition of deprotection and coupling steps afforded heptasaccharide **48** and nonasaccharide **49**.

Analogs **51–56** closely resemble heparin oligosaccharides and their function, but are simpler to synthesize. These so-called "non-glycosamino" glycans contain only *O*-sulfate esters and *O*-alkyl ethers (32). All hydroxyl groups are permanently capped as methyl ethers, thus eliminating the need to discriminate between non-sulfated and sulfated hydroxyl groups. Many analogs with pseudoalternating sequences have been synthesized (105,106).

Pentasaccharides **51–53** contain a common tetrasaccharide composed of 2-*O*-sulfate, 3-*O*-methyl uronic acid moieties, while pentasaccharides **54–56** contain an invariable tetrasaccharide composed of 2,3-di-*O*-methyl uronic acid moieties (Fig. 13). Pentasaccharide **54**, containing not less than seven methyl ethers, displays the highest anti-Xa activity (1611 units/mg) and is the most potent analog of **34** identified to date (Table 2).

To determine whether the $^1C_4$ or the $^2S_0$ conformation of L-iduronic acid is necessary for binding and activation of AT III, octasulfated pentasaccharide **57** containing an L-iduronic acid unit in a fixed $^1C_4$ conformation was synthesized (107).

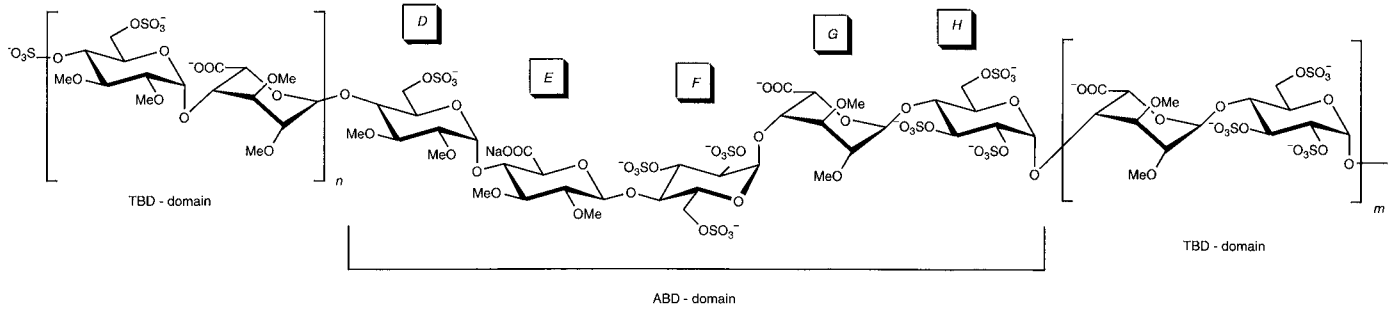

Figure 11 Structure of heparin: a heparin molecule contains an antithrombin-binding domain (ABD) and thrombin binding domains (TBD).

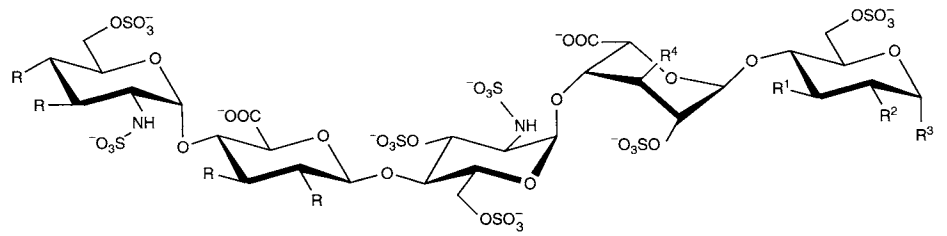

33-39

Figure 12 Different pentasaccharides with Xa affinity.

Table 1

	R	R^1	R^2	R^3	R^4	Anti-Xa activity (units/mg)
33	OH	OH	$NHSO_3^-$	OH	OH	700
34	OH	OH	$NHSO_3^-$	OMe	OH	700
35	OH	OSO_3^-	$NHSO_3^-$	OMe	OH	1270
36	OH	OSO_3^-	OSO_3^-	OMe	OH	1300
37	OH	OSO_3^-	OSO_3^-	OMe	OMe	1110
38	OMe	OSO_3^-	$NHSO_3^-$	OMe	OH	1288
39	OMe	OSO_3^-	OSO_3^-	OMe	OMe	1323

Coupling of triosyl **58** with disaccharide **59** furnished after deprotection and sulfation **57** (Scheme 8). Pentasaccharide **57** exhibited very low anti-Xa activity, indicating that either the $^2S_0$ conformation of L-iduronic acid or a flexible L-iduronic acid residue, presence of both conformers, is essential to bind and activate AT III.

Further studies involving different pentasaccharides indicated that a significant shift of the conformational equilibrium from $^1C_4$ toward the $^2S_0$ conformation was observed when the L-iduronic acid residue is adjacent to a 3-*O*-sulfated glucosamine (unit F) (24). The additional sulfate on unit F is the key structural element responsible for binding to AT III. Pentasaccharides with an extra sulfate group introduced in unit H also show higher affinity for AT III, possibly due to the increased presence of the $^2S_0$ conformation (101).

Replacement of an *O*-glycoside by a *C*-glycoside bond in anti-factor Xa pentasaccharides slightly decreased the affinities of **62** and **63** for AT III and anti-factor Xa (Scheme 9) (108,109).

To increase the $^1C_4$-content of iduronic acid, a C-3-deoxygenated L-iduronic acid residue was incorporated as unit G (Fig. 14) (110).

Decrease of the nonbonding interactions between C-3 and other axial substituents shifts the conformational equilibrium to render unit G predominantly in a $^1C_4$ conformation (65%) of unit G. The $^2S_0$ conformer that predominates in **65** (64%) is now considerably less abundant (24%). Since pentasaccharide **65** has a much higher affinity for AT III than **64**, the conformation of unit G highly

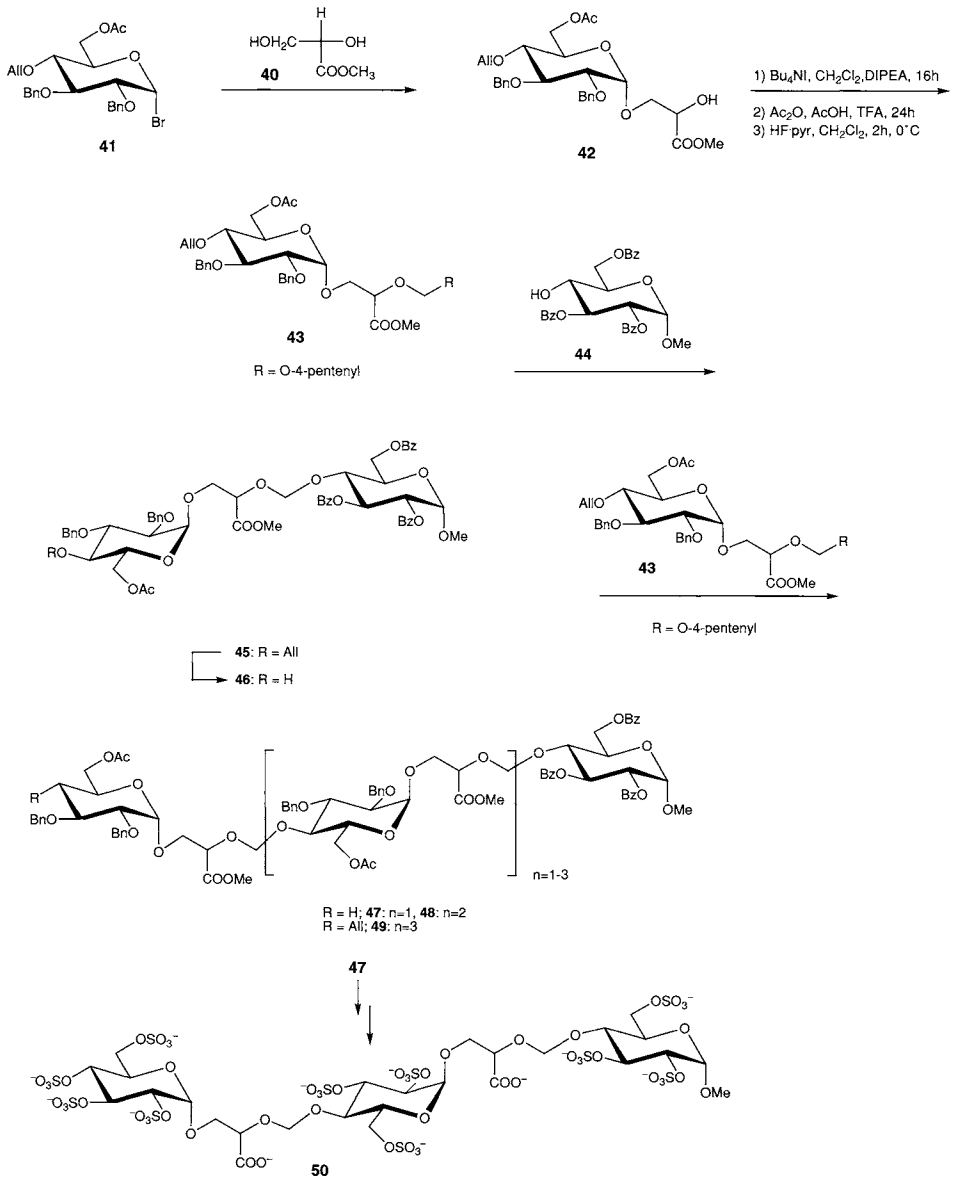

Scheme 7 Synthesis of open-chain oligosaccharides.

influences AT III affinity. To further address the influence of uronic acid conformation on AT III binding, conformationally locked pentasaccharides were prepared. The L-iduronic units were locked in the $^1C_4$ (**66**) or $^2S_0$ (**67**) conformation by covalently bridging the C-2/C-5 and C-3/C-5 ring atoms, or in the $^4C_1$ (**68**) conformation by introducing a methoxymethyl substituent at C-5 (Fig. 15) (58,111).

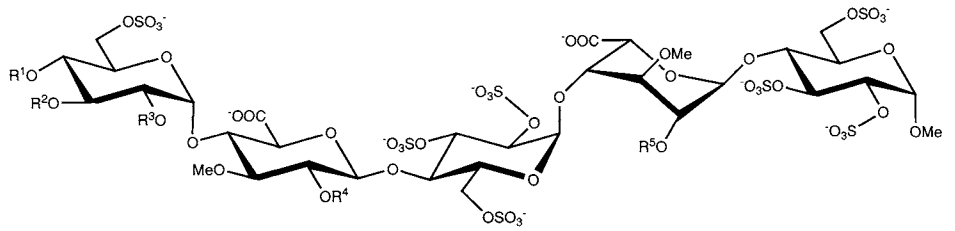

Figure 13 Structures of pentasaccharides with pseudoalternating sequence.

Table 2

Nr	R^1	R^2	R^3	R^4	R^5	Anti-Xa activity (units/mg)
51	Me	Me	Me	SO_3^-	SO_3^-	1217
52	Me	Me	SO_3^-	SO_3^-	SO_3^-	1159
53	Me	SO_3^-	SO_3^-	SO_3^-	SO_3^-	1184
54	Me	Me	Me	Me	Me	1611
55	Me	Me	SO_3^-	Me	Me	1318
56	Me	SO_3^-	SO_3^-	Me	Me	1404

Pentasaccharide **67**, which contains a $^2S_0$ iduronic acid binds to AT III and can inhibit factor Xa. In contrast, the pentasaccharides **66** and **68** containing unit G locked in the $^1C_4$- or $^4C_1$-conformation respectively, exhibit little inhibitory activity. The anti-Xa activity of compound **69** that contains a flexible G unit is similar to reference pentasaccharide **54** (Table 3).

Insertion of one additional bridging carbon atom in pentasaccharide **70** resulted in an iduronic acid that failed to adopt the ideal $^2S_0$ conformation as indicated by ^{1}H-NMR coupling constants (Fig. 16) (35). The anti-factor Xa activity (1198 units/mg) of pentasaccharide **70** is similar to that of pentasaccharide **39** (1323 units/mg) and the biological activity of **70** is slightly better than that of **67** (1073 units/mg) containing one carbon atom to bridge C-2 and C-5.

To determine whether the absence of the noncritical sulfate groups in unit H influences the biological activity, three pentasaccharides (**71–73**) containing the $^2S_0$-locked iduronic acid as well as variously sulfate or methyl groups on the reducing end unit H were synthesized (Table 4) (112). The 3-*O*-sulfate in unit H increases the affinity for AT III and shifts the equilibrium toward the $^2S_0$-conformation. The 6-*O*-sulfate group in H interacts with the 2-*O*-sulfate group on unit G resulting in enhanced biological activity, whereas the removal of one of these sulfate groups results in 10-fold lower activity.

The crystal structure of the AT III–pentasaccharide (**74**) complex illustrates that all carboxylate groups are interacting with the positively charged Lys and Arg residues of AT III (86). The carboxylate groups of Glu113 and Asp117 are separated from the α-*O*-methyl group and the anomeric center. Therefore, the exchange of the α-*O*-methyl group in **54** by a α-*C*-glycosidic ethylamine tether should result

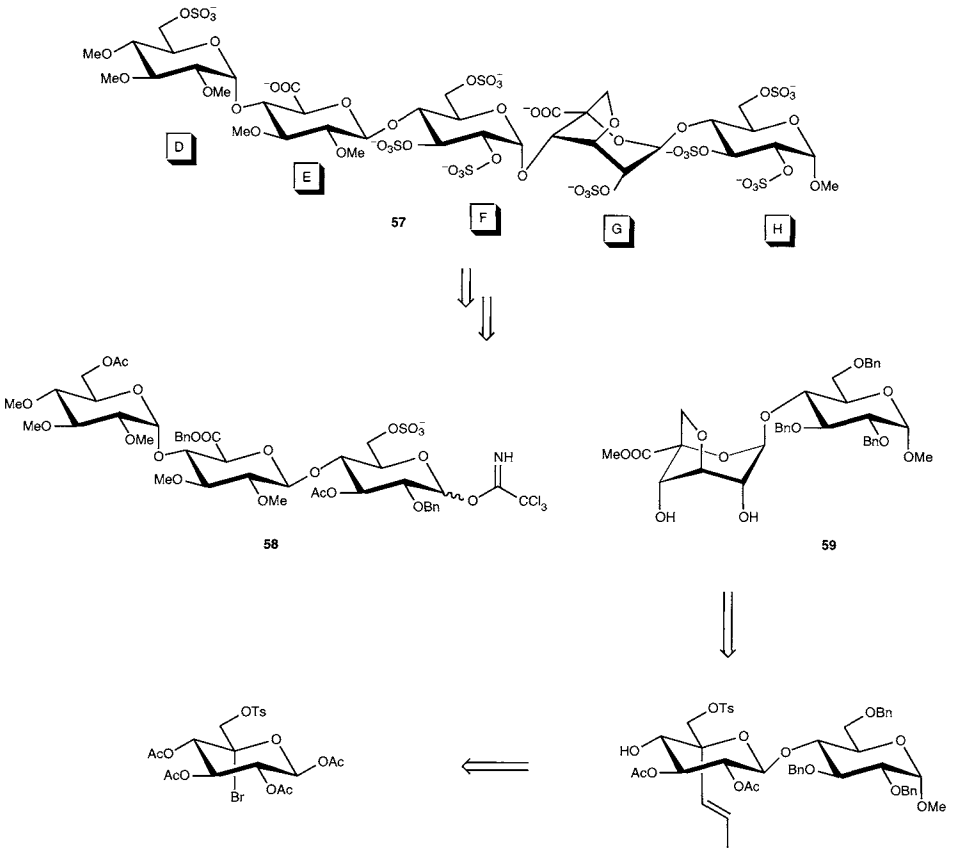

Scheme 8 Retrosynthetic synthesis of a bridged heparin analog.

in an additional binding interaction with Glu113 and Asp117 in AT III. Pentasaccharides (**75–84**) having one or two positively charged amino groups at the reducing end were prepared (Fig. 17) (113). To minimize unwanted intramolecular salt bridges between the terminal amino group and the sulfate groups, the R^1 sulfate of **75** and the R^1 and R^2 sulfates of **80** were replaced by methyl groups in pentasaccharides **76** and **81**. Pentasaccharides **77** and **82** contained additional positively charged amino substituents on the ethylamino tether.

All pentasaccharides were less active than **54** (Table 5). The amino groups in **78** and **83** are not interacting favorably with the negatively charged target amino acids Glu113 and Asp117. Based on the lower activity of **76**, compared to **81**, it can be concluded that the 6-*O*-sulfate may form an intramolecular salt bridge with the amine. Incorporation of two positively charged groups (**77** and **82**) results in decreased activity and further suggests that the amino acid residues are not available for additional binding interactions.

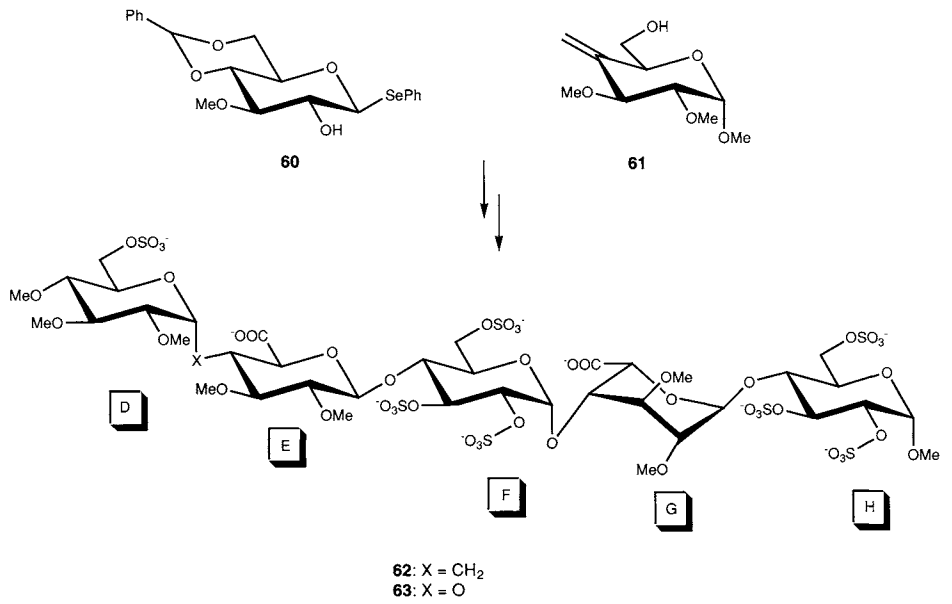

Scheme 9 Synthesis of a pentasaccharide with a C-interglycosidic bond.

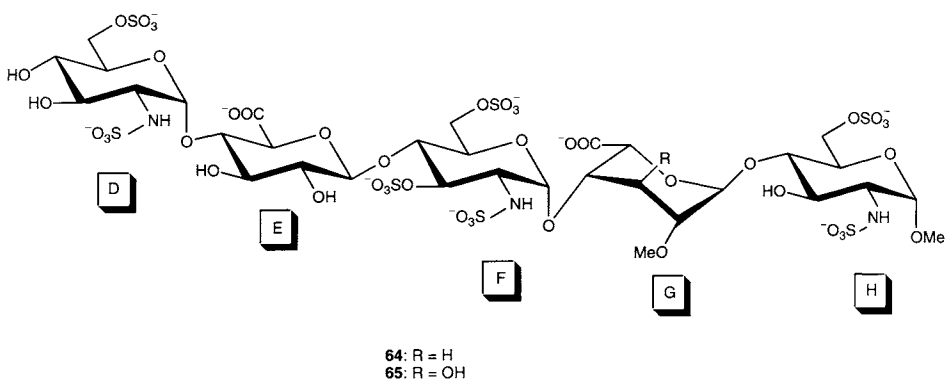

Figure 14 Pentasaccharide **64**, deoxygenated at C-3 of unit G.

b. Heparin Oligosaccharides with Full Anticoagulant Properties

All pentasaccharides described above exhibit strong anti-factor Xa activity but fail to inhibit thrombin. Longer heparin chains (14–20 saccharides) are required for antithrombin activity. Long, sulfated oligosaccharides can be obtained by connecting two sequences such as ABD and TBD through a spacer. Several aspects need to be considered in defining the nature of the spacer: (1) the type of spacer (charged or neutral, linear, flexible or rigid); (2) the direction of chain elongation (from the

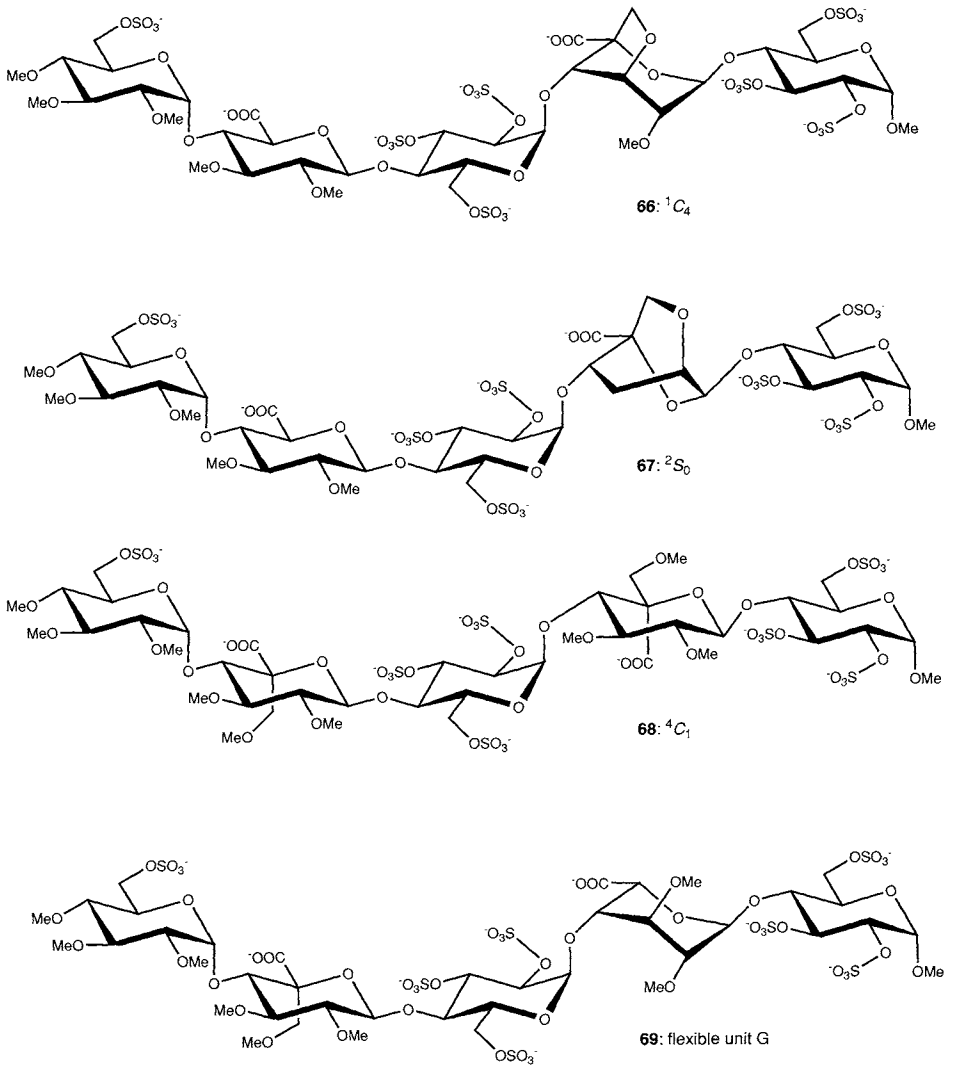

Figure 15 Pentasaccharides containing iduronic acid unit G locked in the $^2S_0$, $^1C_4$, $^4C_1$ conformation.

reducing end or nonreducing end); and (3) the structural requirements of the thrombin-binding domain of heparin.

With these considerations in mind, a model of a heparin/AT III/thrombin complex containing different glycoconjugates in the AT III-binding domain ABD, a linear spacer (50 atoms in length corresponding to an oligosaccharide of 12–18 units), and a persulfated maltotrioside representing the thrombin binding domain TBD was prepared (114). The model suggests that TBD should be attached via the

Table 3

		Anti-Xa activity (units/mg)
54	Reference	1611
66	$^1C_4$	43
67	$^2S_0$	1073
68	$^4C_1$	115
69	Flexible unit G	1345

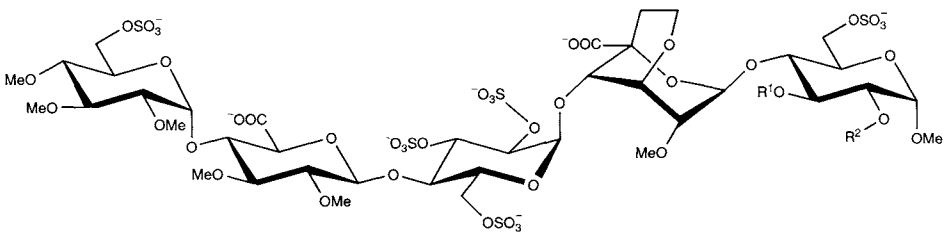

70: R^1, $R^2 = SO_3^-$
71: R^1, R^2 = Me
72: $R^1 = SO_3^-$, R^2 = Me
73: R^1 = Me, $R^2 = SO_3^-$

Figure 16 Pentasaccharides with two carbon atoms in the bridge.

Table 4

	R^1	R^2	Anti-Xa activity (units/mg)
70	SO_3^-	SO_3^-	1198
71	Me	Me	960
72	SO_3^-	Me	886
73	Me	SO_3^-	1078

linker at the nonreducing end of ABD. Different short, persulfated oligosaccharides **90–103** were synthesized and attached to ABD (**54**) to study the binding of TBD to thrombin. The desired ABD unit was obtained over four steps by glycosylation of the tetrasaccharide **85** with **86** (Scheme 10). Coupling of ABD-trisaccharide **87** and the TBD-fragment **88** afforded glycoconjugate **89**. The heparin portions were separated by a 53-atom spacer that corresponds to an 18-mer stretch of oligosaccharide.

Compounds **90–92** display both good AT III-mediated anti-factor Xa and antithrombin activity and indicate that an increase in charge of the TBD unit results higher antithrombin activity (Table 6).

The synthesis of symmetric conjugates that are able to bind AT III on one end and thrombin on the other end was also of interest. Therefore, pentasaccharides **53**,

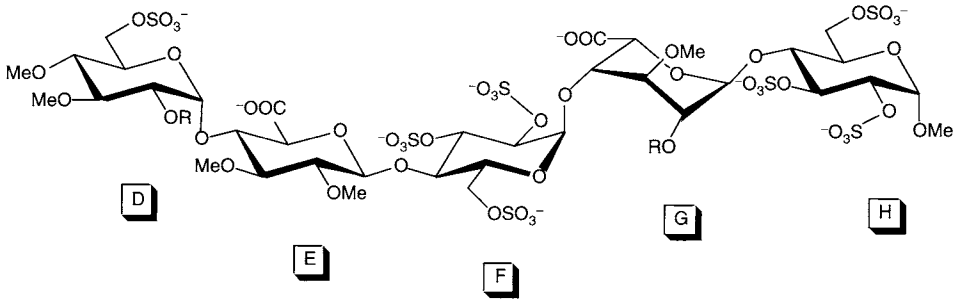

54: R = Me
74: R = SO_3^-

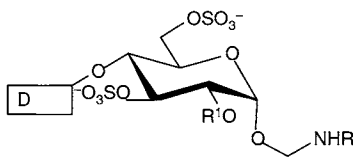

75: $R^1 = SO_3^-, R = H_2^+$
76: R^1 = Me, $R = H_2^+$
77: R^1 = Me, R = 
78: R^1 = Me, R = Z
79: R^1 = Me, R = 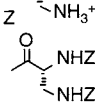

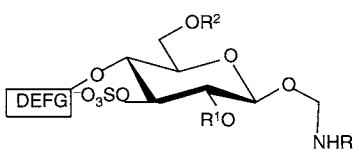

80: $R^1 = SO_3^-, R^2 = SO_3^-, R = H_2^+$
81: R^1, R^2 = Me, $R = H_2^+$
82: R^1, R^2 = Me, R = 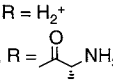
83: R^1, R^2 = Me, R = Z
84: R^1, R^3 = Me, R = 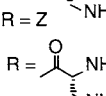

Figure 17 Pentasaccharides containing charged amino groups at the reducing end.

54, **56** containing seven, nine, and eleven sulfates were dimerized to produce glycoconjugates **93–95** (Fig. 18). As observed in previous experiments antithrombin activity increases with the number of sulfate groups.

Based on these findings, it was concluded that antithrombin activity increases with the number of sulfate groups. The number of sulfates in the thrombin-binding domain appeared to be more important than the number of carbohydrates.

Table 5

	Anti-Xa activity (units/mg)
54	938
76	77
77	18
78	105
79	28
81	21
82	18
83	138
84	49

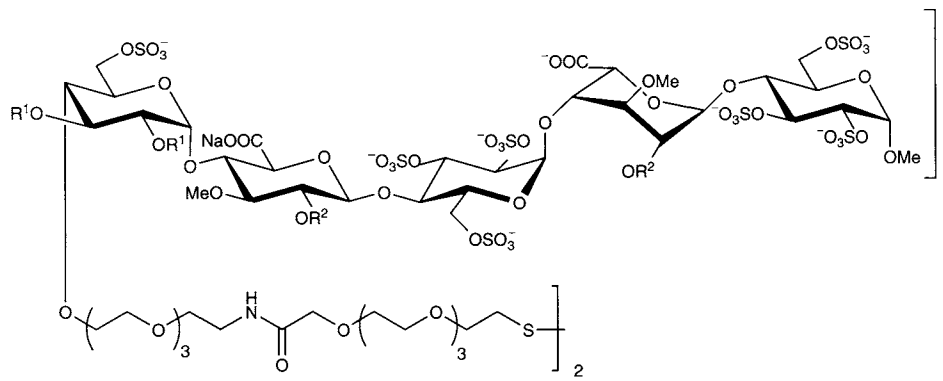

93: R^1, $R^2 = CH_3$
94: $R^1 = SO_3^-$, $R^2 = CH_3$
95: R^1, $R^2 = SO_3^-$

Figure 18 Glycoconjugate derived through dimerization.

The influence of the length of the spacer was investigated using conjugates **96–99**. With an 18-atom spacer only anti-factor Xa activity was observed, whereas incorporation of a 32-atom spacer induces some antithrombin activity. An increase in spacer length to 46 or 59 atoms resulted in a sharp increase in antithrombin activity. Conjugate **100** was synthesized to establish if reduction of the AT III affinity of the pentasaccharide in a conjugate affects both the anti-factor Xa and antithrombin activity. Conjugate **100** is similar to **92**, but contains a pentasaccharide with a 50-fold lower activity for AT III. Surprisingly, the antithrombin activity of **100** is almost identical to that of **92**, but exhibits a sevenfold lower anti-factor Xa activity. An explanation for this phenomenon could be that in the case of conjugate **100** the assembly of the ternary complex occurs through both the expected binary AT III–**100** complex. This leads to an anti-factor Xa and antithrombin activity, and a binary thrombin–**100** complex that lead only to a ATIII-mediated antithrombin

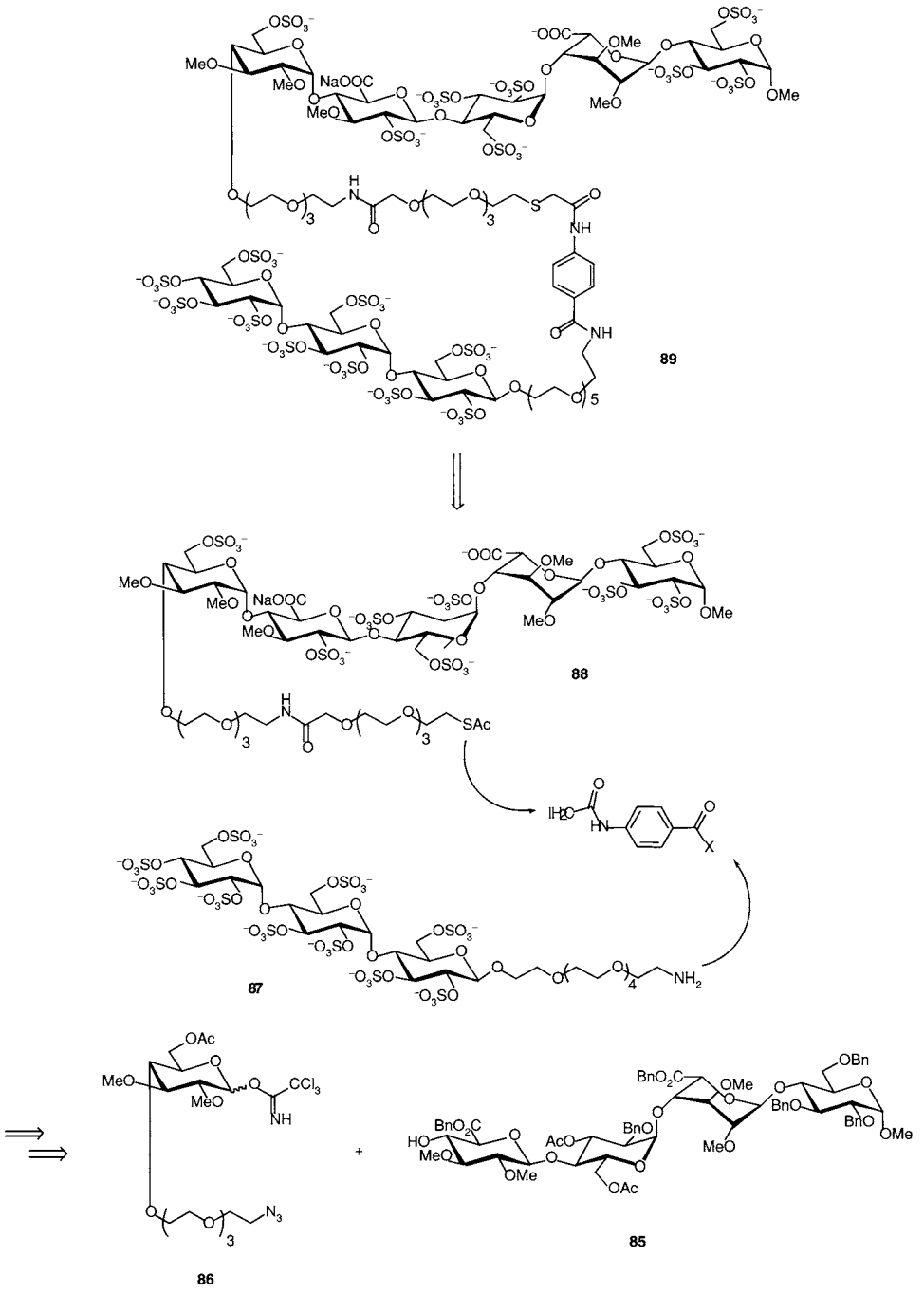

Scheme 10 Strategy for the synthesis of glycoconjugates with a flexible linker.

Table 6

Nr	TBD	Spacer length	ABD	Anti-factor Xa activity (units/mg)	Antithrombin activity (units/mg)
90	Cellobiose (7-S)	53	**54**	740	10
91	Maltotriose (10-S)	53	**54**	490	64
92	Maltopentaose (16-S)	56	**54**	280	330
93	TBD=ABD (7-S)	53	**54**	770	14
94	TBD=ABD (9-S)	53	**56**	640	36
95	TBD=ABD (11-S)	53	**53**	280	160
96	Maltopentaose (10S-)	18	**54**	540	1
97	Maltopentaose (10S-)	32	**54**	700	15
98	Maltopentaose (10-S)	46	**54**	420	20
99	Maltopentaose (10-S)	59	**54**	630	120
100	Maltotriose (16-S)	56	**54**	41	280
101	DS tetra (4-S)	53	**54**		2
102	DS tetra (5-S)	53	**54**		10
103	Heparin tetra (6-S)	53	**54**		10
104	Cellobiose (7-P)	53	**54**	500	22
105	Cellobiose (7-IP)	53	**54**	690	5
106	Maltotriose (10-P)		**54**	1000	167
39	T_{18}-oligonucleotide		**54**	173	5
54		–		1611	–
Heparin	Oligosaccharide	±50		160	160

activity. The formation of the latter binary complex occurs more easily relative to the thrombin–heparin binary complex because the pentasaccharide domain of conjugate **100** has a lower activity for AT III, whereas its thrombin-binding domain should interact more strongly with thrombin.

Heparin-like conjugates **101–103** that contain identical ABD domains but different TBD domains were prepared (115). Conjugate **101** contains a TBD domain with four sulfate groups and exhibited low antithrombin activity. The conjugates **102** and **103** showed an antithrombin activity similar to **90**. The charge density of the TBD moiety determines the antithrombin inhibitory activity, whereas the carbohydrate structure of TBD has no effect.

To probe the effect of the charged group on high-affinity ABD domains, perphosporylated cellobiosyl saccharides **104**, **105** with seven and fourteen negative charges, respectively, as well as maltotrioside **106** carrying 20 negative charges were synthesized (Fig. 19). Incorporation of lipophilic groups into the TBD domain was expected to enhance the interaction with thrombin. The introduction of a phosphate ester in TBD increased the affinity of TBD for thrombin, while the replacement of one sulfate group by a phosphate ester in the ABD decreased the affinity of ABD for AT III.

Based on the observation that oligonucleotides can associate with the heparin-binding site (116), conjugate **107** was prepared where part of the spacer and the

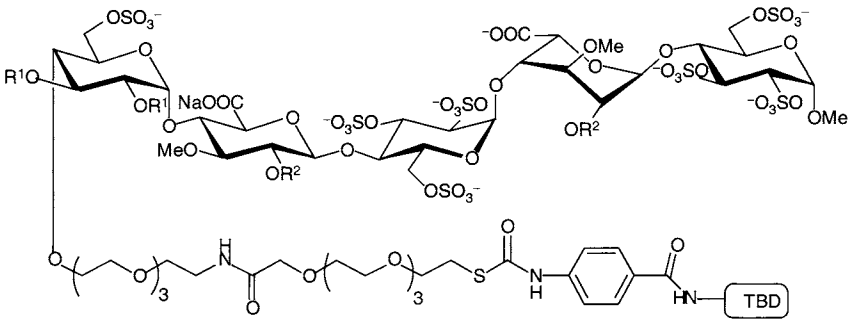

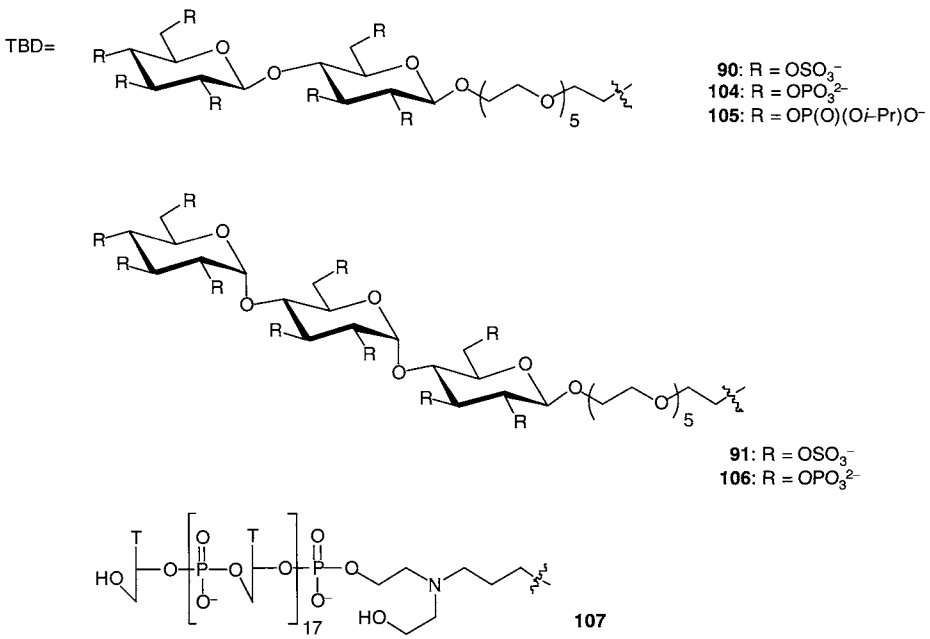

Figure 19 Alternative TBD's for thrombin inhibition.

TBD domain were replaced by an oligonucleotide. The low anti-factor Xa activity (173 units/mg) and antithrombin activity (5 units/mg) of **107** illustrated the existence of a weak interaction of oligonucleotides with the TBD domain. The interaction of the ATB domain with AT III requires more than just the interaction of the TBD domain with thrombin.

N-(2-naphtalenesulfonyl)-glycyl-(D)-4-aminophenyl-alanyl-piperidine (NAPAP) derivate **108** served as another noncarbohydrate TBD (Fig. 20) (117). NAPAP **109** itself binds directly to the active site of thrombin (EC_{50} = 0.75 μM). The NAPAP-conjugate **108** was designed to stimulate AT III-mediated anti-factor Xa activity and to inhibit thrombin. Indeed, conjugate **108** exhibited antithrombin activity (IC_{50} = 0.35 μM) and anti-factor Xa (885 units/mg) and confirmed that the NAPAP-conjugate is a better inhibitor than the combination of the free pentasaccharide and NAPAP.

All approaches discussed thus far incorporated a flexible spacer. Another class of oligosaccharides containing a rigid spacer, and decreased charge density was synthesized. ABD domains with at least six negative charges also served as a TBD because the interaction of thrombin with heparin results from an electrostatic attraction that depends on the density of negative charges. It should be noted that AT III–ABD binding affinity is much higher than thrombin-TBD binding affinity.

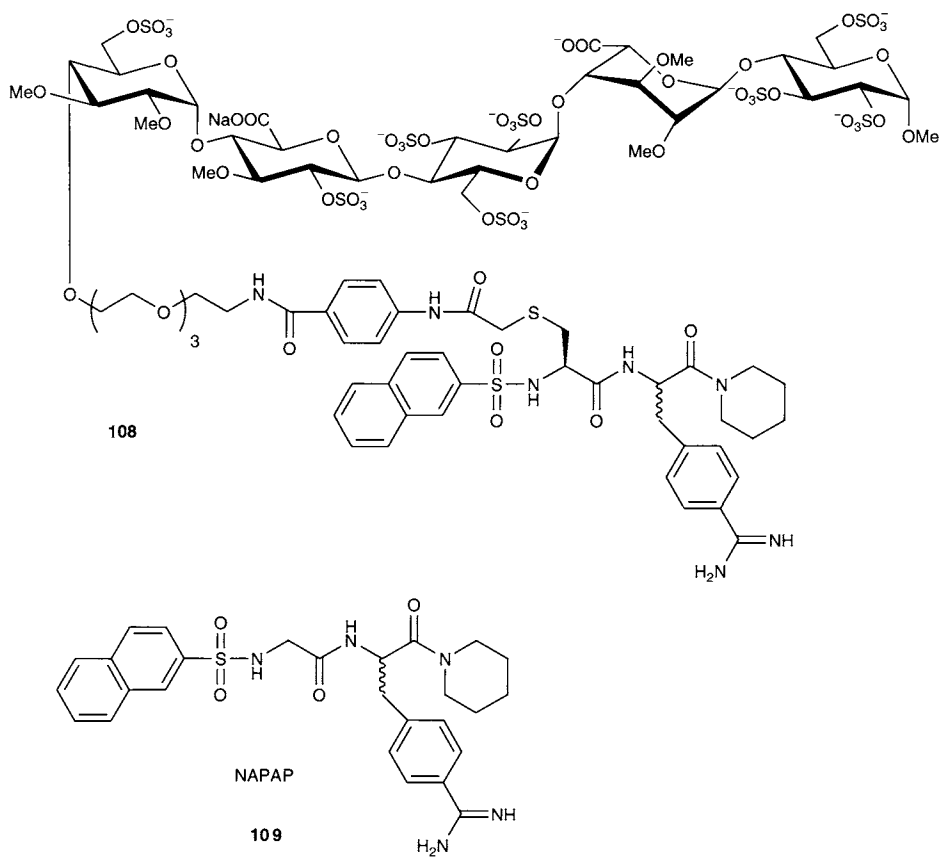

Figure 20 Example for a noncarbohydrate TBD.

A sequence of repeating ABDs would increase the affinity for AT III, but prevent thrombin binding. Oligosaccharides with anti-factor Xa and antithrombin affinity require an affinity of AT III–ABD and thrombin-TBD in the same order of magnitude. Based on the high AT III affinity of pentasaccharide **52**, hexasaccharides consisting of a repeat disaccharide should have a reduced, but still significant affinity for AT III. The highly symmetrical antithrombin binding domain obtained from a single disaccharide results in a much-simplified synthesis of glycoconjugates for drug development. The first carbohydrates exhibiting full heparin anticoagulant properties were synthesized in 1998 (118,119).

Three hexasaccharides that contain one additional trisulfated glucose at the nonreducing end (**109**), a D-glucuronic acid (**110**), and L-iduronic acid as the only uronic acid in the compound (**111**) were synthesized (Fig. 21). The introduction of the additional trisulfated glucose in **109** results in binding to AT III. The binding affinity of **110** that contains only D-glucuronic acids decreased dramatically. Oligomer **111** which contains only L-iduronic acids displayed ideal binding properties with an affinity for AT III ($K_d = 0.35\ \mu M$) that is similar to heparin–thrombin binding ($K_d = 1\ \mu M$). Anti-factor Xa activity of **111** was reported at 325 units/mg.

Based on these findings, larger heparin fragments related to **111** were synthesized (Scheme 11) (120). All compounds (**112–117**) show similar anti-factor Xa activity. The smaller oligosaccharides (hexadecamer, octadecamer, decadecamer,

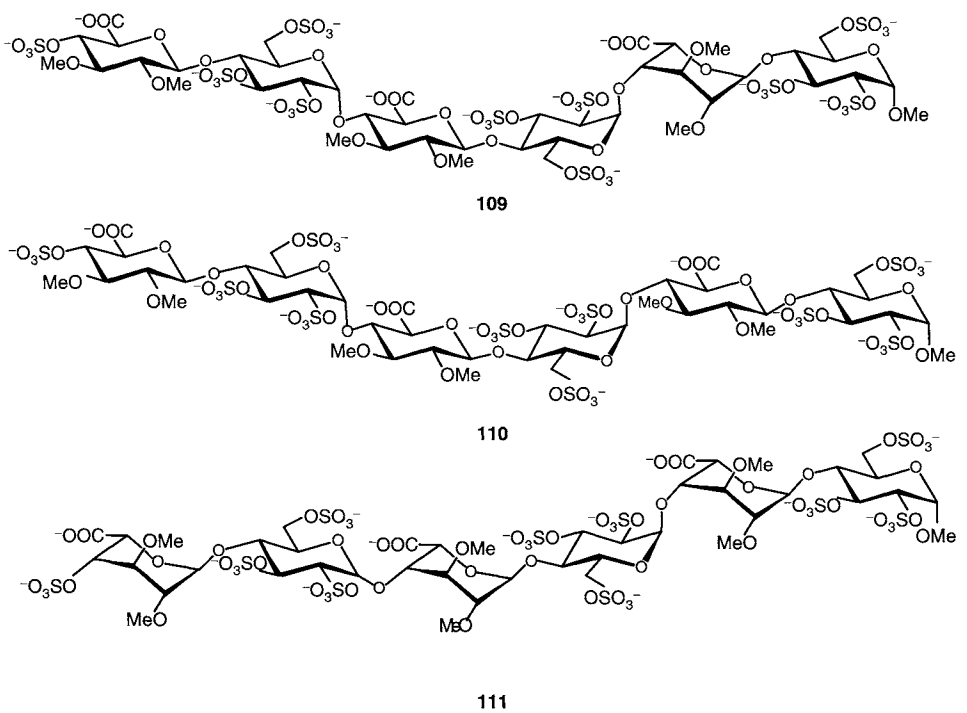

Figure 21 Carbohydrates with full anticoagulant properties for heparin.

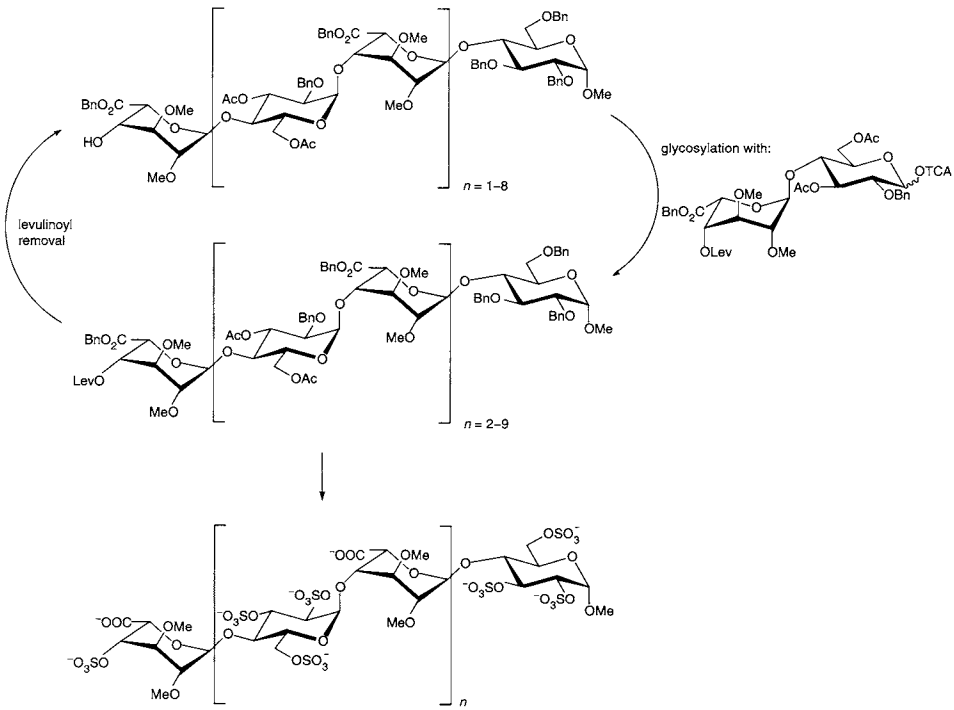

112: $n = 4$; 113: $n = 5$; 114: $n = 6$; 115: $n = 7$; 116: $n = 8$; 117: $n = 9$;

Scheme 11 Strategy for the synthesis of larger oligosaccharides.

dodecadecamer, and tetradecamer) do not inhibit thrombin while for larger oligomers [hexadeca-(**115**), octadeca-(**116**), and eicosasaccharide(**117**)] activity increases with size. The eicosamer is half as potent as standard heparin (Table 7).

Exchange of the polyethylene glycol spacer for a rigid permethylated polymaltose spacer (**118**) increased the antithrombin activity tenfold while anti-factor Xa activity remained similar to **92** (Fig. 22). Due to the lower charge density and the rigidity of the spacer, neutralization of **118** by PF4 was reduced by a factor of 20 when compared with standard heparin (121).

To create oligomers with a charge density similar to that of heparin, glycoconjugates **119–121** possessing a specific ABD domain and a TBD domain that is not recognized by AT III were synthesized (Scheme 12) (122). Synthesis of these structures relied on the elongation of the ABD domain at the nonreducing end by the addition of 3-*O*-methyl-2,6,-di-*O*-sulfo-D-glucose oligomers with alternating α-, and β-(1 → 4) linkages.

Anti-factor Xa activity and affinity for AT III were similar for all compounds, whereby thrombin inhibition increased with growing chain length. Nonadecamer

Table 7

Nr	Size	Anti-factor Xa activity (units/mg)	Antithrombin activity IC_{50} (ng/mL)
112	10-mer	325	>10,000
113	12-mer	405	>10,000
114	14-mer	360	>10,000
115	16-mer	310	130
116	18-mer	360	23
117	20-mer	290	6.7
Heparin	–	170	3
119	15-mer	370	41
120	17-mer	270	5.3
121	19-mer	290	1.7
122	17-mer	270	9.3
123	16-mer	350	490
124	18-mer	260	360
125	20-mer	210	88

121 was as potent as the most active fraction isolated from standard heparin. Heptadecasaccharide **122** that contained even less charge density, exhibited the same anticoagulant properties, but could not be neutralized by PF4 even at very high concentrations (100 μg/mL) (Fig. 23) (Table 7) (123).

A new family of heparin mimetics (**123–125**) combined a pentasaccharide ABD domain with a TBD domain composed of a low sulfated sequence of repeating 2,3-di-*O*-methyl-6-*O*-sodium sulfonato-α-D-glucosyl units (Fig. 24) (124). Only small differences in the AT III affinity and in the inhibition of Xa were observed. These conjugates are less potent than heparin, but none are neutralized by PF4, indicating that this group of molecules may constitute alternatives to standard heparin (Table 7).

Until 2001 there was no experimental proof that the thrombin binding domain in heparin is located at the nonreducing end of the antithrombin binding domain, and that the factor Xa inhibition is not affected by elongation of the antithrombin binding pentasaccharide sequence. Different heparin mimetics were used to investigate this hypothesis (Fig. 25) (33). The *N*-sulfated glucosamine units of heparin were replaced by *O*-sulfated glucose, and *O*-methyl groups were incorporated in place of hydroxyl groups to simplify the synthesis. In the TBD domain, 2,6-di-*O*-sulfonato-β-D-glucose substituted 2-*O*-sulfonato-α-L-iduronic acid to maintain the number of charges per saccharide unit as in heparin.

All analogs (**126–129**) exhibited the same activity for anti-factor Xa and affinity for AT III. Again, inhibition of thrombin was increasing with chain length. Oligosaccharide **129** does not inhibit thrombin in the presence of AT III. These results demonstrate that the TBD must be located at the nonreducing end of ABD to inhibit thrombin.

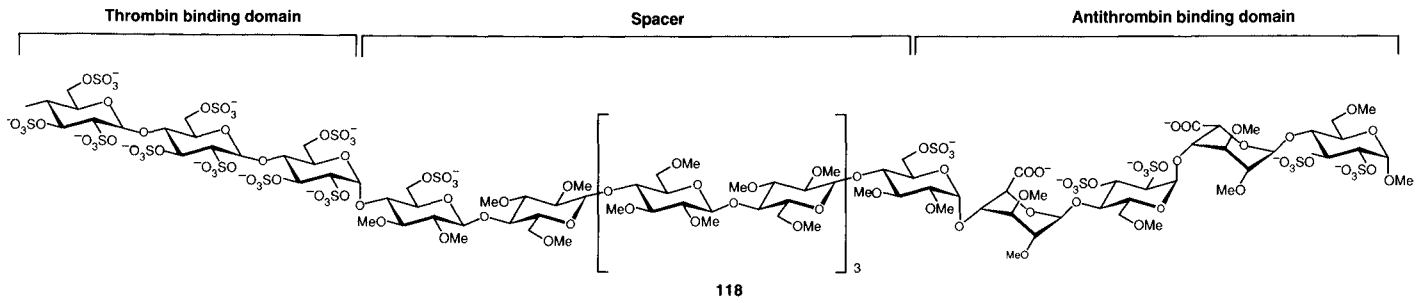

Figure 22 Oligosaccharide with a permethylated polymaltose spacer.

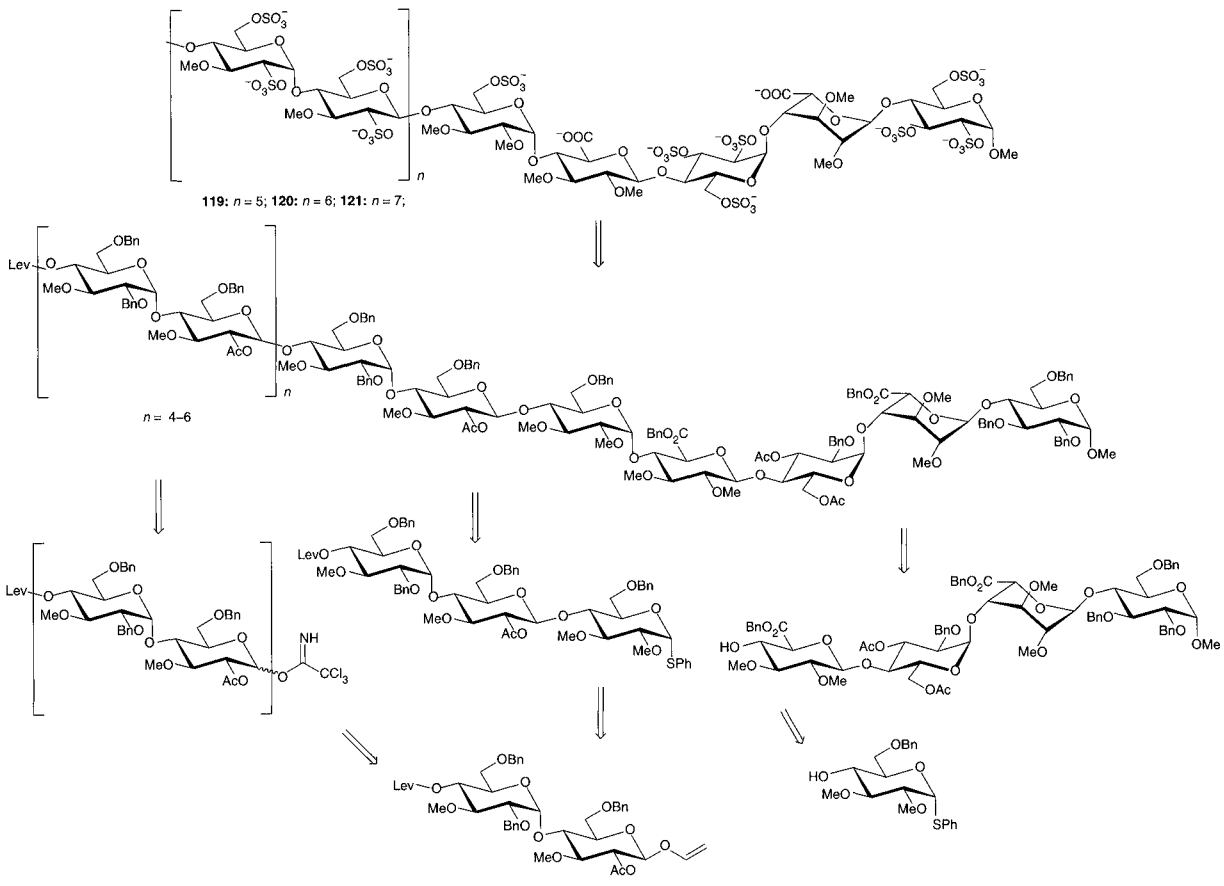

Scheme 12 Retrosynthetic way for the synthesis of glycoconjugates with a rigid spacer.

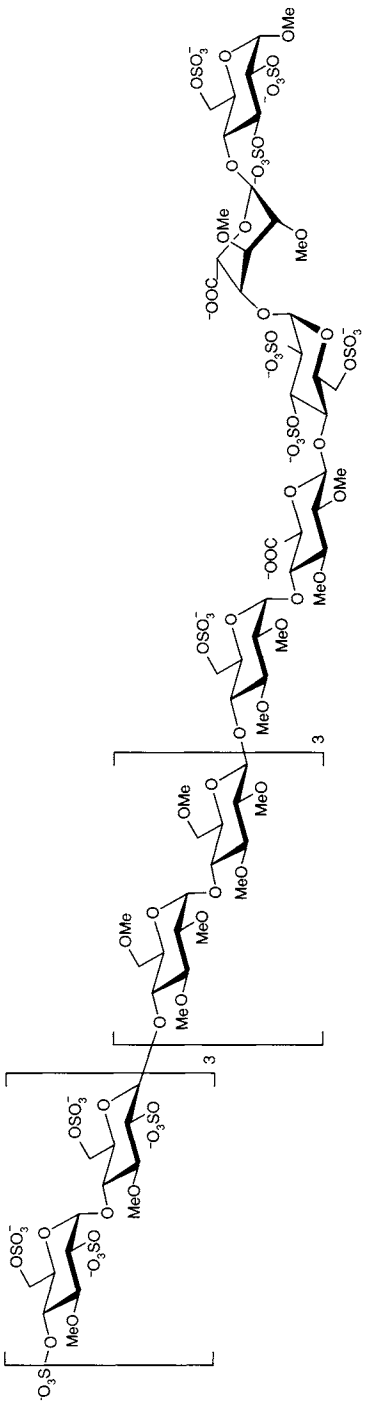

122

Figure 23 Heptadecasaccharide, not neutralized by PF4.

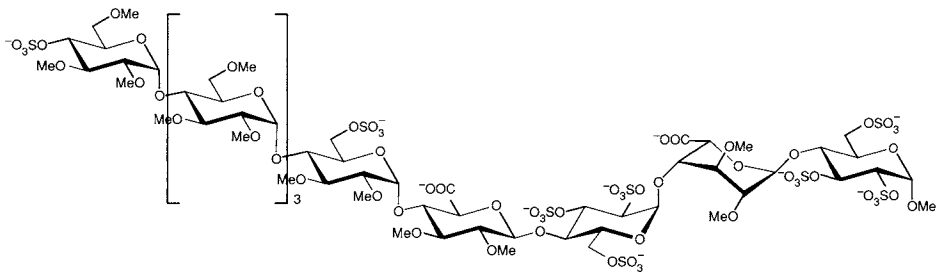

123: $n = 10$
124: $n = 12$
125: $n = 14$

Figure 24 Heparin mimetic with low sulfated sequence.

4. *Interactions with Growth Factors*

Many growth factors, including the fibroblast growth factors (FGFs), bind to the extracellular matrix of target tissues by interacting with GAGs such as heparin and heparan sulfate. The mammalian FGFs belong to a protein family involved in cell proliferation, differentiation, and angiogenesis. Growth factors bind relatively tightly to GAGs (84,125,126).

Heparin interacts directly with the FGF-2 receptor, and mediates a high-affinity FGF–FGFR complex (127). One FGF molecule binds to four to five saccharide units in heparin (128,129). Heparan sulfate stabilizes the formation of FGF oligomers, an essential step in promoting the oligomerization and activation of tyrosine kinase FGF receptor (FGFR). The FGFs interact with two distinct extracellular receptors and proteoglycan modified FGFR dimerization activates the FGF-mediated signal transduction process.

The most thoroughly studied members of the fibroblast growth factor family are FGF-1 (acidic FGF) and FGF-2 (basic FGF) (Fig. 26). The minimum heparin sequences necessary for FGF-1 and FGF-2 to promote assembly of active structures have been determined (130–134). Short oligomers such as trisaccharides and pentasaccharides are able to bind FGF-2 (84,131,135); however longer oligomers are necessary for dimerization and activation of FGFs (Fig. 27) (136). X-ray crystal structures of FGF-1 (137) and FGF-2 (84) complexed with heparin oligosaccharides helped identify functional groups crucial for signaling (20). The binding region for FGF-2 has been identified as a pentasaccharide sequence containing a single, essential, *O*-sulfate group at C-2 of iduronic acid (135) and *N*-sulfated D-glucosamine. For efficient binding of FGF-2, all uronic acid units must be present as L-iduronic acids (138,139). While 6-*O*-sulfate groups are necessary for binding and activation of FGF-1, sulfates are not required for binding to FGF-2 (135,140) but are thought to be required for the mitogenic activity of FGF-2 (141). Crystal structures of FGF–heparin complexes further strengthen these observations (Fig. 26) (84,137,142). Although FGF–heparin interactions are dominated by interactions involving

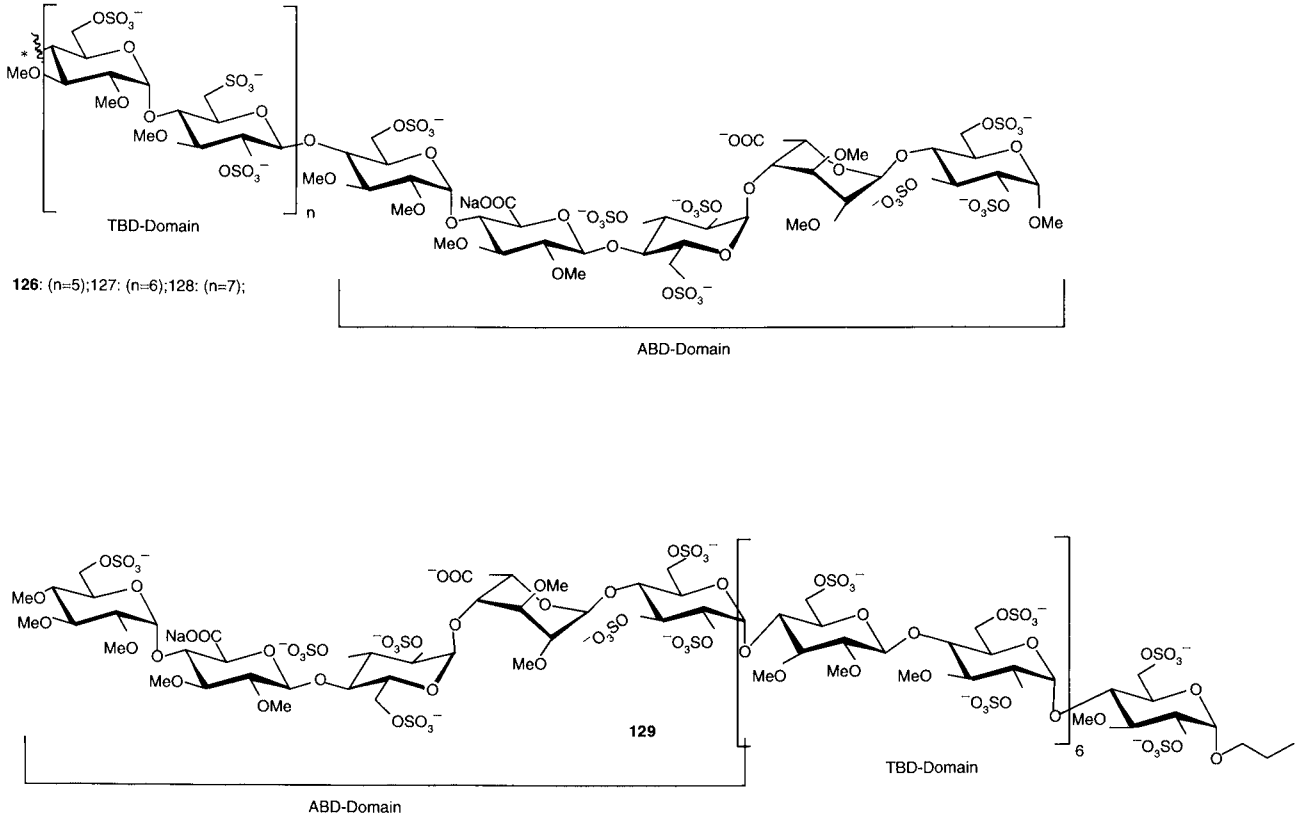

Figure 25 Heparin mimetics to prove the location of the TBD domain.

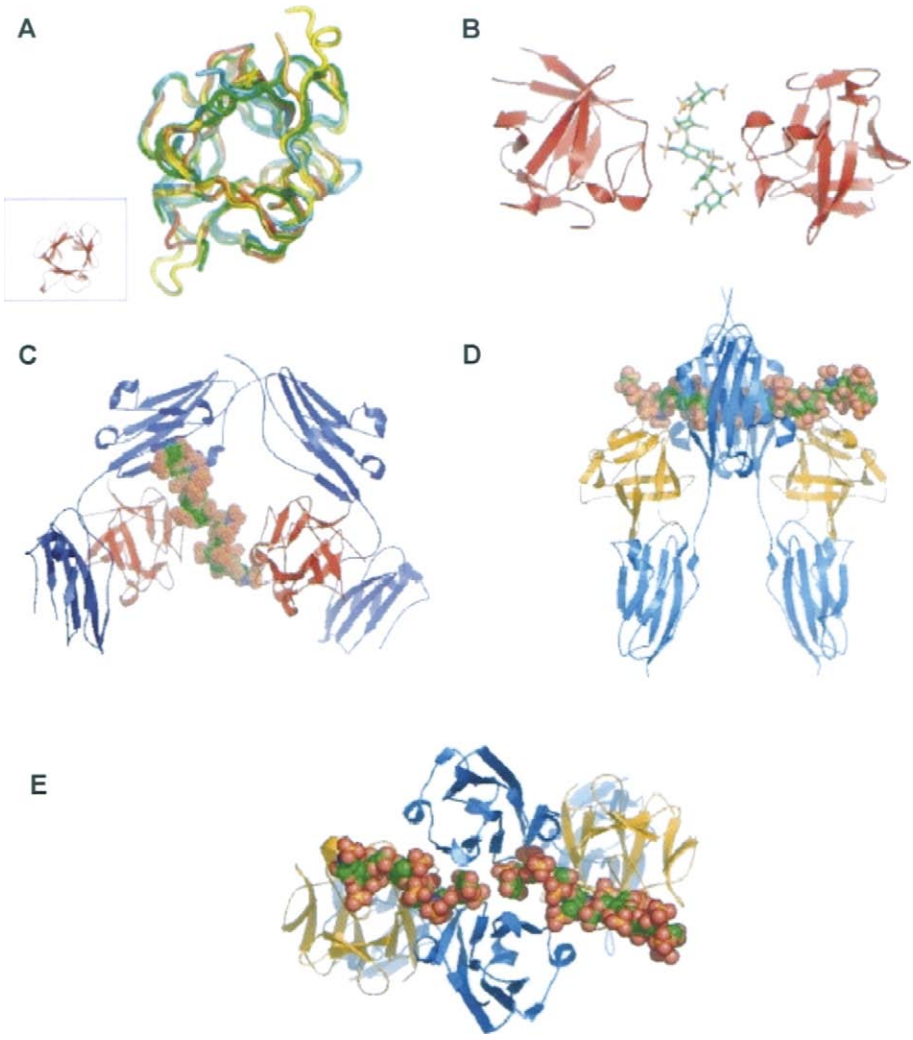

Figure 26 (A) Crystal structures of FGFs. The superimposed structures are shown here as a backbone atom trace, looking down the barrel of the β-trefoil. The inset shown is FGF1 in the traditional cartoon format, in an identical orientation with the main picture. Colors: FGF1, red; FGF2, orange; FGF4, yellow; FGF7, green; FGF9, cyan. (B) Crystal structure of a heparin decamer bridging two FGF1 molecules. FGF1 is shown as a cartoon in red, heparin as sticks with atoms colored by type: carbon, green; oxygen, red; nitrogen, blue; sulfur, orange. (C) A ternary complex of FGF1–FGFR2–heparin showing a 2:2:1 stoichiometry. The Figure shown is taken from the structure 1E0O. FGF1 and FGFR2 are shown in cartoon form, FGF1 in red, FGFR2 in blue. The heparin is shown as spheres. Colors are as in (B). (D) and (E) A ternary complex of FGF2–FGFR1–heparin showing a 2:2:2 stoichiometry. The figure shown is taken from the structure 1FQ9. FGF2 and FGFR1 are shown in cartoon form, FGF2 in red, FGFR1 in blue. The heparin is shown as spheres. Colors are as in (B). The Figures were created using PYMOL (reprinted from *Journal of Molecular Biology*, Towards a resolution of the stoichiometry of the fibroblast growth factor (FGF)–FGIF receptor–heparin complex, 821–834, © 2004 with permission from Elsevier, *www.elsevier.com*).

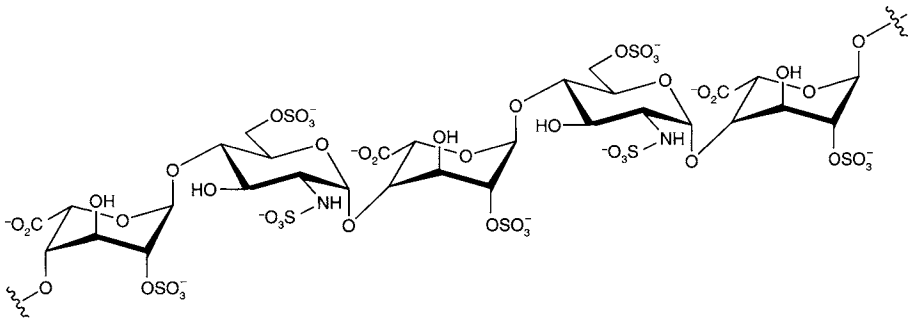

Figure 27 The FGF-binding domain.

sulfate groups, non-sulfated oligosaccharides can also bind to the same site, as the structure of a complex between FGF-2 and a trisaccharide heparin-derivate has shown (131). For the FGF system, only one structure has been determined with sufficient resolution to allow for the direct identification of the structural details of the glycan (84).

a. Synthesis of Heparin Oligosaccharides Involved in FGF Interaction

After the minimum heparin binding sequence for FGF-1 and FGF-2 had been determined (HexA–GlcNS–HexA–GlcNS–IdoA–2OS), different syntheses to access these heparin-fragments were developed. The oligosaccharides differ in the configuration of the HexA units, in the sulfation pattern and in length.

Using a modular strategy, tri-(**130**, **131**), and tetrasaccharide (**132**) derivatives were obtained by coupling disaccharide **133** with alcohols **134** or **135**, respectively (Scheme 13) (143).

This modular strategy also yielded disaccharides **133–138** and trisaccharides **139**, **140** (Fig. 28) (144). Disaccharide **135** and **136** bind FGF-2 less tightly than heparin. The two trisaccharides **139** and **140** bind FGF-2 and show higher affinity for FGF-1.

To elucidate the exact nature of the hexuronic acid unit four different pentasaccharides (**141–144**) were prepared (Table 8) (41,145). All pentasaccharides inhibited FGF-2 binding to heparin or heparan sulfate and the proliferation of FGF-induced human aortic smooth-muscle cells (HASMC). Pentasaccharide **141** is most effective, while **142–144** showed only weak potency. From these observations, it was concluded that iduronic acid is mainly responsible for the interaction between heparin and FGF-2. The conformation of the different iduronic acid residues was analyzed by NMR. The iduronic acid at the nonreducing end is predominantly present in the $^4C_1$-form, the iduronic acid in the center prefers the $^1C_4$-form, and the reducing end iduronic acid adopts the $^2S_0$-conformation.

A tetrasaccharide **145** and hexasaccharide methyl glycoside **146** were prepared from three different disaccharides: seeding disaccharide **149**, elongation disaccharide **148**, and capping disaccharide **147** (Scheme 14) (38). Within each

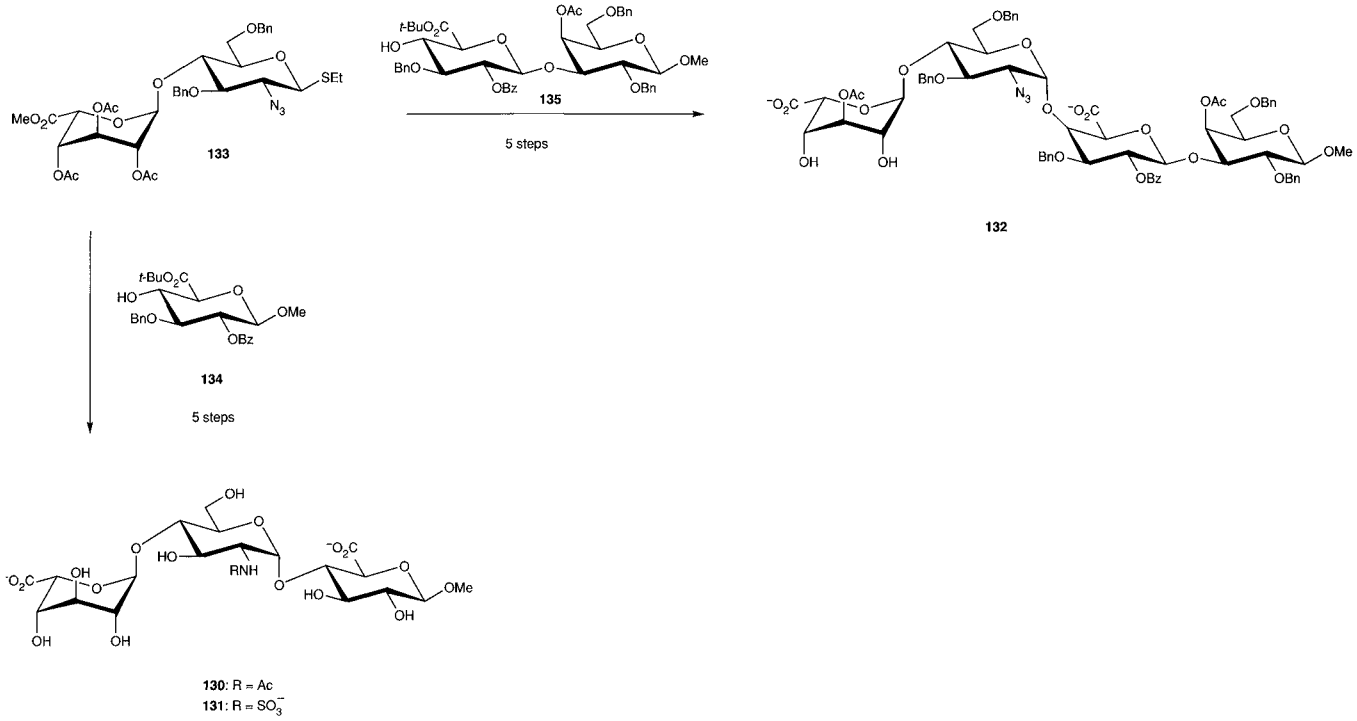

Scheme 13 Synthesis of trisaccharides **130**, **131** and tetrasaccharide **132**.

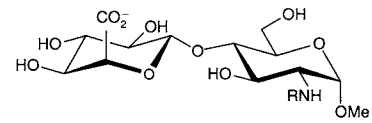

133: R = Ac
134: R = SO_3^-

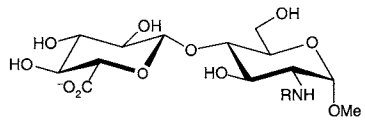

135: R = Ac
136: R = SO_3^-

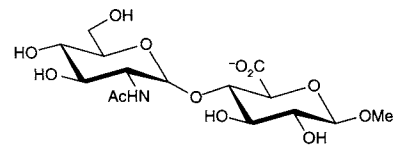

137

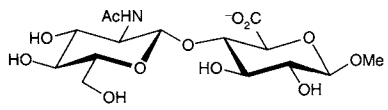

138

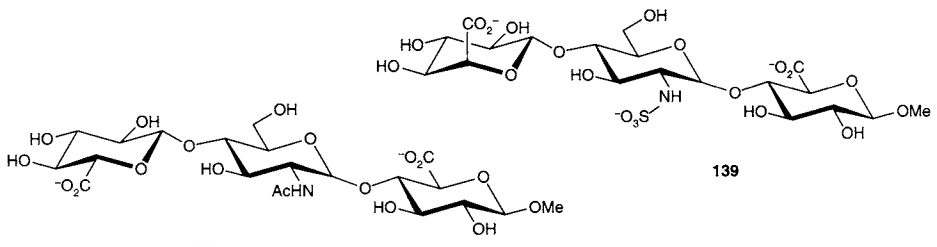

139

140

Figure 28 Different synthetic disaccharides and trisaccharides.

Table 8

Nr	
141	Ido–GlcNS–Ido–GlcNS–Ido
142	Ido–GlcNS–Glc–GlcNS–Ido
143	Glc–GlcNS–Ido–GlcNS–Ido
144	Glc–GlcNS–Glc–GlcNS–Ido

disaccharide, iduronic acid was placed at the nonreducing end and glucosamine at the reducing end. Hexasaccharide **146** antagonized iodinated heparin–FGF-2 binding and inhibited FGF-2-induced proliferation of human aortic smooth-muscle cells (HASMC). Tetrasaccharide **145** showed only weak efficacy (Table 9).

Three tetrasaccharides **150–152** containing the sequence (GlcN–IdoA) and different sulfation patterns at C-6 of the glucosamines were prepared (Fig. 29) (146). The synthesis relied on coupling two versatile disaccharide building blocks with orthogonal protecting groups (66).

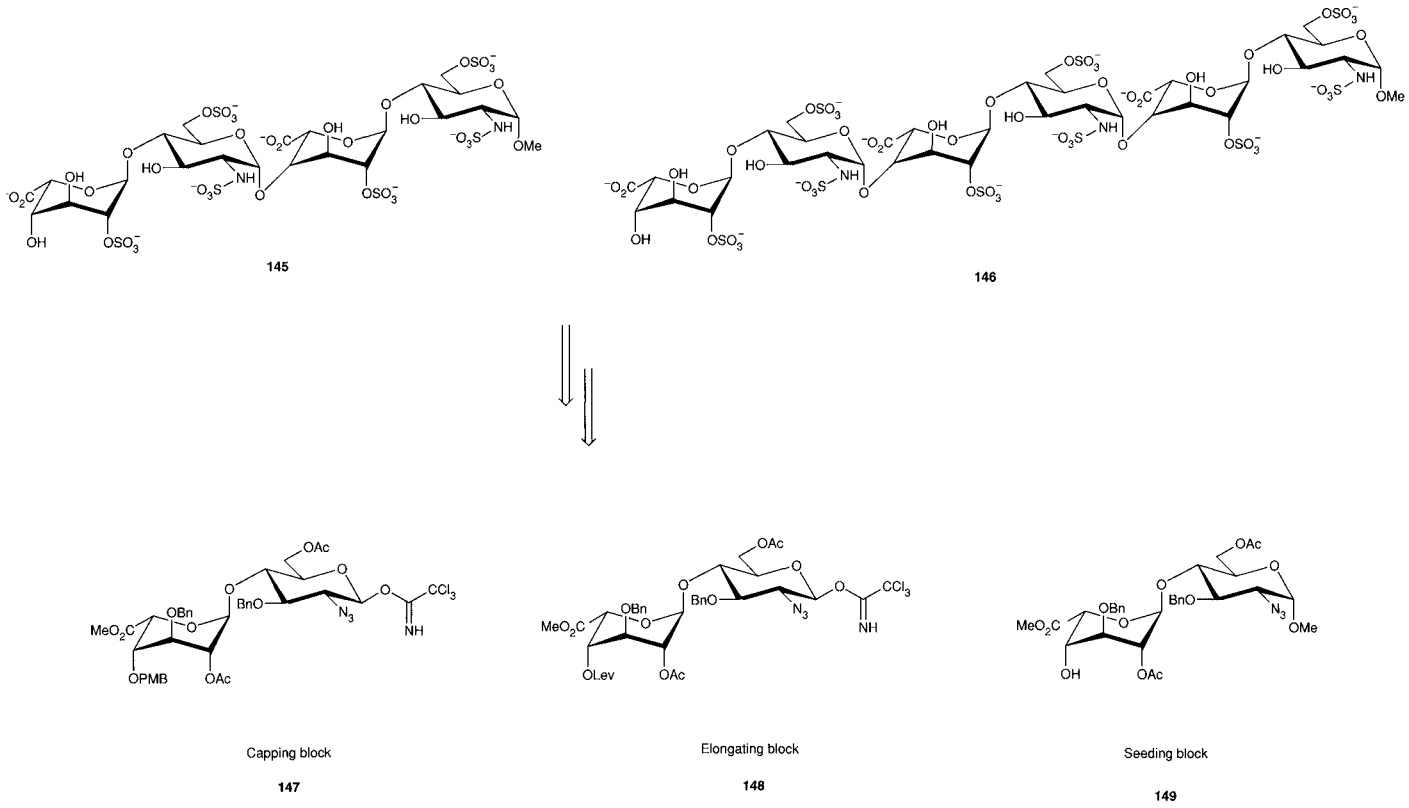

Scheme 14 Strategy for the synthesis of larger oligosaccharides.

Table 9

Nr	Size	Inhibition of FGF-2-binding to HASMC (μg/mL)	Inhibition of FGF-2-induced HASMC proliferation (μg/mL)
145	tetra-mer	127	>100
146	hexa-mer	16	23.7
Heparin		14.8	30.1

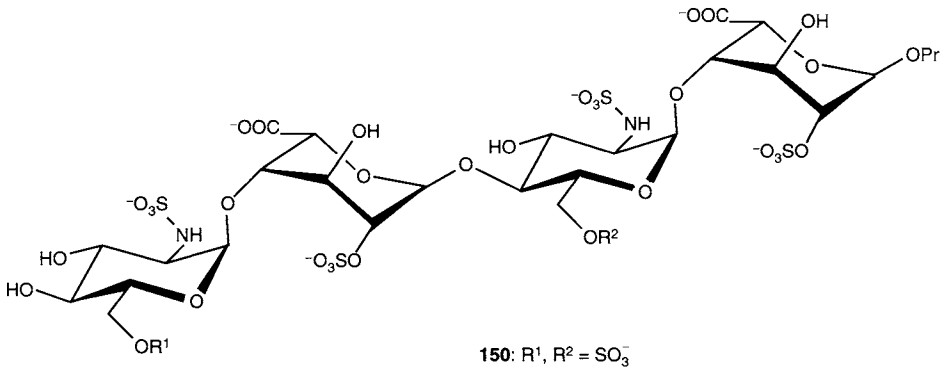

Figure 29 Three tetrasaccharides with different sulfation patterns at C-6.

The same strategy followed by a convergent $(n + 2)$-block approach allowed the preparation of longer oligosaccharides, which are not available by enzymatic or chemical degradation of heparin, with a glucosamine unit at the nonreducing end (Fig. 30) (Table 10) (147–149).

Hexa-**153** and octasaccharide **154** contain the structural motif of the major region of heparin and were tested for activation of FGF-1. Octasaccharide **154** activates the mytogenic signal like heparin, while hexasaccharide **153** was less efficient. From sedimentation experiments, it has been concluded that the active form of FGF-1 is a monomer, assuming that the dimerization of FGF-1 is not necessary for FGF-1-induced signaling. Hexasaccharide **153** prefers a helical

Table 10 Different Sulfated Oligosaccharides

	R^1	R^2	R^3	R^4	R^5	R^6	R^7
153	SO_3^-	SO_3^-	SO_3^-	SO_3^-	SO_3^-	SO_3^-	SO_3^-
156	H	SO_3^-	SO_3^-	Ac	H	H	SO_3^-
158	SO_3^-	H	SO_3^-	SO_3^-	H	SO_3^-	H
159	H	SO_3^-	H	SO_3^-	SO_3^-	H	SO_3^-
154	SO_3^-	SO_3^-	SO_3^-	SO_3^-	SO_3^-	SO_3^-	
157	Ac	H	H	Ac	H	H	

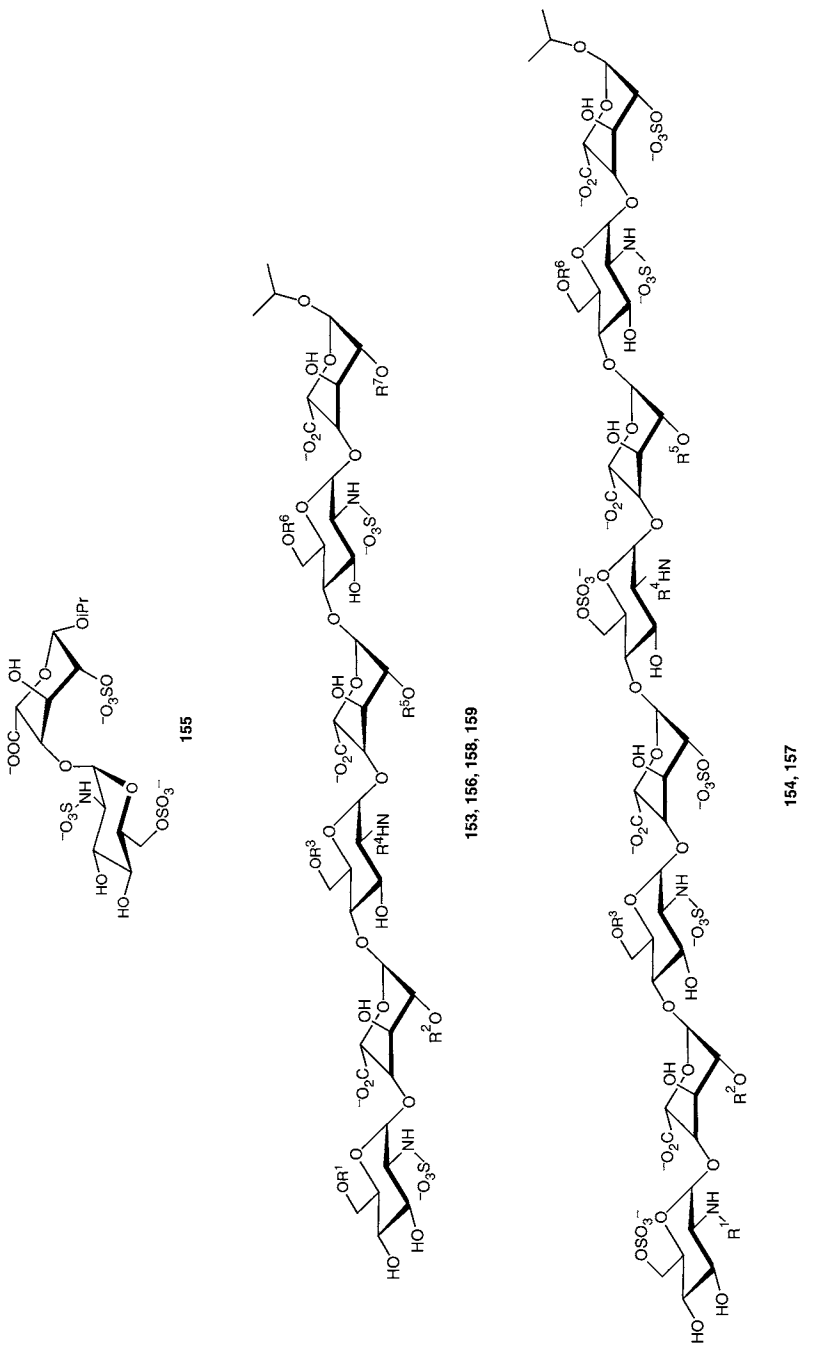

Figure 30 Different sulfated oligosaccharides.

conformation, and the iduronic acid units exist in a fast equilibrium between the $^2S_0$- and the $^1C_4$-form with a slight preference for the latter. Comparison of the conformation of **153** with that of pentasaccharides **141–144** reveals that the sequence of the oligosaccharides (IdoA–GlcN *vs* GlcN–IdoA) can affect the conformation of the iduronic acid units.

Electrostatic interactions of heparin with ions occur via charged saccharide groups. Ca^{2+}–heparin interactions where the cation binds preferentially to the carboxylate groups of the iduronic acid units have been observed. Modification of the carboxylate groups by conversion into methyl esters or by protonation resulted in the loss of binding capability. The lack of the sulfamido group of the glucosamine units results in the loss of Ca^{2+} binding to heparin. Combination of size and charge is responsible for site-specific Ca^{2+} binding, while other ions (e.g., Na^+ and Mg^{2+}) bind more specifically.

Binding of Ca^{2+} to **153** was found to be specific (150,151). The ion influences backbone flexibility, rigidifies the glycosidic linkage, and the conformational equilibrium of the iduronic acid unit may be shifted to the $^1C_4$-conformation. NMR-spectroscopy studies of disaccharide unit **155** confirmed that the $^1C_4$-conformation showed also here the highest affinity for Ca^{2+}. Furthermore, the ion coordinates the carboxylate, and 2-*O*-sulfate groups of the iduronic acid units as well as the *N*-sulfate moiety of glucosamine with the glycosidic and iduronate ring oxygen atoms. Calcium–heparin interaction studies were extended to hexasaccharides **158** and **159** (152). NMR studies in concert with molecular modeling revealed that the 6-*O*-sulfate group of glucosamine is necessary for the interaction of heparin with Ca^{2+}, whereas the sulfate group at C-2 of iduronic acid is not. To test whether the active form of FGF is a monomer, hexasaccharide **156** and octasaccharide **157** were prepared using the convergent $(n + 2)$-block approach (148). Exhibiting charged groups only on one side of the helical structure, a monomeric complex with FGF-1 should be formed exclusively. Conformational analyses showed that the absence of the 2-*O*-sulfate groups in C and G, the 6-*O*-sulfate group in B and F, and the *N*-sulfate group in D and H, do not change the conformation of the iduronic acid rings. Hexasaccharide **156** was found to be biologically active and demonstrated that a 1:1 complex between a heparin fragment and FGF-1 can induce mitogenesis.

The closely related hexasaccharides **158** and **159**, which differ from **153** and **156** only in charge distribution, were used to study the importance of sulfate groups glucosamine C-6 and iduronic acid C-2 while keeping the number of negatively charged groups constant (149).

The oligosaccharides contain the basic structural features of heparin, but different charge distribution and orientation results in different biological behavior. The two oligosaccharides **153** and **154** contain the trisaccharide motif (IdoA–2OS–GlcN–6OS–IdoA–2OS) required for high-affinity binding to FGF-1, while oligosaccharides **156–159** were missing this motif. Oligosaccharides lacking this internal trisaccharide motif can stimulate FGF-1 more efficiently than those with the regular heparin structure (153). Hexasaccharide **156** containing sulfate groups only on one side of the helical structure can activate FGF-1 as effectively as octasaccharide **154**.

These results underscore the importance of charge distribution in the activation process of FGF-1 and suggest that the FGF dimerization is not absolutely required for biological activity.

5. *Synthesis of Heparin Oligosaccharides Recognized by Herpes Simplex Virus*

Heparan sulfate serves as adhesion receptor for bacteria, parasites, and viruses. The negative charges of heparan sulfate can be recognized by viral proteins (154). Herpes simplex viruses are members of the neurotropic subgroup of the herpes virus family. Infection with herpes simplex virus 1 (HSV-1) and herpes simplex virus 2 (HSV-2) are most common in humans. HSV-1 binds to cells through interaction of envelope glycoprotein gB and gC with cell surface heparan sulfate. A third viral glycoprotein, gD, interacts with one of multiple specific receptors, which results in a viral entry of the virion envelope with a cell membrane. This fusion requires the concerted action of the three glycoproteins (gB, gH, and gL) and is triggered by the binding of gD to its cognate receptors. A heparan sulfate octasaccharide (**160**) that binds to HSV-1 gD was identified (Fig. 31) (155,156).

Based on this information, a fully protected *N*-differentiated heparin oligosaccharide was prepared in an effort to establish a structure–activity relationship (157). Based on the limitations of the analytical methods, the nature of one of the uronic acid residues was not known. Therefore, an iduronic acid residue was initially selected in this position. The protecting group strategy was adapted from previous heparin syntheses: *O*-sulfonates were masked as *O*-acetates, hydroxyl groups as *O*-benzyl ethers, carboxylic acids as methyl esters and *N*-sulfonates as azides. In addition, the free amine was protected as benzylcarbamate and the *N*-diacetate as *N*-acetate (Scheme 15).

Two disaccharides **162** and **163** and tetrasaccharide **164** were readily prepared. Coupling of **163** and **164** afforded hexasaccharide **170** as an α/β-mixture (6:1) and the rearranged tetrasaccharide **171** (Scheme 16). The selectivity is decreased by the 2-*N*-CBz glucosamine residue, which could force the iduronic acid unit out of the favorable $^1C_4$ conformation. This finding underscores the fact that the selectivity of glycosylation reactions is greatly influenced by the formation of the nucleophile. This fact has to be taken into consideration for further syntheses of large heparin-like glycosaminoglycans.

6. *Synthesis of Heparin Oligosaccharides Interacting with Platelets*

Heparin binds to platelets and can cause activation and aggregation. To understand how heparin alters platelet function, the platelet-binding site for heparin has to be determined. Given the heterogeneous nature of heparin, this is a challenging task. A disaccharide unit [GlcNS(6-OS)–IdoA(2-OS)] in heparin was found to be key for the binding interaction (158). The disaccharide cannot be obtained by enzymatic or chemical degradation. Therefore, a series of oligomers **172–177** containing this

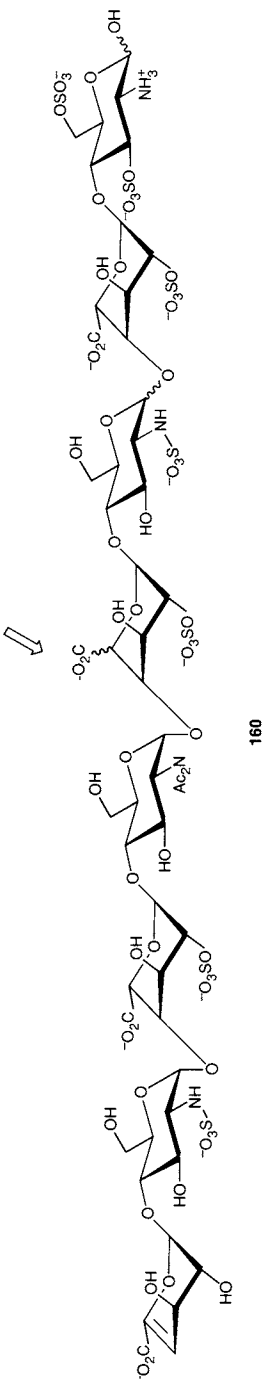

Figure 31 Target structure binding to HSV-1 with unknown stereochemistry at the indicated center.

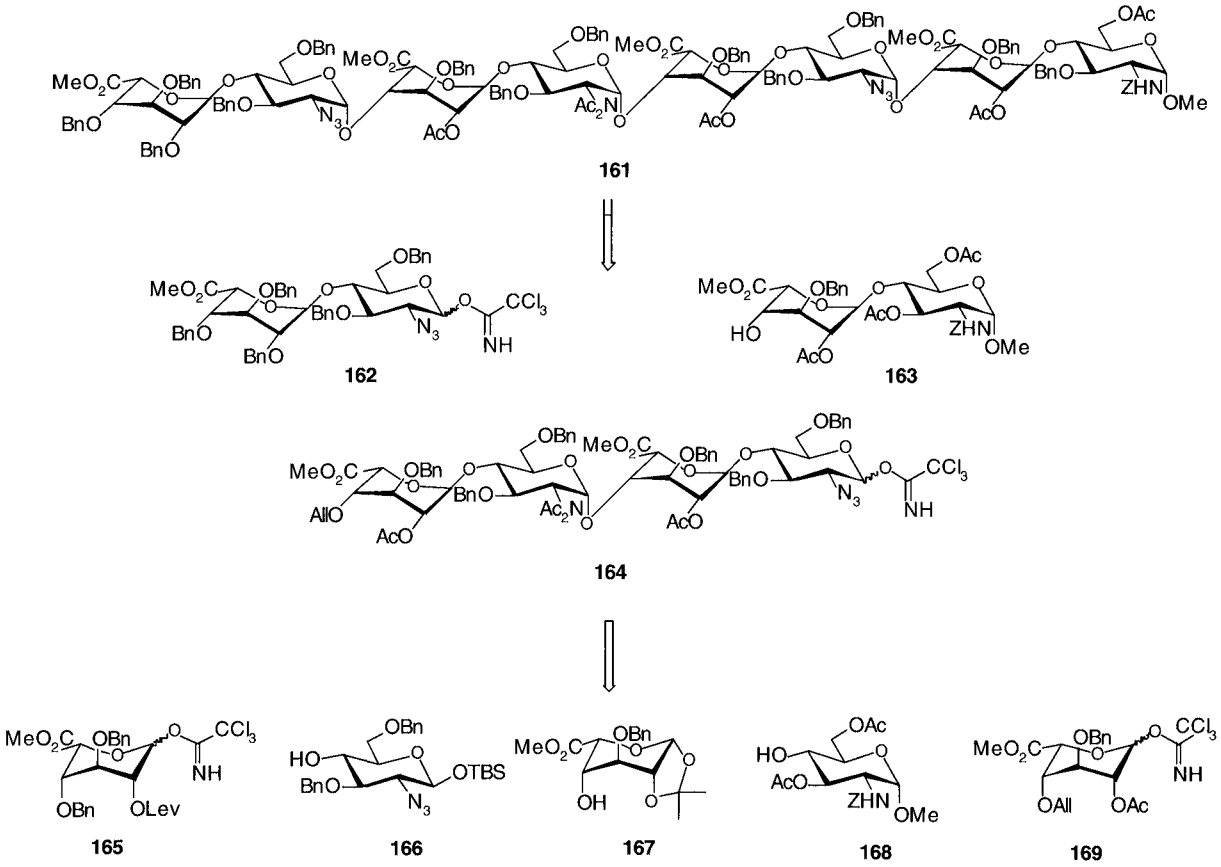

Scheme 15 Retrosynthetic analysis of completely proteced target structure **161**.

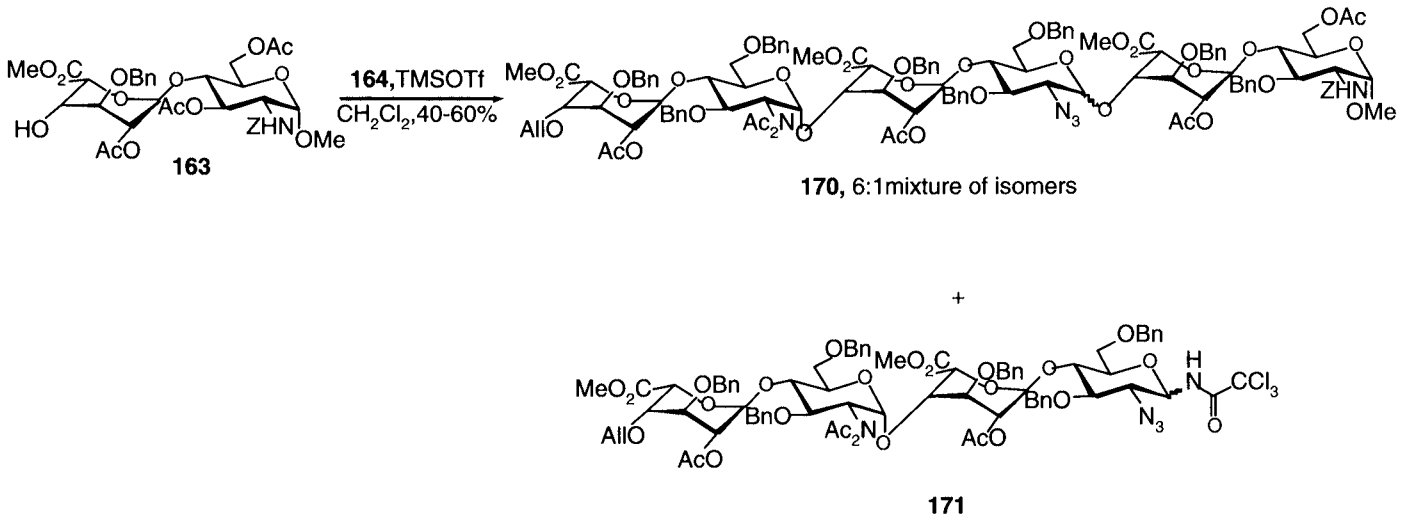

Scheme 16 Glycosylation of **163** and **164** to hexasaccharide **170**.

disaccharide were prepared and their platelet binding activities determined (Fig. 32) (159,160).

Hexasaccharides **173** and **177** that contain three units of GlcNS(6-OS)–IdoA(2-OS) bound stronger than their counterparts **172**, **175**, and **176** that contain only two key disaccharides. This finding underscores the role of the GlcNS(6-OS)–IdoA(2-OS) clustering effect for binding. The binding potency is not influenced by the distance between the GlcNS(6-OS)–IdoA(2-OS) units. Head-to-tail dimer **174** has a higher binding activity than the tail-to-tail dimer **172.** The arrangement of the two units of GlcNS(6-OS)–IdoA(2-OS) has an influence on the activity.

Pentasaccharide **34** that does not contain the key disaccharide GlcNS(6-OS)–IdoA(2-OS) binds to platelets. To determine which part of **34** is responsible for the platelet binding, fragments of **34** were synthesized. The tetrasaccharide that contains the nonreducing fragment *DEF* of **34** does not bind platelets. More detailed studies were focused on the reducing end *FGH* trisaccharide **178**, and on its partially desulfated derivatives **179** and **180** as well as disaccharide derivatives **181** and **182** (Fig. 33). Only trisaccharide **178** bound comparably to **173** and **177**. Based on these results it has been suggested that the sequence GlcNS(3-OS)(6-OS)–IdoA(2-OS)–GlcNS(6-OS) is a high-affinity binding site for platelets.

V. Summary and Outlook

Heparin, the drug of choice for the prevention and treatment of thromboembolic disorders for more than 60 years, has been shown to interact with many proteins. Despite its widespread medical use, little is known about the precise sequences that interact with specific proteins and their structure–activity relationship. Heparin–protein interplay has been studied using defined synthetic heparin sequences. NMR and X-ray crystallography have aided significantly in characterizing the specific interactions of heparin with proteins.

The minimum heparin binding sequence for FGF-1 and FGF-2 necessary to promote signaling was investigated. A characteristic pentasaccharide sequence DEFGH is necessary to accelerate the inhibition of thrombin and factor Xa in the blood-coagulation cascade. A host of oligosaccharides has been synthesized and shows activity for anti-factor Xa and thrombin. Other defined heparin oligosaccharides tightly bind to FGF, HSV, or platelets.

The first synthetic heparin pentasaccharide drug has now been approved in Europe and the US and is sold under the trade name *Arixtra.* Other oligosaccharides with different compositions are under clinical investigation. Despite these successes, many questions remain unanswered. The enormous interest in the assembly of heparin oligosaccharides will stimulate the development of new synthetic approaches. New anticoagulants based on the structure of heparin may avoid undesired interactions with proteins such as PF4. The synthesis of oligosaccharides will have to be simplified in order to access many different structures in large quantities. The automation of heparin oligosaccharide synthesis, similar to that of DNA or peptide synthesis, will play an important role.

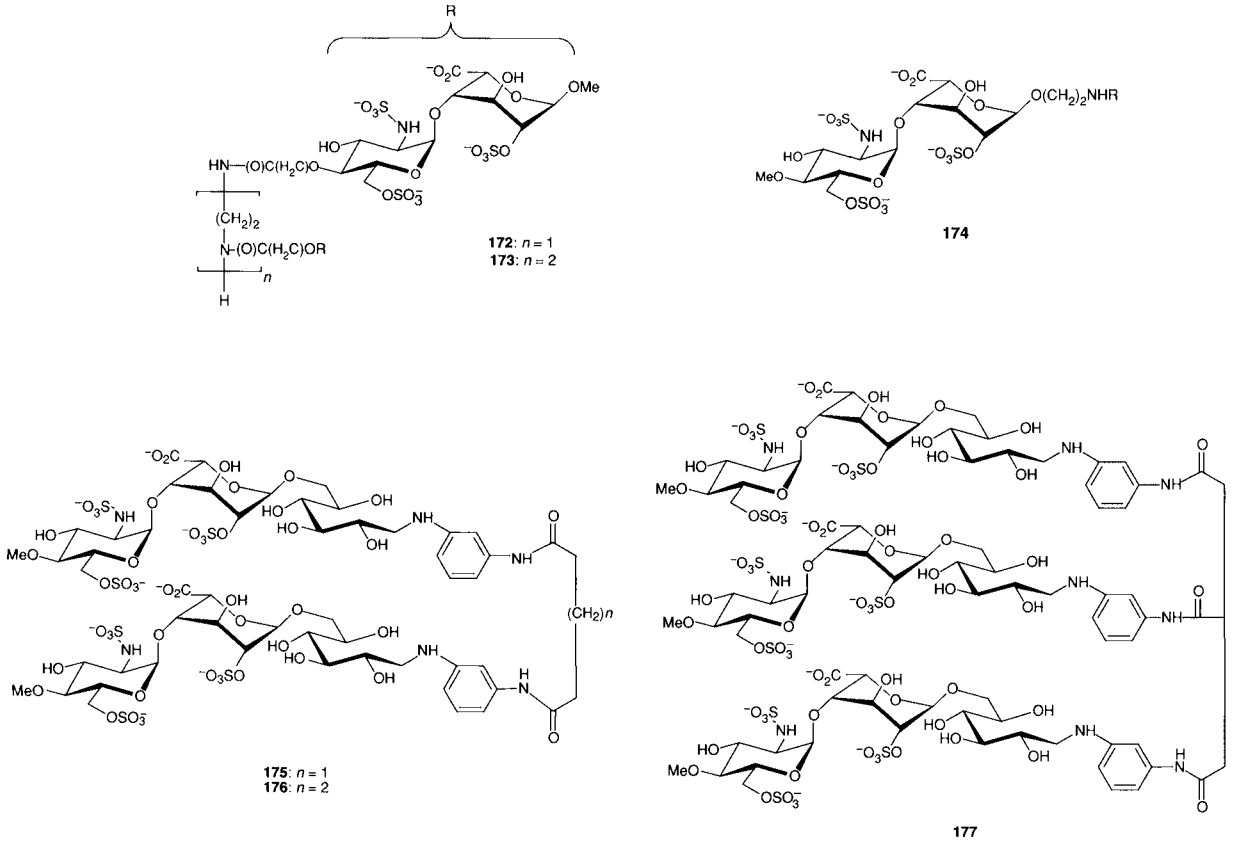

Figure 32 Compounds **172–177** to evaluate platelet-binding activities.

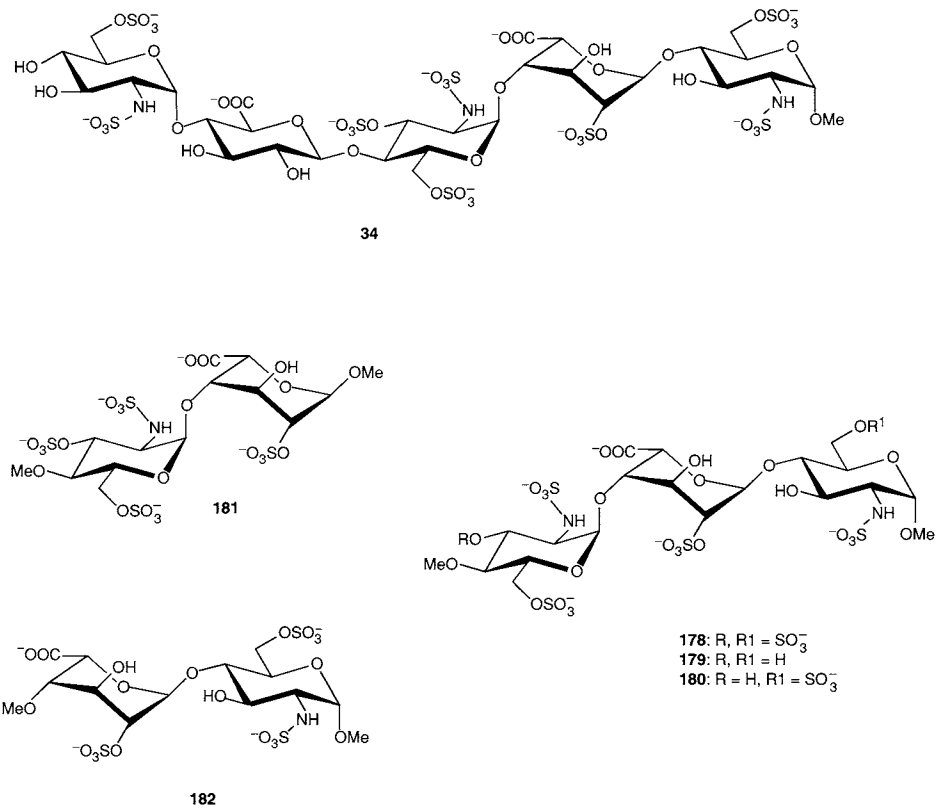

Figure 33 Further compounds to investigate platelet-binding activities.

References

1. Gallagher JT, Turnbull JE. Heparan-sulfate in the binding and activation of basic fibroblast growth-factor. Glycobiology 1992; 2:523–528.
2. Spillmann D, Lindahl U. Glycosaminoglycan protein interactions – a question of specificity. Curr Opin Struct Biol 1994; 4:677–682.
3. Rostand KS, Esko JD. Microbial adherence to and invasion through proteoglycans. Infect Immun 1997; 65:1–8.
4. Capila I, Linhardt RJ. Heparin–protein interactions. Angew Chem Int Edit 2002; 41:391–412.
5. Esko JD, Selleck SB. Order out of chaos: assembly of ligand binding sites in heparan sulfate. Annu Rev Biochem 2002; 71:435–471.
6. Engelberg H. Heparin and the atherosclerotic process. Pharmacol Rev 1984; 36:91–110.
7. Chong BH. Heparin-induced thrombocytopenia. Aust N Z J Med 1992; 22: 145–152.

8. Gavard O, Hersant Y, Alais J, Duverger V, Dilhas A, Bascou A, Bonnaffe D. Efficient preparation of three building blocks for the synthesis of heparan sulfate fragments: Towards the combinatorial synthesis of oligosaccharides from hypervariable regions. Eur J Org Chem 2003:3603–3620.
9. Gallagher JT, Walker A. Molecular distinctions between heparan-sulfate and heparin – analysis of sulfation patterns indicates that heparan-sulfate and heparin are separate families of *N*-sulfated polysaccharides. Biochem J 1985; 230:665–674.
10. van Boeckel CAA, Petitou M. The unique antithrombin-III binding domain of heparin – a lead to new synthetic antithrombotics. Angew Chem Int Edit Engl 1993; 32:1671–1690.
11. Petitou M, van Boeckel CAA. A synthetic antithrombin III binding pentasaccharide is now a drug! What comes next? Angew Chem Int Edit 2004; 43:3118–3133.
12. Poletti L, Lay L. Chemical contributions to understanding heparin activity: synthesis of related sulfated oligosaccharides. Eur J Org Chem 2003:2999–3024.
13. Codee JDC, Overkleeft HS, van der Marel GA, van Boeckel CAA. The synthesis of well-defined heparin and heparan sulfate fragments. Drug Discov Today: Technol 2004; 1:317–326.
14. Powell AK, Yates EA, Fernig DG, Turnbull JE. Interactions of heparin/heparan sulfate with proteins: appraisal of structural factors and experimental approaches. Glycobiology 2004; 14:17R–30R.
15. Rabenstein DL. Heparin and heparan sulfate: structure and function. Nat Prod Rep 2002; 19:312–331.
16. Lindahl U, Feingold DS, Roden L. Biosynthesis of heparin. Trends Biochem Sci 1986; 11:221–225.
17. Bernfield M, Gotte M, Park PW, Reizes O, Fitzgerald ML, Lincecum J, Zako M. Functions of cell surface heparan sulfate proteoglycans. Annu Rev Biochem 1999; 68:729–777.
18. McCormick C, Duncan G, Goutsos KT, Tufaro F. The putative tumor suppressors EXT1 and EXT2 form a stable complex that accumulates in the Golgi apparatus and catalyzes the synthesis of heparan sulfate. Proc Natl Acad Sci USA 2000; 97:668–673.
19. Lidholt K, Lindahl U. The D-glucuronosyl-transferase and *N*-acetyl-D-glucosaminyltransferase reactions and their relation to polymer modification. Biochem J 1992; 287:21–29.
20. Mulloy B, Forster MJ, Jones C, Davies DB. NMR and molecular-modeling studies of the solution conformation of heparin. Biochem J 1993; 293:849–858.
21. Mulloy B, Linhardt RJ. Order out of complexity – protein structures that interact with heparin. Curr Opin Struct Biol 2001; 11:623–628.
22. Hricovini M, Guerrini M, Bisio A, Torri G, Petitou M, Casu B. Conformation of heparin pentasaccharide bound to antithrombin III. Biochem J 2001; 359:265–272.
23. Mulloy B, Forster MJ. Conformation and dynamics of heparin and heparan sulfate. Glycobiology 2000; 10:1147–1156.
24. Casu B, Choay J, Ferro DR, Gatti, G, Jacquinet JC, Petitou M, Provasoli A, Ragazzi M, Sinay P, Torri G. Controversial glycosamino-glycan conformations. Nature 1986; 322:215–216.

25. Ferro DR, Provasoli A, Ragazzi M, Torri G, Casu B, Gatti G, Jacquinet JC, Sinay P, Petitou M, Choay J. Evidence for conformational equilibrium of the sulfated L-iduronate residue in heparin and in synthetic heparin monosaccharides and oligosaccharides – NMR and force-field studies. J Am Chem Soc 1986; 108:6773–6778.
26. Gatti G, Casu B, Hamer GK, Perlin AS. Studies on the conformation of heparin by H-1 and C-13 NMR-spectroscopy. Macromolecules 1979; 12:1001–1007.
27. Yates EA, Santini F, Guerrini M, Naggi A, Torri G, Casu B. H-1 and C-13 NMR spectral assignments of the major sequences of twelve systematically modified heparin derivatives. Carbohydr Res 1996; 294:15–27.
28. Hileman RE, Smith AE, Toida T, Linhardt RJ. Preparation and structure of heparin lyase-derived heparan sulfate oligosaccharides. Glycobiology 1997; 7:231–239.
29. Pervin A, Gallo C, Jandik KA, Han XJ, Linhardt RJ. Preparation and structural characterization of large heparin-derived oligosaccharides. Glycobiology 1995; 5:83–95.
30. Rice KG, Linhardt RJ. Study of structurally defined oligosaccharide substrates of heparin and heparan monosulfate lyases. Carbohydr Res 1989; 190:219–233.
31. Koeners HJ, Verhoeven J, van Boom JH. Synthesis of oligosaccharides by using levulinic ester as an hydroxyl protecting group. Tetrahedron Lett 1980; 21:381–382.
32. Basten J, Jaurand G, Olde-Hanter B, Duchaussoy P, Petitoub, M., van Boeckel, CAA. Biologically active heparin-like fragments with a "non-glycosamino" glycan structure. Part 3. *o*-Alkylated-*o*-sulphated pentasaccharides. Bioorg Med Chem Lett 1992; 2:905–910.
33. Petitou M, Imberty A, Duchaussoy P, Driguez PA, Ceccato ML, Gourvenec F, Sizun P, Herault JP, Perez S, Herbert JM. Experimental proof for the structure of a thrombin-inhibiting heparin molecule. Chem-Eur J 2001; 7:858–873.
34. Zhu T, Boons GJ. A new set of orthogonal-protecting groups for oligosaccharide synthesis on a polymeric support. Tetrahedron-Asymmetry 2000; 11:199–205.
35. Kovensky J, Mallet JM, Esnault J, Driguez PA, Sizun P, Herault JP, Herbert JM, Petitou M, Sinay P. Further evidence for the critical role of a non-chair conformation of L-iduronic acid in the activation of antithrombin. Eur J Org Chem 2002:3595–3603.
36. Haller M, Boons GJ. Towards a modular approach for heparin synthesis. J Chem Soc, Perkin Trans 1 2001:814–822.
37. Jaurand G, Tabeur C, Petitou M. Synthesis of the basic disaccharide unit of heparin. Carbohydr Res 1994; 255:295–301.
38. Tabeur C, Mallet JM, Bono F, Herbert JM, Petitou M, Sinay P. Oligosaccharides corresponding to the regular sequence of heparin: chemical synthesis and interaction with FGF-2. Bioorg Med Chem 1999; 7:2003–2012.
39. Lucas R, Hamza D, Lubineau A, Bonnaffe D. Synthesis of glycosaminoglycan oligosaccharides – an unexpected inhibitory effect of a remote *N*-acetyl group upon trichloroacetimidate-mediated couplings. Eur J Org Chem 2004:2107–2117.

40. Haller MF, Boons GJ. Selectively protected disaccharide building blocks for modular synthesis of heparin fragments – Part 2. Eur J Org Chem 2002:2033–2038.
41. Kovensky J, Duchaussoy P, Bono F, Salmivirta M, Sizun P, Herbert JM, Petitou M, Sinay P. A synthetic heparan sulfate pentasaccharide, exclusively containing -iduronic acid, displays higher affinity for FGF-2 than its L-glucuronic acid-containing isomers. Bioorg Med Chem 1999; 7:1567–1580.
42. Jacquinet JC, Petitou M, Duchaussoy P, Lederman I, Choay J, Torri G, Sinay P. Synthesis of heparin fragments – a chemical synthesis of the trisaccharide *O*-(2-deoxy-2-sulfamido-3,6-di-1-sulfo-alpha-D-glucopyranosyl)-(1-4)-*O*-(2-*O*-sulfo-alpha-L-idopyranosyluronic acid)-(1-4)-2-deoxy-2-sulfamido-6-*O*-sulfo-D-glucopyranose heptasodium salt. Carbohydr Res 1984; 130:221–241.
43. Vlahov IR, Linhardt RJ. Regioselective synthesis of derivatives of L-idopyranuronic acid: a key constituent of glycosaminoglycans. Tetrahedron Lett 1995; 36:8379–8382.
44. Bazin HG, Kerns RJ, Linhardt RJ. Regio and stereoselective conversion of [delta]4-uronic acids to L-ido- and D-glucopyranosiduronic acids. Tetrahedron Lett 1997; 38:923–926.
45. Dromowicz M, Koll P. A convenient synthesis of L-idose. Carbohydr Res 1998; 308:169–171.
46. Hinou H, Kurosawa H, Matsuoka K, Terunuma D, Kuzuhara H. Novel synthesis of -iduronic acid using trehalose as the disaccharidic starting material. Tetrahedron Lett 1999; 40:1501–1504.
47. Medakovic D. An efficient synthesis of methyl 1,2,3,4-tetra-*O*-acetyl-beta-L-idopyranuronate. Carbohydr Res 1994; 253:299–300.
48. Chiba T, Sinay P. Application of a radical reaction to the synthesis of L-iduronic acid-derivatives from D-glucuronic acid analogs. Carbohydr Res 1986; 151:379–389.
49. Baggett N, Samra AK. Re-examination of the acid-hydrolysis of 5,6-anhydro-1,2-*O*-isopropylidene-beta-L-idofuranose. Carbohydr Res 1984; 127:149–153.
50. Macher I, Dax K, Wanek E, Weidmann H. Reactions of D-glucuronic acid. 13. Synthesis of L-idofuranurono-6,3-lactone and its derivatives via hexodialdodifuranoses. Carbohydr Res 1980; 80:45–51.
51. Adinolfi M, Barone G, De Lorenzo F, Iadonisi A. Intramolecular tishchenko reactions of protected hexos-5-uloses: a novel and efficient synthesis of L-idose and L-altrose. Synlett 1999:336–338.
52. RochepeauJobron L, Jacquinet JC. Diastereoselective hydroboration of substituted exo-glucals revisited. A convenient route for the preparation of L-iduronic acid derivatives. Carbohydr Res 1997; 303:395–406.
53. Yu HN, Furukawa J, Ikeda T, Wong CH. Novel efficient routes to heparin monosaccharides and disaccharides achieved via regio- and stereoselective glycosidation. Org Lett 2004; 6:723–726.
54. Lee JC, Chang SW, Liao CC, Chi FC, Chen CS, Wen YS, Wang CC, Kulkarni SS, Puranik R, Liu YH, Hung SC. From D-glucose to biologically potent L-hexose derivatives: synthesis of alpha-L-iduronidase fluorogenic detector and the disaccharide moieties of bleomycin A(2) and heparan sulfate. Chem-Eur J 2004; 10:399–415.

55. Ke W, Whitfield DM, Gill M, Larocque S, Yu SH. A short route to L-iduronic acid building blocks for the syntheses of heparin-like disaccharides. Tetrahedron Lett 2003; 44:7767–7770.
56. Dilhas A, Bonnaffe D. Efficient selective preparation of methyl-1,2,4-tri-*O*-acetyl-3-*O*-benzyl-beta-L-idopyranuronate from methyl 3-*O*-benzyl-L-iduronate. Carbohydr Res 2003; 338:681–686.
57. Schell P, Orgueira HA, Roehrig S, Seeberger PH. Synthesis and transformations of D-glucuronic and L-iduronic acid glycals. Tetrahedron Lett 2001; 42:3811–3814.
58. Das SK, Mallet JM, Esnault J, Driguez PA, Duchaussoy P, Sizun P, Herault JP, Herbert JM, Petitou M, Sinay P. Synthesis of conformationally locked L-iduronic acid derivatives: direct evidence for a critical role of the skew-boat S-2(0) conformer in the activation of antithrombin by heparin. Chem-Eur J 2001; 7:4821–4834.
59. Lubineau A, Gavard O, Alais J, Bonnaffe D. New accesses to L-iduronyl synthons. Tetrahedron Lett 2000; 41:307–311.
60. Ojeda R, de Paz JL, Martin-Lomas M, Lassaletta JM. A new route to L-iduronate building-blocks for the synthesis of heparin-like oligosaccharides. Synlett 1999:1316–1318.
61. Orgueira HA, Bartolozzi A, Schell P, Litjens R, Palmacci ER, Seeberger PH. Modular synthesis of heparin oligosaccharides. Chem-Eur J 2003; 9:140–169.
62. Lohman GJS, Hunt DK, Hogermeier JA, Seeberger PH. Synthesis of iduronic acid building blocks for the modular assembly of glycosaminoglycans. J Org Chem 2003; 68:7559–7561.
63. Prabhu A, Venot A, Boons GJ. New set of orthogonal protecting groups for the modular synthesis of heparan sulfate fragments. Org Lett 2003; 5:4975–4978.
64. Hung SC, Thopate SR, Chi FC, Chang SW, Lee JC, Wang CC, Wen YS. 1,6-Anhydro-beta-L-hexopyranoses as potent synthons in the synthesis of the disaccharide units of bleomycin A(2) and heparin. J Am Chem Soc 2001; 123:3153–3154.
65. Hung SC, Puranik R, Chi FC. Novel synthesis of 1,2:3,5-di-*O*-isopropylidene-[beta]–idofuranoside and its derivatives at C6. Tetrahedron Lett 2000; 41:77–80.
66. La Ferla B, Lay L, Guerrini M, Poletti L, Panza L, Russo G. Synthesis of disaccharidic sub-units of a new series of heparin related oligosaccharides. Tetrahedron 1999; 55:9867–9880.
67. Orgueira HA, Bartolozzi A, Schell P, Seeberger PH. Conformational locking of the glycosyl acceptor for stereocontrol in the key step in the synthesis of heparin. Angew Chem Int Edit 2002; 41:2128–2131.
68. de Paz JL, Ojeda R, Reichardt N, Martin-Lomas M. Some key experimental features of a modular synthesis of heparin-like oligosaccharides. Eur J Org Chem 2003:3308–3324.
69. Seeberger PH, Haase WC. Solid-phase oligosaccharide synthesis and combinatorial carbohydrate libraries. Chem Rev 2000; 100:4349.
70. Ojeda R, de Paz JL, Martin-Lomas M. Synthesis of heparin-like oligosaccharides on a soluble polymer support. Chem Commun 2003:2486–2487.

71. DreefTromp CM, Willems HAM, Westerduin P, van Veelen P, van Boeckel CAA. Polymer-supported solution synthesis of heparan sulphate-like oligomers. Bioorg Med Chem Lett 1997; 7:1175–1180.
72. Ojeda R, Terenti O, de Paz JL, Martin-Lomas M. Synthesis of heparin-like oligosaccharides on polymer supports. Glycoconjugate J 2004; 21:179–195.
73. Muller A, Homey B, Soto H, Ge NF, Catron D, Buchanan ME, McClanahan T, Murphy E, Yuan W, Wagner SN, Barrera JL, Mohar A, Verastegui E, Zlotnik A. Involvement of chemokine receptors in breast cancer metastasis. Nature 2001; 410:50–56.
74. Ibel K, Poland GA, Baldwin JP, Pepper DS, Luscombe M, Holbrook JJ. Low-resolution structure of the complex of human blood platelet factor 4 with heparin determined by small-angle neutron scattering. Biochimica et Biophysica Acta (BBA) *Protein Struct Mol Enzymol* 1986; 870:58–63.
75. Rojas E, Pollard H, Haigler H, Parra C, Burns A. Calcium-activated endonexin II forms calcium channels across acidic phospholipid bilayer membranes. J Biol Chem 1990; 265:21207–21215.
76. Tait J, Gibson D, Fujikawa K. Phospholipid binding properties of human placental anticoagulant protein-I, a member of the lipocortin family. J Biol Chem 1989; 264:7944–7949.
77. Gerke V, Weber K. Identity of P36k phosphorylated upon rous-sarcoma virus transformation with a protein purified from brush-borders – calcium-dependent binding to non-erythroid spectrin and F-actin. EMBO J 1984; 3:227–233.
78. Capila I, van der Noot VA, Mealy TR, Seaton BA, Linhardt RJ. Interaction of heparin with annexin V. FEBS Lett 1999; 446:327–330.
79. Capila I, Hernaiz MJ, Mo YD, Mealy TR, Campos B, Dedman JR, Linhardt RJ, Seaton BA. Annexin V-heparin oligosaccharide complex suggests heparan sulfate-mediated assembly on cell surfaces. Structure 2001; 9:57–64.
80. Ishitsuka R, Kojima K, Utsumi H, Ogawa H, Matsumoto I. Glycosaminoglycan binding properties of annexin IV, V, and VI. J Biol Chem 1998; 273: 9935–9941.
81. Petitou M, Duchaussoy P, Jaurand G, Gourvenec F, Lederman I, Strassel JM, Barzu T, Crepon B, Herault JP, Lormeau JC, Bernat A, Herbert JM. Synthesis and pharmacological properties of a close analogue of an antithrombotic pentasaccharide (SR 90107A ORG 31540). J Med Chem 1997; 40:1600–1607.
82. Koshida S, Suda Y, Sobel M, Ormsby J, Kusumoto S. Synthesis of heparin partial structures and their binding activities to platelets. Bioorg Med Chem Lett 1999; 9:3127–3132.
83. Iacomini M, Casu B, Guerrini M, Naggi A, Pirola A, Torri G. "Linkage Region" sequences of heparins and heparan sulfates: detection and quantification by nuclear magnetic resonance spectroscopy. Anal Biochem 1999; 274:50–58.
84. Faham S, Hileman RE, Fromm JR, Linhardt RJ, Rees DC. Heparin structure and interactions with basic fibroblast growth factor. Science 1996; 271:1116–1120.
85. Schlessinger J, Plotnikov AN, Ibrahimi OA, Eliseenkova AV, Yeh BK, Yayon A, Linhardt RJ, Mohammadi M. Crystal structure of a ternary FGF-FGFR-heparin complex reveals a dual role for heparin in FGFR binding and dimerization. Mol Cell 2000; 6:743–750.

86. Jin L, Abrahams JP, Skinner R, Petitou M, Pike RN, Carrell RW. The anticoagulant activation of antithrombin by heparin. PNAS 1997; 94: 14683–14688.
87. Casu B, Oreste P, Torri G, Zoppetti G, Choay J, Lormeau JC, Petitou M, Sinay P. The structure of heparin oligosaccharide fragments with high anti-(factor-Xa) activity containing the minimal antithrombin-III-binding sequence – chemical and C-13 NMR-studies. Biochem J 1981; 197:599–609.
88. Atha DH, Lormeau JC, Petitou M, Rosenberg RD, Choay J. Contribution of monosaccharide residues in heparin binding to antithrombin-III. Biochemistry 1985; 24:6723–6729.
89. Lindahl U, Backstrom G, Thunberg L. The antithrombin-binding sequence in heparin – identification of an Essential 6-*O*-Sulfate Group. J Biol Chem 1983; 258:9826–9830.
90. Riesenfeld J, Thunberg L, Hook M, Lindahl U. The antithrombin-binding sequence of heparin – location of essential *N*-sulfate Groups. J Biol Chem 1981; 256:2389–2394.
91. Beetz T, van Boeckel CAA. Synthesis of an antithrombin binding heparin-like pentasaccharide lacking 6-0 sulfate at its reducing end. Tetrahedron Lett 1986; 27:5889–5892.
92. Li W, Johnson DJD, Esmon CT, Huntington JA. Structure of the antithrombin–thrombin–heparin ternary complex reveals the antithrombotic mechanism of heparin. Nat Struct Mol Biol 2004; 11:857–862.
93. Dementiev A, Petitou M, Herbert JM, Gettins PGW. The ternary complex of antithrombin-anhydrothrombin heparin reveals the basis of inhibitor specificity. Nat Struct Mol Biol 2004; 11:863–867.
94. van Boeckel CAA, Grootenhuis PDJ, Meuleman D, Westerduin P. Glycosaminoglycans – synthetic fragments and their interaction with serine-protease inhibitors. Pure Appl Chem 1995; 67:1663–1672.
95. Grootenhuis PDJ, Westerduin P, Meuleman D, Petitou M, van Boeckel CAA. Rational design of synthetic heparin analogs with tailor-made coagulation-factor inhibitory activity. Nat Struct Biol 1995; 2:736–739.
96. Petitou M, Herault LP, Bernat A, Driguez PA, Duchaussoy P, Lormeau JC, Herbert JM. Synthesis of thrombin-inhibiting heparin mimetics without side effects. Nature 1999; 398:417–422.
97. Kelton JG. Heparin-induced thrombocytopenia: an overview. Blood Rev 2002; 16:77–80.
98. Petitou M, Duchaussoy P, Lederman I, Choay J, Sinay P, Jacquinet JC, Torri G. Synthesis of heparin fragments – a chemical synthesis of the pentasaccharide *O*-(2-deoxy-2-sulfamido-6-*O*-sulfo-alpha-deuterium-glucopyranosyl)-(1-4)-*O*-(beta-deuterium-glucopyranosyluronic acid)-(1-4)-*O*-(2-deoxy-2-sulfamido-3,6-di-*O*-sulfo-alpha-deuterium-glucopyranosyl)-(1-4)-*O*-(2-*O*-sulfo-alpha-L-idopyranosyluronic acid)-(1-4)-2-deoxy-2-sulfamido-6-*O*-sulfo-deuterium-glucopyranose decasodium salt, a heparin fragment having high-affinity for antithrombin-IIIa. Carbohydr Res 1986; 147:221–236.
99. Sinay P, Jacquinet JC, Petitou M, Duchaussoy P, Lederman I, Choay J, Torri G. Total synthesis of a heparin pentasaccharide fragment having high affinity for antithrombin III. Carbohydr Res 1984; 132:C5–C9.

100. Petitou M, Duchaussoy P, Lederman I, Choay J, Jacquinet JC, Sinay P, Torri G. Synthesis of heparin fragments: a methyl [alpha]-pentaoside with high affinity for antithrombin III. Carbohydr Res 1987; 167:67–75.
101. Petitou, M., Jaurand G, Derrien M, Duchaussoy P, Choay J. A new, highly potent, heparin-like pentasaccharide fragment containing a glucose residue instead of a glucosamine. Bioorg Med Chem Lett 1991; 1:95–98.
102. van Boeckel CAA, Beetz T, van Aelst SF. Synthesis of a potent antithrombin activating pentasaccharide: a new heparin-like fragment containing two 3-*O*-sulphated glucosamines. Tetrahedron Lett 1988; 29:803–806.
103. Jaurand G, Basten J, Lederman I, van Boeckel CAA, Petitou M. Biologically-active heparin-like fragments with a non-glycosamino glycan structure.1. A pentasaccharide containing a 3-*ortho*-methyl iduronic acid unit. Bioorg Med Chem Lett 1992; 2:897–900.
104. Basten J, Jaurand G, Oldehanter B, Petitou M, van Boeckel CAA. Biologically-active heparin-like fragments with a non-glycosamino glycan structure. 2. A tetra-*ortho*-methylated pentasaccharide with high-affinity for antithrombin-III. Bioorg Med Chem Lett 1992; 2:901–904.
105. Lucas H, Basten JEM, Konradsson P, van Boeckel CAA. A short synthetic route towards a biologically-active heparin-like pentasaccharide with a pseudo-alternating sequence. Angew Chem Int Edit Engl 1993; 32:434–436.
106. Westerduin P, van Boeckel CAA, Basten JEM, Broekhoven MA, Lucas H, Rood A, van der Heijden H, van Amsterdam RGM, van Dinther TG, Meuleman DG. Feasible synthesis and biological properties of six "non-glycosamino" glycan analogues of the antithrombin III binding heparin pentasaccharide. Bioorg Med Chem 1994; 2:1267–1280.
107. Sakairi N, Basten JEM, van der Marel GA, van Boeckel CAA, van Boom JH. Synthesis of a conformationally constrained heparin-like pentasaccharide. Chem-Eur J 1996; 2:1007–1013.
108. Petitou M, Herault JP, Lormeau JC, Helmboldt A, Mallet JM, Sinay P, Herbert JM. Introducing a C-interglycosidic bond in a biologically active pentasaccharide hardly affects its biological properties. Bioorg Med Chem 1998; 6:1509–1516.
109. Helmboldt A, Petitou M, Mallet JM, Herault JP, Lormeau JC, Driguez PA, Herbert JM, Sinay P. Synthesis and biological activity of a new anti-factor Xa pentasaccharide with a C-interglycosidic bond. Bioorg Med Chem Lett 1997; 7:1507–1510.
110. Lei PS, Duchaussoy P, Sizun P, Mallet JM, Petitou M, Sinay P. Synthesis of a 3-deoxy-L-iduronic acid containing heparin pentasaccharide to probe the conformation of the antithrombin III binding sequence. Bioorg Med Chem 1998; 6:1337–1346.
111. Das SK, Mallet JM, Esnault J, Driguez PA, Duchaussoy P, Sizun P, Herault JP, Herbert JM, Petitou M, Sinay P. Synthesis of conformationally locked carbohydrates: A skew-boat conformation of L-iduronic acid governs the antithrombotic activity of heparin. Angew Chem Int Edit 2001; 40:1670–1673.
112. Sisu E, Tripathy S, Mallet JM, Driguez PA, Herault JP, Sizun P, Herbert JM, Petitou M, Sinay P. Synthesis of new conformationally constrained pentasaccharides as molecular probes to investigate the biological activity of heparin. Biochimie 2003; 85:91–99.

113. Codee JDC, van der Marel GA, van Boeckel CAA, van Boom JH. Probing the heparin – antithrombin III interaction using synthetic pentasaccharides bearing positively charged groups. Eur J Org Chem 2002:3954–3965.
114. Westerduin P, Basten JEM, Broekhoven MA, de Kimpe V, Kuijpers WHA, van Boeckel CAA. Synthesis of tailor-made glycoconjugates showing ATIII-mediated inhibition of blood coagulation factors Xa and thrombin. Angew Chem Int Edit Engl 1996; 35:331–333.
115. Basten JEM, Dreef-Tromp CM, de Wijs B, van Boeckel CAA. In vitro evaluation of synthetic heparin-like conjugates comprising different thrombin binding domains. Bioorg Med Chem Lett 1998; 8:1201–1206.
116. Buijsman RC, Kuijpers WHA, Basten JEM, KuylYeheskiely E, van der Marel GA, van Boeckel CAA, van Boom JH. Synthesis of a pentasaccharide–oligonucleotide conjugate: a novel antithrombotic agent. Chem-Eur J 1996; 2:1572–1577.
117. Buijsman RC, Basten JEM, van Dinther TG, van der Marel GA, van Boeckel CAA, van Boom JH. Design and synthesis of a novel synthetic NAPAP-penta-saccharide conjugate displaying a dual antithrombotic action. Bioorg Med Chem Lett 1999; 9:2013–2018.
118. Petitou M, Duchaussoy P, Driguez PA, Jaurand G, Herault JP, Lormeau JC, van Boeckel CAA, Herbert JM. First synthetic carbohydrates with the full anticoagulant properties of heparin. Angew Chem Int Edit 1998; 37:3009–3014.
119. Duchaussoy P, Jaurand G, Driguez PA, Lederman I, Gourvenec F, Strassel JM, Sizun P, Petitou M, Herbert JM. Design and synthesis of heparin mimetics able to inhibit thrombin. Part 1. Identification of a hexasaccharide sequence able to inhibit thrombin and suitable for "polymerisation". Carbohydr Res 1999; 317:63–84.
120. Duchaussoy P, Jaurand G, Driguez PA, Lederman I, Ceccato ML, Gourvenec F, Strassel JM, Sizun P, Petitou M, Herbert JM. Assessment through chemical synthesis of the size of the heparin sequence involved in thrombin inhibition. Carbohydr Res 1999; 317:85–99.
121. Dreef-Tromp CM, Basten JEM, Broekhoven MA, van Dinther TG, Petitou M, van Boeckel CAA. Biological properties of synthetic glycoconjugate mimics of heparin comprising different molecular spacers. Bioorg Med Chem Lett 1998; 8:2081–2086.
122. Petitou M, Duchaussoy P, Driguez PA, Herault JP, Lormeau JC, Herbert JM. New synthetic heparin mimetics able to inhibit thrombin and factor Xa. Bioorg Med Chem Lett 1999; 9:1155–1160.
123. Petitou M, Driguez PA, Duchaussoy P, Herault JP, Lormeau JC, Herbert JM. Synthetic oligosaccharides having various functional domains: potent and potentially safe heparin mimetics. Bioorg Med Chem Lett 1999; 9:1161–1166.
124. Driguez PA, Lederman I, Strassel JM, Herbert JM, Petitou M. Synthetic carbohydrate derivatives as low sulfated heparin mimetics. J Org Chem 1999; 64:9512–9520.
125. Pellegrini L, Burke DF, von Delft F, Mulloy B, Blundell TL. Crystal structure of fibroblast growth factor receptor ectodomain bound to ligand and heparin. Nature 2000; 407:1029–1034.
126. Kjellen L, Lindahl U. Proteoglycans – structures and interactions. Annu Rev Biochem 1991; 60:443–475.

127. Kan MK, Wang F, Xu JM, Crabb JW, Hou JZ, McKeehan WL. An essential heparin-binding domain in the fibroblast growth-factor receptor kinase. Science 1993; 259:1918–1921.
128. Mach H, Volkin DB, Burke CJ, Middaugh CR, Linhardt RJ, Fromm JR, Loganathan D, Mattsson L. Nature of the interaction of heparin with acidic fibroblast growth-factor. Biochemistry 1993; 32:5480–5489.
129. Thompson LD, Pantoliano MW, Springer BA. Energetic characterization of the basic fibroblast growth-factor heparin interaction – identification of the heparin-binding domain. Biochemistry 1994; 33:3831–3840.
130. Maccarana M, Casu B, Lindahl U. Minimal sequence in heparin heparan-sulfate required for binding of basic fibroblast growth-factor. J Biol Chem 1994; 269:3903.
131. Ornitz DM, Herr AB, Nilsson M, Westman J, Svahn CM, Waksman G. FGF binding and FGF receptor activation by synthetic heparan-derived disaccharides and trisaccharides. Science 1995; 268:432–436.
132. Herr AB, Ornitz DM, Sasisekharan R, Venkataraman G, Waksman G. Heparin-induced self-association of fibroblast growth factor-alpha – evidence for two oligomerization processes. J Biol Chem 1997; 272:16382–16389.
133. Pellegrini L. Role of heparan sulfate in fibroblast growth factor signalling: a structural view. Curr Opin Struct Biol 2001; 11:629–634.
134. Guerrini M, Agulles T, Bisio A, Hricovini M, Lay L, Naggi A, Poletti L, Sturiale L, Torri G, Casu B. Minimal heparin/heparan sulfate sequences for binding to fibroblast growth factor-1. Biochem Biophys Res Commun 2002; 292:222–230.
135. Maccarana M, Casu B, Lindahl U. Minimal sequence in heparin heparan-Sulfate required for Binding of Basic Fibroblast Growth-Factor. J Biol Chem 1993; 268:23898–23905.
136. Guimond S, Maccarana M, Olwin BB, Lindahl U, Rapraeger AC. Activating and inhibitory heparin sequences for FGF-2 (basic FGF) – distinct requirements for FGF-1, FGF-2, and FGF-4. J Biol Chem 1993; 268:23906–23914.
137. DiGabriele AD, Lax I, Chen DI, Svahn CM, Jaye M, Schlessinger J, Hendrickson WA. Structure of a heparin-linked biologically active dimer of fibroblast growth factor. Nature 1998; 393:812–817.
138. Turnbull JE, Fernig DG, Ke YQ, Wilkinson MC, Gallagher JT. Identification of the basic fibroblast growth-factor binding sequence in fibroblast heparan-sulfate. J Biol Chem 1992; 267:10337–10341.
139. Walker A, Turnbull JE, Gallagher JT. Specific heparan-sulfate saccharides mediate the activity of basic fibroblast growth-factor. J Biol Chem 1994; 269:931–935.
140. Rusnati M, Coltrini D, Caccia P, Dellera P, Zoppetti G, Oreste P, Valsasina B, Presta M. Distinct role of 2-*O*-sulfate, *N*-sulfate, and 6-*O*-sulfate groups of heparin in the formation of the ternary complex with basic fibroblast growth-factor and soluble FGF receptor-1. Biochem Biophys Res Commun 1994; 203:450–458.
141. Wang HM, Toida T, Kim YS, Capila I, Hileman RE, Bernfield M, Linhardt RJ. Glycosaminoglycans can influence fibroblast growth factor-2 mitogenicity without significant growth factor binding. Biochem Biophys Res Commun 1997; 235:369–373.

142. Harmer NJ, Ilag LL, Mulloy B, Pellegrini L, Robinson CV, Blundell TI. Towards a resolution of the stoichiometry of the fibroblast growth factor (FGF)–FGIF receptor–heparin complex. J Mol Biol 2004; 339:821–834.
143. Nilsson M, Svahn CM, Westman J. Synthesis of the methyl glycosides of a tri- and a tetra-saccharide related to heparin and heparan sulphate. Carbohydr Res 1993; 246:161–172.
144. Westman J, Nilsson M, Ornitz DM, Svahn CM. Synthesis and fibroblast growth-factor binding of oligosaccharides related to heparin and heparan-sulfate. J Carbohydr Chem 1995; 14:95–113.
145. Kovensky J, Duchaussoy P, Petitou M, Sinay P. Binding of heparan sulfate to fibroblast growth factor-2 total synthesis of a putative pentasaccharide binding site. Tetrahedron-Asymmetry 1996; 7:3119–3128.
146. Poletti L, Fleischer M, Vogel C, Guerrini M, Torri G, Lay L. A rational approach to heparin-related fragments – synthesis of differently sulfated tetrasaccharides as potential ligands for fibroblast growth factors. Eur J Org Chem 2001:2727–2734.
147. de Paz JL, Angulo J, Lassaletta JM, Nieto PM, Redondo-Horcajo M, Lozano RM, Gimenez-Gallego G, Martin-Lomas M. The activation of fibroblast growth factors by heparin: synthesis, structure, and biological activity of heparin-like oligosaccharides. Chembiochem 2001; 2:673–685.
148. Ojeda R, Angulo J, Nieto PM, Martin-Lomas M. The activation of fibroblast growth factors by heparin: Synthesis and structural study of rationally modified heparin-like oligosaccharides. Can J Chem-Rev Can Chim 2002; 80:917–936.
149. Lucas R, Angulo J, Nieto PM, Martin-Lomas M. Synthesis and structural study of two new heparin-like hexasaccharides. Org Biomol Chem 2003; 1:2253–2266.
150. Angulo J, De Paz JL, Nieto PM, Martin-Lomas M. Interaction of heparin with Ca^{2+}: a model study with a synthetic heparin-like hexasaccharide. Isr J Chem 2000; 40:289–299.
151. Chevalier F, Angulo J, Lucas R, Nieto PM, Martin-Lomas M. The heparin–Ca^{2+} interaction: structure of the Ca^{2+} binding site. Eur J Org Chem 2002; 2367–2376.
152. Chevalier F, Lucas R, Angulo J, Martin-Lomas M, Nieto PM. The heparin–Ca^{2+} interaction: the influence of the *O*-sulfation pattern on binding. Carbohydr Res 2004; 339:975–983.
153. Angulo J, Ojeda R, de Paz JL, Lucas R, Nieto PM, Lozano RM, Redondo-Horcajo M, Gimenez-Gallego G, Martin-Lomas M. The activation of fibroblast growth factors (FGFs) by glycosaminoglycans: Influence of the sulfation pattern on the biological activity of FGF-1. Chembiochem 2004; 5:55–61.
154. Liu J, Thorp SC. Cell surface heparan sulfate and its roles in assisting viral infectious. Med Res Rev 2002; 22:1–25.
155. Liu J, Shriver Z, Pope RM, Thorp SC, Duncan MB, Copeland RJ, Raska CS, Yoshida K, Eisenberg RJ, Cohen G, Linhardt RJ, Sasisekharan R. Characterization of a heparan sulfate octasaccharide that binds to herpes simplex virus type 1 glycoprotein D. J Biol Chem 2002; 277:33456–33467.
156. Shukla D, Liu J, Blaiklock P, Shworak NW, Bai XM, Esko JD, Cohen GH, Eisenberg RJ, Rosenberg RD, Spear PG. A novel role for 3-*O*-sulfated heparan sulfate in herpes simplex virus 1 entry. Glycobiology 1999; 9:155.

157. Lohman GJS, Seeberger PH. A stereochemical surprise at the late stage of the synthesis of fully *N*-differentiated heparin oligosaccharides containing amino, acetamido, and *N*-sulfonate groups. J Org Chem 2004; 69:4081–4093.
158. Sobel M, Fish WR, Toma N, Luo S, Bird K, Mori K, Kusumoto S, Blystone SD, Suda Y. Heparin modulates integrin function in human platelets. J Vasc Surg 2001; 33:587–594.
159. Koshida S, Suda Y, Sobel M, Kusumoto S. Synthesis of oligomeric assemblies of a platelet-binding key disaccharide in heparin and their biological activities. Tetrahedron Lett 2001; 42:1289–1292.
160. Koshida S. Synthesis, designed assembly, and biological activity of heparin fragments responsible for binding interaction to platelets. Trends Glycosci Glycotechnol 2001; 13:209–213.

Chemistry and Biology of Heparin and Heparan Sulfate
H.G. Garg, R.J. Linhardt and C.A. Hales (Editors)

Chapter 5

Biochemical and Pharmacologic Rationale for Synthetic Heparin Polysaccharides

JEANINE M. WALENGA, WALTER P. JESKE

Departments of Thoracic & Cardiovascular Surgery and Pathology, Cardiovascular Institute, Loyola University Chicago, Maywood, IL, USA

and

JAWED FAREED

Department of Pathology, Cardiovascular Institute, Loyola University Chicago, Maywood, IL, USA

I. Introduction

The creation of the synthetic heparin pentasaccharide has addressed an important issue in the pharmacology of heparin on the contribution of the inhibition of factor Xa in the mediation of the antithrombotic effect of low molecular weight heparin and heparin oligosaccharides.

The first studies using heparin derived oligosaccharides failed to demonstrate a functional relevance of the inhibition of factor Xa to an antithrombotic effect in experimental animal models. It was suggested that inactivation of thrombin was required for inhibition of thrombosis and that agents with predominantly anti-factor Xa activity were weakly effective antithrombotic agents. These studies were inconclusive, however, since the agents used were heterogeneous in structure and of relatively low potency. It remained questionable whether a highly active anti-factor Xa agent could be antithrombotic *in vivo*.

Pentasaccharide is a synthetic heparin-related agent representing the minimum saccharidic sequence of critical structure required for the high affinity binding of heparin to the antithrombin (AT) molecule and eliciting solely a high inhibitory action against factor Xa (opposed to the multiple antithrombotic mechanisms of heparin). Since pentasaccharide is synthetic, it is known to be homoge-

neous in molecular size and structure. This oligosaccharide was thus an optimal tool for studies related to antithrombotic agents expressing sole anti-factor Xa activity. Pentasaccharide proved that sole inhibition of factor Xa elicits an antithrombotic effect by decreasing the generation of thrombin, resulting in a controlled and selective modulation of coagulation.

This basic information, initiated to understand the mechanism of action of heparin, was obtained in studies in the 1980s. These findings served as the basis to move ahead with the development of pentasaccharide as a drug for human use. Due to the synthetic nature of this agent, it was logical that chemical derivatives of the original pentasaccharide would be made and evaluated for human pharmacologic purposes. These developments continue to this day.

II. Biological Activities and Mechanisms of Action of Heparin

Multiple discrete structural regions within a heparin molecule are responsible for its ability to complex with AT or other macromolecules to promote or modulate a wide range of biological activities (Fig. 1). These interactions range from nonspecific electrostatic binding to very specific lock and key relationships. Although the AT mediated inhibition of thrombin (factor IIa) and factor Xa are thought to be the primary mechanisms of action of heparin in producing an antithrombotic effect (1–5) other mechanisms have been elucidated.

A. Antithrombin Mediated Heparin Activity

The primary mechanism of the antithrombotic activity of heparin is through association with AT, a 55 kDa single chain plasma glycoprotein (6,7). Heparin binds AT forming equimolar stable complexes through an epsilon–aminolysl residue (8), producing an allosteric alteration in the AT molecule such that the critical arginine_{385} residue of AT is more readily available to interact with the serine active site on specific activated enzymes.

By binding to different regions of the AT molecule, thereby inducing different structural alterations of the inhibitor, different enzymes can be inhibited by the heparin-AT complex (9). Single site binding of heparin to AT is sufficient to inhibit factor Xa, whereas a secondary binding of heparin to AT (therefore a longer saccharidic chain) is required to produce a conformational change in AT that allows for inhibition of thrombin (10). Coagulation factors IXa, XIa, XIIa, as well as plasmin and trypsin can also be neutralized by this complex (11–13). Although a much weaker effect, several investigators have shown that factor VII is also inhibited by heparin (14–16).

In the presence of heparin, the inhibition of these enzymes is accelerated 300–2000-fold above the inhibition rate by AT alone (17). Studies using affinity chromatography established that 30% (gravimetrically) of unfractionated heparin can bind with high affinity to AT (18,19). The high-affinity material is typically of higher

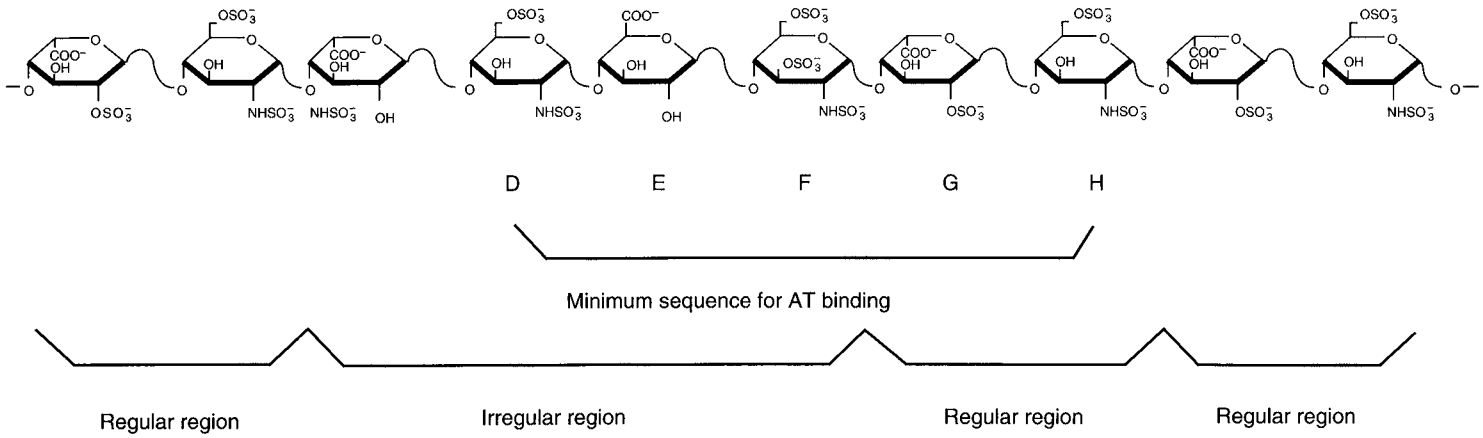

Figure 1 Repeating trisulfated disaccharides represent the regular region of the heparin saccharidic chain with interconnecting irregular regions heterogeneous in structure.

molecular weight. It has also been shown that as molecular weight increased, high-affinity derivatives showed an increased proportion of chains with two binding sites for AT (20).

B. Heparin Cofactor II Mediated Heparin Activity

A second means by which heparin can inhibit thrombin is through heparin cofactor II (HC II). This inhibitor is distinct from AT in structure and function. It is a 66 kDa glycoprotein that is not recognized by antibodies towards AT. HC II is a relatively ineffective inhibitor of factors IXa, Xa, XIa, and plasmin (21). *In vitro*, the thrombin inhibitory effect has only been demonstrated at heparin concentrations greater than 5 U/ml in contrast to the much lower concentrations of heparin ($\geq$0.1 U/ml) required to inhibit thrombin via AT (22). Dermatan sulfate and low affinity heparin are also capable of activating HC II (23,24). HC II-mediated thrombin inhibition may be important *in vivo* as individuals with HC II deficiency have been diagnosed with thrombosis (25,26).

C. Tissue Factor Pathway Inhibitor

The Kunitz-type protease inhibitor tissue factor pathway inhibitor (TFPI) is believed to play an important role as an endogenous inhibitor of tissue factor induced blood coagulation (27,28). TFPI exerts its anticoagulant actions by inhibiting factors Xa and VIIa in a two-step, reversible reaction (29). TFPI is synthesized in vascular endothelium and the majority of the intravascular pool is associated with the endothelial cells (30). This endothelial pool of TFPI is releasable by heparin and other polyanionic substances (31–36) and is believed to contribute to the anticoagulant and antithrombotic effects of these agents. The mechanism of TFPI release is not clear, but may involve displacement from endothelial glycosaminoglycans (27). When measured using a dilute prothrombin time assay, TFPI has been shown to mediate approximately one-third of the observed anticoagulant activity of heparin (37). Infusion of recombinant TFPI decreases mortality of gram-negative bacterial sepsis in a rabbit model (38). Mice with heterozygous TFPI deficiency exhibit a greater degree of atherosclerosis within the vasculature and exhibit a shorter time to occlusive thrombus formation after plaque rupture (39) than wild-type mice. In addition to releasing TFPI from endogenous binding sites, heparin markedly enhances the ability of TFPI to inhibit the tissue factor/factor VIIa complex (40,41) and potentiate the inhibition of thrombin and factor Xa generation by TFPI (42). This may be the result of heparin's ability to prevent TFPI from binding to circulating lipoproteins (43).

Low molecular weight heparins are known to be structurally and biologically diverse (44). Low molecular weight heparins have been shown to release TFPI from the endothelium (31); this effect is related, at least in part, to the molecular weight of the administered heparin (45) and its charge density (46).

D. Non-SERPIN Mediated Heparin Activity

A third mechanism of action of heparin is anti-serine protease in nature but appears to be independent of mediation by AT and HC II. Experimental evidence for this was shown by a low affinity heparin virtually devoid of anti-factor IIa and anti-factor Xa activities *in vitro*, which significantly increased hemorrhage without inducing an *in vivo* antithrombotic effect (47). Additionally, this low affinity heparin was capable of potentiating the antithrombotic effect of a high affinity, 3.5 kDa heparin (48). Further evidence lies in the fact that a low affinity heparin has been shown to induce more platelet pro-aggregatory activity than low molecular weight, high AT affinity fractions (49).

III. Fractionation and Fragmentation of Heparin

Attempts have been made to individually examine the heterogeneous structural features of heparin in order to characterize functionally active domains required for anticoagulant action. To accomplish this objective, fractionation of the components of the natural parent heparin material has been performed based on molecular weight, charge density, solubility characteristics and affinity (usually to AT). Subsequently, chemical procedures to depolymerize the larger molecular weight heparin components into lower molecular weight material were used to generate heparin fragments.

The development of fractions (naturally depolymerized forms) and fragments (chemically or enzymatically depolymerized forms) of heparin added a new dimension in the prophylactic and therapeutic use of heparin. With these more defined materials, efforts were aimed at finding a safer antithrombotic agent that would effectively prevent venous thrombosis, yet would have a lower bleeding risk and a decreased incidence of heparin-induced thrombocytopenia (HIT).

A. Biological Activity

It was found that low molecular weight heparin derivatives did not exhibit strong heparin-like activity in global coagulant assays. A molecular weight dependence of anticoagulant activity was demonstrated (1,50,51) raising doubts as to whether these materials would be effective at inhibiting thrombus formation *in vivo*.

To better understand the depolymerized heparins, a number of *in vitro* methods were developed to analyze their specific rather than overall inhibitory activities (52). The inhibition of factor Xa and thrombin was evaluated by coagulant and amidolytic (colorimetric) assays (53–56). These new assays provided a sensitivity that allowed for the observation of a direct correlation between the inhibitory activity against factors IIa, IXa, and XIa and the molecular weight of heparin. Ultra low molecular weight heparin derivatives were found to be virtually devoid of anti-factor IIa activity (1,57). An octadecasaccharide was found to be the smallest

heparin derivative to possess antithrombin activity (10,58). The inhibitory activity against factor Xa, however, was retained in low molecular weight materials and did not show a similar correlation with molecular weight, anticoagulant activity or antithrombin activity (1,2,4,10,48,51,57–59). A similar lack of molecular weight dependence was shown for the inhibition of factors XIIa and kallikrein (2). A direct molecular weight dependency on the rate of inhibition of factor Xa by heparin existed (60). A 35-fold decrease in the inhibition rate constant was observed between heparin with a molecular weight of 25 kDa ($k_i = 4.2 \times 10^8\,M^{-1}\,min^{-1}$) and the 1.7 kDa pentasaccharide ($k_i = 1.2 \times 10^7\,M^{-1}\,min^{-1}$).

In vitro studies on the prothrombinase complex suggested different inhibitory kinetic rates for low molecular weight heparins and unfractionated heparin. Low molecular weight heparins were found to be progressively less effective, at lower molecular weights than unfractionated heparin, at inhibiting platelet-bound prothrombinase complexes (61). Higher molecular weight heparin derivatives, however, showed a greater discrepancy between the rate of inhibition of free and platelet bound factor Xa such that platelet bound factor Xa was inhibited at a decreased rate from that of unbound factor Xa (61–63). There was, however, no discrepancy observed between the two inhibitory rates for low molecular weight heparins.

In an AT-free system, heparin derivatives demonstrated a weaker inhibition of thrombin-induced platelet factor Va generation and thrombin- and collagen-induced platelet activation of prothrombin than unfractionated heparin (64). In a plasma system, the generation of thrombin was not as strongly inhibited by low molecular weight heparins as it was by unfractionated heparin or heparin derivatives with significant antithrombin activity (65). In addition, the generation of factor Xa following intrinsic pathway activation could not be completely inhibited by high anti-factor Xa activity agents. It was speculated from these results that agents high in anti-factor Xa activity and low in anti-factor IIa activity, known to be poor predictors of anticoagulant activity, would not be effective antithrombotic agents *in vivo*.

Other studies with depolymerized heparins indicated that the charge density (largely the sulfate content) of the heparin was directly related to the anticoagulant activity (66–68). It was difficult, however, to determine a clear relationship between potency and charge density since molecular weight and affinity to AT also varied between the derivatives studied. Further studies showed that carboxyl groups were also essential for anticoagulant activity, whereas acetyl groups were probably non-functional (17,69,70).

B. Neutralization of the Antiprotease Effects of Heparin Derivatives

The antiprotease effects of heparin derivatives can be neutralized by platelet factor 4 (PF4), protamine sulfate, polybrene, and histidine rich glycoprotein. Studies have shown that the specific antiprotease activities of heparin derivatives are differentially neutralized [i.e., the anti-factor IIa activity can be fully neutralized whereas the anti-factor Xa activity of the same agent may only be partially neutralized (71)].

The anti-factor Xa activity of a decasaccharide was found to be insignificantly decreased in the presence of high concentrations of PF4 (72). Measurable but incomplete neutralization of the anti-factor Xa activity of tetradecasaccharides and hexadecasaccharides was observed, whereas complete neutralization of the anti-factor Xa activity of octadecasaccharides and larger oligosaccharides was observed with excess PF4. A similar molecular weight dependency of neutralization of the anticoagulant activity by protamine sulfate has been reported (73). The anti-factor IIa activities of octadecasaccharides and larger oligosaccharides were more readily neutralized by PF4 than were the anti-factor Xa activities (72). Histidine rich-glycoprotein is unable to fully neutralize oligosaccharides of less than 18 monosaccharide units (74). In the same study, an octasaccharide retained 50% of its anti-factor Xa activity even at a histidine rich-glycoprotein:oligosaccharide molar ratio of 500:1.

It has been suggested that the interaction of heparin with histidine rich glycoprotein and PF4 requires an additional saccharidic sequence than that required for binding to AT in order to elicit a full neutralization response (74). It has also been suggested that binding of either of these neutralizing agents to heparin at a site adjacent to the AT binding site either causes a steric interference with the formation of the AT-protease complex or a displacement of AT from the heparin chain, thus inhibiting the effect of the heparins (72,75,76).

Several studies using heparin and low molecular weight heparin, have suggested that the affinity of heparin for protamine sulfate is directly related to sulfation and that this may be more important than molecular weight in determining the degree of neutralization (73,77,78).

C. Interactions Between Platelets and Heparin Derivatives

In vitro studies have demonstrated a decreased level of platelet interactions with low molecular weight heparin as compared to unfractionated heparin. These interactions include spontaneous platelet aggregation upon addition of heparin to platelet rich plasma and augmentation of aggregation induced by ADP, collagen, epinephrine, and thrombin. When performed in platelet rich plasma, a molecular weight dependence to the platelet–heparin interactions was observed with little to no reactivity with very low molecular weight heparins (49,79–82). Platelet reactivity, however, did not parallel anticoagulant activity or AT affinity for high molecular weight heparins. For low molecular weight heparins, on the other hand, high affinity to AT corresponded to enhanced platelet activity. Specific studies examining the binding of fibrinogen to ADP-treated platelets revealed a reduced effect only with certain low molecular heparins. It has been postulated that these effects may be related to the anionic charge of the heparin and, therefore, its degree of sulfation (83). *In vivo* studies have confirmed that low molecular weight heparin is less disruptive of platelet plug formation than unfractionated heparin (84).

In other platelet rich plasma systems, using plasma or serum from patients diagnosed with HIT, a molecular weight dependent effect on heparin-induced aggregation was demonstrated (85).

D. Endothelial Interactions of Heparin Derivatives

Limited studies have shown that low molecular weight heparins have a lower affinity for endothelial cells as compared to unfractionated heparin (86). However, an ultralow molecular weight hexasaccharide binds to endothelial cell growth factor (87). While a pentasaccharide and a hexasaccharide have demonstrated antiproliferative activity against smooth muscle cells, a tetrasaccharide and disaccharide were ineffective (88). Thus, the angiogenic property of heparin appears not to be related to its anticoagulant effect since these non-coagulant derivatives were as effective as unfractionated heparin (89). It was determined, however, that an *O*-sulfate group is required in heparin for the antiproliferative effect and *N*-sulfate and *N*-acetyl groups helped to increase activity (88).

E. Fibrinolytic Effects of Heparin Derivatives

The fibrinolytic effect observed with unfractionated heparin both *in vivo* and *in vitro* has also been observed for the derivatives of heparin (90). Low molecular weight heparins induce a fibrinolytic response in rat and rabbit models and an increase in plasminogen activator was observed in human volunteers (91,92). Anti-fibrinolytic drugs negated the latter effect. Activity levels appear to be dependent on the assays used *in vitro* and possibly on circadian rhythms (93).

F. *In Vivo* Experimental Studies with Heparin Derivatives

The concept of hemostatic control, postulated by Wessler (94) and supported by experimental data of Yin (95), pointed to a pivotal role played by factor Xa in the generation of thrombin. These ideas, coupled with the high anti-factor Xa and low anti-thrombin activities of low molecular weight heparins, stimulated a focus on the specific enhancement of anti-factor Xa activity for the prevention of thrombosis. It was hypothesized that the antithrombin activity, being associated with anticoagulant activity and platelet interactions, was also associated with a hemorrhagic effect (49,80,96). It was subsequently hypothesized that by eliminating this activity, an effective antithrombotic agent might be obtained, which possessed a higher benefit to-risk ratio than unfractionated heparin.

G. *In Vivo* Experimental Antithrombotic Data

Published experimental results with animal models of venous thrombosis have shown that low molecular weight heparins with higher anti-factor Xa:anti-factor IIa activity ratios than unfractionated heparins produce equivalent antithrombotic effects as heparin. Studies have been performed on heparin derivatives that were produced by numerous procedures, using different animal models. Thus, a detailed comparative evaluation of the heparins is difficult, but generalizations can be made.

Heparin fractions from 4.0 to 9.5 kDa prepared by chemical depolymerization produced significant inhibition of thrombosis in rabbit models of stenosis/stasis coupled with an induced hypercoagulable state (96–101).

Similar experimental animal studies were performed on low molecular weight heparins developed for commercial use. Nadroparin (Choay; Sanofi), a 4.5 kDa nitrous acid-derived product, was shown to be at least as effective on a gravimetric basis as unfractionated heparin at inhibiting venous stasis thrombosis in rabbits when administered subcutaneously (102). Enoxaparin (Sanofi-Aventis), a 4.0 kDa product prepared by alkaline cleavage of benzyl esters of heparin, exhibited equivalent activities as heparin at preventing the extension of new or established venous thrombi in a rabbit model following intravenous administration (80,103). Dalteparin (KabiVitrum, Stockholm, Sweden), a 4.5 kDa product prepared by heparinase degradation, prevented thrombosis to the same extent as heparin in a rabbit model of endothelial damage and flow reduction following intravenous administration (99,104).

Experimental studies were extended to determine whether ultralow molecular weight heparins were capable of producing *in vivo* antithrombotic activity. The antithrombotic actions of an octasaccharide in a venous stasis thrombosis model, was the first experimental demonstration of a sole anti-factor Xa oligosaccharide exhibiting antithrombotic actions (105). Subsequent studies deduced that oligosaccharides with high affinity to AT and virtually devoid of antithrombin activity, were incapable of exhibiting *in vivo* antithrombotic activities (99,100,106,107).

Based on several studies of heparin derivatives of varying molecular weight, it was suggested that a minimum molecular weight of 4 kDa was required to produce an antithrombotic effect equal to that of unfractionated heparin, as derivatives with molecular weights of 2.1 and 3.3 kDa were less effective than a 4 kDa derivative (99). This and other experimental data showed a lack of direct correlation between the *in vivo* antithrombotic effect and either the *ex vivo* or *in vitro* anti-factor Xa activity. Although several of the described studies showed partial effectiveness of low molecular weight oligosaccharides at preventing thrombosis, none demonstrated complete inhibition of thrombosis by highly selective anti-factor Xa agents. Since high circulating levels of anti-factor Xa activity were achieved in these studies without total inhibition of thrombosis, it was reasoned that one could not predict an antithrombotic response based on circulating anti-factor Xa levels (100, 106, 107). Results of another study comparing the antithrombotic effects of 2.5 and 5.0 kDa heparin derivatives concluded that the presence of anti-factor IIa activity associated with the anti-factor Xa activity strongly increases the inhibition of thrombosis (108).

H. The Bleeding Effect of Heparin Derivatives

Animal studies have shown that at equal unit doses, heparin derivatives caused less blood loss in animals while exhibiting equal antithrombotic activity as standard heparin. This has been observed for both experimental and commercially developed heparin derivatives (80,84,90,104,109–111).

Conversely, one study has shown that, at a high dose of 10 mg/kg, enoxaparin induced a platelet defect as detected by *ex vivo* collagen-induced platelet aggregation, which was directly correlated to increased blood loss in the rabbit (112). Other studies on low affinity heparin demonstrated that although no *in vitro* anticoagulant

or *in vivo* antithrombotic response could be produced by this material, a bleeding effect was pronounced (47,113).

The mechanism of heparin-induced bleeding is not well understood; however, it has been suggested that bleeding may be related to the anticoagulant effect. Based on current evidence, a heparin-induced antithrombotic effect has not been correlated with an anticoagulant effect in all individuals (114). Furthermore, the low molecular weight heparins have proven to be antithrombotic with reduced bleeding tendencies yet demonstrate little to no anticoagulant effect (4,101). Other factors likely to contribute to the bleeding effect include the effect of heparin on platelet–vessel wall interactions, the endothelium, and fibrinolysis (113). As previously discussed, the low molecular weight heparins have a decreased effect on platelet activation (49).

IV. Elucidation of the Minimum Heparin Sequence for Binding to AT

Initial studies on partially digested heparin demonstrated that anticoagulant activity was directly related to the molecular weight of heparin. Low molecular weight components were found to be more active against activated factor X than against thrombin (1,57). It had been determined that an octadecasaccharide was the minimal saccharidic sequence capable of eliciting an antithrombin effect (10,58). Subsequently, a high AT affinity decasaccharide was isolated, which exhibited high anti-factor Xa activity but very low antithrombin activity (115).

The ^{13}C-nuclear magnetic resonance (NMR) spectroscopy of this decasaccharide revealed an extra signal corresponding to a structural group not commonly observed, a 3-*O*-sulfate group (116). Utilizing a newly discovered 3-*O*-sulfatase from human urine (117), the presence of a 3-*O*-sulfate group in certain oligosaccharides was demonstrated (118). The 3-*O*-sulfate group was not found in oligosaccharides of low affinity.

Subsequent studies were undertaken to further degrade the decasaccharide to obtain even lower molecular weight oligosaccharides. Using enzymatic or nitrous acid depolymerization of heparin, followed by AT affinity chromatography and gel filtration, two octasaccharides were obtained (119,120). These octasaccharides possessed high affinity to AT and extremely high inhibitory effects against factor Xa. NMR studies to determine the saccharidic sequence also revealed the presence of the 3-*O*-sulfate group in both preparations. Comparison of the two structures yielded a common hexasaccharide sequence that was then proposed as the minimal sequence to elicit biological activity.

Preparation of a hexasaccharide by heparinase degradation of the octasaccharide confirmed the hypothesis that such a sequence would retain high affinity to AT and high anti-factor Xa activity without antithrombin activity (Fig. 2) (119,121). Other octasaccharide components of heparin possessing biological activity have been reported; however, these substances were not devoid of antithrombin activity (122). Stepwise, controlled degradation of the previously derived decasaccharides

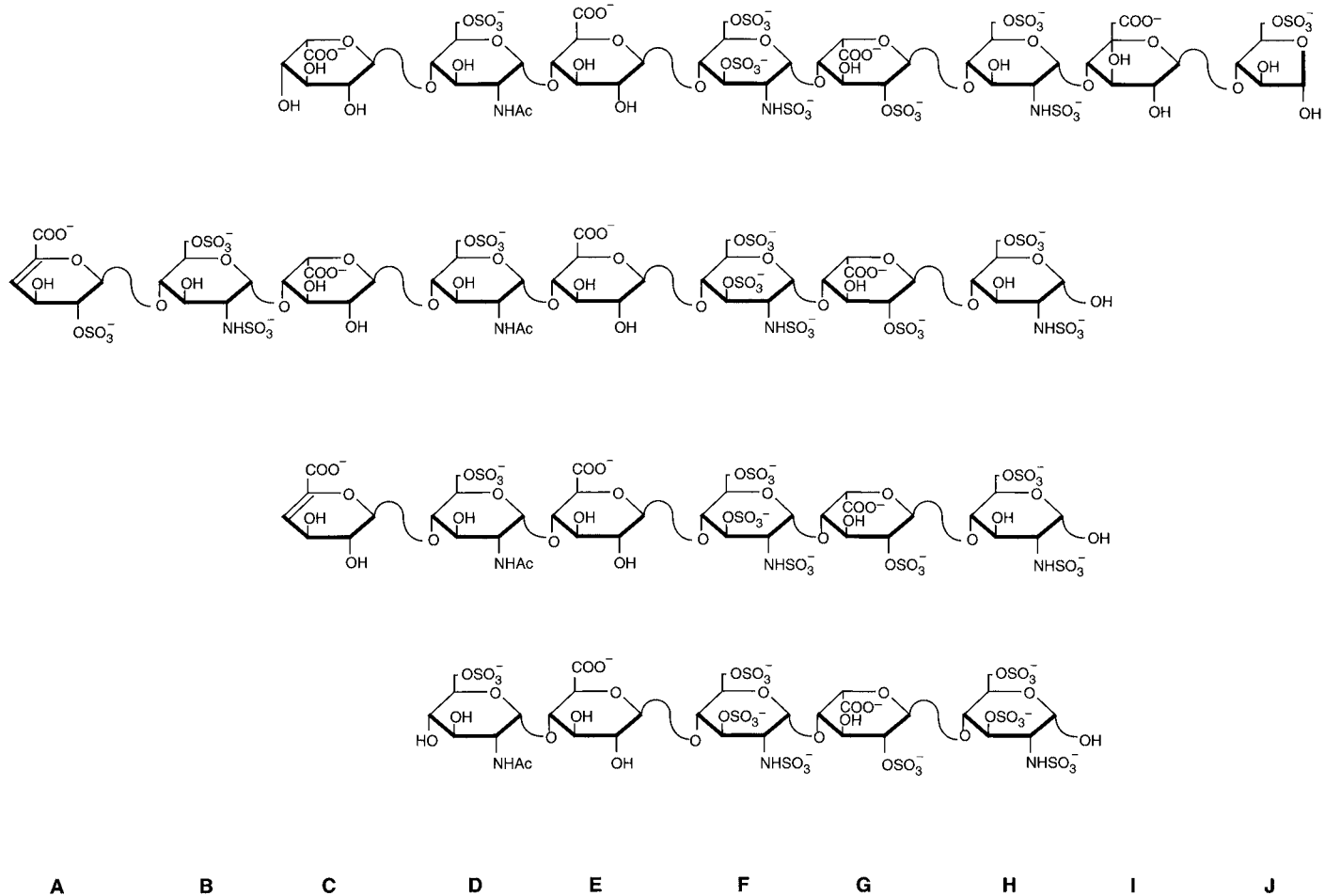

Figure 2 Oligosaccharides of heparin with high binding to AT, which led to the elucidation of the pentasaccharide as the minimal binding site of heparin to AT.

and octasaccharides, produced a hexasaccharide with a defined structure. Close inspection revealed that it contained in unnatural, 4,5-unsaturated uronic acid at the nonreducing end, suggesting that the pentasaccharide structure contained within the hexasaccharide was actually the minimal sequence that would bind to AT and elicit a high anti-factor Xa activity (121,123).

Earlier, Rosenberg had suggested that a tetrasaccharide might be the critical structural element required for anticoagulant activity (124). The isolation of large quantities of a tetrasaccharide derived from exhaustive nitrous acid cleavage of a material with high affinity to AT was reported. Since this tetrasaccharide was absent from low affinity fragments, it was reasoned that it was responsible for the anticoagulant activity; however, no conclusive data was produced.

V. Synthesis of the Pentasaccharide Representing the Critical Binding Site of Heparin to AT

A novel synthetic approach was used to produce the pentasaccharide sequence (Fig. 3) (125,126). The ^{13}C-NMR spectroscopy of the synthesized product revealed the anticipated spectral characteristics consistent with a pentasaccharide structure containing the desired sulfate, carboxyl, and amino groups (127). AT affinity analysis demonstrated a high affinity (3×10^{-8} M) (128). Anti-protease activities of 2800 anti-factor Xa U/mg in human plasma by a clotting method and 4000 anti-factor Xa U/mg in human plasma by an amidolytic method were demonstrated (129). Pharmacologic studies confirmed that this pentasaccharide was biologically active *in vivo* (130).

Due to the hypothesized critical nature of the 3-*O*-sulfate group on unit F of this pentasaccharide for eliciting high affinity to AT, anti-factor Xa activity and thus an antithrombotic effect, a structurally modified pentasaccharide devoid of the 3-*O*-sulfate group was synthesized (Fig. 4) (131,132). Biochemical studies did not show the extra signal in the ^{13}C-NMR spectrum that was previously speculated to result from the 3-*O*-sulfate group. This material did not possess high affinity to AT (5×10^{-4} M) (128), nor did it possess detectable anti-factor Xa activity (133).

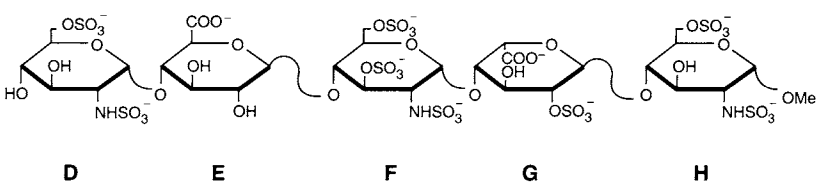

Figure 3 Structure of the pentasaccharide representing the minimal binding site of heparin to AT with high affinity. This is fondaparinux (Arixtra®; GlaxoSmithKline) that has been approved for prophylaxis and treatment of DVT and PE in certain clinical indications. It continues to undergo clinical development.

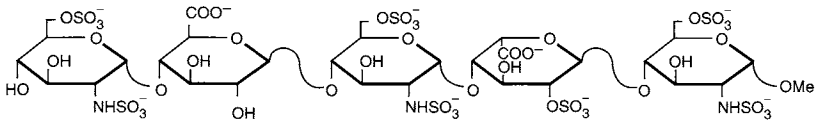

Figure 4 Structure of the 3-*O*-desulfated pentasaccharide. Removal of the 3-*O*-sulfate group on glucosamine residue F (replaced by a hydroxyl group) abolishes binding of the pentasaccharide to AT.

As a certain degree of variability in the structure of the pentasaccharide was thought to be compatible with binding to AT, additional structure–activity relationship studies were performed to more definitively prove the critical nature of the synthetic pentasaccharide structure. Both tetrasaccharides contained within the pentasaccharide (i.e., units D→G and units E→H in Fig. 1) exhibited decreased affinity to AT and decreased anti-factor Xa activity (131,133). It was demonstrated that not only was the 3-*O*-sulfate group on unit F critical for the desired properties of this pentasaccharide, but of an equally essential nature were the 6-*O*-sulfate group on unit D and the 2-*N*-sulfate group on unit F (123,132,134). An *N*-sulfate group on unit H was determined to be important for high AT affinity. Structural work by other investigators provided further evidence that a pentasaccharide was, indeed, the minimal region in heparin for high affinity AT (135).

The binding of pentasaccharide to AT produces an allosteric change in AT that increases its activity 1000-fold. The pentasaccharide-AT complex binds factor Xa via a serine residue on factor Xa that attaches to the arginine_{393}–serine_{394} site of AT. This inhibits factor Xa enzymatic activity in the coagulation cascade (136). Pentasaccharide, like heparin, is reversibly bound to AT and will freely dissociate to bind another AT molecule.

Larger heparin molecules can bind to the "pentasaccharide" site on AT while simultaneously binding to a secondary site. Complex conformational changes are thereby produced in AT allowing for the inhibition of thrombin and other coagulation enzymes (9,12,58,137,138). Due to molecular heterogeneity, heparin possesses multiple functional domains, which can elicit many biological activities. Pentasaccharide, of minimal structure, is only capable of the one inhibitory effect against factor Xa. Furthermore, due to its minimum sequence, none of the pentasaccharide's structure remains outside its binding area of the AT molecule.

VI. Preclinical Pharmacology of Fondaparinux

These basic investigations set the stage for the development of a new class of antithrombotic drugs. The synthetic heparin pentasaccharide (fondaparinux sodium, Arixtra®; GlaxoSmithKline) has the structure methyl-*O*-2-deoxy-6-*O*-sulfo-2-(sulfamino)-α-D-glucopyranosyl-(1→4)-*O*-β-D-glucopyranuronosyl-(1→4)-*O*-2-deoxy-3,6-di-*O*-sulfo-2-(sulfamino)-α-D-glucopyranosyl-(1→4)-*O*-2-*O*-sulfo-α-L-idopyranuronosyl-(1→4)-2-deoxy-6-*O*-sulfo-2-(sulfamino)-α-D-glucopyranoside,

decasodium salt (Fig. 3). Although based on the structure of heparin, fondaparinux differs from heparin and low molecular weight heparin (Table 1).

A. Anti-FXa and Other Activities

Fondaparinux (molecular weight 1.728 kDa.) is a selective and reversible inhibitor of factor Xa dependent on binding to AT to elicit its activity. The K_d of fondaparinux for AT is 48 ± 11 nM (139). Fondaparinux only promotes small increases in the HC II mediated antithrombin activity at high concentration (140). No TFPI release has been detected after intravenous injections of fondaparinux (140–142). There is suggestive evidence that fondaparinux does not affect the function of thrombin activatable fibrinolytic inhibitor (TAFI) as heparin and low molecular weight heparin do via their inhibition of thrombin (143).

The fondaparinux-AT complex inhibits factor VIIa generation and/or its activity (144). It also inhibits the coagulant activity of the tissue factor-FVIIa complex at the same rate as heparin-AT (145). It is suggested that the fondaparinux-AT complex may also inhibit factor IXa (146). It is unclear whether these mechanisms are a direct effect by fondaparinux or an indirect effect due to factor Xa inhibition.

B. AT Saturation

Clinically effective plasma concentrations of fondaparinux for prophylaxis are up to 1 μg/ml; therapeutic plasma concentrations are approximately 1–3 μg/ml

Table 1 Comparison of the Properties of Pentasaccharide, Low Molecular Weight Heparin, and Heparin

	Pentasaccharide	LMW Heparin	Heparin
Molecular weight	1.728 kDa	~5 kDa	~15 kDa
Source	Chemically synthesized	Porcine mucosa, bovine lung	Porcine mucosa, bovine lung
Dispersity	Homogeneous	Heterogeneous (MW 4–9 kDa)	Heterogeneous (MW 3–30 kDa)
Protease specificity	Xa inhibition	Xa and some IIa inhibition	Inhibit most coagulation proteases
AT-mediated activity	Xa inhibition	Xa >IIa inhibition	Inhibit most coagulation proteases
HCII-mediated activity	Only at high concentrations	Weak inhibition of thrombin	Moderate inhibition of thrombin
TFPI release	None	Strong	Strong
HIT response	Not known	Cross-reacts when heparin is positive	Positive
Bioavailability	~100%	≥80%	≤30%
Half-life	Long when bound to AT	Longer than heparin	Relatively short

(approx. 1 μM); effective plasma concentrations for interventional procedures will be > 1 μg/ml (147–151). Since fondaparinux is completely dependent on binding to AT for expression of its anti-factor Xa effect (in a 1:1 molar ratio), low plasma concentrations of AT can be rate limiting for its activity. The normal human plasma level of AT is 2–3 μM. This suggests that with the high concentrations of fondaparinux required for interventional procedures (e.g., dosing that results in plasma levels higher than 3 μg/ml), or in patients with low AT levels due to congenital or acquired deficiencies, the dose-dependent effect of fondaparinux could be reduced. *In vitro* studies demonstrated that for 0.5–2.0 μg/ml fondaparinux, at AT levels of 0.5 U/ml, there is 20% loss of activity in comparison to the activity obtained with 1.0 U/ml AT (152). With 0.25 U/ml AT there is a 45% loss of activity and with 0.125 U/ml AT there is a 65% loss of fondaparinux activity.

AT saturation by fondaparinux at high doses was also shown in a human volunteer study (153). At doses over 17.2 mg, the AUC was lower than expected with an increase in the drug excreted in the urine. The authors suggested that at these high doses, where the plasma molar concentration of fondaparinux exceeds that of plasma AT, excess fondaparinux is excreted in the urine faster than fondaparinux is bound to AT.

C. Anticoagulant Effect

Fondaparinux has no effect on the prothrombin time (PT) or thrombin clotting time (154). It has a very weak effect on the activated partial thromboplastin time (aPTT) such that prolongation is not observed with concentrations < 5.0 μg/ml (154). Laboratory monitoring of fondaparinux is currently not being recommended for prophylactic dosing. If necessary, fondaparinux can be measured by the anti-factor Xa assay available in most special hematology labs. Fondaparinux activity determined by the chromogenic anti-factor Xa assay, Heptest® (Haemachem; St. Louis, MO) and other clot-based anti-factor Xa assays has been shown to correlate with antithrombotic activity in animal models ($r > 0.90$) (154–157). Calibration of the assay is to be made with fondaparinux and not a low molecular weight heparin or unfractionated heparin. Peak plasma concentrations occur 3 h after subcutaneous dosing.

D. Thrombin Generation

Blocking the activity of factor Xa inhibits the generation of thrombin. Fondaparinux produces a dose-dependent inhibition of the amount of thrombin generated and a prolongation of the lag phase of thrombin generation (140,158,159). There is a correlation between the anti-factor Xa activity, inhibition of thrombin generation and *in vivo* antithrombotic activity.

E. Platelet Interactions

Fondaparinux at concentrations of 1–100 μg/ml does not cause platelet aggregation, or influence platelet aggregation induced by epinephrine, ADP, collagen or arachidonic acid (154).

Fondaparinux does not induce *in vitro* platelet aggregation or activation in the presence of heparin antibody obtained from patients clinically diagnosed with HIT (154,160–162). However, data from the clinical trials in orthopedic surgery reveal that platelet counts $<100{,}000\,\mu l^{-1}$ do occur with fondaparinux treatment. In the fondaparinux groups 2.7% and 4.9% of patients *vs* 3.7% and 5.3% of patients treated with enoxaparin developed thrombocytopenia (147,148).

F. Protein Binding

One study of the *in vitro* Plasma to Plasma of fondaparinux showed 97% bound to plasma AT and >94% bound to purified AT (0.125 mg/ml) (163). The protein-bound fraction decreased at higher concentrations of fondaparinux. Scatchard analysis indicated specific binding to a single site coupled with a nonspecific binding component. Specific binding parameters (B_{max}, K_d) were comparable between plasma AT and purified AT. No binding to albumin or α_1-acid glycoprotein was detected.

G. Venous Thrombosis

Fondaparinux produces a dose-dependent inhibition of venous thrombosis as shown in animal models (154–157,164). Complete inhibition is achieved at an intravenous dose of 100 μg/kg as compared to 25 μg/kg heparin (154–157,164). Following subcutaneous administration, the dose of fondaparinux is only 1.5-fold higher than the effective intravenous dose to block the same thrombosis endpoint (155). On the other hand, a nearly 6-fold higher subcutaneous dose of heparin is required to achieve the same thrombosis inhibition endpoint (155).

H. Arterial Thrombosis

Fondaparinux is effective at inhibiting clot formation in the mesenteric arterioles after intravenous administration to animals. A higher dose than needed to suppress venous thrombosis is required against arterial thrombosis (>250 μg/kg) (155). In two arterio-venous shunt models, fondaparinux effectively inhibited arterial-type platelet rich thrombus growth and platelet consumption, as well as venous-type fibrin rich thrombi under static and disturbed blood flow (165–167). Thrombi formed in the presence of fondaparinux (not heparin) became less or non-thrombogenic as determined by a decrease in platelet deposition and a decrease in thrombus-induced thrombin generation *ex vivo* (168). Only at relatively high concentrations did fondaparinux significantly reduce platelet deposits in arterial models. In an *ex vivo* perfusion model, fondaparinux was as effective as heparin and low molecular weight heparin in preventing thrombus formation on mechanical heart valves (169).

I. Hemorrhagic Effect

Fondaparinux administered at 200–20,000 anti-factor Xa U/kg i.v. (up to approx. 25 mg/kg) dosages to rats produced only a mild increase in blood loss (2-fold more

than placebo). In comparison, heparin produced a 5-fold increase in blood loss at a dose of 300 anti-factor Xa U/kg i.v. (approx. 2 mg/kg) (165). In a rabbit model, fondaparinux did not significantly increase the amount of blood loss at doses 50-fold higher than the dose required to produce an antithrombotic effect in the same species (155). Heparin dose-dependently increased blood loss, such that at a dose 10-fold higher than the dose that completely inhibited clot formation, a significant increase in blood loss was observed. No bleeding was observed in a baboon model with fondaparinux (167).

In a subgroup of a human volunteer study, repeated single daily injections of 11.4 or 26.6 mg of fondaparinux were administered to elderly subjects for 7 days (170). In all patients, the bleeding time test was normal. Minor hematomas at the injection/cannula site occurred, as well as one mild transient hematuria on day 3 and re-bleeding in one patient when fondaparinux plasma levels were 3.0 μg/ml (2 anti-factor Xa U/ml).

J. Pharmacokinetics

The elimination half-life of AT-bound fondaparinux is 17–21 h (171,172). The subcutaneous bioavailability of fondaparinux is nearly 100% and it is distributed mainly in the blood (165,173). There is a rapid onset of action as half-maximum activity is reached within 25 min after subcutaneous administration and a peak plasma concentration is reached in 2–3 h (173). Area under the curve (AUC) and maximal concentration (C_{max}) correlate linearly with dose (170). Fondaparinux is predominantly cleared through the kidneys (173), and 77% of a single dose is excreted unchanged in the urine. The renal clearance rate of non-AT-bound fondaparinux is <10 min (172). Steady state plasma concentrations are reached 3–4 days after repeated daily administration of single doses of 2, 4, or 8 mg s.c. fondaparinux (170). In normal individuals, low inter-subject variability is observed. After discontinuation of fondaparinux, its anticoagulant effects may persist for 2–4 days (174).

VII. Clinical Trials of Fondaparinux

Fondaparinux (GlaxoSmithKline) has been evaluated in several clinical trials for the prevention of venous thromboembolism in patients undergoing major orthopedic surgery (148–151,175,176). Approval was obtained for use in hip fracture, hip replacement, and knee replacement surgeries (177). Dosing of fondaparinux is once daily at 2.5 mg s.c. to be started not before 6–8 h after surgery to avoid unwanted bleeding. Patients with low body weight and renal insufficiency require dose adjustment. Overall, there was no reduction in the bleeding risk compared to enoxaparin. Monitoring is not recommended. However, it is advised to closely monitor any thrombocytopenia under fondaparinux treatment. If the platelet count falls to $<100{,}000\,\mu l^{-1}$ fondaparinux should be discontinued, and it should be used with caution in patients with a history of HIT.

Following the success of these trials, fondaparinux was evaluated in several trials of patients undergoing high-risk abdominal surgery and in acutely ill medical patients with restricted mobility (178,179). The global MATISSE trials evaluated fondaparinux for the treatment of patients with acute deep-vein thrombosis (DVT) and acute pulmonary embolism (PE) (180,181). Approval was recently obtained for treatment of acute DVT when administered in conjunction with warfarin and for the treatment of acute PE when administered in conjunction with warfarin when initial therapy is administered in the hospital. The treatment dose is 7.5 mg s.c. daily for patients with a body weight between 50 and 100 kg. Dose adjustment is necessary in patients with low body weight.

Other clinical settings in which fondaparinux is being studied include interventional cardiology procedures, adjunct treatment to thrombolytic agents, acute coronary syndrome, special population studies, and drug interaction studies.

VIII. Derivatives of Pentasaccharide

More efficient means of synthesis of the pentasaccharide that is fondaparinux via enzymatic reactions (182) and the use of defined carbohydrate building blocks (183) have been reported.

A. Synthetic Designs

In an attempt to improve or alter its pharmacologic properties, a number of structural modifications have been made to the original pentasaccharide molecule (fondaparinux). These include linking a thrombin binding domain to the AT binding pentasaccharide (Fig. 5) (184–188), conjugation of the AT-binding pentasaccharide to a direct thrombin inhibitor (Fig. 6) (189), and the synthesis of an *O*-sulfated, *O*-methylated derivative (Fig. 7) (190,191). Addition of a thrombin binding domain to the pentasaccharide resulted in agents that were more effective than heparin at inhibiting clot-bound enzymes and exhibited higher antithrombotic potency in animal models of venous and arterial thrombosis. In addition, these studies demonstrated that by manipulating the total charge or charge density of the oligosaccharides, pharmacologic properties, such as plasma protein binding and elimination half-life, can be modulated.

B. Idraparinux

Idraparinux (SR-34006; Sanofi-Aventis) is an *O*-sulfated, *O*-methylated pentasaccharide derivative of fondaparinux (Fig. 7) (191). Due to the increased sulfation, this agent exhibits a 30-fold higher binding affinity to AT than fondaparinux, and a higher anti-factor Xa potency. Idraparinux exhibits a significantly longer elimination half-life of about 120 h, which allows for once-weekly dosing (191). It has 100% subcutaneous bioavailability (192).

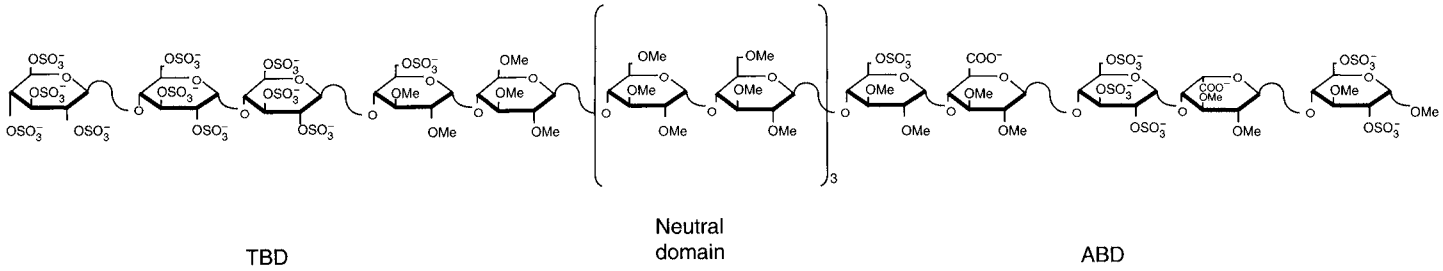

Figure 5 Chemical structure of SR 123781. This pentasaccharide derivative consists of an AT binding domain (ABD) and a thrombin binding domain (TBD) separated by a neutral, methylated hexasaccharide sequence.

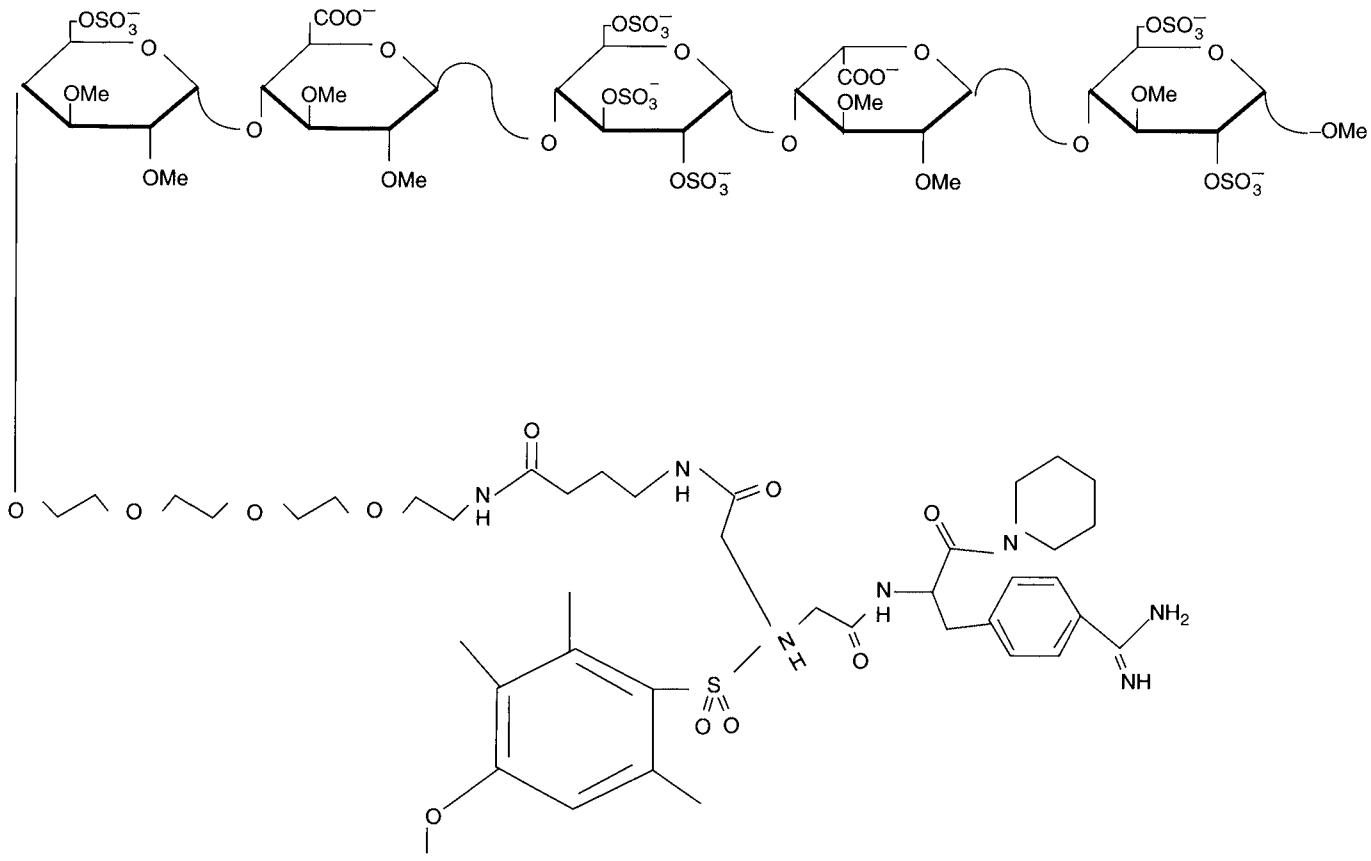

Figure 6 Chemical structure of ORG 42675. This compound consists of an AT binding pentasaccharide conjugated to a direct thrombin inhibitor.

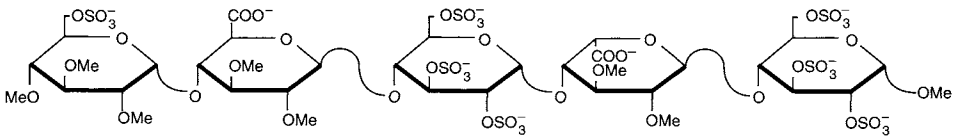

Figure 7 Chemical structure of idraparinux. This 2-*O*-sulfated, *O*-methylated pentasaccharide exhibits higher affinity to AT compared to the native pentasaccharide, a higher anti-factor Xa potency and a longer elimination half-life. Idraparinux (Sanofi-Aventis) is in clinical development.

The PERSIST clinical study compared the efficacy (symptomatic, objectively proven venous thrombosis or a change in thrombotic burden) and safety (clinically overt bleeding) of idraparinux and warfarin in patients with confirmed acute symptomatic proximal DVT. All 659 patients were treated with enoxaparin for 5–7 days and then randomized to receive either idraparinux in a once-weekly dose (2.5, 5.0, 7.5, or 10 mg s.c.) or warfarin (INR 2–3) for an additional 12 weeks. This study demonstrated that a once-weekly 2.5 mg s.c. dose of idraparinux was as efficacious and safe as warfarin (193). There was a dose-dependent increase in major bleeding with an unacceptable frequency in the 10 mg treatment group. Two patients in the 5 mg group experienced fatal bleeding. Unlike heparin, enoxaparin, and fondaparinux, the use of idraparinux was not associated with an increase in plasma liver enzyme levels (194).

Clinical trials investigating the use of idraparinux for the long-term prevention of stroke in patients with atrial fibrillation and for the treatment of DVT and PE include the Van Gogh DVT, the Van Gogh PE, the Van Gogh Extension, and the AMADEUS clinical trials (195, 196).

IX. Summary

Heparin oligosaccharides possess molecular and functional heterogeneity and contain consensus sequences that have different degrees of affinity to endogenous plasma and cellular ligands. Structure–activity studies of heparin have brought about the development of low molecular weight heparins and chemically modified heparins.

To further the understanding of the mechanism of heparin, the interaction of the AT molecule with heparin molecules was studied in-depth. It was deduced that a pentasaccharide sequence was the minimal sequence of heparin able to activate AT to produce antithrombotic activity; in this case only anti-factor Xa activity was observed.

Specifically configured pentasaccharides were then synthesized from 1983–1986 by the group of Choay. By the ^{13}C-NMR, four specific sulfate groups were shown to be critical for optimum binding of the heparin molecule to AT (i.e., the 6-*O*-sulfate on the first saccharide unit, the 3-*O*-sulfate on the third saccharide unit

and two 2-*N*-sulfates on the third and fifth saccharide units). The relative positioning of the individual sulfated saccharides also proved to be of critical importance for AT binding.

These basic investigations set the stage for the development of a new class of antithrombotic drugs. The synthetic heparin pentasaccharide (fondaparinux sodium, Arixtra®; GlaxoSmithKline) is characterized as a selective factor Xa inhibitor, thereby inhibiting thrombin generation, which requires binding to AT to express activity. Although based on the structure of heparin, fondaparinux differs from heparin and low molecular weight heparin with a unique therapeutic profile and cannot be used interchangeably.

Fondaparinux is a homogeneous substance in which all chains are composed of the same specific sulfated pentasaccharide unit. It has an ultralow molecular weight of 1.728 kDa. It has been approved in the US and Europe for prophylaxis of venous thrombosis after major orthopedic surgery (hip fracture, hip replacement, knee replacement surgeries) by a fixed, once daily dose of 2.5 mg s.c. without monitoring. It is also approved for treatment of acute DVT when administered in conjunction with warfarin and for the treatment of acute PE when administered in conjunction with warfarin when initial therapy is administered in the hospital. Treatment dose is 7.5 mg s.c. daily for patients with body weight between 50 and 100 kg. The bleeding risk is not reduced with fondaparinux in comparison to enoxaparin.

Structurally similar analogues of this pentasaccharide can be produced by modifying side groups or adding saccharidic chains. The first derivative of fondaparinux to undergo clinical investigation is idraparinux. Idraparinux (Sanofi-Aventis) differs from fondaparinux in that it contains *O*-methyl groups and exhibits a long half-life leading to once a week dosing. It is developed as an antithrombotic for prevention and treatment of venous and arterial thrombosis, acute coronary syndromes, and as an adjunct to thrombolytic therapy.

The synthetic antithrombotic agents based on the structure–activity relationships within heparin will provide a unique array of designer drugs. Because they are new, questions remain regarding the true pharmacologic potential, full mechanisms of action, clinical limitations, and limitations in efficacy and safety of fondaparinux and its derivatives. The future developments in this area promise to be interesting.

References

1. Andersson L-O, Barrowcliffe TW, Holmer E, Johnson EA. Sims GEC. Anticoagulant properties of heparin fractionated by affinity chromatography on matrix-bound antithrombin III and by gel filtration. Thromb Res 1976; 9:575–583.
2. Holmer E, Kurachi K, Soderstrom G. The molecular-weight dependence of the rate-enhancing effect of heparin on the inhibition of thrombin, factor Xa, factor IXa, factor XIa, factor XIIa and kallikrein by antithrombin. Biochem J 1981; 93:395–400.
3. Johnson E, Mulloy B. The molecular-weight range of mucosal-heparin preparations. Carbohydr Res 1976; 51:119–127.

4. Lane DA, MacGregor IR, Michalski R, Kakkar VV. Anticoagulant activities of four unfractionated and fractionated heparins. Thromb Res 1978; 12:257–271.
5. Nesheim M, Blackburn MH, Lawler CM, Mann KG. Dependence of antithrombin III and thrombin binding stoichiometries and catalytic activity on the molecular weight of affinity purified heparin. J Biol Chem 1986; 261:3214–3221.
6. Brinkhous KM, Smith HP, Warner ED, Seegers WH. The inhibition of blood clotting: an unidentified substance which acts in conjunction with heparin to prevent the conversion of prothrombin into thrombin. Am J Physiol 1939; 125:683–687.
7. Rosenberg RD, Damus PS. The purification and mechanism of action of human antithrombin-heparin cofactor. J Biol Chem 1973; 248:6490–6505.
8. Abildgaard U. Highly purified antithrombin III with heparin cofactor activity by disc electrophoresis. Scand J Clin Lab Invest 1968; 21:89–91.
9. Stone AL, Beeler D, Oosta G, Rosenberg RD. Circular dichroism spectroscopy of heparin–antithrombin interactions. Proc Natl Acad Sci USA 1982; 79:7190–7194.
10. Oosta GM, Gardner WT, Beeler DL, Rosenberg RD. Multiple functional domains of the heparin molecule. Proc Natl Acad Sci 1981; 78:829–833.
11. Beeler DL, Marcum JA, Schiffman S, Rosenberg RD. Interaction of factor XIa and antithrombin in the presence and absence of heparin. Blood 1986; 67:1488–1492.
12. Jordan RE, Oosta GM, Gardner WT, Rosenberg RD. The kinetics of hemostatic enzyme–antithrombin interactions in the presence of low molecular weight heparin. J Biol Chem 1980; 255:10081–10090.
13. McNeely TB, Griffith MJ. The anticoagulant mechanism of action of heparin in contact-activated plasma: inhibition of factor X activation. Blood 1985; 65:1226–1231.
14. Broze GJ, Majerus PW. Purification and properties of human coagulation factor VII. J Biol Chem 1980; 255:1242–1247.
15. Dahl PE, Abildgaard U, Larsen ML, Tjensvoll L. Inhibition of activated coagulation factor VII by normal human plasma. Thromb Haemost 1982; 48:253–256.
16. Godal HC, Ryah M, Laake K. Progressive inactivation of purified factor VII by heparin and antithrombin III. Thromb Res 1974; 5:773–775.
17. Agarwal A, Danishefsky I. Requirement of free carboxyl groups for the anticoagulant activity of heparin. Thromb Res 1986; 42:673–680.
18. Hook M, Bjork I, Hopwood J, Lindahl U. Anticoagulant activity of heparin: separation of high-activity and low-activity heparin species by affinity chromatography on immobilized antithrombin. FEBS Lett 1976; 66:90–93.
19. Lam LH, Silbert JE, Rosenberg RD. The separation of active and inactive forms of heparin. Biochem Biophys Res Commun 1976; 69:570–577.
20. Rosenberg RD, Jordan RE, Favreau LV, Lam LH. Highly active heparin species with multiple binding sites for antithrombin. Biochem Biophys Res Commun 1979; 86:1319–1324.
21. Tollefsen DM, Pestka CA, Monafo WJ. Activation of heparin cofactor II by dermatan sulfate. J Biol Chem 1983; 258:6713–6716.
22. Tollefsen DM, Blank MK. Detection of a new heparin-dependent inhibitor of thrombin in human plasma. J Clin Invest 1981; 68:589–596.

23. Ofosu FA, Modi G, Cerskus AL, Hirsh J, Blajchman MA. Heparin with low affinity to antithrombin III inhibits the activation of prothrombin in normal plasma. Thromb Res 1982; 28:487–497.
24. Sie P, Ofosu F, Fernandez F, Buchanan MR, Petitou M, Boneu B. Respective role of antithrombin III and heparin cofactor II in the in vitro anticoagulant effect of heparin and of various sulfated polysaccharides. Br J Haematol 1986; 64:707–714.
25. Duckert F, Tran TH, Marbet GA. Association of hereditary heparin co-factor II deficiency with thrombosis. Lancet 1985; 2:413–414.
26. Sie P, Dupouy J, Pichon J, Boneu B. Constitutional heparin co-factor II deficiency associated with recurrent thrombosis. Lancet 1985; 2:414–416.
27. Broze GJ. Tissue factor pathway inhibitor. Thromb Haemost 1995; 74:90–93.
28. Sandset PM. Tissue factor pathway inhibitor (TFPI) – an update. Thromb Haemost 1996; 26(Suppl 4):154–156.
29. Broze GJ, Warren LA, Novotny WF, Higuchi DA, Girard JJ, Miletich JP. The lipoprotein-associated coagulation inhibitor that inhibits the factor VII-tissue factor complex also inhibits factor Xa: insights into its possible mechanism of action. Blood 1988; 71:335–343.
30. Bajaj MS, Kuppuswamy MN, Saito H, Spitzer SD, Bajaj SP. Cultured normal human hepatocytes do not synthesize lipoprotein-associated coagulation inhibitor: evidence that endothelium is the principal site of synthesis. Proc Natl Acad Sci 1990; 87:8869–8873.
31. Hoppensteadt DA, Jeske W, Fareed J, Bermes EW. The role of tissue factor pathway inhibitor in the mediation of the antithrombotic actions of heparin and low molecular-weight heparin. Blood Coagul Fibrinolysis 1995; 6:S57–S64.
32. Sandset PM, Abildgaard P, Larsen ML. Heparin induces release of extrinsic coagulation pathway inhibitor (EPI). Thromb Res 1988; 50:803–813.
33. Jeske W, Hoppensteadt D, Klauser R, Kammereit A, Eckenberger P, Haas S, Wyld P, Fareed J. Effect of repeated aprosulate and enoxaparin administration on TFPI antigen levels. Blood Coagul Fibrinolysis 1995; 6:119–124.
34. Demir M, Iqbal O, Hoppensteadt DA, Piccolo P, Ahmad S, Schultz CL, Linhardt RJ, Fareed J. Anticoagulant and antiprotease profiles of a novel natural heparinomimetic mannopentaose phosphate sulfate (PI-88). Clin Appl Thromb Hemost 2001; 7:131–140.
35. Hoppensteadt DA, Fareed J, Raake P, Raake W. Endogenous release of tissue factor pathway inhibitor by topical application of an ointment containing mucopolysaccharide polysulfate to nonhuman primates. Thromb Res 2001; 103:157–163.
36. Cella G, Sbarai A, Mazzaro G, Motta G, Carraro P, Andreozzi GM, Hoppensteadt DA, Fareed J. Tissue factor pathway inhibitor release induced by defibrotide and heparins. Clin Appl Thromb Hemost 2001; 7:225–228.
37. Sandset PM, Bendz B, Hansen JB. Physiological function of tissue factor pathway inhibitor and interaction with heparins. Haemostasis 2000; 30(Suppl 2):48–56.
38. Matyal R, Vin Y, Delude RL, Lee C, Creasey AA, Fink MP. Extremely low doses of tissue factor pathway inhibitor decrease mortality in a rabbit model of septic shock. Inten Care Med 2001; 27:1274–1280.

39. Westrick RJ, Bodary PF, Xu Z, Shen YC, Broze GJ, Fitzman DT. Deficiency of tissue factor pathway inhibitor promotes atherosclerosis and thrombosis in mice. Circulation 2001; 103:3044–3046.
40. Hamamoto T, Kisiel W. The effect of heparin on the regulation of factor VIIa-tissue factor activity by tissue factor pathway inhibitor. Blood Coagul Fibrinolysis 1996; 7:470–476.
41. Jesty J, Wun TC, Lorenz A. Kinetics of the inhibition of factor Xa and the tissue factor–factor VIIa complex by the tissue factor pathway inhibitor in the presence and absence of heparin. Biochemistry 1994; 33:12686–12694.
42. Kaiser B, Hoppensteadt DA, Jeske W, Wun TC, Fareed J. Inhibitory effects of TFPI on thrombin and factor Xa generation in vitro-modulatory action of glycosaminoglycans. Thromb Res 1994; 75:609–616.
43. Alban S. Molecular weight-dependent influence of heparin on the form of tissue factor pathway inhibitor circulating in plasma. Semin Thromb Hemost 2001; 27:503–511.
44. Fareed J, Jeske W, Hoppensteadt D, Clarizio R, Walenga JM. Are the available low-molecular-weight heparin preparations the same? Semin Thromb Hemost 1996; 22(Suppl 1):77–91.
45. Alban S, Gastpar R. Plasma levels of total and free tissue factor pathway inhibitor (TFPI) as individual pharmacological parameters of various heparins. Thromb Haemost 2001; 85:824–829.
46. Valentin S, Larnkjer A, Ostergaard P, Nielsen JI, Nordfang O. Characterization of the binding between tissue factor pathway inhibitor and glycosaminoglycans. Thromb Res 1994; 75:173–183.
47. Ockelford PA, Carter CJ, Cerskus A, Smith CA, Hirsh J. Comparison of the in vivo hemorrhagic and antithrombotic effects of a low antithrombin-III affinity heparin fraction. Thromb Res 1982; 27:679–690.
48. Barrowcliffe TW, Merton RE, Havercroft SJ, Thunberg L, Lindahl U, Thomas DP. Low-affinity heparin potentiates the action of high-affinity heparin oligosaccharides. Thromb Res 1984; 34:125–133.
49. Salzman EW, Rosenberg RD, Smith MH, Lindon JN. Effect of heparin and heparin fractions on platelet aggregation. J Clin Invest 1980; 65:64–73.
50. Andersson L-O, Barrowcliffe TW, Holmer E, Johnson EA, Soderstrom G. Molecular weight dependency of the heparin potentiated inhibition of thrombin and activated factor X. Effect of heparin neutralization in plasma. Thromb Res 1979; 15:531–541.
51. Laurent TC, Tengblad A, Thunberg L, Hook M, Lindahl U. The molecular weight dependence of the anticoagulant activity of heparin. Biochem J 1978; 175:691–701.
52. Walenga JM, Fareed J, Hoppensteadt D, Emanuele RM. In vitro evaluation of heparin fractions: old vs new methods. CRC Crit Rev Clin Lab Sci 1986; 22: 361–389.
53. Denson KWE, Bonnar J. The measurement of heparin. A method based on the potentiation of anti-factor Xa. Thromb Diath Haemorrh 1973; 30:471–479.
54. Handeland F, Abildgaard U. Assay of unfractionated and LMW heparin with chromogenic substrates: twin methods with factor Xa and thrombin. Thromb Res 1984; 35:627–636.

55. Teien AN, Lie M. Evaluation of an amidolytic heparin assay method: increased sensitivity by adding purified antithrombin III. Thromb Res 1977; 10:399–410.
56. Yin ET, Wessler S, Butler JV. Plasma heparin: a unique, practical, submicrogram-sensitive assay. J Lab Clin Med 1973; 81:298–310.
57. Barrowcliffe TW, Johnson EA, Eggleton CA, Thomas DP. Anticoagulant activities of lung and mucous heparins. Thromb Res 1977; 2:27–36.
58. Holmer E, Lindahl U, Backstrom G, Thunberg L, Sandberg H, Soderstrom G, Anderson L-O. Anticoagulant activities and effects on platelets of a heparin fragment with high affinity for antithrombin. Thromb Res 1980; 8:861–869.
59. Thunberg L, Lindahl U. On the molecular-weight-dependence of the anticoagulant activity of heparin. Biochem J 1979; 181:241–243.
60. Ellis V, Scully MF, Kakkar VV. The relative molecular mass dependence of the anti-factor Xa properties of heparin. Biochem J 1986; 238:329–333.
61. Ellis V, Scully M, Kakkar VV. The acceleration of the inhibition of platelet prothrombinase complex by heparin. Biochem J 1986; 233:161–165.
62. Miletich JP, Jackson CM, Majerus PW. Properties of the factor Xa binding site on human platelets. J Biol Chem 1978; 253:6908–6916.
63. Teitel JM, Rosenberg RD. Protection of factor Xa from neutralization by the heparin-antithrombin complex. J Clin Invest 1983; 71:1383–1391.
64. Baruch D, Franssen J, Hemker HC, Lindhout T. Effect of heparin and low molecular weight heparins on thrombin-induced blood platelet activation in the absence of antithrombin III. Thromb Res 1985; 38:447–458.
65. Ofosu FA, Blajchman MA, Modi GJ, Smith LM, Buchanan MR, Hirsh J. The importance of thrombin inhibition for the expression of the anticoagulant activities of heparin, dermatan sulphate, low molecular weight heparin and pentosan polysulphate. Br J Haematol 1985; 60:695–704.
66. Cifonelli JA. The relationship of molecular weight and sulfate content and distribution to anticoagulant activity of heparin preparations. Carbohydr Res 1974; 37:145–154.
67. Hurst RE, West SS, Menter JM. Anticoagulant activity, anionic density, and the conformational properties of heparin. American Chemical Society Symposium Series 1981; 150:251–264.
68. Hurst RE, Poon M-C, Griffith MJ. Structure–activity relationships of heparin. Independence of heparin charge density and antithrombin-binding domains in thrombin inhibition by antithrombin and heparin cofactor II. J Clin Invest 1983; 72:1042–1045.
69. Cofrancesco E, Radaelli F, Pogliani E, Amici N, Torri GG, Casu B. Correlation of sulfate content and degree of carboxylation of heparin and related glycosaminoglycans with anticomplement activity. Relationships to the anticoagulant and platelet-aggregating activities. Thromb Res 1979; 14:179–187.
70. Danishefsky I, Siskovic E. Heparin derivatives prepared by modification of the uronic acid carboxyl groups. Thromb Res 1972; 1:173–182.
71. Racanelli A, Fareed J, Walenga JM, Coyne E. Biochemical and pharmacologic studies on the protamine interactions with heparin, its fractions and fragment. Semin Thromb Hemost 1985; 11:176–189.
72. Lane DA, Denton J, Flynn AM, Thunberg L, Lindahl U. Anticoagulant activities of heparin oligosaccharides and their neutralization by platelet factor 4. Biochem J 1984; 218:725–732.

73. Hubbard AR, Jennings CA. Neutralization of heparan sulfate and low molecular weight heparin by protamine. Thromb Haemost 1985; 53:86–89.
74. Lane DA, Pejler G, Flynn AM, Thompson EA, Lindahl U. Neutralization of heparin-related saccharides by histidine-rich glycoprotein and platelet factor 4. J Biol Chem 1986; 261:3980–3986.
75. Kitani T, Nagarajan SC, Shanberge JN. Effect of protamine on heparin-antithrombin III complexes. In vitro studies. Thromb Res 1980; 17:367–374.
76. Okajima Y, Kanayama S, Maeda Y, Urano S, Kitani T, Watada M, Nakagawa M, Ijichi H. Studies on the neutralizing mechanism of antithrombin activity of heparin by protamine. Thromb Res 1981; 24:21–29.
77. Dawes J, Pepper DS. A sensitive competitive binding assay for exogenous heparins. Thromb Res 1982; 27:387–396.
78. Poon MC, Hurst RE, Rives MS. Platelet factor four and protamine sulfate neutralization of heparin fractionated according to anionic charge density. Thromb Haemost 1982; 47:162–165.
79. Brace LD, Fareed J, Tomeo J, Issleib S. Biochemical and pharmacological studies on the interaction of PK 10169 and its subfractions with human platelets. Haemostasis 1986; 16:93–105.
80. Cade JF, Buchanan MR, Boneu B, Ockelford P, Carter CJ, Cerskus AL, Hirsh J. A comparison of the antithrombotic and haemorrhagic effects of low molecular weight heparin fractions: the influence of the method of preparation. Thromb Res 1984; 35:613–625.
81. Fernandez F, N'guyen P, Van Ryn J, Ofosu F, Hirsh J, Buchanan MR. Hemorrhagic doses of heparin and other glycosaminoglycans induce a platelet defect. Thromb Res 1986; 43:491–495.
82. Westwick J, Scully MF, Poll C, Kakkar VV. Comparison of the effects of low molecular weight heparin and unfractionated heparin on activation of human platelets in vitro. Thromb Res 1986; 42:435–447.
83. Soria C, Soria J, Dunn FW, Thomaidis A, Tobelem G, Caen JP. Interactions of platelets with standard heparin and low molecular weight fractions. Med J Aust 1986; 144:HS32–34.
84. Esquivel CO, Bergqvist D, Bjorck CG, Nilsson B. Comparison between commercial heparin, low molecular weight heparin and pentosan polysulfate on hemostasis and platelets in vivo. Thromb Res 1982; 28:389–400.
85. Huisse MG, Guillin MC, Bezeaud A, Toulemonde F, Kitzis M, Andreassian B. Heparin-associated thrombocytopenia. In vitro effects of different molecular weight heparin fractions. Thromb Res 1982; 27:485–490.
86. Barzu T, Molho P, Tobelem G, Petitou M, Caen J. Binding and endocytosis of heparin by human endothelial cells in culture. Biochim Biophys Acta 1985; 845:196–203.
87. Lormeau JC, Petitou M, Choay J. A heparin hexasaccharide fragment able to bind to anionic endothelial cell growth factor: preparation and structure. XIII International Carbohydrate Symposium: Abstract #C28, 1986.
88. Castellot JJ, Choay J, Lormeau JC, Petitou M, Sache E, Karnovsky MJ. Structural determinants of the capacity of heparin to inhibit the proliferation of vascular smooth muscle cells. II. Evidence for a pentasaccharide sequence that contains a 3-*O* sulfate group. J Cell Biol 1986; 102:1979–1984.
89. Taylor S, Folkman J. Protamine is an inhibitor of angiogenesis. Nature 1982; 297:307–312.

90. Fareed J, Walenga JM, Hoppensteadt D, Messmore HL. Studies on the profibrinolytic actions of heparin and its fractions. Semin Thromb Hemost 1985; 11:199–207.
91. Doutremepuich C, Gestreau JL, Kuttler MC, Fenelon L, Toulemonde F, Variel EG, Quilichini R. Fibrinolytic activity of heparin and heparin fractions. Haemostasis 1984; 14: Abstract #218.
92. Vairel EG, Bouty-Boye H, Toulemonde F, Doutremepuich C, Marsh NA, Gaffney PJ. Heparin and a low molecular weight fraction enhances thrombolysis and by this pathway exercises a protective effect against thrombosis. Thromb Res 1983; 30:219–224.
93. Paques EP, Stohr HA, Heimburger N. Study on the mechanism of action of heparin and related substances on the fibrinolytic system: relationship between plasminogen activators and heparin. Thromb Res 1986; 42:797–807.
94. Wessler S. Small doses of heparin and a new concept of hypercoagulability. Thromb Diath Haemorrh 1974; 33:81–86.
95. Yin ET. Effect of heparin on the neutralization of factor Xa and thrombin by the plasma alpha-2-globulin inhibitor. Thromb Diath Haemorrh 1974; 33:43–50.
96. Carter CJ, Kelton JG, Hirsh J, Cerskus A, Santos AV, Gent M. The relationship between the hemorrhagic and antithrombotic properties of low molecular weight heparin in rabbits. Blood 1982; 59:1239–1245.
97. Bergqvist D, Nilsson B, Hedner U, Pedersen PC, Ostergaard PB. The effect of heparin fragments of different molecular weights on experimental thrombosis and haemostasis. Thromb Res 1985; 38:589–601.
98. Carter CJ, Kelton JG, Hirsh J, Gent M. Relationship between the antithrombotic and anticoagulant effects of low molecular weight heparin. Thromb Res 1981; 21:169–174.
99. Holmer E, Mattsson C, Nilsson S. Anticoagulant and antithrombotic effects of heparin and low molecular weight heparin fragments in rabbits. Thromb Res 1982; 25:475–485.
100. Ockelford PA, Carter CJ, Mitchell L, Hirsh J. Discordance between the anti-Xa activity and the antithrombotic activity of an ultra-low molecular weight heparin fraction. Thromb Res 1982; 28:401–409.
101. Thomas DP, Merton RE, Lewis WE, Barrowcliffe TW. Studies in man and experimental animals of a low molecular weight heparin fraction. Thromb Haemost 1981; 45:214–218.
102. Fareed J, Walenga JM, Williamson K, Emanuele RM, Kumar A, Hoppensteadt DA. Studies on the antithrombotic effects and pharmacokinetics of heparin fractions and fragments. Semin Thromb Hemost 1985; 11:56–74.
103. Boneu B, Buchanan MR, Cade JF, Van Ryn J, Fernandez FF, Ofosu FA, Hirsh J. Effects of heparin, its low molecular weight fractions and other glycosaminoglycans on thrombus growth in vivo. Thromb Res 1985; 40:81–89.
104. Bjorck CG, Bergqvist D, Esquivel C, Nilsson B, Rudsvik Y. Effect of heparin, low molecular weight (LMW) heparin, and a heparin analogue on experimental venous thrombosis in the rabbit. Acta Chir Scand 1984; 150:629–633.
105. Choay J, Lormeau JC, Petitou M, Fareed J, Sinay P. Oligosaccharides de fabile poids moleculaire presentant une activite inhibitrice du facteur Xa en

milieu plasmatique. II. Nouveaux elements de structure et activite antithrombotique. Annales Pharmaceutiques Francaises 1981; 39:267–272.
106. Buchanan MR, Boneu B, Ofosu F, Hirsh J. The relative importance of thrombin inhibition and factor Xa inhibition to the antithrombotic effects of heparin. Blood 1985; 65:198–201.
107. Thomas DP, Merton RE, Barrowcliffe TW, Thunberg L, Lindahl U. Effects of heparin oligosaccharides with high affinity for antithrombin III in experimental venous thrombosis. Thromb Haemost 1982; 47:244–248.
108. Bara L, Trillou M, Mardiguian J, Samama M. Comparison of antithrombotic activity of two heparin fragments PK 10169 (mol. wt. 5000) and EMT 680 (mol. wt. 2500) and unfractionated heparin in a rabbit experimental thrombosis model: relative importance of systemic anti-Xa and anti-IIa activities. Nouv Rev Fr Hematol 1986; 28:355–358.
109. Andriuoli G, Mastacchi R, Barbanti M, Sarret M. Comparison of the antithrombotic and haemorrhagic effects of heparin and a new low molecular weight heparin in rats. Haemostasis 1985; 15:324–330.
110. Bergqvist D, Burmark US, Frisell J, Hallbook T, Lindblad B, Risberg B, Torngren S, Wallin G. Prospective double-blind comparison between Fragmin and conventional low-dose heparin: thromboprophylactic effect and bleeding complications. Haemostasis 1986; 16:11–18.
111. Doutremepuich C, Toulemonde F, Bousquet F, Bonini F. Comparison of the haemorrhagic effects of unfractionated heparin and a low molecular weight heparin fraction (CY 216) in rabbits. Thromb Res 1986; 43:691–695.
112. Fair DS, Sundsmo JS, Schwartz BS, Edgington TS, Muller-Eberhard HJ. Prothrombin activation by factor B (Bb) of the alternative pathway of complement. Thromb Haemost 1981; 46:301.
113. Pangrazzi J, Abbadini M, Zametta M, Casu B, Donati M. Low molecular weight heparins and bleeding. Thromb Haemost 1985; 54:158.
114. Bratt G, Tornebohm E, Widlund L, Lockner L. Low molecular weight heparin (Kabi 2165, Fragmin): pharmacokinetics after intravenous and subcutaneous administration in human volunteers. Thromb Res 1986; 42:613–620.
115. Choay J, Lormeau JC, Petitou M. Anti-Xa active heparin oligosaccharides. Thromb Res 1980; 18:573–578.
116. Casu B, Oreste P, Torri G, Zoppetti G, Choay J, Lormeau JC, Petitou M, Sinay P. The structure of heparin oligosaccharide fragments with high anti-(factor Xa) activity containing the minimal antithrombin III-binding sequence. Biochem J 1981; 197:599–609.
117. Leder IG. A novel 3-*O* sulfatase from human urine acting on methyl 2-deoxy-2-sulfamino-alpha-D-glucopyramoside 3-sulfate. Biochem Biophys Res Comm 1980; 94:1183–1189.
118. Lindahl U, Backstrom G, Thunberg L, Leder IG. Evidence for a 3-*O* sulfated D-glucosamine residue in the antithrombin-binding sequence of heparin. Proc Natl Acad Sci USA 1980; 77:6551–6555.
119. Choay J, Lormeau JC, Petitou M. Oligosaccharides de faible poids moleculaire presentant une activite inhibitrice du facteur Xa en milieu plasmatique. Annales Pharmaceutiques Francaises 1981; 39:37–44.
120. Thunberg L, Backstrom G, Grundberg H, Riesenfeld J, Lindahl U. The molecular size of the antithrombin-binding sequence in heparin. FEBS Lett 1980; 117:203–206.

121. Thunberg L, Backstrom G, Lindahl U. Further characterization of the antithrombin-binding sequence in heparin. Carbohydr Res 1982; 100:393–410.
122. Ototani N, Kikuchi M, Yosizawa Z. Structure and biological activity of finback-whale (*Balaenoptera physalus*) heparin octasaccharide. J Biochem 1982; 205:23–30.
123. Choay J, Lormeau JC, Petitou M, Sinay P, Fareed J. Structural studies on a biologically active hexasaccharide obtained from heparin. Ann NY Acad Sci 1981; 370:644–649.
124. Rosenberg RD, Lam L. Correlation between structure and function of heparin. Proc Natl Acad Sci USA 1979; 76:1218–1222.
125. Petitou M, Duchaussoy P, Lederman I, Choay J, Sinay P, Jacquinet JC, Torri G. Synthesis of heparin fragments. A chemical synthesis of the pentasaccharide *O*-(2-deoxy-2-sulfamido-6-*O*-sulfo-alpha-D-glucopyranosyl)-(1→4)-*O*-(beta-D-glucopyranosyluronic acid)-(1→4)-*O*-(2-deoxy-2-sulfamido-3,6-di-*O*-sulfo-alpha-D-glucopyranosyl)-(1→4)-*O*-(2-*O*-sulfo-alpha-L-idopyranosyluronic acid)-(1→4)-2-deoxy-2-sulfamido-6-*O*-sulfo-D-glucopyranose decasodium salt, a heparin fragment having high affinity for antithrombin III. Carbohydr Res 1986; 147:221–236.
126. Sinay P, Jaquinet JE, Petitou M, Duchaussoy P, Lederman I, Choay J, Torri G. Total synthesis of a heparin pentasaccharide fragment having high affinity for antithrombin III. Carbohydr Res 1984; 132:C5–C9.
127. Torri G, Casu B, Gatti G, Petitou M, Choay J, Jacquinet JC, Sinay P. Mono- and bi-dimensional 500 MHz 1H-NMR spectra of a pentasaccharide corresponding to the binding sequence of heparin to antithrombin-III: evidence for conformational peculiarity of the sulfated iduronate residue. Biochem Biophys Res Comm 1985; 128:134–140.
128. Atha DH, Lormeau JC, Petitou M, Rosenberg RD, Choay J. Contribution of monosaccharide residues in heparin binding to antithrombin III. Biochemistry 1985; 24:6723–6729.
129. Choay J, Petitou M, Lormeau JC, Sinay P, Casu B, Gatti G. Structure–activity relationship in heparin: A synthetic pentasaccharide with high affinity for antithrombin III and eliciting high anti-factor Xa activity. Biochem Biophys Res Commun 1983; 116:492–499.
130. Walenga JM, Fareed J. Preliminary biochemical and pharmacologic studies on a chemically synthesized pentasaccharide. Semin Thromb Hemost 1985; 11:89–99.
131. Choay J. Biologic studies on chemically synthesized pentasaccharide and tetrasaccharide fragments. Semin Thromb Hemost 1985; 11:81–85.
132. Riesenfeld J, Thunberg L, Hook M, Lindahl U. The antithrombin-binding sequence of heparin. Location of essential *N*-sulate groups. J Biol Chem 1981; 256:2389–2394.
133. Petitou M. Synthetic heparin fragments: new and efficient tools for the study of heparin and its interactions. Nouv Rev Fr Hematol 1984; 26:221–226.
134. Lindahl U, Backstrom G, Thunberg L. The antithrombin-binding sequence in heparin. Identification of an essential 6-*O* sulfate group. J Biol Chem 1983; 258:9826–9830.
135. Lindahl U, Thunberg L, Backstrom G, Riesenfeld J, Nordling K, Bjork I. Extension and structural variability of the antithrombin-binding sequence in heparin. J Biol Chem 1984; 259:12368–12376.

136. Jackson CM. Factor X. In: Spaet TH ed. Progress in Hemostasis Thrombosis. New York: Grune & Stratton, 1984; 55–109.
137. Hoylaerts M, Owen WG, Collen D. Involvement of heparin chain length in the heparin-catalyzed inhibition of thrombin by antithrombin III. J Biol Chem 1984; 259:5670–5677.
138. Machovich R, Aranyi P. Effect of thrombin inactivation by antithrombin III. Biochem J 1978; 173:869–875.
139. Herbert JM, Petitou M, Lormeau JC. SR90107A/ORG31540, a novel anti-factor Xa antithrombotic agent. Cardiovasc Drug Rev 1997; 15:1–26.
140. Lormeau JC, Hérault JP. The effect of the synthetic pentasaccharide SR 90107/ORG 31540 on thrombin generation ex vivo is uniquely due to AT-mediated neutralization of factor Xa. Thromb Haemost 1995; 74:1474–1477.
141. Zitoun D, Bara L, Bloch MF, Samama MM. Plasma TFPI activity after intravenous injection of pentasaccharide and unfractionated heparin in rabbits. Thromb Res 1994; 75:577-580.
142. Kaiser B, Hoppensteadt DA, Jeske W, Wun TC, Fareed J. Inhibitory effects of TFPI on thrombin and factor Xa generation in vitro – modulatory action of glycosaminoglycans. Thromb Res 1994; 75:609–616.
143. Walenga JM, Florian M, Hoppensteadt DA, Demir A, Lietz H, Jeske WP, Messmore HL, Leya F, Fareed J. Heparin, LMW heparins and HCII binding oligosaccharides, but not pentasaccharide, regulate TAFI. Thromb Haemost 2001; (July Suppl):2011.
144. Gerotziafas GT, Bara L, Bloch MF, Makris PE, Samama MM. Treatment with LMWHs inhibits factor VIIa generation during in vitro coagulation of whole blood. Thromb Res 1996; 81:491–496.
145. Lormeau JC, Hérault JP, Herbert JM. Antithrombin mediated inhibition of factor VIIa-tissue factor complex by the synthetic pentasaccharide representing the heparin binding site to AT. Thromb Haemost 1996; 76:5–8.
146. Wiebe E, O'Brien L, Stafford A, Fredenburgh J, Weitz J. Heparin catalysis of factor FIXa inhibition by antithrombin: pentasaccharide-induced conformational change in antithrombin predominates over the template effect. Thromb Haemost 2001; (July Suppl):P2101.
147. Turpie AGG, Gallus AS, Hoek JA, for the Pentasaccharide Investigators. A synthetic pentasaccharide for the prevention of deep-vein thrombosis after total hip replacement. N Engl J Med 2001; 344:619–625.
148. Turpie G. The PENTATHLON 2000 study: comparison of the first synthetic factor Xa inhibitor with low molecular weight heparin in the prevention of venous thromboembolism after hip replacement surgery. Thromb Haemost 2001; (July Suppl):OC48.
149. Lassen M. The EHPHESUS study: comparison of the first synthetic factor Xa inhibitor with low molecular weight heparin the prevention of venous thromboembolism after elective hip replacement surgery. Thromb Haemost 2001; (July Suppl):OC45.
150. Eriksson BI, Bauer KA, Lassen MR, Turpie AGG for the Steering Committee of the Pentasaccharide in Hip-Fracture Surgery Study. Fondaparinux compared with enoxaparin for the prevention of venous thromboembolism after hip-fracture surgery. N Engl J Med 2001; 345:1298–1304.
151. Bauer KA, Eriksson BI, Lassen MR, Turpie AGG for the Steering Committee of the Pentasaccharide in Major Knee Surgery Study. Fondaparinux

compared with enoxaparin for the prevention of venous thromboembolism after elective major knee surgery. N Engl J Med 2001; 345:1305–1310.
152. Walenga JM, Hoppensteadt D, Mayuga M, Samama MM, Fareed J. Functionality of pentasaccharide depends on endogenous antithrombin levels. Blood 2000; 96:817a.
153. Boneu B, Necciari J, Cariou R, Sié P, Gabaig AM, Kieffer G, Dickinson J, Lamond G, Moelker H, Mant T, Magnani H. Pharmacokinetics and tolerance of the natural pentasaccharide (SR90107/ORG31540) with high affinity to antithrombin III in man. Thromb Haemost 1995; 74:1468–1473.
154. Walenga JM. Factor Xa Inhibition in Mediating Antithrombotic Actions: Application of a Synthetic Heparin Pentasaccharide, doctoral thesis. Mention tres bien. Universite Pierre et Marie Curie, Paris VI, Paris, France, June 1987.
155. Jeske W. Pharmacologic Studies on Synthetic Analogues of Heparin with Selective Affinity to Endogenous Serine Protease Inhibitors, doctoral thesis. Loyola University Chicago, Chicago, IL, May 1996.
156. Walenga JM, Fareed J, Petitou M, Samama M, Lormeau JC, Choay J. Intravenous antithrombotic activity of a synthetic heparin pentasaccharide in a human serum induced stasis thrombosis model. Thromb Res 1986; 43:243–248.
157. Walenga JM, Petitou M, Lormeau JC, Samama M, Fareed J, Choay J. Antithrombotic activity of a synthetic heparin pentasaccharide in a rabbit stasis thrombosis model using different thrombogenic challenges. Thromb Res 1987; 46:187–198.
158. Walenga JM, Bara L, Petitou M, Samama M, Fareed J, Choay J. The inhibition of the generation of thrombin and the antithrombotic effect of a pentasaccharide with sole anti-factor Xa activity. Thromb Res 1988; 51: 23–33.
159. Beguin S, Choay J, Hemker HC. The action of a synthetic pentasaccharide on thrombin generation in whole plasma. Thromb Haemost 1989; 61: 397–401.
160. Walenga JM, Koza MJ, Lewis BE, Pifarré R. Relative heparin-induced thrombocytopenic potential of low molecular weight heparins and new antithrombotic agents. Clin Appl Thromb Hemost 1996; 2(Suppl 1):S21–S27.
161. Elalamy I, Lecrubier C, Potevin F, Abdelouahed M, Bara L, Marie JP, Samama M. Absence of in vitro cross-reaction of pentasaccharide with the plasma heparin dependent factor of twenty-five patients with heparin associated thrombocytopenia. Thromb Haemost 1995; 74:1384–1385.
162. Ahmad S, Jeske WP, Walenga JM, Hoppensteadt DA, Wood JJ, Herbert JM, Messmore HL, Fareed J. Synthetic pentasaccharides do not cause platelet activation by antiheparin-platelet factor 4 antibodies. Clin Appl Thromb Hemost 1999; 5:259–266.
163. Paolucci F, Clavies MC, Donat F, Necciari J. Fondaparinux sodium mechanism of action: identification of specific binding to purified and human plasma-derived proteins. Clin Pharmacokinet 2002; 2:11–18.
164. Walenga JM, Jeske WP, Bara L, Samama MM, Fareed J. Biochemical and pharmacologic rationale for the development of a synthetic heparin pentasaccharide. Thromb Res 1997; 86:1–36.
165. Hobbelen PM, Van Dinther TG, Vogel GM, van Bieckel CA, Moelker HC, Meuleman DG. Pharmacological profile of the chemically synthesized antith-

rombin III binding fragment of heparin (pentasaccharide) in rats. Thromb Haemost 1990; 63:265–270.
166. Vogel GMT, Meuleman DG, Bourgondien FGM, Hobbelen PMJ. Comparison of two experimental thrombosis models in rats, effects of four glycosaminoglycans. Thromb Res 1989; 54:399–410.
167. Cadroy Y, Hanson SR, Harker LA. Antithrombotic effects of synthetic pentasaccharide with high affinity for plasma antithrombin III in nonhuman primates. Thromb Haemost 1993; 70:631–635.
168. Vogel GM, Van Amsterdam RG, Kop WJ, Meuleman DG. Pentasaccharide and Orgaran arrest, whereas heparin delays thrombus formation in a rat arteriovenous shunt. Thromb Haemost 1993; 69:29–34.
169. Schlitt A, Buerke M, Hauroeder B, Peetz D, Hundt F, Bickel C, Schaefer I, Meyer J, Rupprecht HJ. Fondaparinux and enoxaparin in comparison to unfractionated heparin in preventing thrombus formation on mechanical heart valves in an ex vivo rabbit model. Thromb Haemost 2003; 90:245–251.
170. Boneu B, Necciari J, Cariou R, Sie P, Gabaig AM, Kieffer G, Dickinson J, Lamond G, Moelker H, Mant T. Pharmacokinetics and tolerance of the natural pentasaccharide (SR90107/Org31540) with high affinity to antithrombin III in man. Thromb Haemost 1995; 74:1468–1473.
171. Crepon B, Donat F, Barzu T, Hérault JP. Pharmacokinetic parameters of AT binding pentasaccharides in three animal species: predictive value for humans. Thromb Haemost 1993; 69:654.
172. Van Amsterdam RG, Vogel GM, Visser A, Kop WJ, Buiting MT, Meulemam DG. Synthetic analogues of the antithrombin III-binding pentasaccharide sequence of heparin. Prediction of in vivo residence times. Arterioscler Thromb Vasc Biol 1995; 15:495–503.
173. Donat F, Duret JP, Santoni A, Cariou R, Necciari J, Magnani H, de Greef R. The pharmacokinetics of fondaparinux sodium in healthy volunteers. Clin Pharmacokinet 2002; 2:1–9.
174. Fondaparinux Sodium. In: AHFS Drug Information 2005. American Society of Health-System Pharmacists, Inc., Bethesda 2005; 1446–1448.
175. Eriksson BI, Lassen MR, Pentasaccharide in Hip-Fracture Surgery Plus Investigators. Duration of prophylaxis against venous thromboembolism with fondaparinux after hip fracture surgery: a multicenter, randomized, placebo-controlled, double-blind study. Arch Int Med 2003; 163:1337–1342.
176. Turpie AGG, Bauer KA, Eriksson BI, Lassen MR. Effect on efficacy and safety of the timing of the first pentasaccharide (fondaparinux, Arixtra) administration in the prevention of venous thromboembolism after major orthopedic surgery. Blood 2001; 98:1119.
177. Arixtra® (fondaparinux) Prescribing Information Sheet (GlaxoSmithKline, 2004).
178. Agnelli G, Berqvist D, Cohen AF. A randomized double-blind study to compare the efficacy and safety of fondaparinux with dalteparin in the prevention of venous thromboembolism after high-risk abdominal surgery: the PEGASUS Study. J Thromb Haemost 2003; 1(Suppl):OC006.
179. Cohen AT, Gallus AS, Lassen MR. Fondaparinux vs. placebo for the prevention of venous thromboembolism in acutely ill medical patients (ARTEMIS). J Thromb Haemost 2003; 1(Suppl):P2046.

180. Buller HR, Davidson BL, Decousus H, Gallus A, Gent M, Piovella F, Prins MH, Raskob G, Segers AE, Cariou R, Leeuwenkamp O, Lensing AW, Matisse Investigators. Fondaparinux or enoxaparin for the initial treatment of symptomatic deep venous thrombosis: a randomized trial. Ann Int Med 2004; 140:867–873.
181. Buller HR, Davidson BL, Decousus H, Gallus A, Gent M, Piovella F, Prins MH, Raskob G, van den Berg-Segers AE, Cariou R, Leeuwenkamp O, Lensinig AW, Matisse Investigators. Subcutaneous fondaparinux versus intravenous unfractionated heparin in the initial treatment of pulmonary embolism. New Eng J Med 2003; 349:1695–1702.
182. Kuberan B, Lech MZ, Beeler DL, Wu ZL, Rosenberg RD. Enzymatic synthesis of antithrombin III-binding heparan sulfate pentasaccharide. Nat Biotechnol 2003; 21:1343–1346.
183. Short PL. Sugar chemistry finding markets. Chemical & Engineering News 2004; 82:14–17.
184. Hérault JP, Bernat A, Roye F, Michaux C, Schaeffer P, Bono F, Petitou M, Herbert JM. Pharmacokinetics of new synthetic heparin mimetics. Thromb Haemost 2002; 87:985–989.
185. Hérault JP, Cappelle M, Bernat A, Millet L, Bono F, Schaeffer P, Herbert JM. Effect of SanOrg123781A, a synthetic hexadecasaccharide, on clot-bound thrombin and factor Xa in vitro and in vivo. J Thromb Haemost 2003; 1:1959–1965.
186. Bal Dit Sollier C, Kang C, Berge N, Hérault JP, Bonneau M, Herbert JM, Drouet L. Activity of a synthetic hexadecasaccharide (SanOrg123781A) in a pig model of arterial thrombosis. J Thromb Haemost 2004; 2:925–930.
187. Herbert JM, Hérault JP, Bernat A, Savi P, Schaeffer P, Driguez PA, Duchaussoy P, Petitou M. SR123781A, a synthetic heparin mimetic. Thromb Haemost 2001; 85:852–860.
188. Hérault JP, Bernat A, Gaich C, Herbert JM. Effect of new synthetic heparin mimetics on whole blood thrombin generation in vivo and in vitro in rats. Thromb Haemost 2002; 87:238–244.
189. Vogel GM, Meuleman DG, Van Dinther TG, Buijsman R, Princen AW, Smit MJ. Antithrombotic properties of a direct thrombin inhibitor with a prolonged half-life and AT-mediated factor Xa inhibitory activity. J Thromb Haemost 2003; 1:1945–1954.
190. Gouin-Thibault I, Dingler E, Maris FA, Samama MM. In vitro interaction of the pentasaccharide idraparinux (SanOrg 34006) with unfractionated heparin. J Thromb Haemost 2003; 1:2054–2056.
191. Herbert JM, Hérault JP, Bernat A, van Amsterdam RG, Lormeau JC, Petitou M, van Boeckel C, Hoffmann P, Meuleman DG. Biochemical and Pharmacological Properties of SANORG 34006, a potent and long-acting synthetic pentasaccharide. Blood 1998; 91:4197–4205.
192. Faaij RA, Burggraaf J, Schoemaker RC, Van Amsterdam RGM, Cohen AF. A phase I single rising dose study to investigate the safety, tolerance and pharmacokinetics of subcutaneous SanOrg 34006 in healthy male and female elderly volunteers. Thromb Haemost 1999; (Suppl): Abstract 15547.
193. The Persist Investigators. A novel long-acting synthetic factor Xa inhibitor (SanOrg34006) to replace warfarin for secondary prevention in deep vein thrombosis. A phase II evaluation. Thromb Haemost 2004; 2:47–53.

194. Reiter M, Bucek RA, Koca N, Heger J, Minar E. Idraparinux and liver enzymes: observations for the PERSIST trial. Blood Coagul Fibrinolysis 2003; 14:61–65.
195. Organon's Idraparinux – a novel once weekly anticoagulant enters phase III trials. NV Organon Press Release, 11 June 2003.
196. Ma Q, Fareed J. Idraparinux sodium. IDrugs 2004; 7:1028–1034.

Chemistry and Biology of Heparin and Heparan Sulfate
H.G. Garg, R.J. Linhardt and C.A. Hales (Editors)

Chapter 6

Separation and Sequencing of Heparin and Heparan Sulphate Saccharides

MARK A. SKIDMORE and JEREMY E. TURNBULL

Molecular Glycobiology Group School of Biological Sciences, University of Liverpool, Liverpool, UK

I. Introduction

There is a pressing need to investigate at the structure–function level the many interactions in which heparan sulphate and its oligosaccharides participate. This makes the ability to sequence heparan sulphate oligosaccharides of fundamental importance. In addition, with the ability to probe binding properties of heparan sulphate oligosaccharides (both chemically derived and natural) using a variety of affinity methods, and to identify activators or inhibitors of specific biological processes using bioassays, it is of increasing significance to determine their sequences in order to exploit their potential applications as novel tools for selective chemical intervention, or indeed as new therapeutics. Using current methodologies, this is still a considerable challenge, involving laborious multistage procedures, and requiring significant amounts of starting material. Furthermore, the isolation of heparan sulphate oligosaccharides and their separation to purity is by no means trivial.

Structurally, heparin and heparan sulphate both have a characteristic disaccharide repeat unit comprising of a uronic acid and a glucosamine residue. The uronic acid residue may be present as glucuronic acid or its C5 epimer, iduronic acid. C2 of the glucosamine residue is either *N*-acetylated or *N*-sulphated. Further modifications by means of *O*-sulphation can occur at C6 and C3 of the glucosamine or C2 of the uronic acid residue (1). These modifications theoretically produce 32 possible disaccharide subunit building blocks with which to build heparin or heparan sulphate polysaccharide chains. This array of disaccharide subunits creates potentially one of the

most information-dense molecules in biology (2) and the degree of structural complexity imparted on this molecule explains why heparan sulphate is known to mediate such a large number of biological processes and protein interactions including FGF signaling in a variety of systems, host-cell invasion by pathogenic microorganisms (HSV, dengue virus, malaria, etc.), regulation of APP cleavage in Alzheimer's disease, VEGF regulation in angiogenesis, and GDNF in kidney and brain development (3).

Unfortunately, and in contrast to nucleic acid and protein chemistry, methodology for the analysis of carbohydrates has only recently evolved and with some difficulty. Due to the nature of heparin and heparan sulphate, most traditional chemistries prove problematic, with heparan sulphate and heparin both being sensitive to low (4) and high pH (5) (de-*N*-sulphation occurs at low pH, epoxide formation occurs at high pH), and remaining all but insoluble in most organic solvents. The presence of the reducing end carbonyl (aldehyde) allows for the formation of imines by condensation with amines, but this reaction is sluggish and acid catalysis cannot be used if de-*N*-sulphation is to be avoided. There is also evidence to suggest that the extent of labeling is influenced by the structure of the disaccharide present (4) and the yield can be as low as a few percent (6). Recently a method to attack the nonreducing terminus of heparin/heparan sulphate oligosaccharides by oxymercuration has been developed, taking advantage of the C=C bond generated by bacterial lyase digestion (7). This method may prove more fruitful for labeling and immobilization in comparison to the reducing end strategy. For more detailed information on the chemical properties of heparin and heparan sulphate, readers are referred to the chapter entitled "Surface-Based Studies of Heparin/Heparan Sulfate–Protein Interactions" by Rudd, Skidmore, and Yates in this volume.

The ability to sequence heparin and heparan sulphate is further hampered by the amount of sample available for analysis. Heparin and heparan sulphate preparations are heterogeneous due to the high degree of complexity of the polysaccharide chain, and the presence of many structural isomers. Conventional separation strategies fail to resolve constituent oligosaccharide pools to pure species alone. Commonly, a combination of techniques is required and even then, only a limited number of pure species may be obtained. Isolation and purification is laborious with generally only microgram–milligram amounts being prepared. This can make detection problematic, with the use of fluorophores or radiolabels commonplace. Furthermore, all of the present sequencing strategies rely on some form of sample manipulation, from derivitization to salt extraction and hence sample losses quickly compound. The recent generation of complex analogue libraries by semi-synthetic chemical modification of heparins (8) avoids the problem of low yield but is reliant on the ability to separate similar structures, i.e., oligosaccharides containing many structural isomers.

As could be inferred from above, another problem encountered during heparin and heparan sulphate sequencing is that sample purity. The issues above combined with that of sample purit are the main problems presented by heparin and heparan sulphate sequencing.

Sequencing strategies, which have been used to date, are based on one of three methods:

(i) Direct sequence information from nuclear magnetic resonance (NMR) data, without labeling.
(ii) Treatment of saccharides with various enzymes and their analysis using mass spectrometry.
(iii) Partial hydrolysis (enzymatic or chemical) of end-labeled saccharides (e.g., carrying a fluorophore or radiolabel tag) followed by separation (e.g., on a polyacrylamide gel) and detection of further band shifts or mass changes depending on the action of particular enzymes.

All depend heavily on an ability to separate the oligosaccharide of interest at the outset and subsequent oligosaccharides produced during the sequencing process. Since this is arguably the single biggest obstacle facing the would-be sequencer, a considerable portion of this chapter is devoted to this aspect. The need to isolate pure species is of paramount importance for sequencing methodologies. To date no individual sequencing method possesses the ability to unequivocally determine the structures present within a complex mixture. Therefore, it should be appreciated that this step in the progression from isolation to sequence determination is probably the most difficult and one of the most critical.

II. Separation of Heparin and Heparan Sulphate Oligosaccharides

As mentioned in the introduction, the capacity to separate heparin and heparan sulphate saccharides into single pure species is not an easy task. The chemistry of these molecules gives rise to immense structural diversity. Disaccharide repeats which are structural isomers having the same molecular mass (and the same charge) are common within oligosaccharides and this heterogeneity provides a serious challenge. To complicate matters further, the highly acidic nature of the molecules due to the presence of sulphate and carboxylic acid groups, the sensitivity of the molecules to pH and their insolubility in the vast majority of common organic solvents impairs the use of many conventional separation strategies.

The two physical properties of heparin and heparan sulphate molecules, which are exploited in the separation of oligosaccharides, are their hydrodynamic volume and their charge. The size and conformation of a chain is dictated by the amount and arrangement of disaccharide units present, while the charge of the molecule is dependant on the amount of *O*-sulphate groups and *N*-sulphates present, along with a carboxylic acid group per disaccharide unit. The separation of heparin and heparan sulphate oligosaccharides is conventionally performed by chromatography and/or electrophoresis.

A. Chromatography

The chromatographic separation techniques outlined below arise from the presence of two different phases, the mobile phase, and the stationary phase. The analyte (in our case the carbohydrate oligosaccharides heparin or heparan sulphate) is present in the mobile phase and its interaction with the stationary phase as it passes

throughout the column determines the success and level of separation. A record of the separation is usually obtained in the form of a chromatogram, which gives a correlation between the retention time within the column and the intensity of a peak (representative of an eluting entity) as the analytes pass through an appropriate detector.

In column chromatography (methods detailed below) UV detection at 232 nm is often employed because this is the absorbance maxima for the C=C double bond introduced into the carbohydrates at the nonreducing end following lyase digestion (9). The level of detection by UV at this wavelength is approximately 20–50 pmol using a typical HPLC system. If chemical degradation is performed, detection is possible at 210 nm but with low sensitivity. Sensitive detection of small amounts of saccharides requires a suitable fluorophore or radiolabel at either the reducing or nonreducing termini.

1. *Size-Exclusion Chromatography*

Also known as molecular exclusion, gel filtration or gel permeation chromatography; size-exclusion chromatography, as its name suggests, separates on the basis of size (hydrodynamic volume). This separation is achieved by the interaction of the analytes with a porous stationary phase. The beads, which compose this stationary phase, have a specific assortment of pore sizes which gives rise to a fractionation range within which molecules can be separated. With regard to the separation of heparin and heparan sulphate oligosaccharides, two types of separation are usually encountered, namely the removal of inorganic salts or the fractionation of different sized oligosaccharides. Inorganic salts also need to be removed before further separations, such as ion exchange chromatography, can be carried out. Both of these separations are performed by size-exclusion chromatography, although the fractionation range is markedly different.

For the removal of inorganic salts, such as sodium chloride (NaCl), a column with a relatively small pore size is required. An example is Superdex G25 Superfine (Amersham Biosciences; e.g., PD-10 pre-packed columns). These will quickly and conveniently separate oligosaccharides greater in size than a tetrasaccharide from inorganic salts. Similar columns with improved fractionation properties for disaccharides can be poured using Sephadex G25 Superfine as the matrix of choice by increasing the column length. For semi-preparative separations, Hi-Prep 26/10 columns provide a preparative load-desalting alternative, which can be easily coupled to HPLC systems for automation.

For the separation of oligosaccharide fragments generated from partial cleavage of heparan sulphate chains to oligosaccharides, it has been determined that separations of disaccharides through to hexadecasaccharides can be easily carried out using a column of diameter 1–2 cm and length 1–2 m using Bio-Gel P10 (BioRad) or Sephadex G50 (Amersham) (10). Flow rates are low and thus run times of are usually 24–48 h for these columns. Bio-Gel P10 gives the highest resolution but is the most difficult matrix to handle due to its soft gel nature and thus is less reliable. Alternatively, columns of similar dimensions using the matrix

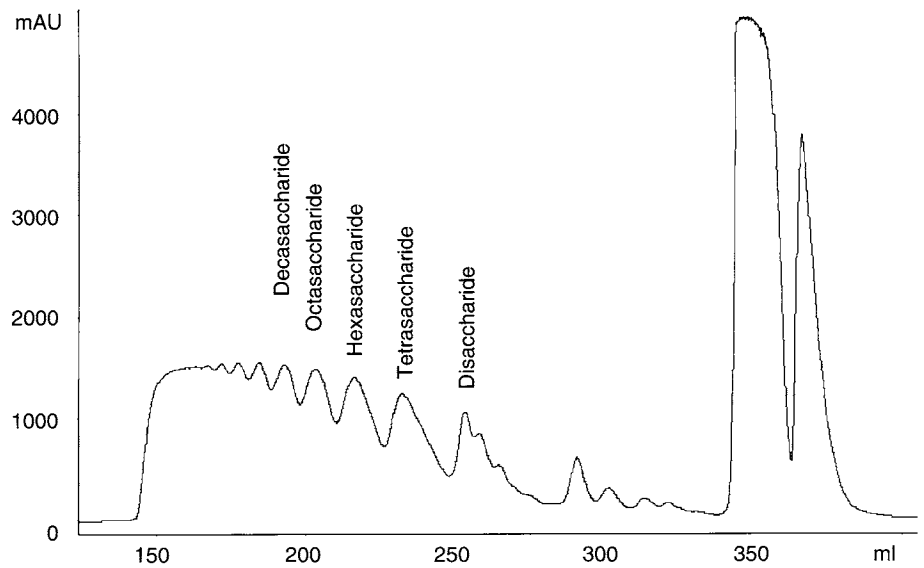

Figure 1 Size-exclusion chromatography elution profile of partial enzymatic digest of porcine mucosal-derived heparan sulphate (PMHS). Separation was carried out on two Amersham XK-16 columns (15 mm × 1 m) connected in series packed with Superdex 30 with a 0–1000 min run time in ammonium bicarbonate 0.5 M at a flow rate of 0.5 ml/min.

Superdex 30n (11) can be employed and give excellent and consistent resolution. In addition this column can be coupled to the HPLC and run at faster flow rates, thus reducing the extended run times necessary with Bio-Gel P10 or Sephadex G50. Using any of these columns, 100–200 mM ammonium bicarbonate is used to ion pair with the negatively charged carboxyl and sulphate groups, hence negating the possibility of charge interactions with the matrix beads. Ammonium bicarbonate is volatile, so it can be readily removed by lyopholization. Examples of a separation profile on a Superdex 30 column is shown in Fig. 1. The choice of column used to separate oligosaccharides depends upon the fractionation range required. As oligosaccharide size increases separation becomes increasingly difficult, and the resolution of oligosaccharides differing by a single disaccharide unit decreases. Thus, it is usually the case in this type of separation that pooled peaks will contain a heterogeneous mixture of oligosaccharides and a certain degree of overlap between peaks is inevitable.

2. High-Performance Strong Anion Exchange Liquid Chromatography

Ion exchange chromatography separates molecules on the basis of their charge. In anion exchange chromatography, the stationary phase or matrix possesses positive charge and interacts with analytes of negative charge. The positive charge on the

matrix is due to a strong base derivatized on to a support medium, which remains positively charged across the pH range of 1–14. The sample mixture is introduced into the mobile phase and will bind ionically to the positively charged matrix. The strength of this interaction is dependent on the number of sulphate groups present in the oligosaccharide and the environmental pH of the mobile phase. The pH of the mobile phase must be above the pK_a of the sulphate and carboxyl groups to de-protonate the acidic groups. If the pH is less than the pK_a of the acidic groups, they will not interact with the column matrix and will pass through the column (although this is unlikely for heparin and heparan sulphate oligosaccharides).

In order to elute the oligosaccharide molecules from the column in a manner, which separates them based on their charge, a counter ion must be introduced that can compete for the basic groups present on the support matrix. The counter ion used for elution is dependent not only on the anion exchange column, but also the charge state of the analytes.

A reliable strong anion exchange column for separation of heparin and heparan sulphate oligosaccharides is the Propac PA1 column (Dionex). This column is polymer based and does not suffer from the steady deterioration problems encountered with its silica-based counterparts (short column life, peak broadening and inconsistent retention times). The Propac PA1 column provides the consistent elution times, which are necessary for the disaccharide analysis described earlier coupled with column longevity (consistent over 250 runs in a 2-year period) (12). Sample loads of between 0.5 and 1 mg can be carried out on a 4 mm × 250 mm analytical column, or up to as high as 5 mg on a semi-prep scale (9 mm × 250 mm) column.

A general separation, which is common in heparin or heparan sulphate structure determination, is disaccharide analysis. This involves the de-polymerization of the glycosaminoglycan chains into their constituent disaccharide components. This is achieved by a cocktail of bacterial lyase enzymes (heparitinase I, heparitinase II and heparinase (see Table 1)) (13). Note that structural information with regard to the hexuronic acid epimer present at the nonreducing terminus (formerly iduronic or glucuronic acid) is lost by the creation of a C=C bond between C4 and C5. A reference chromatogram of structurally defined disaccharide standards can be used to identify the disaccharides present in the sample mixture.

With regards to column choice for disaccharide analysis, the Propac PA1 column separates all eight common disaccharide standards with baseline resolution and consistent and predictable elution times. In order to perform this analysis a linear chloride counter ion gradient, 0–100%, 1 M NaCl, pH 3.5, is used for example over a 45-min period at a flow rate of 1 ml/min. The sample is loaded in double-distilled water adjusted to pH 3.5. An example of the resolution of eight disaccharide standards on Propac PA1 is shown in Fig. 2. Sensitivity is approximately 50 pmol per peak, so a minimum starting sample of about 1 μg is required for a clear compositional analysis.

An alternative to the Propac column is provided by the silica based C18 Hypersil column (Agilent) for disaccharide analysis. This column is derivatized prior to use with cetyltrimethylammonium hydroxide in order to provide the

Table 1 Enzymes for Depolymerising and Sequencing Heparan Sulphate

Enzyme	Substrate specificity*
Polysaccharide lyases	
Heparitinase I (Heparinase III)	GlcNR(± 6S)a1-4GlcA
Heparitinase II (Heparinase II)	GlcNR(± 6S)a1-4GlcA/IdoA
Heparitinase III (Heparinase I)	GlcNS(± 6S)a1-4IdoA(2S)
Exosulphatases	
Iduronate-2-sulphatase	IdoA(2S)
Glucosamine-6-sulphatase	GlcNAc(6S), $GlcNSO_3$(6S)
Sulphamidase (glucosamine-*N*-sulphatase)	$GlcNSO_3$
Glucuronate-2-sulphatase	GlcA(2S)
Glucosamine-3-sulphatase	$GlcNSO_3$(3S)
Exoglycosidases	
Iduronidase	IdoA
Glucuronidase	GlcA
α-*N*-acetylglucosaminidase	GlcNAc
Bacterial exoenzymes	
Δ4,5-Glycuronate-2-sulphatase	ΔUA(2S)
Δ4,5-Glycuronidase	ΔUA

*The specificities are shown as the linkage specificity (for the bacterial polysaccharide lyases), and as the nonreducing terminal group recognized by the enzymes (for the exoenzymes). Sulphatases remove only the sulphate group whereas the glycosidases cleave the whole nonsulphated monosaccharide.

basic group used for anion exchange (14). The column does not appear to have the longevity of the Propac PA1 column in our hands, requiring re-derivitization after 3–4 months. This column does however provide better resolution than the Propac PA1 for disaccharides. This can be seen by the resolution of α- and β-anomers with some of the disaccharide standards. The C18 CTA derivatized column has a mobile phase of double-distilled water brought to pH 3 with methane sulphonic acid. The counter ion is ammonium methane sulphonate and a gradient of 0–100%, 0–2 M ammonium methane sulphonate, pH 2.5 is used over 74 min at a flow rate of 0.22 ml/min. Another advantage of this column is the UV transparency of the mobile phase. This column has also been coupled to gel permeation columns to give a two-dimensional separation (14). An example of the disaccharide separation profile is shown in Fig. 3.

The separation of disaccharides derived from chemical degradation using nitrous acid cleavage poses more of a challenge. This cleavage occurs between the *N*-sulphated glucosamine residue and the hexuronic acid leaving a reducing end anhydromannose residue, which is usually reduced to anhydromannitol (15). One advantage is that the hexuronic acid residue remains intact and can thus be identified. Detection can be achieved by reducing end labeling with radioactivity (3H-borohydride) as there is no C=C double bond at the nonreducing terminus as after lyase digestion. For separation, a silica based column has been used conventionally (e.g., SAX Partisil), but this column appears to give inadequately resolved, broad peaks. This hampers quantitation, identification, and the sensitivity of detection.

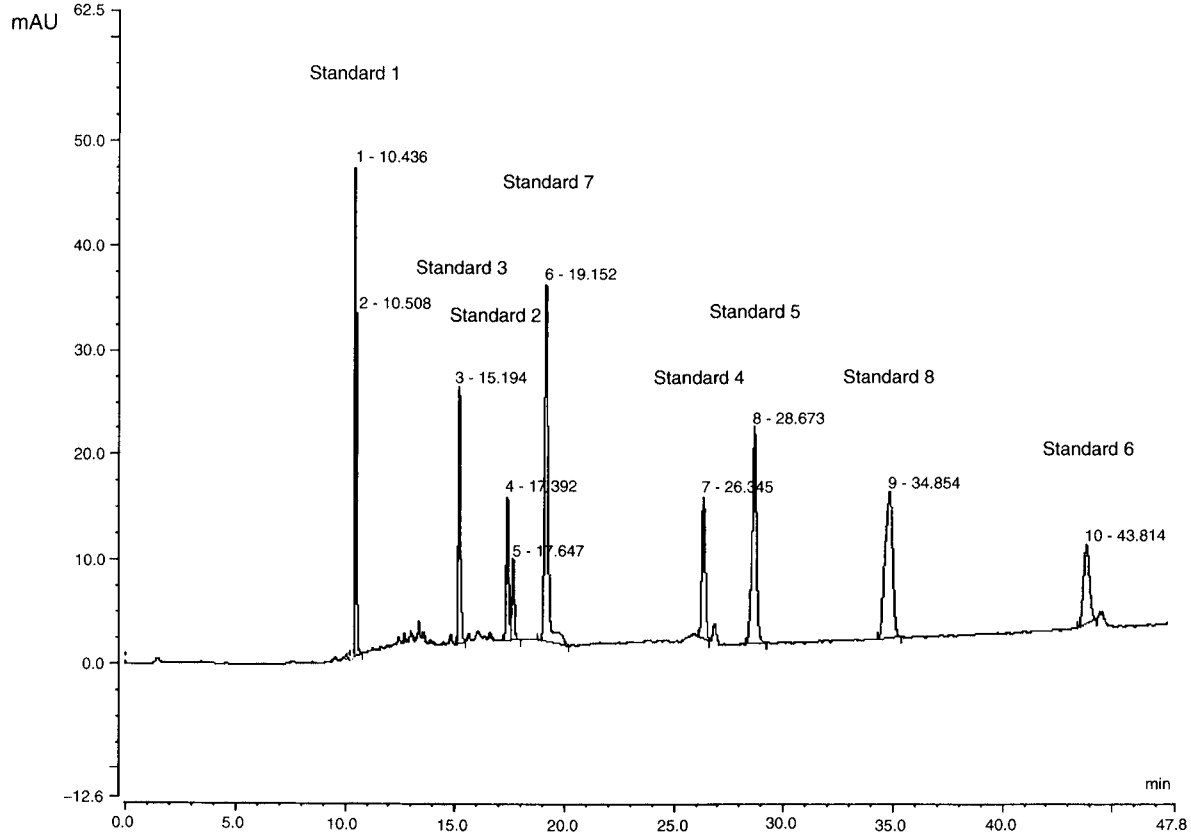

Figure 2 Disaccharide profile for eight common naturally occurring disaccharides derived from heparan sulfate. Separation was achieved using high-performance strong anion exchange chromatography (HPSAX) on a Dionex Propac PA1 column with a 0–45 min, 0–1 M NaCl linear gradient, pH 3.5; flow rate 1 ml/min. Disaccharide peaks: (1) ΔHexA-GlcNAc; (2) ΔHexA-GlcNAc(6S); (3) ΔHexA-$GlcNSO_3$; (4) ΔHexA(2S)-GlcNAc; (5) ΔHexA-$GlcNSO_3$(6S); (6) ΔHexA(2S)-$GlcNSO_3$; (7) ΔHexA(2S)-GlcNAc(6S); (8) ΔHexA(2S)-$GlcNSO_3$(6S).

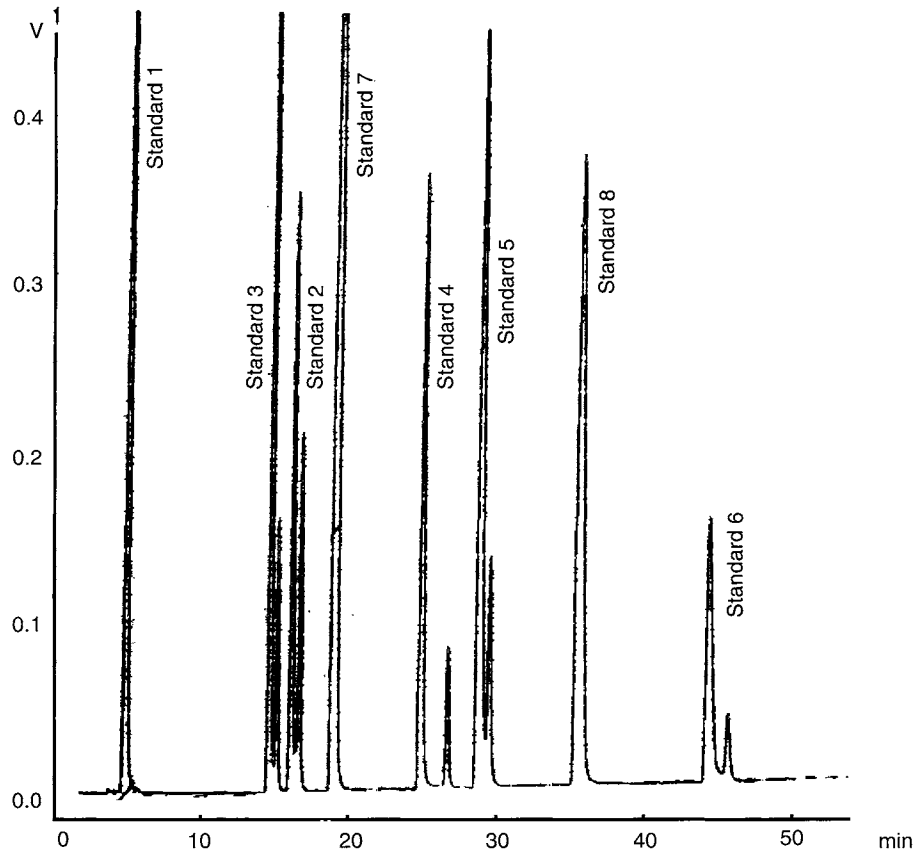

Figure 3 Disaccharide profile for eight common naturally occurring disaccharides derived from heparan sulphate. Separation was achieved using high-performance strong anion exchange chromatography (HPSAX) on a cetyl-triethylammonium ion (CTA) derivatized C18 silica-based column (C18 Hypersil) with a 0–90 min, 0–2 M ammonium methane sulphonate linear gradient, pH 3.5; flow rate 0.22 ml/min. Peaks and structures as defined in Fig. 2.

In contrast, 2 Propac PA1 columns in series provide excellent resolution using shallow linear sodium chloride gradients (e.g., 0–150 mM over 50 min followed by 150–500 mM over 70 min) (12). Furthermore, improved separation of monosulphated disaccharides can be achieved by running a potassium dihydrogen phosphate gradient 0–100%, 1 M over 90 min, with the initial mobile phase being double-distilled water pH 6 (12).

Larger heparin and heparan sulphate oligosaccharides can also be separated using the Propac PA1 column using extended linear NaCl gradients (e.g., 0–100%, 1–2 M NaCl over 90–180 min). Figure 4 shows an example of a decasaccharide fraction from a heparitinase I digest of porcine mucosal heparan sulphate. From the

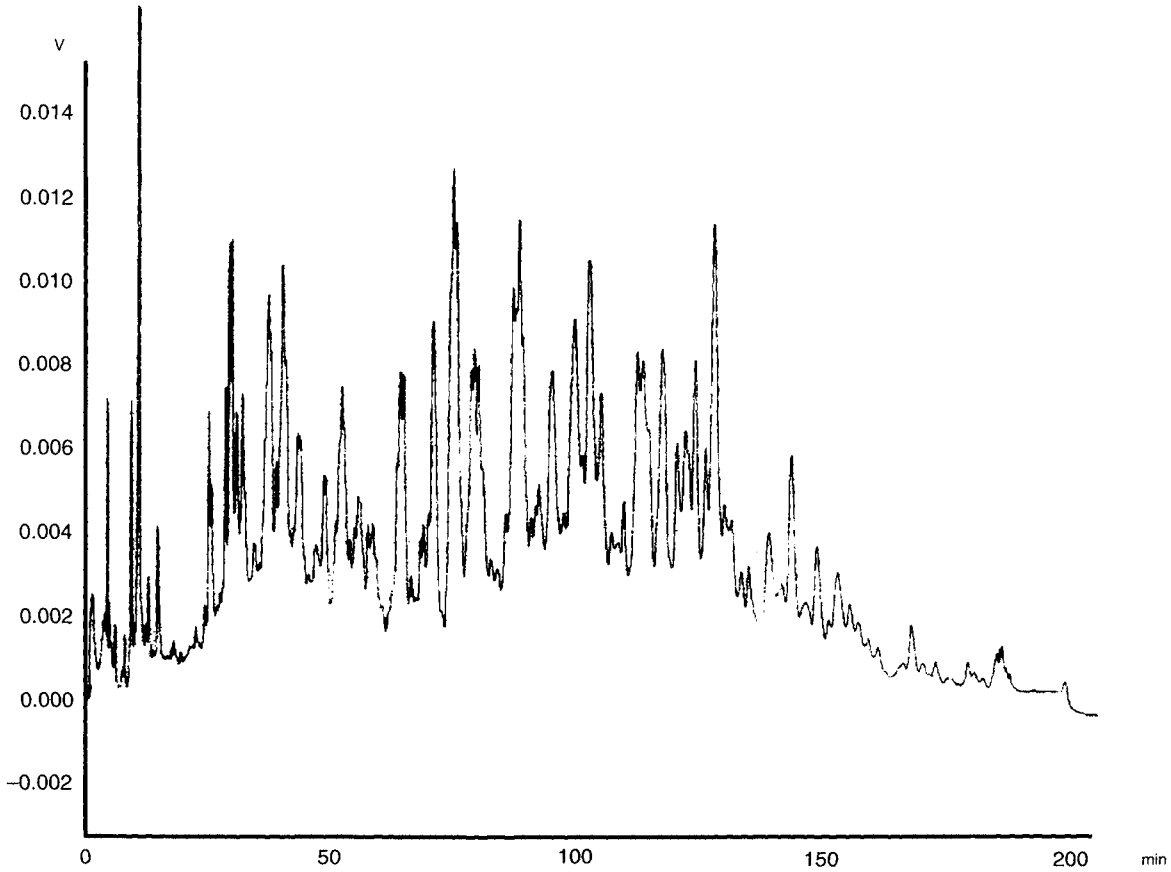

Figure 4 High-performance strong anion exchange (HPSAX) elution profile of size separated porcine mucosal derived heparan sulfate (PMHS) oligosaccharides of uniform size consisting of five disaccharide units. Run conditions were Dionex Propac PA1 column with a 0–180 min, 0–2 M NaCl linear gradient, pH 3.5; flow rate 1 ml/min.

profile both resolved and partially resolved peaks can be observed. It is thought that these peaks are sub-fractions of a particular heparan sulphate saccharides that possess similar or identical charge, but are structural isomers. The C18 CTA column method can also be used to separate larger saccharides (14).

3. Reverse-Phase Ion-Pairing High Performance Liquid Chromatography

Reverse-phase HPLC involves binding an organic molecule to a stationary phase, often silica derivatized with alkyl chains, in a relatively polar environment (the mobile phase), which could contain water, and then eluting the organic molecule using a gradient of a less polar organic solvent. The compounds are therefore separated on account of their differing hydrophobic character. This technique has only been used to separate relatively small oligosaccharides with long run times and problematic desalting making the technique laborious (16). In the case of heparin oligosaccharides, these are first converted into organic salts, often a hydrophobic ammonium salt, for example, tetrabutylammonium by neutralizing the acidic form of the oligosaccharide with, for example, tetrabutylammonium hydroxide (17). Recently this methodology has proved advantageous for linking LC separations directly to electrospray mass spectrometry [see later (16)].

B. Electrophoresis

Electrophoresis is a high-resolution technique, which separates molecules on the basis of their charge, size, and conformation. This separation results from the interaction of an analyte with the gel matrix when a charged molecule experiences a force towards an electrode of opposite charge causing migration. The frictional force experienced by the analyte from the gel is proportional to the distance the analyte migrates within a constant electric field. For the analysis of carbohydrates and especially heparin and heparan sulphate, both agarose and polyacrylamide gels have been used (18). Commonly polyacrylamide gels of high viscosity are used in the order of 30%, but capillary electrophoresis separations have also been developed.

1. Polyacrylamide Gel Electrophoresis

Polyacrylamide gels are created by the polymerization of acrylamide monomers with the *N*,*N*′-methlylenebisacrylamide cross-linker. The pore size, formed within the gel, is dependent on the amount of cross-linking and the lengths of the polymer chains. Ammonium persulphate is usually used as the free radical initiator while *N*,*N*,*N*′,*N*′-tetramethylenediamine (TEMED) stabilizes the polymerization chain reaction. The chain reaction is inhibited by molecular oxygen so the polymerization is conventionally carried out between two thin glass plates with the top of the gel solution covered with water-saturated butanol. Gels used for sequencing, etc. [such as in integral glycan sequencing (IGS)] are generally run on a vertical platform apparatus.

For the analysis of oligosaccharides derived from heparin and heparan sulphate a 33% polyacrylamide gel (with 19:1 acrylamide:bisacrylamide cross-linker) has been found to give good separation. The concentration of the acrylamide solution can however be adjusted though to give more tailored average pore sizes and hence separation ranges. Gradient gels can be used, but these are difficult to cast and reproducibility poses a serious problem. Unlike protein electrophoresis, carbohydrate gels are in the native form and hence the carbohydrate conformation (and thus mobility) will depend on the exact oligosaccharide structures present within. Therefore, a simple direct migration distance to size relationship cannot be achieved.

A common method for visualization of unlabeled oligosaccharides is the blue dye Azure A. Staining occurs due to ionic interactions with the highly negative charge sulphate and carboxylic acid groups present in this class of carbohydrate. Background staining can easily be removed by washing with double-distilled water. The limit of detection is in the order of a few micrograms (13). Detection of oligosaccharides separated on gels can also be achieved using radiolabels (19) or fluorescent tags (20) and preparative scale purification of saccharides is also possible (21).

2. *Capillary Electrophoresis*

Conventional polyacrylamide gel electrophoresis (PAGE) has two main drawbacks. First, only relatively low voltages can be used due to the effect of Joule heating upon the separation gel and the analytes themselves. Second, detection of the molecules is problematic and the level of detection is comparatively low in the slab gel format used in PAGE. To counter these problems capillary electrophoresis (CE) can be employed. The capillary has a high surface to volume ratio, hence radiating heat, allowing for efficient cooling mechanisms to be introduced negating the voltage restrictions that limit PAGE. Detection is performed by directing UV or visible light through a narrow window in the capillary and detecting on the opposing side. This allows for the analysis of much smaller sample quantities. As the voltages used in capillary electrophoresis are very high (typically up to 30 kV) (22), sample run times are usefully short.

Capillary electrophoresis takes place in a narrow bore fused silica capillary. Electrophoresis can occur in free solution or the capillary can be filled with a suitable matrix. Sample loads are minuscule in comparison to conventional PAGE – between 10 and 100 nL of sample is required and consumable costs are significantly reduced (23). Loading on to the capillary is usually achieved by either applied voltage, with only charged molecules entering the capillary (electrokinetic injection), or by a pressure difference being induced across the sample vial and capillary (hydrodynamic injection). It should be noted here that while hydrodynamic injection gives a quantitative representation of the original sample, electrokinetic does not, as the more highly charged analytes will enter the capillary in greater numbers from the starting solution. After electrophoresis the capillary can be flushed, regenerated, and reused.

One consideration, which must be given to capillary electrophoresis, is that of endo-osmotic flow. This occurs due to the presence of silanol groups on the inner surface of the fused capillary. At environmental pHs >2 they donate protons and become ionized. Positively charged ions from the buffer ion-pair with the negatively charged silanol groups lead to the creation of an electric double layer. The positive buffer ions present in the electric double layer are able to migrate towards the negatively charged electrode and in doing so they trap water molecules, which leads to endo-osmotic flow (24). This effect can be diminished by using low pH buffers which protonate the silanol groups and abolish the formation of the electric double layer or by derivitization of the silanol groups, for example with methylcellulose. Various modes of capillary electrophoresis exist. Common ones include capillary zone electrophoresis (CZE), capillary gel electrophoresis, capillary isoelectric focusing, capillary iostachophoresis, and micellar electrokinetic capillary chromatography. As heparan sulphate and heparin oligosaccharides are not amphoteric species, capillary isoelectric focusing is not discussed. Furthermore heparin and heparan sulphate have a high degree of structural diversity so the possibility of micellar electrokinetic capillary chromatography is problematic, although the less diverse disaccharides of dermatan and chondroitin sulphates have been separated using this method (25). Consequently, this form of CE is also omitted.

In regard to heparin/heparan sulphate oligosaccharide separation by CE, the most common mode used is capillary zone electrophoresis (CZE). This involves separation in free solution. To date both normal and reverse polarity separations have been performed (26) on this class of carbohydrate. In normal mode the environmental pH is buffered around neutrality and the capillary wall is negatively charged. Separation will occur due to both electrophoretic and electroendo-osmotic migration/flow. In reverse mode, the pH is usually buffered at around pH 2.5, limiting the effects of endo-osmotic flow, thereby carrying out the separation solely on the basis of electrophoresis.

Detection can be either direct or by derivitization of the carbohydrate molecules with a fluorophore prior to injection. The C=C double bond created upon bacterial lyase digestion mentioned previously allows direct observation using a UV-spectrophotometric detector (27). Carbohydrate analytes can also be derivatized with fluorophores allowing for more highly sensitive detection, including the use of a laser induced fluorescence detection module (28). An example of the power of CE can be seen from the disaccharide analysis performed both by UV and after derivitization with the fluorophore 2-aminoacridone (AMAC). Again, the labeling occurs through reductive amination. Twelve known heparin and heparan sulphate derived disaccharides are resolved in 26 min by UV detection at $\lambda = 232$ nm with the assistance of an imposed pressure gradient (29) and all 12 standards are again resolved using UV and LIF detection (at $\lambda = 255$ and 488 nm, respectively) in just over 30 min (22). Sensitivity of detection of disaccharides labeled with AMAC fluorophore and separated by CE with LIF detection is approx. 50 fmol/peak, and thus nanogram quantities of sample should be required to detect all disaccharides present at >1% level in a typical heparan sulphate.

III. Heparin and Heparan Sulphate Sequencing

The ability to sequence heparin and more specifically heparan sulphate is of fundamental importance in the determination of structure–function relationships between the carbohydrate and its many interacting partners. Unlike protein and nucleic acid sequencing, the sequencing of carbohydrates and more specifically that of glycosaminoglycans has lagged behind with no one individual method allowing for facile, reproducible sequence determination of an oligosaccharide (and certainly not a polysaccharide) chain of any sizeable length.

One of the main obstacles faced is that of obtaining a reasonable amount of starting material in order to perform the multiple stages required with current strategies. This, along with the difficulty in obtaining pure samples, has led to a gap in this aspect of glycosaminoglycan biochemistry.

In general, two approaches to the sequencing of heparan sulphate exist. The first is a direct method, which uses NMR to observe the molecule in question; this method does not require multiple processing steps, yet it does require large amounts of pure sample. The remaining methods can be further subdivided into those, which require oligosaccharide separation methods and which do not (namely mass spectrometry). Associated with all of these methods is the need to generate oligosaccharide fragments from the parental oligosaccharide and the use of a specific sets of endolytic bacterial lyase enzymes and exolytic mammalian lysosomal enzymes in order to identify the presence and positioning of the various sulphate, acetyl and carboxyl groups on the uronic acid and glucosamine residues. The various enzymes used are summarized in Table 1. They are exoglucosidases (e.g., iduronase, which removes the iduronic acid residue present at the terminal nonreducing end, and only acts if there is no 2-*O*-sulphate present), and a class of enzymes known as exosulphatases that remove specific sulphates from nonreducing terminal residues. This information, coupled to the position of *N*-sulphates from the nitrous acid digestion allows for the determination of sequence.

A summary of the different sequencing methods and their merits and limitations are provided in Table 2. Demonstrations of the applications of these various methods have already begun to appear. IGS has been used to sequence heparan sulphate saccharides, which act as specific regulators of signaling by FGFR isoforms (20). Matrix-assisted laser desorbtion ionization (MALDI) and IGS have been used to sequence an antithrombin-binding saccharide with anticoagulant activity (30). In general the methods are designed for the sequencing of purified saccharides, which have been shown to have selective protein-binding characteristics or particular biological activities, as in the above two examples. However, the step sequencing method has also been used to examine structural diversity, by elucidating the sequences of a set of S-domains of different sizes expressed by a single cell type (31).

A. Nuclear Magnetic Resonance

Sequencing oligosaccharides by NMR usually involves several two-dimensional experiments. These are required to obtain firstly, a spectral assignment, to establish

Table 2 Comparison of Sequencing Techniques

Technique	Advantage	Disadvantage
NMR	Isomer information present	Large sample amount needed
	Gives structural information	Spectrum complex for large oligosaccharides
	Nondestructive	Pure saccharides needed
	No labels required	
IGS	Uses common PAGE technique	Loss of sensitivity due to acid digestion
	Small sample amounts	Low yielding reducing end fluorophore
		Enzyme activity is essential
Radiolabel (IGS/step)	Small sample amounts	Radioactivity handling
	Increased detection levels	Disposal of labeled samples
	Metabolic labeling possible	
MALDI-MS	Accurate mass data	Indirect detection
	Mass database	Peptide coupling problems
	Small sample amounts	Ionization problems
ES-MS	Very small sample amounts	Ion-pairing problems
	Tandem MS/MS	Ionization problems
	Accurate mass data	
	Mass database	

which signals arise from particular positions in the sugar units. These are typically three bond $^{1}H - ^{1}H$ COSY and TOCSY experiments. Results from these spectra allow unambiguous assignment of the sugar rings present in the sample but give no information concerning their connectivity. The second set of experiments involves some form of correlation experiment in which the connectivity of residues can be followed. Typically, this involves a NOESY experiment in which space proximity is established and this form of experiment will also establish the proximity of atoms within the ring and allow assignments to be made. Long-range H–C correlation experiments can also be employed to establish connectivity between residues.

There are two principal disadvantages to sequencing heparan sulphate oligosaccharides by NMR. The first is that relatively large amounts of sample are required (usually in the order of a few milligrams) and a high degree of sample purity is required. The second is that the resolution of signals from adjacent disaccharide units becomes more difficult as the length of the oligosaccharide chains increases, and becomes a problem sooner if the disaccharide-repeating units are of the same or similar structure. This is because the signals from those units tend to converge as their environment becomes less distinguishable, i.e., in general, the further they are from the reducing end. In practice, NMR has mainly been used to sequence small saccharides up to hexasaccharide in size, with occasional examples of application to larger oligosaccharides (30).

B. Integral Glycan Sequencing

The IGS technique is based on the observation of band shifts on polyacrylamide gels to yield sequence information (20). In the original PAGE–IGS strategy a purified oligosaccharide is first labeled fluorescently at the reducing end with a fluorophore (e.g., 2-aminobenzoic acid, 2AA) by means of reductive amination. This fluorescent tag provides an essential reading frame for sequence elucidation. 2AA has an excitation maximum in the range of 300–320 nm and an emission maximum between 410 and 420 nm. This allows for easy visualization of subsequent gels on a standard 312-nm UV transilluminator. Improved detection has also been reported using the fluorophore ANDSA (7-aminonapthalene, 1–4-disulfonic acid), since this fluorophore has a greater extinction coefficient than that of 2AA while being less sensitive to cleavage under the acidic conditions experienced during nitrous acid degradation (4).

The second step involves the generation of a ladder of intermediate sized oligosaccharides by partial nitrous acid cleavage of the oligosaccharide. Nitrous acid cleavage occurs between a *N*-sulphated glucosamine residue and its reducing end uronic acid residue. Cleavage does not occur if the glucosamine residue is *N*-acetylated. The resulting ladder of sized oligosaccharides, i.e., di-, tetra-, hexasaccharides, etc. each have a common fluorescently tagged reducing end terminus, with their nonreducing termini corresponding to the original positions of *N*-sulfoglucosamine residues. In the third step, aliquots of these fragments are treated separately with cocktails of various exolytic lysosomal enzymes – exoglucosidases and exosulphatases – that remove specific monosaccharide residues or sulphate groups respectively from the nonreducing ends of the fragments. The resulting products are then separated in separate tracks on a PAGE gel. The specificity of these enzymes, combined with the band shift patterns permits the sugar sequence to be read directly from the resulting fluorescent banding patterns in a manner analogous to DNA sequencing (Fig. 5).

Sequencing using IGS can be achieved with a few nanomoles of starting material (low microgram quantities) but in the future improvements in sensitivity can be expected using better fluorophores and more sensitive detection modes (e.g., LIF detection in CE separations). Note that "breaks" in the sequencing ladder are caused by the presence of GlcNAc residues – to sequence through such a gap additional treatment with the enzyme *N*-acetylglucosaminidase is required to open up access to the next disaccharide unit.

A radiolabel version of the IGS strategy has also been reported, using a ^{3}H radiolabel at the reducing end. This has the advantage of being more resistant to the partial nitrous acid degradation step. Samples are labeled at the reducing end by reduction with the radioactive reducing agent sodium borohydride ($NaB[^{3}H]_4$). Oligosaccharide samples are then treated in a manner analogous to PAGE–IGS. The resulting oligosaccharide products of the various digests (with a ^{3}H-labeled reading frame) are then separated in a series of SAX-HPLC runs with detection achieved by fraction collection and scintillation counting. The elution positions and

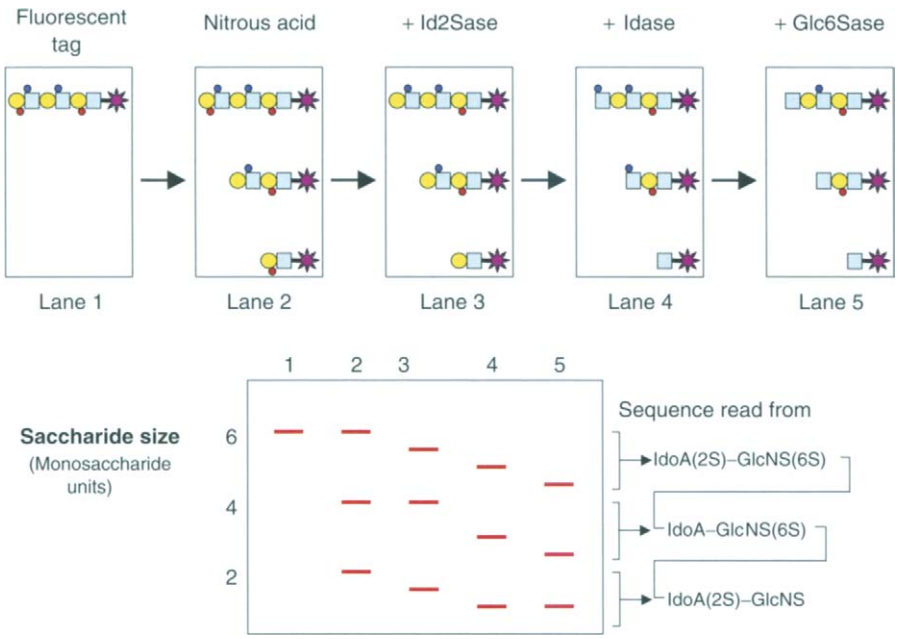

Figure 5 Diagrammatic presentation of the integral glycan sequencing strategy (IGS). This schematic example shows a simple hexasaccharide with the sequence IdoA(2S)–GlcNS(6S)–IdoA–GlcNS(6S)–IdoA(2S)–GlcNS. The saccharide is labeled at its reducing end with a fluorescent tag (track 1; purple star). Partial chemical cleavage at GlcNS residues with nitrous acid "opens up" the structure by creating intermediate fragments differing in size by a disaccharide unit (track 2). Particular combinations of exoenzymes (exosulphatases and exoglycosidases) are used to selectively remove specific sulphate groups or monosaccharide residues. These include 2-*O*-sulphates, IdoA residues and 6-*O*-sulphates in tracks 3, 4, and 5, respectively (Id2S, iduronate-2-sulphatase; Idase, iduronidase; Glc6Sase, glucosamine-6-sulphatase). Critically, these enzymes only act at the nonreducing end disaccharide units of each fragment, newly exposed by the partial fragmentation in the previous step. The products are separated on adjacent tracks of a high density polyacrylamide gel and the resulting fluorescent banding pattern allows the sugar sequence to be read directly from the band shifts in a manner analogous to DNA sequencing.

peak shifts are interpreted to read the sequence of the original saccharide (31). Sensitivity is reported to be similar to that for IGS with the ANDSA label (1–2 nmol of starting material).

C. Sequencing of Metabolically Radio-Labeled Heparan Sulphate Saccharides

The metabolic incorporation of radiolabel (^{3}H and ^{35}S) into heparan sulphate by the use of radioactive precursors permits the sequencing of cell or tissue-derived saccharides. Cells are cultured in the presence of D-[6-^{3}H]glucosamine hydrochloride (20–45 Ci/mmol) and in some cases also $Na_2^{35}SO_4$ (up to 80 mCi/ml), which become

incorporated into the heparin/heparan sulphate polysaccharides produced by the cells. Very small amounts of biosynthetically radio-labeled heparan sulphate saccharides prepared from these radio-labeled polysaccharides by lyase degradation and size exclusion/SAX-HPLC purification can be sequenced using a variant of IGS called "step-sequencing" (32). SAX-HPLC purified heparan sulphate saccharide peaks are partially degraded with nitrous acid to produce intermediate oligosaccharide fragments, and aliquots subjected to various exoenzyme treatments, followed by SAX-HPLC analysis of the products on a Propac PA1 column. Since the saccharides are radio-labeled along their entire length, a key aspect of the step sequencing method is that it relies upon for a "reading frame" differences in elution position of fragments which contain the original nonreducing end hexuronic acid residue *vs* those that do not. By careful interpretation of the SAX profiles, enhanced by knowledge of the elution positions of various known intermediate structures, the sequence of the original saccharide can be deduced. This method is specifically designed for sequencing metabolically labeled heparan sulphate saccharides where sufficient labeled heparan sulphate can be prepared to produce the purified saccharides of interest. It has been used to sequence up to decasaccharides, but larger fragments may prove problematic due to the resolution constraints (problems in detecting shifts) imposed by the strong anion exchange separation itself.

D. Matrix-Assisted Laser Desorbtion Ionization Mass Spectrometry

The use of mass spectrometry to derive the structure of oligosaccharide fragments provides an attractive prospect when the theoretically low amount of material required for analysis is considered. Unfortunately, the ability to ionize and "fly" sulphated saccharides possess something of a problem (33). The high negative charge of the heparin/heparan sulphate saccharides limits ionization, while the high susceptibility of the sulphate group itself to cleavage possess a major obstacle to sequencing. Furthermore, mass spectrometry does not allow for the resolution of the structural isomers arising from the uronic acid epimers or the *O*-sulphates, which can be present at C3 or C6 of the glucosamine residue.

MALDI mass spectrometry has been used to detect oligosaccharide fragments by employing a basic noncovalently bound coupling peptide. This peptide possesses uniform positive charge, which ion-pairs with negatively charged groups contained within the heparan sulphate, hence masking the negative charge and allowing ionization of the molecule. Detection in the mass spectrometer is of the combined mass, i.e., that of the heparan sulphate saccharide and the bound peptide.

A MALDI-peptide approach to sequencing based on a convergent strategy has been developed, linked to use of mass information for intact oligosaccharide fragments that provides a database for mining with the mass signature for any particular saccharide of interest. The database provides the many possible solutions for any single mass (which arise from the extensive potential for structural isomers). In initial studies the further susceptibility of the saccharide to various lyase

enzymes, coupled to knowledge of their specificity and the presence of a reducing end mass tag to identify peaks with a common reducing end, yields a characteristic set of breakdown products that limits the solution possibilities for the initial signature ion observed (34). However, it is rarely possible to fully define a sequence using this approach, so it was further refined by employing various additional treatments with partial nitrous acid and exoenzymes to converge towards a single sequence by the presence or absence of appropriate mass shifts (35,36). Sensitivity is reported to be similar to that for IGS (nmol quantities of starting material), but may be improved with increasing sensitivity of MALDI instruments. However, there are likely to be limitations and the broad applicability still needs to be explored. Coupling is probably favored for heparin/heparan sulphate saccharides with a high degree of charge, and may make sequencing of lower sulphated heparan sulphate saccharides difficult (33). The peptide itself may have to be tailored to the size of the heparin/heparan sulphate fragment under investigation.

E. Electrospray Mass Spectrometry

Effective electrospray mass spectrometry (ES-MS) methods for heparan sulphate saccharides are now emerging. Currently, ES-MS techniques rely on the masking of the negative charge by ion pairing with quaternary ammonium ions, such as tetraethylammonium hydroxide or dibutylammonium acetate. This permits ionization of carbohydrate fragment as well as provides a volatile solvent required for the mass spectrometric technique (37,38).

The use of ES-MS for heparan sulphate sequencing appears to be attractive for a number of reasons. Tandem MS/MS opens up the possibility of overcoming the structural isomer problem by detecting differing fragmentation pathways (39). Another attractive possibility is the direct coupling of liquid chromatography or capillary electrophoresis equipment to the ionization source leading to true two-dimensional analysis. Tributylammonium acetate or dibutyl ammonium acetate are used as the ion pairing agent for direct coupling of liquid chromatography with electrospray. This permits ionization of carbohydrate fragment (especially heparan sulphate) and provides a volatile solvent required for the mass spectrometric technique in order to enhance retention and peak shape (16,38). The characterization of the pentasaccharide responsible for AT III binding and its precursors has been elucidated using LC–ES-MS (38). Furthermore, these methods allow sample concentration prior to ionization.

In addition, coupling of the use of the lyase and exoenzymes with the above methodologies may produce new and powerful sequencing strategies [especially with the use of nano-electrospray ionization techniques (40)] that accurately distinguish between the structural isomers present within differing sequences of equal mass (uronic acid epimers and *O*-sulphate positions), although this may ultimately prove unnecessary if differing fragmentation pathways can be elucidated with tandem MS/MS (40).

IV. Discussion

The separation and sequencing of heparin and heparan sulphate saccharides is by no means a trivial undertaking. Separation of heparan sulphate saccharides is problematic due to the heterogeneity, which is often present within a given sample. Separation techniques, which have greater resolving power, are crucially needed within the field. Pure samples are of fundamental importance if accurate sequence information is to be obtained. Yet, no method provides the ability to unequivocally sequence a complex mixture. Thus, a limiting step in our ability to sequence is sample quantity and purity. Nevertheless, there have been significant advances over the past decade, and there are a number of methods in current use, which with careful experimentation do permit the sequencing of relatively small amounts of saccharide from a range of sources (both cell- and tissue-derived heparan sulphate). The techniques and instrumentation required for these methods are diverse and accessible, putting them within the capabilities of most researchers.

Looking forward, better labeling strategies are needed that provide increased yield (labeling efficiency) and which are more stable in the presence of acid to support the sequencing strategies based on tagging. Better separation techniques should lead to improved purity of heparan sulphate saccharides for sequencing, and more accurate sequencing separations. The increasing sensitivity of detection in mass spectrometry methods, and the possibility of understanding fragmentation pathways for oligosaccharide fragments, can be expected to make an impact and would considerably advance the field. It is reasonable to anticipate that the next decade will see major advances in separation and sequencing techniques for heparin and heparan sulphate saccharides, with the exciting possibility of "glycomics" studies on the structure–activity relationships of these complex molecules.

Acknowledgments

The work of the authors is funded by the Medical Research Council, Biotechnology and Biological Sciences Research Council, European Union and the Human Frontier Science Program. Dr Edwin Yates is thanked for his constructive criticism of the manuscript. The authors would also like to thank Dr Andrew Powell and Yassir Ahmed for provision of the size-exclusion chromatography figure.

References

1. Gallagher JT, Turnbull JE, Lyon M. Patterns of sulphation in heparan sulphate: polymorphism based on a common structural theme. Int J Biochem 1992; 24:553–560.
2. Lindahl U, Kusche-Gullberg M, Kjellen L. Regulated diversity of heparan sulphate. J Biol Chem 1998; 273:24979–24982.
3. Turnbull J, Powell A, Guimond S. Heparan sulphate: decoding a dynamic multifunctional cell regulator. Trends Cell Biol 2001; 11:75–82.

4. Drummond KJ, Yates EA, Turnbull JE. Electrophoretic sequencing of heparin/heparan sulphate oligosaccharides using a highly sensitive fluorescent end label. Proteomics 2001; 1:304–310.
5. Isbell HS, Frush HL, Wade CWR, Hunter CE. Transformations of sugars in alkaline solutions. Carbohydr Res 1969; 9:163–175.
6. Yates EA, Jones MO, Clarke CE, Powell AK, Johnson SR, Porch A, Edwards P, Turnbull JE. Microwave enhanced reaction of carbohydrates with amino-derivatised labels and glass surfaces. J Mater Chem 2003; 13:2061–2063.
7. Skidmore MA, Patey SJ, Thanh NTK, Fernig DG, Turnbull JE, Yates EA. Attachment of glycosaminoglycan oligosaccharides to thiol-derivatised gold surfaces. Chem Commun 2004; 23:2700–2701.
8. Yates EA, Guimond SE, Turnbull JE. Highly diverse heparan sulphate analogue libraries: providing access to expanded areas of sequence space for bioactivity screening. J Med Chem 2004; 47:277–280.
9. Merchant ZM, Kim YS, Rice KG, Linhardt RJ. Structure of heparin-derived tetrasaccharides. Biochem J 1985; 229:369–377.
10. Walker A, Turnbull JE, Gallagher JT. Specific heparan sulphate saccharides mediate the activity of basic fibroblast growth factor. J Biol Chem 1994; 269:931–935.
11. Safaiyan F, Kolset SO, Prydz K, Gottfridsson E, Lindhal U, Salmivirta M. Selective effects of sodium chlorate treatment on the sulphation of heaparan sulphate. J Biol Chem 1999; 274:36267–36273.
12. Turnbull JE. Analytical and preparative strong anion-exchange HPLC of heparan sulphate and heparin saccharides. In: Proteoglycan Protocols. Meth Mol Biol 2001; 171:141–148.
13. Linhardt RJ, Turnbull JE, Wang HM, Loganathan D, Gallagher JT. Examination of the substrate specificity of heparin and heparan sulphate lyases. Biochemistry 1990; 29:2611–2617.
14. Mourier PA, Viskov C. Chromatographic analysis and sequencing approach of heparin oligosaccharides using cetyltrimethylammonium dynamically coated stationary phases. Anal Biochem 2004; 332:299–313.
15. Radoff S, Danishefsky I. Location on heparin of the oligosaccharide section essential for anticoagulant activity. J Biol Chem 1984; 259:166–172.
16. Thanawiroon C, Rice KG, Toida T, Linhardt RJ. Liquid chromatography/mass spectrometry sequencing approach for highly sulphated heparin-derived oligosaccharides. J Biol Chem 2004; 279:2608–2615.
17. Guo YC, Conrad HE. Analysis of oligosaccharides from heparin by reversed-phase ion-pairing high-performance liquid chromatography. Anal Biochem 1988; 168:54–62.
18. Pye DA, Vives RR, Turnbull JE, Hyde P, Gallagher JT. Heparan sulphate oligosaccharides require 6-*O*-sulphation for promotion of basic fibroblast growth factor mitogenic activity. J Biol Chem 1998; 273:22936–22942.
19. Turnbull JE, Gallagher JT. Molecular organization of heparan sulphate from human skin fibroblasts. Biochem J 1990; 265:715–724.
20. Turnbull JE, Hopwood JJ, Gallagher JT. A strategy for rapid sequencing of heparan sulphate and heparin saccharides. Proc Natl Acad Sci USA 1999; 96:2698–2703.
21. Vives RR, Goodger S, Pye DA. Combined strong anion-exchange HPLC and PAGE approach for the purification of heparan sulphate oligosaccharides. Biochem J 2001; 354:141–147.

22. Militsopoulou M, Lecomte C, Bayle C, Couderc F, Karamanos NK. Laser-induced fluorescence as a powerful detection tool for capillary electrophoretic analysis of heparin/heparan sulphate disaccharides. Biomed Chromatogr 2003; 17:39–41.
23. Linhardt RJ, Pervin A. Separation of acidic carbohydrates by capillary electrophoresis. J Chromatogr A 1996; 720:323–335.
24. Mao W, Thanawiroon C, Linhardt RJ. Capillary electrophoresis for the analysis of of glycosaminoglycans and glycosaminoglycan-derived oligosaccharides. Biomed Chromatogr 2002; 16:77–94.
25. Mastrogianni O, Lamari F, Syrokou A, Militsopoulou M, Hjerpe A, Karamanos NK. Microemulsion electrokinetic capillary chromatography of sulphated disaccharides derived from glycosaminoglycans. Electrophoresis 2001; 22:2743–2745.
26. Gunay NS, Linhardt RJ. Capillary electrophoretic separation of heparin oligosaccharides under conditions amenable to mass spectrometric detection. J Chromatogr A 2003; 1014:225–233.
27. Karamanos NK, Vanky P, Tzanakakis GN, Hjerpe A. High performance capillary electrophoresis method to characterize heparin and heparan sulphate disaccharides. Electrophoresis 199; 17:391–395.
28. Militsopoulou M, Lamari FN, Hjerpe A, Karamanos NK. Determination of twelve heparin- and heparan sulphate-derived disaccharides as 2-aminoacridone derivatives by capillary zone electrophoresis using ultraviolet and laser-induced fluorescence detection. Electrophoresis 2002; 23:1104–1109.
29. Ruiz-Calero V, Puignou L, Galceran MT. Use of reversed polarity and a pressure gradient in the analysis ofdisaccharide composition of heparin by capillary electrophoresis. J Chromatogr A 1998; 828:497–508.
30. Shriver Z, Raman R, Venkataraman G, Drummond K, Turnbull J, Toida T, Linhardt R, Biemann K, Sasisekharan R. Sequencing of 3-*O*-sulphate containing heparin decasaccharides with a partial antithrombin III binding site. Proc Natl Acad Sci USA 2000; 97:10359–10364.
31. Vives RR, Pye DA, Salmivirta M, Hopwood JJ, Lindahl U, Gallagher JJ. Sequence analysis of heparan sulphate and heparin oligosaccharides. Biochem J 1999; 339:767–773.
32. Merry CLR, Lyon M, Deakin JA, Hopwood JJ, Gallagher JG. Highly sensitive sequencing of the sulphated domains of heparan sulphate. J Biol Chem 1999; 274:18455–18462.
33. Juhasz P, Biemann K. Utility of non-covalent complexes in the matrix-assisted laser desorption ionization mass spectrometry of heparin-derived oligosaccharides. Carbohydr Res 1995; 270:131–147.
34. Rhomberg AJ, Ernst S, Sasisekharan R, Biemann K. Mass spectrometric and capillary electrophoretic investigation of the enzymatic degradation of heparin-like glycosaminoglycans. Proc Natl Acad Sci USA 1998; 95:4176–4181.
35. Venkataraman G, Shriver Z, Raman R, Sasisekharan R. Sequencing complex polysaccharides. Science 1999; 286:537–542.
36. Keiser N, Venkataraman G, Shriver Z, Sasisekharan R. Direct isolation and sequencing of specific protein-binding glycosaminoglycans. Nat Med 2001; 7:123–128.

37. Gunay NS, Tadano-Aritomi K, Toida T, Ishizuka I, Linhardt RJ. Evaluation of counterions for electrospray ionization mass spectral analysis of a highly sulphated carbohydrate, sucrose octasulphate. Anal Chem 2003; 75:3226–3231.
38. Kuberan B, Lech M, Zhang L, Wu ZL, Beeler DL, Rosenberg RD. Analysis of heparan sulphate oligosaccharides with ion-pair reverse phase capillary high performance liquid chromatography–microelectrospray ionization time-of-flight mass spectrometry. J Am Chem Soc 2002; 124:8707–8718.
39. Naggar EF, Costello CE, Zaia J. Competing fragmentation processes in tandem mass spectra of heparin-like glycosaminoglycans. J Am Soc Mass Spectrom 2004; 15:1534–1544.
40. Pope RM, Raska CS, Thorp SC, Liu J. Analysis of heparan sulphate oligosaccharides by nano-electrospray ionization mass spectrometry. Glycobiology 2001; 6:505–513.

Chemistry and Biology of Heparin and Heparan Sulfate
H.G. Garg, R.J. Linhardt and C.A. Hales (Editors)

Chapter 7

Biosynthesis of Heparin and Heparan Sulfate

SHUJI MIZUMOTO, HIROSHI KITAGAWA and KAZUYUKI SUGAHARA

Kobe Pharmaceutical University, Department of Biochemistry, Higashinada-ku, Kobe, Japan

I. Introduction

Heparin (HP) and heparan sulfate (HS) are structurally the most complex species of the glycosaminoglycan (GAG) family. The backbones of HP and HS are linear polymers composed of repeating disaccharide units, $[-4GlcA\beta1(IdoA\alpha1)\text{-}4GlcNAc\ \alpha1-]_n$ (Fig. 1), where GlcA, IdoA and GlcNAc represent D-glucuronic acid, L-iduronic acid and *N*-acetyl-D-glucosamine, respectively, which are covalently attached to the core proteins through the so-called common GAG-protein linkage tetrasaccharide, GlcAβ1-3Galβ1-3Galβ1-4Xylβ1-*O*-Ser (where Gal, Xyl, and Ser stand for D-galactose, D-xylose and L-serine, respectively). An obvious difference between HP and HS is their cellular localization: HP is mainly present in mast cells, whereas HS exists at the cell surface and extracellular matrix (ECM) in the form of proteoglycans (PGs). In addition, their structural features are different. HP is a highly sulfated species with a high proportion of *N*-sulfated glucosamine (GlcNS) and IdoA, whereas HS is a low-sulfated chain with a high proportion of GlcNAc and GlcA. Although HP meets today's standards for an anticoagulant, it actually controls levels of mast-cell proteases *in vivo*. HSPGs play roles through the HS side chains in various biological processes, such as cell proliferation, tissue morphogenesis, infection by viruses, and interactions with numerous growth factors, morphogens and cytokines (Fig. 2).

The biosynthesis of HP and HS chains that governs the expression of their functions, is initiated by the construction of the tetrasaccharide linkage region, which is assembled by the stepwise transfer of monosaccharides from respective uridine diphosphate (UDP)-sugars to a Ser residue of the core proteins and/or the

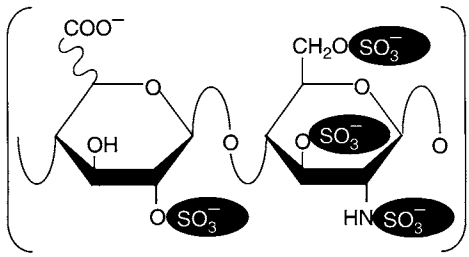

Figure 1 Typical repeating disaccharide units in HP/HS and their potential sulfation sites. HP and HS consist of uronic acids (IdoA and GlcA) and GlcNAc residues with varying proportions of IdoA and GlcA. These sugar residues can be esterified by sulfate at various positions as indicated in the figure.

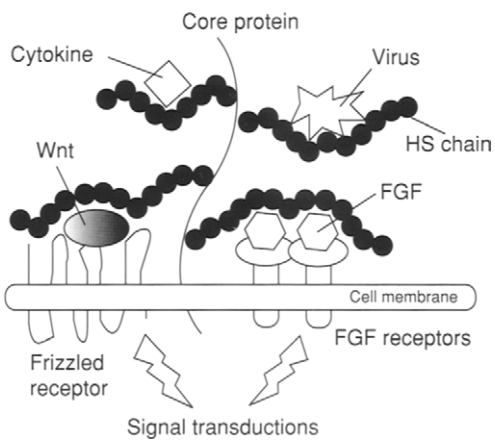

Figure 2 Various functions of HS chains. HS chains expressed on the cell surface interact with various proteins, such as growth factors, morphogens, cytokines, and viral envelope proteins.

naked nonreducing terminus through the action of the respective specific glycosyltransferases. Next, the chain elongation that results in the formation of the repeating disaccharide region of HP and HS, occurs by the action of HS polymerases. Finally, HP and HS are modified by GlcNAc *N*-deacetylase, GlcA epimerase and sulfotransferases. Recently, studies involving cDNA cloning of the genes encoding these enzymes and genetic analyses using knockout mice, zebrafish, fruit flies, and nematodes have led to unanticipated findings of interesting biological phenotypes. This chapter focuses on recent advances in the study of the biosynthesis and functions of HP and HS.

II. Biosynthetic Enzymes and Transporters of Uridine Diphosphate-Sugars and 3′-Phosphoadenosine 5′-Phosphosulfate

A. Uridine Diphosphate-Sugars

During the synthesis of HP and HS chains, glycosyltransferases that have one or two DXD motif(s) for uridine diphosphate (UDP)-sugar binding, utilize nucleotide sugars as donor substrates (1–3). The nucleotide sugars, UDP-Xyl, UDP-Gal, UDP-GlcA, and UDP-GlcNAc, are produced mainly from D-glucose (Glc), D-glucosamine (GlcN) and D-Gal, as shown in Fig. 3 (4). UDP-GlcA is formed by the action of the UDP-Glc dehydrogenase (UGDH) on UDP-Glc in the cytosol (5). On the other hand, UDP-Xyl is formed by the action of UDP-GlcA decarboxylase (UGD) in the endoplasmic reticulum (ER) and Golgi apparatus (Table 1). Moriarity *et al.* however, demonstrated that the rat UGD is localized primarily to the perinuclear Golgi (6). Recently, several groups individually reported the identification and cloning of the *ugdh* gene, *sugarless* in *Drosophila melanogaster* (*D. melanogaster*) and *squashed vulva* (*sqv*)*-4* in *Caenorhabditis elegans* (*C. elegans*),

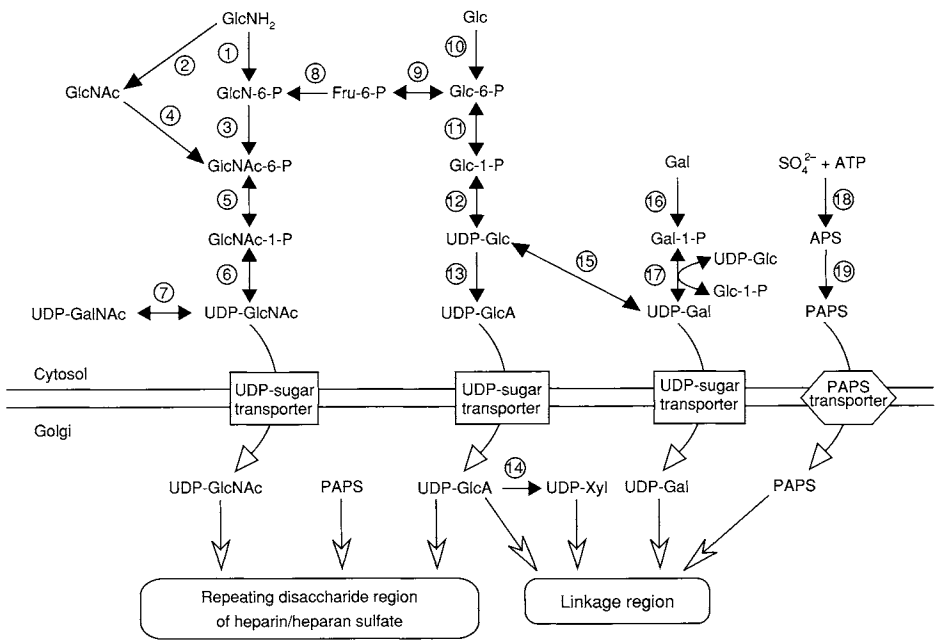

Figure 3 Biosynthetic pathways of UDP-sugars and PAPS. 1, Hexokinase; 2, $GlcNH_2$ acetyltransferase; 3, $GlcNH_2$ 6-phosphate *N*-acetyltransferase; 4, GlcNAc kinase; 5, GlcNAc phosphomutase; 6, UDP-GlcNAc pyrophosphorylase: 7, UDP-GalNAc 4-epimerase; 8, Glutamine-fructose-6-phosphate aminotransferase; 9, Glc-6-phosphate isomerase; 10, Hexokinase; 11, Phosphoglucomutase; 12, UDP-Glc pyrophosphorylase; 13, UDP-Glc dehydrogenase; 14, UDP-GlcA decarboxylase; 15, UDP-Glc 4-epimerase; 16, Galactokinase; 17, Gal-1-phosphate uridylyltransferase; 18, ATP sulfurylase; 19, APS kinase.

Table 1 Human Uridine Diphosphate-Sugars and 3′-Phosphoadenosine 5′-Phosphosulfate Synthases

Name	Abbreviation	Product	Chromosomal location	Amino acid	mRNA expression	mRNA accession
UDP-GlcNAc pyrophosphorylase	UAP1	UDP-GlcNAc	1q23.2	505	Testis, placenta, muscle, liver	NM_003115
Gal-1-phosphate uridylyltransferase	GALT	UDP-Gal	9p13	379	—*	NM_000155
		UDP-Glc		(126)**		(NM_147131)
				(162)**		(NM_147132)
UDP-Glc dehydrogenase	UGDH	UDP-GlcA	4p15.1	494	Ubiquitous	NM_003359
UDP-GlcA decarboxylase (UDP-Xyl synthase)	UGD (UXS1)	UDP-Xyl	2q12.2	420	Ubiquitous	NM_025076
PAPS synthase	PAPSS1	PAPS	4q24	624	Ubiquitous	NM_005443
	PAPSS2		10q23-q24	614	Ubiquitous	NM_004670

—*, not reported.
**, variant form.

both of which produce UDP-GlcA required for the synthesis of HS and chondroitin sulfate (CS) or chondroitin (7–12). These studies of the *sugarless* mutant led to the findings that HS side chains attached to the core proteins are required for signal transduction of Wingless (Wg) and fibroblast growth factor (FGF). These findings are brought about by a defect of HS, but not CS, the synthesis of which also requires UDP-GlcA. On the other hand, the *sqv-4* mutant shows defects in the formation of the vulva and cytokinesis in *C. elegans*. In addition, *sqv-1* encoding UGD was necessary for the morphogenesis (13). It was not clear, however, which type of GAG, chondroitin or HS, was essential for vulval morphogenesis. Recently, Hwang *et al.* and our group independently reported that chondroitin, but not HS, is necessary for cytokinesis and formation of the vulva (14,15). Furthermore, the genes homologous to *jekyll* and *uxs1* that encode UGDH and UGD, respectively, in zebrafish, were reported as requirements for the formation of a cardiac valve and cartilage, respectively (16,17). Also in mice, the mutation of *ugdh*, *lazy mesoderm*, resulted in defects in the migration of mesoderm and endoderm as in the FGF mutants (18).

UDP-sugars synthesized in the cytosol, except for UDP-Xyl, are incorporated into the ER and Golgi lumen through the nucleotide sugar transporters (NSTs) (Fig. 3 and Table 2), which are predicted to contain 6–10 membrane-spanning domains based on hydrophobicity analyses and secondary structure predictions (19,20). The NST genes are found not only in mammals but also in *C. elegans* and

Table 2 Human Uridine Diphosphate-Sugars, 3′-Phosphoadenosine 5′-Phosphosulfate and Sulfate Transporters

Name	Abbreviation	Substrate	Chromosomal location	Amino acid	mRNA expression	mRNA accession
Fringe connection	hfrc1 (UGTrel8)	UDP-GlcNAc UDP-Glc	9q22.32	337	Colon, stomach, lung, leukocyte	NM_007001
UDP-GlcA/ UDP-GalNAc dual transporter	UGTrel7	UDP-GalNAc UDP-GlcA	1p32-p31	355	Ubiquitous	NM_015139
UDP-GlcNAc transporter	UGTrel2	UDP-GlcNAc	1p21	325	Ubiquitous	NM_012243
UDP-Gal transporter	UGT	UDP-Gal UDP-GalNAc	Xp11.23-p11.22	396	Ubiquitous	NM_005660
UDP-Gal transporter-related isozyme 1	UGTrel1	—*	17q21.33	322	—	NM_005827
PAPS transporter	PAPST1 (UGTrel4)	PAPS	6p12.1-p11.2	432	Ubiquitous	NM_178148
Diastrophic dysplasia sulfate transporter	DTDST	Sulfate anion	5q31-q34	739	Ubiquitous	NM_000112

—* not reported.

D. melanogaster, *sqv*-7 and *fringe connection (frc)*, respectively (13, 21–23). SQV-7 translocates UDP-GlcA, UDP-GalNAc, and UDP-Gal *in vitro*. The *sqv-7* mutant perturbs vulval invagination due to a lack of chondroitin. On the other hand, the *frc* mutant displays defects in the signaling of Wg, Hedgehog (Hh), FGF, and Notch. Thus, the enzymes responsible for the biosynthesis of UDP-sugars and NSTs are required not only for the biosynthesis of GAG chains but also for the morphogenesis in early development.

B. 3′-Phosphoadenosine 5′-Phosphosulfate

The sulfation of HP and HS is indispensable for the exertion of their physiological functions. Sulfotransferases, which catalyze the transfer of sulfate from the donor substrate, 3′-phosphoadenosine 5′-phosphosulfate (PAPS), to respective acceptor substrates, have the structural motifs of PAPS-binding sites (24). PAPS is synthesized from inorganic sulfate, which is incorporated into the cytosol through the

sulfate transporter, and adenosine triphosphate (ATP). This reaction occurs in two sequential steps as shown in Fig. 3 (25,26). In the first step, inorganic sulfate reacts with ATP to form adenosine 5′-phosphosulfate (APS) and pyrophosphate by ATP sulfurylase. The second step is the reaction of APS with ATP, which is catalyzed by APS kinase, to form both PAPS and ADP. ATP sulfurylase and APS kinase have been cloned from bacteria, fungi, yeast, and plants, whereas in animals these enzymes are combined and referred to as PAPS synthase (PAPSS), which is composed of the N-terminal APS kinase domain and the C-terminal ATP sulfurylase domain. In humans, the bifunctional PAPSS has been identified as two different isozymes, PAPSS1 and 2 (Table 1). Although PAPSS1 mRNA is expressed in all tissues, the levels of expression are lower in the liver, skeletal muscle, and adrenal gland than in the other tissues. PAPSS2, in contrast, has high levels of expression in cartilage, liver, and adrenal gland. Murine brachymorphism is characterized by a dome-shaped skull, a short thick tail and shortened but not widened limbs and has been attributed to a defective PAPSS2 (27). In humans, spondyloepimetaphyseal dysplasia of Pakistani type that is characterized by short, bowed lower limbs, enlarged knee joints, kyphoscoliosis, a mild generalized brachydactyly and early-onset degenerative joint disease in the hands and knees, also involves a mutation in PAPSS2 but not PAPSS1 (28). In fact, PSPSS1 plays a role in human high endothelial venules for the sulfation of mucin-like glycoproteins, such as GlyCAM-1, CD34, and MAdCAM-1 (29). Furthermore, diastrophic dysplasia (DTD) including atelosteogenesis type 2 and achondrogenesis 1B is an autosomal recessive osteochondrodysplasia that comprises disorders of the skeletal system caused by defects in the DTD sulfate transporter (DTDST) gene (30–32).

Since the sulfation of GAGs occurs in the ER and Golgi apparatus, PAPS formed in the cytosol must be translocated into the Golgi by a specific transporter: the PAPS transporter (PAPST) (Fig. 3). Recently, two groups reported the identification and cloning of the human and *D. melanogaster* PAPST gene (33,34) (Table 2). Human PAPST1 is ubiquitously expressed and localized to the Golgi apparatus but not ER. The *D. melanogaster* PAPST gene mutant, *slalom*, exhibits defects in the Wg and Hh signaling pathways because of a lack of GAG sulfation. These findings suggest that the sulfation of GAG chains might be involved in the early development and onset of diseases involving cartilage and bone metabolism.

III. Biosynthesis of Heparin and Heparan Sulfate Backbones

A. Glycosaminoglycan-Protein Linkage Region

HP and HS chains in addition to CS and dermatan sulfate (DS) contain the common GAG-protein linkage tetrasaccharide, GlcAβ1-3Galβ1-3Galβ1-4Xylβ1-*O*-Ser. After the translation of a core protein, xylosylation of a Ser residue of the core protein is initiated by xylosyltransferase (XylT) in the ER and the *cis*-Golgi (35,36). XylT catalyzes the transfer of a Xyl residue through a β-linkage from UDP-Xyl to a Ser residue in the core protein substrates (Fig. 4), the amino acid sequences of which are conserved as Ser-Gly-X-Gly (where Gly and X stand for

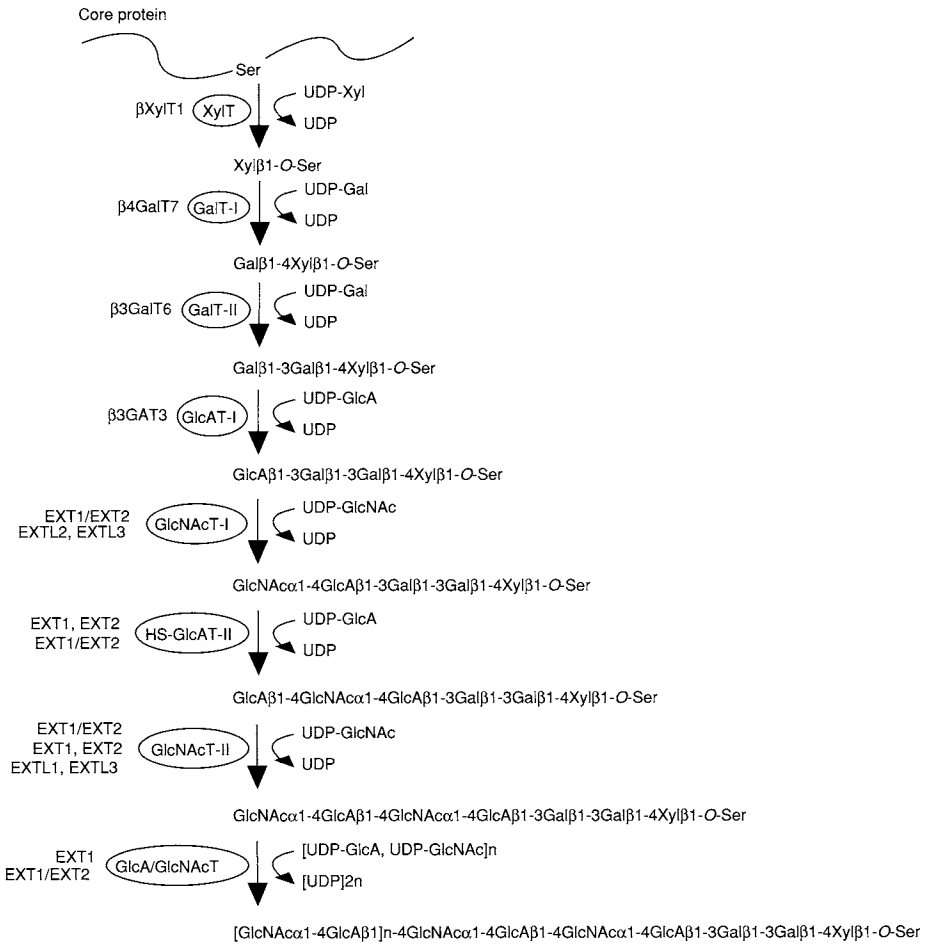

Figure 4 Schema of the assembly of the HP/HS backbones by various glycosyltransferases. Each enzyme shown in an oval requires UDP-sugar as a donor substrate, and then transfers a sugar residue to the nonreducing terminal sugar of an acceptor substrate. The genes encoding respective glycosyltransferases are given next to the enzymes. EXT1/EXT2 indicates a heterodimeric complex. XylT, xylsyltransferase; GlaT-I, galactosyltransferase-I; GlaT-II, galactosyltransferase-II; GlcAT-I, glucuronyltransferase-I; GlcNAcT-I, *N*-acetylglucosaminyltransferase-I; GlcNAcT-II, *N*-acetylglucosaminyltransferase-II; HS-GlcAT-II, HS-glucuronyltransferase-II; GlcA/GlcNAcT, GlcA and GlcNAc transferase.

glycine and any amino acid, respectively) as revealed by comparison with the GAG attachment sites in the core proteins (37). In human and rat, two different β-XylTs have been cloned (38) (Table 3). Human XylT-1 and XylT-2 are 55% identical to each other in the amino acid sequence. XylT-1 can transfer a Xyl residue from UDP-Xyl to the recombinant bikunin and its peptide *in vitro*, whereas the catalytic activity of XylT-2 has not been shown. Thus, the biological role of XylT-2 remains unclear.

Table 3 Human Linkage Region Glycosyltransferases

Name	Abbreviation	Chromosomal location	Amino acid	mRNA expression	mRNA accession
Xyl transferase	XylT-1	16p12	959	Ubiquitous	NM_022166
	XylT-2	17q21.3-17q22	865	Ubiquitous	NM_022167
Gal transferase-I (β1-4Gal transferase-7)	GalT-I (β4GalT7)	5q35.2-q35.3	327	Ubiquitous	NM_007255
Gal transferase-II (β1-3Gal transferase-6)	GalT-II (β3GalT6)	1p36.33	329	Ubiquitous	NM_080605
GlcA transferase-I (β1-3GlcA transferase-3)	GlcAT-I (β3GAT3)	11q12.3	335	Ubiquitous	NM_012200

Subsequently, two Gals are attached to the Xyl residue by galactosyltransferases-I and galactosyltransferases-II (GalT-I, GalT-II) (Fig. 4). GalT-I (β4GalT7) is one of the seven β1-4GalT family members, which appear to have exclusive specificity for the donor substrate UDP-Gal; all transfer Gal through a β1-4 linkage to similar acceptor sugars: GlcNAc, Glc, and Xyl (39, 40). To confirm that this gene product is involved in the biosynthesis of GAG *in vivo*, Chinese hamster ovary (CHO) mutant cells, pgsB-761 that lack GalT-I, were transfected with GalT-I (β4GalT7) (39). The ability to synthesize GAG was restored to the transfectant cells, suggesting that β4GalT7 actually encodes GalT-I *in vivo*. On the other hand, GalT-II (β3GalT6), which transfers Gal from UDP-Gal to a β-linked Gal residue, is one of the six β1-3GalT family members (41). Silencing of the gene β3GalT6 by siRNA blocks the assembly of GAG *in vivo*, ascertaining the identification of β3GalT6 as GAG GalT-II (41).

Finally, the linkage region is completed by the transfer of a GlcA through a β1-3 linkage from UDP-GlcA to Galβ1-3Galβ1-4Xylβ1-*O*-Ser (Fig. 4), which is catalyzed by glucuronyltransferase-I (GlcAT-I) (Table 3) (42,43). GlcAT-I was the first member cloned by PCR using degenerate primers derived from the conserved domain sequences of GlcAT-P (44), which is required for the addition of GlcA to a terminal Galβ1-4GlcNAc-sequence of glycoprotein oligosaccharides and can produce the precursor antigen, GlcAβ1-3Galβ1-4GlcNAcβ1-R, for human natural killer cell carbohydrate antigen-1 (HNK-1). Both GlcAT-I and GlcAT-P are β1-3GlcAT family members along with GlcAT-S (45,46). The transcript of the GlcAT-I gene is broadly expressed in human tissues (47,48), consistent with the ubiquitous distribution of GAGs. On the other hand, GlcAT-P is markedly expressed in the brain (44), corresponding to the expression of the HNK-1 epitope. Remarkably, overexpression of GlcAT-I in COS-1 cells, which do not intrinsically express the HNK-1 epitope, renders the cells capable of synthesizing the HNK-1 epitope as in GlcAT-P transfectants (43). Conversely, overexpression of GlcAT-P in CHO mutant cells lacking endogenous GlcAT-I activity restores the ability to synthesize GAG chains (47). Conceivably, the functions of GlcAT-I and GlcAT-P may be partially redundant in some tissues. Human GlcAT-I is the first GAG glycosyltransferase crystalized (2,3). The crystal structure of GlcAT-I has provided insights

into not only the mechanisms for recognition of their specific substrates and cofactors but also catalytic mechanisms for these reactions.

Mutations of the GalT-I gene cause a progeroidal appearance and symptoms of Ehlers–Danlos syndrome (40,49). Fibroblasts derived from patients with this syndrome synthesize PG core proteins, which are devoid of GAGs (50). In addition, the wild-type GalT-I localizes to the Golgi apparatus, whereas the mutant GalT-I localizes to the cytoplasm (49). Until now, there has been no report that other glycosyltransferases involved in the synthesis of the linkage region are responsible for a progeroid variant of Ehlers–Danlos syndrome. *C. elegans* and *D. melanogaster* have the linkage region tetrasaccharide as in the case of mammalian GAGs (51). The worms have mutations in the genes *sqv-6*, *-3*, *-2*, and *-8* encoding the glycosyltransferases, XylT, GalT-I, GalT-II, and GlcAT-I, respectively (39,52–54). Since these enzymes are required for the biosynthesis of GAG chains, these mutants show reduced synthesis of both HS and chondroitin. The mutant phenotypes show that GAGs play a role in the early developmental stage in *C. elegans*. In addition, *D. melanogaster* also have these glycosyltransferases (41,55–58). *Drosophila* XylT, GalT-I, and GlcAT-I act on the respective acceptor substrates (55–58). Functions of GalT-I have been demonstrated in *D. melanogaster* using the RNA interferance (RNAi) technique, where double-strand RNA (dsRNA) of the target gene sequence is used to suppress the gene expression. In *GalT-I* RNAi-treated flies, the synthesis of both types of GAGs, HS, and CS, is impaired, and the wing and leg morphology is similar to that of flies defective in Hh and Decapentaplegic (Dpp) signaling (56), which needs PGs (59–61). Thus, GAGs are essential for morphogenesis and organogenesis in the regulation of signaling molecules.

B. Modifications of the Glycosaminoglycan-Protein Linkage Region

Several modifications of the GAG-protein linkage region have been reported. 2-*O*-Phosphorylated Xyl has been found in both HP/HS (51,62–64) and CS (51,64–67) from various species. 4-*O*-sulfated and/or 6-*O*-sulfated Gal residues have so far been isolated in CS/DS (64,68–73), but not in HP/HS. Crucial evidence for the selective sulfation of Gal residues in only CS chains has been provided (64). The sulfation of the Gal residue of the linkage region in Syndecan-1 that has both CS and HS chains on the same core protein is observed in CS, but not HS. These observations indicate that the sulfated Gal residues may be sorting signals involved in the biosynthesis or in the intracellular transport of CS/DS, or key factors that control the acceptor activity of the linkage region oligosaccharides for glycosyltransferases involved in the formation of the linkage region. In this regard, it is interesting that α1-4*N*-acetylglucosaminyltransferase-I (GlcNAcT-I), the key enzyme for HP/HS synthesis that also has α1-4*N*-acetylgalactosaminyltransferase (α-GalNAcT) activity towards the linkage region tetrasaccharide, was inhibited by the sulfated Gal residue (74,75). On the other hand, the C-6 sulfation of the nonreducing terminal Gal residue in the linkage region improves the substrate for recombinant GlcAT-I (76). The recombinant GalT-I shows no activity towards the

acceptor substrate containing a C-2 phosphorylated Xyl (76). Whereas the linkage trisaccharide with the phosphorylated Xyl is one of the best acceptors for recombinant GlcAT-I *in vitro* (Tone Y, Pedersen L, Yamamoto T, Kitagawa H, Nishihara J, Tamura J, Darden TA, Negishi M, Sugahara K unpublished data). These observations suggest that the phosphorylation of the Xyl residue may occur after the transfer of the first Gal residue, and stimulate the biosynthesis of GAG by GlcAT-I. The specific kinase, phosphatase, and sulfotransferases that modify the Xyl and Gal residues in the linkage region have not been identified. Thus, the function of these modifications remain to be investigated.

C. Repeating Disaccharide Region

Chain polymerization of the repeating disaccharide region in HP and HS is evoked by the transfer of the αGlcNAc residue from UDP-GlcNAc to the linkage region tetrasaccharide, which is mediated by GlcNAcT-I (Fig. 4). On the other hand, the addition of β1-4-linked GalNAc to the linkage region by β1-4*N*-acetylgalactosaminyltransferase-I (GalNAcT-I) initiates the formation of the repeating disaccharide region of CS and DS chains (77). GlcNAcT-I is encoded by the *exostosin like*-genes 2 and 3 (*EXTL2* and *EXTL3*) (78,79). Three *EXTL* genes are homologous to the tumor suppressors, *exostosins* (*EXTs*), which are associated with hereditary multiple exostoses (HME) and encode HS polymerases (see below) (80). EXTL2 protein is an *N*-acetylhexoaminyltransferase that transfers not only GlcNAc but also GalNAc to the linkage region through an α1-4-linkage (78). The αGalNAcT activity of the recombinant human EXTL2 is much stronger than the GlcNAcT activity. No structure containing α1-4GalNAc, however, has been isolated from any naturally occurring GAG chains. EXTL2 was the first member of the *EXT* gene family to be crystalized, as a ternary complex with UDP and the acceptor substrate, providing important insights into the mechanisms of α1-4*N*-acetylhexoaminyl transfer in the biosynthesis of HS (81). EXTL3 can transfer αGlcNAc to the linkage region, apparently more efficiently than EXTL2 (79). After the attachment of the first αGlcNAc, the resultant nascent pentasaccharide is elongated further by alternate additions of βGlcA and αGlcNAc from UDP-GlcA and UDP-GlcNAc, which are catalyzed by HS-β1-4glucuronyltransferase-II (HS-GlcAT-II) and α1-4*N*-acetylglucosaminyltransferase-II (GlcNAcT-II), respectively (Fig. 4). EXTL1 and EXTL3 but not EXTL2 have GlcNAcT-II activity (78,79) (Table 4). Furthermore, EXT1 and EXT2 have both HS-GlcAT-II and GlcNAcT-II activities (82,83) (Fig. 4). Two independent studies revealed a relation between HS-synthesizing glycosyltransferases and the HME genes (*EXT1* and *EXT2*) (80,84).

Firstly, McCormick *et al.* screened for cDNAs capable of restoring sensitivity to herpes simplex virus (HSV) in HS-deficient and HSV-resistant sog9 cells. A single cDNA, the putative tumor suppressor *EXT1*, was isolated, which sufficiently restored the ability to synthesize HS in the sog9 cell line, thereby rescuing the HSV infectivity (85). Human EXT1 protein has a type II transmembrane topology and consists of 746 amino acids. Overexpression of *EXT1* in sog9 cells induced a slight yet significant increase in both HS-GlcAT-II and GlcNAcT-II activities (86). Secondly, Lind *et al.*

Table 4 Human Heparin/Heparan Sulfate Glycosyltransferases, Sulfotransferases, Epimerase, Sulfatases, and Heparanases

Name	Abbreviation	Chromosoma location	Amino acid	mRNA expression	mRNA accession
GlcA/GlcNAc transferase	EXT1	8q24.11-q24.13	746	Ubiquitous	NM_000127
	EXT2	11p12-p11	718	Ubiquitous	NM_000401
GlcNAc transferase-I	GlcNAcT-I (EXTL2)	1p21	330	Ubiquitous	NM_001439
GlcNAc transferase-II	GlcNAcT-II (EXTL1)	1p36.1	676	Skeletal muscle, brain, heart	NM_004455
GlcNAc transferase-I/II	GlcNAcT-I/II (EXTL3)	8p21	919	Ubiquitous	NM_001440
GlcNAc *N*-deacetylase/ *N*-sulfotransferase	NDST-1	5q33.1	882	Ubiquitous	NM_001543
	NDST-2	10q22	883	Ubiquitous	NM_003635
	NDST-3	4q26	873	Brain, kidney, liver	NM_004784
	NDST-4	4q25-q26	872	—*	NM_022569
GlcA C5-epimerase	Hsepi (GLCE)	15q23	618	Ubiquitous	NM_015554
HS 2-*O*-sulfotransferase	HS2ST	1p31.1-p22.1	356	Ubiquitous	NM_012262
HS 6-*O*-sulfotransferase	HS6ST-1	2q21	401	Ubiquitous	NM_004807
	HS6ST-2	Xq26.2	499	Brain	NM_147174
	HS6ST-2S	Xq26.2	459	Ovary, placenta, fetal kidney	NM_147175
	HS6ST-3	13q32.1	471	—	NM_153456
HS 3-*O*-sulfotransferase	HS3ST-1	4p16	307	Kidney, brain, heart, lung	NM_005114
	HS3ST-2	16p12	367	Brain	NM_006043
	HS3ST-3A	17p12-p11.2	406	Ubiquitous	NM_006042
	HS3ST-3B	17p12-p11.2	390	Ubiquitous	NM_006041
	HS3ST-4	16p11.2	456	Brain	NM_006040
	HS3ST-5	6q22.31	346	Skeletal muscle	NM_153612
	HS3ST-6	16p13.3	311	—	NM_001009606

(*Continued*)

Table 4 *Cont'd*

Name	Abbreviation	Chromosoma location	Amino acid	mRNA expression	mRNA accession
Sulfatase	Sulf-1	8q13.2-q13.3	871	Testis, stomach, skeletal muscle, lung, kidney	NM_015170
	Sulf-2	20q12-q13.2	870 (852)**	Ovary, skeletal muscle, stomach, brain, uterus, heart, kidney, placenta	NM_018837 (NM_198596)
Heparanase	HPSE-1	4q21.3	543	Ubiquitous,	NM_006665
	HPSE-2	10q23-q24	592	Brain, mammary gland, prostate, small intestine, testis, uterus	NM_021828

—*, not reported.
**, variant form.

identified a HS-polymerase, EXT2, by direct peptide sequencing of that purified from bovine serum (86). The bovine EXT2 has a type II transmembrane protein composed of 718 amino acids. The recombinant bovine EXT2 showed both HS-GlcAT-II and GlcNAcT-II activities toward GlcNAc–$[GlcA-GlcNAc]_n$ and $[GlcA-GlcNAc]_n$ oligosaccharide acceptors, respectively.

EXT1 and EXT2 form a hetero-dimeric complex *in vivo*, which leads to the deposition of both proteins in the Golgi apparatus (82,87), although overexpressed EXT1 or EXT2 alone is localized predominantly in the ER (82). The two proteins expressed together exhibit a much higher level of glycosyltransferase activity than the individually expressed proteins (82,83). Recently, we demonstrated that the soluble form of the recombinant EXT1/EXT2 hetero-dimeric complex can synthesize HS polymer chains on various linkage region tetrasaccharide acceptors *in vitro* (88). Likewise, Busse and Kusche-Gullberg reported that recombinant EXT1 alone and the EXT1/EXT2 hetero-dimeric complex catalyze the *in vitro* polymerization of the HS backbone structure on oligosaccharide acceptors (89). These findings explain why mutations in either one can cause HME with very similar clinical pathologies despite the existence of the two HS-polymerases, and suggest that they cannot compensate for each other's loss.

HME is an autosomal dominantly inherited genetic disorder that affects Caucasian populations with an estimated occurrence of 1 in 50,000–100,000. It is characterized by cartilage-capped tumors (exostoses) that develop from the growth plate of endochondral bones, especially of long bones (90). This pathologic feature leads to skeletal abnormalities and a short stature. Malignant transformation from exostoses to chondrosarcomas (91,92) or osteosarcomas (93,94) occurs in approximately 2% of HME patients as a result of loss of heterozygosity in *EXT1* or *EXT2*. Genetic linkage analysis of HME has identified three different loci, 8q24.1, 11p11–13, and 19p, which include *EXT1*, *EXT2*, and *EXT3*, respectively (95–97). In most HME cases, missense or frameshift mutations in *EXT1* and *EXT2* have been identified, although an association of *EXT3* with HME has not been shown (80).

Mice with a targeted disruption of the gene encoding *EXT1* die by embryonic day 8.5–14.5 due to defects in mesoderm formation and a failure of egg cylinder elongation (98–100). $EXT1^{-/-}$ mice show remarkable decreases in GlcA and GlcNAc transferase activities and a complete lack or shortening of HS chains (98,100). Koziel *et al.* suggested that reduced amounts of HS potentiate the signaling of Indian hedgehog (Ihh) and parathyroid hormone-related peptide (PTHrP) in $EXT1^{-/-}$ mice, resulting in delayed hypertrophic differentiation and increased chondrocyte proliferation, and HME patients similarly have clusters of overproliferating chondrocytes (99). Furthermore, Inatani *et al.* generated *EXT1*-null mice in which the *EXT1* gene was selectively disrupted in the central nervous system resulting in serious errors in midline axon guidance through Slit, Sonic hedgehog (Shh) and FGF signalings (101). EXT2 homozygous null mice also failed to develop at the gastrulation stage (102). *EXT1* or *EXT2* heterozygous mice develop exostoses at low frequency. On the other hand, combined heterozygotes ($EXT1^{+/-}EXT2^{+/-}$) show a higher frequency of exostoses (102).

HS is present in genetically tractable model animals as well (51, 103–106), and EXT genes are well conserved in humans, zebrafish (*Danio rerio*) (*ext1*, *ext2/dackel*,

extl3/boxer), *D. melanogaster* (*ttv*, *sotv*, *botv*), and *C. elegans* (*rib-1*, *rib-2*) (107–117) (Fig. 5 and Table 5). Among these genes, *in vitro* glycosyltransferase activities have

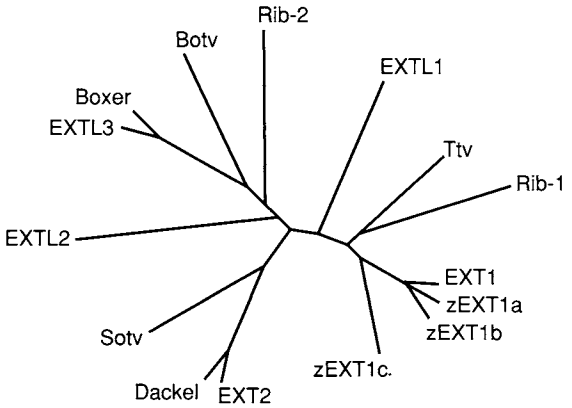

Figure 5 The phylogenetic tree of known EXT family members among *Homo sapiens* (EXT1, EXT2, EXTL1, EXTL2, and EXTL3), *Danio rerio* (zEXT1a, zEXT1b, zEXT1c, Dackel, and Boxer), *D. melanogaster* (Ttv, Sotv, and Botv) and *C. elegans* (Rib-1 and Rib-2). Whole amino acid sequences were used for the ClustalW algorithm.

Table 5 The Model Organisms with the Loss-of-functions or Gain-of-functions Caused by Mutations of the Genes Encoding the Biosynthetic Enzymes of Heparin/Heparan Sulfate, Heparan Sulfate-Proteoglycan Core Proteins and Related Enzymes

Affected genes	Encoded enzymes	Phenotypes	Reference
C. elegans			
sqv-1	UDP-GlcA decarboxylase	Defects in cytokinesis and vulval morphogenesis	13
sqv-2	GalT-II	Defects in cytokinesis and vulval morphogenesis	52
sqv-3	GalT-I	Defects in cytokinesis and vulval morphogenesis	39,54
sqv-4	UDP-Glc dehydrogenase	Defects in cytokinesis and vulval morphogenesis	12
sqv-5	ChSy-1	Defects in cytokinesis and vulval morphogenesis	14,15
sqv-6	XylT	Defects in cytokinesis and vulval morphogenesis	52
sqv-7	UDP-GlcA, UDP-GalNAc, UDP-Gal transporter	Defects in cytokinesis and vulval morphogenesis	13,21
sqv-8	GlcAT-I	Defects in cytokinesis and vulval morphogenesis	54
rib-1	EXT1	—*	115
rib-2	EXTL3	Developmental abnormalities at embryonic stage	116,117

(*Continued*)

Table 5 *Cont'd*

Affected genes	Encoded enzymes	Phenotypes	Reference
hst-1	NDST	Abnormal	118
hst-2	HS2ST	Abnormal axon branching	119,120
hst-3	HS3ST	—	121
hst-6	HS6ST	Suppression of kal-1-dependent axon-branching phenotype	119,122
hse-5	HS GlcA C5-epimerase	Abnormal axon branching	119
srf-3	UDP-Gal, UDP-GlcNAc transporter	Alteration of surface antigenicity and inhibition of bacterial adherence	123,124
unc-52	Perlecan	Defects in the formation or maintenance of the muscle myofilament lattice, affects the regulation of distal tip cell migration	125,126
sdn-1	Syndecan	Defects in vulval morphogenesis	127
agrin	Agrin	Embryonic lethality	128
D. melanogaster			
sugarless	UDP-Glc dehydrogenase	Defects in Wg, FGF signaling	7–10
frc	UDP-sugar transporter	Defects in Wg, Hh, FGF, Notch signaling	22,23
DmUGT	UDP-Gal, UDP-GalNAc transporter	—	129
DmPAPSS	PAPS synthase	—	130
slalom	PAPS transporter	Defects in Wg, Hh signaling	33,34
oxt	XylT	—	55
beta4GalT7	GalT-I	Abnormal wing and leg morphology similar to flies with defective Hh and Dpp signaling	56,57
DmGlcAT-I	GlcAT-I	—	58
ttv	EXT1	Defects in Hh, Wg, Dpp signaling	109–113
sotv	EXT2	Defects in Hh, Wg, Dpp signaling	111–113
botv	EXTL3	Defects in Hh, Wg, Dpp signaling	111–114
sulfateless	NDST	Defects in Wg, FGF signaling	10,131
pipe	HS2ST	Defects in the formation of embryonic dorsal–ventral polarity	132
dHS2ST	HS2ST	—	133
dHS3ST-A	HS3ST	—	134
dHS3ST-B	HS3ST	Defects in Notch signaling	134
dHS6ST	HS6ST	Defects in FGF signaling	135
dally	Glypican	Defects in Wg, Dpp, Hh signaling	131,136–143

(*Continued*)

Table 5 *Cont'd*

Affected genes	Encoded enzymes	Phenotypes	Reference
dally-like	Glypican	Defects in Wg, Hh signaling	143–148
troll	Perlecan	Defects in neuroblast proliferation in the CNS	149
dSyndecan	Syndecan	Interaction with Slit-Robo pathway	150,151
Zebrafish (Danio rerio)			
jekyll	UDP-Glc dehydrogenase	Defects in cardiac valve formation	16
uxs1	UDP-GlcA decarboxylase	Defective cartilage unstained with alcian blue	17
b4galt7	GalT-I	Defective cartilage unstained with alcian blue	152
b3gat3	GlcAT-I	Defective branchial arches and jaw	17
ext1	EXT1	—	107
dackel	EXT2	Defects in optic tract sorting	108
boxer	EXTL3	Defects in optic tract sorting	108
zHS6ST	HS6ST	Defects in muscle differentiation	106
knypek	Glypican	Defects in Wnt signaling	153
syndecan-2	Syndecan-2	Defects in angiogenesis	154
Mouse			
lazme (lazy mesoderm)	UDP-Glc dehydrogenase	Defects in FGF signaling	18
brachymorphic mouse	PAPS synthase 2	Dome-shaped skull, shortened but not widened limbs, short tail	27
DTDST$^{-/-}$	DTDST	Growth retardation, skeletal dysplasia, joint contractures	155
EXT1$^{-/-}$	EXT1	Disruption of gastrulation	98–100
EXT1$^{-/-}$ *(specific for brain)*	EXT1	Defects in the midbrain-hindbrain region, disturbed Wnt-1 distribution	101
EXT2$^{-/-}$	EXT2	Disruption of gastrulation	102
EXT1$^{+/-}$/ *EXT2*$^{+/-}$	EXT1/EXT2	Exostoses	102
EXT2 transgenic mice	EXT2	Upregulation of the formation of trabeculae	156
NDST-1$^{-/-}$	NDST-1	Neonatal lethality due to respiration defects	157–160
NDST-2$^{-/-}$	NDST-2	Loss of heparin, abnormal mast cell	161,162
NDST-1$^{-/-}$/ *NDST-2*$^{-/-}$	NDST-1/NDST-2	Embryonic lethality	159
NDST-3$^{-/-}$	NDST-3	Disortion of the Mendelian distribution	159
HS2ST$^{-/-}$	HS2ST	Renal agenesis, defects in the eye and the skeleton	163–165

(*Continued*)

Table 5 *Cont'd*

Affected genes	Encoded enzymes	Phenotypes	Reference
HS3ST-1$^{-/-}$	HS3ST-1	Genetic background-specific lethality, intrauterine growth retardation	166
Hsepi$^{-/-}$	Hsepi	Neonatal lethality with renal agenesis, lung defects, skeletal malformation	167
Heparanase transgenic mice	Heparanase	Reductions of food consumption and body weight, enhancement of vascularization, and renal failure	168
Syndecan-1$^{-/-}$	Syndecan-1	Defects in the repair of skin and corneal wounds, low susceptibility to Wnt-1 signaling	169,170
Syndecan-3$^{-/-}$	Syndecan-3	Reduction of reflex hyperphagia following food deprivation	171
Syndecan-4$^{-/-}$	Syndecan-4	Impairment of focal adhesion under restricted conditions	172
Gpypican-2$^{-/-}$	Glypican-2	No phenotypes	59
Gpypican-3$^{-/-}$	Glypican-3	Developmental overgrowth typical of human Simpson–Golabi–Behmel syndrome	173
Perlecan$^{-/-}$	Perlecan	Defective cephalic development	174,175
Agrin$^{-/-}$	Agrin	Perinatal lethality owing to breathing failure, defects of neuromuscular synaptogenesis	176
Serglycin$^{-/-}$	Serglycin	Disruption of protease storage in mast cells	177
Human			
Spondylo-epimetaphyseal dysplasia	PAPS synthase 2	Short, bowed lower limbs, enlarged knee joints, kyphoscoliosis, a mild generalized brachydactyly	28
Achondrogenesis type 1B	DTDST	Autosomal recessive, lethal chondrodysplasia with severe underdevelopment of skeleton, extreme micromelia, and death before or immediately after birth	30–32
Ehlers–Danlos syndrome	GalT-I	Aged appearance, developmental delay, dwarfism, craniofacial disproportion, and generalized osteopenia	49,50

(*Continued*)

Table 5 *Cont'd*

Affected genes	Encoded enzymes	Phenotypes	Reference
Hereditary multiple exostoses	EXT1 EXT2	An autosomal dominant disorder characterized by the formation of cartilage-capped tumors (exostoses) that develop from the growth plate of endochondral bones, especially of long bones	80,84

—*, not reported.

been demonstrated only for Botv and Rib-2, both of which have GlcNAcT-I and -II activities (114,116). In zebrafish *dackel* and *boxer* mutants that are defective in *ext2* and *extl3*, respectively, some dorsal retinal ganglion cell axons inappropriately project into the optic tract (108,178). HS was drastically reduced in *dackel* and *boxer*, suggesting that both genes are required for its production (108). On the other hand, *Drosophila* homologs of *EXT* genes, *tout-velu* (*ttv*), *sister of tout-velu* (*sotv*) and *brother of tout-velu* (*botv*) that correspond to vertebrate *EXT1*, *EXT2*, and *EXTL3*, respectively, are involved in the Hh, Wg, and Dpp signalings (109–113). Even though Ttv and Sotv have not been demonstrated to have glycosyltransferase activities, both mutant larvae show a marked reduction in HS but not CS (104,105,113). *Rib-1* and *rib-2* in *C. elegans* show the highest homology to *EXT1* and *EXTL3*, respectively, among human *EXT* genes (Fig. 5). *Rib-2* mutants exhibit anomalous features, such as a developmental delay and egg-laying defects, which are most likely caused by a reduction in HS (117). Thus, EXT1, EXT2, and EXTL3 participate not only in the biosynthesis of HS *in vivo* but also in the development of organisms, especially morphogenesis in the early stages of development. However, the functions of EXTL1 and EXTL2 *in vivo* remain unclear. These proteins might have more specialized or tissue-specific functions since they exist only in vertebrates.

IV. Modifications of the Sugar Backbones of Heparin and Heparan Sulfate

A. *N*-Deacetylation and *N*-Sulfation

N-Deacetylation and *N*-sulfation of GlcNAc residues in HP and HS are initial modifications of precursor chains and essential for all the subsequent modifications (Fig. 6) (179). Both reactions are catalyzed by bifunctional enzymes, GlcNAc *N*-deacetylase/*N*-sulfotransferases (NDSTs). Following the formation of the repeating disaccharide region of HP/HS by EXT proteins, the first modification is the hydrolytic release of acetyl-groups in GlcNAc by the *N*-deacetylase domain of NDSTs. The next step is the transfer of sulfate-groups to unsubstituted GlcN residues from PAPS by the *N*-sulfotransferase domain of NDSTs. The vertebrate NDST family is comprised of four isozymes (Table 4), but only one NDST is found

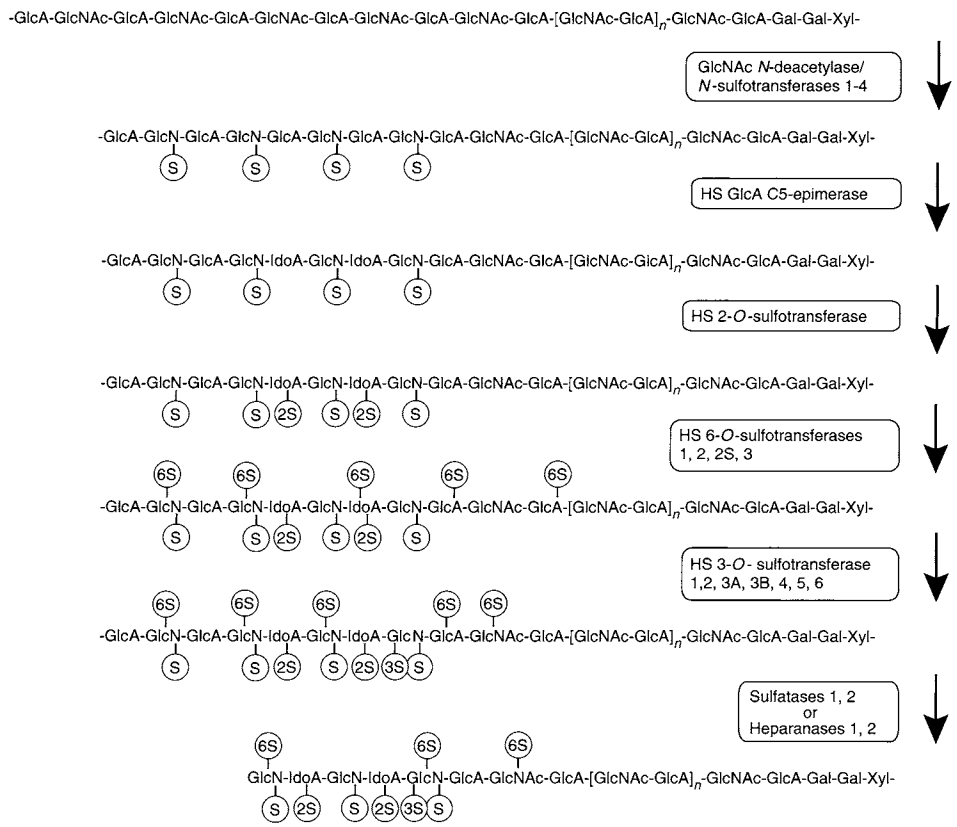

Figure 6 Pathways of biosynthetic modifications of HP and HS chains. Following synthesis of the backbone of HP or HS by HS polymerases belonging to the *EXT* gene family, modifications of the precursor HP/HS chains are conducted by various sulfotransferases and a single epimerase. The first modifications, *N*-deacetylation and *N*-sulfation, are essential for all subsequent reactions. Next, some GlcA residues adjacent to GlcNS residues are converted to IdoA residues by GlcA C5-epimerase. Thereafter, sulfation at C-2 of IdoA residues, and at C-6 and C-3 of GlcNS and/or GlcNAc residues takes place through the actions of specific sulfotransferases. The remodeling of HS through modifications by NDSTs, Hsepi, and sulfotransferases is conducted by sulfatases and heparanases. S, 2-*N*-sulfate; 2S, 2-*O*-sulfate; 3S, 3-*O*-sulfate; 6S, 6-*O*-sulfate; *n*, the number of repeating disaccharide units.

in *D. melanogaster* and *C. elegans* (Table 5). NDST-1 and NDST-2 were originally purified from rat liver and HP-producing mouse mastocytoma, respectively (180,181), and both cDNAs were then isolated based on amino acid sequences (182,183). In addition, NDST-3 and NDST-4 were cloned using the EST database (184,185). *NDST-1* and *NDST-2* are broadly expressed in mouse tissues, whereas *NDST-3* and *NDST-4* are strongly expressed in the brain and at embryonic stages in the mouse (185). Comparison of the enzymatic properties of these isozymes has revealed remarkable differences in *N*-deacetylase and *N*-sulfotransferase activities.

NDST-1 and NDST-2 have much higher levels of both, compared with the other family members. NDST-3 and NDST-4 are characterized by a high level of *N*-deacetylase and *N*-sulfotransferase activity, respectively (185).

Approximately two thirds of *NDST-1*-deficient mouse embryos (*NDST*-$1^{-/-}$) survive until birth, but turn cyanotic and die neonatally with a pathology similar to infant respiratory failure (157,158). The others show skull defects and a disturbed eye development (159). Intriguingly, these abnormalities resemble the mutant phenotypes of Wnt-1, Shh, Chordin and Noggin that are HS-binding morphogens or antagonists of bone morphogenetic protein (BMP) (159). Analysis of *NDST*-$1^{-/-}$ has also demonstrated that HS is involved in Ca^{2+} kinetics in skeletal muscle (160). Structural analysis of HS chains in *NDST*-$1^{-/-}$ mice has revealed significantly reduced *N*-sulfation (158,160). On the other hand, *NDST-2*-deficient mouse embryos (*NDST*-$2^{-/-}$) are viable and fertile, though their mast cells are incapable of synthesizing HP (161,162). The mast cells show changes in morphology and severely reduced amounts of granule proteases, indicating that the storage is controlled by HP. Furthermore, a double knockout (*NDST*-$1^{-/-}$/*NDST*-$2^{-/-}$) of NDST-1 and NDST-2 results in early embryonic lethality, resembling *EXT1*-null mice (159). HS chains of embryonic stem (ES) cells derived from *NDST*-$1^{-/-}$/*NDST*-$2^{-/-}$ completely lack *N*-sulfation, but synthesize 6-*O*-sulfated HS (186), suggesting that 6-*O*-sulfation as well as the generation of *N*-unsubstituted GlcN residues may occur independently of *N*-sulfation. The *Drosophila NDST* gene, *sulfateless*, is essential for Wg and FGF receptor signaling, as in the case of the *sugarless* mutant deficient in UGDH (10,131). HS chains of *sulfateless* completely lack sulfated disaccharides without an effect on the total amount (105). This finding supports the idea that *N*-deacetylation/*N*-sulfation is an early step in the modification of HS required for the subsequent epimerization and sulfation.

B. Glucuronic Acid C5-Epimerization

HP/HS glucuronyl C5-epimerase (Hsepi), which catalyzes *in vitro* the interconversion of GlcA to IdoA and/or IdoA to GlcA in HP/HS but not in CS/DS, was originally purified from bovine liver (187). Hagner-McWhirter *et al.* however, have recently shown using a cellular system that GlcA C5-epimerization is effectively irreversible *in vivo* (188). A cDNA clone encoding *Hsepi* has been isolated from bovine, mouse, human, *C. elegans*, and *D. melanogaster* (189–191). The GFP-tagged and Myc-tagged full-length Hsepi, which is predicted to have a type II transmembrane topology, localizes to the Golgi, whereas an YFP-tagged and N-terminal truncated form of Hsepi, which exhibits weak activity compared with the full-length protein, diffuses in the cytosol (191). Hsepi of a microsomal preparation acts on uronic acids in HP/HS chains when the target residues are located on the nonreducing side of GlcNS, while it does not act on *O*-sulfated uronic acids or on uronic acids on the reducing side of GlcN residues (192). These observations suggest that the GlcA C5-epimerization occurs after the *N*-deacetylation/*N*-sulfation of GlcNAc residues but before the *O*-sulfation of uronic acid (Fig. 6). It has been proposed that IdoA residues in HP/HS provide conformational flexibility to the chain, which facilitates interaction with specific proteins (193).

Targeted disruption of the mouse *Hsepi* results in an almost complete loss of IdoA residues, and alters the sulfation profile (167). The corresponding phenotype is lethal, with renal agenesis, lung defects and skeletal dysplasia as observed for *NDST*-$1^{-/-}$ mice and *HS2ST*$^{-/-}$ mice, which are deficient in HS 2-*O*-sulfotransferase (HS2ST) catalyzing the 2-*O*-sulfation of IdoA and/or GlcA (see later) (157,158,163). In addition, a *C. elegans Hsepi* (*hse-5*) mutant was isolated during the search for suppressors of the *kal-1* gain-of-function phenotype (119,178). *Kal-1* is a homolog, which is deficient in individuals with Kallmann syndrome, a neurological disorder characterized by various behavioral and neuroanatomical defects. The *hse-5* mutant shows defects in many types of axon-guidance behavior and affects Slit and Kal-1 signaling. Thus, GlcA C5-epimerization of HS is required for the subsequent modifications and also for tissue morphogenesis and the nervous system's development.

C. *O*-Sulfation

HS2ST was purified from cultured CHO cells, and the full-length cDNA has been cloned based on the amino acid sequence obtained from the purified enzyme (194,195). HS2ST catalyzes the transfer of sulfate from PAPS to the C-2 position of uronic acids in HP/HS, but the enzyme strongly favors the sulfation of IdoA (196). This observation is further supported by the finding that HS2ST and Hsepi interact with each other *in vivo* (197). A CHO mutant cell line, pgsF-17, has defects in the *HS2ST* gene (198). The HS in pgsF-17 shows a complete lack of 2-*O*-sulfation of both GlcA and IdoA, but exhibits a greater degree of *N*-sulfation and 6-*O*-sulfation of GlcN residues, suggesting that the formation and sulfation of IdoA residues are independent of 2-*O*-sulfation. Mice homozygous for the *HS2ST* gene trap allele die during the neonatal period, showing bilateral renal agenesis and defects in the eyes and skeleton (163). In addition, a significant reduction in cell proliferation, but not cell migration, in the developing cerebral cortex is brought about by the loss of 2-*O*-sulfation (164). The HS chains in *HS2ST*$^{-/-}$ mutant mice exhibit compensatory increases in *N*-sulfation and *O*-sulfation, as in the case of the CHO mutant, pgsF-17 (165). The mutant HS showed no change in affinity for hepatocyte growth factor/sccater factor or fibronectin, but a significant reduction in affinity for FGF-1 and FGF-2. Surprisingly, the *HS2ST*$^{-/-}$ cells are sufficient to allow apparently normal FGF signaling as well as hepatocyte growth factor/sccater factor signaling, suggesting that the synergism between HS and FGF-1 or FGF-2 does not always require a high affinity binding for signal transduction. *Drosophila* mutants of *pipe* that encodes a putative HS2ST, is required for the formation of embryonic dorsal–ventral polarity (132). Another putative *Drosophila HS2ST* gene, *dHS2ST*, has also been identified at the *Segregation disorter* gene locus involved in the meiotic drive system (133). On the other hand, the *C. elegans HS2ST* (*hst-2*) mutant shows not only a disturbance in the axon guidance system as observed for the *hse-5* mutant but also defects in cell migration (119,120,178). These observations indicate that 2-*O*-sulfation of HS is essential for cell migration, tissue morphogenesis, early embryonic development and the formation of the nervous system.

Heparan sulfate 6-*O*-sulfotransferase (HS6ST), which catalyzes the transfer of sulfate to the C-6 position of GlcNAc and GlcNS residues in HP/HS, was originally purified from the culture medium of CHO cells, and *HS6ST-1* cDNA was cloned on the basis of its amino acid sequence (199,200). Furthermore, two additional HS6ST isoforms in mouse, designated HS6ST-2 and HS6ST-3 (201), and a short splicing isoform of human HS6ST-2 lacking 40 amino acids encoded by exons 2 and 3, designated HS6ST-2S, have also been cloned (202) (Table 4). Mouse HS6ST-1, -2 and -3 are type II transmembrane proteins composed of 401, 506, and 470 amino acids, respectively, and the amino acid sequence of mouse HS6ST-1 is 51 and 57% identical to that of HS6ST-2 and HS6ST-3, respectively. These mouse isoforms differ in their sulfotransferase activity toward target GlcN, GlcNS, or GlcNAc residues adjacent to the uronic acids. The recombinant mouse HS6ST-1 exhibits specificity preferring an IdoA residue adjacent to the targeted GlcNS residue, whereas HS6ST-2 prefers GlcA to IdoA, and HS6ST-3 is able to transfer to both structures (201). Moreover, these HS6STs can synthesize the 6-*O*-sulfated GlcNAc that is contained in addition to a GlcNS residue in an AT-binding sequence of HP/HS (203). These mouse HS6STs are localized to the Golgi and the localization requires the stem domain of HS6ST proteins (204). Additionally, their sulfotransferase activities are greatly reduced in HS6STs lacking the stem domain. *Drosophila* HS6ST is 54, 46, and 53% identical to mouse HS6ST-1, -2, and -3, respectively (135). The *HS6ST* RNAi-treated flies showed embryonic lethality and perturbation of the primary branching of the tracheal system similar to the defects observed in fly mutants of FGF signaling components. On the other hand, the *C. elegans HS6ST* (*hst-6*) mutant showed axonal branching and misrouting depending on Kal-1 and Slit signaling (119,122). Furthermore, the knockdown of zebrafish *HS6ST* using a specific antisense morpholino oligonucleotide led to the perturbation of somatic muscle development caused by the reduction of 6-*O*-sulfation in HS (106).

Heparan sulfate 3-*O*-sulfotransferase (HS3ST), which catalyzes the transfer of sulfate to the C-3 position of GlcN residues in HP/HS, is an essential enzyme for the synthesis of the AT-binding domain in HP/HS (205). HS3ST was originally purified to homogeneity from the culture medium of the mouse L cell line, LTA (206), and its cDNA as well as the human counterpart was cloned based on the partial amino acid sequence of the purified enzyme (207). The additional six human isoforms, designated as HS3ST-2, -3A, -3B, -4, -5, and -6, have also been identified based on the sequence homologous to HS3ST-1 or HS3ST-3 (208–211) (Table 4). Human HS3ST-1 is strongly expressed in the brain, kidney, and heart. On the other hand, HS3ST-2 and HS3ST-4 are predominantly expressed in the brain, whereas HS3ST-3A and HS3ST-3B show broad expression patterns (208), and HS3ST-5 is mainly expressed in the skeletal muscle (210), suggesting that human *HS3ST* genes are differentially regulated, have distinct functional roles in tissue, and are cell type-specific. Human recombinant HS3ST-1 can act on the C-3 position of GlcNS or GlcNS(6S) adjacent to the reducing side of GlcA. On the other hand, HS3ST-2 is able to catalyze 3-*O*-sulfation of GlcNS residues in [–GlcA(2S)–GlcNS–] and [–IdoA(2S)–GlcNS–] sequences in HP/HS. Additionally, HS3ST-3 and HS3ST-6 prefer [–IdoA(2S)–GlcNS–] and [–IdoA(2S)–GlcNS(6S)–] sequences to other units, and HS3ST-5 can act on the C-3 position in [–GlcA–GlcNS(6S)–],

[–IdoA(2S)–GlcNS–] and [–IdoA(2S)–GlcNS(6S)–] sequences (209–211). While the 3-*O*-sulfation in HP/HS is uncommon in natural HS chains, it plays crucial roles in the binding to diverse proteins, such as AT (205), envelope glycoprotein D of herpes simplex virus-1 (212), an FGF receptor (213), and FGF-7 (214). HS chains sulfated by HS3ST-1 and HS3ST-5 are able to bind AT (207,210), and those sulfated by HS3ST-3, -5, and -6 can bind glycoprotein D for viral entry (210–212). On the other hand, *HS3ST-2* is involved in the production of melatonin and the regulation of circadian rhythm in the pineal gland (215,216). The CpG islands' methylation of the 5′ region of the *HS3ST-2* gene, which plays important roles in cancer development, is found in a wide range of human cancer cells but not normal cells, suggesting that the *HS3ST-2* gene is expected to be available for the diagnosis and therapy of human cancers (217). The functions of anticoagulant HS *in vivo* have been clarified by the targeted disruption of *HS3ST-1* in mice (166). *HS3ST-1* knockout mice show a large reduction in anticoagulant HS, whereas *HS3ST*-$1^{-/-}$ mice do not display an anticipated procoagulant phenotype, suggesting that the bulk of anticoagulant HS is not essential for normal hemostasis and the hemostatic tone may not be closely linked to the total amount of anticoagulant HS, and that the other HS3ST family members may compensate for the loss of *HS3ST-1*. Two *Drosophila HS3ST* genes, designated *HS3ST-A* and *HS3ST-B*, have been isolated (134). A reduction in *HS3ST-B* functions caused by using the RNAi technique, resulting in neurogenic phenotypes and an abnormal wing margin, affects Notch signaling, suggesting that 3-*O*-sulfation in HS might be involved not only in anticoagulation and viral entry but also in signal transduction.

D. Degradation and Desulfation on Cell Surface

HP and HS chains are degraded by lysosomal enzymes after exerting various functions (218,219). However, there are other catabolic enzymes that are quite different from lysosomal enzymes and mainly expressed on cell surfaces. First, heparanase is an endo-β-glucuronidase that degrades HS chains in the ECM and has been implicated in a variety of biological processes, such as inflammation, tumor angiogenesis, and metastasis (220–223). The cloning of a single human heparanase cDNA, *Hpse-1*, was independently reported by several groups (223–226), and another putative heparanase gene, *Hpse-2*, has also been cloned using the Hpse-1 amino acid sequence (227). No gene homologous to *Hpse* has been found in *D. melanogaster* and *C. elegans*. The expression of human *Hpse-1* mRNA in normal tissues is restricted principally to the placenta and lymphoid organs (224–227). In contrast, the level of *Hpse-2* mRNA is high in the brain, mammary gland, prostate, small intestine, testis, and uterus (227). Furthermore, the expression of both *Hpse-1* and *Hpse-2* was increased in human malignancies and xenografts of carcinomata (227). The recombinant Hpse-1 cleaves in principle the glucuronidic linkage in the –GlcNAc(6S)–GlcA–GlcNS– sequence, whereas this sequence is not sufficient, and an additional sulfate group on this or an adjacent sequence appears to be required (228). For analysis of the functions of Hpse *in vivo*, homozygous transgenic mice overexpressing human *Hpse-1* in all tissues were generated (168). The mice appear

normal and are fertile, but exhibit a reduction in food consumption and body weight, a disruption of the filtration barrier and reabsorption functions in the kidney, and an excess branching and widening of ducts associated with enhanced neovascularization. Altogether, these findings suggest that human Hpse-1 and/or the mature HS chains are involved in food consumption, tissue morphogenesis, and vascularization.

Second, HS 6-*O*-endosulfatase (Sulf), which is distributed on the cell surface and in the Golgi apparatus, is involved in various signal transductions. The cloning of Sulf cDNAs of quail (QSulf1), rat (RsulfFP1), mouse (MSulf-1 and MSulf-2), and human (HSulf-1 and HSulf-2) was independently reported by several groups (229–231). In addition, there are genes homologous to *Sulf* in *D. melanogaster* and *C. elegans*. QSulf1 was identified in a molecular cloning screen for Shh responsive genes, which are activated during somite formation in quail embryos and involved in the regulation of the Wnt signaling (229). On the other hand, RsulfFP1 was isolated from rat embryos by screening for floor plate-specific genes (230). Thereafter, HSulf and MSulf were identified in a search of the GenBank® database (231). HSulf-1, HSulf-2, and QSulf1 remodel 6-*O*-sulfation in the [–IdoA(2S)–GlcNS(6S)–] sequence (231,232). Novel functions of Sulf have been revealed by biochemical experiments with HSPG and QSulf1 on Wnt and BMP signaling activities (232,233). Ai *et al.* proposed a model whereby 6-*O*-sulfated HS on cell surface HSPGs bind Wnt with high affinity to catch Wnt ligands, and 6-*O*-desulfated HS, which exhibits a low affinity binding to Wnt, releases Wnt, which is then presented to the Frizzled receptors (232). Viviano *et al.* showed that the activity of QSulf1 in cells results in the release of Noggin, which is a BMP antagonist, from the cell surface and a restoration of BMP's binding to receptors (233). Furthermore, HSulf-1 is reported to be involved in tumorigenesis (234–236). Thus, the regulation of sulfation of HP/HS is mediated not only by various sulfotransferases but also by extracellular sulfatases.

V. Conclusions

The recent cDNA cloning of enzymes involved in the synthesis and modification of HP and HS chains has led to an understanding of not only the biosynthetic mechanisms but also the functions *in vivo* of HP and HS. Various genes and their products participate in the biosynthesis of HP and HS, as described above. The bioactive HS chains, which have diverse modifications and are covalently attached to various core proteins as HSPGs, play crucial roles in a variety of biological processes, such as cell adhesion (169), cell signaling (61,237), axon guidance (178), cancer biology (84,220), viral entry (35), and the regulation of various growth factors and chemokines (35,169). Further studies on the biosynthesis of HP/HS will help reveal the pathological mechanisms of various human diseases and provide insights into possible therapeutic applications.

Acknowledgments

This work was supported in part by Grant-in-aid for Scientific Research on Priority Areas 14082207 from MEXT and CREST, JST.

References

1. Wiggins CAR, Munro S. Activity of the yeast *MNN1* α-1,3-mannosyltransferase requires a motif conserved in many other families of glycosyltransferases. Proc Natl Acad Sci USA 1998; 95:7945–7950.
2. Pedersen LC, Tsuchida K, Kitagawa H, Sugahara K, Darden TA, Negishi M. Heparan/chondroitin sulfate biosynthesis: structure and mechanism of human glucuronyltransferase I. J Biol Chem 2000; 275:34580–34585.
3. Pedersen LC, Darden TA, Negishi M. Crystal structure of β1,3-glucuronyl transferase I in complex with active donor substrate UDP-GlcUA. J Biol Chem 2002; 277:21869–21873.
4. Silbert JE, Sugumaran G. Biosynthesis of chondroitin/dermatan sulfate. IUBMB Life 2002; 54:177–186.
5. Spicer AP, Kaback LA, Smith TJ, Seldin MF. Molecular cloning and characterization of the human and mouse UDP-glucose dehydrogenase genes. J Biol Chem 1998; 273:25117–25124.
6. Moriarity JL, Hurt KJ, Resnick AC, Storm PB, Laroy W, Schnaar RL, Snyder SH. UDP-glucuronate decarboxylase, a key enzyme in proteoglycan synthesis. J Biol Chem 2002; 277:16968–16975.
7. Binari RC, Staveley BE, Johnson WA, Godavarti R, Sasisekharan R, Manoukian AS. Genetic evidence that heparin-like glycosaminoglycans are involved in Wingless signaling. Development 1997; 124:2623–2632.
8. Haerry TE, Heslip TR, Marsh JL, O'Connor MB. Defects in glucuronate biosynthesis disrupt Wingless signaling in *Drosophila*. Development 1997; 124:3055–3064.
9. Häcker U, Lin X, Perrimon N. The *Drosophila* sugarless gene modulates Wingless signaling and encodes an enzyme involved in polysaccharide biosynthesis. Development 1997; 124:3565–3573.
10. Lin X, Buff EM, Perrimon N, Michelson AM. Heparan sulfate proteoglycans are essential for FGF receptor signaling during *Drosophila* embryonic development. Development 1999; 126:3715–3723.
11. Herman T, Hartwieg E, Horvitz HR. *sqv* mutants of *Caenorhabditis elegans* are defective in vulval epithelial invagination. Proc Natl Acad Sci USA 1999; 96:968–973.
12. Hwang HY, Horvitz HR. The *Caenorhabditis elegans* vulval morphogenesis gene *sqv-4* encodes a UDP-glucose dehydrogenase that is temporally and spatially regulated. Proc Natl Acad Sci USA 2002; 99:14224–14229.
13. Hwang HY, Horvitz HR. The *SQV-1* UDP-glucuronic acid decarboxylase and the *SQV-7* nucleotide-sugar transporter may act in the Golgi apparatus to affect *Caenorhabditis elegans* vulval morphogenesis and embryonic development. Proc Natl Acad Sci USA 2002; 99:14218–14223.

14. Mizuguchi S, Uyama T, Kitagawa H, Nomura KH, Dejima K, Gengyo-Ando K, Mitani S, Sugahara K, Nomura K. Chondroitin proteoglycans are involved in cell division of *Caenorhabditis elegans*. Nature 2003; 423:443–448.
15. Hwang HY, Olson SK, Esko JD, Horvitz HR. *Caenorhabditis elegans* early embryogenesis and vulval morphogenesis require chondroitin biosynthesis. Nature 2003; 423:439–443.
16. Walsh EC, Stainier DYR. UDP-Glucose dehydrogenase required for cardiac valve formation in zebrafish. Science 2001; 293:1670–1673.
17. Golling G, Amsterdam A, Sun Z, Antonelli M, Maldonado E, Chen W, Burgess S, Haldi M, Artzt K, Farrington S, Lin SY, Nissen RM, Hopkins N. Insertional mutagenesis in zebrafish rapidly identifies genes essential for early vertebrate development. Nat Genet 2002; 31:135–140.
18. García-García MJ, Anderson KV. Essential role of glycosaminoglycans in Fgf signaling during mouse gastrulation. Cell 2003; 114:727–737.
19. Hirschberg CB, Robbins PW, Abeijon C. Trasporters of nucleotide sugars, ATP, and nucleotide sulfate in the endoplasmic reticulum and Golgi apparatus. Annu Rev Biochem 1998; 67:49–69.
20. Berninsone PM, Hirschberg CB. Nucleotide sugar transporters of the Golgi apparatus. Curr Opin Struct Biol 2000; 10:542–547.
21. Berninsone P, Hwang HY, Zemtseve I, Horvitz HR, Hirschberg CB. *SQV-7*, a protein involved in *Caenorhabditis elegans* epithelial invagination and early embryogenesis, transports UDP-glucuronic acid, UDP-*N*-acetylgalactosamine, and UDP-galactose. Proc Natl Acad Sci USA 2001; 98:3738–3743.
22. Selva EM, Hong K, Baeg GH, Beverley SM, Turco SJ, Perrimon N, Häcker U. Dual role of the *fringe connection* gene in both heparan sulphate and *fringe*-dependent signalling events. Nat Cell Biol 2001; 3:809–815.
23. Goto S, Taniguchi M, Muraoka M, Toyoda H, Sado Y, Kawakita M, Hayashi S. UDP-sugar transporter implicated in glycosylation and processing of Notch. Nat Cell Biol 2001; 3:816–822.
24. Negishi M, Pedersen LG, Petrotchenko E, Shevtsov S, Gorokhov A, Kakuta Y, Pedersen LC. Structure and function of sulfotransferases. Arch Biochem Biophys 2001; 390:149–157.
25. Schwartz NB, Lyle S, Ozeran JD, Li H, Deyrup A, Ng K, Westley J. Sulfate activation and transport in mammals: system components and mechanisms. Chem Biol Interact 1998; 109:143–151.
26. Venkatachalam KV. Human 3′-phosphoadenosine 5′-phosphosulfate (PAPS) synthase: biochemistry, molecular biology and genetic deficiency. IUBMB Life 2003; 55:1–11.
27. Kurima K, Warman ML, Krishnan S, Domowicz M, Krueger RC, Deyrup A, Schwartz NB. A member of a family of sulfate-activating enzymes causes murine brachymorphism. Proc Natl Acad Sci USA 1998; 95:8681–8685.
28. ul Haque MF, King LM, Krakow D, Cantor RM, Rusiniak ME, Swank RT, Superti-Furga A, Haque S, Abbas H, Ahmad W, Ahmad M, Cohn DH. Mutations in orthologous genes in human spondyloepimetaphyseal dysplasia and the brachymorphic mouse. Nat Genet 1998; 20:157–162.
29. Girard JP, Baekkevold ES, Amalric F. Sulfation in high endothelial venules: cloning and expression of the human PAPS synthetase. FASEB J 1998; 12:603–612.

30. Hästbacka J, de la Chapelle A, Mahtani MM, Clines G, Reeve-Daly MP, Daly M, Hamilton BA, Kusumi K, Trivedi B, Weaver A, Coloma A, Lovett M, Buckler A, Kaitila I, Lander ES. The diastrophic dysplasia gene encodes a novel sulfate transporter: positional cloning by fine-structure linkage disequilibrium mapping. Cell 1994; 78:1073–1087.
31. Hästbacka J, Superti-Furga A, Wilcox WR, Rimoin DL, Cohn DH, Lander ES. Atelosteogenesis type II is caused by mutations in the diastrophic dysplasia sulfate-transporter gene (DTDST): evidence for a phenotypic series involving three chondrodysplasias. Am J Hum Genet 1996; 58:255–262.
32. Superti-Furga A, Hästbacka J, Wilcox WR, Cohn DH, van der Harten HJ, Rossi A, Blau N, Rimoin DL, Steinmann B, Lander ES, Gitzelmann R. Achondrogenesis type IB is caused by mutations in the diastrophic dysplasia sulphate transporter gene. Nat Genet 1996; 12:100–102.
33. Lüders F, Segawa H, Stein D, Selva EM, Perrimon N, Turco SJ, Häcker, U. *slalom* encodes an adenosine 3′-phosphate 5′-phosphosulfate transporter essential for development in *Drosophila*. EMBO J 2003; 22:3635–3644.
34. Kamiyama S, Suda T, Ueda R, Suzuki M, Okubo R, Kikuchi N, Chiba Y, Goto S, Toyoda H, Saigo K, Watanabe M, Narimatsu H, Jigami Y, Nishihara S. Molecular cloning and identification of 3′-phosphoadenosine 5′-phosphosulfate transporter. J Biol Chem 2003; 278:25958–25963.
35. Esko JD, Selleck SB. Order out of chaos: assembly of ligand binding sites in heparan sulfate. Annu Rev Biochem 2002; 71:435–471.
36. Prydz K, Dalen KT. Synthesis and sorting of proteoglycans. J Cell Sci 2000; 113:193–205.
37. Esko JD, Zhang L. Influence of core protein sequence on glycosaminoglycan assembly. Curr Opin Struct Biol 1996; 6:663–670.
38. Götting C, Kuhn J, Zahn R, Brinkmann T, Kleesiek K. Molecular cloning and expression of human UDP-D-xylose: proteoglycan core protein β-D-xylosyltransferase and its first isoform XT-II. J Mol Biol 2000; 304:517–528.
39. Okajima T, Yoshida K, Kondo T, Furukawa K. Human homolog of *Caenorhabditis elegans sqv-3* gene is galactosyltransferase I involved in the biosynthesis of the glycosaminoglycan-protein linkage region of proteoglycans. J Biol Chem 1999; 274:22915–22918.
40. Almeida R, Levery SB, Mandel U, Kresse H, Schwientek T, Bennett EP, Clausen H. Cloning and expression of a proteoglycan UDP-galactose: β-xylose β1,4-galactosyltransferase I: a seventh member of the human β4-galactosyltransferase gene family. J Biol Chem 1999; 274:26165–26171.
41. Bai X, Zhou D, Brown JR, Crawford BE, Hennet T, Esko JD. Biosynthesis of the linkage region of glycosaminoglycans: cloning and activity of galactosyltransferase II, the sixth member of the β1,3-galactosyltransferase family (β3GalT6). J Biol Chem 2001; 276:48189–48195.
42. Kitagawa H, Tone Y, Tamura J, Neumann KW, Ogawa T, Oka S, Kawasaki T, Sugahara K. Molecular cloning and expression of glucuronyltransferase I involved in the biosynthesis of the glycosaminoglycan-protein linkage region of proteoglycans. J Biol Chem 1998; 273:6615–6618.
43. Tone Y, Kitagawa H, Imiya K, Oka S, Kawasaki T, Sugahara K. Characterization of recombinant human glucuronyltransferase I involved in the biosynthesis of the glycosaminoglycan-protein linkage region of proteoglycans. FEBS Lett 1999; 459:415–420.

44. Terayama K, Oka S, Seiki T, Miki Y, Nakamura A, Kozutsumi Y, Takio K, Kawasaki T. Cloning and functional expression of a novel glucuronyltransferase involved in the biosynthesis of the carbohydrate epitope HNK-1. Proc Natl Acad Sci USA 1997; 94:6093–6098.
45. Seiki T, Oka S, Terayama K, Imiya K, Kawasaki T. Molecular cloning and expression of a second glucuronyltransferase involved in the biosynthesis of the HNK-1 carbohydrate epitope. Biochem Biophys Res Commun 1999; 255:182–187.
46. Shimoda Y, Tajima Y, Nagase T, Harii K, Osumi N, Sanai Y. Cloning and expression of a novel galactoside β1,3-glucuronyltransferase involved in the biosynthesis of HNK-1 epitope. J Biol Chem 1999; 274:17115–17122.
47. Wei G, Bai X, Sarkar AK, Esko JD. Formation of HNK-1 determinants and the glycosaminoglycan tetrasaccharide linkage region by UDP-GlcUA: galactose β1,3-glucuronosyltransferases. J Biol Chem 1999; 274:7857–7864.
48. Kitagawa H, Taoka M, Tone Y, Sugahara K. Human glycosaminoglycan glucuronyltransferase I gene and a related processed pseudogene: genomic structure, chromosomal mapping and characterization. Biochem J 2001; 358:539–546.
49. Okajima T, Fukumoto S, Furukawa K, Urano T, Furukawa K. Molecular basis for the progeroid variant of Ehlers–Danlos syndrome: identification and characterization of two mutations in galactosyltransferase I gene. J Biol Chem 1999; 274:28841–28844.
50. Quentin E, Gladen A, Roden L, Kresse H. A genetic defect in the biosynthesis of dermatan sulfate proteoglycan: galactosyltransferase I deficiency in fibroblasts from a patient with a progeroid syndrome. Proc Natl Acad Sci USA 1990; 87:1342–1346.
51. Yamada S, Okada Y, Ueno M, Iwata S, Deepa SS, Nishimura S, Fujita M, Van Die I, Hirabayashi Y, Sugahara K. Determination of the glycosaminoglycan-protein linkage region oligosaccharide structures of proteoglycans from *Drosophila melanogaster* and *Caenorhabditis elegans*. J Biol Chem 2002; 277:31877–31886.
52. Hwang HY, Olson SK, Brown JR, Esko JD, Horvitz HR. The *Caenorhabditis elegans* genes *sqv-2* and *sqv-6*, which are required for vulval morphogenesis, encode glycosaminoglycan galactosyltransferase II and xylosyltransferase. J Biol Chem 2003; 278:11735–11738.
53. Herman T, Horvitz HR. Three proteins involved in *Caenorhabditis elegans* vulval invagination are similar to components of a glycosylation pathway. Proc Natl Acad Sci USA 1999; 96:974–979.
54. Bulik DA, Wei G, Toyoda H, Kinoshita-Toyoda A, Waldrip WR, Esko JD, Robbins PW, Selleck SB. *sqv-3*, *-7*, and *-8*, a set of genes affecting morphogenesis in *Caenorhabditis elegans*, encode enzymes required for glycosaminoglycan biosynthesis. Proc Natl Acad Sci USA 2000; 97:10838–10843.
55. Wilson IBH. Functional characterization of *Drosophila melanogaster* peptide *O*-xylosyltransferase, the key enzyme for proteoglycan chain initiation and member of the core 2/I *N*-acetylglucosaminyltransferase family. J Biol Chem 2002; 277:21207–21212.
56. Nakamura Y, Haines N, Chen J, Okajima T, Furukawa K, Urano T, Stanley P, Irvine KD, Furukawa K. Identification of a *Drosophila* gene encoding xylosylprotein β4-galactosyltransferase that is essential for the synthesis

of glycosaminoglycans and for morphogenesis. J Biol Chem 2002; 277: 46280–46288.
57. Takemae H, Ueda R, Okubo R, Nakato H, Izumi S, Saigo K, Nishihara S. Proteoglycan UDP-galactose: β-xylose β1,4-galactosyltransferase I is essential for viability in *Drosophila melanogaster*. J Biol Chem 2003; 278:15571–15578.
58. Kim BT, Tsuchida K, Lincecum J, Kitagawa H, Bernfield M, Sugahara K. Identification and characterization of three *Drosophila melanogaster* glucuronyltransferases responsible for the synthesis of the conserved glycosaminoglycan-protein linkage region of proteoglycans: two novel homologs exhibit broad specificity toward oligosaccharides from proteoglycans, glycoproteins, and glycosphingolipids. J Biol Chem 2003; 278:9116–9124.
59. Perrimon N, Bernfield M. Specificities of heparan sulfate proteoglycans in developmental processes. Nature 2000; 404:725–728.
60. Selleck SB. Proteoglycans and pattern formation: sugar biochemistry meets developmental genetics. Trends Genet 2000; 16:206–212.
61. Lin X. Functions of heparan sulfate proteoglycans in cell signaling during development. Development 2004; 131:6009–6021.
62. Fransson LÅ, Silverberg I, Carlstedt I. Structure of the heparan sulfate-protein linkage region: demonstration of the sequence galactosyl-galactosyl-xylose-2-phosphate. J Biol Chem 1985; 260:14722–14726.
63. Rosenfeld L, Danishefsky I. Location of specific oligosaccharides in heparin in terms of their distance from the protein linkage region in the native proteoglycan. J Biol Chem 1988; 263:262–266.
64. Ueno M, Yamada S, Zako M, Bernfield M, Sugahara K. Structural characterization of heparan sulfate and chondroitin sulfate of syndecan-1 purified from normal murine mammary gland epithelial cells: common phosphorylation of xylose and differential sulfation of galactose in the protein linkage region tetrasaccharide sequence. J Biol Chem 2001; 276:29134–29140.
65. Sugahara K, Mizuno N, Okumura Y, Kawasaki T. The phosphorylated and/or sulfated structure of the carbohydrate-protein-linkage region isolated from chondroitin sulfate in the hybrid proteoglycans of Engelbreth–Holm–Swarm mouse tumor. Eur J Biochem 1992; 204:401–406.
66. Sugahara K, Ohi Y, Harada T, de Waard P, Vliegenthart JFG. Structural studies on sulfated oligosaccharides derived from the carbohydrate-protein linkage region of chondroitin 6-sulfate proteoglycans of shark cartilage: I. six compounds containing 0 or 1 sulfate and/or phosphate residues. J Biol Chem 1992; 267:6027–6035.
67. Moses J, Oldberg Å, Cheng F, Fransson LÅ. Biosynthesis of the proteoglycan decorin: transient 2-phosphorylation of xylose during formation of the trisaccharide linkage region. Eur J Biochem 1997; 248:521–526.
68. Sugahara K, Yamashina I, de Waard P, Van Halbeek H, Vliegenthart JFG. Structural studies on sulfated glycopeptides from the carbohydrate-protein linkage region of chondroitin 4-sulfate proteoglycans of swarm rat chondrosarcoma: demonstration of the structure Gal(4-*O*-sulfate)β1-3Galβ1-4Xylβ1-*O*-Ser. J Biol Chem 1988; 263:10168–10174.
69. de Waard P, Vliegenthart JFG, Harada T, Sugahara K. Structural studies on sulfated oligosaccharides derived from the carbohydrate-protein linkage region of chondroitin 6-sulfate proteoglycans of shark cartilage: II. seven compounds containing 2 or 3 sulfate residues. J Biol Chem 1992; 267:6036–6043.

70. Yamada S, Oyama M, Yuki Y, Kato K, Sugahara K. The uniform galactose 4-sulfate structure in the carbohydrate-protein linkage region of human urinary trypsin inhibitor. Eur J Biochem 1995; 233:687–693.
71. Sugahara K, Ohkita Y, Shibata Y, Yoshida K, Ikegami A. Structural studies on the hexasaccharide alditols isolated from the carbohydrate-protein linkage region of dermatan sulfate proteoglycans of bovine aorta: demonstration of iduronic acid-containing components. J Biol Chem 1995; 270:7204–7212.
72. Tsuchida K, Shioi J, Yamada S, Boghosian G, Wu A, Cai H, Sugahara K, Robakis NK. Appican, the proteoglycan form of the amyloid precursor protein, contains chondroitin sulfate E in the repeating disaccharide region and 4-*O*-sulfated galactose in the linkage region. J Biol Chem 2001; 276: 37155–37160.
73. Lauder RM, Huckerby TN, Brown GM, Bayliss MT, Nieduszynski IA. Age-related changes in the sulphation of the chondroitin sulphate linkage region from human articular cartilage aggrecan. Biochem J 2001; 358:523–528.
74. Kitagawa H, Tanaka Y, Tsuchida K, Goto F, Ogawa T, Lidholt K, Lindahl U, Sugahara K. *N*-acetylgalactosamine (GalNAc) transfer to the common carbohydrate-protein linkage region of sulfated glycosaminoglycans: identification of UDP-GalNAc: chondro-oligosaccharide α-*N*-acetylgalactosaminyltransferase in fetal bovine serum. J Biol Chem 1995; 270:22190–22195.
75. Lidholt K, Fjelstad M, Lindahl U, Goto F, Ogawa T, Kitagawa H, Sugahara K. Assessment of glycosaminoglycan-protein linkage tetrasaccharides as acceptors for GalNAc- and GlcNAc-transferases from mouse mastocytoma. Glycoconj J 1997; 14:737–742.
76. Gulberti S, Lattard V, Fondeur M, Jacquinet JC, Mulliert G, Netter P, Magdalou J, Ouzzine M, Fournel-Gigleux S. Phosphorylation and sulfation of oligosaccharide substrates critically influence the activity of human β1,4-galactosyltransferase 7 (GalT-I) and β1,3-glucuronosyltransferase I (GlcAT-I) involved in the biosynthesis of the glycosaminoglycan-protein linkage region of proteoglycans. J Biol Chem 2005; 280:1417–1425.
77. Sugahara K, Kitagawa H. Recent advances in the study of the biosynthesis and functions of sulfated glycosaminoglycans. Curr Opin Struct Biol 2000; 10: 518–527.
78. Kitagawa H, Shimakawa H, Sugahara K. The tumor suppressor EXT-like gene *EXTL2* encodes an α1,4-*N*-acetylhexosaminyltransferase that transfers *N*-acetylgalactosamine and *N*-acetylglucosamine to the common glycosaminoglycan-protein linkage region: the key enzyme for the chain initiation of heparan sulfate. J Biol Chem 1999; 274:13933–13937.
79. Kim BT, Kitagawa H, Tamura J, Saito T, Kusche-Gullberg M, Lindahl U, Sugahara K. Human tumor suppressor *EXT* gene family members *EXTL1* and *EXTL3* encode α1,4-*N*-acetylglucosaminyltransferases that likely are involved in heparan sulfate/heparin biosynthesis. Proc Natl Acad Sci USA 2001; 98:7176–7181.
80. Zak BM, Crawford BE, Esko JD. Hereditary multiple exostoses and heparan sulfate polymerization. Biochem Biophys Acta 2002; 1573:346–355.
81. Pedersen LC, Dong J, Taniguchi F, Kitagawa H, Krahn JM, Pedersen LG, Sugahara K, Negishi M. Crystal structure of an α1,4-*N*-acetylhexosaminyltransferase (EXTL2), a member of the exostosin gene family involved in heparan sulfate biosynthesis. J Biol Chem 2003; 278:14420–14428.

82. McCormick C, Duncan G, Goutsos T, Tufaro F. The putative tumor suppressors EXT1 and EXT2 form a stable complex that accumulates in the Golgi apparatus and catalyzes the synthesis of heparan sulfate. Proc Natl Acad Sci USA 2000; 97:668–673.
83. Senay C, Lind T, Muguruma K, Tone Y, Kitagawa H, Sugahara K, Lidholt K, Lindahl U, Kusche-Gullberg M. The EXT1/EXT2 tumor suppressors: catalytic activities and role in heparan sulfate biosynthesis. EMBO Rep. 2000; 1:282–286.
84. Duncan G, McCormick C, Tufaro F. The link between heparan sulfate and hereditary bone disease: finding a function for the EXT family of putative tumor suppressor proteins. J Clin Invest 2001; 108:511–516
85. McCormick C, Leduc Y, Martindale D, Mattison K, Esford LE, Dyer AP, Tufaro F. The putative tumour suppressor EXT1 alters the expression of cell-surface heparan sulfate. Nat Genet 1998; 19:158–161.
86. Lind T, Tufaro F, McCormick C, Lindahl U, Lidholt K. The Putative tumor suppressors EXT1 and EXT2 are glycosyltransferases required for the biosynthesis of heparan sulfate. J Biol Chem 1998; 273:26265–26268.
87. Kobayashi S, Morimoto K, Shimizu T, Takahashi M, Kurosawa H, Shirasawa T. Association of EXT1 and EXT2, hereditary multiple exostoses gene products, in Golgi apparatus. Biochem Biophys Res Commun 2000; 268:860–867.
88. Kim BT, Kitagawa H, Tanaka J, Tamura J, Sugahara K. *In vitro* heparan sulfate polymerization: crucial roles of core protein moieties of primer substrates in addition to the EXT1–EXT2 interaction. J Biol Chem 2003; 278:41618–41623.
89. Busse M, Kusche-Gullberg M. *In vitro* polymerization of heparan sulfate backbone by the EXT proteins. J Biol Chem 2003; 278:41333–41337.
90. Solomon L. Hereditary multiple exostosis. J Bone Joint Surg Br 1963; 45:292–304.
91. Leone NC, Shupe JL, Gardner EJ, Millar EA, Olson AE, Phillips EC. Hereditary multiple exostosis: a comparative human-equine-epidemiologic study. J Hered 1987; 78:171–177.
92. Hennekam RC. Hereditary multiple exostoses. J Med Genet 1991; 28: 262–266.
93. Schmale GA, Conrad EU, Raskind WH. The natural history of hereditary multiple exostoses. J Bone Joint Surg Am 1994; 76:986–992.
94. Wicklund CL, Pauri RM, Johnston D, Hecht JT. Natural history study of hereditary multiple exostoses. Am J Med Genet 1995; 55:43–46.
95. Cook A, Raskind W, Blanton SH, Pauli RM, Gregg RG, Francomano CA, Puffenberger E, Conrad EU, Schmale G, Schellenberg G, Wijsman E, Hecht JT, Wells D, Wagner MJ. Genetic heterogeneity in families with hereditary multiple exostoses. Am J Hum Genet 1993; 53:71–79.
96. Wu YQ, Heutink P, de Vries BB, Sandkuijl LA, van den Ouweland AM, Niermeijer MF, Galjaard H, Reyniers E, Willems PJ, Halley DJ. Assignment of a second locus for multiple exostoses to the pericentromeric region of chromosome 11. Hum Mol Genet 1994; 3:167–171.
97. Le Merrer M, Legeai-Mallet L, Jeannin PM, Horsthemke B, Schinzel A, Plauchu H, Toutain A, Achard F, Munnich A, Maroteaux P. A gene for hereditary multiple exostoses maps to chromosome 19p. Hum Mol Genet 1994; 3:717–722.

98. Lin X, Wei G, Shi Z, Dryer L, Esko JD, Wells DE, Matzuk MM. Disruption of gastrulation and heparan sulfate biosynthesis in EXT1-deficient mice. Dev Biol 2000; 224:299–311.
99. Koziel L, Kunath M, Kelly OG, Vortkamp A. Ext1-dependent heparan sulfate regulates the range of Ihh signaling during endochondral ossification. Dev Cell 2004; 6:801–813.
100. Yamada S, Busse M, Ueno M, Kelly OG, Skarnes WC, Sugahara K, Kusche-Gullberg M. Embryonic fibroblasts with a gene trap mutation in *Ext1* produce short heparan sulfate chains. J Biol Chem 2004; 279:32134–32141.
101. Inatani M, Irie F, Plump AS, Tessier-Lavigne M, Yamaguchi Y. Mammalian brain morphogenesis and midline axon guidance require heparan sulfate. Science 2003; 302:1044–1046.
102. Zak BM, Stickens D, Wells D, Evans G, Esko JD. A Murine model for hereditary multiple exostoses (HME). Glycobiology 2002; 12:642–643.
103. Yamada S, Van Die I, Van den Eijnden DH, Yokota A, Kitagawa H, Sugahara K. Demonstration of glycosaminoglycans in *Caenorhabditis elegans*. FEBS Lett 1999; 459:327–331.
104. Toyoda H, Kinoshita-Toyoda A, Selleck SB. Structural analysis of glycosaminoglycans in *Drosophila* and *Caenorhabditis elegans* and demonstration that *tout-velu*, a *Drosophila* gene related to EXT tumor suppressors, affects heparan sulfate *in vivo*. J Biol Chem 2000; 275:2269–2275.
105. Toyoda H, Kinoshita-Toyoda A, Fox B, Selleck SB. Structural analysis of glycosaminoglycans in animals bearing mutations in *sugarless, sulfateless*, and *tout-velu*: *Drosophila* homologues of vertebrate genes encoding glycosaminoglycan biosynthetic enzymes. J Biol Chem 2000; 275:21856–21861.
106. Bink RJ, Habuchi H, Lele Z, Dolk E, Joore J, Rauch GJ, Geisler R, Wilson SW, Den Hertog J, Kimata K, Zivkovic D. Heparan sulfate 6-*O*-sulfotransferase is essential for muscle development in zebrafish. J Biol Chem 2003; 278:31118–31127.
107. Siekmann AF, Brand M. Distinct tissue-specificity of three zebrafish *ext1* genes encoding proteoglycan modifying enzymes and their relationship to somitic *sonic hedgehog* signaling. Dev Dyn 2005; 232:498–505.
108. Lee JS, von der Hardt S, Rusch MA, Stringer SE, Stickney HL, Talbot WS, Geisler R, Nüsslein-Volhard C, Selleck SB, Chien CB, Roehl H. Axon sorting in the optic tract requires HSPG synthesis by *ext2* (*dackel*) and *extl3* (*boxer*). Neuron 2004; 44:947–960.
109. Bellaiche Y, The I, Perrimon N. *Tout-velu* is a *Drosophila* homologue of the putative tumour suppressor *EXT-1* and is needed for Hh diffusion. Nature 1998; 394:85–88.
110. The I, Bellaiche Y, Perrimon N. Hedgehog movement is regulated through *tout velu*-dependent synthesis of a heparan sulfate proteoglycan. Mol Cell 1999; 4:633–639.
111. Takei Y, Ozawa Y, Sato M, Watanabe A, Tabata T. Three *Drosophila* EXT genes shape morphogen gradients through synthesis of heparan sulfate proteoglycans. Development 2004; 131:73–82.
112. Han C, Belenkaya TY, Khodoun M, Tauchi M, Lin X. Distinct and collaborative roles of *Drosophila* EXT family proteins in morphogen signalling and gradient formation. Development 2004; 131:1563–1575.

113. Bornemann DJ, Duncan JE, Staatz W, Selleck S, Warrior R. Abrogation of heparan sulfate synthesis in *Drosophila* disrupts the Wingless, Hedgehog and Decapentaplegic signaling pathways. Development 2004; 131:1927–1938.
114. Kim BT, Kitagawa H, Tamura J, Kusche-Gullberg M, Lindahl U, Sugahara K. Demonstration of a novel gene *DEXT3* of *Drosophila melanogaster* as the essential *N*-acetylglucosamine transferase in the heparan sulfate biosynthesis: chain initiation and elongation. J Biol Chem 2002; 277:13659–13665.
115. Clines GA, Ashley JA, Shah S, Lovett M. The structure of the human multiple *exostoses 2* gene and characterization of homologs in mouse and *Caenorhabditis elegans*. Genome Res 1997; 7:359–367.
116. Kitagawa H, Egusa N, Tamura J, Kusche-Gullberg M, Lindahl U, Sugahara K. *rib-2*, a *Caenorhabditis elegans* homolog of the human tumor suppressor *EXT* genes encodes a novel α1,4-*N*-acetylglucosaminyltransferase involved in the biosynthetic initiation and elongation of heparan sulfate. J Biol Chem 2001; 276:4834–4838.
117. Morio H, Honda Y, Toyoda H, Nakajima M, Kurosawa H, Shirasawa T. EXT gene family member *rib-2* is essential for embryonic development and heparan sulfate biosynthesis in *Caenorhabditis elegans*. Biochem Biophys Res Commun 2003; 301:317–323.
118. Schachter H. Protein glycosylation lessons from *Caenorhabditis elegans*. Curr Opin Struct Biol 2004; 14:607–616.
119. Bülow HE, Hobert O. Differential sulfations and epimerization define heparan sulfate specificity in nervous system development. Neuron 2004; 41:723–736
120. Kinnunen T, Huang Z, Townsend J, Gatdula MM, Brown JR, Esko JD, Turnbull JE. Heparan 2-*O*-sulfotransferase, *hst-2*, is essential for normal cell migration in *Caenorhabditis elegans*. Proc Nat Acad Sci USA 2005; 102: 1507–1512.
121. Turnbull J, Drummond K, Huang Z, Kinnunen T, Ford-Perriss M, Murphy M, Guimond S. Heparan sulphate sulphotransferase expression in mice and *Caenorhabditis elegans*. Biochem Soc Trans 2003; 31:343–348.
122. Bülow HE, Berry KL, Topper LH, Peles E, Hobert O. Heparan sulfate proteoglycan-dependent induction of axon branching and axon misrouting by the Kallmann syndrome gene *kal-1*. Proc Natl Acad Sci USA 2002; 99:6346–6351.
123. Höflich J, Berninsone P, Göbel C, Gravato-Nobre MJ, Libby BJ, Darby C, Politz SM, Hodgkin J, Hirschberg CB, Baumeister R. Loss of *srf-3*-encoded nucleotide sugar transporter activity in *Caenorhabditis elegans* alters surface antigenicity and prevents bacterial adherence. J Biol Chem 2004; 279: 30440–30448.
124. Cipollo JF, Awad AM, Costello CE, Hirschberg CB. *srf-3*, a mutant of *Caenorhabditis elegans*, resistant to bacterial infection and to biofilm binding, is deficient in glycoconjugates. J Biol Chem 2004; 279:52893–52903.
125. Merz DC, Alves G, Kawano T, Zheng H, Culotti JG. UNC-52/Perlecan affects gonadal leader cell migrations in *C. elegans* hermaphrodites through alterations in growth factor signaling. Dev Biol 2003; 256:174–187.
126. Rogalski TM, Mullen GP, Bush JA, Gilchrist EJ, Moerman DG. UNC-52/ perlecan isoform diversity and function in *Caenorhabditis elegans*. Biochem Soc Trans 2001; 29:171–176.

127. Minniti AN, Labarca M, Hurtado C, Brandan E. *Caenorhabditis elegans* syndecan (SDN-1) is required for normal egg laying and associates with the nervous system and the vulva. J Cell Sci 2004; 117:5179–5190.
128. Maeda I, Kohara Y, Yamamoto M, Sugimoto A. Large-scale analysis of gene function in *Caenorhabditis elegans* by high-throughput RNAi. Curr Biol 2001; 11:171–176.
129. Segawa H, Kawakita M, Ishida N. Human and *Drosophila* UDP-galactose transporters transport UDP-*N*-acetylgalactosamine in addition to UDP-galactose. Eur J Biochem 2002; 269:128–138.
130. Jullien D, Crozatier M, Käs E. cDNA sequence and expression pattern of the *Drosophila melanogaster* PAPS synthetase gene: a new salivary gland marker. Mech Dev 1997; 68:179–186.
131. Lin X, Perrimon N. Dally cooperates with *Drosophila* Frizzled 2 to transduce Wingless signalling. Nature 1999; 400:281–284.
132. Sen J, Golts JS, Stevens L, Stein D. Spatially restricted expression of *pipe* in the *Drosophila* egg chamber defines embryonic dorsal–ventral polarity. Cell 1998; 95:471–481.
133. Merrill C, Bayraktaroglu L, Kusano A, Ganetzky B. Truncated RanGAP encoded by the *segregation distorter* locus of *Drosophila*. Science 1999; 283:1742–1745.
134. Kamimura K, Rhodes JM, Ueda R, McNeely M, Shukla D, Kimata K, Spear PG, Shworak NW, Nakato H. Regulation of Notch signaling by *Drosophila* heparan sulfate 3-*O* sulfotransferase. J Cell Biol 2004; 166:1069–1079.
135. Kamimura K, Fujise M, Villa F, Izumi S, Habuchi H, Kimata K, Nakato H. *Drosophila* heparan sulfate 6-*O*-sulfotransferase (*dHS6ST*) gene: structure, expression, and function in the formation of the tracheal system. J Biol Chem 2001; 276:17014–17021.
136. Nakato H, Futch TA, Selleck SB. The *division abnormally delayed* (*dally*) gene: a putative integral membrane proteoglycan required for cell division patterning during postembryonic development of the nervous system in *Drosophila*. Development 1995; 121:3687–3702.
137. Jackson SM, Nakato H, Sugiura M, Jannuzi A, Oakes R, Kaluza V, Golden C, Selleck SB. *dally*, a *Drosophila* glypican, controls cellular responses to the TGF-β-related morphogen, Dpp. Development 1997; 124:4113–4120.
138. Tsuda M, Kamimura K, Nakato H, Archer M, Staatz W, Fox B, Humphrey M, Olson S, Futch T, Kaluza V, Siegfried E, Stam L, Selleck SB. The cell-surface proteoglycan Dally regulates Wingless signalling in *Drosophila*. Nature 1999; 400:276–280.
139. Fujise M, Takeo S, Kamimura K, Matsuo T, Aigaki T, Izumi S, Nakato H. Dally regulates Dpp morphogen gradient formation in the *Drosophila* wing. Development 2003; 130:1515–1522.
140. Han C, Belenkaya TY, Wang B, Lin X. *Drosophila* glypicans control the cell-to-cell movement of Hedgehog by a dynamin-independent process. Development 2004; 131:601–611.
141. Belenkaya TY, Han C, Yan D, Opoka RJ, Khodoun M, Liu H, Lin X. *Drosophila* Dpp morphogen movement is independent of dynamin-mediated endocytosis but regulated by the glypican members of heparan sulfate proteoglycans. Cell 2004; 119:231–244.

142. Franch-Marro X, Marchand O, Piddini E, Ricardo S, Alexandre C, Vincent JP. Glypicans shunt the Wingless signal between local signalling and further transport. Development 2005; 132:659–666.
143. Han C, Yan D, Belenkaya TY, Lin X. *Drosophila* glypicans Dally and Dally-like shape the extracellular Wingless morphogen gradient in the wing disc. Development 2005; 132:667–679.
144. Baeg GH, Lin X, Khare N, Baumgartner S, Perrimon N. Heparan sulfate proteoglycans are critical for the organization of the extracellular distribution of Wingless. Development 2001; 128:87–94.
145. Desbordes SC, Sanson B. The glypican Dally-like is required for Hedgehog signalling in the embryonic epidermis of *Drosophila*. Development 2003; 130:6245–6255.
146. Kreuger J, Perez L, Giraldez AJ, Cohen SM. Opposing activities of Dally-like glypican at high and low levels of Wingless morphogen activity. Dev Cell 2004; 7:503–512.
147. Kirkpatrick CA, Dimitroff BD, Rawson JM, Selleck SB. Spatial regulation of Wingless morphogen distribution and signaling by Dally-like protein. Dev Cell 2004; 7:513–523.
148. Baeg GH, Selva EM, Goodman RM, Dasgupta R, Perrimon N. The Wingless morphogen gradient is established by the cooperative action of Frizzled and heparan sulfate proteoglycan receptors. Dev Biol 2004; 276:89–100.
149. Voigt A, Pflanz R, Schäfer U, Jäckle H. Perlecan participates in proliferation activation of quiescent *Drosophila* neuroblasts. Dev Dyn 2002; 224:403–412.
150. Steigemann P, Molitor A, Fellert S, Jäckle H, Vorbrüggen G. Heparan sulfate proteoglycan syndecan promotes axonal and myotube guidance by Slit/Robo signaling. Curr Biol 2004; 14:225–230.
151. Johnson KG, Ghose A, Epstein E, Lincecum J, O'Connor MB,Van Vactor D. Axonal heparan sulfate proteoglycans regulate the distribution and efficiency of the repellent Slit during midline axon guidance. Curr Biol 2004; 14:499–504.
152. Amsterdam A, Nissen RM, Sun Z, Swindell EC, Farrington S, Hopkins N. Identification of 315 genes essential for early zebrafish development. Proc Nat Acad Sci USA 2004; 101:12792–12797.
153. Topczewski J, Sepich DS, Myers DC, Walker C, Amores A, Lele Z, Hammerschmidt M, Postlethwait J, Solnica-Krezel L. The zebrafish glypican knypek controls cell polarity during gastrulation movements of convergent extension. Dev Cell 2001; 1:251–264.
154. Chen E, Hermanson S, Ekker SC. Syndecan-2 is essential for angiogenic sprouting during zebrafish development. Blood 2004; 103:1710–1719.
155. Forlino A, Piazza R, Tiveron C, Torre SD, Tatangelo L, Bonafé L, Gualeni B, Romano A, Pecora F, Superti-Furga A, Cetta G, Rossi A. A diastrophic dysplasia sulfate transporter (SLC26A2) mutant mouse: morphological and biochemical characterization of the resulting chondrodysplasia phenotype. Hum Mol Genet 2005; 14:859–871.
156. Morimoto K, Shimizu T, Furukawa K, Morio H, Kurosawa H, Shirasawa T. Transgenic expression of the EXT2 gene in developing chondrocytes enhances the synthesis of heparan sulfate and bone formation in mice. Biochem Biophys Res Commun 2002; 292:999–1009.

157. Fan G, Xiao L, Cheng L, Wang X, Sun B, Hu G. Targeted disruption of NDST-1 gene leads to pulmonary hypoplasia and neonatal respiratory distress in mice. FEBS Lett 2000; 467:7–11.
158. Ringvall M, Ledin J, Holmborn K, van Kuppevelt T, Ellin F, Eriksson I, Olofsson AM, Kjellén L, Forsberg E. Defective Heparan sulfate biosynthesis and neonatal lethality in mice lacking *N*-deacetylase/*N*-sulfotransferase-1. J Biol Chem 2000; 275:25926–25930.
159. Grobe K, Ledin J, Ringvall M, Holmborn K, Forsberg E, Esko JD, Kjellén L. Heparan sulfate and development: differential roles of the *N*-acetylglucosamine *N*-deacetylase/*N*-sulfotransferase isozymes. Biochim Biophys Acta 2002; 1573:209–215.
160. Jenniskens GJ, Ringvall M, Koopman WJH, Ledin J, Kjellén L, Willems PHGM, Forsberg E, Veerkamp JH, van Kuppevelt TH. Disturbed Ca^{2+} kinetics in *N*-deacetylase/*N*-sulfotransferase-1 defective myotubes. J Cell Sci 2003; 116:2187–2193.
161. Humphries DE, Wong GW, Friend DS, Gurish MF, Qiu WT, Huang C, Sharpe AH, Stevens RL. Heparin is essential for the storage of specific granule proteases in mast cells. Nature 1999; 400:769–772.
162. Forsberg E, Pejler G, Ringvall M, Lunderius C, Tomasini-Johansson B, Kusche-Gullberg M, Eriksson I, Ledin J, Hellman L, Kjellén L. Abnormal mast cells in mice deficient in a heparin-synthesizing enzyme. Nature 1999; 400:773–776.
163. Bullock SL, Fletcher JM, Beddington RSP, Wilson VA. Renal agenesis in mice homozygous for a gene trap mutation in the gene encoding heparan sulfate 2-sulfotransferase. Genes Dev 1998; 12:1894–1906.
164. McLaughlin D, Karlsson F, Tian N, Pratt T, Bullock SL, Wilson VA, Price DJ, Mason JO. Specific modification of heparan sulphate is required for normal cerebral cortical development. Mech Dev 2003; 120:1481–1488.
165. Merry CLR, Bullock SL, Swan DC, Backen AC, Lyon M, Beddington RSP, Wilson VA, Gallagher JT. The molecular phenotype of heparan sulfate in the *Hs2st*$^{-/-}$ mutant mouse. J Biol Chem 2001; 276:35429–35434.
166. HajMohammadi S, Enjyoji K, Princivalle M, Christi P, Lech M, Beeler D, Rayburn H, Schwartz JJ, Barzegar S, de Agostini AI, Post MJ, Rosenberg RD, Shworak NW. Normal levels of anticoagulant heparan sulfate are not essential for normal hemostasis. J Clin Invest 2003; 111:989–999.
167. Li JP, Gong F, Hagner-McWhirter Å, Forsberg E, Åbrink M, Kisilevsky R, Zhang X, Lindahl U. Targeted disruption of a murine glucuronyl C5-epimerase gene results in heparan sulfate lacking L-iduronic acid and in neonatal lethality. J Biol Chem 2003; 278:28363–28366.
168. Zcharia E, Metzger S, Chajek-Shaul T, Aingorn H, Elkin M, Friedmann Y, Weinstein T, Li JP, Lindahl U, Vlodavsky I. Transgenic expression of mammalian heparanase uncovers physiological functions of heparan sulfate in tissue morphogenesis, vascularization, and feeding behavior. FASEB J 2004; 18:252–263.
169. Bernfield M, Götte M, Park PW, Reizes O, Fitzgerald ML, Lincecum J, Zako M. Functions of cell surface heparan sulfate proteoglycans. Annu Rev Biochem 1999; 68:729–777.

170. Alexander CM, Reichsman F, Hinkes MT, Lincecum J, Becker KA, Cumberledge S, Bernfield M. Syndecan-1 is required for Wnt-1-induced mammary tumorigenesis in mice. Nat Genet 2000; 25:329–332.
171. Reizes O, Lincecum J, Wang Z, Goldberger O, Huang L, Kaksonen M, Ahima R, Hinkes MT, Barsh GS, Rauvala H, Bernfield M. Transgenic expression of Syndecan-1 uncovers a physiological control of feeding behavior by Syndecan-3. Cell 2001; 106:105–116.
172. Ishiguro K, Kadomatsu K, Kojima T, Muramatsu H, Tsuzuki S, Nakamura E, Kusugami K, Saito H, Muramatsu T. Syndecan-4 deficiency impairs focal adhesion formation only under restricted conditions. J Biol Chem 2000; 275:5249–5252.
173. Cano-Gauci DF, Song HH, Yang H, McKerlie C, Choo B, Shi W, Pullano R, Piscione TD, Grisaru S, Soon S, Sedlackova L, Tanswell AK, Mak TW, Yeger H, Lockwood GA, Rosenblum ND, Filmus J. Glypican-3–deficient mice exhibit developmental overgrowth and some of the abnormalities typical of Simpson-Golabi-Behmel syndrome. J Cell Biol 1999; 146:255–264.
174. Aikawa-Hirasawa E, Watanabe H, Takami H, Hassell JR, Yamada Y. Perlecan is essential for cartilage and cephalic development. Nat Genet 1999; 23:354–358.
175. Costell M, Gustafsson E, Aszódi A, Mörgelin M, Bloch W, Hunziker E, Addicks K, Timpl R, Fässler R. Perlecan maintains the integrity of cartilage and some basement membranes. J Cell Biol 1999; 147:1109–1122.
176. Gautam M, Noakes PG, Moscoso L, Rupp F, Scheller RH, Merlie JP, Sanes JR. Defective neuromuscular synaptogenesis in agrin-deficient mutant mice. Cell 1996; 85:525–535.
177. Åbrink M, Grujic M, Pejler G. Serglycin is essential for maturation of mast cell secretory granule. J Biol Chem 2004; 279:40897–40905.
178. Lee JS, Chien CB. When sugars guide axons: insights from heparan sulphate proteoglycan mutants. Nat Rev Genet 2004; 5:923–935.
179. Sugahara K, Kitagawa H. Heparin and heparan sulfate biosynthesis. IUBMB Life 2002; 54:163–175.
180. Brandan E, Hirschberg CB. Purification of rat liver *N*-heparan-sulfate sulfotransferase. J Biol Chem 1988; 263:2417–2422.
181. Pettersson I, Kusche M, Unger E, Wlad H, Nylund L, Lindahl U, Kjellén L. Biosynthesis of heparin: purification of a 110-kDa mouse mastocytoma protein required for both glucosaminyl *N*-deacetylation and *N*-sulfation. J Biol Chem 1991; 266:8044–8049.
182. Hashimoto Y, Orellana A, Gil G, Hirschberg CB. Molecular cloning and expression of rat liver *N*-heparan sulfate sulfotransferase. J Biol Chem 1992; 267:15744–15750.
183. Eriksson I, Sandbäck D, Ek B, Lindahl U, Kjellén L. cDNA cloning and sequencing of mouse mastocytoma glucosaminyl *N*-deacetylase/*N*-sulfotransferase, an enzyme involved in the biosynthesis of heparin. J Biol Chem 1994; 269:10438–10443.
184. Aikawa J, Esko JD. Molecular cloning and expression of a third member of the heparan sulfate/heparin GlcNAc *N*-deacetylase/*N*-sulfotransferase Family. J Biol Chem 1999; 274:2690–2695.
185. Aikawa J, Grobe K, Tsujimoto M, Esko JD. Multiple isozymes of heparan sulfate/heparin GlcNAc *N*-deacetylase/GlcN *N*-sulfotransferase: structure

and activity of the fourth member, NDST4. J Biol Chem 2001; 276:5876–5882.
186. Holmborn K, Ledin J, Smeds E, Eriksson I, Kusche-Gullberg M, Kjellén L. Heparan sulfate synthesized by mouse embryonic stem cells deficient in NDST1 and NDST2 is 6-*O*-sulfated but contains no *N*-sulfate groups. J Biol Chem 2004; 279:42355–42358.
187. Campbell P, Hannesson HH, Sandbäck D, Rodén L, Lindahl U, Li JP. Biosynthesis of heparin/heparan sulfate: purification of the D-glucuronyl C-5 epimerase from bovine liver. J Biol Chem 1994; 269:26953–26958.
188. Hagner-McWhirter Å, Li JP, Oscarson S, Lindahl U. Irreversible glucuronyl C5-epimerization in the biosynthesis of heparan sulfate. J Biol Chem 2004, 279:14631–14638.
189. Li JP, Hagner-McWhirter Å, Kjellén L, Palgi J, Jalkanen M, Lindahl U. Biosynthesis of heparin/heparan sulfate: cDNA cloning and expression of D-glucuronyl C5-epimerase from bovine lung. J Biol Chem 1997; 272: 28158–28163.
190. Li JP, Gong F, Darwish KE, Jalkanen M, Lindahl U. Characterization of the D-glucuronyl C5-epimerase involved in the biosynthesis of heparin and heparan sulfate. J Biol Chem 2001; 276:20069–20077.
191. Crawford BE, Olson SK, Esko JD, Pinhal MAS. Cloning, Golgi localization, and enzyme activity of the full-length heparin/heparan sulfate-glucuronic acid C5-epimerase. J Biol Chem 2001; 276:21538–21543.
192. Jacobsson I, Bäckström G, Höök M, Lindahl U, Feingold DS, Malmström A, Rodén L. Biosynthesis of heparin: assay and properties of the microsomal uronosyl C-5 epimerase. J Biol Chem 1979; 254:2975–2982.
193. Casu B, Petitou M, Provasoli M, Sinaÿ P. Conformational flexibility: a new concept for explaining binding and biological properties of iduronic acid-containing glycosaminoglycans. Trends Biochem Sci 1988; 13:221–225.
194. Kobayashi M, Habuchi H, Habuchi O, Saito M, Kimata K. Purification and characterization of heparan sulfate 2-sulfotransferase from cultured chinese hamster ovary cells. J Biol Chem 1996; 271:7645–7653.
195. Kobayashi M, Habuchi H, Yoneda M, Habuchi O, Kimata K. Molecular cloning and expression of chinese hamster ovary cell heparan-sulfate 2-sulfotransferase. J Biol Chem 1997; 272:13980–13985.
196. Rong J, Habuchi H, Kimata K, Lindahl U, Kusche-Gullberg M. Substrate specificity of the heparan sulfate hexuronic acid 2-*O*-sulfotransferase. Biochemistry 2001; 40:5548–5555.
197. Pinhal MAS, Smith B, Olson S, Aikawa J, Kimata K, Esko JD. Enzyme interactions in heparan sulfate biosynthesis: uronosyl 5-epimerase and 2-*O*-sulfotransferase interact *in vivo*. Proc Natl Acad Sci USA 2001; 98: 12984–12989.
198. Bai X, Esko JD. An animal cell mutant defective in heparan sulfate hexuronic acid 2-*O*-sulfation. J Biol Chem 1996; 271:17711–17717.
199. Habuchi H, Habuchi O, Kimata K. Purification and characterization of heparan sulfate 6-sulfotransferase from the culture medium of chinese hamster ovary cells. J Biol Chem 1995; 270:4172–4179.
200. Habuchi H, Kobayashi M, Kimata K. Molecular characterization and expression of heparan-sulfate 6-sulfotransferase: complete cDNA cloning in human

and partial cloning in chinese hamster ovary cells. J Biol Chem 1998; 273:9208–9213.
201. Habuchi H, Tanaka M, Habuchi O, Yoshida K, Suzuki H, Ban K, Kimata K. The occurrence of three isoforms of heparan sulfate 6-*O*-sulfotransferase having different specificities for hexuronic acid adjacent to the targeted *N*-sulfoglucosamine. J Biol Chem 2000; 275:2859–2868.
202. Habuchi H, Miyake G, Nogami K, Kuroiwa A, Matsuda Y, Kusche-Gullberg M, Habuchi O, Tanaka M, Kimata K. Biosynthesis of heparan sulphate with diverse structures and functions: two alternatively spliced forms of human heparan sulphate 6-*O*-sulphotransferase-2 having different expression patterns and properties. Biochem J 2003; 371:131–142.
203. Smeds E, Habuchi H, Do AT, Hjertson E, Grundberg H, Kimata K, Lindahl U, Kuche-Gullberg M. Substrate specificities of mouse heparan sulphate glucosaminyl 6-O-sulphotransferases. Biochem J 2003; 372:371–380.
204. Nagai N, Habuchi H, Esko JD, Kimata K. Stem domains of heparan sulfate 6-*O*-sulfotransferase are required for Golgi localization, oligomer formation and enzyme activity. J Cell Sci 2004; 117:3331–3341.
205. Lindahl U, Bäckström G, Thunberg L, Leder IG. Evidence for a 3-*O*-sulfated D-glucosamine Residue in the Antithrombin-Binding Sequence of Heparin. Proc Nat Acad Sci USA 1980; 77:6551–6555.
206. Liu J, Shworak NW, Fritze LMS, Edelberg JM, Rosenberg RD. Purification of heparan sulfate D-glucosaminyl 3-*O*-sulfotransferase. J Biol Chem 1996; 271:27072–27082.
207. Shworak NW, Liu J, Fritze LMS, Schwartz JJ, Zhang L, Logeart D, Rosenberg RD. Molecular cloning and expression of mouse and human cDNAs encoding heparan sulfate D-glucosaminyl 3-*O*-sulfotransferase. J Biol Chem 1997; 272:28008–28019.
208. Shworak NW, Liu J, Petros LM, Zhang L, Kobayashi M, Copeland NG, Jenkins NA, Rosenberg RD. Multiple isoforms of heparan sulfate D-glucosaminyl 3-*O*-sulfotransferase: isolation, characterization, and expression of human cDNAs and identification of distinct genomic loci. J Biol Chem 1999; 274:5170–5184.
209. Liu J, Shworak NW, Sinaÿ P, Schwartz JJ, Zhang L, Fritze LMS, Rosenberg RD. Expression of heparan sulfate D-glucosaminyl 3-*O*-sulfotransferase isoforms reveals novel substrate specificities. J Biol Chem 1999; 274:5185–5192.
210. Xia G, Chen J, Tiwari V, Ju W, Li JP, Malmström A, Shukla D, Liu J. Heparan sulfate 3-*O*-sulfotransferase isoform 5 generates both an antithrombin-binding site and an entry receptor for herpes simplex virus, type 1. J Biol Chem 2002; 277:37912–37919.
211. Xu D, Tiwari V, Xia G, Clement C, Shukla D, Liu J. Characterization of heparan sulphate 3-O-sulphotransferase isoform 6 and its role in assisting the entry of herpes simplex virus type 1. Biochem J 2005; 385:451–459.
212. Shukla D, Liu J, Blaiklock P, Shworak NW, Bai X, Esko JD, Cohen GH, Eisenberg RJ, Rosenberg RD, Spear PG. A novel role for 3-*O*-sulfated heparan sulfate in herpes simplex virus 1 entry. Cell 1999; 99:13–22.
213. McKeehan WL, Wu X, Kan M. Requirement for anticoagulant heparan sulfate in the fibroblast growth factor receptor complex. J Biol Chem 1999; 274:21511–21514.

214. Ye S, Luo Y, Lu W, Jones RB, Linhardt RJ, Capila I, Toida T, Kan M, Pelletier H, McKeehan WL. Structural basis for interaction of FGF-1, FGF-2, and FGF-7 with different heparan sulfate motifs. Biochemistry 2001; 40:14429–14439.
215. Borjigin J, Deng J, Sun X, De Jesus M, Liu T, Wang MM. Diurnal pineal 3-*O*-sulphotransferase 2 expression controlled by β-adrenergic repression. J Biol Chem 2003; 278:16315–16319.
216. Kuberan B, Lech M, Borjigin J, Rosenberg RD. Light-induced 3-*O*-sulfotransferase expression alters pineal heparan sulfate fine structure: a surprising link to circadian rhythm. J Biol Chem 2004; 279:5053–5054.
217. Miyamoto K, Asada K, Fukutomi T, Okochi E, Yagi Y, Hasegawa T, Asahara T, Sugimura T, Ushijima T. Methylation-associated silencing of *heparan sulfate* D-*glucosaminyl 3-O-sulfotransferase-2* (*3-OST-2*) in human breast, colon, lung and pancreatic cancers. Oncogene 2003; 22:274–280.
218. Desnick RJ, Schuchman EH. Enzyme replacement and enhancement therapies: lessons from lysosomal disorders. Nat Rev Genet 2002; 3:954–966.
219. Futerman AH, van Meer G. The cell biology of lysosomal storage disorders. Nat Rev Mol Cell Biol 2004; 5:554–565.
220. Sasisekharan R, Shriver Z, Venkataraman G, Narayanasami U. Roles of heparan-sulphate glycosaminoglycans in cancer. Nat Rev Cancer 2002; 2:521–528.
221. Vlodavsky I, Friedmann Y. Molecular properties and involvement of heparanase in cancer metastasis and angiogenesis. J Clin Invest 2001; 108:341–347.
222. Parish CR, Freeman C, Hulett MD. Heparanase: a key enzyme involved in cell invasion. Biochim Biophys Acta 2001; 1471:M99–M108.
223. Bame KJ. Heparanases: endoglycosidases that degrade heparan sulfate proteoglycans. Glycobiology 2001; 11:91R–98R.
224. Vlodavsky I, Friedmann Y, Elkin M, Aingorn H, Atzmon R, Ishai-Michaeli R, Bitan M, Pappo O, Peretz T, Michal I, Spector L, Pecker I. Mammalian heparanase: gene cloning, expression and function in tumor progression and metastasis. Nat Med 1999; 5:793–802.
225. Hulett MD, Freeman C, Hamdorf BJ, Baker RT, Harris MJ, Parish CR. Cloning of mammalian heparanase, an important enzyme in tumor invasion and metastasis. Nat Med 1999; 5:803–809.
226. Toyoshima M, Nakajima M. Human heparanase: purification, characterization, cloning, and expression. J Biol Chem 1999; 274:24153–24160.
227. McKenzie E, Tyson K, Stamps A, Smith P, Turner P, Barry R, Hircock M, Patel S, Barry E, Stubberfield C, Terrett J, Page M. Cloning and expression profiling of Hpa2, a novel mammalian heparanase family member. Biochem Biophys Res Commun 2000; 276:1170–1177.
228. Okada Y, Yamada S, Toyoshima M, Dong J, Nakajima M, Sugahara K. Structural recognition by recombinant human heparanase that plays critical roles in tumor metastasis: hierarchical sulfate groups with differential effects and the essential target disulfated trisaccharide sequence. J Biol Chem 2002; 277:42488–42495.
229. Dhoot GK, Gustafsson MK, Ai X, Sun W, Standiford DM, Emerson Jr CP. Regulation of Wnt signaling and embryo patterning by an extracellular sulfatase. Science 2001; 293:1663–1666.

230. Ohto T, Uchida H, Yamazaki H, Keino-Masu K, Matsui A, Masu M. Identification of a novel nonlysosomal sulphatase expressed in the floor plate, choroid plexus and cartilage. Genes Cells 2002; 7:173–185.
231. Morimoto-Tomita M, Uchimura K, Werb Z, Hemmerich S, Rosen SD. Cloning and characterization of two extracellular heparin-degrading endosulfatases in mice and humans. J Biol Chem 2002; 277:49175–49185.
232. Ai X, Do AT, Lozynska O, Kusche-Gullberg M, Lindahl U, Emerson Jr CP. QSulf1 remodels the 6-O sulfation states of cell surface heparan sulfate proteoglycans to promote Wnt signaling. J Cell Biol 2003; 162:341–351.
233. Viviano BL, Paine-Saunders S, Gasiunas N, Gallagher J, Saunders S. Domain-specific modification of heparan sulfate by Qsulf1 modulates the binding of the bone morphogenetic protein antagonist Noggin. J Biol Chem 2004; 279:5604–5611.
234. Morimoto-Tomita M, Uchimura K, Rosen SD. Novel extracellular sulfatases: potential roles in cancer. Trends Glycosci Glycotechnol 2003; 15: 159–164.
235. Lai J, Chien J, Staub J, Avula R, Greene EL, Matthews TA, Smith DI, Kaufmann SH, Roberts LR, Shridhar V. Loss of HSulf-1 up-regulates heparin-binding growth factor signaling in cancer. J Biol Chem 2003; 278: 23107–23117.
236. Lai JP, Chien J, Strome SE, Staub J, Montoya DP, Greene EL, Smith DI, Roberts LR, Shridhar V. HSulf-1 modulates HGF-mediated tumor cell invasion and signaling in head and neck squamous carcinoma. Oncogene 2004; 23:1439–1447.
237. Kramer KL, Yost HJ. Heparan sulfate core proteins in cell-cell signaling. Annu Rev Genet 2003; 37:461–484.

Chemistry and Biology of Heparin and Heparan Sulfate
H.G. Garg, R.J. Linhardt and C.A. Hales (Editors)

Chapter 8

Remodeling of Heparan Sulfate Sulfation by Extracellular Endosulfatases

XINGBIN AI

Boston Biomedical Research Institute, Watertown, MA, USA

MARION KUSCHE-GULLBERG

University of Bergen, Department of Biomedicine, Borgen, Norway

ULF LINDAHL

Uppsala University, IMBIM, The Biomedical Center, Uppsala, Sweden

and

CHARLES P. EMERSON Jr.

Boston Biomedical Research Institute, Watertown, MA, USA

I. Introduction

Cell surface heparan sulfate proteoglycans (HSPGs) have key developmental signaling functions in the control of cell growth and differentiation. Heparan sulfate proteoglycans signaling functions are mediated both through the HSPG core protein signaling (1–3) as well as through the interactions of growth factors and receptors with heparan sulfate (HS) chains linked to core proteins. The signaling functions of HS are dependent on the 6-*O*-, 2-*O*-, and *N*-sulfation of the disaccharides units of HS chains, which have defined domains of high, low, and no sulfation along their chain lengths (4). The sulfation states of HSPGs are tissue specific and dynamically regulated in embryonic cells during development and in adult normal and cancer cells responding to growth factor signals (5–8). Specifically, the 6-*O*-sulfation states of HS are major determinants of the growth factor signaling and coreceptor functions of proteoglycans. The dynamic patterns of HS sulfation generally have been thought to be controlled by the differential activities of HS sulfyltransferase isoforms during HSPG biosynthesis.

Recently a novel family of cell surface 6-*O*-HS endosulfatases (Sulfs) has been discovered (9). Extracellular sulfatases function as HS modifying enzymes of the 6-*O*-sulfation states of HS chains on cell surface HSPGs to regulate extracellular HS-mediated growth factor signaling (10–14). In this chapter, we review current knowledge of Sulf enzymes, including their unique structural and enzymatic properties as novel extracellular heparan endosulfatases, their regulatory functions in extracellular HS-dependent Wnt and FGF signaling in stem cell progenitors, and their roles and therapeutic applications in the control of tumor growth and angiogenesis.

II. Identification of Sulf Enzymes

Sulf enzymes are members of Sulfatase gene family. *QSulf1* was discovered in an RNA expression screen designed to identify Sonic hedgehog target genes expressed in mesoderm and neural stem cell progenitors in developing avian embryos (9). Homology search analyses identified *QSulf1* orthologues in a diversity of multicellular invertebrate and vertebrate animals, including Drosophila, *C. elegans*, Xenopus, Zebra fish, chicken, mouse, rat, and humans (15,16; unpublished data). Vertebrates express a second, closely related isoform, *Sulf2* (10; unpublished data). The closest relative of Sulf1 and Sulf2 in the Sulfatase gene family is *N*-acetyl glucosamine (GlcN) 6-*O*-sulfatase (GlcNR6Sase), a heparan 6-*O*-exosulfatase involved in lysosomal degradation of heparin sulfate chains (17,18). Amino acid sequence alignments reveal that QSulf1 and GlcNR6Sase proteins are highly homologous within their catalytic domains, likely reflecting their common functions as GlcN 6-*O*-sulfatases (9), as well as within their C-terminal domain, which has unknown function (Fig. 1). Within the conserved catalytic domain, QSulf1 shares a conserved cysteine residue that is predicted to be posttranslationally modified to form a formalglycine residue required for catalytic activity of all sulfatases (19). Consistent with this function, an alanine substitution mutation of this conserved cysteine inactivates QSulf1 activity, both *in vitro* and *in vivo* (9,11,13). In addition to these conserved sequence features, Sulf1 and Sulf2 have two unique structural domains: (1) an N-terminal secretion signal peptide, which is processed during secretion (9,10; unpublished data); and (2) a "hydrophilic domain" (HD) located between the catalytic domain and the C-terminus, making Sulf enzymes significantly larger than their closest GlcNR6Sase relatives. The HD domain has a predicted coiled-coil structure with a striking abundance of clustered positively and negatively charged amino acids and 12 cysteine residues positionally conserved in the sequences of all members of the Sulf family. The HD domain is evolutionarily conserved and is the unique signature sequence for Sulf proteins, based on genome-wide database analyses. Conservation of the HD sequence in association with catalytic and C-terminal domains has enabled identification of Sulf proteins in vertebrates and invertebrates. Vertebrates Sulf1 and Sulf2 are highly homologous in all domains, consistent with their redundant functions (10; unpublished data), although the HD domain has sequence regions of isoform-specific conservation, suggesting isoform-specific differences in HD function that remain to be defined.

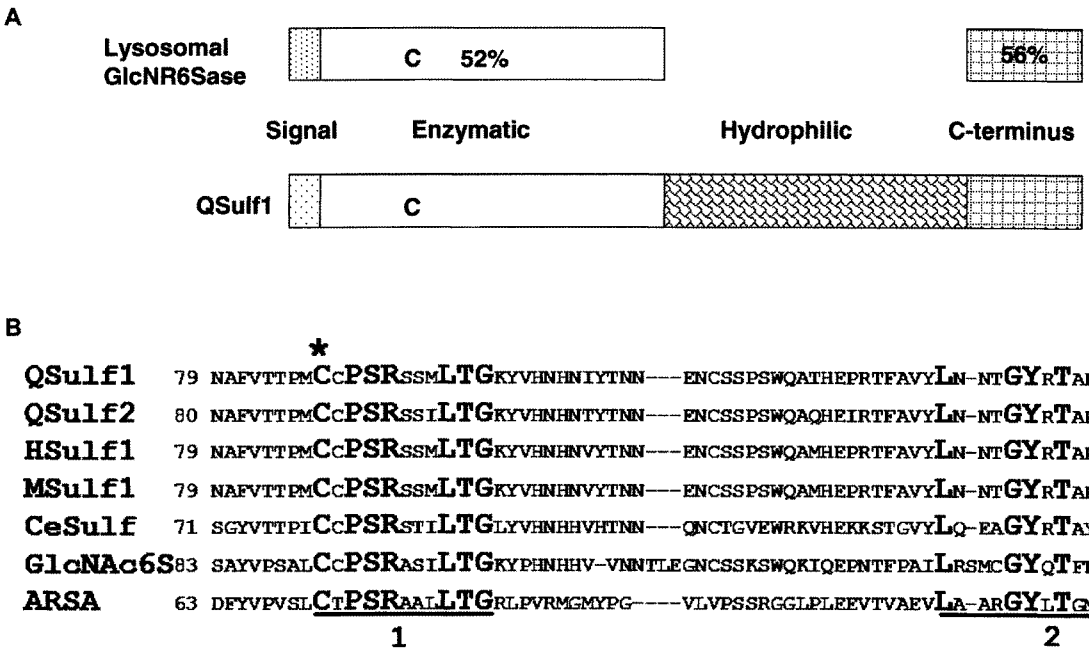

Figure 1 Domain structure and sequence homology comparisons of cell surface Sulfs and lysosomal sulfatases. (A) Sulfs and lysosomal GlcNR6Sase share sequence homology in the enzymatic domain including the critical cysteine residue ("C") that normally undergoes formalglycine modification, as well as in the C-terminal domain. Sulfs also have characteristic secretion signal peptide, distinct from the lysosomal targeting peptide of GlcNR6Sase, and a unique hydrophilic domain. (B) Two signature sequences in the catalytic site of the enzymatic domain (labeled 1 and 2) are conserved in all sulfatases. The critical formalglycine-modified cysteine residue in domain 1 is marked by a star. Sulf sequences in the catalytic site are conserved across the species and are more homologous to the lysosomal heparan sulfatase, GlcNR6Sase, than to aryl sulfatase, ARSA, and other sulfatases with different substrate specificities.

III. Expression and Enzymatic Activity of Sulf Enzymes

Sulf enzymes are functionally distinct from other sulfatases, including GlcNR6Sase, in their restricted expression in stem cells, in their localization on the cell surface, and in their substrate specificity and activity as heparan sulfate-specific 6-*O*-endosulfatases (9–11,14). In avian and mouse embryos, *Sulf1* is expressed dynamically in somite muscle progenitors and motor neuron progenitors under the control of Sonic hedgehog signaling, as well as in the notochord, floor plate, and the limb bud (9; unpublished data). *Sulf2* has overlapping, localized patterns of expression in neural and mesodermal tissues (unpublished data). The dynamic, lineage-specific expression of *Sulf1* and *Sulf2* in embryonic neural and mesodermal (somite) tissues provided initial evidence that Sulf proteins have developmental regulatory functions in stem cell progenitor specification in embryonic tissues, as confirmed by antisense gene knockdown experiments described below (9). In adult mice and humans, *Sulf1* and *Sulf2* mRNAs are expressed in a diversity of adult tissues, including muscle, digestive tract, ovaries, uterus, testis, and brain (10,12), although the specific populations of cells expressing *Sulf1* and *Sulf2* within these tissues remain to be defined.

Sulf enzymes are secreted and docked on the cell surfaces of expressing cells (9,11,12,15). Cell surface docking is controlled by HD domain interactions with cell surface components that are not yet defined, but do not involve GAGs (9). The cell surface localization of Sulf on expressing cells suggests its cell autonomous function. Supporting this interpretation, QSulf1 expression has been shown to modify the 6-*O*-sulfation states of HS of expressing cells (11), but not neighboring cells, as assayed by loss of cell surface 10E4 epitope expression (11). Rosen's group (10) reported their controversial results that human HSulf1 and HSulf2 proteins expressed in tissue culture cells in part are secreted into the medium, suggesting that HSulfs can function non-cell autonomously, leaving open the possibility that HSulfs modify HS on neighboring, nonexpressing cells.

Enzymological studies reveal that Sulfs have unique 6-*O*-endosulfatase activities that functionally distinguish Sulf enzymes from lysosomal GlcNR6Sase, which is a 6-*O*-exosulfatase (11). Heparan Sulfate degradation is a process that is initiated by restricted endo-β-D -glucuronidase cleavage by a "heparanase" that may act extracellularly as well as intracellularly (17). Further degradation of the resultant oligosaccharides is accomplished by the concerted action of a series of lysosomal glycosidases and sulfatases that all operate in exolytic fashion (18). By contrast, Sulf enzymes differ from the lysosomal sulfatases by their endolytic mode of action during postbiosynthetic modification of HS chains (11).

The Sulfs were predicted to act on GlcN 6-*O*-sulfate residues in HS based on their sequence homology with lysosomal GlcNR6Sase, an exoenzyme that removes 6-*O*-sulfate groups from the nonreducing-terminal GlcN residue of HS, heparin, and keratan sulfate chains (9,18). The first evidence indirectly implicating HS as a physiological target for QSulf1 was obtained from studies of QSulf1 effects on the cellular responsiveness to HS-dependent Wnt-signaling (9). Biochemical and cell-biologic studies subsequently identified QSulf1 as an HS-specific 6-*O*-endosulfatase

that selectively removes 6-*O*-sulfate groups from GlcNS6S residues within a subdomain of cell-associated HS chains (11). Detailed structural analyses showed that QSulf1 preferentially releases 6-*O*-sulfate groups from the trisulfated -IdoA2S-GlcNS6S- units, with less pronounced activity on -GlcA-GlcNS6S- units, and no detectable effect on -IdoA-GlcNS6S- sequences. 6-*O*-sulfated GlcNAc or GlcNS residues within the alternating NA/NS domains are not targeted by QSulf1 (Fig. 2) (14). These findings suggested that the target disaccharide unit occurs predominantly in -GlcNS ± 6S-IdoA2S-Glc NS6S-IdoA ± 2S-GlcN-sequences within NS-domains. QSulf1 is an endosulfatase and, in contrast to the lysosomal GlcNR6Sase, does not desulfate the monosaccharide substrate GlcNAc6S (11). The pH optimum for Sulf enzyme activity is in the neutral range, consistent with an extracellular function, and the catalytic activity depends on the conserved cysteine residue in the active site. Additionally, QSulf1 is able to release sulfate groups from cell-associated HSPG, confirming its role as a postbiosynthetic modifier of extracellular HS chains (11). Human Sulf1 and Sulf2 enzymes were found to desulfate -IdoA2S-GlcNS6S- units in heparin (10), which can be considered an extended *N*-sulfated HS sequence rich in -IdoA2S-GlcNS6S- units. The current challenge is to define more exactly the sequence specificity of Sulf1 and Sulf2 on biologic HS substrates to understand the molecular basis for Sulf function in the modification of HS interactions with FGF, EGF, and Wnt signaling ligands and receptors, as discussed later.

IV. Signaling Regulatory Functions of Extracellular Sulfatases

A. Sulf Enhancement of Wnt Signaling

Sulfs are positive regulators of Wnt signaling. Wnts are signaling ligands that control tissue patterning in embryos and stem cell renewal in adults (20,21). Nineteen Wnts have been identified in man and mice. In response to binding to its Frizzled receptor and complexed with an LDL receptor isoform, Lrp5/6, Wnts activate canonical pathway signaling by releasing β-catenin from the APC-axin-kinases degradation complex to activate nuclear transcription with its Lef/Tcf cofactors. Wnts also transduce noncanonical signal transduction through the planar cell polarity (PCP) and Wnt/Ca^{2+} pathways.

Both canonical and noncanonical Wnt signaling require extracellular HSPGs, as evidenced by loss of Wnt signaling activity in *Drosophila* mutant for the biosynthesis of either the protein core or HS side chains of HSPGs (3,22–24). Significantly, HS sulfation is required for Wnt signaling. The *Drosophila sulfateless* mutants, which are deficient in HS *N*-deacetylase/*N*-sulfotransferase, lack HS sulfation and display disrupted Wg signaling (22). In addition, blockade of HS sulfation by chlorate inhibits Wg/Wnt signaling in *Drosophila* and mammalian cultured cells (25,9). Considering Wnt proteins are posttranslationally lipid-modified (26), it is intriguing that HSPGs control Wnt signaling. Two models have been proposed to explain HSPGs regulation of Wnt signaling. Heparan sulfate proteoglycans, which bind to Wnt ligands, may stabilize and restrict the diffusion of the Wnt proteins.

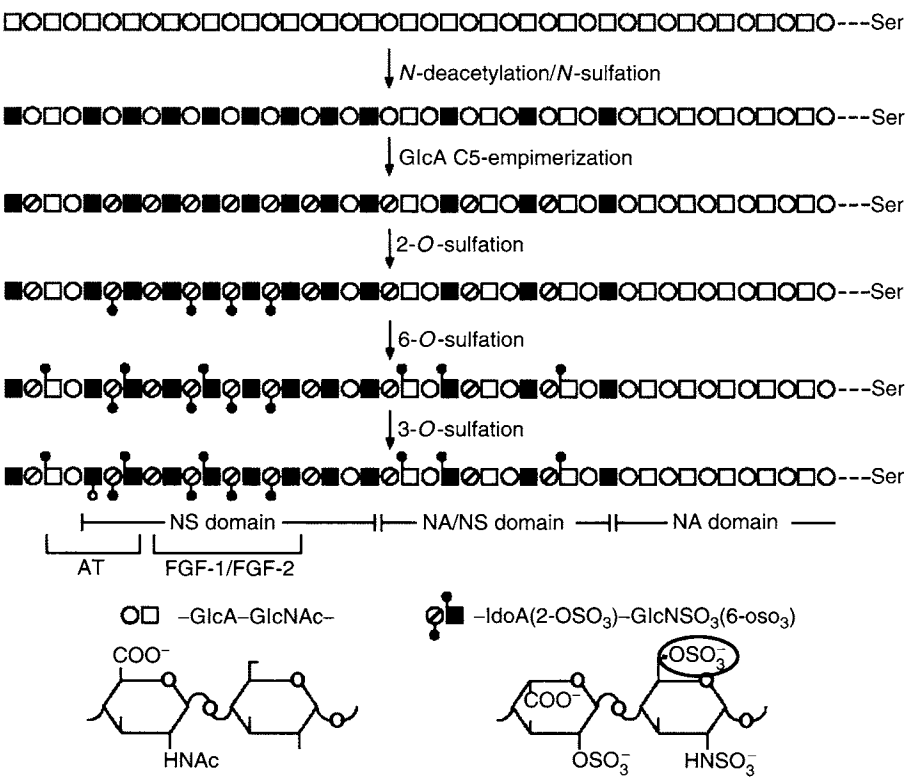

Figure 2 HS domain diversity and Sulf endosulfatase substrate activity. Structural heterogeneity of HS sulfation is generated during HS biosynthesis. The "linkage tetrasaccharide" for attachment of HS chains to core protein is not shown. The different sulfation structural domains (NA, NA/NS, and NS) are defined with regard to the distribution of GlcN *N*-substituents, as indicated. Also shown are domain regions implicated in binding of protein ligands, such as FGF-1/FGF-2 and antithrombin (AT). *Large circles*, hexuronic acid residues; *open squares*, GlcNAc residues, *closed small circles*, 2-*O*- and 6-*O*-sulfate groups, *open small circle*, single GlcN 3-*O*-sulfate group in the AT-binding sequence. Sulfs are endosulfatases that remove 6-*O*-sulfate groups (as indicated by the black oval) from trisulfated disaccharides that are prevalent in NS domain of HS chains.

Alternatively, HSPGs may function as coreceptors to promote the formation of Frizzled receptor–Wnt complexes (3).

QSulf1 is a positive regulator of canonical Wnt signaling through modification of the binding of Wnt ligands to cell surface HSPGs (11). QSulf1 expression in C2C12 myoblasts enhances Wnt1 canonical signaling by 2- to 3-fold above basal Wnt1 induction. Enzymatically inactive QSulf1(C-A) mutant protein does not enhance Wnt1 signaling, establishing that 6-*O*-endosulfatase activity of QSulf1 is required for its Wnt1 signaling activity. QSulf1 also is required for Wnt-responsive

gene expression in embryos. *QSulf1* antisense oligos block *MyoD* mRNA expression, but not *Myf5* expression in somite myogenic progenitors (9). *MyoD* expression is primarily controlled by Wnt signaling, while *Myf5*, like *QSulf1*, is a target gene of Sonic Hedgehog signaling.

Biochemical studies provide insight into the mechanisms of QSulf1 function in Wnt regulation. These studies show that QSulf1 6-*O*-endosulfatase activity reduces the binding affinity between Wnt8 ligand to HS chains of Glypican1 HSPG, in both *in vitro* and *in vivo* binding assays (11). Heparinase treatment totaly eliminates the interaction between Glypican1 and Wnt8, establishing that Glypican1 binds to Wnt8 through its HS chains and not its protein core. The binding of Glypican1 to Wnt8 is significantly reduced when Glypican1 is treated with enzymatically active QSulf1, and not by inactive QSulf1(C-A). In addition, cellular Wnt1 signaling is unaffected by extracellular chemically 6-*O*-desulfated heparin, whereas highly sulfated heparin or 2-*O*-desulfated heparin block Wnt1 signaling activity, providing further evidence that 6-*O*-sulfation of HS promotes Wnt binding and inhibits Wnt signaling. Together, these findings are consistent with a two-state "catch and presentation" model in which QSulf1 enzymatically converts cell surface HS from a high affinity Wnt binding state to a low affinity Wnt binding state that in turn mobilizes the presentation of Wnt ligand to the Frizzled receptor to activate signaling (Fig. 3).

B. Sulf Repression of FGF Signaling

Fibroblast growth factors (FGFs) constitute a family of signaling proteins of fundamental importance in embryonic development and adult physiology. A total of 23 FGFs and 4 FGF-receptors (FGFRs), receptor tyrosine kinases, are currently known (27). Fibroblast growth factors depend on HSPGs for cell-signaling activity. The formation of FGF–HSPG–FGFR ternary complexes at the cell surface leads to activation and phosporylation of the receptor tyrosine kinase that triggers various intracellular signaling cascades (28,29). Both the FGF and FGFR components of such complexes appear to interact with the same HS chain in tightly knit structures.

While the presence of sulfate groups in HS is clearly important for complex formation with the proteins, the need for distinct sulfation patterns on its HS chains remains an open question. Studies of ternary complex formation at different stages of mouse embryo development suggested that complexation of different FGF–FGFR pairs requires distinct HS structures (30). On the other hand, various FGF-dependent processes in development appear normal in 2-*O*-sulfotransferase- or GlcA C5-epimerase-deficient mice, in spite of severely perturbed HS structure (no 2-*O*-sulfated IdoA residues, but essentially unchanged overall sulfate density compared to wild-type HS) (31,32). Binding of FGFs alone to HS oligosaccharides is generally promoted by increased sulfate density (33–35). Fibroblast growth factor2 provides an interesting model, in that 2-*O*-sulfate groups alone suffice to mediate strong binding of the growth factor to HS, whereas 6-*O*-sulfate groups, in addition, are required to induce FGFR signaling (36). More recent findings suggested that *N*-sulfated HS oligosaccharides, depending on their *O*-sulfation patterns, could either promote or inhibit FGF-mediated cell proliferation (37).

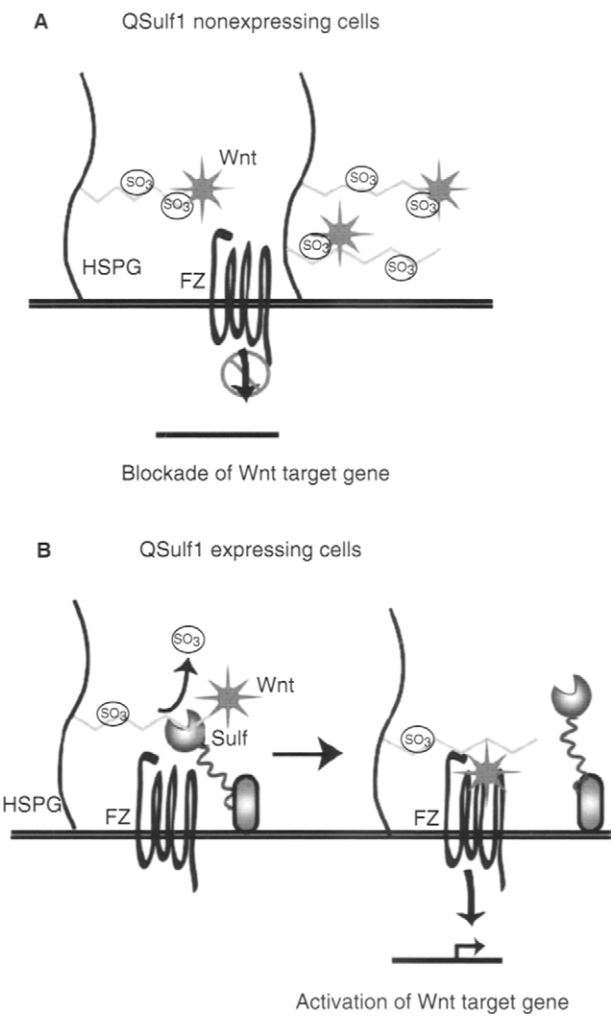

Figure 3 A two-state "catch and presentation" model of QSulf1 regulation of Wnt signaling. (A) In QSulf1-nonexpressing embryonic cells, HS chains on cell surface HSPGs are in a 6-*O*-sulfated state, which binds with high affinities to catch Wnt ligands, preventing functional interactions of bound Wnts with their Frizzled receptors. (B) In QSulf1-expressing cells, selective 6-*O*-desulfation activity of QSulf1 removes 6-*O*-sulfates from HS chains on cell surface HSPGs to convert HS to a low affinity binding state for Wnts. 6-*O*-desulfated HS then can present Wnt ligands to Frizzled receptor and can form functionally active Wnt–HS–frizzled receptor complexes for initiation of Wnt signal transduction.

Taken together, these findings indicate that sulfation of HS is essential for its ability to promote FGF signaling, and further, that signaling may be regulated by modulation of HS sulfation patterns.

Until recently, HS sulfation was thought to be exclusively controlled by the action of sulfotransferases during HS biosynthesis. The Sulf enzymes introduce a novel level of control in protein binding to HS. The Sulfs located at the cell surface, presumably close to HS chains, are strong candidates for roles as modulators of HS-mediated signaling. Indeed, over-expression of QSulf1 affects FGF-dependent signaling, although, contrary to Wnt signaling that is stimulated by QSulf1 (9), FGF-2 and FGF-4 signaling is suppressed. Expression of QSulf1 inhibits FGF-2- and FGF-4-dependent mesoderm induction in *Xenopus* embryos and FGF-2-induced angiogenesis in chick embryos (13). Furthermore, QSulf1 expression in *Xenopus* and expression of human Sulf1 in cancer cell lines result in down-regulation of the FGF-dependent activation of extracellular signal regulated kinase (ERK) (12,13,38). The inhibitory effect of QSulf1 on FGF signaling is dependent on catalytic sulfatase activity, as over-expression of catalytically inactive QSulf1, with the conserved cysteine residue in the active site exchanged for an alanine, has no effect on FGF-signaling (13).

Cell-surface HS that has been 6-*O*-desulfated by QSulf1 will still bind FGF-2 through 2-*O*-sulfate groups, but cannot bind receptor, which requires both 2-*O*- and 6-*O*-sulfate groups. Reduced binding affinity of 6-*O*-desulfated HS and its bound FGF ligand to FGFR1 receptor suppresses FGFR1 dimerization to block signal transduction. Thus, QSulf1 most likely inhibits HS-dependent FGF-signaling by attenuating formation of the FGF–HS–FGFR ternary complex (Fig. 4) (13).

C. Sulf1 Regulates Noggin Function to Enhance BMP Signaling

BMPs are TGF-β family signaling proteins that function cooperatively with Hedgehog, Wnt, and FGF to control progenitor stem cell differentiation in the embryo and adult tissues (3). BMP signaling activity is localized in embryos and tissues by Noggin and several other proteins that bind at high affinity to BMPs to inhibit their activity, to achieve spatially localized signaling (39). Noggin is a heparin binding protein, and enzymatic treatment of heparin with QSulf1 reduces the binding affinity of Noggin for heparin, establishing that binding is mediated through HS 6-*O*-sulfation (14). Additionally, QSulf1 expression significantly enhances BMP signaling response in Noggin-expressing cells, further supporting that QSulf1 is a positive regulator of BMP signaling. Studies to establish the *in vivo* regulatory function of Sulf enzymes in Noggin inhibition of BMP signaling remain to be undertaken.

V. Sulf Function in Tumor Growth and Angiogenesis

Heparan sulfate proteoglycans have a major role in tumor growth through their roles in cell attachment and migration, growth factor-dependent cell proliferation and angiogenesis (2). HSulf1 mRNA expression is differentially expressed in

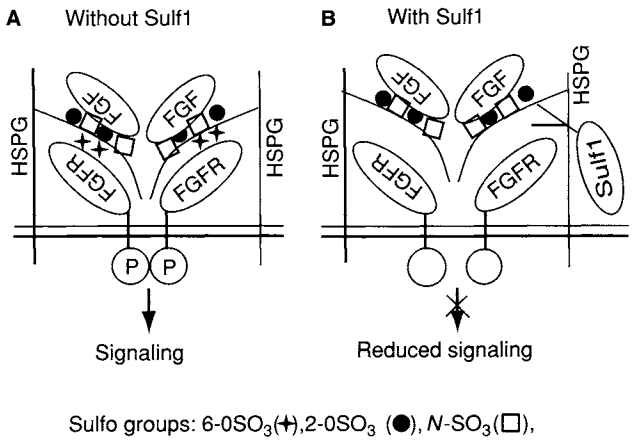

Figure 4 A "ternary complex inhibition" model for QSulf regulation of FGF signaling. A 2:2:2 model (two ligands, two HS chains, and two receptors) has been proposed for ternary complex formation of FGF-2–HS–FGFR1 during signaling. (A) In the absence of QSulf1 expression, sulfated HS chains on cell surface HSPGs promote FGF ligand–receptor interaction, receptor dimerization, and activation of intracellular signaling. (B) Expression of cell surface QSulf leads to the selective 6-*O*-desulfation of critical 6-*O*-sulfates from trisulfated disaccharides in the NS domain of HS chains on cell surface, reducing FGF ligand–receptor binding without effecting FGF ligand binding to HS. Reduced binding affinity of 6-*O*-desulfated HS and its bound FGF ligand to FGFR1 receptor suppresses FGFR1 dimerization and thus blocks receptor signal transduction.

different primary human tumors, suggesting that Sulf enzymes have diverse roles in tumorigenesis (12,38,40). A majority of ovarian cancers, hepatocellular carcinomas, and head and neck squamous carcinomas have down-regulated HSulf1 mRNA expression. Primary tumor cells from these carcinomas exhibit enhanced proliferation and motility in response to FGF and HGF, which also is an HS-regulated signaling ligand. Additionally, hepatocellular carcinomas and head and neck squamous cell carcinoma cell lines show resistance to staurosporine- and cisplatin-induced apoptosis (38,40). HSulf1 transfected carcinoma cells, however, becomes refractory to growth stimulation by FGF and HGF as well as sensitive to apoptosis by apoptotic inducers, providing further evidence for the negative signaling regulatory function of Sulf1. These findings, therefore, indicate that HSulf1 is a tumor suppressor for ovarian and hepatocellular carcinomas, and for head and neck squamous carcinomas. Finally, it is notable that QSulf1 enzymatic treatment of heparin produces modified heparin compounds that inhibit FGF-induced angiogenesis in chick embryo CAM graft assays (13), suggesting that Sulf-modified heparin compounds will be useful therapeutic drugs to inhibit growth of carcinomas as well as block tumor neovascularization.

In contrast to carcinomas, about 50% of pancreatic carcinomas have increased HSulf1 mRNA expression compared to normal pancreatic tissue. A significant number of pancreatic carcinomas have deregulated Hedgehog signaling, and likely are dependent on growth factor signaling that does not require HS, specifically insulin growth factors (41). In theses tumors, HSulf1 overexpression may have alterative pathological functions to potentiate cell migration and matrix detachment, to promote metastasis.

VI. CONCLUSIONS

The recent discovery of Sulf enzymes has opened up new avenues of investigation into the regulatory mechanisms of HSPG-mediated signaling in development and cancer. Future genetic, biochemical and cellular studies can be expected to provide additional insights into the role of HSPGs in extracellular signaling for stem cell progenitor growth and differentiation, as well as provide a basis for the development of novel cancer therapeutics.

References

1. Rapraeger AC. Heparan sulfate-growth factor interactions. Meth Cell Biol 2002; 69:83–109.
2. Sasisekharan R, Shriver Z, Venkataraman G, Narayanasami U. Roles of heparan-sulphate glycosaminoglycans in cancer. Nat Rev Cancer 2002; 2:521–518.
3. Lin X. Functions of heparan sulfate proteoglycans in cell signaling during development. Development 2004; 131:6009–6021.
4. Esko JD, Lindahl U. Molecular diversity of heparan sulfate. J Clin Invest 2001; 108:169–173.
5. Brickman YG, Ford MD, Gallagher JT, Nurcombe V, Bartlett PF, Turnbull JE. Structural modification of fibroblast growth factor-binding heparan sulfate at a determinative stage of neural development. J Biol Chem 1998; 273:4350–4359.
6. Merry CL, Lyon M, Deakin JA, Hopwood JJ, Gallagher JT. Highly sensitive sequencing of the sulfated domains of heparan sulfate. J Biol Chem 1999; 274:18455–18462.
7. Safaiyan F, Lindahl U, Salmivirta M. Structural diversity of *N*-sulfated heparan sulfate domains: distinct modes of glucoronyl C5 epimerization, iduronic acid 2-*O*-sulfation, and glucosamine 6-*O*-sulfation. Biochemistry 2000; 39:10823–10830.
8. Jayson GC, Vives C, Paraskeva C, Schofield K, Coutts J, Fleetwood A, Gallagher JT. Coordinated modulation of the fibroblast growth factor dual receptor mechanism during transformation from human colon adenoma to carcinoma. Int J Cancer 1999; 82:298–304.
9. Dhoot GK, Gustafsson MK, Ai X, Sun W, Standiford DM, Emerson CP, Jr. Regulation of Wnt signaling and embryo patterning by an extracellular sulfatase. Science 2001; 293:1663–1666.
10. Morimoto-Tomita M, Uchimura K, Werb Z, Hemmerich S, Rosen SD. Cloning and characterization of two extracellular heparin-degrading endosulfatases in mouse and human. J Biol Chem 2002; 277:49175–49185.

11. Ai X, Do A, Lozynska O, Kusche-Gullberg M, Lindahl U, Emerson CP, Jr. QSulf1 remodels the 6-*O* sulfation states of cell surface heparan sulfate proteoglycans to promote Wnt signaling. J Cell Biol 2003; 162:341–351.
12. Lai J, Chien J, Staub J, Avula R, Greene EL, Matthews TA, Smith DI, Kaufmann SH, Roberts LR, Shridhar V. Loss of HSulf-1 up-regulates heparin-binding growth factor signaling in cancer. J Biol Chem 2003; 278:23107–23117.
13. Wang S, Ai X, Freeman SD, Pownall ME, Lu Q, Kessler DS, Emerson CP, Jr. QSulf1, a heparan sulfate 6-*O*-endosulfatase, inhibits fibroblast growth factor signaling in mesoderm induction and angiogenesis. Proc Natl Acad Sci USA 2004;101:4833–4838.
14. Viviano BL, Paine-Saunders S, Gasiunas N, Gallagher J, Saunders S. Domain-specific modification of heparan sulfate by Qsulf1 modulates the binding of the bone morphogenetic protein antagonist Noggin. J Biol Chem 2004; 279: 5604–5611.
15. Ohto T, Uchida H, Yamazaki H, Keino-Masu K, Matsui A, Masayuki M. Identification of a novel nonlysosomal sulphatase expressed in the floor plate, choroid plexus and cartilage. Genes Cells 2002; 7:173–185.
16. Braquart-Varnier C, Danesin C, Clouscard-Martinato C, Agius E, Escalas N, Benazeraf B, Ai X, Emerson C, Cochard P, Soula C. A subtractive approach to characterize genes with regionalized expression in the gliogenic ventral neuroepithelium: identification of chick sulfatase 1 as a new oligodendrocyte lineage gene. Mol Cell Neurosci 2004; 25:612–628.
17. Vlodavsky I, Goldshmidt O, Zcharia E, Atzmon R, Rangini-Guatta Z, Elkin M, Peretz T, Friedmann Y. Mammalian heparanase: involvement in cancer metastasis, angiogenesis and normal development. Semin Cancer Biol 2002;12:121–129.
18. Freeman C, Hopwood J. Human alpha-L-iduronidase. Catalytic properties and an integrated role in the lysosomal degradation of heparan sulphate. Adv Exp Med Biol 1992; 313, 121–134.
19. Schmidt B, Selmer T, Ingendoh A, von Figura K. A novel amino acid modification in sulfatases that is defective in multiple sulfatase deficiency. Cell 1995; 82:271–278.
20. Reya T, Clevers H. Wnt signalling in stem cells and cancer. Nature 2005; 434:843–850.
21. Nusse R. Wnt signaling in disease and in development. Cell Res 2005; 15: 28–32.
22. Lin X, Perrimon N. Dally cooperates with Drosophila Frizzled to transduce Wingless signaling. Nature 1999; 400:281–284.
23. Tsuda M, Kamimura K, Nakato H, Archer M, Staaz W, Fox B, Humphrey M, Olson S, Futch T, Kaluza V, Kaluza V, Siegfried E, Stam L, Selleck SB. The cell-surface proteoglycan Dally regulates Wingless signaling in Drosophila. Nature 1999; 400:276–280.
24. Baeg GH, Lin X, Khare N, Baumgartner S, Perrimon N. Heparan sulfate proteoglycans are critical for the organization of the extracellular distribution of Wingless. Development 2001; 128:87–94.
25. Reichsman F, Smith L, Cumberledge S. Glycosaminoglycans can modulate extracellular localization of the wingless protein and promote signal transduction. J Cell Biol 1996; 135:819–827.

26. Willert K, Brown JD, Danenberg E, Duncan AW, Weissman IL, Reya T, Yates JR III, Nusse R. Wnt proteins are lipid-modified and can act as stem cell growth factors. Nature 2003; 423:448–452.
27. Itoh N, Ornitz DM. Evolution of the Fgf and Fgfr gene families. Trends Genet 2004; 20:563–569.
28. Schlessinger J, Plotnikov AN, Ibrahimi OA, Eliseenkova AV, Yeh BK, Yayon A, Linhardt R, Mohammadi M. Crystal structure of a ternary FGF–FGFR–heparin complex reveals a dual role for heparin in FGFR binding and dimerization. Mol Cell 2000; 6:743–750.
29. Pellegrini L, Burke DF, von Delft F, Mulloy B, Blundell TL. Crystal structure of fibroblast growth factor receptor ectodomain bound to ligand and heparin. Nature 2000; 407:1029–1034.
30. Allen BL, Rapraeger AC. Spatial and temporal expression of heparan sulfate in mouse development regulates FGF and FGF receptor assembly. J Cell Biol 2003; 163:63–648.
31. Bullock SL, Fletcher JM, Beddington RS, Wilson VA. Renal agenesis in mice homozygous for a gene trap mutation in the gene encoding heparan sulfate 2-sulfotransferase. Genes Dev 1998; 12:1894–1906.
32. Merry CL, Bullock SL, Swan DC, Backen AC, Lyon M, Beddington RS, Wilson VA, Gallagher JT. The molecular phenotype of heparan sulfate in the Hs2st−/− mutant mouse. J Biol Chem 2001; 276:35429–35434.
33. Kreuger J, Salmivirta M, Sturiale L, Gimenez-Gallego G, Lindahl U. Sequence analysis of heparan sulfate epitopes with graded affinities for fibroblast growth factors 1 and 2. J Biol Chem 2001; 276:30744–30752.
34. Jemth P, Kreuger J, Kusche-Gullberg M, Sturiale L, Gimenez-Gallego G. Lindahl U. Biosynthetic oligosaccharide libraries for identification of protein-binding heparan sulfate motifs. Exploring the structural diversity by screening for fibroblast growth factor (FGF)1 and FGF-2 binding. J Biol Chem 2002; 277:30567–30573.
35. Kreuger J, Jemth P, Sanders-Lindberg E, Eliahu L, Ron D, Basilico C, Salmivirta M, Lindahl U. Fibroblast growth factors share binding sites in heparan sulfate. Biochem J 2005; 389:145–150.
36. Guimond SE, Turnbull JE. Fibroblast growth factor receptor signalling is dictated by specific heparan sulphate saccharides. Curr Biol 1999; 9: 1343–1346.
37. Pye DA, Vives RR, Hyde P, Gallagher JT. Regulation of FGF-1 mitogenic activity by heparan sulfate oligosaccharides is dependent on specific structural features: differential requirement for the modulation of FGF-1 and FGF-2. Glycobiology 2000; 10:1183–1192.
38. Lai J, Chien J, Strome SE, Staub J, Montoya DP, Greene EL, Smith DI, Roberts LR, Shridhar V. HSulf-1 modulates HGF-mediated tumor cell invasion and signaling in head and neck squamous carcinoma. Oncogene 2004; 23:1439–1447.
39. Balemans W, Van Hul W. Extracellular regulation of BMP signaling in vertebrates: a cocktail of modulators. Dev Biol 2002; 250:231–250.
40. Lai JP, Chien JR, Moser DR, Staub JK, Aderca I, Montoya DP, Matthews TA, Nagorney DM, Cunningham JM, Smith DI, Greene EL, Shridhar V, Roberts LR. hSulf1 Sulfatase promotes apoptosis of hepatocellular cancer

cells by decreasing heparin-binding growth factor signaling. Gastroenterology 2004; 126:231–248.
41. Li J, Kleeff J, Abiatari I, Kayed H, Giese NA, Felix K, Giese T, Buchler MW, Friess H. Enhanced levels of Hsulf-1 interfere with heparin-binding growth factor signaling in pancreatic cancer. Mol Cancer 2005; 4:14.

Chemistry and Biology of Heparin and Heparan Sulfate
H.G. Garg, R.J. Linhardt and C.A. Hales (Editors)

Chapter 9

Heparan Sulfate Degradation by Heparanases

KAREN J. BAME

School of Biological Sciences,
University of Missouri-Kansas City,
Kansas City, MO, USA

I. Heparanase Proteins

Interactions between the extracellular environment and the cell surface influence the growth and differentiation of cells and their organization into organs and tissues. As components of basement and plasma membranes, heparan sulfate proteoglycans (HSPGs) are important players in these functional interactions (1,2). The anionic heparan sulfate (HS) glycosaminoglycans bind to extracellular matrix and cell surface proteins (1,3), providing a framework for cell–cell or cell–matrix interactions, and initiating processes that regulate cell shape and motility (4). As receptors, cell surface and matrix HSPG bind a variety of growth factors, chemokines, and enzymes and regulate processes as diverse as cell growth and differentiation, lipoprotein metabolism, and blood coagulation (1–6). Because of their functional and structural roles, the expression of cell associated and matrix HSPGs must be tightly regulated. One way to do this is to degrade the HS glycosaminoglycan through the action of intracellular and extracellular endoglycosidases or heparanases. Heparanases may remove all binding sites from proteoglycans by cleaving the HS chain off the core protein, or they may destroy specific binding sites when degrading the chain to shorter oligosaccharides.

Heparanase activities have been described in a number of cells and tissues since the 1970s (7). However, because of difficulties in designing simple assays and maintaining enzymatic activity, it was not until the late 1990s that several groups reported the purification of a 40 to 50 kDa glycoprotein with heparanase activity from placenta (8) and platelets (9,10). When the proteins were cloned (11–14) it

became clear the enzymes were identical. This novel enzyme has been given the designation heparanase 1 or Hpa1, and in addition to humans, has been found in mouse, rat, bovine, and chicken. The human Hpa1 gene has been localized to chromosome 4q22 (15) and consists of 14 exons spanning over 50 kb. Differential splicing of exon 1 and exon 14 generate two Hpa1 transcripts, a 1.7-kb mRNA and a 5.0-kb mRNA (15). Northern analysis and RT-PCR studies show Hpa1 expression is primarily restricted to placenta and lymphoid organs (12,13,16,17), where the 1.7-kb transcript is expressed. The restriction of Hpa1 expression to lymphoid tissues suggests it primarily acts outside the cell, degrading basement membrane and extracellular HSPG at sites of inflammation or injury, releasing growth factors from their extracellular stores, and regulating embryo implantation and pregnancy (17–20). Increased Hpa1 mRNA expression is also observed in a variety of human carcinomas (16,19,20), suggesting the enzyme plays a role in tumor progression and metastatic potential.

The apparent lack of Hpa1 expression in normal, non-lymphoid tissue raises the question of whether there are other heparanase enzymes. In 1995, Hoogewerf et al. (21) reported the purification of a 9 to 10 kDa heparanase from platelets. This enzyme was identified as the chemokine CTAP-III (connective tissue activating peptide-III), which is derived from proteolytic processing of platelet basic protein and participates in inflammation, wound healing, and growth regulation (22). Although expression of a CTAP-III fusion protein in *Escherichia coli* confirmed the peptide has heparanase activity (23), the importance and role of this enzyme is unclear. Others have shown that the major heparanase activity in platelets can be attributed to Hpa1 (9,24), while studies with neutrophils show heparanase activity is associated with CTAP-III but as the larger 80 kDa chemokine precursor (25). It may be that only certain types of immune cells express an enzymatically active CTAP-III to supplement the actions of Hpa1 heparanase.

A putative Hpa2 heparanase, which is 35% identical to Hpa1, was identified by a BLAST search using the Hpa1 amino acid sequence (16). Analysis of the Hpa2 transcripts shows it may be differentially spliced, generating three different Hpa2 proteins (16). RT-PCR shows Hpa2 mRNA is expressed in a different set of tissues than hpa1 mRNA (16), suggesting it may be the primary enzyme to degrade HSPGs in nonlymphoid organs. However, it is still unknown whether the hpa2 mRNA actually encodes a functional heparanase enzyme.

Intracellular heparanase activities, responsible for the catabolism of endocytosed cell surface HSPGs, have been studied in Chinese hamster ovary (CHO) cells (7). Analysis of the short HS products generated in CHO cells (26) suggested there may be multiple heparanase enzymes, and indeed two activities that could be separated by cation exchange chromatography, C1A and C2, were purified (27). Since Northern analysis of purified CHO mRNA did not detect an hpa1 transcript (28), the CHO heparanase activities were proposed to be different proteins. In support of this hypothesis, initial amino acid sequence data and protein characterization studies suggested C1A heparanase was homologous to the N-terminal domain, or FERM-domain, of ezrin, radixin, and moesin, proteins that link the cytoskeleton to the plasma membrane (28). However, recent study shows that while

the C1A and C2 heparanases share properties with FERM-domains (28), they are the hamster homologues of Hpa1 (KJ Bame, in preparation). This finding suggests the intracellular catabolism of HSPGs in nonlymphoid tissue is due to low levels of expressed Hpa1 rather than the expression of a different heparanase enzyme.

Hpa1 appears to be the primary heparanase in mammals, so this chapter will examine what is known about the expression, activity, and functions of this enzyme. Because Hpa1 is not highly expressed in normal cells (12,13,16,17), most of these studies have been done in tumor cell lines or in cell lines engineered to overexpress recombinant protein. Therefore, the reader needs to keep in mind that some of these findings may be due to overexpression of the enzyme and may not apply to those tissues that express low levels of Hpa1.

II. Synthesis of Heparanase 1

A. Transcriptional Regulation

In 2002, a 3.5-kb Hpa1 promoter was cloned from a thyroid tumor cell line, and analysis of the GC-rich, TATA-less promoter (Fig. 1) suggested transcription factors of the Sp1 and Ets families act cooperatively to regulate basal expression of the Hpa1 gene (29). A minimal promoter region from −1 to −310 bp was defined, which contains three binding sites for Sp1 (29), a transcription factor that binds to GC boxes and plays a role in transcription of many genes (30). This minimal promoter region also contains two binding sites for the Ets family member GA-binding protein (GABP) (29), which has been shown to regulate transcription of both lineage-restricted and "housekeeping" genes (31). Functional studies suggest GABP cooperates with Sp1 to regulate the promoter activity of the Hpa1 gene (29), which is likely due to physical interactions between the transcription factors (31). Studies with breast cancer cell lines identified two additional Ets binding sites upstream of the GABP sites in the minimal promoter (Fig. 1) that are functionally important in regulating Hpa1 expression (32).

In addition to the factors regulating basal transcription of the Hpa1 gene, studies have been done to see what factors might be involved in induction of

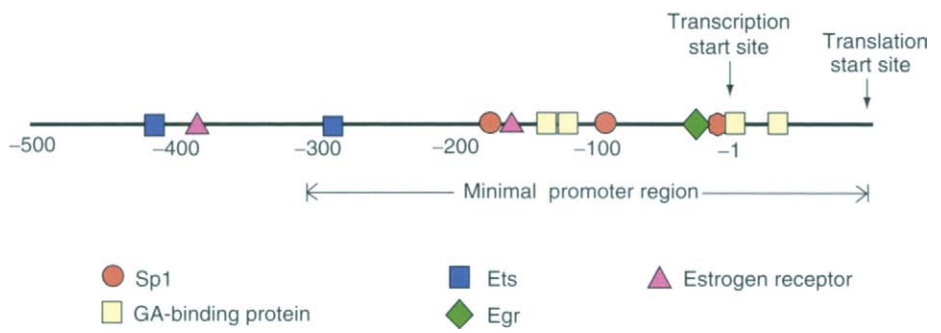

Figure 1 Human heparanase 1 promoter.

heparanase expression in physiological and pathological processes. When Jurkat T cells are incubated with PMA to mimic T cell activation there is an increase in Hpa1 expression (33). Using a 280-bp fragment of the Hpa1 promoter, the increase was shown to be due to an Egr1 (early gene response) transcription factor binding to the Egr binding site directly upstream of the first Sp1 site (33) (Fig. 1). The increased expression is inhibited if the cells are exposed to the MEK inhibitor PD98059, providing evidence that induction of Hpa1 in T cell activation may occur through the MEK/ERK pathway (33). Heparanase expression in endothelial cells is induced by inflammation, and studies suggest oleic acid plays a role in this process by enhancing the interaction of Sp1 with the Hpa1 promoter (34). Steroid hormones may also be involved in regulating Hpa1 expression, since physiological concentrations of estrogen induced the synthesis of Hpa1 mRNA in breast carcinoma cell lines with active estrogen receptors but not in cell lines lacking the receptor (35). The authors of this study (35) identified four putative estrogen response elements in the 1700-bp upstream of the transcription start site (two sites are shown in Fig. 1), but they did not do any experiments to identify which sites were involved in the induced expression of the enzyme.

Studies with carcinoma cell lines and tumor tissue also suggest the expression of Hpa1 may be regulated by the methylation state of the Hpa1 promoter. The 483-bp sequence immediately upstream of the translation start site defines a CpG island (36,37), a cluster of generally underrepresented CpG dinucleotides. These islands are often associated with the 5′-region of housekeeping and tissue-specific genes, and it has been shown that methylation of the CpG sequences correlates inversely with transcriptional activity (36). Studies examining the Hpa1 promoter in 22 human cancer cell lines found a good correlation between heparanase activity and the methylation state of the promoter (37). Similar results were seen in studies examining samples of prostate cancer and benign prostate hyperplasia, where overall the Hpa1 promoter was more methylated in the benign samples than the cancer tissue (38). In studies where heparanase-minus cells with hypermethylated promoters were incubated in media containing the methylation inhibitor 5-aza-2dC, the Hpa1 promoters became hypomethylated, and this was accompanied by increased expression of heparanase activity and protein (37–39). These findings suggest the low levels of heparanase mRNA, seen in most normal human tissues, (12,13,16,17) may be maintained by DNA methylation, and that demethylation may play a role in the increased synthesis of Hpa1 seen in human cancers.

B. Posttranslational Processing

Cloning showed the 50 kDa Hpa1 enzyme was encoded by a 65 kDa proheparanase (11,12), suggesting proteolytic processing was necessary to generate the active enzyme (Fig. 2). Attempts to express active enzyme from an engineered cDNA that only encoded the 50 kDa portion of the proheparanase were unsuccessful (12), indicating sequences at the N-terminal end of the protein were required. The first clue of the importance of this N-terminal portion came from studies of the enzyme purified from platelet lysates, which showed an 8 kDa peptide was associated with

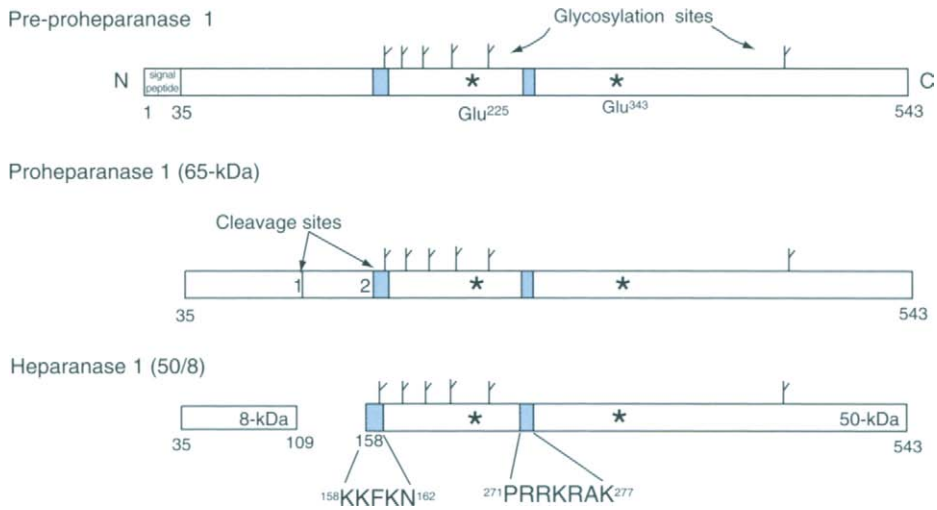

Figure 2 Posttranslational processing of human Heparanase 1 protein. The proposed active site residues, Glu^{225} and Glu^{343} are indicated by asterisks. The shaded boxes show the location of the two proposed HS binding sequences, $K^{157} - N^{162}$ and $P^{271} - K^{277}$.

the purified 50 kDa protein (40). Analysis of the purified 8 kDa peptide showed it was derived from the N-terminal end of the 65 kDa proheparanase (40) and suggested that both the 8 kDa and 50 kDa pieces were required for active enzyme. This hypothesis was confirmed by expression studies in baculovirus-infected Sf9 cells (41) and mammalian HEK 293 cells (42), which showed active heparanase required coexpression of both the 8 kDa and 50 kDa subunits. Subsequent studies with a proheparanase cDNA, bioengineered to contain tobacco etch virus–protease cleavage sequences at the normal processing site, showed proteolytic cleavage at both sites is required to generate the active enzyme (43).

The structural requirements for proheparanase processing have been examined by site-directed mutagenesis studies using recombinant proteins transiently expressed in JAR cells (44). Neither protein processing nor enzyme activity is affected when mutations are made at or near cleavage site 1 (Fig. 2), suggesting a relatively nonspecific protease acts at this site. While mutagenesis studies show the amino acid at position 157 is not critical, cleavage at site 2 does require a bulky, hydrophobic residue at position 156, suggesting a capthepsin-L-like activity is responsible (44). Additional evidence for a cysteine protease activity in Hpa1 activation is that cathepsin inhibitors prevent processing and activation of proheparanase when the protein is transiently expressed in JAR cells or incubated with JAR cell extracts (44), and purified recombinant proheparanase is converted to a processed, active form when incubated with partially purified cathepsin-L (44).

How does proteolytic processing activate Hpa1? Sequence analysis and secondary structure predictions suggest Hpa1 is a member of the glycosyl hydrolase clan, GH-A (45). Members of this clan have been proposed to have an $(\alpha/\beta)_8$ TIM-barrel fold architecture, and within the 50 kDa subunit there is clear homology for six (α/β) units (45). Since secondary structure predictions indicate the presence of a $(\beta/\alpha/\beta)$ element in the 8 kDa subunit, Nardella et al. (43) hypothesized proteolytic processing may be a mechanism to provide the two additional (α/β) folds found in the classical $(\alpha/\beta)_8$ motif. To test this hypothesis, they designed single-chain heparanase variants, where residues 110-156 were removed and replaced with short linker peptides chosen by multiple sequence alignment (43). One of the linker sequences came from *Hirudinaria manillensis* hyaluronidase, an enzyme with 35% sequence identity to Hpa1 but active without proteolytic processing. Two of the six recombinant proteins tested were active as single-chain polypeptides, including the variant with the *H. manillensis* sequence (43). These results support the notion that the 8 kDa N-terminal subunit is contributing the missing structural units of the TIM barrel fold to generate the active enzyme. To prove this hypothesis, however, the X-ray crystal structure of the Hpa1 protein must be solved.

In addition to providing the additional structural elements, proteolytic processing of proheparanase may be necessary to generate the HS substrate-binding site. When the human Hpa1 amino acid sequence is mapped onto the three-dimensional structure of the *Penicillium simplicissimum* endo-1,4-β-xylanase, two basic amino acid clusters are predicted to be on the top of the TIM-barrel fold, in proximity to the proposed active site (45). One of these clusters is the N-terminal end of the 50 kDa subunit, residues 158–162 (Fig. 2). Thus, proteolytic processing of proheparanase may be necessary for exposing or altering the structure of these basic residues so they can participate in binding the negatively charged glycosaminoglycan substrate. In support of this hypothesis, expression studies show if the 50 kDa subunit has extra amino acids at the N-terminal end it is not active (41,44), suggesting these additional residues prevent HS from binding to the enzyme.

Hpa1 was originally purified using ConA chromatography (8–10), suggesting the protein was glycosylated, and indeed, the cloned human Hpa1 has six potential *N*-glycosylation sites (Fig. 2). Studies indicate all six sites are glycosylated when the human protein is expressed in baculovirus-infected Sf9 cells (41) and HepG2 cells (46) and that glycosylation is not required for heparanase activity (11,41,46). Incubation of recombinant protein with Endo H or PNGase F showed the Hpa1 protein expressed in HepG2 cells has both high mannose and complex *N*-linked oligosaccharides (46), but further analysis of the type of oligosaccharide at each site has not been done. The Hpa1 enzymes from other species are also believed to be glycoproteins, but based on amino acid sequence they have fewer potential *N*-glycosylation sites than the human enzyme. There are four putative *N*-glycosylation sites on the mouse, rat, and bovine Hpa1 proteins and three *N*-glycosylation sites on the chicken enzyme.

C. Maturation Pathway

Based on the cells that express it, Hpa1 is thought to act primarily outside the cell, where it degrades basement membrane and extracellular matrix HSPGs (7). Two basic approaches have been taken to look at how Hpa1 is synthesized and secreted, and the cellular location where the proheparanase is proteolytically processed to the active enzyme. In one approach, tumor-derived cell lines that endogenously express Hpa1 (47) or tumor-derived cell lines with transiently transfected or stably transfected human Hpa1 cDNA (46–49) are used to follow the synthesis and processing of the enzyme. In the other approach, normal or tumor-derived cell lines are incubated with purified, recombinant Hpa1 protein, and its internalization into the cell is examined (48–50). Together these studies propose a model for the synthesis of Hpa1 and its processing to the active enzyme (Fig. 3).

It was assumed Hpa1 was synthesized in the secretory pathway (Fig. 3) because of its signal sequence and the presence of N-linked oligosaccharides (Fig. 2). The first direct evidence for this synthetic route used immunoelectron microscopy and showed Hpa1 was present in the Golgi stacks of breast carcinoma

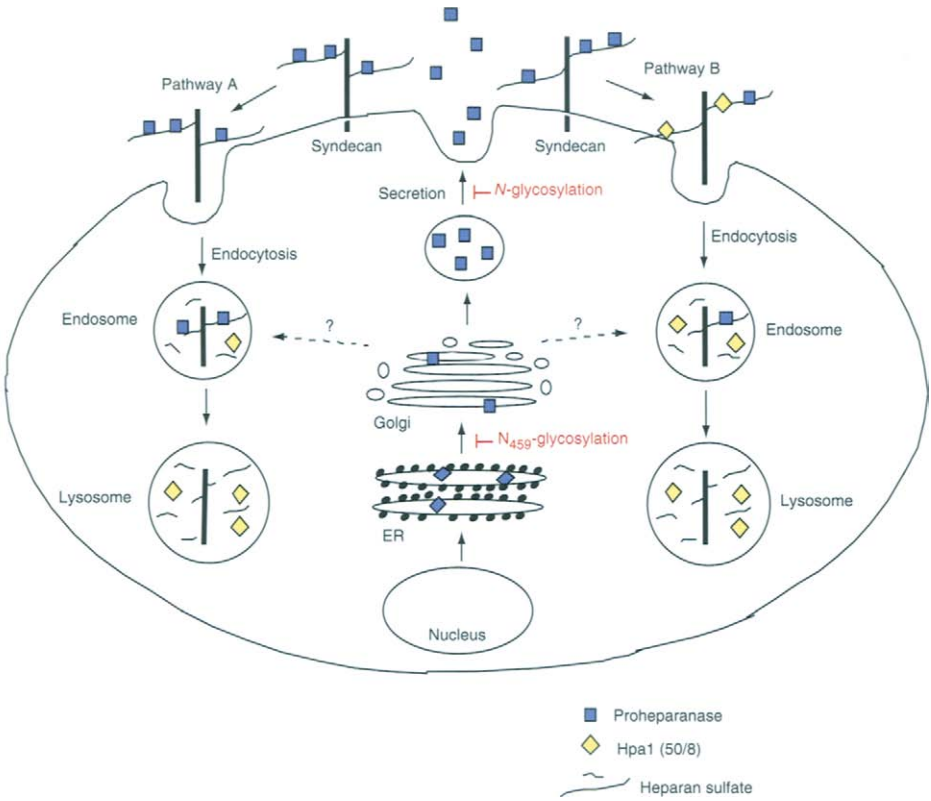

Figure 3 Maturation of Hpa1 to the processed, active enzyme.

MDA-231 cells that endogenously synthesize the enzyme (47). These studies also showed that when the cultured MDA-231 cells were treated with Brefeldin A, a compound that causes disassembly of the Golgi apparatus, there was a reduction in the synthesis of active Hpa1 (47), suggesting the integrity of the Golgi is necessary for the production of the enzyme. The glycosylation state of Hpa1 appears to play a role in its movement through the secretory pathway as well. If the asparagine at the C-terminal end of the 50-kDa protein, N^{459} (Fig. 2), is mutated to glutamine, Hpa1 is not efficiently transported from the ER to the Golgi in transiently transfected HeLa cells (46). Mutation of the other five *N*-glycosylation sites (Fig. 2) does not affect trafficking of the enzyme within the cell (46) but does affect whether Hpa1 is secreted. Lack of glycosylation at either N^{200} or N^{217} causes the secretion rate of Hpa1 to decrease to one-third of that observed with the fully glycosylated protein, and no enzyme is secreted from HepG2 cells if glycosylation is absent at N^{162}, N^{178}, or N^{238} (46). While the number of *N*-glycosylation sites varies on the other Hpa1 proteins that have been cloned, all four nonhuman Hpa1 enzymes have putative glycosylation sites at N^{162}, N^{217}, and N^{459}, suggesting glycosylation may play a role in the trafficking and secretion of all Hpa1 proteins.

The secretion of Hpa1 protein into the media of cultured cells appears to depend on what cells express it. While both HepG2 (46) and HEK-293 (49) cells secrete recombinantly expressed Hpa1 into the culture media, MDA-435 human breast carcinoma cells, U87 human glioma cells, and C6 rat glioma cells do not (49). These differences could be due to how much of the recombinant protein is being expressed, or whether the recombinant protein has been modified to contain a C-terminal tag (46). However, since secretion of Hpa1 from MDA-435, U97, and C6 cells is observed if heparin is included in the culture media (49), it suggests that instead of being released, the enzyme is retained at the plasma membrane by binding to cell surface HSPGs. This result is not surprising, since previous studies of heparanase activity suggested the enzyme bound to extracellular matrix or cell surface HSPGs, so that it would be available when inflammation or tissue damage occurred (17,51,52). Further evidence for the role of cell surface HSPG comes from studies that look at the internalization of recombinant enzyme. When purified recombinant Hpa1 is added to the culture media, it is taken up into a variety of cells (48–50). This uptake is inhibited if heparin is included in the media, the cells are pretreated with bacterial heparinases, or the studies are done in a CHO mutant, pgs-745, which does not synthesize HSPGs (49,50). Antibodies against cell associated HSPGs show syndecans move from the plasma membrane to intracellular vesicles after recombinant Hpa1 is added to the culture media of U87 glioma cells, while glypican remains at the cell surface (49), suggesting Hpa1 comes into the cell complexed to the HS chains on syndecan core proteins (Fig. 3). The authors of this study (49) also speculate the uptake of exogenous enzyme may be the mechanism by which nonlymphoid tissue obtains the Hpa1 needed for intracellular catabolism of cell associated HSPGs. However, since it appears that normal non-lymphoid tissues do express Hpa1, albeit at very low levels (K.J. Bame, in preparation), these cells most likely generate their own active Hpa1 through a similar synthesis and maturation pathway.

One important question is whether Hpa1 has been processed to the active form before it is secreted from the cell. Studies with tumor-derived cell lines suggest it has not (48,49). Using antibodies that can distinguish between proheparanase and processed Hpa1, Zetser and colleagues (48) used immunofluorescence and immunoblots to look at the uptake and proteolysis of recombinant Hpa1 added to the culture media of MDA-435 breast carcinoma cells. The cells rapidly take up the recombinant 65 kDa proheparanase, where it is initially associated with the plasma membrane. After 1 h, the proheparanase is distributed in the perinuclear region of the cell cytoplasm, but very little of it has been converted to the processed form. Processed Hpa1 starts to accumulate inside the cell after 2–3 h, indicating proteolysis is an intracellular event. Immunostaining shows cathepsin-D co-localizes with the processed Hpa1, suggesting the active enzyme is accumulating in lysosomes. To verify proteolysis occurs inside the cell, the authors looked at the processing of an Hpa1 variant that had the PDGF-receptor transmembrane domain added at the C-terminus of the 50 kDa subunit (48). Cells stably transfected with this cDNA express high-level of the Hpa1 variant at the plasma membrane, and it has been processed to the expected 50 kDa form (48). However, when the cells are incubated with chloroquine, a primary amine that raises lysosomal pH, the variant protein was not proteolytically cleaved (48), suggesting the appearance of the processed Hpa1 variant at the cell surface is due to membrane recycling from endosomal/lysosomal compartments. A different approach was employed by Gingis-Velitski et al. (49), who used pulse-chase studies to look at the synthesis and processing of Hpa1 in stably transfected HEK-293 cells. Initially, the 65-kDa proheparanase was the only species associated with the cell, and over the next 2 h the level of cell associated ^{35}S-proheparanase decreased, and began to appear in the culture media (49). Processed Hpa1 was not evident until 4 h of chase and was only found associated with the cell. From these studies, the authors concluded the enzyme is secreted as the 65 kDa proheparanase and must be endocytosed back into the cell to be proteolytically processed to the active form.

Together, these studies indicate the proteolytic processing of Hpa1 occurs after the secreted proheparanase is endocytosed into the cell (Fig. 3). However, it is not clear where inside the cells this processing occurs. An acidic compartment is necessary for proteolysis, since the conversion of the 65 kDa proheparanase to the processed species is inhibited when chloroquine, which raises lysosomal pH, or bafilomycin A, an inhibitor of the vacuolar protein pump, is added to the culture media (48). Zetser et al. (48) proposed lysosomes to be this acidic compartment (Fig. 3, pathway A), based on their immunofluorescence experiments and studies that showed LysoTracker dye co-localizes with Hpa1 in MDA-231 breast carcinoma cells (47). However, when the uptake of recombinant Hpa1 was examined in primary skin fibroblasts the internalized enzyme co-localized with markers for endosomes, not lysosomes (50), suggesting the proteolysis of proheparanase to the active enzyme occurs in this acidic compartment (Fig. 3, pathway B). Additional evidence that supports an endosomal location for proheparanase processing comes from studies looking at the intracellular catabolism of HSPGs. Pulse-chase studies in CHO cells show short HS chains are generated as soon as the cell surface HSPG

is internalized, suggesting heparanase-catalyzed degradation occurs very close to the cell surface, presumably in endosomes (53). When rat ovarian granulosa cells (54) or human skin fibroblasts (55) are cultured with chloroquine or NH_4Cl, agents which raise the intralysosomal pH, the long-HS chains are still cleaved to shorter oligosaccharides, suggesting the endoglycosidic cleavage occurs before the glycosaminoglycans enter the lysosome. An endosomal site for heparanase-catalyzed degradation was confirmed by fractionation studies in CHO cells (56). They showed the HS chains were already cleaved to the 5 to 6 kDa pieces before they were transported to lysosomes, and that heparanase activity co-localized with the endosomal fractions (56). Why do there appear to be different intracellular locations for Hpa1 processing? One possibility is the over-expression of recombinant Hpa1 protein, used to more easily follow the maturation of the enzyme, may overwhelm the cell's trafficking pathways so that proteins are localized to places where they are not found normally. Another possibility is the location of Hpa1 processing depends on the cells used to express or internalize the protein. The studies suggesting a lysosomal location of Hpa1 processing were done primarily with cultured cells derived from tumors. It has been observed in a wide variety of human tumors and transformed cells that lysosomal enzymes are redistributed to vesicles that are more closely associated with the plasma membrane (57). If the redistribution of lysosomal components had occurred in the tumor tissue, it may have been maintained when cells derived from the tumor were cultured. Thus, the processing of Hpa1 in these cells may appear to occur in lysosomes because the lysosomes have been affected.

These studies provide a working hypothesis for how Hpa1 is synthesized and proteolytically processed to the active enzyme; however, there are still some important unanswered questions. Expression of Hpa1 is observed in immune cells, such as neutrophils, macrophages, and platelets, which are thought to secrete active enzyme in order to degrade extracellular HSPGs (16,58–60). However, as yet there is no evidence that active, processed Hpa1 protein is released from cells. One possibility is that these immune cells secrete the proheparanase, which is then processed to the active enzyme extracellularly. A more likely explanation and one that fits with the intracellular location of heparanase activity in these cells (9, 58–60) is that the processed Hpa1 is stored in secretory lysosomes. Secretory lysosomes are found in cells of haemopoetic origin and, like conventional lysosomes, contain hydrolases and lysosome-specific membrane proteins (61). However, unlike conventional lysosomes, stimulation of the cell can cause these secretory lysosomes to fuse with the plasma membrane and release their contents into the extracellular environment. There are a variety of mechanisms to deliver molecules to secretory lysosomes (61), and it may be the secretion/endocytosis pathway proposed for Hpa1 is how active enzyme is generated for stimulated secretion in immune cells (58–60). Another question is whether an alternate maturation pathway exists, where the proheparanase is transported to endosomes directly from the *trans*-Golgi (Fig. 3). This pathway might be preferred in nonlymphoid tissues that only synthesize Hpa1 to degrade internalized cell associated HSPGs.

III. Heparanase 1 Catalytic Activity

A. Catalytic and Substrate Binding Sites

By the mid-1990s it was firmly established that heparanase activities in cells and tissues are β-endoglucuronidases that cleave long HS chains to 5 to 6 kDa oligosaccharides (7). Unlike the bacterial heparanases, which are polysaccharide lyases, Hpa1 is a hydrolytic enzyme that uses water to cleave the glycosidic bond (7). Therefore, it was not surprising when database searches indicated Hpa1 was related to other glycosyl hydrolases (45). Glycosyl hydrolases are grouped into families based on amino acid sequence similarities and then further grouped into clans based on known or predicted three-dimensional structure (62). Based on the amino acid sequence, Hpa1 is thought to be a member of family 51, which belongs to clan GH-A (45). Clan GH-A family members cleave the glycosidic bond via a general acid catalysis mechanism (Fig. 4), with retention of the anomeric configuration (62). Two amino acids are critical for catalysis, a proton donor and a nucleophilic base, which are usually glutamate or aspartate residues (62). Using the predicted three-dimensional structure of clan GH-A enzymes, site-directed mutagenesis identified two glutamate residues, E^{225} and E^{343} (Fig. 2), which act as the proton donor and nucleophile respectively (45). The importance of these residues in catalysis is supported by the fact that they are conserved in the nonhuman Hpa1 proteins.

Hpa1 has two regions of clustered basic amino acids (17,45,63) that conform to HS-binding protein consensus sequences (64), suggesting they may be involved in binding the HS substrate. When the human sequence is mapped onto the three-dimensional structure of a clan GH-A member, both clusters, residues 158–162 and residues 271–277 (Fig. 2) are found close to the putative active site (45). Studies with competitor peptides and deletion mutants indicate both sequences are important for enzyme–HS interactions (63). If a peptide of residues 158–172, corresponding to the first basic cluster, is included in the enzyme assay, heparanase activity is inhibited (63), suggesting this cluster, found at the N-terminus of the 50 kDa subunit (41,44), is important for catalytic activity. Similar results were observed when an antibody made against the N-terminal peptide was included in the heparanase assay (48). However, activity is not affected when a peptide of residues 270–280 is added to the enzyme assay (63), suggesting the second basic cluster is not as important as the N-terminus for binding the HS substrate. Support for the significance of the first basic cluster in the binding and cleavage of the HS substrate is that both K^{158} and K^{159} are close to the active site glutamate residues when the human Hpa1 sequence is modeled on the three-dimensional structure of *Thermoanaerobacterium saccharolyticum* β-xylosidase (63). When either residues 158–172 or residues 270–280 are deleted, the mutant 50 kDa subunits form heterodimers when co-transfected with the 8 kDa subunit (63), indicating neither cluster is involved in protein–protein interactions to form the dimer. However, both mutant heterodimers are enzymatically inactive (63). This finding suggests that while only the sequence at the N-terminus is important for catalysis; both HS-binding sites may be required to position the substrate correctly on the enzyme protein. A similar hypothesis was proposed from studies in CHO cells that suggested the enzyme

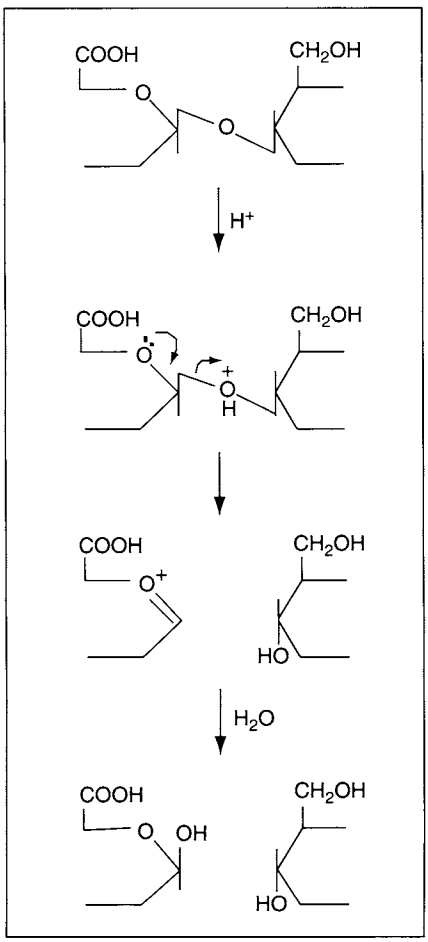

Figure 4 Hpa1 hydrolytic cleavage mechanism with retention of the anomeric configuration at the cleaved glycosidic bond.

recognizes the HS substrate by its domain structure (26,65) and may require the glycosaminoglycan to bind to multiple sites on the protein. Both basic clusters also appear to be important in the interaction of the enzyme with cell surface HSPG (Fig. 3), since the 158–172 peptide blocks binding of iodinated enzyme to cells, while the heterodimer with the 270–280 deletion accumulates in the culture media and is not internalized (63).

B. Heparan Sulfate Substrate Specificity

In order to understand how Hpa1 might recognize and cleave the HS substrate, it is necessary to first look at how the synthesis of the glycosaminoglycan generates its

domain structure. HS glycosaminoglycans are synthesized as polysaccharides of alternating *N*-acetylglucosamine and glucuronic acid residues, which are modified in the Golgi by a series of enzymatic reactions (66). These reactions replace acetyl groups with sulfate groups, epimerize glucuronic acid to iduronic acid, and add sulfate to the C6 and C2 hydroxyl groups of glucosamine and iduronic acid, respectively. Because these reactions are interdependent and incomplete, the final HS molecule has a domain structure (Fig. 5), where S-domains, rich in *N*- and *O*-sulfate groups and iduronic acid residues, are separated by stretches of unmodified sequences (66,67). Bridging these two regions are short stretches of mixed sequences, where *N*-acetylated and *N*-sulfated disaccharides, alternate (67). The S-domains range in size from 2 to 8 disaccharides and are separated on the chain by unmodified and mixed sequences of about 15 disaccharides (67). The short heparanase-derived HS chains generated in human fibroblasts (68) or CHO cells (26,69) contain a single S-domain, suggesting the domain structure of the HS molecule plays a role in how Hpa1 recognizes and cleaves the glycosaminoglycan.

One mechanism by which Hpa1 may bind to and cleave the HS substrate is by recognizing a specific sequence or modification in the S-domain or flanking mixed sequences. Examples of this type of sequence specificity have been observed with the binding of antithrombin III and bFGF to the HS glycosaminoglycan (67). By using defined HS polysaccharides (70), specific HS or heparin-derived oligosaccharides (70,71), and chemically modified heparins (72), it is clear the HS substrate must be sulfated for it to be recognized and cleaved by Hpa1 (7,70–72). *O*-sulfate groups appear to be more important in this interaction than *N*-sulfate groups (70), although since *N*-sulfation precedes *O*-sulfation (66) both modifications are required. It was initially suggested that 2-*O*-sulfate groups were required for Hpa1 to cleave the HS chain (70), but this finding has not been supported in studies using heparin-derived oligosaccharide substrates (71) or studies examining the inhibition of Hpa1 activity in the presence of chemically modified heparins (72). To date, none of these types of studies has defined a particular sequence or sulfate modification that is essential for Hpa1 to recognize and cleave the HS substrate, although they do suggest the enzyme has a preference for cleaving the glycosaminoglycan at –GlcNAc(6S)–GlcUA–GlcN(NS) sequences (26,71,73–75). These findings are not surprising, because while the S-domains are enriched in sulfate groups and iduronic acid residues, the actual sugar sequence in the domains is usually different from one another due to the randomness of the modification reactions (66). Thus, it is

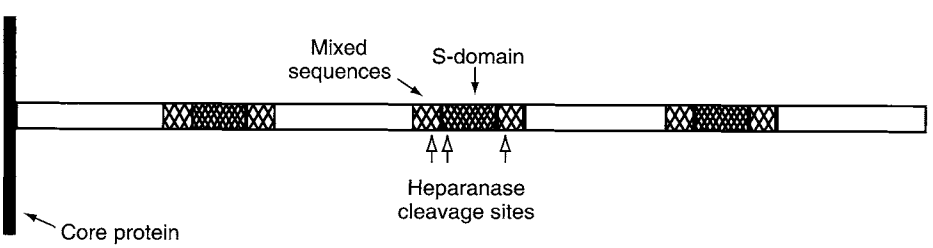

Figure 5 Heparan sulfate domain structure and proposed Hpa1 cleavage sites.

unlikely that every S-domain on the HS chain would have the same specific cleavage sequence.

Although the sequence of sulfate groups and uronic acid residues vary between S-domains (66), the three-dimensional structure of all the S-domains on a HS chain is similar because of the conformational flexibility of the iduronic acid residues (76). Studies with heparin oligosaccharides show the conformation of the iduronic acid residues also cause the 2-*O*-sulfate and 6-*O*-sulfate groups in the S-domains to be clustered on one side of the polysaccharide (76). This suggests a model where Hpa1 is able to use the three-dimensional structure of the glycosaminoglycan to easily discriminate between the sulfated S-domains and the nonsulfated regions and bind the chain so that the polysaccharide is cleaved at the junction between them (Fig. 5). A structural recognition model was first proposed by Bame and colleagues (65), based on studies of HS catabolism in CHO cells that show heparanase cleavage required a substrate with at least two S-domains. Recent studies looking at heparin inhibitors of Hpa1 activity (72) also support a domain-structure recognition model. When heparin is treated with periodate, the C2–C3 bond of unmodified glucuronic acid residues will be cleaved, which should result in the sugar having increased conformational freedom. Periodate-treated heparin is a better inhibitor of Hpa1 activity than heparin itself (72), suggesting the cleaved glucuronic acid residues in the nonsulfated regions are able to adopt the S-domain structure, which causes the treated chain to bind Hpa1 with better affinity.

A model where Hpa1 recognizes and cleaves the HS chain because of structural differences between S-domains and unmodified sequences is appealing because it fits with what is known about HS substrate specificity. The HS substrate must be sulfated because *N*-sulfation is required to generate the S-domains, and *O*-sulfate groups better differentiate the S-domains from the unmodified regions of the glycosaminoglycan. However, as shown experimentally (71,72), the type of *O*-sulfate group should not matter, since both the 2-*O*-sulfate and 6-*O*-sulfate groups are clustered on the same side of the S-domain. Hpa1 does not cleave heparin as well as it cleaves HS (73), because the extensive modifications to the heparin chain means it lacks a distinctive domain structure (77). However, heparin should be an inhibitor of the enzyme (72), since it has S-domain sequences that could bind to the HS binding site(s) on the enzyme. The size-dependence of the HS substrate (26,54,56,73) can also be explained if Hpa1 requires that there be multiple S-domains to properly orient the HS substrate at the enzyme active site. Finally, a structural recognition model can explain the subtle HS sequence differences seen on either side of the cleaved glycosidic bond (26,71,73–75). If Hpa1 recognizes a general structure, rather than a specific sequence, there could be slight differences in where the glycosaminoglycan is cleaved, based on how the HS substrate is sitting at the active site.

C. Modulation of Activity

The recent finding that heparanase activities in CHO cells are due to the hamster Hpa1 homologue (KJ Bame, in preparation), indicate Hpa1 is also the primary enzyme responsible for the intracellular catabolism of HSPGs. This finding is

difficult to reconcile with studies from cultured cells that, based on the size and structure of the HS products, suggest there are multiple heparanases with different substrate specificities (26,27,54,78). One possibility for these apparent differences may be that additional posttranslational processing of the Hpa1 protein inside the cell affects its enzyme properties. Two different heparanase activities, C1A and C2, have been purified from CHO cells (27). Although they are similar in size, and are both recognized by anti-Hpa1 antibodies (Fig. 6), the C1A heparanase activity releases HS chains from proteoglycan core proteins but the C2 enzyme does not (27). Since the C2 enzyme requires higher salt to elute from a cation exchange column than the C1A enzyme (27), it suggests substrate specificity may be related to differences in posttranslational modifications of the enzyme protein.

Additional proteolytic processing of Hpa1 may also affect its catalytic activity. Four different sizes of Hpa1 were detected when chloroquine was added to the culture media of heparanase-transfected NMU cells (48), suggesting there may be intermediates in the intracellular processing of the enzyme. When a recombinant proheparanase with a C-terminal myc-tag was added to the media of cultured CHO cells, the tag was lost after the protein was internalized and converted to the active form (49), indicating the C-terminus of the 50 kDa subunit may be proteolytically

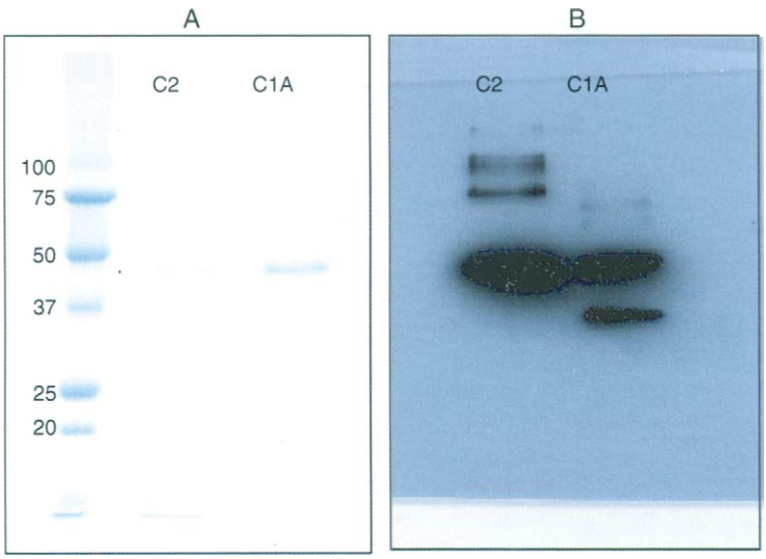

Figure 6 C1A and C2 heparanases from CHO cells are recognized by anti-Hpa1 antibodies. Purified C1A and C2 heparanases were electrophoresed and stained with Coomassie blue (A) or blotted to nitrocellulose and probed with an anti-heparanase antibody (B). The antibody used is Mab HP3/17 made against a polypeptide from the 50-kDa subunit of human Hpa1 (InSight Biopharmaceuticals, Ltd.). Because it is difficult to see, the dot on the Coomassie stained gel is at the position of the C2 protein band.

processed. Anti-heparanase antibodies recognize a smaller molecular weight protein in the purified C1A preparation (Fig. 6B) that is similar to the 30 kDa C1B heparanase originally identified in CHO cells (27). In those studies, partially purified C1B activity generated 9 kDa HS products, while partially purified C1A activity generated 6 kDa products (27), suggesting the enzymes were binding to and cleaving the HS substrate differently. Thus, it may be that removal of amino acids from the enzyme may alter how the HS chain binds to Hpa1, resulting in products of different sizes or structures.

The pH of the environment may also affect Hpa1 catalytic activity. Depending on how it is assayed, Hpa1 is active from pH 3.5 to 7.5, with maximal activity around pH 5.5 (9,27,28,41,52). This broad pH profile makes sense for the intracellular actions of Hpa1, since the pH varies from 6.5 to 4.5 as molecules move through the endocytic pathway. It also explains why the secreted enzyme will not act unless conditions, such as inflammation, cause the pH of the extracellular environment to be lowered (51,52). Studies suggest the inactivation of Hpa1 at physiological pH may be due to changes in the protein structure so that while HS is still able to bind to the enzyme, it cannot be cleaved (52). It is possible that as the pH drops, changes in protein structure will alter how HS sits at the active site so that different types of HS products are generated. For example, the CHO Hpa1/C2 activity generates longer HS oligosaccharide products when assayed at pH 6.5 than when assayed at pH 5.5 (27), suggesting the pH of the environment affects the specificity of the enzyme.

Another explanation for the appearance of multiple heparanase activities is that Hpa1 may interact with other proteins, resulting in changes in catalytic activity. The initial characterization of heparanase activities in CHO cells suggested the enzyme has a FERM-domain (28), a 300-amino acid domain that links proteins to the plasma membrane via protein–protein interactions (79). Although subsequent analysis shows the CHO enzyme is the hamster Hpa1 homologue (Fig. 6), the enzyme does share properties with FERM-domains, in that it can bind to acidic phospholipids and the C-terminal domain (CTD) of radixin (28). Interactions with the radixin-CTD affect the pH profile of heparanase (28). When assayed in the absence of the radixin-CTD, the enzyme is active from pH 3.5 to 6.0, with optimal activity at pH 4.0. But if the radixin-CTD is included in the assay, the optimal activity shifts to pH 6.0, and the enzyme is now active at pH 7.5 but not at pH 4.0 (28). Thus, instead of requiring an acidic environment to bind the HS substrate and cleave the glycosidic bond, the interaction between Hpa1 and the radixin-CTD has altered the enzyme conformation, or provided additional functional groups, so that now the heparanase acts at a more neutral pH. It is doubtful the Hpa1/radixin-CTD interaction is physiologically relevant; however, these findings do suggest interactions with proteins inside the cell may regulate the catalytic activity of Hpa1. These interactions could make sure that the enzyme is active at the appropriate pH, or be responsible for the different HS populations seen in cultured cells (26,54). It will be important to identify what types of proteins can interact with Hpa1 inside cells, and how these interactions affect enzyme activity.

IV. Biological Functions of Heparanase 1

Because Hpa1 is overexpressed in a number of human tumors (80), and the level of enzyme expression in the tumor correlates with malignant potential and poor prognosis (81–84), most studies of heparanase function have concentrated on its role in cancer metastasis (19,20,80). Experimental evidence supports a role of extracellular Hpa1 in this process (85). Hpa1 will degrade HPSG in basement membranes, allowing cancer cells to escape the vasculature and invade surrounding tissue. In addition, the Hpa1-catalyzed degradation of extracellular HSPG will release HS-binding factors, necessary for cell proliferation and angiogenesis, from their storage sites. Hpa1 may play similar roles in chronic inflammation (20,33,34,86), allowing extravasion of leukocytes through the blood vessel wall and releasing cytokines that cause the accumulation of leukocytes at inflammatory sites. Hpa1 has also been implicated in the pathogenesis of proteinuria seen in passive Heymann nephritis (87). In this disease, there is loss of HSPG from the glomerular basement membrane that changes its permeability properties. Diseased animals have higher expression of Hpa1 in glomeruli than normal animals (87), suggesting the enzyme may be responsible for the observed loss of HS. This is supported by studies that show proteinuria is reduced if animals are treated with a synthetic heparanase inhibitor (88). Similar findings were observed in transgenic mice engineered to overexpress Hpa1 protein (89). Compared to normal mice, the transgenic *hpa-tg* mice had higher levels of protein and creatine in their urine, suggesting the actions of the overexpressed enzyme may have disrupted the filtration barrier of the kidney (89).

In addition to pathological processes, Hpa1 has been proposed to play roles in normal development and tissue remodeling. Embryo implantation in the uterine wall has been likened to malignant tumor invasion (90), so the expression of Hpa1 in trophoblasts (91) may be essential for breaking down the extracellular matrix and releasing growth and angiogenic factors that establish and maintain the placenta. The homozygous *hpa-tg* mice have a higher number of embryos in the uterus during the first trimester of pregnancy (89), suggesting the over-expression of Hpa1 promoted embryo implantation. The litter sizes of *hpa-tg* mice and normal mice were the same (89), suggesting increased levels of Hpa1 might also contribute to a higher rate of miscarriage or embryonic death. The over-expression of Hpa1 in the *hpa-tg* mice also affected mammary gland development. Upon pregnancy, the basement membrane surrounding the mammary ducts is degraded, which allows the epithelial cells to form aveolar structures. Virgin *hpa-tg* mice had alveolar development and maturation comparable to the gland at 9–12 days of pregnancy (89). This suggests the over-expression of Hpa1 in the mice resulted in basement membrane disruption and the release of matrix-bound growth factors that stimulated cell proliferation and differentiation in the absence of normal signals. Hpa1-catalyzed release of HS-bound factors is also necessary for the tissue repair and remodeling seen with wound healing (92). Hpa1 is normally expressed in skin, and upon wounding there is increased expression of the enzyme in keratinocytes adjacent to the wound margin, suggesting Hpa1 acts to enhance cell migration.

Wound healing is accelerated if recombinant Hpa1 is topically applied to the wound or if the experiment is done with *hpa-tg* mice (92), indicating increased levels of the enzyme enhances the release of factors that promote cell proliferation and tissue vascularization.

All the physiological functions ascribed thus far to Hpa1 are due to the enzyme acting extracellularly. However, even though it is not highly expressed in non-lymphoid tissues (12,13,16,17), evidence suggests Hpa1 is the enzyme inside cells that degrade internalized cell surface and extracellular matrix HSPGs (Fig. 6). Cell surface HSPGs act as receptors for numerous ligands involved in cell differentiation, lipoprotein metabolism, blood coagulation, and wound healing (1,3,6). Once brought into the cell, endosomal Hpa1 may cleave the HS chain to release the ligand from the internalized core protein and generate short HS chains that activate the ligand, protect it from degradation, or direct it to another location inside the cell (56,93). Thus, deficiencies in intracellular Hpa1 activity may affect cell and tissue development (94) or lead to increased risk of diseases such as athlerosclerosis (6,95). Moreover, since intracellular Hpa1 catalyzes the first step in the complete catabolism of HS glycosaminoglycans (96), lack of the enzyme may contribute to an, as yet, unidentified form of mucopolysaccharidosis. When rats were given the anti-parasitic drug suramin, it induced mucopolysaccharidosis in the animals, which was proposed to be due to suramin's inhibitory action on the lysosomal enzymes iduronate-2-sulfatase and β-glucuronidase (97). However, it might also have resulted from inhibition of intracellular Hpa1 activity, since suramin has been shown to inhibit the enzyme (98,99). As strategies are developed to treat pathological conditions that result from over-expression of Hpa1 such as cancer, inflammation, or kidney disease (20,80,88,92,99). It will be important to elucidate the roles of the enzyme in intracellular catabolism of HSPGs so that the normal functions of the enzyme are not severely affected.

References

1. Bernfield M, Götte M, Park PW, Reizes O, Fitzgerald MI, Lincecum J, Zako M. Functions of cell surface heparan sulfate proteoglycans. Annu Rev Biochem 1999; 68:729–777.
2. Iozzo RV. Matrix proteoglycans: from molecular design to cellular function. Ann Rev Biochem 1998; 67:609–652.
3. Gallagher JT, Lyon M. Heparan sulfate: molecular structure and interactions with growth factors and morphogens. In: Iozzo RV, ed. Proteoglycans: Structure, Biology and Molecular Interactions. New York: Marcel-Dekker, 2000; 27–60.
4. Couchman JR, Woods A. Signalling through the syndecan proteoglycans. In: Iozzo RV, ed. Proteoglycans: Structure, Biology and Molecular Interactions. New York: Marcel-Dekker, 2000; 147–159.
5. Colin S, Jearing J-C, Mascorelli F, Vienet R, Al-Mahmood S, Bourtois Y, Labarre J. In vivo involvement of heparan sulfate proteoglycan in the bioavailability, internalization, and catabolism of exogenous basic fibroblast growth factor. Mol Pharmacol 1999; 1:74–82.

6. Mahley RW, Ji Z-S. Remnant lipoprotein metabolism: key pathways involving cell surface heparan sulfate proteoglycans and apolipoprotein E. J Lip Res 1999; 40:1–16.
7. Bame KJ. Heparanases: endoglycosidases that degrade heparan sulfate proteoglycans. Glycobiology 2001; 11:91R–98R.
8. Goshen R, Hochberg AA, Korner G, Levy E, Ishai-Michaeli R, Elkin M, de Groot N, Vlodavsky I. Purification and characterization of placental heparanase and its expression by cultured cytotrophoblasts. Mol Hum Reprod 1996; 2:679–684.
9. Freeman C, Parish CR. Human platelet heparanase: purification, characterization and catalytic activity. Biochem J 1998; 330:1341–1350.
10. Gonzalez-Stawinski GV, Parker W, Holzknecht ZE, Huber NS, Platt JL. Partial sequence of human platelet heparitinase and evidence of its ability to polymerize. Biochem Biophys Acta 1999; 1429:431–438.
11. Vlodavsky I, Friedman Y, Elkin M, Aingorn H, Atzmon R, Ishai-Michaeli R, Bitan M, Pappo O, Peretz T, Michal I, Spector L, Pecker I. Mammalian heparanase: gene cloning, expression and function in tumor progression and metastasis. Nat Med 1999; 5:793–802.
12. Hulett MD, Freeman C, Hamdorf BJ, Baker RT, Harris MJ, Parish CR. Cloning of mammalian heparanase, an important enzyme in tumor invasion and metastasis. Nat Med 1999; 5:803–809.
13. Kussie PH, Hulmes JD, Ludwig DL, Patel S, Navarro EC, Seddon AP, Giorgio NA, Bohlen P. Cloning and functional expression of a human heparanase gene. Biochem Biophys Res Commun 1999; 261:183–187.
14. Toyoshima M, Nakajima M. Human heparanase: purification, characterization, cloning and expression. J Biol Chem 1999; 274:24153–24160.
15. Dong, J, Kukula AK, Toyoshima M, Nakajima M. Genomic organization and chromosome localization of the newly identified human heparanase gene. Gene 2000; 253:171–178.
16. McKenzie E, Tyson K, Stamps A, Smith P, Turner P, Barry R, Hircock M, Pastel S, Barry E, Stubberfield C, Terret J, Page M. Cloning and expression profiling of Hpa2, a novel mammalian heparanase family member. Biochem Biophys Res Commun 2000; 276:1170–1177.
17. Dempsey LA, Plummer TB, Coombes SL, Platt JL. Heparanase expression in invasive trophoblasts and acute vascular damage. Glycobiology 2000; 10:467–475.
18. Dempsey LA, Brunn GJ, Platt JL. Heparanase, a potent regulator of cell matrix interactions. Trends Biol Sci 2000; 25:349–355.
19. Vlodavsky I, Friedman Y. Molecular properties and involvement of heparanase in cancer metastasis and angiogenesis. J Clin Invest 2001; 108:341–347.
20. Parish CR, Freeman C, Hulett MD. Heparanase: a key enzyme involved in cell invasion. Biochem Biophys Acta 2001; 1471:M99–M108.
21. Hoogewerf AJ, Leone JW, Reardon IM, Howe WJ, Asa D, Heinrikson RL, Ledbetter SR. CXC chemokines connective tissue activating peptide-III and neutrophil activating peptide-2 are heparin/heparan sulfate-degrading enzymes. J Biol Chem 1995; 270:3268–3277.
22. Proudfoot AE, Peitsch MC, Power CA, Allet B, Mermod JJ, Bacon K, Wells TN. Structure and bioactivity of recombinant human CTAP-III and NAP-2. J Protein Chem 1997; 16:37–49.

23. Rechter M, Lider O, Cahalon L, Baharav E, Dekel M, Seigel D, Vlodavsky I, Aingorn H, Cohen IR, Shoseyov O. A cellulose-binding domain-fused recombinant human T Cell connective tissue-activating peptide-III manifests heparanase activity. Biochem Biophys Res Commun 1999; 255:657–662.
24. Castor CW, Kotlyar A, Edwards BE. Connective tissue activation XXXVIII: heparin/heparanase activity of human platelets resides in a high molecular weight protein, not in connective tissue activating peptide III. J Rheumatol 2002; 29:2337–2344.
25. Kosir MA, Foley-Loudon PA, Finkernauer R, Tenneberg SD. Multiple heparanases are expressed in polymorphonuclear cells. J Surg Res 2002; 103:100–108.
26. Bame KJ, Robson K. Heparanases produce distinct populations of heparan sulfate glycosaminoglycans in Chinese hamster ovary cells. J Biol Chem 1997; 272:2245–2251.
27. Bame KJ, Hassall A, Sanderson C, Venkatesan I, Sun C. Partial purification of heparanase activity in Chinese hamster ovary cells. Evidence for multiple heparanases. Biochem J 1998; 336:191–200.
28. Bame KJ, Venkatesan I, Dehdashti J, McFarlane J, Burfeind R. Characterization of a novel intracellular heparanase that has a FERM domain. Biochem J 2002; 364:265–274.
29. Jiang P, Kumar A, Parrillo JE, Dempsey LA, Platt JL, Prinz RA, Xu X. Cloning and characterization of the human heparanase-1 (HPR1) gene promoter. Role of GA-binding protein and Sp1 in regulating HPR1 basal promoter activity. J Biol Chem 2002; 277:8989–8998.
30. Suske G. The Sp-family of transcription factors. Gene 1999; 238:291–300.
31. Rosmarin AG, Resendes KK, Yang Z, McMillan JN, Fleming SL. GA-binding protein transcription factor: a review of GABP as an integrator of intracellular signaling and protein-protein interactions. Blood Cells Mol Dis 2004; 32:143–154.
32. Lu WC, Liu YN, Kang BB, Chen JH. Trans-activation of heparanase promoter by ETS transcription factors. Oncogene 2003; 22:919–923.
33. de Mestre AM, Khachigian LM, Santiago FS, Staykova MA, Hulett MD. Regulation of inducible heparanase gene transcription in activated T cells by early growth response 1. J Biol Chem 2003; 278:50377–50385.
34. Chen G, Wang D, Vikramadithyan R, Yagyu H, Saxena U, Pillarisetti S, Goldberg IJ. Inflammatory cytokines and fatty acids regulate endothelial cell heparanase expression. Biochemistry 2004; 43:4971–4977.
35. Elkin M, Cohen I, Zcharia E, Orgel A, Guatta-Rangini Z, Peretz T, Vlodavsky I, Kleinman HK. Regulation of heparanase gene expression by estrogen in breast cancer. Cancer Res 2003; 63:8821–8826.
36. Antequera F. Structure, functions and evolution of CpG island promoters. Cell Mol Life Sci 2003; 60:1647–1658.
37. Shteper PJ, Zcharia E, Ashhab Y, Peretz T, Vlodavsky I, Ben-Yehuda D. Role of promoter methylation in regulation of the mammalian heparanase gene. Oncogene 2003; 22:7737–7749.
38. Ogishima T, Shiina H, Breault JE, Tabatabai L, Bassett WW, Enokida H, Li L-C, Kawakami T, Urakami S, Ribeiro-Filho LA, Terashma M, Fujime M, Igawa M, Dahiya R. Increased heparanase expression is caused by promoter hypomethylation and up-regulation of transcriptional factor early

growth response-1 in human prostate cancer. Clin Canc Res 2005; 11: 1028–1036.
39. Simizu S, Ishida K, Wierzba MK, Sator T-A, Osada H. Expression of heparanase in human tumor cell lines and human head and neck tumors. Cancer Lett 2003; 193:83–89.
40. Fairbanks MB, Mildner AM, Leone JW, Cavey GS, Mathews WR, Drong RF, Slightom JL, Bienkowski MJ, Smith CW, Bannow CA, Heinrikson RL. Processing of the human heparanase precursor, and evidence that the active enzyme is a heterodimer. J Biol Chem 1999; 274:29587–29590.
41. McKenzie E, Young K, Hircock M, Bennett J, Bhaman M, Felix R, Turner P, Stamps A, McMillan D, Saville G, Ng S, Mason S, Snell D, Schofield D, Gong H, Townsend T, Gallagher J, Page M, Parekh R, Stubberfield C. Biochemical characterization of the active heterodimer form of human heparanase (Hpa1) protein expressed in insect cells. Biochem J 2003; 373:423–435.
42. Levy-Adam F, Miao H-Q, Heinrikson RL, Vlodavsky I, Ilan N. Heterodimer formation is essential for heparanase enzyme activity. Biochem Biophys Res Commun 2003; 308:885–891.
43. Nardella C, Lahm A, Pallaoro M, Brunetti M, Vannini A, Steinkühler C. Mechanism of activation of human heparanase investigated by protein engineering. Biochemistry 2004; 43:1862–1873.
44. Abboud-Jarrous G, Aingorn H, Rangini-Guetta Z, Atzmon R, Elgavish S, Peretz T, Vlodavsky I. Heparanase processing: site-directed mutatgenesis, proteolytic cleavage and activation. J Biol Chem 2005; 280:13568–13575.
45. Hulett MD, Hornby JR, Ohms SJ, Zuegg J, Freeman C, Gready JE, Parish CR. Identification of active-site residues of the pro-metastatic endoglycosidase heparanase. Biochemistry 2000; 39:15659–15667.
46. Simizu S, Ishida K, Wierzba MK, Osada H. Secretion of heparanase protein is regulated by glycosylation in human tumor cell lines. J Biol Chem 2004; 279:2697–2703.
47. Goldshmidt O, Nadev L, Aingorn H, Irit C, Feinstein N, Ilan N, Zamir E, Geiger B, Vlodavsky I, Katz B-Z. Human heparanase is localized within lyosomes in a stable form. Exp Cell Res 2002; 281:50–62.
48. Zetser A, Levy-Adam F, Kaplan V, Gingis-Velitski S, Bashenko Y, Schubert S, Flugelman MY, Vlodavsky I, Ilan N. Processing and activation of latent heparanase occurs in lysosomes. J Cell Sci 2004; 117:2249–2258.
49. Gingis-Velitski S, Zetser A, Kaplan V, Ben-Zaken O, Cohen E, Levy-Adam F, Bashenko Y, Flugelman MY, Vlodavsky I, Ilan N. Heparanase uptake is mediated by cell membrane heparan sulfate proteoglycans. J Biol Chem 2004; 279:44084–44092.
50. Nadev L, Eldor A, Yacoby-Zeevi O, Zamir E, Pecker I, Ilan N, Geiger B, Vlodavsky I, Katz B-Z. Activation, processing and trafficking of extracellular heparanase by primary human fibroblasts. J Cell Sci 2002; 115:2179–2187.
51. Gilat D, Hershkoviz R, Goldkorn I, Cahalon L, Korner G, Vlodavsky I, Lider O. Molecular behavior adapts to context: heparanase functions as an extracellular matrix-degrading enzyme or as a T cell adhesion molecule, depending on the local pH. J Exp Med 1995; 181:1929–1934.
52. Ihrcke NS, Parker W, Reissner KJ, Platt JL. Regulation of platelet heparanase during inflammation: role of pH and proteinases. J Cell Physiol 1998; 175: 255–267.

53. Bame KJ. Release of heparan sulfate glycosaminoglycans from proteoglycans in Chinese hamster ovary cells does not require proteolysis of the core protein. J Biol Chem 1993; 268:19956–19964.
54. Yanagishita M, Hascall VC. Cell surface heparan sulfate proteoglycans. J Biol Chem 1992; 267:9451–9454.
55. Brauker JH, Wang JL. Non-lysosomal processing of cell surface heparan sulfate proteoglycans. Studies of I-cells and NH_4Cl-treated normal cells. J Biol Chem 1987; 262:13093–13101.
56. Tumova S, Hatch BA, Law DJ, Bame KJ. bFGF does not prevent heparan sulphate proteoglycan catabolism in intact cells, but it alters the distribution of the glycosaminoglycan degradation products. Biochem J 1999; 337:471–481.
57. Sameni M, Elliot E, Ziegler G, Fortgens PH, Dennison C, Sloane BF. Cathepsin B and D are localized at the surface of human breast cancer cells. Pathol Oncol Res 1995; 1:43–53.
58. Matzner Y, Vlodavsky I, Bar-Ner M, Ishai-Michaeli R, Tauber AI. Subcellular localization of heparanase in human neutrophils. J Leukoc Biol 1992; 51:519–524.
59. Mollinedo F, Nakajima M, Llorens A, Barbosa E, Callejo S, Gajate C, Fabra A. Major co-localization of the extracellular-matrix degradative enzymes heparanase and gelatinase in tertiary granules of human neutrophils. Biochem J 1997; 327:917–923.
60. Sasaki N, Higashi N, Taka T, Nakajima M, Irimura I. Cell surface localization of heparanase on macrophages regulates degradation of extracellular matrix heparan sulfate. J Immunol 2004; 172:3830–3835.
61. Blott EJ, Griffiths GM. Secretory lysosomes. Nat Rev Mol Cell Biol 2002; 3:122–131.
62. Henrissat B, Davies G. Structural and sequence-based classification of glycoside hydrolases. Curr Opin Struct Biol 1997; 7:637–644.
63. Levy-Adam F, Abboud-Jarrous G, Fuerrini M, Beccoti D, Vlodavsky I, Ilan N. Identification and characterization of heparin/heparan sulfate binding domains of the endoglycosidase heparanase. J Biol Chem 2005; 280:20457–20466.
64. Hileman RE, Fromm JR, Weiler JM, Linhardt RJ. Glycosaminoglycan-protein interactions: definitions of consensus sites in glycosaminoglycan binding proteins. Bioessays 1998; 20:156–167.
65. Bame KJ, Venkatesan I, Stelling HD, Tumova S. The spacing of S-domains on HS glycosaminoglycans determines whether the chain is a substrate for intracellular heparanases. Glycobiology 2000; 10:715–726.
66. Esko JD, Lindahl U. Molecular diversity of heparan sulfate. J Clin Invest 2001; 108:169–173.
67. Gallagher JT. Heparan sulfate: growth control with a restricted sequence motif. J Clin Invest 2001; 108:357–361.
68. Schmidtchen A, Fransson L-Å. Analysis of heparan-sulphate chains and oligosaccharides form proliferating and quiescent fibroblasts. A proposed model for endoheparanase activity. Eur J Biochem 1994; 223:211–221.
69. Tumova S, Bame KJ. The interaction between basic fibroblast growth factor and heparan sulfate can prevent the in vitro degradation of the glycosaminoglycan by Chinese hamster ovary cell heparanases. J Biol Chem 1997; 272:9078–9085.

70. Pikas DS, Li J, Vlodavsky I, Lindahl U. Substrate specificity of heparanases from human hepatoma and platelets. J Biol Chem 1998; 273:18770–1877.
71. Okada Y, Yamada S, Toyoshima M, Dong J, Nakajima M, Sugahara K. Structural recognition by recombinant human heparanase that plays critical roles in tumor metastasis. Hierarchical sulfate groups with differential effects and the essential target disulfated trisaccharide sequence. J Biol Chem 2002; 277:42488–42495.
72. Naggi A, Casu B, Perez M, Torri G, Cassinelli G, Penco S, Pisano C, Giannini G, Ishai-Michaeli R, Vlodavsky I. Modulation of the heparanase-inhibiting activity of heparin through selective desulfation, graded *N*-acetylation and glycol-splitting. J Biol Chem 2005; 280:12103–12113.
73. Klein U, von Figura K. Substrate specificity of a heparan sulfate-degrading endoglucuronidase from human placenta. Hoppe-Seyler's Z Physiol Chem 1979; 360:1465–1471.
74. Oldberg Å, Heldin C-H, Wasteson Å, Busch C, Höök M. Characterization of a platelet endoglycosidase degrading heparin-like polysaccharides. Biochemistry 1980; 19:5755–5762.
75. Podyma-Inoue KA, Yokote H, Sakaguchi K, Ikuta M, Yanagishita M. Characterization of heparanase from a rat parathyroid cell line. J Biol Chem 2002; 277:32459–32465.
76. Mulloy B, Foster MJ. Conformation and dynamics of heparin and heparan sulfate. Glycobiology 2000; 10:1147–1156.
77. Lyon M, Gallagher JT. Bio-specific sequences and domains in heparan sulphate and the regulation of cell growth and adhesion. Matrix Biol 1998; 17:485–493.
78. Iozzo RV. Turnover of heparan sulfate proteoglycans in human colon carcinoma cells. A quantitative biochemical and autoradiographic study. J Biol Chem 1987; 262:1888–1900.
79. Tsukita Sa, Yonemura S. Cortical actin organization: lessons from ERM (Ezrin/Radixin/Moesin) proteins. J Biol Chem 1999; 274:34507–34510.
80. Simizu S, Ishida K, Osada H. Heparanase as a molecular target of cancer chemotherapy. Cancer Sci 2004; 95:553–558.
81. Rohloff J, Zinke J, Schoppmeyer K, Tannapfel A, Witzigmann H, Mossner J, Wittekind C, Caca K. Heparanase expression is a prognostic indicator for postoperative survival in pancreatic adenocarcinoma. Br J Cancer 2002; 86:1270–1275.
82. Ohkawa T, Naomoto Y, Takaoka M, Nobuhisa T, Noma K, Motoki T, Murata T, Uetsuka H, Kobayashi M, Shirakawa Y, Yamatsuji T, Matsubara N, Matsuoka J, Haisa M, Gunduz M, Tsujigiwa H, Nagatsuka H, Hosokawa M, Nakajima M, Tanaka N. Localization of heparanase in esophageal cancer cells: respective roles in prognosis and differentiation. Lab Invest 2004; 8410:1289–1304.
83. Sato T, Yamaguchi A, Goi T, Hirono Y, Takeuchi K, Katayama K, Matsukawa S. Heparanase expression in human colorectal cancer and its relationship to tumor angiogenesis, hematogenous metastasis, and prognosis. J Surg Oncol 2004; 87:174–181.
84. Nobuhisa T, Naomoto Y, Ohkawa T, Takaoka M, Ono R, Murata T, Gunduz M, Shirakawa Y, Yamatsuji T, Haisa M, Matsuoka J, Tsuhigiwa H, Nagatsuka H,

Nakajima M, Tanaka N. Heparanase expression correlates with malignant potential in human colon cancer. J Cancer Res Clin Oncol 2005; 131:229–237.
85. Goldshmidt O, Zcharia E, Abramovitch R, Metzger S, Aingorn H, Friedmann Y, Schirrmacher V, Mitrani E, Vlodavsky I. Cell surface expression and secretion of heparanase markedly promote tumor angiogenesis and metastasis. Proc Natl Acad Sci USA 2002; 99:10031–10036.
86. Vaday GG, Lider O. Extracellular matrix moieties, cytokines and enzymes: dynamic effects on immune cell behavior and inflammation. J Leukoc Biol 2000; 67:149–159.
87. Levidiotis V, Freeman C, Tikellis C, Cooper ME, Power DA. Heparanase is involved in the pathogenesis of proteinuria as a result of glomerulonephritis. J Am Soc Nephrol 2004; 15:68–78.
88. Levidiotis V, Freeman C, Punler M, Martinello P, Creese B, Ferro V, van der Vlag J, Berden JH, Parish CR, Power DA. A synthetic heparanase inhibitor reduces proteinuria in passive Heymann nephritis. J Am Soc Nephrol 2004; 15:2882–2892.
89. Zcharia E, Metzger S, Chajek-Shaul T, Aingorn H, Elkin M, Friedmann Y, Weinstein T, Li J-P, Lindahl U, Vlodavsky I. Transgenic expression of mammalian heparanase uncovers physiological functions of heparan sulfate in tissue morphogenesis, vascularization and feeding behavior. FASEB J 2004; 18:252–263.
90. Soundararajan R, Rao AJ. Trophoblast "psuedo-tumorigenesis": significance and contributory factors. Reprod Biol Endocrinol 2004; 2:15–26.
91. Haimov-Kochman R, Friedmann Y, Prus D, Goldman-Wohl DS, Greenfield C, Anteby EY, Aviv A, Vlodavsky I, Yagel S. Localization of heparanase in normal and pathological human placenta. Mol Human Reprod 2002; 8: 566–573.
92. Zcharia E, Zilka R, Yaar A, Yacoby-Zeevi O, Zetser A, Metzger S, Sarid R, Naggi A, Casu B, Ilan N, Vlodavsky I, Abramovitch R. Heparanase accelerates wound angiogenesis and wound healing in mouse and rat models. FASEB J 2005; 19:211–221.
93. Ji Z-S, Pitas RE, Mahley RW. Differential cellular accumulation/retention of apolipoprotein E mediated by cell surface heparan sulfate proteoglycans. J Biol Chem 1998; 273:13452–13460.
94. Nurcombe V, Ford MD, Wildshot JA, Bartlett PF. Developmental regulation of neural response to FGF-1 and FGF-2 by heparan sulfate proteoglycans. Science 1993; 260:103–106.
95. Lutz EP, Merkel M, Kako Y, Melford K, Radner H, Breslow JL, Bensadoun A, Goldberg IJ. Heparin-binding defective lipoprotein lipase is unstable and causes abnormalities in lipid delivery to tissues. J Clin Invest 2001; 107:1183–1192.
96. Kresse H, Glössl J. Glycosaminoglycan degradation. Adv Enzymol 1987; 60:217–311.
97. Constantopoulos G, Rees S, Cragg BG, Barranger JA, Brady RO. Experimental animal model for mucopolysaccharidosis: suramin-induced glycosaminoglycan and sphingolipid accumulation in the rat. Proc Natl Acad Sci USA 1980; 77:3700–3704.

98. Marchetti D, Reiland J, Erwin B, Roy M. Inhibition of heparanase activity and heparanase-induced angiogenesis by suramin analogues. Int J Cancer 2003; 104:167–174.
99. Fransson LÅ, Egren G, Havsmark B, Schmidtchen A. Recycling of a glycosylphosphatidylinositol-anchored heparan sulfate proteoglycan (glypican) in skin fibroblasts. Glycobiology 1995; 5:407–415.

Chemistry and Biology of Heparin and Heparan Sulfate
H.G. Garg, R.J. Linhardt and C.A. Hales (Editors)

Chapter 10

Lysosomal Degradation of Heparin and Heparan Sulfate

PETER J. MEIKLE, MARIA FULLER, and JOHN J. HOPWOOD

Lysosomal Diseases Research Unit, Department of Genetic Medicine, Women's and Children's Hospital and Department of Pediatrics, University of Adelaide, Adelaide, Australia

I. Introduction

A question to answer: what is the difference between heparin and heparan sulfate (HS)? In some publications the terms heparin, HS, and heparin-like polysaccharides have been used to describe similar materials. An accepted definition of heparin is a polysaccharide, in which more than 80% of the glucosamine residues are *N*-sulfated and the concentration of *O*-sulfated residues exceed the *N*-sulfated residues. Gallagher and Walker (1) suggested that heparin will only occur in connective tissue mast cells, whereas HS is distributed widely throughout the body. Further, there is a very special and specific process for heparin modification that operates to produce active-blood coagulation-oligosaccharides; within the endosome, *endo*-glycosidase activity produces heparin chains that are held/stored in mast cells for controlled release. The limited distribution of heparin proteoglycans to skin, lung, and a few other tissues reflect the specialized function of these proteoglycans, whereas HS proteoglycans are ubiquitously present on the surface and matrix of all cells, dramatically influencing many cell functions.

Heparin and HS proteoglycans are composed of linear sulfated glycosaminoglycan (GAG) chains of up to several hundred alternating uronic acid and *N*-acetylglucosamine residues that are modified through a series of reactions to produce a complex pattern of *O*- and *N*-sulfated monosaccharide and epimerized uronic acid residues. The GAG chains are linked through their reducing ends via a specific linkage region, xylosyl–serine residue, to the protein core of the proteoglycan. In this chapter, the breakdown of the GAG component of these proteoglycans in the lysosome is reviewed.

Following internalization from the cell surface, HS proteoglycans are trafficked through the endocytic pathway, where they undergo proteolytic cleavage to produce single GAG chains that are then subject to *endo*-degradation resulting in a series of oligosaccharide structures that are ultimately trafficked to the lysosome. Within the lysosome, a series of *exo*-enzymes and one acetyltransferase degrade these oligosaccharides, from the nonreducing end, to produce monosaccharides and inorganic sulfate. These molecules are actively transported out of the lysosome for reutilization by the cell. Much of our knowledge of the degradative action of lysosomes on heparin and HS have come from the study of genetic diseases, where a gene defects lead to deficiencies of the enzymes involved in this process. These deficiencies result in the lysosomal storage and the excretion in the urine of excessive amounts of HS fragments that are substrates for these enzymes. Genetic disorders that store HS fragments in lysosomes are part of a group of disorders known as the mucopolysaccharidoses (MPS). The MPS are part of a large group of lysosomal storage disorders (LSD) currently numbering more than 50 individual gene defects (2). Some of the MPS that store HS substrates may also store another GAG substrate, dermatan sulfate (DS) that also requires the action of three hydrolases, also common to HS degradation. Seven of the nine enzymes involved in lysosomal HS degradation have been associated with specific MPS types (Table 1). As the same lysosomal pathway is used for the degradation of both heparin and HS, this review will cover the process that is common to both.

II. Transport of Heparin and Heparan Sulfate to the Lysosome

The uptake pathway of heparin from its site of action has not been defined. HS proteoglycans destined for turn over, traffic through the endocytic vacuolar network to the lysosome for degradation. The HS proteoglycans are routed from the cell surface via clathrin-coated vesicles that fuse with early endosomes. Labeled molecules have been shown to traverse the endocytic network, and three relatively distinct compartments have been suggested: early endosome, endosome carrier vesicle, and the prelysosome (3). Endosome organelles have a mildly acidic pH that is optimal for the working of proteolytic and hydrolytic enzymes, as well as harbouring acidic dissociation reactions. Cleavage of the protein core of HS proteoglycans begins in the endosomal compartment. Although lysosomes are distinguished from late endosomes and prelysosomes by the absence of the cation-independent mannose-6-phosphate receptor, the exact location of each of the degradative processes of HS is still unknown.

III. *endo*-Degradation of Heparin and Heparan Sulfate

The degradation of heparin and HS begins with *endo*-hydrolysis to clip the long chain polysaccharides or GAG chains to shorter oligosaccharide fragments with the action of *endo*-glycosidases, called heparanases (4). A number of heparanase

Table 1 Genetic Defects in the Lysosomal Degradation of Heparan Sulfate and Other Structurally Related Glycosaminoglycans

Disease	Clinical phenotype	Enzyme deficiency	EC	OMIM	Gene locus	Australian prevalence[a]	Primary storage substrates
Mucopolysaccharidoses							
MPS type I	Hurler/Scheie syndrome	α-L-Iduronidase	EC 3.2.1.76	252,800	4p16.3	1 in 88,000	HS, DS, oligosaccharides
MPS type II	Hunter syndrome	Iduronate-2-sulfatase	EC 3.1.6.13	309,900	Xq28	1 in 136,000	HS, DS, oligosaccharides
MPS type IIIA	Sanfilippo syndrome	Heparan-*N*-sulfatase	EC 3.10.1.1	252,900	17q25.3	1 in 114,000	HS, oligosaccharides
MPS type IIIB	Sanfilippo syndrome	α-*N*-Acetylglucosaminidase	EC 3.2.1.50	252,920	17q21	1 in 211,000	HS, oligosaccharides
MPS type IIIC	Sanfilippo syndrome	Acetyl-CoA: *N*-acetyltransferase	EC 2.3.1.3	252,930	Chr.14	1 in 1,407,000	HS, oligosaccharides
MPS type IIID	Sanfilippo syndrome	*N*-acetylglucosamine-6-sulfatase	EC 3.1.6.14	252,940	12q14	1 in 1,056,000	HS, oligosaccharides
MPS type VII	Sly syndrome	β-Glucuronidase	EC 3.2.1.31	253,220	7q21.11	1 in 2,111,000	HS, DS, CS oligosaccharides
Biogenesis defects							
Multiple sulfatase deficiency	MSD	Processing enzyme/multiple sulfatases		272,200	3p26	1 in 1,407,000	HS, DS, CS, oligosaccharides
Mucolipidosis types II / III	I-cell disease, pseudo-Hurler polydystrophy	Phosphotransferase		252,500	4q21-q23/16p	1 in 325,000	HS, DS, oligosaccharides

(*Continued*)

Table 1 *Cont'd*

Disease	Clinical phenotype	Enzyme deficiency	EC	OMIM	Gene locus	Australian prevalence[a]	Primary storage substrates
Transporter defect							
Sialic acid storage disease	Sialuria; Salla disease; infantile sialic acid storage disease	Sialic acid transporter		269,920, 604,369	6q14-q15	1 in 528,000	sialic acid, uronic acid
No known defect							
		Glucuronate-2-sulfatase					
		Glucosamine-3-sulfatase					

[a]Prevalence figures from (82).

activities have been reported (5), but cloning of the enzyme from a variety of different tissues indicates that mammalian cells express primarily one heparanase (6). This heparanase cDNA encodes a 65-kDa polypeptide of 543 amino acids. This inactive precursor form of heparanase undergoes proteolytic processing to yield 50- and 8-kDa subunits that exist as a heterodimer resulting in active heparanase (7).

Increased heparanase activity has been shown in a number of tumours (8), and other pathological conditions, such as nephrosis (9) and cirrhosis (10). Heparanase activity has also been demonstrated in a variety of tissues, such as the placenta and skin in non-diseased states (11). Furthermore, heparanase activity is elevated in diabetes and consequently detected in urine from diabetics suggesting that heparanase is secreted (12). Nonetheless, localization studies indicate that heparanase resides in the endosome–lysosome network for a relatively long period and is activated upon the conversion of endosomes to lysosomes (13,14). This activation enables heparanase to act in the lysosome to cleave the β-glucuronosyl bonds in heparin and HS producing smaller oligosaccharide chains. It seems that the acidic microenvironment of the lysosome provides optimal conditions for heparanase activity and storage (15). Moreover, the proteolytic enzymes present in lysosomes may facilitate the conversion of the 65-kDa inactive heparanase to its 50- and 8-kDa heterodimer active form (16). The lysosome may also serve as a compartment to confine heparanase for its primary function in heparin and HS degradation, thereby limiting its secretion and extracellular activities associated with cell invasion and angiogenesis.

Heparanase is an *endo*-β-glucuronidase that produces variable sized fragments, because only a limited number of glucuronidic linkages are susceptible to degradation. Originally, it was thought that heparanase isolated from platelets could cleave the glucuronosyl bonds in the antithrombin binding pentasaccharide region of heparin, thereby producing products lacking anticoagulant activity (17). However, it now seems that heparin has a strong inhibitory effect on heparanase activity (18). A repeating inhibitory disaccharide (α-L-iduronic acid 2-sulfate linked to *N*- and 6-sulfated glucosamine) is present in greater number on heparin compared to HS, which may explain the relative resistance of heparin to heparanase digestion. Several reports now identify heparanase cleavage at sites distinct from the antithrombin binding sequence (18).

Attempts to define the substrate specificity of heparanase have highlighted the relevance of sulfation but have not presented a unified picture (18). Several studies have suggested that *O*-sulfate groups are necessary for substrate recognition by heparanase, but the precise position of the sulfate moieties has not been elucidated (19,20). A trisaccharide composed of a 6-sulfated glucosamine, β-D-glucuronic acid, and *N*-sulfated glucosamine has been postulated to be essential for substrate recognition (19). Furthermore, exolytic cleavage of heparanase has been demonstrated at terminal β-D-glucuronic or α-L-iduronic acid residues adjacent to a glucosamine that is *N*- and 6-sulfated, (18). From studies on the relative susceptibility of various oligosaccharides to heparanase cleavage, it has been proposed that 3-*O*-sulfate groups on adjacent glucosamine residues in highly

sulfated domains of HS exert an inhibitory effect on heparanase activity (19). The effect of inhibitory and substrate motifs in HS in relation to heparanase cleavage is difficult to determine because the various domains are not readily amenable to kinetic analysis.

More recently, an *endo*-α-*N*-acetylglucosaminidase activity towards HS has been suggested (21). No enzyme has been identified with this *endo*-activity and it is not clear whether this is a new function of an already-reported enzyme. This activity was identified based on the appearance of HS-derived oligosaccharides that were clipped at internal β-linked glycosidic bonds between *N*-acetylglucosamine and uronic acid residues. Hylauronidases are another class of *endo*-enzyme activities that have broad substrate specificities. There are six hyluronidase-like sequences present in mammals which are *endo*-hexosaminidases (22). Their primary substrate is believed to be hyaluronan, but they have been shown to cleave chondroitin, chondroitin sulfate (CS), and DS producing predominantly tetrasaccharides and hexasaccharides as end products. To date, mammalian hylauronidases are not known to have any activity toward HS. However, hyaluronidases that are *endo*-β-glucuronidases have been described in leeches (23).

A relatively new class of evolutionary conserved HS *endo*-sulfatases, that remove sulfate from the 6-O position from glucosamine residues in HS, has been identified (24,25). They are secreted through the Golgi complex and docked at the cell surface where they function. As yet, there is no evidence that *endo*-sulfatases act in the lysosome and are involved in the endosomal/lysosomal degradation of HS. Rather, it seems their function is in the subtle changing of sulfation patterns of HS on the cell surface, enabling the molecule to carry out key biological processes that are tightly linked to its sulfation pattern (26). Notwithstanding this observed role, *endo*-sulfatases cannot be ignored as possible players in the lysosomal degradation of HS.

There is no doubt that the fine structure of HS and the structurally related heparin is both spatially and temporarily regulated to impart the diverse biological functions that these two molecules have. Nonetheless, how this structural diversity is produced is quite complex. *endo*-Enzyme activities toward HS have yet to be fully elucidated; their roles have already been shown to be quite diverse. For example, human heparanase is known to be associated with cell invasion, angiogenesis, inflammation, and tissue remodeling (11,27,28). Although, if present in the lysosome, *endo*-enzyme activity is directed towards the degradation of GAG, *endo*-enzyme activities are likely to also play a part in the generation of the fine sequence of HS at the cell surface.

Thus far, there have been no reports of patients with genetic defects in the *endo*-degradation of HS. Defects in these processes may be lethal in utero, or alternatively, such defects may have no clinical outcome and there may be a level of redundancy in these processes. This may be expected in the case of the *endo*-enzymes as there are thought to be at least two *endo*-enzymes that can degrade HS (21). In addition, even in the absence of any *endo*-activity, the lysosomal degradation of HS may proceed through the action of the *exo*-enzymes.

IV. *exo*-Degradation of Heparin and Heparan Sulfate

Following partial catabolism of HS by *endo*-enzymes, which are believed to digest GAG to fragments of approximately 5 kDa, lysosomal *exo*-enzyme activities reduce these oligosaccharides to monosaccharides and sulfate to enable egress from the lysosome. This *exo*-degradative process occurs in the lysosome and requires the activity of three glycosidases, potentially four sulfatases, and an acetyltransferase. These lysosomal *exo*-enzymes are only able to hydrolyse linkages at the nonreducing termini of HS and must therefore act sequentially. The concerted action of these *exo*-enzymes is depicted in Fig. 1. The degradation of HS is suggested to occur in a highly organized and coordinated fashion, such that the *exo*-enzymes involved function as a multienzyme complex (29,30).

The lysosomal *exo*-enzymes are synthesized and processed in the endoplasmic reticulum and the Golgi apparatus. A signal sequence is required to direct mRNA and the ribosome complex to the rough endoplasmic reticulum to commence protein synthesis. Within the lumen of the endoplasmic reticulum, protein processing and folding occur, as the polypeptide is translocated (31). *N*-linked oligosaccharide structures are attached in the endoplasmic reticulum and these are modified in the Golgi apparatus; the latter also being where *O*-linked saccharides are attached (32). The phosphorylation of *N*-linked mannose oligosaccharides in the Golgi is crucial for directing *exo*-enzymes to the lysosome. *exo*-Enzymes leaving the Golgi are either trafficked to the endosome/lysosome network, or the cell surface. The former relies heavily on mannose-6-phosphate receptors, which direct protein traffic into the endosomal network for delivery to lysosomes (33). The majority of lysosomal enzymes undergo a maturation process as they are generally synthesized as polypeptide precursors that are converted to their mature active form by limited proteolytic cleavage after entering the endosome/lysosome network.

Mucolipidosis type II/III (I-cell disease, pseudo-Hurler polydystrophy) are genetic disorders that result from a defect in the processing and trafficking of lysosomal enzymes. In mucolipidosis II/III, the enzyme involved in the introduction of the mannose-6-phosphate residue onto the newly synthesized enzyme, *N*-acetylglucosamine 1-phosphotransferase, is deficient (34). This results in the mistargetting of lysosomal enzymes, with most being secreted from the cell rather than trafficked to the lysosome (35). The storage in this disorder includes primarily oligosaccharides and lipids in addition to some mucopolysaccharides. The phosphotransferase exists as a hexameric complex with the composition alpha-2/beta-2/gamma-2 (36). Mutations have been reported in both the genes encoding the alpha/beta subunits (37), and the gamma subunit (38,39).

Mucolipidosis II/III can present with a range of clinical phenotypes. The severe form (mucolipidosis type II) can present with multiple pathologies reflecting the different enzyme deficiencies; these include developmental delay, skeletal deformities, coarse facial features, and hepatomegaly. The clinical course is rapid with death usually occurring between five and eight years. Mucolipidosis type III is the more attenuated form with many of the same features, but a slower clinical evolution and normal intelligence. This is similar to the phenotype seen in the

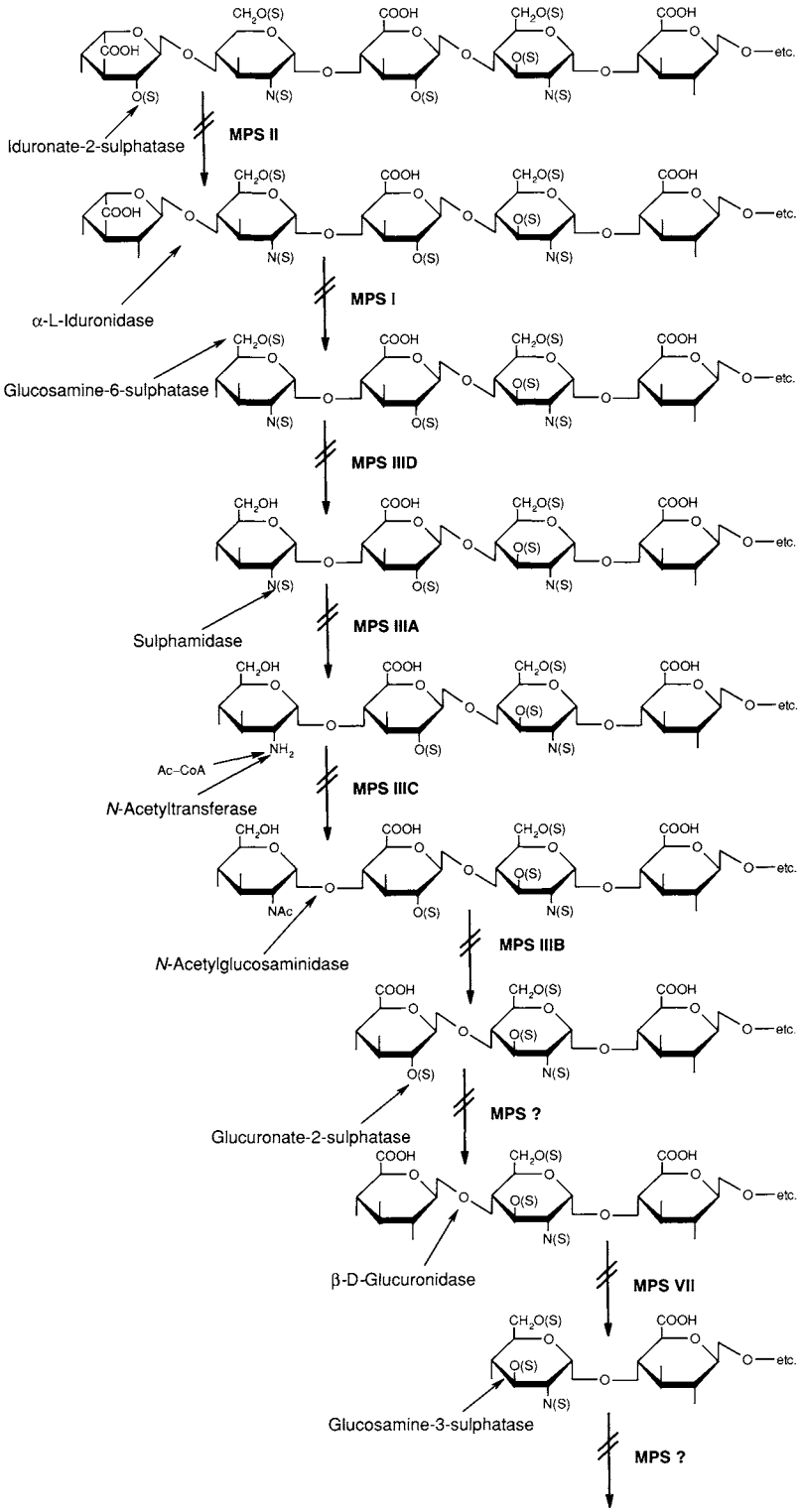
Iduronate-2-sulphatase
MPS II
α-L-Iduronidase
MPS I
Glucosamine-6-sulphatase
MPS IIID
Sulphamidase
MPS IIIA
Ac-CoA
N-Acetyltransferase
MPS IIIC
N-Acetylglucosaminidase
MPS IIIB
Glucuronate-2-sulphatase
MPS ?
β-D-Glucuronidase
MPS VII
Glucosamine-3-sulphatase
MPS ?

attenuated form of Hurler syndrome (MPS II), although the mucopolysaccharidu ria is not seen, suggesting the level of HS and DS stored are not as great as in the MPS.

A second defect in lysosomal protein processing, leading to the disrupted degradation of HS and other GAG, is multiple sulfatase deficiency. Multiple sulfatase deficiency (MSD) results from a defect in the enzyme that generates the C-α-formylglycine residue in the active site of eukaryotic sulfatases (40). This residue is posttranslationally generated from a cysteine in the endoplasmic reticulum by the enzyme SUMF-1. A deficiency in this enzyme results in the biosynthesis of inactive sulfatases leading to the accumulation of the substrates for these enzymes, including HS and other GAG, as well as sulfatide and steroid sulfates. Mutations in the gene encoding SUMF-1 have been identified in some patients (41,42). The MSD patients have a combination of the features seen with deficiency of the individual sulfatases. These include: metachromatic leukodystrophy (*250100*), X-linked ichthyosis (*308100*) and MPS II (*309900*), MPS IIIA (*252900*), MPS IIID (*252940*), MPS IVA (*253000*), and MPS VI (*253200*), although as with all LSD, a range of severity is observed.

A. *exo*-Glycosidases

The glycosidases (EC 3.2.1–3.2.3) are a group of hydrolyases that act either by retention or inversion of configuration of the anomeric carbon of their substrate (43). Both of these activities involve a pair of carboxylic acid residues, nominally aspartic acid or glutamic acid. At least two out of the three *exo*-glycosidases, α-L-iduronidase and β-D-glucuronidase involved in the catabolism of HS execute their hydrolytic activities by the retention mechanism. This requires the two carboxylic acid groups that are involved in a catalytic reaction, to be positioned on either side of the glycosidic bond and separated by 5.5 Å (44). In a two-step mechanism, a nucleophilic attack occurs at the anomeric carbon from one of the acid residues, whilst the other carboxylic acid operates as an acid/base assisting aglycon departure by protonating the glycosidic oxygen. This results in the formation of a covalent glycosyl–enzyme intermediate. Following this, the deprotonated acid/base abstracts a proton from water that subsequently attacks the glycosyl–enzyme releasing the product that has identical stereochemistry to that of the substrate.

Figure 1 *exo*-Hydrolytic degradation of heparan sulfate (HS). HS is composed of alternating uronic acid and hexosamine residues. The uronic acid residues can be iduronic or glucuronic acid that may contain 2-*O*-sulfate resudues. The glucosamine can be *N*-acetylated or *N*-sulfated in addition to containing variable levels of 6-*O*- and 3-*O*-sulfate. Within the lysosome, HS is degraded by a series of *exo*-enzymes that act sequentially at the nonreducing end. A deficiency of one of these enzymes results in one of several disorders known collectively as the *mucopolysaccharidoses*.

1. α-L-*Iduronidase*

Hydrolysis of nonreducing end α-L-iduronic acid glycosidic bonds in HS results from the action of an *exo*-hydrolase, α-L-iduronidase (Fig. 1). Lysosomal degration of DS also requires the action of α-L-iduronidase. As with the majority of lysosomal *exo*-enzymes, this hydrolase has been well characterized and purified to homogeneity from a variety of human tissues including liver, lung, kidney, and urine (45). Different catalytic properties have been attributed to α-L-iduronidase isolated from different human tissues (30). Freeman and Hopwood (46) have determined the catalytic properties of α-L-iduronidase purified from human liver toward heparin-derived oligosaccharide substrates. The aglycone residue present on these oligosaccharides was shown to influence the ability of α-L-iduronidase to bind and release iduronic acid. The presence of a C6 sulfate on the aglycone *N*-sulfated or acetylated hexosamine had a several hundred-fold effect on the catalytic efficiency [Km/Kcat] of the enzyme. The gene for human α-L-iduronidase has been cloned. The enzyme is synthesized in the endoplasmic reticulum as a 653 amino acid precursor polypeptide with a 26 amino acid signal peptide, that is cleaved at the amino terminus and contains six *N*-glycosylation sites (47). The precursor polypeptide is 85 kDa, which is proteolytically processed to a 74-kDa active monomer. The recombinant form has been shown to have pH optimum and kinetic parameters that differ from those of the mature enzyme purified from human liver (48). The active enzyme exists in monomeric form and contains the mannose-6-phosphate receptor for effective lysosomal targeting (49). Although α-L-iduronidase is yet to be crystallized, a three-dimensional structure of the active site has been postulated (50).

A mutation in the α-L-iduronidase gene results in MPS type I (MPS I). Because of the enzyme deficiency, HS and DS accumulate in the lysosomes of affected cells and are excreted in the urine of affected individuals. MPS I is the most prevalent of the MPS subtypes with a reported incidence of 1:88,000 births. A number of mutations have been described for MPS I including two common premature termination mutations W402X and Q70X (51) that make up 45 and 15% of mutations, respectively, in the UK (52). However, the frequency of these alleles varies in different populations (53–55), and they are not found in the Israeli Arab population (56). These mutations result in the severe form of MPS I known as Hurler syndrome. Other mutations that reduce the α-L-iduronidase activity to about 1% of unaffected levels result in less lysosomal storage of HS and DS, and lead to more attenuated forms of the disease (Scheie syndrome) (51,57,58). However, as with all MPS subtypes, MPS I phenotypes represent a continuum from severe to attenuated.

2. β-D-*Glucuronidase*

Terminal β-D-glucuronic acid residues are hydrolyzed from HS in the lysosome by the *exo*-glycosidase, β-D-glucuronidase (Fig. 1). As with α-L-iduronidase, β-D-glucuronidase has been isolated and purified to homogeneity from a number of mammalian tissues (59). β-D-Glucuronidase is unusual in that it has a dual localization, being present in both lysosomes and microsomes in some tissues.

For example, in mouse liver, β-D-glucuronidase is present in microsomes, retained there by binding through the C-terminus to the protein egasyn (60). The fraction of cellular β-D-glucuronidase in excess of egasyn is transported to the lysosome (61). The human gene for β-D-glucuronidase has been isolated and cloned (62). The full-length cDNA encodes a polypeptide of 651 amino acids with four potential glycosylation sites, of which two are preferentially phosphorylated (63). The active enzyme exists as a tetramer of 75 kDa subunits that are synthesized as precursor polypeptides and proteolytically processed (64). The crystal structure for β-D-glucuronidase has been elucidated (65). MPS VII, resulting from a deficiency of β-D-glucuronidase, is a relatively rare MPS subtype with many patients presenting with the very severe fetal, or neonatal forms of the disease. More than 35 mutations have been described, with no common mutations reported (66). In addition to HS, MPS VII patients also store DS and CS.

3. α-*N*-Acetylglucosaminidase

α-*N*-Acetylglucosaminidase acts to hydrolyse the α-linked *N*-acetylglucosamine residues in HS (Fig. 1). These moieties either exist naturally in GAG or are produced during their lysosomal degradation from the action of acetyl-CoA: α-glucosaminide transferase. α-*N*-Acetylglucosaminidase has been purified from a number of human tissues and contains all the usual properties of lysosomal glycosidases (67). The cDNA encoding the human enzyme has been cloned and it predicts a protein of 743 amino acids including the signal peptide (68,69). The recombinant form of the active enzyme has been reported as a monomer and dimer, compared with α-*N*-acetylglucosaminidase isolated from human tissues that exists in monomeric and oligomeric forms (70,71). A deficiency of α-*N*-acetylglucosaminidase leads to MPS IIIB. Over 80 mutations have been described in MPS IIIB patients with no common mutations (72). The storage material in MPS IIIB is restricted to HS and its endolytic degradation products.

B. *exo*-Sulfatases

1. Iduronate-2-sulfatase

Iduronate-2-sulfatase is an *exo*-sulfatase that hydrolyzes the C2-sulfate ester bond from nonreducing terminal α-L-iduronic acid residues in HS (Fig. 1), as well as DS. This enzyme has been purified 500,000-fold to homogeneity from human liver (73). Bielicki et al. (73) observed that the purified sulfatase displayed maximum catalytic efficiency toward HS oligosaccharides with sulfated aglycone residues. The cDNA encoding the entire human iduronate-2-sulfatase sequence has been isolated (74). The cDNA sequence predicts a 550 amino acid precursor polypeptide with a 25 amino acid signal sequence. Some proteolytic processing occurs in lysosomes to yield a 42-kDa active polypeptide with similar catalytic properties to iduronate-2-sulfatase isolated from human liver. The full iduronate-2-sulfatase sequence contains seven possible *N*-glycosylation sites, but the number used in the 42-kDa

polypeptide is not known. MPS II, resulting from a deficiency of iduronate-2-sulfatase, is the only x-linked MPS, with most mutations being restricted to individual families (75–77). Affected females are rare but have been reported, and are thought to result from nonrandom inactivation of the X-chromosome (66,78). As with MPS I, MPS II patients store both HS and DS within the lysosomes of affected cells and excrete these in their urine.

2. Glucuronate-2-sulfatase

Glucuronate-2-sulfatase specifically breaks the C2-sulfate ester from nonreducing end β-D-glucuronate residues (79) (Fig. 1). Relatively few sulfated β-D-glucuronic acid residues exist in HS and even less are found in heparin. The enzyme has been purified two million-fold to homogeneity from human liver (80), but the gene encoding glucuronate-2-sulfatase has not yet been isolated. The enzyme has been shown to be distinct from iduronate-2-sulfatase by demonstrating glucuronate-2-sulfatase activity in cultured fibroblasts from patients lacking iduronate-2-sulfatase activity (81). No patients with a deficiency in glucuronate-2-sulfatase have been reported to date. It seems unlikely that deficiencies in this enzyme would be lethal *in utero* as deficiencies in other enzymes involved in the degradation of HS (MPS III subtypes) lead to a normal presentation at birth with pathology usually developing over the first decade of life. However, the structural motifs that are the substrate for this enzyme are relatively uncommon in HS; so, the accumulation of substrate in the absence of the enzyme may not be at a level high enough to result in clinical pathology. Alternatively, the gene encoding this enzyme may be relatively stable with regard to the introduction of mutations and the incidence of the disease is not high enough to have been clinically identified. The incidence within the MPS III subtypes ranges from 1:114,000 for MPS IIIA to less than 1:1,000,000 for MPS IIIC and IIID (82).

3. N-Acetylglucosamine-6-sulfatase

N-Acetylglucosamine-6-sulfatase desulfates the terminal C6-sulfated *N*-acetylglucosamine residues in HS. As well as cleaving sulfate from these α-linked residues, *N*-acetylglucosamine-6-sulfatase also removes the C6-sulfate ester from β-linked *N*-acetylglucosamine residues in keratan sulfate (83). The human liver enzyme has been purified and was shown to exist in two forms: one with a single subunit of 78- kDa and the other composed of two subunits of 32- and 48-kDa (88). The human cDNA has also been isolated and the sequence predicts a polypeptide of 552 amino acids with a 36 amino acid leader sequence (85). The protein contains 13 potential *N*-glycosylation sites, of which 10 are likely to be occupied (85). A deficiency of *N*-acetylglucosamine-6-sulfatase results in MPS IIID, one of the rarer MPS. The first mutation, a single base pair deletion (c1169delA), which will cause a frameshift and premature termination of the protein has only recently been reported (86). Although *N*-acetylglucosamine-6-sulfatase is involved in the degradation of both

HS and keratan sulfate (KS), only the former is stored in this disorder. An alternate pathway for the degradation of KS involving the removal of terminal *N*-acetylglucosamine-6-sulfate residues by β-hexosaminidase has been described (87). This leads to the accumulation of *N*-acetylglucosamine-6-sulfate in addition to HS in MPS IIID.

4. *Heparan N-sulfatase*

Heparan *N*-sulfatase removes sulfate groups from the amino group of glucosamine residues present in HS. Structurally, this moiety is a sulphamate, distinct from sulfate, and therefore the enzyme is commonly referred to as sulphamidase. Heparan *N*-sulfatase has been purified to homogeneity from a number of human tissues (88). A series of HS oligosaccharide substrates were constructed and used to evaluate the influence of aglycone structure on catalytic efficiency of the purified sulphamidase to hydrolyze the sulphamate bond (88). Some substrates were turned over more than a million-fold more efficiently than others. The most important residues on the aglycone monosaccharide were a C2-sulfate ester and a C6-carboxyl group. The cDNA encoding heparan *N*-sulfatase has been isolated, and it predicts a polypeptide of 502 amino acids including a 20 amino acid signal peptide (89). The precursor protein has a molecular mass of 62-kDa, which is proteolytically processed to give a mature form at 56-kDa. The enzyme contains five potential glycosylation sites, of which all five are believed to be utilized (90). Over 60 mutations in the heparan *N*-sulfatase gene have now been defined for MPS IIIA (72); some common mutations have been reported, although these appear to be varying between different populations. Thus, the R245H mutation is common in Australian, Dutch, and German groups (91), R74C in the Polish (92), S66W in the Italian (93), and the 1091delC mutation is common in the Spanish (94). Only HS, together with its *endo*-degradation products are stored in MPS IIIA.

5. *Glucosamine-3-sulfatase*

In addition to glucosamine being *N*-sulfated and 6-*O*-sulfated, it can also be 3-*O*-sulfated. Using *N*-sulfate-D-glucosamine-3-sulfate as a substate, Leder (95) identified a glucosamine-3-sulfatase activity needed to degrade this structure. This 3-*O*-sulfatase identified in human urine required the glucosamine to be *N*-sulfated (95). The enzyme was found to be active toward the nonreducing end 3-*O*-sulfate ester on a pentasaccharide derived from the antithrombic-binding site of heparin (96). These authors also proposed that as the 3-*O*-sulphase was inactive toward the glucosamine residue if 6-sulfated, then a glucosamine-6-sulfatase needs to act first followed by the 3-*O*-sulfatase, and then sulphamidase to completely desulfate this glucosamine residue. The 3-*O*-sulfatase has not been purified to homogeneity, nor its gene identified. No MPS subtype has been associated with a deficiency in this activity.

C. Acetyltransferase

Acetyl-CoA:α-glucosaminide *N*-acetyltransferase is the only lysosomal enzyme known to be involved in making a bond rather than hydrolysing one. The enzyme catalyzes the acetylation of the glucosamine amino group resulting from the action of heparan *N*-sulfatase (Fig. 1). This is a biosynthetic reaction in what is a cascade of degradative process occurring in the lysosome to reduce heparin and HS to monosaccharides and inorganic sulfate. Adding to the enigma of this enzyme is its presence in the lysosomal membrane. The enzyme has not yet been purified to homogeneity, but partial purification has revealed much about its activity. On the cytoplasmic side, at neutral pH, the enzyme self-acetylates by transferring an acetyl group from acetyl-CoA. On the lysosomal side, at acidic pH, the enzyme transfers the acetyl group to a glucosamine residue (97). Evidence has also been provided that acetyl-CoA: α-glucosaminide *N*-acetyltransferase acts via a random-order ternary complex mechanism, which involves the utilization of cytosolic acetyl-CoA to transfer acetyl groups on to the terminal glucosamine residues of HS (98). The cDNA encoding this transferase remains to be isolated, although a deficiency in the enzyme has been associated with MPS IIIC, another of the more rare MPS subtypes. Here also the storage substrate is restricted to HS and its *endo*-degradation products.

V. Transport of Degradation Products out of the Lysosome

Following catabolism of heparin and HS, the inorganic sulfate and monosaccharide products are transported out of the lysosome for reutilization by the cell or excretion. Over 20 lysosomal transporters have been described for molecules, such as amino acids, ions, nucleosides, sugars, and vitamins (99). However, relatively little is known about the structure and regulation of these lysosomal transport systems. There is evidence that ATP has a role in the regulation of lysosomal transporters through the action of the membrane-bound lysosomal H^+-ATPase (100). This lysosomal proton pump maintains the intralysosomal pH at 4.6 through the translocation of protons (101).

A. Monosaccharide Transporters

One of the major products from the lysosomal degradation of HS is free monosaccharides. These monosaccharides are transported out of the lysosome for recycling within the cell. *N*-Acetyl-D-glucosamine is believed to exit from the lysosomal by a specific transporter. This transporter was shown to selectively transport *N*-acetyl-D-glucosamine and *N*-acetyl-D-galactosamine, and not other sugars or amino acids, thereby demonstrating independence from other amino acid and carbohydrate transport systems (102). To date, the protein has not been isolated.

The other monosaccharides generated from HS are β-D-glucuronic and α-L-iduronic acid, which also egress from the lysosome using a specific transporter, the lysosomal sialic acid transporter. This transporter was shown to have substrate specificity for the acidic monosaccharides sialic acid, uronic acids, and alduronic

acids (103). This monocarboxylate transporter has since been purified to apparent homogeneity from lysosomal membranes of rat liver (104). A 57-kDa protein was found to correlate with transport activity and was shown to recognize structurally different forms of acidic monosaccharides, like sialic acid, glucuronic, and iduronic acid. Interestingly, this lysosomal monocarboxylate transporter has biochemical and structural properties, very similar to the monocarboxylate transporters of the plasma membrane.

A deficiency in the sialic acid transporter results in the accumulation of sialic and uronic acids within lysosomes of affected cells. Sialic acid storage disease may present as a severe infantile form (ISSD), or as a slowly progressive adult form that is prevalent in Finland (Salla disease). The main symptoms are hypotonia, cerebellar ataxia, and mental retardation; visceromegaly and coarse features are also present in the infantile cases. The gene encoding the sialic acid transporter has been cloned and encodes a protein, sialin, which belongs to a family of anion/cation symporters (105). A homozygous mutation (R39C) was identified in five Finnish patients with Salla disease, and six different mutations identified in six infantile sialic acid storage disease (ISSD) patients of non-Finnish origins (105).

B. Sulfate Transporters

Inorganic sulfate is also a product generated from the lysosomal degradation of heparin and HS. A sulfate transporter, that is distinct from other lysosomal anion transport systems, enables efflux of sulfate from the lysosome (106). This sulfate transport system exhibits saturation kinetics and is inhibited by known inhibitors of anion transporters and requires the lysosomal acidic pH for optimal activity. The action of the lysosomal H^+-ATPase maintains the acidic conditions of the lysosome against a neutral exterior, which should favor the egress of sulfate from the lysosome. Nevertheless, evidence now suggests that lysosomal sulfate transport is modulated by ATP, which is independent from the action of the lysosomal H^+-ATPase (107).

VI. Diagnostic and Clinical Aspects of the Mucopolysaccharidoses

A. Additional Mucopolysaccharidoses Subtypes

Four MPS subtypes result from deficiencies in enzymes not involved in HS degradation. These are: MPS IVA (galactose-6-sulfatase) and IVB (β-galactosidase), where the enzyme deficiencies lead to lysosomal accumulation of KS; MPS VI, where a deficiency of *N*-acetylgalactosamine-4-sulphatase leads to the accumulation of DS and CS; and MPS IX where hyaluronidase is the deficient enzyme leading to lysosomal accumulation of hyaluronan.

B. Biochemical Phenotype of the Mucopolysaccharidoses

For the majority of mutations leading to an MPS subtype, the resulting enzyme/protein is unstable and is removed by the quality control mechanisms that operate

to remove miss-folded protein during the posttranslational modification process that occurs within the endoplasmic reticulum and Golgi apparatus (108). In most cases these proteins also have reduced activity or catalytic capacity, although for some mutations the resulting protein is more active than the native protein, but much less stable, thereby, leading to a deficiency of the enzyme activity (108). Other mutations result in a protein that is stable to the cells quality control machinery, but has very low or null activity (108). While in other patients, the resulting protein has altered specificity for the substrate leading to a deficiency in some specific activities rather than a deficiency in a particular protein.

In the MPS, the level of residual activity required for a normal phenotype is relatively low. Typically, 1–2% of the mean normal activity level is sufficient to produce a normal clinical phenotype. Thus, the range from 0 to 2% of normal enzyme activity covers the clinical spectrum from the severe infantile forms to the attenuated adult onset forms of these diseases.

The deficiency of specific enzyme activities leads to the accumulation of the substrates for the deficient enzymes. The trafficking of the GAG substrates to the lysosome coincides with the *endo*-degradation of these GAG substrates from the large proteoglycans that are internalized from the cell surface, to the low molecular weight forms that ultimately accumulate within lysosomes of affected cells. The nature of this storage material appears to be critical to the resulting clinical phenotype for each disorder. While the source of the storage material for each MPS subtype has been known for many years (Table 1), it is only recently that the size and composition of the storage substrates have been characterized. Byers et al. (109) have analyzed the storage material present in the urine of MPS patients by gradient PAGE. This showed characteristic patterns for the accumulated GAG fragments in these disorders, ranging in size from disaccharides to large oligosaccharides containing more than 50 sugar residues. In addition, the pattern resulting from each disorders, subtype was unique, providing a means for the determination of the MPS subtype (109). The mechanism for the generation of these GAG derived oligosaccharides is described in Section III, where the internalized proteoglycans are acted upon by a series of *endo*-enzymes to produce oligosaccharides. These oligosaccharides are then further degraded by a series of *exo*-enzymes until the nonreducing terminal residue is the substrate for the deficient enzyme. At this point, the degradative process is arrested and these oligosaccharide structures accumulate within the lysosomes of affected cells. Recently, the use of electrospray ionization-tandem mass spectrometry (ESI-MS/MS) has provided a new method to characterize and quantify the stored substrates in these disorders. Fuller et al. (21) demonstrated that the oligosaccharides that accumulate in MPS I (a deficiency of α-L-iduronidase) have an iduronic acid at the nonreducing terminus. Similarly, oligosaccharides derived from MPS II patients (iduronate-2-sulfatase deficiency) have iduronate-2-sulfate at the nonreducing terminus and oligosaccarides derived from MPS IIIA patients (sulphamidase deficiency) have a glucosamine-*N*-sulfate resudue at the nonreducing terminus (unpublished observations).

In addition to the primary storage of the GAG-derived oligosaccharides, patients with MPS subtypes, where HS accumulates, also store the gangliosides,

G_{M2}, and G_{M3}, particularly in the brain (110–114). One long-held view of why gangliosides accumulate in the brain of MPS patients, when they are not substrates for the deficient enzymes, proposes that the HS storage material inhibits several hydrolases involved in the degradation of the gangliosides. Liour et al. (115) have demonstrated a reduction in sialidase activity in MPS IIID caprine brain homogenates. If hydrolase inhibition is the sole mechanism for ganglioside accumulation, then it would be predicted that the stored gangliosides were located in the same storage vacuoles as the HS storage material. However, recent studies of MPS mouse models have shown that, in addition to gangliosides, cholesterol also accumulates in neurons in a manner similar to that observed in the related glycosphingolipid storage disorders (116). The cholesterol was shown to be co-localized with G_{M3} but not with G_{M2}, suggesting different mechanisms for each ganglioside, and that the mechanism leading to the accumulation of gangliosides in MPS brain is likely to be more complex than previously thought.

C. Clinical Phenotype of the Mucopolysaccharidoses

Of the 10 enzyme deficiencies known to result in an MPS, only four are exclusively involved in the degradation of HS. These are sulphamidase, *N*-acetylglucosaminidase, acetyl-CoA:α-glucosaminide *N*-acetyltransferase, and glucosamine-6-sulfatase, corresponding to the MPS subtypes IIIA, IIIB, IIIC, and IIID, respectively. Examination of the clinical presentation of these enzyme deficiencies provides us with an isolated view of the pathology resulting from a block in the lysosomal degradation of heparin and HS, while comparison with other MPS subtypes can provide a delineation of the phenotypes resulting from the storage of different GAG. All four subtypes of MPS III present with similar clinical phenotypes. This group of MPS is characterized by severe central nervous system degeneration, but only mild somatic disease. Onset is usually between 2 and 6 years of age, and presenting symptoms can include hyperactivity, aggressive behavior, delayed development, coarse hair, hirsutism, sleep disorders, and mild hepatosplenomegaly. Skeletal involvement is minimal with most patients showing normal stature for age and only mild dystosis multiplex and joint stiffness. The relatively mild presentation makes MPS III difficult to recognize, often leading to long delays in obtaining a diagnosis. As with all MPS subtypes, MPS III patients can present within a broad clinical spectrum, from the classical severe form described above to more attenuated variants, in which neurological function is close to normal.

The enzyme deficiencies in MPS I, MPS II, and MPS VII, all lead to the accumulation and storage of HS in addition to other GAG. DS is stored in all of these subtypes with CS also being stored in MPS VII. The phenotypes that result from the combined storage of HS and DS contain the combined clinical features of MPS III and MPS types that store DS leading to skeletal abnormalities. Thus in severe forms of MPS I and II, patients display both the neuropathology associated with the storage of HS and the skeletal abnormalities associated with the storage of DS. Infants typically appear normal at birth but are commonly diagnosed between 4 and 18 months of age. Developmental delay, skeletal deformities, coarse facial features, hepatomegaly, and

enlarged tongue are early symptoms. At the attenuated end of the clinical spectrum, Scheie syndrome in MPS I, intelligence and stature are normal and patients are characterized by joint stiffness, corneal clouding, aortic valve disease, and coarse facial features. Patients can have close to a normal life span. MPS VII also presents with a broad spectrum of clinical severity. The severe neonatal form is characterized by hydrops fetalis, dysostosis multiplex, and dysmorphic features. Patients who present beyond the neonatal form but still with the severe form of the disease, are clinically similar to the severe form of MPS I (Hurler syndrome).

D. Prediction of Phenotype in the Mucopolysaccharidoses

The genetic and biochemical basis for the clinical heterogeneity observed between patients with a specific MPS subtype has not been fully elucidated. Correlations between geneotype and phenotype have been performed (51,117), and for some patients these enable a prediction of disease severity. For example, MPS I patients homozygous for the common mutation W402X will have the severe form of the disease including the neuropathology. In contrast, patients containing the mutation R89Q have been reported to have a more attenuated form of MPS I (Hurler/Scheie syndrome), even when this is combined with a severe mutation. However, in many instances, patients do not have common mutations, limiting the usefulness of direct genotype/phenotype correlations.

In addition to genotype, residual enzyme activity and catalytic capacity have been used to correlate to phenotype. Bunge et al. (118) measured the residual α-L-iduronidase protein in skin fibroblasts from MPS I patients, and used this with activity and kinetic measurements to calculate a catalytic capacity of each cell line. This showed a strong correlation to clinical severity in MPS I patients. The combination of genotype and structural analysis of the mutant enzyme may also provide additional information to genotype analysis alone. Thus, with appropriate enzyme models, it may be possible to map new mutations to predict their effect on the protein structure and thereby the resulting phenotype.

The amount of stored substrate has also been proposed as a marker to predict clinical severity in the MPS. Early observations have reported that the level of urinary GAG correlates to the clinical severity in MPS I (119). Fuller et al. (120) have also used ESI-MS/MS to quantify several sulfated oligosaccharides in cultured skin fibroblasts from MPS I patients and showed a clear correlation between oligosaccharide level and clinical severity. This method enabled the discrimination of the severe patients, with neuropathology, from the more attenuated patients with no neurological symptoms.

At this time, it seems likely that the best prediction of disease severity will come from a combination of genotype, residual enzyme protein/activity measurements and the determination of stored substrates. However, even with this information, there is still likely to be differences in the way individuals respond to the accumulation and storage of these substrates. Additional secondary markers, such as the gangliosides in those MPS that store HS, may increase the predictive power of this type of genetic/biochemical profile.

VII. Summary and Future Challenges in the Field

The detailed study of the MPS and other LSD has contributed to our understanding of lysosomal degradation of heparin and HS. We now have a clear understanding of the sequential order of events required to degrade these macromolecules within the endosomal/lysosomal vacuolar network. Most of the hydrolytic enzymes involved in this process have been well characterized and the genes encoding them have been cloned. In many cases, those genes have been expressed and recombinant proteins have been used to further characterize the structure and function of these enzymes. The notable exceptions are the genes for glucuronate-2-sulfatase, glucosamine-3-sulfatase, and the *N*-acetyltransferase. In addition, only one of the three lysosomal membrane transporters involved in the turnover of heparin and HS have been cloned. The sulfate and *N*-acetylglucosamine transporters have not been fully characterized and the genes remain to be identified.

Most LSD have been well characterized at the protein and molecular level although there are likely to be subtypes that remain to be recognized clinically. These may include deficiencies in glucuronate-2-sulfatase and glucosamine-3-sulfatase. However, mechanisms of pathology for the MPS and other LSD are still largely unknown. How does the storage of heparin and HS fragments within lysosomes lead to the range of pathologies associated with the MPS and other LSD? Studies of these disorders will continue to provide us with models to improve our understanding of the molecular basis of heparin and HS biology.

References

1. Gallagher JT, Walker A. Molecular distinctions between heparan sulphate and heparin. Analysis of sulphation patterns indicates that heparan sulphate and heparin are separate families of *N*-sulphated polysaccharides. Biochem J 1985; 230:665–674.
2. Meikle PJ, Fietz MJ, Hopwood JJ. Diagnosis of lysosomal storage disorders: current techniques and future directions. Expert Rev Mol Diagn 2004; 4:677–691.
3. Griffiths G, Gruenberg J. The arguments for pre-existing early and late endosomes. Trends Cell Biol 1991; 1:5–9.
4. Hulett MD, Freeman C, Hamdorf BJ, Baker RT, Harris MJ, Parish CR. Cloning of mammalian heparanase, an important enzyme in tumor invasion and metastasis. Nat Med 1999; 5:803–809.
5. Bame KJ. Heparanases: endoglycosidases that degrade heparan sulfate proteoglycans. Glycobiology 2001; 11:91R–98R.
6. Toyoshima M, Nakajima M. Human heparanase. Purification, characterization, cloning, and expression. J Biol Chem 1999; 274:24153–24160.
7. McKenzie E, Young K, Hircock M, Bennett J, Bhaman M, Felix R, Turner P, Stamps A, McMillan D, Saville G, Ng S, Mason S, Snell D, Schofield D, Gong H, Townsend R, Gallagher J, Page M, Parekh R, Stubberfield C. Biochemical characterization of the active heterodimer form of human heparanase (Hpa1) protein expressed in insect cells. Biochem J 2003; 373:423–435.

8. Vlodavsky I, Goldshmidt O, Zcharia E, Atzmon R, Rangini-Guatta Z, Elkin M, Peretz T, Friedmann Y. Mammalian heparanase: involvement in cancer metastasis, angiogenesis and normal development. Semin Cancer Biol 2002; 12:121–129.
9. Levidiotis V, Kanellis J, Ierino FL, Power DA. Increased expression of heparanase in puromycin aminonucleoside nephrosis. Kidney Int 2001; 60:1287–1296.
10. Xiao Y, Kleeff J, Shi X, Buchler MW, Friess H. Heparanase expression in hepatocellular carcinoma and the cirrhotic liver. Hepatol Res 2003; 26:192–198.
11. Dempsey LA, Brunn GJ, Platt JL. Heparanase, a potential regulator of cell-matrix interactions. Trends Biochem Sci 2000; 25:349–351.
12. Katz A, Van-Dijk DJ, Aingorn H, Erman A, Davies M, Darmon D, Hurvitz H, Vlodavsky I. Involvement of human heparanase in the pathogenesis of diabetic nephropathy. Isr Med Assoc J 2002; 4:996–1002.
13. Gingis-Velitski S, Zetser A, Flugelman MY, Vlodavsky I, Ilan N. Heparanase induces endothelial cell migration via protein kinase B/Akt activation. J Biol Chem 2004; 279:23536–23541.
14. Nadav L, Eldor A, Yacoby-Zeevi O, Zamir E, Pecker I, Ilan N, Geiger B, Vlodavsky I, Katz BZ. Activation, processing and trafficking of extracellular heparanase by primary human fibroblasts. J Cell Sci 2002; 115:2179–2187.
15. Kjellen L, Pertoft H, Oldberg A, Hook M. Oligosaccharides generated by an endoglucuronidase are intermediates in the intracellular degradation of heparan sulfate proteoglycans. J Biol Chem 1985; 260:8416–8422.
16. Fairbanks MB, Mildner AM, Leone JW, Cavey GS, Mathews WR, Drong RF, Slightom JL, Bienkowski MJ, Smith CW, Bannow CA, Heinrikson RL. Processing of the human heparanase precursor and evidence that the active enzyme is a heterodimer. J Biol Chem 1999; 274:29587–29590.
17. Thunberg L, Backstrom G, Wasteson A, Robinson HC, Ogren S, Lindahl U. Enzymatic depolymerization of heparin-related polysaccharides. Substrate specificities of mouse mastocytoma and human platelet endo-beta-D-glucuronidases. J Biol Chem 1982; 257:10278–10282.
18. Gong F, Jemth P, Escobar Galvis ML, Vlodavsky I, Horner A, Lindahl U, Li JP. Processing of macromolecular heparin by heparanase. J Biol Chem 2003; 278:35152–35158.
19. Okada Y, Yamada S, Toyoshima M, Dong J, Nakajima M, Sugahara K. Structural recognition by recombinant human heparanase that plays critical roles in tumor metastasis. Hierarchical sulfate groups with different effects and the essential target disulfated trisaccharide sequence. J Biol Chem 2002; 277:42488–42495.
20. Pikas DS, Li JP, Vlodavsky I, Lindahl U. Substrate specificity of heparanases from human hepatoma and platelets. J Biol Chem 1998; 273:18770–18777.
21. Fuller M, Meikle PJ, Hopwood JJ. Glycosaminoglycan degradation fragments in mucopolysaccharidosis I. Glycobiology 2004; 14:443–450.
22. Csoka AB, Frost GI, Stern R. The six hyaluronidase-like genes in the human and mouse genomes. Matrix Biol 2001; 20:499–508.
23. Hovingh P, Linker A. Hyaluronidase activity in leeches (Hirudinea). Comp Biochem Physiol B Biochem Mol Biol 1999; 124:319–326.

24. Ai X, Do AT, Lozynska O, Kusche-Gullberg M, Lindahl U, Emerson CP, Jr. QSulf1 remodels the 6-O sulfation states of cell surface heparan sulfate proteoglycans to promote Wnt signaling. J Cell Biol 2003; 162:341–351.
25. Morimoto-Tomita M, Uchimura K, Werb Z, Hemmerich S, Rosen SD. Cloning and characterization of two extracellular heparin-degrading endosulfatases in mice and humans. J Biol Chem 2002; 277:49175–49185.
26. Viviano BL, Paine-Saunders S, Gasiunas N, Gallagher J, Saunders S. Domain-specific modification of heparan sulfate by Qsulf1 modulates the binding of the bone morphogenetic protein antagonist Noggin. J Biol Chem 2004; 279:5604–5611.
27. Parish CR, Freeman C, Hulett MD. Heparanase: a key enzyme involved in cell invasion. Biochim Biophys Acta 2001; 1471:M99–M108.
28. Vlodavsky I, Friedmann Y. Molecular properties and involvement of heparanase in cancer metastasis and angiogenesis. J Clin Invest 2001; 108:341–347.
29. Freeman C, Hopwood J. Lysosomal degradation of heparin and heparan sulphate. Adv Exp Med Biol 1992; 313:121–134.
30. Hopwood JJ. Heparin: enzymes that degrade heparin and heparan sulphate. In: Lane D, Lindahl U, eds. Heparin: chemical and Biological Properties, Clinical Applications. Edward Arnold, 1989: 191–228.
31. Gorlich D, Rapoport TA. Protein translocation into proteoliposomes reconstituted from purified components of the endoplasmic reticulum membrane. Cell 1993; 75:615–630.
32. Lis H, Sharon N. Protein glycosylation. Structural and functional aspects. Eur J Biochem 1993; 218:1–27.
33. Hille-Rehfeld A. Mannose 6-phosphate receptors in sorting and transport of lysosomal enzymes. Biochim Biophys Acta 1995; 1241:177–194.
34. Reitman ML, Varki A, Kornfeld S. Fibroblasts from patients with I-cell disease and pseudo-Hurler polydystrophy are deficient in uridine 5′-diphosphate-*N*-acetylglucosamine: glycoprotein *N*-acetylglucosaminylphosphotransferase activity. J Clin Invest 1981; 67:1574–1579.
35. Kornfeld S. Trafficking of lysosomal enzymes in normal and disease states. J Clin Invest 1986; 77:1–6.
36. Bao M, Booth JL, Elmendorf BJ, Canfield WM. Bovine UDP-*N*-acetylglucosamine: lysosomal-enzyme *N*-acetylglucosamine-1-phosphotransferase. I. Purification and subunit structure. J Biol Chem 1996; 271:31437–31445.
37. Steet RA, Hullin R, Kudo M, Martinelli M, Bosshard NU, Schaffner T, Kornfeld S, Steinmann B. A splicing mutation in the alpha/beta GlcNAc-1 -phosphotransferase gene results in an adult onset form of mucolipidosis III associated with sensory neuropathy and cardiomyopathy. Am J Med Genet A 2005; 132:369–375.
38. Tiede S, Cantz M, Raas-Rothschild A, Muschol N, Burger F, Ullrich K, Braulke T. A novel mutation in UDP-*N*-acetylglucosamine-1-phosphotransferase gamma subunit (GNPTAG) in two siblings with mucolipidosis type III alters a used glycosylation site. Hum Mutat 2004; 24:535.
39. Raas-Rothschild A, Bargal R, Goldman O, Ben-Asher E, Groener JE, Toutain A, Stemmer E, Ben-Neriah Z, Flusser H, Beemer FA, Penttinen M, Olender T, Rein AJ, Bach G, Zeigler M. Genomic organisation of the UDP-*N*-acetylglucosamine-1-phosphotransferase gamma subunit (GNPTAG) and its mutations in mucolipidosis III. J Med Genet 2004; 41:e52.

40. Schmidt B, Selmer T, Ingendoh A, von Figura K. A novel amino acid modification in sulfatases that is defective in multiple sulfatase deficiency. Cell 1995; 82:271–278.
41. Cosma MP, Pepe S, Annunziata I, Newbold RF, Grompe M, Parenti G, Ballabio A. The multiple sulfatase deficiency gene encodes an essential and limiting factor for the activity of sulfatases. Cell 2003; 113:445–456.
42. Dierks T, Schmidt B, Borissenko LV, Peng J, Preusser A, Mariappan M, von Figura K. Multiple sulfatase deficiency is caused by mutations in the gene encoding the human C(alpha)-formylglycine generating enzyme. Cell 2003; 113:435–444.
43. Davies G, Henrissat B. Structures and mechanisms of glycosyl hydrolases. Structure 1995; 3:853–859.
44. McCarter JD, Withers SG. Mechanisms of enzymatic glycoside hydrolysis. Curr Opin Struct Biol 1994; 4:885–892.
45. Clements PR, Brooks DA, McCourt PA, Hopwood JJ. Immunopurification and characterization of human alpha-L-iduronidase with the use of monoclonal antibodies. Biochem J 1989; 259:199–208.
46. Freeman C, Hopwood JJ. Human alpha-L-iduronidase. Catalytic properties and an integrated role in the lysosomal degradation of heparan sulphate. Biochem J 1992; 282 (Part 3):899–908.
47. Scott HS, Anson DS, Orsborn AM, Nelson PV, Clements PR, Morris CP, Hopwood JJ. Human alpha-L-iduronidase: cDNA isolation and expression. Proc Natl Acad Sci USA 1991; 88:9695–9699.
48. Unger EG, Durrant J, Anson DS, Hopwood JJ. Recombinant alpha-L-iduronidase: characterization of the purified enzyme and correction of mucopolysaccharidosis type I fibroblasts. Biochem J 1994; 304 (Part 1):43–49.
49. Zhao KW, Faull KF, Kakkis ED, Neufeld EF. Carbohydrate structures of recombinant human alpha-L-iduronidase secreted by Chinese hamster ovary cells. J Biol Chem 1997; 272:22758–22765.
50. Durand P, Lehn P, Callebaut I, Fabrega S, Henrissat B, Mornon JP. Active-site motifs of lysosomal acid hydrolases: invariant features of clan GH-A glycosyl hydrolases deduced from hydrophobic cluster analysis. Glycobiology 1997; 7:277–284.
51. Scott HS, Bunge S, Gal A, Clarke LA, Morris CP, Hopwood JJ. Molecular genetics of mucopolysaccharidosis type I: diagnostic, clinical, and biological implications. Hum Mutat 1995; 6:288–302.
52. Beesley CE, Meaney CA, Greenland G, Adams V, Vellodi A, Young EP, Winchester BG. Mutational analysis of 85 mucopolysaccharidosis type I families: frequency of known mutations, identification of 17 novel mutations and in vitro expression of missense mutations. Hum Genet 2001; 109:503–511.
53. Voskoboeva EY, Krasnopolskaya XD, Mirenburg TV, Weber B, Hopwood JJ. Molecular genetics of mucopolysaccharidosis type I: mutation analysis among the patients of the former Soviet Union. Mol Genet Metab 1998; 65:174–180.
54. Bunge S, Kleijer WJ, Steglich C, Beck M, Zuther C, Morris CP, Schwinger E, Hopwood JJ, Scott HS, Gal A. Mucopolysaccharidosis type I: identification of 8 novel mutations and determination of the frequency of the two common alpha-L-iduronidase mutations (W402X and Q70X) among European patients. Hum Mol Genet 1994; 3:861–866.

55. Gort L, Chabas A, Coll MJ. Analysis of five mutations in 20 mucopolysaccharidois type 1 patients: high prevalence of the W402X mutation. Mutations in brief no. 121. Online Hum Mutat 1998; 11:332–333.
56. Bach G, Moskowitz SM, Tieu PT, Matynia A, Neufeld EF. Molecular analysis of Hurler syndrome in Druze and Muslim Arab patients in Israel: multiple allelic mutations of the IDUA gene in a small geographic area. Am J Hum Genet 1993; 53:330–338.
57. Tieu PT, Bach G, Matynia A, Hwang M, Neufeld EF. Four novel mutations underlying mild or intermediate forms of alpha-L-iduronidase deficiency (MPS IS and MPS IH/S). Hum Mutat 1995; 6:55–59.
58. Clarke LA, Scott HS. Two novel mutations causing mucopolysaccharidosis type I detected by single strand conformational analysis of the alpha-L-iduronidase gene. Hum Mol Genet 1993; 2:1311–1312.
59. Paigen K. Mammalian beta-glucuronidase: genetics, molecular biology, and cell biology. Prog Nucleic Acid Res Mol Biol 1989; 37:155–205.
60. Medda S, Chemelli RM, Martin JL, Pohl LR, Swank RT. Involvement of the carboxyl-terminal propeptide of beta-glucuronidase in its compartmentalization within the endoplasmic reticulum as determined by a synthetic peptide approach. J Biol Chem 1989; 264:15824–15828.
61. Lusis AJ, Paigen K. Relationships between levels of membrane-bound glucuronidase and the associated protein egasyn in mouse tissues. J Cell Biol 1977; 73:728–735.
62. Oshima A, Kyle JW, Miller RD, Hoffmann JW, Powell PP, Grubb JH, Sly WS, Tropak M, Guise KS, Gravel RA. Cloning, sequencing, and expression of cDNA for human beta-glucuronidase. Proc Natl Acad Sci USA 1987; 84: 685–689.
63. Shipley JM, Grubb JH, Sly WS. The role of glycosylation and phosphorylation in the expression of active human beta-glucuronidase. J Biol Chem 1993; 268:12193–12198.
64. Erickson AH, Blobel G. Carboxyl-terminal proteolytic processing during biosynthesis of the lysosomal enzymes beta-glucuronidase and cathepsin D. Biochemistry 1983; 22:5201–5205.
65. Jain S, Drendel WB, Chen ZW, Mathews FS, Sly WS, Grubb JH. Structure of human beta-glucuronidase reveals candidate lysosomal targeting and active-site motifs. Nat Struct Biol 1996; 3:375–381.
66. Neufeld EF, Meunzer J. The Mucopolysaccharidoses. In: Scriver CR, Beaudet AL, Sly WS, Valle D, eds. The Molecular Basis of Inherited Disease. New York: McGraw-Hill, 2001: 3421–3452.
67. von Figura K. Human alpha-*N*-acetylglucosaminidase. 1. Purification and properties. Eur J Biochem 1977; 80:523–533.
68. Weber B, Blanch L, Clements PR, Scott HS, Hopwood JJ. Cloning and expression of the gene involved in Sanfilippo B syndrome (mucopolysaccharidosis III B). Hum Mol Genet 1996; 5:771–777.
69. Zhao HG, Li HH, Bach G, Schmidtchen A, Neufeld EF. The molecular basis of Sanfilippo syndrome type B. Proc Natl Acad Sci USA 1996; 93:6101–6105.
70. Zhao KW, Neufeld EF. Purification and characterization of recombinant human alpha-*N*-acetylglucosaminidase secreted by Chinese hamster ovary cells. Protein Exp Purif 2000; 19:202–211.

71. Weber B, Hopwood JJ, Yogalingam G. Expression and characterization of human recombinant and alpha-*N*-acetylglucosaminidase. Protein Exp Purif 2001; 21:251–259.
72. Yogalingam G, Hopwood JJ. Molecular genetics of mucopolysaccharidosis type IIIA and IIIB: diagnostic, clinical, and biological implications. Hum Mutat 2001; 18:264–281.
73. Bielicki J, Freeman C, Clements PR, Hopwood JJ. Human liver iduronate-2-sulphatase. Purification, characterization and catalytic properties. Biochem J 1990; 271:75–86.
74. Wilson PJ, Morris CP, Anson DS, Occhiodoro T, Bielicki J, Clements PR, Hopwood JJ. Hunter syndrome: isolation of an iduronate-2-sulfatase cDNA clone and analysis of patient DNA. Proc Natl Acad Sci USA 1990; 87:8531–8535.
75. Hopwood JJ, Bunge S, Morris CP, Wilson PJ, Steglich C, Beck M, Schwinger E, Gal A. Molecular basis of mucopolysaccharidosis type II: mutations in the iduronate-2-sulphatase gene. Hum Mutat 1993; 2:435–442.
76. Li P, Bellows AB, Thompson JN. Molecular basis of iduronate-2-sulphatase gene mutations in patients with mucopolysaccharidosis type II (Hunter syndrome). J Med Genet 1999; 36:21–27.
77. Filocamo M, Bonuccelli G, Corsolini F, Mazzotti R, Cusano R, Gatti R. Molecular analysis of 40 Italian patients with mucopolysaccharidosis type II: new mutations in the iduronate-2-sulfatase (IDS) gene. Hum Mutat 2001; 18:164–165.
78. Clarke JT, Wilson PJ, Morris CP, Hopwood JJ, Richards RI, Sutherland GR, Ray PN. Characterization of a deletion at Xq27–q28 associated with unbalanced inactivation of the nonmutant X chromosome. Am J Hum Genet 1992; 51:316–322.
79. Shaklee PN, Glaser JH, Conrad HE. A sulfatase specific for glucuronic acid 2-sulfate residues in glycosaminoglycans. J Biol Chem 1985; 260:9146–9149.
80. Freeman C, Hopwood JJ. Human liver glucuronate 2-sulphatase. Purification, characterization and catalytic properties. Biochem J 1989; 259:209–216.
81. Freeman C, Hopwood JJ. Glucuronate-2-sulphatase activity in cultured human skin fibroblast homogenates. Biochem J 1991; 279 (Part 2):399–405.
82. Meikle PJ, Hopwood JJ, Clague AE, Carey WF. Prevalence of lysosomal storage disorders. JAMA 1999; 281:249–254.
83. Kresse H, Paschke E, von Figura K, Gilberg W, Fuchs W. Sanfilippo disease type D: deficiency of *N*-acetylglucosamine-6-sulfate sulfatase required for heparan sulfate degradation. Proc Natl Acad Sci USA 1980; 77:6822–6826.
84. Freeman C, Clements PR, Hopwood JJ. Human liver *N*-acetylglucosamine-6-sulphate sulphatase. Purification and characterization. Biochem J 1987; 246:347–354.
85. Robertson DA, Freeman C, Morris CP, Hopwood JJ. A cDNA clone for human glucosamine-6-sulphatase reveals differences between arylsulphatases and non-arylsulphatases. Biochem J 1992; 288 (Part 2):539–544.
86. Beesley CE, Burke D, Jackson M, Vellodi A, Winchester BG, Young EP. Sanfilippo syndrome type D: identification of the first mutation in the *N*-acetylglucosamine-6-sulphatase gene. J Med Genet 2003; 40:192–194.

87. Hopwood JJ, Elliott H. *N*-acetylglucosamine 6-sulfate residues in keratan sulfate and heparan sulfate are desulfated by the same enzyme. Biochem Int 1983; 6:141–148.
88. Freeman C, Hopwood JJ. Human liver sulphamate sulphohydrolase. Determinations of native protein and subunit Mr values and influence of substrate agylcone structure on catalytic properties. Biochem J 1986; 234:83–92.
89. Scott HS, Blanch L, Guo XH, Freeman C, Orsborn A, Baker E, Sutherland GR, Morris CP, Hopwood JJ. Cloning of the sulphamidase gene and identification of mutations in Sanfilippo A syndrome. Nat Genet 1995; 11:465–467.
90. Perkins KJ, Byers S, Yogalingam G, Weber B, Hopwood JJ. Expression and characterization of wild type and mutant recombinant human sulfamidase. Implications for Sanfilippo (Mucopolysaccharidosis IIIA) syndrome. J Biol Chem 1999; 274:37193–37199.
91. Weber B, van de Kamp JJ, Kleijer WJ, Guo XH, Blanch L, van Diggelen OP, Wevers R, Poorthuis BJ, Hopwood JJ. Identification of a common mutation (R245H) in Sanfilippo A patients from the Netherlands. J Inherit Metab Dis 1998; 21:416–422.
92. Bunge S, Ince H, Steglich C, Kleijer WJ, Beck M, Zaremba J, van Diggelen OP, Weber B, Hopwood JJ, Gal A. Identification of 16 sulfamidase gene mutations including the common R74C in patients with mucopolysaccharidosis type IIIA (Sanfilippo A). Hum Mutat 1997; 10:479–485.
93. Di Natale P, Balzano N, Esposito S, Villani GR. Identification of molecular defects in Italian Sanfilippo A patients including 13 novel mutations. Hum Mutat 1998; 11:313–320.
94. Montfort M, Vilageliu L, Garcia-Giralt N, Guidi S, Coll MJ, Chabas A, Grinberg D. Mutation 1091delC is highly prevalent in Spanish Sanfilippo syndrome type A patients. Hum Mutat 1998; 12:274–279.
95. Leder IG. A novel 3-*O*-sulfatase from human urine acting on methyl-2-deoxy-2-sulfamino-alpha-D-glucopyranoside 3-sulfate. Biochem Biophys Res Commun 1980; 94:1183–1189.
96. Lindahl U, Backstrom G, Thunberg L, Leder IG. Evidence for a 3-*O*-sulfated D-glucosamine residue in the antithrombin-binding sequence of heparin. Proc Natl Acad Sci USA 1980; 77:6551–6555.
97. Bame KJ, Rome LH. Acetyl coenzyme A: alpha-glucosaminide *N*-acetyltransferase. Evidence for a transmembrane acetylation mechanism. J Biol Chem 1985; 260:11293–11299.
98. Meikle PJ, Whittle AM, Hopwood JJ. Human acetyl-coenzyme A: alpha-glucosaminide *N*-acetyltransferase. Kinetic characterization and mechanistic interpretation. Biochem J 1995; 308 (Part 1):327–333.
99. Pisoni RL, Thoene JG. The transport systems of mammalian lysosomes. Biochim Biophys Acta 1991; 1071:351–373.
100. Ohkuma S, Moriyama Y, Takano T. Identification and characterization of a proton pump on lysosomes by fluorescein-isothiocyanate-dextran fluorescence. Proc Natl Acad Sci USA 1982; 79:2758–2762.
101. Schneider DL. ATP-dependent acidification of intact and disrupted lysosomes. Evidence for an ATP-driven proton pump. J Biol Chem 1981; 256:3858–3864.

102. Jonas AJ, Speller RJ, Conrad PB, Dubinsky WP. Transport of *N*-acetyl-D-glucosamine and *N*-acetyl-D-galactosamine by rat liver lysosomes. J Biol Chem 1989; 264:4953–4956.
103. Mancini GM, de Jonge HR, Galjaard H, Verheijen FW. Characterization of a proton-driven carrier for sialic acid in the lysosomal membrane. Evidence for a group-specific transport system for acidic monosaccharides. J Biol Chem 1989; 264:15247–15254.
104. Havelaar AC, Mancini GM, Beerens CE, Souren RM, Verheijen FW. Purification of the lysosomal sialic acid transporter. Functional characteristics of a monocarboxylate transporter. J Biol Chem 1998; 273:34568–34574.
105. Verheijen FW, Verbeek E, Aula N, Beerens CE, Havelaar AC, Joosse M, Peltonen L, Aula P, Galjaard H, van der Spek PJ, Mancini GM. A new gene, encoding an anion transporter, is mutated in sialic acid storage diseases. Nat Genet 1999; 23:462–465.
106. Jonas AJ, Jobe H. Sulfate transport by rat liver lysosomes. J Biol Chem 1990; 265:17545–17549.
107. Chou HF, Passage M, Jonas AJ. ATP stimulates lysosomal sulphate transport at neutral pH: evidence for phosphorylation of the lysosomal sulphate carrier. Biochem J 1997; 327 (Part 3):781–786.
108. Hopwood JJ, Brooks DA. An introduction to the basic science and biology of the lysosome and storage diseases. In: Applegarth DA, Dimmick JE, Hall JG, eds. Organelle Diseases. London: Chapman and Hall Medical, 1997; 7–36.
109. Byers S, Rozaklis T, Brumfield LK, Ranieri E, Hopwood JJ. Glycosaminoglycan accumulation and excretion in the mucopolysaccharidoses: characterization and basis of a diagnostic test for MPS. Mol Genet Metab 1998; 65:282–290.
110. Constantopoulos G, Dekaban AS. Neurochemistry of the mucopolysaccharidoses: brain lipids and lysosomal enzymes in patients with four types of mucopolysaccharidosis and in normal controls. J Neurochem 1978; 30: 965–973.
111. Constantopoulos G, Iqbal K, Dekaban AS. Mucopolysaccharidosis types IH, IS, II, and IIIA: glycosaminoglycans and lipids of isolated brain cells and other fractions from autopsied tissues. J Neurochem 1980; 34:1399–1411.
112. Li HH, Yu WH, Rozengurt N, Zhao HZ, Lyons KM, Anagnostaras S, Fanselow MS, Suzuki K, Vanier MT, Neufeld EF. Mouse model of Sanfilippo syndrome type B produced by targeted disruption of the gene encoding alpha-*N*-acetylglucosaminidase. Proc Natl Acad Sci USA 1999; 96:14505–14510.
113. Jones MZ, Alroy J, Rutledge JC, Taylor JW, Alvord Jr EC, Toone J, Applegarth D, Hopwood JJ, Skutelsky E, Ianelli C, Thorley-Lawson D, Mitchell-Herpolsheimer C, Arias A, Sharp P, Evans W, Sillence D, Cavanagh KT. Human mucopolysaccharidosis IIID: clinical, biochemical, morphological and immunohistochemical characteristics. J Neuropathol Exp Neurol 1997; 56:1158–1167.
114. Siegel DA, Walkley SU. Growth of ectopic dendrites on cortical pyramidal neurons in neuronal storage diseases correlates with abnormal accumulation of GM2 ganglioside. J Neurochem 1994; 62:1852–1862.

115. Liour SS, Jones MZ, Suzuki M, Bieberich E, Yu RK. Metabolic studies of glycosphingolipid accumulation in mucopolysaccharidosis IIID. Mol Genet Metab 2001; 72:239–247.
116. McGlynn R, Dobrenis K, Walkley SU. Differential subcellular localization of cholesterol, gangliosides, and glycosaminoglycans in murine models of mucopolysaccharide storage disorders. J Comp Neurol 2004; 480:415–426.
117. Terlato NJ, Cox GF. Can mucopolysaccharidosis type I disease severity be predicted based on a patient's genotype? A comprehensive review of the literature. Genet Med 2003; 5:286–294.
118. Bunge S, Clements PR, Byers S, Kleijer WJ, Brooks DA, Hopwood JJ. Genotype-phenotype correlations in mucopolysaccharidosis type I using enzyme kinetics, immunoquantification and in vitro turnover studies. Biochim Biophys Acta 1998; 30:249–256.
119. Hopwood JJ, Morris CP. The mucopolysaccharidoses. Diagnosis, molecular genetics and treatment. Mol Biol Med 1990; 7:381–404.
120. Fuller M, Brooks DA, Evangelista M, Hein LK, Hopwood JJ, Meikle PJ. Prediction of neuropathology in mucopolysaccharidosis I patients. Mol Genet Metab 2005; 84:18–24.

Chemistry and Biology of Heparin and Heparan Sulfate
H.G. Garg, R.J. Linhardt and C.A. Hales (Editors)

Chapter 11

Heparin Regulation of the Complement System

HAINING YU

Department of Medicinal and Natural Product, College of Pharmacy, University of Iowa, Iowa City, IA, USA

EVA M. MUÑOZ

Department of Chemistry and Chemical Biology, Biology and Chemical and Biological Engineering, Rensselaer Polytechnic Institute, Troy, NY, USA

R. ERIK EDENS

Department of Pediatrics, College of Medicine, University of Arkansas Medical Sciences, Arkansas Children's Hospital, Little Rock, AR, USA

and

ROBERT J. LINHARDT

Department of Chemistry and Chemical Biology, Biology and Chemical and Biological Engineering, Rensselaer Polytechnic Institute, Troy, NY, USA

I. Introduction

The complement system consists of approximately 25 proteins that work to complement the activity of antibodies in destroying bacteria, either by facilitating phagocytosis or by puncturing the bacterial cell membrane resulting in bacterial cell lysis (1). Heparin, a clinically used anticoagulant, is a polydisperse, highly sulfated, linear polysaccharide consisting of $1 \rightarrow 4$ linked uronic acid and glucosamine residues (2,3). The biological activities of pharmaceutical heparin are reviewed elsewhere (2–6).

Heparin can bind to a variety of proteins, including growth factors (7), proinflammatory chemokines and cytokines (6), extracellular matrix proteins (8), and complement proteins (9). Binding takes place primarily through electrostatic interactions between heparin's anionic groups (sulfo and carboxyl), and the positively charged amino acid residues (arginine and lysine) of the heparin-binding proteins (10,11). Heparin–protein interactions regulate such diverse processes as coagulation, homeostasis (12), cell adhesion (8), lipid metabolism (13), growth factor signal

transduction (7), and complement-mediated cell lysis (9), which is the subject of this chapter.

II. Background and History

A. Heparin

1. Structure

Heparin is acidic (average negative charge of −100) and polydisperse (chains ranging in molecular weight from 5000 to 40,000) (2,14). It is comprised of a major (75–95%) alternating disaccharide having the structure *N*-sulfo-6-*O*-sulfo-β-D-glucosamine (1→4) 2-*O*-sulfo-α-L-iduronic acid. Minor sequences containing variable levels of *O*- and *N*-sulfo groups and containing glucuronic acid in place of iduronic acid are also found in heparin (15) (Fig. 1A). Heparin, localized intracellularly in the cell granules of mast cells and basophils, is biosynthesized as serglycin proteoglycan (PG, M_r ~1500 kDa), consisting of the central core protein, from which approximately 11 long-linear polysaccharide chains (M_r ~100 kDa) extend (Fig 1B) (16). Once released from core protein, the polysaccharide chains are cleaved by proteases to form peptidoglycan heparin, a single long polysaccharide chain attached to a small peptide (M_r 100 kDa), which is immediately processed by a β-endoglucuronidase to generate a number of smaller polysaccharide chains called glycosaminoglycan (GAG) heparin (12).

2. Biological Activities and Therapeutic Potential

Heparin has a variety of biological activities, many of which are of interest because of their potential therapeutic utility (17,18). By regulating the activity of heparin-binding proteins, heparin and the related GAG, heparan sulfate, can influence various biological processes giving heparin therapeutic applications as an antithrombotic, antiatherosclerotic, anticomplement, antiinfective, anticancer, and antiinflammatory agent (16,19–29). The heparin-binding proteins that represent therapeutic targets include enzymes, protease inhibitors, lipoproteins, growth factors, chemokines, selectins, extracellular matrix proteins, receptor proteins, viral coat proteins, and nuclear proteins (30).

B. Complement System

1. General Description of the Complement System

Complement is a major defense and clearance system in the bloodstream and is comprised of a series of approximately 25 different proteins (Table 1) (1,30,31). The complement system can be activated in three main ways: the classical pathway, the alternative pathway, and the mannose-binding lectin pathway. The most potent activation occurs when antibody (IgG or IgM) binds to antigen at the surface of a cell (Fig. 2). This results in the immune triggering of the classical pathway.

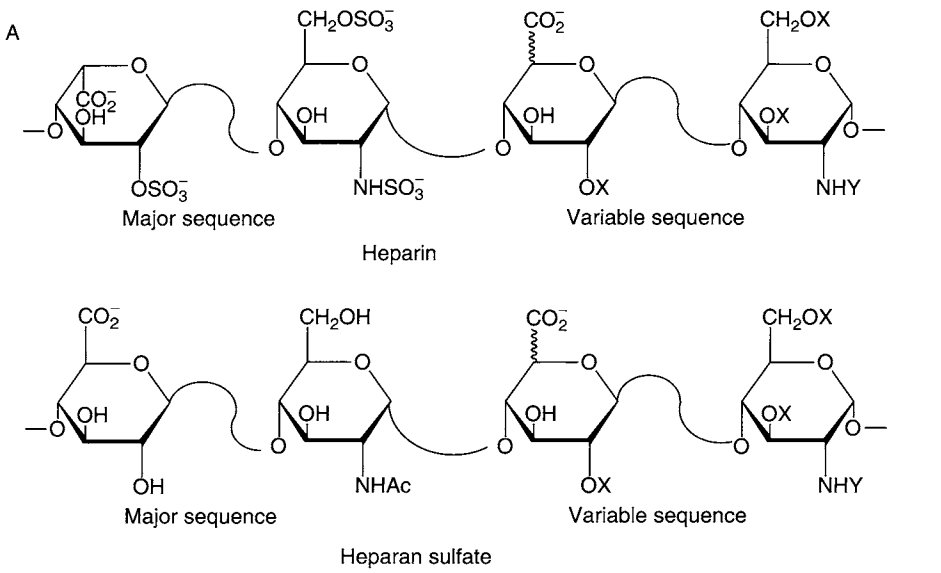

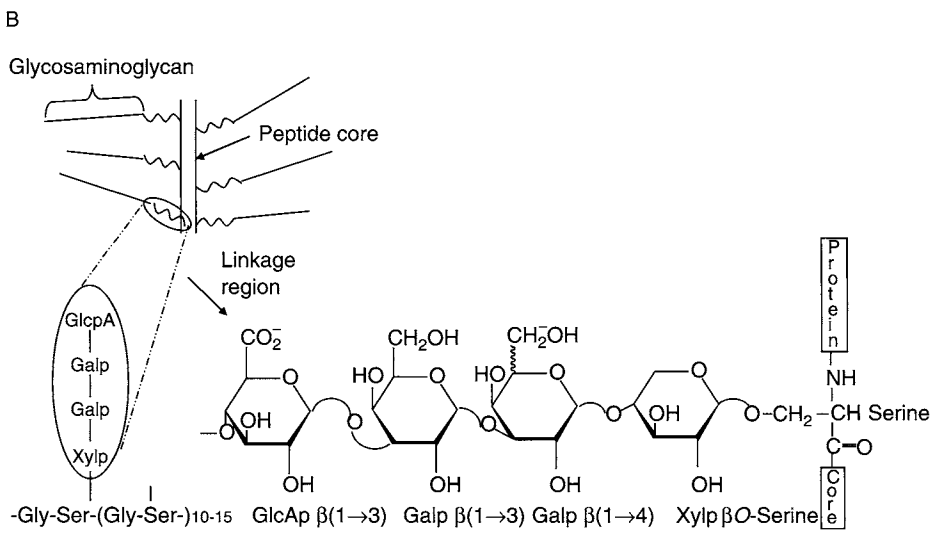

Figure 1 Heparin structure. (A) The sequence of heparin and the related heparan sulfate are shown, where X, SO_3^-, or H and Y, SO_3^-, $COCH_3$, or H. (B) The structure of heparin proteoglycan serglycin and the linkage region between core protein and GAG chain.

Table 1 Serum Concentrations of Selected Complement Proteins

Complement protein	Concentration in serum (μg/ml)	Concentration in serum (nM)
C1q	75	182
C1r	34	178
C1s	30	344
C2	15–20	130–173
C3	1500	8333
C4	430	2047
C5	75	394
C6	60	468
C7	60	495
C8	80	490
C9	58	734
C1INH	262.5	2500
C4BP	250	454
Factor B	120–300	1290–3225
Factor D	1	41
Factor P	20	90
Factor H	470	3133
Factor I	34	386
Factor J	2.6–8.2	130–410
MBL (mannan binding lectin)	1	1.85

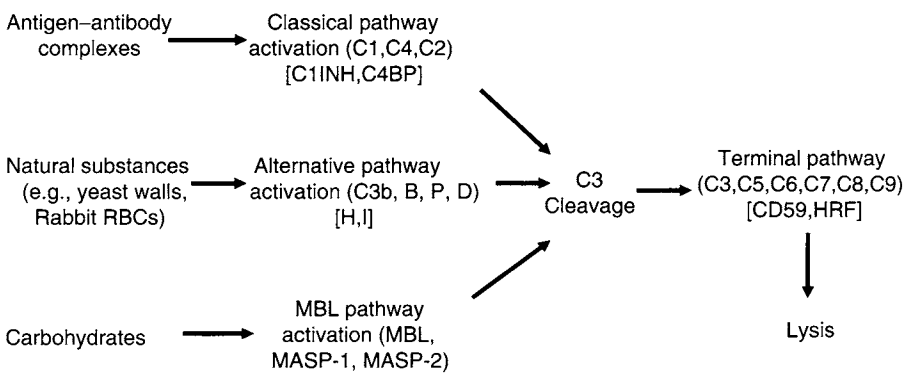

Figure 2 Overview of the three pathways of complement cascade.

The second means of activation, associated with the alternative or properdin pathway, is activated by direct contact with activated C3 that is deposited on a variety of surfaces including pathogens, such as viruses, and fungi, but also host cells in autoimmune disorders (30). The mannose-binding lectin (MBL) pathway, the most recently recognized activation pathway, leads to complement activation after contact with mannose on the cell surface of pathogens such as bacteria (Fig. 2).

In all three cases, a cascade of events follows, in which each step leads to the next. At the center of the cascade are steps, in which the proteolysis of a complement protein (C) leads to a smaller protein and a peptide (usually designated Ca, Cb). The smaller protein remains bound to the complex at the surface of the microorganism, while the peptide diffuses away. Both pathways converge at the fifth complement protein, C5, ultimately leading to the assembly of a multiprotein complex on the bacterial cell membrane known as the membrane attack complex (MAC), which lyses the bacterial cell.

2. Role of Complement in Health and Disease

a. *Biosynthesis of Complement Components*

Soluble complement components, with the exception C1q, factor D, properdin, and C7, are primarily synthesized in the liver (32). Extrahepatic biosynthesis also has been observed for most components. Complement protein secretion is increased by various mediators of inflammation, such as cytokines/chemokines, including tumor necrosis factor (TNF), interleukin-1 (IL-1), and interleukin-6 (IL-6). C1q is biosynthesized primarily in macrophages. The spleen appears to be the major organ involved in properdin biosynthesis. Adipocytes in the fat tissue are responsible for factor D biosynthesis.

b. *Disease Associated with Complement System*

Complement deficiencies result in frequent infections and immune complex diseases (33). With the exception of C9, deficiencies have been identified in all of the complement factors, including Factor D and properdin. Deficiencies have also been identified in the complement regulatory proteins C1INH, Factors I and H, DAF (complement decay accelerating factor), and HRF (homologous restriction factor). In general, deficiencies in complement components result in increased bacterial infections, especially with *Neisseria* species, resulting from reduced bacterial opsonization and phagocytosis (34).

The immune complex diseases are quite varied. These diseases include rheumatoid arthritis, where an inflammatory response is induced by antibody–antigen complexes in the synovial fluid; types of glomerulonephritis, due to complex trapping within the glomerulus, or retention of antibody–antigen in the glomerulus; extrinsic allergic alveolitis, as in "farmer's lung", where antigens are inhaled; filariasis, where antigens released from parasites in the lymphatic vessels; and erythema nodosum, where the chemotherapy treatment of patients with high levels of antibody against the leprosy bacillus results in antigen release and immune complex formation.

A series of inflammatory activities, including the induction of smooth muscle contraction, vasodilation, and an increase in vascular permeability have been attributed in large part to the activation of two peptides (C3a and C5a), released by the proteolytic action of the convertases on C3 and C5 (Fig. 3).

III. Heparin Regulation of the Complement System

A. Early Studies of Heparin-Complement Interaction

Ecker and Gross (35) reported nearly 70 years ago that heparin-like polyanions exhibit anticomplementary activity through the direct interaction of heparin with complement proteins. Ecker and Gross also showed that heparin did not inhibit lysis by binding to red cell membranes (9,35). Rosenberg and coworkers (36) reported in the early 1980s that heparin interacted with C1q, subsequently Kazatchkine and coworkers (37) demonstrated multiple sites in the classical and the alternative amplification pathways of complement, at which heparin may act. In 1993, Sahu and Pangburn (38) examined the binding activity of the normal human serum on heparin-agarose using affinity chromatography. They found that 13 complement proteins (C1q, C2, C4, C4bp, C1INH, B, D, H, P, C6, C8, C9, and vitronectin) bound heparin, while nine complement proteins (C1r, C1s, C3, Factor I, C5, C7, C3b, Ba, and Bb) did not bind heparin. Factor J, a highly glycosylated complement inhibitor glycoprotein, which acts on the classical and the alternative pathways, was also found to strongly interact with heparin and the structurally related heparan sulfate (39). Heparin directly inhibits C1q binding to immune complexes, inhibits the interaction of C1s with C4 and C2, and inhibits the binding of C2 to C4b (40). Heparin also inhibits formation or binding of the complement protein trimolecular complex, C5b67 (41). Heparin inhibits cobra venom factor (CoVF)-dependent C3 inactivation in whole serum, thereby having an impact on the generation and action of the C3 convertase formed from CoVF, factors B and D (42). Edens et al. (9) described the multiple effects of heparin on the classical and

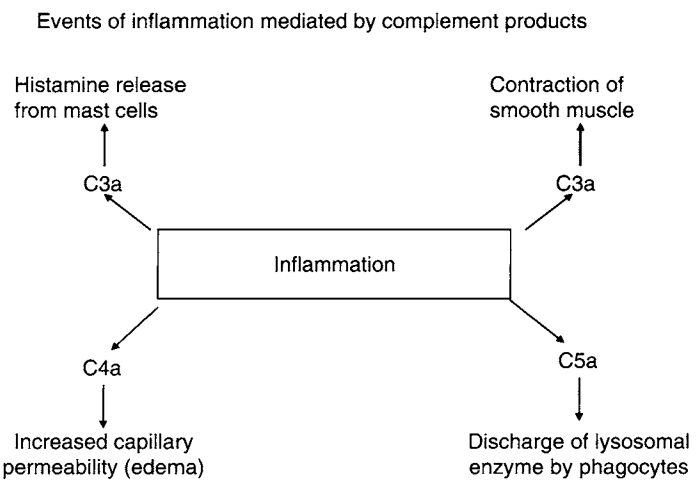

Figure 3 The role of complement components in the events of inflammation.

alternative pathways (Fig. 4). The MBL consists of a carbohydrate recognition domain (CRD) that binds to side chains on glycoconjugates rich in D-mannose and *N*-acetylglucosamine (43). However, little is known about the specific effects of sulfated polysaccharides on the recently described MBL pathway of complement activation.

Cofrancesco et al. (44) observed that heparin's inhibitory effect on the complement cascade is time-dependent and reversible. In addition, the size of the heparin chain and its chemical modification can influence and extent of its inhibitory activity (19). However, these previous reports on heparin-complement interactions are generally qualitative and lack kinetic and thermodynamic data, making it difficult to conclude what the real impact heparin has in the complement proteins of the classical and alternative pathways. This is particularly important when comparing the very low endogenous levels of circulating heparin and heparan sulfate with the high conventional therapeutic concentrations of exogenously administered heparin. More recently developed technologies, such as surface plasmon resonance (described later), better permit kinetic and thermodynamic determination of polysaccharide-complement interactions.

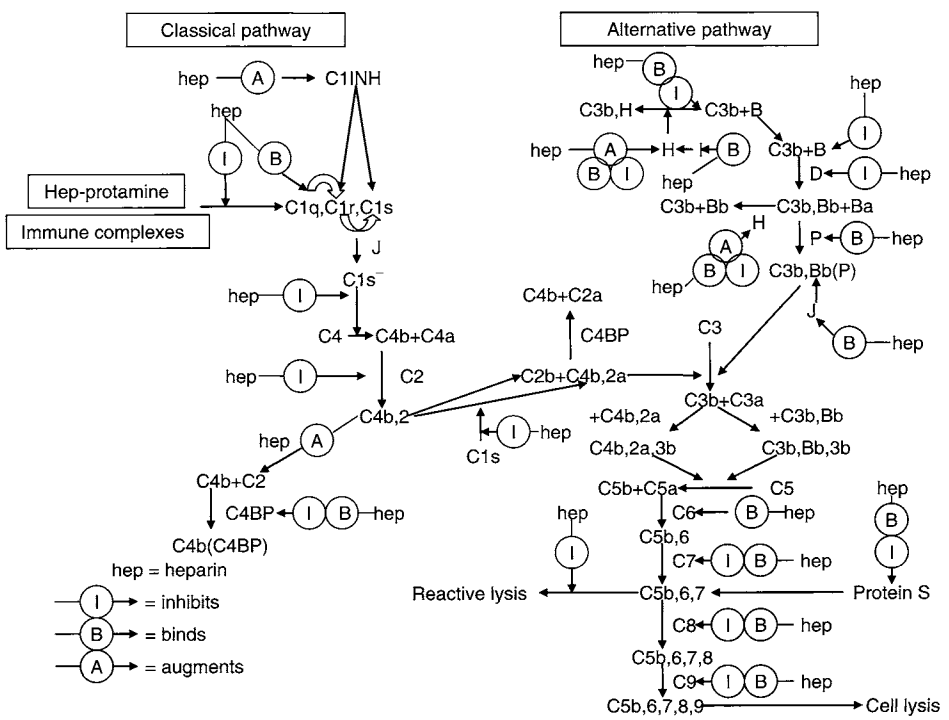

Figure 4 Current view of heparin effects on the classical and alternative pathways.

B. The Effects of Heparin on the Classical Pathway

1. *Heparin Inhibition of C1 Activity*

The classical pathway is triggered by C1, a protein composed of three functionally different subunits: C1q, C1r, and C1s. The recognition protein C1q (~75 μg/ml in normal adult serum) binds to the Fc portion of an antibody. The catalytic subunit is the tetramer C1s–C1r–C1r–C1s that is formed in a calcium-dependent manner (45). C1s enzymatically cleaves the next complement protein, C4, while C1r acts as a bridge connecting C1q to C1s (46). Most C1-complexing ligands are recognized by the C1q moiety, generating a conformational signal that triggers self-activation of C1r that in turn activates C1s (47).

The interaction of heparin with C1 was examined using both affinity chromatography on heparin-Sepharose and by fluorescence polarization measurement using fluorescein-labeled heparin (48). Almeda et al. (36) measured the interaction of a radiolabeled low molecular weight (LMW) heparin (M_r = 8500) (6), and found two K_d values for C1q binding, high-affinity binding constant of 76.6 nM a low-affinity binding constant of 1.01 μM. They also reported that LMW–Hep (2.5 nM) inhibited the ability of C1q (0.5 nM) to recombine with C1r (1.4 nM) and C1s (1.6 nM) to form hemolytically active C1 and at 250 mM, LMW–Hep inhibited the hemolytic activity of reconstituted C1.

In a recent study in our laboratory (49), surface plasmon resonance (SPR) spectrometry was utilized to determine the kinetic and thermodynamic parameters for C1q-heparin interaction. Biotinylated heparin, immobilized to a streptavidin chip, interacted with fluid phase C1q. A sensorgram for interaction of C1 and heparin is shown in Fig 6A. Immobilized heparin interacted with C1, giving an on-rate constant (k_{on}) value of $1.95 \times 10^5\ M^{-1}s^{-1}$, off-rate constant ($k_{off}$) of 5.39×10^{-3} M, and K_d of 27.6 nM (Table 2). The calculated K_d is comparable to the high affinity heparin-binding data for C1q, obtained by Almeda. Therefore, our result confirms that the interaction between C1 and heparin can primarily be attributed to the C1q. Based on the structure of C1 complex (Fig. 5) and 1:1 stoichiometry of the binding, we suggest that heparin binds only to the collagenous stalk region of C1q, showing no interaction with the C1q globular region.

Heparin inhibits C1 functional activity when it binds to C1. Raepple et al. (40) reported that incubation of heparin, or other selected polyanions (including dextran sulfate, polyvinyl sulfate, and chondroitin sulfate), with C1, C4, and C2 separately, reduced most of the hemolytic activity of C1, but had no effect on that of C2 and C4. These experiments demonstrated that all the tested polyanions strongly inactivated C1 and that the extent of this inactivation differed with each polyanion. In addition, all the polyanions examined also inhibited the consumption of C2 and C4 by C1, prevented the uptake of C2a by C4b and promoted the dissociation of C4b2a. This report was further confirmed by Strunk and Colten (50), who found that heparin noncompetitively inhibited the cleavage of C4 and C2 by C1. Heparin has a more pronounced effect on C2 cleavage than on C4 cleavage (50,51).

Table 2 Kinetic and Affinity Constants for Heparin-Complement Protein Binding

Complement protein	Chip surface	$k_{on}(M^{-1}s^{-1})$	$k_{off}(s^{-1})$	K_d (nM)
C1	DEX-SA	1.95×10^5	5.39×10^{-3}	27.6
C2	DEX-SA	4.13×10^3	1.32×10^{-3}	320
C3	DEX-SA	1.83×10^4	5.73×10^{-4}	31.2
C4	DEX-SA	9.64×10^4	3.46×10^{-3}	60.8
C5	DEX-SA	2.43×10^5	1.35×10^{-3}	21.9
C6	DEX-SA	1.72×10^4	5.58×10^{-4}	31.3
C7	DEX-SA	6.25×10^4	9.60×10^{-4}	12.8
C8	DEX-SA	4.17×10^4	5.74×10^{-3}	173
C9	DEX-SA	3.43×10^4	4.51×10^{-3}	131
C1INH	DEX-SA	1.58×10^4	4.64×10^{-4}	29.4
Factor I	DEX-SA	4.45×10^4	1.03×10^{-3}	36.2
Factor H	DEX-SA	1.84×10^4	7.25×10^{-3}	399
Factor B	PEG-NA	2.58×10^5	2.77×10^{-4}	2.10
Factor P	PEG-NA	3.84×10^4	8.74×10^{-5}	26.8

Two chips were used to acquire these data: the dextran-streptavidin (DEX-SA) chip and the poly(ethylene glycol)-neutravidin (PEG-NA) chip.

2. *Heparin Augmentation of C1 Inhibitor (C1INH) Activity*

C1 inhibitor (C1INH) is a 105 kDa plasma protein, which is the only serine protease inhibitor known to dissociate the activated C1r and C1s from C1q, thus limiting the time this complex is active (51,52). C1 inhibitor also blocks spontaneous activation of C1 by plasma proteases. A deficiency in C1INH is associated with sudden, life-threatening episodes of angioedema.

As early as 1976, Nagaki and Inai (53) found the presence of heparin in the reaction mixture of C1INH, and C1s substantially enhanced C1INH inhibition of

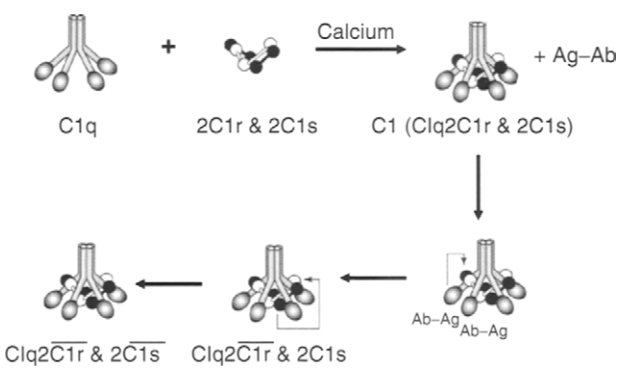

Figure 5 Schematic representation of activation of three components of C1: C1q, C1r, and C1s. The globular region and the collagenous stalk region of C1q were also specified.

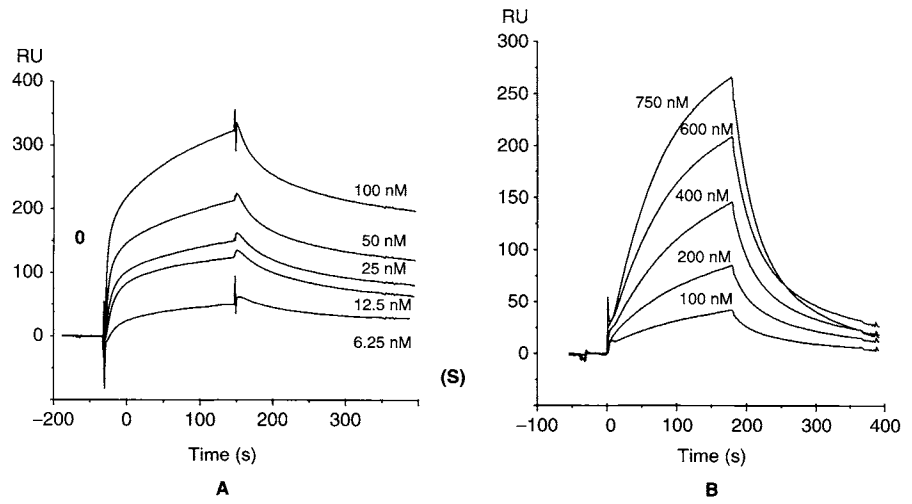

Figure 6 SPR analysis of (A) C1 ($C1qC1r_2C1s_2$)-heparin interaction; (B) C1INH-heparin. Increasing concentrations of C1 (100, 50, 25, 12.5, and 6.25 nM) and C1INH (100, 200, 400, 600, and 750 nM) were injected over sensor chip containing biotinylated heparin, which was bound to immobilized streptavidin. The amount of protein associating with the heparin was measured in resonance units. Identical samples were also injected over a control chip containing streptavidin but no heparin (nonspecific binding), and the sensorgrams shown in this figure were obtained after subtraction of nonspecific binding.

C1s (54–56). Other GAGs including chondroitin sulfate A, B, and C were also found effective in augmenting the C1INH inhibition of C1s, but to a lesser extent than heparin. Kinetic studies indicated that heparin potentiated C1IHN inhibitory activity by up to 15- to 35-fold. The SPR studies of the interaction of heparin and heparan sulfate with C1INH were first reported by our laboratory in 1999 (57). Heparin, immobilized on a biosensor chip gave a K_a value of $7 \times 10^6\,M^{-1}$. These data showed somewhat weaker binding than our recently obtained results (49) (Fig. 6B), which affords a K_a of $3.41 \times 10^7\,M^{-1}$ and K_d of $2.94 \times 10^{-8}\,M$, respectively (Table 2). The discrepancy in these results may be caused by differences in the heparin–biotin conjugates or the surface density of the immobilized heparin. The proximity of the protein-binding site to the point of immobilization might interfere with protein binding, having a major impact on the measured affinity constants.

The order of interaction between C1, C1INH, and heparin was also determined by protease inhibition experiment (57). The results suggest that heparin must interact with C1 and with C1INH prior to, or at the same time that C1INH interacts with C1 for heparin augmentation to occur. Summarily, heparin interacts with C1INH and augments its inhibition of C1. The concentrations of heparin required for binding and augmentation are within those achieved by inhalation therapy in patients (58,59). Future studies will be required to determine if the heparin–C1INH

interaction has biological significance *in vivo* and, if this is the case, suggests a potential new therapy for treating hereditary angioedema.

C. Effect of Heparin on C2 and C4 Activity

C2 is one of the least abundant of the complement components in the human plasma, present at a concentration of 15–20 μg/ml (Table 1) (60). C2 is a single chain glycoprotein with an M_r of 100 kDa (61). C4 is the second complement protein to undergo reaction in the classical pathway of the complement cascade. C4 is a β-globulin with an M_r of 240 kDa and is found at a serum concentration of 430 μg/ml (Table 1) (62).

The role of C2 and C4 in the classical pathway has been reviewed extensively (9,54,60,61). C4 is cleaved by the C1s domain of the membrane bound C1qC1rC1s complex with the release of a small and inactive peptide, C4a. The larger C4b (M_r = 198 kDa) fragment binds covalently to sugar residues on cell-surface glycoproteins through ester bond formation (63). C4b serves as a receptor for C2 by forming an Mg^{2+}-dependent complex with C2. C2 is then rapidly cleaved by C1s with the loss of hemolytic activity to yield a small, inactive, fragment of C2b (M_r = 34 kDa) that diffuses away. C2a (M_r = 73 kDa) binds noncovalently to a site on membrane-bound C4b. The complex of C4b2a is referred to as "C3 convertase" since it cleaves C3 into C3a and C3b (Fig. 7).

In 1976, Loos and coworkers (40,64) demonstrated that heparin interfered with the components of the classical pathway in at least three different ways. Heparin binds to C1q, preventing the consumption of C4 and C2 by C1s by interfering with its C4 and C2 binding sites, and inhibiting the binding of C2 to C4b by sequestering the Mg^{2+}. Almost a decade later, Sahu and Pangburn (38) determined a relative affinity of C2 for heparin represented as an IC_{50}

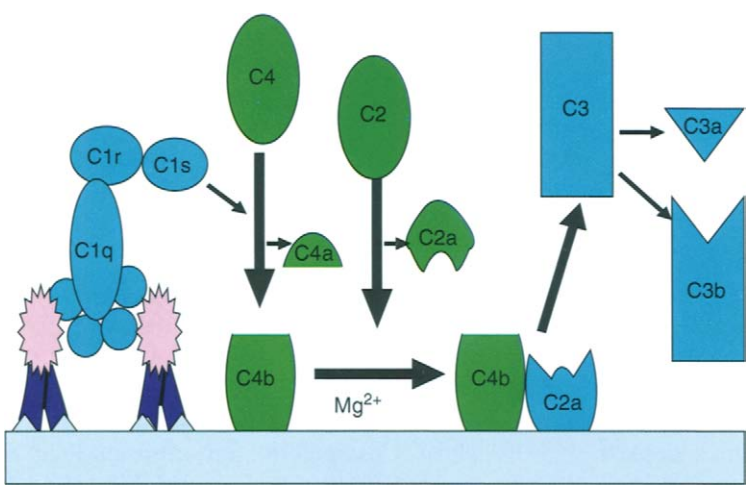

Figure 7 The formation of C3 convertase (C4b2a) and its cleavage of C3.

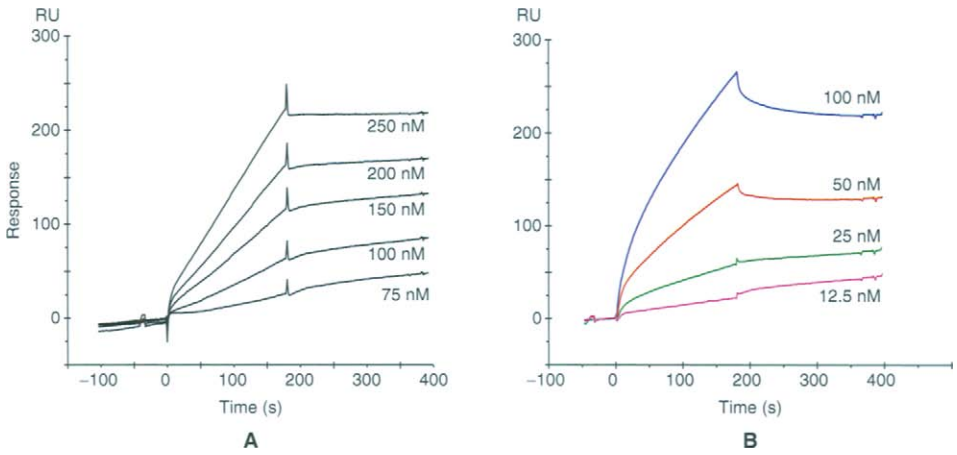

Figure 8 Sensorgram shows the interaction of biotinylated heparin on a streptavidin chip with: (A) soluble complement C2 at five representative concentrations (75, 100, 150, 200, and 250 nM) and (B) C3 at 12.5, 25, 50, 75, and 100 nM.

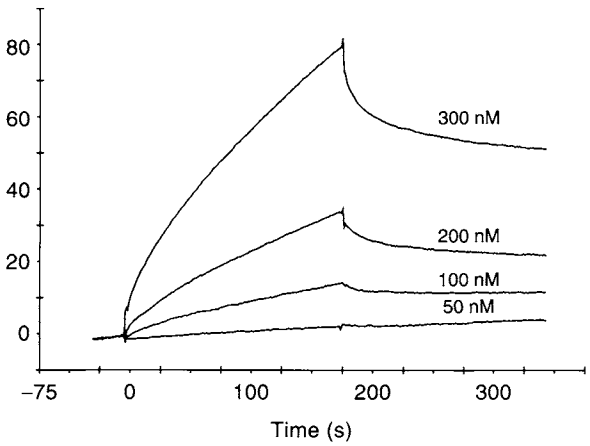

Figure 9 SPR sensorgrams of interaction between C4 at 50, 100, 200, and 300 nM with biotinylated heparin immobilized on a streptavidin (SA) chip.

(concentration of free heparin needed to inhibit C2 protein binding to heparin-agarose by 50%) of 12 μg/ml. In contrast, other studies performed by incubating C4 and C2 with heparin, and determining their residual activity showed that heparin had no direct effect on purified C4 and C2. Our laboratory recently determined the kinetic interactions of heparin with C4 using SPR (49). We measured the kinetic interaction of heparin with C2 and C4 using SPR. Sensorgram (Figs. 8A and 9) clearly show that *in vitro* heparin binds C2 with K_d of 320 nM; binds C4 with a K_d of 6.08 nM (Table 2).

D. Effect of Heparin on C4 Binding Protein (C4BP)

C4 binding protein (C4BP) is a glycoprotein that is capable of specifically binding to C4b. The main function of C4BP is believed to be the inhibition of the activity of the C3 convertase (C4b2a) of the classical pathway. There are two forms of C4BP having similar functional properties present in human plasma. These forms differ in molecular weight (590 and 540 kDa) and net charge (65). C4 binding protein contributes to the regulation of the classical pathway of the complement system and plays an important role in blood coagulation. It binds specifically to C4b to control the assembly and function of the C3 convertase (C4b2a), and accelerates the decay of this convertase in a concentration-dependent fashion (66).

Scharfstein et al. (67) first reported that the formation of C4/C4BP complex could be prevented in the presence of heparin, suggesting that heparin bound to C4BP. Schwalbe et al. (68) reached the same conclusion by examining heparin's effect on serum amyloid protein (SAP) interaction with C4BP. Subsequently, Hessing et al. (69) reported that the heparin-binding domain was localized on, or close to the C4b-binding site in C4BP. The interaction between heparin and C4BP was first studied using SPR by Blom et al. (70). They found C4BP interaction with heparin showed a high-association rate constant (k_{on}), and low-dissociation rate constant (k_{off}), suggesting this was a high-affinity interaction (70). However, in these experiments, the interaction between the fluid phase multimeric C4BP and the immobilized heterogeneous heparin was too complex to calculate meaningful affinity constants for this interaction.

E. Effect of Heparin on C3 and C3 Convertase

C3, a prominent complement protein, with the plasma level of 1500 μg/ml (Table 1) holds a key position in the complement cascade since it is found at the convergence of the classical and the alternative pathways (Fig. 10).

C3 has an M_r of 180 kDa and is made up of two different polypeptide chains held together through disulfide bonds and noncovalent interactions. The larger α-chain has an M_r of 110 kDa and the smaller β-chain an M_r of 70 kDa (71,72).

In the classical pathway C3 convertase, C4b2a cleaves an arginine–serine peptide bond at position 77 of the C3 α-chain (Fig. 7) to generate the 9 kDa C3a and the 171 kDa C3b. In the alternative pathway, the same fragments are formed from C3 through the action of a complex of C3b and factor B fragment Bb (C3bBb). Subsequently, C3b binds to the C4b2a of classical pathway, or C3bBb of alternative pathway already attached to a biological membrane to form a new membrane-bound enzyme complex that recognizes C5 as its substrate. In 1981, Sim et al. (73) established the mechanism, by which C3b formed a covalent bond with surfaces, such as protein or glycoprotein, carbohydrate, and phospholipids (Fig. 11).

Four decades of studies have established that C3 functions like a double-edged sword: on one hand it promotes phagocytosis, inducing inflammatory responses against pathogens; on the other hand, unregulated activity of C3 resulting in host cell damage. C3b also serves the important function of distinguishing between cells of different species. Hence, the human alternative and MBL pathways can only

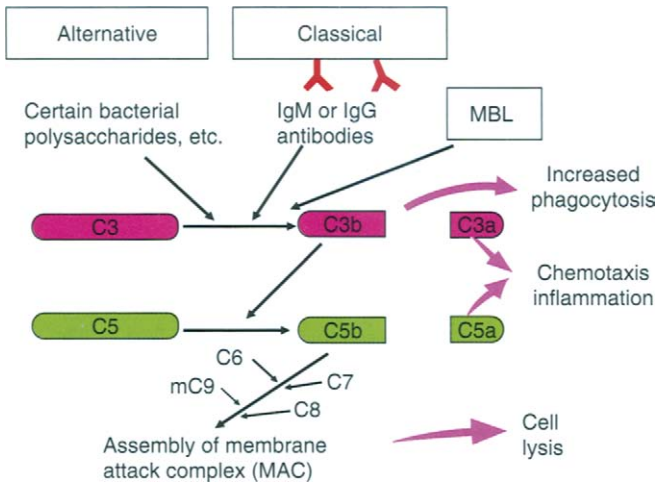

Figure 10 C3 is a central component in all three pathways of the complement activation.

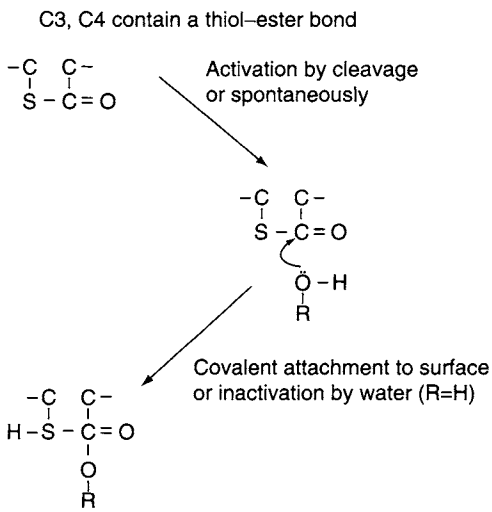

Figure 11 Schematic representation of the chemistry taking place upon C3 immobilization on the cell surface.

be activated by cell walls of other species and by certain bacteria, but not by human erythrocytes.

The effect of heparin on C3 activity has been examined both *in vivo* (20) and *in vitro*. Heparin inhibitory activity on the alternative pathway convertase formation (Fig. 4) is independent of its anticoagulant activity and requires the presence of *O*-sulfo groups (74). Pangburn (75) observed that C3b binding to polysaccharide caused a reduction of C3 activity, which depended in part on the size of the

oligosaccharide. Monosaccharide and disaccharides with structural similarities to dextran did not cause a detectable decrease in C3b-factor H binding, while sugar polymers caused large decreases in the affinity between C3b and factor H, due to the polysaccharide occupying the binding site in C3b or in factor H, preventing their interaction. An earlier finding by Weiler et al. (76) suggested that heparin could reversibly inhibit C3b binding to factor B. They believed that the inhibiting action of heparin had nothing to do with the chelation of Mg^{2+}, but came about preventing B utilization during the fluid phase interaction of C3b, B, and D.

SPR was used to characterizing the heparin and C3 interaction. The SA chip immobilized with biotinylated heparin was also used in this experiment. Sensorgram (Fig. 8B) was fitted with the Langmuir 1:1 binding model to afford a k_{on} value of $1.83 \times 10^4\,M^{-1}s^{-1}$ and k_{off} value of $5.73 \times 10^{-4}\,s^{-1}$. Thus, the overall approximate K_d for heparin–C3 binding is 31.2 nM.

Recent studies on the antimicrobial activities of heparin-binding peptides by Andersson et al. (77) showed that the heparin-binding peptides derived from complement factor C3 exerted antimicrobial activities against Gram-positive and Gram-negative bacteria. An improved understanding of the features of GAG-complement protein binding, such as heparin–C3 binding, may aid in the search for endogenous antimicrobial peptides from complex biological sources. It may also provide a logical rationale for evaluating possible antimicrobial properties of GAG-binding proteins or peptides not yet considered as antimicrobials.

F. The Effects of Heparin on the Terminal Pathway

1. *Effect of Heparin on the Membrane Attack Complex (MAC) and Reactive Lysis*

The final step of the complement cascade common to all three activation pathways is referred to as the terminal pathway. C5 convertases are membrane assemblies of C4b2a (classical pathway) or C3bBb (alternative pathway), and additional C3b molecules corresponding to C4b2a3b and C3bBb3b, respectively (78). The major difference observed between the two convertases is in their rates of C5 cleavage. The classical pathway C5 convertase cleaves C5 about six to nine times faster than does the alternative pathway C5 convertase. C5, present at a plasma concentration of 0.37 μM (Table 1) (79), is cleaved by these convertases into two biologically important products, corresponding to the last enzymatic step in the complement activation cascade (54). The smaller fragment, C5a, is chemotactic, regulating inflammatory responses by stimulating neutrophils and phagocytes. The larger fragment, C5b, initiates the formation of the MAC (C5b-9) (Fig. 12), resulting in the lysis of bacteria and other pathogens (80). Activated C5 provides the nucleus for the sequential and essentially nonreversible addition of single copies of components C6, C7, and C8, and multiple copies of C9 to produce the MAC at the targeted site. The MAC is regulated by S protein, also called vitronectin, which controls the activity of C5b67. MAC assembly is also regulated by homologous restriction factor (HRF), SP40, and CD59, which regulates C8, C9 activity.

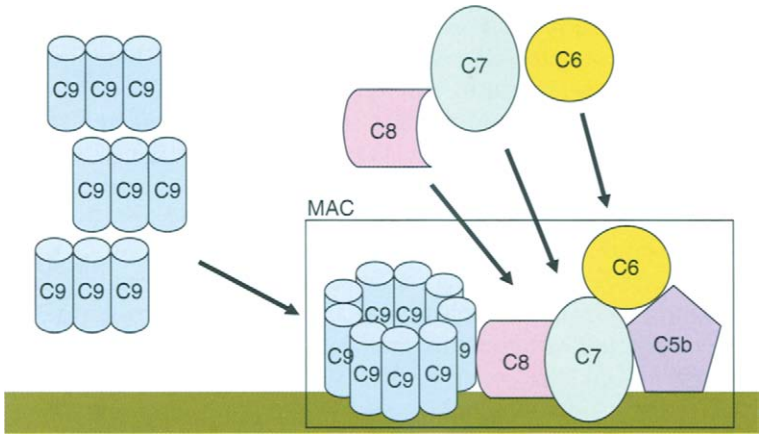

Figure 12 The formation of the membrane attack complex (C5b–9).

Baker et al. (41) first reported that heparin and other polyanions including polyanethol sulfonate and dextran sulfate, inhibited MAC promoted reactive lysis. By contrast, polycations, including polybrene, protamine, and polyornithine, potentiated the formation of C567, which can attach to erythrocyte membranes rendering them susceptible to lysis in the presence of C8 and C9. They observed that the heparin polyanion inhibited the formation of C567 from C56, C7, and sheep erythrocytes, suggesting that the reaction C567 → EAC567 (erythrocytes sensitized by antibody and the C567 complex) was susceptible to manipulation by a spectrum of polymers based on their charge and size (41). Heparin at 2 μg/ml causes 50% inhibition of the formation of C5b67 while as much as 250 μg/ml of chondroitin sulfates A or B or C or hyaluronic acid (a nonsulfated GAG) has no effect on the formation of C5b67. These findings were confirmed by Tschopp and Masson (81), who found that negatively charged GAGs, such as heparin, inhibited hemolytic activity by blocking the lytic activities of C6, C7, C8, and C9 by interfering with the incorporation of these terminal components into the MAC.

Surface plasmon resonance studies were conducted to better understand the numerous interactions between heparin and components of terminal pathway (49). Figures. 13A–D and 14 show SPR sensorgrams for a surface immobilized heparin pulsed with varying concentrations of C5, C6, C7, C8, and C9. The equilibrium and kinetic constants from SPR for the interaction of C5, C6, C7, C8, and C9, as well as all other C proteins are listed in Table 2.

2. *Heparin Interaction with Vitronectin*

Vitronection is a 70 kDa protein found in both the extracellular matrix as well as serum. Vitronectin regulates the complement terminal pathway in two ways, by binding soluble C5b67 promoting its formation and attenuating its ability to bind to membranes and by preventing C9 polymerization (81). Heparin binds vitronectin

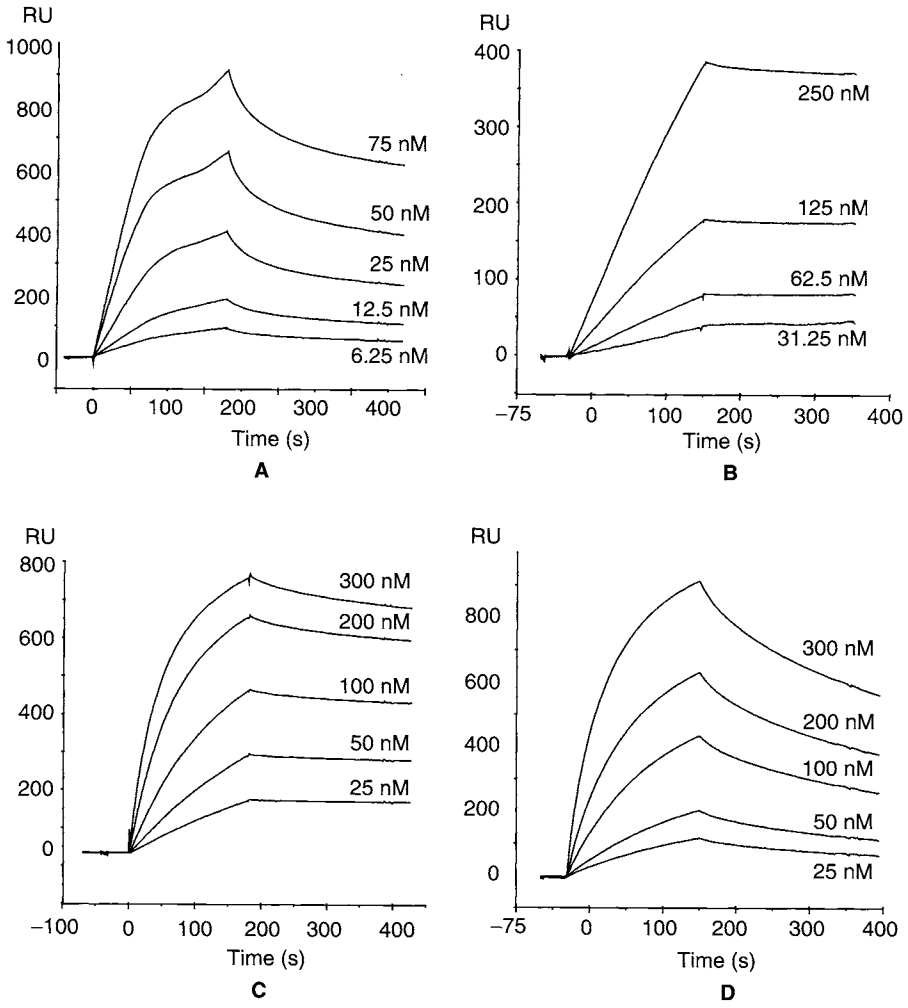

Figure 13 Kinetic binding studies of heparin and complement proteins C5, C6, C7, and C8. Biotinylated heparin was immobilized on a streptavidin-coated sensor chip and complement protein was injected at increasing concentrations (indicated in the legend box of each sensorgram) over the surface. The curves represent injections performed at 30 μl/min for 90 s, followed by 3 min of buffer flow. Injections (repeated at least four times) were aligned at $t = 0$. (A) C5 at 6.25, 12.5, 25, 50, and 75 nM; (B) C6 at 31.25, 62.5, 125, and 250 nM; (C) C7 at 25, 50, 100, 200, and 300 nM; and (D) C8 at 25, 50, 100, 200, and 300 nM. All the complement components listed here nearly have the same association rate, while compared with other complement proteins; C6 is described by a much slower dissociation rate (as seen by the nearly flat in signal during the dissociation phase).

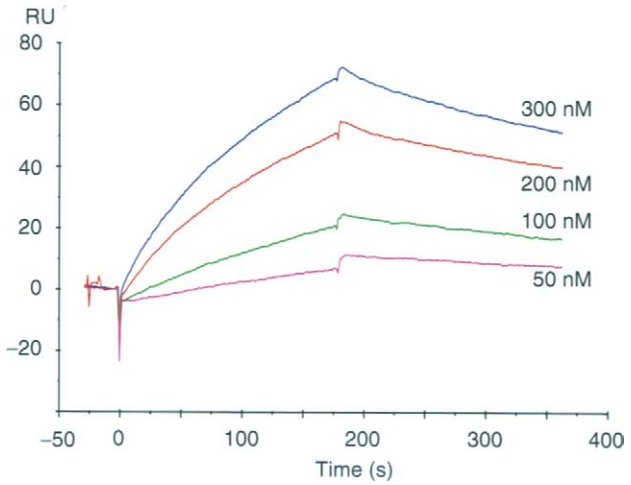

Figure 14 Interaction of C9 with heparin as studied using SPR, C9 at 50, 100, 200, and 300 nM.

and diminishes its inhibition of complement activity (82). The highly basic region of vitronectin ($Ala^{341}-Arg^{379}$) is important in its interaction with heparin. Using an affinity electrophoresis technique, Edens et al. (8) demonstrated that specific heparin chain of $M_r > 8000$-bound vitronectin with high affinity ($K_d \sim 6.7 \times 10^{-6}$ M), whereas most high molecular weight chains showed little, or no affinity for vitronectin. Previous K_d reports for the interation of heparin with vitronectin ranged from 4 to 40 $\times 10^{-6}$ M with most results centered around 5×10^{-6} M (83).

IV. The Effects of Heparin on the Alternative Pathway

In the alternative pathway, complement is activated directly by microbial components (Fig. 15). This is an important and biologically primitive form of complement activation. The alternative pathway begins with spontaneous self-activation of C3. As previously discussed, C3bBb is the C3 convertase of the alternative pathway of complement. The enzyme is controlled by the serum proteins, factors H and I, and properdin. The formation of the enzyme requires C3b, factors B and D, and Mg^{2+}. In solution, C3 undergoes a slow conformational change, similar to that produced by cleavage or hydrolysis, exposing its reactive thioester bond. This activated fluid-phase C3* resembles C3b and is rapidly inactivated by factors H and I. Its lifetime is prolonged by binding to an "activator surface," such as a bacteria capsule. There it may persist long enough to bind factor B and allow cleavage and activation by factor D. The activated Bb subunit of the resulting C3bBb complex can bind and activate additional molecules of C3. This C3 convertase of the alternative pathway is stabilized by the binding of a protein, properdin (P). The C3bBbP will cleave

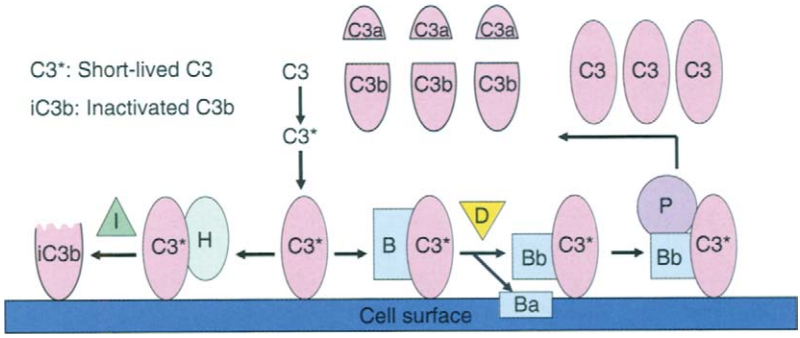

Figure 15 Cartoon showing the activation of C3 in the alternative pathway.

more C3 molecules and form a C3bBbP ($C3b_n$) complex, which in turn binds and activates C5.

There are multiple sites in the alternative pathway where heparin exerts regulatory activity (84). The ability of heparin to mediate the alternative pathway can be correlated to its size and degree of sulfation (85). At a given concentration, the inhibitory activity of heparin on the alternative pathway is much greater than its inhibitory activity on the classical pathway (63). Weiler (86) reported a comparison of a series of polyanions with a series of polycations for ability to inhibit either the classical or the alternative pathways. They also observed that polyanions have more activity on the alternative pathway, while polycations have more activity on the classical pathway on a weight basis. It remains unclear why polycations preferentially inhibit the classical pathway and polyanions preferentially inhibit the alternative pathway.

A. Heparin Interaction with Factors H and I

There are six complement glycoproteins: C3 and factors B, D, H, I, and P. Factor H is an elongated $\approx$ 150 kDa plasma glycoprotein composed of a single polypeptide chain containing 9.3% carbohydrate. C3b and factor H are directly involved in the discrimination between activators and nonactivators (87–89). Whether C3b is inactivated or initiates its amplification most frequently depends on the affinity of bound C3b for regulatory factor H. This affinity is mediated by the interaction of factor H with polyanions, such as heparin and sialic acids, on glycoproteins and glycolipids (90,91). Heparin's effect on factor H seems to be inconsistent because heparin has been reported to activate both pathways of complement (92), and also inhibit alternative pathway activation, suggesting that heparin simultaneously has opposing effects on the functions of factor H. Heparin in a concentration range of 0.54–8.66 μg per 10^7 erythrocytes inhibits the activity of factor H to accelerate the decay of unstabilized convertase (90). In contrast, polyanions-like heparin on surfaces can prevent activation of the alternative pathway by enhancing the binding of factor H to C3b. The reason for such apparent discrepancy is likely because of a

difference in experimental design. Studies investigating the classical or alternative pathways, examining effects of fluid-phase heparin, or of immobilized heparin led to different outcomes. In addition, the varied concentrations used in these different studies might also have caused this apparent discrepancy (93).

In 1994, Meri and Pangburn (94) compared the ability of heparin and chemically modified heparins (M_r~11kDa) to enhance factor H binding to zymosan (an insoluble polysaccharide fraction of yeast cell walls used as a support) C3b by measuring the binding of radiolabeled factor H to activator-bound C3b in the presence of heparin. They found the magnitude of this enhancement effect was much reduced in the case of LMW heparin, and the effect also decreased in a concentration-dependent manner if *N*-sulfo groups were removed from heparin, indicating that these negatively charged *N*-sulfo groups were essential for heparin's activity (Fig. 16). Although the heparin-binding domain on factor H has been identified (95,96), the mechanism of heparin augmentation of factor H function is still not clear. One assumption is that heparin causes a conformational change in factor H, which in turn facilitates a high-affinity interaction between factor H and surface-associated C3b (97).

Factor I, also referred to as C3b inactivator, is composed of two disulfide-linked polypeptide chains (M_r 50 and 38 kDa, respectively), and is found in plasma at a concentration of ~34 μg/ml (Table 1). Factor I is a regulatory protein of the alternative pathway exerting its control with the help of its cofactor, factor H, by the enzymatic inactivation of soluble C3b, cleaving the α′ chain of C3b into two fragments (M_r 67 and 40 kDa) (98,99). If C3b is attached to particulate activators (polysaccharides, fungi, bacteria, viruses, certain mammalian cells, and aggregates of immunoglobulins), C3b can be cleaved by factor I alone, but the rate of cleavage is enhanced 30-fold by factor H (97).

Meri and Pangburn (89) demonstrated that heparin not only augmented the binding of factor H to zymosan-bound C3b, but at the same concentration it also enhanced the cofactor function of factor I with factor H, on C3b linked to soluble dextran support. In another report, Koistinen (100) showed that neither heparin nor LMW dextran sulfate had regulatory effect on the activity of factor I cofactor, using C3b bound to Sepharose 4B as a support. In contrast, high molecular weight

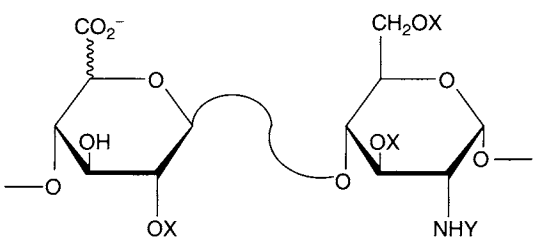

Figure 16 Summary of the structural requirements of heparin acting on complement. Some X substituents must be sulfo and Y substituents can be sulfo or acetyl. If no X is sulfo, or if Y is a hydrogen, no complement inhibitory activity is observed.

dextran sulfate strongly inhibited factor I. However, when Koistinen (100) incubated fluid phase C3b with factors I and H, either in the presence or absence of polyanions, no effect was observed on factor I. This discrepancy may also result from different experimental parameters. No direct kinetic binding data for heparin and factor I had been reported.

Recent studies in our laboratory (49) performed kinetic analysis to study the binding of heparin and factors I and H (Fig. 17A and B), the kinetic constants obtained for factor I are k_{on} ($M^{-1}s^{-1}$) = 4.45×10^4, k_{off} (s^{-1}) = 1.03×10^{-3}, K_d (M) = 3.62×10^{-8}; for factor H are k_{on} ($M^{-1}s^{-1}$) = 1.84×10^4, $k_{off}(s^{-1})$ = 7.25×10^{-3}, K_d (M) = 3.99×10^{-7} (Table 2).

B. Heparin Activity on Factors B and D

Factor B, also called C3 proactivator, is a glycine-rich, heat-labile, β-glycoprotein with an M_r of 93 kDa found in blood at concentrations of 120–300 μg/ml (Table 1) (101). Factor B, the precursor of the catalytic subunit of the C3 convertase in the alternative pathway, is converted by factor D to two fragments (102,103). The larger fragment, Bb, M_r of 60 kDa, possesses the active site of C3 convertase, C3bBb. Factor D is an enzyme consisting of a single polypeptide chain that is involved in the assembly of the C3 convertase in the alternative pathway (104). Factor D cleaves factor B, its only-known substrate, in the context of the biomolecular complex C3bB. It has been proposed that binding to C3b induces a conformational change in factor B, thus allowing it to fit into the substrate-binding site of factor D.

There are few reports about effects of heparin on factors B and D. One of these, by Kazatchkine and coworkers (42) showed that fluid phase heparin inhibited

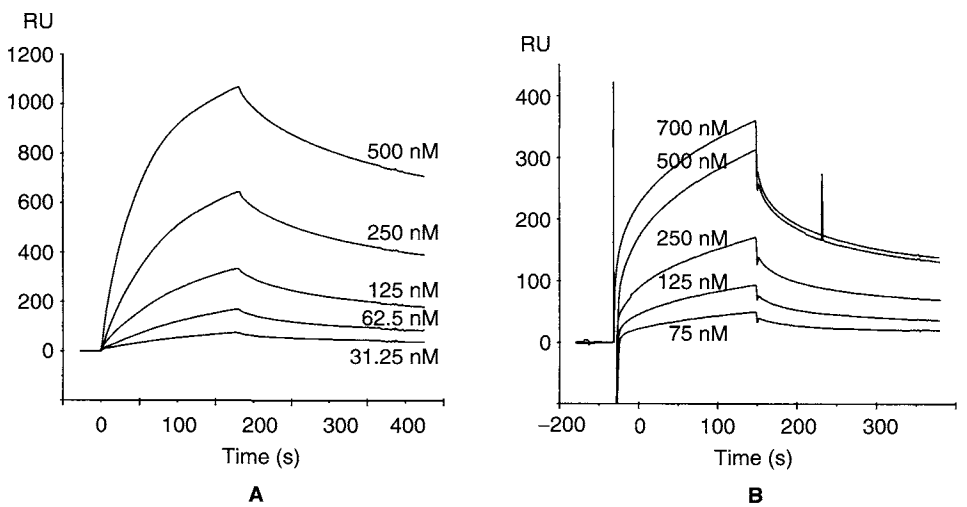

Figure 17 SPR sensorgrams of interaction between biotinylated heparin immobilized on a streptavidin (SA) chip with (A) factor I at 12.5, 50, 75, and 100 nM; (B) factor H at 75, 125, 250, 500, and 700 nM.

C3 convertase C3bBb formation by preventing the interaction of cell-bound C3b binding with factor B in the presence and absence of factor D. They found this effect of heparin was concentration-dependent and required the presence of sulfo groups, because no inhibition effect was observed in the presence of completely (*N*- and *O*-) desulfonated heparin (42). They also demonstrated that this inhibition effect resulted from the binding of heparin to the cell-bound C3b and masking the factor B binding in C3b. Furthermore, they suggested that heparin does not inactivate factor B, or directly affect its binding affinity (105), but instead inhibits consumption of factor B by factor D in a fluid phase.

To study the binding of heparin and factor B, our group performed kinetic analysis using SPR (Fig. 18A) (49) and obtained kinetic constants for this binding: k_{on} ($M^{-1}s^{-1}$) = 2.58×10^5, k_{off} (s^{-1}) = 2.77×10^{-4}, K_d (M) = 2.1×10^{-9} (Table 2).

C. Heparin Regulation of Properdin (Factor P)

Properdin has an M_r of 224 kDa and is composed of four identical polypeptide chains held together noncovalently. Properdin functions as an enhancing regulator and stabilizes the C3 convertase during the activation of the alternative pathway (106,107). The native properdin (nP) then becomes activated properdin (aP), which retards C3bBb decay, thus enhancing C3 cleavage.

The role that sulfated glycoconjugates exert on properdin function has been studied (76,84,108). Heparin proteoglycan or GAG from rat peritoneal mast cells and heparin inhibits the formation of C3 convertase in the presence or absence of properdin. This capacity of GAG depends largely on whether the convertase is

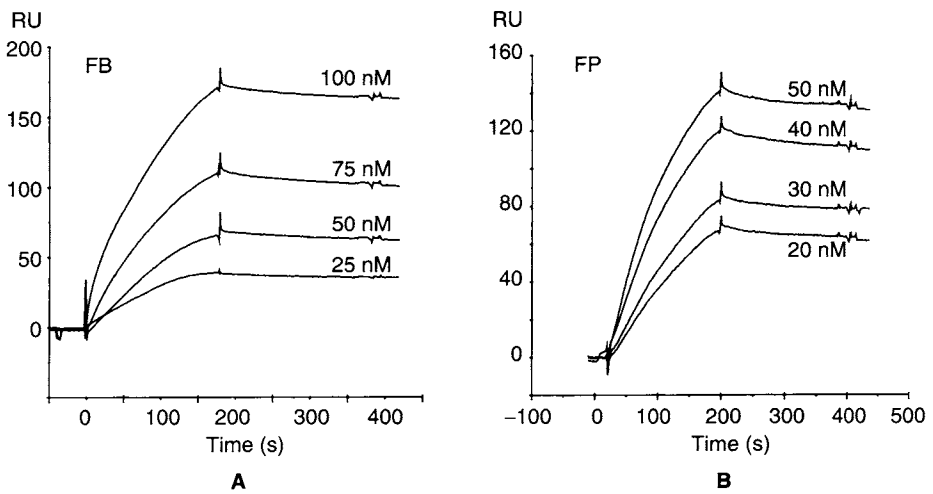

Figure 18 SPR sensorgrams of interaction between factor B (A) at 12.5, 50, 75, and 100 nM; factor P (B) at 20, 30, 40, and 50 nM, with biotinylated heparin immobilized on a poly(ethylene glycol) (PEG)-based chip.

destabilized, or stabilized with nP or aP. Heparin has no effect on the decay of preformed convertase either stabilized or destabilized or with nP or aP (107). Weiler and Linhardt (63) found that much higher concentrations of heparin could achieve accelerating decay of the properdin-stabilized convertase than that was needed to prevent its formation.

The interaction between properdin and carbohydrate was not clearly described until Holt et al. (109) examined the binding of nP and aP to glycoconjugates. Their report showed that both forms of properdin specifically binds sulfatide (Gal (3-SO_4)$\beta 1 \rightarrow 1'$ ceramide, probe to study glycolipid dynamics in model membranes), and some natural or synthetic carbohydrate polymers. Dextran sulfate ($M_r \sim 5$ kDa) had the greatest affinity for aP, followed by dextran sulfate ($M_r \sim 500$ kDa), fucoidan and heparin showing the lowest affinity. They also found that aP bound to sulfatide with higher affinity than nP, and the binding of nP to sulfatide was not prevented by dextran sulfate. The possible reason could be that the polymerization of nP to the activated form aP requires a conformational change that may convert a low-affinity binding site to high-affinity binding sites.

The kinetic examination of the interaction between heparin and factor P has been recently completed by our group using SPR (49). The sensorgram of this binding is shown in Fig. 18B and the kinetic constants are k_{on} ($M^{-1}s^{-1}$) = 3.84×10^4, k_{off} (s^{-1}) = 8.74×10^{-5}, K_d (M) = 2.68×10^{-8} (Table 2).

D. Heparin Regulation of Factor J

Factor J is a cationic glycoprotein and inhibits both the classical and the alternative pathways (110). In the classical pathway, factor J inhibits C1 activity (111), and in the alternative pathway, Factor J prevents the generation of the fluid-phase and cell-bound C3 convertase and accelerates the decay of preformed convertase by directly interacting with C3b and Bb to disrupt C3bBb formation (107,112).

It has been reported that factor J binds heparin strongly (39), and its inhibitory activity in the alternative pathway can be regulated by heparin. A concentration-dependent increase in inhibition of convertase generation has been reported (112). Factor J is capable of neutralizing heparin's inhibitory activity through the mechanism of charge neutralization. Hence, the relative concentrations of factor J and heparin could well control the balance between activation and inhibition of complement. No qualitative binding constants or binding kinetics for the factor J-heparin interaction has been reported.

All the binding data of heparin with complement proteins are best analyzed in light of the relative concentrations that these proteins are found within the serum (Table 1). The dissociation constant K_d represents the ratio of free complement components in equilibrium with complement protein–heparin complex (a smaller K_d indicates high affinity). The ratio of K_d (nM)/serum concentration (nM) gives a dimensionless value (Table 3). For a given K_d, the higher the protein concentration, the higher the percentage of serum complement protein is bound to heparin, or heparan sulfate. For example, the K_d of heparin–C4 binding is 60.8 nM and the reported serum concentration is 2047 nM giving a ratio of 0.03. The ratio of

Table 3 Serum Concentrations of Selected Complement Proteins and Their Relationship to K_d

Complement protein	Conc. in serum (μg/ml)	Conc. in serum nM	K_d (nM)/Serum conc. (nM)	[AB]/[A] + [AB] at 0.1 U/ml heparin	[AB]/[A] + [AB] at 1.0 U/ml heparin
C1	<17	<89	>0.31	0.406–1	0.944–1
C2	15–20	130–173	1.85–2.46	0.104–0.11	0.58–0.60
C3	1500	8333	0.004	0.0066	0.066
C4	430	2047	0.03	0.03	0.26
C5	75	394	0.06	0.13	0.90
C6	60	468	0.07	0.11	0.84
C7	60	495	0.03	0.11	0.89
C8	80	490	0.35	0.08	0.60
C9	58	734	0.53	0.05	0.16
C1INH	262.5	2500	0.01	0.02	0.22
B	120–300	1290–3225	0.0006–0.0016	0.02–0.04	0.17–0.43
P	20	90	0.30	0.41	0.95
I	34	386	0.09	0.13	0.86
H	470	3133	0.096	0.016	0.16

The concentration of complement protein bound to heparin [AB] is divided by the total (free and bound) concentration of complement protein ([A] + [AB]) at two concentrations 0.1 U/ml (55 nM) and 1.0 U/ml (550 nM).

K_d/serum concentration for the 14 complement proteins studied mostly ranged from 0.01 to 0.53 (Table 3). Thus, these data suggest as much as a 50-fold difference in the fraction of heparin-bound complement proteins in the serum. Neither the soluble concentration of endogenous heparin (or heparan sulfate) in human blood, nor its concentration on the endothelium, is known. Thus, we decided to consider the effect, on complement, of exogenous heparin, administered at two standard therapeutic doses.

Heparin is normally administered at doses designed to result in plasma concentrations ranging from 0.1 to 1.0 U/ml corresponding to 55–550 nM, based on a specific activity of 150 U/mg and an average molecule weight of 12,000 Da. From these two concentrations and the K_d/serum concentration value, the fraction of bound complement protein ([AB]/([A] + [AB])) was calculated and is presented in Table 3. Among all the complement proteins examined, factor P binds to heparin most strongly. Low-dose heparin results in 41% of the heparin bound and that value increases to 95% bound at a plasma–heparin concentration of 1 U/ml. In contrast, even at a 1 U/ml heparin concentration, we calculate < 26% of C3, C4, C9, C1INH, and factor H are bound to heparin, among which C3 binds to heparin with the smallest proportion. These values only represent estimated values as they do not take into account competition for heparin with other heparin-binding proteins in the circulation. Despite this complication, it is clear that some complement proteins are certainly present primarily in their bound state while others in their unbound state in heparinized patients.

The studies reported here are the first to demonstrate the quantitative information in the form of affinity constants for some complex formation using a surface plasmon resonance biosensor instead of conventional solid-phase assays. The major advantage of biosensor data, compared to other measurement of macromolecular interaction, is that the formation and breakdown of complexes can be monitored in real time, which offers the possibility to determine the interaction mechanism and kinetic rate constants associated with a binding event. The data presented in this report represent the essential first step for understanding how heparin and heparan sulfate regulate multiple steps in the complement system including ones in both the classical and alternative pathways. Furthermore, these data provide insights at the molecular level required for the design of new therapeutic approaches for regulating complement activation.

V. Conclusions

Heparin and the structurally similar heparan sulfate regulate multiple steps in the complement system including ones in both the classical and alternative pathways. Quantitative data in the form of association rates, dissociation rates, and affinity constants for complex formation are provided for many of these interactions. Based on the serum concentration of complement proteins, an understanding of the relative impact of clinical doses of heparin has been assessed. These data should provide some insight into the design of therapeutic approaches to regulate complement activation.

References

1. Makrides SC. Therapeutic inhibition of the complement system. Pharmacol Rev 1998; 50:59–88.
2. Linhardt RJ. Heparin: structure and activity. J Med Chem 2003; 46:2551–2564.
3. Casu B, Lindahl U. Structure and biological interactions of heparin and heparan sulfate. Adv Carbohydr Chem Biochem 2001; 57:159–206.
4. Jacques LB. Heparin: an old drug with a new paradigm. Science 1979; 206: 528–533.
5. Linhardt RJ. Heparin: an important drug enters its seventh decade. Chem Ind 1991; 2:45–50.
6. Linhardt RJ, Toida T. Role of glycosaminoglycans in cellular communication. Acc Chem Res 2004; 37:431–438.
7. Faham S, Linhardt RJ, Rees DC. Diversity does make a difference: fibroblast growth factor-heparin interactions. Curr Opin Struct Biol 1998; 8:578–586.
8. Edens RE, LeBrun LA, Linhardt RJ, Kaul PR, Weiler JM. Certain high molecular weight heparin chains have high affinity for vitronectin. Arch Biochem Biophys 2001; 391:278–285.
9. Edens RE, Linhardt RJ, Weiler JM. Heparin is not just an anticoagulant anymore: six and one-half decades of studies on the ability of heparin to regulate complement activity. Complement Profiles 1993; 1:96–120.

10. Hileman RE, Fromm JR, Weiler JM, Linhardt RJ. Glycosaminoglycan-protein interactions: definition of consensus sites in glycosaminoglycan binding proteins. Bioessays 1998; 20:156–167.
11. Capila I, Linhardt RJ. Heparin-protein interactions. Angew Chem Int Ed Engl 2002; 41:391–412.
12. Kolset SO, Prydz K, Pejler G. Intracellular proteoglycans. Biochem J 2004; 379:217–227.
13. Engelberg H. Actions of heparin in the atherosclerotic process. Pharmacol Rev 1996; 48:327–352.
14. Rabenstein DL. Heparin and heparan sulfate: structure and function. Nat Prod Rep 2002; 19:312–331.
15. Gunay NS, Linhardt RJ. Heparinoids: structure, biological activities and therapeutic applications. Planta Medica 1999; 65:301–306.
16. Munoz EM, Linhardt RJ. Heparin-binding domains in vascular biology. Arterioscler Thromb Vasc Biol 2004; 24:1549–1557.
17. Islam T, Linhardt RJ. Chemistry, Biochemistry and Pharmaceutical Potential of Glycosaminoglycans and Related Saccharides in Carbohydrate-based Drug Discovery. 2003. 1:407–433.
18. Tyrrell DJ, Kilfeather S, Page CP. Therapeutic uses of heparin beyond its traditional role as an anticoagulant. Trends Pharmacol Sci 1995; 16:198–204.
19. Linhardt RJ, Rice KG, Kim YS, Engelken JD, Weiler JM. Homogeneous, structurally defined heparin-oligosaccharides with low anticoagulant activity inhibit the generation of the amplification pathway C3 convertase in vitro. J Biol Chem 1988; 263:13090–13096.
20. Weiler JM, Edens RE, Linhardt RJ, Kapelanski DP. Heparin and modified heparin inhibit complement activation in vivo. J Immunol 1992; 148: 3210–3215.
21. Akiyama H, Sakai S, Linhardt RJ, Goda Y, Toida T, Maitani T. Chondroitin sulphate structure affects its immunological activities on murine splenocytes sensitized with ovalbumin. Biochem J 2004; 382:269–278.
22. Rathore D, McCutchan TF, Garboczi DN, Toida T, Hernaiz MJ, LeBrun LA, Lang SC, Linhardt RJ. Direct measurement of the interactions of glycosaminoglycans and a heparin decasaccharide with the malaria circumsporozoite protein. Biochemistry 2001; 40:11518–11524.
23. Barth H, Schafer C, Adah MI, Zhang F, Linhardt RJ, Toyoda H, Kinoshita-Toyoda A, Toida T, Van Kuppevelt TH, Depla E, Von Weizsacker F, Blum HE, Baumert TF. Cellular binding of hepatitis C virus envelope glycoprotein E2 requires cell surface heparan sulfate. J Biol Chem 2003; 278:41003–41012.
24. Borsig L, Wong R, Feramisco J, Nadeau DR, Varki NM, Varki A. Heparin and cancer revisited: mechanistic connections involving platelets, P-selectin, carcinoma mucins, and tumor metastasis. Proc Natl Acad Sci USA 2001; 98:3352–3357.
25. Lee YS, Yang HO, Shin KH, Choi HS, Jung SH, Kim YM, Oh DK, Linhardt RJ, Kim YS. Suppression of tumor growth by a new glycosaminoglycan isolated from the African giant snail Achatina fulica. Eur J Pharmacol 2003; 465:191–198.
26. Linhardt RJ. Heparin-induced cancer cell death. Chem Biol 2004; 11:420–422.
27. Joo EJ, ten Dam GB, van Kuppevelt TH, Toida T, Linhardt RJ, Kim YS. Nucleolin: acharan sulfate-binding protein on the surface of cancer cells. Glycobiology 2005; 15:1–9.

28. Smorenburg SM, Van Noorden. The complex effects of heparins on cancer progression and metastasis in experimental studies. Pharmacol. Rev 2001 53:93–106.
29. Feng B, Yao PM, Li Y, Devlin CM, Zhang D, Harding HP, Sweeney M, Rong JX, Kuriakose G, Fisher EA, Marks AR, Ron D, Tabas I. The endoplasmic reticulum is the site of cholesterol-induced cytotoxicity in macrophages. Nat Cell Biol 2003; 5:781–792.
30. Muller-Eberhard HJ. Complement. Annu Rev Biochem 1969; 38:389–414.
31. Muller-Eberhard HJ. Molecular organization and function of the complement system. Annu Rev Biochem 1988; 57:321–347.
32. Whaley K, Schwaeble W. Complement and complement deficiencies. Semin Liver Dis 1997; 17:297–310.
33. Colten HR, Rosen FS. Complement deficiencies. Annu Rev Immunol 1992; 10:809–834.
34. Frank MM. Complement deficiencies. Pediatr Clin North Am 2000; 47: 1339–1354.
35. Ecker EE, Gross P. Anticomplementary power of heparin. J Infect Dis 1929; 44:250–253.
36. Almeda S, Rosenberg RD, Bing DH. The binding properties of human complement component C1q. Interaction with mucopolysaccharides. J Biol Chem 1983; 258:785–791.
37. Blondin C, Fischer E, Boisson-Vidal C, Kazatchkine MD, Jozefonvicz J. Inhibition of complement activation by natural sulfated polysaccharides (fucans) from brown seaweed. Mol Immunol 1994; 31:247–253.
38. Sahu A, Pangburn MK. Identification of multiple sites of interaction between heparin and the complement system. Mol Immunol 1993; 30:679–684.
39. Larrucea S, Gonzalez-Rubio C, Cambronero R, Ballou B, Bonay P, Lopez-Granados E, Bouvet P, Fontan G, Fresno M, Lopez-Trascasa M. Cellular adhesion mediated by factor J, a complement inhibitor. Evidence for nucleolin involvement. J Biol Chem 1998; 273:31718–31725.
40. Raepple E, Hill HU, Loos M. Mode of interaction of different polyanions with the first (C1, C1), the second (C2) and the fourth (C4) component of complement—I. Effect on fluid phase C1 and on C1 bound to EA or to EAC4. Immunochemistry 1976; 13:251–255.
41. Baker PJ, Lint TF, McLeod BC, Behrends CL, Gewurz H. Studies on the inhibition of C56-induced lysis (reactive lysis). VI. Modulation of C56-induced lysis polyanions and polycations. J Immunol 1975; 114:554–558.
42. Maillet F, Kazatchkine MD, Glotz D, Fischer E, Rowe M. Heparin prevents formation of the human C3 amplification convertase by inhibiting the binding site for B on C3b. Mol Immunol 1983; 20:1401–1404.
43. Kase TSY, Kawai T, Sakamoto T, Ohtani K, Eda S, Maeda A, Okuno Y, Kurimura T, Wakamiya N. Human mannan-binding lectin inhibits the infection of influenza a virus without complement. Immunology 1999; 97:385–392.
44. Cofrancesco E, Radaelli F, Pogliani E, Amici N, Torri GG, Casu B. Correlation of sulfate content and degree of carboxylation of heparin and related glycosaminoglycans with anticomplement activity. Relationships to the anticoagulant and platelet-aggregating activities. Thromb Res 1979; 14:179–187.
45. Sim RB. The first component of human complement—C1. Methods Enzymol 1981; 80 (Part C): 6–16.

46. Arlaud GJ, Gaboriaud C, Thielens NM, Rossi V. Structural biology of C1. Biochem Soc Trans 2002; 30:1001–1006.
47. Sim RB. The human complement system serine proteases C1r and C1s and their proenzymes. Methods Enzymol 1981; 80 (Part C): 26–42.
48. Lennick M, Brew SA, Ingham KC. Kinetics of interaction of C1 inhibitor with complement C1s. Biochem 1986; 25:3890–3898.
49. Yu H, Muñoz EM, Zhang F, Edens RE, Linhardt RJ. Kinetic studies on the interaction of heparin and complement proteins using surface plasmon resonance. Biochim Biophys Acta 2005; 1726:168–176.
50. Strunk R, Colten HR. Inhibition of the enzymatic activity of the first component of complement (C1) by heparin. Clin Immunol Immunopathol 1976; 6:248–255.
51. Loos M, Volanakis JE, Stroud RM. Mode of interaction of different polyanions with the first (C1, C1), the second (C2), and the fourth (C4) component of complement—III. Inhibition of C4 and C2 binding site(s) on C1s by polyanions. Immunochem 1976; 13:789–791.
52. Hortin GL, Trimpe BL. C1 inhibitor: different mechanisms of reaction with complement component C1 and C1s. Immunol Invest 1991; 20:75–82.
53. Nagaki K, Inai S. Inactivator of the first component of human complement (C1INA). Enhancement of C1INA activity against C1s by acidic mucopolysaccharides. Int Arch Allergy Appl Immunol 1976; 50:172–180.
54. Tack BF, Janatova J, Thomas ML, Harrison RA, Hammer CH. The third, fourth, and fifth components of human complement: isolation and biochemical properties. Methods in Enzymology 1981; 80:64–101.
55. Sim RB, Arlaud GJ, Colomb MG. Kinetics of reaction of human C1-inhibitor with the human complement system proteases C1r and C1s. Biochim Biophys Acta 1980; 612:433–449.
56. Caldwell EE, Andreasen AM, Blietz MA, Serrahn JN, VanderNoot V, Park Y, Yu G, Linhardt RJ, Weiler JM. Heparin binding and augmentation of C1 inhibitor activity. Arch Biochem Biophys 1999; 361:215–222.
57. Caldwell EE, Andreasen AM, Blietz MA, Serrahn JN, VanderNoot V, Park Y, Yu G, Linhardt RJ, Weiler JM. Heparin binding and augmentation of C1 inhibitor activity. Arch Biochem Biophys 1999; 361:215–222.
58. Weiler JM, Stechschulte DJ, Levine HT, Edens RE, Maves KK. Inhaled heparin in the treatment of hereditary angioedema. Complement Inflammation 1991; 8:240–241.
59. Levine HT, Stechschulte DJ. Possible efficacy of nebulized heparin therapy in hereditary angioedema. Immunol. Allergy Pract 1992; 14:162–167.
60. Kerr MA. The second component of human complement. Methods Enzymol 1981; 80:54–64.
61. Akama H, Johnson CA, Colten HR. Human complement protein C2. Alternative splicing generates templates for secreted and intracellular C2 proteins. J Biol Chem 1995; 270:2674–2678.
62. Kulics J, Circolo A, Strunk RC, Colten HR. Regulation of synthesis of complement protein C4 in human fibroblasts: cell- and gene-specific effects of cytokines and lipopolysaccharide. Immunology 1994; 82:509–515.
63. Weiler JM, Linhardt RJ. Comparison of the activity of polyanions and polycations on the classical and alternative pathways of complement. Immunopharmacology 1989; 17:65–72.

64. Loos M, Bitter-Suermann D. Mode of interaction of different polyanions with the first (C1, C1), the second (C2), and the fourth (C4) component of complement. IV. Activation of C1 in serum by polyanions. Immunol 1976; 31:931–934.
65. Nussenzweig V, Melton R. Human C4-binding protein (C4-bp). Methods Enzymol 1981; 80:124–133.
66. Gigli I, Fujita T, Nussenzweig V. Modulation of the classical pathway C3 convertase by plasma proteins C4 binding protein and C3b inactivator. Proc Natl Acad Sci USA 1979; 76:6596–6600.
67. Scharfstein J, Ferreira A, Gigli I, Nussenzweig V. Human C4-binding protein. I. Isolation and characterization. J Exp Med 1978; 148:207–222.
68. Schwalbe RA, Dahlback B, Nelsestuen GL. Heparin influence on the complex of serum amyloid P component and complement C4b-binding protein. J Biol Chem 1991; 266:12896–12901.
69. Hessing M, Vlooswijk RA, Hackeng TM, Kanters D, Bouma BN. The localization of heparin-binding fragments on human C4b-binding protein. J Immunol 1990; 144:204–208.
70. Blom AM, Webb J, Villoutreix BO, Dahlback B. A cluster of positively charged amino acids in the C4BP alpha-chain is crucial for C4b binding and factor I cofactor function. J Biol Chem 1999; 274:19237–19245.
71. Law SK, Dodds AW. The internal thioester and the covalent binding properties of the complement proteins C3 and C4. Protein Sci 1997; 6:263–274.
72. Sahu A, Lambris JD. Structure and biology of complement protein C3, a connecting link between innate and acquired immunity. Immunol Rev 2001; 180:35–48.
73. Sim RB, Twose TM, Paterson DS, Sim E. The covalent-binding reaction of complement component C3. Biochem J 1981; 193:115–127.
74. Kazatchkine MD, Maillet F, Fischer E, Glotz D. Modulation of the formation of the human C-3 amplification convertase of complement by polyelectrolytes. Agents Actions 1981; 11:645–646.
75. Pangburn MK. Analysis of recognition in the alternative pathway of complement. Effect of polysaccharide size. J Immunol 1989; 142:2766–2770.
76. Weiler JM, Yurt RW, Fearon DT, Austen KF. Modulation of the formation of the amplification convertase of complement, C3b, Bb, by native and commercial heparin. J Exp Med 1978; 147:409–421.
77. Andersson E, Rydengard V, Sonesson A, Morgelin M, Bjorck L. Antimicrobial activities of heparin-binding peptides. Eur J Biochem 2004; 271:1219–1226.
78. Pangburn MK, Rawal N. Structure and function of complement C5 convertase enzymes. Biochem Soc Trans 2002; 30:1006–1010.
79. Rawal N, Pangburn MK. Formation of high affinity C5 convertase of the classical pathway of complement. J Biol Chem 2003; 278:38476–38483.
80. Rawal N, Pangburn MK. Functional role of the noncatalytic subunit of complement C5 convertase. J Immunol 2000; 164:1379–1385.
81. Tschopp J, Masson D, Schafer S, Peitsch M, Preissner KT. The heparin binding domain of S-protein/vitronectin binds to complement components C7, C8, and C9 and perforin from cytolytic T-cells and inhibits their lytic activities. Biochem 1988; 27:4103–4109.
82. Francois PP, Preissner KT, Herrmann M, Haugland RP, Vaudaux P, Lew DP, Krause KH. Vitronectin interaction with glycosaminoglycans. Kinetics, structural determinants, and role in binding to endothelial cells. J Biol Chem 1999; 274:37611–37619.

83. Gibson AD, Lamerdin JA, Zhuang P, Baburaj K, Serpersu EH, Peterson CB. Orientation of heparin-binding sites in native vitronectin. Analyses of ligand binding to the primary glycosaminoglycan-binding site indicate that putative secondary sites are not functional. J Biol Chem 1999; 274:6432–6442.
84. Kazatchkine MD, Fearon DT, Metcalfe DD, Rosenberg RD, Austen KF. Structural determinants of the capacity of heparin to inhibit the formation of the human amplification C3 convertase. J Clin Invest 1981; 67:223–228.
85. Sharath MD, Merchant ZM, Kim YS, Rice KG, Linhardt RJ, Weiler JM. Small heparin fragments regulate the amplification pathway of complement. Immunopharmacol 1985; 9:73–80.
86. Weiler JM. Polyions regulate the alternative amplification pathway of complement. Immunopharmacol 1983; 6:245–255.
87. Zipfel PF, Skerka C, Hellwage J, Jokiranta ST, Meri S, Brade V, Kraiczy P, Noris M, Remuzzi G. Factor H family proteins: on complement, microbes and human diseases. Biochem Soc Trans 2002; 30:971–978.
88. Pangburn MK, Pangburn KL, Koistinen V, Meri S, Sharma AK. Molecular mechanisms of target recognition in an innate immune system: interactions among factor H, C3b, and target in the alternative pathway of human complement. J Immunol 2000; 164:4742–4751.
89. Meri S, Pangburn MK. Discrimination between activators and nonactivators of the alternative pathway of complement: regulation via a sialic acid/polyanion binding site on factor H. Proc Natl Acad Sci USA 1990; 87:3982–3986.
90. Pangburn MK. Analysis of the mechanism of recognition in the complement alternative pathway using C3b-bound low molecular weight polysaccharides. J Immunol 1989; 142:2759–2765.
91. Boackle RJ, Caughman GB, Vesely J, Medgyesi G, Fudenberg HH. Potentiation of factor H by heparin: a rate-limiting mechanism for inhibition of the alternative complement pathway. Mol Immunol 1983; 20:1157–1164.
92. Bitter-Suermann D, Burger R, Hadding U. Activation of the alternative pathway of complement: efficient fluid-phase amplification by blockade of the regulatory complement protein beta1H through sulfated polyanions. Eur J Immunol 1981; 11:291–295.
93. Cheung AK, Parker CJ, Janatova J, Brynda E. Modulation of complement activation on hemodialysis membranes by immobilized heparin. J Am Soc Nephrol 1992; 2:328–337.
94. Meri S, Pangburn MK. Regulation of alternative pathway complement activation by glycosaminoglycans: specificity of the polyanion binding site on factor H. Biochem Biophys Res Commun 1994; 198:52–59.
95. Pangburn MK, Atkinson MA, Meri S. Localization of the heparin-binding site on complement factor H. J Biol Chem 1991; 266:16847–16853.
96. Blackmore TK, Hellwage J, Sadlon TA, Higgs N, Zipfel PF, Ward HM, Gordon DL. Identification of the second heparin-binding domain in human complement factor H. J Immunol 1998; 160:3342–3348.
97. Pangburn MK, Muller-Eberhard HJ. Complement C3 convertase: cell surface restriction of beta1H control and generation of restriction on neuraminidase-treated cells. Proc Natl Acad Sci USA 1978; 75:2416–2420.
98. Soames CJ, Sim RB. Interactions between human complement components factor H, factor I and C3b. Biochem J 1997; 326:553–561.

99. Pangburn MK, Muller-Eberhard HJ. Kinetic and thermodynamic analysis of the control of C3b by the complement regulatory proteins factors H and I. Biochem 1983; 22:178–185.
100. Koistinen V. Effects of sulphated polyanions on functions of complement factor H. Mol Immunol 1993; 30:113–118.
101. Kerr MA. Human factor B. Methods Enzymol 1981; 80:102–112.
102. Jing H, Xu YY, Carson M, Moore D, Macon KJ, Volanakis JE, Narayana SVL. New structural motifs on the chymotrypsin fold and their potential roles in complement factor B. EMBO J 2000; 19:164–173.
103. Kam CM, McRae BJ, Harper JW, Niemann MA, Volanakis JE, Powers JC. Human complement proteins D, C2, and B. Active site mapping with peptide thioester substrates. J Biol Chem 1987; 262:3444–3451.
104. Narayana SV, Carson M, el-Kabbani O, Kilpatrick JM, Moore D, Chen X, Bugg CE, Volanakis JE, DeLucas LJ. Structure of human factor D. A complement system protein at 2.0 A resolution. J Mol Biol 1994; 235: 695–708.
105. Kazatchkine MD, Fearon DT, Silbert JE, Austen KF. Surface-associated heparin inhibits zymosan-induced activation of the human alternative complement pathway by augmenting the regulatory action of the control proteins on particle-bound C3b. J Exp Med 1979; 150:1202–1215.
106. Ruddy S. Complement and properdin: biologic and clinical importance. Orthop Clin North Am 1975; 6:609–617.
107. Maves KK, Weiler JM. Properdin: approaching four decades of research. Immunol Res 1993; 12:233–243.
108. Wilson JG, Fearon DT, Stevens RL, Seno N, Austen KF. Inhibition of the function of activated properdin by squid chondroitin sulfate E glycosaminoglycan and murine bone marrow-derived mast cell chondroitin sulfate E proteoglycan. J Immunol 1984; 132:3058–3063.
109. Holt GD, Pangburn MK, Ginsburg V. Properdin binds to sulfatide [Gal (3-SO4)beta 1-1 Cer] and has a sequence homology with other proteins that bind sulfated glycoconjugates. J Biol Chem 1990; 265:2852–2855.
110. Gonzalez-Rubio C, Gonzalez-Muniz R, Jimenez-Clavero MA, Fontan G, Lopez-Trascasa M. Factor J, an inhibitor of the classical and alternative complement pathway, does not inhibit esterolysis by factor D. Biochim Biophys Acta 1996; 1295:174–178.
111. Lopez-Trascasa M, Bing DH, Rivard M, Nicholson-Weller A. Factor J: isolation and characterization of a new polypeptide inhibitor of complement C1. J Biol Chem 1989; 264:16214–16221.
112. Gonzalez-Rubio C, Jimenez-Clavero MA, Fontan G, Lopez-Trascasa M. The inhibitory effect of factor J on the alternative complement pathway. J Biol Chem 1994; 269:26017–26024.

Chemistry and Biology of Heparin and Heparan Sulfate
H.G. Garg, R.J. Linhardt and C.A. Hales (Editors)

Chapter 12

Surface-Based Studies of Heparin/Heparan Sulfate–Protein Interactions: Considerations for Surface Immobilisation of HS/Heparin Saccharides and Monitoring Their Interactions with Binding Proteins

TIM RUDD, MARK A. SKIDMORE and EDWIN A. YATES

School of Biological Sciences,
University of Liverpool,
Liverpool, UK

I. Introduction

Heparin has been widely employed as an anticoagulant for many years but it is only relatively recently that its ability to interact with manifold proteins involved in a wide range of biological processes has been recognised. These include enzymes, extracellular matrix proteins, growth factors, and the surface proteins of many pathogens. Most of these activities rely on the ability of heparin to mimic heparan sulfate (HS), which shares the same biosynthetic route and constituent monosaccharides. Indeed, heparin is held by many authorities to be a specialised form of heparan sulfate.

The possibility of using heparin, which is much more readily available than tissue derived HS, to influence these biological processes suggests obvious medical applications. Some loss of selectivity due to heparin's higher levels of homogeneity and sulfation is generally observed but heparin is still widely used as a model for HS and, when chemically modified, as a probe for structure–activity studies of HS mediated biological activities. The generation of oligosaccharides from heparin, chemically modified heparin and heparan sulfate is usually motivated by two aims. The first is to investigate the structure–activity relationship for particular

saccharides from the point of view of answering biological questions and the second is to identify potential pharmaceutical agents. This may include experiments to isolate a minimum size of active saccharide, a defined active sequence or the simplest active structure for a given activity. The attachment of this class of saccharide to surfaces will permit a large number of structures to be tested for binding with a protein of interest through microarrays or detailed biochemical binding data to be obtained through surface plasmon techniques. Furthermore, a large number of potential applications await the development of controllable surface coating with selected saccharides possessing known activities in both the medical and technological arenas, most notably perhaps in tissue engineering.

The attachment of heparin/HS and their oligosaccharide fragments to surfaces for the purposes of conducting kinetic studies of their interactions with binding partners will form the subject of the first part of this chapter. We will review the chemical properties of this class of molecule as they relate to surface attachment as well as the effects that chemical treatments, widely employed for derivatising heparin for structure–activity studies, can have. Means of detecting and quantifying surface coverage with sugars and detecting their binding partners, which are usually but not exclusively proteins, will form the second part. Although we will not deal explicitly with the problem of screening these compounds on surfaces in microarray formats, some of our remarks will also be relevant to such an approach. All of the material that will be covered here is equally applicable to HS and heparin and much of it will also be relevant to other members of the GAG family, such as chondroitin sulfate, hyaluronan or keratan sulfate, many of which share some chemical and structural properties with heparin. For the purposes of much of this discussion, heparin and HS can be considered synonymous and henceforth we will refer to both as HS and will only distinguish between them when necessary. The attachment of other classes of glycans (for example, N-linked glycans) will not be covered here and the interested reader is referred to reviews in that area.

Heparan sulfate is a linear sulfated anionic polysaccharide typically between 50 and 200 sugar units in length (25–100 kDa) which is synthesised on a tetrasaccharide (GlcA–Gal–Gal–Xyl) linker, attached to serine residues in proteoglycans by means of an *O*-ether linkage, the growing linear chain being added repetitively in the order *N*-acetyl glucosamine-glucuronic acid. Several incomplete enzymatic modifications then follow, including conversion of *N*-acetylglucosamine to glucosamine-*N*-sulfate, epimerisation of D-glucuronic acid to L-iduronic acid, and *O*-sulfations at position 2 of the uronic acid residues and positions 6, or more rarely, 3 of the glucosamine residue. The general repeating disaccharide structure is shown in Fig. 1. In the case of heparin, the result is a relatively homogeneous and highly sulfated polysaccharide, but for HS (and not heparin), the further subtlety of a domain structure (1,2) is introduced. Together with expression of distinct heparan sulfate structures in tissues, the regulation of which is not yet well understood, these are the origins of the ability of HS to mediate wide-ranging biological activities. Both of these polysaccharides therefore share a common underlying structure and hence similar chemistry. For more detailed discussions of their biosynthesis and bioactivity, the reader is referred to chapter 7.

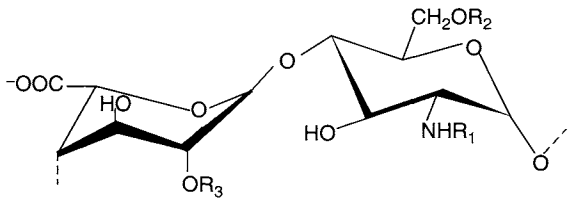

R_1: SO_3^- or $COCH_3$
R_2: H or SO_3^-
R_3: H or SO_3^-

Figure 1 General repeating unit of HS and heparin with principal positions of substitution. Heparan sulfate and heparin differ in their detailed structure (see text) although they share a common biosynthetic route and constituent monosaccharides.

The relative difficulty of attaching proteins or other binding partners to surfaces combined with that of detecting GAGs (and most other sugars) by optical techniques (they are difficult to detect by differences in refractive index in surface plasmon resonance instruments) has dictated that it is usually the sugar that is attached to the surface. Thus, it is usually the attachment or detachment of the binding partner, usually a protein that is detected at the surface. This is the approach that we will adopt for this review.

II. Attachment

The aim is to achieve facile binding of HS sugars to surfaces (derivatised with appropriate reactive chemical groups) with consistent coverage, reproducible reactivity and preferably to attach them with high yields. Ideally, the process would avoid the need to react each saccharide separately because this becomes prohibitively laborious for high throughput applications, especially arrays although for surface plasmon experiments it is less of a problem. Some properties of HS that make some of these aims difficult to achieve are examined in the following sections. These points also cover chemically modified derivatives of HS, which can serve as useful indicators of the structural dependence of protein binding or may be screened for binding in their own right.

A. Chemical Properties of HS Derived Saccharides and Implications for their Attachment to Surfaces

It seems reasonable that the cleavage of the polysaccharide from the proteoglycan could release a consistent reducing end suitable for further derivatisation, including attachment to appropriate surfaces. At first sight, this appears to represent a

desirable situation because all the saccharides would contain common structural features at their reducing ends and consistent attachment to a surface would be feasible. Exposure of the proteoglycan to base cleaves the Xyl-*O*-Ser linkage and unhindered, this will then proceed to degrade the HS chain. To avoid this, it is usual to include a reducing agent, which converts reducing end residues to unreactive alcohols, thereby destroying the principal means of attachment to surfaces. The production of HS polysaccharides by this method with uniform reducing ends is therefore difficult. However, in practice, it is relatively rare that attachment of a full-length polysaccharide is desired because these contain a large number of potential binding sites, making results difficult to interpret, and the aim is more commonly to identify or study an oligosaccharide fragment that (ideally) contains only one binding site.

Once an HS polysaccharide has been released, several cleavage methods, employing nitrous acid, acid hydrolysis, free radical, or enzymatic cleavage are usually employed, either to partial extent or completion, to obtain oligosaccharide fragments. All result in the production of oligosaccharides of various lengths and, in some cases also include a number of other structural modifications, which are relevant to the present discussion. Most of these are dealt with later in this section. The attachment of this class of sugar to surfaces has, until recently, almost entirely depended on the chemistry of the reducing end aldehyde group and this will now be considered in some detail.

B. Some Relevant Properties of Reducing Sugars

The rate of mutarotation (the process by which reducing sugars may undergo structural changes in solution, for example between α- and β-anomers via an open-chain aldehyde containing form) increases with temperature and is affected by pH, bases being particularly effective. For pyranose–pyranose interconversions, the minimum rate is observed in acidic conditions (pH 2.5–6) but the exact value for HS oligosaccharides has not, to our knowledge, been determined. The polarity of the solvent is also a factor, with polar solvents promoting mutarotation (3–5). These factors have important ramifications for the attachment of HS oligosaccharides to surfaces and in particular for the attachment via Schiff base formation, which remains the most common means of attachment (Fig. 2). In general, the reactions are carried out in ampholytic polar solvents, which are necessary both to dissolve the highly polar sugars and allow mutarotation to occur. Schiff base formation is catalysed by mild acidity (by protonation of the carbonyl function of the sugar) and this might reduce the rate of mutarotation of α- and β-pyranose ring forms further although it can be offset to some extent by heating. In addition, acid conditions protonate a proportion of the inevitably limited numbers of surface-borne amine or hydrazide groups (which act as nucleophiles in attacking the aldehyde group of the sugar) further reducing the yield. Under basic conditions, protonation of the carbonyl function of the sugar becomes less likely and the reducing end residue is subject to inter-conversions, which will be discussed in some detail later.

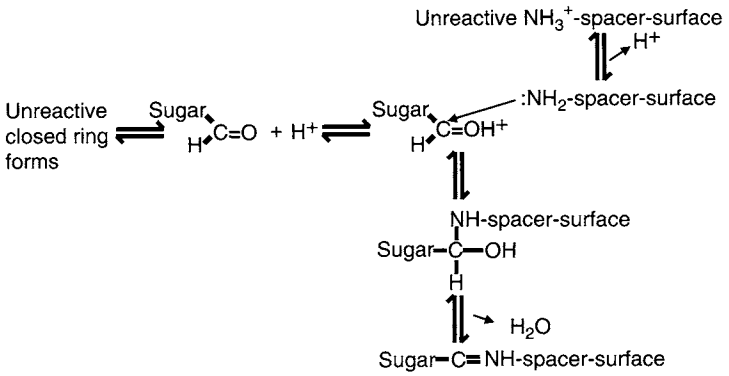

Figure 2 Mechanism for the attachment of reducing sugars to amino-derivatised surfaces to form Schiff bases.

C. Sensitivity of Heparin/HS Oligosaccharides and Polysaccharides to Acids and Bases

The dominant characteristics of HS that restrict the range of chemical conditions to which they can be exposed are their sensitivity to acids and bases. Although this is frequently overlooked, unwitting exposure can result in widespread modification, which will alter the structure of the saccharide under investigation and could, in extreme cases, render the results of surface attachment and subsequent binding studies invalid. In many cases, these modifications could be made inadvertently and could remain undetected.

The motivation for discussing these characteristics here encompasses two aims. The first is to stress that attention to the conditions to which these molecules are exposed must be paid throughout the process of generation, purification, and attachment of a saccharide as well as during any experiment. The second is that, as will become clear, several of these modifications are exploited in the preparation of chemically modified heparin. Since the use of these derivatives is widespread (they are frequently employed as models of HS, with their many biological and medically related activities), it is important to bear in mind their susceptibility to these conditions.

We will divide the sensitivity of HS polysaccharides or oligosaccharides into those resulting from acid- or base-derived phenomena although the site of action may vary from reducing end modifications to wholesale changes along the length of the saccharide chain. Saccharides with modified reducing ends are likely to attach to different extents to derivatised surfaces compared to intact samples while those containing modifications along the length of the chain will be more heterogeneous and possess different activities.

1. Acid Sensitivity

Mildly acidic conditions enhance the reactivity of the reducing end carbonyl group towards suitably derivatised surfaces through increased protonation of the carbonyl group but, at pH 4 or below, de-*N*-sulfation can begin to occur especially if accompanied by heating (for information on de-*N*-sulfation in general, see Refs. 6 and 7) although a definitive study of this phenomenon in HS has yet to be reported. However, inter-conversion between pyranose forms (by mutarotation via the reactive aldehyde containing open chain form) is slowest under acidic conditions and is another contributing factor to the low reaction rate characteristic of Schiff base formation in this class of sugars.

The possibility that de-*N*-sulfated artifacts remain following partial scission by nitrous acid (a common method for the degradation of HS) has not been studied but warrants investigation. In more extreme acidic conditions, de-*O*-sulfation can also occur in the order 6 (of glucosamine) and then 2 (of iduronate). In fact, this difference in reactivity is exploited during chemical modification procedures although the selective removal of 6-over 2-*O*-sulfates is not absolute. It is, however, possible to replace *N*-sulfate groups in samples in which their loss is suspected, employing well-established re-*N*-sulfation procedures (8) although details of the following section on base sensitivity should be born in mind.

2. Base Sensitivity

Heparan sulfate and oligosaccharides derived from it are also sensitive to basic conditions and these can be divided into those effects which occur at the reducing end residue, which we will deal with first, and several that result in modifications along the length of the saccharide chain.

The rates at which the unreactive closed forms of reducing sugars convert to the reactive, open-chain aldehyde (by mutarotation) as well as their different tendencies to undergo conversion to ene-diols (Fig. 3) both influence the rate of reactions proceeding via the carbonyl groups of terminal reducing sugar units. Mutarotation requires an ampholytic agent, usually the solvent, and occurs at different rates in different solvents, proceeding faster in more polar solvents (3–5). Modifications to the reducing end residue proceeding via 1,2-ene-diol formation are favoured in basic conditions (reported to occur down to 0.01 mM ammonium hydroxide) (9) similar to the Lobry de Bruyn–van Eckenstein rearrangement observed in reducing monosaccharides (10). Conversion of GlcNAc to ManNAc has also been reported (11). The result of this, although not usually serious for the activity of larger oligosaccharides or polysaccharides, can only add to the already considerable heterogeneity of reducing end amino sugar moieties and further augments the varied rates observed for the reaction of reducing end units. An additional problem is that these species are often difficult to detect, particularly for the small amounts of material likely to be relevant to this discussion.

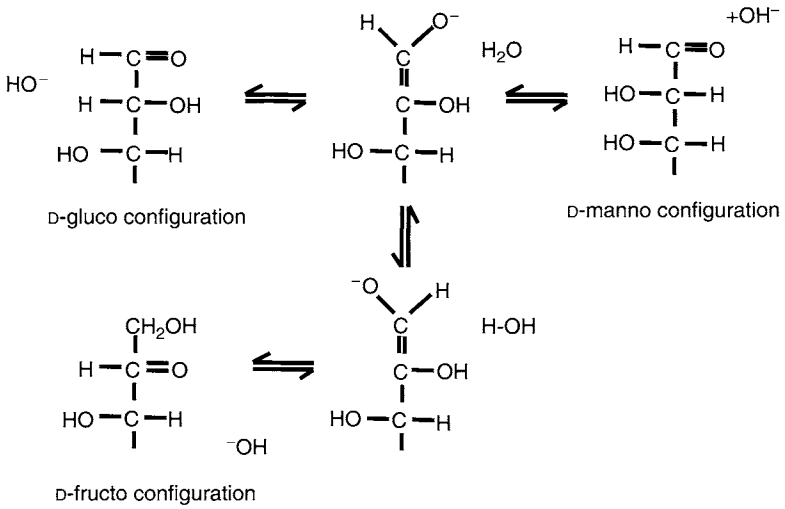

Figure 3 Proposed general mechanism for the transformation of D-*gluco* sugars to D-*manno* and D-*fructo* sugars via base catalysed ene-diol formation.

3. *Epoxide Formation and de-O-Sulfation in Iduronate 2-Sulfate Residues*

Under more basic conditions, the electronegative 2-*O*-sulfate group present in iduronate residues provides an opportunity for attack at the relatively electron poor C-2 atom by the adjacent oxygen (of the former hydroxyl group at position 3), now denuded of its hydrogen atom. At moderately high pH ranges (>9 and especially with heating), this results in the loss of the sulfate group and formation of 2,3-epoxide groups (12–14) (Fig. 4A). If, at this point, yet harsher basic conditions are applied, nucleophilic attack by a hydroxide ion at C-2 results in stereoselective opening of the epoxide and formation of an iduronate residue. This is also exploited in the selective de-*O*-sulfation (in iduronate) of HS. It is likely that this reaction is also accompanied by β-elimination resulting in de-polymerisation as well as another modification which occurs in the glucosamine residues carrying both *N*- and 3-*O*-sulfate groups (see the following section). If, on the other hand, the intact epoxide is exposed to acidic conditions (for example, following the accidental addition of excessive acid during neutralisation), the epoxide is opened to form L-galacturonic residues (13,14) (Fig. 4A). It is not known whether these conditions have a similar effect on the relatively rare glucuronic acid-2-*O*-sulfate residues, which have been observed at low levels in HS (15). The probable higher stability of the glucuronic acid rings (presumably $^4C_1$) may preclude this possibility although the authors have been unable to find conclusive evidence in the literature either way concerning these modifications.

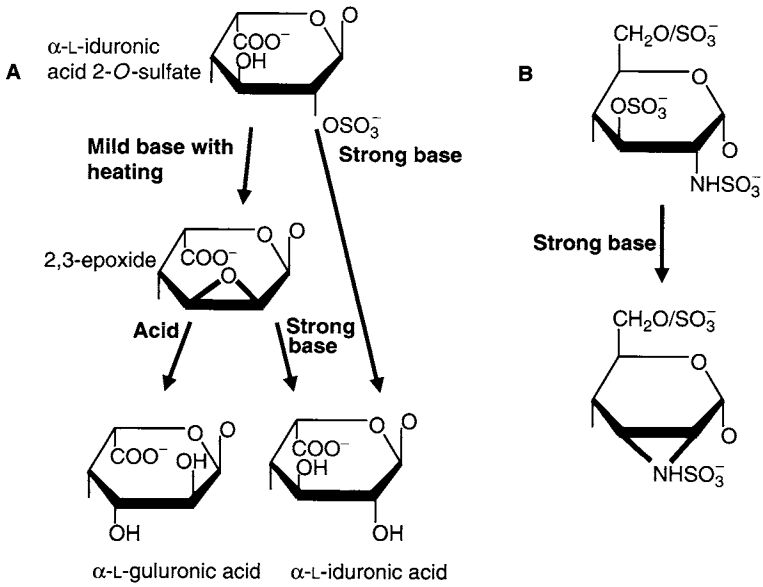

Figure 4 (A) Formation of 2,3-epoxide ring in iduronate 2-*O*-sulfate residues of HS in a moderate alkaline environment and of de-*O*-sulfated iduronate under strong alkaline conditions. (B) Formation of 2,3-*N*-sulfoaziridine groups under strong alkaline conditions in 2,3- and 2,3,6 sulfated glucosamine residues of HS. The reaction does not occur in the absence of the *N*-sulfate group.

4. *Aziridine Formation in 2,3- and 2,3,6-Glucosamine Sulfate Residues*

Under the extreme basic conditions employed for the selective de-*O*-sulfation of iduronate residues in heparin, a further modification has been observed in the small proportion of glucosamine residues containing either 2,3- or 2,3,6-sulfation patterns (Fig. 4B). In this case, the nitrogen atom of the *N*-sulfate group (presumably having lost its proton) at C-2 of glucosamine attacks the electron deficient carbon atom at C-3 resulting in de-*O*-sulfation, inversion of stereochemistry at C-3 and the formation of an *N*-sulfated-aziridine derivative. This reaction does not appear to occur without the *N*-sulfate group present nor under conditions where only epoxide formation is observed (16,17).

5. *Means of Producing Oligosaccharides from HS*

The means by which oligosaccharides are produced also have important consequences for their attachment to surfaces. They can be classified into two groups: those produced by chemical, or by enzymatic means.

D. Chemical Means

1. Nitrous Acid Cleavage

Nitrous acid cleaves HS chains at glucosamine residues where the glucosamine is either *N*-unsubstituted or *N*-sulfated (18) to produce pair-wise oligosaccharides in which the reducing end glucosamine is modified to a 2,5-anhydromannose unit. This has the advantage that it is more reactive than its parent glucosamine residue because it bears an aldehyde group that is not in equilibrium with a series of unreactive closed ring forms, but lacks a convenient chromophore reducing the sensitivity of detection during separation. The technique can preferentially cut unsubstituted or *N*-sulfated glucosamine residues [employing pH <2.5 to cut *N*-sulfated residues while pH 2.5–4.0 cleaves at unsubstituted glucosamine residues (12,18)] although the rate of scission can be influenced by the adjacent substituents. There is also the possibility of unwanted modifications in the saccharide chain, which are difficult to monitor. However, the improved reactivity of the reducing end probably outweighs these disadvantages when considering their attachment to surfaces.

2. Free Radical Degradation

The free radical degradation of polysaccharide chains has been achieved mediated by copper(I) ions (19). The mechanisms of this method has not been studied in great detail and has been relatively little used but has one crucial advantage over other methods in that it results in cleavage of HS to produce both odd and even oligosaccharides, apparently cutting predominantly at the glycosidic linkages (19). Apart from a small amount of unwanted modification, the chains produced are apparently intact (i.e., do not suffer from de-*O*- or de-*N*-sulfation) and bear a conventional glucosamine or uronic acid derivative at their reducing ends, thereby increasing still further the range of species involved in any subsequent surface attachment. As far as we are aware, little work has been conducted on the relative reactivities of uronic acid derivatives compared to glucosamine residues on surfaces.

E. Enzymatic Means

Bacterial derived lyase enzymes also produce pair-wise oligosaccharide fragments but these contain intact glucosamine residues at their reducing ends. Instead, the non-reducing end uronic acid residue is modified to a 4,5 unsaturated derivative (Fig. 5). This is a convenient chromophore, useful during subsequent separation steps but the unmodified reducing end residues lead to poor surface attachment via Schiff base formation. The 4,5 unsaturated bond, on the other hand, has recently been exploited for surface attachment through the formation of a mercury derivative (see Section IIIC).

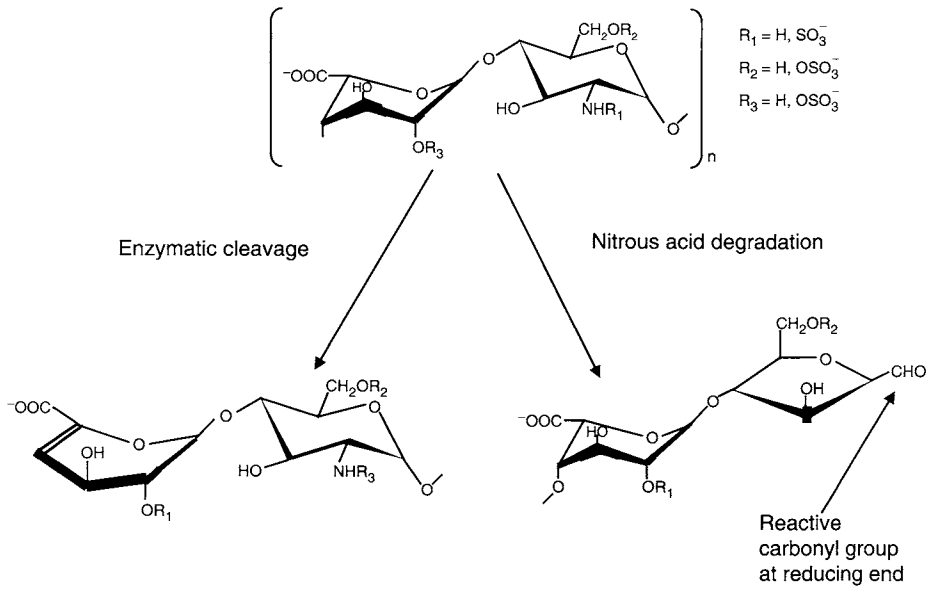

Figure 5 The production of saccharides by nitrous acid and enzymatic degradation both result in modifications to their structure. Nitrous acid introduces a 2,5-anhydromannose residue bearing a reactive aldehyde group at the reducing end while enzymatic cleavage modifies the non-reducing terminal uronic acid to a 4,5 unsaturated derivative which can be either 2-*O*-sulfated or underivatised and the identity of the acid (glcA or idoA) is lost.

III. Methods of Attachment to Surfaces

A. Formation of Schiff Base or Imine

One of the most common methods for attachment of sugars to surfaces involves the formation of a Schiff base or imine between an amino-derivatised group on a surface and the carbonyl function of a reducing sugar. As mentioned above, several factors compete, effectively limiting the yield of this reaction and considerable heterogeneity may be present in the coupled products. The attacking nucleophile, usually an amine or hydrazide group, is constrained on the surface, and this further reduces reactivity with the carbonyl group of the saccharide. The yields in uncatalysed labelling reactions are typically as low as a few per cent, even after considerable reaction periods, but any attempts to improve this are hamstrung by the sluggish equilibrium between unreactive and reactive forms of the sugar ring (see Section IIB) as well as the acid sensitivity of the *N*-sulfate group (see Section IIC1). Reaction on a derivatised surface may be expected to be at least as low yielding and it would be difficult to detect the presence or extent of de-*N*-sulfation if it occurred during the attachment process. High rate improvement, although not yield, has been reported by employing microwave-enhanced solvent heating (20)

for the convenient attachment of heparin oligosaccharides to aminosilane-derivatised glass slides. This approach employed the polar and non-volatile ampholytic solvent formamide, which permitted rapid mutarotation and allowed nanolitre drop size to be efficiently heated with microwave radiation on a glass surface, where aqueous and most other solvents suffered from very rapid evaporation.

An example of the above is the attachment of HS to a thiol-derivatised gold surface via thiolundecanoic acid, followed by 1-ethyl-3-(3-dimethylaminopropyl)-carbodi-imide (EDC) to activate the carboxylic acid and subsequent reaction with hydrazine to yield a hydrazide surface. Reaction of the sugar was then achieved via the reducing end aldehyde to form a Schiff base (21).

B. Attachment in the Chain with Esters or via Esters

Alternatives to attachment via the reducing end include derivatisation within the saccharide chain employing reagents such as succinimidyl esters, which react with free-amino groups (and possibly *N*-sulfate groups) or EDC ester activation of the carboxylic acid groups and subsequent attack with suitable nucleophiles. This approach is rarely used because it suffers from several serious drawbacks. The first is that such derivatives cannot normally be made homogeneous [and behave differently to the parent molecule (22)] and the second is that attachment to a surface will almost inevitably lead to a significant proportion of the molecules being held close to the surface, leading to steric restrictions for any potential binding partner.

Biotin can be attached (23,24) to either the reducing end (e.g., via a hydrazide linkage) or along the chain (usually to amino groups via an activated ester derivatised biotin derivative). The issues involved in both of these types of procedure are the same as those mentioned above with the additional consideration that binding of the protein binding partner to the immobilised streptavidin on the surface will need to be minimised.

C. Attachment at the Non-Reducing End via Attack of the Double Bond

The cleavage of HS polysaccharides by bacterial lyase enzymes (see above) provides one important modification to the structure of the oligosaccharides it produces. At the point of cleavage, the fragment terminating at the freshly generated reducing end is released with a conventional reducing end. In contrast, the neighbouring fragment, terminating at the new non-reducing end with a uronic acid moiety, is converted into a 4,5 unsaturated derivative (see above). Both GlcA and idoA derivatives are converted to the same unsaturated residue in this process (Fig. 5). The unsaturated uronic acid unit is present in all bacterial lyase-derived fragments except those originating from the extreme non-reducing end of the parent polysaccharide and only exists in two forms: either bearing a 2-*O*-sulfate group, or lacking this substituent. This represents considerably reduced heterogeneity compared to that present at the reducing end of oligosaccharides derived by other techniques. Recently, attention has focused on whether this feature can serve

as an alternative means of attachment to surfaces. The presence of the double bond has been exploited via the formation of oxymercurinium intermediates, to attach heparin oligosaccharides to a thiol-derivatised gold surface (25) (Fig. 6). A potential advantage of this approach is that it offers an alternative to the very low yielding, uncatalysed attachment via the reducing end.

IV Detection of Binding Partners

From the point of view of HS–protein interaction studies, there are a number of types of information that can be gleaned. These are the qualitative assessment of binding with partners (almost always proteins) or screening, in which the sugars are attached to a surface and probed for binding with labelled proteins of interest. A more rigorous approach, less prone to false negative results, involves quantitative screening in which careful controls and statistical analyses are undertaken.

Optical biosensors can be employed for the determination of both binding affinity determination and kinetics but these require careful experimental design and the correct application of models in order to interpret binding curves. In particular, the widespread but erroneous practice of employing a one-site model for interactions with a multi-dentate nature should be avoided while careful analysis with appropriate models or selection of oligosaccharides with a true mono-dentate nature can yield valuable data (12).

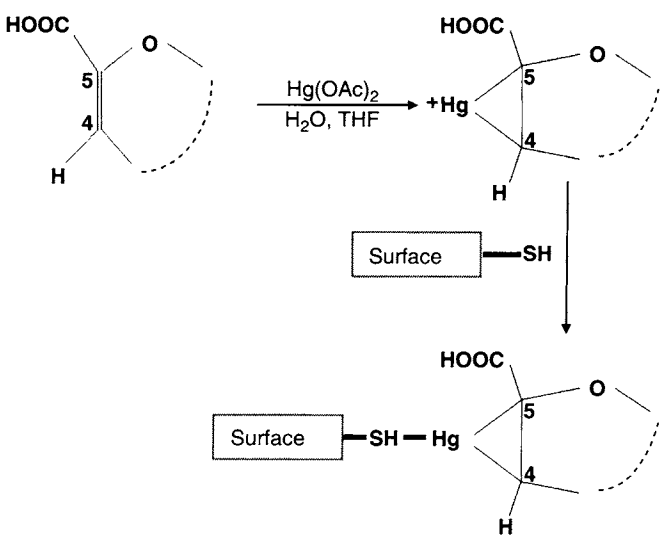

Figure 6 Derivatisation of the unsaturated 4,5-uronic acid residue of enzyme cleaved HS saccharides with mercury acetate and their subsequent attachment to thiol-derivatised gold surfaces.

However, with all of these techniques, there are a number of factors, which could influence the outcome but are often difficult to assess. These include the nature of the linkage between surface and sugar and its geometry in relation to the surface and its dimensions (it may or may not include a spacer). Furthermore, the density of coverage on the surface, the distribution of the attached sugars and their orientation in relation to the surface will also influence binding. In the following section, some of the means at our disposal for determining these parameters and methods for determining the extent of binding of partners are outlined.

A. Detecting Interactions at a Surface

The detection of interactions especially those involving biological molecules at surfaces is a problem that researchers have been trying to solve for many years. Early techniques such as quartz crystal microbalance (QCM) simply detected the mass of material absorbed to a surface, which has now developed in to a much more sophisticated technique; quartz crystal microbalance-dissipation (QCM-D). Several other useful techniques operate by measuring the change in refractive index of a surface that includes Biacore, the Affinity sensors IAsys plus and the Farfield Analight. The topology and morphology of surfaces can be investigated using scanning probe microscopy (SPM) techniques, such as atomic force microscopy (AFM) and scanning tunnelling microscopy (STM). In the following sections, each of these techniques is briefly explained and some examples given (Table 1).

1. Quartz Crystal Microbalance-Dissipation

Quartz Crystal Microbalance-Dissipation (QCM-D) is a technique that measures the mass of material adsorbed to a surface and the viscoelastic changes that occur. The technique is based on the piezoelectric properties of quartz. Briefly, when an alternating potential is placed across a quartz crystal it will vibrate at a frequency that is dependent on its mass. When additional material (i.e., mass) adsorbs to its surface the frequency will decrease. An analogy is a tuning fork; the more massive the tuning fork the lower its pitch. This relationship is expressed by the Sauerbrey equation:

$$\Delta m = \frac{-\Delta f \cdot c}{n} \tag{1}$$

where Δf is the change in frequency due to material binding to the surface, Δm, the change in mass, c, a proportionality constant, and n, the overtone.

The other quantity that QCM-D can measure is the "damping" of the surface. The driving alternating potential is switched off and the rate at which the oscillations decay is measured. This quantity is known as dissipation and is expressed as a ratio of the energy lost to the energy stored in the crystal:

$$D = \frac{E_{\text{lost}}}{2\pi E_{\text{stored}}} \tag{2}$$

where D is the dissipation, and E, the energy lost or stored from the quartz crystal.

Table 1 Comparison of Techniques

Device	Advantages	Disadvantages
QCM-D	Gold surface	Large sample volume needed
	Gives structural information	Only one reaction cell
	Surfaces easy to clean	Measures average across the surface
	No labels required	Uses downward flow and mass transport
	Detects all materials	
RM [IAsys]	Two-channel cuvette	Measures average across the surface
	No labels required	Detection dependent on optical properties of adsorbate
	Uses small volumes	
	Has a sonic stirrer	
SPR [BIAcore]	Gold Surface	Nanofluidics – has problems with very viscous solutions
	Nanofluidics – results can vary	Measures only one variable
	Small volumes	Detection dependent on optical properties of adsorbate
	No labels required	
DPI [Farfield Analight]	Two channels	Fluidics – has problems with very viscous solutions
	No labels required	Surfaces sensitive to high pH
	Fluidic system	
	Can measure surface thickness	
Ellipsometry	Non-invasive	Dry sample only
	Works on any reflective surface	
	Angstrom sensitivity	
PM-IRRAS	Non-invasive	Orientation specific
	Works on any reflective surface	
	Dry and wet samples	

If the material bound to the quartz crystal surface forms a very rigid structure [in this example, a self-assembled monolayer (SAM)], then the decay rate of the oscillations will be very small and will have a small dissipation. Conversely, if the structure is very flexible then the oscillations will decay very quickly and it will have a large dissipation.

By measuring the rate at which the oscillations decay information about the order and structure of the surface can be obtained and modelling software can be used to determine viscoelastic parameters providing quantitative information of the dissipation measurement. Quartz crystal surfaces are covered in a selection of metals and semiconductors, the most common being gold which, as described earlier in this chapter, is amenable to the attachment of HS saccharides by several methods (21,26–28).

2. Optical Biosensors

All optical biosensors measure or sense a change in refractive index at a surface, the surface being situated just outside a waveguide. The three devices that will be discussed here, surface plasmon resonance (SPR), resonant mirror (RM) and dual polarisation interferometry (DPI), do this in very different ways.

a. Surface Plasmon Resonance (e.g., BIAcore™)

Surface Plasmon Resonance (SPR) is used to monitor the change of refractive index at a surface. SPR occurs when polarised light undergoes total internal reflection at a metal film (Fig. 7). When the energy of the light is sufficient, electron waves or plasmons, will be created in the gold film. These surface plasmons can be detected by a decrease in the intensity of the reflected light. The plasmons generated will interact with the material on the surface and, as the refractive index of the surface changes, will alter the angle at which light is reflected. The change in angle linearly corresponds to the change in refractive index, which is proportional to the mass attached to the gold surface (25,29–31).

b. Dual Polarisation Interferometer (e.g., Farfield Analight™)

The Analight™ is a dual polarisation interferometer; Fig. 8 shows the two-tier waveguide of the Analight™, which is constructed of silicon oxynitride. There are two parts to the waveguide; the reference guide, which is totally shielded and the measurement waveguide, which is not shielded. Light can "leak" from the measurement waveguide and interact with matter on and close to the surface. The light that leaks from the measurement waveguide is transmitted when total internal reflection occurs; this is also known as evanescent light. The evanescent light will only be transmitted if the refractive index of the material on or close to the surface is greater than the refractive index of the measurement waveguide. The transmission

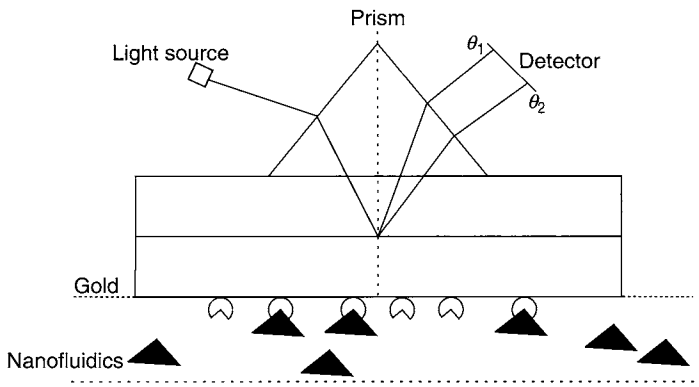

Figure 7 BIAcore, as material binds to the reactive surface the reflected angle of the lighted is changed (θ_1 and θ_2).

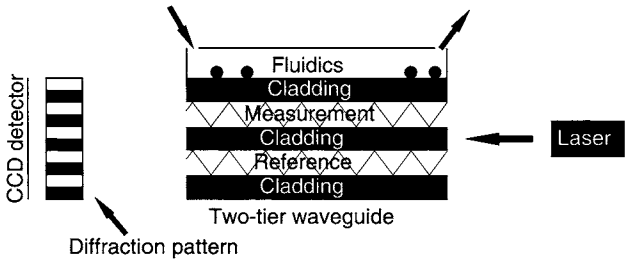

Figure 8 Farfield Analight, the diagram shows the two-tier waveguide of the Analight, light from the top (measurement) and bottom (reference) tiers interfere with each other producing a diffraction pattern.

of the light across the cladding costs energy and changes the phase of the light in the measurement waveguide. When laser light is passed through the waveguides, it emerges at the other end of the waveguide producing an interference pattern. This pattern will change depending on how the phase of the light in the measurement waveguide has changed. By monitoring the change in the interference pattern, the refractive index of the material on, or close to, the surface can be determined, and can be used to determine the materials mass. In addition, the thickness of layers can be calculated.

The surface of the Analight™ waveguide is functionalised using silane chemistry, allowing the production of surfaces terminated with a variety of chemical groups including methyl, thiol or amino, some of which facilitate binding of sugars (32–34).

c. Resonant Mirror (e.g., Affinity Sensors, IAsys plus™)

The IAsys plus uses an evanescent wave to monitor the adsorption of material to a cuvette surface. Light from a diode undergoes total internal reflection in a waveguide coated with a metal oxide, the evanescent wave (an electric field) is transmitted across this film (Fig. 9). Interactions between the evanescent wave and the material in the cuvette (sample) cause a change in velocity and therefore momentum of the light in the waveguide. This causes the angle at which total internal reflection occurs to change. The greater the ratio of mass to refractive index of the material, the greater the change in angle. The IAsys plus is a cuvette based system in which the waveguide makes up the bottom half, the top half being the cuvette itself with the metal oxide surface. The latter can be supplied underivatised or functionalised with carboxymethyl dextran (35–37).

d. Scanning Probe Microscopy

SPM techniques rely on a feedback loop allowing a probe to be moved across a surface very closely. The two most common SPM techniques are STM and AFM (Fig. 10).

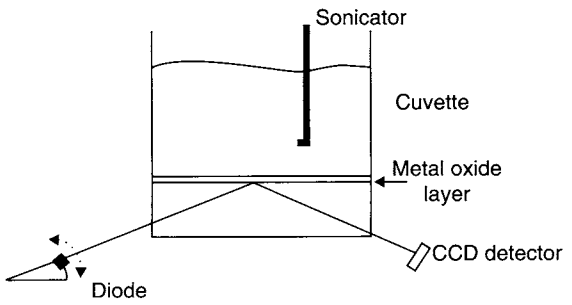

Figure 9 Affinity sensors, IAsys plus; the diagram shows the cuvette system employed by the IAsys plus. The cuvette contains a stirrer to overcome diffusion-restrained interactions. While the sensor itself is made up of an arcing diode and a CCD detector, which collects the reflected light.

i. Scanning Tunnelling Microscopy

STM is used to give an electronic picture of a surface. The technique relies on a quantum mechanical effect known as tunnelling. Quantum mechanics predicts that an electron can tunnel across a potential barrier. In the case of STM, this barrier is arranged between the surface and a metal tip. A potential is applied between the tip and surface, and the tip is scanned (or rastered) across the surface in mutually perpendicular directions parallel to the surface, producing an electron density map of the surface.

$$I \propto V\, e^{-s} \tag{3}$$

where I is the tunnelling current, V, the bias voltage and s, the separation between the tip and surface.

The device can be run in two different modes; under constant voltage, where the tip is kept at a constant height over the surface and the current is measured (Eq. 3) or under constant current, in which the tip height is allowed to follow the topology of the surface. STM can provide a wealth of information on the electronic state of the surface, this can be related back to gain structural and topographical information, and can be used to investigate the electrochemical state also (38–40).

ii. Atomic Force Microscopy

Atomic Force Microscopy (AFM) is used to give a physical picture of a surface. A tip is rastered over a surface with constant force to give a three-dimensional picture of a surface and its features. The tip is moved across the surface using piezoelectric motors, the force between the tip and surface is kept constant by measuring the position of the tip using light reflected from it. With a feedback loop, this prevents the tip from touching the surface. The device can either be run in contact mode for hard samples, or in tapping/vibrational/intermittent contact mode for soft samples such as biological samples. AFM can also be used to measure the interaction forces

between a sample and the tip. Molecules can be immobilised on the surface and another molecule known to interact with the immobilised molecule can be attached to the tip (Fig. 10). When the tip is rastered across the surface and an interaction is observed, the tip can be pulled away from the surface and the force diagram produced shows the force that was required to break the interaction (41–44).

iii. Ellipsometry

Ellipsometry is a technique that measures the polarisation of reflected light. The name derives from the fact that reflected light is elliptically polarised.

$$\tan \varphi \, e^{i\Delta} = \frac{r_p}{r_s} \tag{4}$$

where Δ is the relative phase change, φ, the relative amplitude change and r_s and r_p are the Fresnel reflection coefficients for p- and s-polarised light.

During an experiment Δ and φ (Eq. 4) are measured, the thickness of the film can be determined from these two parameters as Δ, the relative phase change, is linearly related to the thickness of the film. The technique is non-invasive; any surface can be used as long as it is flat and reflective. Ellipsometry provides information on the thickness of thin inorganic films, through monitoring the change of polarisation the surface causes to the incident light (45).

iv. Polarisation Modulation Infrared Reflection Adsorption Spectroscopy
Polarisation modulation infrared reflection adsorption spectroscopy (PM-IRRAS) is a highly sensitive surface specific infrared technique arising only from radiation that is perpendicular to the surface contributing to the spectrum (i.e., fulfilling the selection rules). The technique is very versatile and as long as the substrate being used is flat and reflective, the technique can be used. With a little modification, the technique can also be employed with a sample in air or in solution. As well as providing spectrographic information about a surface, the orientation of adsorbed species can be deduced by comparison with signals of relevant chemical groups in the sample from solution and surface spectra (46–48).

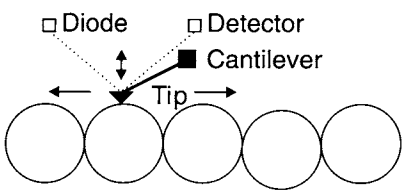

Figure 10 Atomic force microscopy. This depicts the tip of an AFM moving across a surface. The *Z*-position of the tip is monitored by the light reflected from it and the tip is moved across the surface by piezoelectric motors.

3. Summary

Using the techniques mentioned above it is possible to gain insights into the interactions between an immobilised heparin or HS oligosaccharide and a binding partner. With the QCM-D, IAsys plus, Biacore and Analight, the mass change when a ligand is added to the surface can be obtained. The QCM-D and Analight can also extract other information. The former provides viscoelastic properties of the surface, such as the shear modulus and viscosity, while the latter provides thickness and density measurements. Using the SPM technique topographical information, such as the orientation of the immobilised proteins or other molecules can be gained and with AFM, the interaction forces. STM can produce topographical data but also electronic data, which can be analysed spectrographically. The study of HS–protein interactions and the molecular details underlying them are increasingly employing techniques that involve attachment of HS saccharides to a derivatised surface. In this chapter we have highlighted some of the considerations that need to be borne in mind when undertaking such experiments on both naturally occurring and chemically or enzymatically modified HS or heparin and oligosaccharides derived from them. We have also described some of the principal surface-based techniques that are currently in use. No doubt, considerable advances will continue to be made in this, as in other areas of research, which will allow a more accurate and increasingly detailed picture of these biologically important interactions to be formed.

Acknowledgments

The work of the authors is funded by BBSRC. Drs Scott Guimond and Andrew Powell are thanked for their constructive criticism of the manuscript.

References

1. Turnbull JE, Gallagher JT. Sequence analysis of heparan sulphate indicates defined location of *N*-sulphated glucosamine and iduronate 2-sulphate residues proximal to the protein-linkage region. Biochem J 1991; 15:297–303.
2. Lindahl U, Kusche-Gullberg M, Kjellen L. Regulated diversity of heparan sulfate. J Biol Chem 1998; 273:24979–24982.
3. Shallenberger RS. Advanced Sugar Chemistry Principles of Sugar Stereochemistry. Westport, CT: AVI Publishing, 1982.
4. Isbell HS, Frush HL, Wade CWR, Hunter CE. Transformations of sugars in alkaline solutions. Carbohydr Res 1969; 9:163–175.
5. Isbell HS, Pigman W. Mutarotation of sugars in solution. Part II. Catalytic processes, isotope effects, reaction mechanisms and biochemical aspects. Adv Carbohydr Chem Biochem 1969; 24:13–65.
6. Inoue Y, Nagasawa K. Selective *N*-desulfation of heparin with dimethyl sulfoxide containing water or methanol. Carbohydr Res 1976; 46:87–95.
7. Nagasawa K, Inoue Y, Kamata T. Solvolytic desulfation of glycosaminoglycuronan sulfates with dimethyl sulfoxide containing water or methanol. Carbohydr Res 1977; 58:47–55.

8. Lloyd AG, Embrey G, Fowler LJ. Studies on heparin degradation. I. Preparation of (35 S) sulphamate derivatives for studies on heparin degrading enzymes of mammalian origin. Biochem Pharmacol 1971; 20:637–648.
9. Yamada S, Watanabe M, Sugahara K. Conversion of *N*-sulfated glucosamine to *N*-sulfated mannosamine in an unsaturated heparin disaccharide by non-enzymatic, base-catalyzed C-2 epimeization during enzymatic oligosaccharide preparation. Carbohydr Res 1998; 309:261–268.
10. Lobry de Bruyn CA, van Ekenstein W. Action of alkalies on the sugars. Reciprocal transformation of glucose, fructose and mannose. Rec Trav Chim Pays-Bas 1895; 14:203–216.
11. Toida T, Vlahov IR, Smith AE, Hileman RE, Linhardt RJ. C-2 epimerization of *N*-acetylglucosamine in an oligosaccharide derived from heparan sulfate. J Carbohydr Chem 1996; 15:351–360.
12. Powell AK, Yates EA, Fernig DG, Turnbull JE. Interactions of heparin/heparin sulfate with proteins: appraisal of structural factors and experimental approaches. Glycobiology 2004; 14:17R–30R.
13. Jaseja M, Rej RN, Sauriol F, Perlin AS. Novel region- and stereoselective modifications of heparin in alkaline solution. Nuclear magnetic resonance spectroscopic evidence. Can J Chem 1989; 67:1449–1457.
14. Rej RN, Perlin AS. Base-catalyzed conversion of the alpha-L-iduronic acid 2-sulfate unit of heparin into a unit of alpha-L-galacturonic acid and related reactions. Carbohydr Res 1990; 200:437–447.
15. Yamada S, Murakami T, Tsuda H, Yoshida K, Sugahara K. Isolation of the porcine heparin tetrasaccharides with glucuronate 2-*O*-sulfate. Heparinase cleaves glucuronate 2-*O*-sulfate-containing disaccharides in highly sulfated blocks in heparin. J Biol Chem 1995; 270:8695–8705.
16. Yates EA, Santini F, Bisio A, Cosentino C. Evidence for a heparin derivative containing an *N*-sulfated aziridine ring that retains high anti-factor Xa activity. Carbohydr Res 1997; 298:335–340.
17. Santini F, Bisio A, Guerrini M, Yates EA. Modifications under basic conditions of the minor sequences of heparin containing 2,3- or 2,3,6-sulfated D-glucosamine residues. Carbohydr Res 1997; 302:103–108.
18. Shively JE, Conrad HE. Formation of anhydrosugars in the chemical depolymerisation of heparin. Biochemistry 1976; 15:3932–3942.
19. Liu Z, Perlin AS. Evidence of a selective free radical degradation of heparin, mediated by cupric ion. Carbohydr Res 1994; 255:183–191.
20. Yates EA, Jones MO, Clarke CE, Powell AK, Johnson SR, Porch A, Edwards PP, Turnbull JE. Microwave enhanced reaction of carbohydrates with amino-derivatised labels and glass surfaces. J Mater Chem 2003; 13:2061–2063.
21. Rudd T, Gallagher JT, Ron D, Nichols RJ, Fernig DG. Biological functions of sulphated glycoproteins. Biochem Soc Trans 2003; 31:349–351.
22. Osmond RI, Kett WC, Skett SE, Coombe DR. Protein–heparin interactions measured by BIAcore 2000 are affected by the method of heparin immobilization. Anal Biochem 2002; 310:199–207.
23. Lee WT, Conrad DH. The murine lymphocyte receptor for IgE. II. Characterization of the multivalent nature of the B lymphocyte receptor for IgE. J Exp Med 1984; 159:1790–1795.

24. Norgard-Sumnicht Rand Varki A. Endothelial heparan sulfate proteoglycans that bind to L-selectin have glucosamine residues with unsubstituted amino groups. J Biol Chem 1995; 270:12012–12024.
25. Skidmore MA, Patey SJ, Thanh NTK, Fernig DG, Turnbull JE, Yates EA. Attachment of glycosaminoglycan oligosaccharides to thiol-derivatised gold surfaces Chem Comm 2004; 2700–2701.
26. Sauerbrey G. Verwendung von schwingquarzen zur wagung dunner schichten und zur mikrowagung. Z Physik 1959; 155(2):206–222.
27. Höök F, Rodahl M, Fredriksson C, Brzezinski P, Keller CA, Voinova M, Krozer A, Kasemo B. Simultaneous frequency and dissipation factor QCM measurements of biomolecular adsorption and cell adhesion. Faraday Discuss 1997; 107:229–246.
28. Kristensen EME, Rensmo H, Larsson R, Siegbahn H. Characterization of heparin surfaces using photoelectron spectroscopy and quartz crystal microbalance. Biomaterials 2003; 24:4153–4159.
29. Jonsson U, Fagerstam L, Ivarsson B, Johnsson B, Karlsson R, Lundh K, Lofas S, Persson B, Roos H, Ronnberg I, Sjolander S, Stenberg GE, Stahlberg GR, Urbaniczky C, Ostlin H, Malmqvist M. Real-time biospecific interaction analysis using surface plasmon resonance and a sensor chip technology. Biotechniques 1991; 11:620–627.
30. Ricard-Blum S, Feraud O, Lortat-Jacob H, Rencurosi A, Fukai N, Dkhissi F, Vittet D, Imberty A, Olsen BR, van der Rest M. Characterization of endostatin binding to heparin and heparan sulfate by surface plasmon resonance and molecular modeling – role of divalent cations. J Biol Chem 2004; 279:2927–2936.
31. Osmond RIW, Kett WC, Skett SE, Coombe DR. Protein–heparin interactions measured by BIAcore 2000 are affected by the method of heparin immobilization. Anal Biochem 2002; 310:199–207.
32. Swann MJ, Peel LL, Carrington S, Freeman NJ. Dual-polarization interferometry: an analytical technique to measure changes in protein structure in real time, to determine the stoichiometry of binding events, and to differentiate between specific and nonspecific interactions. Anal Biochem 2004; 329:190–198.
33. Cross GH, Reeves A, Brand S, Swann MJ, Peel LL, Freeman NJ, Lu JR. The metrics of surface adsorbed small molecules on the Young's fringe dual-slab waveguide interferometer. J Phys D Appl Phys 2004; 37:74–80.
34. Cross GH, Reeves AA, Brand S, Popplewell JF, Peel LL, Swann MJ, Freeman NJ. A new quantitative optical biosensor for protein characterisation. Biosens Bioelectron 2003; 19:383–390.
35. Cush R, Cronin JM, Stewart WJ, Maule CH, Molloy J, Goddard NJ. The resonant mirror: a novel optical biosensor for direct sensing of biomolecular interactions. Part I. Principle of operation and associated instrumentation. Biosens Bioelectron 1993; 8:347–354.
36. Delehedde M, Lyon M, Vidyasagar R, McDonnell TJ, Fernig DG. Hepatocyte growth factor/scatter factor binds to small heparin-derived oligosaccharides and stimulates the proliferation of human HaCaT keratinocytes. J Biol Chem 2002; 277:12456–12462.
37. Xu XY, Takano R, Nagai Y, Yanagida T, Kamei K, Kato H, Kamikubo Y, Nakahara Y, Kumeda K, Hara S. Effect of heparin chain length on the

interaction with tissue factor pathway inhibitor (TFPI). Int J Biol Macro 2002; 30:151–160.
38. Binning G, Rohrer H. Scanning tunneling microscopy. Helv Phys Acta 1982; 55:726–735.
39. Halliwell CM, Davies JA, Gallop JC, Josephs-Franks R. Real-time scanning tunnelling microscopy imaging of protein motion at electrode surfaces. Bioelectrochemistry 2004; 63:225–228.
40. Leggett GJ, Davies MC, Jackson DE, Tendler SJB. Scanning probe microscopy of biomolecules and polymeric biomaterials. J Electron Spectrosc 1996; 81:249–268.
41. Binning G, Quate CF, Gerber Ch. Atomic Force Microscope. Phys Rev Lett 1980; 56:930–933.
42. Marszalek PE, Oberhauser AF, Li HB, Fernandez JM. The force-driven conformations of heparin studied with single molecule force microscopy. Biophys J 2003; 85:2696–2704.
43. Chen CH, Hansma HG. Basement membrane macromolecules: insights from atomic force microscopy. J Struct Biol 2000; 131:44–55.
44. Negishi A, Chen J, McCarty DM, Samulski JR, Jian L, Superfine R. Analysis of the interaction between adeno-associated virus and heparan sulfate using atomicforce microscopy. Glycobiology 2004; 14:969–977.
45. Arwin H. Spectroscopic ellipsometry and biology: recent developments and challenges. Thin Solid Films 1998; 313:764–774.
46. Ronzon F, Desbat B, Buffeteau T, Mingotaud C, Chauvet JP, Roux B. Structure and orientation of a glycosylphosphatidyl inositol anchored protein at the air/water interface. J Phys Chem B 2002; 106:3307–3315.
47. Bellet-Amalric E, Blaudez D, Desbat B, Graner F, Gauthier F, Renault A. Interaction of the third helix of Antennapedia homeodomain and a phospholipid monolayer, studied by ellipsometry and PM-IRRAS at the air–water interface. Biochim Biophys Acta 2000; 1467:131–143.
48. Buffeteau T, Desbat B, Turlet JM. Polarization modulation FT-IR spectroscopy of surface and ultra-thin films – experimental procedure and quantitative-analysis. Appl Spectrosc 1991; 45:380–389.

Chemistry and Biology of Heparin and Heparan Sulfate
H.G. Garg, R.J. Linhardt and C.A. Hales (Editors)

Chapter 13

Heparin Activation of Serpins

JAMES A. HUNTINGTON

Department of Haematology, University of Cambridge, Division of Structural Medicine, Thrombosis Research Unit, Cambridge Institute for Medical Research, Wellcome Trust/MRC Building, Hills Road, Cambridge, UK

I. Introduction

The family of serine protease inhibitors known as the serpins is represented in all branches of life and predominates in the higher organisms, including man (1). They have evolved an extraordinary mechanism to inhibit proteases (2), which distinguishes them from the 20 other families of serine protease inhibitors (3,4) (see http://merops.sanger.ac.uk), and renders them uniquely qualified to control the proteolytic pathways essential to life. The mechanism is best described as a spring-loaded mousetrap (5), where nibbling of the peptide loop bait springs the trap and crushes the unsuspecting protease. As with a set mousetrap, the active state of a serpin is metastable, and the energy released upon conversion to its more stable form is used to trap the protease. The complexity of the serpin mechanism provides many advantages over the simpler lock-and-key type mechanism utilized by all other serine protease inhibitor families; serpins provide stoichiometric, irreversible inhibition, and the dependence on serpin and protease conformational change is exploited for regulation, signalling, and clearance. Regulation of serpin activity is best illustrated by the heparin activation of serpins. Thirty-five serpins have been identified in the human genome, and only five are known to bind heparin-like glycosaminoglycans (GAGs): antithrombin (AT), heparin cofactor II (HCII), plasminogen activator inhibitor-1 (PAI-1), protease nexin 1 (PN1), and protein C inhibitor (PCI) (6). All are implicated in hemostatic or fibrinolytic mechanisms,

but also have important extravascular functions. AT is the principal inhibitor of the coagulation proteases, and is the effector molecule for therapeutic heparin. Its heparin binding mechanism is the best characterized of the five, and therefore AT serves as the prototype heparin binding serpin. Recent crystallographic structures have shed new light on how heparin binding fine-tunes the inhibitory mechanism of serpins, and how seemingly disparate mechanisms of heparin binding and activation can share critical elements. This chapter describes recent developments in our understanding of the molecular mechanisms involved in the heparin activation of serpins.

II. General Features of Heparin Binding Serpins

A. Serpin Structure

Serpins were identified as a protein family by Hunt and Dayhoff in 1980 based on the sequence similarities of AT, α_1-antitrypsin and ovalbumin (7). To date, over 1500 serpins have been identified in the genomes of organisms representing all branches of life, and have been implicated in diverse physiological processes (1,8). Although most serpins are inhibitors of serine proteases, as the acronym suggests (serine protease inhibitor), many are incapable of protease inhibition and others possess additional functions (e.g., cell signalling, hormone carriers) (6). Some serpins inhibit intracellular cysteine proteases to control apoptotic pathways (9). Although the serpins were initially identified by sequence identity, it is generally weak compared to the level of observed structural homology. The highly conserved serpin-fold consists of three β-sheets (A, B, and C) and nine α-helices (A-I), organised into an upper β-barrel domain and a lower α-helical domain, which are bridged by the five-stranded β-sheet A (Fig. 1A). In the classic serpin orientation, β-sheet A is facing, and the reactive center loop (RCL), the region that interacts with the protease, is on top. Unlike all other families of serine protease inhibitors, the RCL of serpins is long and flexible, and serves as bait by presenting a favourable protease cleavage site. The serpin-fold is also unusual in its thermodynamic properties, as the native state is not the most stable. Under certain conditions, serpins undergo a change in topology to a hyperstable state, with the insertion of the RCL as the fourth strand in the now six-stranded β-sheet A. This transition is triggered by proteolytic nicking of the RCL to generate the cleaved form (Fig. 1C), or in the absence of cleavage to generate the so-called 'latent' form (10) (Fig. 1D) (11,12).

B. The Suicide Substrate Mechanism

Serpins utilise a suicide substrate mechanism for the inhibition of serine proteases (2), which is best described by the kinetic model of protease substrate hydrolysis (Fig. 2A). Unlike the typical reversible lock-and-key type inhibitors (e.g., Kunitz family inhibitors such as BPTI), the serpin is consumed during inhibition (hence *suicide-substrate*). However, serpins have evolved to be very poor substrates of serine proteases, with the very last step in the proteolytic cycle, deacylation (k_{hyd}), slowed several orders of magnitude. How deacylation is slowed has been revealed by the

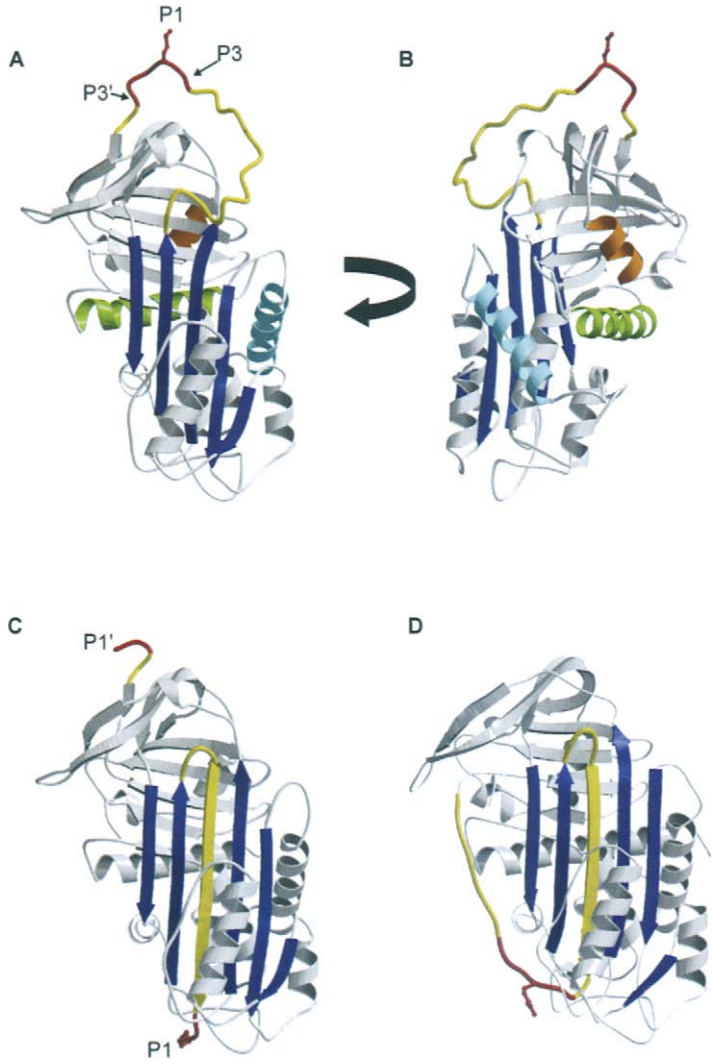

Figure 1 The serpin architecture. (A) The typical native serpin fold, shown here in the classic orientation (β-sheet A facing with RCL on top), is composed of a lower helical domain and an upper β-barrel domain, bridged by β-sheet A (blue). Proteases recognise target peptide sequences expressed on the flexible serpin RCL (yellow and red). Most critical in determining inhibitory specificity of serpins is the composition of the reactive centre residue (P1, red ball-and-stick) and the N- and C-terminal flanking regions from P3 to P3′ (red) (13). The helices involved in heparin binding are A (green), D (cyan), and H (orange). (B) A rotation along the long axis 90° from the standard orientation shows the relative positions of the three heparin binding helices. (C) The stability of the serpin is typically doubled by the incorporation of the RCL as the fourth strand of the now six-stranded β-sheet A through cleavage of the RCL. (D) Loop insertion can also occur in the absence of RCL cleavage to form the so-called latent conformer. This figure and others were made using Bobscript (14) and Raster3D (15).

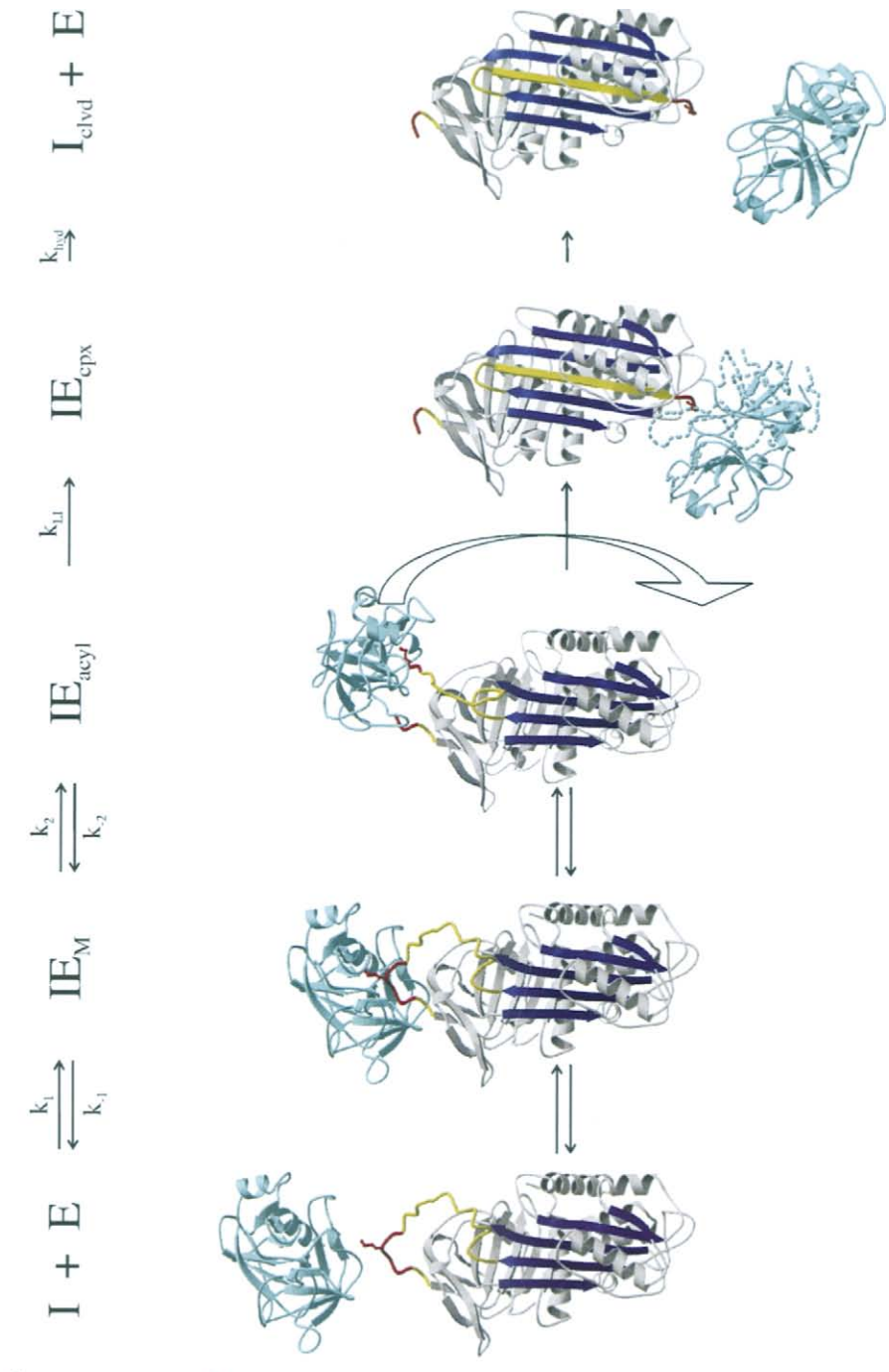
A
B
I + E
k_1
k_{-1}
IE_M
k_2
k_{-2}
IE_{acyl}
k_{L1}
IE_{cpx}
k_{hyd}
I_{clvd} + E

Figure 2 The serpin mechanism of protease inhibition. (A) The kinetic scheme which describes the serpin mechanism of protease inhibition is very similar to that describing the proteolytic cleavage of a substrate. The serpin (I) interacts rapidly with the protease (E) to form a Michaelis complex (IE_M). This step, defined by the Michaelis constant K_m, tends to be rate limiting, with k_1 indistinguishable from the overall second-order rate constant of inhibition. The Michaelis complex is quickly converted to the acyl-enzyme intermediate (IE_{acyl}), and upon separation of the C-terminal portion of the RCL from the active site of the protease, the N-terminal portion rapidly inserts into β-sheet A (k_{LI}). At high concentrations of reactants, the limiting rate of complex formation is the separation of the C-terminus of the RCL from the active site of the protease, not the rate of loop insertion (16). The insertion of the RCL and the 70 Å translocation of the covalently attached protease from the top to the bottom of the serpin results in the final serpin-protease complex (IE_{cpx}). Destruction of the proteolytic architecture slows the final step of hydrolysis of the acyl-enzyme linkage by several orders of magnitude (k_{hyd} is very slow), but the reaction will eventually result in cleaved serpin (I_{clvd}) and regenerated protease. (B) Each step of the serpin mechanism is illustrated by structures of the reactants and complexes involved. The protease is coloured cyan and the serpin is coloured as in Fig. 1. The structure of the intermediate IE_{acyl} is inferred from the adjacent structures of the Michaelis (17) and final complexes (18).

recent structure of the final serpin–protease complex (18). As shown in Fig. 2B, rapid recognition of the serpin RCL by the protease (formation of the Michaelis complex) is followed by the formation of the acyl-enzyme intermediate and separation of the C-terminal peptide of the serpin RCL from the active site of the protease (16). At the acyl-enzyme intermediate step, where the serpin and protease are covalently linked via an ester bond between the reactive centre P1 residue and the active site Ser of the protease, the serpin rapidly inserts the RCL into β-sheet A. The protease is thus flung 70 Å from the top of the serpin to the bottom, and the now hyperstable serpin crushes the protease by exerting a pulling force on the active site loop. The effect of the pulling force is a stretching out of the catalytic loop of the protease, which contains the active site serine and the residues which form the oxyanion hole, thus rendering the protease catalytically inert. Clashes between the hyperstable serpin and the protease also lead to the unfolding of roughly 40% of the protease structure, as evidenced by the lack of density in the crystal structure (18), the acquisition of profound proteolytic susceptibility (19,20) and the change of NMR resonances (21).

C. Heparin Acceleration of Protease Inhibition

The hallmark of the heparin binding serpins is that target protease inhibition is accelerated in the presence of heparin. Table 1 is a list of second-order rate constants of inhibition for selected serpin–protease pairs, in the absence and presence of heparin. Acceleration is generally through a 'bridging' mechanism where the protease and serpin bind to the same heparin chain, resulting in improved encounter rate (k_1) and stabilisation of the Michaelis complex by reducing the initial dissociation rate (k_{-1}) (Fig. 2A). The promiscuity of the serpin mechanism allows serpins to inhibit proteases *in vitro* which would not normally be encountered under physiological conditions, and in some cases there is a small rate enhancing effect conferred by heparin, even though the protease does not bind heparin. Examples are the trypsin inhibition by AT and PN1, and the chymotrypsin inhibition by PCI. Such behaviour suggests a change in the conformation of the serpin RCL in response to heparin binding, so that reactivity with proteases is improved (generally referred to as allosteric activation).

D. Heparin Binding Sites

The heparin binding site of serpins was identified through structural alignment on the template of RCL-cleaved α_1-antitrypsin (35,36). The alignment revealed a cluster of basic residues at the N-terminus of helix A and along the length of helix D. Figure 3 is a new alignment based on superposition of the known structures of AT, HCII, PAI-1, and PCI; and although no structure of PN1 is currently available, molecular modelling suggests the exclusive contribution of the D helix. PCI is the only heparin binding serpin without several basic residues on helix D, and its heparin binding motifs are found on its N-terminal insertion loop and on helix H. The surface electrostatic potentials of the heparin binding sites are shown in Fig. 4.

Table 1 Heparin Acceleration of Protease Inhibition by Serpins

Serpin	Protease	Rate constant ($M^{-1}s^{-1}$) −Heparin	+Heparin	Fold acceleration	References
AT	Factor IXa†	58	3.1×10^7	530,000	(22)
AT	Factor IXa†,♣	58	3.1×10^4	530	(22)
AT	Factor Xa†	2.6×10^3	1.4×10^8	53,800	(23)
AT	Factor Xa†,♣	2.6×10^3	8.2×10^5	315	(23)
AT	Thrombin†	6.8×10^3	1.2×10^8	17,650	(23)
AT	Thrombin†,♣	6.8×10^3	1.1×10^4	1.6	(23)
AT	Trypsin*	1.5×10^5	1.1×10^6	7	(24)
AT	Trypsin*,♣	1.4×10^5	4.0×10^5	3	(25)
HCII	Thrombin	1.0×10^3	7.4×10^7	74,000	(26,27)
HCII	Chymotrypsin*	3.7×10^3	4.0×10^3	1	(26)
PAI-1	Thrombin	7.9×10^2	1.6×10^5	200	(28)
PN1	Thrombin	1.4×10^6	1.2×10^9	860	(29)
PN1	Factor Xa	5.1×10^3	3.5×10^5	70	(30)
PN1	Factor XIa	8.0×10^4	1.7×10^6	21	(31)
PN1	Trypsin*	2.2×10^6	1.0×10^7	5	(30)
PCI	APC	4.8×10^2	2.5×10^4	52	(32)
PCI	Thrombin	2.0×10^4	1.9×10^5	10	(32)
PCI	Acrosin	2.4×10^5	5.6×10^7	230	(33)
PCI	Tissue kallikrein	2.3×10^4	~0	–	(34)
PCI	Chymotrypsin*	1.1×10^6	3.3×10^6	3	(32)

*Non-target protease, which is incapable of binding to heparin.
†At physiological Ca^{2+} levels.
♣With pentasaccharide.

III. Antithrombin

A. Physiological Functions

Antithrombin (AT) is the most important serpin in hemostasis (37). It is a plasma serpin which circulates at 2.3 μM and is capable of inhibiting all of the serine proteases that promote blood coagulation, but based on rates of inhibition, its primary targets are factors IXa, Xa, and thrombin. The importance of AT is demonstrated by the high association of deficiency with venous thrombosis (38), by the embryonic lethal consumptive coagulopathy in the knockout mouse (39), and by the continued success of therapeutic heparin. The anticoagulant effect of natural heparin and the new synthetic heparins, is mediated primarily through the activation of AT as an inhibitor of the coagulation proteases (40,41). Of course, heparin, which is produced and secreted exclusively by mast cells, is not a physiological activator of AT; instead it is the closely related cousin heparan sulfate which lines the vascular wall, and which, through interaction with a fraction of the circulating AT, ensures the fluidity of the microvasculature (42). Heparin differs from heparan sulfate only in degree of sulfation and in the fraction of the highly flexible iduronic acid; both factors are key in determining affinity for AT. Heparan

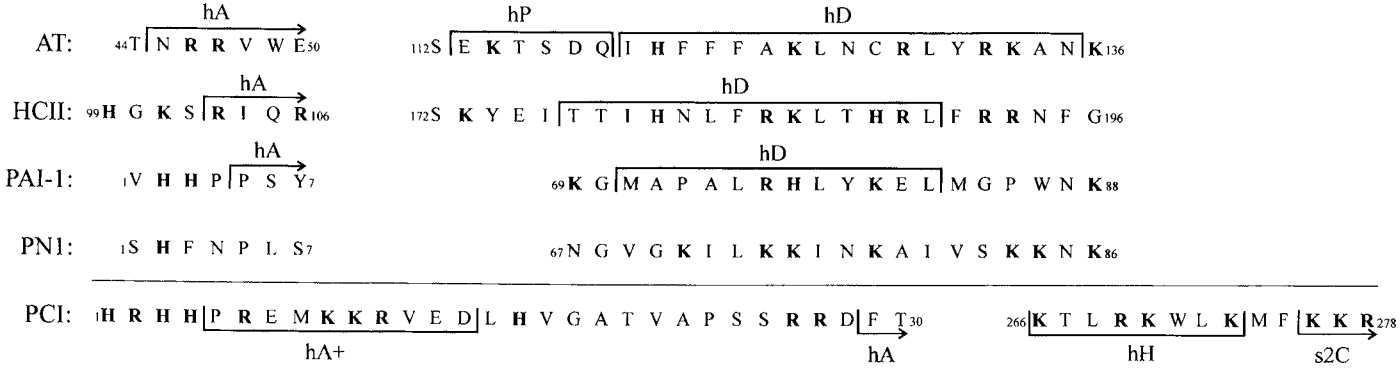

Figure 3 Manual alignment of serpin heparin binding sequences based on superposition of available structures. The heparin binding site of serpins is primarily at the N-terminus of helix A (hA) and all along the face of helix D (hD). The sequences are aligned on the structure of AT bound to its pentasaccharide heparin fragment, and the positions of the helices are indicated. When AT binds to heparin a new helix P (hP), named after the pentasaccharide, forms on the N-terminus of helix D. The basic residues are shown in bold. No structure of PN1 is known, and consequently no secondary structure identification is made. PCI does not have its heparin binding site along helix D, rather the basic N-terminal loop and helix H are implicated in heparin binding.

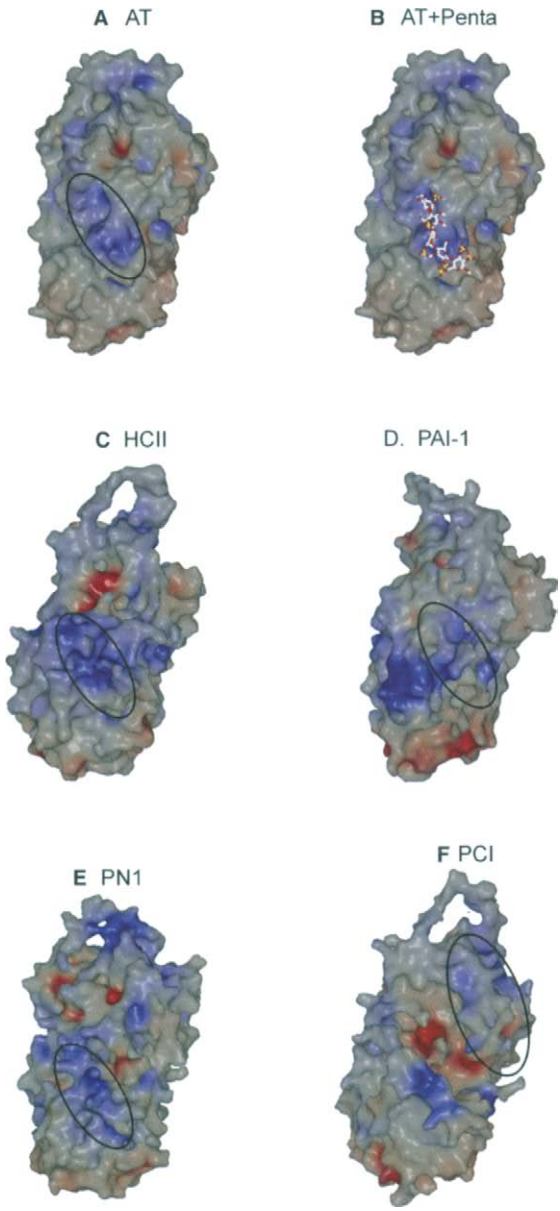

Figure 4 Surface electrostatic properties of heparin binding serpins. The surface representations of heparin binding serpins are coloured according to electrostatic properties, with blue indicating positively charged regions and red negatively charged regions. Heparin binding sites of proteins tend to be highly basic (blue) surfaces. The pentasaccharide interaction with AT has been observed crystallographically, and the surfaces in the absence (A) and presence (B) of the pentasaccharide are shown. The proposed heparin binding sites are indicated by a black oval, and the orientation for all serpins is as for Fig. 1B. The surfaces of HCII (C) and PAI-1 (D) were calculated on known structures, but that of PN1 (E) is based on a molecular model built on the native AT structure, and that of PCI (F) is based on a model of native PCI built on the structure of cleaved PCI. Figures were made using the program Spock.

sulfate is highly heterogeneous and contains patches of high sulfation and iduronic acid levels, providing the sites of interaction with AT (43). While some 30% of heparin chains bind AT with high affinity, only a small fraction of heparan sulfate chains possess the high affinity site (42). The early identification of AT as the effector of heparin anticoagulant activity has spurned intense research effort aimed at understanding how it binds to, and is activated by heparin. The AT–heparin interaction now serves as a paradigm for the heparin binding serpins as a whole.

B. Mechanism of Heparin Binding

The high affinity AT binding site on heparin is a five monosaccharide fragment (44,45) commonly referred to as the 'pentasaccharide'. The interaction is exquisitely specific and small alterations in either the sulfation pattern of the pentasaccharide or in the sequence of the heparin binding region of AT can significantly reduce binding affinity [reviewed in (46)]. The region of AT which binds to heparin was initially identified from a heparin binding deficient variant of AT found in a patient who had experienced a thrombotic event (47). Subsequent alignment of the sequence of AT on the template of the first serpin structure by Huber and Carrell (36) revealed the heparin binding site, and it has since been confirmed by mutagenesis (48) and crystallographic (49–51) studies. A diagram detailing the individual interactions between the pentasaccharide and AT is given as Fig. 5. The heparin binding residues of AT have been mutated to determine their individual contributions to the free energy of pentasaccharide binding; by far the most important

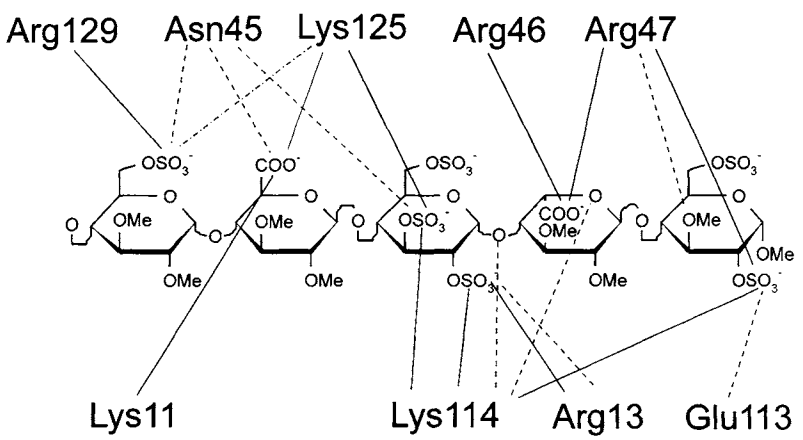

Figure 5 AT pentasaccharide interactions. The interactions between AT and a pentasaccharide mimetic are indicated by lines: solid lines indicate a salt-bridge, dashed lines H-bonds, and dashed-dotted lines water mediated H-bonds. Although several structures of AT bound to pentasaccharide mimetics have been published, the structure of the natural pentasaccharide has not. The interactions shown here are from the highest resolution AT–pentasaccharide structure solved to date, that of AT bound to the mimetic SR123781 (50). Residues from the N-terminal loop, and the A, D and P helices are making significant contacts, with the most important residue, Lys114, making more than any other.

residue is Lys114 (52,53), found on the loop just N-terminal to helix D, which is induced into a helical conformation through interaction with the pentasaccharide, and two other residues, Lys125 and Arg129, also contribute significantly to the energy of binding (54,55). It is interesting to note that the sum of energetic contributions of the three residues, Lys114, Lys125, and Arg129, is greater than the total free energy of binding, implying cooperativity. AT also has an N-terminal loop containing Lys11 and Arg13, which contacts the pentasaccharide and may serve a capping role (56). Of the eight-to-ten negatively charged groups on the pentasaccharide available for interaction with AT, six interact with AT; this is consistent with the number of ionic interactions inferred from the dependence of binding affinity on ionic strength (five-to-six) (57).

It had been established through biochemical studies that heparin binding induces a large-scale conformational change in AT (58–60), and this has subsequently been confirmed by crystallographic structures of native and pentasaccharide bound AT. The structure of native AT was published in 1994 (61,62), and the first structure of pentasaccharide-complexed AT in was published three years later (49). The heparin binding mechanism of AT is summarized in Fig. 6. AT binds the pentasaccharide by an induced-fit mechanism involving an initial weak interaction ($K_1 = \frac{k_{-1}}{k_1} \sim 25\,\mu M$), followed by a conformational change (k_2) to the high-affinity state, with an overall dissociation constant of ~50 nM (60). The structures of AT reveal conformational changes in the vicinity of the pentasaccharide and in other regions, indicating a global conformational change in response to heparin binding. In the heparin binding region, helix D is extended towards its C-terminus, a new helix P extends from its N-terminus, and helix A appears to extend towards its N-terminus. The global conformational change involves the expulsion of the RCL from β-sheet A, and the consequent closing of β-sheet A to the five-stranded form seen for other native serpin structures. The tertiary structure of AT is also altered by heparin binding, with a 10° rotation of helix D and the repositioning of the upper β-barrel domain relative to the lower helical domain [described in detail in (63)]. Just how local changes in the heparin binding region result in the expulsion of the RCL and the closure of sheet A is unclear. Molecular modelling (64) and biochemical studies (65,66) suggest a link between the C-terminal elongation of helix D and loop expulsion, and this has been supported by the recent crystal structure of AT in an intermediate pentasaccharide-bound conformation (51). Cleavage of the RCL of AT reverses the induced fit, causing a 1000-fold loss in affinity for the pentasaccharide (67,68). It is expected that such a mechanism would allow AT–protease complexes to be released from heparan sulfate for receptor-based clearance.

C. Acceleration of Protease Inhibition

Heparin acceleration of protease inhibition by AT involves two distinct mechanisms, depending on the targets involved (69). Pentasaccharide binding to AT is sufficient to accelerate the inhibition of factors IXa and Xa by 300–500-fold, and as the pentasaccharide binds only to AT and induces a conformational change, this mechanism of activation is considered allosteric. In contrast, activation of thrombin

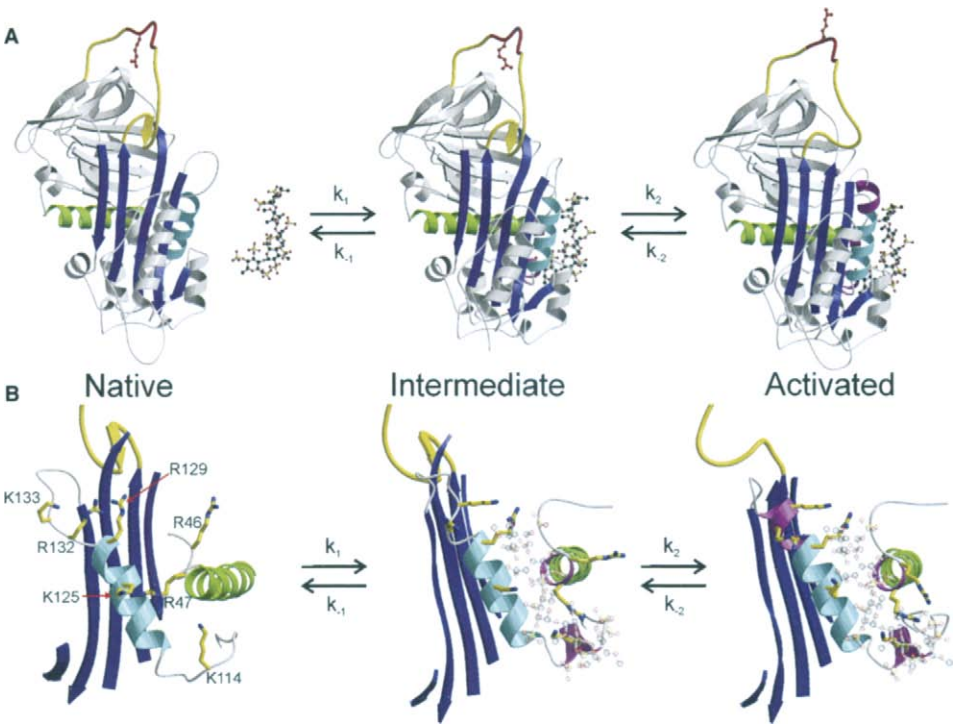

Figure 6 Pentasaccharide binding mechanism of AT. AT binds to the pentasaccharide via an induced-fit mechanism, where after the initial rapid formation of an intermediate complex, a conformational change to leads to tight binding. AT is coloured as before, and the pentasaccharide is shown in a ball-and-stick representation. The mechanism is shown here in the classic orientation (A) and as a close-up of the heparin binding site with only helices A, D, and P, β-sheet A and the RCL shown for clarity (B, the heparin binding residues are shown as yellow rods and the pentasaccharide is transparent). All three structures have been solved by X-ray crystallography. AT interacts weakly to form the intermediate complex, where the conformational changes are limited to the formation of helix P and the stabilisation/elongation of the N-terminus of helix A (all structural changes in the heparin binding region are coloured magenta). Expulsion of the RCL from β-sheet A and the C-terminal extension of helix D are coupled events, which lock AT in the high affinity state.

inhibition requires both AT and thrombin to bind to the same heparin chain [at least 18 monosaccharide units in length (70)], with heparin serving a bridging function. A schematic of the allosteric and bridging mechanisms is given in Fig. 7A. Although convenient to consider the two mechanisms as distinct, recent studies have demonstrated that in the presence of physiological levels of Ca^{2+} factor Xa (and IXa) inhibition is further accelerated through the addition of a bridging component to the allosteric mechanism (22,23). The molecular basis of improved protease recognition by AT in the presence of heparin is currently under investigation, and it has become clear that exosite contacts, outside the RCL of AT, are critical (72,73). Two crystal structures of AT in complex with inert thrombin and a synthetic heparin mimetic (SR123781) have recently been published (50,74). In the higher resolution structure by Li et al., electron density was observed for the entire heparin chain and revealed the expected thrombin–heparin interactions; it is thus considered more likely to represent the bridged complex (Fig. 7C). The position of thrombin relative to AT in the structure explains why the rate of thrombin inhibition is insensitive to the expulsion of the hinge region, as partial insertion of the hinge is observed. In contrast, heparin acceleration of factor IXa and Xa inhibition is completely dependent on the expulsion of the hinge region from β-sheet A (71), probably due to the requirement of exosite contacts towards the back of AT (75) (Fig. 7B).

IV. Heparin Cofactor II

A. Physiological Functions

Heparin cofactor II (HCII) circulates at a concentration comparable to that of AT and is a potent inhibitor of thrombin when activated by heparin (76), but its physiological functions are unclear. HCII deficiency has been found in patients with thrombotic disorders, but the frequency is similar to that found in the general population (77,78). Recent studies have established a link between HCII levels and restenosis after stent angioplasty (79,80) and risk for carotid atherosclerosis (81), and the properties of challenged HCII-deficient mice support a role of HCII in limiting arterial thrombus formation (82). Although HCII deficiency is not a significant risk factor for thrombosis, the high circulating levels (1.2 μM) and an ability to bind to and be activated by the GAGs suggests that it may add to the antithrombotic protection afforded by AT. HCII can be activated by GAGs other than heparin and appears to have some specificity for dermatan sulfate, indicating that dermatan sulfate may provide a potential alternative to heparin for the prevention and treatment of thrombosis (83,84). This is particularly true for clot-bound thrombin which is protected from inhibition by heparin activated AT, but is vulnerable to dermatan sulfate activated HCII (85). The fact that HCII binds to dermatan sulfate, which is found in the extravascular tissues, suggests functions unrelated to hemostasis, such as to providing protection from thrombin after tissue damage (86,87). Consistent with such a function is the observation that neutrophil proteases can cleave the N-terminus of HCII to produce a chemotactic peptide corresponding

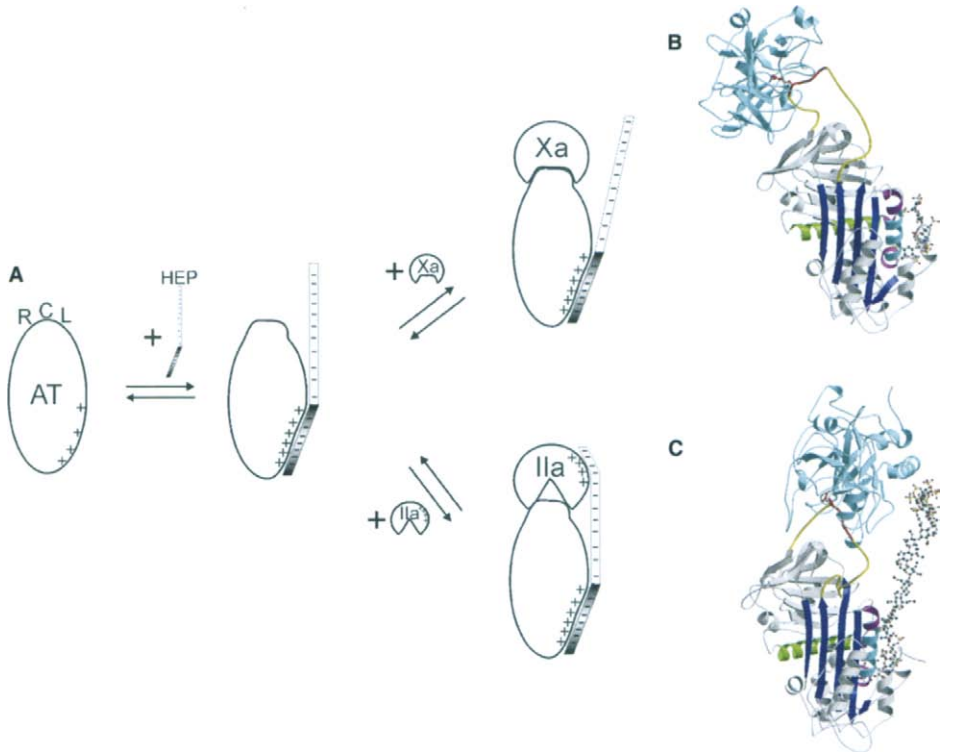

Figure 7 Heparin activation mechanism of AT. The heparin acceleration of AT inhibition of its three principal targets occurs by two distinct mechanisms, illustrated in the schematic (A). When heparin (HEP) binds to AT via the high affinity site (shaded) AT undergoes a conformational change, which alters the conformation of the RCL (see Fig. 6). The activated form is recognised better by factors IXa and Xa, but not by thrombin. Thus, inhibition of factors IXa and Xa is accelerated by an allosteric mechanism, where AT conformational change improves its ability form a Michaelis complex. Further acceleration can be achieved through a bridging mechanism in the presence of Ca^{2+}, and with heparin chains of at least 30 monosaccharide units in length. Acceleration of thrombin (IIa) inhibition, however, is fully dependent on the formation of a heparin bridged Michaelis complex. A model of the factor Xa (identical for IXa) Michaelis complex with AT, based on the thrombin–HCII complex, is given in panel (B). Recent work has demonstrated that the activating conformational change is the expulsion of the hinge region from β-sheet A (71), which allows the protease to interact at the back of AT. The crystal structure of the ternary AT–thrombin–heparin complex is shown in (C). It revealed why hinge region expulsion is not a part of the activation mechanism, as thrombin is oriented towards the front of AT and the RCL is partially inserted into β-sheet A. AT and proteases are coloured as before, with heparin in the ball-and-stick representation.

to residues 49–60 (88). HCII might thus serve a minor role as a circulating anticoagulant, but its main function may be found in the extravascular tissues.

B. Heparin Binding Mechanism

The heparin binding site of HCII is similar to that of AT, with the critical residues for the AT–pentasaccharide interaction conserved in HCII (Fig. 3). The predicted involvement of helix A and D residues in heparin binding to HCII (36) has been confirmed by mutagenesis studies (89–94). The apparent conservation of heparin binding residues is somewhat surprising, as AT and HCII have evolved independently (95,96), and because HCII is incapable of binding to the AT-specific pentasaccharide (97). Attempts to fractionate heparin according to HCII affinity have not resulted in the identification of a high affinity sequence akin to the AT-specific pentasaccharide (98–100), and although much effort has been made to fractionate other GAGs, no sequence with significantly greater affinity has ever been found (101). HCII binds heparin 1000-fold more weakly (97) (Kd = 26 μM) than does AT to heparin chains containing the specific pentasaccharide (102) (Kd = 20 nM), thus explaining why therapeutic heparin does not exert an appreciable HCII-mediated anticoagulant effect (70). A recent study has demonstrated that HCII binds heparin according to a non-specific binding model, where the apparent binding affinity is affected by heparin chain length and ionic strength in the predicted fashion (97). The minimal heparin length which fully occupies the binding site on HCII is 13 monosaccharide units; more than twice as long as the minimal AT-specific pentasaccharide. However, the minimal binding site size for AT is not known for heparin chains devoid of the pentasaccharide sequence (so-called 'low-affinity heparin'). Interestingly, the affinities of HCII and AT for low-affinity heparin are identical (Kd ~25 μM) (103). The recently solved structures of native and activated HCII suggested an unexpected similarity between the heparin activation mechanisms of AT and HCII (104). Native HCII possesses a partially inserted RCL, identical to native AT, and activated HCII has an expelled RCL, as does activated AT (Fig. 8A). The structure of native HCII also illustrates the similarity of the heparin binding sites, with important residues for the binding of heparin to AT spatially conserved in the structure of HCII (Fig. 8B). These observations combine to suggest an AT-like heparin binding mechanism for HCII, involving an initial weak interaction with heparin followed by a conformational change. The hallmark of such an induced-fit mechanism, the hyperbolic dependence of rate of heparin binding on heparin concentration (60), has recently been demonstrated for HCII (97). Thus, the heparin binding mechanism of HCII is fully analogous to that of AT, with the caveat that no specific HCII GAG sequence has yet been found, and that cleavage of the RCL does not appear to reduce the affinity of HCII for heparin (105).

C. Heparin Activation Mechanism

Unlike all other heparin binding serpins which have a P1 Arg residue, the reactive centre residue of HCII is a Leu, rendering it an inhibitor of the chymotrypsin-like serine proteases, not the trypsin-like proteases such as thrombin (106–108). Its

specificity for thrombin is conferred by an 80-residue N-terminal insertion loop which contains two cryptic hirudin-like repeats, PEGEEDDDY(SO_4) and IFSEDDDY(SO_4)IDI, that are somehow exposed by GAG binding (109). The improved heparin affinity of N-terminal variants (91,109,110) and the activating effect of heparin binding site mutations (111) support the hypothesis that the acidic N-terminal tail interacts with the basic heparin binding site of native HCII, and that the tail is released from its electrostatic interactions with the heparin binding site by competition of GAGs for the same site (76) (Fig. 9A). Unfortunately, the crystal structure of native HCII lacked electron density for the majority of the acidic tail, and thus its interaction with the body of HCII has not been determined. It is clear, however, that the tail does not fold into ordered structure, so that its interactions with the body of HCII will extend over a large surface area. The surface electrostatic representation of the body of HCII reveals a highly basic nature, which is not limited to the heparin binding site (75) (Fig. 4C). Thus, if electrostatic interactions are a critical part of the sequestration of the acidic tail onto the body of HCII, they need not be limited to the heparin binding site. There is also evidence that the tail may be somewhat mobile in native HCII (112). Wherever the tail is bound, the AT-like heparin binding mechanism of HCII suggests that a global conformational change is responsible for breaking the extended interactions between the acidic tail and the body of HCII (104). The structure of the Michaelis complex between HCII and thrombin further supports the mechanistic similarity to AT, and reveals the requirement of HCII conformational change and the contacts which confer thrombin specificity. A modified hypothesis for the heparin activation mechanism of HCII towards thrombin inhibition has been formulated on the basis of the crystal structures of HCII and the mechanistic similarity to AT (Fig. 9B). It differs from the original hypothesis (Fig. 9A) in that it is does not depend upon the direct displacement of the acidic tail by heparin binding, rather the tail is released from extended interactions by the global conformational change associated with heparin binding. The mechanism is thus fully allosteric, although, like the heparin activation of AT towards factors IXa and Xa, long GAG chains will further improve the rate of inhibition through the addition of a bridging element (111,113).

V. The Others

A. Plasminogen Activator Inhibitor-1

Plasminogen activator inhibitor-1 (PAI-1) is a plasma serpin, which circulates at very low (nM) concentrations (114). It is a typical serpin in its structure (115,116) and in its inhibitory promiscuity; PAI-1 inhibits all trypsin-like serine proteases with appreciable rates (with the exception of factor Xa) (6). The inclusion of PAI-1 in the heparin binding serpins is based on an ability to bind heparin Sepharose and the accelerating effect of heparin on the rate of thrombin inhibition (28,117). The physiological role of PAI-1, however, does not appear to involve thrombin inhibition, as elevated levels of PAI-1 are associated with thrombosis (118), and PAI-1

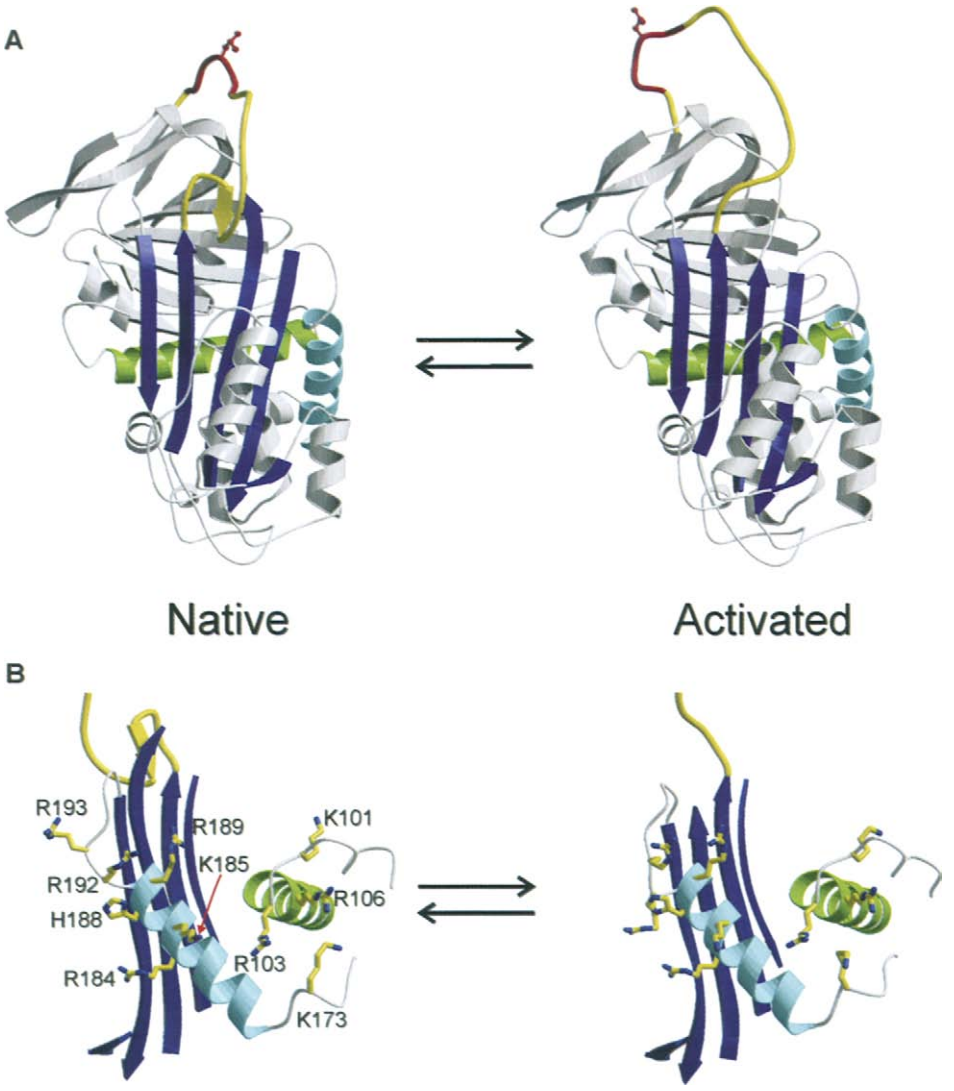

Figure 8 AT-like structural changes and heparin binding site of HCII. The crystal structures of native and activated HCII have been solved, revealing structural changes similar to those observed upon activation of AT. Native HCII has an inserted hinge region, which restrains the RCL, and activation releases the RCL to allow thrombin to dock towards the back of HCII (shown in Fig. 9). The structures are shown in the classic orientation in (A), and the heparin binding site is highlighted in (B) (as for AT in Fig. 7B). The residues involved in GAG binding are shown as rods, and although no conformational change is seen, the structure of activated HCII did not have heparin bound.

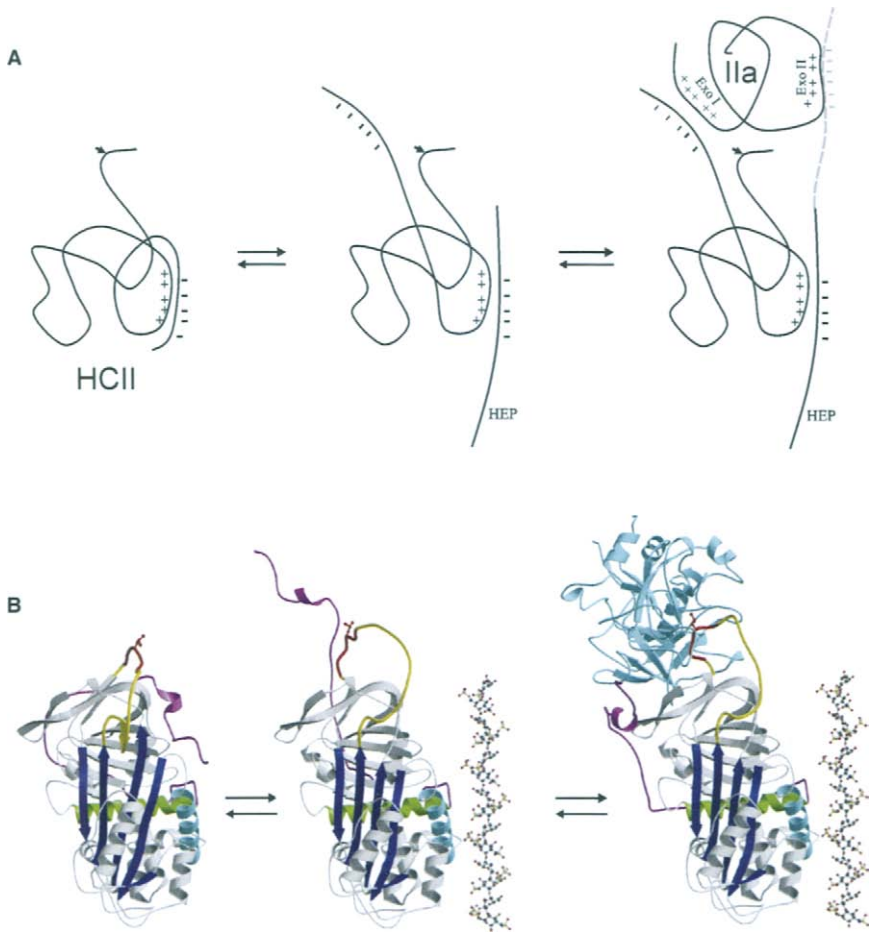

Figure 9 Heparin activation mechanism of HCII. A schematic of the originally proposed heparin activation mechanism of HCII (A) is contrasted to the mechanism based on HCII structures and analogy to AT (B). The original hypothesis was that the acidic N-terminal tail (negative charges) was sequestered through direct interaction with the heparin binding site (positive charges), and that heparin (HEP) displaced the tail through direct competition. The reactive centre (arrow) accessibility was not altered as part of this mechanism. The liberated acidic tail would be free to recruit thrombin (IIa) through interaction with exosite I (Exo I) followed by active site docking on the RCL of HCII. This mechanism was proposed to be primarily allosteric, but could be further enhanced through a heparin bridging component (grey heparin with exosite II of thrombin). The refined hypothesis (B) does not involve direct competition for the heparin binding site. The acidic tail (magenta) is proposed to interact in an extended manner with the body of HCII, and although it may be near the heparin binding site, it does not block it from binding to heparin. Rather, heparin binding would cause a conformational change in HCII, which would weaken its interaction with the tail. The released tail then recognises exosite I (as proposed previously) and is subsequently sandwiched between the top of HCII and thrombin (coloured as before). This mechanism is fully allosteric, and depends on the expulsion of the hinge region of the RCL for the global conformational change, which releases the tail, and allows the docking of thrombin towards the back of HCII.

deficiency causes bleeding (119). These effects support a primary physiological role of PAI-1 in fibrinolysis (120), with its principal targets being plasminogen activators, tPA and uPA, and plasmin (117,121). Although PAI-1 levels are very low in the circulation, the concentration near the blood clot is enhanced by its secretion from activated platelets as part the procoagulant/antifibrinolytic platelet function (122,123). Although potentially artifactual, thrombin inhibition by PAI-1 is accelerated by almost 100-fold in the presence of heparin chains of 14 monosaccharide units or greater in length (124). The heparin size dependency is consistent with acceleration through a bridging mechanism, analogous to that of AT.

The heparin binding site of PAI-1 is similar, but not identical, to that of AT. As shown in Fig. 3, PAI-1 has several basic amino acids along helix D and on the N-terminus of helix A. The importance of the helix D residues has been demonstrated by mutagenesis studies (125), but the two histidines preceding helix A have never been evaluated. Two residues on the adjacent helix E have also been implicated in heparin binding, Arg115 and Arg118 (126). Little is known about the details of the PAI-1 heparin interaction, but its elution from heparin Sepharose around 0.5 M NaCl suggests similar affinity as the other heparin binding serpins (127). The crystallographic structure of a stable variant of native PAI-1 revealed a typical serpin-fold (115,116), with no evidence of the partial RCL incorporation observed for AT and HCII, however, there is some evidence that wild-type PAI-1 may exist in an equilibrium between RCL inserted and expelled states (128).

B. Protease Nexin 1

Protease nexin 1 (PN1, also known as glia-derived nexin) is a serpin with multiple functions and targets. It is expressed in several cell types, such as fibroblasts, glial cells and platelets, but is not secreted by the liver, and thus does not circulate in the plasma as do the other heparin binding serpins (129–131). Rather, PN1 is found bound to cell surfaces and extracellular matrix components, where it functions to regulate wound healing (132–136), neurite outgrowth (137), and possibly platelet activation (130). Consistent with these functions, its major targets appear to be uPA (138), plasmin (138), thrombin (139), and factor XIa (31). As with all serpins with an Arg at the reactive centre position, PN1 inhibits all trypsin-like serine proteases, making it difficult to determine its physiological targets. However, PN1 is definitely a physiological inhibitor of thrombin for many of its proposed physiological functions. Thrombin inhibition by PN1 is extremely rapid, and in the presence of heparin, is about 10 times faster than heparin activated AT. Inhibition of thrombin, factors Xa and XIa, and trypsin (among others) is accelerated in the presence of heparin, but inhibition of plasmin is not (30). Acceleration is presumably through a template mechanism, similar to that of AT and thrombin, due to the dependence on heparin chain length (30), and to the bell-shaped dependence of inhibition rate on heparin concentration (29).

The heparin binding site of PN1 is homologous to that of AT, with several basic residues aligned on the same face of helix D (Fig. 3). A single His residue is found N-terminal to helix A, but is unlikely to contribute significantly to heparin

binding. The heparin affinity of PN1 is similar to that of AT ($Kd = 20$ nM) (140), but without any apparent sequence specificity (139,141). The structure of native PN1 is unknown, but it may resemble that of native AT, based on a similar high affinity for heparin and the apparent allosteric activation towards trypsin inhibition, similar to the pentasaccharide acceleration of AT inhibition of thrombin and trypsin (2–7-fold). If the native conformation of PN1 were similar to that of AT, then it would follow that the mechanism of heparin binding would involve the expulsion of the hinge region as part of an induced-fit mechanism. An argument against such analogy between PN1 and AT heparin binding mechanisms is that RCL-cleaved PN1 appears to bind to heparin with the same affinity as intact PN1 (by elution from heparin Sepharose) (30); whereas the affinity of AT for heparin is reduced by 1000-fold upon cleavage of the RCL. However, the affinity of AT for low-affinity heparin is independent of RCL cleavage, and this may represent a better comparison to PN1 where no specific sequence has been identified.

C. Protein C Inhibitor

Protein C inhibitor (also known as PAI-3) is found in many tissues and fluids, including blood, urine, seminal plasma, etc., and has several possible physiological roles (142–144). In blood plasma, PCI functions as a procoagulant by inhibiting activated protein C (APC) (145) and the thrombin–thrombomodulin complex (146,147). Increased PCI levels have been associated with venous and arterial thrombosis, and high-circulating concentrations of the PCI–APC complex is a marker for thrombotic states (148–151). The highest concentrations of PCI are found in the reproductive tract where it inhibits prostate specific antigen, acrosin, tPA and uPA, and plays a role in spermatozoid development and storage (152,153). Mice do not express PCI in the liver, and consequently have no circulating PCI (154). Thus, the PCI knockout mouse does not possess the otherwise expected bleeding phenotype; rather the fertility of the male knockout mouse is reduced, due to impaired spermatogenesis and a sperm storage disorder (155). As for the other heparin binding serpins, heparin acceleration of protease inhibition by PCI involves heparin binding to both the protease and PCI, thus implying a bridging mechanism. In addition to the accelerating effect of heparin on PCI, heparin binding to PCI also alters inhibitory specificity by blocking the inhibition of tissue kallikrein (34). Thus, heparin can regulate the activity of PCI by favouring and disfavouring certain targets. Although PCI inhibits trypsin-like serine proteases due to the Arg at the reactive centre position, the Trp at P2 can also be employed as a reactive centre by chymotrypsin-like proteases (32). The functional significance of the dual reactive centres of PCI is unknown.

PCI binds heparin with moderate affinity, based on its elution from heparin Sepharose at 0.5 M NaCl (156). Unlike all other heparin binding serpins, the heparin binding site of PCI is not found on helix D. Based on a molecular model of PCI constructed on the cleaved α_1-antitrypsin structure, the heparin binding site was proposed to be comprised of helix H and a predicted helical portion of the N-terminal loop, termed helix A+ (157). Subsequent mutagenesis studies have confirmed the role

of helix H in heparin binding (158,159), but conflicting reports have been published on the importance of the A+ helix. Although monoclonal antibody binding to the A+ helix abrogates heparin binding and activation (157), mutations in the region have no effect (160). A recent structure of RCL cleaved PCI (161) has led to a refinement of the hypothesised heparin binding site, which includes residues on and contiguous with helix H, nearby residues on other secondary structural elements (Arg229, Arg234, and Arg362), and two Arg residues on the N-terminus of helix A (Arg26 and Arg27) (Fig. 10A and B). A heparin binding site adjacent to helix H, as opposed to helix D, has the potential to directly influence the initial interaction between PCI and proteases, as it is located at the top of the serpin. Such a mechanism is consistent with the ability of short heparin chains, roughly seven monosaccharide units in length, to appreciably accelerate the inhibition of APC (162). As with other heparin binding serpins, a significant acceleration effect is provided by the one-dimensional diffusion of protease and inhibitor along the heparin chain, but the ability of short chains to accelerate protease inhibition and the accelerated inhibition of non-heparin binding proteases are an indication that an additional mechanism is at work. In the case of AT and HCII (and maybe PN1), global conformational change upon heparin binding results in improved accessibility of the RCL through hinge region expulsion. This is unlikely for PCI. Rather, the binding of heparin near helix H will alter the properties of the protease docking site to either favour or disfavour the formation of a Michaelis complex (161). The proposed heparin activation mechanism of PCI is given in Fig. 10C.

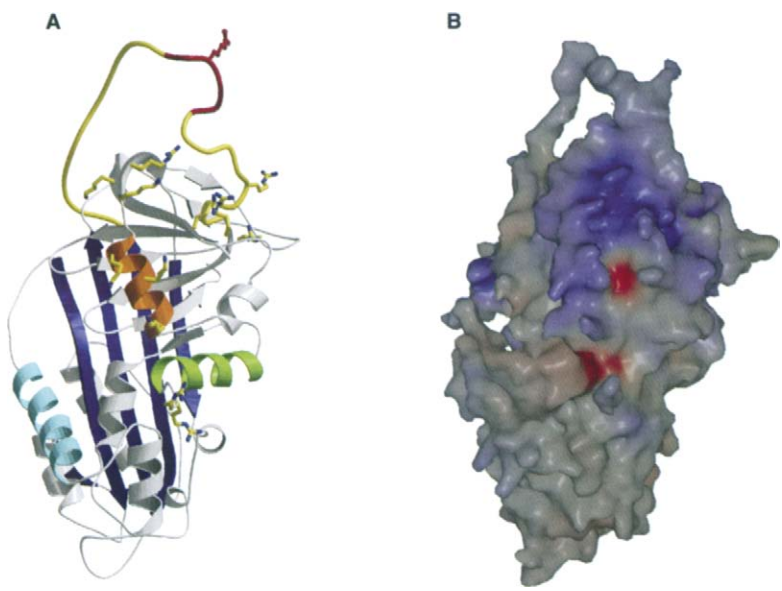

Figure 10 Proposed heparin binding site and activation mechanism of PCI. (A) A model of native PCI (coloured as in Fig. 1A) based on the structure of RCL cleaved PCI is rotated 140° from the classic orientation to show the proposed heparin binding site. The basic residues in the site are shown as rods, and their contribution to the surface electrostatics is shown in (B). It is clear that helix H is only a small part of the basic site, with other residues much closer to the RCL involved. *(Continued on next page.)*

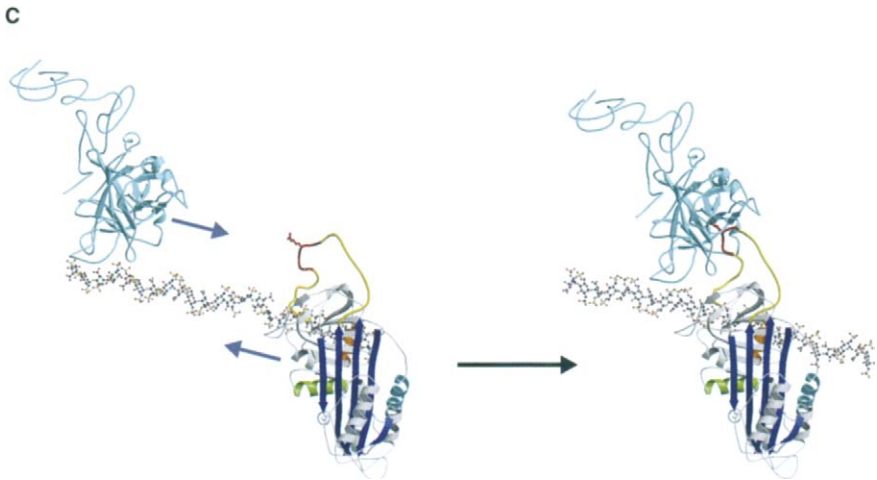

Figure 10 Cont'd The mechanism of heparin activation (C) would involve rapid translocation of both PCI and APC (cyan, with EGF domains as a coil) to a single shared heparin site. The binding of heparin would thus accelerate the formation of the encounter complex, but also stabilise the Michaelis complex by providing a shared exosite interface.

VI. Conclusions

Heparin is not the physiological activator of any of the human heparin binding serpins, but serves only as a convenient model for the GAGs found in the vascular and extravascular spaces. These include heparan sulfate, chondroitin sulfate, dermatan sulfate, hyaluronan, and karatan sulfate, which differ in saccharide linkage and sulfation, but are all linear polysaccharides decorating the proteoglycans attached to the surface of cells or secreted into the extracellular matrix. It is thus unsurprising that, with the exception of AT, the so-called heparin binding serpins do not bind to heparin with any apparent specificity. In fact, the only exquisitely specific interaction between heparin and a heparin binding *protein is that of AT binding to its pentasaccharide sequence. The AT–pentasaccharide interaction illustrates the potential for GAG binding specificity, and provides a useful starting point for the evaluation of other serpin activation mechanisms.*

Acknowledgments

I would like to acknowledge the support of the Medical Research Council and the British Heart Foundation (UK).

References

1. Silverman GA, Bird PI, Carrell RW, Church FC, Coughlin PB, Gettins PGW, Irving JA, Lomas DA, Luke CJ, Moyer RW, Pemberton PA, Remold-O'Donnell E, Salvesen GS, Travis J, Whisstock JC. The serpins are an

expanding superfamily of structurally similar but functionally diverse proteins. J Biol Chem 2001; 276:33293–33296.
2. Gettins PG. Serpin structure, mechanism, and function. Chem Rev 2002; 102:4751–4804.
3. Rawlings ND, Tolle DP, Barrett AJ. MEROPS: the peptidase database. Nucleic Acids Res 2004; 32:D160–D164.
4. Barrett AJ, Salvesen G., eds. Protease Inhibitors. Amsterdam: Elsevier, 1986.
5. Huntington JA, Carrell RW. The serpins: nature's molecular mousetraps. Sci Prog 2001; 84:125–136.
6. Gettins PGW, Patston PA, Olson ST. Serpins: Structure, Function and Biology. Austin, TX: R.G. Landes Co., 1996.
7. Hunt LT, Dayhoff MO. A surprising new protein superfamily containing ovalbumin, antithrombin-III, and alpha 1-proteinase inhibitor. Biochem Biophys Res Commun 1980; 95:864–871.
8. Irving JA, Steenbakkers PJ, Lesk AM, Op dCH, Pike RN, Whisstock JC. Serpins in prokaryotes. Mol Biol Evol 2002; 19:1881–1890.
9. Bird PI. Serpins and regulation of cell death. Results Probl Cell Differ 1998; 24:63–89.
10. Carrell RW, Evans DL, Stein PE. Mobile reactive centre of serpins and the control of thrombosis [published erratum appears in Nature 1993; 364 (6439):737]. Nature 1991; 353:576–578.
11. Mottonen J, Strand A, Symersky J, Sweet RM, Danley DE, Geoghegan KF, Gerard RD, Goldsmith EJ. Structural basis of latency in plasminogen activator inhibitor-1. Nature 1992; 355:270–273.
12. Zhou A, Huntington JA, Carrell RW. Formation of the antithrombin heterodimer In vivo and the onset of thrombosis. Blood 1999; 94:3388–3396.
13. Schechter I, Berger A. On the size of the active site in proteases. I. Papain. Biochem Biophys Res Commun 1967; 27:157–162.
14. Esnouf RM. An extensively modified version of MolScript that includes greatly enhanced coloring capabilities. J Mol Graph Modell 1997; 15:132.
15. Merritt EA, Murphy MEP. Raster3d version-2.0 – a program for photorealistic molecular graphics. Acta Crystalogr 1994; D50:869–873.
16. Olson ST, Swanson R, Day D, Verhamme I, Kvassman J, Shore JD. Resolution of Michaelis complex, acylation, and conformational change steps in the reactions of the serpin, plasminogen activator inhibitor-1, with tissue plasminogen activator and trypsin. Biochemistry 2001; 40:11742–11756.
17. Ye S, Chech AL, Belmares R, Bergstrom RC, Tong Y, Corey DR, Kanost MR, Goldsmith EJ. The structure of a Michaelis serpin–protease complex. Nat Struct Biol 2001; 8:979–983.
18. Huntington JA, Read RJ, Carrell RW. Structure of a serpin–protease complex shows inhibition by deformation. Nature 2000; 407:923–926.
19. Kaslik G, Patthy A, Balint M, Graf L. Trypsin complexed with alpha 1-proteinase inhibitor has an increased structural flexibility. FEBS Lett 1995; 370:179–183.
20. Stavridi ES, O'Malley K, Lukacs CM, Moore WT, Lambris JD, Christianson DW, Rubin H, Cooperman BS. Structural change in alpha-chymotrypsin induced by complexation with alpha 1-antichymotrypsin as seen by enhanced sensitivity to proteolysis. Biochemistry 1996; 35:10608–10615.

21. Peterson FC, Gettins PG. Insight into the mechanism of serpin–proteinase inhibition from 2D [1H-15N] NMR studies of the 69 kDa alpha 1-proteinase inhibitor Pittsburgh-trypsin covalent complex. Biochemistry 2001; 40:6284–6292.
22. Bedsted T, Swanson R, Chuang YJ, Bock PE, Bjork I, Olson ST. Heparin and calcium ions dramatically enhance antithrombin reactivity with factor IXa by generating new interaction exosites. Biochemistry 2003; 42:8143–8152.
23. Rezaie AR, Olson ST. Calcium enhances heparin catalysis of the antithrombin-factor Xa reaction by promoting the assembly of an intermediate heparin–antithrombin-factor Xa bridging complex. Demonstration by rapid kinetics studies. Biochemistry 2000; 39:12083–12090.
24. Danielsson A, Bjork I. Mechanism of inactivation of trypsin by antithrombin. Biochem J 1982; 207:21–28.
25. Chuang YJ, Swanson R, Raja SM, Bock SC, Olson ST. The antithrombin P1 residue is important for target proteinase specificity but not for heparin activation of the serpin. Characterization of P1 antithrombin variants with altered proteinase specificity but normal heparin activation. Biochemistry 2001; 40:6670–6679.
26. Derechin VM, Blinder MA, Tollefsen DM. Substitution of arginine for Leu444 in the reactive site of heparin cofactor II enhances the rate of thrombin inhibition. J Biol Chem 1990; 265:5623–5628.
27. Verhamme IM, Bock PE, Jackson CM. The preferred pathway of glycosaminoglycan-accelerated inactivation of thrombin by heparin cofactor II. J Biol Chem 2004; 279:9785–9795.
28. Rezaie AR. Role of exosites 1 and 2 in thrombin reaction with plasminogen activator inhibitor-1 in the absence and presence of cofactors. Biochemistry 1999; 38:14592–14599.
29. Wallace A, Rovelli G, Hofsteenge J, Stone SR. Effect of heparin on the glia-derived-nexin-thrombin interaction. Biochem J 1989; 257:191–196.
30. Evans DL, McGrogan M, Scott RW, Carrell RW. Protease specificity and heparin binding and activation of recombinant protease nexin I. J Biol Chem 1991; 266:22307–22312.
31. Knauer DJ, Majumdar D, Fong PC, Knauer MF. SERPIN regulation of factor XIa. The novel observation that protease nexin 1 in the presence of heparin is a more potent inhibitor of factor XIa than C1 inhibitor. J Biol Chem 2000; 275:37340–37346.
32. Pratt CW, Church FC. Heparin binding to protein C inhibitor. J Biol Chem 1992; 267:8789–8794.
33. Hermans JM, Jones R, Stone SR. Rapid inhibition of the sperm protease acrosin by protein C inhibitor. Biochemistry 1994; 33:5440–5444.
34. Ecke S, Geiger M, Resch I, Jerabek I, Sting L, Maier M, Binder BR. Inhibition of tissue kallikrein by protein C inhibitor. Evidence for identity of protein C inhibitor with the kallikrein binding protein. J Biol Chem 1992; 267:7048–7052.
35. Loebermann H, Tokuoka R, Deisenhofer J, Huber R. Human alpha 1-proteinase inhibitor. Crystal structure analysis of two crystal modifications, molecular model and preliminary analysis of the implications for function. J Mol Biol 1984; 177:531–557.

36. Huber R, Carrell RW. Implications of the three-dimensional structure of alpha 1-antitrypsin for structure and function of serpins. Biochemistry 1989; 28:8951–8966.
37. Bjork I, Olson ST. Antithrombin. A bloody important serpin. Adv Exp Med Biol 1997; 425:17–33.
38. Hirsh J. Blood tests for the diagnosis of venous and arterial thrombosis. Blood 1981; 57:1–8.
39. Kojima T. Targeted gene disruption of natural anticoagulant proteins in mice. Int J Hematol 2002; 76 (Suppl 2):36–39.
40. Desai UR. New antithrombin-based anticoagulants. Med Res Rev 2004; 24:151–181.
41. Sie P, Ofosu F, Fernandez F, Buchanan MR, Petitou M, Boneu B. Respective role of antithrombin III and heparin cofactor II in the in vitro anticoagulant effect of heparin and of various sulphated polysaccharides. Br J Haematol 1986; 64:707–714.
42. Casu B, Lindahl U. Structure and biological interactions of heparin and heparan sulfate. Adv Carbohydr Chem Biochem 2001; 57:159–206.
43. Esko JD, Selleck SB. Order out of chaos: assembly of ligand binding sites in heparan sulfate. Annu Rev Biochem 1905; 71:435–471.
44. Lindahl U, Thunberg L, Backstrom G, Riesenfeld J. The antithrombin-binding sequence of heparin. Biochem Soc Trans 1981; 9:499–51.
45. Casu B, Oreste P, Torri G, Zoppetti G, Choay J, Lormeau JC, Petitou M, Sinay P. The structure of heparin oligosaccharide fragments with high anti-(factor Xa) activity containing the minimal antithrombin III-binding sequence. Chemical and 13C nuclear-magnetic-resonance studies. Biochem J 1981; 197:599–609.
46. Petitou M, Casu B, Lindahl U. 1976–1983, a critical period in the history of heparin: the discovery of the antithrombin binding site. Biochimie 2003; 85:83–89.
47. Borg JY, Owen MC, Soria C, Soria J, Caen J, Carrell RW. Proposed heparin binding site in antithrombin based on arginine 47. A new variant Rouen-II, 47 Arg to Ser. J Clin Invest 1988; 81:1292–1296.
48. Olson ST, Bjork I, Bock SC. Identification of critical molecular interactions mediating heparin activation of antithrombin: implications for the design of improved heparin anticoagulants. Trends Cardiovasc Med 2002; 12:198–205.
49. Jin L, Abrahams JP, Skinner R, Petitou M, Pike RN, Carrell RW. The anticoagulant activation of antithrombin by heparin. Proc Natl Acad Sci USA 1997; 94:14683–14688.
50. Li W, Johnson DJ, Esmon CT, Huntington JA. Structure of the antithrombin–thrombin–heparin ternary complex reveals the antithrombotic mechanism of heparin. Nat Struct Mol Biol 2004; 11:857–862.
51. Johnson DJ, Huntington JA. Crystal structure of antithrombin in a heparin-bound intermediate state. Biochemistry 2003; 42:8712–8719.
52. Arocas V, Bock SC, Raja S, Olson ST, Bjork I. Lysine 114 of antithrombin is of crucial importance for the affinity and kinetics of heparin pentasaccharide binding. J Biol Chem 2001; 276:43809–43817.

53. Mushunje A, Zhou A, Huntington JA, Conard J, Carrell RW. Antithrombin 'DREUX' (Lys 114Glu): a variant with complete loss of heparin affinity. Thromb Haemost 2002; 88:436–443.
54. Desai U, Swanson R, Bock SC, Bjork I, Olson ST. Role of arginine 129 in heparin binding and activation of antithrombin. J Biol Chem 2000; 275: 18976–18984.
55. Schedin-Weiss S, Desai UR, Bock SC, Gettins PG, Olson ST, Bjork I. Importance of lysine 125 for heparin binding and activation of antithrombin. Biochemistry 2002; 41:4779–4788.
56. Schedin-Weiss S, Desai UR, Bock SC, Olson ST, Bjork I. Roles of N-terminal region residues Lys11, Arg13, and Arg24 of antithrombin in heparin recognition and in promotion and stabilization of the heparin-induced conformational change. Biochemistry 2004; 43:675–683.
57. Nordenman B, Bjork I. Influence of ionic strength and pH on the interaction between high-affinity heparin and antithrombin. Biochim Biophys Acta 1981; 672:227–238.
58. Nordenman B, Bjork I. Binding of low-affinity and high-affinity heparin to antithrombin. Ultraviolet difference spectroscopy and circular dichroism studies. Biochemistry 1978; 17:3339–3344.
59. Olson ST, Shore JD. Binding of high affinity heparin to antithrombin III. Characterization of the protein fluorescence enhancement. J Biol Chem 1981; 256:11065–11072.
60. Olson ST, Srinivasan KR, Bjork I, Shore JD. Binding of high affinity heparin to antithrombin III. Stopped flow kinetic studies of the binding interaction. J Biol Chem 1981; 256:11073–11079.
61. Carrell RW, Stein PE, Fermi G, Wardell MR. Biological implications of a 3A structure of dimeric antithrombin. Structure 1994; 2:257–270.
62. Schreuder HA, de Boer B, Dijkema R, Mulders J, Theunissen HJ, Grootenhuis PD, Hol WG. The intact and cleaved human antithrombin III complex as a model for serpin–proteinase interactions. Nat Struct Biol 1994; 1:48–54.
63. Whisstock JC, Pike RN, Jin L, Skinner R, Pei XY, Carrell RW, Lesk AM. Conformational changes in serpins. II. The mechanism of activation of antithrombin by heparindagger. J Mol Biol 2000; 301:1287–1305.
64. van Boeckel CA, Grootenhuis PD, Visser A. A mechanism for heparin-induced potentiation of antithrombin III. Nat Struct Biol 1994; 1:423–425.
65. Meagher JL, Olson ST, Gettins PG. Critical role of the linker region between helix D and strand 2A in heparin activation of antithrombin. J Biol Chem 2000; 275:2698–2704.
66. Belzar KJ, Zhou A, Carrell RW, Gettins PG, Huntington JA. Helix D elongation and allosteric activation of antithrombin. J Biol Chem 2002; 277:8551–8558.
67. Bjork I, Fish WW. Production in vitro and properties of a modified form of bovine antithrombin, cleaved at the active site by thrombin. J Biol Chem 1982; 257:9487–9493.
68. Skinner R, Chang WS, Jin L, Pei X, Huntington JA, Abrahams JP, Carrell RW, Lomas DA. Implications for function and therapy of a 2.9A structure of binary-complexed antithrombin. J Mol Biol 1998; 283:9–14.

69. Olson ST, Bjork I. Role of protein conformational changes, surface approximation and protein cofactors in heparin-accelerated antithrombin–proteinase reactions. Adv Exp Med Biol 1992; 313:155–165.
70. Bray B, Lane DA, Freyssinet JM, Pejler G, Lindahl U. Anti-thrombin activities of heparin. Effect of saccharide chain length on thrombin inhibition by heparin cofactor II and by antithrombin. Biochem J 1989; 262:225–232.
71. Langdown J, Johnson DJ, Baglin TP, Huntington JA. Allosteric activation of antithrombin critically depends upon hinge region extension. J Biol Chem 2004; 279:47288–47297.
72. Izaguirre G, Zhang W, Swanson R, Bedsted T, Olson ST. Localization of an antithrombin exosite that promotes rapid inhibition of factors Xa and IXa dependent on heparin activation of the serpin. J Biol Chem 2003; 278:51433–51440.
73. Olson ST, Chuang YJ. Heparin activates antithrombin anticoagulant function by generating new interaction sites (exosites) for blood clotting proteinases. Trends Cardiovasc Med 2002; 12:331–338.
74. Dementiev A, Petitou M, Herbert JM, Gettins PG. The ternary complex of antithrombin–anhydrothrombin–heparin reveals the basis of inhibitor specificity. Nat Struct Mol Biol 2004; 11:863–867.
75. Huntington JA. Mechanisms of glycosaminoglycan activation of the serpins in hemostasis. J Thromb Haemost 2003; 1:1535–1549.
76. Tollefsen DM. Heparin cofactor II. Adv Exp Med Biol 1997; 425:35–44.
77. Andersson TR, Larsen ML, Handeland GF, Abildgaard U. Heparin cofactor II activity in plasma: application of an automated assay method to the study of a normal adult population. Scand J Haematol 1986; 36:96–102.
78. Bertina RM, van dL I, Engesser L, Muller HP, Brommer EJ. Hereditary heparin cofactor II deficiency and the risk of development of thrombosis. Thromb Haemost 1987; 57:196–200.
79. Schillinger M, Exner M, Sabeti S, Mlekusch W, Amighi J, Handler S, Quehenberger P, Kalifeh N, Wagner O, Minar E. High plasma heparin cofactor II activity protects from restenosis after femoropopliteal stenting. Thromb Haemost 2004; 92:1108–1113.
80. Takamori N, Azuma H, Kato M, Hashizume S, Aihara K, Akaike M, Tamura K, Matsumoto T. High plasma heparin cofactor II activity is associated with reduced incidence of in-stent restenosis after percutaneous coronary intervention. Circulation 2004; 109:481–486.
81. Aihara K, Azuma H, Takamori N, Kanagawa Y, Akaike M, Fujimura M, Yoshida T, Hashizume S, Kato M, Yamaguchi H, Kato S, Ikeda Y, Arase T, Kondo A, Matsumoto T. Heparin cofactor II is a novel protective factor against carotid atherosclerosis in elderly individuals. Circulation 2004; 109:2761–2765.
82. He L, Vicente CP, Westrick RJ, Eitzman DT, Tollefsen DM. Heparin cofactor II inhibits arterial thrombosis after endothelial injury. J Clin Invest 2002; 109:213–219.
83. Fernandez F, Van Ryn J, Ofosu FA, Hirsh J, Buchanan MR. The haemorrhagic and antithrombotic effects of dermatan sulphate. Br J Haematol 1986; 64:309–317.

84. Carrie D, Caranobe C, Gabaig AM, Larroche M, Boneu B. Effects of heparin, dermatan sulfate and of their association on the inhibition of venous thrombosis growth in the rabbit. Thromb Haemost 1992; 68:637–641.
85. Liaw PC, Becker DL, Stafford AR, Fredenburgh JC, Weitz JI. Molecular basis for the susceptibility of fibrin-bound thrombin to inactivation by heparin cofactor ii in the presence of dermatan sulfate but not heparin. J Biol Chem 2001; 276:20959–20965.
86. McGuire EA, Tollefsen DM. Activation of heparin cofactor II by fibroblasts and vascular smooth muscle cells. J Biol Chem 1987; 262:169–175.
87. Whinna HC, Choi HU, Rosenberg LC, Church FC. Interaction of heparin cofactor II with biglycan and decorin. J Biol Chem 1993; 268:3920–3924.
88. Church FC, Pratt CW, Hoffman M. Leukocyte chemoattractant peptides from the serpin heparin cofactor II. J Biol Chem 1991; 266:704–709.
89. Hayakawa Y, Hirashima Y, Kurimoto M, Hayashi N, Hamada H, Kuwayama N, Endo S. Contribution of basic residues of the A helix of heparin cofactor II to heparin- or dermatan sulfate-mediated thrombin inhibition. FEBS Lett 2002; 522:147–150.
90. Blinder MA, Tollefsen DM. Site-directed mutagenesis of arginine 103 and lysine 185 in the proposed glycosaminoglycan-binding site of heparin cofactor II. J Biol Chem 1990; 265:286–291.
91. Ragg H, Ulshofer T, Gerewitz J. On the activation of human leuserpin-2, a thrombin inhibitor, by glycosaminoglycans. J Biol Chem 1990; 265:5211–5218.
92. Blinder MA, Andersson TR, Abildgaard U, Tollefsen DM. Heparin cofactor II Oslo. Mutation of Arg-189 to His decreases the affinity for dermatan sulfate. J Biol Chem 1989; 264:5128–5133.
93. Whinna HC, Blinder MA, Szewczyk M, Tollefsen DM, Church FC. Role of lysine 173 in heparin binding to heparin cofactor II. J Biol Chem 1991; 266:8129–8135.
94. Colwell NS, Grupe MJ, Tollefsen DM. Amino acid residues of heparin cofactor II required for stimulation of thrombin inhibition by sulphated polyanions. Biochim Biophys Acta 1999; 1431:148–156.
95. Atchley WR, Lokot T, Wollenberg K, Dress A, Ragg H. Phylogenetic analyses of amino acid variation in the serpin proteins. Mol Biol Evol 2001; 18:1502–1511.
96. Ragg H, Lokot T, Kamp PB, Atchley WR, Dress A. Vertebrate serpins: construction of a conflict-free phylogeny by combining exon–intron and diagnostic site analyses. Mol Biol Evol 2001; 18:577–584.
97. O'Keeffe D, Olson ST, Gasiunas N, Gallagher J, Baglin TP, Huntington JA. The heparin binding properties of heparin cofactor II suggest an antithrombin-like activation mechanism. J Biol Chem 2004; 279:50267–50273.
98. Petitou M, Lormeau JC, Perly B, Berthault P, Bossennec V, Sie P, Choay J. Is there a unique sequence in heparin for interaction with heparin cofactor II? Structural and biological studies of heparin-derived oligosaccharides. J Biol Chem 1988; 263:8685–8690.
99. Sie P, Petitou M, Lormeau JC, Dupouy D, Boneu B, Choay J. Studies on the structural requirements of heparin for the catalysis of thrombin inhibition by heparin cofactor II. Biochim Biophys Acta 1988; 966:188–195.
100. Hurst RE, Poon MC, Griffith MJ. Structure–activity relationships of heparin. Independence of heparin charge density and antithrombin-binding domains

in thrombin inhibition by antithrombin and heparin cofactor II. J Clin Invest 1983; 72:1042–1045.
101. Maimone MM, Tollefsen DM. Structure of a dermatan sulfate hexasaccharide that binds to heparin cofactor II with high affinity [published erratum appears in J Biol Chem 1991; 266 (22):14830]. J Biol Chem 1990; 265:18263–18271.
102. Turk B, Brieditis I, Bock SC, Olson ST, Bjork I. The oligosaccharide side chain on Asn-135 of alpha-antithrombin, absent in beta-antithrombin, decreases the heparin affinity of the inhibitor by affecting the heparin-induced conformational change. Biochemistry 1997; 36:6682–6691.
103. Streusand VJ, Bjork I, Gettins PG, Petitou M, Olson ST. Mechanism of acceleration of antithrombin–proteinase reactions by low affinity heparin. Role of the antithrombin binding pentasaccharide in heparin rate enhancement. J Biol Chem 1995; 270:9043–9051.
104. Baglin TP, Carrell RW, Church FC, Esmon CT, Huntington JA. Crystal structures of native and thrombin-complexed heparin cofactor II reveal a multistep allosteric mechanism. Proc Natl Acad Sci USA 2002; 99: 11079–11084.
105. Maekawa H, Sato H, Tollefsen DM. Thrombin inhibition by HCII in the presence of elastase-cleaved HCII and thrombin–HCII complex. Thromb Res 2000; 100:443–451.
106. Griffith MJ, Noyes CM, Tyndall JA, Church FC. Structural evidence for leucine at the reactive site of heparin cofactor II. Biochemistry 1985; 24:6777–6782.
107. Church FC, Noyes CM, Griffith MJ. Inhibition of chymotrypsin by heparin cofactor II. Proc Natl Acad Sci USA 1985; 82:6431–6434.
108. Pratt CW, Tobin RB, Church FC. Interaction of heparin cofactor II with neutrophil elastase and cathepsin G. J Biol Chem 1990; 265:6092–6097.
109. Van DV, Tollefsen DM. The N-terminal acidic domain of heparin cofactor II mediates the inhibition of alpha-thrombin in the presence of glycosaminoglycans. J Biol Chem 1991; 266:20223–20231.
110. Ragg H, Ulshofer T, Gerewitz J. Glycosaminoglycan-mediated leuserpin-2/thrombin interaction. Structure–function relationships. J Biol Chem 1990; 265:22386–22391.
111. Liaw PC, Austin RC, Fredenburgh JC, Stafford AR, Weitz JI. Comparison of heparin- and dermatan sulfate-mediated catalysis of thrombin inactivation by heparin cofactor II. J Biol Chem 1999; 274:27597–27604.
112. Brinkmeyer S, Eckert R, Ragg H. Reformable intramolecular cross-linking of the N-terminal domain of heparin cofactor II: effects on enzyme inhibition. Eur J Biochem 2004; 271:4275–4283.
113. Sheehan JP, Tollefsen DM, Sadler JE. Heparin cofactor II is regulated allosterically and not primarily by template effects. Studies with mutant thrombins and glycosaminoglycans. J Biol Chem 1994; 269:32747–32751.
114. Juhan-Vague I, Moerman B, De Cock F, Aillaud MF, Collen D. Plasma levels of a specific inhibitor of tissue-type plasminogen activator (and urokinase) in normal and pathological conditions. Thromb Res 1984; 33:523–530.
115. Sharp AM, Stein PE, Pannu NS, Carrell RW, Berkenpas MB, Ginsburg D, Lawrence DA, Read RJ. The active conformation of plasminogen activator inhibitor 1, a target for drugs to control fibrinolysis and cell adhesion. Struct Fold Design 1999; 7:111–118.

116. Nar H, Bauer M, Stassen JM, Lang D, Gils A, Declerck PJ. Plasminogen activator inhibitor 1. Structure of the native serpin, comparison to its other conformers and implications for serpin inactivation. J Mol Biol 2000; 297:683–695.
117. Keijer J, Linders M, Wegman JJ, Ehrlich HJ, Mertens K, Pannekoek H. On the target specificity of plasminogen activator inhibitor 1: the role of heparin, vitronectin, and the reactive site. Blood 1991; 78:1254–1261.
118. Hamsten A, Wiman B, de Faire U, Blomback M. Increased plasma levels of a rapid inhibitor of tissue plasminogen activator in young survivors of myocardial infarction. N Engl J Med 1985; 313:1557–1563.
119. Fay WP, Parker AC, Condrey LR, Shapiro AD. Human plasminogen activator inhibitor-1 (PAI-1) deficiency: characterization of a large kindred with a null mutation in the PAI-1 gene. Blood 1997; 90:204–208.
120. Agirbasli M. Pivotal role of plasminogen-activator inhibitor 1 in vascular disease. Int J Clin Pract 2005; 59:102–106.
121. Gils A, Declerck PJ. Plasminogen activator inhibitor-1. Curr Med Chem 2004; 11:2323–2334.
122. Booth NA, Simpson AJ, Croll A, Bennett B, MacGregor IR. Plasminogen activator inhibitor (PAI-1) in plasma and platelets. Br J Haematol 1988; 70:327–333.
123. Erickson LA, Ginsberg MH, Loskutoff DJ. Detection and partial characterization of an inhibitor of plasminogen activator in human platelets. J Clin Invest 1984; 74:1465–1472.
124. Gebbink RK, Reynolds CH, Tollefsen DM, Mertens K, Pannekoek H. Specific glycosaminoglycans support the inhibition of thrombin by plasminogen activator inhibitor 1. Biochemistry 1993; 32:1675–1680.
125. Ehrlich HJ, Gebbink RK, Keijer J, Pannekoek H. Elucidation of structural requirements on plasminogen activator inhibitor 1 for binding to heparin. J Biol Chem 1992; 267:11606–11611.
126. Sui GC, Wiman B. Functional effects of single amino acid substitutions in the region of Phe113 to Asp138 in the plasminogen activator inhibitor 1 molecule. Biochem J 1998; 331 (Pt 2):409–415.
127. Ehrlich HJ, Keijer J, Preissner KT, Gebbink RK, Pannekoek H. Functional interaction of plasminogen activator inhibitor type 1 (PAI-1) and heparin. Biochemistry 1991; 30:1021–1028.
128. Hagglof P, Bergstrom F, Wilczynska M, Johansson LB, Ny T. The reactive-center loop of active PAI-1 is folded close to the protein core and can be partially inserted. J Mol Biol 2004; 335:823–832.
129. Baker JB, Low DA, Simmer RL, Cunningham DD. Protease-nexin: a cellular component that links thrombin and plasminogen activator and mediates their binding to cells. Cell 1980; 21:37–45.
130. Gronke RS, Knauer DJ, Veeraraghavan S, Baker JB. A form of protease nexin I is expressed on the platelet surface during platelet activation. Blood 1989; 73:472–478.
131. Gloor S, Odink K, Guenther J, Nick H, Monard D. A glia-derived neurite promoting factor with protease inhibitory activity belongs to the protease nexins. Cell 1986; 47:687–693.
132. Houenou LJ, Turner PL, Li L, Oppenheim RW, Festoff BW. A serine protease inhibitor, protease nexin I, rescues motoneurons from naturally

occurring and axotomy-induced cell death. Proc Natl Acad Sci USA 1995; 92:895–899.
133. Guttridge DC, Lau AL, Cunningham DD. Protease nexin-1, a thrombin inhibitor, is regulated by interleukin-1 and dexamethasone in normal human fibroblasts. J Biol Chem 1993; 268:18966–18974.
134. Cunningham DD, Pulliam L, Vaughan PJ. Protease nexin-1 and thrombin: injury-related processes in the brain. Thromb Haemost 1993; 70:168–171.
135. Vaughan PJ, Cunningham DD. Regulation of protease nexin-1 synthesis and secretion in cultured brain cells by injury-related factors. J Biol Chem 1993; 268:3720–3727.
136. Mbebi C, Hantai D, Jandrot-Perrus M, Doyennette MA, Verdiere-Sahuque M. Protease nexin I expression is up-regulated in human skeletal muscle by injury-related factors. J Cell Physiol 1999; 179:305–314.
137. Monard D. Cell-derived proteases and protease inhibitors as regulators of neurite outgrowth. Trends Neurosci 1988; 11:541–544.
138. Scott RW, Bergman BL, Bajpai A, Hersh RT, Rodriguez H, Jones BN, Barreda C, Watts S, Baker JB. Protease nexin. Properties and a modified purification procedure. J Biol Chem 1985; 260:7029–7034.
139. Rovelli G, Stone SR, Guidolin A, Sommer J, Monard D. Characterization of the heparin-binding site of glia-derived nexin/protease nexin-1. Biochemistry 1992; 31:3542–3549.
140. Herndon ME, Stipp CS, Lander AD. Interactions of neural glycosaminoglycans and proteoglycans with protein ligands: assessment of selectivity, heterogeneity and the participation of core proteins in binding. Glycobiology 1999; 9:143–155.
141. Farrell DH, Cunningham DD. Glycosaminoglycans on fibroblasts accelerate thrombin inhibition by protease nexin-1. Biochem J 1987; 245:543–550.
142. Cooper ST, Church FC. PCI: protein C inhibitor? Adv Exp Med Biol 1997; 425:45–54.
143. Geiger M, Krebs M, Jerabek I, Binder BR. Protein C inhibitor (PCI) and heparin cofactor II (HCII): possible alternative roles of these heparin-binding serpins outside the hemostatic system. Immunopharmacology 1997; 36:279–284.
144. Geiger M, Zechmeister-Machhart M, Uhrin P, Hufnagl P, Ecke S, Priglinger U, Xu J, Zheng X, Binder BR. Protein C inhibitor (PCI). Immunopharmacology 1996; 32:53–56.
145. Heeb MJ, Espana F, Griffin JH. Inhibition and complexation of activated protein C by two major inhibitors in plasma. Blood 1989; 73:446–454.
146. Rezaie AR, Cooper ST, Church FC, Esmon CT. Protein C inhibitor is a potent inhibitor of the thrombin–thrombomodulin complex. J Biol Chem 1995; 270:25336–25339.
147. Elisen MG, von dem B, Bouma BN, Meijers JC. Protein C inhibitor acts as a procoagulant by inhibiting the thrombomodulin-induced activation of protein C in human plasma. Blood 1998; 91:1542–1547.
148. Espana F, Vicente V, Tabernero D, Scharrer I, Griffin JH. Determination of plasma protein C inhibitor and of two activated protein C-inhibitor complexes in normals and in patients with intravascular coagulation and thrombotic disease. Thromb Res 1990; 59:593–608.

149. Minamikawa K, Wada H, Wakita Y, Ohiwa M, Tanigawa M, Deguchi K, Hiraoka N, Huzioka H, Nishioka J, Hayashi T. Increased activated protein C-protein C inhibitor complex levels in patients with pulmonary embolism. Thromb Haemost 1994; 71:192–194.
150. Watanabe R, Wada H, Sakakura M, Mori Y, Nakasaki T, Okugawa Y, Gabazza EC, Hayashi T, Nishioka J, Suzuki K, Shiku H, Nobori T. Plasma levels of activated protein C-protein C inhibitor complex in patients with hypercoagulable states. Am J Hematol 2000; 65:35–40.
151. Meijers JC, Marquart JA, Bertina RM, Bouma BN, Rosendaal FR. Protein C inhibitor (plasminogen activator inhibitor-3) and the risk of venous thrombosis. Br J Haematol 2002; 118:604–609.
152. Espana F, Gilabert J, Estelles A, Romeu A, Aznar J, Cabo A. Functionally active protein C inhibitor/plasminogen activator inhibitor-3 (PCI/PAI-3) is secreted in seminal vesicles, occurs at high concentrations in human seminal plasma and complexes with prostate-specific antigen. Thromb Res 1991; 64:309–320.
153. Laurell M, Christensson A, Abrahamsson PA, Stenflo J, Lilja H. Protein C inhibitor in human body fluids. Seminal plasma is rich in inhibitor antigen deriving from cells throughout the male reproductive system. J Clin Invest 1992; 89:1094–1101.
154. Zechmeister-Machhart M, Hufnagl P, Uhrin P, Xu J, Geiger M, Binder BR. Molecular cloning and tissue distribution of mouse protein C inhibitor (PCI). Immunopharmacology 1996; 32:96–98.
155. Uhrin P, Dewerchin M, Hilpert M, Chrenek P, Schofer C, Zechmeister-Machhart M, Kronke G, Vales A, Carmeliet P, Binder BR, Geiger M. Disruption of the protein C inhibitor gene results in impaired spermatogenesis and male infertility. J Clin Invest 2000; 106:1531–1539.
156. Pratt CW, Whinna HC, Church FC. A comparison of three heparin-binding serine proteinase inhibitors. J Biol Chem 1992; 267:8795–8801.
157. Kuhn LA, Griffin JH, Fisher CL, Greengard JS, Bouma BN, Espana F, Tainer JA. Elucidating the structural chemistry of glycosaminoglycan recognition by protein C inhibitor. Proc Natl Acad Sci USA 1990; 87:8506–8510.
158. Neese LL, Wolfe CA, Church FC. Contribution of basic residues of the D and H helices in heparin binding to protein C inhibitor. Arch Biochem Biophys 1998; 355:101–108.
159. Shirk RA, Elisen MG, Meijers JC, Church FC. Role of the H helix in heparin binding to protein C inhibitor. J Biol Chem 1994; 269:28690–28695.
160. Elisen MG, Maseland MH, Church FC, Bouma BN, Meijers JC. Role of the A+ helix in heparin binding to protein C inhibitor. Thromb Haemost 1996; 75:760–766.
161. Huntington JA, Kjellberg M, Stenflo J. Crystal structure of protein C inhibitor provides insights into hormone binding and heparin activation. Structure 2003; 11:205–215.
162. Aznar J, Espana F, Estelles A, Royo M. Heparin stimulation of the inhibition of activated protein C and other enzymes by human protein C inhibitor – influence of the molecular weight of heparin and ionic strength. Thromb Haemost 1996; 76:983–988.

Chemistry and Biology of Heparin and Heparan Sulfate
H.G. Garg, R.J. Linhardt and C.A. Hales (Editors)

Chapter 14

Role of Heparan Sulfate in Fibroblast Growth Factor Signaling

NICHOLAS J. HARMER

University of Cambridge, Cambridge, UK

I. Introduction and Perspective

The fibroblast growth factors (FGFs) are a family of extracellular animal proteins that act as mediators of cell–cell signaling (1,2). Since the first FGF was discovered in 1973 (3), members of the family have been found to be required for the correct development and homeostasis of virtually every tissue and organ in the human body. FGFs have also aroused great interest due to the fact that, in addition to their high affinity cell surface receptors, the FGF receptors (FGFRs), the FGFs bind with a high affinity to heparan sulfate (HS) and its analogue, heparin (2,4). FGFs therefore are one of the heparin-binding growth factors, a group that includes hepatocyte growth factor (5), transforming growth factor β and hedgehog (6). FGFs are an excellent study model for the interactions of proteins with HS because HS is required for the correct signaling of the FGFs (7–9). Furthermore, the intimate interactions between HS, FGFs, and FGFRs have been revealed by X-ray crystallography, revealing the nature of the contacts between the molecules (10,11). Finally, the FGFs and their receptors have excited interest as they have been heavily implicated in the mechanisms of pathogenesis of several important diseases, most notably arthritis (12,13) and many cancers (2).

This chapter presents salient features of the biology of the FGFs and FGFRs, the biochemical characterization of the FGF/FGFR interactions with heparin and HS, and the crystal structures that have been solved of FGFs, FGF–FGFR complexes, and complexes of these with heparin.

II. Fibroblast Growth Factors

A. Overview

The FGF family comprises 22 members in humans, mice, and rats, with smaller numbers in lower eukaryotes (14). These proteins are usually expressed to signal to neighboring or local cells, although some members of the family signal over longer ranges (15). Cellular responses to exposure to FGFs include proliferation (3,16), differentiation (7), survival (17), migration (18,19), and the alteration of cellular metabolism (15). The effect produced is dependent on the FGF, the receptor that it activates on the target cell, and the dose of FGF that is presented to the cell.

A phylogenetic analysis of the 22 human FGFs suggests that they fall within seven subfamilies (Fig. 1). The members of each subfamily tend to be similar to one another in terms of their physiological action and tend to bind to similar receptors. In many cases, the different members of a subfamily are expressed in different tissues or are expressed predominantly at different developmental stages (particularly in either the embryo or postnatally).

Deletion of the FGF genes from mice has led to a variety of results (14): in some cases, this leads to embryonic lethality. However, in many cases, the conse-

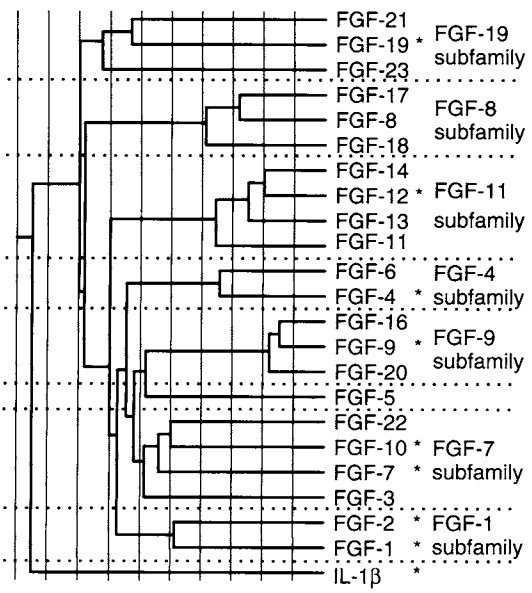

Figure 1 Evolutionary trace of the FGF family. A structure-based sequence alignment of the conserved cores of the 22 human FGFs (20) was used to generate an evolutionary trace of the FGF family using Tracesuite II (21). From this evolutionary trace, it is clear that the FGFs fall into seven subfamilies (with FGF-5 unplaced within these subfamilies). The sequence of interleukin-1β (IL-1β) was used to as a root for this analysis. FGFs with solved crystal structures are marked *.

quences of the knockout are extremely subtle, if not undetectable in the laboratory environment. This implies that there is a degree of redundancy in the FGF genes, as might be expected from the high sequence and functional homology between some of the FGFs. This suggests that it can be useful to examine a single member of a family of FGFs, as this helps to gain information that can be extended to other members of this family.

B. Features of Key FGF Subfamilies

1. FGF-1 Subfamily (FGFs 1 and 2)

FGFs 1 and 2 were the first FGFs to be identified, as proteins that could support the proliferation of fibroblasts (3,16). Because they were discovered much earlier than the other FGFs, and because recombinant FGF-1 and FGF-2 can be produced straightforwardly in *Escherichia coli*, these FGFs have been studied far more extensively than other FGFs. This is perhaps unfortunate, as their functions (especially those of FGF-1) are somewhat nebulous: both genes can be deleted from mice at the same time without significant phenotypes (22), although a wide variety of roles have been proposed, especially angiogenesis (23). The majority of the studies in this chapter will concern these FGFs.

2. FGF-4 Subfamily (FGFs 4 and 6)

FGFs 4 and 6 form the best example of a family pair of FGFs that are split between developmental (FGF-4) (24) and postnatal (FGF-6) (25) expression. In this case, the distinction is absolute, with no evidence existing for FGF-4 expression in the adult, whilst FGF-6 has no developmental role at all. FGF-4 is required for the formation of multiple tissues, but most crucially in the inner cell mass of the early embryo: FGF-6 expression is limited to the adult skeleton.

3. FGF-7 Subfamily (FGFs 3, 7, 10, and 22) and FGF 8 Subfamily (FGFs 8, 17, and 18)

These two subfamilies of FGFs have been extensively studied *in vivo* due to the involvement of FGFs 8 and 10 in limb patterning (26), and because FGFs 8 and 10 are required for gastrulation (27) and lung formation (28), respectively. The FGF-7 subfamily are primarily involved in signaling to epithelial cell types (29), whilst the FGF-8 subfamily often provide reciprocal signals from mesenchymal tissue (26). The importance of these FGFs for development has led to some significant studies on their binding to heparin and HS.

4. FGFs 9, 11, and 19 Subfamilies

Little data is available on the heparin binding of these FGFs, and consequently they will be mentioned little in the remainder of the chapter. In particular, FGFs 11–14

appear to have no FGFR or HS binding activity (30) and have been proposed to function as intracellular molecular scaffolds (31). Although the FGF-9 and FGF-19 subfamilies have vital functions in many systems (particularly the neuronal system in the case the FGF-9 subfamily), their binding to HS has not been studied in any detail.

III. FGF RECEPTORS

A. Perspective

The protein receptors for FGFs (FGFRs) are integral membrane proteins that are responsible for transmitting the FGF signal from the extracellular space to the inside of the cell (32). There are five FGFR genes, all of which are conserved in mice and rats (14,33). These are all capable of binding both FGFs and HS, and both of these are required for signal transduction.

B. Receptor Structure

The five FGFRs are all type I transmembrane proteins (i.e., they have a single membrane-spanning helix). They have a common extracellular architecture, consisting of three immunoglobulin (Ig)-like domains (Ig domain 1, Ig domain 2, and Ig domain 3) (34). Both biochemical (35–37) and crystallographic (10,37–41) studies have shown that the two membrane proximal Ig domains (Ig domain 2 and Ig domain 3) are responsible for binding to FGFs. Ig domain 3 appears to have the central role in providing specificity between the FGFs (39,41). Ig domain 2 binds to heparin as well as to the FGF (42), indicating that the FGFR will bind to both the FGF and the HS that the FGF binds. This allows several interactions to combine creating a complex with very high affinity amongst the component members, and exquisite specificity of the FGFR for its cognate FGFs (5). The function of Ig domain 1 is, at present, unclear. This domain can be dispensed with entirely for FGF binding (35–37), and indeed FGF binding is stronger in the absence of Ig domain 1. The linker between Ig domains 1 and 2 has a short sequence of consecutive negatively charged residues, known as the acid box, that has been hypothesized to bind to Ig domain 2 in the absence of HS or HS–FGF, and so reduce the affinity of the FGFR for FGFs, improving the specificity (36).

The intracellular regions of FGFRs 1–4 consist of a juxta-membrane region (a loosely structured region of approximately 70 amino acids), and a tyrosine kinase domain of the split kinase family (34). FGFR 5 has no signaling intracellular domain and does not appear to produce signals in response to FGF binding (33). Consequently, little data is available on its FGF or HS binding.

C. Receptor Splicing

FGFRs 1–3 are notable in that they have a number of possible alternative splicings (Fig. 2) (2). Out of the range of alternative splicings, the key splicing events are those that lead to the removal of Ig domain 1, and those that alter Ig domain 3

(Fig. 2). Ig domain 1 (and the acid box in some FGFR 2 splicings) is removed by alternative splicing in FGFRs 1 and 2. This splicing event leads to the affinity for FGFs being increased, as the inhibitory effect of Ig domain 1 (and the acid box) is relieved. A constitutive shift to this splice form has been observed during the progression of some cancers (43).

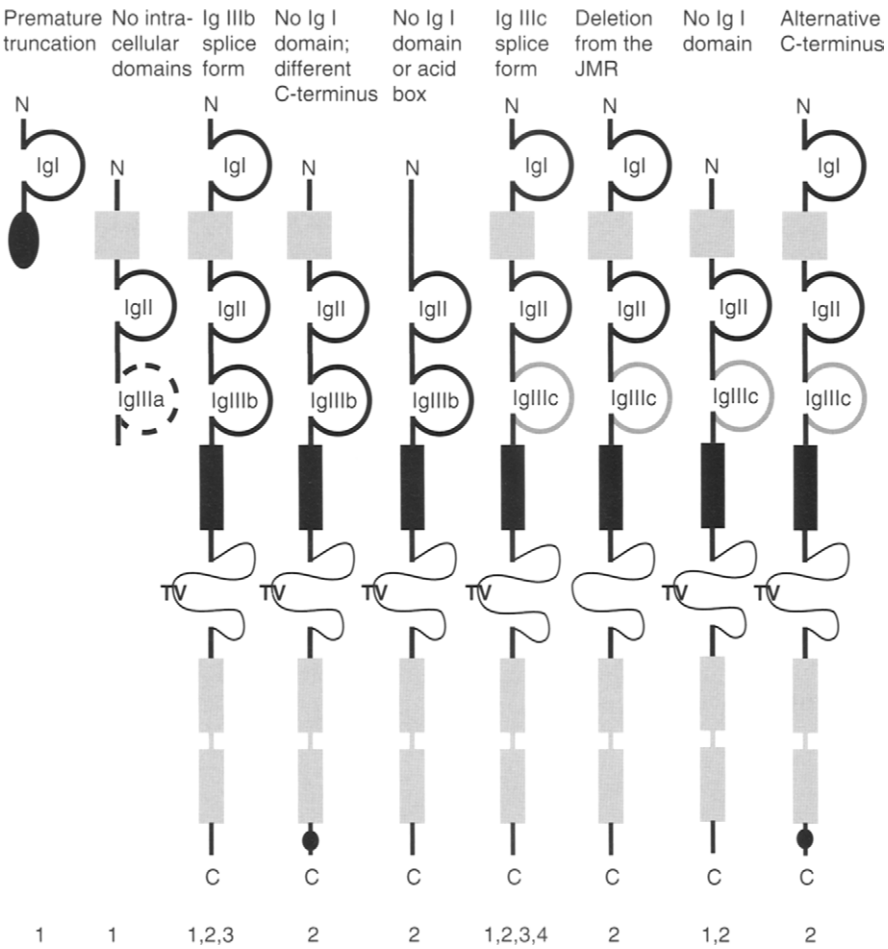

Figure 2 Splicing variations in the fibroblast growth factor receptors. Ig domains 1–3 are marked as Ig I, Ig II, and Ig III. The alternative splicings of Ig domain III are shown by different coloring of the loop: broken black – "a" splice variant, black – "b" splice variant, gray – "c" splice variant. Gray box: "acid box." Dark cylinder: transmembrane domain. Curved line: juxtamembrane region (JMR); the TV dipeptide shown in the JMR is present to show the splice form where this is eliminated. Light gray double cylinder: tyrosine kinase domain. N, C: N- and C-termini. Numbers underneath each splice form detail the receptors that display each splice variant. Adapted from Ref. (2).

The second major splicing event occurs in Ig domain 3. Here, FGFRs 1–3 have two alternative, mutually exclusive, sequences for the second half of the Ig domain. As this half of the Ig domain contains the majority of the FGF binding surface, the result of this alternative splicing is to radically alter the affinity of the FGFR for the various FGFs. The alteration in affinity is so great that the two alternative splice forms for FGFRs 1–3 can be considered to be different receptors, and are referred to as the "b" and "c" splice forms (i.e., FGFR 1c is the "c" splice form of FGFR 1). Therefore, it is generally considered that there are seven signaling FGFRs.

D. FGFR Binding to FGFs

Due to the large number of different FGFs and FGFRs, there has been great interest in determining the specificity of the interaction between each FGF and the various FGFRs. The best data is available for FGFs 1–9, the affinity of which for FGFRs 1–4 (considering both the "b" and "c" splice forms of FGFRs 1–3) has been thoroughly assessed (Table 1) (44). FGF-1, as is clear from these data, is an extremely promiscuous protein and will bind to and activate all of the FGFRs. In general, the FGFs bind to more than one FGFR, and each FGFR binds to several FGFs. FGF-7 is an exception to this rule in that it binds to only one of the signaling FGFRs, FGFR 2b. The "b" splice forms of the FGFRs are also less promiscuous than the "c" forms: the "c" forms each bind to at least four FGFs (in addition to FGF-1). FGFR 3b, in contrast, appears to be the most specific FGFR, binding only to FGF-9 in addition to FGF-1. Members of each subfamily of FGFs, in general, bind to similar receptors, depending upon the extent of the homology between the FGFs. As can be seen from the above data, FGFs 4 and 6 broadly bind to the same receptors (FGFR 1c, FGFR 2c, and FGFR 4), with FGF-6 additionally binding to FGFR-3c, whilst FGF-3 binds to FGFR 2b (like FGF-7), and additionally FGFR 1b. Similar patterns have been found in other studies that have tested a more limited dataset outside this range.

Table 1 Affinities of FGFRs for FGFs 1–9

	FGF-1	FGF-2	FGF-3	FGF-4	FGF-5	FGF-6	FGF-7	FGF-8	FGF-9
FGFR 1b	100	59.9	34.4	15.6	3.8	4.6	6.3	3.5	3.5
FGFR 1c	100	104	0.3	102	59	54.9	0.3	0.7	21.1
FGFR 2b	100	9.0	44.6	14.9	5.0	5.4	80.6	3.8	7.3
FGFR 2c	100	64.0	4.2	94.3	25.0	60.7	2.5	16.1	89.2
FGFR 3b	100	1.2	1.5	1.0	1.0	0.9	1.2	0.9	41.5
FGFR 3c	100	107	0.6	69.1	11.8	8.8	1.0	40.5	95.6
FGFR 4	100	113	5.8	108	7.0	79.4	1.9	76.1	75.4

The figures shown are the amounts of proliferation of BaF3 cells after 36–48-h incubation with the FGF shown, normalized for each receptor so that FGF-1 gives 100. Proliferation was measured by incorporation of ^{3}H-thymidine into the DNA of the cells. Data taken from Ref. (44).

The most striking consequence of the relative affinities of FGFRs for FGFs that are observed is that, as most FGFRs can be activated by more than one of the FGFs that the body is expressing at any one time, the potential interactions are extremely complicated. Furthermore, since a single FGF can activate different receptors on the same, or even different cells at the same time, it seems likely that there will be further levels of specificity, other than the FGF–FGFR interaction to ensure that the signals are correctly interpreted by the receiving cells.

E. Downstream Signaling from FGFRs

The actions that lead to the formation of a mature signaling complex on the extracellular face of the membrane must be understood in the context of what will result inside the cell. Receptor tyrosine kinases are activated by ligand(s) binding to two receptors in close proximity. Following the binding of the ligand(s), the intracellular tyrosine kinase domains phosphorylate one another at several sites (45). These phosphorylation events set the kinase in the activated form and create docking sites for cellular proteins that bind to peptides containing a phosphorylated tyrosine. Proteins that bind to the activated receptor are then either themselves activated by phosphorylation, or as adaptors or scaffolds recruit other molecules to the signaling complex (32). These additional molecules will be activated either by phosphorylation or by co-localization with molecular partners.

The FGF receptors generate intracellular signals via several downstream signaling pathways, involving the proteins phospholipase Cγ (PLCγ) Ras and MAP kinase (MAPK), Src, STATs, and phosphoinositol-3-kinase (PI3K) (45,46). These pathways generate "second messengers," signaling molecules diffusible in the membrane or the cytoplasm that transmit the signal inside the cell: these molecules can be either activated proteins (STATs, Src, MAPK), or small molecules (PLCγ and PI3K). These second messengers activate a range of molecules in the cell and communicate the message from the FGFR. The combination of these, in addition to other signals that the cell may be receiving, will determine the eventual cellular response to the FGF signal.

IV. Interactions of the FGFs and FGFRs with Heparin

A. Methods of Study

The study of the interactions of HS with the FGFs and their receptors has broadly fallen into two approaches. One approach has been to purify the isolated components of the complex, in particular the FGF and HS or heparin, and to assess the interaction of these components (Chapter 29) (47). The second approach has been to take an intact system (usually a cell expressing FGFRs, with separately purified FGF added to induce a response), remove the endogenous HS from the cell by chlorate treatment, and assess the capacity of exogenously added HS or heparin to reconstitute the system. Both of these approaches to the problem have their limitations: the first, like all reductionist strategies, assesses a single interaction,

far from its physiological context, in the hope that what is observed in this limited system is also true when all other components are present. In particular, the potentially dramatic effects of the cellular membrane are ignored in this approach. There are also considerable caveats to the second approach: heparin or HS fragments that are free in solution, rather than attached to the cell in distinct locations, may allow the possibility of complexes forming that could not with natural HS; FGFR–HS interactions that would exist on resting cells will not be present; and the other cellular components that cooperate in processing the FGF signal will vary between cell lines, particularly in cases where FGFRs are transfected into cell lines that lack FGFR expression, and so may lack some components of the full FGFR signaling machinery. These factors may be the cause of the variety in the conclusions that are drawn by different groups. With these potential pitfalls in mind, however, clear conclusions can be drawn from the mass of available data.

B. FGF–Heparin Interactions

The interaction between the FGFs and heparin has been of great interest since the discovery that FGFs (especially FGF-2) have an extremely high affinity for heparin. That this affinity was a specific property of a face of the FGF was confirmed by site-directed mutagenesis (48): mutagenesis of individual FGF-1 side chains to alanine considerably weakens the binding to heparin, suggesting two sites on the FGF as the source of the FGF affinity. This finding, together with crystal structures of FGFs in complex with heparin (Section V) (49,50), suggested that the FGF might selectively bind to regions of the heparin or HS with a specific sulfation pattern. In recent years, tools for determining the sulfation patterns of isolated heparin species, and removing defined sets of sulfates from a heparin sample, have become more sophisticated and sensitive. These improvements have made it possible to make great strides towards determining the minimal sulfation requirements for various FGFs to bind to heparin fragments.

Information about the HS (or heparin) sulfate pattern preferences has been elucidated for FGFs 1, 2, 4, 7, 8, 10, and 18. The best information exists for FGFs 1 and 2. The precise structures of HS fragments that bound to these two molecules have been determined (51), and a consensus pattern obtained from those that showed selectively higher affinity. These data confirmed and elaborated many other results. FGF-1 binds HS octamers containing the trisaccharide motif IdoA(2-OSO_3)GlcNSO_3(6-OSO_3)IdoA(2-OSO_3) most strongly, although further sulfations flanking this sequence increase the apparent affinity for the immobilized FGF-1; whilst in the case of FGF-2, samples with the sequence GlcNSO_3IdoA (2-OSO_3)GlcNSO_3 bound to the FGF with as high an affinity as more heavily sulfated species (Fig. 3).

Information on the sulfation requirements of the other FGFs is rather limited, and in many cases the data are gathered from only one or two studies. FGF-4 has been shown to require the *N*-, 2-*O*, and 6-*O*-sulfations for binding to heparin, by the binding of synthetically sulfated heparins to an FGF 4 affinity column (52), cell proliferation studies (53), and structure-based mutagenesis (54). H-S samples from

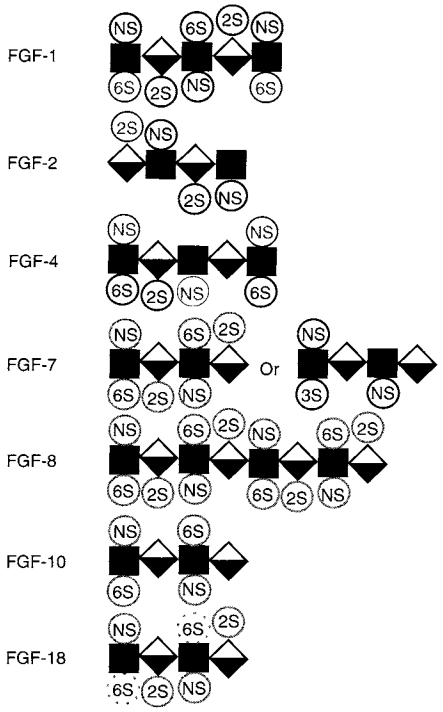

Figure 3 Summary of *in vitro* data of the heparin sulfation requirements for FGF binding. Key: dark rectangles – glucosamine. Half-filled diamonds – iduronic acid. Sulfate groups required for binding are shown. Sulfate with dark ring: known to be required, position determined. Sulfate with thick gray ring: sulfate type known to be required, position in sequence not determined. Sulfate with thin gray ring: not required, but presence increases affinity, position determined. Sulfate with dashed ring: not required, but presence increases affinity, position not determined.

vascular tissues are incapable of activating FGF-4, consistent with FGF-4 requiring a specific, highly sulfated species to bind to (55).

The HS binding pattern required for the binding of FGF-7 is currently unclear. One study has suggested that FGF-7 requires glucosamine *N*- and 6-*O*-sulfation and uronic acid 2-*O*-sulfation (52). However, a previous result found that FGF-7 binds heparin fragments with similar properties to those bound by antithrombin (56). This suggests that FGF-7 requires the glucosamine 3-*O*-sulfation modification in oligosaccharides to which it binds tightly. As the former result used semi-synthetically prepared heparin, the extent of 3-*O*-sulfation was not determined, and further confirmation of these data will be required.

Heparin fragments that bind to FGF are rich in glucosamine *N*- and 6-*O*-sulfations and iduronic acid 2-*O*-sulfations, especially in trisulfated disaccharides. FGF-8 tends to bind heparin fragments that are longer than those observed to bind to the other studied

FGFs (57). FGF-8 is sensitive to the source of HS in an analogous manner to FGF-4, supporting a role for all of the sulfations (58). FGF-10, in contrast, binds strongly to heparin octasaccharides with only glucosamine *N*- and 6-*O*-sulfation, whilst FGF-18 has affinity to octasaccharides with the *N*-sulfation and either 6-*O*-sulfation or 2-*O*-sulfation, with the latter giving the stronger affinity (Fig. 3) (52). Finally, FGF-19 has been found to have extremely weak interactions with heparin, in comparison to other FGFs (20).

One limitation of many of these experiments is that the HS samples studied were fully sulfated at the amine group, and so these investigations did not reveal the requirements for *N*-sulfation for FGF binding. HS contains sequences of mixed *N*-sulfation, and these may be important for the binding of FGFs (or FGFRs) when signaling complexes are being formed. Thorough studies elucidating the requirements for the *N*-sulfation of HS for FGF binding will reveal the relevance of these sequences to FGF signaling.

The conclusion from all these data is that any notion that the binding of FGFs to heparin or HS is uniform is misguided, as each FGF appears to require a different consensus sequence in the HS chain to obtain the highest affinity interaction (Fig. 3). Differences are observed between the members of each FGF subfamily: FGF-10 binds to *N*- and 6-*O*-sulfated heparins, whilst FGF-7 requires a more extensive range of sulfation; FGF-18 will bind to a range of octasaccharides, whilst FGF-8 requires a longer, highly sulfated oligosaccharide. It is not yet clear whether the subfamilies show entirely different heparin binding patterns, or whether these represent variations on a common mode of binding. This suggests that the relative proportions of the HS biosynthetic enzymes in Golgi apparatus of each cell type may be a potential site of regulation for the FGFs that the cell will ultimately bind. A broader picture of the requirements for HS binding of the other FGFs, and an extension of the current data to examine the role of *N*-sulfation, will help to elucidate the extent to which this is the case.

C. FGFR–Heparin Interactions

FGFR–heparin interactions have been studied far less extensively than FGF–heparin interactions. This is principally because, whereas most FGFs can be conveniently expressed in bacterial cells, FGFRs must be either refolded from inclusion bodies following expression in *E. coli*, or expressed in insect cells. The first key observation into the interaction was that the FGFRs themselves are capable of binding to heparin. Mutational analysis of the FGFR 2 extracellular domain (42) identified a strongly basic sequence (termed the K18K loop), containing six lysine, arginine, or histidine residues, whose mutation abolished FGFR binding to heparin. The mutation of no other regions of the FGFR caused a significant drop in the affinity of the FGFR for heparin. The K18K loop is strongly conserved between the FGFRs (as indeed is most of FGFR Ig domain 2), suggesting that the binding to heparin is likely to be similar for all of the FGFRs. Nevertheless, the existing data suggests that FGFR 2 binds to heparin fragments more strongly than FGFR 1 (59), whilst FGFR 4 binds extremely avidly to heparin (60,61). These observations suggest that subtle changes in the structure of Ig

domain 2 may be important in determining heparin binding. Analyses of HS fragments that bind to FGFR 4 (61) suggest that the strongest binding is provided by a tetrasaccharide of IdoA(2-OSO_3)GlcNSO_3IdoA(2-OSO_3)GlcNSO_3. Sulfations at the glucosamine 6-*O* position increased the affinity, but unlike the other sulfations these could not be exactly placed within the consensus sequence of the HS fragments isolated, suggesting that this is an electrostatic effect. It therefore appears that the FGFRs, as well as the FGFs, bind HS with the highest affinity to specific sequences on an HS chain.

The affinity of FGFs to FGFRs is considerably increased by the presence of heparin or HS (62), which strongly suggests that the heparin binding sites of the two molecules will be close together in the complex (which has been confirmed by X-ray crystallography) (10,11). The consensus sequences for both FGF and FGFR must therefore necessary occur consecutively to allow both to bind with high affinity to the HS, and to each other. This suggests that the sites on the HS chains that will permit high affinity binding will be rare, perhaps only a few percent of all the HS on any cell for a given FGF–FGFR pair. This will clearly have implications for the mechanism by which the ternary complex of FGF, FGFR, and HS is built up.

D. FGF–FGFR–Heparin Complex Formation *In Vivo*

The HS requirements for forming constructive complexes of FGF, FGFR, and HS *in vivo* have been studied by removing the endogenous cellular HS by treatment with sodium chlorate, followed by the addition of exogenous heparins. The responses assayed have been either the capacity to drive cells into mitosis (measured by cell density, the rate of DNA synthesis, or by monitoring the cell cycle status of the cellular population), or the phosphorylation of the p42/p44 Erk kinase (which acts as a terminal effector in the signaling pathway initiated by FGFR activation of Ras). FGFs are now known to be able to elicit a partial response from the FGFRs in the absence of HS, resulting in the transient phosphorylation of Erk, but not in either sustained phosphorylation or the entry of the cells into the cell cycle (63). Therefore, the HS is a requirement for the sustained signaling of FGFRs. Experiments to determine the capacity of polysaccharide fragments to replace the endogenous HS have yielded a wide variety of results. Nevertheless, clear conclusions can be drawn from these data, even if some results pose tantalizing questions that remain unanswered.

This method has been used to show that FGFs can utilize glucosaminoglycans other than HS to form complexes with their receptors. Chondroitin sulfate (64), dermatan sulfate (65), and hybrids of the two (66) have all been shown to compensate for HS in chlorate treated cells. The response to these polysaccharides does not match the response to endogenous HS. Nevertheless, these data suggest that these alternative polysaccharides may have a role in mediating FGF–FGFR interactions in locations where HS is limiting. The results also indicate that all the other data must be treated with a note of caution: species of limited physiological relevance can potentiate FGF signaling in the absence of HS.

Thorough studies of the effect of small heparin-derived saccharides on chlorate treated cells (67) suggest that, for FGF-2, a fully sulfated tetrasaccharide is capable of driving a complete response from the FGFRs (Fig. 4). However, this response is observed only when the heparin is added at high concentrations. Heparin decamers, in contrast, are active at much lower concentrations (Fig. 4). These data suggest that the composition of the complexes that are forming is complicated, and that the shorter heparins are capable of forming a less stable complex that is nevertheless sufficient to drive the cells into the cell cycle. Some reports have suggested that heparin fragments as short as two saccharide units in length can compensate for HS to some extent (68,69). It generally appears that species of eight to ten saccharides in length are required for the full activation of cells by FGFs 1 and 2 (70).

Similar studies have examined the effects of using different FGF–FGFR pairs. These studies showed that whilst very short oligosaccharides (even disaccharides) are sufficient to potentiate the signaling via certain FGF–FGFR pairs (FGF-1 and FGFR 2b or FGFR 4), other FGF–FGFR pairs (FGF-1 and FGFR 1c or FGF-7 and FGFR 2b) require a far longer oligosaccharide (such as a decasaccharide) to drive the cells into the cell cycle (70). More recent studies have shown that the FGF-1 and

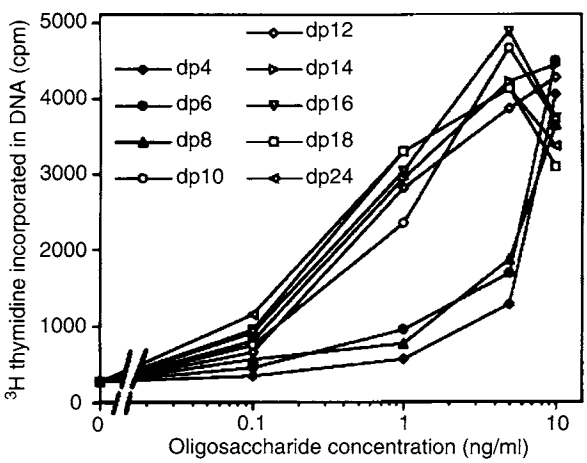

Figure 4 Dose response of active heparin oligosaccharides of different lengths added with FGF-2 (10 ng/ml). FGF-2 and heparin oligosaccharides (both 10 ng/ml) were added to serum-starved chlorate-treated Rama 27 fibroblasts. DNA synthesis was measured by the incorporation of (^{3}H)thymidine into the DNA of the cells. In a separate experiment, FGF-2 stimulated the incorporation of 7527 ± 376 cpm of (^{3}H)thymidine into the DNA of untreated serum-starved cells. Results are the mean of triplicate wells of one of four experiments. The S.D. was less than 10% of the mean and is omitted for clarity. Reproduced, with permission, from Delehedde, Lyon, Gallagher, Rudland, Fernig, *Biochem J* 2000, 366:235–244. © The Biochemical Society.

FGF-2 pairs with FGFR 1c and FGFR 3c show different levels of sensitivity to digestion of the HS chains with heparinases (71). This implies that the HS structures that are required for the formation of FGFR clusters differs between the FGF–FGFR pairs.

The patterns of HS sulfation that are required for full activity of the FGF–FGFR pair have also been investigated. It has become apparent that the 2-*O*- and 6-*O*-sulfations are not required for FGF-1–FGFR 2b signaling, but neither sulfation can be dispensed with for FGF 1–FGFR 1c and FGF-7–FGFR 2b signaling (70). As the data above (Fig. 3) showed that FGF-1 binds most strongly to species that have both of the 2-*O*- and 6-*O*-sulfations, this suggests that the FGF–FGFR interaction can compensate for the lack of the most favored sulfations on the HS. In contrast, Sulf1, a soluble mammalian extracellular 6-*O*-endosulfatase, inhibits FGF-2 and FGF-4 signaling through FGFR 1 in *Xenopus* embryos (72). This suggests that the removal of the 6-*O*-sulfates is sufficient to block the FGF–FGFR signaling with these FGF–FGFR pairs. The deletion of the sulfotransferase genes in mice (73) and *Drosophila* (74,75) result in catastrophic developmental incompleteness, due to the lack of appropriate FGF signaling (in addition to the signaling of other heparin binding growth factors), demonstrating that the lack of these sulfations cannot be compensated for with all FGF–FGFR pairs. Indeed, heparins with the 6-*O*-sulfates enzymatically removed proved to be excellent inhibitors of angiogenesis *in vitro* (72). It therefore appears that all of the sulfations are absolutely required for certain FGF–FGFR pairs, but for other pairs, some sulfations can be dispensed with. The likelihood is that, as with the FGFs and FGFRs in isolation, each pair of FGF and FGFR will have a consensus pattern of sulfations for binding with the highest affinity (76).

E. Biophysical Analysis of FGF, FGFR, and Heparin Complexes

A number of biophysical techniques have been employed to gain greater insight into the FGF–FGFR–heparin complex. These approaches are all far more costly in materials than the biochemical and *in vivo* approaches that have yielded information on the length and sulfation patterns of the HS that binds to FGFs and FGFRs. As a result, the majority of the data is only available for FGFs 1 and 2, and FGFRs 1 and 2, and the conclusions may not apply for the remainder of the family (given the earlier data).

Isothermal calorimetry (a technique where the heat of binding between two species is measured experimentally) yields information on the stoichiometries and thermodynamics of complexes. Application of this technique to the FGF–FGFR–heparin complex (62,77) confirmed that FGFs and FGFRs bind to one another with a 1:1 stoichiometry. The affinity of this interaction is greatly increased when HS is present, with a 10-fold drop in the value of the dissociation constant (62). In addition, the presence of HS makes the binding of a second FGFR to the FGF 1 observable, although the dissociation constant is extremely high (1.2 μM) in

comparison to the primary binding event (5.3 nM). In addition, it has been shown that FGFR 1 is capable of binding to heparin fragments (62): although the observed dissociation constant is high ($\approx 100\,\mu M$), the high concentration of HS on the cell surface makes it likely that the FGFR will be bound to HS in the physiological context (59). In contrast, FGF-1 binds with a high affinity ($k_D \approx 500\,nM$) to heparin, and the number of FGF-1 molecules that will bind increases with the length of the heparin, with no apparent reduction in the dissociation constant (77). These data are extremely helpful in building ideas as to how a complex involving two FGFRs might form: FGFs and FGFRs will predominantly form 1:1 complexes, with the presence of the HS making these complexes considerably stronger. The route to involving a second FGFR molecule could come either from the tendency of multiple FGFs to bind to a single HS chain: or from the potential for the FGF to bind a second FGFR in the presence of HS. These studies provide useful data against which proposed models can be tested.

A complementary technique to this is surface plasmon resonance. Using this method, both the affinity of binary interactions, and the rates of binding and dissociation can be evaluated. Surface plasmon resonance data on the binding of a range of FGFs to FGFRs (78,79) broadly supported the results obtained from studies on cells, although FGFR 3c appeared to bind to a more limited range of FGFs in the absence of HS. A thorough investigation of the interactions of FGFR 1c, FGF-2, and heparin yielded dissociation constants for the binary interactions that are of the same order as those obtained using calorimetry (80). The rates of the associations between the components were also determined (Table 2). The association between FGF-2 and heparin is far faster (over 100 times) than the association of FGFR 1c with either FGF-2 or heparin. Furthermore, the rate of association between the FGF–heparin complex and FGFR 1c is much faster (over 60 times) than the rate for an FGF-2–FGFR 1c complex with heparin. It is therefore clear that, when a cell is exposed to FGF-2, the first step in the process of forming a complex will be the binding of FGF-2 to its cognate HS, following which the FGF-2-heparin complex will bind to FGFR 1c. It is notable that the fastest dissociation of all of the complexes tested is also the FGF-2–heparin complex. This suggests that

Table 2 Association and Dissociation Rates, and Dissociation Constants Between FGF-2, FGFR 1, and Heparin Calculated Using Surface Plasmon Resonance

	k_a ($M^{-1}s^{-1}$)	k_d (s^{-1})	K_D (M)
FGF-2/FGFR 1	$9.64 \pm 0.08 \times 10^4$	$6 \pm 6 \times 10^{-3}$	6.19×10^{-8}
FGF-2/heparin	$1.10 \pm 0.05 \times 10^7$	0.43 ± 0.02	3.9×10^{-8}
FGFR 1/heparin	$5.9 \pm 0.3 \times 10^3$	$1.90 \pm 0.08 \times 10^{-4}$	3.2×10^{-6}
FGF-2/heparin[a]	144 ± 2	$1.18 \pm 0.08 \times 10^{-5}$	8.21×10^{-8}
FGF-2-FGFR 1/heparin[a]	90 ± 2	$8.63 \pm 0.09 \times 10^{-3}$	9.60×10^{-5}
FGF-2-heparin/FGFR 1[a]	$6.1 \pm 0.5 \times 10^3$	$1.6 \pm 0.1 \times 10^{-5}$	2.71×10^{-9}

Data adapted from Ref. (79). The values for the interactions labeled with superscript "a" were derived indirectly from FGF-2–FGFR 1–heparin interactions.

the FGF-2 can dissociate from the HS if it binds first to a less favorable sequence, and then bind to a different HS sequence that may have higher affinity for the FGF-2 or the FGFR. This suggests that the FGF–HS complex formation is of fundamental importance in determining the progress of the signaling in the physiological context: the HS is clearly the first species that the FGF will interact with on the cell surface, both because of the high concentration of HS and the extremely fast association between the two species. This will have the effect of localizing the FGF on the membrane, where the dimensionality is reduced from three to two dimensions.

Another biophysical investigation that has proved fruitful is the examination of FGF–FGFR–heparin complexes by size exclusion chromatography. This technique involves mixing purified FGFs, FGFRs, and heparin or HS fragments in a variety of stoichiometries, and separating the complexes that are formed using a chromatography column that separates samples on the basis of shape and size. By comparing the elution of species in comparison to each purified sample, a profile of the binding requirements can be built up (Fig. 5). The length of heparin required to

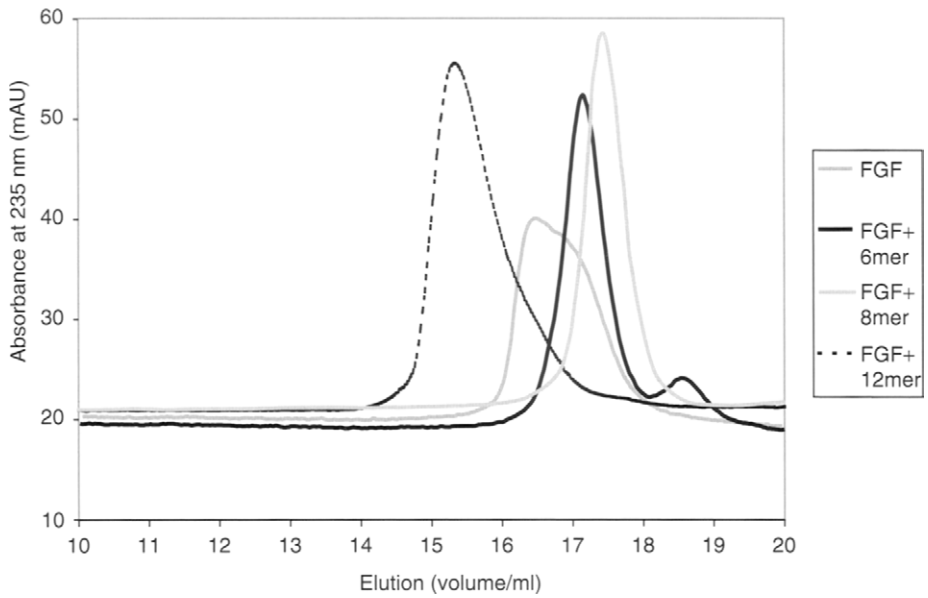

Figure 5 Size-exclusion chromatography of FGF and heparin samples. FGF-1 and heparin fragments (from porcine mucosa) of defined sizes were mixed and applied to a size exclusion chromatography column. Successive applications with heparins of different sizes allow the change in the mobility of the FGF to be established. Shifts to lower elution volumes indicate an increase in size of the complex. With this heparin preparation, the addition of heparin hexamers and octamers form complexes of a size similar to the FGF alone, whilst the addition of a dodecamer leads to dimerization of the FGF.

form a dimer of FGF-1 has been determined using this technique (50). A shift in the apparent mass of the eluted species is observed when an octamer of heparin was added to FGF-1, whereas little change was observed with a hexamer. A further small increase in mass was observed when a heparin decamer was the added species. Sedimentation analytical ultracentrifugation on the same samples confirmed the interpretations of the size exclusion. The same technique has been used to study the heparin length requirements for forming FGF–FGFR complexes. Using preformed FGF–FGFR pairs and heparin, a heparin hexamer is required to form a dimer of FGF-2–FGFR 1 (11), whilst an octamer is required for FGF-1–FGFR 2 (81). These data show again that the choice of FGF and FGFR is crucial for the heparin pattern that is required for the formation of biologically interesting complexes of saccharide and protein. Finally, using separately purified FGF-1 and FGFR 2, an octamer of heparin is again required for the formation of a complex of two FGFs and two FGFRs (81).

V. Structural Studies of FGF, FGFR, and Heparin Complexes

A. Motivation for Structural Studies of the FGF–FGFR–HS Complex

High-resolution structures have become increasingly important in recent years not only as a tool for improving our understanding of proteins and their complexes, but also for establishing or optimizing potential drugs (82). A well-understood structural model of the FGF–FGFR–HS complexes that drive signaling would be of great importance to efforts to generate specific inhibitors of FGF signaling. Models of the structure of the biologically relevant complexes have been built up over recent years, and are continuing to be explored and refined. However, at present these models have not proved sufficient for the generation of specific inhibitors of FGF signaling at the stage of complex formation.

B. Heparin and HS Structure

The structure of heparin has been studied extensively in the solid and solution states (reviewed in Ref. 83). The conclusion of these experiments, especially NMR studies (84,85) is that the heparin chain is unusually rigid compared with other polysaccharides, with little flexibility about the glycosidic bonds. This rigidity is also exhibited in both tetrasaccharides (86) and hexasaccharides (87). The intrinsic variability of HS makes such experiments on HS impracticable, as NMR requires homogeneous samples. However, glycosidic linkages equivalent to those that are found in the low sulfated region of HS are found in other carbohydrates that have been studied by NMR. These investigations have showed that these linkages have multiple favorable conformations (88–90), and so the less sulfated regions of the HS chain will have considerably more flexibility than the S domains. These results must be borne in mind when considering the complexes with FGFs and FGFRs: these have all been prepared using heparin, and so may bias against possible conformations that are sampled by HS.

C. FGF and FGF–FGFR Structures

The structures of eight of the FGFs have been solved using X-ray crystallography, enabling an extremely good comparison of the features of the entire family. Structures of FGF-1 (91), FGF-2 (92,93), FGF-4 (54), FGF-7 (56), FGF-9 (94,95), FGF-12 (30), and FGF-19 (20) have been solved on their own, whilst FGF-10 has been solved in complex with its receptor (41). The FGFs have a common core structure, the β-trefoil. The fold consists of a β-barrel formed from six β-strands at the base of the molecule, with three β-hairpins at the upper end of the molecule (Fig. 6). In

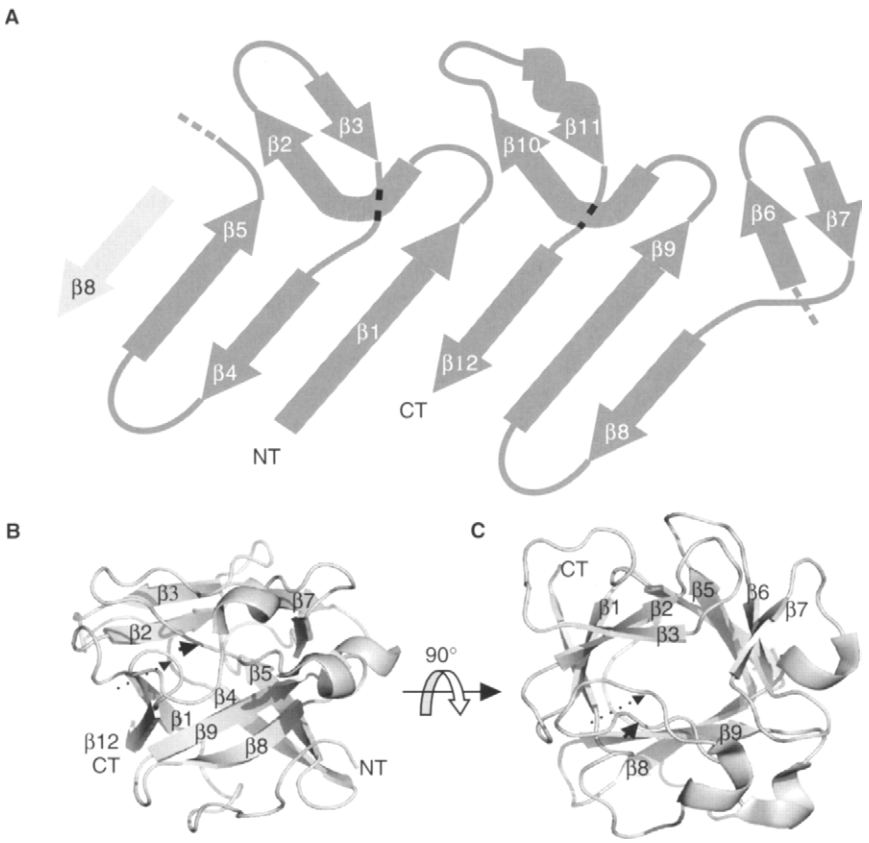

Figure 6 Overview of the structure of the FGF core. (A) Illustrated representation of the FGF structure. β-Sheets are shown as block arrows. NT, CT represent the N- and C-termini, respectively. Strand β-11 is shown as a waved arrow, as it does not form a conventional β-strand. Strand β-8 is shown twice (once in a light shade) to illustrate the β-barrel at the base of the FGF. (B, C) Structure of FGF-1. Strands are labeled as in (A). (B) β-Barrel shown at the base of the structure. (C) 90° rotation looking down the pseudo-3-fold axis of the FGF (β-barrel at the bottom) illustrates the symmetry in the fold. Figure generated using Pymol (96).

spite of the moderate sequence identity between the solved structures, there is very little structural difference in the core, with a small root-mean-squared difference in the positions of the backbone atoms (Table 3). The most significant structural differences between the members of the FGF family occur in the loops connecting the β-strands: these alter in both length and conformation in the various FGFs. The full significance of all of these changes has yet to be determined; however, these are likely to have an impact on the specificity of binding of the FGFs to the receptors.

Six structures of complexes of one FGF and one FGFR have been solved (37–41). Each of these structures includes the FGFR Ig domains 2 and 3 and the FGF core. All six of these structures show a very similar arrangement of the FGF and FGFR with respect to one another, and of the two domains of the FGFR with respect to one another (Fig. 7). The FGF interacts with both Ig domains of the receptor, and with the linker region between the two domains. The FGF region that interacts with the FGFR primarily consists of four strands of the FGF β-barrel, with loops connecting strands in the β-barrel contributing to the structure. The largest interaction area is formed between Ig domain 3 and the FGF, with an invariant orientation of the Ig domain being invariant between the FGF–FGFR dimer structures (41). Because this is the largest interface between the FGF and the FGFR, Ig domain 3 displays a little more sequence variation than Ig domain 2, and because this is the site of the most significant of the FGFR splice variants, the Ig domain 3–FGF interaction is thought to play the major part in determining the specificity of the FGF for the FGFR (39,41). Whilst the interaction between Ig domain 2 and the FGF is well conserved between most FGF–FGFR pairs (38,39), the one structure that did not include FGF-1 or FGF-2 showed a small alteration in the conformation of Ig domain 2 (Fig. 7) and a change in the nature of the interaction (41). This indicates that the FGF–Ig domain 2 interaction differs for at least some FGF–FGFR pairs, and can be a feature of the specificity of the FGF for its receptor.

Table 3 Sequence Identities and Backbone Atom Root-Mean-Squared Deviations (RMSD) for the Solved FGF Structures

	FGF-1	FGF-2	FGF-4	FGF-7	FGF-9	FGF-10	FGF-12	FGF-19
FGF-1	*****	56	38	37	40	32	33	33
FGF-2	0.517	*****	44	38	41	36	33	36
FGF-4	0.626	0.579	*****	36	44	34	41	34
FGF-7	0.876	0.811	0.848	*****	42	55	35	38
FGF-9	0.627	0.598	0.582	0.866	*****	42	35	32
FGF-10	0.615	0.668	0.533	0.789	0.676	*****	34	34
FGF-12	0.885	0.867	0.800	0.743	0.833	0.763	*****	29
FGF-19	0.985	0.864	0.860	1.067	0.863	0.967	1.089	*****

RMSDs were calculated for structurally equivalent backbone atoms using the program COMPARER (97). An alignment of the core regions of the FGFs was generated using FUGUE (98) to calculate sequence identities. Sequence identities (%) are shown above the diagonal, backbone atom RMSDs (Å) are shown below the diagonal. Data updated from Ref. (20).

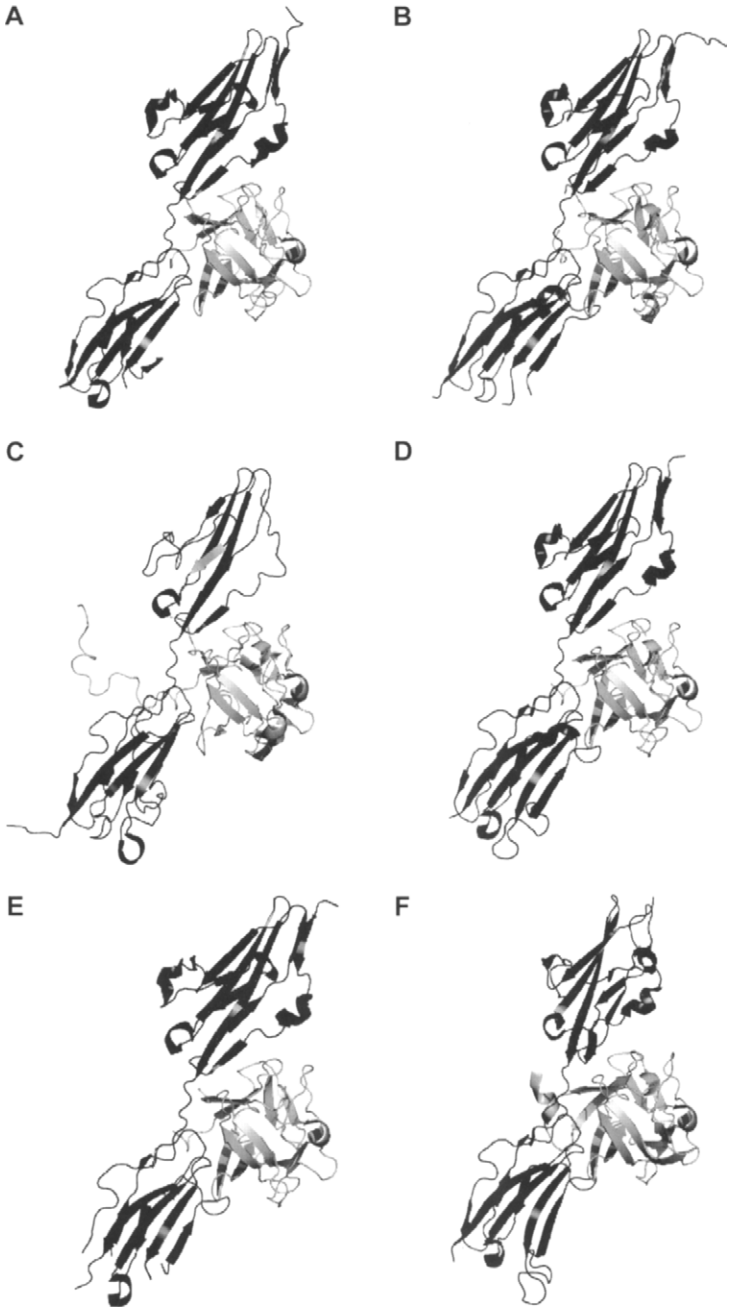

Figure 7 Comparison of the FGF–FGFR structures. The FGFs of the six FGF–FGFR structures were superimposed. An image of each individual FGF–FGFR is shown following the superposition, with FGFR Ig domain 2 at the top of each image, Ig domain 3 at the bottom. FGFs shown in light gray, FGFRs in black. (A) FGF-1–FGFR 1c (39); (B) FGF-1–FGFR 2c (40); (C) FGF-1–FGFR 3c (37); (D) FGF-2–FGFR 1c (38); (E) FGF-2–FGFR 2c (39); (F) FGF-10–FGFR 2b (41). Note that the orientations of the FGFRs are very similar, but that the orientation of Ig domain 2 in (F) is rotated with respect to the others.

D. Structures of FGF and FGFR Complexes with Heparin

The structures of complexes of FGFs (and FGFRs) and heparin have been determined by X-ray crystallography to show the precise binding sites for the heparin, and the nature of the heparin–protein interactions. Two structures have been solved of complexes of heparin fragments and FGFs. The first showed FGF-2 bound to a heparin 6-mer (49), whilst the second demonstrated a complex of FGF-1 with a heparin 10-mer (50). These two structures both suggest that the heparin binding domains of the FGF are located at the apex of the FGF structure. They are formed principally by the region extending around strand β11, with a small contribution from another loop (β1 – β2 loop; Fig. 8). These are the same regions that were identified by site-directed mutagenesis as heparin binding domains (48). The former region is rich in (positively charged) arginine and lysine side chains. The structure of this heparin binding region appears to be optimized to give a high affinity interaction with the polysaccharide: what is generally referred to as strand β11 does not form the regular hydrogen bonding pattern or backbone conformations usually associated with a β-strand (20), whilst NMR measurements of FGF-1 (99) and FGF-2 (100) suggest that the structure is not a regular strand. Thus, it appears that this region of the FGF is structurally altered, compared to the homologous non-heparin binding growth factor interleukin-1β, to accommodate a more stable interaction with the polysaccharide.

Both of the crystal structures showed that the FGF has a minimal structural change upon binding to heparin: the root-mean-squared deviation in the protein main chain is similar to that observed between different crystal structures of the same FGF (50,56). Therefore, it appears that the native FGF fold is primed to interact with heparin, and that the only rearrangements required are in the side chains that interact with heparin and that are close to the binding site. The two structures suggest that the FGF interacts primarily with the heparin sulfate and carboxylate groups, with between three and four side chains interacting per FGF monomer. These side chains are (in FGF-1) Asn18 (from the β1 – β2 loop), Lys118, and one or two of the other residues in the main heparin binding region. These features are relatively well conserved amongst the FGFs, with a potential binding residue in the β1–β2 loop, and positively charged residues in most of the

Figure 8 FGF binding to heparin. (A) FGF-2 interaction with heparin hexamer (49). FGF is shown in the illustrated representation, heparin in stick representation. Heparin sulfur atoms are shown in black. Interaction point between the FGF β1–β2 loop and heparin: dashed arrow. Interaction points between the β10–β11 region and heparin: black arrows. (B) FGF-1 interaction with heparin (50). Interactions shown as in (A). Note that the heparin has a different orientation of the reducing and nonreducing ends with respect to the FGF compared with (A). (C) Detail of the FGF-1–heparin interactions: FGF-1 interacting residues shown as sticks, with nitrogen atoms shown dark gray, oxygen atoms light gray. Black dashed lines: hydrogen bonds to protein side chain atoms; gray lines: hydrogen bonds to protein main-chain amides. Dashed arrow: side chain from the β1–β2 loop interacts with heparin. Gray arrowheads: main-chain nitrogen atoms from the β10–β11 region make hydrogen bonds with heparin.

equivalent positions in the heparin binding region, for almost all of the heparin binding FGFs (i.e., not the FGF-11 subfamily) (20,101). These features are, however, extremely poorly conserved in the FGF-19 subfamily. FGF-19 itself shows a rather weaker interaction with heparin than the canonical FGFs (20). The features of the FGF and heparin suggested by these FGF–heparin structures are therefore likely to be the major determinants of FGF–heparin affinity for all FGFs.

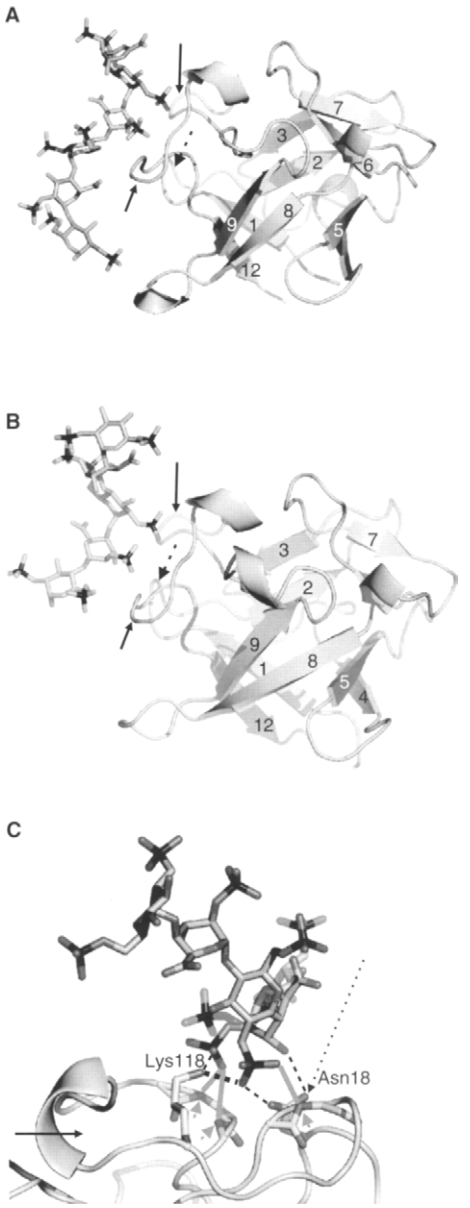

A crucial difference observed between the structure of FGF-1 in complex with a heparin decamer, and the structure of FGF in complex with a heparin hexamer, is that the polarity of the heparin species is reversed between the two structures. A superimposition of the two FGFs shows that the reducing ends of the heparins are at opposite ends of the FGF (101,102). Examination of the structures of FGFs, FGFRs and heparin in a ternary complex (see later) suggest that the conformation of heparin observed with FGF-1 binding to a heparin decamer (50) is the more biologically relevant one: this conformation of heparin appears to be required for the most favorable interaction of the heparin with the FGFR. Since the FGF–FGFR complex appears to have a single conformation that is likely to be favored by all FGF–FGFR pairs, this implies that a single orientation of the heparin–FGF interaction is likely to exist for all the FGFs.

The structure of FGF-1 in complex with a heparin decamer demonstrates a dimer of FGFs (Fig. 9). This dimer is constructed in a most unusual manner, with a protein forming a dimer on a saccharide without any contact at all between the protein molecules: the only contacts between the molecules in the complex are the FGF–heparin interactions. This suggests a mechanism by which the FGF may be dimerized, so that the binding of the FGFs to FGFRs may dimerize or alter the conformation of the FGFRs, and so allow the signal of the FGF to be passed inside the cell. The crystal that was used to solve this structure contained four separate FGF-1 dimers upon heparin, which showed a variety of conformations for the position of the second FGF in relation to the first FGF (50). This suggests that there may be a number of favorable conformations for the location of the second molecule, allowing the most optimal binding of the FGF to the heparin, so that the FGF may then bind also to FGFRs. However, this may also be a consequence of the crystallization process, with the alternative conformations required to form the crystal.

Understanding of the role of HS in FGF signaling has been greatly advanced by two crystal structures of complexes of FGFs, FGFRs, and heparin (Fig. 10) (10,11). The first of these complexes (10) describes a complex of two FGF-1 molecules, two FGFR 2 molecules, and one heparin decamer; the second (11) describes a complex of two molecules each of FGF-2, FGFR 1, and heparin decamers, and so the complexes differ in their stoichiometry as well as the FGFs and FGFRs used. The two complexes appear considerably dissimilar: the location of the FGFRs and the heparin in particular are very different. The FGFRs are broadly central and the heparin peripheral in the 2:2:2 FGF-2:FGFR 1:heparin structure, whilst the 2:2:1 FGF-1:FGFR 2:heparin structure shows the heparin as the center of the complex whilst the FGFRs are at the extremes. However, the interaction between the FGF-1, the Ig domain 2 of the FGFR, and heparin is well conserved between the two complexes (Fig. 11) (102). This conservation, in the face of the apparent differences between the two complexes, strongly suggests that these interactions are physiologically relevant ones. This has considerable implications for the interaction of HS with the FGFs and the FGFRs. The structures confirm that the orientation of heparin with respect to the FGF observed in the FGF-1 dimer on

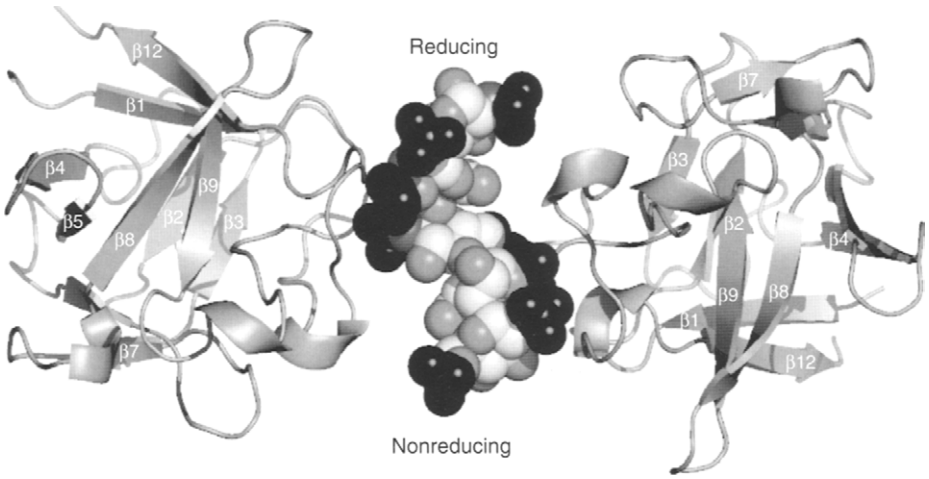

Figure 9 Heparin decamers induce the formation of dimers of FGF-1 (50). FGF-1 shown as in illustration, heparin as an all-atom sphere model, with sulfates colored black. The reducing and nonreducing ends of the heparin are labeled. Notice that similar regions of the FGF-1 interact with heparin on both sides of the heparin molecule, and that there is no protein–protein interaction in the complex.

a heparin decamer (50) is likely to be the physiologically relevant one. Furthermore, the structures demonstrate the precise nature of the binding of heparin to the FGFR. In both structures, all of the heparin interactions with FGFR are found in the Ig domain 2. The contacts that are made involve the heparin sulfate and carboxylate groups and the side chains of residues in the "K18K loop", most of which are lysines or arginines. In one structure, hydrogen bonds were also observed between sulfate groups and protein main chain amide groups (10). Therefore, the primary energetic contribution is from charge–charge and hydrogen bonding interactions involving the sulfate groups of the heparin, and lysine and arginine side chains together with the protein main chain. These data show that the interaction between the heparin and the FGFR is similar in nature to that between heparin and FGFs.

As the two complexes share a common binding site for heparin on both the FGF and the FGFR, this suggests that these sites are likely to be responsible for generating the affinity for heparin throughout both families. Although the various FGF–FGFR dimer structures show flexibility in the orientation of FGFR Ig domain 2 relative to the FGF (41), this is sufficiently limited that the binding to heparin is unlikely to be severely affected. These findings provide a scaffold on which the various data regarding the required modifications of HS that are most favorable for binding to each member of the FGF and FGFR families, and the protein sequences of the FGFs and FGFRs, may be brought together to gain insight into the binding of

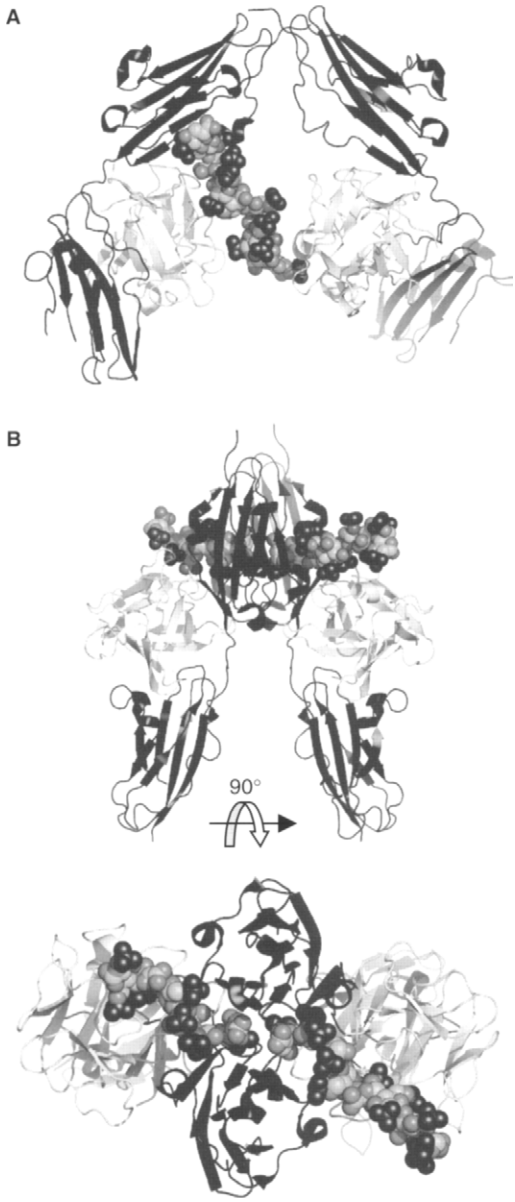

Figure 10 Ternary complexes of FGF, FGFR, and heparin. FGFs shown as light illustrations – FGFRs as dark illustrations – heparin as all-atom sphere models, with sulfates colored dark gray. FGFRs are shown with Ig domain 2 at the top of the image, Ig domain 3 at the bottom of the image. (A) Complex of 2 FGF-1:2 FGFR 2c:1 heparin decamer (10). (B) Complex of 2 FGF-2:2 FGFR 1c:2 heparin decamers (11). Rotation of 90° around the horizontal axis (FGFR Ig domain 2 nearest) shows the twofold symmetry of this complex, and that two molecules of heparin meet at the apex of the structure.

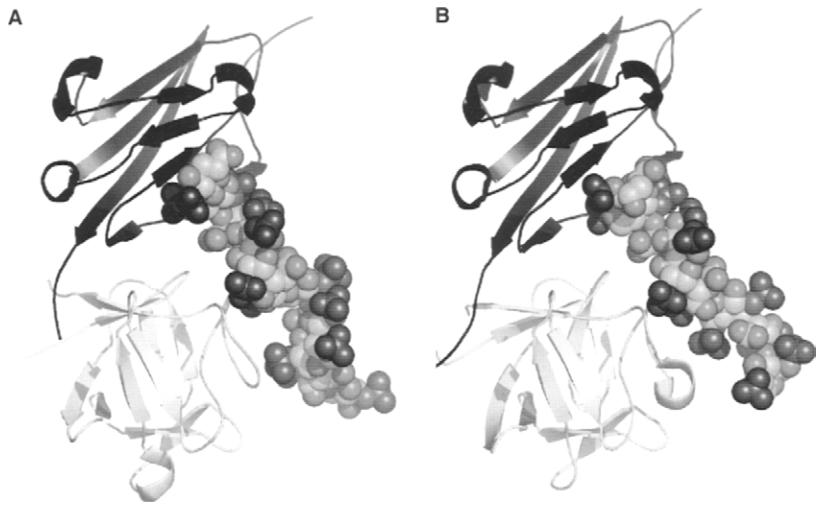

Figure 11 A conserved unit of 1 FGF, 1 FGFR Ig domain 2, and one heparin molecule are common to the two structures of ternary complexes of FGF, FGFR, and heparin (101). FGF shown as light illustrations – FGFR as dark illustrations – heparin as all-atom sphere model, with sulfates colored dark gray. Structures were superimposed using the FGF units, with separate images of each FGF–FGFR–heparin complex shown following the superposition. Note the similarity in the position of the heparin, and the orientation of the FGFR Ig domain. (A) 2 FGF-1–2 FGFR 2c–heparin structure; (B) 2 FGF-2–2 FGFR 1c–2 heparin structure.

FGFs and FGFRs whose structures have not yet been solved in complex with heparin.

Within the differences between the two structures of ternary complexes of FGFs, FGFRs and heparin lie potential additional interactions between the protein and the heparin, which are involved in generating stable complexes involving two FGFRs. The structure of the 2:2:1 FGF-1:FGFR 2:heparin complex shows an FGF-1 dimer upon the heparin decamer with no protein–protein interaction between the two FGFs: the dimerization of the FGF-1 (and therefore, the FGFR 2) is mediated solely by heparin (Fig. 12). The second FGF molecule in the complex binds to heparin using the β10 – β11 region, as has been observed in the other FGF–heparin structures, and makes additional hydrogen bonds via the preceding loop. This structure suggests that HS fragments that are competent to form complexes with FGFs and FGFRs that will lead to signal transduction will be at least eight saccharide units in length, and that the sulfations that are required will be spread along the length of this octasaccharide fragment.

In contrast, the structure of a 2:2:2 FGF-2:FGFR 1:heparin complex (11) shows the dimerization being principally achieved by interactions between the FGFR in each FGF–FGFR pair, and the FGF in the opposing pair (Fig. 13). The additional interactions would appear sufficient to drive the formation of a complex

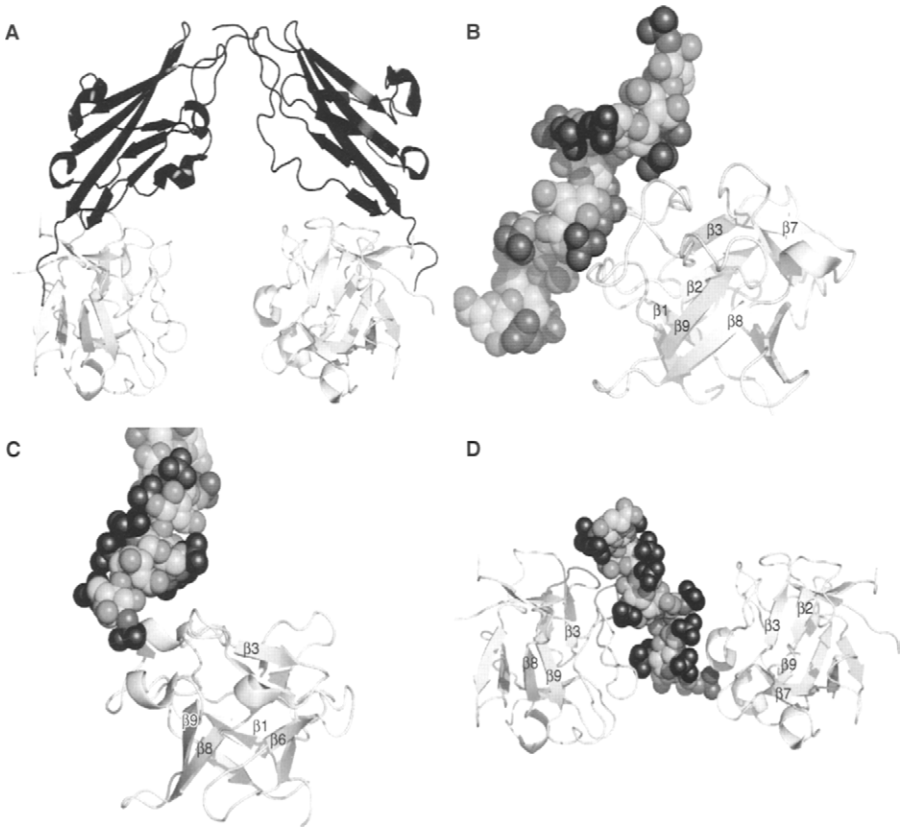

Figure 12 Formation of an FGFR dimer in the 2 FGF:2 FGFR:1 heparin model (10). FGFs shown as light illustration, FGFRs as dark illustration, heparin as all-atom sphere model with sulfates colored dark gray. FGFR Ig domain 2 only is shown for clarity. (A) Structure with the heparin molecule removed shows that there is very little protein–protein contact – not sufficient to form a complex. (B, C) Interaction of the two FGFs with the heparin molecule. Each FGF is rotated to show the β-barrel at the base of the structure; β-strands are annotated for comparison: (B) represents the FGF bound to the FGFR that also interacts with heparin; (C) represents the FGF bound to the FGFR that does not interact with the heparin. Note how the heparin interacts with the same regions of the two FGFs, but that the conformation of the heparin is somewhat different. Part (D) focuses on the two FGFs bound to the heparin. Notice that the orientation of the FGF on the right is dissimilar to the equivalent FGF in the FGF-1–heparin structure (Fig. 9) (50): in each case, the two FGFs are related by a 180° rotation, but the axis of rotation differs between the two cases.

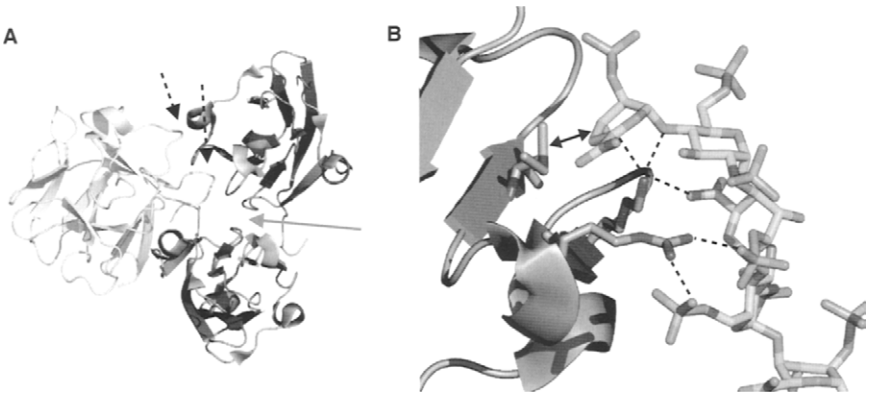

Figure 13 Formation of an FGFR dimer in the 2 FGF:2 FGFR:2 heparin model (11). (A) View down the axis of symmetry of the complex highlights protein–protein interactions driving the complex formation. FGF shown as light illustrations: FGFRs as dark illustrations. Only one FGF, and the FGFR Ig domain 2s, are shown for clarity. The complex is formed by an FGFR–FGFR interaction (gray arrow), and two interactions between each FGFR and the FGF primarily bound to the other FGFR (black dashed arrows). (B) Interactions between each FGFR and the heparin primarily bound to the other FGFR. Heparin shown as all-atom sticks model, FGFR Ig domain 2 shown as dark illustration, with heparin binding residues shown as all-atom sticks model, with nitrogen atoms in black. Interactions consist of hydrogen bonds between FGFR lysine and arginine side chains and heparin (dashed lines), and hydrophobic interaction between FGFR isoleucine side chain and heparin (double headed arrow).

of the two FGF–FGFR dimers under some conditions. However, the complex formed contains an extremely positively charged canyon (38,40), and it appears that one role of the heparin is to help neutralize this positive charge. In this complex, the heparin makes additional interactions with the second FGFR, largely involving hydrogen bonds between sulfate ions and positively charged side chains. This structure predicts that a hexasaccharide would be the smallest heparin fragment capable of forming the complex, and that this hexasaccharide would require a high level of sulfation, as it is interacting with both FGFRs and the FGF. A more controversial conclusion that has been drawn from this structure is that the FGF–FGFR–HS complex will form at the ends of two molecules of HS. In the structure, the two heparin molecules modeled are found with their nonreducing ends meeting at a central point in the complex (Fig. 10b). For this to represent a physiological state, it would require that the observed heparins are analogous to the termini of the HS chains. Two models that have been proposed for how this might occur are that the FGF–FGFR complexes might form at any point along the HS chain, and then migrate to the end to form a complex with another FGF–FGFR–HS complex (103); or that the HS chains could be cleaved *in vivo* at S-domains, resulting in a higher concentration of sulfation rich HS ends that would be the sites of FGF signaling (104). However, neither of these models has been experimentally validated.

Further experimental data have supported both of the structural models. Firstly, several of the crystal structures show the pair of FGF–FGFR dimers in the form observed in the 2:2:2 FGF-2:FGFR 1:heparin structure (10,40,41), including the crystal structure from which the alternative model was proposed. A study of FGF:FGFR:heparin complexes using gel mobility shift assays concluded that the 2:2:2 FGF-2:FGFR 1:heparin model was most consistent with all of their data (105). A comparison of the two complexes by biophysical methods (81) demonstrated that both of the complexes could be formed from identical protein preparations. However, mass spectrometry demonstrated that for both complexes, the most abundant species had one molecule of heparin only. A careful study of the 2:2:2 FGF-2:FGFR 1:heparin complex demonstrated that mutagenesis of the FGF side chains that form additional interactions with a second FGFR in the dimer reduces the potency of FGF-10 to induce DNA synthesis in a normally responsive cell line (106). This study also presented semi-quantitative mass spectrometry data supporting the role of a contact between the FGFRs in forming the ternary complex. These studies suggest that both of the complexes observed in these crystal structures can be stably formed in solution. Both of the proposed models for the FGF–FGFR–heparin complex explain some of the wide range of data that has been obtained using *in vitro* and cell-based studies for this system, and fail to explain other data. It would appear that both models may have relevance to the formation of complexes upon the cell surface, as the true signaling entities for transmembrane signaling appear to be large aggregates of activated receptors, and multiple interactions between the molecules may be required at the extracellular surface. Whilst some findings have cast doubt on specific aspects of each model [e.g., a *cis*-proline in the 2:2:1 FGF:FGFR:heparin model (106), or the presence of a second heparin molecule in the 2:2:2 FGF:FGFR:heparin model (80)], the overall architectures are both likely to be relevant, and many of the interactions with heparin appear to be in agreement between the two models.

VI. Conclusions and Future Perspectives

The FGF–FGFR–HS system is amongst the richest extracellular signaling systems in terms of its complexity and specificity. The introduction of HS as a third part of the signaling complex, required for the biological activity, vastly increases the capacity for cells to alter their specificities for the FGFs that will bind, and so to tune the signaling system appropriately. When this is added to the variations in affinities that the seven FGFR splice forms have for the 18 signaling FGFs, and to the differing cellular responses that are observed when differing doses of FGFs are added, the capacity for exquisite regulation is immense. Our current understanding of the system demonstrates the crucial role of HS: crystal structures show how heparin intimately binds to both FGF and FGFR, and brings together two FGF–FGFR dimers to form a ternary complex. Biophysical studies have shown that the heparin is key to the capture of FGF upon the cell surface, and that heparin dramatically increases the affinity of the FGF for the FGFR. The studies of heparin

fragments have demonstrated that each FGF and FGFR has a different affinity for sulfation patterns upon the polysaccharide, and that subtle alterations to the polysaccharide can dramatically affect the cellular responses to FGF signaling.

Future advances in our understanding of the FGF–FGFR–HS system are likely to involve moves towards the physiological state. This will involve a general shift towards using HS rather than heparin, as improvements in technologies permit the HS fragments used to be characterized in smaller quantities. A more thorough analysis of the interactions with HS of FGFs other than FGF-1 and FGF-2 will give a broader view of the binding of the FGFs to HS. Studies of the HS complement of individual cell types, and a correlation with the FGFs that the cells are exposed to, will give a broader view of the likely responsiveness of cells to each FGF. Finally, at some stage it will be necessary to attempt to view the FGF complexes that are found upon an active cell, so that the true nature of the signaling entities can be accurately determined. The combination of these approaches may allow the development of HS analogues that are active in specifically inhibiting single FGF–FGFR pairs, which could then be used to combat the various diseases associated with the FGF family.

References

1. Ornitz DM. FGFs, heparan sulphate and FGFRs: complex interactions essential for development. Bioessays 2000; 22:108–112.
2. Powers CJ, McLeskey SW, Wellstein A. Fibroblast growth factors, their receptors and signaling. End-Rel Cancer 2000; 7:165–197.
3. Armelin HA. Pituitary extracts and steroid hormones in the control of 3T3 cell growth. Proc Nat Acad Sci USA 1973; 70:2702–2706.
4. Ornitz DM, Itoh N. Fibroblast growth factors. Genome Biol 2001; 2:reviews3005.1–3005.12.
5. Harmer NJ, Chirgadze D, Kim KH, Pellegrini L, Blundell TL. The structural biology of growth factor receptor activation. Biophys Chem 2003; 100:545–553.
6. Lin X. Functions of heparan sulphate proteoglycans in cell signaling during development. Development 2004; 131:6009–6021.
7. Rapraeger AC, Krufka A, Olwin BB. Requirement of heparan sulfate for bFGF-mediated fibroblast growth and myoblast differentiation. Science 1991; 252:1705–1708.
8. Ornitz DM, Yayon A, Flanagan JG, Svahn CM, Levi E, Leder P. Heparin is required for cell-free binding of basic fibroblast growth factor to a soluble receptor and for mitogenesis in whole cells. Mol Cell Biol 1992; 12:240–247.
9. Walker A, Turnbull JE, Gallagher JT. Specific heparan sulfate saccharides mediate the activity of basic fibroblast growth factor. J Biol Chem 1994; 269:931–935.
10. Pellegrini L, Burke DF, von Delft F, Mulloy B, Blundell T. Crystal structure of fibroblast growth factor receptor ectodomain bound to ligand and heparin. Nature 2000; 407:1029–1034.

11. Schlessinger J, Plotnikov AN, Ibrahimi OA, Eliseenkova AV, Yeh BK, Yayon A, Linhardt RJ, Mohammadi M. Crystal structure of a ternary FGF–FGFR–heparin complex reveals a dual role for heparin in FGFR binding and dimerization. Mol Cell 2000; 6:743–750.
12. Sano H, Forough R, Maier JAM, Case JP, Jackson A, Engleka K, Macaig T, Wilder RL. Detection of high levels of heparin binding growth factor-1 (acidic fibroblast growth factor) in inflammatory arthritic joints. J Cell Biol 1990; 110:1417–1426.
13. Nedvetzki S, Golan I, Assayag N, Gonen E, Caspi D, Gladnikoff M, Yayon A, Naor D. A mutation in a CD44 variant of inflammatory cells enhances the mitogenic interaction of FGF with its receptor. J Clin Invest 2003; 111:1211–1220.
14. Itoh N, Ornitz DM. Evolution of the FGF and FGFR gene families. Trends Genet 2004; 20:563–569.
15. The ADHR Consortium. Autosomal dominant hypophosphataemic rickets is associated with mutations in FGF23. Nat Genet 2000; 26:345–348.
16. Gospodarowicz D. Localisation of a fibroblast growth factor and its effect alone and with hydrocortisone on 3T3 cell growth. Nature 1974; 249:123–127.
17. Detillieux KA, Sheikh F, Kardami E, Cattini PA. Biological activites of fibroblast growth factor-2 in the adult myocardium. Cardiovasc Res 2003; 57:8–19.
18. Sutherland D, Samakovlis C, Krasnow MA. Branchless encodes a *Drosophila* FGF homolog that controls tracheal cell migration and the pattern of branching. Cell 1996; 87:1091–1101.
19. Burdine RD, Chen EB, Kwok SF, Stern MJ. *egl-17* encodes an invertebrate fibroblast growth factor family member required specifically for sex myoblast migration in *Caenorhabditis elegans*. Proc Nat Acad Sci USA 1997; 94: 2433–2437.
20. Harmer NJ, Chirgadze D, Pellegrini L, Fernandez-Recio J, Blundell TL. The crystal structure of fibroblast growth factor (FGF) 19 reveals novel features of the FGF family and offers a structural basis for its unusual receptor affinity. Biochemistry 2004; 43:629–640.
21. Innis CA, Shi J, Blundell TL. Evolutionary trace analysis of TGF-beta and related growth factors: implications for site-directed mutagenesis. Prot Engin 2000; 13:839–847.
22. Miller DL, Ortega S, Bashayan O, Basch R, Basilico C. Compensation by fibroblast growth factor 1 (FGF1) does not account for the mild phenotypic defects observed in FGF2 null mice. Mol Cell Biol 2000; 20:2260–2268.
23. Folkman J, Shing J. Angiogenesis. J Biol Chem 1992; 267:10931–10934.
24. Feldman B, Poueymirou W, Papaioannou VE, DeChiara TM, Goldfarb M. Requirement of FGF-4 for postimplantation mouse development. Science 1995; 267:246–249.
25. Han JK, Martin GR. Embryonic expression of FGF-6 is restricted to the skeletal muscle lineage. Dev Biol 1993; 158:549–554.
26. Naski MC, Ornitz DM. FGF signalling in skeletal development. Frontiers Biosci 1998; 3:d781–d794.
27. Meyers EN, Lewandoski M, Martin GR. An Fgf8 mutant allelic series generated by Cre- and Flp-mediated recombination. Nat Genet 1998; 18:136–141.

28. Min H, Danilenko DM, Scully S, Bolon B, Ring DB, Tarpley JE, DeRose M, Simonet WS. FGF-10 is required for both limb and lung development and exhibits striking functional similarity to Drosophila branchless. Genes Dev 1998; 12:3156–3161.
29. Igarashi M, Finch PW, Aaronson SA. Characterization of recombinant human fibroblast growth factor (FGF)-10 reveals functional similarities with keratinocyte growth factor (FGF-7). J Biol Chem 1998; 273:13230–13235.
30. Olsen SK, Garbi M, Zampieri N, Eliseenkova AV, Ornitz DM, Glodfarb M, Mohammadi M. FHFs share structural but not functional homology to FGFs. J Biol Chem 2003; 278:34226–34236.
31. Schoorlemmer J, Goldfarb M. Fibroblast growth factor homologous factors are intracellular signaling proteins. Curr Biol 2001; 11:793–797.
32. Schlessinger J. Common and distinct elements in cellular signaling via EGF and FGF receptors. Science 2004; 306:1506–1507.
33. Sleeman M, Fraser J, McDonald M, Yuan S, White D, Grandison P, Kumble K, Watson JD, Murison JG. Identification of a new fibroblast growth factor, FGFR5. Gene 2001; 271:171–182.
34. Burke DF, Wilkes D, Blundell TL, Malcolm S. Fibroblast growth factor receptors: lessons from the genes. Trends Biochem Sci 1998; 23:59–62.
35. Xu J, Nakahara M, Crabb JW, Shi E, Matou Y, Fraser M, Kan M, Hou J, McKeehan WL. Expression and immunochemical analysis of rat and human fibroblast growth factor receptor (flg) isoforms. J Biol Chem 1992; 267:17792–17803.
36. Wang F, Kan M, Xu J, Yan G, McKeehan WL. Ligand-specific structural domains in the fibroblast growth factor receptor. J Biol Chem 1995; 270:10222–10230.
37. Olsen SK, Ibrahimi OA, Raucci A, Zhang F, Eliseenkova AV, Yayon A, Basilico C, Linhardt RJ, Schlessinger J, Mohammadi M. Insights into the molecular basis for fibroblast growth factor receptor autoinhibition and ligand-binding promiscuity. Proc Nat Acad Sci USA 2004; 101:935–1040.
38. Plotnikov AN, Schlessinger J, Hubbard SR, Mohammadi M. Structural basis for FGF receptor dimerization and activation. Cell 1999; 98:641–650.
39. Plotnikov AN, Hubbard SR, Schlessinger J, Mohammadi M. Crystal structures of two FGF–FGFR complexes reveal the determinants of ligand–receptor specificity. Cell 2000; 101:413–424.
40. Stauber DJ, DiGabriele AD, Hendrickson WA. Structural interactions of fibroblast growth factor receptor with its ligands. Proc Nat Acad Sci USA 2000; 97:49–54.
41. Yeh BK, Igarashi M, Eliseenkova AV, Plotnikov AN, Sher I, Ron D, Aaronson SA, Mohammadi M. Structural basis by which alternative splicing confers specificity in fibroblast growth factor receptors. Proc Nat Acad Sci USA 2003; 100:2266–2271.
42. Kan M, Wang F, Xu J, Crabb JW, Hou J, McKeehan WL. An essential heparin-binding domain in the fibroblast growth factor receptor kinase. Science 1993; 259:1918–1921.
43. Vickers SM, Huang Z-Q, MacMillan-Crow L, Greendorfer JS, Thompson JA. Ligand activation of alternatively spliced fibroblast growth factor receptor-1 modulates pancreatic adenocarcinoma cell malignancy. J Gastrointest Surg 2002; 6:546–553.

44. Ornitz DM, Xu J, Colvin JS, McEwan DG, MacArthur CA, Coulier F, Gao G, Goldfarb M. Receptor specificity of the fibroblast growth factor family. J Biol Chem 1996; 271:15292–15297.
45. Schlessinger J. Cell signaling by receptor tyrosine kinases. Cell 2000; 103: 211–225.
46. Li X, Brunton VG, Burgar HR, Wheldon LM, Heath JK. FRS2-dependent SRC activation is required for fibroblast growth factor receptor-induced phosphorylation of Sprouty and suppression of ERK activation. J Cell Sci 2004; 117:6007–6017.
47. Powell AK, Yates EA, Fernig DG, Turnbull JE. Interactions of heparin/heparan sulfate with proteins: appraisal of structural factors and experimental approaches. Glycobiology 2004; 14:17R–30R.
48. Thompson LD, Pantoliano MW, Springer BA. Energetic characterization of the basic fibroblast growth factor–heparin interaction: identification of the heparin binding domain. Biochemistry 1994; 33:3831–3840.
49. Faham S, Hileman RE, Fromm JR, Linhardt RJ, Rees DC. Heparin structure and interactions with basic fibroblast growth factor. Science 1996; 271:1116–1120.
50. DiGabriele AD, Lax I, Chen DI, Svahn CM, Jaye M, Schlessinger J, Hendrickson WA. Structure of a heparin-linked biologically active dimmer of fibroblast growth factor. Nature 1998; 393:812–817.
51. Kreuger J, Salmivirta M, Sturiale L, Giménez-Gallego G, Lindahl U. Sequence analysis of heparan sulfate epitopes with graded affinities for fibroblast growth factors 1 and 2. J Biol Chem 2001; 276:30744–30754.
52. Ashikari-Hada S, Habuchi H, Kariya Y, Itoh N, Reddi AH, Kimata K. Characterization of growth factor-binding structures in heparin/heparan sulfate using an octasaccharide library. J Biol Chem 2004; 279:12346–12354.
53. Guimond S, Maccarana M, Olwin BB, Lindahl U, Rapraeger AC. Activating and inhibitory heparin sequences for FGF-2 (basic FGF). Distinct requirements for FGF-1, FGF-2, and FGF-4. J Biol Chem 1993; 268:23906–23914.
54. Bellosta P, Iwahori A, Plotnikov AN, Eliseenkova AV, Basilico C, Mohammadi M. Identification of receptor and heparin binding sites in fibroblast growth factor 4 by structure-based mutagenesis. Mol Cell Biol 2001; 21:5946–5957.
55. Allen BL, Filla MS, Rapraeger AC. Role of heparan sulfate as a tissue-specific regulator of FGF-4 and FGF receptor recognition. J Cell Biol 2001; 155: 845–857.
56. Ye S, Luo Y, Lu W, Jones RB, Linhardt RJ, Capila I, Toida T, Kan M, Pelletier H, McKeehan WL. Structural basis for interaction of FGF-1, FGF-2, and FGF-7 with different heparan sulfate motifs. Biochemistry 2001; 40:14429–14439.
57. Loo B-M, Salmivirta M. Heparin/heparan sulfate domains in binding and signaling of fibroblast growth factor 8b. J Biol Chem 2002; 277:32616–32623.
58. Ford-Perriss M, Guimond SE, Greferath U, Kita M, Grobe K, Habuchi H, Kimata K, Esko JD, Murphy M, Turnbull JE. Variant heparan sulfates synthesized in developing mouse brain differentially regulate FGF signaling. Glycobiology 2002; 12:721–727.

59. Powell AK, Fernig DG, Turnbull JE. Fibroblast growth factor receptors 1 and 2 interact differently with heparin/heparan sulfate. J Biol Chem 2002; 277:28554–28563.
60. Gao G, Goldfarb M. Heparin can activate a receptor tyrosine kinase. EMBO J 1995; 14:2183–2190.
61. Loo B-M, Kreuger J, Jalkanen M, Lindahl U, Salmivirta M. Binding of heparin/heparan sulfate to fibroblast growth factor receptor 4. J Biol Chem 2001; 276:16868–16876.
62. Pantoliano MW, Horlick RA, Springer BA, Van Dyk DE, Tobery T, Wetmore DR, Lear JD, Nahapetian AT, Bradley JD, Sisk WP. Multivalent ligand–receptor binding interactions in the fibroblast growth factor system produce a cooperative growth factor and heparin mechanism for receptor dimerization. Biochemistry 1994; 33:10229–10248.
63. Delehedde M, Seve M, Sergeant N, Wartelle I, Lyon M, Rudland PS, Fernig DG. Fibroblast growth factor-2 stimulation of $p42/44^{MAPK}$ phosphorylation and IkB degradation is regulated by heparan sulfate/heparin in rat mammary fibroblasts. J Biol Chem 2000; 275:33905–33910.
64. Deepa SS, Umehara Y, Higashiyama S, Itoh N, Sugahara K. Specific molecular interactions of oversulfated chondroitin sulfate E with various heparin-binding growth factors. J Biol Chem 2002; 277:43707–43716.
65. Villena J, Brandan E. Dermatan sulfate exerts an enhanced growth factor response on skeletal muscle satellite cell proliferation and migration. J Cell Physiol 2004; 198:169–178.
66. Nandini CD, Mikami T, Ohta M, Itoh N, Akiyama-Nambu F, Sugahara K. Structural and functional characterization of oversulfated chondroitin sulfate/dermatan sulfate hybrid chains from the notochord of hagfish. Neuritogenic and binding activities for growth factors and neurotrophic factors. J Biol Chem 2004; 279:50799–50809.
67. Delehedde M, Lyon M, Gallagher J, Rudland PS, Fernig DG. Fibroblast growth factor-2 binds to small heparin-derived oligosaccharides and stimulates a sustained phosphorylation of p42/44 mitogen-activated protein kinase and proliferation of rat mammary fibroblasts. Biochem J 2002; 366:235–244.
68. Maccarana M, Casu B, Lindahl U. Minimal sequence in heparin/heparan sulfate required for binding of basic fibroblast growth factor. J Biol Chem 1993; 268:23898–23905.
69. Ornitz DM, Herr AB, Nilsson M, Westman J, Svahn CM, Waksman G. FGF binding and FGF receptor activation by synthetic heparan-derived di- and trisaccharides. Science 1995; 268:432–436.
70. Ostrovsky O, Berman B, Gallagher J, Mulloy B, Fernig DG, Delehedde M, Ron D. Differential effects of heparin saccharides on the formation of specific fibroblast growth factor (FGF) and FGF receptor complexes. J Biol Chem 2002; 277:2444–2453.
71. Berry D, Shriver Z, Venkataraman G, Sasisekharan R. Quantitative assessment of FGF regulation by cell surface heparan sulfates. Biochem Biophys Res Commun 2004; 314:994–1000.
72. Wang S, Ai X, Freeman SD, Pownall ME, Lu Q, Kessler DS, Emerson Jr CP. QSulf1, a heparan sulfate 6-*O*-endosulfatase, inhibits fibroblast growth factor signaling in mesoderm indction and angiogenesis. Proc Nat Acad Sci USA 2004; 101:4833–4838.

73. Merry CL, Bullock SL, Swan DC, Backen AC, Lyon M, Beddington RS, Wilson VA, Gallagher JT. The molecular phenotype of heparan sulfate in the Hs2st−/− mutant mouse. J Biol Chem 2001; 276:35429–35434.
74. Toyoda H, Kinoshita-Toyoda A, Fox B, Selleck SB. Structural analysis of glycosaminoglycans in animals bearing mutations in sugarless, sulfateless, and tout-velu. Drosophila homologues of vertebrate genes encoding glycosaminoglycan biosynthetic enzymes. J Biol Chem 2000; 275:21856–21861.
75. Luders F, Segawa H, Stein D, Selva EM, Perrimon N, Turco SJ, Hacker U. Slalom encodes an adenosine 3′-phosphate 5′-phosphosulfate transporter essential for development in Drosophila. EMBO J 2003; 22:3635–3644.
76. Allen BL, Rapraeger AC. Spatial and temporal expression of heparan sulfate in mouse development regulates FGF and FGF receptor mediated assembly. J Cell Biol 2003; 163:637–648.
77. Spivak-Kroizman T, Lemmon MA, Dikic I, Ladbury JE, Pinchasi D, Huang J, Jaye M, Crumley G, Schlessinger J, Lax I. Heparin-induced oligomerization of FGF molecules is responsible for FGF receptor dimerization, activation, and cell proliferation. Cell 1994; 79:1015–1024.
78. Anderson J, Burns HD, Enriquez-Harris P, Wilkie AOM, Heath JK. Apert syndrome mutations in fibroblast growth factor receptor 2 exhibit increased affinity for FGF ligand. Hum Mol Genet 1998; 7:1475–1483.
79. Ibrahimi OA, Zhang F, Eliseenikova AV, Linhardt RJ, Mohammadi M. Proline to arginine mutations in FGF receptors 1 and 3 result in Pfeiffer and Muenke craniosynostosis syndromes through enhancement of FGF binding affinity. Hum Mol Genet 2004; 13:69–78.
80. Ibrahimi OA, Zhang F, Hrstka SC, Mohammadi M, Linhardt RJ. Kinetic model for FGF, FGFR, and proteoglycan signal transduction complex assembly. Biochemistry 2004; 43:4724–4730.
81. Harmer NJ, Ilag LL, Pellegrini L, Mulloy B, Robinson CV, Blundell TL. Towards a resolution of the stoichiometry of the fibroblast growth factor (FGF)–FGF receptor–heparin complex. J Mol Biol 2004; 339:821–834.
82. Anderson AC. The process of structure-based drug design. Chem Biol 2003; 10:787–797.
83. Mulloy B, Forster MJ. Conformation and dynamics of heparin and heparan sulfate. Glycobiology 2000; 10:1147–1156.
84. Mulloy B, Forster MJ, Jones C, Davies DB. NMR and molecular-modelling studies of the solution conformation of heparin. Biochem J 1993; 293:849–858.
85. Mulloy B, Forster MJ, Jones C, Drake AF, Johnson EA, Davies DB. The effect of variation of substitution on the solution conformation of heparin: a spectroscopic and molecular modelling study. Carbohydr Res 1994; 255:1–26.
86. Mikhailov D, Mayo KH, Vlahov IR, Toida T, Pervin A, Linhardt RJ. NMR solution conformation of heparin-derived tetrasaccharide. Biochem J 1996; 318:93–102.
87. Mikhailov D, Linhardt RJ, Mayo KH. NMR solution conformation of heparin-derived hexasaccharide. Biochem J 1997; 328:51–61.
88. Stevens EJ, Sathyanarayama BK. Potential energy surfaces of cellobiose and maltose in aqueous solution: a new treatment of disaccharide optical rotation. J Am Chem Soc 1989; 111:4149–4154.

89. Dowd MK, French AD, Reilly PJ. Conformational analysis of the anomeric forms of sophorose, laminarabiose and cellobiose using MM3. Carbohydr Res 1992; 233:15–34.
90. Dowd MK, Zeng J, French AD, Reilly PJ. Conformational analysis of the anomeric forms of kojibiose, nigerose and maltose using MM3. Carbohydr Res 1992; 230:223–244.
91. Eriksson AE, Cousens LS, Weaver LH, Matthews BW. Three-dimensional structure of human basic fibroblast growth factor. Proc Nat Acad Sci USA 1991; 88:3441–3445.
92. Zhu X, Komiya H, Chirino A, Faham S, Fox GM, Arakawa T, Hsu BT, Rees DC. Three-dimensional structures of acidic and basic fibroblast growth factors. Science 1991; 251:90–93.
93. Zhang JD, Cousens LS, Barr PJ, Sprang SR. Three-dimensional structure of human basic fibroblast growth factor, a structural homolog of interleukin 1 beta. Proc Nat Acad Sci USA 1991; 88:3446–3450.
94. Hecht HJ, Adar R, Hofmann B, Bogin O, Weich H, Yayon A. Structure of fibroblast growth factor 9 shows a symmetric dimer with unique receptor- and heparin-binding interfaces. Acta Crystallogr D: Biol Crystallogr 2001; 57:378–384.
95. Plotnikov AN, Eliseenkova AV, Ibrahimi OA, Shriver Z, Sasisekharan R, Lemmon MA, Mohammadi M. Crystal structure of fibroblast growth factor 9 reveals regions implicated in dimerization and autoinhibition. J Biol Chem 2001; 276:4322–4329.
96. DeLano WL. The Pymol Molecular Graphics System. San Carlos, CA: DeLano Scientific, 2002.
97. Sali A, Blundell TL. Definition of general topological equivalence in protein structures: a procedure involving comparison of properties and relationships through simulated annealing and dynamic programming. J Mol Biol 1990; 212:403–428.
98. Shi J, Blundell TL, Mizuguchi K. FUGUE: sequence–structure homology recognition using environment-specific substitution tables and structure-dependent gap penalties. J Mol Biol 2001; 310:243–257.
99. Ogura K, Nagata K, Hatanaka H, Habuchi H, Kimata K, Tate S-I, Ravera MW, Jaye M, Schlessinger J, Inagaki K. Solution structure of human acidic fibroblast growth factor and interaction with heparin-derived hexasaccharide. J Biomol NMR 1999; 13:11–24.
100. Moy FJ, Seddon AP, Campell EB, Bohlen P, Powers R. 1H, 15N, 13C and 13CO assignments and secondary structure determination of basic fibroblast growth factor using 3D heteronuclear NMR spectroscopy. J Biomol NMR 1995; 6:245–254.
101. Faham S, Linhardt RJ, Rees DC. Diversity does make a difference: fibroblast growth factor-heparin interactions. Curr Opin Struct Biol 1998; 8:578–586.
102. Pellegrini L. Role of heparan sulphate in fibroblast growth factor signalling: a structural view. Curr Opin Struct Biol 2001; 11:629–634.
103. Ibrahimi OA, Zhang F, Eliseenikova AV, Itoh N, Linhardt RJ, Mohammadi M. Biochemical analysis of pathogenic ligand-dependent FGFR2 mutations suggests distinct pathophysiological mechanisms for craniofacial and limb abnormalities. Hum Mol Genet 2004; 13:2313–2324.

104. Zhang Z, Coomans C, David G. Membrane heparan sulfate proteoglycan-supported FGF2–FGFR1 signaling: evidence in support of the "cooperative end structures" model. J Biol Chem 2001; 276:41921–41929.
105. Wu ZL, Zhang L, Yabe T, Kuberan B, Beeler DL, Love A, Rosenberg RD. The involvement of heparan sulfate (HS) in FGF1/HS/FGFR1 signaling complex. J Biol Chem 2003; 278:17121–17129.
106. Ibrahimi OA, Yeh BK, Eliseenikova AV, Zhang F, Olsen SK, Igarashi M, Aaronson SA, Linhardt RJ, Mohammadi M. Analysis of mutations in fibroblast growth factor (FGF) and a pathogenic mutation in FGF receptor (FGFR) provides direct evidence for the symmetric two-end model for FGFR dimerization. Mol Cell Biol 2005; 25:671–684.

Chemistry and Biology of Heparin and Heparan Sulfate
H.G. Garg, R.J. Linhardt and C.A. Hales (Editors)

Chapter 15

Role of Anticoagulant Heparan Sulfate in Mammalian Reproduction

ARIANE I. DE AGOSTINI, GHAMARTAJ HOSSEINI, MARC PRINCIVALLE and JI-CUI DONG

Department of Gynecology and Obstetrics,
Unit of Medicine of Reproduction and Endocrinology,
Geneva University Hospital, Geneva, Switzerland

I. Introduction

Major tissue remodeling occurs in hormone-responsive tissues of the female genital tract, at ovulation and during gestation, involving proteolysis, fibrin deposition and tightly controlled inflammation. Anticoagulant heparan sulfate proteoglycans (aHSPG) bind and activate the hemostatic protease inhibitor antithrombin III (AT). The expression of aHSPG in extravascular compartments and the reproductive defects of knockout mice deficient in aHSPG suggest that they play additional functions in mammalian reproduction. In this chapter, the characterization and tissue distribution of aHSPG in the female reproductive tract is presented and their emerging role in the control of tissue remodeling in reproduction is discussed.

II. Anticoagulant Heparan Sulfate Proteoglycans

A. Heparan Sulfate Proteoglycans

Heparan sulfate proteoglycans (HSPG) are ubiquitously distributed on the surfaces of animal cells and in the extracellular matrix and have numerous important biological activities through interactions with diverse proteins. HSPG are composed of a core protein with covalently attached HS chains formed by repetitive sulfated disaccharides of uronic acid and glucosamine (GlcN). The different length

and variable sequence of sulfated disaccharides generate the structural diversity required to form specific oligosaccharide binding sites for proteins, such as growth factors, protease inhibitors, or cell adhesion molecules. Binding of proteins to their HS binding sites affects their reactivity, and in the case of heparin and anticoagulant HS (aHS), accelerates the rate at which AT inhibits serine proteases in the blood-clotting cascade (1).

B. Anticoagulant Heparan Sulfate Proteoglycans

The AT-binding pentasaccharide of heparin and aHS is the best characterized biologically active structure of HS. It specifically binds and activates AT by inducing a conformational change in the inhibitor that stabilizes its active conformer. This pentasaccharide bears a cardinal 3-*O*-sulfated glucosamine essential for AT binding (2,3). 3-*O*-sulfates are added late in the biosynthetic pathway of HS by 3-*O*-sulfotransferases. Six different isoforms of 3-*O*-sulfotransferases have been identified, with different tissue expression pattern and acceptor substrate specificities. The 3-*O*-sulfotransferase-1 (3-OST-1) is expressed in many tissues with a particularly high expression in endothelial cells. It is the predominant form that can produce AT-binding pentasaccharides in aHS, while other forms, such as 3-OST-3, introduce 3-*O*-sulfates in HS chains but without forming the active pentasaccharide (4–6). The 3-OST-5 can also generate aHS but its expression pattern is more limited (4,7).

In addition to AT, 3-*O*-sulfated HS also have functional interactions with a viral envelope protein mediating the binding and entry into cells of Herpes Simplex virus (5). Moreover, the co-receptor activity of HS for FGF-7 interaction with its epithelial cell receptor FGFR2IIIb is due to aHS chains containing the AT binding 3-*O*-sulfated pentasaccharide responsible for their anticoagulant activity (8). These data suggest that aHSPG might have additional co-receptor activities toward certain protein ligands such as cytokines.

aHSPG were first characterized in endothelial cells (9–12). ^{125}I-AT-binding to endothelial cell aHSPG was shown on cultured microvascular endothelial cells and visualized by microscopic autoradiography. aHSPG were found in the extracellular matrix of cultured cells and were concentrated beneath the endothelium in the basement membrane of rat aorta (Fig. 1) (10). Endothelial aHSPG are thought to endow the vascular wall with antithrombotic properties, in particular in the subendothelial basement membrane. aHSPG were detected on cell surfaces as well as in soluble form in cell conditioned medium showing that aHSPG can be released from the cell surface by secretion or by shedding their extracellular domain (13).

Besides endothelial cells, aHSPG have also been detected in Reichert's membrane during embryonic development, in cultured fibroblasts (14,15) and in various cell lines of fibroblastic or epithelial origin (16–19). In addition, aHSPG are synthesized by ovarian granulosa cells (20,21). Thus, the biosynthesis of aHSPG appears not to be restricted to endothelial cells and to occur selectively in extravascular cell types but their function outside the vascular bed is unknown.

The observation that most aHSPG are located underneath the vascular endothelium suggests that they have a protective biological function to limit fibrin

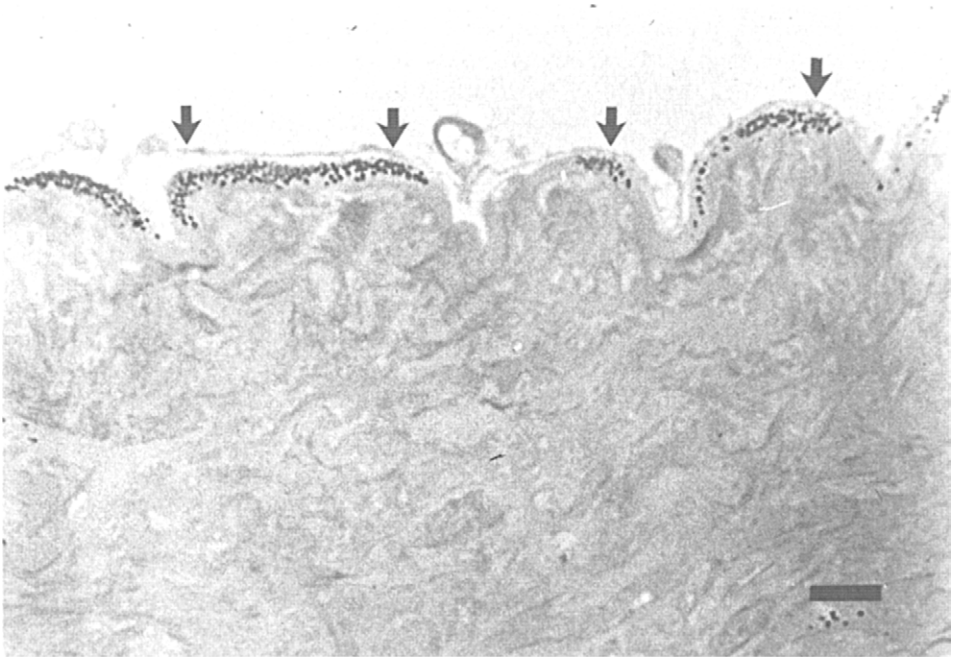

Figure 1 Light micrographic autoradiograph of rat aorta after perfusion with ^{125}I-AT. The intense labeling is noted in the basement membrane beneath the endothelial cells (arrows). Bar, 10 μm (10).

deposition in the case of increased vascular permeability. In this context, the synthesis of aHSPG by nonvascular cells is evocative of a role for aHSPG in the control of proteolysis and fibrin deposition in tissue remodeling.

III. Anticoagulant Heparan Sulfate Proteoglycans in the Reproductive Tract

A. Development of the Ovarian Follicle and Ovulation

The development of the ovarian follicle, its rupture at ovulation, and the subsequent formation of corpus luteum constitute one of the most striking examples of tissue remodeling in adult mammals. This process is hormonally orchestrated and involves important proteolysis. The inner follicle, constituted by the oocyte and granulosa cells, is separated from outer theca layers by a basement membrane and remains avascular until ovulation. As ovulation approaches, the ovarian basement membrane of preovulatory follicles is progressively permeabilized and plasma proteins accumulate in follicular fluid (22).

The ovulatory surge of luteinizing hormone (LH) triggers a cascade of events resulting in follicular rupture and oocyte expulsion. Proteolytic enzymes from the

plasmin generating system and collagenases are activated and acute inflammation takes place, involving vascular permeabilization, edema, extravasation of plasma proteins, and fibrin deposition (23,24). As a result, plasma proteins extravasate into the follicular cavity where they form a fibrin clot. Subsequently, luteinized granulosa and theca cells and an extensive network of blood vessels grow inward, using the fibrin clot as provisional matrix, to fill the former antral cavity with highly vascularized luteal tissue (25). Thus, multiple proteolytic events take place during the ovarian cycle, involving serine proteases of the plasminogen activator and coagulation cascades. HSPG are widely expressed in ovarian follicles and their turnover, synthesis, internalization and release is regulated by gonadotrophins (26). Granulosa cells are steroidogenic cells and their development and metabolism is profoundly affected by gonadotrophins during the estrous cycle.

B. Ovarian Granulosa Cell Anticoagulant Heparan Sulfate Proteoglycans

We have characterized aHSPG from rat ovarian granulosa cells and shown that cultured primary cells synthesize considerable amounts of aHSPG, similar to that found in endothelial cells. ^{35}S-labeled HS were fractionated in aHS and anticoagulantly inactive HS (iHS) by affinity chromatography on AT immobilized on concanavalin A Sepharose. aHS from granulosa cells are large glycosaminoglycans with an average modal M_r of 57,000, they represent 6.5% of the total HS and they contain 13% 3-*O*-sulfated disaccharides (Table 1). The biological activity of granulosa cell aHSPG was shown by their ability to bind AT (Fig. 2) and to accelerate the formation of thrombin-AT complexes (Fig. 3).

Stimulation of granulosa cells by gonadotrophins altered the distribution between cell-bound and soluble forms of aHSPG, as determined using ^{125}I-labeled AT (^{125}I-AT) cell-binding and ligand-binding assays. Cultured granulosa cells responded to stimulation by follicle-stimulating hormone (FSH) and luteinizing hormone (LH), by increasing their synthesis of estradiol and progesterone, respectively, while they responded to both FSH and LH by increasing their aHSPG output in favor of the liberation of cell-bound aHSPG into the culture medium (Table 2)

Table 1 Disaccharide Composition of aHS and iHS from Granulosa Cells

Sulfated disaccharide[a]	aHS	iHS
GlcA → AMN 3-*O*-SO_3	8.0 ± 0.0	0.2 ± 0.3
IdA 2-*O*-SO_3 → AMN	29.2 ± 0.4	40.6 ± 0.9
GlcA → AMN 6-*O*-SO_3	16.4 ± 0.5	17.0 ± 1.2
IdA → AMN 6-*O*-SO_3	13.2 ± 0.4	14.4 ± 0.9
GlcA → AMN 3,6-*O*-$(SO_3)_2$	4.9 ± 0.2	0.8 ± 0.2
IdA 2-*O*-SO_3 → AMN 6-*O*-SO_3	28.0 ± 0.7	27.0 ± 1.0

[a] Abbreviations: GlcA, glucuronic acid; IdA, iduronic acid; AMN, anhydromannitol.
^{35}S-Labeled aHS and iHS were prepared by AT affinity chromatography, and sulfated disaccharides were resolved by reverse phase ion pairing HPLC. Results are presented as the percentage of sulfated disaccharides (mean ± SD) from four determinations (21).

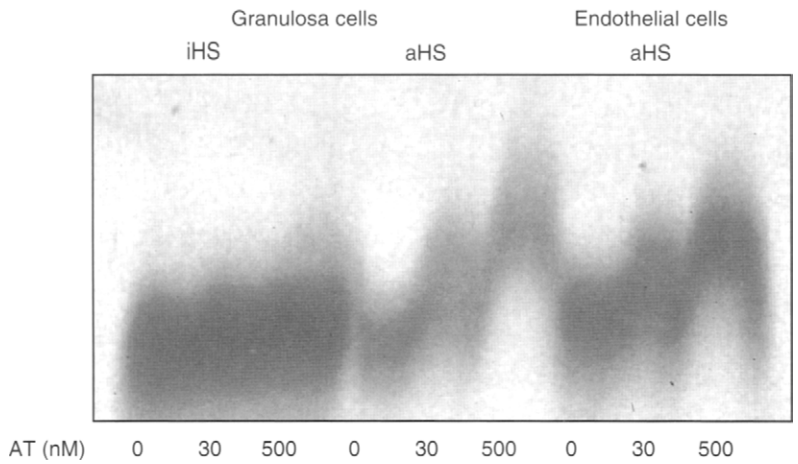

Figure 2 Complex formation between aHS and AT. Autoradiography of ^{35}S-labeled HS electrophoresed in an agarose gel containing the indicated concentrations of AT. Binding to AT retarded the migration of HS and was observed for the entire population of aHS from granulosa and endothelial cells, whereas only traces of AT-binding species were detected in iHS (21).

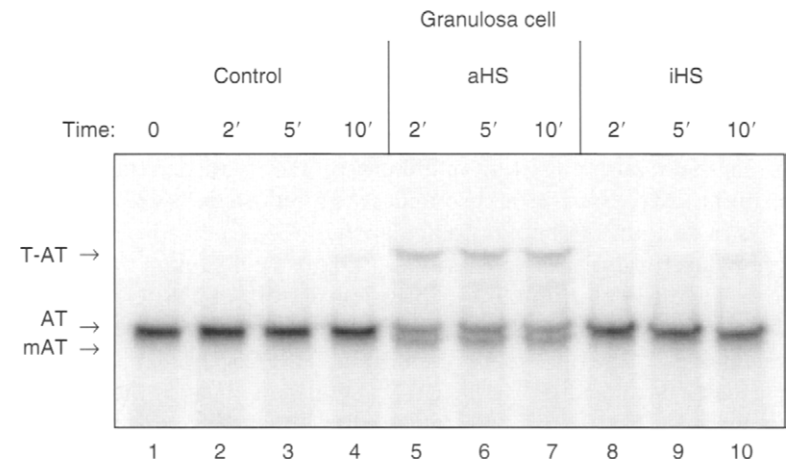

Figure 3 The formation of thrombin-AT complexes is accelerated by granulosa cell aHS. Autoradiography of SDS-PAGE analysis of mixtures of thrombin (50 mM) and ^{125}I-AT (2 nM, 0.5×10^6cpm/ml) with or without HS. Control without HS (lanes 1–4), granulosa cell aHS (49 ng/ml, 0.86 nM) (lanes 5–7), granulosa cell iHS (426 ng/ml, 7.5 nM) (lane-10). In each case, the enzyme and the inhibitor were incubated at 37 °C for 2, 5 and 10 min, respectively. Arrows indicate the migration position of AT, modified AT (mAT) and the thrombin-AT complex (T-AT) (21).

Table 2 Distribution of Cell-Bound and Soluble aHSPG in Cultured Granulosa Cells

	Cell layer			Culture medium		
	Basal	FSH-primed	LH	Basal	FSH-primed	LH
% aHSPG average	83	59*	47**	17	41*	53**
SD	8	20	14	8	20	14

Student's paired *t*-test, $**p < 0.01$, $*p < 0.05$. Data from seven independent experiments, average ± SD (27).

(21,27). These data show that aHSPG distribution is affected by gonadotrophins and thus could be modulated according to the stage of follicular development.

C. Heparan Sulfate Proteoglycans Core Proteins in Granulosa Cells

Biologically active HSPG are bound to the cell surface through their core protein (syndecans and glypicans), integrated in extracellular matrix, and basement membranes (perlecan), or released in soluble form from the cell surface by shedding. Alternatively, their HS chains can be degraded by heparanase. The half-life of HSPG on the cell surface is generally considered to be short (a few hours) allowing for highly dynamic modulation of their biological activities (28). Each cell type expresses a particular set of HSPG core proteins that varies according to their differentiation stage (29). The specific attachment of HS chains endowed with particular biological activities to defined core proteins is not firmly established and in endothelial cells aHS chains can be attached to all core proteins expressed (2,30–33). In the ovary, the four members of the syndecan family, glypican-1 and perlecan are expressed in mouse and rat granulosa cells (27,34). In addition, perlecan has been found in human follicular fluid (35,36).

We have used rat ovaries or purified granulosa cells taken at different stages of the estrus cycle to determine the expression pattern of HSPG core proteins by northern blot analysis. Five distinct HSPG core proteins expressed in granulosa cells were analyzed: the basement membrane HSPG perlecan, the membrane-spanning HSPG syndecan-1, syndecan-2, syndecan-4, and the GPI-anchored HSPG glypican-1. The coordinate expression of these core proteins and of aHSPG in granulosa cells suggests that aHS is associated with both membrane-bound and secreted HSPG. No major variation in core protein expression was detected during the cycle, indicating that the differences observed in aHSPG are due to modulations of the aHS biosynthesis, likely involving 3-OST-1, the limiting factor in aHS biosynthetic pathway. Indeed, synthesis of 3-OST-1 has been shown in the rat ovary and in isolated granulosa cells by RT-PCR and northern blot analysis (Fig. 4) (27).

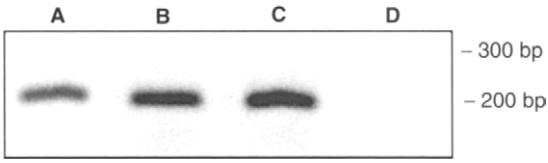

Figure 4 D-glucosaminyl-3-*O*-sulfotransferase-1 expression in the rat ovary and in granulosa cells. Resolution of RT-PCR products (219 bp) by 2% agarose gel electrophoresis with SYBR green staining. The positions of relevant DNA size markers are indicated. A: rat ovary, B: rat endothelial cells (RFP), C: isolated rat granulosa cells, and D: negative control, rat ovary control with RT omitted (27).

D. Localization of Anticoagulant Heparan Sulfates in Ovary Cryosections

To evaluate the pattern of expression of aHSPG during the cyclic development of ovarian follicles *in vivo*, we have established a method of detection based on the specific binding of aHSPG by ^{125}I-AT, revealed by microscopic autoradiography (27).

The aHSPG could be visualized on granulosa cells in culture and in ovary cryosections, and the specificity of aHSPG labeling was demonstrated using glycosidases digestions and polysaccharide competitors (Fig. 5). The aHSPG were seen on granulosa cell layers of follicles and as punctuated labeling on vascular endothelial cells. Digestion of the ovary sections with heparitinase abolished subsequent ^{125}I-AT binding to the cryosection while chondroitinase ABC had no effect, and incubation of ^{125}I-AT in the presence of heparin, but not of dextran sulfate, decreased the signal to background levels. Moreover, no labeling was observed when ^{125}I-AT was incubated in the presence of excess unlabeled AT or of the heparin AT-binding pentasaccharide.

E. Distribution of Anticoagulant Heparan Sulfates in the Rat Ovary During the Reproductive Cycle

The dynamics of expression of aHSPG in ovarian follicles during the reproductive cycle was revealed in ovaries from immature female rats in which ovulation was induced by gonadotrophin treatment, as well as in ovaries from mature cycling female rats. In immature animals, the ovary contains numerous dormant primordial follicles and small follicles developing to gonadotrophin-independent preantral stages. During gonadotrophin stimulation, one single oversized cohort of follicles can be followed in detail until ovulation. In contrast, in naturally cycling adults, several cohorts of follicles overlap in the ovary, but physiological levels of hormones ensure the formation of fully mature corpus luteum. Thus, localization of aHSPG in these two complementary models has allowed us to draw the following scenario for aHSPG synthesis in the rat ovary (Fig. 6) (27,37).

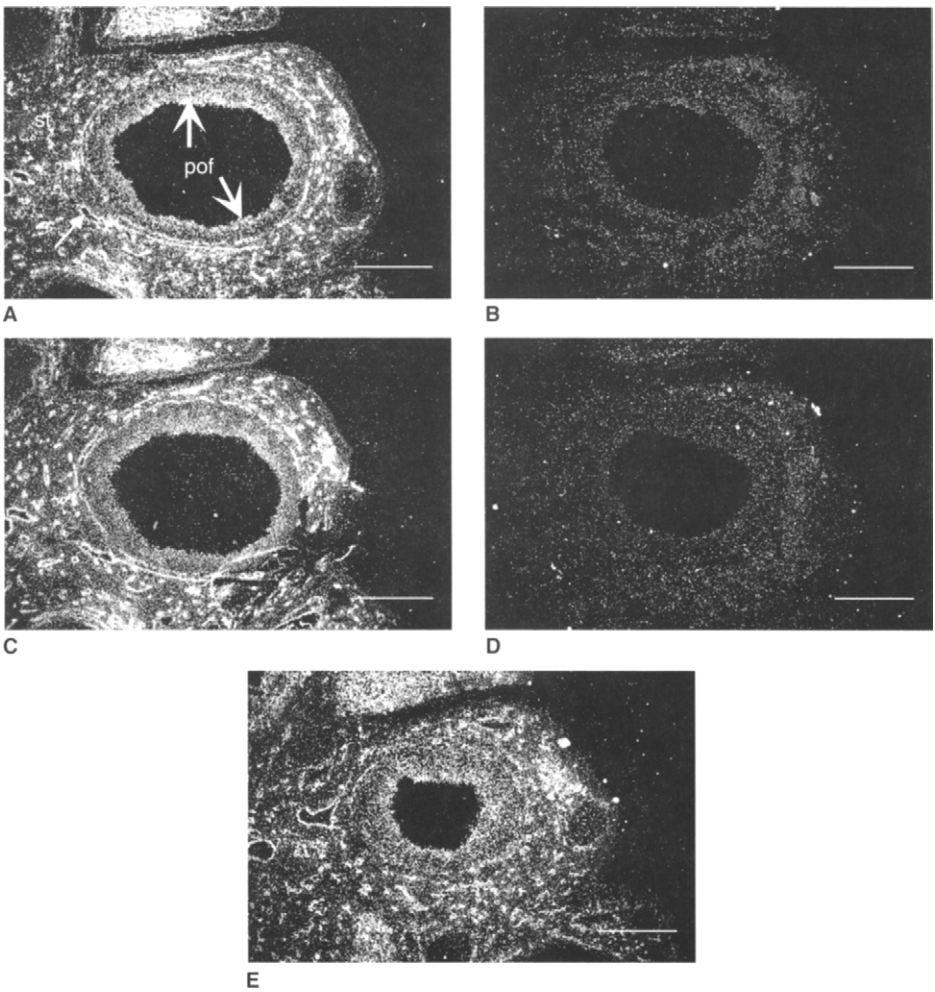

Figure 5 Specificity of ^{125}I-AT-binding to aHSPGs in ovary cryosections. Autoradiography of ^{125}I-AT-labeled ovary cryosections in dark field exposure, oxidized silver grains appearing in white. (A) Incubation with ^{125}I-AT alone. Preovulatory follicle (pof); stroma (st); granulosa cells (bold arrows), blood vessels (arrow). Intense labeling reveals aHSPG on granulosa cells and in capillary vessel walls; (B, C) preincubation of the cryosection with heparitinase (B) or with chondroitinase ABC (C) and subsequent incubation with ^{125}I-AT; (D, E) incubation of ^{125}I-AT in the presence of 100 μg/ml of the competitors heparin (D) or dextran sulfate (E). Scale bar 200 μm (27).

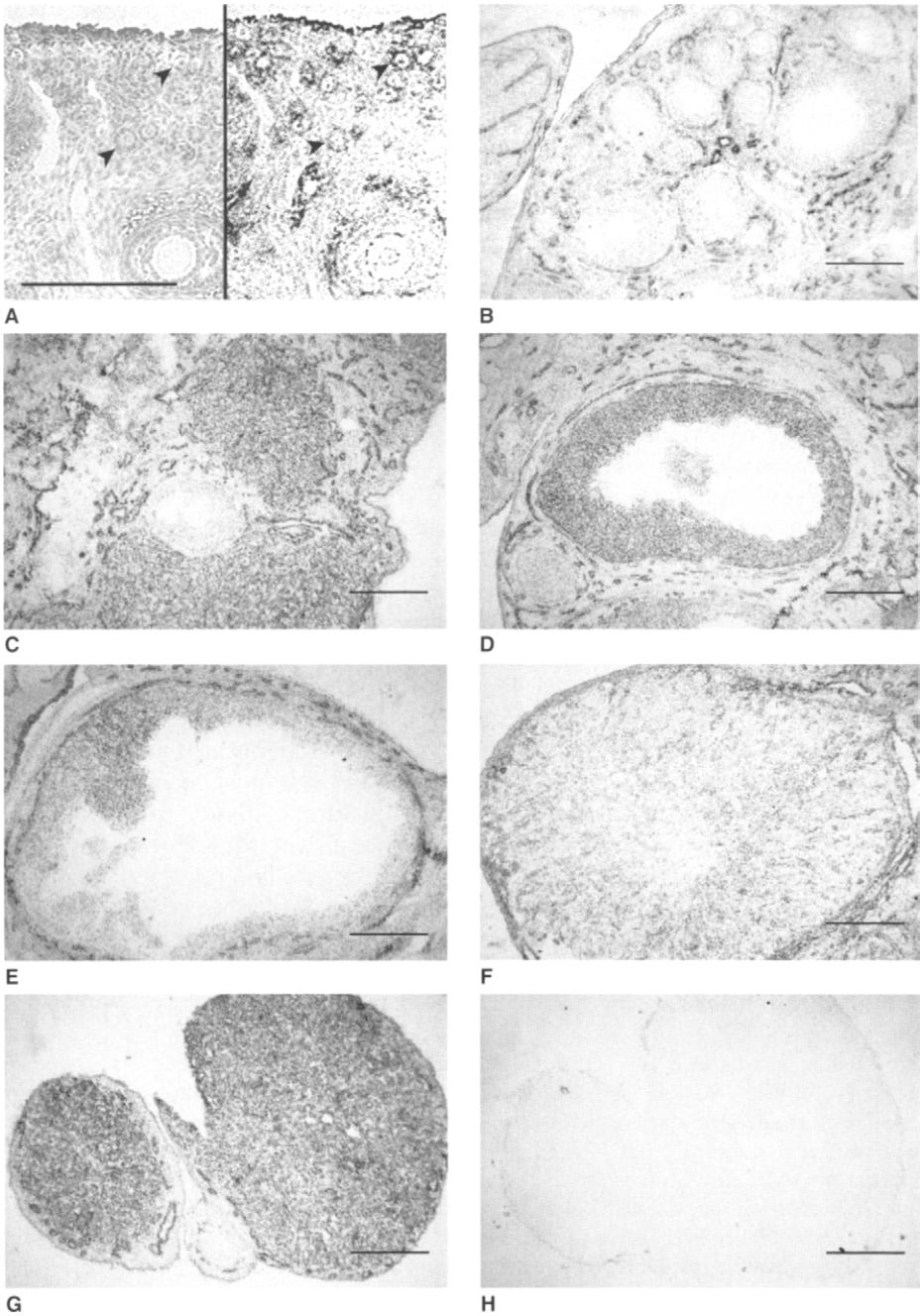

Figure 6 aHSPG localization in the rat ovary during the estrous cycle. Autoradiographic detection of ^{125}I-AT-labeled aHSPG on ovary cryosections. (A) Immature ovary, serial sections; left: histological staining, right: autoradiography; primordial follicles

In primordial follicles, aHSPG were present at the boundary between the single granulosa cell layer and ovarian stroma and might serve to protect dormant follicles from the active proteolysis occurring in neighboring developing follicles, by virtue of their ability to activate serine protease inhibitors. At the onset of follicular development in response to estrogen, aHSPG quickly disappeared and they remained absent from actively growing follicles with proliferating granulosa cells up to the early antral stage. After FSH induction aHSPG were then strongly expressed during the maturation of preovulatory follicles, granulosa cells from large antral follicles were heavily labeled for aHSPG and this labeling was consistently found until ovulation. These observations are in agreement with the increased production of aHSPG induced by gonadotrophins in cultured granulosa cells. Moreover, aHSPG were present in rat follicular fluid, where they could accumulate to be released at ovulation. At ovulation, granulosa cell aHSPG were transiently decreased during the remodeling of the follicular wall of ovulatory follicles. During the formation of corpus luteum, aHSPG were weakly expressed on luteal cells and mainly associated with invading capillaries, while in mature corpus luteum a very intense aHSPG labeling was restored, due to superimposed aHSPG signals in luteal and endothelial cells.

In summary, aHSPG are very strongly expressed on granulosa cells of ovulatory follicles until ovulation. Hence, we postulate that the inner follicle displays a strongly anticoagulant surface protecting it from fibrin deposition, which ensures the maintenance of fluidity of follicular fluid until expulsion of the oocyte at ovulation. The widespread localization of aHSPG on the entire granulosa cells volume, and most likely also in follicular fluid, is probably necessary to control the large influx of procoagulant plasma proteins that leak from blood vessels, during the inflammatory vascular permeabilization occurring at ovulation (38). The rapid decrease in aHSPG observed on the surface of luteinized granulosa cells after ovulation corresponds to a change to a more procoagulant surface, which is permissive for a fibrin clot to form, filling the antral cavity with a provisional matrix for invading luteal cells. Alternatively, aHSPG could interact with other heparin-activated serine protease inhibitors present in the follicle, such as protease nexin-1 (PN-1) and plasminogen activator inhibitor-1 (PAI-1), and be involved in the control of the proteolytic breakdown of the follicular wall at ovulation.

(arrowheads) are labeled for aHSPG. (B) Immature ovary with unlabeled primary and secondary follicles. Various stages of a natural cycle of ovary are shown (C–H): after ovulation, a small secondary follicles beginning the next cycle is not labeled for aHSPGs, unlike adjacent corpora lutea (C). In preovulatory stage, the granulosa cells of a large preovulatory follicles are intensely labeled for aHSPG (D). At ovulation, intense remodeling of the follicular wall occurs, aHSPG are less abundant and the labeling is less homogeneous on granulosa luteal cells (E). After ovulation, aHSPG labeling in the forming corpus luteum is marked on invading capillaries and weak and diffuse on luteal cells (F). During the luteal phase, mature functional corpora lutea are strongly labeled for aHSPG (G). Serial section to (G) incubated with ^{125}I-AT in the presence of 100 μm/ml heparin, which abolishes all binding to the tissue (H). Scale bar 200 μm (27,37).

F. Coordinate Localization of Anticoagulant Heparan Sulfates and of Serpin in Ovarian Follicles

To test the hypothesis of interactions between granulosa cell aHSPG and follicular protease inhibitors, we have coordinately localized aHSPG and the serine protease inhibitors (serpins) AT, PN-1, and PAI-1 in the ovary along the reproductive cycle.

The ovulatory surge of LH triggers a rapid cascade of events resulting in follicular rupture and oocyte expulsion that involves serine proteases of the plasminogen activation and coagulation cascades. The activity of these enzymes is controlled by inhibitors of the serpins superfamily, which are often modulated by heparin (39). The serpins PAI-1, PN-1 and AT have been described in the ovary (40–45).

AT distribution in tissues is mainly restricted to vascular walls where it is bound to aHSPG (10,12,46) but in the ovary, AT appears in extravascular tissue around ovulation and remains elevated thereafter. AT is abundant on granulosa cells of preovulatory follicles; however, its mRNA could not be detected by northern blot analysis, suggesting that AT leaks from permeabilized vessels to bathe the ovarian tissue and concentrates on granulosa cell aHSPG (37). PN-1 is found exclusively on granulosa cells of developing follicles, where it accumulates until the onset of ovulation, quickly disappearing thereafter. PAI-1 is present in developing follicles, strictly confined in basement membranes of follicular theca until ovulation and then is abundant in corpus luteum (37,40,41).

These data demonstrate overlapping localization of the serpins AT, PN-1, and PAI-1 during the follicular cycle. To reveal the scenario of interactions connecting aHSPG to these serpins in the ovary we have localized them in the same follicles, along the cycle.

Coordinate localization on rat ovary serial sections has shown that aHSPG are co-localized with PN-1 during follicular growth, and then in preovulatory stage, with both PN-1 and AT. After ovulation, aHSPG coincide with AT and PAI-1 during corpus luteum formation. Maximal labeling of aHSPG, AT, and PN-1 on granulosa cells is observed shortly before the oocyte expulsion, 6 h after ovulation induction (Fig. 7). Thus, aHSPG are adequately positioned in the follicle in time and space to activate sequentially the three serpins PN-1, AT, and PAI-1 (27,37).

Binding of AT to heparin or aHSPG activates it by stabilizing its conformation with a fully exposed reactive loop (3,47). The serpins AT, PN-1, and PAI-1 share a common binding site for heparin on their D helix (48). The structural requirements on heparin for activation of PAI-1 and PN-1 are less restrictive than for AT (49,50), but their binding sites on heparin might overlap the AT-activating pentasaccharide (51). Moreover, HS are formed of alternating domains with low sulfate and high sulfate content (52), and several AT-binding sites can be clustered in highly sulfated domains (53); thus, aHS likely contain adequate structures to activate PN-1 and PAI-1. Therefore, we postulate that the localization of aHS in the ovary by ^{125}I-AT-binding identifies aHSPG species susceptible to also activate PN-1 and PAI-1.

In light of these considerations, we have analyzed the effects that follicular aHSPG could exert on PN-1, PAI-1, and AT during the reproductive cycle. PN-1 is a potent thrombin inhibitor, it inhibits plasminogen activators at lower reaction

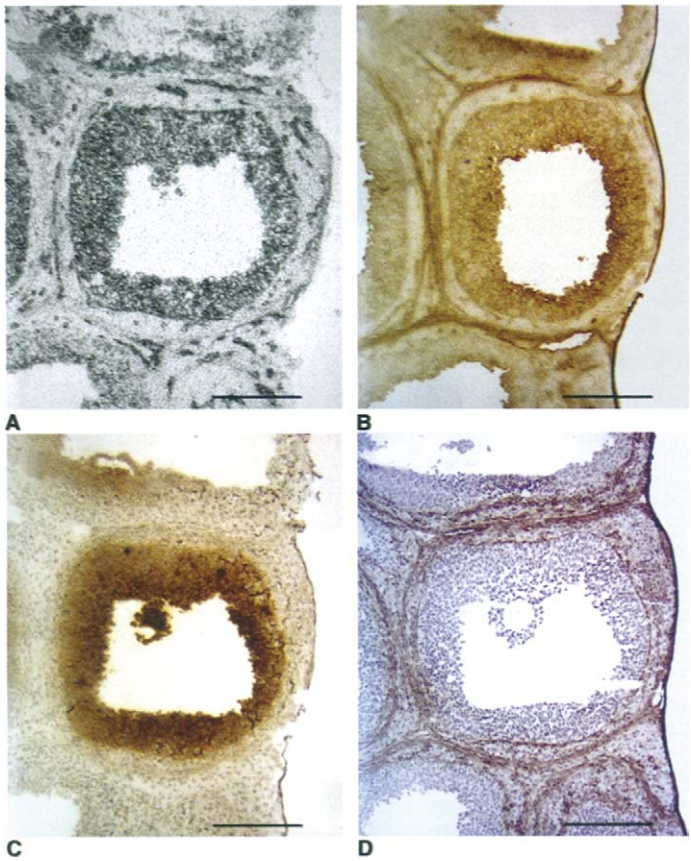

Figure 7 Co-localization of aHSPG and of serine protease inhibitors in rat ovarian follicles. Serial cryosections stained for aHSPG by ^{125}I-AT-binding revealed by autoradiography (A), and for AT (B), PN-1 (C), and PAI-1 (D) by immunohistochemistry. Gonadotrophin-induced cycle, preovulatory follicle 6 h after ovulation induction. Shortly before ovulation, aHSPG, AT, and PN-1 labeling is maximal showing that AT and PN-1 are exactly co-localized with aHSPG on the whole surface of the granulosa cell layer (A, B, C), while PAI-1 is strictly restricted to basement membranes (D). Scale bar 200 μm (37).

rates and its reactivity towards these enzymes is increased by heparin (54). The reactivity of PN-1 towards thrombin and plasminogen activators could thus increase in developing follicles as aHSPG appear on granulosa cells. The quick disappearance of PN-1 at the onset of ovulation suggests that it could be prohibitive for the follicular wall breakdown. PAI-1 primary targets are the plasminogen activators, but in the presence of heparin its reaction rate towards thrombin is markedly increased (55), suggesting that when co-localized with aHSPG, PAI-1 could control thrombin activity. AT activation by aHSPG increases its reactivity towards

coagulation enzymes, mainly Factor Xa and thrombin (56). AT circulates in a conformation with minimal anticoagulant activity (47), and as it leaks from the vasculature into the ovary stroma where no aHS are present, fibrin deposition occurs (57). In contrast, the abundant expression of aHSPG on granulosa cells of developing follicles could stabilize AT in a fully active conformation and prevent fibrin formation in the inner follicle until ovulation.

Thus, AT is critically located on granulosa cell aHSPG to control thrombin activity in the follicle. Moreover, both PN-1 and PAI-1 could play dual roles in the regulation of serine protease activities in the follicle, and be involved in controlling plasminogen activator activity, until their interaction with aHSPG redirects them toward the control of thrombin activity. According to this model, aHSPG increase greatly the inhibitory potential of PN-1 and AT in the inner follicle before ovulation. At ovulation, this inhibition is released, due to the rapid disappearance of PN-1 and to the decrease in aHSPG, which greatly reduce the thrombin inhibition potential in the follicle. As a result, a fibrin clot can form in the former antral cavity and serve as a provisional matrix for invading luteal cells. Altogether, the thrombin-inhibitory potential successively present in the follicle along the cycle is impressive, with the redundant presence of three potent thrombin inhibitors AT, PN-1, and PAI-1, which are likely activated by aHSPG.

To further investigate the role of aHSPG in the regulation of serpin activity in the ovary we have manipulated the proteolytic balance at the time of ovulation by injecting an inactive form of AT, R393C-AT.

G. Mobilization of Anticoagulant Heparan Sulfates by an Inactive Variant of Antithrombin III: Impact on Ovulation

The R393C-AT variant lacks thrombin inhibitory activity as a result of the replacement of the specificity-determining arginine at position P1 by a cysteine, but retains normal heparin binding (58) and thus it can occupy AT-binding sites on aHSPG.

The impact of aHSPG mobilization by R393C-AT on ovulation was examined *in vivo* by injection in the ovarian bursa during gonadotrophin-induced cycles in immature rats (59). R393C-AT was injected at the time of ovulation induction, ovulation was scored 24 h later by counting oocytes present in oviducts (Table 3) and the deposition of cross-linked fibrin in the ovary was visualized by immunohistochemistry (Fig. 8). R393C-AT significantly reduced the number of ovulated oocytes, in a dose-dependant manner. The histology of R393C-AT injected ovaries was comparable to controls but with an increased incidence of oocyte retention in luteinized follicles, a pattern reminiscent of the luteinized unruptured follicle syndrome in humans (60). In addition, R393C-AT induced heavy cross-linked fibrin deposits in the ovary, both in luteinized follicles and in small developing follicles. These results indicate that the serpin-activating potential of aHSPG plays an active role in the control of the proteolytic balance in the ovary (37).

Altogether, the data presented show that aHSPG are critically expressed in the rat ovary to promote thrombin inhibition in the follicle and therefore to maintain the fluidity of the oocyte environment at ovulation.

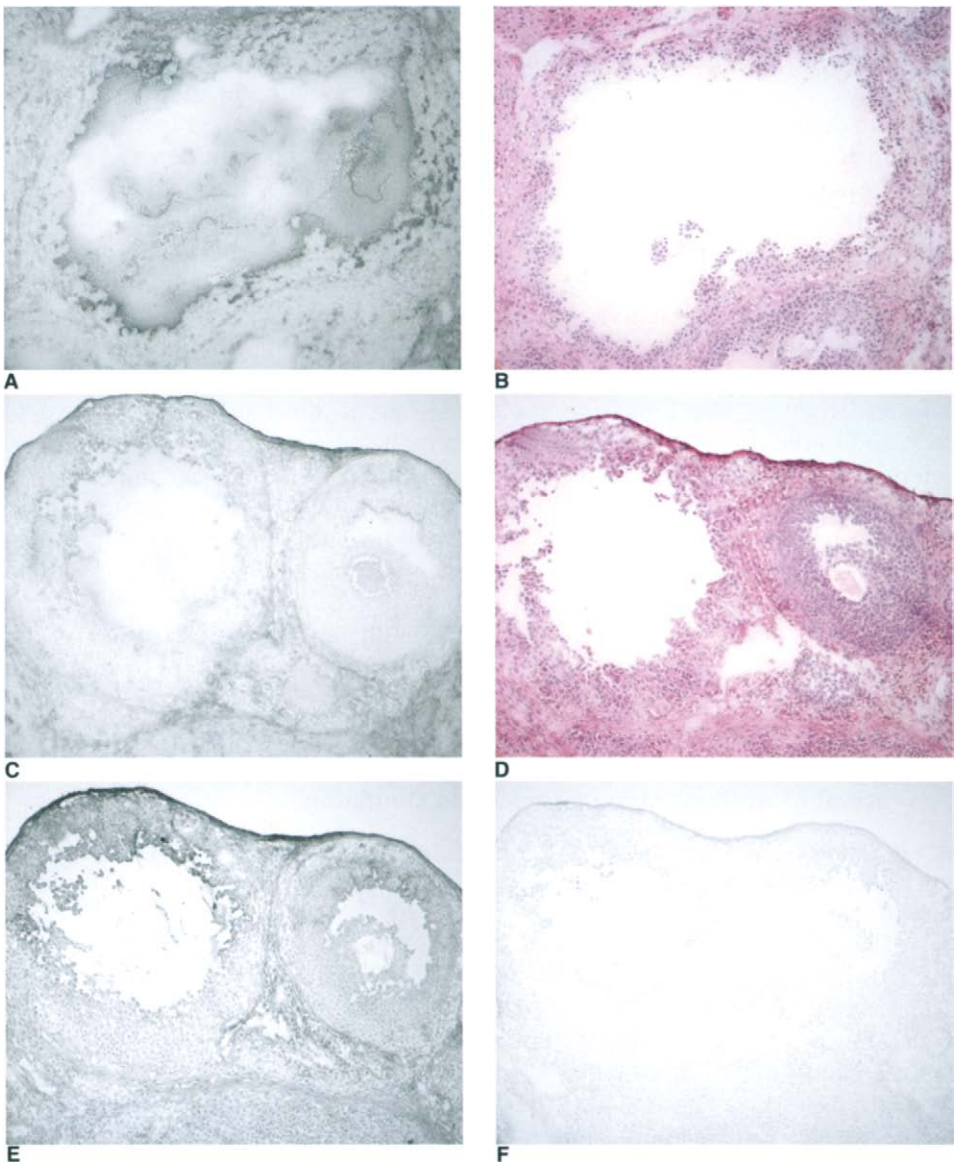

Figure 8 Fibrin deposition in rat ovaries injected with R393C-AT. Fibrin immunostaining of ovaries injected in the ovarian bursa with 85 μg R393C-AT (A, B) or vehicle (C–F). Serial sections were used for fibrin immunostaining (A, C, E) and for histological staining (B, D). Specific staining of cross-linked fibrin (A, C), is observed as compared to cumulative staining of fibrinogen and fibrin (E), and to the absence of signal with a control antibody (F). In the R393C-AT injected ovary, a luteinized follicle contains an entrapped oocyte (B) and heavy cross-linked fibrin deposits, that are interspersed in the cell layers of the luteinizing follicle, as well as covering much of the follicular cavity and embedding the oocyte. Fibrin deposits are also evident in granulosa cell layers of a small follicle that does not belong to the ovulatory cohort (lower-right corner of Fig. 7A and B). In the control ovary, a luteinized follicle (D) contains moderate cross-linked fibrin deposits and a small follicle is not stained. Scale bar 100 μm (37).

Table 3 Injection of R393C-AT in the Ovarian Bursa

Number of ovulated oocytes per ovary			
Effector injected	NaCl	R393C-AT (9 μg)	R393C-AT (85 μg)
	25	14	19
	25	21	52
	31	13	17
	16	28	1
	21	5	6
	10	18	19
	18	30	3
	27	21	2
	25	26	5
	28	10	8
	34	21	4
	31	15	27
Median	25	19.5	7
Intequartile range	20.3–28.8	13.8–22.3	3.8–19.0
Mann–Witney *U*-test, *P* (R393C-AT *vs* NaCl)		0.075	0.009

The number of oocytes ovulated by ovaries injected with 85 μg R393-AT was significantly less than in ovaries injected with NaCl vehicle. With a smaller dose of R393-AT (9 μg), there was a smaller decrease in the number of ovulated oocytes, suggesting a dose-dependent effect of R393-AT in the occupation of available aHSPG AT-binding sites (37).

H. Human Follicular Fluid Contains Anticoagulant Heparan Sulfate Proteoglycans

Soluble aHSPG have been observed in cultured rat granulosa cells and in rat follicular fluid, suggesting that in addition to their function in the follicle before ovulation, aHSPG might be released with follicular fluid at ovulation and play a distal role in the female genital tract.

We have detected aHSPG in the human follicular fluid collected from luteinized follicles of women undergoing oocyte pickup for *in vitro* fertilization treatments. aHSPG was detected by ^{125}I-AT ligand-binding assay and showed a very strong signal, which prompted us to purify human follicular fluid aHSPG (hFF-aHS) (unpublished observations). Purification of hFF-aHS was done as for rat granulosa cell aHS (21), follicular fluid was fractionated by MonoQ ion exchange chromatography, aHSPG followed by ^{125}I-AT ligand binding assay and positive fractions, eluting at approximately 1 M NaCl ionic strength were used for purification of aHS. Purified HS were obtained by β-elimination and chondroitinase ABC treatment and aHS were isolated by affinity fractionation on AT immobilized on concanavalin A-Sepharose as described (21). HS and aHS were followed by uronic acid analysis by the carbazole method or by micro-colorimetric assay using alcian

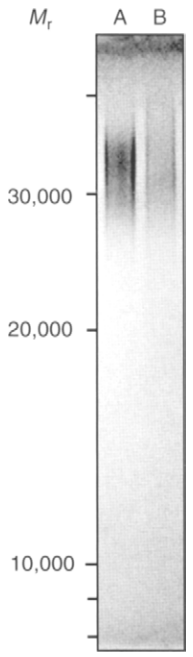

Figure 9 Human follicular fluid aHS and iHS size distribution. h-FF aHS and iHS were analyzed on a 11–22% gradient PAGE in the presence of 0.1 M NaCl as described (63). HS (3 μg/lane) were visualized by azure A staining. The modal M_r was determined using calibrated GAG standards and was of 32,000 Da for both aHS (A) and iHS (B).

blue (61,62). The size distribution of hFF, HS and aHS was determined by PAGE, aHS, and iHS had the same modal M_r of 32,000 Da (Fig. 9) and these chains were degraded to lower M_r species by heparitinase digestion. The amount of aHS recovered from hFF comprised between 1 and 10 μg/ml with variations that were probably due to differences in the individual response to gonadotrophin stimulation. The presence of soluble aHSPG in follicular fluid suggests that they could play a role distally from the ovary, in the oviduct at fertilization, or in the uterus at implantation.

The notion that aHSPG could play a role outside the ovarian follicle prompted us to examine the distribution of aHSPG in other compartments of the genital tract. In parallel, a mouse model was produced that was deficient in the key synthetic enzyme of aHS, which revealed the role of aHSPG in reproduction.

IV. Reproduction in Mice Deficient in Anticoagulant Heparan Sulfate Proteoglycans

A. Knockout Mouse Model with Deficient Anticoagulant Heparan Sulfate Synthesis: the *Hs3st1*$^{-/-}$ Mice

Endothelial cell production of aHS is controlled by the *Hs3st1* gene, which encodes the rate-limiting enzyme 3-OST-1. The *in vivo* role of aHS was evaluated by generating *Hs3st1*$^{-/-}$ knockout mice. *Hs3st1*$^{-/-}$ animals were devoid of 3-OST-1 enzyme activity in plasma and tissue extracts. Nulls showed dramatic reductions in tissue levels of aHS but maintained wild-type levels of tissue fibrin accumulation and did not show an obvious pro-coagulant phenotype (Fig. 10). Instead, *Hs3st1*$^{-/-}$ mice exhibited genetic background specific lethality and intrauterine growth restriction (IUGR), without evidence of a gross coagulopathy. These results demonstrate that the 3-OST-1 enzyme produces the majority of tissue aHS. Surprisingly, this bulk of aHS is not absolutely essential for normal hemostasis in mice. Instead, 3-OST-1-deficient mice exhibited unanticipated phenotypes suggesting that aHS or additional 3-OST-1-derived structures may serve alternate biologic roles (64).

B. Expression of Anticoagulant Heparan Sulfate in the Genital Tract of Wild-Type and *Hs3st1*$^{-/-}$ Mice

We have analyzed the expression pattern of aHSPG in the male and female genital tracts by specific ^{125}I-AT binding, on tissue cryosections by autoradiography and in tissue extract by ligand-binding assay (13,27). In addition to endothelial and granulosa cells, AT-binding aHSPG were strongly expressed by epithelial cells in the female genital tract, where they accumulate in the basolateral basement membranes (Fig. 11). In particular, continuous labeling was seen on the lumenal and glandular epithelium of the uterus, while it was absent from the squamous epithelium of the cervix and vagina. In *Hs3st1*$^{-/-}$ mice, labeling was completely abolished in all tissues. In the male genital tract, aHSPG were present in all epithelia in wild-type and absent in *Hs3st1*$^{-/-}$ mice (data not shown). The tissue distribution of aHSPG and their absence in *Hs3st1*$^{-/-}$ mice were confirmed by quantitative measurements of aHSPG in tissue extracts. The highest amount of aHSPG was detected in the ovary. aHSPG were elevated in the female genital tract, in the oviduct and in the uterus, as well as in the male genital tract and also in some nonreproductive tissues, such as the lung or kidney. In contrast, many other tissues, like muscle or vagina, had low aHSPG content, and were considered negative for aHSPG (Fig. 12). In *Hs3st1*$^{-/-}$ mice, a steep decrease in the AT-binding signal was shown in all organs tested (not shown). The residual signal observed in some tissues could be due to the activity of other 3-OST isoforms; however, it is noteworthy that the discrete localization of aHSPG seen in wild-type tissues is abolished in *Hs3st1*$^{-/-}$, suggesting that their biological activity is compromised.

The physiological importance of aHSPG in the reproductive tract was revealed by the observation that both male and female *Hs3st1*$^{-/-}$ mice suffered from markedly decreased fertility. We have further investigated the reproductive dysfunctions in female *Hs3st1*$^{-/-}$ mice.

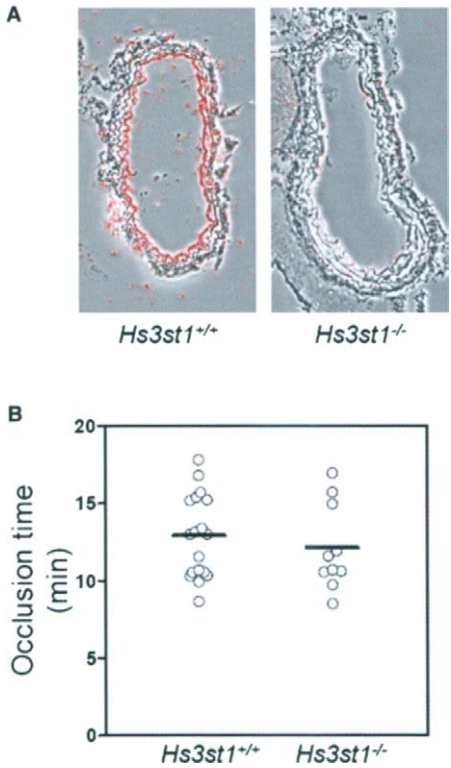

Figure 10 *Hs3st1* disruption reduces carotid artery AT-binding sites but does not alter thrombotic response to acute arterial injury. (A) Autoradiographic detection of ^{125}I-AT-labeled aHSPG on carotid artery cryosections. Silver grains were digitally false colored red and resulting images were superimposed over the corresponding phase contrast image. (B) Acute endothelial injury was initiated by $FeCl_3$ application to the outer surface of a common carotid artery. Blood flow was monitored with extravascular micro Doppler probes to detect the occlusion time – from $FeCl_3$ application to complete cessation of blood flow (64).

C. Reproduction Defects of Female *Hs3st1*$^{-/-}$

We have examined the reproductive performance of female *Hs3st1*$^{-/-}$ mice and observed multiple defects at different levels (unpublished observations).

Despite the fact that young *Hs3st1*$^{-/-}$ females underwent normal puberty and cycled normally, they had significantly decreased litter numbers and size compared with wild-type littermates over a 4-month fertility test. Moreover, the pups born from *Hs3st1*$^{-/-}$ mothers had a significantly reduced body weight during the first 2 days of life, followed by catch-up growth, a pattern typical for IUGR due to placental insufficiency during gestation. In addition, *Hs3st1*$^{-/-}$ females produced decreased numbers of preimplantation embryos compared with wild-type controls. These data indicate that ovulation is impaired in aHSPG deficient females, contributing to the smaller litter size observed at birth. The impairment of ovulation in

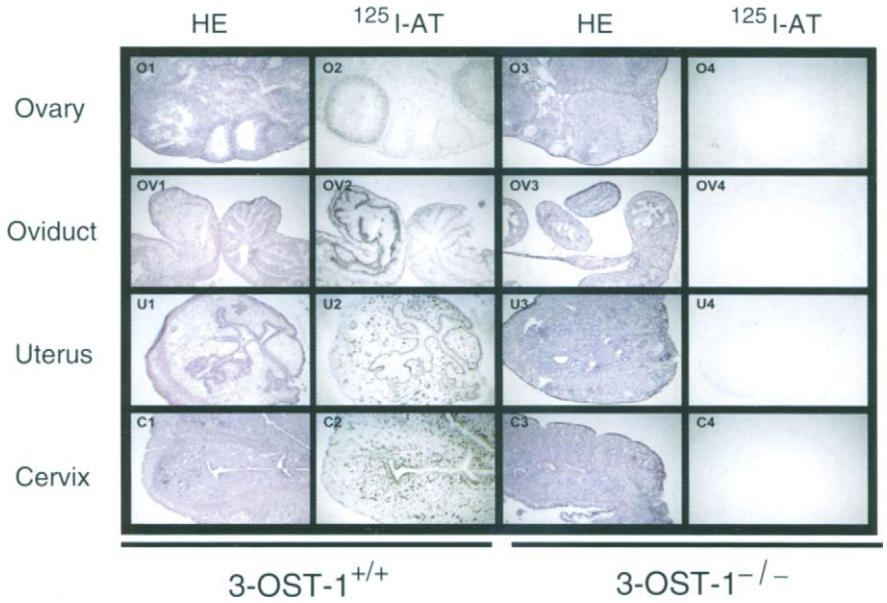

Figure 11 aHSPG localization in the mouse female genital tract. Autoradiographic detection of ^{125}I-AT-labeled aHSPG on cryosections (columns 2 and 4), and histological staining of serial sections (column 1 and 3) of ovary (line 1), oviduct (line 2), uterus (line 3) and cervix (line 4). In wild-type mice, aHSPG are strongly labeled on the surface of granulosa Cells from preovulatory ovarian follicles, and aHSPG are also detected in the oviduct and uterus, associated with epithelial cell basement membranes. In *Hs3st1*$^{-/-}$ mice, aHSPG signal was abolished.

Hs3st1$^{-/-}$ females is concordant with the demonstration in the rat that mobilization of aHSPG with inactive AT variant compromises ovulation (37). Finally, the most striking reproductive phenotype observed was a high incidence of mortality in breeding *Hs3st1*$^{-/-}$ females. This mortality occurred abruptly at mid-gestation in the course of miscarriage. Altogether, these data demonstrate fertility defects in *Hs3st1*$^{-/-}$ females, associated with ovarian and gestational dysfunction.

V. Perspectives

The histological examination of *Hs3st1*$^{-/-}$ females at mid-gestation revealed acute local inflammation with strong PMN infiltration and extended fibrin deposition around the placenta, in close proximity to the maternal-fetal interface. These observations suggest the following scenario to explain the occurrence of IUGR and maternal mortality in *Hs3st1*$^{-/-}$ mice. The deficiency in aHSPG of *Hs3st1*$^{-/-}$ mothers appears to trigger an acute inflammatory reaction at the maternal–fetal interface during placentation. This inflammation is later controlled and the placenta recovers but its development is delayed, leading to the IUGR observed at birth.

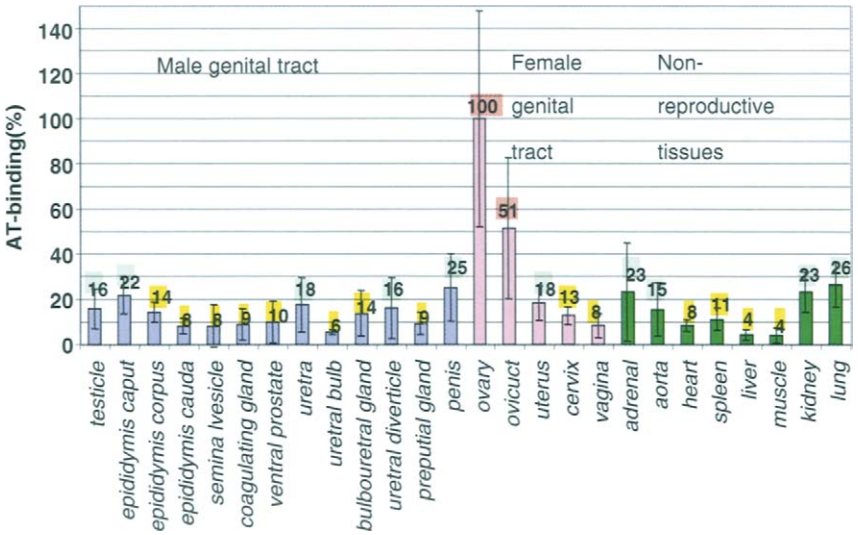

Figure 12 Quantitative measurement of aHSPG in tissue extracts. The distribution of aHSPG in the male and female genital tracts was measured by ^{125}I-AT ligand binding assay on tissue extracts (13,4). The signals were normalized to the highest value, in the ovary. The maximal amount of aHSPG was detected in the ovary, and in the oviduct. In addition, we found positive signals, representing 15–25% of the ovary signal in a discrete number of tissues, in the male and female genital tract: testicle, penis in the male and uterus in the female. In addition, several other organs, such as the kidney or the lung had similar signals. In contrast, in many other tissues the binding of AT was around 10% of the ovary. We consider these organs as negative, the low signal being due to endothelial cell aHSPG.

Occasionally, the inflammation overspills, eventually resulting in miscarriage and maternal death. These data strongly indicate the involvement of aHSPG in the control of inflammation in this system.

The reproductive phenotypes observed in *Hs3st1*$^{-/-}$ female mice are responsible for their decreased fertility and affect the ovary at ovulation and the placenta during gestation. In these two systems, intense tissue remodeling occurs, driven by hormonal stimulation and involving a limited and reversible acute local inflammation that destabilizes existing tissue and allows its reorganization. The hormonally controlled expression of aHSPG in the genital tract could serve to limit the extent of inflammation and proteolysis occurring during tissue remodeling.

HSPG are involved in inflammatory reactions at several levels: they bind and modulate the activity of inflammatory mediators, cytokines, chemokines and their receptors (65,66). Binding of aHSPG to AT can mediate the antiinflammatory properties of AT, either in a thrombin-independent way through syndecan-4 signaling, or by promoting thrombin inhibition and affecting proinflammatory stimuli, such as fibrin deposition and protease activated receptors signaling (67,68).

Further studies are needed to elucidate the level of control of the inflammatory reaction exerted by aHSPG in hormone driven tissue remodeling of the reproductive tract and to identify the mediators involved in this process.

Acknowledgments

The work presented in this chapter has been done in part by talented young scientists working in the laboratory: Shereen Hasan, and Valerie Martin with the expert technical help of Marie-Andrée Ramus and Isabelle Dentand-Quadri. We thank R.D. Rosenberg and N.W. Shworak for a long-standing collaboration and for providing us the *Hs3st1*$^{-/-}$ mice. This project has been supported by the Swiss National Fund for Scientific Research (Grant No. 3200B0-10148/1).

References

1. Capila I, Linhardt RJ. Heparin–protein interactions. Angew Chem Int Ed Engl 2002; 41:390–412.
2. Rosenberg RD, Shworak NW, Liu J, Schwartz JJ, Zhang L. Heparan sulfate proteoglycans of the cardiovascular system. Specific structures emerge but how is synthesis regulated? J Clin Invest 1997; 99:2062–2070.
3. Carrell R, Skinner R, Jin L, Abrahams JP. Structural mobility of antithrombin and its modulation by heparin. Thromb Haemost 1997; 78:516–519.
4. Shworak NW, Liu J, Petros LM, et al. Multiple isoforms of heparan sulfate D-glucosaminyl 3-*O*-sulfotransferase. Isolation, characterization, and expression of human cDNAs and identification of distinct genomic loci. J Biol Chem 1999; 274:5170–5184.
5. Liu J, Shworak NW, Sinay P, et al. Expression of heparan sulfate D-glucosaminyl 3-*O*-sulfotransferase isoforms reveals novel substrate specificities. J Biol Chem 1999; 274:5185–5192.
6. Liu J, Shriver Z, Blaiklock P, Yoshida K, Sasisekharan R, Rosenberg RD. Heparan sulfate D-glucosaminyl 3-*O*-sulfotransferase-3A sulfates N-unsubstituted glucosamine residues. J Biol Chem 1999; 274:38155–38162.
7. Xia G, Chen J, Tiwari V, et al. Heparan sulfate 3-*O*-sulfotransferase isoform 5 generates both an antithrombin-binding site and an entry receptor for herpes simplex virus, type 1. J Biol Chem 2002; 277:37912–37919.
8. Ye S, Luo Y, Lu W, et al. Structural basis for interaction of FGF-1, FGF-2, and FGF-7 with different heparan sulfate motifs. Biochemistry 2001; 40:14429–14439.
9. Marcum JA, Atha DH, Fritze LMS, Nawroth P, Stern D, Rosenberg RD. Cloned bovine aortic endothelial cells synthesize anticoagulantly active heparan sulfate proteoglycan. J Biol Chem 1986; 261:7507–7517.
10. de Agostini AI, Watkins SC, Slayter HS, Youssoufian H, Rosenberg RD. Localization of anticoagulantly active heparan sulfate proteoglycans in vascular endothelium: antithrombin binding on cultured endothelial cells and perfused rat aorta. J Cell Biol 1990; 111:1293–1304.
11. Marcum JA, McKenny JB, Rosenberg RD. Acceleration of thrombin-antithrombin complex formation in rat hindquarters via heparinlike molecules bound to the endothelium. J Clin Invest 1984; 74:341–350.
12. Xu Y, Slayter HS. Immunocytochemical localization of endogenous antithrombin III in the vasculature of rat tissues reveals locations of anticoagulantly active heparan sulfate proteoglycans. J Histochem Cytochem 1994; 42:1365–1376.

13. de Agostini AI, Ramus MA, Rosenberg RD. Differential partition of anticoagulant heparan sulfate proteoglycans synthesized by endothelial and fibroblastic cell lines. J Cell Biochem 1994; 54:174–185.
14. Pejler G, Backstrom G, Lindahl U, et al. Structure and affinity for antithrombin of heparan sulfate chains derived from basement membrane proteoglycans. J Biol Chem 1987; 262:5036–5043.
15. Marcum JA, Conway EM, Youssoufian H, Rosenberg RD. Anticoagulantly active heparin-like molecules from cultured fibroblasts. Exp Cell Res 1986; 166:253–258.
16. Pejler G, David G. Basement-membrane heparan sulfate with high affinity for antithrombin synthesized by normal and transformed mouse mammary epithelial cells. Biochem J 1987; 248:69–77.
17. de Agostini AI, Lau HK, Leone CW, Youssoufian H, Rosenberg RD. Cell mutants defective in synthesizing a heparan sulfate proteoglycan with regions of defined monosaccharide sequence. Proc Natl Acad Sci USA 1990; 87: 9784–9788.
18. Piepkorn M, Hovingh P, Hentschel WM. Isolation of heparan sulfate with antithrombin III affinity and anticoagulant potency from Balb/c 3T3, B16.F10 melanoma and cutaneous fibrosarcoma cell lines. Biochem Biophys Res Commun 1988; 151:327–332.
19. Berry L, Andrew M, Post M, Ofosu F, O'Brodovich H. A549 lung epithelial cells synthesize anticoagulant molecules on the cell surface and matrix and in conditioned media. Am J Respir Cell Mol Biol 1991; 4:338–346.
20. Andrade-Gordon P, Wang SY, Strickland S. Heparin-like activity in porcine follicular fluid and rat granulosa cells. Thromb Res 1992; 66:475–487.
21. Hosseini G, Liu J, de Agostini A. Characterization and hormonal modulation of anticoagulant heparan sulfate proteoglycans synthesized by rat ovarian granulosa cells. J Biol Chem 1996; 271:22090–22099.
22. Shalgi R, Kraicer P, Rimon A, Pinto M, Soferman N. Proteins of human follicular fluid: the blood-follicle barrier. Fertil Steril 1973; 24:429–434.
23. Ny T, Peng XR, Ohlsson M. Hormonal regulation of the fibrinolytic components in the ovary. Thromb Res 1993; 71:1–45.
24. Tsafriri A, Reich R. Molecular aspects of mammalian ovulation. Exp Clin Endocrinol Diabetes 1999; 107:1–11.
25. Kamat BR, Brown LF, Manseau EJ, Senger DR, Dvorak HF. Expression of vascular permeability factor/vascular endothelial growth factor by human granulosa and theca lutein cells. Role in corpus luteum development. Am J Pathol 1995; 146:157–165.
26. Yanagishita M. Proteoglycans and hyaluronan in female reproductive organs. Experientia 1994; 70:179–190.
27. Princivalle M, Hasan S, Hosseini G, de Agostini AI. Anticoagulant heparan sulfate proteoglycans expression in the rat ovary peaks in preovulatory granulosa cells. Glycobiol 2001; 11:183–194.
28. Esko JD, Selleck SB. Order out of chaos: assembly of ligand binding sites in heparan sulfate. Annu Rev Biochem 2002; 71:435–471.
29. Carey DJ. Syndecans: multifunctional cell-surface co-receptors. Biochem J 1997; 327:1–16.
30. Liu W, Litwack ED, Stanley MJ, Langford JK, Lander AD, Sanderson RD. Heparan sulfate proteoglycans as adhesive and anti-invasive molecules.

Syndecans and glypican have distinct functions. J Biol Chem 1998; 273: 22825–22832.
31. Kojima T, Shworak NW, Rosenberg RD. Molecular cloning and expression of two distinct cDNA-encoding heparan sulfate proteoglycan core proteins from a rat endothelial cell line. J Biol Chem 1992; 267:4870–4877.
32. Kojima T, Leone CW, Marchildon GA, Marcum JA, Rosenberg RD. Isolation and characterization of heparan sulfate proteoglycans produced by cloned rat microvascular endothelial cells. J Biol Chem 1992; 267:4859–4869.
33. Mertens G, Cassiman J-J, Van den Berghe H, Vermylen J, David G. Cell surface heparan sulfate proteoglycans from human vascular endothelial cells. Core protein characterization and antithrombin III binding properties. J Biol Chem 1992; 267:20435–20443.
34. Ishiguro K, Kojima T, Taguchi O, Saito H, Muramatsu T, Kadomatsu K. Syndecan-4 expression is associated with follicular atresia in mouse ovary. Histochem Cell Biol 1999; 112:25–33.
35. Murdoch AD, Liu B, Schwarting R, Tuan RS, Iozzo RV. Widespread expression of perlecan proteoglycan in basement membranes and extracellular matrices of human tissues as detected by a novel monoclonal antibody against domain III and by in situ hybridization. J Histochem Cytochem 1994; 42: 239–249.
36. Eriksen GV, Carlstedt I, Morgelin M, Uldbjerg N, Malmstrom A. Isolation and characterization of proteoglycans from human follicular fluid. Biochem J 1999; 340:613–620.
37. Hasan S, Hosseini G, Princivalle M, et al. Co-ordinate expression of anticoagulant heparan sulfate proteoglycans and serine protease inhibitors in the rat ovary: a potent system of proteolysis control. Biol Reprod 2001; 66: 144–158.
38. Dvorak HF, Nagy JA, Feng D, Brown LF, Dvorak AM. Vascular permeability factor/vascular endothelial growth factor and the significance of microvascular hyperpermeability in angiogenesis. Curr Top Microbiol Immunol 1999; 237: 97–132.
39. Huntington JA, Read RJ, Carrell RW. Structure of a serpin-protease complex shows inhibition by deformation. Nature 2000; 407:923–926.
40. Liu K, Brandstrom A, Liu YX, Ny T, Selstam G. Coordinated expression of tissue-type plasminogen activator and plasminogen activator inhibitor type 1 during corpus luteum formation and luteolysis in the adult pseudopregnant rat. Endocrinology 1996; 137:2126–2132.
41. Peng XR, Hsueh AJ, Ny T. Transient and cell-specific expression of tissue-type plasminogen activator and plasminogen-activator-inhibitor type 1 results in controlled and directed proteolysis during gonadotropin-induced ovulation. Eur J Biochem 1993; 214:147–156.
42. Hagglund AC, Ny A, Liu K, Ny T. Coordinated and cell-specific induction of both physiological plasminogen activators creates functionally redundant mechanisms for plasmin formation during ovulation. Endocrinology 1996; 137:5671–5677.
43. Vassalli JD, Huarte J, Bosco D, et al. Protease-nexin I as an androgen-dependent secretory product of the murine seminal vesicle. EMBO J 1993; 12:1871–1878.
44. Gulamali-Majid F, Ackerman S, Veeck L, Acosta A, Pleban P. Kinetic immunonephelometric determination of protein concentrations in follicular fluid. Clin Chem 1987; 33:1185–1189.

45. Suchanek E, Mujkic Klaric A, Grizelj V, Simunic V, Kopjar B. Protein concentration in pre-ovulatory follicular fluid related to ovarian stimulation. Int J Gynaecol Obstet 1990; 32:53–59.
46. Kourteva Y, Schapira M, Patston PA. The effect of sex and age on antithrombin biosynthesis in the rat. Thromb Res 1995; 78:521–529.
47. Jin L, Abrahams JP, Skinner R, Petitou M, Pike RN, Carrell RW. The anticoagulant activation of antithrombin by heparin. Proc Natl Acad Sci USA 1997; 94:14683–14688.
48. Carrell RW, Evans DLI. Serpins: mobile conformations in a family of proteinase inhibitors. Curr Opin Struct Biol 1992; 2:438–446.
49. Evans DL, McGrogan M, Scott RW, Carrell RW. Protease specificity and heparin binding and activation of recombinant protease nexin I. J Biol Chem 1991; 266:22307–22312.
50. Ehrlich HJ, Keijer J, Preissner KT, Gebbink RK, Pannekoek H. Functional interaction of plasminogen activator inhibitor type 1 (PAI-1) and heparin. Biochemistry 1991; 30:1021–1028.
51. Rovelli G, Stone SR, Guidolin A, Sommer J, Monard D. Characterization of the heparin-binding site of glia-derived nexin/protease nexin-1. Biochemistry 1992; 31:3542–3549.
52. Gallagher JT. Structure–activity relationship of heparan sulphate. Biochem Soc Trans 1997; 25:1206–1209.
53. Zhang L, Yoshida K, Liu J, Rosenberg RD. Anticoagulant heparan sulfate precursor structures in F9 embryonal carcinoma cells. J Biol Chem 1999; 274:5681–5691.
54. Wallace A, Rovelli G, Hofsteenge J, Stone SR. Effect of heparin on the glia-derived-nexin-thrombin interaction. Biochem J 1989; 257:191–196.
55. Gebbink RK, Reynolds CH, Tollefsen DM, Mertens K, Pannekoek H. Specific glycosaminoglycans support the inhibition of thrombin by plasminogen activator inhibitor 1. Biochemistry 1993; 32:1675–1680.
56. Rosenberg RD, Aird WC. Vascular-bed – specific hemostasis and hypercoagulable states. N Engl J Med 1999; 340:1555–1564.
57. Dvorak HF, Senger DR, Dvorak AM, Harvey VS, McDonagh J. Regulation of extravascular coagulation by microvascular permeability. Science 1985; 227:1059–1061.
58. Gettins PG, Fan B, Crews BC, Turko IV, Olson ST, Streusand VJ. Transmission of conformational change from the heparin binding site to the reactive center of antithrombin. Biochemistry 1993; 32:8385–8389.
59. Bronson FH, Dagg CP, Snell GD. Reproduction. In: Green EL, Coleman DL, Fahey EU, eds. Biology of the Laboratory Mouse. New York: McGraw Hill, 1966; 187–200.
60. Bateman BG, Kolp LA, Nunley WC, Thomas TS, Mills SE. Oocyte retention after follicle luteinization. Fertil Steril 1990; 54:793–798.
61. Bitter T, Muir HM. A modified uronic acid carbazole reaction. Anal Biochem 1962; 4:330–334.
62. Bjornsson S. Simultaneous preparation and quantitation of proteoglycans by precipitation with alcian blue. Anal Biochem 1993; 210:282–291.
63. Matorras R, Garcia F, Corcostegui B, Ramon O, Montoya F, Rodriguez Escudero FJ. Factors that influence the outcome of the intrauterine insemination with husband's sperm. Clin Exp Obstet Gynecol 1994; 21:38–44.

64. HajMohammadi S, Enjoyji K, Princivalle M, et al. The majority of anticoagulant heparan sulfate is not absolutely essential for normal hemostasis. J Clin Invest 2003; 111:989–999.
65. Gotte M. Syndecans in inflammation. FASEB J 2003; 17:575–591.
66. Hoogewerf AJ, Kuschert GS, Proudfoot AE, et al. Glycosaminoglycans mediate cell surface oligomerization of chemokines. Biochem 1997; 36:13570–13578.
67. Coughlin SR. How the protease thrombin talks to cells. Proc Natl Acad Sci USA 1999; 96:11023–11027.
68. Griffin CT, Srinivasan Y, Zheng YW, Huang W, Coughlin SR. A role for thrombin receptor signaling in endothelial cells during embryonic development. Science 2001; 293:1666–1670.

Chemistry and Biology of Heparin and Heparan Sulfate
H.G. Garg, R.J. Linhardt and C.A. Hales (Editors)

Chapter 16

Glycol-Splitting as a Device for Modulating Inhibition of Growth Factors and Heparanase by Heparin and Heparin Derivatives

ANNAMARIA NAGGI

G. Ronzoni Institute for Chemical and Biochemical Research, G. Colombo, Milan, Italy

I. Introduction

The anticoagulant activity of heparin (H) has been extensively exploited in clinics. Although heparin remains a major drug in the prevention of thromboembolic diseases, its anticoagulant activity is usually seen as an adverse effect in the exploitation of the several other biological activities found for this polysaccharide. Both earlier and more recent knowledge of the relationships between the structure and biological activity of heparin has been summarized in reviews covering heparin/heparansulfate–protein interactions and associated biological activities (1–4).

Part of our studies on heparin have focused on periodate oxidation studies leading to glycol-split derivatives. Glycol-splitting of all non-sulfated uronic acid residues of heparin, including the glucuronic acid (GlcA) residue essential for high-affinity binding to antithrombin (5–7), involves a dramatic drop in the anticoagulant activity (8). In contrast, glycol-splitting did not impair the nonantithrombin-mediated biological activities of heparin, such as lipid clearing and heparin cofactor II-mediated anticoagulant activity, mainly associated with regular sulfated regions ($IdoA2SO_3$–$GlcNS6SO_3$) (9,10).

The versatility of heparin as a ligand for many proteins is associated in part with the ability of its iduronic acid (IdoA) residues to undergo rapid conformational changes involving a variety of arrangements of its anionic groups on the two sides of the polymer chains (11). Earlier studies (12) suggested that an extra

flexibility can be induced in heparin chains by opening the uronic acid rings by periodate oxidation, thus favoring the interaction with target proteins. This kind of modification (glycol-splitting) is illustrated in a simplified way in Fig. 1.

In view of this expected extra flexibility, a systematic study of glycol-splitting of heparin was undertaken, with the particular aim of studying the influence of glycol-splitting on the interaction of heparin with proteins involved in induction of growth and metastatic spread of cancer cells. The targets for these studies were growth factors, such as fibroblast growth factor 2 (FGF-2), vascular endothelial growth factor (VEGF), and the enzyme heparanase. FGF-2 and VEGF are among the major inducers of angiogenesis (13) and heparanase is implicated in angiogenesis and metastasis, both through the release of growth factors from endothelium and the disruption of extracellular matrix, thus facilitating extravasation and migration of cancer cells (14).

Glycol-splitting was performed by periodate oxidation of preexisting GlcA and IdoA of natural heparins, as well as of heparins in which additional non-sulfated uronic acid residues were generated by systematic alkali-induced 2-*O*-desulfation. These undersulfated and glycol-split derivatives were also studied with the aim of validating the concept that the generation of sulfation gaps along the heparin chains should destabilize binding with proteins requiring, especially in the formation of ternary complexes, relatively long, fully sulfated heparin sequences (15,16). The primary products of periodate oxidation were stabilized by borohydride reduction, obtaining well-defined compounds that were studied for their interaction with FGF-2 and heparanase, and for other biological activities associated with these interactions. The dialdehyde groups of the primary products of periodate oxidation were also exploited to obtain glycine and taurine derivatives of glycol-split heparins. Most of the glycol-split derivatives were more effective than unmodified heparin as inhibitors of both growth factors and heparanase. A dramatic increase in the heparanase-inhibiting activity was induced by glycol-splitting of *N*-acetylated heparins (NAH). Since these products are poor releasers of growth factors from endothelium, they are promising candidates as antiangiogenic and antimetastatic agents.

II. Glycol-Split Heparins

A. Glycol-Splitting at the Level of Preexisting Non-sulfated Uronic Acid Units

Periodate oxidation is a classic reaction in carbohydrate chemistry used to split bonds between vicinal carbons bearing unsubstituted hydroxyl or amino groups (17). As shown in Fig. 1, heparin bonds cleavable by periodate are those of non-sulfated uronic acid residues, i.e., GlcA and IdoA. Under standardized reaction conditions, glycosidic bonds are barely affected by periodate oxidation and the products retain the same molecular size of the parent heparin or undergo only a slight molecular weight decrease. Primary products of the reaction are polydialdehydes ("oxyheparins", O·H), which are usually stabilized by borohydride reduction, leading to "reduced oxyheparins" (RO·H).

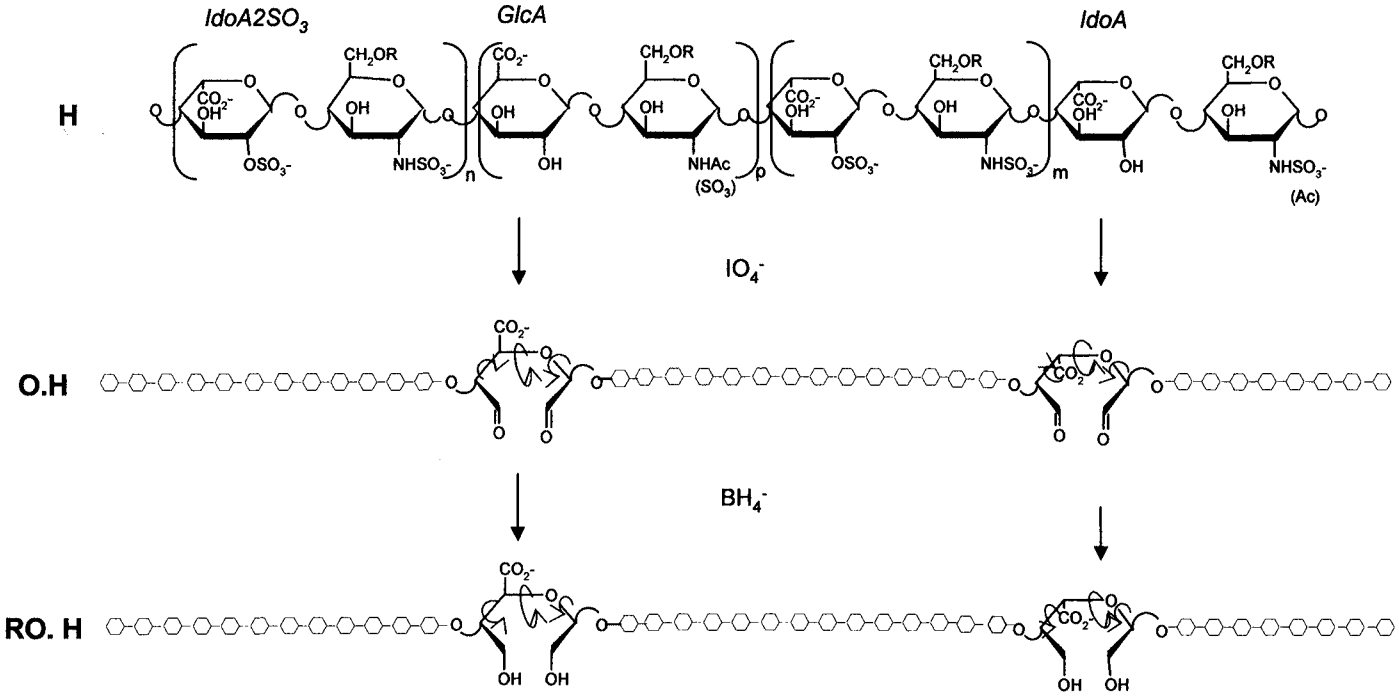

Figure 1 Schematic representation of glycol-splitting of preexisting non-sulfated uronic acid residues of heparin (H) to yield corresponding dialdehydes ("oxyheparins", O·H), and "reduced oxyheparins", RO·H.

Periodate oxidation was first exploited to prepare nonanticoagulant heparins (9,10,18) and as an analytical tool for the determination of unsubstituted uronic acids and as a method of depolymerizing heparin. It is also part of a depolymerizing strategy to generate fragments for further structural analysis (19) and for biological screenings (20). The analytical approach is based on treatment of RO·H with acid (Smith degradation) or of O·H with alkali, to specifically cleave the glycosidic bonds of the glycol-split residues. Assessment of the extent of splitting is made either through determination of the consumption of the periodate reagent (21), or by chromatographic analysis of oligosaccharidic fragments (22). Extensive periodate oxidation also splits the non-sulfated GlcA residue within the pentasaccharide of the antithrombin binding domain (ATbd) (Fig. 2) (6), thus explaining the dramatic drop of the anticoagulant activity observed for RO·Hs as compared with the parent unmodified heparins (23–24). Figure 1 illustrates the preparation of O·H and RO·H, showing that the chemical modification affects only a few residues of the original structure, i.e., the naturally preexisting GlcA and IdoA, usually accounting for 20–25% of total uronic acid in pig mucosal heparins (25). Figure 2 shows the pentasaccharidic segment of heparin corresponding to the ATbd and the same after glycol-splitting, showing that glycol-splitting modifies the GlcA residue essential for anticoagulant activity (26,27).

To confirm that periodate oxidation of heparin does not affect the major part of the heparin structure, RO·H remains a good substrate for heparinase I, with just some reduction of the yields in the di- and tetrasaccharidic fractions with respect to the untreated material (28,29). Glycol-splitting was also performed on heparan sulfates (HS), which became less susceptible to digestion by heparitinase than the original GAGs (29,30).

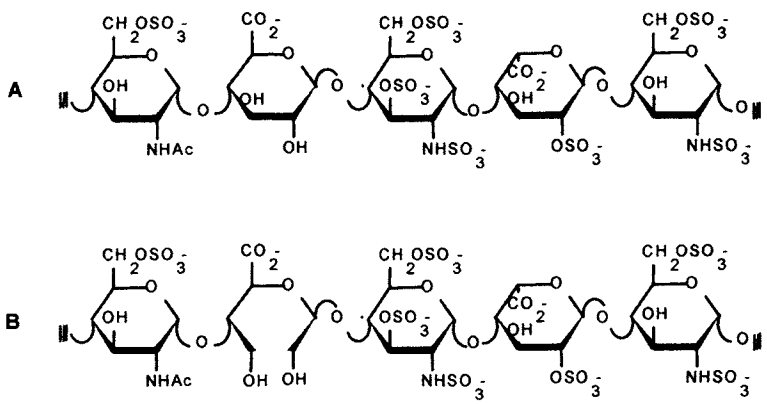

Figure 2 Pentasaccharidic sequence of the heparin/HS active site for AT before (A) and after glycol-splitting of the glucuronic acid (GlcA) residue (B).

B. Glycol-Splitting of Uronic Acid Residues Generated by Selective Desulfation of 2-*O*-Sulfated Iduronic Acid Residues

2-*O*-desulfation of heparin can be performed using different procedures. Lyofilization of alkaline solutions allows the direct and complete conversion of $IdoA2SO_3$ to IdoA residues. A second procedure based on controlled heating of heparin alkaline solutions is more easily modulated in order to generate also partially 2-*O*-desulfated heparins. As shown in Fig. 3, this reaction occurs through formation of epoxide derivatives (step a). The hydrolysis of the resulting epoxide rings with inversion of configuration leads to heparin derivatives containing L-galacturonic acid (GalA) residues (step b) (31–33). All non-sulfated uronic acids, i.e., the preexisting non-sulfated GlcA and IdoA residues and the newly generated GalA ones, were subsequently oxidized with periodate (step c) and either reduced with borohydride (step d) or converted by aminative reduction to glycine and taurine derivatives (step e) (34).

A number of heparin derivatives with degrees of conversion to "GalA heparins" ranging from 14% to 42% of the original content of $IdoA2SO_3$ residues and the corresponding glycol-split derivatives were thus obtained. These compounds consist of chains constituted by regular sequences of trisulfated disaccharides ($IdoA2SO_3$–$GlcNS6SO_3$) spaced by flexible joints. In fact, the glycol-split residues interrupt the natural 2-*O*-sulfated sequences and generate new ones of different lengths depending on the extent of splitting. The idealized structures shown in Fig. 4 illustrate the prevalent structures obtained for different degrees of 2-*O*-desulfation/glycol-splitting in the NS regions of heparin. Whereas splitting one out of four uronic acid residues "frames" heptasaccharidic sequences, splitting one out of three or one out of two residues results in pentasaccharidic and trisaccharidic sequences between glycol-split residues, respectively.

The same procedure was applied to obtain glycol-split derivatives of *N*-acetyl heparins of various degrees of *N*-acetylation and 2-*O*-desulfation (34), as shown in the general scheme of Fig. 5A for a fully and ~50% NAH (Fig. 5B).

C. Structural Characterization of Glycol-Split Heparins

All products and their intermediates can be easily characterized by their ^{13}C and ^{1}H-NMR spectra, which also permit the determination of the mole percent of the modified residues. Figure 6 shows the ^{13}C-NMR spectrum of a typical glycol-split heparin containing a total of approximately 50% glycol-split uronic acids arising from the non-sulfated uronic acids originally present in the parent heparin (22% GlcA and 9% IdoA), in addition to the newly formed GalA residues (approximately 25%) generated by controlled 2-*O*-desulfation.

The spectrum is remarkably clean, consisting of a major pattern of signals superimposed on weak signals mostly associated with the minor GlcNAc-containing sequences of the NA and mixed NS/NA regions of the original heparin. The spectrum is fully compatible with a uniform distribution of split residues along the NS regions of the heparin chains. Independent proof of structure was provided

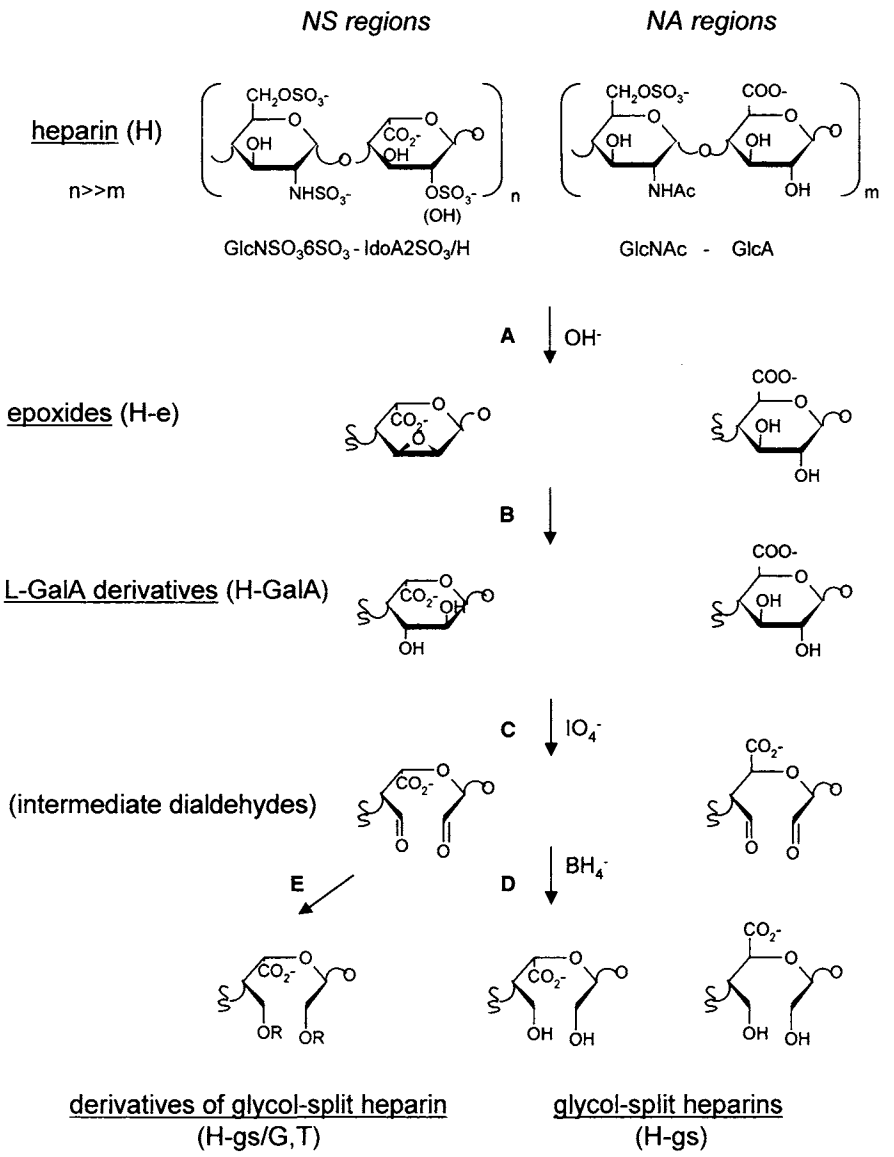

Figure 3 Structure of disaccharide units of heparin and modified uronic acid residues following: (A) alkali treatment; (B) heating at 70 °C/pH 7; (C) reaction with periodate; (D) borohydride reduction of dialdehydes; (E) derivatization of dialdehydes with glycine (G) and taurine (T). Reactions (C–E) involve L-iduronic acid residues of the prevalent, *N*-sulfated (NS) regions as well as D-glucuronic acid residues of the *N*-acetylated (NA) regions.

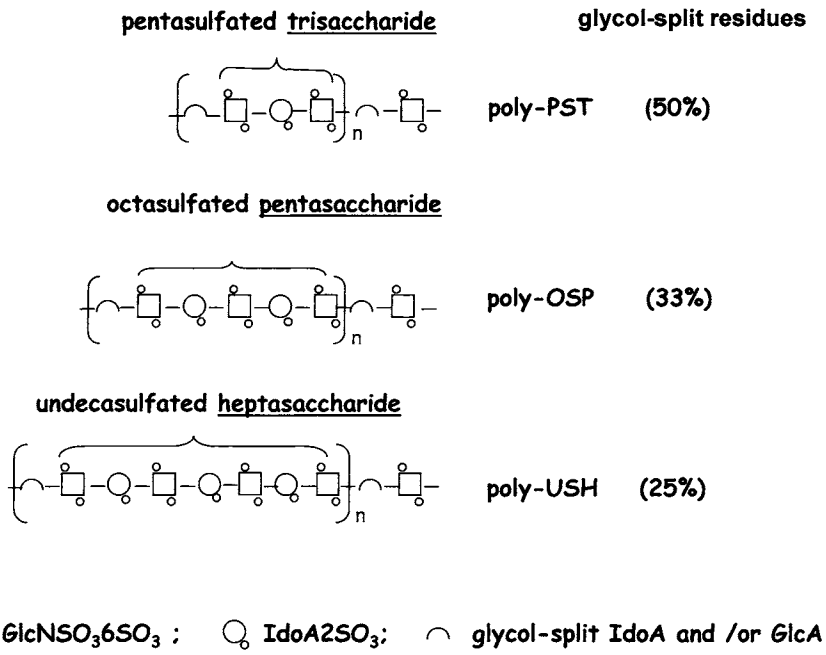

Figure 4 Schematic representation of regularly sulfated heparin sequences (NS regions) separated by glycol-split uronic acid residues, obtained by controlled 2-*O*-desulfation/glycol splitting. Modification of one-fourth of $IdoA2SO_3$ residues in the NS region chiefly affords sequences of undecasulfated heptasaccharides; modification of one-third and one-half or more of these residues generate shorter regularly sulfated sequences (octasulfated pentasaccharides and pentasulfated trisaccharide, respectively).

by Smith degradation with mild acid, which generated a trisaccharide linked to the remnant of a glycol-split uronic acid as the major hydrolysis product.

III. Protein-Binding and Associated Biological Properties of Glycol-Split Heparins

A. Interaction with Fibroblast Growth Factor 2

Binding of HS to fibroblast growth factors usually involves only some of the sulfate groups present in its heparin-like sequences (13). Exogenous heparin competes with HS chains of cell-surface HSPGs for binding FGF-2 and this essentially involves only two sulfate groups (the NSO_3 of a GlcN residue and the OSO_3 of an $IdoA2SO_3$ residue) of a disaccharidic unit of heparin. Activation of the growth factor involves formation of ternary complexes with FGFs and FGFRs and requires several pairs of these groups (as well as some 6-*O*-sulfate groups in the case of

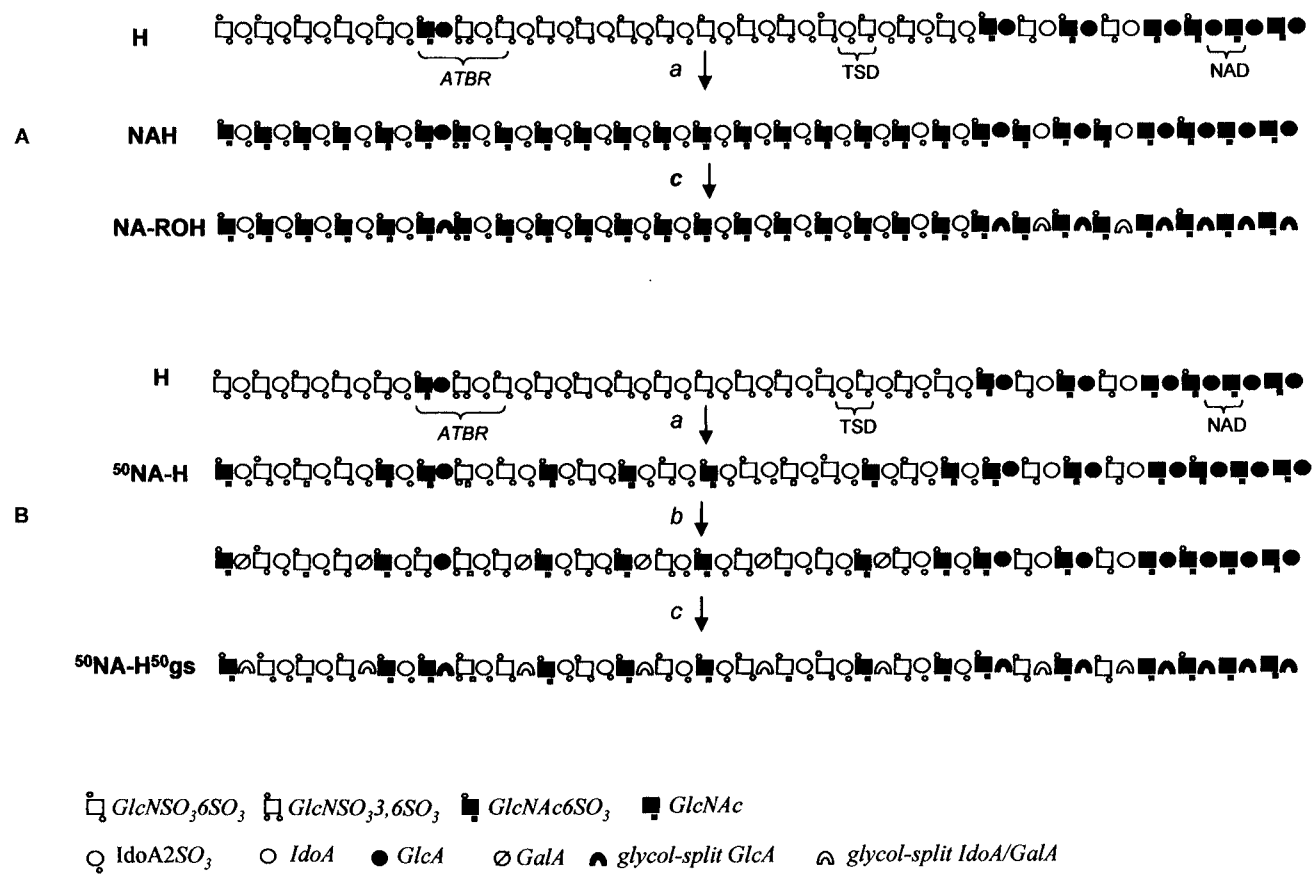

Figure 5 Schematic representation of glycol-splitting of the preexisting (A) and both the preexisting and the newly generated nonsulfated uronic acid residues of *N*-acetylated heparin (B). Examples A and B refer to fully *N*-acetylated heparin (NAH) and 50% *N*-acetylated heparin (^{50}NAH), respectively. The part (A) shows the model of 25% glycol-split (gs) fully *N*-acetylated heparin derivative (NAH^{25} gs).

FGF-2) along heparin chains longer than 8–10 monosaccharidic units (35,36). Reported strategies to develop antiangiogenic agents based on competition with HSPGs for binding FGF-2 while preventing formation of FGF-2/FGFR complexes involve use of small heparin oligosaccharides (37) or removal of heparin 6-*O*-sulfate groups necessary for activation of the FGF-2–FGFR complexes (38).

The partially (50%) 2-*O*-desulfated glycol-split heparin (p-PST.sU) retains the heparin properties to bind FGF-2. In fact, it prevents the triptic digestion of FGF-2 (15,39) and displaces the growth factor from the extracellular matrix (40). However, unlike heparin, it is unable to induce FGF-2 oligomerization. The heparin derivative p-PST.sU was a potent inhibitor for FGF-2-induced [^{3}H]-thymidine incorporation in BAE cells (ID_{50} of 1, 100, and >100 μg/ml for p-PST.sU, unmodified heparin, and *N*-acetyl heparin, respectively) (15). Moreover, p-PST.sU inhibited the mitogenic activity exerted by FGF-2, with a potency significantly higher than those of the other tested GAGs (ID_{50} corresponding to 0.1, 2.0, and >100 μg/ml for p-PST.sU, unmodified heparin, and *N*-acetyl heparin, respectively). This glycol-split heparin derivative also inhibits *in vitro* FGF-2-stimulated endothelial cell proliferation and prevents the formation of FGFR/FGF-2/HSPG ternary complex in a FGF-2-mediated cell–cell adhesion assay (Fig. 7).

A significant correlation exists between the potency shown by the various glycol-split heparins in the two *in vitro* assays and their degree of splitting (Fig. 7), indicating that the FGF-2-antagonist activity of these derivatives increases with increasing the number of glycol-split uronic acid residues along the heparin chain independently of their molecular weights.

B. Interaction with Vascular Endothelial Growth Factor

Vascular endothelial growth factor (VEGF) also appears to play a major role in angiogenesis (41) through binding heparansulfate (HS) of cell surface proteoglycans (HSPGs) (42,43). Heparin–HS interaction can modulate the activity and fate of VEGF. In addition, cell surface HSPGs are required for the interaction of VEGF with VEGFRs (42–44). Vascular endothelial growth factor and VEGFR antagonists affect tumor growth and vascularization in different experimental animal models (45). It was demonstrated by polyacrilamide gel electrophoresis that a low molecular weight (LMW) derivative of p-PST.sU binds to $VEGF_{165}$ isoform and exerts a significant $VEGF_{165}$ antagonist activity *in vitro* (46). Moreover, surface plasmon resonance experiments confirmed the ability of LMW p-PST.sU to bind directly to $VEGF_{165}$ even though with an ID_{50} value (46) higher than that of heparin, but close to that of LMW heparin (100 nM).

Unlike heparin, the LMW glycol-split derivative was unable to increase the binding of ^{125}I-$VEGF_{165}$ to HUVE cells. In contrast, it caused a significant decrease of the ^{125}I-$VEGF_{165}$ binding to its receptors, both in the absence and in the presence of 1.0 μg/ml heparin. Scatchard plot analysis of the binding data demonstrated that LMW p-PST.sU causes an apparent three-fold decrease in the number of cell surface binding sites without affecting their affinity for the ligand, in keeping with a competitive mechanism of inhibition. These data indicate that, unlike

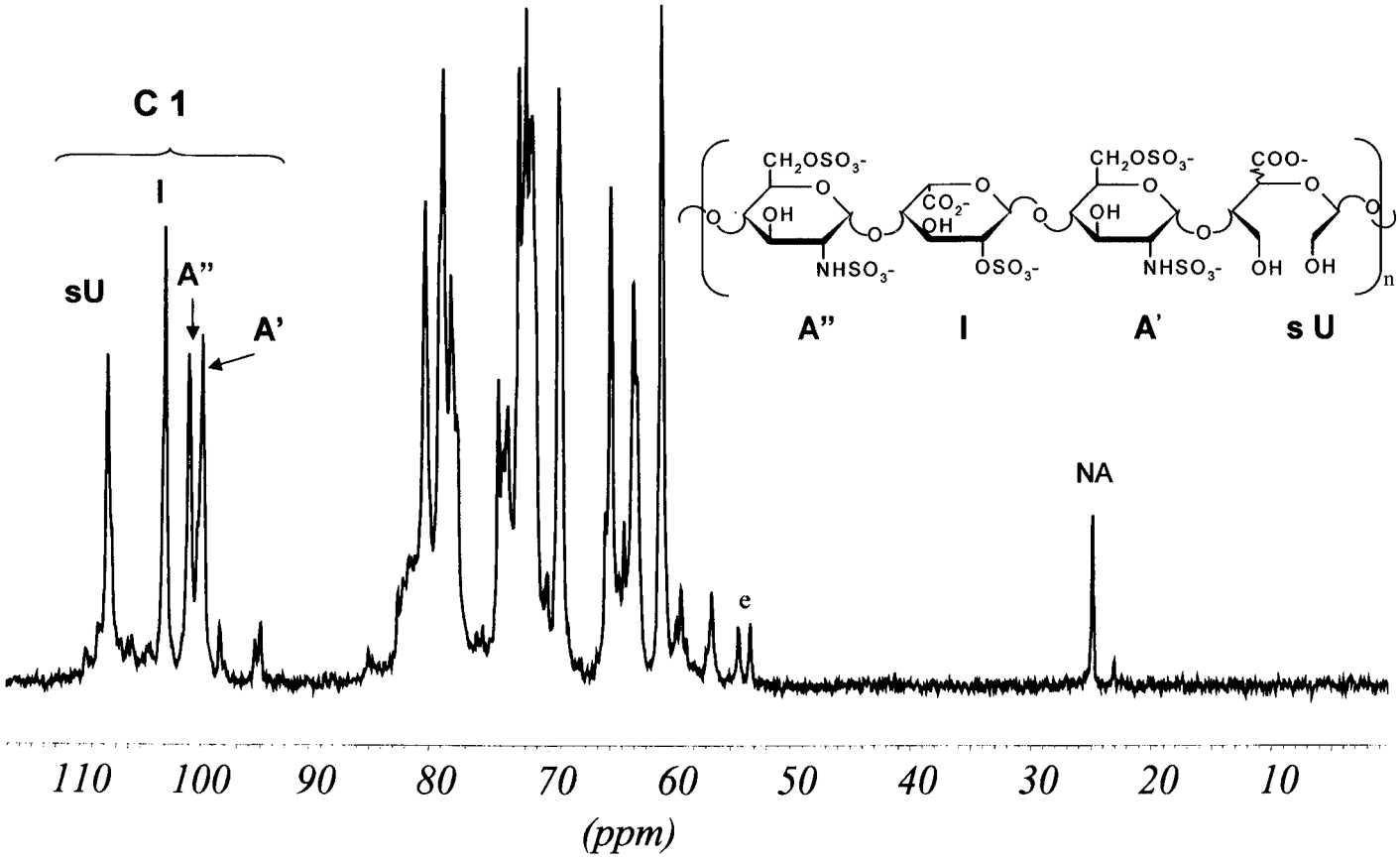

Figure 6 ^{13}C-NMR spectra (100 MHz,D_2O) of a prototype of 50% glycol-split heparin. Weak signals are associated with heterogeneities in the original heparin [such as *N*-acetylated GlcN (NA) residues] and with residual intermediates [such as epoxidated (e) residues].

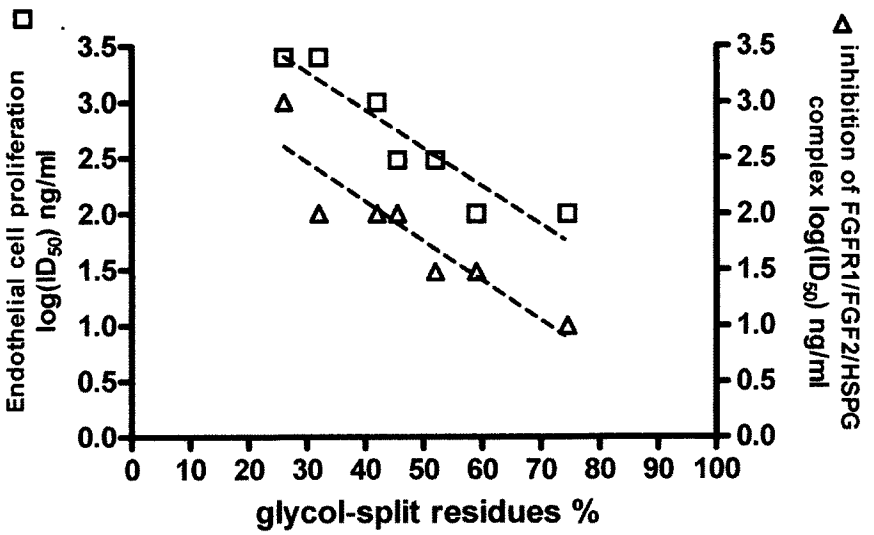

Figure 7 Effect of glycol-splitting on the FGF-2-antagonist, antiangiogenic activities of heparin derivatives. The potencies of glycol-split heparins in the endothelial cell proliferation assay (□) and in the FGF-2-mediated cell–cell adhesion assay (Δ) are significantly related to their degree of glycol-splitting (34).

heparin, LMW p-PST.sU is unable to efficiently present VEGF to its high-affinity receptors, thus sequestering the growth factor and hampering its receptor interaction. In fact, it inhibited the $VEGF_{165}$-induced proliferation of HUVE cells in a dose-dependent manner with an IC_{50} value of 100 μg/ml.

C. Interaction with Heparanase

Even highly efficient FGF inhibitors may not be sufficient to suppress FGF-induced signaling. Accordingly, it is desirable to minimize the concentration of growth factors in circulation by preventing, as much as possible, their release from HSPGs. In principle, such a release can be prevented by inhibiting heparanase, the β-endo glycosidase, which cleaves the HS chains at the level of GlcA residues and can release FGFs in active form and then favor the invasion of cancer cells through the connective tissue (47–49). Inhibition of heparanase is also expected to prevent disruption of the HSPGs of the extracellular matrix and migration of cancer cells causing an antimetastatic effect (50).

Heparin is a known heparanase inhibitor (~70% inhibition at 1 μg/ml) and its 2-*O*-desulfation does not significantly decrease its inhibitory activity. On the other hand, this activity can be enhanced by introduction of glycol-split residues in the heparin chain (42). Figure 8A shows the inhibition activity of heparin, RO·H (25% gs) and of a partially *O*-desulfated glycol-split heparin tested at two different concentrations. An increase of inhibition activity as a function of the number of glycol-split

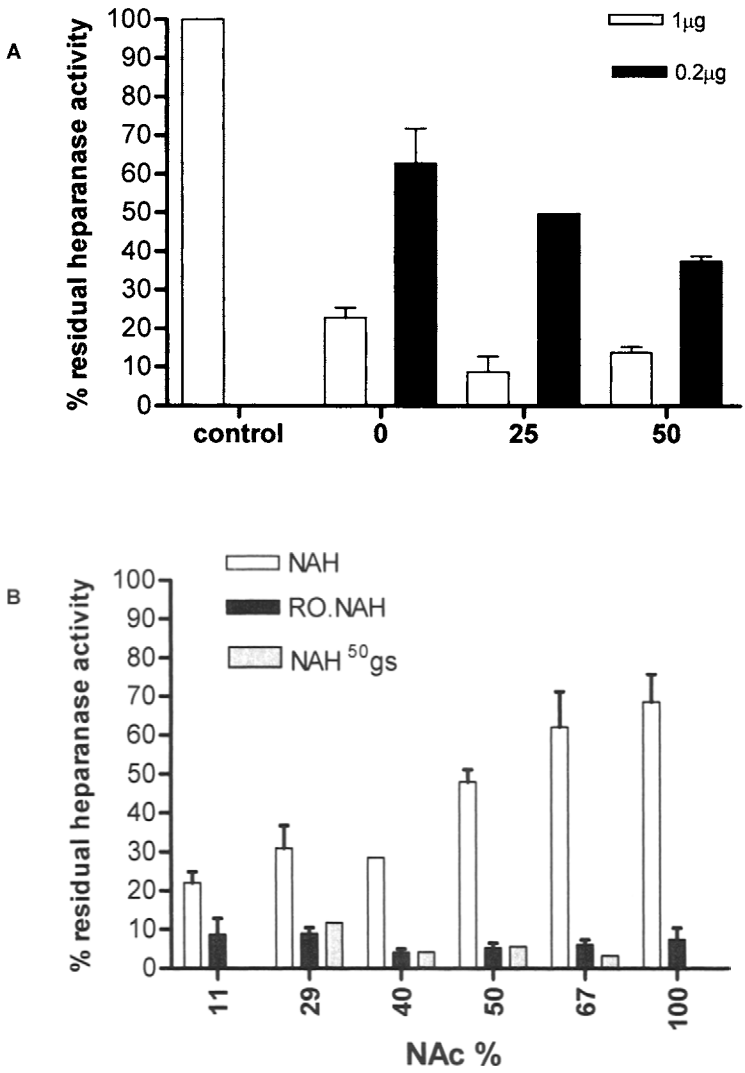

Figure 8 Heparanase inhibitory activity in the absence (control) and presence of 1 μg/ml (white bars) or 0.2 μg/ml (black bars) of glycol-split heparins (A), and in presence of 1 μg/ml of fully *N*-acetylated heparin (white bars), 25% glycol-split *N*-acetylated heparins(black bars) and 50% glycol-split *N*-acetylated heparin (grey bars) (B). Sulfate labeled ECM was incubated (4 h, 37 °C, pH 6.0) with 40 μg/ml of recombinant heparanase in absence (control) and presence of inhibitor.

residues in the polysaccharide is evident. This effect was even more evident when the glycol-split residues were generated on chains of NAH (Fig. 8B). In fact, while removal of up to 50% of *N*-sulfate groups followed by *N*-acetylation resulted in a substantial decrease of the inhibitory activity, glycol-splitting enhanced the heparanase inhibitory activity of *N*-acetyl heparins for any tested degree of *N*-acetylation and this was more evident for *N*-acetylation degrees higher than approximately 50%. Glycol-splitting extended to newly-generated non-sulfated GalA residues in heparin and NAH gave products showing high heparanase inhibitory activity (42).

D. Inhibition of Angiogenesis and Metastasis

The chick embryo chorioallantoic membrane (CAM) is supplied by an extensive capillary network expressing FGF-2, which plays a limiting role in the development of the vascular system of this embryonic membrane (51,52). Chorioallantoic membrane is thus a well-established assay for studying the effects of growth factors on blood vessel, and it represents an *in vivo* system suitable for assessing the impact of putative anti-angiogenic FGF-2 antagonists on blood vessel formation during development.

In the basal CAM assay, where heparin is inactive in inhibiting neovascularization or somewhat proangiogenic, most of the glycol-split tested products exert an antiangiogenic effect, as shown in Fig. 9. The highest activities (inhibition of 60–90%) were observed for heparins glycol-split to extents higher than 45%, and for their derivatives with a maximum activity of around 50%. *N*-acetyl heparin, 50% *N*-acetylated heparin, and its RO derivative were essentially inactive (34).

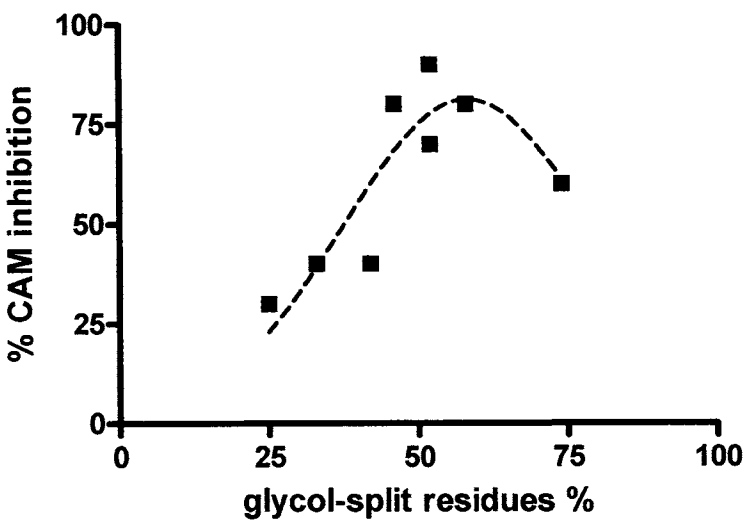

Figure 9 Effect of glycol-splitting compounds (100 μg/embryo) on the angiostatic activity in CAM assay (34).

The glycol-split derivative p-PST.sU showed inhibitory properties on vessel proliferation also in the CAM angiogenesis induced by FGF-2 or VEGF.

In heparanase-overexpressing transgenic mice, glycol-split heparin p-PST.sU inhibited wound angiogenesis (53). Like unmodified heparin, a number of glycol-split heparins effectively abolish experimental lung colonization of intravenously administered B16-BL6 mouse melanoma cells (54–56).

IV. Conformational Implications of Glycol-Splitting

The antiangiogenic properties of glycol-split heparins can be explained by their three-dimensional structures and molecular dynamics in water solution as compared with heparin. The overall and internal motion parameters of both heparin and its glycol-split derivative p-PST.sU were calculated from NMR relaxation data. The nature of overall motion and the rates of overall and internal motions have been estimated using the model-free approach (57). Heparin and its derivative can be approximated with a symmetric top model (it was assumed that both molecules adopt a cylindrical shape in water solution). The main axis of the cylinder is identified along the molecular chain. Although the axial motion ratio ($\tau_\perp/\tau_\parallel$) is comparable in both molecules, significant differences were found in the internal motion correlation times (τ_e) and general order parameters (S^2_{C-H}) (58). These results support the assumption that glycol-split residues act as flexible joints and confirm the results of early small-angle X-ray scattering studies (59, Table 1), indicating a more spherical or coiling configuration of RO·H as compared with the original heparin.

As illustrated in Fig. 10 for one of the major conformers compatible with measured nuclear Overhauser effects (NOE), the chain of glycol-split derivative deviates from the linear propagation of the heparin helix (60), which facilitates accommodation in the basic canyon of FGF/FGFR assemblies.

In order to investigate whether conformational properties induced by glycol-splitting in the heparin sequences could influence binding to FGF-2 and account for the observed induction of FGF-2-antagonist properties, the coordinates of a heparin hexasaccharidic fragment (H-Hexa) co-crystallized with FGF-2 (61–63) were used to model, by molecular dynamics calculations, the corresponding glycol-split

Table 1 Solution Parameters of Heparin in Water at 25 °C, from SAXS Measurements*

	Pig mucosal H	Pig mucosal RO·H	Beef lung H	Beef lung RO·H
$\langle S^2\rangle^{1/2}$ (Å)	43.1	59.1	26.0	29.2
M_w (Da)	16,100	16,300	8800	8900
$\nu_{hyd} \times 10^{-4}$(Å)	24.5	28.5	8.0	10.0

*Data from (59).

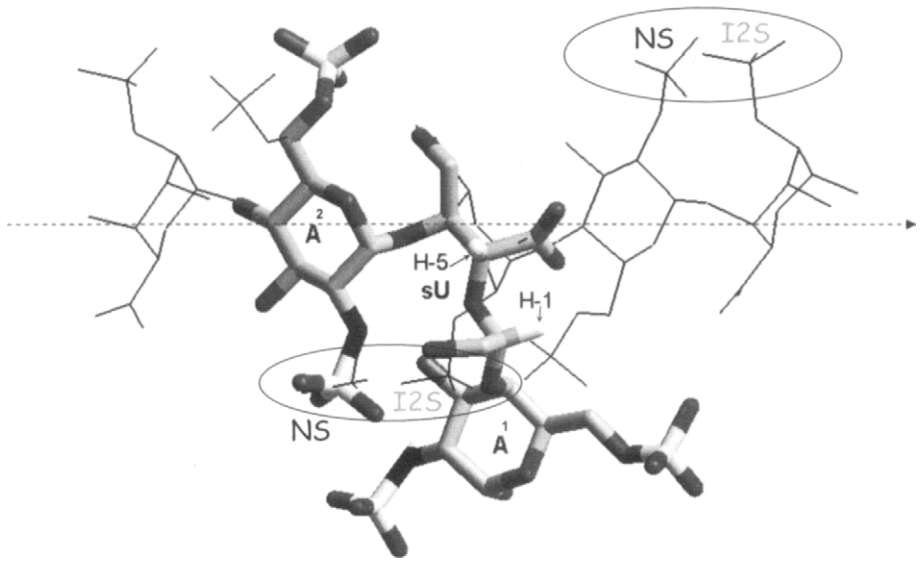

Figure 10 Molecular model of a trisaccharidic segment of p-PST.sU (stick model) compared with unmodified heparin, thin line (54). For comparison purposes, the aminosugar residue A2 is superimposed on the corresponding residue of heparin.

hexasaccharide (sU-Hexa). As illustrated in Fig. 11, in some of the favored geometries the reducing end of the glycol-split hexasaccharide is spread away from FGF-2, whereas in others it is closer to the protein surface, suggesting that, at least at the hexasaccharide level, some conformers of glycol-split chains could favor 1:1 complexes with FGF-2 also through the interaction of their sulfamino group A3-NS with the Lys27 residue of the protein. In conclusion, while still able to form 1:1 complexes with the growth factor, the modified product (where glycol-splitting induced a divergence of the heparin chain from the linear propagation) seems unable to induce formation of the active higher-order complexes needed to induce mitogenic signals. The results from modeling studies thus confirm that glycol-splitting does not impair the ability of heparin to form 1:1 complexes with FGF-2, while supporting the assumption that chains of glycol-split derivatives are consistently more flexible than those of heparins with unmodified backbones.

Regarding heparanase, heparin molecules contain both recognition, cleavage, and inhibition sites (64). Because of modification of the GlcA residues that are the natural substrates for heparanase, glycol-split heparins are not cleaved by the enzyme and exert their inhibitory effect in a noncompetitive way (35). As illustrated in Fig. 12, glycol-split residues are thought to act as flexible joints between heparin sequences involved in binding (and inhibition) of heparanase, thus facilitating fitting of these sequences in the active site of the enzyme.

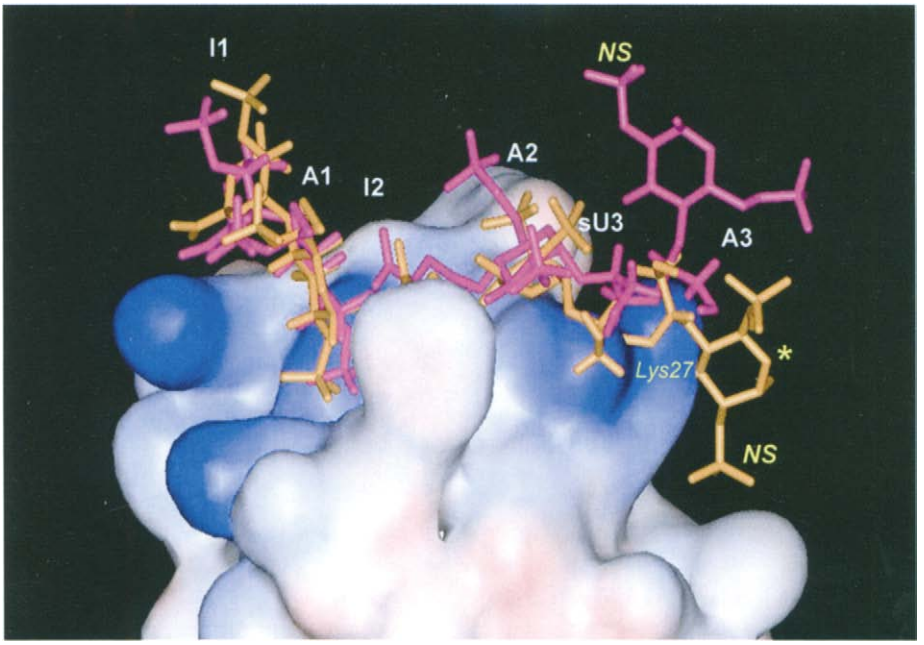

Figure 11 FGF-2 hexasaccharide complexes of glycol-split hexasaccharide (sU-Hexa) conformers with the largest (violet) and smallest (orange) A3-NS ↔ N-Lys27 distance obtained by MCSD calculation. $GlcNSO_3$ (A1-NS) and $IdoA2SO_3$ (I2-2S) were locked into the protein-binding site. The asterisk indicates the position of *N*-sulfate group in the A3-NS residue of the heparin hexasaccharide complexed with FGF-2 from X-ray structure (34).

V. Conclusions

The strategy for designing heparin-like FGF-2 inhibitors with potential antiangiogenic activity described in this chapter was based on the generation of sulfation gaps along the regular NS regions of heparin chains, followed by glycol-splitting of all non-sulfated uronic acid residues. This way, FGF-binding sequences were interrupted by flexible joints along the heparin chains and were unable to promote oligomerization of the growth factor. Accordingly, these novel nonanticoagulant heparin derivatives maintain the FGF-2-binding properties of heparin but do not induce mitogenic signals, as indicated by their antiangiogenic activity in a CAM model in which heparin is inactive. Unlike 6-*O*-desulfated heparin, they also inhibit VEGF (65) and the enzyme heparanase. Current studies on prototypes and their LMW derivatives indicate that glycol-split heparins and their *N*-acetylated analogs also inhibit angiogenesis in a number of *in vivo* tests and are antimetastatic in experimental animal models (54).

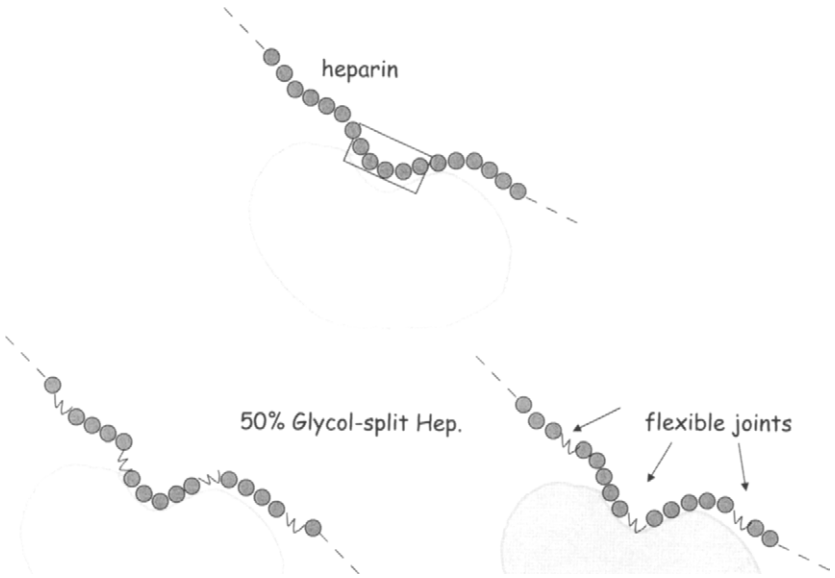

Figure 12 Idealized representation of glycol-split heparin–heparanase interaction.

In conclusion, glycol-splitting can lead to antiangiogenic and antimetastatic agents devoid of anticoagulant activity. Selected glycol-split heparin derivatives can be further exploited as eclectic protein-binding molecules for a variety of potential therapeutic applications.

References

1. Casu B. Structure and biological activity of heparin. Adv Carbohydr Chem Biochem 1985; 43:51–132.
2. Conrad HE. Heparin Binding Proteins. San Diego, CA: Academic Press, 1998.
3. Capila I, Linhardt RJ. Heparin-protein interactions. Angew Chem Int 2002; 41:390–412.
4. Linhardt RJ. Heparin: Structure and activity. J Med Chem 2003; 46:2551–2564.
5. Choay J, Lormeau JC, Petitou M, Fareed P, Sinay P. Low molecular weight oligosaccharides active in plasma against factor Xa. II New structural elements and antithrombotic activity. Ann Pharma Fr 1981; 39:267–272.
6. Casu B, Oreste P, Torri G, Zoppetti G, Choay J, Lormeau CJ, Petitou M, Sinay P. The structure of heparin oligosaccharide fragments with high anti-(factor Xa) activity containing the minimal antithrombin III-binding sequence. Chemical and ^{13}C nuclear-magnetic-resonance studies. Biochem J 1981; 197:599–609.

7. Hricovini M, Guerrini M, Bisio A, Torri G, Petitou M, Casu B. Conformation of heparin pentasaccharide bound to Antithrombin III. Biochem J 2001; 359:265–272.
8. Conrad HE, Guo Y. Structural analysis of periodate-oxidized heparin. In: Lane DA, Björk I, Lindahl U, eds. Advances in Experimental Medicine and Biology. New York: Plenum Press, 1992; vol. 313:31–36.
9. Foster AB, Webber JM. The structure of heparin. Biochem J 1964; 91:1P.
10. Casu B, Diamantini G, Fedeli G, Mantovani M, Oreste P, Pescador R, Porta R, Prino G, Torri G, Zoppetti G. Retention of antilipemic activity by periodate-oxidized non-anticoagulant heparins. Arzneim Forsch/Drug Res 1986; 36(4):637–642.
11. Ferro DR, Provasoli A, Ragazzi M, Casu B, Torri G, Bossennec V, Perly B, Sinay P, Petitou M, Choay J. Conformer populations of L-iduronic acid residues in glycosaminoglycan sequences. Carbohydr Res 1990; 19:157–167.
12. Casu B. Structure, shape and function of glycosaminoglycans. In: Harenberg J, Heene DL, Stehle G, Schettler G, eds. New Trends in Haemostasis: Coagulation Proteins, Endothelium, and Tissue Factors. Heidelberg: Springer-Verlag, 1990; 2–11.
13. Cross, MJ, Claesson-Welsh L. FGF and VEGF function in angiogenesis: Signaling pathways, biological responses and therapeutic inhibition. Trends Pharmacologic Sci 2001; 22:201–207.
14. Vlodavskyl I, Goldshmidt O, Zcharia E, Atzmon R, Rangini-Guatta Z, Elkin M, Peretz T, Friedmann Y. Mammalian heparanase: Involvement in cancer metastasis, angiogenesis and normal development. Semin Cancer Biol 2002; 12 (2):121–129.
15. Casu B, Guerrini M, Naggi A, Perez M, Torri G, Ribatti D, Carminati P, Giannini G, Penco S, Pisano C, Belleri M, Rusnati M, Presta M. Short heparin sequences spaced by glycol-split uronate residues are antagonists of fibroblast growth factor 2 and angiogenesis inhibitors. Biochemistry 2002; 41:10519–10528.
16. Pellegrini L. Role of heparan sulfate in fibroblast growth factor signaling: A structural view. Curr Opin Struct Biol 2001; 11:629–634.
17. Perlin AS. Glycol-cleavage oxidation. In: Pigman W, Horton D, Wander J, eds. The Carbohydrates Chemistry and Biochemistry. New York: Academic Press, 1980; IB:1167–1207.
18. Timms ID, Tomaszewski JE, Shlansky-Goldberg RD. Effect of nonanticoagulant heparin (Astenose) on restenosis after balloon angioplasty in the atherosclerotic rabbit. J Vasc Intervent Radiol 1995; 6:365–378.
19. Fransson LÅ, Malmström A, Sjöberg I, Huckeberry TN. Periodate oxidation and alkaline degradation of heparin-related glycans. Carbohydr Res 1980; 80:131–145.
20. Sache E, Maillard M, Malazzi P, Bertrand H. Partially *N*-desulfated heparin as a non-anticoagulant heparin: some physico-chemical and biological properties. Thromb Res 1989; 55:247–258.
21. Scott JE. Periodate oxidation, pK_a and conformation of hexuronic acids in polyuronides and mucopolysaccharides. Biochimica Biophysica Acta 1968; 170 (2):471–473.
22. Conrad HE, Guo G. Structural analysis of periodate-oxidized heparin. In: Lane DA, ed. Heparin and Related Polysaccharides. New York: Plenum Press, 1992; 31–36.

23. Fransson LÅ, Lewis W. Relationship between anticoagulant activity of heparin and susceptibility to periodate oxidation. FEBS Lett 1979; 97:119–123.
24. Thunberg L, Bäckström G, Grundberg H, Riesenfeld J, Lindahl U. The molecular size of the antithrombin-binding sequence in heparin. FEBS Lett 1980; 117:203–206.
25. Guerrini M, Bisio A, Torri G. Combined quantitative ^{1}H and ^{13}C-NMR spectroscopy for characterization of heparin preparations. Semin Thromb Hemost 2001; 27:473–482.
26. Hricovini M, Guerrini M, Bisio A, Torri G, Petitou M, Casu B. Conformation of heparin pentasaccharide bound to Antithrombin III. Biochem J 2001; 359:265–272.
27. Islam T, Butler M, Sikkander SA, Toida T, Linhardt RJ. Further evidence that periodate cleavage of heparin occurs primarily through the antithrombin binding site. Carbohydr Res 2002; 337:2239–2243.
28. Linker A, Hovingh P. Enzymatic degradation of heparin as a tool for structural analysis. In: McDuffie NM, ed. Heparin: Structure, Cellular Functions, and Clinical Application. New York: Academic Press, 1979; 3–24.
29. Nader H, Dietrich C, Oreste P, Dell'Eva M. Substrate specificity of heparinase and heparitinases. Cleavage of chemically-modified heparins and heparin sulfate. In: Crescenzi V, Dea I, Paoletti S, Stivala S, eds. Biomedical and Biotechnological Advances in Industrial Polysaccharides. New York: Gordon and Breach, 1989; 89–100.
30. Kovensky J, Cirelli AF. Chemical modification of glycosaminoglycans. Sulfation of heparansulfate derivatives obtained by periodate oxidation/borohydride reduction. Carbohydr Polymers 1996; 31:211–214.
31. Jaseja M, Rej RN, Sauriol F, Perlin AS. Novel regio- and stereoselective modifications of heparin in alkaline solution. Nuclear magnetic resonance spectroscopic evidence. Can J Chem 1989; 67:1449–1456.
32. Rej RN, Perlin AS. Base-catalyzed conversion of the α-L-iduronic acid 2-sulfate unit into a unit of α-L-galacturonic acid, and related reactions. Carbohydr Res 1990; 200:427–447.
33. Piani S, Casu B, Marchi EG, Torri G, Ungarelli F. Alkali induced optical rotation changes in heparins and heparin sulfates, and their relation to iduronic acid-containing sequences. J Carbohydr Chem 1995; 12:507–521.
34. Casu B, Guerrini M, Guglieri S, Naggi A, Perez M, Torri G, Cassinelli G, Ribatti D, Carminati P, Giannini G, Penco S, Pisano C, Belleri M, Rusnati M, Presta M. Undersulfated and glycol-split heparins endowed with antiangiogenic activity. J Med Chem 2004; 47:838–848.
35. Pellegrini L. Role of heparan sulfate in fibroblast growth factor signaling: a structural view. Curr Opin Struct Biol 2001; 11:629–634.
36. Guimond S, Maccarana M, Olvin BB, Lindahl U, Rapraeger AC. Activating and inhibitory heparin sequences for FGF-2 (basic FGF). J Biol Chem 1993; 268:23906–23914.
37. Ornitz DM, Herr AB, Nilsson M, Westman J, Svahn CM, Waksman G. FGF binding and FGF receptor activation by synthetic heparan-derived di- and trisaccharides. Science 1995; 268:432–436.
38. Lundin L, Larsson H, Krueger J, Kanda S, Lindahl U, Salvimirta M, Claesson-Welsh L. Selectively desulfated heparin inhibits fibroblast growth factor-induced mitogeneity and angiogenesis. J Biol Chem 2000; 275:24653–24660.

39. Ornitz DM, Yayon A, Flanagan JG, Svahn CM, Levi E, Leder P. Heparin is required for cell-free binding of basic fibroblast growth factor to a soluble receptor and for mitogenesis in whole cells. Mol Cell Biol 1992; 12:240–247.
40. Naggi A, Casu B, Perez M, Torri G, Cassinelli G, Penco S, Pisano C, Giannini G, Ishai-Michaeli R, Vlodavsky I. Modulation of the heparanase-inhibiting activity of heparin through selective desulfation, graded *N*-acetylation, and glycol-splitting. J Biol Chem 2005; 280:12103–12113.
41. Ferrara N, Gerberet HP, Le Couter J. The biology of VEGF and its receptors. Nat Med 2003; 9:669–676.
42. Gitay-Goren SS, Vlodavsky I, Neufed G. The binding of vascular endothelial growth factor to its receptors is dependent on cell surface-associated heparin-like molecules. J Biol Chem 1992; 267:6093–6098.
43. Tessler S, Rockwell P, Hicklin D, Cohen T, Levi BZ, Witte L, Lemischka IR, Neufeld G. Heparin modulates the interaction of VEGF165 with soluble and cell associated flk-1 receptors. J Biol Chem 1994; 69:12456–12461.
44. Cohen T, Gitay-Goren H, Sharon R, Shibuya M, Halaban R, Levi BZ, Neufeld G. VEGG121, a vascular endothelial growth factor (VEGF) isoform lacking heparin binding ability, requires cell-surface heparin sulphate for efficient binding to the VEGF receptors of human melanoma cells. J Biol Chem 1995; 270:11322–11326.
45. Margolin K. Inhibition of vascular endothelial growth factor in the treatment of solid tumors. Curr Oncol Rep 2002; 4:20–28.
46. Pisano C, Aulicino C, Vesci L, Casu B, Naggi A, Torri G, Ribatti D, Belleri M, Rusnati M, Presta M. Undersulfated, low-molecular-weight glycol-split heparin as an antiangiogenic VEGF antagonist. Glycobiology 2005; 15 (2):1C–6C.
47. Vlodavsky I, Friedmann Y. Molecular properties and involvement of heparanase in cancer metastasis and angiogenesis. J Clin Invest 2001; 108:341–347.
48. Parish CR, Freeman C, Hulett MD. Heparanase: A key enzyme involved in cell invasion. Biochim Biophys Acta 2001; 1471:M99–108.
49. Dempsey LA, Brunn GT, Platt JL. Heparanase, a potential regulator of cell-matrix interactions. Trends Biol Sci 2000; 25:349–351.
50. Vlodavsky I, Eldor A, Haimovitz-Friedman A, Matzner Y, Ishai-Michaeli R, Lide O, Naparstek Y, Cohen IR, Fuks Z. Expression of heparanase by platelets and circulating cells of the immune system: possible involvement in diapedesis and extravasation. Invasion Metastasis 1992; 12:112–127.
51. Ribatti D, Gualandris A, Bastaki M, Vacca A, Roncali L, Presta M. New model for the study of angiogenesis and antiangiogenesis in the chick embryo chorioallantoic membrane: the gelatin sponge/chorioallantoic membrane assay. J Vasc Res 1997; 34:445–463.
52. Ribatti D, Bertossi M, Nico B, Vacca A, Ria R, Riva A, Roncali L, Presta M. Role of basic fibroblast growth factor in the formation of the capillary plexus in the chick embryo chorioallantoic membrane. An in situ hybridization, immunohistochemical and ultrastructural study. J Submicrosc Cytol Pathol 1998; 30:127–136.
53. Zcharia E, Zilka R, Yaar A, Yacoby-Zeevi O, Zetser A, Metzger S, Sarid R, Naggi A, Casu B, Ilan N, Vlodavsky I, Abramovitch R. Heparanase accelerates wound angiogenesis and wound healing in mouse and rat models. FASEB J 2005; 19:211–222.

54. Vlodavsky I, Zcharia E, Goldshmidt O, Eshel R, Katz BZ, Minucci S, Kovalchuk O, Penco S, Pisano C, Naggi A, Casu B. Involvement of heparanase in tumor progression and normal differentiation. Pathophysiol Haemost Thromb 2003; 33:59–61.
55. Lapierre F, Holme K, Lam L, Tressler RJ, Storm N, Wee J. Chemical modifications of heparin that diminish its anticoagulant but preserve its heparanase-inhibitory, angiostatic, anti-tumor and anti-metastatic properties. Glycobiology 1996; 6:355–366.
56. Yoshitomi Y, Nakanishi H, Kusano Y, Munesue S, Oguri K, Tatematsu M, Yamashina I, Okayama M. Inhibition of experimental lung metastases of Lewis lung carcinoma cells by chemical modified heparin with reduced anticoagulant activity. Cancer Lett 2004; 207:165–174.
57. Lipari G, Szabo A, Model-free approach to the interpretation of nuclear magnetic resonance relaxation in macromolecules. 1. Theory and range of validity. J Am Chem Soc 1982; 104:4546–4559.
58. Guerrini M, Hricovini M, Naggi A, Torri G, Guglieri S, Casu B. Influence of molecular motion on activation of growth factors by heparin derivatives. Seventh European NMR Large Scale Facilities User Meeting, 2003; p 43.
59. Korramian BA. Small-angle X-ray scattering of reduced oxyheparins. In: Stivala SS, Crescenzi V, Dea ICM, eds. Industrial Polysaccharides. New York: Gordon and Breach, 1987; 339–347.
60. Mulloy B, Forster MJ, Jones C, Davies DB. NMR and molecular-modelling studies of the solution conformation of heparin. Biochem J 1993; 293:849–858.
61. Still WC, Tempczyk A, Hawlely R, Hendrickson TA. General treatment of solvation for molecular mechanics. J Am Chem Soc 1990; 112:6127–6129.
62. Venkataraman G, Shriver Z, Davis JC, Sasisekharan R. Fibroblast growth factors 1 and 2 are distinct in oligomerization in the presence of heparin-like glycosaminoglycans. Acad Sci USA 1999; 96:1892–1897.
63. Faham S, Hileman RE, Fromm JR, Linhardt RJ, Rees DC. Heparin structure and interactions with basic fibroblast growth factor. Science 1996; 271: 1116–1120.
64. Okada Y, Yamada S, Toyoshima M, Dong J, Nakajima M, Sugahara K. Structural recognition by recombinant human heparanase that plays critical roles in tumor metastasis. Hierarchical sulfate groups with different effects and the essential target disulfated trisaccharide sequence. J Biol Chem 2002; 277:42488–42495.
65. Ono K, Hattori H, Takeshita S, Kurita A, Ishihara M. Structural features in heparin that interact with VEGF165 and modulate its biological activity. Glycobiology 1999; 9:705–711.

Chemistry and Biology of Heparin and Heparan Sulfate
H.G. Garg, R.J. Linhardt and C.A. Hales (Editors)

Chapter 17

Antithrombin Activation and Designing Novel Heparin Mimics

UMESH R. DESAI

Department of Medicinal Chemistry and Institute for Structural Biology and Drug Discovery, Virginia Commonwealth University, Richmond, VA, USA

I. Introduction

Antithrombin (AT) is a key molecule regulating the clotting cascade in humans. The importance of antithrombin can be assessed from numerous cases of deficiencies, congenital or acquired, which lead to enhanced risk for thrombosis in the affected individuals (1–4). More importantly, targeted disruption of the antithrombin gene in mice resulted in death of all $AT^{-/-}$ embryos due to consumptive coagulopathy and/or liver dysfunction supporting its central role in regulation of blood coagulation in the myocardium and liver (5,6). Antithrombin is a plasma glycoprotein that inhibits several enzymes of the coagulation cascade, thereby functioning as a principal anticoagulant agent. Yet, current knowledge indicates that the physiological targets of antithrombin are factor IXa (fIXa), factor Xa (fXa), and thrombin (fIIa).

The circulating form of human antithrombin has 432 residues with a molecular weight of 58,200 Da. α-Antithrombin, the major form circulating in plasma, has four Asn residues glycosylated, while the minor form (β-antithrombin) has an unglycosylated Asn135. The inhibitor is present in human plasma in fairly high concentration (2–3 μM) and for a long time served as a principal source of material for study. Nowadays, recombinant antithrombin is routinely expressed in a number of cell systems including baculovirus infected insect cells and mammalian cells, with properties similar to the plasma protein. In addition, the milk of transgenic dairy

goats has been exploited to provide a homogeneous, well defined, and abundant supply of this inhibitor for commercial purposes (7).

Antithrombin belongs to the *serpin* superfamily of proteins, in which most members inhibit serine proteinases, although several are known to inhibit cysteine proteinases, while some are non-inhibitory (8,9). Antithrombin shows structural and functional similarity with prototypic serpin members including α_1-proteinase inhibitor, heparin cofactor II, and plasminogen activator inhibitor I. Like these inhibitory serpins, antithrombin inhibits fIXa, fXa, and fIIa through the formation of stable complex. The serpin inhibition mechanism, studied extensively in the past decade, can be referred to as the "mousetrap"mechanism. In this mechanism, the inhibitor (**I**) acts as bait to trap the target enzyme (**E**) in an equimolar, covalent, inactive complex (**E*–I***) (Fig. 1). The reactive center loop (RCL), an exposed sequence of residues containing the enzyme recognition site, first interacts with the active site of the proteinase as in a normal substrate reaction to form a Michaelis complex (**E:I**). This is rapidly followed by cleavage of the scissile bond P1–P1′ in the RCL to form an acyl-enzyme intermediate (**E–I**), which undergoes a major rearrangement to disrupt the enzyme catalytic triad (10,11) resulting in inhibition (**E*–I***) (inhibition pathway, Fig. 1). A competing process, called the substrate pathway (Fig. 1), may operate

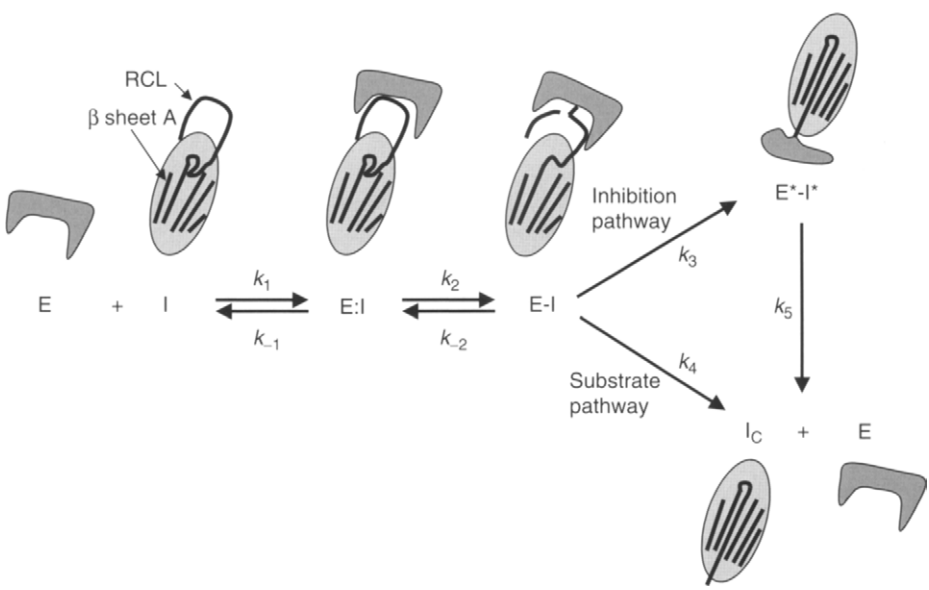

Figure 1 A model of the antithrombin inhibition mechanism. E, target enzyme (fIXa, fXa, or thrombin); AT, antithrombin; E:AT, Michaelis–Menten complex; E–AT, acyl-enzyme intermediate; E^*–AT^*, antithrombin–enzyme complex; AT_C, cleaved antithrombin; RCL, reactive center loop; "*k*", microscopic rate constants. See text for details. Reprinted with permission from Desai (2004) *Med. Res. Rev.* 24:151–181. Wiley Periodicals, Inc.

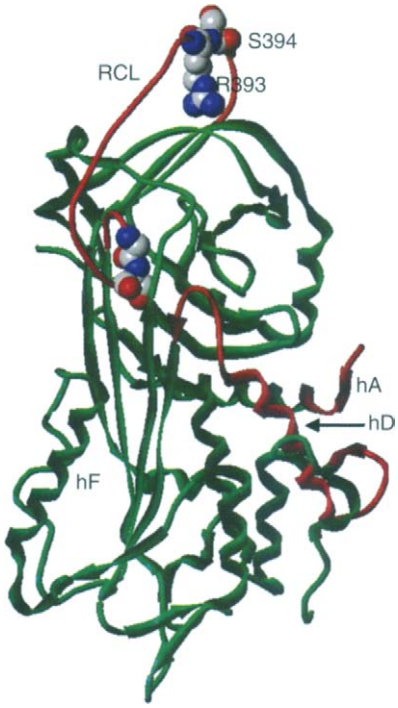

Figure 2 Structure of native antithrombin showing partially inserted reactive center loop and the main body of the inhibitor. The structure of inhibitory form of plasma antithrombin was obtained from RCSB (file name "1E04" – chain I). Arg393 (P1)–Ser394 (P1′) bond and partially inserted P14–P15 residues (Ser380–Gly379) of the RCL are shown in ball and stick representation. hD, helix D; hA, helix A; hF, helix F; sA, β-sheet A; see text for details.

in parallel and diminish the efficacy of inhibition. In the substrate pathway, structural perturbations in antithrombin (e.g., mutational changes) may facilitate rapid hydrolysis of the acyl enzyme intermediate **E–I** to yield an active enzyme (**E**) and a cleaved inhibitor ($\mathbf{I_C}$). *In vitro*, inhibition of fIXa, fXa, and thrombin by plasma antithrombin has no contribution from the substrate pathway, thus the reaction has a stoichiometry of inhibition of 1. However, alterations in the structure of the inhibitor (e.g., introduction of certain mutations) may enhance the contribution of the substrate pathway, thereby increasing the inhibition stoichiometry significantly. Such antithrombins may not function well as anticoagulants.

The central role of antithrombin has resulted in some 18 crystal structures, in which the inhibitor is either present alone or in complex with other molecules. Interestingly, each reported crystal structure is a dimer containing antithrombin in either the inhibitory, cleaved or latent form. To date, monomeric antithrombin has not been crystallized, thus the exact structure of the circulating form remains unclear. The structure of intact, uncleaved free antithrombin shows 9 α-helices

surrounding 3 β-sheets (12–14). Of these secondary structures, two features are striking – a dominant five-stranded β-sheet approximately in the center of the inhibitor and an exposed 15-residue sequence containing the reactive bond Arg393–Ser394, the so-called RCL at the "top"of the molecule (Fig. 2). These features are common to all serpins. In addition, antithrombin shows an extremely interesting feature known to be present in only one other serpin todate, heparin cofactor II (15). Two residues, P15-P14 (Gly379–Ser380) at the N-terminal end of the RCL, are inserted as a short β-strand in-between strands 3 and 4 of β-sheet A in the inhibitor (Fig. 2). This feature is called the partial insertion of RCL, and the reason(s) for such a preferential fold in antithrombin is not clear.

II. Antithrombin Inhibition of Procoagulant Proteinases

Antithrombin has been reported to inhibit most enzymes of the clotting cascade including kallikrein, fXIIa, fXIa, fIXa, fXa, thrombin, and factor VIIa. Yet, the rates of antithrombin inhibition of these procoagulant proteinases under physiological conditions are small (Table 1). Typical uncatalyzed inhibition rate constants (k_{UNCAT}) lie in the range of 10–10,000 $M^{-1}s^{-1}$, thus suggesting that antithrombin alone is not very effective in inhibiting these enzymes. The reason for the slow inhibition likely resides in the structure of antithrombin. Previously, it was believed that partial insertion of the RCL introduces a structural constraint in antithrombin that is not conducive for rapid reaction with procoagulant proteinases (16,17), yet recent evidence suggests proteinase recognition by native antithrombin is encoded primarily in the P1Arg residue, and that the conformation of RCL plays a minimal role (18–20).

The slow rates of antithrombin inhibition of these enzymes are greatly enhanced (Table 1) in the presence of heparin, a natural linear sulfated polysaccharide. Whereas, the inactivation of thrombin, fXa, and fIXa reached nearly diffusion-controlled second-order rate constants of 10^6–10^7 $M^{-1}s^{-1}$ in the presence of full-length heparin, the inhibition of other proteinases was some 20-fold slower

Table 1 Rates of Antithrombin Inhibition of Pro-Coagulant Proteinases Under Physiological Conditions

	fIXa[a] ($M^{-1}s^{-1}$)	fXa[b] ($M^{-1}s^{-1}$)	fIIa[c] ($M^{-1}s^{-1}$)
AT	5.8×10^1	2.6×10^3	8.7×10^3
AT:H_5[d]	3.1×10^4	81.2×10^5	14.6×10^3
AT:H[e]	$\sim 2 \times 10^7$	140×10^6	37×10^6

[a]Data taken from Bedsted et al. (2003) *Biochemistry* 42:8143.
[b]Data taken from Rezaie and Olson (2000) *Biochemistry* 39:12083.
[c]Data taken from Olson et al. (1992) *J. Biol. Chem.* 267:12528.
[d]Antithrombin–heparin pentasaccharide complex.
[e]Antithrombin–high-affinity-heparin complex.

(11,21–24). These increases in rate constants represent an acceleration of ~600-fold for fXa, ~2000-fold for thrombin, and ~ 10^6-fold for fIXa. These dramatic enhancements in inhibition of three key enzymes form the basis for heparin's clinical use as an anticoagulant since 1940s. Likewise, the manifold activity of polysaccharide heparin on other proteinases of the coagulation and fibrinolysis systems may also be responsible for the bleeding complications observed with heparin therapy.

III. Structure of Heparin and Heparin Pentasaccharide

Heparin is a 1 → 4-linked linear copolymer of glucosamine (2-amino-2-deoxyglucopyranose) and uronic acid (pyranosyluronic acid) residues that are variously sulfated (in this chapter, the $NHSO_3^-$ group is called *N*-sulfate and the OSO_3^- group is called sulfate) (Fig. 3). This structure, called glycosaminoglycan (GAG), is obtained by chemical processing of proteoglycan heparin present in porcine or bovine intestinal mucosa and lung (25). Glycosaminoglycan heparin is a complex mixture of polymeric chains. The structural complexity arises primarily from the apparently incomplete biosynthesis of proteoglycan heparin, in which multiple enzyme systems are involved (26,27), and secondarily from its preparative processing with alkali, enzymes, and/or bleaching agents.

Glycosaminoglycan heparin, referred to as unfractionated heparin (UFH), consists of polysaccharide chains having molecular weights in the range of 5000–40,000 Da with an average molecular weight of ~14,000 Da. Several substitutions are possible in the glucosamine and uronic acid residues. The β-D-glucosamines may be *N*-sulfated or acetylated and may also contain sulfates at 2-, 3-, and 6-positions, while the uronic acid residues may be either β-D-glucuronic acid (GlcAp)

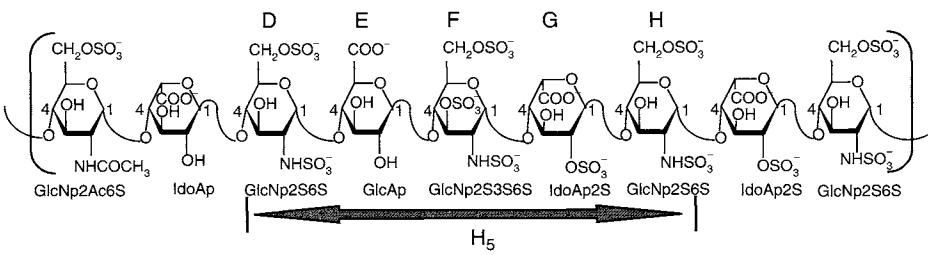

Figure 3 Plausible structure of a high-affinity heparin chain containing heparin pentasaccharide sequence H_5 (also called DEFGH). GlcNp, β-D-2-amino-2-deoxy-glucopyranose; GlcAp, β-D-glucopyranosyluronic acid; IdoAp, α-L-idopyranosyluronic acid; S, sulfate group; Ac, acetate group. The glucosamines may have sulfate groups at 3- or 6-positions, while the uronic acids may have sulfate at the 2-position. The glucosamines may be *N*-acetylated or *N*-sulfated. Heparin chain is 1 → 4-linked. H_5 sequence, marked as a double-headed arrow, consists of → 4)-GlcNp2S6S–(1 → 4)-GlcAp–(1 → 4)-GlcNp2S3S6S–(1 → 4)-IdoAp2S–(1 → 4) –GlcNp2S6S-(1 →.

or α-L-iduronic acid (IdoAp) and may be sulfated at 2-position (Fig. 3). Typically, there are more *N*-sulfated glucosamines than *N*-acetylated, and more IdoAp residues than GlcAp. Heparin is the strongest acid in our body (pK_a of sulfate groups = ~0.2) and consequently, is highly anionic at physiological pH. The molecular weight dispersity, structural variability, and polyanionic character introduce some novel and challenging properties in heparin.

Heparin is an anticoagulant because it recognizes antithrombin with high affinity and activates the inhibitor, as discussed above. The high-affinity interaction arises from a specific sequence $\mathbf{H_5}$ in a polymeric chain of heparin – called the high-affinity heparin (HAH) chain (Fig. 3). $\mathbf{H_5}$ is composed of three 2-*N*- and 6-sulfated glucosamines (β-D-GlcNp2S, 6S) interspersed with a 2-sulfated iduronic acid (α-L-IdoAp2S) and a glucuronic acid (β-D-GlcAp), in which the central glucosamine residue has a unique 3-sulfate group. This sequence is labeled as **DEFGH** (28–31), which reflects its history of identification. High-affinity heparin binds to plasma antithrombin, mostly α-antithrombin, with an affinity of ~10 nM at physiological pH. This high affinity originates from a combination of multiple ionic and nonionic interactions between the sulfate and carboxylate groups of DEFGH and positively charged residues of antithrombin (22).

IV. Mechanism of Heparin Activation of Antithrombin

Nature has engineered two distinct mechanisms for heparin acceleration of antithrombin inhibition of fIXa, fXa, and thrombin. These two mechanisms are: (i) allosteric activation of antithrombin by heparin pentasaccharide DEFGH; and (ii) activation through bridging of the inhibitor and the enzyme (Fig. 4).

The allosteric activation of antithrombin, also called the conformational activation mechanism, is an important mechanism that enhances the rate of inhibition of fXa and fIXa. The binding of heparin pentasaccharide DEFGH to antithrombin increases the second-order rate constant nearly 300-fold for fXa (22) and ~300–500-fold for fIXa (23). Up until a couple of years ago, the conformational activation mechanism was thought to occur through the expulsion of the partially inserted RCL residues. In this mechanism, first proposed by van Boeckel et al. (32) the binding of DEFGH in the heparin-binding site of antithrombin results in elongation of helix D by 1–2 turns introduces some pressure in sheet A, thereby causing it to close with concomitant exposure of the RCL. This expulsion of the partially inserted residues was expected to significantly change the conformation of RCL residues, especially the P1–P1′ reactive center, making it more favorable for recognition and cleavage by the proteinase (33,34) (Fig. 4).

Several discrete steps of the hypothesis have found support. For example, mutagenesis of C-terminal end residues of helix D to prevent elongation resulted in impaired heparin activation (35,36), while mutation of the critical hinge region residue P14Ser to Glu (additional charge), Trp (steric bulk), or Cys-fluorescein (bulk) resulted in activation without the need for heparin (37–39). Likewise, comparison of the X-ray crystal structures of native and pentasaccharide-complexed

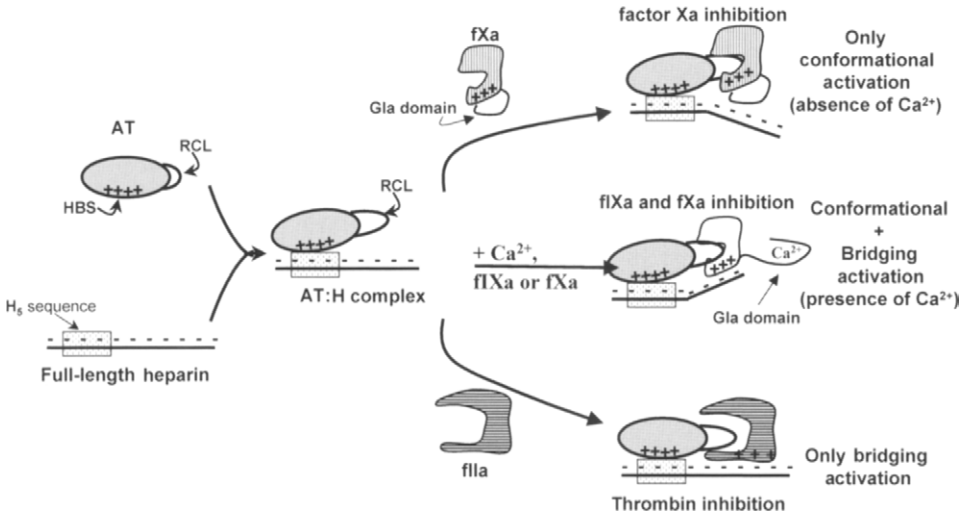

Figure 4 Bridging and conformational activation mechanism of antithrombin inhibition of factor Xa, factor IXa, and thrombin in the presence of heparin. AT:H, antithrombin–heparin complex; H_5, high-affinity pentasaccharide sequence in heparin; RCL, reactive center loop; fXa, factor Xa; fIXa, factor IXa; Gla, Gla domain on fIXa/fXa; "+ + +", exosite on enzyme; HBS, heparin-binding site. See text for details.

antithrombin (14,33) shows a clear difference in conformation of the hinge region residues, although the P1Arg was still directed inward and bound to Glu255. Despite this apparent lack of structural change in the critical P1 residue in the crystalline state, heparin-dependent modification of P1Arg residue in solution supported the idea that this critical proteinase recognition site becomes available in the activated form (16). In addition, earlier it had been demonstrated that NBD fluorophore at the P1Cys position underwent a dramatic increase in fluorescence on DEFGH binding, thereby supporting significant changes in the conformation of RCL hypothesis (40).

Although these experiments supported the idea of heparin-induced RCL conformational change, another body of experiments suggested that the changes introduced are not enough to explain the 300–500-fold accelerations achieved. Specifically, when Olson and coworkers mutated the antithrombin RCL sequence to a more thrombin specific sequence, a maximal acceleration achieved was only 2–9-fold due to heparin binding (18,19,41). Interestingly, these RCL mutations did not decrease pentasaccharide acceleration of fXa inhibition, thus supporting the idea that RCL sequence, except for P1Arg, or conformation had little to do with heparin activation of antithrombin for fXa (20). Thus, it was hypothesized that there must be exosites outside of RCL in antithrombin that recognize the target proteinases and that these exosites become available only in the activated state of the inhibitor. This exosite has now been localized using chimeric antithrombins to strand 3 of β-sheet C, which when changed to α1-proteinase inhibitor sequence

shows no enhancement in the rate of fXa/fIXa inhibition (42). The strand 3C sequence contains three conserved residues, Tyr253, Glu255, and Lys257, which appear to be good candidates as exosites. An alternative proposal, based on modeling antithrombin–fXa Michaelis complex, suggests strands 1B, 3B, and 4C as the likely proteinase recognition domains (43).

Complementing the antithrombin exosite hypothesis are studies on identifying the exosite(s) on fXa that is involved in the acceleration phenomenon. Through a series of mutations in the surface loops on fXa, including the 39, 60, sodium-binding, and the autolysis loop, Rezaie and coworkers (44,45) have identified Arg150 of the autolysis loop as a primary determinant of the recognition of the activation conformation of antithrombin. Interestingly, when the autolysis loop of fXa was introduced into corresponding positions in thrombin and activated protein C, the acceleration achieved with heparin pentasaccharide was 37- and 375-fold, respectively, thus suggesting that the autolysis loop of fXa plays a major role (46).

Taking these studies on the importance of RCL structure and exosites in antithrombin and the role of exosites in fXa/fIXa into consideration, Olson and Chuang (20) hypothesize that antithrombin RCL sequence evolved to *not* optimally recognize proteinases for a specific reason. In addition to inhibiting procoagulant proteinases, antithrombin can also possibly inhibit activated protein C because of its P1Arg specificity. Activated protein C is a natural anticoagulant, and thus to avoid being simultaneously conflicting, anticoagulant when inhibiting fIXa, fXa or thrombin and procoagulant when inhibiting activated protein C, antithrombin evolved to not recognize its potential targets properly! In fact, antithrombin is an extremely poor inhibitor of activated protein C even in the presence of heparin (47). The use of exosites as a means to introduce specificity and reactivity is nature's ingenuity in regulation.

In contrast to fXa inhibition, thrombin inhibition is accelerated only 1.7-fold through allosteric activation of antithrombin by heparin pentasaccharide (22). The predominant effect of heparin in accelerating thrombin inhibition arises from a bridging mechanism. Tight binding of antithrombin to the $\mathbf{H_5}$ sequence in full-length heparin is followed by the binding of thrombin to the same chain to form an antithrombin–heparin–thrombin ternary complex (Fig. 4). The binding of heparin to thrombin at the so-called exosite II is electrostatically driven resulting in poor heparin structure specificity (21,48). Thrombin then diffuses along the polyanionic chain to encounter the inhibitor resulting in a ~2000-fold acceleration in inhibition under physiological conditions. The lack of specificity with respect to heparin structure is probably necessary for thrombin to glide along the sulfated polysaccharide chain. A chain length of ~18 residues is needed to simultaneously hold thrombin and antithrombin for the accelerated inhibition (49,50). Thus, while sequence-specific $\mathbf{H_5}$ is necessary for tight binding of heparin chains, $\mathbf{H_5}$ alone cannot potentiate antithrombin inhibition of thrombin. The bridging mechanism exemplifies the fine use of specificity and nonspecificity to enhance recognition and reactivity.

The bridging mechanism, also called the template or approximation mechanism, also plays an important role in accelerated inhibition of fIXa and fXa

(23,24,51–53). Under physiological concentrations of Ca^{2+} ions, additional enhancement in the inhibition rate is observed. For fXa, polysaccharide heparin accelerated antithrombin inhibition more than 100-fold in the presence of 2.5 mM Ca^{2+} over and above the acceleration achieved in the presence of DEFGH (51,52), while for fIXa this acceleration reaches 130–1000-fold (23). The increased acceleration in the presence of Ca^{2+} is mediated by a bridging of the proteinase and the inhibitor on polysaccharide heparin chains. In the absence of Ca^{2+} ions, the N-terminal Gla domain containing several γ-carboxy glutamic acid residues, which are negatively charged, folds over an electropositive exosite that recognizes heparin. Binding of calcium ions to the Gla domain of both fIXa and fXa results in the release of the positively charged exosite on the proteinase, thus facilitating ternary complex formation with full-length heparin (Fig. 4) (54,55). For fXa, the maximal effect due to Ca^{2+} was observed with HAH containing ~35 (or higher) saccharide residues, while for fIXa nearly half as long a polysaccharide appears to be necessary (53).

V. The Heparin Binding Site in Antithrombin

The heparin-binding site in antithrombin is an engineering masterpiece (Fig. 5). The binding site is located some 20 Å away from the RCL, and hence the mechanism of conformational activation is called the allosteric activation mechanism. This binding site specifically recognizes $\mathbf{H_5}$ with high affinity, yet is capable of binding to numerous structurally different molecules that bear resemblance to the pentasaccharide. The heparin-binding domain in antithrombin is formed by positively charged residues of helices A and D, and the polypeptide N-terminus. The crystal structure of antithrombin–pentasaccharide co-complex shows that residues Lys114, Lys125, and Arg129 in this region interact strongly with $\mathbf{H_5}$ (33). Biochemical studies with antithrombin mutants suggest that the three residues contribute ~50, ~25–33, and ~28–35% of the total binding energy, respectively (56–58). Interestingly, Lys114 and Arg129 cannot be interchanged, while Lys125 → Arg interchange was essentially silent, indicating a high level of structural specificity (59). The domain formed by these three residues is called the pentasaccharide-binding site (PBS, Fig. 6). The PBS also contains other residues that play a smaller role in heparin binding. These residues include Lys11, Arg13, Arg24, Arg46, Arg47, and Trp49 (60–62). Each of these residues contributes 5–15% of total binding energy, except for Trp49, which contributes nearly 20% binding energy (62). It is to be expected that the many charged interaction points in PBS, each capable of hydrogen bonding in addition, raise the level of specificity as well as enhance affinity for a molecule with perfect fit (e.g., the heparin pentasaccharide DEFGH).

In addition to interacting with PBS, full-length heparin binds to an extended region formed by residues Arg132, Lys133, and Lys136 at the C-terminal end of helix D. This extended region is designated as the extended heparin-binding site (EHBS, Fig. 5) (63). This interaction is supported by biochemical studies that show that mutation of Arg132 and Lys133 selectively impairs the binding of polysaccharide

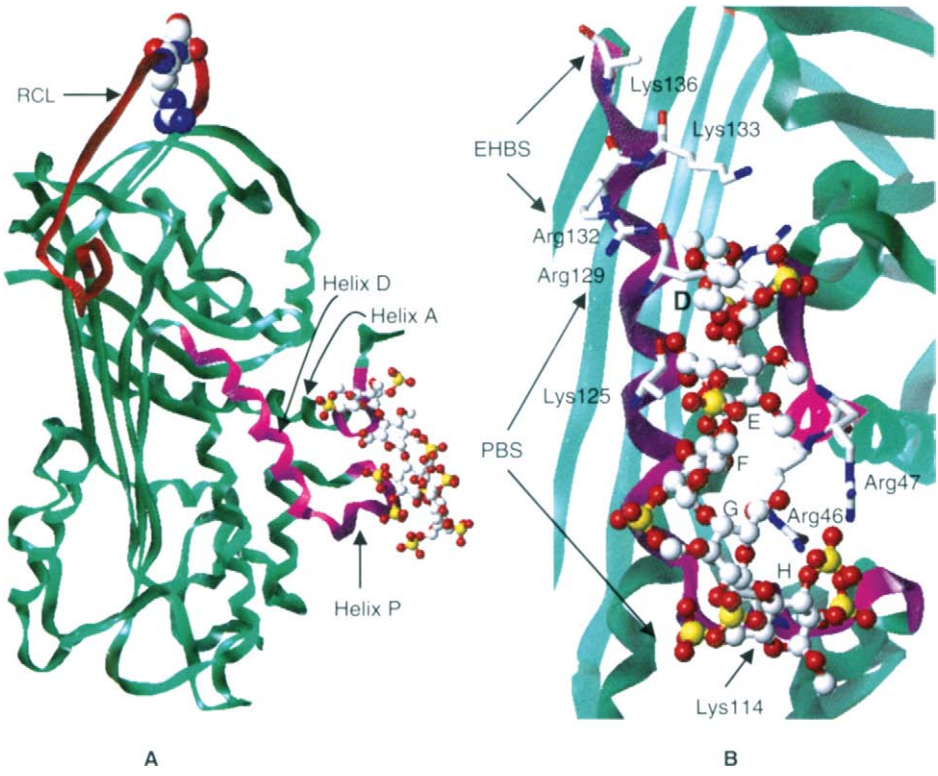

Figure 5 Structure of heparin-binding site of antithrombin: (A) shows plasma antithrombin complexed to natural pentasaccharide DEFGH, while (B) shows a close up view of the heparin-binding site. The structure of co-complex was obtained from RCSB (filename "1E03"). In both figures, green ribbon shows antithrombin, red represents RCL, and magenta represents the heparin-binding site. Pentasaccharide DEFGH is shown in ball-and-stick representation and individual residues are marked in (B). Helices D, P, and A (C-terminal end) form the heparin-binding site. Helix D extends by 1.5 turns in the complex as compared to free antithrombin (Fig. 2). In addition, helix P is not present in uncomplexed antithrombin. Arg46, Arg47, Lys114 [hidden in (B)], Lys125 and Arg129 form the pentasaccharide binding site (PBS), while Arg132, Lys133, and Lys136 form the extended heparin-binding site (EHBS). See text for details. Reprinted with permission from Desai (2004) *Med. Res. Rev.* 24:151–181. Wiley Periodicals, Inc.

heparin, but not of DEFGH (64). In addition, salt dependence of binding affinity shows that whereas DEFGH forms 4 ion-pair interactions, full-length heparin forms 5 (22). Finally, crystallographic studies on antithrombin–heparin–thrombin ternary complexes also suggest that these positively charged residues could form ion-pairs with sulfate groups on heparin (65,66), although the heparin used in these studies had a neutral linker.

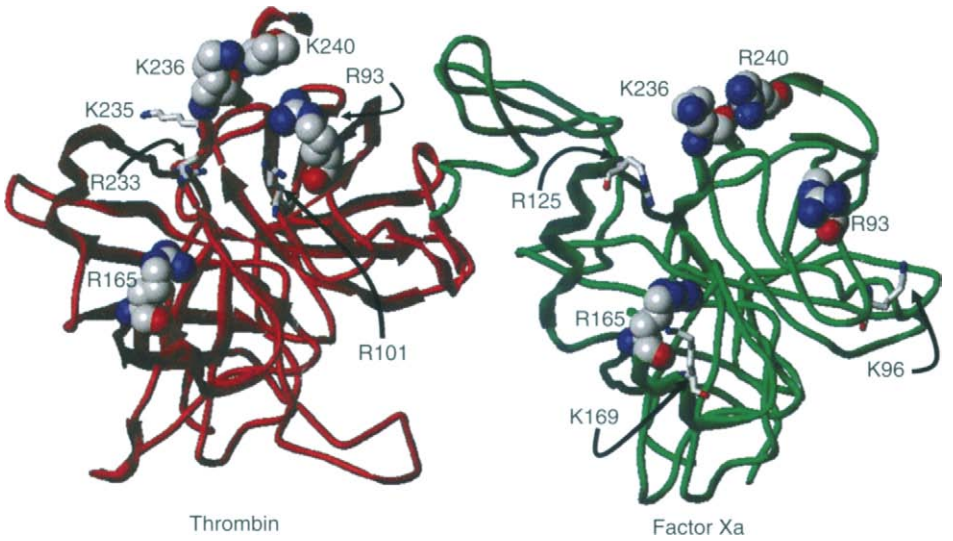

Figure 6 Comparison of heparin-binding exosite in factor Xa and thrombin. The X-ray crystal structures of Gla-domainless fXa (RCSB file "*1hcg*") and thrombin (from RCSB file "*1tb6*") were used for comparison. The enzymes are placed in approximately similar orientation. Key heparin-binding residues common in both proteinases are shown in space-filling model, while other residues implicated in heparin binding are shown in capped stick representation. See text for details.

It is important to recognize that the allosteric activation phenomenon involves the conformational changes at both ends – at the RCL as well as at the heparin-binding site. At a molecular level, following heparin binding at least three changes occur in the HBS. One, a short 3_{10} P helix, containing the critical Lys114 residue, is formed at the N-terminal end of helix D. Two, a small kink present in helix D before heparin binding is straightened out, and three, helix D is extended by 1.5 turns, the elongation discussed above. These changes in the heparin-binding site are coupled to changes in the RCL and the exosite in β-strand 3C. Whereas the molecular details at the two ends of the allosteric activation mechanism are fairly well understood, much less is understood regarding the molecular mechanism of transmission of heparin binding energy.

VI. The Heparin Binding Site in Factor Xa and Thrombin

Both fXa and thrombin can bind heparin polysaccharide, under appropriate conditions, as can be concluded from the above discussion. Heparin affinity of fXa and thrombin has been mostly inferred from indirect experiments involving formation of ternary complexes at high concentrations of full-length heparin, although direct titrations have been performed for thrombin to ascertain the apparent affinities so

measured (67,68). High- and low-affinity heparin (for antithrombin) bind to thrombin at physiological pH 7.4 and ionic strength I 0.15 but in absence of Ca^{2+}, with an apparent K_D of 0.7–2 μM. This indistinguishable apparent affinity for the two forms of heparin polysaccharide indicates less stringent structural specificity. Moreover, affinity may be different in the presence of calcium ions. In contrast, the wild-type fXa–high affinity heparin complex, in which the proteinase lacks the N-terminal Gla domain, has an apparent dissociation constant of ~ 0.4 μM in the presence of 2.5 mM Ca^{2+}. Whether the affinity of fXa for heparin is dependent on the sequence of the polysaccharide remains to be tested, although one can expect minimal structural specificity. It is interesting that there is a small ~2–5-fold difference in affinity for heparin between the two proteinases, although the Ca^{2+} concentrations were different.

Both fXa and thrombin contain electropositive domains, called exosites that bind heparin. A number of mutagenesis experiments have identified the amino acid residues that interact with sulfate groups on heparin. The residues identified common in both enzymes include Arg93, Arg165, Lys236, and Lys/Arg240 [residues are numbered following the chymotrypsin numbering system (69)] (68,70–72, Fig. 6). In addition, Arg101, Arg233, and Lys235 of thrombin have been implicated (70–72), while for fXa the additional residues include Lys96, Arg125, and Lys169 (68). According to the defect introduced in heparin binding, the rank order of importance of these residues in thrombin is Arg93 > Lys236 > Lys240 > Arg101 > Arg233, for fXa the order is Arg240 > Lys236 > Lys96, Lys169 > Arg165 > Arg93.

Whereas the crystal structure of fXa–heparin complex remains unknown, that for thrombin has recently been solved (73). In addition, the crystal structure of antithrombin–heparin–thrombin ternary complex (65) also provides an indepth view of the structure of heparin binding exosite II in thrombin. Compiling this structural information with the crystal structure of γ-Gla, domainless fXa shows striking similarity between the exosites (Fig. 6). The residues common to both (R93, R165, K236, and K/R240) are in identical positions on exposed surfaces scattered across helices and loops. Yet, other residues are positioned differently, especially Arg101 of thrombin, and Lys96 and Lys169 of fXa. Thus, differences do exist that may result in small changes in affinity and specificity. It is likely that the electropositive density of thrombin exosite is more than that of fXa. Finally, the reason for the difference in the rank order of importance of residues is not obvious. A simple calculation suggests that both exosites are nearly 15–20 Å long capable of binding 4–5 saccharide residues.

VII. Thermodynamics and Kinetics of Heparin Binding to Antithrombin

The high-affinity interaction between heparin and antithrombin is mediated through heparin pentasaccharide DEFGH that contains a unique 3-*O*-sulfate substituent on glucosamine F (see Fig. 3, 28–31). DEFGH accounts for ~95% of the free energy of binding of the HAH species to antithrombin (22), which arises

primarily due to sulfates and carboxylates of DEFGH interacting with positively charged residues, identified above, of the PBS. Ionic binding energy contributes ~40% of the total standard free energy of binding under physiological conditions (22) arising from nearly four ion-pair interactions (22,74,75). In addition, our molecular modeling study using hydropathic interaction (HINT) analysis, based on the crystal structure of pentasaccharide–antithrombin complex, indicates that the remaining 60% ΔG° also arises from the hydrogen bond-type interactions between these positively and negatively charged groups (76). This implies that according to HINT analysis, the saccharide backbone makes minimal contribution to the binding affinity. It is likely that the pentasaccharide backbone is important to primarily position the critical OSO_3^- and COO^- groups for optimal interaction with antithrombin, a concept deemed extremely important for designing new antithrombin activators.

The binding of DEFGH, or HAH, to antithrombin is a two-step process involving the formation of an initial low-affinity complex (AT:H) in rapid equilibrium. This process may be called the "recognition" process. This is followed by a major conformational change to give a high-affinity AT*:H complex in which antithrombin has been conformationally activated (Scheme I, Fig. 7) (22,77). This process may be thought of as the "activation" process. This conformational change has been linked to the expulsion of the RCL for accelerated inhibition of fXa (40). Analysis of the two-step induced fit binding process for antithrombin mutants and heparin pentasaccharide derivatives has yielded some important insight into how activation occurs at a molecular level on the heparin side. Our investigations with the truncated forms of DEFGH indicate that full conformational activation of antithrombin (~300-fold acceleration) can also be achieved with trisaccharide DEF under saturating conditions suggesting that recognition and activation is built-in in the trisaccharide (74). Thus, DEF residues play a major role in both the first and second step of the induced-fit pathway interacting with all three critical residues, Arg129, Lys125, and Lys114, of the PBS (56–59). Of these, only Lys125 is known to play a major role in the recognition of DEF, although it is likely that other point charges are involved to lesser extent (57). Yet, the affinity of DEF for antithrombin is much weaker ($K_D \sim 66\,\mu M$) under physiological conditions. This affinity is dramatically enhanced by the presence of disaccharide unit GH that interacts with Lys114. Thus, residues GH play an important role in the conformational activation step to greatly stabilize the activated state of antithrombin (58,74) (Fig. 7). Overall, in addition to the three critical residues, many other positively

$$\mathrm{AT} + \mathrm{H} \underset{k_{-1}}{\overset{k_1}{\rightleftharpoons}} \mathrm{AT{:}H} \underset{k_{-2}}{\overset{k_2}{\rightleftharpoons}} \mathrm{AT^*{:}H}$$

$$\text{where } K_1 = \frac{k_{-1}}{k_1} \text{ and } K_2 = \frac{k_{-2}}{k_2}$$

Scheme 1

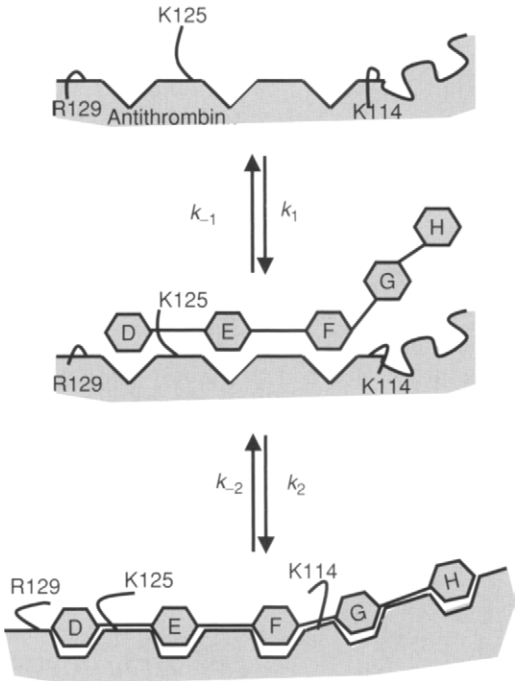

Figure 7 A model of conformational changes occurring in the pentasaccharide-binding site of antithrombin during the two-step binding process. The PBS in native antithrombin can recognize only the DEF part of the pentasaccharide (step 1). In addition, it is not fully complementary to the trisaccharide unit result in weaker affinity. In this first step, only K125 residue appears to play a major role. The small amount of binding energy made available due to this initial recognition results in conformational changes in the PBS that generates binding sites for residues G and H, as well as introduces greater complementarity for residues D, E, and F. In this second step, Arg129 and Lys114 play a major role. It is important to note that many other positively charged residues of the PBS take part in this process. See text for details.

charged residues play a secondary role, primarily in the second step. Activation of antithrombin aligns these residues to make optimal contacts with the heparin pentasaccharide, thus enhancing the stability of the activated form (see Fig. 9B).

VIII. Rationale for Designing Functional Mimics of Heparin

Despite the phenomenal success of heparin as an anticoagulant drug, heparin therapy is beset with a number of drawbacks. Natural product heparin is a highly heterogeneous, polydisperse polymer that forms indiscriminate, ionic interactions with numerous soluble proteins and cell surface receptors (11,78). This introduces several problems: (i) appreciable patient-to-patient variability in response, thus

requiring continuous monitoring and hospital stay; (ii) enhanced risk for bleeding; (iii) possibility of heparin-induced-thrombocytopenia (HIT) and osteoporosis; (iv) poor bioavailability; and (v) short half-life.

This nonspecific binding, and the problems thereof, can be greatly reduced by decreasing the size and the highly anionic character of heparins. Low-molecular weight heparins (LMWHs), developed in the past decade, have much better defined chemical and biological properties. These agents are prepared using chemical or enzymatic depolymerization of heparin and possess distinct pharmacologic profile that is largely determined by their composition. Depolymerization reduces the average molecular weight to ~3000–6000 Da. The multitude of preparative methods makes each product a distinct entity (79). Moreover, several reports show that the critical antithrombin binding sequence, DEFGH, may be lost in some of the preparative methods (80,81). Yet, LMWHs possess several advantages. These include better bioavailability, fewer HIT incidences, and lesser risk of bleeding complications (79). With the use of these advantages, LMWHs have significantly changed outpatient anticoagulant management. Thus, the introduction of LMWHs represents a major advance in improving the use of heparin and to a large extent the LMWHs have replaced unfractionated heparin in most subcutaneous indications.

In 2001, a heparin pentasaccharide fondaparinux, based on sequence DEFGH, was introduced as a selective fXa inactivating agent. Fondaparinux, originally synthesized in 1983 by Choay et al. (82), represents a major advance in anticoagulation therapy, in terms of its applicability and its unprecedented massive preparation. It broke apart two commonly held beliefs surrounding heparins. One, that fXa inhibition only cannot be effective, and two, that the half-life of molecules smaller than full-length heparin will be much shorter. Current evidence indicates that fondaparinux is much better than both UFH and LMWHs. It has greater efficacy over LMWHs, is useful in both arterial and venous thrombosis, has a longer half-life (17 h), no HIT adverse effects, and limited patient-to-patient variability (83–86). The bleeding risk seems to not have been completely eliminated.

Although anticoagulation therapy has advanced dramatically in the last few years, the risk for bleeding seems to persist. The synthetic challenge with oligosaccharides introduces high costs (87). Additionally, we are way away from orally active heparins.

IX. Heparin Mimics

A. Heparin Mimics that Selectively Utilize Conformational Activation Pathway

Enormous effort has been directed toward discovering and/or designing new molecules with heparin-like anticoagulant activity. These new molecules can be classified into natural polysaccharides, synthetic modified heparins, synthetic oligosaccharides, and synthetic nonsugar heparin mimics (88). Recent efforts in designing novel heparin pentasaccharide derivatives have also been reviewed (89).

Petitou and coworkers (89,90) have made major inroads into pentasaccharide derivatives that are better than the native molecule. The natural pentasaccharide sequence has two variations of unequal activity arising from the nonreducing end glucosamine residue D being either *N*-sulfated (DEFGH) or *N*-acetylated (D′EFGH) (Fig. 8). The *N*-sulfated pentasaccharide (700 units/mg anti-fXa) is about twice as active as the *N*-acetylated variant. Structure–activity relationships were derived using synthetic variants of DEFGH. It was established that 4-sulfate groups, at the 6-position of residue D, 3- and 2-positions of residue F, and 2-position of residue H, are critical for high-affinity binding to antithrombin (Fig. 8). Of these, the 3-*O*-sulfate group on residue F was found to be most important for antithrombin

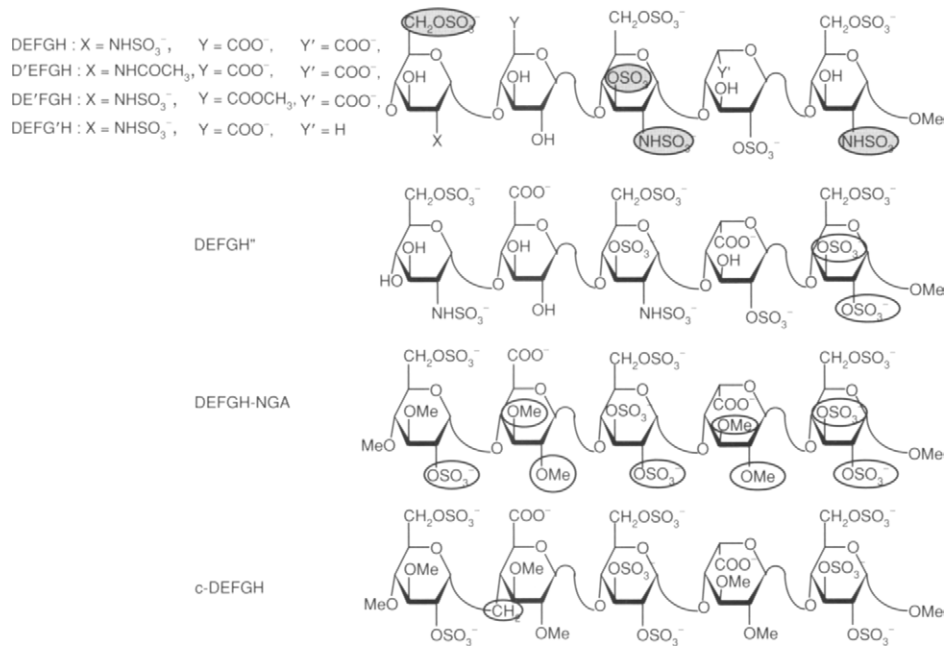

Figure 8 Structure of natural pentasaccharide DEFGH and its derivatives. Molecules with *primes* have a residue whose structure differs slightly from natural pentasaccharide DEFGH. Sulfate groups in DEFGH highlighted as filled ovals (◯) are critical for high-affinity interaction with antithrombin. Pentasaccharide "DEFGH" has residue H-containing sulfates at 2- and 3-positions (highlighted as empty ovals). DEFGH-NGA, the "*n*onglycos*a*mino" derivative of the natural pentasaccharide, has no *N*-sulfates and contains uronic acids that have 2-OMe groups. Note the number of changes introduced in DEFGH-NGA to ease the synthesis and enhance the anti-fXa activity. C-DEFGH contains a methylene (–CH2) group replacing the interglycosidic oxygen atom between residues D and E. Reprinted with permission from Desai (2004) *Med. Res. Rev.* 24:151–181. Wiley Periodicals, Inc.

activation. Its antithrombin interaction counterpart is Lys114 (33), which has also been implicated as the most important residue (58,59). The carboxylate groups of GlcAp and IdoAp2S are also important as demonstrated by pentasaccharides DE'FGH and DEFG'H (Fig. 8) that exhibit less than 5% of the activity of the reference DEFGH.

Studies with DEFGH' and DEFGH-NGA (Fig. 8) led Petitou and coworkers to two major advances. Replacement of $NHSO_3^-$ group in all three glucosamine residues with OSO_3^- and introduction of alkyl ethers at the available free hydroxyl groups not only retained anti-fXa activity, but enhanced it ~200% (90). The new "non-glycosamino" pentasaccharide DEFGH-NGA contains glucose residues, instead of glucosamines, thus easing their synthesis significantly. The "non-glycosamino" pentasaccharide preserves the distribution of critical sulfate and carboxylate groups of the natural pentasaccharide sequence. Further, it is likely that the new pentasaccharide retains the conformational preference and flexibility of the parent molecule. Further, a C-pentasaccharide, consisting of a carbon (CH_2)-based interglycosidic bond between residues D and E (Fig. 8), was shown to hardly affect the biological properties of the natural pentasaccharide (91). This C-pentasaccharide shows an anti-fXa activity ~34% better than DEFGH and represents the first member of new anti-fXa pentasaccharides.

Recently, major advances on chemoenzymatic front have been made by Rosenberg and coworkers (92–94) to synthesize the high-affinity saccharides. This approach utilizes the tremendous advances made in cloning and expressing heparan sulfate sulfotransferases (*N*-deacetylase *N*-sulfotransferase, 2-*O*-sulfotransferase, 3-*O*-sulfotransferase and 6-*O*-sulfotransferase). The availability of these enzymes for *in vitro* use coupled with the availability of a polysaccharide from *Escherichia coli* strain K5 has resulted in a two-step enzymatic synthesis of HAH (93) and a six-step synthesis of heparin pentasaccharide (92) with reasonably good yields and in short time. In addition, the HAH prepared in this approach was found to be 3–4-fold better than commercial heparin because of the higher proportion of the $\mathbf{H_5}$ sequence per full-length chain. Another chemoenzymatic approach, which relied more on chemical sulfation/de-sulfation steps, was used by Lindahl et al. (95) to prepare HAH from bacterial K5 capsular polysaccharide. These chemoenzymatic approaches are likely to be extremely useful in generating heparin (heparan sulfate) structures tailored to specific sulfation pattern (94).

B. Heparin Mimics that Use the Bridging Mechanism of Inhibition

As discussed above the dominant mechanism in heparin action appears to be the bridging pathway. Thus, it was reasoned that a heparin mimic could be easily designed based on a three-domain structure – an antithrombin-binding domain (ABD), a thrombin binding domain (TBD) and a linker joining the two. Essentially, heparin is a three-domain structure. Whereas the structure of ABD (i.e. DEFGH)

could not be changed greatly, the structure of TBD in heparin could be altered readily because thrombin–heparin interaction is relatively nonspecific (21,48). The TBD was predicted to compose of ~5–6 negative charges, recently confirmed by the crystal structure of thrombin–heparin complex (73), distributed on either 2 or 3 saccharides, most probably representing the dominant disaccharide sequence, → 4)-IdoAp2S–(1 → 4)-GlcNp2S,6S–(1 →, of heparin. Previous molecular modeling studies (96), later confirmed by a crystallography study (33), had suggested that TBD was located on the nonreducing end of the DEFGH sequence. Thus, the relative orientation of the two domains could be fixed. However, questions remained on the constitution and length of spacer, as well as the fine structure of TBD.

Chemical synthesis of oligosaccharides, containing the heparin pentasaccharide at the reducing end and heparin disaccharide at the nonreducing end of the chain, established that for accelerated thrombin inhibition a minimum chain length of either 15 or 16 residues is needed (97,98). Several different spacer structures were utilized (Fig. 9). A flexible polyethylene glycol type spacer was less active as anti-factor IIa inactivation agent than a rigid polyglucose type spacer (99). Finally,

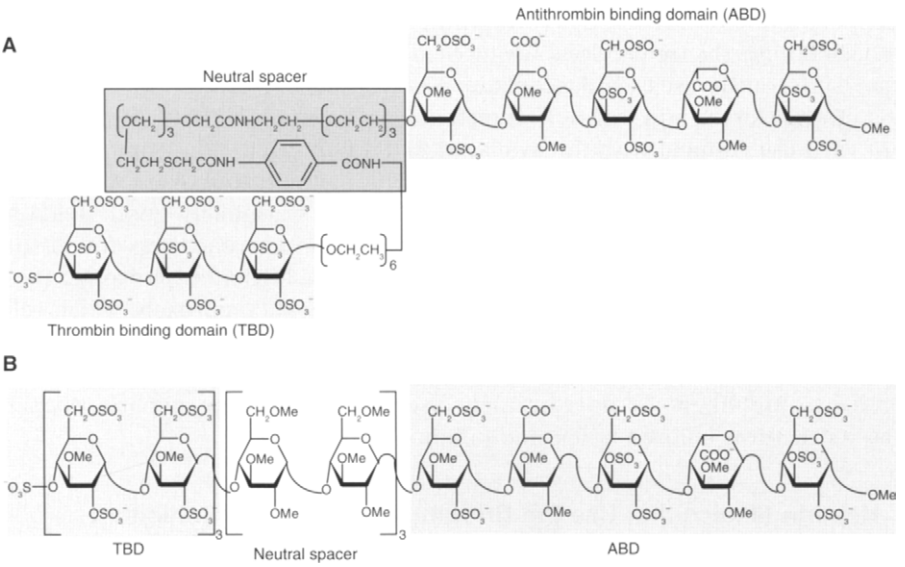

Figure 9 Structure of novel molecules designed to inhibit both factor Xa and factor IIa using the bridging mechanism: (A) shows antithrombin-binding domain (ABD) linked to a thrombin-binding domain (TBD) using a flexible polyethylene glycol type neutral linker to arrive at an appropriate length so as to facilitate ternary complex formation. The ABD is extended at its nonreducing terminus. (B) shows a similar concept, however with a relatively more rigid neutral spacer consisting of glucose units. The anti-fIIa activity of molecule (A) is much lower than that of molecule (B).

a heparin mimic was engineered that has the ABD connected to TBD through an uncharged hexasaccharide spacer. To ease the synthesis, the TBD was constructed of a disulfated glucose-based hexasaccharide (Fig. 9) (100,101). This heptadecasaccharide is an extremely potent anti-fXa and anti-factor IIa molecule and cannot be neutralized by PF4. It is likely that this molecule has negligible HIT adverse effect. Recently, a heparin mimic containing TBD, which is perphosphorylated rather than persulfated, has been found to exhibit an increase in antithrombin activity (102). Phosphate groups appear to be more potent at interacting with TBD than sulfate group. These full-length heparin mimics show tremendous promise of moving into clinical trials.

C. Heparin Mimics with Nonheparin Scaffold

As may be apparent from the above discussion, all functional mimics of heparin started with a heparin scaffold. We questioned this fundamental tenet of the assumed requirement of saccharide skeleton for high-affinity interaction with antithrombin. A major concern with the saccharide-based approach is the difficulty of oligosaccharide synthesis that reduces the cost effectiveness. We have recently designed synthetic nonsugar molecules that exhibit antithrombin activation for accelerated inhibition of fXa (103,104). These molecules represent the first in the class of small, nonsugar activators.

To rationally design nonsugar activators a robust modeling tool was required that accurately simulates the interactions of antithrombin at a molecular level. First, hydropathic interaction (HINT) analysis was used to quantitate the interactions of antithrombin (103). Hydropathic interaction is molecular modeling tool that provides quantitative information regarding intermolecular interactions at an atomic level. Hydropathic interaction accurately identifies and quantitiates three common interactions, charge–charge interactions, hydrogen bonding interactions, van der Waals interactions, between proteins and its ligands. For antithrombin–pentasaccharide interaction, HINT map showed favorable interactions between positively charged residues of helix A, helix D, and the polypeptide N terminus and the sulfate and carboxylate groups of the pentasaccharide (105). Further, HINT predicted reasonably well the interaction of DEFGH with heparin-binding mutants of antithrombin (103) (Fig. 10). Using this as a basis, the interaction profile of designed *de novo* ligands was studied.

We reasoned that mimicking trisaccharide DEF would be a good starting point for designing heparin mimics for several reasons. DEF is nearly equivalent to pentasaccharide DEFGH in inducing acceleration in antithrombin inhibition of fXa, it is that part of the heparin pentasaccharide structure that exhibits considerable rigidity, and it is small enough for rapid synthesis of mimics. To design an antithrombin activator, a "pharmacophore" was deduced from the DEF portion of the natural pentasaccharide, DEFGH. This assumed pharmacophore was built from four negatively charged residues, at the 6-position of residues D and E and at the 3- and 2-positions of residue F (see Fig. 8), groups that are thought to be important for antithrombin activation. Numerous molecular frameworks were

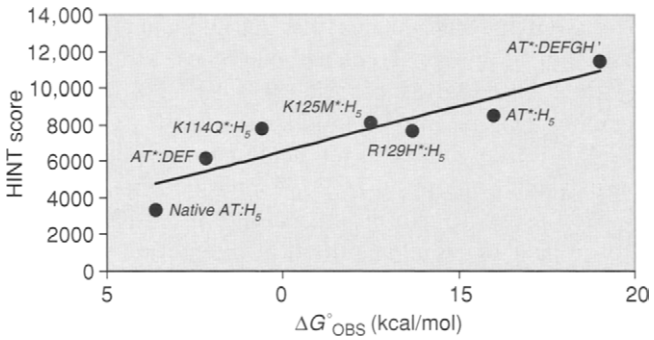

Figure 10 Predictability of affinity of heparin ligands for binding to antithrombin using HINT technique. Total HINT scores were obtained for heparin oligosaccharides binding to native antithrombin and its mutants *in silico* for which the affinities had been previously obtained. A linear correlation with correlation coefficient of 0.81 was obtained for standard free energy of binding (ΔG°_{OBS}) range of 4–20 kcal/mol suggesting high predictability. Asterisk (*) represents activated state. The solid line is a linear regression obtained by fitting data with slope of 491 ± 105 HINT score/kcal/mol and an intercept of 1622 ± 1346 HINT score. Adapted from Gunnarsson and Desai (2002) *J. Med. Chem.* 45:1233–1243.

screened based on their ability to satisfy the three-dimensional organization of the pharmacophore (Fig. 11). These frameworks are constituted of saturated or unsaturated 6- or 10-membered rings joined by a linker that is one, two, or three bonds long. The essence of our rational approach to arrive at the first nonsugar heparin-mimic scaffold was repetitive docking and scoring analysis to answer questions, such as: (i) does the new mimic form ion-pair interactions of the type formed by heparin pentasaccharide? (ii) does the mimic have HINT score comparable to DEF or DEFGH? (iii) does the mimic show interactions with R129, K125 and/or K114 (Fig. 11)? After a series of structural screens, a small nonsugar skeleton, (−)-epicatechin sulfate (ECS, Fig. 12A), was designed. Epicatechin sulfate was found to interact with antithrombin with an affinity comparable to DEF. More interestingly, it accelerated the inhibition of fXa nearly eight-fold, the first small nonsugar molecule known to activate antithrombin (103).

The design of the first nonsugar heparin mimic, albeit with a weak acceleration in inhibition of fXa, indicated a strong possibility of discovering more active molecules. Hence we screened several related molecules (Fig. 12A). However, the activation of antithrombin did not increase beyond ~20-fold in comparison to that known for DEF (~300-fold) (104,106,107). To examine the reason for this poor activation, we performed detailed competitive binding and molecular modeling studies. These experiments indicate although designed to bind to the PBS in antithrombin, our designed small molecules prefer to bind in an electropositive domain adjacent to the pentasaccharide binding site and formed by residues Arg132, Lys133, and Lys136, a site called the extended heparin-binding site (EHBS) (104). This site is known to play a secondary role in antithrombin activation

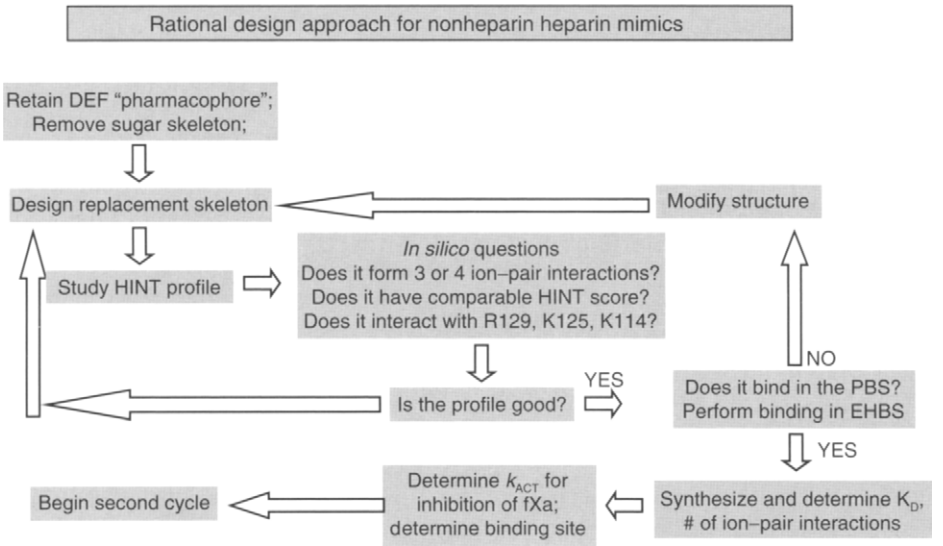

Figure 11 Strategy for rational design of nonsaccharide mimics of heparin. We started with DEF pharmacophore, rather than DEFGH, and used HINT and biochemical studies extensively to derive the first organic nonsugar mimics of heparin. See text for details.

and thus, the weaker activation potential of flavanoids and flavonoids could be rationalized. This exercise has given rise to a modified search algorithm that goes beyond the initial screening of new scaffolds. The new search algorithm requires an answer to the question whether the heparin-mimic is likely to prefer to bind to the PBS or the EHBS. Answer to this question may sometimes come only from biochemical studies using competitive inhibition experiments (Fig. 11).

Simultaneously we have exploited the bridging mechanism to arrive at nonheparin skeletons for antithrombin activation. A major advantage of the bridging mechanism is that it obviates conformational change in antithrombin. This is important because inducing conformational change in antithrombin is likely to be difficult with nonheparin mimics, although not impossible. Thus, we reasoned that activation should be possible with nonsulfated activators, based only on carboxylic acid groups. As a proof of the principle, linear poly(acrylic acid)s (PAAs) (Fig. 12B) have been found to bind to antithrombin and accelerate inhibition of fXa and thrombin (108). The acceleration in thrombin inhibition achieved with linear PAAs was in the range of 100–1100-fold depending on the length of the polymer, which is extremely encouraging. The affinity of these PAAs for antithrombin under physiological conditions is poor ($\sim 100\,\mu M$) and hence impossible to succeed as a drug. Yet, our work demonstrates that molecules completely devoid of sulfate groups can activate antithrombin effectively. These initial studies highlight the possibility that rational design of nonheparinoid molecules that recognize the PBS in antithrombin and that effectively bridge proteinases is possible.

A

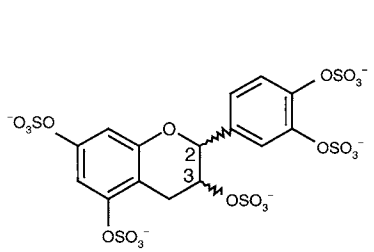

ECS = (2S, 3S)
(+)-CS = (2S, 3R)

R_7	R_6	R_5	R_3	R'_2	R'_3	R'_4	R'_5
H	OS	H	H	H	H	OS	OS
OS	H	OS	H	H	OS	H	H
OS	H	OS	H	H	OS	OS	H
H	OS	H	OS	H	H	OS	OS
OS	H	OS	OS	H	OS	OS	H
OS	H	OS	OS	OS	H	OS	H
OS	H	OS	H	OS	OS	OS	H

B

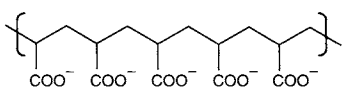

	Monomers	Length	Acceleration
PAA1500	~21-mer	~40 Å	114-fold
PAA2280	~32-mer	~61 Å	259-fold
PAA3450	~48-mer	~91 Å	597-fold
PAA6200	~86-mer	~164 Å	1109-fold

Figure 12 Structures of novel nonsugar activators of antithrombin. (A) Structure of flavanoids and flavonoids shown to interact with plasma antithrombin with μM affinity and inducing a 8–20-fold acceleration in inhibition of fXa. ECS [(–)-epicatechin sulfate] was the first rationally designed molecule to mimic trisaccharide DEF. "OS" in the substitution grid represents the sulfate group (OSO_3^-). (B) Structure of poly(acrylic acid)s used to test the hypothesis that antithrombin can be activated in the absence of sulfate groups and in the presence of carboxylate groups only. Acceleration (k_{CAT}/k_{UNCAT} ratio) in thrombin inhibition shown here was determined in pH 7.4, I 0.05 buffer, wherein the affinity of these molecules for antithrombin is very poor. See text for details.

X. Conclusions

Detailed knowledge on the mechanism of antithrombin activation, the structure of heparin-binding site in antithrombin, and the structure–function relationships in the heparin pentasaccharide sequence has made possible the rational design of new heparin mimics. Several interesting pentasaccharide derivatives have been made for selective inhibition of fXa. Longer chain polysaccharides have also been developed for effective simultaneous inhibition of fXa and thrombin. Novel small, rationally

designed, nonsugar molecules have shown early promise of antithrombin activation. Finally, good acceleration in antithrombin inhibition of thrombin has been achieved with nonsulfated polymers. These advances bode well for rational design of high-affinity, high-activity indirect anticoagulants with minimal adverse effects.

Acknowledgments

The author thanks Drs Gunnarsson and Monien for their comments on the manuscript. This work was made possible through grants from the National Heart, Lung and Blood Institute, American Heart Association, and the A. D. Williams Foundation.

References

1. Franco RF, Reitsma PH. Genetic risk factors of venous thrombosis. Hum Genet 2001; 109:369–384.
2. van Boven HH, Lane DA. Antithrombin and its inherited deficiency states. Semin Hematol 1997; 34:188–204.
3. Lane DA, Bayston T, Olds RJ, Fitches AC, Cooper DN, Millar DS, Jochmans K, Perry DJ, Okajima K, Thein SL, Emmerich J. Antithrombin mutation database: 2nd (1997) update. For the Plasma Coagulation Inhibitors Subcommittee of the Scientific and Standardization Committee of the International Society on Thrombosis and Haemostasis. Thromb Haemost 1997; 77:197–211.
4. Lane DA, Kunz G, Olds RJ, Thein SL. Molecular genetics of antithrombin deficiency. Blood Rev 1996; 10:59–74.
5. Ishiguro K, Kojima T, Kadomatsu K, Nakayama Y, Takagi A, Suzuki M, Takeda N, Ito M, Yamamoto K, Matsushita T, Kusugami K, Muramatsu T, Saito H. Complete antithrombin deficiency in mice results in embryonic lethality. J Clin Invest 2000; 106:873–878.
6. Yanada M, Kojima T, Ishiguro K, Nakayama Y, Yamamoto K, Matsushita T, Kadomatsu K, Nishimura M, Muramatsu T, Saito H. Impact of antithrombin deficiency in thrombogenesis: lipopolysaccharide and stress-induced thrombus formation in heterozygous antithrombin-deficient mice. Blood 2002; 99: 2455–2458.
7. Levy JH, Weisinger A, Ziomek CA, Echelard Y. Recombinant antithrombin: production and role in cardiovascular disorder. Semin Thromb Hemost 2001; 27:405–416.
8. Gettins PGW, Patston PA, Olson ST. Serpins: Structure, Function and Biology. New York: R G Landes Company, 1996.
9. Gettins PGW. Serpin structure, mechanism and function. Chem Rev 2002; 102:4751–4803.
10. Huntington JA, Read RJ, Carrell RW. Structure of a serpin – protease complex shows inhibition by deformation. Nature 2000; 407:923–926.
11. Björk I, Olson ST. Antithrombin: a bloody important serpin. In: Church FC, et al., eds. Chemistry and Biology of Serpins. New York: Plenum Press, 1997; 17–33.
12. Schreuder HA, de Boer B, Dijkema R, Mulders J, Theunissen HJM, Grootenhuis PDJ, Hol WGJ. The intact and cleaved human antithrombin

III complex as a model for serpin-proteinase interactions. Nature Struct Biol 1994; 1:48–54.
13. Carrell RW, Stein PE, Fermi G, Wardell MR. Biological implications of a 3 Å structure of dimeric antithrombin. Structure 1994; 2:257–270.
14. Skinner R, Abrahams J-P, Whisstock JC, Lesk AM, Carrell RW, Wardell MR. The 2.6 Å structure of antithrombin indicates a conformational change at the heparin-binding site. J Mol Biol 1997; 266:601–609.
15. Baglin T, Carrell RW, Church FC, Esmon CT, Huntington JA. Crystal structures of native and thrombin-complexed heparin cofactor II reveal a multistep allosteric mechanism. Proc Natl Acad Sci USA 2002; 99:11079–11084.
16. Pike RN, Potempa J, Skinner R, Fitton HL, McGraw WT, Travis J, Owen M, Jin L, Carrell RW. Heparin-dependent modification of the reactive center arginine of antithrombin and consequent increase in heparin binding affinity. J Biol Chem 1997; 272:19652–19655.
17. Jairajpuri MA, Lu A, Bock SC. Elimination of P1 arginine 393 interaction with underlying glutamic acid 255 partially activates antithrombin III for thrombin inhibition but not factor Xa inhibition. J Biol Chem 2002; 277:24460–24465.
18. Chuang Y-J, Swanson R, Raja SM, Bock SC, Olson ST. The antithrombin P1 residue is important for target proteinase specificity but not for heparin activation of the serpin. Characterization of P1 antithrombin variants with altered proteinase specificity but normal heparin activation. Biochemistry 2001; 40:6670–6679.
19. Chuang Y-J, Gettins PGW, Olson ST. Importance of the P2 glycine of antithrombin in target proteinase specificity, heparin activation, and the efficiency of proteinase trapping as revealed by a P2 Gly → Pro mutation. J Biol Chem 1999; 274:28142–28149.
20. Olson ST, Chuang Y-J. Heparin activates antithrombin anticoagulant function by generating new interaction sites (exosites) for blood clotting proteinases. Trends Cardiovasc Med 2002; 12:331–338.
21. Olson ST, Björk I. Predominant contribution of surface approximation to the mechanism of heparin acceleration of the antithrombin-thrombin reaction. Elucidation from salt concentration effects. J Biol Chem 1991; 266:6353–6364.
22. Olson ST, Björk I, Sheffer R, Craig PA, Shore JD, Choay J. Role of the antithrombin-binding pentasaccharide in heparin acceleration of antithrombin-proteinase reactions. Resolution of the antithrombin conformational change contribution to heparin rate enhancement. J Biol Chem 1992; 267:12528–12538.
23. Bedsted T, Swanson R, Chuang Y-J, Bock PE, Björk I, Olson ST. Heparin and calcium ions dramatically enhance antithrombin reactivity with factor IXa by generating new interaction exosites. Biochemistry 2003; 42:8143–8152.
24. Olson ST, Swanson R, Raub-Segall E, Bedsted T, Sadri M, Petitou M, Herault JP, Herbert JM, Björk I. Accelerating ability of synthetic oligosaccharides on antithrombin inhibition of proteinases of the clotting and fibrinolytic systems. Comparison with heparin and low-molecular-weight heparins. Thromb Haemost 2004; 92:929–939.
25. Linhardt RJ, Loganathan D. Heparin, heparinoids and heparin oligosaccharides: structure and biological activities. In: Gebelein CG, ed. Biomimetic Polymers. New York: Plenum Press, 1990; 135–173.

26. Sasisekharan R, Venkataraman G. Heparin and heparan sulfate: biosynthesis, structure and function. Curr Opin Chem Biol 2000; 4:626–631.
27. Rabenstein DL. Heparin and heparan sulfate: structure and function. Nat Prod Rep 2002; 19:312–331.
28. Lindahl U, Backström G, Thunberg L, Leder IG. Evidence for a 3-*O*-sulfated D-glucosamine residue in the antithrombin-binding sequence of heparin. Proc Natl Acad Sci USA 1980; 77:6551–6555.
29. Atha DH, Stephens AW, Rimon A, Rosenberg RD. Sequence variation in heparin octasaccharides with high affinity from antithrombin III. Biochemistry 1984; 23:5801–5812.
30. Lindahl U, Thunberg L, Backström G, Riesenfeld J, Nordling K, Björk I. Extension and structural variability of the antithrombin-binding sequence in heparin. J Biol Chem 1984; 259:12368–12376.
31. Atha DH, Lormeau J-C, Petitou M, Rosenberg RD, Choay J. Contribution of monosaccharide residues in heparin binding to antithrombin III. Biochemistry 1985; 24:6723–6729.
32. van Boeckel CAA, Grootenhuis PDJ, Visser A. A mechanism for heparin induced potentiation of antithrombin III. Nat Struct Biol 1994; 1:423–425.
33. Jin L, Abrahams J-P, Skinner R, Petitou M, Pike RN, Carrell RW. The anticoagulant activation of antithrombin by heparin. Proc Natl Acad Sci USA 1997; 94:14683–14688.
34. Whisstock JC, Pike RN, Jin L, Skinner R, Pei XY, Carrell RW, Lesk AM. Conformational changes in serpins: II. The mechanism of activation of antithrombin by heparin. J Mol Biol 2000; 301:1287–1305.
35. Meagher JL, Olson ST, Gettins PGW. Critical role of the linker region between helix D and strand 2A in heparin activation of antithrombin. J Biol Chem 2000; 275:2698–2704.
36. Belzar KJ, Zhou A, Carrell RW, Gettins PGW, Huntington JA. Helix D elongation and allosteric activation of antithrombin. J Biol Chem 2002; 277:8551–8558.
37. Huntington JA, Olson ST, Fan B, Gettins PGW. Mechanism of heparin activation of antithrombin: Evidence for reactive center loop preinsertion with expulsion upon heparin binding. Biochemistry 1996; 35:8495–8503.
38. Futamura A, Gettins PGW. Serine 380 (P14) → glutamate mutation activates antithrombin as an inhibitor of factor Xa. J Biol Chem 2000; 275:4092–4098.
39. Huntington JA, McCoy A, Belzar KJ, Pei XY, Gettins PGW, Carrell RW. The conformational activation of antithrombin: a 2.85 Å structure of a fluorescein derivative reveals an electrostatic link between the hinge and heparin binding regions. J Biol Chem 2000; 275:15377–15383.
40. Gettins PGW, Fan B, Crews BC, Turko IV. Transmission of conformational change from the heparin binding site to the reactive center of antithrombin. Biochemistry 1993; 32:8385–8389.
41. Chuang Y-J, Swanson R, Raja SM, Olson ST. Heparin enhances the specificity of antithrombin for thrombin and factor Xa independent of the reactive center loop sequence. Evidence for an exosite determinant of factor Xa specificity in heparin-activated antithrombin. J Biol Chem 2001; 276:14961–14971.
42. Izaguirre G, Zhang W, Swanson R, Bedsted T, Olson ST. Localization of an antithrombin exosite that promotes rapid inhibition of factors Xa and

IXa dependent on heparin activation of the serpin. J Biol Chem 2003; 278: 51433–51440.
43. Huntington JA. Mechanisms of glycosaminoglycan activation of the serpins in hemostasis. J Thromb Haemost 2003; 1:1535–1549.
44. Manithody C, Yang L, Rezaie AR. Role of basic residues of the autolysis loop in the catalytic function of factor Xa. Biochemistry 2002; 41:6780–6788.
45. Rezaie AR, Yang L, Manithody C. Mutagenesis studies toward understanding the mechanism of differential reactivity of factor Xa with the native and heparin-activated antithrombin. Biochemistry 2004; 43:2898–2905.
46. Yang L, Manithody C, Rezaie AR. Heparin-activated antithrombin interacts with the autolysis loop of target coagulation proteases. Blood 2004; 104: 1753–1759.
47. Hermans JM, Stone SR. Interaction of activated protein C with serpins. Biochem J 1993; 295:239–245.
48. Olson ST, Halvorson HR, Björk I. Quantitative characterization of the thrombin-heparin interaction. Discrimination between specific and nonspecific binding models. J Biol Chem 1991; 266:6342–6352.
49. Duchaussoy P, Jaurand G, Driguez P-A, Lederman I, Ceccato M-L, Gourvenec F, Strassel J-M, Sizun P, Petitou M, Herbert J-M. Assessment through chemical synthesis of the size of the heparin sequence involved in thrombin inhibition. Carbohydr Res 1999; 317:85–99.
50. Petitou M, Herault J-P, Bernat A, Driguez P-A, Duchaussoy P, Lormeau J-C, Herbert J-M. Synthesis of thrombin-inhibiting heparin mimetics without side effects. Nature 1999; 398:417–422.
51. Rezaie AR. Calcium enhances heparin catalysis of the antithrombin-factor Xa reaction by a template mechanism. J Biol Chem 1998; 273:16824–16827.
52. Rezaie AR, Olson ST. Calcium enhances heparin catalysis of the antithrombin-factor Xa reaction by promoting the assembly of an intermediate heparin-antithrombin-factor Xa binding complex. Demonstration by rapid kinetics studies. Biochemistry 2000; 39:12083–12090.
53. Herault JP, Gaich C, Bono F, Driguez PA, Duchaussoy P, Petitou M, Herbert JM. The structure of synthetic oligosaccharides in relation to factor IXa inhibition. Thromb Haemost 2002; 88:432–435.
54. Rezaie AR. Heparin-binding exosite of factor Xa. Trends Cardiovasc Med 2000; 10:333–338.
55. Whinna HC, Lesesky EB, Monroe DM, High KA, Larson PJ, Church FC. Role of the γ-carboxyglutamic acid domain of activated factor X in the presence of calcium during inhibition by antithrombin-heparin. J Thromb Haemost 2004; 2:1127–1134.
56. Desai UR, Swanson RS, Bock SC, Björk I, Olson ST. The role of arginine 129 in heparin binding and activation of antithrombin. J Biol Chem 2000; 275: 18976–18984.
57. Schedin-Weiss S, Desai UR, Bock SC, Gettins PGW, Björk I, Olson ST. The importance of lysine 125 for heparin binding and activation of antithrombin. Biochemistry 2002; 41:4779–4788.
58. Arocas V, Bock SC, Raja S, Olson ST, Björk I. Lysine 114 of antithrombin is of crucial importance for the affinity and kinetics of heparin pentasaccharide binding. J Biol Chem 2001; 276:43809–43817.

59. Schedin-Weiss S, Arocas V, Bock SC, Olson ST, Björk I. Specificity of the basic side chains of Lys114, Lys125 and Arg129 of antithrombin in heparin binding. Biochemistry 2002; 41:12369–12376.
60. Arocas V, Bock SC, Olson ST, Bjork I. The role of Arg46 and Arg47 of antithrombin in heparin binding. Biochemistry 1999; 38:10196–10204.
61. Schedin-Weiss S, Desai UR, Bock SC, Olson ST, Björk I. Roles of N-terminal region residues Lys11, Arg13, and Arg24 of antithrombin in heparin recognition and in promotion and stabilization of the heparin-induced conformational change. Biochemistry 2004; 43:675–683.
62. Monien BH, Krishnasamy C, Olson ST, Desai UR. Importance of tryptophan 49 of antithrombin in heparin binding and conformational activation. Biochemistry 2005; 44:11660–11668.
63. Arocas V, Turk B, Bock SC, Olson ST, Björk I. The region of antithrombin interacting with full-length heparin chains outside the high-affinity pentasaccharide sequence extends to Lys136 but not to Lys139. Biochemistry 2000; 39:8512–8518.
64. Meagher JL, Huntington JA, Gettins PGW. Role of arginine 132 and lysine 133 in heparin binding to and activation of antithrombin. J Biol Chem 1996; 271:29353–29358.
65. Li W, Johnson DJD, Esmon CT, Huntington JA. Structure of the antithrombin-thrombin-heparin ternary complex reveals the antithrombotic mechanism of heparin. Nat Struct Mol Biol 2004; 11:857–862.
66. Dementiev A, Petitou M, Herbert J-M, Gettins PGW. The ternary complex of antithrombin-anhydrothrombin-heparin reveals the basis of inhibitor specificity. Nat Struct Mol Biol 2004; 11:863–867.
67. Streusand VJ, Björk I, Gettins PG, Petitou M, Olson ST. Mechanism of acceleration of antithrombin-proteinase reactions by low affinity heparin. Role of the antithrombin binding pentasaccharide in heparin rate enhancement. J Biol Chem 1995; 270:9043–9051.
68. Rezaie AR. Identification of basic residues in the heparin-binding exosite of factor Xa critical for heparin and factor Va binding. J Biol Chem 2000; 275:3320–3327.
69. Bode W, Mayr I, Baumann U, Huber R, Stone SR, Hofsteenge J. The refined 1.9 Å crystal structure of human α-thrombin. Interaction with D-Phe-Pro-Arg-chloromethylketone and significance of the Tyr-Pro-Pro-Trp insertion segment. EMBO J 1989; 8:3467–3475.
70. Gan ZR, Li Y, Chen Z, Lewis SD, Shafer JA. Identification of basic amino acid residues in thrombin essential for heparin-catalyzed inactivation by antithrombin III. J Biol Chem 1994; 269:1301–1305.
71. Sheehan JP, Sadler JE. Molecular mapping of the heparin-binding exosite of thrombin. Proc Natl Acad Sci USA 1994; 91:5518–5522.
72. Tsiang M, Jain AK, Gibbs CS. Functional requirements for inhibition of thrombin by antithrombin III in the presence and absence of heparin. J Biol Chem 1997; 272:12024–12029.
73. Carter WJ, Cama E, Huntington JA. Crystal structure of thrombin bound to heparin. J Biol Chem 2005; 280:2745–2749.
74. Desai UR, Petitou M, Björk I, Olson ST. Mechanism of heparin activation of antithrombin. Role of individual residues of the pentasaccharide activating sequence in the recognition of native and activated states of antithrombin. J Biol Chem 1998; 273:7478–7487.

75. Desai UR, Petitou M, Björk I, Olson ST. Mechanism of heparin activation of antithrombin: evidence for an induced-fit model of allosteric activation involving two interaction subsites. Biochemistry 1998; 37:13033–13041.
76. Desai UR, Gunnarsson G. Hydropathic interaction analysis of sequence-specific heparin pentasaccharide binding to antithrombin. Med Chem Res 1999; 9:643–655.
77. Olson ST, Srinivasan KR, Björk I, Shore JD. Binding of high affinity heparin to antithrombin III: stopped flow kinetic studies of the binding interaction. J Biol Chem 1981; 256:11073–11079.
78. Capila I, Linhardt RJ. Heparin-protein interactions. Angew Chem Int Ed 2002; 41:390–412.
79. Fareed J, Hoppensteadt DA, Bick RL. An update on heparins at the beginning of the new millennium. Semin Thromb Hemost 2000; 26 (Suppl 1):5–21.
80. Shriver Z, Sundaram M, Venkataraman G, Fareed J, Linhardt R, Biemann K, Sasisekharan R. Cleavage of the antithrombin III binding site in heparin by heparinases and its implication in the generation of low molecular weight heparin. Proc Natl Acad Sci USA 2000; 97:10365–10370.
81. Islam T, Butler M, Sikkander SA, Toida T, Linhardt RJ. Further evidence that periodate cleavage of heparin occurs primarily through the antithrombin binding site. Carbohydr Res 2002; 337:2239–2243.
82. Choay J, Petitou M, Lormeau JC, Sinay P, Casu B, Gatti G. Structure-activity relationship in heparin: a synthetic pentasaccharide with high affinity for antithrombin III and eliciting high anti-factor Xa activity. Biochem Biophys Res Commun 1983; 116:492–499.
83. Cheng JWM. Fondaparinux: a new antithrombotic agent. Clin Ther 2002; 24:1757–1769.
84. Samama M-M, Gerotziafas GT. Evaluation of the pharmacological properties and clinical results of the synthetic pentasaccharide (fondaparinux). Thromb Res 2003; 109:1–11.
85. Tran AH, Lee G. Fondaparinux for prevention of venous thromboembolism in major orthopedic surgery. Ann Pharmacother 2003; 37:1632–1643.
86. Bauer KA. New pentasaccharides for prophylaxis of deep vein thrombosis. Chest 2003; 124:364S–370S.
87. Orgueira HA, Bartolozzi A, Schell P, Litjens RE, Palmacci ER, Seeberger PH. Modular synthesis of heparin oligosaccharides. Chemistry 2003; 9:140–169.
88. Desai UR. New antithrombin-based anticoagulants. Med Res Rev 2004; 24:151–184.
89. Petitou M, van Boeckel CAA. A synthetic antithrombin III binding pentasaccharide is now a drug! What comes next? Angew Chem Int Ed 2004; 43:3118–3133.
90. van Boeckel CAA, Petitou M. The unique antithrombin III binding domain of heparin: a lead to new synthetic antithrombotics. Angew Chem Int Ed 1993; 32:1671–1818.
91. Petitou M, Hérault JP, Lormeau JC, Helmboldt A, Mallet J-M, Sinaÿ P, Herbert J-M. Introducing a C-interglycosidic bond in a biologically active pentasaccharide hardly affects its biological properties. Bioorg Med Chem 1998; 6:1509–1516.

92. Kuberan B, Lech MZ, Beeler DL, Wu ZL, Rosenberg RD. Enzymatic synthesis of antithrombin III-binding heparan sulfate pentasaccharide. Nat Biotech 2003; 21:1343–1346.
93. Kuberan B, Beeler DL, Lawrence R, Lech M, Rosenberg RD. Rapid two-step synthesis of mitrin from heparosan: a replacement for heparin. J Am Chem Soc 2003; 125:12424–12425.
94. Kuberan B, Beeler DL, Lech M, Wu ZL, Rosenberg RD. Chemoenzymatic synthesis of classical and non-classical anticoagulant heparan sulfate polysaccharides. J Biol Chem 2003; 278:52613–52621.
95. Lindahl U, Li JP, Kusche-Gullberg M, Salmivirta M, Alaranta S, Veromaa T, Emeis J, Roberts I, Taylor C, Oreste P, Zoppetti G, Naggi A, Torri G, Casu B. Generation of "eoheparin" from *E. coli* K5 capsular polysaccharide. J Med Chem 2005; 48:349–352.
96. Grootenhuis PDJ, van Boeckel CAA. Constructing a molecular model of the interaction between antithrombin III and a potent heparin analogue. J Am Chem Soc 1991; 113:2743–2747.
97. Duchaussoy P, Jaurand G, Driquez P-A, Lederman I, Gourvenec F, Strassel J-M, Sizun P, Petitou M, Herbert J-M. Identification of a hexasaccharide sequence able to inhibit thrombin and suitable for 'polymerisation'. Carbohydr Res 1999; 317:63–84.
98. Duchaussoy P, Jaurand G, Driquez P-A, Lederman I, Ceccato M-L, Gourvenec F, Strassel J-M, Sizun P, Petitou M, Herbert J-M. Assessment through chemical synthesis of the size of the heparin sequence involved in thrombin inhibition. Carbohydr Res 1999; 317:85–99.
99. Dreef-Tromp CM, Basten JEM, Broekhoven MA, van Dinther TG, Petitou M, van Boeckel CAA. Biological properties of synthetic glycoconjugate mimics of heparin comprising different molecular spacers. Bioorg Med Chem Lett 1998; 8:2081–2086.
100. Petitou M, Driguez PA, Duchaussoy P, Hérault J-P, Lormeau J-C, Herbert J-M. Synthetic oligosaccharides having various functional domains: potent and potentially safe heparin mimetics. Bioorg Med Chem Lett 1999; 9:1161–1166.
101. Sinaÿ P. Sugars slide into heparin activity. Nature 1999; 398:377–378.
102. Buijsman RC, Basten JE, Dreef-Tromp CM, van der Marel GA, van Boeckel CAA, van Boom JH. Synthesis of heparin-like antithrombotics having perphosphorylated thrombin binding domains. Bioorg Med Chem 1999; 7:1881–1890.
103. Gunnarsson GT, Desai UR. Designing small, non-sugar activators of antithrombin using hydropathic interaction analyses. J Med Chem 2002; 45:1233–1243.
104. Gunnarsson GT, Desai UR. Interaction of sulfated flavanoids with antithrombin: lessons on the design of organic activators. J Med Chem 2002; 45:4460–4470.
105. Desai UR, Gunnarsson GT. Hydropathic interaction analysis of the sequence-specific heparin pentasaccharide binding to antithrombin. Med Chem Res 1999; 9:643–655.
106. Gunnarsson GT, Desai UR. Exploring new non-sugar sulfated molecules as activators of antithrombin. Bioorg Med Chem Lett 2003; 13:579–583.

107. Gunnarsson GT, Riaz M, Adams J, Desai UR. Synthesis of per-sulfated flavonoids using 2,2,2-trichloro ethyl protecting group and their factor Xa inhibition potential. Bioorg Med Chem 2005; 13:1783–1789.
108. Monien BH, Desai UR. Antithrombin activation by nonsulfated, non-polysaccharide organic polymer. J Med Chem 2005; 48:1269–1273.

Chemistry and Biology of Heparin and Heparan Sulfate
H.G. Garg, R.J. Linhardt and C.A. Hales (Editors)

Chapter 18

Influence of Heparin Chemical Modifications on its Antiproliferative Properties

HARI G. GARG

Massachusetts General Hospital, Harvard Medical School, Boston, MA, USA

ROBERT J. LINHARDT

Rensselaer Polytechnic Institute, Troy, NY, USA
and
CHARLES A. HALES

Massachusetts General Hospital, Harvard Medical School, Boston, MA, USA

I. Introduction

Pulmonary hypertension due to chronic hypoxia is associated with increased quantities of smooth muscle cells (SMCs) in pulmonary arteries, due to thickening of the medial muscle layer in the proximal arteries and extension of the smooth muscle investment into preripheral, normally nonmuscular vessels (1–4). A number of factors are known to cause SMCs migration, such as serum, platelet-derived growth factor (PDGF)-BB (5,6), transforming growth factor β (7), fibrinogen (8), oxidized low-density lipoprotein (9,10), and angeotensin II (11,12). Heparin inhibits hypoxic pulmonary hypertension, possibly by an antiproliferative effect on SMCs (13–15).

Heparin consists of alternating residues of a uronic acid (either β-D-glucuronic acid or α-L-iduronic acid) with a hexosamine (α-D-glucosamine) linked by $1 \rightarrow 4$ glycosadic linkage and covalently bound to serine residues of the core protein. It has various *O*-sulfo, *N*-sulfo, and *N*-acetyl substituents that are usually heterogeneously distributed along the glycosaminoglycan (GAG) chains.

The possible 48 repeating disaccharide sequences in heparin are given in Fig. 1. Many but not all of these sequences have been reported to date (16).

The most common repeating disaccharide sequence ($70 \pm 16\%$) occurring in heparin is the trisulfated disaccharide with a sulfonate group at position 2 of the

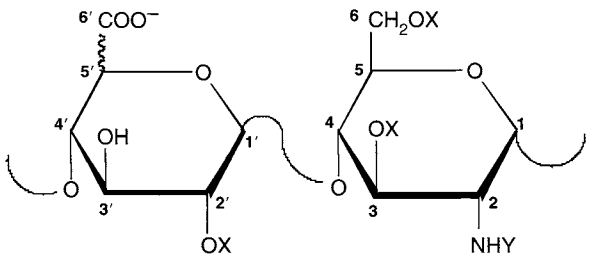

Four uronate residues		Twelve glucosamine residues		
2'X	5'	2Y	3X	6X
hydrogen	iduronate	sulfo	hydrogen	hydrogen
sulfo	iduronate	sulfo	hydrogen	sulfo
hydrogen	glucuronate	sulfo	sulfo	hydrogen
sulfo	glucuronate	sulfo	sulfo	sulfo
		acetyl	hydrogen	hydrogen
		acetyl	hydrogen	sulfo
		acetyl	sulfo	hydrogen
		acetyl	sulfo	sulfo
		hydrogen	hydrogen	hydrogen
		hydrogen	hydrogen	sulfo
		hydrogen	sulfo	hydrogen
		hydrogen	sulfo	sulfo

Figure 1 The possible 48 disaccharide sequences in heparin.

uronate residue and at positions 2 and 6 of the glucosamine residue (17). This structure is shown in Fig. 2 as the major sequence.

However, a number of structural variations of repeating disaccharide units have been observed, leading to the microheterogeneity of heparin (Fig. 2, variable sequence). The amino group at position 2 of the glucosamine residue may be substituted with an acetyl, or sulfo group or unsubsituted. The 3- and 6-positions of the glucosamine residues can either be substituted with an *O*-sulfo group or unsubstituted. The uronic acid, which can either be L-iduronic or D-glucuronic acid may also contain a 2-*O*-sulfo group (18). An average negative charge in the heparin macromolecule is approximately −75, (i.e., due to SO_3^- and COO^-) (18).

II. Background and Significance of Chemical Modification of Heparin

Chronic pulmonary hypertension is characterized by structural changes in the pulmonary vasculature, which along with variable degrees of vasoconstriction are responsible for the high pulmonary vascular resistance and associated right heart failure (19,20). The vascular structural changes associated with exposure to chronic hypoxia have been most extensively studied and are characterized by hyperplasia, hypertrophy, and migration of vascular smooth SMC in the media of muscular and

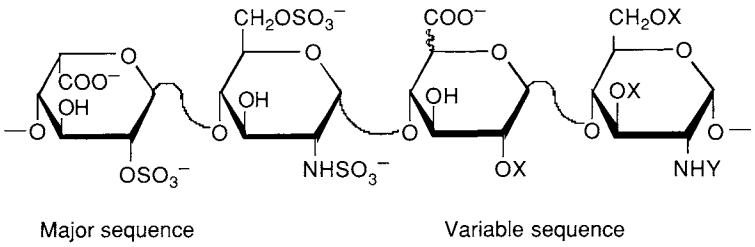

Figure 2 Major and variable sequence disaccharide repeating units in heparin (X = H or SO_3^- and Y = Ac[CH_3CO] or SO_3^- or H).

partially muscular pulmonary arteries (19,20). To develop a potential therapeutic agent to reverse vascular remodeling, which occurs in pulmonary hypertension, we and others have examined the antiproliferative activity of heparin including chemically modified heparin derivatives.

III. Mechanisms Contributing to Heparin Inhibition of Smooth Muscle Cell Growth

Several laboratories have demonstrated that heparin inhibits cell proliferation (21–28). Although much attention has been focused on the factors that stimulate smooth muscle cell (SMC) proliferation (29), very little is known about the mechanisms maintaining these cells in a quiescent state or about the reestablishment of a quiescent state after their proliferative response has been initiated.

Circulating HP binds to endothelial cells and is taken up by the reticuloendothelial system where it enters a cellular pool to be released at a later stage (30). Furthermore, HP binds to specific binding sites on SMCs and is internalized (24). Some antiproliferative effects are mediated by specific binding, although it is not clear whether internalization is essential. HP blocks the cell cycle at either the G_0/G_1 transition point (22) or at mid to late G_1 progression (24,27,31) and may inhibit such cellular intermediate processes as protein kinase C activation, c-Fos and c-Myc induction (32,33), activator protein-1/Fos-Jun binding activity, and posttransitional modification of Jun B (34–36). HP has also been shown to selectively block the protein kinase C pathway of mitogenic signaling (37) and the phosphorylation of mitogen-activated protein kinase (38). However, these mechanisms responsible for the antiproliferative effects of heparin are not very well understood.

We have demonstrated that PASMC mitogens, such as platelet-derived growth factor and epidermal growth factor, act through the Na^+/H^+ antiporter by stimulating a one-for-one exchange of extracellular Na^+ for intracellular H^+ to cause intracellular alkalinization, a permissive first step for cell division (39). Dahlberg et al. (40) have demonstrated that antiproliferative HPs block Na^+/H^+ exchange in a manner directly related to antiproliferative activity.

IV. Importance of 3-*O*-Sulfo Group on the Internal Glucosamine Residue of Pentasaccharide for Antiproliferative Activity

Using a synthetically prepared pentasaccharide (Fig. 3), Castellot et al. (25) presented evidence that the 3-*O*-sulfonate on the internal glucosamine is critical for antiproliferative capacity of the pentasaccharide.

To evaluate whether 3-*O*-sulfo group containing glucosamine residues in whole commercial HPs are essential for native HP's antiproliferative effect on pulmonary artery smooth muscle cells, we treated three commercial available HPs of varying potency with heparinases I and II (41). These enzymes degrade heparin fragments containing 3-*O*-sulfo groups to unsaturated Δ-tetrasaccharides only (Fig. 4). The above study clearly demonstrated that the 3-*O*-sulfo group of

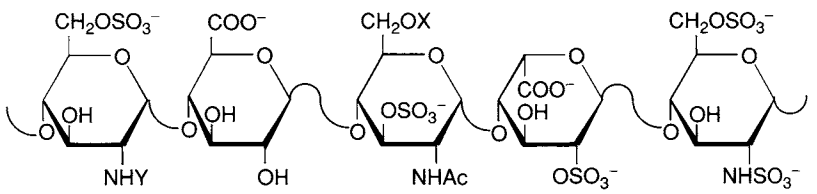

Figure 3 Antiproliferative pentasaccharide demonstrating the structure critical for growth inhibition (10).

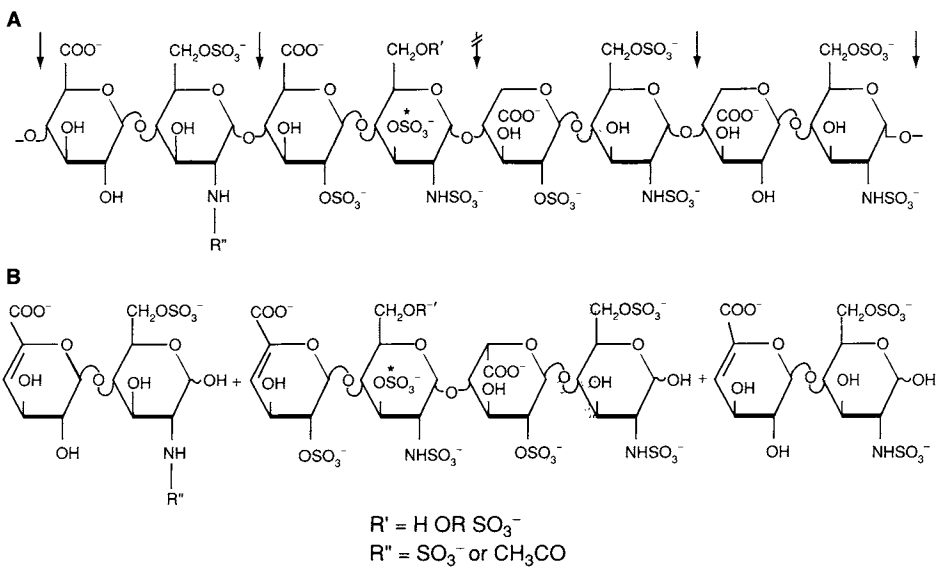

Figure 4 (A) Heparin sequences with different sulfation patterns arbitrarily assigned, and (B) cleavage pattern of heparin containing 3-*O*-sulfated glucosamine residue by heparinases I and II.

glucosamine residues is not critical in whole heparin for antiproliferative activity as the most potent HP preparation generated the least amount of Δ-tetrasaccharide (Table 1). Different heparin preparations also differ in the contents of the released mono-, di-, and tri-sulfated Δ-disaccharides as shown in Table 2.

V. Minimal Heparin Oligosaccharide Size Necessary for Antiproliferative Activity

Wright et al. prepared oligosaccharides of defined length by nitrous acid cleavage of heparin followed by gel filteration and tested them for their antiproliferative potency in three cell types (42). They reported that the size requirement is similar but not identical for different cell types. Decasaccharides have the same antiproliferative activity as native heparin. Experiments with rat and calf vascular smooth muscle cells growth inhibition showed that dodecasaccharide and larger fragments (Table 3) are essential for the growth inhibitory effect (43). To evaluate the minimum oligosaccharide size necessary to retain full antiproliferative activity, a commercially available heparin preparation under mild enzymatic conditions was cleaved to give oligosaccharides of different sizes. The structure of these oligosaccharides is given in Fig. 5 (44).

The above oligosaccharides (Fig. 5) were assayed for their antiproliferative activities against bovine pulmonary artery smooth muscle cells and the results are summarized in Fig. 6.

Table 1 Unsaturated Δ-Tetrasaccharide Released after Heparinases I and II Treatments (17)

No.	Heparin preparation	Δ-Tetrasaccharide released (%)
1	Upjohn #1438	1.7
2	Choay #IC86-1772	17.3
3	Elkins-Sinn #26390	1.9

Table 2 Disaccharide Composition of Heparins from Different Manufacturers[a]

Disaccharide	X^6	Y^2	$X^{2'}$	Upjohn	Elkins-Sinn	Choay
1	H	Ac	H	0.9	3.9	14.5
2	H	SO_3^-	H	0.3	2.0	–
3	SO_3	AC	H	–	3.9	–
4	H	Ac	SO_3	–	1.7	–
5	SO_3	SO_3	II	5.4	11.5	–
6	H	SO_3	SO_3	4.8	6.3	18.0
7	SO_3	Ac	SO_3	0.4	1.5	1.5
8	SO_3	SO_3	SO_3	86.8	66.3	66.0

[a]Disaccharides were released by treating exhaustively with heparin lyase I and III. Results are expressed as percentage of total disaccharide released (17).

Table 3 Comparison of the Antiproliferative Activity and Degree of Sulfation of Heparin Fragments (43)

	Antiproliferative activity[a]		
	1 μg/ml	100 μg/ml	Sulfation degree[b]
Native heparin	36	75	2.7
Disaccharide	0	4	1.8
Tetrasaccharide	2	12	2.3
Hexasaccharide	21	46	2.7
Octasaccharide	29	65	2.7
Decasaccharide	40	71	2.7
Dodecasaccharide	43	82	2.7
~20 saccharide	42	80	2.7

[a]Percent inhibition of rat aortic smooth muscle cells grown in media containing fetal bovine serum (FBS) plus heparin fragment.
[b]Moles sulfate/mole glucosamine (approximate).

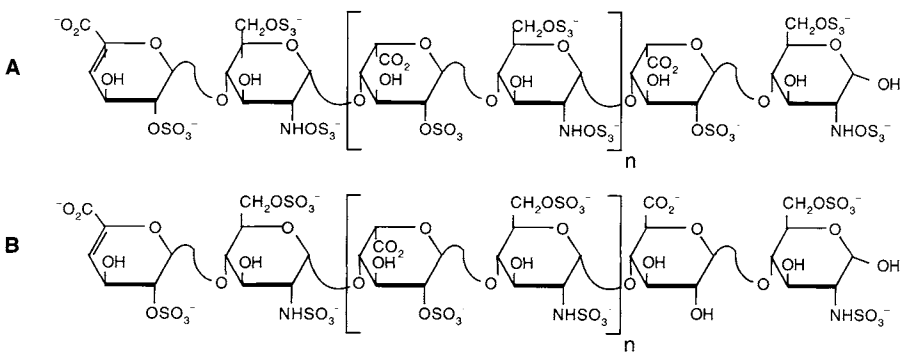

Figure 5 Structure of heparin-derived oligosaccharides. Shown is a fully sulfated structure (A) corresponding to tetrasaccharide (1), decasaccharide (3), dodecasaccharide (7), and the major component in the purified tetradecasaccharide (8), hexadecasaccharide (9), and octadecasaccharide (10) fractions, where $n = 0$, 3, 4, 5, 6, and 7. Also shown is undersulfated structure (B) corresponding to decasaccharide (2) and dodecasaccharide (4), where $n = 3$ and 4, respectively.

These results suggest that the 14-mer (Fig. 5a, $n = 5$) and above, 16- and 18-mers (Fig. 5a, $n = 6$ and 7), have as full antiproliferative potency as native heparin. This difference in the size of the oligomer required for antiproliferative activity suggests the origin of vascular smooth muscle cells (i.e., pulmonary or aortic) is important to determine the size of the oligomer.

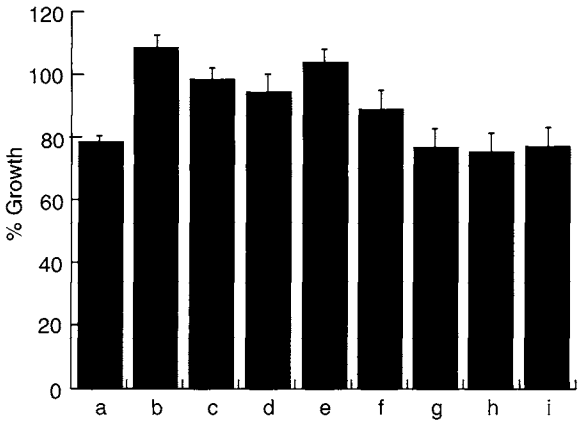

Figure 6 Percent growth of bovine pulmonary artery smooth muscle cells grown in media containing 10% fetal bovine serum (FBS) plus: Column a, native heparin; Column b, 4-mer (Fig. 5a, $n = 0$); Column c, 10-mer (undersulfated) (Fig. 5b, $n = 3$); Column d, 10-mer (Fig. 5a, $n = 3$); Column e, 12-mer (undersulfated) (Fig. 5b, $n = 4$); Column f, 12-mer (undersulfated) (Fig. 5b, $n = 4$); Column f, 12-mer (Fig. 5a, $n = 4$); Column g, 14-mer (Fig. 5a, $n = 5$); Column h, 16-mer (Fig. 5a, $n = 6$); and Column i, 18-mer (Fig. 5a, $n = 6$ and 7).

VI. Effect of Chemical Modification of Heparin on Its Antiproliferative Activity

To establish which domain of the heparin is especially responsible for antiproliferative activity, the following strategies have been adopted: (a) chemical modification; (b) fractionation of heparin molecule; and (c) preparation of oligosaccharides with a defined chemical structure. The present chapter includes the effects of heparin modifications on the antiproliferative activity.

A. *N*-Desulfonated, re-*N*-Sulfonated and re-*N*-Acetylated Heparin Derivatives

Castellot et al. (43) examined the antiproliferative activity of chemically modified heparins with native heparin (45). Comparison of the antiproliferative activity and degree of sulfation of chemically modified heparins are summarized in Table 4. All these modifications retained a high degree of antiproliferative activity. Wright et al. (42) found that the presence of 2-*O*-sulfo glucuronic acid was not required for antiproliferative activity.

Tiozzo et al. (46) also determined the role of *N*-linked and *O*-linked sulfo groups on the antiproliferative effect in two different cell types; BHK-21 (hamster fibroblasts) and human arterial smooth muscle cells. In the case of 2-*O*-desulfonated heparins the antiproliferative activity decreased compared to unfractionated

Table 4 Comparison of the Antiproliferative Activity Against Rat Aorta Smooth Muscle Cells and Degree of Sulfation of Chemically Modified Heparins (43)

	Antiproliferative activity[a]		Sulfation degree[b]	
	1 μg/ml	100 μg/ml	*N*-sulfo groups	Total sulfo groups
Native heparin	36	75	0.96	2.69
N-desulfonated	10	18	0	1.43
N-desulfonated → *N*-resulfonated	41	82	0.92	2.31
N-desulfonated → *N*-reacetylated	24	64	0	1.03
Totally desulfonated	7	10	0	0
Totally desulfonated → *N*-resulfonated	15	26	0.96	1.03
Totally desulfonated → *N*-reacetylated	3	12	0	

[a]Per cent inhibition in rat aortic smooth muscle cells grown in media containing fetal bovine serum (FBS) plus individual heparin preparation. Essentially identical results were obtained with calf aortic smooth muscle cells.
[b]Moles SO_4^{2-}/moles glucosamine.

heparin from intestinal mucosa. Although *N*-desulfonation also reduced antiproliferative potency of heparin, the relationship between the degree of sulfonation and the inhibition of cell growth forward is less straightforward. In contrast, these studies suggest that the negative charge, particularly *O*-sulfo group content is important in determining the antiproliferative potency.

B. Influence of Protein/Peptide Core and Glycosaminoglycan Chains of Heparin

The core protein/peptide of heparin was isolated by digesting with heparinases I and II in sodium acetate buffer (47). The reaction mixture was dialyzed against water and lyophilized to yield core protein/peptide. This process removed the GAG chains, leaving the protein/peptide core with linkage region intact. The released protein/peptide core significantly lost the antiproliferative activity of bovine pulmonary smooth muscle cells in comparison to whole heparin 88.3 ± 2.8 *vs* 48.8 ± 1.9, respectively, (Fig. 7) (48).

Glycosaminoglycan chains of heparin were liberated with alkaline borohydride treatment (49). This procedure cleaved the carbohydrate–protein of heparin of HP GAG chains by converting the xylose residue linked with Ser/Thr into xylatol thereby cleaving and degrading the protein core. These peptides were removed by dialyzing against water, leaving the GAG chains. The GAG chains released have similar antiproliferative activity (45.5 ± 3.0%) as the parent heparin (44.6 ± 2.7%) (Fig. 8) (48).

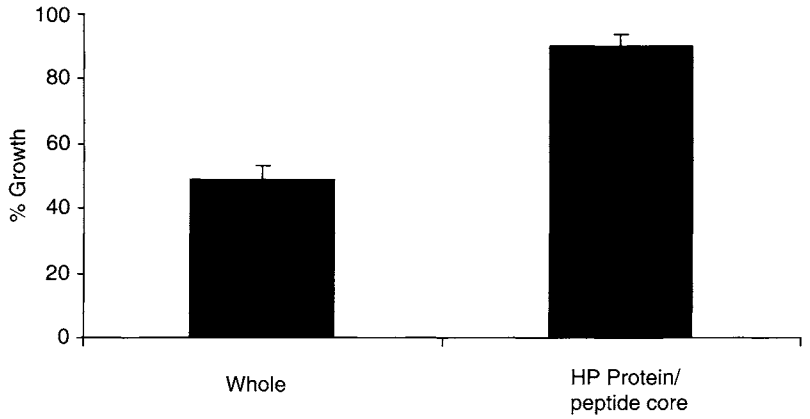

Figure 7 Percent growth in bovine pulmonary artery SMC grown in media containing 10% FBS plus native heparin or protein/peptide core (10 mg/ml).

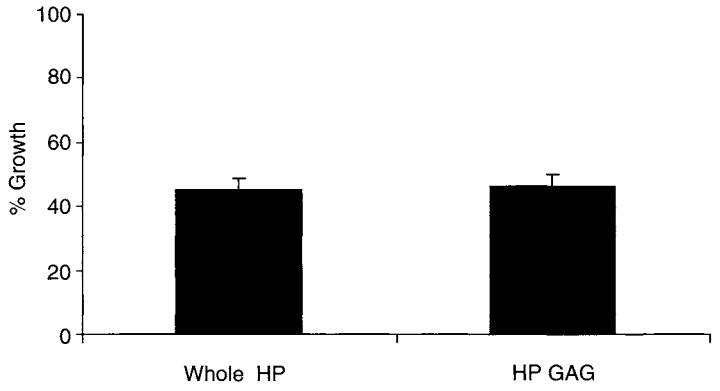

Figure 8 Percent growth in bovine pulmonary artery SMC in media containing 10% FBS plus native heparin or GAG chains (10 mg/ml).

C. Influence of Full sulfation of Heparin and Other Glycosaminoglycans

Fully sulfated heparin and other GAGS (Fig. 9) were prepared by treating tributylammonium salt of these with sulfur trioxide (50). Physical properties are summarized in Table 5 (51). All these derivatives were assayed for antiproliferative activity on cultured bovine pulmonary artery SMC (Fig. 10).

No appreciable difference was found between heparin and fully sulfated heparin on the growth of pulmonary artery smooth muscle cells. Chondroitin and dermatan sulfates stimulated the pulmonary artery smooth muscle cells. Hyaluronan was not antiproliferative but full sulfation made HA strongly antiproliferative against pulmonary smooth muscle cells (Fig. 10) (51).

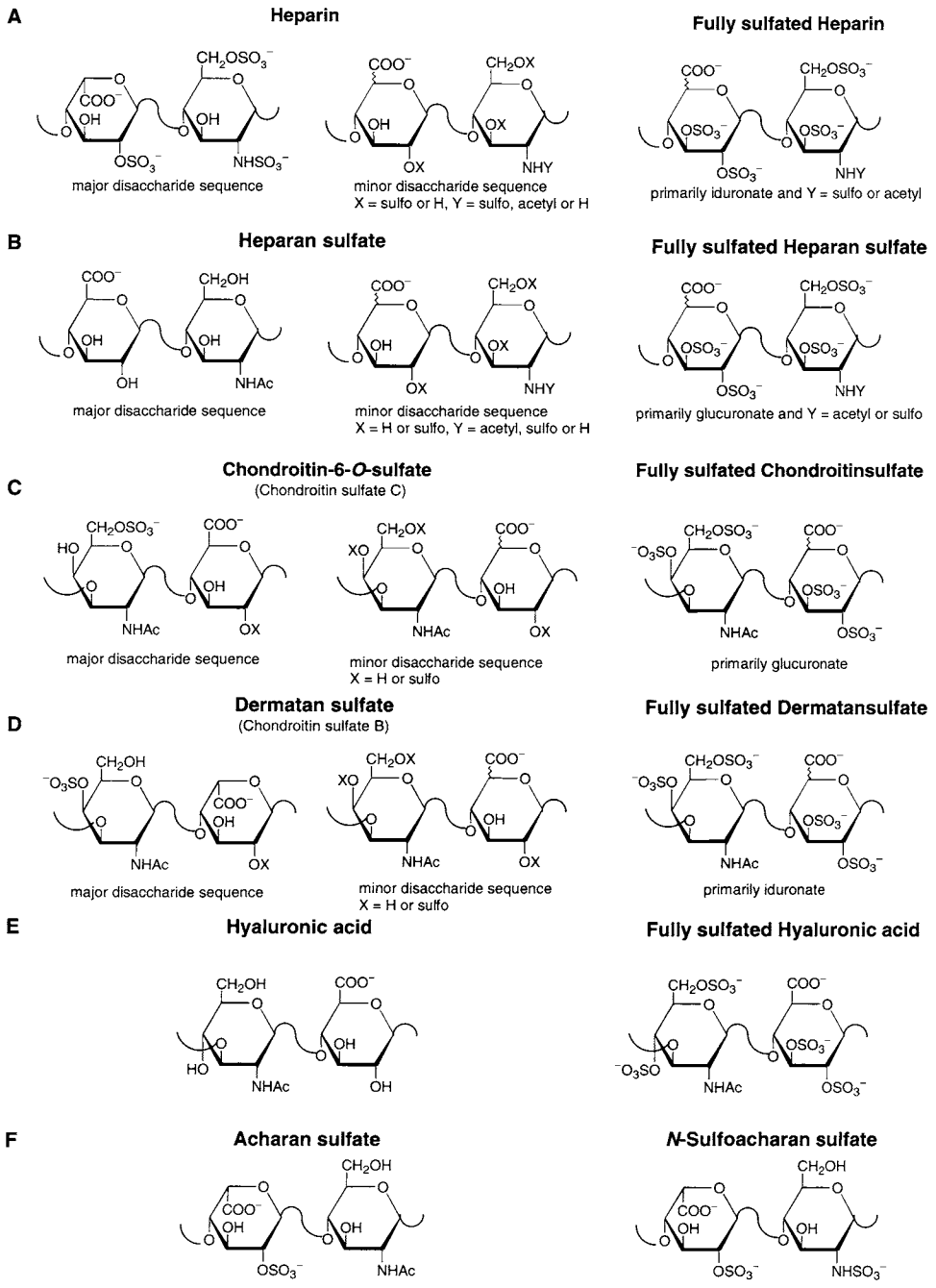

Figure 9 Major and variable sequences of original and fully sulfated GAGs: (A) heparin; (B) heparan sulfate; (C) chondroitin sulfate; (D) dermatan sulfate; (E), hyaluronan; (F) acharan sulfate and *N*-sulfoacharan sulfate; X = H or SO_3^-, Y = CH_3CO or SO_3^-.

Table 5 Physical Properties of Heparin and other Glycosaminoglycans, Acharan Sulfate, and Their Fully Sulfated Derivatives (51)

Disaccharide unit Compound rotation	Mol *O*-SO_3^- groups	Mol *N*-SO_3^- groups	Average molecular weight	Optical [α] D
Heparin (HP)	2.0	0.88	16.0	+46.5
Fully sulfated HP	4.0	0.68	20.0	+22.3
Heparan sulfate (HS)	1.0	0.22	14.8	+70.0
Fully sulfated HS	4.0	0.22	24.0	+31.5
Chondroitin sulfate (CS)	1.0	0	15.0	−30.0
Fully sulfated CS	4.0	0	23.8	−8.0
Dermatan sulfate (DS)	1.0	0	30.0	−41.5
Fully sulfated DS	4.0	0	47.5	−10.5
Hyaluronan (HA)	0	0	100	−32.5
Fully sulfated HA	4.0	0	198	−25.0
Acharan sulfate (AS)	1.0	0	29	nd
N-sulfo AS	1.0	1.0	8	nd

Note: nd, not determined.

D. Effect of Sulfonation Patterns in Heparin and Heparan Sulfate on the Proliferation of SMC

Sulfo groups in HP appear to play an important role in the growth inhibitory effect on smooth muscle cell proliferation. Removal of *N*-sulfo groups from HP reportedly negates its growth inhibitory effect on SMC (46). To understand the significance of *N*- and 6-*O*-sulfo groups in heparin/heparan sulfate for SMC proliferation, six chemically modified HP and HS (Fig. 11) were prepared, which fell into three groups. One group consisted of fully *O*-sulfonated-*N*-acetylated, the second group consisted de-*N*-sulfonated and re-*N*-acetylated, and the third group consisted of 6-*O*-desulfonated HP and HS derivatives (52). Properties of HP and HS derivatives (1–8) are given in Table 6.

These six preparations were assayed for their antiproliferative potency on pulmonary artery SMC (Fig. 12).

The results of this assay showed that (a) full-*O*-sulfonation of both HP and HS increases antiproliferative potency, (b) substitution of hexosamine with *N*-acetyl diminishes antiproliferative activity in both HP and HS, and (c) 6-*O*-desulfonation of HP and HS diminishes antiproliferative potency (52).

Importance of both the *N*-acetylation and *N*-sulfo groups of glucosamine residues in heparin for growth inhibition of SMC is not very well understood. This was studied recently (53) by quantifying the relative *N*-acetylation of three commercial heparins of known antiproliferative activities, using Fourier transform infrared (FTIR) band areas at 1381–1387 and 1320–1317 cm^{-1}, which combined resulted in 1.0, 1.0, and 1.3 cm^2 for Choay, Elkins-Sinn, and Upjohn HP, respectively. These data show that Upjohn HP, which is at least 44% more antiproliferative than the other two (40), is 30% more *N*-acetylated. Further, Upjohn HP on

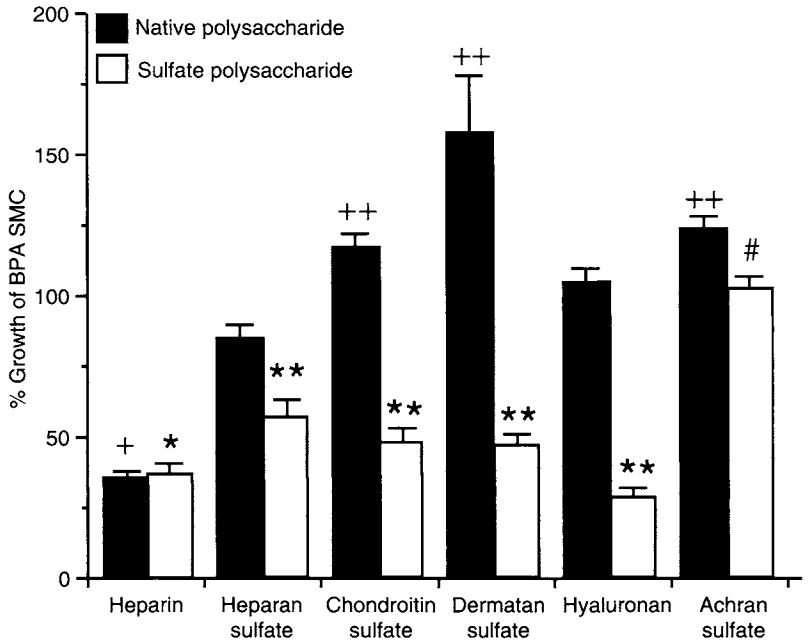

Figure 10 Effect of various polysaccharides on bovine pulmonary artery smooth muscle cells grown in media containing 10% FBS plus either original (solid bars) or fully sulfated GAG (open bars) or acharan sulfated (solid bar) or *N*-sulfoacharan sulfated (open bar). Samples are standardized to growth in media containing 10% serum without polysaccharide. +, significant reduction in cell growth as compared to the standard ($p < 0.05$); ++, significant increase in cell growth as compared to the standard ($p < 0.05$); *, significant reduction in cell growth as compared to the standard ($p < 0.05$), but no difference as compared to the parent polysaccharide; **, significant reduction in cell growth as compared to both the standard and parent polysaccharide ($p < 0.05$); #, significant reduction in cell growth as compared to parent acharan sulfate ($p < 0.05$), but not to the standard.

chemically *N*-desulfonation resulted in a 67% decrease in the growth inhibitory potency. The above results show that both *N*-acetyl and *N*-sulfo groups are essential for antiproliferative activity.

VII. Effect of the Type of Serum on Antiproliferative Activity

Underwood et al. (54) have recently demonstrated that while HP inhibited proliferation of vascular SMC in fetal bovine serum (FBS) as a growth supplement in culture medium, it was ineffective in the presence of human serum. We (55) examined the growth inhibitory effect of our most antiproliferative HP preparation from Upjohn in the presence of FBS as well as human serum on pulmonary artery SMC (Fig. 13) and on aortic SMC (Fig. 14). We also examined the growth

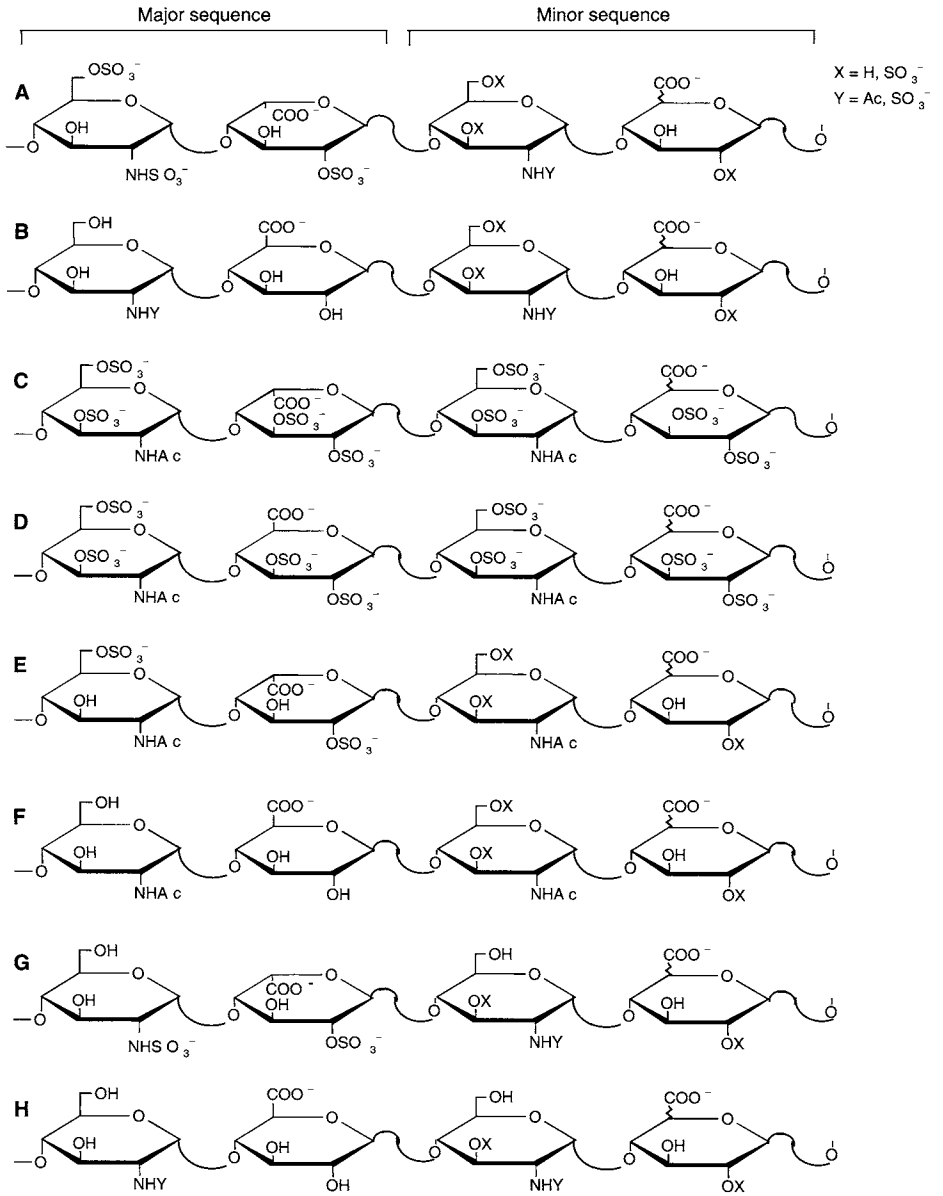

Figure 11 Structural formulae of major and variable sequences of repeating disaccharide units of HP and HS preparations. (A) heparin (HP); (B) heparan sulfate (HS); (C) fully *O*-sulfonated and re-*N*-acetylated HP; (D), fully *O*-sulfonated and re-*N*-acetylated HS; (E) de-*N*-sulfonated and re-*N*-acetylated HP; (F) de-*N*-sulfonated and re-*N*-acetylated HS; (G) 6-*O*-desulfonated HP; 6-*O*-desulfonated HS.

Table 6 Properties of Heparin and Heparan Sulfate Derivatives (1–8) (52)

Compound	SO_3^-/COO^-	2-*O*-SO_3^- (%)	6-*O*-SO_3^- (%)	*N*-SO_3^- (%)	IdoA/GlcA (%)
HP 1	2.68	86.2	89.7	90.4	92.3/7.7
3	3.88	100	100	<0.5	92.3/7.7
5	1.74	86.2	89.7	<0.5	92.3/7.7
7	1.66	86.2	<0.5	90.4	92.3/7.7
HS 2	0.25	1.6	6.4	17.5	26.7/73.3
4	3.92	100	100	<0.5	26.7/73.3
6	0.10	1.6	6.4	<0.5	26.7/73.3
8	0.19	1.6	<0.5	17.1	26.7/73.3

inhibitory effect of the above heparin preparation in the presence of human serum on human pulmonary artery SMC (Fig. 15) (55).

Our results are opposite to those reported by Underwood et al. (54). The variance in resistance to heparin in human serum could be due to the potency of the HP preparations. A potent antiproliferative heparin was effective in either bovine or human serum whether it be for aortic or pulmonary artery SMC.

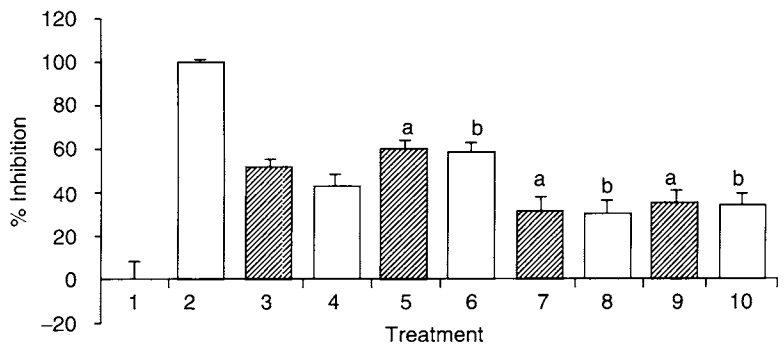

Figure 12 Inhibition of pulmonary artery SMC proliferation by modified HP, HS preparations including starting HP and HS. Percent inhibition of bovine pulmonary artery smooth muscle cell grown in media containing 10% FBS without HP and HS as negative control, Column (1); 0.1% fatal bovine serum (FBS) without HP or HS positive control (+), Column (2); 10% FBS plus HP (1), Column (3); 10% FBS plus HS (2), Column (4); containing 10% FBS plus fully *O*-sulfonated-re-*N*-acetylated HP (3), Column (5); containing 10% FBS plus fully *O*-sulfonated-re-*N*-acetylated HS (4), Column (6); 10% FBS plus de-*N*-sulfonated-re-*N*-acetylated HP (5), Column (7); containing 10% FBS plus de-*N*-sulfonated-re-*N*-acetylated HS (6), Column (8); 10% FBS plus 6-*O*-desulfonated HP (7), Column (9); 10% FBS plus 6-*O*-desulfonated HS (8), Column (10). Letter "a" represents a significant inhibition in cell growth compared to HP, and "b" represents a significant inhibition in cell growth compared to HS.

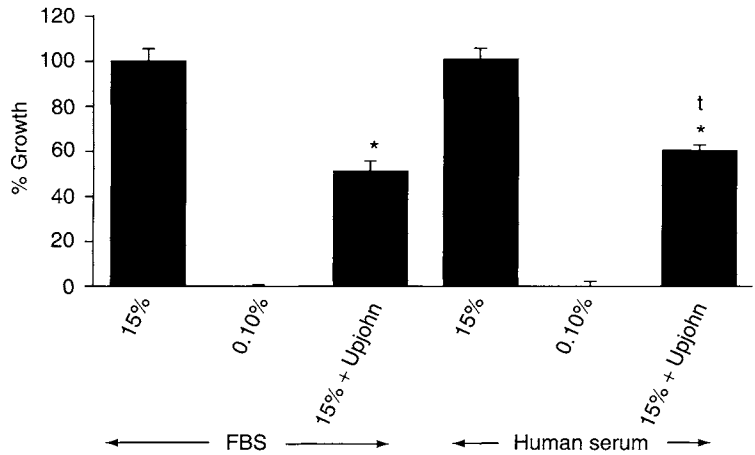

Figure 13 Bovine pulmonary artery smooth muscle cells (BPASMC) treated with Upjohn heparin in fetal bovine serum (FBS) and human serum. BPASMC were treated with standard medium (RPMI-1640 supplemented with antibiotics) + 15% FBS, standard medium + 15% human serum, standard medium + 0.1% FBS (growth arrest), standard medium + 0.1% human serum (growth arrest), standard medium containing 10 μg/ml Upjohn heparin + 15% FBS, and standard medium containing 10 μg/ml Upjohn heparin (Upjohn) + 15% human serum. After 4 days of treatment, cells harvested and the cell number and percent growth were determined; $^{*}p < 0.0001$ *vs* 15%; $^{t}p < 0.05$ *vs* 15% human + HP. Values are means ± SE; $n = 15$ in each group.

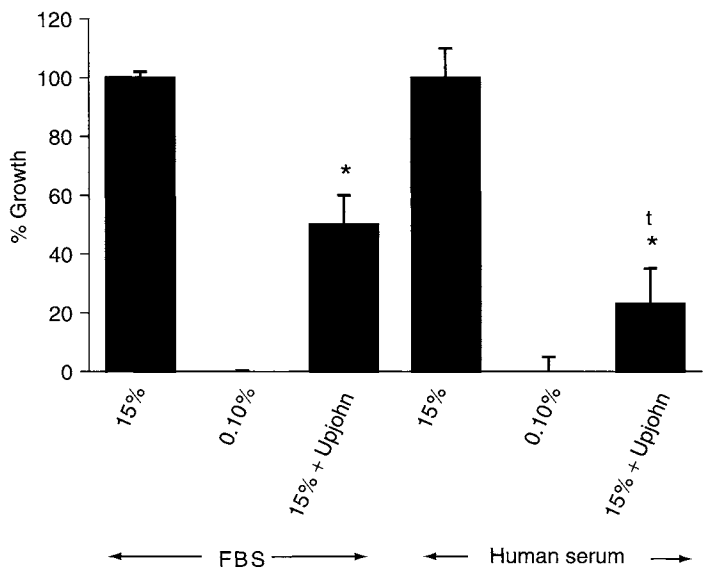

For Legend see page 528

Figure 14 Bovine aortic smooth muscle cells (BAOSMC) treated with Upjohn heparin in fetal bovine serum (FBS) and human serum. BPAOMC were treated with standard medium (RPMI-1640 supplemented with antibiotics) + 15% FBS, standard medium + 15% human serum, standard medium + 0.1% FBS (growth arrest), standard medium + 0.1% human serum (growth arrest), standard medium containing 10 μg/ml Upjohn heparin + 15% FBS, and standard medium containing 10 μg/ml Upjohn heparin (Upjohn) + 15% human serum. After 4 days of treatment, cells harvested and the cell number and percent growth were determined; * $p < 0.0001$ *vs* 15%; $^{t}p < 0.05$ *vs* 15% human + HP. Values are means ± SE; $n = 15$ in each group.

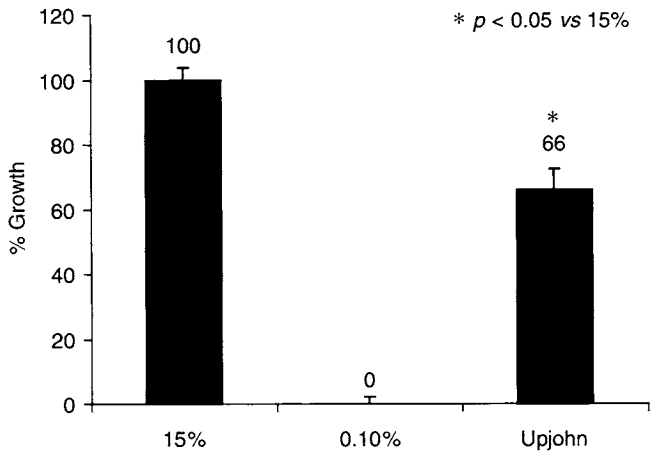

Figure 15 Human pulmonary artery smooth muscle cells (HPASMc) treated with Upjohn heparin in human serum. HPASMC were treated with standard medium (RPMI-1640 supplemented with antibiotics) + 15% human serum, standard medium + 0.1% human serum (growth arrest), and standard medium containing 10 μg/ml Upjohn heparin + 15% human serum. After 4 days of treatment, cells were harvested and the cell number and percent growth were determined; *$p < 0.0001$ *vs* 15%. Values are means ± SE; $n = 15$ in each group.

VIII. Conclusions

In conclusion, although the structural requirements for antiproliferative activity of heparin are not fully understood, the above studies demonstrate that: (a) an increase in the charge density affects the antiproliferative activity; (b) the molecular size of the HP does not affect the potency of growth inhibition; (c) the HP protein core prepared by digesting with heparitinases I and II significantly loses the antiproliferative activity; (d) the HP GAG chains are responsible for the antiprolifera-

tive activity; (e) 3-*O*-sulfo group on the internal glucosamine residues is not critical for native HP's antiproliferative activity; (f) both *N*-acetyl and *N*-sulfo groups in HP are important for antiproliferative properties; (g) 14-mer is the minimum size of oligosaccharide, which is essential for full antiproliferative activity; (h) loss of *N*-sulfo and 6-*O*-sulfo groups in the glucosamine residues of heparin reduces antiproliferative potency.

References

1. Geggel RL, Reid LM. The structure basis of PPHN. Clin Perinatol 1985; 11:525–549.
2. Hales CA, Kradin RL, Branstetter RD, Zhu YJ. Impairment of hypoxic pulmonary artery remodeling by heparin in mice. Am Rev Respir Dis 1983; 128:747–751.
3. Meyrick B, Reid L. The effect of chronic hypoxia on pulmonary arteries in young rats. Exp Lung Res 1981; 2:257–271.
4. Hislop A, Reid L. New findings in pulmonary arteries of rats with hypoxia-induced pulmonary hypertension. Br J Exp Pathol 1976; 57:542–554.
5. Grotendorst GR, Seppa HEJ, Kleinman HK, Martin GR. Attachment of smooth muscle cells to collagen and their migration toward platelet-derived growth factor. Proc Natl Acad Sci USA 1981; 78:3669–3672.
6. Ikeda M, Kohno M, Yasunari K, Yokokawa K, Horio T, Ueda M, Morisaki N, Yoshikawa J. Natriuretic peptide as a novel antimigration factor of vascular smooth muscle cells. Arterioscler Thromb Vasc Biol 1997; 17:731–736.
7. Koyama N, Koshikawa T, Morisaki N, Saito Y, Yoshida S. Bifunctional effects of transforming growth factor β on migration of cultured rat aortic smooth muscle cells. Biochem Biophys Res Commun 1990; 169:725–729.
8. Naito M, Hayashi T, Kuzuya M, Funaki C, Asai K, Kuzuya F. Fibrogen in chemotactic for vascular smooth muscle cells. FEBS Lett 1989; 247:358–360.
9. Autio I, Jakkola O, Solakivi T, Nikkari T. Oxidized low density lipoprotein in chemotactic for arterial smooth muscle cells in culture. FEBB Lett 1990; 277:247–249.
10. Kohno M, Yokokawa K, Yasunari K, Kano H, Minami M, Ueda M, Yoshikawa J. Effect of natriuretic family on the oxidized LDL-induced migration of human coronary artery smooth muscle cells. Circ Res 1997; 81:585–590.
11. Dubey RK, Jackson EK, Lucher TF. Nitric oxide inhibits angiotensin-II induced migration of rat aortic smooth muscle cells: role of cyclic nucleotides and angeotensin I receptors. J Clin Invest 1995; 96:141–149.
12. Kohno M, Yokokawa K, Kano H, Yasunari K, Minami M, Hanehara T, Yoshikawa J. Adrenomedullin, is a potent inhibitor of angiotensin-II induced migration of human coronary artery smooth muscle cells. Hypertension 1997; 29:1309–1313.
13. Lee S-L, Wong W-W, Joseph PM, Hales CA, Fanburg BL. Inhibitory effect of heparin on serotonin-induced hyperplasia and hypertrophy of smooth muscle cells. Am J Respir Cell Mol Biol 1997; 17:78–83.
14. Thomson BT, Spence CR, Janssens SP, Joseph PM, Hales CA. Inhibition of hypoxic pulmonary hypertension by heparins of differing in vitro antiproliferative potency. Am J Respir Crit Care Med 1994; 149:1512–1517.

15. Hassoun PM, Thomson BT, Steigman D, Hales CA. Effect of heparin and warfarin on chronic hypoxic pulmonary hypertension and vascular remodeling in the guinea pig. Am Rev Respir Dis 1994; 139:763–7681.
16. Garg HG, Linhardt RJ, Hales HA. Heparin as a potential therapeutic agent to reverse vascular remodeling. In: Garg HG, Roughley PJ, Hales CA, eds. Proteoglycans in Lung Disease. New York: Marcel-Dekker, 2002; 377–398.
17. Garg HG, Joseph PAM, Yoshida K, Thompson BT, Hales CA. Antiproliferative role of 3-*O*-sulfate glucosamine in heparin on cultured plumanary artery smooth muscle cells. Biochem Biophys Res Commun 1996; 224:468–473.
18. Capila I, Linhardt RJ. Heparin-protein interactions. Angew Chem Int Ed 2002; 41:390–412.
19. Reid L. The pulmonary circulation: remodeling in growth and disease. J Burns Amberson Lecture. Am J Respir Dis 1979; 119:431–436.
20. Rabinovitch M. Pulmonary vascular remodeling in hypoxic pulmonary hypertension. In: Yuan J, ed. Hypoxic Pulmonary Vasoconstriction. Cellular and Molecular Molecular Mechanisms. Boston: Kulwar Academic Publisher, 2004; 403–418.
21. Benitz WE, Lessler Ds, Coulson JD, Bernfield M. Heparin inhibits proliferation of fetal vascular smooth muscle cells in the absence of platelet-derived growth factor. J Cell Physiol 1986; 127:1–7.
22. Castellot Jr JJ, Favreau LV, Karnovsky MJ, Rosenberg RD. Inhibition of vascular smooth muscle cell growth by endothelial cell-derived heparin. Possible role of a platelet endoglycosidase. J Biol Chem 1982; 257:11256–11260.
23. Castellot Jr JJ, Cochran DL, Karnovsky MJ. Effect of heparin on vascular smooth muscle cells. I. Cell metabolism. J Cell Physiol 1985; 124:21–28.
24. Castellot Jr JJ, Wong K, Herman B, Hoover RL, Albertini DF, Wright TC, Caleb BL, Karnovsky MJ. Binding and internalization of heparin by vascular smooth muscle cells. J Cell Physiol 1985; 124:13–20.
25. Castellot Jr JJ, Choay J, Lormeau JC, Pettitou M, Sache E, Karnovsky MJ. Structural determinants of the capacity of heparin to inhibit the proliferation of vascular smooth muscle cells. II. Evidence for a pentasaccharide sequence that contain a 3-*O*-sulfate group. J Cell Biol 1986; 102:1979–1984.
26. Reilly CF, Fritze MS, Rosenberg RD. Heparin inhibition of smooth muscle cell proliferation: a cellular site of action. J Cell Physiol 1986; 129:11–19.
27. Reilly CF, Kindy MS, Brown KE, Rosenberg RD. Heparin prevents vascular smooth muscle cell progression through the G1 phase of the cell cycle. J Biol Chem 1989; 264:6990–6995.
28. Jackson RL, Busch SJ, Cardin AD. Glycosaminoglycans: Molecular properties, protein interactions and role in physiological processes. Physiol Rev 1991; 71:481–539.
29. Schwartz SM, Gajdusek CM, Owens GK. Vessel growth and control. In: Nossel HL, Vogel HT, eds. Pathology of the Endothelial Cell. New York: Academic Press, 1982; 63–78.
30. Jaques LB. Heparins—anionic polyelectrolyte drugs. Pharmacol Rev 1980; 31:99–106.
31. Majesky MW, Schwartz SM, Clowes MM, Clowes AW. Heparin regulates smooth muscle S phase entry in the injured rat carotid. Circ Res 1987; 61:296–300.

32. Castellot Jr JJ, Pujac LA, Caleb BL, Wright TC, Karnovsky MJ. Heparin selectively inhibits a protein kinase C-dependent mechanism of cell cycle progression in calf aortic smooth muscle cells. J Cell Biol 1989; 116:31–42.
33. Wright Jr TC, Pukac LA, Castellot Jr JJ, Karnovsky MJ, Levine RA, Kim-Park HY, Campisi J. Heparin suppresses the inhibition of c-fos and c-myc RNA in murine fibroblasts by selective induction of protein kinase C-dependent pathway. Proc Natl Acad Sci USA 1989; 86:3199–3209.
34. Au YPT, Dobrowolska G, Morris DR, Clowes AW. Heparin decreases activator protein-1 binding to DNA in part by posttranslational modification of junB. Circ Res 1994; 75:15–22.
35. Busch SJ, Martin GA, Barnhart RL, Mano M, Cardin AD, Jackson RL. Trans-repressor activity of nuclear glycosaminoglycans of fos and jun/AP-1 on coprotein-mediated transcription. J Cell Biol 1992; 116:31–42.
36. Pukac LA, Castellot Jr JJ, Wright TC, Caleb BL, Karnovsky MJ. Heparin inhibits c-fos c-myc mRNA expression in vascular smooth muscle cells. Cell Regul 1990; 1:435–443.
37. Daum G, Hedin U, Wang Y, Wang T, Clowes AW. Diverse effects of heparin on mitogen-activated protein kinase-dependent signal transduction in vascular smooth muscle cells. Circ Res 1997; 81:17–23.
38. Mishra-Goruk K, Castellot Jr JJ. Heparin rapidly and selectively regulates protein tyrosine phosphorylation in vascular smooth muscle cells. J Cell Physiol 1999; 178:205–215.
39. Quinn DA, Dahlberg CGW, Boventre JP, Sceid CR, Honeyman T, Joseph PM, Thompson BT, Hales CA. The role of Na^+/H^+ exchange and growth factors in pulmonary artery smooth muscle cell proliferation. Am J Respir Cell Mol Biol 1996; 14:139–145.
40. Dahlberg CGW, Thompson BT, Joseph PM, Garg HG, Spence CR, Quinn DA, Boventre JV, Hales CA. Differential effect of three commercial heparins on Na^+/H^+ exchange and growth of PASMC. Am J Physiol Lung Cell Mol Physiol 1996; 270:L260–L265.
41. Garg HG, Joseph PAM, Yoshida K, Thompson BT, Hales CA. Antiproliferative role of 3-*O*-sulfate glucosamine in heparin on cultured pulmonary artery smooth muscle cells. Biochem Biophys Res Commun 1996; 224:468–473.
42. Wright Jr TC, Castellot Jr JJ, Petitou M, Lormeau J -C, Choay J, Karnovsky MJ. Structural determinants of heparin's growth inhibitory activity. Interdependence of oligosaccharide size and charge. J Biol Chem 1989; 264:1534–1542.
43. Castellot Jr JJ, Beeler DL, Rosenberg RD, Karnovsky MJ. Structural determinants of the capacity of heparin to inhibit the proliferation of vascular smooth muscle cells. J Cell Physiol 1984; 120:315–320.
44. Garg HG, Cindhuchao N, Quinn DA, Hales CA, Thanawiroon C, Capila I, Linhardt RJ. Heparin oligosaccharide sequence and size essential for inhibition of pulmonary artery smooth muscle cell proliferation. Carbohydr Res 2002; 337:2359–2364.
45. Kazatchkine M, Fearon DT, Metcalfe DD, Rosenberg RD, Austen KF. Structural determinants of the capacity of heparin to inhibit the formation of the human amplification C3 convertase. J Clin Invest 1981; 67:223–228.
46. Tiozzo R, Cingi MR, Reggiani D, Andreoli T, Calandra S, Milani MR, Piani S, Marchi E, Barbanti M. Effect of the desulfation of heparin on its anticoagulant and anti-proliferative activity. Thromb Res 1993; 70:99–106.

47. Kariya Y, Yoshida K, Morikawa K, Tawada A, Miyazono H, Kikuchi H, Tokuyasu K. Preparation of unsaturated disaccharides by eliminative cleavage of heparin and heparan sulfate with heparitinases. Comp Biochem Physiol 1992; 103B:473–479.
48. Joseph PAM, Garg HG, Thompson BT, Liu X, Hales CA. Influence of molecular weight, protein core and charge of native heparin fractions on pulmonary artery smooth muscle cell proliferation. Biochem Biophys Res Commun 1997; 241:18–23.
49. Carlson DM. Structures and immunochemical properties of oligosaccharides isolated from pig submaxillary mucins. J Biol Chem 1968; 243;616–626.
50. Maruyama T, Toida T, Imanari T, Yu G, Linhardt RJ. Conformational changes and anticoagulant activity of chondroitin sulfate following its *O*-sulfonation. Carbohydr Res 1998; 306:35–43.
51. Garg HG, Joseph PAM, Thompson BT, Hales CA, Toida T, Imanhari T, Capila I, Linhardt RJ. Effect of fully sulfated glycosaminoglycans on pulmonary artery smooth mucle cell proliferation. Arch Biochem Biophys 1999; 371:228–233.
52. Garg HG, Yu L, Hales CA, Toida T, Islam T, Linhardt RJ. Sulfation patterns in heparin and heparan sulfate: effects on the proliferation of bovine plumanary artery smooth muscle cells. Biochim Biophys Acta 2003; 1639:225–231.
53. Longas MO, Garg HG, Trinkle-Pereira M, Hales CA. Heparin antiproliferative activity on bovine pulmonary artery smooth muscle cells requires both *N*-acetylation and *N*-sulfonation. Carbohydr Res 2003; 338:251–256.
54. Underwood PA, Mitchell SM, Whitelock JM. Heparin fails to inhibit the proliferation of human vascular smooth muscle cells in the presence of human serum. J Vas Res 1998; 35:449–460.
55. Cindhuchao N, Quinn DA, Garg HG, Hales CA. Heparin inhibits SMC growth in the presence of human and fetal bovine serum. Biochem Biophys Res Commun 2003; 302:84–88.

Chemistry and Biology of Heparin and Heparan Sulfate
H.G. Garg, R.J. Linhardt and C.A. Hales (Editors)

Chapter 19

Mechanisms of Cell Growth Regulation by Heparin and Heparan Sulfate

MATTHEW A. NUGENT

Boston University School of Medicine, Boston, MA, USA

KIMBERLY FORSTEN-WILLIAMS

Virginia Polytechnic Institute and State University, Blacksburg, VA, USA

MORRIS J. KARNOVSKY

Harvard Medical School, Boston, MA, USA
and

ELAZER R. EDELMAN

Massachusetts Institute of Technology, Cambridge, MA, USA and Harvard Medical School, Boston, MA, USA

I. Introduction

Heparin has been widely used as an effective anticoagulant drug for 70 years; however, it was not until the 1970s that its mechanism of action began to be revealed (1). Today it is clear that the anticoagulant activity of heparin is mediated, in large part, by binding to antithrombin III causing a conformational change leading to a greatly accelerated reaction with and inactivation of thrombin (2–4). This ability of heparin to facilitate protein–protein interactions likely underlies many of its biological activities. Indeed, since the original observation that heparin is a potent inhibitor of vascular smooth muscle cell growth (5), it has become clear that heparin and heparan sulfate interact with, and profoundly affect, a wide range of growth factors and cytokines (3,6,7). Thus, it has become increasingly appreciated that heparin and heparan sulfate play key roles in promoting and inhibiting cell proliferation during normal tissue growth and development as well as in disease states. These findings, and the growing understanding of the mechanisms underlying the cell growth regulatory activity of heparin and heparan sulfate, have generated considerable enthusiasm regarding the potential clinical applications of

these polysaccharides for the treatment of disorders associated with insufficient and excessive cell proliferation. However, this enthusiasm has met with the sobering reality that the mechanisms underlying the growth regulatory activities of heparin and heparan sulfate are dauntingly complex, wide ranging and remain incompletely understood. In this chapter we will provide an overview of the direct and indirect mechanisms that heparin and heparan sulfate use to modulate cell growth in a variety of normal and pathological states.

II. Modulation of Growth Factor Action

A. Heparin and Heparan Sulfate Structure

Heparin and heparan sulfate (HS) are members of a large class of linear polysaccharides characterized by repeating disaccharide units of alternating N-substituted glucosamine and hexuronic (glucuronic or iduronic) acid residues (Fig. 1) (1). HS chains are subject to extensive modification during biosynthesis, including sulfation of the *N*-position as well as at the C-6 and C-3 *O*-positions of the glucosamine and at the C-2 *O*-position of the uronic acid (8,9). Thus, there are theoretically as many as 48 potential disaccharide units that together make this class of compounds one of the most information dense in biology. The high degree of structural complexity likely underlies the ability of heparin and HS to play critical roles in a large and diverse number of biological processes (7–12).

Heparin is a highly sulfated form of HS that is made predominantly by connective tissue mast cells as a large heparin proteoglycan (750–1000 kDa) consisting of a small core protein, serglycin, with multiple heparin polysaccharide chains (1,13). After synthesis, the heparin chains are randomly cleaved into smaller polysaccharides (5–25 kDa) that are stored in secretory granules bound to proteases. Approximately 90% of the uronic acid within heparin is iduronic acid, and an average heparin disaccharide contains 2.7 sulfate groups (14). HS from other cell and tissue sources contains less than one sulfate per disaccharide and the majority of the uronic residues are glucuronic acid (15,16). In addition, HS has domain structures made up of extended sequences of high or low levels of sulfation making its overall structure and sequence considerably more complex than that of heparin (17). In contrast to the intragranule localization of heparin, HS chains are physically positioned on the cell surface, within the extracellular matrix, or in soluble form, through covalent linkage to core proteins as heparan sulfate proteoglycans (HSPG) (Fig. 1). Approximately 20 HSPG core proteins have been identified. They include the syndecans 1–4 and the glypicans 1–6, which are widely expressed in nearly all mammalian cell types and tissues where they are linked to plasma membrane surfaces either through a transmembrane core protein (syndecans) or by a glycosylphosphatidylinositol tail (glypicans) (18,19). In addition, the ectodomain of the syndecans, which contains the attached HS chains, can be shed from the cell surface through the action of extracellular proteases to produce "soluble" HSPG fragments (20–23). In contrast to the cell surface HSPG, several HSPG, such as perlecan, are localized to basement membranes and other extracellular matrices where their HS

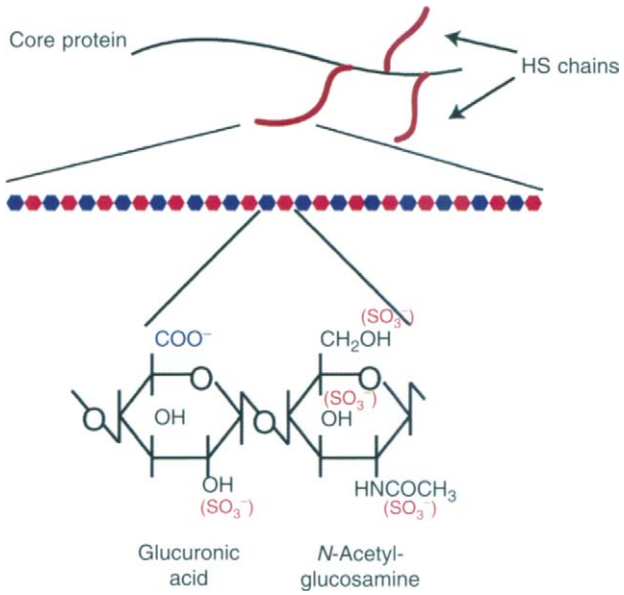

Figure 1 Structure of heparin and heparan sulfate proteoglycans. Heparin and HS are comprised of linear chains of repeating disaccharide units, which can be modified by sulfations, as indicated in the expanded chemical structure, at four positions. In addition to sulfation, the nitrogen on the glucosamine residues can be acetylated or unmodified. The majority of the disaccharide residues in heparin contain iduronic acid in place of the glucuronic acid shown. HSPG are composed of generally 1–6 HS chains linked to a protein core. The protein core can carry additional GAG chains (i.e., chondroitin sulfate) as well as additional branched oligosaccharides.

chains modulate matrix structure and molecular transport (24). In addition to the traditional role of HSPG within the extracellular space, evidence has also suggested roles for these molecules within cells (25–30). Indeed, the principal role of the highly sulfated HS produced by mast cells (heparin) is to store mast cell proteases in an inactive form within secretory granules (31,32). Consequently, the physical location and specific HS structure allow HSPG to alternatively inhibit or promote cell proliferation through direct and indirect mechanisms (33–35).

B. Control of Growth Factor Receptor Binding

Growth factors are a class of relatively small soluble proteins that act, principally, through the binding and activation of specific cell surface receptor proteins to induce a wide range of cellular responses such as: proliferation, migration, differentiation, and survival. Binding of many growth factors to their receptors induces dimerization and tyrosine phosphorylation of the receptors through the activation of intrinsic tyrosine kinase activity (36,37). The autophosphorylation of tyrosine residues participates in signal transduction by often leading to increased kinase

activity of the receptors toward other protein substrates as well as by creating docking sites for other enzymes and adaptor proteins. Ultimately, the cellular response is mediated by the combination of the various second messengers, and as such, is related to the extent and duration of receptor activation. During the development of methods for the isolation and purification of growth factors it was noted that many bound tightly to heparin-agarose affinity columns (38). Consequently heparin-affinity has been used to identify several potent growth factors; most prominently the fibroblast growth factor (FGF) family, which now includes 23 separate members (39). Since the original observation that members of the FGF family bind heparin, many growth factors have been demonstrated to bind to heparin (Table 1); and it is now accepted that this interaction is indicative of important regulatory activities of HS chains on HSPG. The importance of these interactions for the prototypic heparin-binding growth factor, FGF-2, was originally revealed in cells that were rendered HS deficient either through genetic mutation, or treatment with heparinase or the sulfation inhibitor chlorate (40,41). In these instances it was observed that FGF-2 binding to its receptor was significantly reduced in the absence of HS. The data indicate that HS participates in forming a ternary complex such that binding of FGF-2 is stabilized through the simultaneous binding to both its receptor and HS (Fig. 2) (42,43). Hence, kinetic analysis of these binding events suggested that the principal impact of HS is to reduce the rate of FGF-2 dissociation from its receptor without significantly altering the association rate (42,44,45). While the majority of the studies on the coreceptor activity of HS have focused on FGF-2, high affinity binding of a number of growth factors for their receptors has similarly been shown to depend on HS. For example, receptor binding of vascular endothelial growth factor (VEGF) is reduced in endothelial cells treated with heparinase or chlorate (46–50), and the binding and activity of heparin-binding epidermal growth factor-like growth factor to EGF receptors on vascular smooth muscle cells is reduced by chlorate treatment (51). Thus, HS likely plays a general role in enhancing the sensitivity of receptors for heparin-binding growth factors through their ability to increase the observed affinity for binding.

The chemical and physical mechanisms underlying the ability of HS to function as a coreceptor for FGF-2 have received considerable attention over the past 10–15 years. The use of oligosaccharides and chemically modified forms of heparin and HS have demonstrated that a pentasaccharide with *N*-sulfated glucosamine residues and at least one iduronic acid containing a sulfate in the 2-*O*-position is the minimal heparin unit that can bind FGF-2 (52,53). However, longer oligosaccharides (dodecasaccharide) containing 6-*O*-sulfate groups in addition to 2-*O*- and *N*-sulfation are required to facilitate FGF-2 binding to its receptor (52,54). The additional requirements for ternary complex formation likely reflect the 6-*O*-sulfated glucosamine dependent binding of HS to FGF receptors (43,52,55,56). Thus, the HS-FGF-2-receptor complex likely consists of two FGF-2 molecules bound to two FGF receptors with a sufficiently long HS chain that makes contacts with all the protein components to effectively stabilize the complex. However, the exact stoichiometry and physical orientation of the various components remain an area of open investigation in spite of the availability of several FGF-receptor crystal

Table 1 A Partial List of Heparin-Binding Proteins that Relate to Cell Growth Control

Growth factors/ morphogens	ECM Components	Inflammation/ antiangiogenesis
FGFs (1–23)	Fibronectin	IL2,3,4,5,7,8,12
TGF β 1 and 2	Interstitial collagens	GM-CSF
VEGF145, 165, 183, 189, 206	Laminins	Interferon γ
PDGF-AA	Fibrin	TNF α
EGF family ligands	Tenascin	L-selectin
• Amphiregulin	Thrombospondin	P-selectin
• Heparin binding EGF	Vitronectin	Endostatin
• Betacellulin	Pleiotropin	Angiostatin
• Neuregulin		N-CAM
IGF-II	Proteases/coagulation	MAC-1
Activin	Neutrophil elastase	PECAM-1
Sonic Hedgehog	Cathepsin	Serum amyloid A
Sprouty peptides	Factor Xa	Bac-5 and 7
Wnts (1–13)	Antithrombin III	PR-39
IGF binding proteins 3 and 5	Thrombin	Platelet factor 4
TGF β binding protein	Tissue plasminogen activator	Neutrophil activating factor
BMP 2 and 4	Plasminogen activator inhibitor	RANTES
HGF	Protease nexin I	MCP-1

A selection of heparin-binding proteins was compiled from a number of sources (3,6,10,67,238), and grouped into four categories. Growth factors and morphogens represent proteins that are considered direct growth regulatory factors. ECM components are proteins that have been identified to have a role within the extracellular matrix. Inflammation and anti-angiogenesis refer to a number of proteins that are involved in inflammatory cell activation, recruitment, adhesion and inhibition of angiogenesis. The abbreviations are: EGF, epidermal growth factor; FGF, fibroblast growth factor; IL, interleukin; IGF, insulin-like growth factor; BMP, bone morphogenic protein; PDGF-AA, platelet-derived growth factor AA; TGF, transforming growth factor; TNF, tumor necrosis factor; GM-CSF, granulocyte-macrophage colony stimulating factor; N-CAM, neural cell adhesion molecule; PECAM-1, platelet/endothelial cell adhesion molecule-1; MCP-1, monocyte *chemottractant* protein-1; PR-39, proline-rich peptide 39.

structures (57–62). Differences in the various cocrystal structures potentially reflect intrinsic differences between the components used in the various studies (i.e., FGF-1 *vs* FGF-2, receptor ectodomain, oligosaccharide). In particular, the structural details of the HS within these complexes are poorly resolved and the exact positioning of HS is often modeled theoretically or inferred from the use of analogs. In any case, the distinct HS structural requirements for binding to FGF-2 *vs* those for enhanced receptor binding provide an explanation for why some HS species facilitate FGF-2 activity while others inhibit. Indeed, short oligosaccharides and 6-*O*-desulfated heparin have been shown to be potent inhibitors of FGF-2 through the ability to sequester FGF-2 from its receptor (52,63). Even heparin and HS containing sequences capable of binding both FGF-2 and its receptor can inhibit

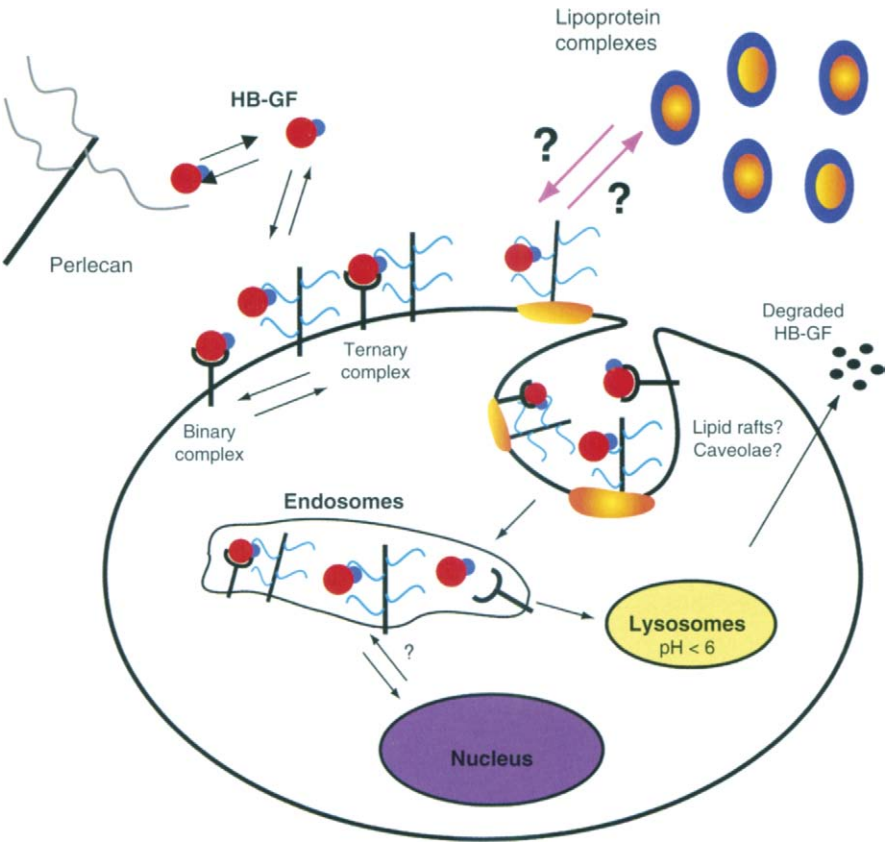

Figure 2 Complex regulation of heparin-binding growth factors by HSPG. HSPG can alter heparin-binding growth factor (HB-GF) interactions with cells at multiple levels. HSPG within the extracellular matrix (shown as perlecan) can sequester or store growth factor, while HSPG on the cell surface can facilitate the formation of signaling complexes alone and in conjunction with receptor tyrosine kinases. The particular signaling pathways activated might relate to membrane localization within cholesterol-rich lipid rafts, which would relate to cholesterol homeostasis (i.e., lipoprotein delivery). HSPG also modulate internalization, degradation, and intracellular trafficking of HB-GF.

receptor binding and activation. This is generally under conditions where these molecules are not able to associate with the cell surface to be put in proximity to receptors (35,64–66). Thus, HS structure and physical localization, as well as the state of the cell surface of the target cell, are all likely to contribute to the ability of particular HS species to modulate growth factor receptor binding.

C. Regulation of Growth Factor Receptor Signaling

The ability of HS to modulate FGF-2 binding to its receptor has also been demonstrated to alter receptor signaling; however, these two activities of HS have not always correlated completely (35,45,54,67–71). While some studies note a nearly

direct correlation between HS-regulated receptor binding and biological activity (72–74), it is often difficult to link the direct consequences of receptor binding, which might occur in minutes, to an endpoint biological response such as cell growth which requires hours to days to be revealed. Thus, more detailed evaluation of receptor signaling kinetics have begun to reveal a complex process whereby HS not only alters the ability of FGF-2 to elicit a signal from its receptor, but also alters the nature (magnitude and duration) of the signal (69–71,75). This area is further complicated by the fact that HS and HSPG can directly modulate cell growth through mechanisms that are independent of growth factor receptors (see Section III). Therefore, the consequences of HS on growth factor receptor binding and signaling are clearly profound, yet currently defy simple categorization. A more detailed and quantitative understanding of these processes is required before growth factor receptor binding and signaling can be predictably modulated in a controlled manner within tissue environments.

The ability of HS to function as a coreceptor for FGF through the stabilization of FGF-receptor complexes is the best characterized activity of HS in growth factor biology. Consequently, it is tempting to speculate that this type of mechanism is mirrored throughout the large family of heparin-binding growth factors. However, it is important to cautiously consider the individual details of each growth factor-receptor system, as it has become clear that significant distinctions exist between various growth factor systems. For example, Cohen et al. noted that removal of HS from endothelial cells with heparinase results in a significant reduction in the binding of VEGF121, even though this isoform of VEGF does not contain the consensus heparin-binding domain contained within the other VEGF isoforms (47). Thus, it is suggested that HS can alter growth factor receptor binding even under conditions where the HS and growth factor do not directly interact, possibly through mechanisms involving cell surface interactions between HSPG and growth factor receptors. Consistent with a possible requirement for cell surface HSPG in the VEGF system, the addition of heparin does not rescue the lost VEGF121 binding in heparinase treated cells (47). These results and others might reflect a mechanism whereby HSPG acts to position growth factor receptors on the plasma membrane with respect to signaling molecules within the pericytoplasmic region. Consistent with this potential function, certain HSPG, such as syndecan 4 and glypicans, have recently been demonstrated to preferentially distribute to cholesterol-rich and sphingolipid-rich lipid rafts, which can act as depots for signaling molecules (76–80). Thus, in addition to the direct cofactor function whereby HS chains act as a bridging device to facilitate growth factor–receptor binding and activation; HSPG might also effectively enhance interactions between the cytoplasmic domain of these receptors with signaling molecules by recruiting receptors to subdomains (i.e., rafts) on the plasma membrane. In a sense, HS chains might be able to transfer their ability to influence protein–protein interactions across the plasma membrane. This transmembrane communication also suggests important roles for HSPG core proteins in growth factor signaling (77,81–85). However, it remains to be determined how significant these types of processes are in modulating growth factor signaling and activity.

D. Intracellular Regulation of Growth Factor Function

Most studies on HS regulation of growth factor–receptor interactions have focused on events occurring on the cell surface. However, there is considerable evidence that growth factors and their receptors have intracellular functions after endocytosis. Thus, it is likely that HS influences intracellular growth factor-driven events in addition to cell surface processes. Indeed, there has long been an association between cell growth and HS within the nuclei of some cells (27,28,86). These observations, coupled with the growing evidence that several growth factors are targeted to the nucleus after internalization (87,88), suggest that nuclear translocation of some growth factors might be mediated by HS.

This appears to be the case for FGF-2, which is translocated to the nucleus more efficiently in cells under conditions (i.e., on a fibronectin matrix) where nuclear HS is more prevalent (25,26). Moreover, FGF-2 nuclear translocation is reduced when cell surface HS is removed by heparinase treatment, or when HS synthesis is inhibited by treatment with chlorate (26,45). While the consequences of nuclear translocation of growth factors and HS are not completely clear, there are a number of studies indicating that these factors might directly interact with nuclear machinery involved in regulating cell growth (29,89–95). For example, FGF-2 interacts with and activates CK2, a ubiquitous serine/threonine kinase that functions within the nucleus to control cell growth (93). The ability of FGF-2 to bind and activate CK2 appears to be critical to its proliferative activity as a point mutation in FGF-2 (ser 117) does not alter FGF-2 binding to or activation of its receptors, yet result in the loss of CK2 binding and elimination of mitogenic activity (93). HS, in addition to modulating growth factor nuclear translocation, may also have direct activities associated with cell growth control within the nucleus. HS has been shown to inhibit DNA topoisomerase I, and to bind to nucleosomes and participate in chromatin clearance (29,89,90), suggesting a general means for regulating nuclear activity. Heparin added to cells has also been demonstrated to be translocated to the nucleus where it competes with DNA for binding to transcription factors and causes apoptosis (96). The process by which HS and growth factors are translocated from the cell surface to the nucleus is not well characterized. However, it is interesting to note that HS-growth factor complexes are likely to resist the normal process of endosomal acidification that is often associated with ligand-receptor dissociation after endocytosis, indicating a mechanism whereby HS protects growth factors from the classic degradative fate associated with ligand internalization (45,50,97,98). In addition, it has also been demonstrated that HSPG can direct bound FGF-2 to a nonclathrin mediated-lipid raft dependent pathway of cellular uptake that might circumvent the normal lysosomal fate (76,77,99–101). A more complete understanding of how HS and HSPG core proteins dictate intracellular processing of growth factors in conjunction with identification of their function is required to fully appreciate the scope of HS control of growth factor action (Fig. 2).

E. Storage and Release of Growth Factors in the Extracellular Matrix

The original observation that many growth factors bind to heparin suggested that HS within the extracellular matrix might function as a storage depot for these potent growth regulatory proteins. Subsequently, several studies have confirmed that members of the FGF family are deposited within basement membrane bound to HS (102–106). The interaction of FGFs and VEGF with HS has also been demonstrated to protect these proteins against proteases and physical denaturation (107–111). Moreover, extracellular matrix, containing stored growth factors, can function as a prolonged platform for the release of stored active growth factor, suggesting that HSPG within the extracellular matrices *in vivo* plays important roles as reservoirs of active growth factor (112–115). A mechanism involving storage of presynthesized mitogenic proteins within the ECM would provide a highly tuned system for rapid local growth regulation, which would avoid the delay associated with *de novo* synthesis. Toward this end, several studies have demonstrated that degradation of HSPG, or ECM in general, by heparanase or inflammatory proteases can result in the release of active growth factor that might participate in the tissue response to injury (23,116–119). The clinical application of this regulated storage and release system has already begun to be realized with the development of synthetic heparin-based controlled drug delivery systems, which are currently being evaluated in clinical trials (120–123). The storage and release of growth factors from ECM is likely controlled at many levels. Obviously, alterations in the local synthesis and deposition of HS and growth factors would alter the dynamics of this process, particularly when one considers the rapid binding kinetics of most growth factor–HS interactions. The high rates of association and dissociation indicate that the "stored" growth factors are not simply bound in a static and locked state, but are in constant dynamic equilibrium with matrix resident HS (42,44,124,125). Consequently, changes in the structure and density of growth factor binding sites within HS, as a result of altered biosynthesis, or through the action of extracellular enzymes such as the 6-*O*-sulfatases, could modulate the binding kinetics of growth factors to the resident HS chains and alter growth factor availability to nearby cells (126–130). In addition, the interactions of growth factors with HS within the ECM might also be modulated by changes in the extracellular environment. As a specific example of this type of process, we have found that VEGF binding to HS is dramatically stabilized at low pH, suggesting that VEGF deposition in ECM would be controlled by factors such as hypoxia, which lead to decreased local pH (50,131). Together this myriad of actions has been demonstrated to provide a means for HSPG within the ECM to modulate the molecular transport of growth factors, and in turn, the formation of growth factor and morphogen gradients that are required for coordinated tissue development (12,129,130,132,133). In addition, HS can interact with many of the structural protein (i.e., fibronectin, collagens, and laminin) components of the ECM through specific HS domains and these interactions can alter the structure of the matrix proteins (6,134).

In addition to the generalized ability of HS within the ECM to control cell proliferation and tissue development by regulating the availability of growth factors, there is considerable evidence that the specific HSPG, perlecan, influences growth factor activity during tissue repair and disease (11,24,64,66,135–139). Perlecan is a large (~1000 kDa) HSPG that is found predominantly within the vascular ECM. Consequently, there is considerable evidence that perlecan regulates vascular cell growth. Expression of perlecan in vascular smooth muscle cells (SMC) correlates inversely with cell proliferation suggesting that it participates in cell cycle exit and quiescence in these cells (140–142). This observation is consistent with the long-standing observation that HS acts as a potent inhibitor of SMC proliferation independent of anticoagulant activity (5,143–148). One possible mechanism for the inhibition of SMC is through the ability of perlecan to bind and sequester FGF-2 (66,73,138). However, it has also been demonstrated, in other cell systems, that perlecan can actually potentiate the action of FGFs, and is required for tumors angiogenesis (135,136). It is possible that the ability of perlecan to alternatively inhibit or potentiate FGF action is related to the fine structure of the HS chains, as endothelial perlecan with longer HS chains is a more potent inhibitor of FGF activity in SMC (66). These apparently conflicting activities of perlecan might also relate to the pericellular localization of perlecan. For example, cells that are able to effectively bind perlecan and place their HS chains in proximity to cell surface growth factor receptors might show enhanced growth factor responsiveness, while situations where perlecan remains excluded from the proximal cell surface might relate to growth factor inhibition (35,64,65). The concept that perlecan is critical to growth control *in vivo* has been supported by several studies. In particular, the growth suppressive role of perlecan within the arterial wall is supported by perlecan gene knockout (149) and knockdown (138) studies, as well as in situations where perlecan containing preparations were delivered to injured blood vessels (150,151), and by correlative analysis of perlecan expression in injured arteries (142). While many of the growth regulating activities of perlecan relate to its HS chains, it is important to note that the very large perlecan core protein has significant proliferative and antiproliferative activities independent of HS as well (152–156). Therefore, it is clear that HSPG, and perlecan in particular, have important functions within the ECM that involve the modulation of cell growth.

F. Quantitative Models of Growth Factor Control

Clearly the regulation of heparin-binding growth factors by HS or HSPG is complex, and interpreting the apparent contradictory experimental evidence regarding activity is difficult. Mathematical or computational modeling is one tool being exploited to assist in this process (Fig. 3). Modeling combined with quantitative experimentation allows one to explore possible mechanisms of action and to determine if the proposed system is consistent with experimental evidence. These models can rapidly evaluate a range of conditions that could never be reproduced in

culture or *in vivo*, and when coupled with experimentally derived physicochemical parameters are a remarkably powerful analytical resource. Complex models of binding, processing and signal transduction have been described for both the epidermal growth factor (EGF) and platelet-derived growth factor (PDGF) systems and have proven to have valuable predictive power (157–160). However, additional complexities exist for heparin-binding growth factors due to the association of these growth factors with HS and HSPG.

Being the most studied of the heparin-binding growth factors, it is perhaps not surprising that computational modeling efforts in this area have primarily focused on FGF-2. Computational models have been used primarily in two ways: (1) to assist in determining quantitative parameter values critical for elucidating HS/HSPG mechanisms of action and (2) to test hypotheses based on experimental observation. For example, our early work indicating that HSPG association with FGF-2 and FGF receptors stabilizes the complex and reduces dissociation was aided by the use of a simple model for surface binding enabling us to quantify critical interactions (42). Sperinde and Nugent (2000) added internalization and degradation to the simple model in order to interpret and compare receptor-mediated and HSPG-mediated degradation data (45,98). More recently, Ibrahimi et al. (2004), applied a simple surface binding model to surface plasmon resonance data and concluded that FGF-2–heparin interactions occur preferentially to FGF-2–FGFR interactions prior to FGF-2–FGFR–heparin triad formation suggesting FGF-2 binding to HSPG is a more likely initial step in cellular association (44).

Studies using computational modeling to test hypotheses suggest future experiments have also been performed. FGF-2 binding regulation by heparin and heparin-like molecules in solution were investigated using a system of ordinary differential equations describing the relevant binding events (64,65). Despite being a relatively simple model that included triad formation between FGF-2, FGF receptors, and HSPG or heparin but not higher order complexes, we were, for example, able to demonstrate the importance of cell surface localization to explain both the enhancement and inhibition of FGF-2 binding by heparin. We extended these early models to investigate FGF receptor signaling dynamics in response to FGF-2 providing support for MAP kinase phosphorylation studies indicating HSPG signaling by FGF-2 in the absence of receptor input (71,161). Filion and Popel developed a compartmental model of the myocardium, which they used to investigate how HS and HSPG might impact FGF-2 retention following intracoronary administration of the growth factor and to provide testable predictions (162). It should be noted that two recent papers by Mac Gabhann and Popel have presented simple models of VEGF interactions with cell surface receptors as a means to interpret experimental observations but have incorporated the role of HSPG in the system via kinetic rate constants rather than as explicit regulatory elements (163,164). As more quantitative data becomes available, mathematical models of the role of HS/HSPG in modulating growth factor action will likely prove to be necessary in order to effectively evaluate the underlying complex mechanisms of these processes.

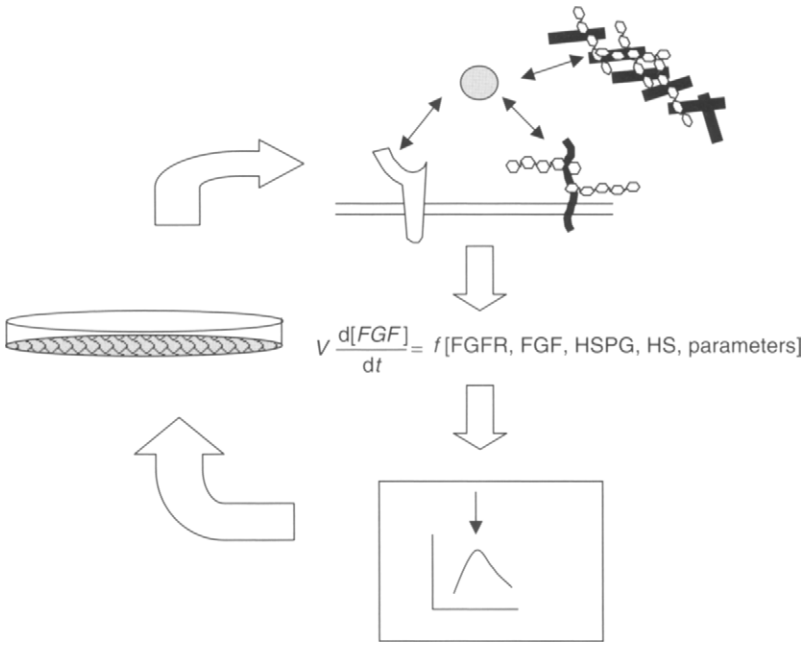

Figure 3 Role of computational modeling in experimental biology. A cyclic relationship exists between experimental cell studies and computational modeling. The experimental results lead to the formulation of a conceptual model, which can then be translated into mathematical terms relating the change in variables (such as the concentration of FGF) to the other variables and parameters describing the system. The model can then be solved and computational results produced and experimentally testable predictions generated. These predictions can then prompt new experimental studies, the results of which are then fed back to modify and expand the mathematic model.

III. Direct Regulation of Cell Growth

A. Heparin Receptors and Signaling

In addition to the ability of heparin and HS to regulate cell growth through the modulation of growth factor action, there is considerable evidence of direct effects on cells as well. Since the original observation that heparin inhibits SMC growth in culture and within the blood vessel wall, studies have indicated that heparin regulates cells through direct interaction with cell associated "heparin receptors" on a variety of cells (145,165,166). Specific binding, internalization and metabolism of heparin have been demonstrated in SMC (145,167–170). While these binding events have been demonstrated to be specific, the ability of heparin to interact with so many proteins on the cell surface has restricted the formal isolation, identification or verification of heparin receptors. However, it has been demonstrated that heparin can stimulate an intracellular signal transduction response that relates to that observed for growth factors, cytokines, and hormones. In particular, heparin

has been shown to suppress the expression of the serum and glucocorticoid-regulated kinase, which is an early response gene that is associated with cell proliferation (171). Heparin has also been demonstrated to selectively regulate tyrosine kinase activity, inhibit the activation of mitogen-activated protein kinases and to inhibit the activity of Ca^{2+}/calmodulin regulated protein kinase II in SMC (172–174). Consistent with its growth inhibitory activity in SMC, heparin has also been found to inhibit c-fos and c-myc mRNA expression in these cells (175). Thus, heparin, and by analogy, HS as well as soluble HSPG ectodomains likely regulate cell growth through a combination of processes whereby direct and indirect mechanisms combine to alternatively stimulate or inhibit cell growth. While it remains to be shown that there are "true" receptors that are dedicated to respond to heparin/HS, it is important to consider the possibility that linear polysaccharides can directly modulate receptor activation in the absence of protein ligands when evaluating potential growth regulation by heparin and HS.

B. Heparan Sulfate Proteoglycan Signaling

Cell surface HSPG, particularly the syndecans 1–4, is capable of direct cell activation in response to interaction with extracellular ligands. Several studies, in particular, have demonstrated that the major and widely distributed HSPG, syndecan-4, can signal through the activation of protein kinase Cα (PKCα) (81,82,84,85,176–181). The activation of PKCα by syndecan-4 requires multimerization (dimers and higher order aggregates) of syndecan-4 via the interaction of phosphatidylinositol 4,5-bisphosphate (PIP2) with the syndecan-4 cytoplasmic tail (177,179,181). The PIP2 interaction with syndecan-4 stabilizes the formation of syndecan-4 dimers, which can then bind to and activate PKCα (181). This syndecan-4 signaling pathway is regulated by phosphorylation of the syndecan-4 cytoplasmic domain on a key serine residue (ser183), whereby dephosphorylation of ser183 is required before PIP2 will bind (85,176,177). FGF-2 can induce this response by stimulating the association of a serine/threonine phosphatase type 1/2A with the cytoplasmic tail of syndecan via postsynaptic density 95, disk large, zona occludens-1 (PDZ)-dependent binding (85,176). The FGF-2-mediated activation of phosphatase activity leads to decreased phosphorylation of ser183, which stimulates PIP2 association, dimerization (and oligomerization) and activation of PKCα (76,77,85,176). The activation of PKCα via FGF-2-syndecan-4 interactions mediates the FGF-2 response in vascular cells (81,85). Genetic manipulation of syndecan-4 has also provided considerable additional evidence that dimerization induced by FGF-2 is required for signaling (76,77,81,83,85). For example, mutation in the PIP2 or PDZ binding domains of the cytoplasmic tail of syndecan-4 results in a loss of FGF-2 mediated signaling in spite of the fact that FGF-2 can still bind to syndecan-4 monomers (85). Ligand induced HSPG signaling has also been demonstrated to lead to the activation of the extracellular regulated kinases (Erk 1/2) in SMC, which is associated with regulation of growth and migration in these cells (71,161).

The elaborate mechanisms involved in FGF-2-mediated signaling through syndecan-4 are likely reflective of a more general process whereby extracellular

ligands can signal through cell surface HSPG. Indeed, syndecan-1 and syndecan 3 have been demonstrated to signal in response extracellular matrix and soluble ligands to regulate cell spreading and neurite outgrowth, respectively (182,183). In a more general process, integrins, and most extracellular matrix proteins have heparin-binding domains reflecting a mechanism where HSPG participate in modulating integrin signaling and cell adhesion (184,185). The complex relationship between cell adhesion and cell proliferation indicates that integrin modulation by HSPG is also likely to have significant consequences on cell growth (186).

IV. Growth Control in Disease

A. Atherosclerosis and Restenosis

The complex geometry and relationship of cells and compartments within the blood vessel wall contribute to the retention of structural integrity of the vasculature. Minor modification or disruption of vascular architecture and health can create profound effects. When the normal vascular anatomy is disrupted, cascades of events amplify injury and insult, and can occlude blood flow to distal organs. We now understand that biochemical regulation by adjacent structures plays an equally important role in this regard, and that loss of this form of control, even in the presence of seemingly normal anatomy, can be just as devastating as loss of physical elements. Potent heparin-like products secreted by vascular cells play a central role in the biochemical regulation of vascular wall homeostasis through a wide range of paracrine and autocrine mechanisms.

The hallmark of the normal blood vessel is the retention of a normal relationship between the smooth muscle cells and the overlying endothelial monolayer. The endothelial monolayer serves as a thromboresistant lining with the remarkable ability to allow for the selective rejection of cell and circulating material infiltration into the wall of the artery. Vascular tone and luminal diameter are carefully regulated by synchronous contraction and relaxation of vascular smooth muscle cells (SMC). When the endothelium is injured and denuded, or is simply dysfunctional, a complex sequence of events ensues. The normally quiescent SMC are stimulated. Intimal resident SMC proliferate and medial SMC migrate into the intima, where further proliferation occurs. The resultant bulky lesion creates myointimal thickening and vascular occlusion. Coupled with alterations in local lipid metabolism, thrombosis and hemostasis and leukocyte/monocyte adhesion, lesions slowly evolve over the course of 40–60 years into fixed obstructive arterial disease. When more severe endothelial injury is imposed exogenously, such as following balloon angioplasty, endovascular stent implantation vascular bypass surgery or organ transplantation, these events progress rapidly and may culminate in blood flow compromise within weeks to months (187–193).

The earliest pathogenic events underlying the development of myointimal thickening are thought to involve adhesion of platelets and/or leukocytes (usually monocytes) to the luminal surface of the dysfunctional or denuded endothelium (EC). The platelets either spread or aggregate, depending on the nature of the

injury, and secrete chemotactic and mitogenic factors for SMC, such as PDGF. Adherent monocytes invade the intimal space, develop into macrophages, and secrete chemotactic and mitogenic factors for SMC. Thus, the migration of SMC into the intima and SMC proliferation are the consequence of platelet-based and macrophage-based events. This sequence of events is essentially that proposed by Ross in his reaction-to-injury hypothesis for SMC proliferation (194–196). More recently, and with the advent of permanent implants like endovascular stents there has been an increasing appreciation for the role of chronic smoldering inflammation (197). Stents and other similar interventions elicit a polymorphonuclear and monocytic reaction that not only remains active long after implantation but also contributes as well to the bulk and mass of the obstructing intimal lesion (198).

B. Heparin and Control of Smooth Muscle Cell Proliferation

Many of the events associated with vascular disease development and progression are potentially controlled by heparin. Karnovsky and associates initially reasoned that antithrombotic approach to vascular proliferative disease was reasonable as vascular occlusion was likely governed by thrombin generation. Their initial studies examined whether inhibition of thrombin with heparin might reduce intimal hyperplasia following removal of the endothelium, (147,199,200). Continuous intravenous infusion of heparin markedly decreased the myointimal thickening and SMC proliferation after the artery injury (5,201–203). Most interestingly however was that the control of SMC events elicited by heparin was independent of its anticoagulant or antithrombin III-binding activity (204–206). Indeed, heparin inhibits the growth of SMC derived from a variety of species and vessels, including rat, calf and primate aortae, rat mesenteric and carotid arteries and human umbilical vein (143,207), and fetal bovine pulmonary artery (202,208). While many forms of heparin, with and without antithrombin activity, effectively controlled SMC proliferation *in vitro*, other charged GAGs such as dermatan sulfate, chondroitin-4-sulfate, chondroitin-6-sulfate and hyaluronic acid were ineffective (143). Heparin block in the cell cycle was in mid-to-late G_1, was fully reversible upon removal of the drug (167,209) and must be administered before the cells enter S-phase (207,210,211).

Heparin regulation of vascular repair is complex. Indeed, when agents that degrade or reduced HS were delivered to the blood vessel wall, both increased and decreased SMC hyperplasia was observed (212–216). Heparin is a highly soluble and readily diffusible compound. In fact its linear conformation allows for this compound to *reptate* (i.e., move like a reptile with rapid permeation through the vessel wall). These features probably explain the fascinating dichotomy between the dramatic reduction in intimal hyperplasia and smooth muscle cell proliferation with continuous intravenous infusion or controlled perivascular release of heparin (217) and the increased lesion size and cell proliferation with intermittent delivery (218). Moreover, the rapid movement of this compound through the artery contributes to the ability of stent-based release of heparin to inhibit thrombosis but not intimal hyperplasia (219).

Similarly heparin binding to antithrombin III and growth factors is size specific, so too, is its antiproliferative effect on SMC (144), which requires hexasaccharides or greater. Decasaccharides lacking anticoagulant activity were antiproliferative (144). *O*-sulfation is required for both anticoagulant and antiproliferative activity. *N*-sulfation is required for anticoagulant, but not for antiproliferative activity. For the latter, a neutral or negative charge at the N-position is necessary. Thus, *N*-desulfated re-*N*-acetylated heparin lacks antithrombin activity, but retains antiproliferative activity (144). The more highly negatively charged polymers are more antiproliferative than the less negatively charged. Oversulfation at the *O*-positions increases antiproliferative activity, whereas decarboxylation decreases such activity (220). Pentasaccharides with 3-*O*-sulfate on the internal D-glucosamine that specifically bind antithrombin III were minimally antiproliferative, and highly antiproliferative fractions lacked this sequence (220).

C. Possible Mechanisms of Heparin/Heparan Sulfate Effects on SMC Behavior

Despite the wealth of knowledge relating to the effects of heparin/heparan sulfate on SMC behavior, the full form of this control remains incompletely understood. Each of the mechanisms noted above likely plays a role including regulation of leukocyte/monocyte adhesion, SMC adhesion, migration, and proliferation, extracellular matrix production and phenotypic modulation, all of which may underlie various aspects of the pathogenesis of the legion of myointimal thickening. Some time ago we set out to create a unified model proposing how the body makes use of heparin and like compounds to regulate vascular events. We listed (221) a series of observations to support the notion that heparin-like compounds produced by the endothelial cells and smooth muscle cells (143,222) bind to the cell surface and extracellular matrix and govern SMC proliferation as well as a large number of cellular and molecular events and interactions. These observations include:

1. Intimal hyperplasia with substantial SMC proliferation follows removal of the vascular endothelium (5,200).
2. Intimal hyperplasia and SMC proliferation reach a peak in experimental systems and then stop; cessation of SMC growth corresponds to the restoration of the endothelial layer (199).
3. Endothelial cell mitogens like FGF-1 and VEGF enhance restoration of endothelial integrity and regression of SMC proliferation (191,223–228).
4. Heparin/heparan sulfate inhibits SMC proliferation in culture (143), and the infusion of heparin inhibits intimal SMC accumulation *in vivo* (5,200).
5. Cultured endothelial cells produce a heparin-like inhibitor of SMC when confluent and a SMC mitogen when sparsely plated (143).
6. Cultured media from confluent, but not from exponentially growing SMC synthesize a highly antiproliferative HS species (222).
7. Protamine removes the ability of exogenous heparin preparations to mitigate vascular injury and when administered alone exacerbates vascular injury (229).

8. FGF-2 is a potent SMC mitogen in culture, but has no effect *in vivo* if the endothelium is present or if heparin is administered to deendothelialized arteries (230–232).
9. Heparin inhibition of FGF-2 binding to SMC correlates with heparin inhibition of FGF-2 mitogenicity (73).

One potential model of proliferative vascular diseases that incorporates all of these observations revolves about two related ideas that are heparin-centric. First, it is the endothelium that is the primary modulator of the system, keeping the vascular wall quiescent in health, and, with endothelial injury, leading to disease. Second, endothelial regulation in all likelihood arises from a sophisticated autocrine/paracrine system to which heparin/heparan sulfate is crucial. Vasculo-proliferative states may well be appreciated like deficiency diseases of the endocrine system. Just as diabetes mellitus runs the full spectrum from absolute insulinopenia to hyperinsulinemia and insulin resistance, so too, vasculo-proliferative diseases may be seen as encompassing the range of states from a situation wherein the *amount* of heparin/HS is insufficient to inhibit growth, to one wherein the *activity* of heparin/HS is neutralized and/or their binding inhibited.

In the normal state the intact endothelial monolayer produces growth suppressive heparan sulfate, as do confluent cultured endothelial cells (143), and confluent SMC (222). The heparan sulfate percolates throughout the vascular wall, binds to or surrounds SMC and the extracellular matrix, and maintains growth homeostasis. The growth inhibitory arterial wall heparan sulfate fractions isolated by Schmidt et al. possess 2-*O*-sulfated residues (233,234), and heparin induces the production of a heparan sulfate with 2-*O*-glucuronic sulfation by porcine SMC (235). It is possible that the effects of endothelial cell-derived heparan sulfate arise in part from stimulation of SMC production of a growth inhibitory heparan sulfate.

Physical removal of the endothelial monolayer, or injury that impairs the synthetic or secretory ability of the cells, imposes two important effects. First, the subendothelial space is exposed, and second a critical source of heparan sulfate is lost. The exposure of the underlying basement membrane excites a cascade of events including: platelet activation, adhesion, and aggregation, which when coupled with the loss of endothelial based antithrombotic compounds provides for the potential for thrombosis; leukocyte adhesion, leading to the infiltration of monocytes, lymphocytes and neutrophils, bearing growth factors, cytokines, and hydrolytic and proteolytic compounds; insudation and modification of lipid allowing for the increase in lesion size and enhanced cytoxicity and injury; loss of vasodilators and enhanced production of vasoconstrictors, followed by the potential for spasm and paradoxical vasoconstriction, etc. When these various events begin to interact, injury is amplified still further. As injury progresses one can envision that the reservoir of heparan sulfate surrounding the medial SMC is threatened. Both monocytes and platelets secrete potent endoglycosidases and heparanases (216,236,237) that have the potential to cleave heparan sulfate and other heparin-like compounds. Furthermore, platelet factor 4 released by the platelets inactivates

heparin/heparan sulfate because of its high affinity binding for these species. The loss of the source and stores of the inhibitor allow the SMC to begin to respond to the high concentration of potent mitogens (e.g., PDGF, FGF-2, IL-2, TNF, etc.) that begins to be released from activated cells and HS storage sites within the extracellular matrix (Table 1) (3,6,10,67,238). The exogenous administration of growth factors, inactive in the presence of an intact endothelium, now produces significant mitogenesis (232,239). As evidence that the action of the endothelium as a barrier preventing contact of circulating growth factor with the target SMC is of secondary importance to the biochemical regulation by the endothelium we demonstrated that extravascular FGF-2 was deposited within the media-intima identically for native and denuded arteries, but was only mitogenic in the latter (240). Furthermore, we showed that confluent endothelial cells and endothelial cell conditioned media produced a heparin-like compound that interfered with FGF-2 binding to SMC and in doing so prevented mitogenesis (66,73).

The observations that only confluent, and not exponentially growing, cells produce HS species that interfere with FGF-2 binding and SMC growth (73,143) may be reflective of the difference between the intact and damaged endothelial monolayer. SMC accumulation within the *intima* ceases with restoration of the endothelium (199,241), and regression of intimal hyperplasia is maximized where endothelial restoration is maximized (191,199,223,242,243). It may well be that restoring the endothelial monolayer reverses the state of relative heparan sulfate deficiency. Indeed the administration of exogenous preparations of heparin intravenously (5,210), or to the perivascular space (217), reduces intimal hyperplasia, and prevents the additional growth stimulatory effects of exogenously administered mitogens (232). However, if the activity of endogenous heparan sulfate or exogenous heparin preparations are interfered with, vascular injury is made all the worse (229). This occurs with the cation protamine. Protamine binds avidly to heparin and is routinely used to reverse systemic heparin anticoagulation. For example, virtually all procedures requiring heparin anticoagulation during cardiopulmonary bypass or arteriography are reversed by protamine infusion. We found that protamine neutralized the inhibitory effects of heparin on SMC both *in vitro* and *in vivo*. Furthermore, protamine stimulated SMC proliferation in culture, and exacerbated vascular injury in the absence of heparin. This last finding provides further evidence for the existence of a natural vascular reparative process that revolves about the elaboration of exogenous heparin-like compounds.

The validation of this model was established from cell culture and animal studies. Conditioned media from cultured confluent EC was fractionated into HS and non-HS components. The latter had no influence on intimal hyperplasia but the HS alone was still capable of inhibiting SMC proliferation 50–60% as well as intact conditioned media (244). When the two components were recombined full inhibition was restored. Similar results were observed *in vivo*. EC were incorporated within three-dimensional matrices and placed adjacent to balloon-injured porcine arteries (138,245). While, intact EC that secreted perlecan inhibited resultant intimal hyperplasia by almost 75% and entirely eliminated thrombosis, implants of EC genetically programmed to secrete reduced amounts of the HS perlecan were

less effective at inhibiting experimental restenosis and completely incapable of preventing thrombosis (138). Taken together these results not only directly implicate this HSPG as an important regulator of intimal hyperplasia and occlusive thrombosis that follow vascular interventions, but also show the complexity of the regulatory role of this class of compounds. The HS is absolutely necessary to control the occlusive thrombotic reaction to deep vascular injury, and its contribution to the hyperplastic reaction is part of the overall regulation that the intact endothelium elicits. It is likely that endothelial control over intimal thickening results from the action of the HS in concert with other secreted products such as nitric oxide, endothelins, prostaglandins and a myriad of growth factors, cytokines and vasoreactive agents. HS is essential and other factors may be required to enhance this regulatory activity. Removal of either diminishes the ability of the cell to enact the full extent of its homeostatic regulation; loss of the HS eliminates all of the beneficial effects.

D. Cancer and Angiogenesis

The ability of heparin and HS to modulate cell proliferation suggests the involvement of these polysaccharides in proliferative disorders such as cancer. Indeed, there has been a long-standing anecdotal relationship suggesting that heparin has antitumor activity (246–248). Cancer patients have an increased risk of thromboembolism, often because of an activated coagulation system. Consequently, cancer patients are often treated with anticoagulants including heparin and low molecular weight heparins (LMWH), and these treatments appear to lead to increased cancer survival and regression of primary tumors in some instances (246–248). While there is evidence that these clinical benefits reflect the role of blood coagulation in cancer; the observation that heparin and LMWH show noticeable advantages over other anticoagulants, such as warfarin, suggests that other mechanisms are also involved (249). The development and progression of cancer is complex and involves a series of coordinated steps (250). These steps include the initial transformation of a normal cell followed by unregulated growth and the recruitment of new blood vessels to facilitate growth and invasion of the tumor into the surrounding tissue. Access to blood and lymphatic vessels provides a means for tumors to further metastasize to distant sites within the organism. These steps involve a myriad of biological processes including: cell proliferation, adhesion, migration, ECM turnover, the immune system, and blood clotting. Heparin and HS have been implicated, to some degree, in controlling all of these processes. We will focus our discussion on the role of heparin and HS in modulating tumor and endothelial cell growth. For a more complete discourse on the role of heparin and HS in cancer, the reader is directed to a number of recent comprehensive reviews (251–254).

The initiation of tumor transformation is associated with genetic changes involving the activation of oncogenes and/or the inactivation of tumor suppressor genes leading to a loss in normal cell growth control. Changes in tumor cell HSPG expression level and structure have been associated with the transformation process. For example, downregulation of syndecans and glypicans has been correlated

with transformation (255,256). In addition, changes in HS fine structure and function (growth inhibitory or stimulatory) have also been associated with tumorigenesis (257–259). It has also been demonstrated that inhibition of perlecan expression in tumor cells, through the use of antisense mRNA expression, results in reduced tumor growth (136). In humans, mutations in the glypican-3 gene are linked to the complex overgrowth condition known as Simpson-Golabi-Behmel syndrome, which is associated with an increased risk of certain malignancies (260). In addition to the role that HSPG appear to play in the initial transformation process, the ability of HS to modulate the access and activity of mitogenic proteins (see Section II) has been implicated in regulating the progression of tumor cell growth. Thus, direct and indirect activities of cell associated and ECM HSPG play important roles in modulating tumor cell growth, invasion, and metastasis.

In addition to the effects of HSPG in regulating tumor cells, HSPG also act as critical mediators of angiogenesis (11). Without access to the circulation, tumors are limited by diffusion of nutrients and waste to a size of only 1–2 mm (261). Hence, the switch from the preangiogenic to the angiogenic phenotype has been identified as the critical event in the conversion from the benign to malignant state. As such, the regulation of the growth of new blood vessels, specifically, the ability of tumors to stimulate endothelial cells from the surrounding vasculature to actively proliferate, is a crucial component to the development of malignant disease. Members of the VEGF and FGF families of growth factors have been demonstrated to be the key mediators of endothelial cell growth that is necessary for tumor vascularization (116,262). As evidence of this, low oxygen tension (hypoxia) within preangiogenenic tumors upregulates VEGF and HSPG expression (263–266). An additional consequence of hypoxia is the generation of an acidic extracellular environment within tumors as the result of high rates of anaerobic glycolysis (267,268). VEGF binding to HS is stabilized by decreased pH, indicating that tumor acidification would increase the deposition of VEGF within the surrounding ECM, which could lead to the formation of stable HSPG-mediated VEGF gradients to direct the growth of new blood vessels to the tumor (50,131) (Fig. 4). Interestingly, even VEGF121, which lacks the VEGF heparin-binding domain, acquires the ability to bind to HS under acidic conditions, indicating that this interaction is via a new pH sensitive heparin-binding domain. Thus, modulation of HS–VEGF interactions by physical environmental factors (i.e., pH) as well as through the coordinated regulation of HSPG expression and structure are likely important components of the angiogenic switch. Taken together, the involvement of heparin, HS and HSPG in the biology of tumor initiation and progression at multiple levels highlights the potential for interventions aimed at targeting the functional role of HS. Recent advances in structural and chemical analysis of complex polysaccharides coupled with new approaches to chemical synthesis and separation technology will potentially provide the foundation for the development of target-specific polysaccharide drugs for the treatment of cancer (269–274).

V. Conclusions

Heparin and HS are able to modulate cell proliferation through a number of interrelated direct and indirect mechanisms. A large number of growth factors that modulate tissue development and repair bind to and are regulated by HSPG on the surface of cells and within the extracellular matrix. There are also a number of potential direct targets of heparin and HS action on the cell surface and within intracellular compartments such as the nucleus. With recent advances in molecular methods for modulating the biosynthesis of HS and analytical methods for determining polysaccharide structure, a more complete understanding of the complex mechanisms used by these polysaccharides to modulate cell growth will continue to emerge. The central role that HS appears to play in orchestrating the delicate balance between cell growth stimulation and inhibition that is in place to maintain normal tissue function, identifies this class of complex polysaccharides as important targets for the design of rational therapies aimed at reestablishing proliferative balance in disease states.

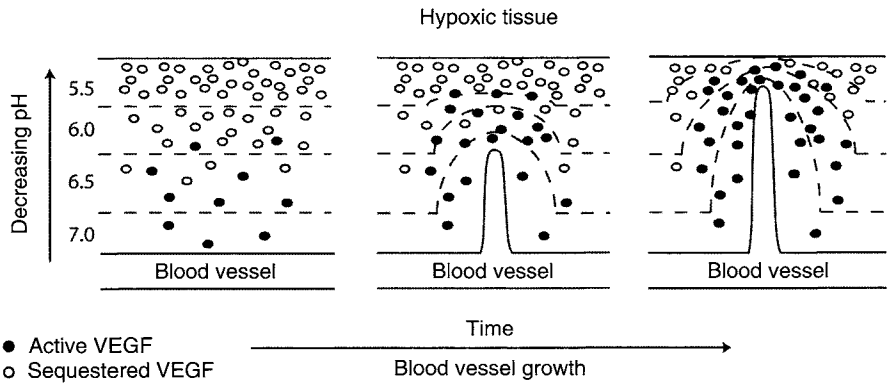

Figure 4 Regulation of directed angiogenesis by pH sensitive binding of VEGF to HSPG. Schematic representation of how pH sensitive binding of VEGF to HS could contribute to directed angiogenesis into a hypoxic tissue. VEGF is predicted to be distributed such that the area of the tissue that is most hypoxic (lowest pH) would contain the most VEGF because of the high binding to HSPG as well as the increased expression of VEGF. Thus, variable matrix binding of VEGF would allow a stable VEGF gradient to be established from the most acidic to the least acidic region of the tissue. Hence, the region of the tissue that is closest to the existing vasculature would contain the least amount of deposited VEGF, yet this VEGF would be in the active state (free from the ECM) such that it could participate in initiating angiogenesis. As the blood vessel grows into the acidic tissue the extracellular pH would increase causing the release and activation of the high levels of stored VEGF, further propagating the directed growth of the blood vessel toward the regions of tissue containing the highest levels of VEGF. Figure reprinted from (131).

Acknowledgments

Our research on heparin and heparan sulfate is funded by National Institutes of Health grants HL56200, HL46902, EY14007 (M.A.N.), and GM49039 and HL67246 (E.R.E.). We thank Dr Jo Ann Buczek-Thomas for critically reading this manuscript. We are grateful to Drs Chia Chu and Adrienne Goerges for assistance in preparing the figures.

References

1. Rabenstein DL. Heparin and heparan sulfate: structure and function. Nat Prod Rep 2002; 19:312–331.
2. Rosenberg RD, Damus PS. The purification and mechanism of action of human antithrombin-heparin cofactor. J Biol Chem 1973; 248:6490–6505.
3. Capila I, Linhardt RJ. Heparin–protein interactions. Angew Chem Int Ed Engl 2002; 41:391–412.
4. Bjork I, Lindahl U. Mechanism of the anticoagulant action of heparin. Mol Cell Biochem 1982; 48:161–182.
5. Clowes AW, Karnovsky MJ. Suppression by heparin of smooth muscle cell proliferation in injured arteries. Nature 1977; 265:625–626.
6. Conrad HE. Heparin-Binding Proteins. San Diego: Academic Press, 1998.
7. Gallagher JT. Heparan sulfate: growth control with a restricted sequence menu. J Clin Invest 2001; 108:357–361.
8. Esko JD, Selleck SB. Order out of chaos: assembly of ligand binding sites in heparan sulfate. Annu Rev Biochem 2002; 71:435–471.
9. Turnbull J, Powell A, Guimond S. Heparan sulfate: decoding a dynamic multifunctional cell regulator. Trends Cell Biol 2001; 11:75–82.
10. Shriver Z, Liu D, Sasisekharan R. Emerging views of heparan sulfate glycosaminoglycan structure/activity relationships modulating dynamic biological functions. Trends Cardiovasc Med 2002; 12:71–77.
11. Iozzo RV, San Antonio JD. Heparan sulfate proteoglycans: heavy hitters in the angiogenesis arena. J Clin Invest 2001; 108:349–355.
12. Perrimon N, Bernfield M. Specificities of heparan sulphate proteoglycans in developmental processes. Nature 2000; 404:725–728.
13. Robinson HC, Horner AA, Hook M, Ogren S, Lindahl U. A proteoglycan form of heparin and its degradation to single-chain molecules. J Biol Chem 1978; 253:6687–6693.
14. Linhardt RJ, Ampofo SA, Fareed J, Hoppensteadt D, Mulliken JB, Folkman J. Isolation and characterization of human heparin. Biochemistry 1992; 31:12441–12445.
15. Griffin CC, Linhardt RJ, Van Gorp CL, Toida T, Hileman RE, Schubert RL, 2nd, Brown SE. Isolation and characterization of heparan sulfate from crude porcine intestinal mucosal peptidoglycan heparin. Carbohydr Res 1995; 276:183–197.
16. Hileman RE, Fromm JR, Weiler JM, Linhardt RJ. Glycosaminoglycan-protein interactions: definition of consensus sites in glycosaminoglycan binding proteins. Bioessays 1998; 20:156–167.

17. Gallagher JT, Turnbull JE, Lyon M. Heparan sulphate proteoglycans: molecular organisation of membrane – associated species and an approach to polysaccharide sequence analysis. Adv Exp Med Biol 1992; 313:49–57.
18. Bernfield M, Gotte M, Park PW, Reizes O, Fitzgerald ML, Lincecum J, Zaka M. Functions of cell surface heparan sulfate proteoglycans. Annu Rev Biochem 1999; 68:729–777.
19. Park PW, Reizes O, Bernfield M. Cell surface heparan sulfate proteoglycans: selective regulators of ligand-receptor encounters. J Biol Chem 2000; 275:29923–29926.
20. Subramanian SV, Fitzgerald ML, Bernfield M. Regulated shedding of syndecan-1 and -4 ectodomains by thrombin and growth factor receptor activation. J Biol Chem 1997; 272:14713–14720.
21. Rapraeger A, Bernfield M. Cell surface proteoglycan of mammary epithelial cells. Protease releases a heparan sulfate-rich ectodomain from a putative membrane-anchored domain. J Biol Chem 1985; 260:4103–4109.
22. Fitzgerald ML, Wang Z, Park PW, Murphy G, Bernfield M. Shedding of syndecan-1 and -4 ectodomains is regulated by multiple signaling pathways and mediated by a TIMP-3-sensitive metalloproteinase. J Cell Biol 2000; 148:811–824.
23. Buczek-Thomas JA, Nugent MA. Elastase-mediated release of heparan sulfate proteoglycans from pulmonary fibroblast cultures. A mechanism for basic fibroblast growth factor (bFGF) release and attenuation of bFGF binding following elastase-induced injury. J Biol Chem 1999; 274:25167–25172.
24. Iozzo RV. Matrix proteoglycans: from molecular design to cellular function. Annu Rev Biochem 1998; 67:609–652.
25. Richardson TP, Trinkaus-Randall V, Nugent MA. Regulation of heparan sulfate proteoglycan nuclear localization by fibronectin. J Cell Sci 2001; 114:1613–1623.
26. Hsia E, Richardson TP, Nugent MA. Nuclear localization of basic fibroblast growth factor is mediated by heparan sulfate proteoglycans through protein kinase C signaling. J Cell Biochem 2003; 88:1214–1225.
27. Ishihara M, Fedarko NS, Conrad HE. Transport of heparan sulfate into the nuclei of hepatocytes. J Biol Chem 1986; 261:13575–13580.
28. Fedarko NS, Conrad HE. A unique heparan sulfate in the nuclei of hepatocytes: structural changes with the growth state of the cells. J Cell Biol 1986; 102:587–599.
29. Kovalszky I, Dudas J, Olah-Nagy J, Pogany G, Tovary J, Timar J, Kopper L, Jeney A, Iozzo RV. Inhibition of DNA topoisomerase I activity by heparan sulfate and modulation by basic fibroblast growth factor. Mol Cell Biochem 1998; 183:11–23.
30. Kolset SO, Prydz K, Pejler G. Intracellular proteoglycans. Biochem J 2004; 379:217–227.
31. Humphries DE, Wong GW, Friend DS, Gurish MF, Qiu WT, Huang C, Sharpe AH, Stevens RL. Heparin is essential for the storage of specific granule proteases in mast cells. Nature 1999; 400:769–772.
32. Humphries DE, Wong GW, Friend DS, Gurish MF, Stevens RL. 14 heparin-null transgenic mice are unable to store certain granule proteases in their mast cells. J Histochem Cytochem 1999; 47:1645D–1646.

33. Segev A, Nili N, Strauss BH. The role of perlecan in arterial injury and angiogenesis. Cardiovasc Res 2004; 63:603–610.
34. Nugent MA, Iozzo RV. Fibroblast growth factor-2. Int J Biochem Cell Biol 2000; 32:115–120.
35. Fannon M, Forsten KE, Nugent MA. Potentiation and inhibition of bFGF binding by heparin: A model for regulation of cellular response. Biochemistry 2000; 39:1434–1445.
36. Lemmon MA, Schlessinger J. Transmembrane signaling by receptor oligomerization. Methods Mol Biol 1998; 84:49–71.
37. Fantl WJ, Johnson DE, Williams LT. Signalling by receptor tyrosine kinases. Annu Rev Biochem 1993; 62:453–481.
38. Shing Y, Folkman J, Sullivan R, Butterfield C, Murray J, Klagsbrun M. Heparin affinity: purification of a tumor-derived capillary endothelial cell growth factor. Science 1984; 223:1296–1299.
39. Burgess WH, Maciag T. The heparin-binding (fibroblast) growth factor family of proteins. Annu Rev Biochem 1989; 58:575–606.
40. Yayon A, Klagsbrun M, Esko JD, Leder P, Ornitz DM. Cell surface, heparin-like molecules are required for binding basic fibroblast growth factor to its high affinity receptor. Cell 1991; 64: 841–848.
41. Rapraeger A, Krufka A, Olwin B. Requirement of heparan sulfate for bFGF-mediated fibroblast growth and myoblast differentiation. Science 1991; 252:1705–1708.
42. Nugent MA, Edelman ER. Kinetics of basic fibroblast growth factor binding to its receptor and heparan sulfate proteoglycan: a mechanism for cooperativity. Biochemistry 1992; 31:8876–8883.
43. Pantoliano MW, Horlick RA, Springer BA, Van Dyk DE, Tobery T, Wetmore DR, Lear JD, Nahapetian AT, Bradley JD, Sisk WP. Multivalent ligand-receptor binding interactions in the fibroblast growth factor system produce a cooperative growth factor and heparin mechanism for receptor dimerization. Biochemistry 1994; 33:10229–10248.
44. Ibrahimi OA, Zhang F, Hrstka SC, Mohammadi M, Linhardt RJ. Kinetic model for FGF, FGFR, and proteoglycan signal transduction complex assembly. Biochemistry 2004; 43:4724–4730.
45. Sperinde GV, Nugent MA. Heparan sulfate proteoglycans control bFGF processing in vascular smooth muscle cells. Biochemistry 1998; 37:13153–13164.
46. Gitay-Goren H, Soker S, Vlodavsky I, Neufeld G. The binding of vascular endothelial growth factor to its receptors is dependent on cell surface-associated heparin-like molecules. J Biol Chem 1992; 267:6093–6098.
47. Cohen T, Gitay-Goren H, Sharon R, Shibuya M, Halaban R, Levi BZ, Neufeld G. VEGF121, a vascular endothelial growth factor (VEGF) isoform lacking heparin binding ability, requires cell-surface heparan sulfates for efficient binding to the VEGF receptors of human melanoma cells. J Biol Chem 1995; 270:11322–11326.
48. Neufeld G, Cohen T, Gengrinovitch S, Poltorak Z. Vascular endothelial growth factor (VEGF) and its receptors. FASEB J 1999; 13:9–22.
49. Gengrinovitch S, Berman B, David G, Witte L, Neufeld G, Ron D. Glypican-1 is a VEGF165 binding proteoglycan that acts as an extracellular chaperone for VEGF165. J Biol Chem 1999; 274:10816–10822.

50. Goerges AL, Nugent MA. Regulation of vascular endothelial growth factor binding and activity by extracellular pH. J Biol Chem 2003; 278:19518–19525.
51. Higashiyama S, Abraham JA, Klagsbrun M. Heparin-binding EGF-like growth factor stimulation of smooth muscle cell migration: dependence on interactions with cell surface heparan sulfate. J Cell Biol 1993; 122:933–940.
52. Guimond S, Maccarana M, Olwin BB, Lindahl U, Rapraeger AC. Activating and inhibitory heparin sequences for FGF-2 (basic FGF). Distinct requirements for FGF-1, FGF-2, and FGF-4. J Biol Chem 1993; 268:23906–23914.
53. Turnbull JE, Fernig DG, Ke Y, Wilkinson MC, Gallagher JT. Identification of the basic fibroblast growth factor binding sequence in fibroblast heparan sulfate. J Biol Chem 1992; 267:10337–10341.
54. Pye DA, Vives RR, Turnbull JE, Hyde P, Gallagher JT. Heparan sulfate oligosaccharides require 6-*O*-sulfation for promotion of basic fibroblast growth factor mitogenic activity. J Biol Chem 1998; 273:22936–22942.
55. Kan M, Wang F, Xu J, Crabb JW, Hou J, McKeehan WL. An essential heparin-binding domain in the fibroblast growth factor receptor kinase. Science 1993; 259:1918–1921.
56. Loo BM, Kreuger J, Jalkanen M, Lindahl U, Salmivirta M. Binding of heparin/heparan sulfate to fibroblast growth factor receptor 4. J Biol Chem 2001; 276:16868–16876.
57. Stauber DJ, DiGabriele AD, Hendrickson WA. Structural interactions of fibroblast growth factor receptor with its ligands. Proc Natl Acad Sci USA 2000; 97:49–54.
58. Schlessinger J, Plotnikov AN, Ibrahimi OA, Eliseenkova AV, Yeh BK, Yayon A, Linhardt RJ, Mohammadi M. Crystal structure of a ternary FGF-FGFR-heparin complex reveals a dual role for heparin in FGFR binding and dimerization. Mol Cell 2000; 6:743–750.
59. Plotnikov AN, Hubbard SR, Schlessinger J, Mohammadi M. Crystal structures of two FGF-FGFR complexes reveal the determinants of ligand-receptor specificity. Cell 2000; 101:413–424.
60. Plotnikov AN, Schlessinger J, Hubbard SR, Mohammadi M. Structural basis for FGF receptor dimerization and activation. Cell 1999; 98:641–650.
61. Pellegrini L. Role of heparan sulfate in fibroblast growth factor signalling: a structural view. Curr Opin Struct Biol 2001; 11:629–634.
62. Pellegrini L, Burke DF, von Delft F, Mulloy B, Blundell TL. Crystal structure of fibroblast growth factor receptor ectodomain bound to ligand and heparin. Nature 2000; 407:1029–1034.
63. Lundin L, Larsson H, Kreuger J, Kanda S, Lindahl U, Salmivirta M, Claesson-Welsh L. Selectively desulfated heparin inhibits fibroblast growth factor-induced mitogenicity and angiogenesis. J Biol Chem 2000; 275:24653–24660.
64. Fannon M, Forsten-Williams K, Dowd CJ, Freedman DA, Folkman J, Nugent MA. Binding inhibition of angiogenic factors by heparan sulfate proteoglycans in aqueous humor: potential mechanism for maintenance of an avascular environment. FASEB J 2003; 17:902–904.
65. Forsten KE, Fannon M, Nugent MA. Potential mechanisms for the regulation of growth factor binding by heparin. J Theor Biol 2000; 205:215–230.
66. Forsten KE, Courant NA, Nugent MA. Endothelial proteoglycans inhibit bFGF binding and mitogenesis. J Cell Physiol 1997; 172:209–220.

67. Gallagher JT. Structure–activity relationship of heparan sulphate. Biochem Soc Trans 1997; 25:1206–1209.
68. Walker A, Turnbull JE, Gallagher JT. Specific heparan sulfate saccharides mediate the activity of basic fibroblast growth factor. J Biol Chem 1994; 269:931–935.
69. Delehedde M, Lyon M, Gallagher JT, Rudland PS, Fernig DG. Fibroblast growth factor-2 binds to small heparin-derived oligosaccharides and stimulates a sustained phosphorylation of p42/44 mitogen-activated protein kinase and proliferation of rat mammary fibroblasts. Biochem J 2002; 366:235–244.
70. Delehedde M, Seve M, Sergeant N, Wartelle I, Lyon M, Rudland PS, Fernig DG. Fibroblast growth factor-2 stimulation of p42/44MAPK phosphorylation and IkappaB degradation is regulated by heparan sulfate/heparin in rat mammary fibroblasts. J Biol Chem 2000; 275:33905–33910.
71. Chua CC, Rahimi N, Forsten-Williams K, Nugent MA. Heparan sulfate proteoglycans function as receptors for fibroblast growth factor-2 activation of extracellular signal-regulated kinases 1 and 2. Circ Res 2004; 94:316–323.
72. Padera R, Venkataraman G, Berry D, Godavarti R, Sasisekharan R. FGF-2/fibroblast growth factor receptor/heparin-like glycosaminoglycan interactions: a compensation model for FGF-2 signaling. FASEB J 1999; 13:1677–1687.
73. Nugent MA, Karnovsky MJ, Edelman ER. Vascular cell-derived heparan sulfate shows coupled inhibition of bFGF binding and mitogenesis in vascular smooth muscle cells. Circ Res 1993; 73:1051–1060.
74. Fannon M, Nugent MA. FGF binds its receptors, is internalized and stimulates DNA synthesis in Balb/c3T3 cells in the absence of heparan sulfate. J Biol Chem 1996; 271:17949–17956.
75. Delehedde M, Lyon M, Sergeant N, Rahmoune H, Fernig DG. Proteoglycans: pericellular and cell surface multireceptors that integrate external stimuli in the mammary gland. J Mammary Gland Biol Neoplasia 2001; 6:253–273.
76. Tkachenko E, Simons M. Clustering induces redistribution of syndecan-4 core protein into raft membrane domains. J Biol Chem 2002; 277:19946–19951.
77. Tkachenko E, Lutgens E, Stan RV, Simons M. Fibroblast growth factor 2 endocytosis in endothelial cells proceed via syndecan-4-dependent activation of Rac1 and a Cdc42-dependent macropinocytic pathway. J Cell Sci 2004; 117:3189–3199.
78. Chu CL, Buczek-Thomas JA, Nugent MA. Heparan sulphate proteoglycans modulate fibroblast growth factor-2 binding through a lipid raft-mediated mechanism. Biochem J 2004; 379:331–341.
79. Fuki IV, Meyer ME, Williams KJ. Transmembrane and cytoplasmic domains of syndecan mediate a multistep endocytic pathway involving detergent-insoluble membrane rafts. Biochem J 2000; 351 (Part 3):607–612.
80. Fuki II, Iozzo RV, Williams KJ. Perlecan heparan sulfate proteoglycan. A novel receptor that mediates a distinct pathway for ligand catabolism. J Biol Chem 2000; 275:25742–25750.
81. Volk R, Schwartz JJ, Li J, Rosenberg RD, Simons M. The role of syndecan cytoplasmic domain in basic fibroblast growth factor-dependent signal transduction. J Biol Chem 1999; 274:24417–24424.
82. Horowitz A, Murakami M, Gao Y, Simons M. Phosphatidylinositol-4, 5-bisphosphate mediates the interaction of syndecan-4 with protein kinase C. Biochemistry 1999; 38:15871–15877.

83. Zhang Y, Li J, Partovian C, Sellke FW, Simons M. Syndecan-4 modulates basic fibroblast growth factor 2 signaling in vivo. Am J Physiol Heart Circ Physiol 2003; 284:H2078–2082.
84. Oh ES, Woods A, Lim ST, Theibert AW, Couchman JR. Syndecan-4 proteoglycan cytoplasmic domain and phosphatidylinositol 4,5-bisphosphate coordinately regulate protein kinase C activity. J Biol Chem 1998; 273:10624–10629.
85. Horowitz A, Tkachenko E, Simons M. Fibroblast growth factor-specific modulation of cellular response by syndecan-4. J Cell Biol 2002; 157:715–725.
86. Fedarko NS, Ishihara M, Conrad E. Control of cell division in hepatoma cells by exogenous heparan sulfate proteoglycan. J Cell Physiol 1989; 139:287–294.
87. Clevenger CV. Nuclear localization and function of polypeptide ligands and their receptors: a new paradigm for hormone specificity within the mammary gland? Breast Cancer Res 2003; 5:181–187.
88. Johnson HM, Subramaniam PS, Olsnes S, Jans DA. Trafficking and signaling pathways of nuclear localizing protein ligands and their receptors. Bioessays 2004; 26:993–1004.
89. Watson K, Gooderham NJ, Davies DS, Edwards RJ. Nucleosomes bind to cell surface proteoglycans. J Biol Chem 1999; 274:21707–21713.
90. Du Clos TW, Volzer MA, Hahn FF, Xiao R, Mold C, Searles RP. Chromatin clearance in C57Bl/10 mice: interaction with heparan sulphate proteoglycans and receptors on Kupffer cells. Clin Exp Immunol 1999; 117:403–411.
91. O'Farrell F, Loog M, Janson IM, Ek P. Kinetic study of the inhibition of CK2 by heparin fragments of different length. Biochim Biophys Acta 1999; 1433:68–75.
92. Hathaway GM, Lubben TH, Traugh JA. Inhibition of casein kinase II by heparin. J Biol Chem 1980; 255:8038–8041.
93. Bailly K, Soulet F, Leroy D, Amalric F, Bouche G. Uncoupling of cell proliferation and differentiation activities of basic fibroblast growth factor. FASEB J 2000; 14:333–344.
94. Amalric F, Bouche G, Bonnet H, Brethenou P, Roman AM, Truchet I, Quarto N. Fibroblast growth Factor-2 (FGF-2) in the nucleus: Translocation process and targets. Biochem Pharm 1994; 47:111–115.
95. Jans DA, Hassan G. Nuclear targeting by growth factors, cytokines, and their receptors: a role in signaling? Bioessays 1998; 20:400–411.
96. Berry D, Lynn DM, Sasisekharan R, Langer R. Poly(beta-amino ester)s promote cellular uptake of heparin and cancer cell death. Chem Biol 2004; 11:487–498.
97. Forsten KE, Akers RM, San Antonio JD. Insulin-like growth factor (IGF) binding protein-3 regulation of IGF-I is altered in an acidic extracellular environment. J Cell Physiol 2001; 189:356–365.
98. Sperinde GV, Nugent MA. Mechanisms of FGF-2 intracellular processing: a kinetic analysis of the role of heparan sulfate proteoglycans. Biochemistry 2000; 39:3788–3796.
99. Gleizes PE, Noaillac-Depeyre J, Dupont MA, Gas N. Basic fibroblast growth factor (FGF-2) is addressed to caveolae after binding to the plasma membrane of BHK cells. Eur J Cell Biol 1996; 71:144–153.
100. Gleizes PE, Noaillac-Depeyre J, Amalric F, Gas N. Basic fibroblast growth factor (FGF-2) internalization through the heparan sulfate proteoglycans-mediated pathway: an ultrastructural approach. Eur J Cell Biol 1995; 66:47–59.

101. Reilly JF, Mizukoshi E, Maher PA. Ligand dependent and independent internalization and nuclear translocation of fibroblast growth factor (FGF) receptor 1. DNA Cell Biol 2004; 23:538–548.
102. Folkman J, Klagsbrun M, Sasse J, Wadzinski M, Ingber D, Vlodavsky I. A heparin-binding angiogenic protein – basic fibroblast growth factor – is stored within basement membrane. Am J Pathol 1988; 130:393–400.
103. Vlodavsky I, Folkman J, Sullivan R, Fridman R, Ishai-Michaeli R, Sasse J, Klagsbrun M. Endothelial cell-derived basic fibroblast growth factor: synthesis and deposition into the subendothelial extracellular matrix. Proc Natl Acad Sci USA 1987; 84:2292–2296.
104. Whalen GF, Shing Y, Folkman J. The fate of intravenously administered bFGF and the effect of heparin. Growth Factors 1989; 1:157–164.
105. Friedl A, Filla M, Rapraeger AC. Tissue-specific binding by FGF and FGF receptors to endogenous heparan sulfates. Methods Mol Biol 2001; 171:535–546.
106. Friedl A, Chang Z, Tierney A, Rapraeger AC. Differential binding of fibroblast growth factor-2 and -7 to basement membrane heparan sulfate: comparison of normal and abnormal human tissues. Am J Pathol 1997; 150:1443–1455.
107. Gospodarowicz D, Cheng J. Heparin protects basic and acidic FGF from inactivation. J Cell Physiol 1986; 128:475–484.
108. Edelman ER, Nugent MA. Controlled release of basic fibroblast growth factor. Drug News and Perspectives 1991; 4:352–357.
109. Sommer A, Rifkin DB. Interaction of heparin with human basic fibroblast growth factor: protection of the angiogenic protein from proteolytic degradation by a glycosaminoglycan. J Cell Physiol 1989; 138:215–220.
110. Saksela O, Moscatelli D, Sommer A, Rifkin DB. Endothelial cell-derived heparan sulfate binds basic fibroblast growth factor and protects it from proteolytic degradation. J Cell Biol 1988; 107:743–751.
111. Gitay-Goren H, Cohen T, Tessler S, Soker S, Gengrinovitch S, Rockwell P, Klagsbrun M, Levi BZ, Neufeld G. Selective binding of VEGF121 to one of the three vascular endothelial growth factor receptors of vascular endothelial cells. J Biol Chem 1996; 271:5519–5523.
112. Rogelj S, Klagsbrun M, Atzmon R, Kurokawa M, Haimovitz AZF, Vlodavsky I. Basic fibroblast growth factor is an extracellular matrix component required for supporting the proliferation of vascular endothelial cells and the differentiation of PC12 cells. J Cell Biol 1989; 109:823–831.
113. Nugent MA, Edelman ER. Transforming growth factor β1 stimulates the production of basic fibroblast growth factor binding proteoglycans in Balb/c3T3 cells. J Biol Chem 1992; 267:21256–21264.
114. Presta M, Maier JAM, Rusnati M, Ragnotti G. Basic fibroblast growth factor is released from endothelial extracellular matrix in a biologically active form. J Cell Physiol 1989; 140:68–74.
115. Bashkin P, Doctrow S, Klagsbrun M, Svahn CM, Folkman JIV. Basic fibroblast growth factor binds to subendothelial extracellular matrix and is released by heparitinase and heparin-like molecules. Biochemistry 1989; 28:1737–1743.
116. Vlodavsky I, Korner G, Ishai-Michaeli R, Bashkin P, Bar-Shavit R, Fuks Z. Extracellular matrix-resident growth factors and enzymes: possible

involvement in tumor metastasis and angiogenesis. Cancer and Metast Rev 1990; 9:203–226.
117. Rich CB, Nugent MA, Stone P, Foster JA. Elastase release of basic fibroblast growth factor in pulmonary fibroblast cultures results in down regulation of elastin gene transcription. J Biol Chem 1996; 271:23043–23048.
118. Liu J, Rich CB, Buczek-Thomas JA, Nugent MA, Panchenko MP, Foster JA. Heparin-binding EGF-like growth factor regulates elastin and FGF-2 expression in pulmonary fibroblasts. Am J Physiol Lung Cell Mol Physiol 2003; 285:L1106–1115.
119. Buczek-Thomas JA, Lucey EC, Stone PJ, Chu CL, Rich CB, Carreras I, Goldstein RH, Foster JA, Nugent MA. Elastase mediates the release of growth factors from lung in vivo. Am J Respir Cell Mol Biol 2004; 31:344–350.
120. Sellke FW, Laham RJ, Edelman ER, Pearlman JD, Simons M. Therapeutic angiogenesis with basic fibroblast growth factor: technique and early results. Ann Thorac Surg 1998; 65:1540–1544.
121. Laham RJ, Sellke FW, Edelman ER, Pearlman JD, Ware JA, Brown DL, Gold JP, Simons M. Local perivascular delivery of basic fibroblast growth factor in patients undergoing coronary bypass surgery: results of a phase I randomized, double-blind, placebo-controlled trial. Circulation 1999; 100:1865–1871.
122. Edelman ER, Mathiowitz E, Langer R, Klagsbrun M. Controlled and modulated release of basic fibroblast growth factor. Biomaterials 1991; 12:619–626.
123. Nugent MA, Chen OS, Edelman ER. Controlled release of fibroblast growth factor: activity in cell culture. Mat Res Soc Symp Proc 1992; 252:273–284.
124. Moscatelli D. Basic fibroblast growth factor (bFGF) dissociates rapidly from heparan sulfate but slowly from receptors. J Biol Chem 1992; 267: 25803–25809.
125. Dowd CJ, Cooney CL, Nugent MA. Heparan sulfate mediates bFGF transport through basement membrane by diffusion with rapid reversible binding. J Biol Chem 1999; 274:5236–5244.
126. Wang S, Ai X, Freeman SD, Pownall ME, Lu Q, Kessler DS, Emerson Jr CP. QSulf1, a heparan sulfate 6-*O*-endosulfatase, inhibits fibroblast growth factor signaling in mesoderm induction and angiogenesis. Proc Natl Acad Sci USA 2004; 101:4833–4838.
127. Ai X, Do AT, Lozynska O, Kusche-Gullberg M, Lindahl U, Emerson Jr CP. QSulf1 remodels the 6-*O*-sulfation states of cell surface heparan sulfate proteoglycans to promote Wnt signaling. J Cell Biol 2003; 162:341–351.
128. Dhoot GK, Gustafsson MK, Ai X, Sun W, Standiford DM, Emerson Jr CP. Regulation of Wnt signaling and embryo patterning by an extracellular sulfatase. Science 2001; 293:1663–1666.
129. Izvolsky KI, Zhong L, Wei L, Yu Q, Nugent MA, Cardoso WV. Heparan sulfates expressed in the distal lung are required for Fgf10 binding to the epithelium and for airway branching. Am J Physiol Lung Cell Mol Physiol 2003; 285:L838–846.
130. Izvolsky KI, Shoykhet D, Yang Y, Yu Q, Nugent MA, Cardoso WV. Heparan sulfate–FGF10 interactions during lung morphogenesis. Dev Biol 2003; 258:185–200.

131. Goerges AL, Nugent MA. pH regulates vascular endothelial growth factor binding to fibronectin: a mechanism for control of extracellular matrix storage and release. J Biol Chem 2004; 279:2307–2315.
132. Lin X, Buff EM, Perrimon N, Michelson AM. Heparan sulfate proteoglycans are essential for FGF receptor signaling during *Drosophila* embryonic development. Development 1999; 126:3715–3723.
133. Lin X, Perrimon N. Developmental roles of heparan sulfate proteoglycans in *Drosophila*. Glycoconj J 2002; 19:363–368.
134. San Antonio JD, Slover J, Lawler J, Karnovsky MJ, Lander AD. Specificity in the interactions of extracellular matrix proteins with subpopulations of the glycosaminoglycan heparin. Biochemistry 1993; 32:4746–4755.
135. Aviezer D, Hecht D, Safran M, Eisinger M, David G, Yayon A. Perlecan, basal lamina proteoglycan, promotes basic fibroblast growth factor binding, mitogenesis, and angiogenesis. Cell 1994; 79:1005–1013.
136. Sharma B, Handler M, Eichstetter I, Whitelock JM, Nugent MA, Iozzo RV. Antisense targeting of perlecan blocks tumor growth and angiogenesis in vivo. J Clin Invest 1998; 102:1599–1608.
137. Whitelock JM, Graham LD, Melrose J, Murdoch AD, Iozzo RV, Underwood PA. Human perlecan immunopurified from different endothelial cell sources has different adhesive properties for vascular cells. Matrix Biol 1999; 18:163–178.
138. Nugent MA, Nugent HM, Iozzo RV, Sanchack K, Edelman ER. Perlecan is required to inhibit thrombosis after deep vascular injury and contributes to endothelial cell-mediated inhibition of intimal hyperplasia. Proc Natl Acad Sci USA 2000; 97:6722–6727.
139. Whitelock JM, Murdoch AD, Iozzo RV, Underwood PA. The degradation of human endothelial cell-derived perlecan and release of bound basic fibroblast growth factor by stromelysin, collagenase, plasmin, and heparanases. J Biol Chem 1996; 271:10079–10086.
140. Weiser MC, Belknap JK, Grieshaber SS, Kinsella MG, Majack RA. Developmental regulation of perlecan gene expression in aortic smooth muscle cells. Matrix Biol 1996; 15:331–340.
141. Belknap JK, Weiser-Evans MC, Grieshaber SS, Majack RA, Stenmark KR. Relationship between perlecan and tropoelastin gene expression and cell replication in the developing rat pulmonary vasculature. Am J Respir Cell Mol Biol 1999; 20:24–34.
142. Kinsella MG, Tran PK, Weiser-Evans MC, Reidy M, Majack RA, Wight TN. Changes in perlecan expression during vascular injury: role in the inhibition of smooth muscle cell proliferation in the late lesion. Arterioscler Thromb Vasc Biol 2003; 23:608–614.
143. Castellot JJ, Addonizio ML, Rosenberg RD, Karnovsky MJ. Cultured endothelial cells produce a heparin-like inhibitor of smooth muscle growth. J Cell Biol 1981; 90:372–379.
144. Castellot JJ, Beeler DL, Rosenberg RD, Karnovsky MJ. Structural determinants of the capacity of heparin to inhibit the proliferation of vascular smooth muscle cells. J Cell Physiol 1984; 120:315–320.
145. Castellot JJ, Wong K, Herman B, Hoover RL, Albertini DF, Wright TC, Caleb BL, Karnovsky MJ. Binding and internalization of heparin by vascular smooth muscle cells. J Cell Physiol 1985; 124:13–20.

146. Castellot JJ, Rosenberg RD, Karnovsky MJ. Endothelium, heparin, and the regulation of vascular smooth muscle cell growth. In: Jaffe EA, ed. Biology of Endothelial Cells. Boston: Martinus Nijhoff Publishers, 1984; 118–128.
147. Clowes AW, Karnovsky MJ. Suppression by heparin of injury-induced myointimal thickening. J Surg Res 1978; 24:161–168.
148. Castellot JJ, Wright TC, Karnovsky MJ. Regulation of vascular smooth muscle cell growth by heparin and heparan sulfate. Semin Thromb Hemost 1987; 13:489–503.
149. Tran PK, Tran-Lundmark K, Soininen R, Tryggvason K, Thyberg J, Hedin U. Increased intimal hyperplasia and smooth muscle cell proliferation in transgenic mice with heparan sulfate-deficient perlecan. Circ Res 2004; 94: 550–558.
150. Bingley JA, Hayward IP, Campbell JH, Campbell GR. Arterial heparan sulfate proteoglycans inhibit vascular smooth muscle cell proliferation and phenotype change in vitro and neointimal formation in vivo. J Vasc Surg 1998; 28:308–318.
151. Bingley JA, Campbell JH, Hayward IP, Campbell GR. Inhibition of neointimal formation by natural heparan sulfate proteoglycans of the arterial wall. Ann NY Acad Sci 1997; 811:238–244.
152. Bix G, Fu J, Gonzalez EM, Macro L, Barker A, Campbell S, Zutter MM, Santoro SA, Kim JK, Hook M, Reed CC, Iozzo RV. Endorepellin causes endothelial cell disassembly of actin cytoskeleton and focal adhesions through alpha2beta1 integrin. J Cell Biol 2004; 166:97–109.
153. Gonzalez EM, Mongiat M, Slater SJ, Baffa R, Iozzo RV. A novel interaction between perlecan protein core and progranulin: potential effects on tumor growth. J Biol Chem 2003; 278:38113–38116.
154. Mongiat M, Fu J, Oldershaw R, Greenhalgh R, Gown AM, Iozzo RV. Perlecan protein core interacts with extracellular matrix protein 1 (ECM1), a glycoprotein involved in bone formation and angiogenesis. J Biol Chem 2003; 278:17491–17499.
155. Mongiat M, Sweeney SM, San Antonio JD, Fu J, Iozzo RV. Endorepellin, a novel inhibitor of angiogenesis derived from the *C terminus* of perlecan. J Biol Chem 2003; 278:4238–4249.
156. Ghiselli G, Eichstetter I, Iozzo RV. A role for the perlecan protein core in the activation of the keratinocyte growth factor receptor. Biochem J 2001; 359:153–163.
157. Moehren G, Markevich N, Demin O, Kiyatkin A, Goryanin I, Hoek JB, Kholodenko BN. Temperature dependence of the epidermal growth factor receptor signaling network can be accounted for by a kinetic model. Biochemistry 2002; 41:306–320.
158. Wiley HS, Shvartsman SY, Lauffenburger DA. Computational modeling of the EGF-receptor system: a paradigm for systems biology. Trends Cell Biol 2003; 13:43–50.
159. Kholodenko BN, Demin OV, Moehren G, Hoek JB. Quantification of short term signaling by the epidermal growth factor receptor. J Biol Chem 1999; 274:30169–30181.
160. Park CS, Schneider IC, Haugh JM. Kinetic analysis of platelet-derived growth factor receptor/phosphoinositide 3-kinase/Akt signaling in fibroblasts. J Biol Chem 2003; 278:37064–37072.

161. Forsten-Williams K, Chua CC, Nugent MA. The kinetics of FGF-2 binding to heparan sulfate proteoglycans and MAP kinase signaling. J Theo Biol 2005:483–499.
162. Filion RJ, Popel AS. A reaction-diffusion model of basic fibroblast growth factor interactions with cell surface receptors. Ann Biomed Eng 2004; 32:645–663.
163. Mac Gabhann F, Popel AS. Differential binding of VEGF isoforms to VEGF receptor 2 in the presence of Neuropilin-1: a computational model. Am J Physiol Heart Circ Physiol 2005; 288:H2851–2860.
164. Mac Gabhann F, Popel AS. Model of competitive binding of vascular endothelial growth factor and placental growth factor to VEGF receptors on endothelial cells. Am J Physiol Heart Circ Physiol 2004; 286:H153–164.
165. Patton WA, 2nd, Granzow CA, Getts LA, Thomas SC, Zotter LM, Gunzel KA, Lowe-Krentz LJ. Identification of a heparin-binding protein using monoclonal antibodies that block heparin binding to porcine aortic endothelial cells. Biochem J 1995; 311 (Part 2):461–469.
166. Glimelius B, Busch C, Hook M. Binding of heparin on the surface of cultured human endothelial cells. Thromb Res 1978; 12:773–782.
167. Castellot JJ, Cochran DL, Karnovsky MJ. Effect of heparin on vascular smooth muscle cells. I. Cell metabolism. J Cell Physiol 1985; 124:21–28.
168. Letourneur D, Caleb BL, Castellot Jr JJ. Heparin binding, internalization, and metabolism in vascular smooth muscle cells. I. Upregulation of heparin binding correlates with antiproliferative activity. J Cell Physiol 1995; 165:676–686.
169. Letourneur D, Caleb BL, Castellot Jr JJ. Heparin binding, internalization, and metabolism in vascular smooth muscle cells. II. Degradation and secretion in sensitive and resistant cells. J Cell Physiol 1995; 165:687–695.
170. Karnovsky MJ, Wright Jr TC, Castellot Jr JJ, Choay J, Lormeau JC, Petitou M. Heparin, heparan sulfate, smooth muscle cells, and atherosclerosis. Ann NY Acad Sci 1989; 556:268–281.
171. Delmolino LM, Castellot Jr JJ. Heparin suppresses sgk, an early response gene in proliferating vascular smooth muscle cells. J Cell Physiol 1997; 173:371–379.
172. Mishra-Gorur K, Castellot Jr JJ. Heparin rapidly and selectively regulates protein tyrosine phosphorylation in vascular smooth muscle cells. J Cell Physiol 1999; 178:205–215.
173. Mishra-Gorur K, Singer HA, Castellot Jr JJ. Heparin inhibits phosphorylation and autonomous activity of Ca(2+)/calmodulin-dependent protein kinase II in vascular smooth muscle cells. Am J Pathol 2002; 161:1893–1901.
174. Daum G, Hedin U, Wang Y, Wang T, Clowes AW. Diverse effects of heparin on mitogen-activated protein kinase-dependent signal transduction in vascular smooth muscle cells. Circ Res 1997; 81:17–23.
175. Pukac LA, Castellot Jr JJ, Wright Jr TC, Caleb BL, Karnovsky MJ. Heparin inhibits c-fos and c-myc mRNA expression in vascular smooth muscle cells. Cell Regul 1990; 1:435–443.
176. Horowitz A, Simons M. Regulation of syndecan-4 phosphorylation in vivo. J Biol Chem 1998; 273:10914–10918.

177. Horowitz A, Simons M. Phosphorylation of the cytoplasmic tail of syndecan-4 regulates activation of protein kinase Calpha. J Biol Chem 1998; 273:25548–25551.
178. Oh ES, Couchman JR, Woods A. Serine phosphorylation of syndecan-2 proteoglycan cytoplasmic domain. Arch Biochem Biophys 1997; 344:67–74.
179. Oh ES, Woods A, Couchman JR. Multimerization of the cytoplasmic domain of syndecan-4 is required for its ability to activate protein kinase C. J Biol Chem 1997; 272:11805–11811.
180. Oh ES, Woods A, Couchman JR. Syndecan-4 proteoglycan regulates the distribution and activity of protein kinase C. J Biol Chem 1997; 272:8133–8136.
181. Lee D, Oh ES, Woods A, Couchman JR, Lee W. Solution structure of a syndecan-4 cytoplasmic domain and its interaction with phosphatidylinositol 4,5-bisphosphate. J Biol Chem 1998; 273:13022–13029.
182. Kinnunen T, Kaksonen M, Saarinen J, Kalkkinen N, Peng HB, Rauvala H. Cortactin-Src kinase signaling pathway is involved in *N*-syndecan-dependent neurite outgrowth. J Biol Chem 1998; 273:10702–10708.
183. Lebakken CS, McQuade KJ, Rapraeger AC. Syndecan-1 signals independently of beta1 integrins during Raji cell spreading. Exp Cell Res 2000; 259:315–325.
184. Beauvais DM, Rapraeger AC. Syndecans in tumor cell adhesion and signaling. Reprod Biol Endocrinol 2004; 2:3.
185. Beauvais DM, Burbach BJ, Rapraeger AC. The syndecan-1 ectodomain regulates $\alpha v \beta 3$ integrin activity in human mammary carcinoma cells. J Cell Biol 2004; 167:171–181.
186. Asthagiri AR, Nelson CM, Horwitz AF, Lauffenburger DA. Quantitative relationship among integrin-ligand binding, adhesion, and signaling via focal adhesion kinase and extracellular signal-regulated kinase 2. J Biol Chem 1999; 274:27119–27127.
187. O'Keefe Jr JH, Hartzler GO. Restenosis after coronary angioplasty. J Inv Car 1989; 1:109–122.
188. McBride W, Lange RA, Hillis LD. Restenosis after successful coronary angioplasty: pathophysiology and prevention. New Engl J Med 1988; 318:1734–1738.
189. Ip JH, Fuster V, Badimon L, Badimon J, Taubman MB, Chesebro JH. Syndromes of accelerated atherosclerosis: role of vascular injury and smooth muscle proliferation. J Am Coll Cardiol 1990; 15:1667–1687.
190. Bhargava B, Karthikeyan G, Abizaid AS, Mehran R. New approaches to preventing restenosis. BMJ 2003; 327:274–279.
191. Losordo DW, Isner JM, Diaz-Sandoval LJ. Endothelial recovery: the next target in restenosis prevention. Circulation 2003; 107:2635–2637.
192. Association AH. Cardiovascular disease statistics. www.americanheartorg 2000:Heart_and_Stroke_A_Z_Guide/cvds.html.
193. Association AH. Heart Disease and Stroke Statistics – 2004 Update. Dallas: American Heart Association, Inc 2004; 1–52.
194. Ross R, Glomset JA. The pathogenesis of atherosclerosis (first of two parts). N Engl J Med 1976; 295:369–377.
195. Ross R. The pathogenesis of atherosclerosis – an update. N Engl J Med 1986; 314:488–500.

196. Ross R. The pathogenesis of atherosclerosis: a perspective for the 1990s. Nature 1993; 362:801–808.
197. Ross R. Atherosclerosis – an inflammatory disease [see comments]. N Engl J Med 1999; 340:115–126.
198. Moreno PR, Palacios IF, Leon MN, Rhodes J, Fuster V, Fallon JT. Histopathologic comparison of human coronary in-stent and post-balloon angioplasty restenotic tissue. Am J Cardiol 1999; 84:462–466.
199. Fishman JA, Ryan GB, Karnovsky MJ. Endothelial regeneration in the rat carotid artery and significance of endothelial denudation in the pathogenesis of myointimal thickening. Lab Invest 1975; 32:339–351.
200. Clowes AW, Reidy MA, Clowes MM. Kinetics of cellular proliferation after arterial injury I. Smooth muscle growth in the absence of endothelium. Lab Invest 1983; 49:327–333.
201. Clowes AW, Clowes MM. Kinetics of cellular proliferation after arterial injury II. Inhibition of smooth muscle growth by heparin. Lab Invest 1985; 52:611–616.
202. Hales CA, Kradin RL, Brandstetter RD, Zhu YJ. Impairment of hypoxic pulmonary artery remodeling by heparin in mice. Am Rev Respir Dis 1983; 128:747–751.
203. Hirsch GM, Karnovsky MJ. Inhibition of vein graft intimal proliferative lesions in the rat by heparin. Am J Pathol 1991; 139:581–587.
204. Hopwood J, Hook M, Linker A, Lindahl U. Anticoagulant activity of heparin: isolation of antithrombin-binding sites. FEBS Lett 1976; 69:51–54.
205. Beeler D, Rosenberg R, Jordan R. Fractionation of low molecular weight heparin species and their interaction with antithrombin. J Biol Chem 1979; 254:2902–2913.
206. Guyton JR, Rosenberg RD, Clowes AW, Karnovsky MJ. Inhibition of rat arterial smooth muscle cell proliferation by heparin I. In vivo studies with anticoagulant and non-anticoagulant heparin. Circ Res 1980; 46:625–634.
207. Hoover RL, Rosenberg R, Haering W, Karnovsky MJ. Inhibition of rat arterial smooth muscle cell proliferation by heparin II. In vitro studies. Circ Res 1980; 47:578–583.
208. Benitz WE, Lessler DS, Coulson JD, Bernfield M. Heparin inhibits proliferation of fetal vascular smooth muscle cells in the absence of platelet-derived growth factor. J Cell Physiol 1986; 127:1–7.
209. Castellot Jr JJ, Hoover RL, Harper PA, Karnovsky MJ. Heparin and glomerular epithelial cell-secreted heparin-like species inhibit mesangial-cell proliferation. Am J Pathol 1985; 120:427–435.
210. Clowes AW, Clowes MM. Kinetics of cellular proliferation after arterial injury II. Inhibition of smooth muscle growth by heparin. Lab Invest 1985; 52:611–616.
211. Majesky MW, Schwartz SM, Clowes MM, Clowes AW. Heparin regulates smooth muscle S phase entry in the injured rat carotid artery. Circ Res 1987; 61:296–300.
212. Kinsella MG, Irvin C, Reidy MA, Wight TN. Removal of heparan sulfate by heparinase treatment inhibits FGF-2-dependent smooth muscle cell proliferation in injured rat carotid arteries. Atherosclerosis 2004; 175:51–57.
213. Francis DJ, Parish CR, McGarry M, Santiago FS, Lowe HC, Brown KJ, Bingley JA, Hayward IP, Cowden WB, Campbell JH, Campbell GR,

Chesterman CN, Khachigian LM. Blockade of vascular smooth muscle cell proliferation and intimal thickening after balloon injury by the sulfated oligosaccharide PI-88: phosphomannopentaose sulfate directly binds FGF-2, blocks cellular signaling, and inhibits proliferation. Circ Res 2003; 92:e70–77.

214. Myler HA, West JL. Heparanase and platelet factor-4 induce smooth muscle cell proliferation and migration via bFGF release from the ECM. J Biochem (Tokyo) 2002; 131:913–922.
215. Silver PJ, Moreau JP, Denholm E, Lin YQ, Nguyen L, Bennett C, Recktenwald A, DeBlois D, Baker S, Ranger S. Heparinase III limits rat arterial smooth muscle cell proliferation in vitro and in vivo. Eur J Pharmacol 1998; 351:79–83.
216. Campbell JH, Rennick RE, Kalevitch SG, Campbell GR. Heparan sulfate-degrading enzymes induce modulation of smooth muscle phenotype. Exp Cell Res 1992; 200:156–167.
217. Edelman ER, Adams DA, Karnovsky MJ. Effect of controlled adventitial heparin delivery on smooth muscle cell proliferation following endothelial injury. Proc Natl Acad Sci USA 1990; 87:3773–3777.
218. Edelman ER, Karnovsky MJ. Contrasting effects of the intermittent and continuous administration of heparin in experimental restenosis. Circulation 1994; 89:770–776.
219. Rogers C, Karnovsky MJ, Edelman ER. Inhibition of experimental neointimal hyperplasia and thrombosis depends on the type of vascular injury and the site of drug administration. Circulation 1993; 88:1215–1221.
220. Wright TC, Castellot JJ, Petitou M, Lormeau J-C, Choay J, Karnovsky MJ. Structural determinants of heparin's growth inhibitory activity. J Biol Chem 1989; 264:1534–1542.
221. Edelman ER, Karnovsky MJ. Heparin/heparan sulfate regulation of vascular smooth muscle cell behavior. In: Page C, Black J, eds. Airway and Vascular Remodeling in Asthma and Cadiovascular Diseases: Implications for Therapeutic Interventions. London: Academic Press, 1994; 45–70.
222. Fritze L, Reilly C, Rosenberg R. An antiproliferative heparan sulfate species produced by postconfluent smooth muscle cells. J Cell Biol 1985; 100: 1041–1049.
223. Bjornsson TD, Dryjski M, Tluczek J, Mennie R, Ronan J, Mellin TN, Thomas KA. Acidic fibroblast growth factor promotes vascular repair. PNAS (USA) 1991; 88:8661–8665.
224. Asahara T, Bauters C, Pastore C, Kearney M, Rossow S, Bunting S, Ferrara N, Symes JF, Isner JM. Local delivery of vascular endothelial growth factor accelerates re-endothelialization and attenuates intimal hyperplasia in balloon-injured rat carotid artery. Circulation 1995; 91:2793–2801.
225. Asahara T, Chen D, Tsurumi Y, Kearney M, Rossow S, Passeri J, Symes JF, Isner JM. Accelerated restitution of endothelial integrity and endothelium-dependent function after phVEGF165 gene transfer. Circulation 1996; 94:3291–3302.
226. Swanson N, Hogrefe K, Javed Q, Malik N, Gershlick AH. Vascular endothelial growth factor (VEGF)-eluting stents: in vivo effects on thrombosis, endothelialization and intimal hyperplasia. J Invasive Cardiol 2003; 15: 688–692.

227. Van Belle E, Tio FO, Chen D, Maillard L, Kearney M, Isner JM. Passivation of metallic stents after arterial gene transfer of phVEGF165 inhibits thrombus formation and intimal thickening. J Am Coll Cardiol 1997; 29:1371–1379.
228. Hedman M, Hartikainen J, Syvanne M, Stjernvall J, Hedman A, Kivela A, Vanninen E, Mussalo H, Kauppila E, Simula S, Narvanen O, Rantala A, Peuhkurinen K, Nieminen MS, Laakso M, Yla-Herttuala S. Safety and feasibility of catheter-based local intracoronary vascular endothelial growth factor gene transfer in the prevention of postangioplasty and in-stent restenosis and in the treatment of chronic myocardial ischemia: phase II results of the Kuopio Angiogenesis Trial (KAT). Circulation 2003; 107:2677–2683.
229. Edelman ER, Pukac LA, Karnovsky MJ. Protamine and protamine insulins exacerbate vascular injury. J Clin Invest 1993; 91:2308–2313.
230. Lindner V, Olson NE, Clowes AW, Reidy MA. Inhibition of smooth muscle cell proliferation in injured rat arteries. Interaction of heparin with basic fibroblast growth factor. J Clin Invest 1992; 90:2044–2049.
231. Lindner V, Reidy MA. Role of basic fibroblast growth factor in proliferation of endothelium and smooth muscle after denuding injury in vivo. Exs 1992; 61:386–388.
232. Edelman ER, Nugent MA, Smith LT, Karnovsky MJ. Basic fibroblast growth factor enhances the coupling of intimal hyperplasia and proliferation of vasa vasorum in injured rat arteries. J Clin Invest 1992; 89:465–473.
233. Schmidt A, Yoshida K, Buddecke E. The antiproliferative activity of arterial heparan sulfate residues in domains enriched with 2-*O*-sulfated uronic acid residues. J Biol Chem 1992; 267:19242–19247.
234. Schmidt A, Lemming G, Yoshida K, Buddecke E. Molecular organization and antiproliferative domains of arterial tissue heparan sulfate. Eur J Cell Biol 1992; 59:322–328.
235. Nader HB, Buonassisi V, Colburn P, Dietrich CP. Heparin stimulates the synthesis and modifies the sulfation pattern of heparan sulfate proteoglycan from endothelial cells. J Cell Physiol 1989; 140:305–310.
236. Vlodavsky I, Eldor A, Haimovitz-Friedman A, Matzner Y, Ishai-Michaeli R, Lider O, Naparstek Y, Cohen IR, Fuks Z. Expression of heparanase by platelets and circulating cells of the immune system: possible involvement in diapedesis and extravasation. Invasion Metastasis 1992; 12:112–127.
237. Ishai-Michaeli R, Eldor A, Vlodavsky I. Heparanase activity expressed by platelets, neutrophils, and lymphoma cells releases active fibroblast growth factor from extracellular matrix. Cell Regul 1990; 1:833–842.
238. Mulloy B, Linhardt RJ. Order out of complexity – protein structures that interact with heparin. Curr Opin Struct Biol 2001; 11:623–628.
239. Lindner V, Lappi DA, Baird A, Majack RA, Reidy MA. Role of basic fibroblast growth factor in vascular lesion formation. Circ Res 1991; 68:106–113.
240. Edelman ER, Nugent MA, Karnovsky MJ. Perivascular and intravenous administration of basic fibroblast growth factor: vascular and solid organ deposition. Proc Natl Acad Sci USA 1993; 90:1513–1517.
241. Schwartz SM, Gajdusek CM, Reidy MA, Selden SCd, Haudenschild CC. Maintenance of integrity in aortic endothelium. Fed Proc 1980; 39: 2618–2625.

242. Rubanyi GM. The role of endothelium in cardiovascular homeostasis and diseases. J Cardiovasc Pharmacol 1993; 22:S1–14.
243. Schwartz SM, Reidy MA, O'Brien ER. Assessment of factors important in atherosclerotic occlusion and restenosis. Thromb Haemost 1995; 74:541–551.
244. Han RO, Ettenson DS, Koo EW, Edelman ER. Heparin/heparan sulfate chelation inhibits control of vascular repair by tissue-engineered endothelial cells. Am J Physiol 1997; 273:H2586–2595.
245. Nugent HM, Rogers C, Edelman ER. Endothelial implants inhibit intimal hyperplasia after porcine angioplasty. Circ Res 1999; 84:384–391.
246. Zacharski LR, Ornstein DL, Mamourian AC. Low-molecular-weight heparin and cancer. Semin Thromb Hemost 2000; 26 (Suppl 1):69–77.
247. Hettiarachchi RJ, Smorenburg SM, Ginsberg J, Levine M, Prins MH, Buller HR. Do heparins do more than just treat thrombosis? The influence of heparins on cancer spread. Thromb Haemost 1999; 82:947–952.
248. Cosgrove RH, Zacharski LR, Racine E, Andersen JC. Improved cancer mortality with low-molecular-weight heparin treatment: a review of the evidence. Semin Thromb Hemost 2002; 28:79–87.
249. Bobek V, Kovarik J. Antitumor and antimetastatic effect of warfarin and heparins. Biomed Pharmacother 2004; 58:213–219.
250. Kumar V, Abbas AK, Fausto N, Robbins SL, Cotran RS. Robbins and Cotran Pathologic Basis of Disease, 7th ed. Philadelphia: Elsevier Saunders, 2005.
251. Liu D, Shriver Z, Qi Y, Venkataraman G, Sasisekharan R. Dynamic regulation of tumor growth and metastasis by heparan sulfate glycosaminoglycans. Semin Thromb Hemost 2002; 28:67–78.
252. Sasisekharan R, Shriver Z, Venkataraman G, Narayanasami U. Roles of heparan-sulphate glycosaminoglycans in cancer. Nat Rev Cancer 2002; 2:521–528.
253. Smorenburg SM, Van Noorden CJ. The complex effects of heparins on cancer progression and metastasis in experimental studies. Pharmacol Rev 2001; 53:93–105.
254. Castelli R, Porro F, Tarsia P. The heparins and cancer: review of clinical trials and biological properties. Vasc Med 2004; 9:205–213.
255. Sanderson RD. Heparan sulfate proteoglycans in invasion and metastasis. Semin Cell Dev Biol 2001; 12:89–98.
256. Filmus J. Glypicans in growth control and cancer. Glycobiology 2001; 11:19R–23R.
257. Liu D, Shriver Z, Venkataraman G, El Shabrawi Y, Sasisekharan R. Tumor cell surface heparan sulfate as cryptic promoters or inhibitors of tumor growth and metastasis. Proc Natl Acad Sci USA 2002; 99:568–573.
258. Jayson GC, Lyon M, Paraskeva C, Turnbull JE, Deakin JA, Gallagher JT. Heparan sulfate undergoes specific structural changes during the progression from human colon adenoma to carcinoma in vitro. J Biol Chem 1998; 273: 51–57.
259. Iozzo RV. Presence of unsulfated heparan chains on the heparan sulfate proteoglycan of human colon carcinoma cells. Implications for heparan sulfate proteoglycan biosynthesis. J Biol Chem 1989; 264:2690–2699.

260. DeBaun MR, Ess J, Saunders S. Simpson Golabi Behmel syndrome: progress toward understanding the molecular basis for overgrowth, malformation, and cancer predisposition. Mol Genet Metab 2001; 72:279–286.
261. Folkman J. Angiogenesis-dependent diseases. Semin Oncol 2001; 28: 536–542.
262. Dvorak HF. Vascular permeability factor/vascular endothelial growth factor: a critical cytokine in tumor angiogenesis and a potential target for diagnosis and therapy. J Clin Oncol 2002; 20:4368–4380.
263. Levene CI, Kapoor R, Heale G. The effect of hypoxia on the synthesis of collagen and glycosaminoglycans by cultured pig aortic endothelium. Atherosclerosis 1982; 44:327–337.
264. Li J, Shworak NW, Simons M. Increased responsiveness of hypoxic endothelial cells to FGF2 is mediated by HIF-1alpha-dependent regulation of enzymes involved in synthesis of heparan sulfate FGF2-binding sites. J Cell Sci 2002; 115:1951–1959.
265. Furuta GT, Dzus AL, Taylor CT, Colgan SP. Parallel induction of epithelial surface-associated chemokine and proteoglycan by cellular hypoxia: implications for neutrophil activation. J Leukoc Biol 2000; 68:251–259.
266. Detmar M, Brown LF, Berse B, Jackman RW, Elicker BM, Dvorak HF, Claffey KP. Hypoxia regulates the expression of vascular permeability factor/vascular endothelial growth factor (VPF/VEGF) and its receptors in human skin. J Invest Dermatol 1997; 108:263–268.
267. Fukumura D, Xu L, Chen Y, Gohongi T, Seed B, Jain RK. Hypoxia and acidosis independently up-regulate vascular endothelial growth factor transcription in brain tumors in vivo. Cancer Res 2001; 61:6020–6024.
268. Jain RK. Molecular regulation of vessel maturation. Nat Med 2003; 9:685–693.
269. Venkataraman G, Shriver Z, Raman R, Sasisekharan R. Sequencing complex polysaccharides. Science 1999; 286:537–542.
270. Nugent MA. Heparin sequencing brings structure to the function of complex oligosaccharides. Proc Natl Acad Sci USA 2000; 97:10301–10303.
271. Sears P, Wong CH. Toward automated synthesis of oligosaccharides and glycoproteins. Science 2001; 291:2344–2350.
272. Plante OJ, Palmacci ER, Seeberger PH. Automated solid-phase synthesis of oligosaccharides. Science 2001; 291:1523–1527.
273. Naggar EF, Costello CE, Zaia J. Competing fragmentation processes in tandem mass spectra of heparin-like glycosaminoglycans. J Am Soc Mass Spectrom 2004; 15:1534–1544.
274. Zaia J, Li XQ, Chan SY, Costello CE. Tandem mass spectrometric strategies for determination of sulfation positions and uronic acid epimerization in chondroitin sulfate oligosaccharides. J Am Soc Mass Spectrom 2003; 14:1270–1281.

Chemistry and Biology of Heparin and Heparan Sulfate
H.G. Garg, R.J. Linhardt and C.A. Hales (Editors)

Chapter 20

Heparin and Low Molecular Weight Heparin in Thrombosis and Inflammation: Emerging Links

SHAKER A. MOUSA

The Pharmaceutical Research Institute and Albany College of Pharmacy, Albany, NY, USA

I. Introduction

In recent years, clinical data and studies have clarified the potential and shortcomings of anticoagulant therapy in the prevention and treatment of thromboembolic disorders. The discovery and introduction of heparin derivatives such as low molecular weight heparins (LMWHs) have enhanced the clinical options for the management of thromboembolic disorders while enhancing the safety of therapy. In the United States, LMWHs are currently approved for the prophylaxis and treatment of deep vein thrombosis (DVT). LMWH uses are also being expanded for additional indications for the management of unstable angina and non-Q-wave myocardial infarction (1–4). In addition to the approved uses, LMWHs are currently being tested for several newer indications. Being polypharmacological agents, these drugs are expected to find uses in several other clinical indications, such inflammatory diseases and cancer. Additional pharmacological studies and well-designed clinical trials in which various pharmacokinetic and pharmacodynamic parameters are studied will provide additional evidence on the clinical individuality of each member of this class of novel agents (1–4). The key reason behind the success of heparin in thrombosis and beyond is its polypharmacological site of action for the prevention and treatment of multifactorial diseases that will only benefit slightly with a single pharmacological mechanism-based agent. Thromboembolic disorders are driven by hypercoaguable, hyperactive platelet, pro-inflammatory, endothelial dysfunction, and pro-angiogenesis

states. Heparin can effectively modulate all of those multifactorial components as well as the interface among those components.

Because heparin was discovered over a half century ago, our knowledge of the chemical structure and molecular interactions of this fascinating poly-component was limited at the early stages of its development. Through the efforts of major multidisciplinary groups of researchers and clinicians, it is now well recognized that heparin has multiple sites of actions and can be used in multiple indications. In the not-too-distant future, we may witness the impact of these drugs on the management of various diseases.

II. Emerging Links Between Thrombosis and Inflammation: Potential Role of Heparin

Several lines of evidence demonstrated the interplay between the platelet/leukocyte in the activated state and the coagulation cascade. That led to the exposure of the platelet GPIIb/IIIa receptors in its active state, leading to platelet fibrinogen binding and amplification of platelet aggregate formation. Activated platelets also interact with leukocytes, leading to platelet–leukocyte cohesion and leukocyte activation. Hyperactive platelets also provide a surface for thrombin generation and platelet–leukocyte interactions. Additionally, there is significant interplay among the coagulation cascade, platelets, and the vessel wall in the promotion of thromboembolic disorders. Depending upon the shear level venous (low shear) *vs* arterial (high shear), platelet/fibrin proportions and contributions vary.

For example, infection leading to the initiation of pro-inflammatory stimuli could be a major predisposing factor in propagation of thromboembolic disorders. Endotoxin that can be liberated from *Escherichia coli* and other bacteria can induce a pro-inflammatory state with the increase of tissue necrosis factor-α (TNF-α) and other cytokines (Fig. 1). That would lead to the activation of leukocytes, with increased expression of membrane L-selectin and the shedding of soluble L-selectin, which can serve as a surrogate marker of leukocyte activation. Activation of leukocyte leads to the propagation and generation of tissue factor, which initiates and amplifies a hypercoaguable state as well as the up-regulation of TNF-α production (Fig. 1). A hypercoaguable state with the generation of thrombin activates the platelets, leading to the overexpression of platelet membrane p-selectin and the shedding of soluble p-selectin, which can act as a surrogate marker of platelet activation (5). Additionally, the pro-inflammatory state can induce endothelial cell (EC) insult, leading to increased EC membrane expression and shedding of soluble vascular adhesion molecule-1 (VCAM-1), intracellular adhesion molecule-1 (ICAM-1), and E-selectin (Fig. 1). Furthermore, emerging links are shown between thrombosis, angiogenesis, and inflammation in vascular, cardiovascular, and inflammatory disorders (Fig. 2).

Heparin is a glycoaminoglycan formed by sulfated oligosaccharides and it varies in the length of polymeric units and therefore has different molecular weights. LMWH is made by partial hydrolysis or enzymatic degradation of unfractionated

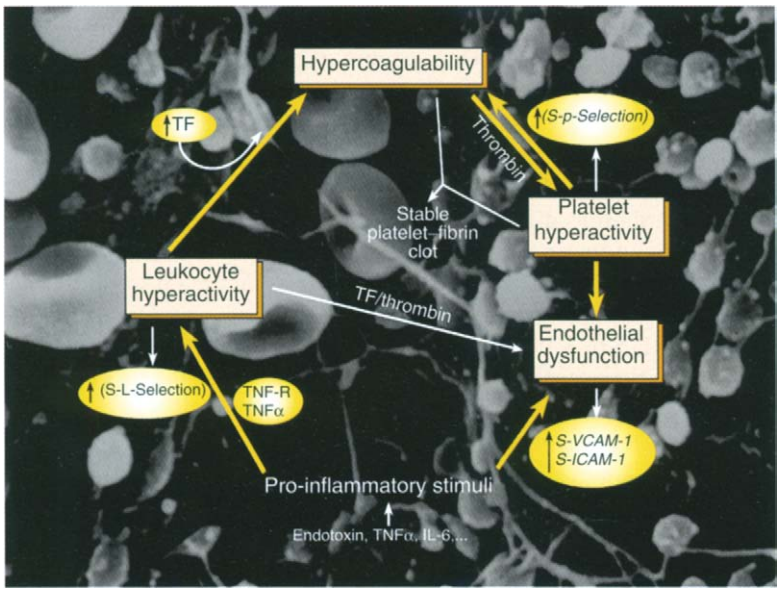

Figure 1 Amplifications of thrombosis by pro-inflammatory stimuli and the generation of soluble markers reflecting hypercoagulation, platelet hyperactivity, and endothelial cell activation.

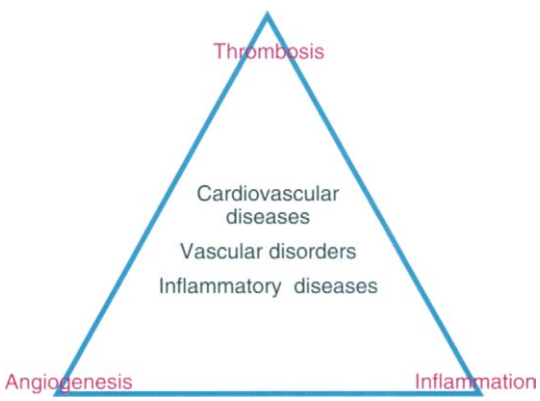

Figure 2 Emerging links between thrombosis, angiogenesis, and inflammation in vascular, cardiovascular, and inflammatory diseases.

heparin (UFH). Heparin and LMWH prevent the process of blood coagulation and have a natural anti-thrombin effect. In recent years, several studies have shown that heparin and LMWH have an obvious anti-inflammatory activity in addition to its traditional anticoagulant effects (6,7). In animal models, heparin disaccharides inhibited TNF-α production by macrophages and decreased immune inflammation (8). Heparin accelerated the healing process of mucosa in colitis in several clinical studies and had anti-inflammatory effects (9–14). Therefore, administration of heparin can afford both anti-inflammatory and anticoagulant effects. The effects of heparin on platelet surface P-selectin and interleukin (IL)-8 have not been studied. The present study was designed to observe the effects of LMWH on platelet surface P-selectin expression, serum IL-8 production, and TNF-α expression in mucosa of rats with trinitrobenzene sulphonic acid (TNBS)-induced colitis, as well as to clarify the anti-inflammatory mechanisms of LMWH in the treatment of colitis.

A. Heparin and Asthma

The significant reduction in symptoms within 10 min might be related to the ability of heparin to prevent the release of histamine from mast cells. Heparin may interfere with stimulation of mast cell mediator secretion by blocking internal calcium release. Later on, heparin may reduce eosinophil recruitment through different mechanisms: by preventing mast cell mediator release, heparin could indirectly down-regulate adhesion molecules on EC, and thus limit eosinophil migration into the nasal mucosa (15–17). Furthermore, the heavily anionic heparin may inactivate platelet-activating factor, a cationic protein with a potent chemotactic activity for human eosinophils. Intranasal heparin attenuated the nasal response to an allergic challenge in atopic rhinitic subjects, and no adverse reaction was noted (15–17). More studies are needed to completely explain the mechanisms by which heparin produces its anti-inflammatory activity; this will allow us to optimize heparin use in allergic diseases, such as rhinitis and asthma.

The anti-inflammatory activity of heparin has been reinforced by positive, although small, clinical trials in patients suffering from a range of inflammatory diseases, including rheumatoid arthritis and bronchial asthma (18,19). In addition, a number of clinical studies have recently demonstrated the anti-inflammatory activity of heparin in the treatment of inflammatory bowel disease at doses that do not produce antihemorrhagic complications (20). Given that it is now well recognized that different portions of the heparin molecule exhibit anti-inflammatory activity and that a pentasaccharide sequence retains the ability to inhibit antithrombin III (21), it is possible that the anti-inflammatory actions of heparin are distinct from its anticoagulant activity (22).

B. Heparin/Low Molecular Weight Heparin and Inflammatory Bowel Diseases

Under various experimental and clinical conditions, heparin was found to actively reduce the process of leukocyte recruitment into the site of injury or of application

of inflammatory stimuli. Salas et al. (23) provided evidence for the first *in vivo* mechanism responsible for the anti-migratory action of heparin. In fact, intravital microscopy techniques have allowed direct observation of inflamed microvascular beds with definition of the paradigm of white blood cell extravasation. Leukocyte interaction with the endothelium of an inflamed post-capillary venule is initially intermittent and dynamic (cell rolling); it then becomes static (firm adhesion) and is finally followed by diapedesis (24). Using the potent cytokine, TNF-α, to promote this cascade of events *in vivo*, Salas et al. (23) reported that heparin down-regulated TNF-α-induced leukocyte rolling, adhesion, and migration into gut tissue without affecting changes in vascular permeability. These data extend and confirm previous studies in which heparin reduced leukocyte adhesion to vascular ECS *in vitro* (25) and recruitment of inflammatory cells into other tissues during an experimental inflammatory reaction (22).

Several uncontrolled studies have suggested that heparin may be potentially therapeutic in the clinical management of both ulcerative colitis and Crohn's disease. Although these studies included only a limited number of patients, they demonstrated apparent beneficial effects of heparin with no associated hemorrhagic complications (26–33). In addition, heparin has been shown to prevent macroscopic inflammatory lesions in an animal model of experimental colitis (5). However, the molecular mechanisms by which heparin may help patients with inflammatory bowel disease (IBD) are unknown.

A large body of evidence supports the concept that heparin has anti-inflammatory actions; among these include modulation of some of the pathophysiological effects of endotoxin and TNF-α, such as neutrophil migration, edema formation, pulmonary hypertension, and hypoxemia (6–11). Moreover, heparin has been shown to suppress selected neutrophil functions, such as superoxide generation (12) and chemotaxis *in vitro* (13,14), to reduce eosinophil migration (12), and to diminish vascular permeability (34,35). Among the mechanisms that may account for the anti-inflammatory actions of heparin, binding of this glycosaminoglycan to adhesion molecules expressed on the surface of activated ECs and/or leukocytes has been proposed. Recent *in vitro* studies have demonstrated the ability of heparin to effectively bind to endothelial P-selectin but not E-selectin (6,36), as well as L-selectin and CD11b/CD18 expressed on neutrophils (37,38). Taken together, these reports suggest that the therapeutic actions of heparin observed in IBD patients may involve attenuation of inflammatory processes as well as a hypercoaguable state associated with clinical exacerbation of IBD, effects that may promote mucosal repair.

III. Heparin *vs* Low Molecular Weight Heparin

In contrast to UFH, LMWHs have a lower affinity to bind to plasma proteins, ECs, and macrophages. This difference in binding profile explains the pharmacokinetic differences observed between LMWHs and UFH. The binding of UFH to plasma proteins reduces its anticoagulant activity, which combined with the variations in

plasma concentrations of heparin-binding proteins, is reflected in its unpredictable anticoagulant response (Table 1).

LMWHs exhibit improved subcutaneous bioavailability; lower protein binding; longer half-life; variable number of antithrombin III binding sites; variable glycosaminoglycan contents; variable anti-serine protease activities (anti-Xa, anti-IIa, anti-Xa/anti-IIa ratio, and other anti-coagulation factors); variable potency in releasing tissue factor pathway inhibitor (TFPI); and variable levels of vascular EC binding kinetics (39–42). For these reasons, over the last decade LMWHs have increasingly replaced UFH in the prevention and treatment of venous thromboembolic disorders (VTE). Randomized clinical trials have demonstrated that individual LMWHs used at optimized dosages are at least as effective as and probably safer than UFH. The convenient once or twice daily SC dosing regimen without the need for monitoring has encouraged the wide use of LMWHs. It is well established that different LMWHs vary in their physical and chemical properties due to the differences in their methods of manufacturing. These differences translate into differences in their pharmacodynamic and pharmacokinetic characteristics (40). The World Health Organization (WHO) and United States Food and Drug Administration (US-FDA) regard LMWHs as individual drugs that cannot be used interchangeably (40).

Bioavailability of LMWHs after IV or SC administration is greater than for UFH and was determined to be between ~87% and 98%. UFH, by contrast, has a bioavailability of 15–25% after SC administration. LMWHs have biological $t_{1/2}$ (based on anti-Xa clearance) nearly double that of UFH. The $t_{1/2}$ of LMWHs enoxaparin, deltaparin, tinzaparin, and others has been documented to be between ~100 and 360 min, depending on whether the administration of LMWH was IV or SC. The anti-Xa activity persists longer than antithrombin activity, which reflects the faster clearance of longer heparin chains (43).

Table 1 UFH *vs* LMWH

UFH	LMWH
• Continuous, IV infusion	• BID or QD subcutaneous injection
• Primarily administered in hospital	• Administered in hospital, office, or home
• Usually administered by health care professionals	• Administered by patient, caregiver, or professional
• Monitoring and dosing adjustments	• No monitoring, fixed or weight-based dosing
• Frequent dosing errors	• More precise dosing
• Risk of thrombocytopenia and osteoporosis	• Decreased risk of adverse events
• Cheap, but not cost-effective	• Demonstrated pharmacoeconomic benefits
• Requires 5–7 days in the hospital	• Requires 0–2 days in the hospital

LMWH, low molecular weight heparin; UFH, unfractionated heparin.

LMWH, in doses based on patient weight, needs no monitoring, possibly because of the better bioavailability, longer plasma $t_{1/2}$, and more predictable anticoagulant response of LMWHs compared with UFH, when administered SC. Though LMWHs are more expensive than UFH, a pilot study in pediatric patients found SC LMWH administration to reduce the number of necessary laboratory assays, nursing hours, and phlebotomy time (44).

LMWHs are expected to continue to erode UFH use, through development programs for new indications and increased clinician comfort with use of the drugs. In addition, as both patients and health care providers recognize the relative simplicity of administration with an SC injection, together with real cost savings and quality-of-life benefits by reducing hospital stays, the trend toward outpatient use will continue.

IV. Heparin as an Anti-Inflammatory Molecule: Potential Mechanisms

Heparin is used in the treatment and prevention of thrombotic and thromboembolic conditions like DVT, pulmonary embolism (PE), and crescendo angina (45–47). Heparin activates antithrombin III to prevent conversion of fibrinogen to fibrin; it accelerates inhibition of factors IX-a, X-a, XI-a, and XII-a. Heparin also possesses non-anticoagulant properties, including modulation of various proteases, anti-complement activity, and anti-inflammatory actions. Inhaled heparin has been shown to reduce early phase of asthmatic reaction and suppress allergen-induced rise in bronchial hyper-reactivity. Heparin also inhibits the acute cutaneous reaction due to allergens. The ubiquitous distribution of heparin in tissue spaces may serve to limit inflammatory responses in various tissues where leukocytes accumulate following an inflammatory challenge. It is interesting that heparin is found in high concentrations in the gastrointestinal tract and the lung (45,46), the two organs exposed to external environment.

Few studies have reported an effect of heparin on reactive oxygen species (ROS) generation (48) and cytokine secretion (49) by leukocytes, *in vitro*. It has been recently demonstrated that heparin, when injected intravenously, into normal subjects at a dose of 10,000 IU inhibits ROS generation by mononuclear cells (MNC) and polymorphonucleocytes (PMN) (50). Heparin has been also shown in a series of experiments using *N*-acetyl heparin to protect the heart from ischemia-reperfusion injury both *in vivo* and *in vitro*, independently of its anti-thrombin mechanism (51,52). It was suggested that this protection might be due to a reduction in complement activation-mediated injury to the heart (52). Since ischemia-reperfusion injury may also be mediated by oxidative damage (53), it is therefore possible that the protective effect of heparin may be due to an inhibition of ROS generation. A reduction in superoxide radical formation by heparin is likely to allow a greater bioavailability of nitric oxide (NO) for vasodilatation. In fact, heparin has been shown to exert a vasodilatory effect in normal subjects, *in vivo* (54). Increased bioavailability of NO may have an additional beneficial effect:

inhibition of leukocyte adhesion to the endothelium, which would, in turn, inhibit or retard inflammation (55). In addition, NO inhibits the pro-inflammatory transcription nuclear factor (NF-kB), which plays a central role in the triggering and coordination of both innate and adaptive immune responses.

V. Conclusions

Available uncontrolled data show that heparin may be effective in steroid-resistant ulcerative colitis, with a percentage of complete clinical remission of over 70% after an average of 4–6 weeks of therapy. The administration of heparin is not currently justified by the very limited available data. LMWH was used in a single trial in patients with steroid-refractory ulcerative colitis, with results similar to those observed with heparin. Since a pro-thrombotic state has been described in IBD, and microvascular intestinal occlusion seems to play a role in the pathogenesis of IBD, it is reasonable that part of the beneficial effects of heparin in IBD may result from its anticoagulant properties. However, beyond its well-known anticoagulant activity, heparin also exhibits a broad spectrum of immune-modulating and anti-inflammatory properties, by inhibiting the recruitment of neutrophils and by reducing pro-inflammatory cytokines. In conclusion, heparin or heparin derivatives may represent a safe therapeutic option for severe, steroid-resistant ulcerative colitis and other inflammatory disorders, although randomized, controlled trials are needed to confirm these data.

References

1. Weitz JI. Low-molecular-weight heparin. N Engl J Med 1997; 337:688–698.
2. Mousa SA, Fareed JW. Advances in anticoagulant, antithrombotic and thrombolytic drugs. Exp Opin Invest Drugs 2001; 10:157–162.
3. Mousa SA. Comparative efficacy among different low molecular weight heparin (LMWHs) & drug interaction: implications in the management of vascular disorders. Thromb Haemost 2000; 26 (Suppl 1):39–46.
4. Aguilar D, Goldhaber SZ. Clinical uses of low molecular weight heparin. Chest 1999; 115:1418–1423.
5. Taheri SA, Lazar L, Haddad G, Castaldo R, Wilson M, Mousa S. Diagnosis of deep venous thrombosis by use of soluble necrosis factor receptor. Angiology 1998; 49:537–541.
6. Nelson RM, Cecconi O, Roberts WG, Aruffo A, Linhardt RJ, Bevilacqua MP. Heparin oligosaccharides bind L- and P-selectin and inhibit acute inflammation. Blood 1993; 82:3253–3258.
7. Lantz M, Thysell H, Nilsson E, Olsson I. On the binding of tumor necrosis factor (TNF) to heparin and the release *in vivo* of the TNF-binding protein I by heparin. J Clin Invest 1991; 88:2026–2031.
8. Tyrell DJ, Kilfeather S, Page CP. Therapeutic uses of heparin beyond its traditional role as an anticoagulant. Trends Pharmacol Sci 1995; 16:198–204.
9. Hocking D, Ferro TJ, Johnson A. Dextran sulfate and heparin sulfate inhibit platelet-activating factor-induced pulmonary edema. J Appl Physiol 1992; 72:179–185.

10. Darien BJ, Fareed J, Centgraf KS, Hart AP, MacWilliams PS, Clayton MK, Wolf H, Kruse-Elliott KT. Low molecular weight heparin prevents the pulmonary hemodynamic and pathomorphologic effects of endotoxin in a porcine acute lung injury model. Shock 1998; 9:274–281.
11. Meyer J, Cox CS, Herndon DN, Nakazawa H, Lentz CW, Traber LD, Traber DL. Heparin in experimental hyperdynamic sepsis. Crit Care Med 1993; 21:84–89.
12. Hiebert LM, Liu JM. Heparin protects cultured arterial endothelial cells from damage by toxic oxygen metabolites. Atherosclerosis 1990; 83:47–51.
13. Matzner Y, Marx G, Drexler R, Eldor A. The inhibitory effect of heparin and related glycosaminoglycans on neutrophil chemotaxis. Thromb Haemost 1984; 52:134–137.
14. Bazzoni G, Beltran Nunez A, Mascellani G, Bianchini P, Dejana E, Del Maschio A. Effect of heparin, dermatan sulfate, and related oligo-derivatives on human polymorphonuclear leukocyte functions. J Lab Clin Med 1993; 121:268–275.
15. Vancheri C, Mastruzzo C, Armato F, Tomaselli V, Magri S, Pistorio MP, LaMicela M, D'amico L, Crimi N. Intranasal heparin reduces eosinophil recruitment after nasal allergen challenge in patients with allergic rhinitis. J Allergy Clin Immunol 2001; 108:703–708.
16. Diamant Z, Timmers MC, van der Veen H, Page CP, van der Meer FJ, Sterk PJ. Effect of inhaled heparin on allergen-induced early and late asthmatic responses in patients with atopic asthma. Am J Respir Crit Care Med 1996; 153:1790–1795.
17. Garrigo J, Danta I, Ahmed T. Time course of the protective effect of inhaled heparin on exercise-induced asthma. Am J Respir Crit Care Med 1996; 153:1702–1707.
18. Gaffney A, Gaffney P. Rheumatoid arthritis and heparin. Br J Rheumatol 1996; 35:808.
19. Bowler SD, Smith SM, Lavercombe PS. Heparin inhibits the immediate response to antigen in the skin and lungs of allergic subjects. Am Rev Respir Dis 1993; 147:160–163.
20. Dwarakanath AD, Yu LG, Brookes C, Pryce D, Rhodes JM. Sticky neutrophils, pathergic arthritis, and response to heparin in pyoderma gangrenosum complicating ulcerative colitis. Gut 1995; 37:585–588.
21. Petitou M, Hérault J-P, Bernat A, Driguez PA, Duchaussoy P, Lormeau JC, Herbert JM. Synthesis of thrombin-inhibiting heparin mimetics without side effects. Nature 1999; 398:417–422.
22. Tyrrel DJ, Horne AP, Holme KR, Preuss JMH, Page CP. Heparin in inflammation: potential therapeutic applications beyond anticoagulation. Adv Pharmacol 1999; 46:151–208.
23. Salas A, Sans M, Soriano A, Reverter JC, Anderson DC, Pique JM, Panes J. Heparin attenuates TNF-α induced inflammatory response through a CD11b dependent mechanism. Gut 2000; 47:88–96.
24. Panés J, Perry M, Granger DN. Leukocyte-endothelial cell adhesion: avenues for therapeutic intervention. Br J Pharmacol 1999; 126:537–550.
25. Lever R, Hoult JRS, Page CP. The effects of heparin and related molecules upon the adhesion of human polymorphonuclear leukocytes to vascular endothelium in vitro. Br J Pharmacol 2000; 129:533–540.

26. Gaffney PR, Doyle CT, Gaffney A, Hogan J, Hayes DP, Annis P. Paradoxical response to heparin in 10 patients with ulcerative colitis. Am J Gastroenterol 1995; 90:220–223.
27. Gaffney P, Gaffney A. Heparin therapy in refractory ulcerative colitis—an update. Gastroenterology 1996; 110:A913.
28. Evans RC, Rhodes JM. Treatment of corticosteroid-resistant ulcerative colitis with heparin. A report of nine cases. Gut 1995; 37:A49.
29. Brazier F, Dupas JL. Medical management of severe acute colitis. Rev Prat 1998; 48:1165–1167.
30. Malhotra S, Bhasin D, Shafiq N, Pandhi P. Drug treatment of ulcerative colitis: unfractionated heparin, low molecular weight heparins and beyond. Expert Opin Pharmacother 2004; 5:329–334.
31. Prajapati DN, Newcomer JR, Emmons J, Abu-Hajir M, Binion DG. Successful treatment of an acute flare of steroid-resistant Crohn's colitis during pregnancy with unfractionated heparin. Inflamm Bowel Dis 2002; 8:192–195.
32. He SH. Key role of mast cells and their major secretory products in inflammatory bowel disease. World J Gastroenterol 2004; 10 (3):309–318.
33. Dwarakanath AD, Yu LG, Brookes C, Pryce D, Rhodes JM. "Sticky" neutrophils, pathergic arthritis, and response to heparin in pyoderma gangrenosum complicating ulcerative colitis. Gut 1995; 37:585–588.
34. Teixeira MM, Hellewell PG. Suppression by intradermal administration of heparin of eosinophil accumulation but not edema formation in inflammatory reactions in guinea-pig skin. Br J Pharmacol 1993; 110:1496–1500.
35. Carr J. The anti-inflammatory action of heparin: heparin as an antagonist to histamine, bradykinin and prostaglandin E1. Thromb Res 1979; 16:507–516.
36. Koenig A, Norgard-Sumnicht K, Linhardt R, Varki A. Differential interactions of heparin and heparan sulfate glycosaminoglycans with the selectins. Implications for the use of unfractionated and low molecular weight heparins as therapeutic agents. J Clin Invest 1998; 101:877–889.
37. Diamond MS, Alon R, Parkos CA, Quinn MT, Springer TA. Heparin is an adhesive ligand for the leukocyte integrin Mac-1 (CD11b/CD18). J Cell Biol 1995; 130:1473–1482.
38. Benimetskaya L, Loike JD, Khaled Z, Loike G, Silverstein SC, Cao L, el Khoury J, Cai TQ, Stein CA. Mac-1 (CD11b/CD18) is an oligodeoxynucleotide-binding protein. Nat Med 1997; 3:414–420.
39. Emmanuele RM, Fareed J. The effect of molecular weight on the bioavailability of heparin. Thromb Res 1987; 48:591–596.
40. Brieger D, Dawes J. Production method affects the pharmacokinetic and ex vivo biological properties of low molecular weight heparins. Thromb Haemost 1997; 77:317–322.
41. Mousa SA, Mohamed S. Inhibition of endothelial cell tube formation by the low molecular weight heparin, tinzaparin, is mediated by tissue factor pathway inhibitor. Thromb Haemost 2004; 92:627–633.
42. Mousa SA, Kaiser B. Tissue factor pathway inhibitor in thrombosis and beyond: role of heparin. Drugs Future 2004; 29:751–766.
43. Boneu B, Caranobe C, Cadroy Y, Dol F, Gabaig AM, Dupouy D, Sie P. Pharmacokinetic studies of standard unfractionated heparin, and low molecular weight heparins in the rabbit. Semin Thromb Hemost 1988; 14:18–27.

44. Sutor AH, Massicotte P, Leaker M, Andrew M. Heparin therapy in pediatric patients. Semin Thromb Hemost 1997; 23:303–319.
45. Majerus P, Broze JG, Miletich J. Anticoagulant, thrombolytic and antiplatelet drugs. In: Hardman J, Limbird L, Molinoff P, Ruddon R, Goodman A, eds. Goodman & Gilman's, The Pharmacological Basis of Therapeutics, 9th ed. New York: McGraw-Hill, 1996; 1341–1359.
46. Silverstein R. Drugs affecting hemostosis. In: Munson P, Mueller R, Breeze G, eds. Munson's Principles of Pharmacology. New York: Chapman & Hall, 1995; 1123–1143.
47. Theroux P, Waters D, Qiu S, McCans J, de Guise P, Juneau M. Aspirin versus heparin to prevent myocardial infarction during the acute phase of unstable angina. Circulation 1993; 88:2045–2048.
48. Itoh K, Nakao A, Kishimoto W, Takagi H. Heparin effects on superoxide production by neutrophils. Eur Surg Res 1995; 27:184–188.
49. Attanasio M, Gori AM, Giusti B, Pepe G, Comeglio P, Brunelli T, Prisco D, Abbate R, Gensini GF, Neri Serneri GG. Cytokine gene expression in human LPS- and IFN-gamma-stimulated mononuclear cells is inhibited by heparin. Thromb Haemost 1998; 79:959–962.
50. Dandona P, Qutob T, Hamouda W, Bakri F, Aljada A, Kumbkarni Y. Heparin inhibits reactive oxygen species generation by polymorphonuclear and mononuclear leucocytes. Thromb Res 1999; 96:437–443.
51. Friedrichs GS, Kilgore KS, Manley PJ, Gralinski MR, Lucchesi BR. Effects of heparin and *N*-acetyl heparin on ischemia/reperfusion-induced alterations in myocardial function in the rabbit isolated heart. Circ Res 1994; 75:701–710.
52. Black SC, Gralinski MR, Friedrichs GS, Kilgore KS, Driscoll EM, Lucchesi BR. Cardioprotective effects of heparin or *N*-acetylheparin in an in vivo model of myocardial ischaemic and reperfusion injury. Cardiovasc Res 1995; 29:629–636.
53. Lucchesi BR, Kilgore KS. Complement inhibitors in myocardial ischemia/reperfusion injury. Immunopharmacology 1997; 38:27–42.
54. Hawari FI, Shykoff BE, Izzo JL Jr. Heparin attenuates norepinephrine-induced venoconstriction. Vasc Med 1998; 3:95–100.
55. De Caterina R, Libby P, Peng HB, Thannickal VJ, Rajavashisth TB, Gimbrone Jr MA, Shin WS, Liao JK. Nitric oxide decreases cytokine-induced endothelial activation. Nitric oxide selectively reduces endothelial expression of adhesion molecules and pro-inflammatory cytokines. J Clin Invest 1995; 96:60–68.

Chemistry and Biology of Heparin and Heparan Sulfate
H.G. Garg, R.J. Linhardt and C.A. Hales (Editors)

Chapter 21

Basic and Clinical Differences of Heparin and Low Molecular Weight Heparin Treatment

DEBRA HOPPENSTEADT, OMER IQBAL and JAWED FAREED

Hemostasis & Thrombosis Research Laboratories, Department of Pathology and Pharmacology, Loyola University Medical Center, Maywood, IL, USA

I. Introduction

Recent developments in antithrombotic drugs are significant and contribute to the management of thrombotic disorders. Many advanced techniques to develop antithrombotic drugs are being used at present. Developments in organic synthetic, biotechnology, and separation techniques have contributed to the introduction of novel antithrombotic drugs (1–2). Drugs, such as the antithrombin, and anti-Xa agents are claimed to have a better efficacy in the control of thrombogenesis and its treatment. Newly developed antithrombotic drugs markedly differ in their mechanism and sites of action. Knowledge of the pathogenic triggers is helpful in the optimization of therapeutic or prophylactic use of these drugs.

It is widely appreciated that antithrombotic drugs represent a broad spectrum of natural, synthetic, semisynthetic, and biotechnology-produced agents with marked differences in chemical composition, physicochemical properties, biochemical actions, and pharmacologic effects. Figure 1 depicts the molecular diversities in the structure of various classes of new anticoagulant drugs. These represent proteins, peptides, peptidomimetics, carbohydrates, synthetic oligosaccharides, and their conjugates. Beside the structural heterogeneity, each of these agents also shows distinct functional properties. Many of these agents produce their antithrombotic effects via indirect mechanisms, such as the modulation of endogenous

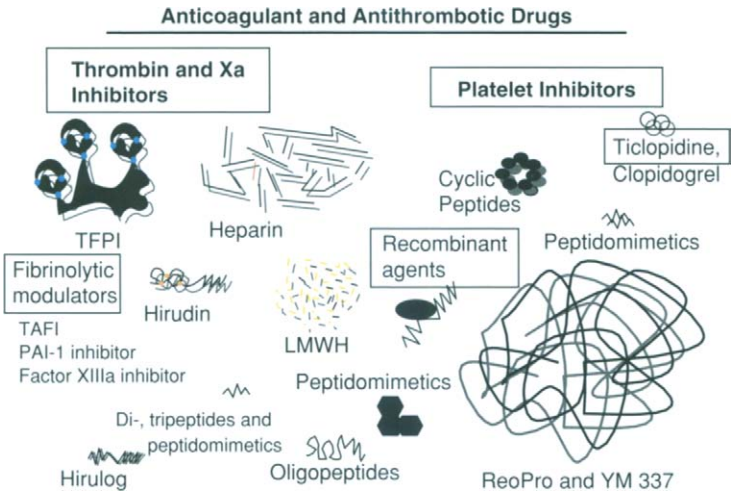

Figure 1 Molecular and structural diversity in the newer anticoagulant and antithrombotic drugs. The newer drug classes include thrombin and Xa inhibitors, which are prepared by biotechnology, isolation, and purification from the natural sources and utilize newer biotechnology-based methods.

antithrombotic processes (TFPI release), modulation of adhesion molecules, enhancement of fibrinolysis, and a reduction in inflammatory cytokines.

II. Unfractionated Heparin and Newer Anticoagulant and Antithrombotic Drugs

A. Unfractionated Heparin

Unfractionated heparin is primarily used as an anticoagulant for both therapeutic and prophylactic indications. Usually beef lung and porcine mucosal-derived products are used. Unfractionated heparins have recently been employed for the following additional clinical applications:

1. management of unstable angina;
2. adjunct to chemotherapeutic agents;
3. adjunct to antiinflammatory drugs;
4. modulatory agent for growth factors;
5. treatment of hemodynamic disorders;
6. surface coating of biomedical devices; and
7. management of vascular deficit.

The heparins are heterogeneous in nature, as depicted in Figure 2. Based on their origin, the molecular weight of these anticoagulant drugs varies. The beef lung heparin preparations are usually of higher molecular weight, in comparison to porcine mucosal heparin. However, charge density and serpin affinity is similar

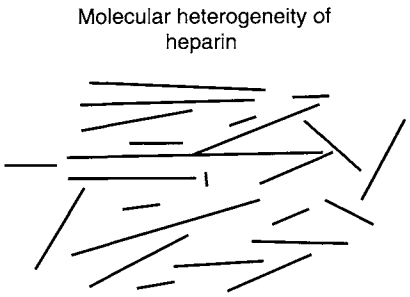

Figure 2 A diagrammatic representation of the molecular heterogeneity of unfractionated heparin. The mean molecular weight of unfractionated heparin range is between 12,000 and 16,000 Da.

for both preparations. The low molecular weight heparins are derived from the unfractionated heparin by controlled depolymerization processes and/or fractionation methods.

Chemical modification of unfractionated heparin, such as desulfation, deamination, or coupling with various agents has resulted in (non-anticoagulant) products with selective actions on enzymes and cellular receptors. These heparin derivatives are currently being tested for such indications as sepsis, viral infections, and the treatment of proliferative disorders.

More recently, newer oral formulations of unfractionated heparin have been successfully tested in several preclinical and clinical settings. Unfractionated heparin in oral formulation is currently undergoing phase III clinical trials for the prophylaxis of deep vein thrombosis (DVT) in orthopedic surgical patients (3). Both liquid and soluble forms have been developed. Additional formulations to deliver heparin through other routes are also under investigation.

B. Newer Anticoagulant/Antithrombotic Drugs in Comparison to Unfractionated Heparin

There are several newer drugs that have become available for clinical use in the USA. The synthetic heparin pentasaccharide, fondaparinux, a chemically synthesized heparin analogue, has recently been introduced. It is now approved for the prevention of DVT in orthopedic patients. Currently, there are three low molecular weight heparins (LMWHs) approved for DVT prophylaxis in the US. However, the approved indications differ for these agents. Two of these drugs, enoxaparin and dalteparin, are also approved for the management of acute coronary syndromes. These agents are widely used for the treatment of established thrombosis throughout the world. Antithrombin agents, namely refludan (hirudin) and argatroban (novostan) have been approved for therapeutic anticoagulation in patients who are not treatable with heparin. Hirulog (angiomax) is also an antithrombin agent, which is now optimized for anticoagulant and cardiovascular indications in heparin compromised patients.

The ADP antagonist, clopidogrel (Plavix) was initially approved by the US FDA and the EMEA for the management of thrombotic stroke. However, it is now used widely for various cardiovascular indications. This drug has gradually replaced the original ADP antagonist namely, ticlopidine, because of the side effects associated with this agent. Plavix has been used by cardiologists for interventional purposes in combination with aspirin to prevent coronary stent thrombosis. In addition, the FDA has recently approved the combination of low dose aspirin with sustained released dipyridamole for the secondary prevention of stroke. Another old drug namely, cilostazol (Pletal), is approved for intermittant claudication. Presently, two additional IIb/IIIa antagonists, integrilin and aggrastat, have been approved. The future recommendations of the experts in the field will point to the use of some of these agents in specific indications.

Despite these dramatic basic and clinical developments, unfractionated heparin has continued to play a pivotal role in the management of thrombotic disorders for over half a century. While bleeding and heparin-induced thrombocytopenia represent major side effects of this drug, it has remained the anticoagulant of choice for the treatment of arterial thrombotic disorders, surgical anticoagulation in open heart surgery, and interventional usage (Fig. 3).

It is the understanding of the structure of heparin, which led to the development of LMWHs, synthetic heparinomimetics, antithrombin, and anti-Xa agents. These drugs may compete with unfractionated heparin for specific indications. However, it is unlikely they will totally replace heparin.

The first generation of heparin represented unfractionated heparin (bovine, porcine, ovine); the second generation included the LMWHs, whereas the third generation encompasses chemically modified heparin, heparin derivatives, oral heparin formulations, and synthetic- and biotechnology-derived heparinomimetics (Fig. 4). One of the major advances in this area is the synthesis of heparin–pentasaccharide and its derivatives, which represent the minimal anticoagulation binding portion of heparin. In addition, chemically synthesized conjugates of pentasaccharide, including both the anti-Xa and anti-IIa derivatives, have been synthesized. The pentasaccharide has undergone several clinical trials for the prevention of venous and arterial thrombosis. Based on the available data, it is now approved for the management of DVT prophylaxis in orthopedic patients. While the pentasaccharide may represent a major advance in the understanding of the structural and functional properties of heparin, it does not mimic the overall pharmacologic profile of heparin. For this reason, pentasaccharide conjugates with both the anti-Xa and anti-IIa activities are also being developed.

The pharmaceutical industry has allocated sizable resources in the last two decades to finding an alternative for heparin therapy. Despite the major impact of recombinant technology and advanced chemical methods at this time, a suitable substitute for heparin is not available for several specific indications. Heparin remains the anticoagulant of choice for therapeutic and surgical indications because of shorter half-life of heparin and its ability to be neutralized with protamine sulfate. The most significant advances in this area are the development of LMWHs. As shown in Figure 5, the LMWHs are obtained by chemical, enzymatic,

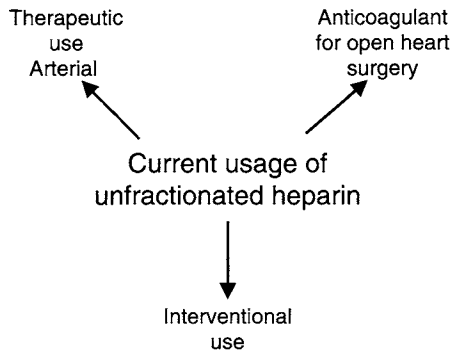

Figure 3 Current usage of unfractionated heparin. Despite bleeding and heparin-induce thrombocytopenia as side effects, heparin still remains the anticoagulant of choice for the treatment of arterial disorders, surgical anticoagulation in open heart surgery, and interventional usage.

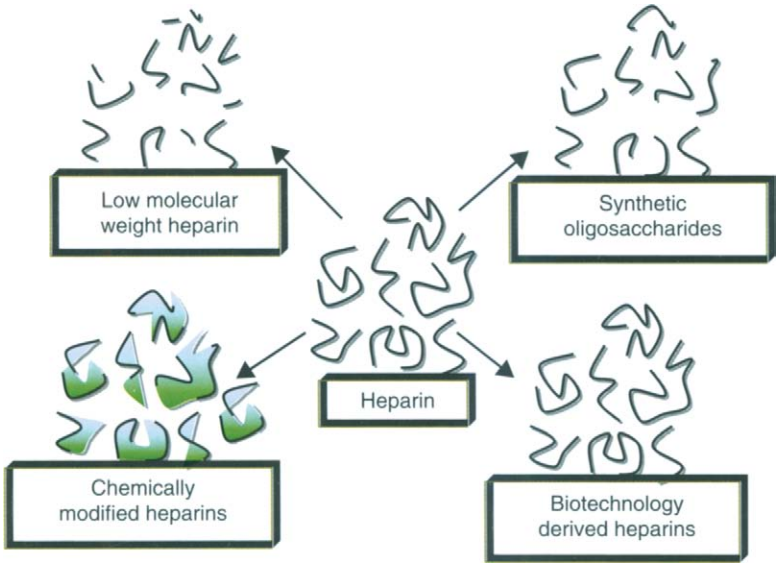

Figure 4 The low molecular weight heparins (LMWHs), synthetic oligosaccharides, biotechnology-derived heparins, and chemically modified heparins are all derived from unfractionated heparin.

or physical depolymerization of heparin. These drugs were first introduced some 20 years ago for the prophylaxis of surgery-related thrombosis. Today these drugs are used for additional indications beyond thrombotic disorders. The LMWHs are not only optimized for the prophylaxis and treatment of venous thrombosis, but are also used for inflammatory, proliferative, and ischemic disorders. Because of their polypharmacologic nature, LMWHs are being developed for expanded indications, such as cancer, transplantation, and immunologic disorders. More recently, these agents are evaluated as anticoagulants in percutaneous intervention (4).

The recognition of heparin-induced thrombocytopenia as a catastrophic complication of heparin therapy is rather paradoxical. Some 20 years ago the occurrence of this syndrome was hardly recognized. Alternate medication and improved processing of heparin may eventually lead to heparin with lesser thrombocytopenic potential. The identification of patients with predisposing factors may also reduce the incidence of thrombocytopenia. It is already known that the incidence of heparin-induced thrombocytopenia with LMWHs is lower than that with heparin; and the pentasaccharide anticoagulant fondaparinux does not produce any thrombocytopenic reaction. Thus, in optimized dosages, heparins can be safely used. Oral formulations of heparin are currently in phase III clinical trials for various indications. In this formulation, heparin may exhibit a better safety profile. Furthermore, with the newer diagnostic methods, patients at risk of developing heparin-induced thrombocytopenia may be identified and treated with alternate forms of therapy.

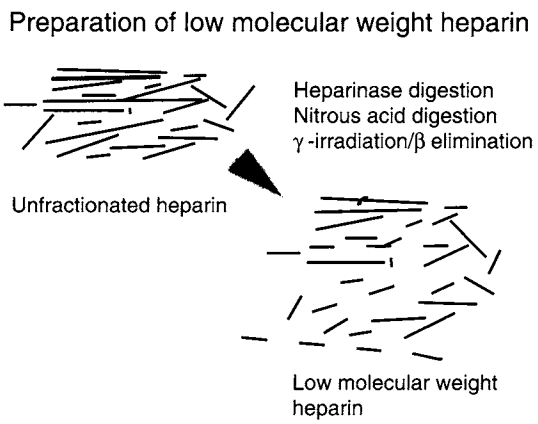

Figure 5 A diagrammatic illustration of the manufacturing processes for low molecular weight heparins and their derivatives. Both the chemical and enzymatic depolymerization result in a depolymerization of heparins, eventually leading to heparin-derived oligosaccharides. If the depolymerization is exhaustive, it may result in the degeneration of heparin-derived disaccharides and trisaccharides.

III. Low Molecular Weight Heparins and Their Impact on the Management of Thrombotic and Vascular Disorders

The LMWHs represent a refined version of heparin (5). About 20–30% of low molecular weight heparin components are already present in the unfractionated heparin. Chemical and enzymatic depolymerization have resulted in the formation of products, which mimic the function of the low molecular weight heparin components. Almost all of these agents are produced by chemical or enzymatic digestion of porcine mucosal heparin. Depolymerization induced specific changes in each of the LMWH products make each of these agents a distinct drug entity. Thus, depending on the patented depolymerization procedure, different products are formed. These products exhibit not only physical and chemical heterogeneity, but also show variations in biologic actions, which are translated into differences in the clinical effect. Whether various LMWHs can replace heparin for all its indications remains unclear at this time.

From initial studies, it became evident that low dose subcutaneous heparin produced prophylactic antithrombotic effects in surgical patients. This is due to the subcutaneous absorption of the low molecular weight components of heparin, which exhibit mostly on anti-Xa activity and produce a long-lasting effect. The bioavailability of smaller molecular weight heparin components is markedly high. This observation led to the development of LMWHs, which exhibit similar properties to low molecular weight components of unfractionated heparin. Not only the bioavailability, but the duration of action of these agents is much longer than heparin. In addition, these agents show decreased toxicity profiles.

The LMWHs are now globally regarded as drugs of choice for postsurgical prophylaxis of DVT and the management of acute coronary syndromes. Recently, these agents have also been approved for the treatment of thrombotic disorders. Several products are currently available for clinical use worldwide. Because of manufacturing differences, each of the LMWHs exhibits distinct pharmacologic and biochemical profiles (5). The specific activity of these agents in the anticoagulant assays ranges from 35 to 45 anti-IIa U/mg, whereas the specific activity in terms of anti-Xa units is designated as 80–120 anti-Xa U/mg. The LMWHs are capable of producing product-specific dose and time-dependent antithrombotic effects in animal models of thrombosis. While the anticoagulant effects are initially present at dosages that are antithrombotic, these agents have been found to produce sustained antithrombotic effects without any detectable *ex vivo* anticoagulant actions. In experimental animal models and in various clinical trials, these agents have been found to release tissue factor pathway inhibitor (TFPI) after both intravenous (IV) and subcutaneous (SC) administration (6). Repeated administration of LMWHs produces progressively stronger antithrombotic effects. However, the hemorrhagic responses vary and are largely dependent on products. The release of TFPI following IV and SC administration in humans has demonstrated the product individuality and the relevance of this inhibitor to the actions of LMWHs (7). Antithrombotic and hemorrhagic studies are reported that compare the pharmacologic profile of some of the available LMWHs. Product individuality in terms of relative potency in

different assays and the failure of standardization protocols to provide any guidelines for product substitution and prediction of the clinical effects has remained a major consideration (8).

Initially, the clinical batches of LMWHs were prepared by ethanolic fractionation of heparin. However, because of cost and limited availability of heparin for the sizeable isolation of these agents, chemical and enzymatic depolymerization procedures were developed. Physical methods, such as γ irradiation and ultrasonification process, have also been employed in the preparation of these agents.

Although the depolymerization process results in LMWH products (MW 4–8 kDa), these products exhibit differences in both their molecular, structural, and functional properties. Optimized methods are currently employed to prepare LMWHs, which exhibit a similar molecular profile. However, due to the significant differences in the chemical or enzymatic procedures, structural variations are found in all of these agents. These differences, therefore, exert significant influence on the biologic action of these products (6). Safety and efficacy comparison of these agents in well-designed clinical trials to demonstrate clinical differences in each of the individual products have only become available recently. Initial attempts to standardize LMWHs on the basis of their biologic actions, such as anti-Xa potency, have failed. A potency designation on the basis of the anti-Xa actions only represents one of the several properties of these agents. Furthermore, this assay only measures the AT-AT affinity based actions of some of the components of these agents. Many of the pharmacologic actions of LMWHs are based on the non-AT non-AT affinity components of the drugs. These include the release of TFPI, t-PA, inhibition of adhesion molecule release, decrease in the circulating von Willebrand factor, and modulation of blood flow. Most of these effects are not measurable by using conventional methods to assay heparin, such as the anti-Xa, anti-IIa, and global anticoagulant tests. Despite the clinical effectiveness of the LMWHs in various indications, the mechanism of action of these agents is not completely understood. It has been suggested that endogenous release of a Kunitz-type inhibitor, TFPI, may be a contributing factor to the mediation of the antithrombotic actions of these agents. It is interesting to note that most of the studies on LMWH have alluded to the relevance of the anti-Xa effect with the antithrombotic action of these agents. However, after subcutaneous administration of these agents, circulating anti-Xa activity is not detectable in samples collected 12 h after the administration of prophylactic dosages. Despite this, the patients remain in an antithrombotic state. Thus, additional mechanisms, such as the release of TFPI, may contribute to the overall action of these agents. LMWHs are also known to produce endothelial modulation and may release fibrinolytic activators, such as t-PA and antiplatelet substances, such as prostacyclin and nitric oxide. Endothelial dysfunction, platelet activation, white cell activation, and plasmatic process contribute to this process. Since LMWHs are polycomponent drugs with multiple sites of action, these agents are capable of controlling of thrombogenesis at several target sites.

Unfortunately, most of the clinical trials have been designed to determine the clinical outcome with these drugs and very little is known of the pharmacologic mechanisms involved in the mediation of their action. Pharmacologic differences

and nonequivalence of these agents have been reported previously (5,6). Recent clinical trial results also show that each of these drugs produces its own product-specific therapeutic index. Thus, unlike unfractionated heparin, these drugs are not interchangeable on the potency-adjusted dosage.

Unfractionated heparin's anticoagulant potency is usually measured in terms of USP U/mg. This method, however, is not applicable to the LMWHs because of their relatively weaker and varied effect on the coagulation process. However, since LMWHs exhibit anticoagulant action at higher concentrations (>5.0 μg/mL), their anticoagulant actions can be compared in this assay. The anti-Xa activity of various LMWHs is now considered to be of limited importance in the potency evaluation and marketing of these agents. Similarly, the anti-Xa/IIa ratio is only of pharmaceutical value and may not have any clinical meaning. The relative anti-Xa anti-IIa ratio also changes after the administration of these agents and is dependent on several factors.

The first clinical trial on LMWH for the prophylaxis of postsurgical DVT was published in 1986 (10). The initial clinical development of LMWHs remained restricted to the European continent for the first few years. Almost 10 years later, these drugs were introduced in the US. In the initial stages of the development of these drugs, only nadroparin, dalteparin, and enoxaparin were used. Subsequently, several other LMWHs, such as ardeparin, tinzaparin, reviparin, and parnaparin were introduced. Today, some eight LMWHs constitute a group of important medications with total sales reaching nearly 2.5 billion dollars with expanded indications reaching far beyond the initial indications for the prophylaxis of post-surgical DVT. Only two of the LMWHs identified have been approved for multiple indications (1,4,6,10,11).

In addition to the currently approved indications, these drugs are also used in several off-label indications. Figure 6 depicts the wide range of indications for the LMWHs. In addition to these indications, LMWHs are currently being evaluated for anticoagulant use in percutaneous interventions and surgical procedures. Whether or not, the ultra-LMWHs and pentasaccharide can be used in all indications is unclear at this time. Clinical trials have clearly demonstrated the safety and efficacy of some of the LMWHs in the outpatient prophylaxis and treatment of thromboembolic diseases (11–13). In addition, these drugs have also been used for the management of acute coronary syndrome. Additional clinical evidence has also provided supportive evidence for the efficacy of these agents in such patient groups as thrombotic and vascular stroke, peripheral arterial diseases, cancer, thrombotic process associated with pregnancy, old age, and inflammatory disorders (13–18). While the clinical studies have only been performed on a select number of LMWHs, it is likely that different products at individually optimized dosages may prove to be effective. In this regard, product individuality and the available clinical trial data should be considered prior to a recommendation being made for a given LMWH. This poses a challenge to the clinicians and requires a clear decision on the selection of a given product for single or multiple indications. Since the pharmacologic profile of each of these drugs is different and some of the comparative data have shown varying clinical performance, it is likely that the optimized dosage for

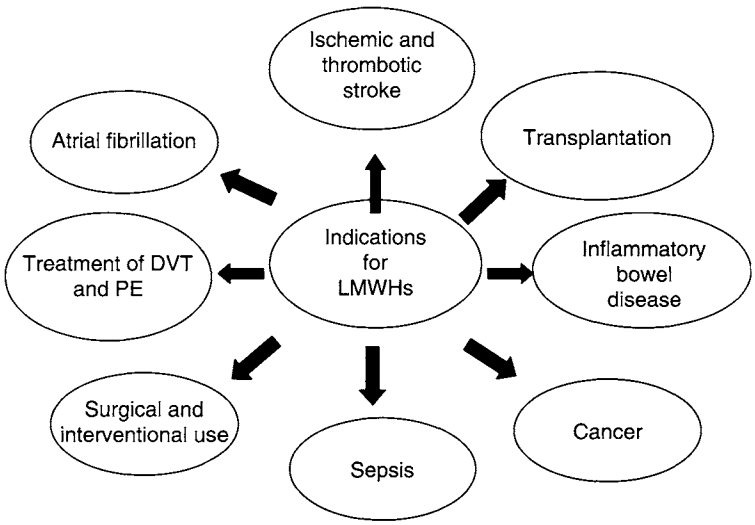

Figure 6 There is a wide range of indication for the potential use of low molecular weight heparins (LMWHs). These include treatment of DVT/PE, surgical and interventional usage, sepsis, cancer, inflammatory bowel disease, transplantation, ischemic and thrombotic stroke, and atrial fibrillation.

these agents may be significantly different, requiring individual dosing recommendations. Thus, it is of crucial importance to consider each of these products as different drugs, and make each of these different agents available for specific indications.

Although venous thromboembolism (VTE) occurs more often in patients with gastrointenstinal malignancies, essentially, all cancer patients have increased risk of VTE. Various factors contribute to VTE in cancer patients, including increased plasma levels of fibrinogen and factors V, VIII, IX, and XI, decreased plasma level of antithrombin III, production of procoagulants by tumor cells, increased production of procoagulants by immune mediator, endothelial damage by tumor, as well as tumor compression related venous stasis worsened by reduced mobility, and inherited risk factors. Persistent malignancy increases the incidence of VTE, resulting in frequent hospitalizations. Prandoni (19) reported an incidence of VTE of 10.3% (6/58) in cancer patients treated with oral anticoagulants compared to 4.7% (14/297) in a noncancer population. Similarly, the Columbus (20) investigators reported an 8.6% (20/232) VTE rate in patients with cancer compared to 4.1% (32/789) in noncancer patients. The American College of Chest Physician's recommends that patients with continuing risk factor, such as cancer, inhibitor deficiency states, antiphospholipid antibody syndrome, or patients with recurrent venous thrombosis should be treated with anticoagulation (21,22). Therefore, effective antithrombotic management, without compromising the quality of life of patients, is an important clinical issue and warrants clinical research.

Current studies have also provided evidence that LMWHs may exhibit drug interactions with other anticoagulants (hirudin, pentasaccharide, and heparin), antiplatelet drugs (clopidogrel, aspirin, GP IIb/IIIa inhibitors), and thrombolytics. These interactions may alter the safety and efficacy profile of not only these drugs but also the effects of the LMWHs. These interactions have to be clearly understood both at the basic and clinical levels. The dosage of heparin and other anticoagulants have been arbitrarily reduced in some clinical trials when these drugs are administered with antiplatelet drugs. However, a study, where the antiplatelet drug is reduced rather than heparin, has not been done. LMWHs may exhibit synergistic interaction with not only antiplatelet drugs, but can also strongly modulate the effects of antithrombin and anti-Xa agents. Dose adjustments, optimization of drug combinations, and assurance of the safety of combined drugs are areas where clinical trials will be very helpful. Despite the expanded use of LMWHs in thrombotic and cardiovascular indications, several issues remain unresolved.

Although these agents are used in high dosages for anticoagulation purpose, there still is no available antidote at this time (22,23). In addition, there are no guidelines available for the management of bleeding with these agents with the exception of the use of protamine sulfate. The adjustment of dosage in weight compromised patients, dosing in pediatrics, and geriatric patients remains to be unclear. Furthermore, the guidelines for the monitoring of the effect of these agents especially in drug combinations are not available.

As newer clinical trials are now based on polytherapeutic approaches, it is important to consider the clinical consequences of the drug combinations with LMWHs. Many of the trials in acute coronary syndromes now utilize aspirin, front loading of ADP receptors antagonists in combination with glycoprotein IIb/IIIa inhibitors, and thrombolytic agents. Markedly different outcomes in terms of safety and efficacy are expected despite drug–dosage adjustments. It is widely expected that these drug combinations at adjusted dosages will improve the clinical outcome in terms of improved efficacy. However, such combinations may also have a profound impact on the safety index. It is therefore important that drug combinations should only be considered in specific conditions, where multiple pathophysiologic events contribute to the thrombotic event, and then they should be used with caution. It is also important not to use multiple drug combinations indiscriminately in a given indication. Such combinations may be more useful in specific clinical situations.

Anticoagulation with heparin represents an indispensable pharmacologic modality for all of the patients with ischemic and occlusive cardiovascular and cerebrovascular events. The dosage of heparins (unfractionated heparins and LMWHs) has been optimized after careful trials/observations. Thus, an adjustment of the use of heparin and LMWHs should be based on valid preclinical observations. Objective clinical trials should be carried out to determine the relative effects of each drug component. While combination therapy will be of major value in years to come, it will require a careful assessment of clinical implications.

In the coming years, the role of LMWHs will be expanded in both thrombotic and nonthrombotic indications. A greater emphasis is currently placed on the

non-anticoagulant properties of these agents. Some of the clinical effects of many of these products are not explainable in terms of anticoagulant effects. Newer formulations, drug combinations, extended use, and long-term effects of these drugs will be important in the optimization of these drugs. Pharmacoeconomics will play a key role in the expanded usage of these drugs and the optimization in years to come. Selection of a proper agent for a given indication, dosing, management of adverse reactions, and substitution therapy represent some of the areas where valid clinical trials are needed. Cost remains an important factor in providing optimized medical care. An objective approach is crucial in streamlining critical pathways and optimizing pharmacoeconomics. Identification of products for specific indications and knowledge of individual LMWHs will be extremely helpful in the proper usage of these agents.

IV. Monitoring of Heparin and Low Molecular Weight Heparins

A. Prophylactic and Therapeutic Dosages

The current recommendation is that most patients receiving prophylactic and therapeutic LMWHs heparin do not require monitoring (24–26). This includes patients who are clinically stable and receiving prophylaxis for postoperative VTE. Uncomplicated patients under treatment with higher doses of LMWHs for established VTE by a weight adjusted, fixed dose also do not require monitoring. In these patients, there is little to no risk of having circulating drug concentrations outside the target range due to the pharmacokinetic behavior of LMWHs.

Patients receiving LMWHs who do require monitoring include those who are obese, have renal insufficiency, or are pediatric patients or newborns (24,26). Women should be monitored periodically throughout pregnancy due to changing physiologic requirements as the pregnancy proceeds. Patients receiving LMWHs for long-term therapeutic treatment, such as for malignancy, and those receiving LMWHs if they are refractory to warfarin (antiphospholipid, myeloproliferative disorders), or if warfarin derivatives are contraindicated, should be monitored.

One of the mechanisms of action of LMWHs is inhibition of factor Xa via AT (24). LMWHs (and heparin) can be assayed by clot or chromogenic-based anti-FXa assays (24,26,27). It should be appreciated that monitoring LMWHs by an anti-FXa assay will not always give a complete measure of the drug effect, because these drugs have antithrombotic activities other than factor Xa inhibition. Moreover, the half-life of LMWHs measured by different assays can be different. It has been observed that the anti-FXa activity is longer than the half-life of the anticoagulant effect measured by the activated clotting time test (ACT) after protamine neutralization. Similar discrepancies are observed for heparin between these assays where, for example, results from the activated partial thromboplastin time test (aPTT) do not necessarily reflect the same results from the chromogenic anti-FXa assay (Fig. 7).

When LMWHs monitoring is needed, the chromogenic anti-FXa assay is the currently recommended assay (24,26). The clot-based aPTT is only sensitive

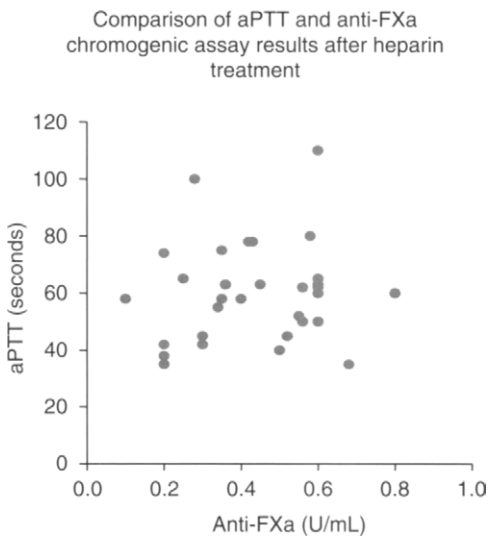

Figure 7 The activated partial thromboplastin time test (aPTT) and the chromogenic anti-factor Xa assay can both be used for monitoring heparin; however, they produce results that do not necessarily reflect the same activity of heparin. The assays also have differing sensitivities and interfering substances.

to very high levels of LMWHs (Fig. 8). The chromogenic anti-FXa assay has sensitivity to LMWHs while the aPTT does not, and it is a specific assay for LMWHs; however, reproducibility and interlaboratory results (accuracy) can vary.

Blood samples for LMWHs monitoring should be obtained 3–4 h after a subcutaneous injection to obtain the peak circulating concentration. Target peak level for treatment of VTE is 0.5–1.1 anti-FXa U/mL. Newborns may need a higher dose (1.6 mg/kg) than older pediatric, or adult patients (1.0 mg/kg) to reach the target range (9). If the patient is receiving the drug intravenously, the blood specimen is to be drawn from a different extremity than the one used for drug infusion.

B. Interventional Procedure Dosages

At higher therapeutic doses, the aPTT may have sufficient sensitivity towards LMWHs, but this assay is typically not used clinically. It has been shown that the same ACT as used for heparin can be used for monitoring high doses of the LMWHs, dalteparin, for interventional cardiology procedures (27). Because dalteparin, enoxaparin, tinzaparin, and reviparin produce markedly different anticoagulant effects in the ACT (Figure 9), each LMWHs has to be individually optimized in this setting.

The LMWHs respond differently than heparin in the same monitoring assay system. It is important to recognize that the ACT target guidelines for LMWHs,

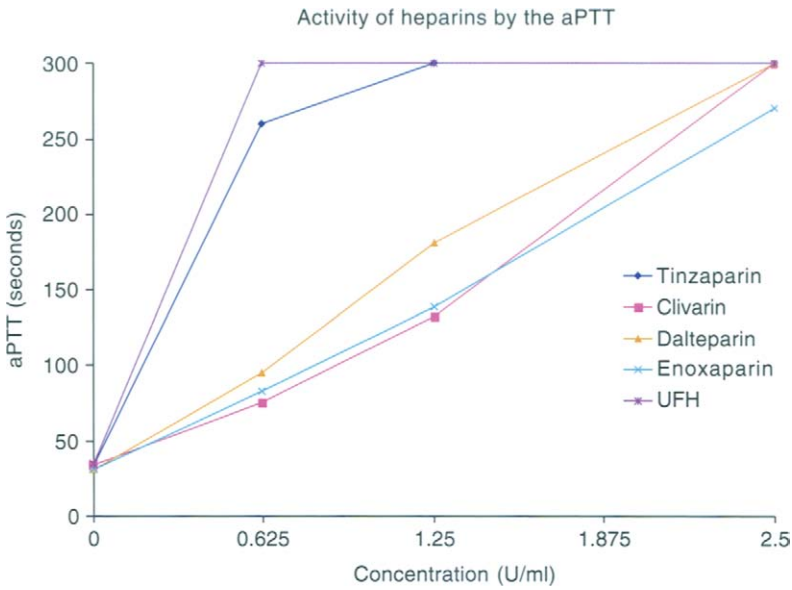

Figure 8 At low (prophylactic concentrations), LMWHs do not have activity that is detectable by the activated partial thromboplastin time test (aPTT). At higher concentrations, such as those used for interventional cardiology, the aPTT does produce a dose-dependent response to LMWHs. Each LMWHs has an individual response.

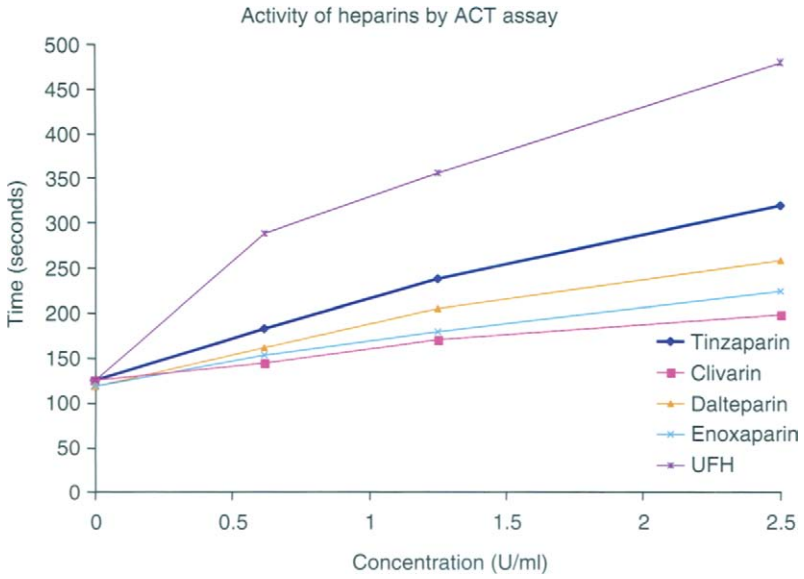

Figure 9 At high concentrations, such as those used for interventional cardiology, the celite activated clotting time test (ACT) produces a dose-dependent response to LMWHs. Each LMWHs has an individual response.

when used in interventional procedures, are different from those for heparin. The NICE and DREAM studies have provided data to individualize the dosing guidelines for enoxaparin and dalteparin, respectively, in the interventional cardiology setting (28). Although aPTT is not a useful test for the monitoring of LMWHs for prophylactic and therapeutic indications, this test can be used for the monitoring of the interventional dosage of LMWHs.

V. Clinical Trials with Low Molecular Weight Heparins

There are several newer clinical trials in progress using different products in indication-specific protocols. Each of these trials is designed either empirically, or by considering results of pilot trials on a given product. The dosages used are product specific. Some of these trials employ relatively high dosage for long periods. In these situations, each product will have its own clinical profile. The results of these trials will certainly validate the notion that all LMWHs are not the same. Future consensus conferences will also consider the product based differences and a collective statement based on the performance of LMWHs as a group must be based on valid meta-analyses.

The LMWHs were initially developed for the prophylaxis of postsurgical thromboembolism, and at this time these drugs represent the gold standard for this indication. Ever since their introduction, more than 10 years ago, the polypharmacologic properties of these agents were quite evident. Coupled with the outpatient compliance and the safety profile of these agents, their use in the management of acute coronary syndromes, in particular, unstable angina and non-Q-wave myocardial infarction provided an important indication, for which a standard of care drug was not available and only the inpatient use of UFH was practiced (29–31). Thus, several clinical trials to test the efficacy and safety of these agents began some 7 years ago. The initial trial carried out on fraxiparin and dalteparin provided evidence that LMWH in fact produced beneficial effects in comparison to placebo and UFH in this indication. Because of the safety issues with long-term use of heparin and the need for monitoring the LMWHs, offered a unique drug to the clinical community to manage acute coronary syndromes. Several newer indications in both cardiovascular and cerebrovascular indications are proposed at this time. Beside the US FDA, several other regulatory agencies in Europe have recently approved the use of enoxaparin and dalteparin for this indication. Thus, the same or better therapeutic benefit has been achieved with the outpatient use of these agents as with UFH without any monitoring and hospitalization. Since there are several different LMWHs available at this time, the relative efficacy of each agent should be individually optimized. Interestingly, in the clinical trials, differences in the safety and efficacy profiles have already started to emerge (22,32).

The LMWHs also provide a useful antithrombotic agent for various hematologic and oncologic indications (14). Because of the relatively higher therapeutic index, these drugs may prove to be very useful in the prophylaxis and treatment of thromboembolic disorders associated with various hematologic and oncologic

disorders. In the area of hematology, LMWHs have been tested in the following indications:

1. prophylaxis and treatment of DVT and pulmonary embolism associated with hematologic disorders (leukemia, sickle cell anemia, hypercoagulable states);
2. antiphospholipid syndrome;
3. bone marrow transplantation associated vasculopathies;
4. congenital and acquired thrombophlebitis; and
5. vasculitis and related disorders.

These agents have also been used as adjunctive drugs in several therapeutic protocols and have been found to augment the therapeutic effects of various drugs.

The clinical potential of LMWHs in the management of cancer-related thrombotic disorders has been recognized from the early days of the development of these agents. In the substudy analysis of various clinical trials, it has been clearly known that patients administered LMWHs exhibit a reduced mortality rate. Currently, several clinical trials have been designed to test the efficacy of these agents in prevention and treatment of thromboembolic complications associated with cancer. Some of the areas where these agents are currently tested are listed below.

1. Prophylaxis and treatment of radiation associated thrombotic and vascular disorders.
2. Prophylaxis and treatment of chemotherapy associated thrombotic and vascular disorders.
3. Prevention of thrombosis in drug delivery devices.
4. Control of metastases (prevention of angiogenesis).
5. Prevention and treatment of cancer procoagulant mediated thrombotic syndrome.
6. Postsurgical prophylaxis after surgical intervention.

The LMWHs may also be useful in the prophylaxis of thromboembolic complications in several other indications, such as pheresis, cell preservation, and other interventional procedures in both hematology and oncology.

Several trials are currently underway on the use of LMWHs in thrombotic and ischemic stroke. These trials were prompted due to the favorable outcome in a clinical study with Fraxiparin. However, when this study was repeated in an expanded population group (FISS-BIS) the results were disappointing (33). It is important to note that the same drug was used in both clinical trials. However, the first study was mainly carried out in Hong Kong, whereas the other study was carried out in Europe. Once again, differences in the study design may be considered as the key factor in the different outcome of these studies.

VI. Generic Low Molecular Weight Heparins

There is considerable debate on the development of generic versions of branded LMWHs, such as dalteparin, enoxaparin, tinzaparin, and others. As the patents of some of these drugs have already expired, or are reaching term, there is a consider-

able interest in the major suppliers of generic drugs to introduce the generic versions of the branded products at a lower cost. The LMWHs are unique as these products are of biologic origin, yet, there is significant chemical processing, which make each drug different. The current pharmacopial description of the LMWHs have an oversimplistic description of these products without taking into account their unique molecular, structural, and biological features. Not having proper guidelines, the generic industry has already introduced products with the molecular profile specifications and biologic activity in terms of anti-Xa U/mg. Products manufactured by different chemical processes are not the same and generic versions of these products do not control for each LMWH distinct characteristics. Thus, these products cannot be interchanged on the basis of the claimed generic equivalence.

The primary aim of drug interchangeability is to reduce costs without compromising patient care (i.e., drug acquisition cost) (34). There are two types of drug interchangeability: (1) therapeutic and (2) generic. Therapeutic interchangeability is the substitution of chemically distinct drugs, which exhibit therapeutic equivalence (34). Therapeutically equivalent drugs may be interchanged, or used as substitutes because they are expected to produce almost identical therapeutic outcomes and adverse reactions (35). Guidelines are usually provided to assist with therapeutic interchangeability (substitutions) for specific medical conditions.

There are six criteria for scientifically justifiable and pharmacoeconomically beneficial therapeutic interchangeability. If chemically unique drugs fail to meet any *one* of the following six criteria, then therapeutic interchangeability is not accepted (34).

1. Pharmacologic equivalence.
2. Clinical evidence supporting the therapeutic interchange in a given indication.
3. Cost/availability.
4. Thorough evaluation process (e.g., Pharmacy and Therapeutics Committee).
5. Regular monitoring of patient outcomes.
6. Response variations.

There are heated debates about therapeutic interchangeability for LMWHs (33,35–37). The brand name LMWH products, such as dalteparin (fragmin), enoxaparin (lovenox), nadroparin (fraxiparin), and tinzaparin (innohep), are chemically and biologically unique drugs (39–41). Rulings by federal health authorities based on scientific and clinical data state that these drugs are not interchangeable.

Pharmacologic equivalence between LMWHs has not been established (34). There have been no head-to-head, large scale comparative clinical trials establishing clincial evidence in support of equivalent dosing regimens for two different LMWHs, although, there has been for fondarparinux. For those LMWHs, where a dosage for a given indication has been objectively established based on valid clinical trials, there are medicolegal implications for the indiscriminate interchange of another LMWH for the branded LMWH using indication-specific dosing only established for the branded LMWH.

On the other hand, generic LMWH interchangeability with the branded LMWH products may be more acceptable in the future. Because it appears that the manufacturing process for LMWHs must be preserved in order to produce an identical antithrombotic drug with similar clinical outcomes, generic LMWHs are expected to be pharmacologically equivalent to the branded LMWH. Prior to the acceptance, however, studies will need to be performed proving this equivalence. The bioequivalence and pharmacodynamic comparative data for generic LMWHs will need to include antithrombotic markers, such as anti-Xa activity, anti-IIa activity, anti-Xa to anti-IIa ratio, aPTT, INR, etc. In addition, head-to-head clinical trials in specific indications will also prove the safety and efficacy of the generic LMWH in comparison to the branded LMWH.

VII. American College of Chest Physicians Consensus Recommendations

Recognizing the clinical usefulness of LMWHs, the American College of Chest Physicians (ACCP) Consensus Conferences have constantly endorsed the use of UFH and LMWHs in high-risk major surgery, hip replacement, knee replacement, and high risk multiple trauma. The recent consensus statements also include favorable comments for LMWHs in contrast to the use of UFH and oral anticoagulant drugs for knee surgery. These recommendations are based on well-designed clinical trials and were objectively developed by a panel of experts. It is also important that such recommendations have taken into account the product-specific clinical outcome. The 7th ACCP consensus statement has provided additional supportive data for the expanded use of LMWHs in various indications (42). Besides the prophylaxis of postsurgical and medical DVT/PE, guidelines for the treatment have also been endorsed. In addition, two of the LMWHs, namely enoxaparin and dalteparin are now approved for the management of acute coronary syndromes. Thus, the ACCP consensus statements have continually endorsed the use of these agents in various indications. In addition, the ongoing consensus discussions at global levels, such as the European community, and International Union of Angiology, will continue to provide objective guidelines for the use of these drugs.

A. Prevention of Venous Thromboembolism

Mechanical methods of prophylaxis are recommended in patients who are at high risk of bleeding, or as adjunct to anticoagulant therapy. In general surgery, for moderate and high-risk patients prophylaxis with low dose UFH (5000 U bid) or LMWH (<3400 U 9d for moderate; >3400 U d for high risk) is recommended (43). Specific guidelines for different types of surgery are also given in the ACCP guidelines. The dosage varies widely for the individual products.

In orthopedic surgery, the recommendations for elective hip surgery, or elective knee surgery include one of the following three treatments:

1. LMWH at a high-risk dosage started 12 h before surgery, or 12–24 h after surgery, or half the high-risk dose 4–6 h after surgery, then increase the dosage to full dose the next day (43);
2. fondaparinux 2.5 mg started 6–8 h after surgery (43); and
3. adjusted dose vitamin K antagonists started preoperatively, or the evening after surgery (INR target 2.5) (43).

The panel also recommended that treatment duration should be at least 10 days.

In medical patients and cancer patients, prophylaxis with low dose UFH or LMWH were recommended. In cancer patients undergoing surgery, prophylaxis that is appropriate for the current risk status of the patient should be considered (43).

B. Treatment of Venous Thromboembolic Disease

For the initial treatment of acute DVT of the leg for patients with confirmed DVT, short-term treatment with SC LMWH, or IV UFH, or SC UFH for at least five days was recommended. Initiation of vitamin K antagonists together with LMWH or UFH until the INR is stable (>2.0) was also recommended (21). For long-term treatment, vitamin K antagonists were recommended for at least three months, or longer depending on the other risk factors, and if the patient has some other underlying problems (21). LMWH was recommended for long-term treatment of DVT in most cancer patients (21).

In patients who develop a pulmonary embolism, IV UFH or LMWH for the initial treatment was recommended. For confirmed nonmassive PE, short-term treatment with SC LMWH or IV UFH was recommended (21). In acute nonmassive PE, LMWH was recommended over UFH (21).

C. Acute Coronary Syndromes

Unfractionated heparin has remained useful in the management of acute coronary syndrome. The 7th ACCP recommendations endorse the use of unfractionated heparin on patients presenting with NSTR, ACS over no anticoagulation with heparin therapy for short-term use with antiplatelet therapies (44). Weight-based dosing of UFH and maintenance of the aPTT between 50 and 75 s is also recommended (44).

The LMWHs are now widely used in the management of ACS. For the acute treatment of patients with non-ST segment elevation (NSTE) ACS, the ACCP recommended LMWHs over UFH (44). The panel recommended against routine monitoring of the anticoagulant effect of LMWHs (44). It was also suggested to continue LMWHs during PCI treatment of the NSTE ACS patients when it has been started as the upstream anticoagulant (44). For patients receiving GP IIb/IIa inhibitors as upstream treatment of NSTE ACS, LMWH is suggested over UFH as the anticoagulant of choice (44).

Although the panel recommended against the use of direct thrombin inhibitors in patients presenting with NSTE ACS, as a routine initial anticoagulant therapy, it is important to note that agents, such as argatroban, and angiomax may be useful in heparin compromised patients, such as those with heparin-induced thrombocytopenia (44).

D. Patients Undergoing Precutaneous Coronary Intervention with Unfractionated Heparin

UFH has remained the anticoagulant of choice in most PCI procedures. The ACCP panel recommended in patients receiving a GP-IIb/IIa inhibitor a heparin bolus of 50–70 IU/kg to achieve a target ACT >200 s (45). However, in those patients not receiving GP IIb/IIa inhibitors, it was recommended that UFH be administered in doses sufficient to produce an ACT of 250–350 s (45). It was also suggested that a weight-adjusted bolus of UFH of 60–100 IU/kg be given (45). In patients after uncomplicated PCI, the panel advised against routine post-procedural infusion of UFH (45).

E. Low Molecular Weight Heparins in Patients Undergoing Precutaneous Coronary Intervention

Several clinical trials on the use of LMWHs in PCI have been reported. The use of LMWH for PCI is not approved by the FDA. The panel recommends that in patients who received LMWH prior to PCI, that administration of additional anticoagulant therapy is dependent on the timing of the last dose of LMWH (45). If the last dose of enoxaparin was administered <8 h prior to PCI, it was suggested not to use any additional anticoagulant therapy (45). If the last dose of enoxaparin was administered between 8 and 12 h before PCI, it was advised to use a 0.3 mg/kg bolus of enoxaparin at the time of PCI (45). If the last enoxaparin dose was administered >12 h before PCI, the panel suggested conventional anticoagulation with UFH during PCI (45).

F. Direct Thrombin Inhibitors in Patients Undergoing Precutaneous Coronary Intervention

Direct thrombin inhibitors were also considered by the ACCP panel. It was recommended that in patients undergoing PCI, who were not treated with a GP II/IIIa antagonist, that a bolus of angiomax (0.75 mg/kg followed by an infusion of 1.75 mg/kg/h for the duration of PCI) was treatment of choice over UFH during PCI (45). In PCI patients who are low risk for complications, the panel recommended angiomax as an alternative to UFH as an adjunct to GP IIb/IIIa antagonist (45). For PCI patients who are at high risk for bleeding, the panel recommended angiomax over UFH as adjunct to GP IIb/IIIa antagonists (45). These recommendations were based on a rather limited trial on angiomax. Furthermore, long-term implications of anticoagulation with angiomax are not known at this time.

G. Anticoagulation in Patients with Heparin-Induced Thrombocytopenia

The ACCP panel recommended against the use of LMWHs in patients suspected with HIT regardless of associated thrombotic complications (46). It was recommended that these patients should be treated with direct thrombin inhibitors, such as the lepirudin, argatroban, angiomax, or a heparinoid namely danaparoid (46).

H. Protamine Neutralization of the Bleeding Effects of Low Molecular Weight Heparins

At present, there are no formal guidelines on the protamine neutralization of the bleeding effects of LMWHs. It is however recommended that if the LMWH were administered within 8 h (SC), protamine may be given in a dose of 1 mg/kg IV per 100 U LMWH as most of the LMWH are administered at 80–100 U/mg with the exception of dalteparin (150 U/kg) (47). An additional dose of 0.5 mg per 100 units of LMWHs may be administered if bleeding continues. Additional dosages of protamine may be needed to counteract bleeding associated with the subcutaneously administered dosage of LMWHs (47). No guidelines are available for IV administration.

VIII. Summary

Owing to advanced technology, dramatic developments in the area of new anticoagulant and antithrombotic drugs appears to have made a profound impact on the use of LMWHs. Furthermore, since porcine mucosal heparin has been used for the preparation of these agents, it is likely that alternate drugs with comparable pharmacologic and clinical efficacy will be sought. Antithrombin drugs, such as argatroban and hirudin, are already approved for alternate management of patients with heparin-induced thrombocytopenia. However, their efficacy in other indications is somewhat less superior. None of these drugs are capable of mimicking the polytherapeutic effects of LMWHs. Biotechnology using bacterial and yeast cultures, aqua cultures from marine products, and plant carbohydrates have been the focus of developing heparin analogues. The development of these agents is in early phases. However, it is likely that this approach may provide a reasonable alternate to the LMWHs. Despite these developments, it is unlikely that any of these drugs will have a profound impact on the use of LMWHs in the near future.

Despite these developments, it is likely that unfractionated heparin will continue to be used for some specific indications. Drug combinations with heparin may necessitate dose adjustments. However, it is not clear at this time, that a unilateral reduction of heparins will be optimal. The coming years will provide useful clinical and applied data on improved usage of unfractionated heparin, LMWHs, and pentasaccharide in the management of thrombotic and cardiovascular disorders. In addition, these drugs will also be used in many expanded indications, such as cancer, inflammation, sepsis, and autoimmune diseases. Polytherapeutic approaches emphasizing the LMWHs as primary and secondary drugs will also impact on the

management of thrombotic and nonthrombotic disorders with these drugs. However, ultra-LMWHs and synthetic heparinomimetics, such as fondaparinux exhibiting a narrow pharmacologic spectrum will only be useful in specific indications and in combination with other drugs.

References

1. Fareed J, Hoppensteadt DA, Bick RL. New antithrombotic drugs: a perspective. Curr Opin Cardiovasc Pulm Ren Investig Drugs 1999; 1:40–55.
2. Fareed J, Bacher P, Messmore HL, Walenga JM, Hoppensteadt DA, Strano A, Pifarre R. Pharmacological modulation of fibrinolysis by antithrombotic and cardiovascular drugs. Prog Cardiovas Dis 1992; 6:379–398.
3. Berkowitz SD, Marder VJ, Kosutic G, Baughman RA. Oral heparin administration with a novel drug delivery agent (SNAC) in healthy volunteers and patients undergoing elective total hip arthroplasty. J Thromb Haemost 2003; 1 (9):1914–1919.
4. Rabah MM, Premmereur J, Graham M, Fareed J, Hoppensteadt D, Grines LL, Grines CL. Usefulness of intravenous enoxaparin for percutaneous coronary intervention instable angina pectoris. Am J Cardiol 1999; 84:1391–1395.
5. Hirsh J, Warkentin T, Raschke R, Granger C, Ohman E, Dalen J. Heparin and low molecular weight heparin. Mechanism of action, pharmacokinetics, dosing considerations, monitoring safety and efficacy. Chest 1998; 114: 489S–501S.
6. Fareed J. Basic and applied pharmacology of low molecular weight heparins. Pharm Ther 1995; 16S–24S.
7. Hoppensteadt DA, Jeske W, Fareed J, Bermes Jr EW. The role of tissue factor pathway inhibitor in the mediation of the antithrombotic actions of heparin and low molecular weight heparin. Blood Coagul Fibrinolysis 1995; (Suppl 1):S57–S64.
8. Fareed J, Walenga JM, Hoppensteadt D, Huam X, Racanelli R. Comparative study on the in vitro and in vivo activities of seven low-molecular weight heparins. Haemostasis 1988; 18 (Suppl 3):3–15.
9. Beguin S, Welzel D, Diere RA, Hemker HC. Conjectures and refutations on the mode of action of heparins. Haemostasis 1999; 29:170–178.
10. Planes A, Vochelle N, Ferru J, Przyrowski D, Clerc J, Fagola M, Planes M. Enoxaparin, low molecular weight heparin: its use in the prevention of deep vein thrombosis following total hip replacement. Haemostasis 1986; 16:152–158.
11. Koopman MMW, Prandoni P, Piovella F. Treatment of venous thrombosis with intravenous unfractionated heparin administered in the hospital as compared with subcutaneous low molecular weight heparin administered at home. N Engl J Med 1996; 334:682–687.
12. Levine M, Gent M, Hirsch J. A comparison of low-molecular-weight administered primarily at home with unfractionated heparin administered in the hospital for proximal deep-vein thrombosis. N Engl J Med 1996; 334:677–681.
13. Samama MM, Cohen AT, Darmon JY, Desjardins L, Eldor A, Janbon C, Leizorovicz A, Nguyen H, Olsson CG, Turpie AG, Weisslinger N. A comparison with placebo for the prevention of venous thromboembolism in acutely ill medical patients. N Engl J Med 1999; 341:793–800.

14. Zacharski LR, Ornsteing DL. Heparin and cancer. Thromb Haemost 1998; 80:10–23.
15. Kay R, Wong KS, Lu UL. Low-molecular-weight heparin for the treatment of acute ischemic stroke. N Engl J Med 1995; 333:1588–1593.
16. Gillis S, Dann EJ, Eldor A. A low molecular weight heparin in the prophylaxis and treatment of disseminated intravascular coagulation in acute promyeloctic leukemia. Eur J Haematol 1995; 54:59–60.
17. Aguilar D, Goldhaber SZ. Clinical uses of low molecular weight heparins. Chest 1999; 115:1418–1423.
18. Hirsh J, Raschke R. Heparin and low-molecular-weight heparin. Chest 2004; 126:179S–203S.
19. Prandoni P. Antithrombotic strategies in patients with cancer. Thromb Haemost 1997; 78:141–144.
20. The Columbus Investigators. Low-molecular-weight heparin in the treatment of patients with venous thromboembolism. N Engl J Med 1997; 337:657–662.
21. Dalen JE, Hirsch J. Fifth ACCP concensus conference on antithrombotic therapy. Chest 1998; 114S–127S.
22. Weitz JI. Low-molecular-weight heparins. N Engl J Med 1997; 337:688–698.
23. Hirsh J, Warkentin TE, Shaughnessy SG. Heparin and low-molecular-weight heparin. mechanisms of action, pharmacokinetic, dosing, monitoring, efficacy, and safety. Chest 2001; 119:64S–94S.
24. Olson JD, Arkin CF, Brandt JT. College of American Pathologist Conference XXXI on laboratory monitoring of anticoagulant therapy. Laboratory monitoring of unfractionated heparin therapy. Arch Pathol Lab Med 1998; 122:782–798.
25. Laposata M, Green D, Van Cott EM, Barrowcliffe TW, Goodnight SH, Sosolik RC. College of American Pathologists Conference XXXI on laboratory monitoring of anticoagulant therapy. The clinical use of laboratory monitoring of low-molecular-weight heparin, danaparoid, hirudin and related compounds, and argatroban. Arch Pathol Lab Med 998; 122:799–807.
26. Walenga J, Fareed J, Messmore HL. Newer avenues in the monitoring of antithromboitc therapy: the role of automation. Semin Thromb Hemost 983; 9:346–354.
27. Marmur JD, Anand SC, Bagga RS. The activated clotting time can be used to monitor the low molecular weight heparin dalteparin after intravenous administration. J Am Coll Cardiol 2003; 4:394–402.
28. Kereiakes DJ, Grines C, Fry E, Esente P, Hoppensteadt D, Midel M, Barr L, Matthai W, Todd M, Broderick T, Rubinstein R, Fareed J, Santoian E, Neiderman A, Brodie B, Zidar J, Ferguson JJ, Cohen M, for the NICE 1 and NICE 4 investigators. Enoxaparin and abciximab adjunctive pharmacotherapy during percutaneous coronary intervention. J Invas Cardiol 2001; 13:272–278.
29. Fareed J, Walenga JM, Pifarre R. Newer approaches to the pharmacologic management of acute myocardial infarction. Cardiac Surg: Art Rev 1992; 6:101–112.
30. Fox KAA, Antman EM. Treatment options in unstable angina. A clinical update. Eur Heart J 1998; 19:KO10.

31. Cohen M, Demers C, Gurfinkel EP. For the ESSENCE investigators. A comparison of low-molecular-weight heparin with unfractionated heparin for unstable coronary artery disease. N Engl J Med 1997; 337:447–454.
32. Kerekiakes DJ, Young J, Broderick TM, Shimshak TM, Abbottsmith CW. Therapeutic adjuncts for immediate transfer to the catheterization laboratory in patients with acute coronary syndromes. J AM Coll Cardiol 2000; 86 (Suppl):10M–17M.
33. Munoz-Torrero JJ, Mora FJ, Diez-Tejedor E. Specific treatment of the acute cerebral infarct. Rev Neurol 2000; 31:959–982.
34. Merli G, Vanscoy G, Rihn TL, Groce JB. Applying scientific criteria to therapeutic interchange: a balanced analysis of low molecular weight heparins. J Thromb Thrombolysis 2001; 11:247–259.
35. American Society of Hospital Pharmacists. ASHP statement on the formulary system. Am J Hosp Pharm 1988; 43:2839–2841.
36. McCart GM, Kayser S. Therapeutic equivalency of low molecular weight heparins. Ann Pharmcotherap 2002; 36:1042–1057.
37. Prandoni P. Low molecular weight heparins: are they interchangeable? Yes. J Thromb Hemostasis 2003; 1:10–11.
38. Nenci G. Low molecular weight heparins: are they interchangeable? No. J Thromb Hemostasis 2003; 1:12–13.
39. Bick RL, Fareed J. Low molecular weight heparin: differences and similarities in approved preparations in the United States. Clin Appl Throm Hemost 1999; 5 (Suppl 1):S63–S66.
40. Fareed J, Hoppensteadt D, Jeske W, Clarizio R, Walenga JM. Low molecular weight heparins. Are they different? Can J Cardiol 1998; 14 (Suppl E): 28E–34E.
41. Leong W, Hoppensteadt DA. Generic forms of low molecular weight heparins: some practical considerations. Clin Appl Thromb Hemost 2003; 9:293–297.
42. Geerts WH, Pinoe GF, Heit JA, Bergqvist D, Lassen MR, Colwell CW, Bay JG. Prevention of venous thromboembolism. Chest 2004; 126:338S–400S.
43. Buller HR, Agnelli G, Hull R, Hyers TM, Prins MH, Raskob GE. Antithrombotic therapy for venous thromboembolic disease. Chest 2004; 126: 401S–428S.
44. Harrington RA, Becker RC, Ezekowitz M, Meader TW, O'Connor CM, Vorchheimer DA, Guyatt GH. Antithrombotic therapy for coronary artery disease. Chest 2004; 126:513S–548S.
45. Popma JJ, Berger P, Ohman EM, Harrington RA, Grines C, Weitz JI. Antithrombotic therapy during percutaneous coronary intervention. Chest 2004; 126:576S–599S.
46. Warkentin TE, Greinacher A. Heparin-induced thrombocytopenia; recognition, treatment and prevention. Chest 2004; 126:338S–400S.
47. Hirsh J, Raschke R. Heparin and low molecular weight heparin. Chest 2004; 126:188S–203S.

Chemistry and Biology of Heparin and Heparan Sulfate
H.G. Garg, R.J. Linhardt and C.A. Hales (Editors)

Chapter 22

Perlecan: An Extracellular Matrix Heparan Sulfate Proteoglycan that Regulates Key Events in Vascular Development and Disease

MICHAEL G. KINSELLA and THOMAS N. WIGHT

Benaroya Research Institute at Virginia Mason, Seattle, WA, USA

I. Introduction

Perlecan is a large heparan sulfate proteoglycan (HSPG) that is synthesized by vascular cells such as endothelial cells (ECs) and smooth muscle cells (SMCs) and is found in basement membranes below ECs and as part of the external lamina (basal lamina) that surrounds SMCs. This highly interactive molecule plays a structural role in the assembly of these specialized extracellular matrices (ECMs), as well as a physiological role in regulating many phenotypic properties of the vascular cells such as adhesion, proliferation, and migration. This involvement places this macromolecule at the heart of events associated with vascular development and disease.

II. Perlecan – The Gene, the Protein Core, and the Glycosaminoglycans

Unlike other principal HSPG gene families, such as the syndecans and glypicans, which have multiple related members, perlecan is the product of a single gene and has no close relatives. The 94 exons of the human perlecan gene, HSPG2 (1), are located on the short arm of chromosome 1 at 1p36.1-p35 (2,3) and are distributed over >140 kb of contiguous genomic DNA (Fig. 1). The murine perlecan gene is located on a syntenic region mouse chromosome 4 (4), and perlecan homologues

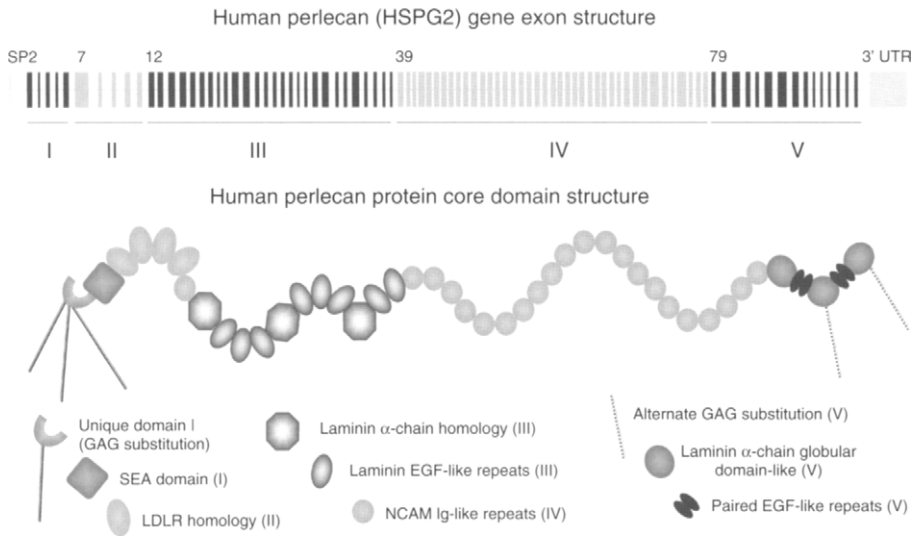

Figure 1 Gene and protein structure of perlecan. The human perlecan gene is composed of 94 exons distributed over >140 kb of genomic sequence, with exon one encoding the signal peptide, and exon 3 encoding the principal GAG substitution sites. Several of the introns are very large (>10 kb), and are not drawn to scale. The protein domains, except for domain I, are composed of repetitive patterns of subdomains with homology to a variety of other proteins.

have been identified in *Drosophila* (5,6) and the nematode, *Caenorhabditis elegans* (7,8). The 5′ flanking region upstream from the exon 1 transcriptional start site of the human perlecan gene has been sequenced (1) and characterized by reporter assay to contain a TGF-β1 responsive element that binds TGF-β-inducible nuclear proteins (9).

Perlecan was first isolated from the reduplicated basement membranes of the mouse Engelbreth–Holm–Swarm sarcoma (10). The structures of the mouse (11) and human (3,12) core proteins were subsequently deduced from cDNA clones. The core proteins of human (467 kDa) and mouse (396 kDa) perlecan are divided into 5 domains based on homology to modules first identified in other proteins. The small amino terminal domain I includes three glycosaminoglycan attachment motifs. Domain II has 4 repeats of a domain homologous to the low-density lipoprotein receptor followed by an immunoglobin (Ig)-like repeat. Domain III has a repetitive homology to the laminin α-chain and contains a pattern of a single laminin domain IV-like module followed by three laminin EGF-like sequences, repeated three times, with the final repeat including only two EGF-like sequences. The largest core protein domain of perlecan is domain IV that includes an extended series of repetitive sequences with homology to the Ig-like repeats in N-CAM. Domain V is homologous to the globular carboxyl terminal domain of laminin α-chain, and contains three repeats of the laminin modules separated by two pairs of EGF-homology modules. The extensive modular repeats within all of

the perlecan domains except domain I suggest that mammalian perlecan gene structure has evolved by a series of reduplication events.

Perlecan that was originally isolated from EHS sarcoma (10,13) and other sources (14) was characterized as containing exclusively heparan sulfate (HS) chains. Subsequently, a subclass of perlecan isolated from a cultured cell line was found to also bear chondroitin/dermatan sulfate chains, either exclusively, or together with HS (15,16), suggesting that perlecan could exist as a hybrid proteoglycan bearing both types of GAG chains. Questions concerning the determinants and sites of GAG chain substitution in the perlecan core protein have been investigated largely by the expression of recombinant perlecan domains in cultured cells. Expression of recombinant domain I in cultured mammalian cells (17,18) demonstrated that this domain could support HS or chondroitin sulfate chain substitution, and deletion mutagenesis the serine residues (ser 65, ser 71, and ser 76) of both human and murine perlecan domain I unambiguously identified these sites of GAG chain substitution (19,20). A single HS or chondroitin/dermatan sulfate chain can be substituted in domain V (21–23). No evidence for GAG substitution of domains II, III, or IV of mammalian perlecan has been found, despite the presence of many potential consensus GAG chain substitution motifs. Thus, mammalian perlecan is primarily substituted with HS at three sites in domain I, but can also bear an additional HS chain in domain V. Alternative minor substitution with chondroitin sulfate can also occur in both domains I and V, although the biological consequences of such alternative glycanation is not known.

HS chain substitution begins by the xylosyltransferase-catalyzed addition of xylose to a serine within a heparan sulfate substitution motif. Sequential additions of two galactose residues and the first glucuronic acid (GlcA) and *N*-acetyl glucosamine (GlcNAc) disaccharide complete the linkage region. HS biosynthesis then occurs by alternating addition of GlcA and GlcNAc residues to the nonreducing end of the growing polymer. HS chain extension is catalyzed by a family of transferases (EXT1, EXT2, and EXT3) that are products of the exostosin-related genes (24). This polymer is then modified by *N*-deacetylation and *N*-sulfation of selected GlcNAc residues, 2-*O*-sulfation, 6-*O*-sulfation, 3-*O*-sulfation, and GlcA epimerization (25). These modifications of the HS chain are carried out by families of *N*-deacetylase: *N*-sulfotransferases (NDSTs), *O*-sulfotransferases, and a C5-epimerase (26) and result in the formation of blocks of highly sulfated HS disaccharide residues interspersed among less highly modified segments of the HS chain. The sequence complexity of HS chains is responsible for the selective differential binding of a large number of ligands, for which the specific HS binding sequences have been determined for several, including antithrombin III and fibroblast growth factor 2 (FGF-2) (27,28). Because HS chain modification results in the formation of ligand binding sequences independent of HSPG protein core sequence, different HSPGs may all bind a given heparin-binding ligand. Thus, the tissue specificity and functional consequence of that binding may often be dependent upon tissue-specific expression of the different proteoglycan core proteins and the differential localization of proteoglycans due to protein core interactions with other macromolecules at the cell surface or within the ECM. As an example, heparin, a particularly heavily

sulfated form of heparan sulfate that is synthesized by mast cells, owes its pharmacological anticoagulant activity to the amplification of antithrombin III activity via interaction through a specific HS pentasaccharide sequence (29,30). However, endothelial cell surface (glypican and syndecan), as well as ECM (perlecan) HSPGs all bind antithrombin III, suggesting that any of these proteoglycans could act as tissue site-specific modulators of thrombosis (31). Interestingly, the localization of anticoagulantly active HSPGs *in vitro* and *in vivo* by determination of antithrombin binding sites suggested that such binding was predominantly found in the subendothelial cell basement membrane (32). Consistent with the suggestion that perlecan may be particularly important in this regard, increased perlecan synthesis by EC was found to correlate with increased antithrombin binding (33).

III. Perlecan Is a Key Extracellular Matrix Component in Basement Membranes and in the Development of the Vascular System

Perlecan, because of its interaction with many of the other principal structural proteins of basal and external laminae, is a reasonable candidate for a central role in basement membrane structure. Perlecan has been found to interact with components of these extracellular structures, including laminin, type IV collagen, and nidogen (34–36). In these studies, laminin and collagen IV bound perlecan HS chains, while nidogens 1 and 2 interacted with the Ig-like modules within perlecan domain IV (36). Site-directed mutagenesis of serine residues in the domain I GAG substitution motif has more recently demonstrated the necessity of HS chains in laminin-1 binding (19). Interactions between perlecan and other minor basement membrane proteins occur as well, although their importance in providing basement membrane stability are not clear. For example, perlecan is known to interact with a C-terminal globular domain proteolytic fragment of collagen type XVIII that co-localizes with perlecan in epithelial and vascular basement membranes (37).

Perlecan is first expressed early in developing mouse heart and major vasculature (e 10.5), (38) and in the aorta of rats (e19) (39), and increases during vascular development. Consistent with a proposed role for basement membrane proteins in promoting cellular differentiation, the expression of perlecan is correlated with the later onset of differentiation in the parenchyma of kidney, lung, liver, spleen, and the gastrointestinal tract (38). Deletional mutations of perlecan that target either exon 6 (40) or exon 7 (41) result in animals that are functionally null for perlecan gene expression. Perlecan null mice are generally embryonic lethal, with critical developmental stages at about e10 and birth (40). The earlier time appears consistent with the timing of perlecan expression in normal mouse heart and large vessels (38), while lethality at the later critical time point is associated with a failure of cartilage differentiation and perichondrial ossification (40,41). The human perlecan null mutation causes Silverman–Handmaker type dyssegmental dysplasia (42), consistent with a major cartilage interstitial matrix defect. These models have provided critical observations that address the function of perlecan in the formation of basement membranes during in vascular development. Interestingly, homozygous perlecan

null mouse embryos form basement membranes that appear morphologically normal, but rupture at sites of increased tensional forces generated with tissue growth or movement, such as during heart contraction (40). Such defects in vascular basement membranes allow blood loss pericardially and result in lethality at the earlier critical stage. Perlecan, as a major HSPG of basal laminae has long been thought to provide anionic charges to critical to filtration of charged solutes (see, e.g., Ref. 43). Indeed, decreased synthesis and content of basement membrane heparan sulfate has been reported in diabetic glomeruli (44,45), which during diabetic nephropathy develop thickened glomerular basement membranes with decreased charge density. Somewhat surprisingly however, mice with a targeted deletion of exon 3, which encodes the principal N-terminal GAG substitution sites of perlecan, show no obvious ultrastructural changes in kidney glomerular basal laminae, and had no apparent defect in kidney filtration (46). Despite the apparently normal structure of kidney basement membrane in this model, the lens capsule basement membrane is disrupted and results in lens degeneration shortly after birth (46). Thus, it appears that a principal function of perlecan is to maintain the structural integrity of basement membranes.

IV. Phenotypic Regulation of Vascular Cells by Perlecan

A. Adhesion

In addition to contributing to the integrity of basement membranes, perlecan binds cell surface proteins and receptors. These interactions both organize cell surface proteins and mediate cellular adhesion to extracellular matrix proteins. For example, the leucine-rich protein, PRELP, binds to perlecan and has been proposed as an anchor for the basement membrane on the cell surface (47). Perlecan also interacts via its HS chains with other matricellular proteins, including fibronectin (36) and thrombospondin-1 (48). It has been proposed that the interaction of cell surface HSPGs, such as syndecans, with heparin-binding domains on matricellular proteins that serve as ligands for integrins modify cell adhesion site formation (49). Perlecan, in contrast, has been reported to inhibit cell adhesion to fibronectin in HS-dependent manner (50), presumably through its interaction with fibronectin. However, perlecan has itself been shown to serve as a ligand for cell surface receptors including integrins. For example, vascular endothelial and SMCs adhere to the perlecan, and removal of the HS chains increases binding (51,52). The adhesion to the perlecan core protein could be blocked by combinations of anti-β1 and anti-β3 integrin antibodies, and was partially inhibited by RGD-containing peptides, including a peptide sequence present in domain III of mouse perlecan core protein (52). Other work has agreed that cell adhesion to perlecan is mediated by β1 integrins, but found that the binding is not RGD-dependent, and that removal of HS from perlecan decreases binding, suggesting that the perlecan core protein and HS chains cooperate in the interaction (53). Analysis of recombinant perlecan protein core domains has also identified a site in domain V for β1 integrin-dependent binding (21).

B. Proliferation

Perlecan expression by SMCs in the developing vasculature is negatively correlated with levels of cell proliferation (39). Thus, SMC proliferation is high early during development of rat aorta, and perlecan protein and mRNA first becomes detectable on day e19, a time at which proliferation of smooth muscle within the aortic media is reduced. Examination of individual cells within the developing aorta indicated that only cells that did not stain for a proliferative marker had detectable perlecan mRNA as determined by *in situ* hybridization (39). Perlecan null mouse embryos that escape lethal critical periods during heart development have a large incidence of transposition of the great arteries (54). Examination of early embryos indicates that the heart develops with hyperplastic conotruncal endocardial cushions, which are populated by neural crest-derived secondary mesenchyme that emigrate from the aortic arches. It is possible that the hypercellularity of the perlecan-null conotruncus predicts a role for perlecan in limiting the extent of migration of secondary mesenchyme, as has been proposed (55). However, it is also possible that perlecan is critical to limit proliferation of the mesenchyme at the time of their differentiation into embryonic smooth muscle of the arterial tree.

A key question continues to be the mechanism by which perlecan downregulates the proliferative response of vascular SMCs. An obvious possibility for perlecan-dependent inhibition of vascular smooth muscle growth is suggested by the binding of heparan binding growth factors, such as bFGF, by perlecan (Fig. 2). In this model, sequestration of heparin-binding growth factors (HBGFs) in extracellular matrix prevents the requisite interaction of the growth factor, such as FGF-2, with cell-surface HSPGs and their high affinity receptor (56). This model is similar to the proposed blockade of HBGF activity by heparin, which has been proposed for FGF-2 within wall of the injured rat vessel (57), and for the inhibition of the transactivation of the EGF receptor by heparin-binding EGF after thrombin treatment of vascular SMCs is culture (58,59). However, sequestration of HB-GF by perlecan is not sufficient to explain all examples of matrix HSPG-dependent inhibition of vascular SMC proliferation. For example, heparitinase digestion of rat neointimal lesions *in vitro* allows induction of proliferation by exogenous PDGF in previously refractive intimal SMCs (60) (Fig. 3), although in the absence of endogenous HS, HBGFs such as FGF-2, could not induce proliferation (M.G. Kinsella, unpublished observations). This observation suggests that a mechanism other than sequestration of HB-GF in the perlecan-rich intimal extracellular matrix is involved in HS-dependent inhibition intimal SMC proliferation.

In addition, or as an alternative to the sequestration hypothesis, there is evidence for direct effects of perlecan on signaling mechanisms activated by growth factors. Following the earlier discovery that heparin infusion could limit vascular smooth muscle proliferation, vascular SMC signaling pathways downstream from growth factor-activated receptor tyrosine kinase were examined for evidence of sensitivity to heparin inhibition. Among the diverse effects of heparin on mitogen-activated protein kinase-dependent signal transduction in vascular SMCs, PDGF-BB receptor activation and stimulation of the Ras-ERK pathway are heparin-insensitive,

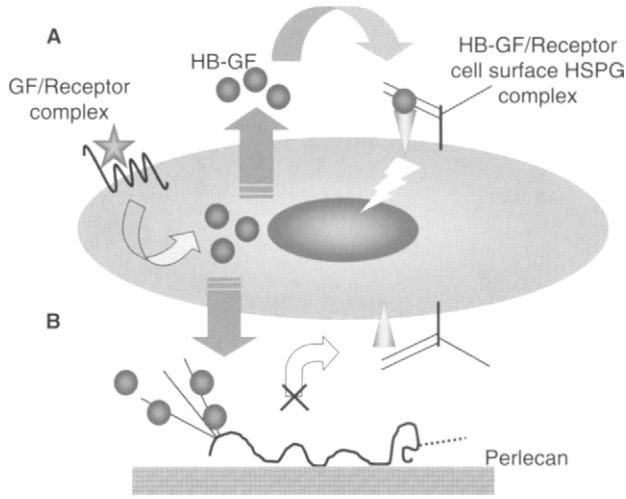

Figure 2 Model of inhibition of heparin-binding growth factor activity by perlecan HS-chain sequestration. (A) Heparin-binding growth factors (HB-GF), such as HB-EGF and FGF-2, released as a result of cell injury or upon cellular activation by signaling through mitogen/receptors (GF/receptor complex), bind cell surface HSPGs and their receptor tyrosine kinase to activate signaling. (B) Release of HB-GF into an environment rich in ECM-bound perlecan sequesters the HB-GF in the ECM and prevents interaction with cell surface HSPGs and their receptor tyrosine kinase.

but MAP kinase activation was found to be affected by heparin inhibition of protein kinase C-dependent signaling (61–63). In addition to suppression of early response genes of proliferating SMC, such as serum and glucocorticoid-regulated kinase (64), as would be expected, heparin also induces the expression of growth arrest specific genes such as COP-1 (65). Examination of perlecan-specific inhibition of proliferation indicated that the expression of the growth-associated transcription factor, Oct-1, which is constitutively expressed by SMC *in vitro* and upregulated during phenotypic modulation of quiescent vascular SMC *in vivo*, is downregulated when cells are grown on perlecan (66). More recently, Garl et al. (68) reported that the regulatory phosphatase and tumor suppressor, PTEN that blocks phosphoinositide-3 kinase (PI3K) signaling at a point upstream from the activation of Akt/PKB (67), is upregulated in SMC that are growth-inhibited by attachment to perlecan. This data is particularly exciting, as downstream targets of Akt activation are associated with constitutive growth of vascular SMC (69), and transgenic mice with a targeted deletion of PTEN (70,71) have a hypercellularity defect that is lethal for homozygous animals. Moreover, PTEN null fibroblasts undergo decreased cell death in response to a variety of apoptotic stimuli because of the constitutive activation of Akt-dependent cell survival mechanisms (72). Thus, PTEN regulation by perlecan may influence apoptotic signaling in neointimal and atherosclerotic lesions, where death of SMCs can contribute to the progression of the disease.

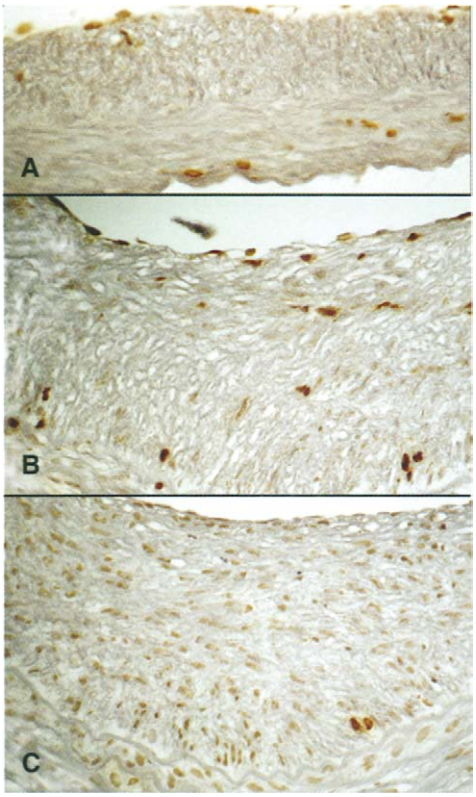

Figure 3 Acquisition of growth factor responsiveness by intimal smooth muscle cells after heparitinase digestion. In 35 weeks after balloon injury to the rat carotid artery, neointimal explants dissected, and treated with buffer alone (A) or heparin lyases I and II (B, C) prior to 48-h organ culture without growth factors (B) or with PDGF-BB (A, C). Nuclei of proliferating cells (dark nuclei) were stained to detect bromodeoxyuridine incorporated during the culture period. Note that dramatically increased intimal SMC growth stimulation by PDGF occurs only after heparin lyase treatment (C).

It is still unclear what receptor(s) might be involved in the transduction of perlecan-dependent growth inhibitory signals. Heparin and HS can bind to a variety of cell surface and transmembrane proteins, although it has yet to be demonstrated that such specific interactions are required to transduce perlecan-mediated inhibitory signals. Perlecan core protein is known to serve as a ligand for integrins and the HS chains of perlecan may modulate integrin interactions with other matrix protein ligands, as discussed above. These interactions may modify integrin-dependent signaling, particularly in regard to the formation of signaling complexes, such as focal adhesions, to influence smooth muscle growth inhibition. For example, the inhibition of SMC growth by apolipoprotein depends upon the induction of perlecan expression (73). The inhibition is reversed by an anti-perlecan domain III antibody. Because integrins have been found to bind perlecan core protein domain

III (52), the authors suggest that the inhibitory effect may be mediated by integrin-dependent signaling. In this regard, it is interesting that the focal adhesion kinase-related nonkinase (FRNK) that is an endogenous inhibitor of focal adhesion kinase (FAK) signaling, is activated in vascular SMC by adhesion of cells to perlecan (74).

C. Extracellular Matrix Assembly

It is important to note that perlecan is associated with the pericellular and extracellular matrix in addition to its involvement in the structure and function of the basement membrane. Within those matrices, perlecan has been found to bind microfibrillar proteins, including fibrillin-1 (75) and fibulin-2 (36,76). Perlecan and fibrillin-1 were co-localized by immunohistochemical approaches in cultured cells as well as at regions near the surface of basement membranes in tissue samples (75). This interaction was mapped to perlecan domains I and II and a central region of fibrillin-1 *in vitro* binding assays, and the authors suggest a role for perlecan in anchoring microfibrils to basement membranes. Fibrillin-1 and fibulin-2 containing microfibrils also bind tropoelastin (77), and serve as a template for elastin fiber formation (78). Interestingly, tropoelastin also interacts with perlecan in binding assays (77), although these two molecules show different patterns of expression in the developing rat pulmonary vasculature and in vascular SMCs in culture (79).

V. Perlecan in Intimal Hyperplasia

Quiescent SMC within the normal media of arteries are in close contact with an external lamina that contains basement membrane components, including type IV collagen, laminin, and perlecan. During intimal hyperplasia in response to arterial injury, medial SMCs are induced to migrate and proliferate in response to the release of growth factors both from injured cells and/or from platelets that bind to the lumenal surface of the vessel at sites of endothelial damage or denudation. The activation of medial SMCs is accompanied by changes in cellular structure, which has been termed phenotypic modulation, in which cellular contractile function and structure is decreased, and synthetic machinery in the cell is increased (80,81). Such proliferative cells have a distinctive profile of ECM protein synthesis, including the synthesis of hyaluronan and versican, fibronectin and interstitial collagens, while decreasing the synthesis of basement membrane components, such as perlecan and laminins (82–84). It has been proposed that after arterial injury SMC transiently express a growth autonomic phenotype that has been associated with rapidly proliferating embryonic vessel wall SMCs (85). This phenotype is associated with the constitutive activation of distinctive signaling pathways, including those involving Akt, mTOR, and p70S6K (69), that are downstream from potential inhibitory signals engendered by cellular interaction with perlecan (68,74).

During the proliferative and migratory stage of vascular smooth muscle response to injury, perlecan expression is low and little perlecan is evident in the developing neointima during the first week after balloon catheterization of the rat

carotid artery (60,86,87) (Fig. 4). The proliferation of SMCs during the first few days after injury is driven largely by the HBGF, FGF-2 (88–90). FGF-2 signaling, like signal transduction by many other heparin binding growth factors and cytokines, requires binding of the growth factor to the HS chains of a cell surface HSPG co-receptor (syndecans and/or glypicans) that also binds to the cognate high affinity receptor (91–93). This interaction of FGF-2 with HS chains on proteoglycans is competitively inhibited by heparin, which thereby inhibits FGF-2 dependent signaling. The heparin-inhibitable SMC proliferation caused by other factors, such as PDGF (94), and thrombin (58,95), also depend upon the induced release of HBGFs, such as HB-EGF and FGF-2, and the transactivation of receptors for these growth factors.

Heparin infusion inhibits SMC proliferation and neointimal formation in the rat carotid injury model (96–98). In addition, incubation of carotid arteries with heparinase immediately after balloon catheter injury inhibits FGF-2-dependent SMC proliferation in injured rat carotid arteries during the first 48 h after injury (86,99). Interestingly, implantation of biomaterial scaffolds containing perlecan-secreting endothelial cells (100), or the periadvential administration of arterial HSPGs (101) inhibit thrombus formation and development of neointimal lesions in injured rat and rabbit carotids, respectively. Conversely, when endothelial cells in which perlecan expression was downregulated with antisense were implanted adventitially to injured porcine carotid arteries, the vessels had increased neointimal proliferation. These experiments suggest that perlecan is responsible for the endothelial cell-mediated inhibition of intimal hyperplasia (102), presumably by sequestration of FGF-2 and the competitive inhibition of interaction of the growth factor with cell surface HSPG co-receptors.

After an early proliferative phase, neointimal cell proliferation is progressively decreased and the lesion volume increases with continued deposition of neointimal extracellular matrix. Perlecan expression is greatly increased during this latter phase of neointimal development, and perlecan is heavily deposited in the neointima (60,87). Interestingly, perlecan accumulation in the neointima occurs when rat carotid arteries are infused with heparin during the development of the neointima after balloon injury (103). This observation has been replicated with cultured rat aortic SMCs in which inhibition of cell proliferation by either serum starvation or heparin treatment results in the accumulation of perlecan (39). Heparin, in addition to its effects on gene expression and HBGF utilization (104), also inhibits HSPG turnover by arterial SMCs (105), which may aid in perlecan accumulation by the cells. Clearly, other factors released from vascular cells by injury may influence perlecan synthesis. Lee and his coworkers have reported that mechanical strain induces perlecan synthesis by cultured vascular SMCs (106), but the mechanism for upregulation, and whether it involves release of growth factors from the cells was not examined. Other factors such as TGF-β1, which regulates extracellular matrix accumulation during neointimal formation (107,108), activate the upstream promoter of human perlecan (9), and induces perlecan expression in endothelial cells (109). Thrombin, which is activated during the coagulation cascade, induces perlecan mRNA and core protein expression in coronary SMCs (110). Conversely, perlecan expression by endothelial cells is downregulated by antithrombin (111).

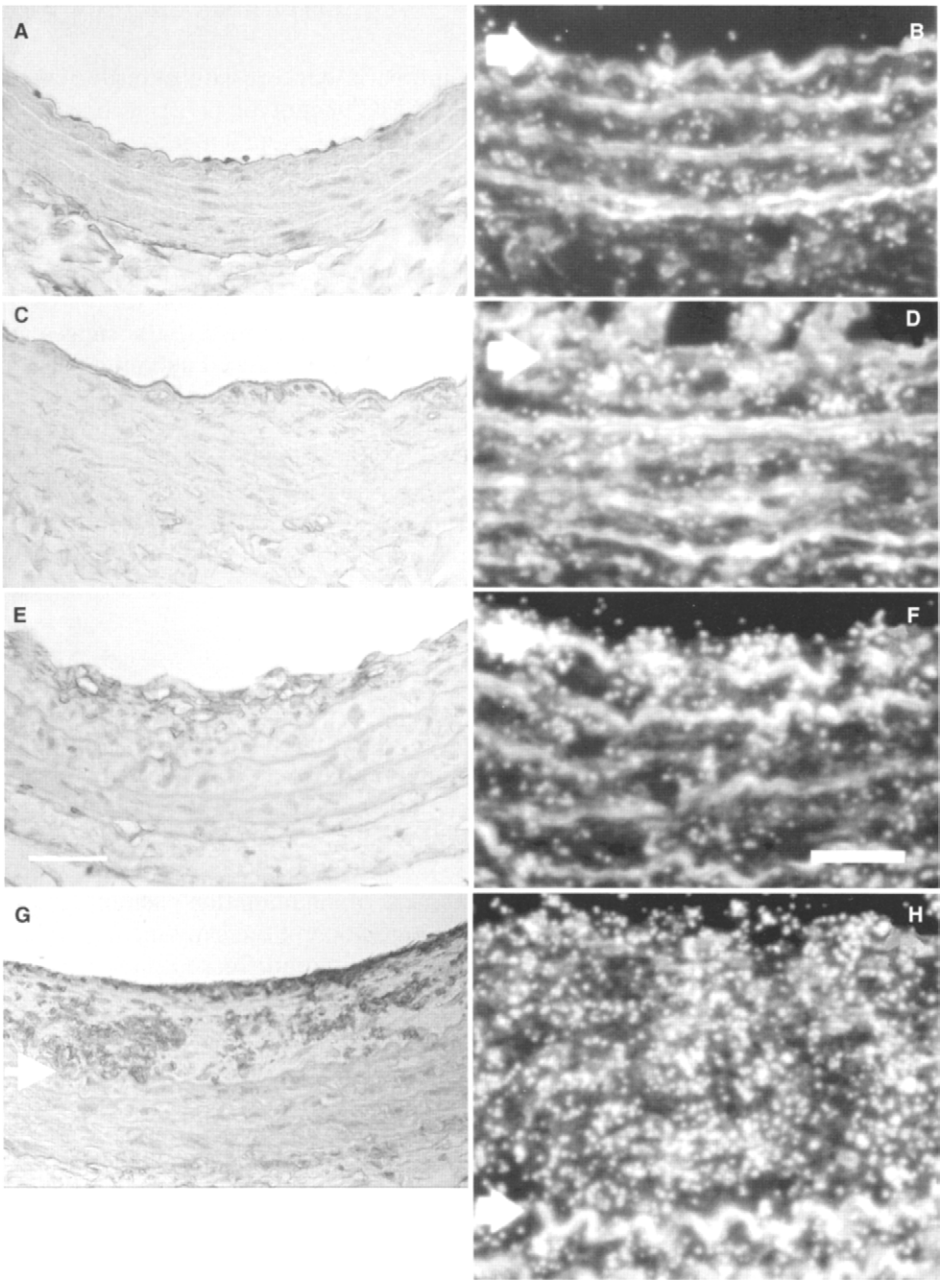

Figure 4 Perlecan core protein (A, C, E, G) and mRNA (B, D, F, G) detected by respectively, immunoperoxidase localization (bar = 150 μm) and *in situ* hybridization (bar = 50 μm), in rat carotid artery sections after experimental injury (A and B, uninjured; C and D, 2–4 days; E and F, 7 days; G and H, 14 days). Arrow marks the internal elastic lamina, which delimits the boundary of the neointima. Lumen of the vessel is at top. Note that substantial increases in perlecan deposition do not occur until a significant neointima is formed at about 14 days in this model, at a time when growth factor responsiveness and cell proliferation of neointimal SMC is decreased.

Perlecan accumulates in the late neointima in concert with other basement membrane components that clearly influence SMC phenotype (112), such as laminin (84). However, evidence suggests that perlecan itself is sufficient to inhibit SMC proliferation *in vitro* (39). In the rat carotid neointima, SMCs return to quiescence as perlecan accumulates (60), and are refractive to stimulation by infusion of exogenous growth factors, such as FGF-2 (113) and platelet-derived growth factor (PDGF), in contrast to medial SMCs that are activated in the first 48 h following injury (114). The refractivity to growth factor stimulation can be overcome in organ-cultured neointima by heparitinase treatment (60), suggesting that HSPGs deposited in the extracellular matrix of the advanced neointimal lesion are responsible for the growth inhibition. In agreement with this observation, when mice with a targeted deletion of perlecan exon 3 that have reduced HS substitution were subjected to carotid artery ligation injury, SMC proliferation was increased and the intimal lesions were larger when compared to the lesions seen in control animals (115). These experiments strongly suggest that perlecan is the critical HSPG that limits smooth muscle proliferation in the advanced neointimal lesion.

VI. Perlecan in Atherosclerosis

Models of arterial injury such as rat carotid artery balloon catheterization induce intimal hyperplasia without substantial inflammation. However, atherosclerosis is a complicated vascular disease that develops largely in response to inflammatory stimuli, including the accumulation of lipoproteins and other proteins, such as serum amyloid protein (SAA) (116–118). In this environment, perlecan may have several influences, including the entrapment of inflammation promoting lipoproteins and SAA within the vessel wall, and regulation of the cytokine-dependent events that affect leukocyte trafficking and differentiation. In addition, as previously discussed, perlecan may influence the extent of vascular SMC hyperplasia within the lesion, and the assembly of extracellular matrix proteins to limit the expansion of the lesion and promote cellular and tissue stability. In this environment, perlecan appears to play a key role.

A. Perlecan Involvement in Arterial Lipoprotein Retention

A principal inductive agent in atherosclerosis in humans, and in mouse and rabbit models, is the accumulation of lipoproteins within the vessel wall. Lipoproteins are known to bind to glycosaminoglycans, including the HS chains borne on perlecan (119). Although domain II of perlecan core protein has homology to the LDL receptor and has been proposed to mediate interaction of lipoprotein, such a direct interaction has not been demonstrated. The binding of lipoproteins by perlecan may be important in the entrapment of serum-borne lipoproteins within the vessel wall, which has been proposed as a critical element in the promotion of atherosclerosis as the "response-to-retention" hypothesis (120). In an examination of

atherosclerotic lesions induced by fat feeding in the primate, *Macaca nemestrina*, perlecan was heavily deposited in the advanced lesion adjacent to the lipid-rich lesion core (121). In the fat-fed mouse $LDLR^{-/-}$ model of atherosclerosis, perlecan immunostaining was localized throughout the intima in intermediate and advanced lesions in association with extracellular deposits of lipoproteins (122). These observations indicate that perlecan is a major proteoglycan that accumulates in atherosclerotic lesions, in addition to other chondroitin/dermatan sulfate proteoglycans, such as biglycan and versican that also contribute to lipoprotein binding within the developing lesion (123).

Perlecan may also be important for systemic catabolism of lipoproteins *in vivo* (124). To test the importance of perlecan in lipoprotein retention in the mouse models of atherosclerosis, mice that had a heterozygous deletion of perlecan were crossed into apoE and LDL receptor knockout backgrounds (125). Examination of atherosclerosis in apolipoprotein E null mice with a heterozygous perlecan deletion, which have reduced perlecan levels, did not detect altered lipoprotein profiles, suggesting that perlecan HS is not a limiting factor for systemic lipoprotein remnant removal (125). However, these studies confirmed the previously reported distribution of perlecan in developing atheromas, although the presence of a perlecan null allele did not significantly alter the size of the lesion that was ultimately formed. Perlecan was detected in subendothelial regions adjacent to small fatty streaks that formed at the earliest time point. The authors suggest that proteoglycan accumulation and subsequent lipoprotein deposition may represent the earliest morphological evidence of disease in this model, and that perlecan, may specifically be important for the binding of apolipoprotein A-I containing HDL particles, which have important anti-atherogenic and pro-atherogenic properties (122,126,127). LDL binds weakly to HS *in vitro* and it is likely that other molecules such as lipoprotein lipase act as bridges between perlecan and the lipoprotein (128–130).

Serum amyloid is another plasma lipoprotein (HDL)-associated molecule that interacts with HS-containing proteoglycans such as perlecan (131) and accumulates in lesions of atherosclerosis (132). In fact, elevated serum amyloid A levels are associated with increased cardiovascular risk in humans. Of interest is that SAA are major acute phase reactants (133) that increase dramatically with inflammation (133,134). Recent studies show that SAA is deposited in murine atherosclerosis co-localized with extracellular perlecan (132)(Fig. 5). Also, HDL isolated from LPS-injected mice with elevated SAA levels bound to a greater extent than HDL isolated from normal mice to perlecan isolated from human arterial SMC cultures (132). These results are consistent for a role of SAA and perlecan in the retention of lipoproteins during the formation of atherosclerotic lesions.

B. A Role for Perlecan in Inflammatory Vascular Disease

At very early times after induction of atherosclerosis in mouse models, monocytes and T cells bind activated endothelial cells and infiltrate the arterial wall, and compose the major part of the early lesion. The monocytes that initially traffic

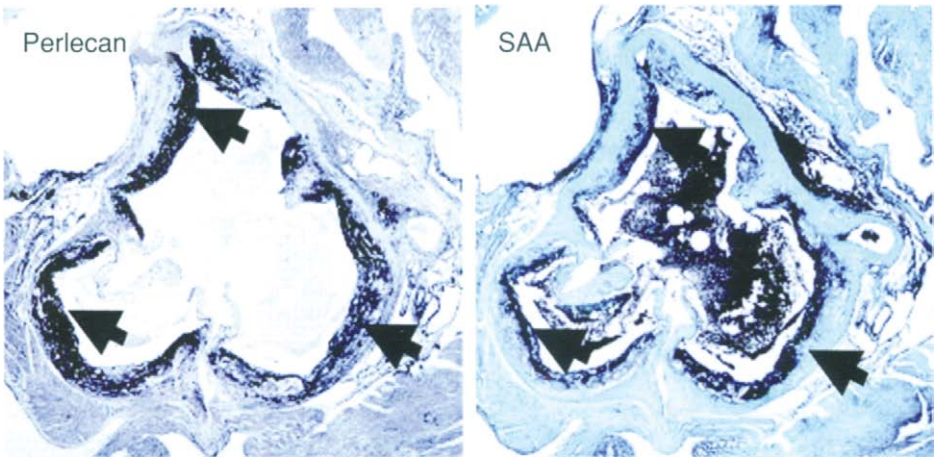

Figure 5 Immunohistochemical detection of serum amyloid A (SAA) and perlecan (arrows) in sections of late (70 weeks) atherosclerotic lesions in the aortic sinus from chow-fed low-density lipoprotein receptor null ($LDLR^{-/-}$) mice. SAA co-localizes with extracellular perlecan in murine atherosclerosis.

into the developing lesion, and the macrophages into which they rapidly differentiate probably do not make large quantities of perlecan (135), although the monocytic cell line, THP-1, has recently been shown to synthesize perlecan (136). In addition to binding lipoproteins that, particularly when modified, are important antigens involved in the induction of an immune response, perlecan binds chemokines that direct activation, differentiation and targeting of leukocytes during inflammatory events. HS chains bind a large number of chemokines involved in leukocyte activation and trafficking, including IL-2, IL-8, RANTES, MCP-1 and MIP-1α (137–139). As perlecan is deposited early during inflammatory lesion formation, it may mediate leukocyte-modified and modifying activities within the developing lesion. However, perlecan is also a component of extracellular matrix structures in immune organs such as the spleen, where it is important for binding and presenting cytokines such as IL-2 (139). Therefore, perlecan may also have a systemic role in driving T-cell proliferation and homeostasis in response to cytokine-dependent activation (140).

HS chains can also serve directly as a ligand for cell surface receptors of leukocytes and may modify their adhesion to other matrix protein ligands. For example, treatment of activated endothelial cells to remove HS inhibited L-selectin-dependent monocyte adhesion under flow conditions (141). Although the interaction of the apical surface of endothelial cells probably involved cell surface HSPGs in that study, the interaction of L-selectins with HS suggests that perlecan heparan chains may also play a role in mediating monocytes post-trafficking events in the development of the atherosclerotic lesion. The high-affinity binding of specific HS tetrasaccharides to P-selectin and L-selectin affinity columns

has led to the suggestion that these compounds might be useful as therapeutic agents in inflammatory disease (142). In addition, as discussed above, β1 and β3 integrins interact with the core protein of perlecan, and perlecan can modify integrin-dependent leukocyte adhesion to other ligands, such as fibronectin (50,143). Interestingly, alteration of perlecan HS chain structure occurs under conditions such as hyperglycemia (144) or treatment of cells with a component of modified lipoproteins (143) that increases atherosclerosis susceptibility and alters monocytes adhesion. Such changes in heparan sulfate chain structure remain incompletely characterized, but may derive from several mechanisms. For example, HS chain length and composition may be affected by catabolic mechanisms such as the induced expression of extracellularly active sulfatases and heparanases (33,143) or the effects of NO generation, which has been shown to depolymerize HS at levels comparable to those induced in tissue (145). Alternatively, such changes may be caused by altered expression of HS modifying enzymes, such as the *N*-deacetylase/*N*-sulfotransferases (NDSTs) (146), which may influence the binding of growth factors that modify vascular SMC proliferation and phenotype (147), and cytokines that mediate in inflammatory responses (148).

VII. Perlecan and Angiogenesis

It is important to note that under certain conditions heparin/heparan sulfate and perlecan can stimulate cell growth. For example, low concentrations of heparin support FGFR activation by FGF-2, particularly in the absence of endogenous HS, thus promoting cell growth associated with angiogenesis (93). Moreover, perlecan cannot only bind FGF-2, but is capable of supporting HS-dependent FGF receptor activation by the growth factor as well (59,149). In these experiments, antisense downregulation of perlecan synthesis in mouse 3T3 cells or a melanoma cell line abrogated FGF-2-dependent cell proliferation and FGF receptor activation. These effects were rescued by the addition of perlecan or heparin. Similar effects have been recognized after perlecan downregulation in a number of tumor cell lines (150–152). Moreover, mice with a targeted deletion of perlecan exon 3 that synthesize HS-deficient perlecan have impaired angiogenesis and slower wound healing (153). These studies and others have suggested a role for perlecan in the promotion of tumor-directed angiogenesis, primarily through the presentation of proangiogenic factors, such as FGF and vascular endothelial cell growth factor (VEGF) [see (154) for an excellent review]. These observations suggest that perlecan can either inhibit or promote cellular response to HBGFs, an apparent duality of function that has been termed a paradox [e.g., see (155)]. However, several explanations may account for the apparent disparity in perlecan function. HS chains bind many effectors through distinct sulfated oligosaccharide sequences (27). It has been noted that perlecan isolated from different vascular tissues bears HS chains that differentially bind FGF-2 and FGFR (156). Moreover, hyperglycemia appears to alter perlecan heparan chain structure and HS-dependent cell adhesion (144). Similarly, increased proliferative responsiveness to HB-EGF of vascular SMCs of

diabetic rats or SMC cultured in high glucose is dependent on altered HS produced by the cells (157,158). HS synthesis and structure are also altered by the murine J774 macrophage cell line as they take up lipid to form foam cells *in vitro* (159). Therefore, it is possible that the HS chains synthesized by different cell types, or under different metabolic conditions, may have altered ability to bind various growth and angiogenic factors and thereby alter the balance of HS-dependent inhibitory and stimulatory activities. Another likely explanation for the apparent duality of perlecan function also may relate to changes in environmental conditions. If a key requirement of the inhibition of HBGF action by perlecan is the ability to sequester such factors at extracellular matrix sites in which interaction with the high affinity receptors at the cell surface is precluded, then release of active HS–HBGF complexes by heparanase or proteolytic activity may reverse the inhibition. Clearly, treatment of HSPGs with a variety of proteases and mammalian heparanase or exogenous bacterial heparinase releases HBGFs, such as FGF-2 and VEGF in a bioactive form (160–162). Moreover, expression of metalloproteinases and serine proteases, such as plasmin, is activated during activation of SMCs at early times during neointimal formation after arterial injury and during atherosclerosis and angiogenesis (163,164). Perlecan is degraded by neutrophil elastase and myeloperoxidase (165) and by proteases during ischemia (166), a condition that is commonly present in vascular disease. Recent interest in a cell-associated endogenous heparanase has also led to studies of the involvement of this enzyme in the regulation of metastatic cell growth and angiogenesis (167). Mammalian heparanase has been found to degrade HS chains on perlecan (168) and to be induced by inflammatory cytokines and fatty acids that are contributing factors in atherosclerosis (169). Thus, it seems likely, particularly in the molecular environment of a growing tumor, or during induction of vascular disease by injury or inflammation, that the role of perlecan as an inhibitor of vascular cell proliferation could be reversed by cleavage by proteases and heparanase to release fragments that activate cell proliferation (Fig. 6).

Proteolytic cleavage of basement membrane proteins such as type XVIII collagen and perlecan also releases C-terminal globular domains that have important inhibitory activities for vascular cell growth and angiogenesis, and are being analyzed as potential agents for suppression of tumor cell growth (170). The proteolytically generated C-terminal of type XVIII collagen, termed "endostatin," has been shown to bind to laminin and HS and co-localizes with perlecan in basement membranes (37,171,172). Endostatin does not compete for FGF2 binding to HS chains (171), and recent studies have defined a distinct HS oligosaccharide sequence that mediates endostatin binding that is distinct from the determinants that mediate FGF-2 binding (173). A similar anti-angiogenic activity has recently been associated with a proteolytically derived C-terminal globular portion of perlecan domain V (174), which was named "endorepellin". This perlecan cleavage product can be generated by the metalloproteinase, BMP-1 (175), and may influence endothelial cell biology by causing cytoskeleton and focal adhesions disassembly through integrin destabilization (176). Recently, in a study of anti-apoptotic factors released by apoptotic endothelial cells, Raymond et al. found that a

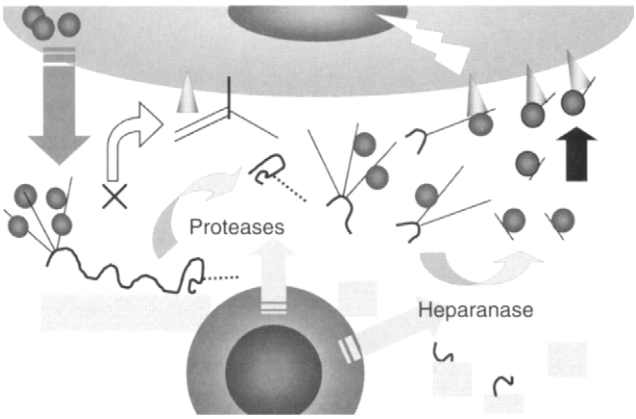

Figure 6 Reversal of perlecan-mediated inhibition of growth factor responsiveness (top, left) by ECM degradation. Secretion of proteases and heparanase by activated tumor cells, leukocytes or endothelial cells (bottom, center) release heparin-binding growth factors and proangiogeneic factors from binding sites on perlecan HS-chains within the ECM (bottom left), and allow activation of cell surface HSPG/receptor tyrosine kinase complexes at the cell surface (right).

proteolytic product of perlecan domain V, released endogenously by a protease dependent upon caspase activity, inhibited apoptotic mechanisms in vascular SMC. Interestingly, either the EGF motif of perlecan domain V or chondroitin 4-sulfate, which may be substituted on this domain, were found to have the same activity (177). Since endothelial cells damage, and death and decreased apoptosis of vascular SMC are central events during vascular disease leading to neointimal thickening, such proteolytically generated fragments may have a previously unrecognized role in the control of vascular cell biology in development and disease.

VIII. Conclusions

The large HSPG, perlecan, is expressed in a regulated manner during development and disease by vascular endothelial and smooth muscle cells. The interactions of both the perlecan protein core and the HS chains with ligands at the cell surface and within the ECM are critical to the assembly of ECM structures, such as basement membranes, and to the interaction of cells with those structures. The binding of growth factors by perlecan HS chains regulates key aspects of vascular cell growth and may control, in part, the extent of intimal hyperplasia and angiogenesis. Finally, the interactions of perlecan HS with antithrombin, cytokines and lipoproteins have an important role in the response of vascular tissue to injury, including modulation of blood coagulation, and the regulation of inflammation during atherosclerosis.

Acknowledgments

This work was funded by a Grant-in-Aid from the American Heart Association, Pacific Mountain Affiliate (M.G.K.) and HL18645 and HL030086 (T.N.W.).

References

1. Cohen IR, Grässel S, Murdoch AD, Iozzo RV. Structural characterization of the complete human perlecan gene and its promoter. Proc Natl Acad Sci USA 1993; 90:10404–10408.
2. Dodge GR, Kovalszky I, Chu ML, Hassell JR, McBride OW, Yi HF, Iozzo RV. Heparan sulfate proteoglycan of human colon: partial molecular cloning, cellular expression, and mapping of the gene (HSPG2) to the short arm of human chromosome 1. Genomics 1991; 10:673–680.
3. Kallunki P, Eddy RL, Byers MG, Kestila M, Shows TB, Tryggvason K. Cloning of human heparan sulfate proteoglycan core protein, assignment of the gene (HSPG2) to 1p36.1-p35 and identification of a BamHI restriction fragment length polymorphism. Genomics 1991; 11:389–396.
4. Chakravarti S, Phillips SL, Hassell JR. Assignment of the perlecan (heparan sulfate proteoglycan) gene to mouse chromosome 4. Mamm Genome 1991; 1:270–272.
5. Friedrich MV, Schneider M, Timpl R, Baumgartner S. Perlecan domain V of Drosophila melanogaster. Sequence, recombinant analysis and tissue expression. Eur J Biochem 2000; 267:3149–3159.
6. Park Y, Rangel C, Reynolds MM, Caldwell MC, Johns M, Nayak M, Welsh CJ, McDermott S, Datta S. Drosophila perlecan modulates FGF and hedgehog signals to activate neural stem cell division. Dev Biol 2003; 253:247–257.
7. Rogalski TM, Williams BD, Mullen GP, Moerman DG. Products of the unc-52 gene in Caenorhabditis elegans are homologous to the core protein of the mammalian basement membrane heparan sulfate proteoglycan. Genes Dev 1993; 7:1471–1484.
8. Rogalski TM, Mullen GP, Gilbert MM, Williams BD, Moerman DG. The UNC-112 gene in Caenorhabditis elegans encodes a novel component of cell-matrix adhesion structures required for integrin localization in the muscle cell membrane. J Cell Biol 2000; 150:253–264.
9. Iozzo RV, Pillarisetti J, Sharma B, Murdoch AD, Danielson KG, Uitto J, Mauviel A. Structural and functional characterization of the human perlecan gene promoter. Transcriptional activation by transforming growth factor-beta via a nuclear factor 1-binding element. J Biol Chem 1997; 272:5219–5228.
10. Hassell JR, Robey PG, Barrach HJ, Wilczek J, Rennard SI, Martin GR. Isolation of a heparan sulfate-containing proteoglycan from basement membrane. Proc Natl Acad Sci USA 1980; 77:4494–4498.
11. Noonan DM, Horigan EA, Ledbetter SR, Vogeli G, Sasaki M, Yamada Y, Hassell JR. Identification of cDNA clones encoding different domains of the basement membrane heparan sulfate proteoglycan. J Biol Chem 1988; 263:16379–16387.

12. Murdoch AD, Dodge GR, Cohen I, Tuan RS, Iozzo RV. Primary structure of the human heparan sulfate proteoglycan from basement membrane (HSPG2/perlecan). A chimeric molecule with multiple domains homologous to the low density lipoprotein receptor, laminin, neural cell adhesion molecules, and epidermal growth factor. J Biol Chem 1992; 267:8544–8557.
13. Fujiwara S, Wiedemann H, Timpl R, Lustig A, Engel J. Structure and interactions of heparan sulfate proteoglycans from a mouse tumor basement membrane. Eur J Biochem 1984; 143:145–157.
14. Saku T, Furthmayr H. Characterization of the major heparan sulfate proteoglycan secreted by bovine aortic endothelial cells in culture. Homology to the large molecular weight molecule of basement membranes. J Biol Chem 1989; 264:3514–3523.
15. Danielson KG, Martinez-Hernandez A, Hassell JR, Iozzo RV. Establishment of a cell line from the EHS tumor: biosynthesis of basement membrane constituents and characterization of a hybrid proteoglycan containing heparan and chondroitin sulfate chains. Matrix 1992; 11:22–35.
16. Couchman JR, Kapoor R, Sthanam M, Wu RR. Perlecan and basement membrane-chondroitin sulfate proteoglycan (bamacan) are two basement membrane chondroitin/dermatan sulfate proteoglycans in the Engelbreth–Holm–Swarm tumor matrix. J Biol Chem 1996; 271:9595–9602.
17. Kokenyesi R, Silbert JE. Formation of heparan sulfate or chondroitin/dermatan sulfate on recombinant domain I of mouse perlecan expressed in Chinese hamster ovary cells. Biochem Biophys Res Commun 1995; 211:262–267.
18. Dolan M, Horchar T, Rigatti B, Hassell JR. Identification of sites in domain I of perlecan that regulate heparan sulfate synthesis. J Biol Chem 1997; 272:4316–4322.
19. Sasaki T, Costell M, Mann K, Timpl R. Inhibition of glycosaminoglycan modification of perlecan domain I by site-directed mutagenesis changes protease sensitivity and laminin-1 binding activity. FEBS Lett 1998; 435:169–172.
20. Costell M, Mann K, Yamada Y, Timpl R. Characterization of recombinant perlecan domain I and its substitution by glycosaminoglycans and oligosaccharides. Eur J Biochem 1997; 243:115–121.
21. Brown JC, Sasaki T, Gohring W, Yamada Y, Timpl R. The C-terminal domain V of perlecan promotes beta1 integrin-mediated cell adhesion, binds heparin, nidogen and fibulin-2 and can be modified by glycosaminoglycans. Eur J Biochem 1997; 250:39–46.
22. Tapanadechopone P, Hassell JR, Rigatti B, Couchman JR. Localization of glycosaminoglycan substitution sites on domain V of mouse perlecan. Biochem Biophys Res Commun 1999; 265:680–690.
23. Friedrich MV, Gohring W, Morgelin M, Brancaccio A, David G, Timpl R. Structural basis of glycosaminoglycan modification and of heterotypic interactions of perlecan domain V. J Mol Biol 1999; 294:259–270.
24. Zak BM, Crawford BE, Esko JD. Hereditary multiple exostoses and heparan sulfate polymerization. Biochim Biophys Acta 2002; 1573:346–355.
25. Lindahl U, Kusche-Gullberg M, Kjellen L. Regulated diversity of heparan sulfate. J Biol Chem 1998; 273:24979–24982.
26. Kusche-Gullberg M, Kjellen L. Sulfotransferases in glycosaminoglycan biosynthesis. Curr Opin Struct Biol 2003; 13:605–611.

27. Esko JD, Selleck SB. Order out of chaos: assembly of ligand binding sites in heparan sulfate. Annu Rev Biochem 2002; 71:435–471.
28. Esko JD, Lindahl U. Molecular diversity of heparan sulfate. J Clin Invest 2001; 108:169–173.
29. Rosenberg RD, Bauer KA, Marcum JA. The heparin-antithrombin system. In: Murano E, ed. Reviews in Hematology. P.D.J. Publications, Ltd, 1984.
30. Hovingh P, Piepkorn M, Linker A. Biological implications of the structural, antithrombin affinity and anticoagulant activity relationships among vertebrate heparins and heparan sulfates. Biochem J 1986; 237:573–581.
31. Mertens G, Cassiman JJ, Van den Berghe H, Vermylen J, David G. Cell surface heparan sulfate proteoglycans from human vascular endothelial cells. Core protein characterization and antithrombin III binding properties. J Biol Chem 1992; 267:20435–20443.
32. de Agostini AI, Watkins SC, Slayter HS, Youssoufian H, Rosenberg RD. Localization of anticoagulantly active heparan sulfate proteoglycans in vascular endothelium: antithrombin binding on cultured endothelial cells and perfused rat aorta. J Cell Biol 1990; 111:1293–1304.
33. Pillarisetti S. Lipoprotein modulation of sub-endothelial heparan sulfate proteoglycans (perlecan) and atherogenicity. Trends Cardiovasc Med 2000; 10:60–65.
34. Battaglia C, Mayer U, Aumailley M, Timpl R. Basement-membrane heparan sulfate proteoglycan binds to laminin by its heparan sulfate chains and to nidogen by sites in the protein core. Eur J Biochem 1992; 208:359–366.
35. Timpl R, Brown JC. Supramolecular assembly of basement membranes. Bioessays 1996; 18:123–132.
36. Hopf M, Gohring W, Mann K, Timpl R. Mapping of binding sites for nidogens, fibulin-2, fibronectin and heparin to different IG modules of perlecan. J Mol Biol 2001; 311:529–541.
37. Miosge N, Simniok T, Sprysch P, Herken R. The collagen type XVIII endostatin domain is co-localized with perlecan in basement membranes in vivo. J Histochem Cytochem 2003; 51:285–296.
38. Handler M, Yurchenco PD, Iozzo RV. Developmental expression of perlecan during murine embryogenesis. Dev Dyn 1997; 210:130–145.
39. Weiser MC, Belknap JK, Grieshaber SS, Kinsella MG, Majack RA. Developmental regulation of perlecan gene expression in aortic smooth muscle cells. Matrix Biol 1996; 15:331–340.
40. Costell M, Gustafsson E, Aszodi A, Morgelin M, Bloch W, Hunziker E, Addicks K, Timpl R, Fassler R. Perlecan maintains the integrity of cartilage and some basement membranes. J Cell Biol 1999; 147:1109–1122.
41. Arikawa-Hirasawa E, Watanabe H, Takami H, Hassell JR, Yamada Y. Perlecan is essential for cartilage and cephalic development. Nat Genet 1999; 23:354–358.
42. Arikawa-Hirasawa E, Wilcox WR, Le AH, Silverman N, Govindraj P, Hassell JR, Yamada Y. Dyssegmental dysplasia, Silverman–Handmaker type, is caused by functional null mutations of the perlecan gene. Nat Genet 2001; 27:431–434.
43. Conde-Knape K. Heparan sulfate proteoglycans in experimental models of diabetes: a role for perlecan in diabetes complications. Diabetes Metab Res Rev 2001; 17:412–421.

44. Brown DM, Klein DJ, Michael AF, Oegema TR. 35S-glycosaminoglycan and 35S-glycopeptide metabolism by diabetic glomeruli and aorta. Diabetes 1982; 31:418–425.
45. Parthasarathy N, Spiro RG. Effect of diabetes on the glycosaminoglycan component of the human glomerular basement membrane. Diabetes 1982; 31:738–741.
46. Rossi M, Morita H, Sormunen R, Airenne S, Kreivi M, Wang L, Fukai N, Olsen BR, Tryggvason K, Soininen R. Heparan sulfate chains of perlecan are indispensable in the lens capsule but not in the kidney. EMBO J 2003; 22: 236–245.
47. Bengtsson E, Morgelin M, Sasaki T, Timpl R, Heinegard D, Aspberg A. The leucine-rich repeat protein PRELP binds perlecan and collagens and may function as a basement membrane anchor. J Biol Chem 2002; 277: 15061–15068.
48. Vischer P, Völker W, Schmidt A, Sinclair N. Association of thrombospondin of endothelial cells with other matrix proteins and cell attachment sites and migration tracks. Eur J Biochem 1988; 47:36–46.
49. Hook M, Woods A, Johansson S, Kjellen L, Couchman JR. Functions of proteoglycans at the cell surface. Ciba Found Symp 1986; 124:143–157.
50. Lundmark K, Tran PK, Kinsella MG, Clowes AW, Wight TN, Hedin U. Perlecan inhibits smooth muscle cell adhesion to fibronectin: role of heparan sulfate. J Cell Physiol 2001; 188:67–74.
51. Whitelock JM, Graham LD, Melrose J, Murdoch AD, Iozzo RV, Underwood PA. Human perlecan immunopurified from different endothelial cell sources has different adhesive properties for vascular cells. Matrix Biol 1999; 18:163–178.
52. Hayashi K, Madri JA, Yurchenco PD. Endothelial cells interact with the core protein of basement membrane perlecan through beta 1 and beta 3 integrins: an adhesion modulated by glycosaminoglycan. J Cell Biol 1992; 119:945–959.
53. Battaglia C, Aumailley M, Mann K, Mayer U, Timpl R. Structural basis of beta 1 integrin-mediated cell adhesion to a large heparan sulfate proteoglycan from basement membranes. Eur J Cell Biol 1993; 61:92–99.
54. Costell M, Carmona R, Gustafsson E, Gonzalez-Iriarte M, Fassler R, Munoz-Chapuli R. Hyperplastic conotruncal endocardial cushions and transposition of great arteries in perlecan-null mice. Circ Res 2002; 91:158–164.
55. Kirby ML. Embryogenesis of transposition of the great arteries: a lesson from the heart. Circ Res 2002; 91:87–89.
56. Nugent MA, Karnovsky MJ, Edelman ER. Vascular cell-derived heparan sulfate shows coupled inhibition of basic fibroblast growth factor binding and mitogenesis in vascular smooth muscle cells. Circ Res 1993; 73:1051–1060.
57. Lindner V, Olson NE, Clowes AW, Reidy MA. Inhibition of smooth muscle cell proliferation in injured rat arteries. Interaction of heparin with basic fibroblast growth factor. J Clin Invest 1992; 90:2044–2049.
58. Kalmes A, Vesti BR, Daum G, Abraham JA, Clowes AW. Heparin blockade of thrombin-induced smooth muscle cell migration involves inhibition of epidermal growth factor (EGF) receptor transactivation by heparin-binding EGF-like growth factor. Circ Res 2000; 87:92–98.

59. Aviezer D, Hecht D, Safran M, Eisinger M, David G, Yayon A. Perlecan, basal lamina proteoglycan, promotes basic fibroblast growth factor-receptor binding, mitogenesis, and angiogenesis. Cell 1994; 79:1005–1013.
60. Kinsella MG, Tran PK, Weiser-Evans MC, Reidy M, Majack RA, Wight TN. Changes in perlecan expression during vascular injury: role in the inhibition of smooth muscle cell proliferation in the late lesion. Arterioscler Thromb Vasc Biol 2003; 23:608–614.
61. Pukac LA, Ottlinger ME, Karnovsky MJ. Heparin suppresses specific second messenger pathways for protooncogene expression in rat vascular smooth muscle cells. J Biol Chem 1992; 267:3707–3711.
62. Daum G, Hedin U, Wang Y, Wang T, Clowes AW. Diverse effects of heparin on mitogen-activated protein kinase-dependent signal transduction in vascular smooth muscle cells. Circ Res 1997; 81:17–23.
63. Pukac LA, Carter JE, Ottlinger ME, Karnovsky MJ. Mechanisms of inhibition by heparin of PDGF stimulated MAP kinase activation in vascular smooth muscle cells. J Cell Physiol 1997; 172:69–78.
64. Delmolino LM, Castellot Jr JJ. Heparin suppresses sgk, an early response gene in proliferating vascular smooth muscle cells. J Cell Physiol 1997; 173:371–379.
65. Delmolino LM, Stearns NA, Castellot Jr JJ. COP-1, a member of the CCN family, is a heparin-induced growth arrest specific gene in vascular smooth muscle cells. J Cell Physiol 2001; 188:45–55.
66. Weiser MC, Grieshaber NA, Schwartz PE, Majack RA. Perlecan regulates Oct-1 gene expression in vascular smooth muscle cells. Mol Biol Cell 1997; 8:999–1011.
67. Oudit GY, Sun H, Kerfant BG, Crackower MA, Penninger JM, Backx PH. The role of phosphoinositide-3 kinase and PTEN in cardiovascular physiology and disease. J Mol Cell Cardiol 2004; 37:449–471.
68. Garl PJ, Wenzlau JM, Walker HA, Whitelock JM, Costell M, Weiser-Evans MC. Perlecan-induced suppression of smooth muscle cell proliferation is mediated through increased activity of the tumor suppressor PTEN. Circ Res 2004; 94:175–183.
69. Mourani PM, Garl PJ, Wenzlau JM, Carpenter TC, Stenmark KR, Weiser-Evans MC. Unique, highly proliferative growth phenotype expressed by embryonic and neointimal smooth muscle cells is driven by constitutive Akt, mTOR, and p70S6K signaling and is actively repressed by PTEN. Circulation 2004; 109:1299–1306.
70. Suzuki A, de la Pompa JL, Stambolic V, Elia AJ, Sasaki T, del Barco Barrantes I, Ho A, Wakeham A, Itie A, Khoo W, Fukumoto M, Mak TW. High cancer susceptibility and embryonic lethality associated with mutation of the PTEN tumor suppressor gene in mice. Curr Biol 1998; 8:1169–1178.
71. Di Cristofano A, Pesce B, Cordon-Cardo C, Pandolfi PP. Pten is essential for embryonic development and tumour suppression. Nat Genet 1998; 19: 348–355.
72. Stambolic V, Suzuki A, de la Pompa JL, Brothers GM, Mirtsos C, Sasaki T, Ruland J, Penninger JM, Siderovski DP, Mak TW. Negative regulation of PKB/Akt-dependent cell survival by the tumor suppressor PTEN. Cell 1998; 95:29–39.

73. Paka L, Goldberg IJ, Obunike JC, Choi SY, Saxena U, Goldberg ID, Pillarisetti S. Perlecan mediates the antiproliferative effect of apolipoprotein E on smooth muscle cells. J Biol Chem 1999; 274:36403–36408.
74. Walker HA, Whitelock JM, Garl PJ, Nemenoff RA, Stenmark KR, Weiser-Evans MC. Perlecan up-regulation of FRNK suppresses smooth muscle cell proliferation via inhibition of FAK signaling. Mol Biol Cell 2003; 14: 1941–1952.
75. Tiedemann K, Sasaki T, Gustafsson E, Gohring W, Batge B, Notbohm H, Timpl R, Wedel T, Schlotzer-Schrehardt U, Reinhardt DP. Microfibrils at basement membrane zones interact with perlecan via fibrillin-1. J Biol Chem 2005; 280:11404–11412.
76. Sasaki T, Gohring W, Pan TC, Chu ML, Timpl R. Binding of mouse and human fibulin-2 to extracellular matrix ligands. J Mol Biol 1995; 254:892–899.
77. Sasaki T, Gohring W, Miosge N, Abrams WR, Rosenbloom J, Timpl R. Tropoelastin binding to fibulins, nidogen-2 and other extracellular matrix proteins. FEBS Lett 1999; 460:280–284.
78. Timpl R, Sasaki T, Kostka G, Chu ML. Fibulins: a versatile family of extracellular matrix proteins. Nat Rev Mol Cell Biol 2003; 4:479–489.
79. Belknap JK, Weiser-Evans MC, Grieshaber SS, Majack RA, Stenmark KR. Relationship between perlecan and tropoelastin gene expression and cell replication in the developing rat pulmonary vasculature. Am J Respir Cell Mol Biol 1999; 20:24–34.
80. Campbell GR, Campbell JH. Smooth muscle phenotypic changes in arterial wall homeostasis: implications for the pathogenesis of atherosclerosis. Exp Mol Pathol 1985; 42:139–162.
81. Thyberg J. Phenotypic modulation of smooth muscle cells during formation of neointimal thickenings following vascular injury. Histol Histopathol 1998; 13:871–891.
82. Wight TN. Proteoglycans and hyaluronan in vascular disease. In: Ernst B, Hart G, Sinay P, eds. Oligosaccharides in Chemistry and Biology. New York: Wiley-VCH, 1999.
83. Wight TN, Lara S, Reissen R, LeBaron R, Isner J. Selective deposits of versican in the extracellular matrix of restenotic lesions from human peripheral arteries. Am J Pathol 1997; 151:963–973.
84. Thyberg J, Blomgren K, Roy J, Tran PK, Hedin U. Phenotypic modulation of smooth muscle cells after arterial injury is associated with changes in the distribution of laminin and fibronectin. J Histochem Cytochem 1997; 45: 837–846.
85. Weiser-Evans MC, Quinn BE, Burkard MR, Stenmark KR. Transient reexpression of an embryonic autonomous growth phenotype by adult carotid artery smooth muscle cells after vascular injury. J Cell Physiol 2000; 182:12–23.
86. Kinsella MG, Irvin C, Reidy MA, Wight TN. Removal of heparan sulfate by heparinase treatment inhibits FGF-2-dependent smooth muscle cell proliferation in injured rat carotid arteries. Atherosclerosis 2004; 175:51–57.
87. Nikkari ST, Järveläinen HT, Wight TN, Ferguson M, Clowes AW. Smooth muscle cell expression of extracellular matrix genes after arterial injury. Am J Pathol 1994; 144:1348–1356.

88. Lindner V, Reidy MA. Proliferation of smooth muscle cells after vascular injury is inhibited by an antibody against basic fibroblast growth factor. Proc Natl Acad Sci USA 1991; 88:3739–3743.
89. Olson NE, Chao S, Lindner V, Reidy MA. Intimal smooth muscle cell proliferation after balloon catheter injury. The role of basic fibroblast growth factor. Am J Pathol 1992; 140:1017–1023.
90. Edelman ER, Nugent MA, Smith LT, Karnovsky MJ. Basic fibroblast growth factor enhances the coupling of intimal hyperplasia and proliferation of vasa vasorum in injured rat arteries. J Clin Invest 1992; 89:465–473.
91. Nugent MA, Edelman ER. Kinetics of basic fibroblast growth factor binding to its receptor and heparan sulfate proteoglycan: a mechanism for cooperactivity. Biochemistry 1992; 31:8876–8883.
92. Gallagher JT, Turnbull JE. Heparan sulphate in the binding and activation of basic fibroblast growth factor. Glycobiology 1992; 2:523–528.
93. Folkman J, Shing Y. Control of angiogenesis by heparin and other sulfated polysaccharides. Adv Exp Med Biol 1992; 313:355–364.
94. Millette E, Rauch BH, Defawe O, Kenagy RD, Daum G, Clowes AW. Platelet-derived growth factor-BB-induced human smooth muscle cell proliferation depends on basic FGF release and FGFR-1 activation. Circ Res 2005; 96:172–179.
95. Rauch BH, Millette E, Kenagy RD, Daum G, Clowes AW. Thrombin- and factor Xa-induced DNA synthesis is mediated by transactivation of fibroblast growth factor receptor-1 in human vascular smooth muscle cells. Circ Res 2004; 94:340–345.
96. Clowes AW, Karnovsky MJ. Suppression by heparin of smooth muscle proliferation in injured arteries. Nature 1977; 265:625–626.
97. Clowes AW, Clowes MM. Kinetics of cellular proliferation after arterial injury. II. Inhibition of smooth muscle growth by heparin. Lab Invest 1985; 52:611–616.
98. Strauss BH, Chisholm RJ, Keeley FW, Gotlieb AI, Logan RA, Armstrong PW. Extracellular matrix remodeling after balloon angioplasty injury in a rabbit model of restenosis. Circ Res 1994; 75:650–658.
99. Silver P, Moreau J, Denholm E, Lin Y, Nguyen L, Bennett C, Recktenwald A, DeBlois D, Baker S, Ranger S. Heparinase III limits rat arterial smooth muscle cell proliferation in vitro and in vivo. Eur J Pharmacol 1998; 351: 79–83.
100. Nathan A, Nugent MA, Edelman ER. Tissue engineered perivascular endothelial cell implants regulate vascular injury. Proc Natl Acad Sci USA 1995; 92:8130–8134.
101. Bingley JA, Hayward IP, Campbell JH, Campbell GR. Arterial heparan sulfate proteoglycans inhibit vascular smooth muscle cell proliferation and phenotype change in vitro and neointimal formation in vivo. J Vasc Surg 1998; 28:308–318.
102. Nugent MA, Nugent HM, Iozzo RV, Sanchack K, Edelman ER. Perlecan is required to inhibit thrombosis after deep vascular injury and contributes to endothelial cell-mediated inhibition of intimal hyperplasia. Proc Natl Acad Sci USA 2000; 97:6722–6727.

103. Snow AD, Bolender RP, Wight TN, Clowes AW. Heparin modulates the composition of the extracellular matrix domain surrounding arterial smooth muscle cells. Am J Pathol 1990; 137:313–330.
104. Kalmes A, Daum G, Clowes AW. EGFR transactivation in the regulation of SMC function. Ann NY Acad Sci 2001; 947:42–54; discussion 54–45.
105. Potter-Perigo S, Wight TN. Heparin causes the accumulation of heparan sulfate in cultures of arterial smooth muscle cells. Arch Biochem Biophys 1996; 336:19–26.
106. Lee RT, Yamamoto C, Feng Y, Potter-Perigo S, Briggs WH, Landschulz KT, Turi TG, Thompson JF, Libby P, Wight TN. Mechanical strain induces specific changes in the synthesis and organization of proteoglycans by vascular smooth muscle cells. J Biol Chem 2001; 276:13847–13851.
107. Merrilees M, Beaumont B, Scott L, Hermanutz V, Fennessy P. Effect of TGF-beta(1) antisense S-oligonucleotide on synthesis and accumulation of matrix proteoglycans in balloon catheter-injured neointima of rabbit carotid arteries. J Vasc Res 2000; 37:50–60.
108. Nabel EG, Shum L, Pompili VJ, Yang ZY, San H, Shu HB, Liptay S, Gold L, Gordon D, Derynck R, Nabel GJ. Direct gene transfer of transforming growth factor b1 into arteries stimulates fibrocellular hyperplasia. Proc Natl Acad Sci USA 1993; 90:10759–10763.
109. Kaji T, Yamada A, Miyajima S, Yamamoto C, Fujiwara Y, Wight TN, Kinsella MG. Cell density-dependent regulation of proteoglycan synthesis by transforming growth factor-beta(1) in cultured bovine aortic endothelial cells. J Biol Chem 2000; 275:1463–1470.
110. Yamamoto C, Wakata T, Fujiwara Y, Kaji T. Induction of synthesis of a large heparan sulfate proteoglycan, perlecan, by thrombin in cultured human coronary smooth muscle cells. Biochim Biophys Acta 2005; 1722:92–102.
111. Zhang W, Chuang YJ, Swanson R, Li J, Seo K, Leung L, Lau LF, Olson ST. Antiangiogenic antithrombin down-regulates the expression of the proangiogenic heparan sulfate proteoglycan, perlecan, in endothelial cells. Blood 2004; 103:1185–1191.
112. Hedin U, Roy J, Tran PK. Control of smooth muscle cell proliferation in vascular disease. Curr Opin Lipidol 2004; 15:559–565.
113. Olson NE, Kozlowski J, Reidy MA. Proliferation of intimal smooth muscle cells. Attenuation of basic fibroblast growth factor 2-stimulated proliferation is associated with increased expression of cell cycle inhibitors. J Biol Chem 2000; 275:11270–11277.
114. Reidy MA. Growth factors and arterial smooth muscle cell proliferation. Ann NY Acad Sci 1994; 714:225–230.
115. Tran PK, Tran-Lundmark K, Soininen R, Tryggvason K, Thyberg J, Hedin U. Increased intimal hyperplasia and smooth muscle cell proliferation in transgenic mice with heparan sulfate-deficient perlecan. Circ Res 2004; 94: 550–558.
116. Xu Q. Mouse models of arteriosclerosis: from arterial injuries to vascular grafts. Am J Pathol 2004; 165:1–10.
117. Hansson GK, Libby P, Schonbeck U, Yan ZQ. Innate and adaptive immunity in the pathogenesis of atherosclerosis. Circ Res 2002; 91:281–291.
118. Hansson GK. Inflammation, atherosclerosis, and coronary artery disease. N Engl J Med 2005; 352:1685–1695.

119. Olsson U, Ostergren-Lunden G, Moses J. Glycosaminoglycan–lipoprotein interaction. Glycoconjugate J 2001; 18:789–797.
120. Williams KJ, Tabas I. The response-to-retention hypothesis of atherogenesis reinforced. Curr Opin Lipidol 1998; 9:471–474.
121. Evanko SP, Raines EW, Ross R, Gold LI, Wight TN. Proteoglycan distribution in lesions of atherosclerosis depends on lesion severity, structural characteristics and the proximity of PDGF and TGF-b1. Am J Pathol 1998; 152:533–546.
122. Kunjathoor VV, Chiu DS, O'Brien KD, LeBoeuf RC. Accumulation of biglycan and perlecan, but not versican, in lesions of murine models of atherosclerosis. Arterioscler Thromb Vasc Biol 2002; 22:462–468.
123. Wight TN, Merrilees MJ. Proteoglycans in atherosclerosis and restenosis: key roles for versican. Circ Res 2004; 94:1158–1167.
124. Fuki II, Iozzo RV, Williams KJ. Perlecan heparan sulfate proteoglycan. A novel receptor that mediates a distinct pathway for ligand catabolism. J Biol Chem 2000; 275:31554.
125. Vikramadithyan RK, Kako Y, Chen G, Hu Y, Arikawa-Hirasawa E, Yamada Y, Goldberg IJ. Atherosclerosis in perlecan heterozygous mice. J Lipid Res 2004; 45:1806–1812.
126. Chait A, Wight TN. Interaction of native and modified low density lipoproteins with extracellular matrix. Curr Opin Lipidol 2000; 11:457–463.
127. Chait A, Han CY, Oram JF, Heinecke JW. Thematic review series: The immune system and atherogenesis. Lipoprotein-associated inflammatory proteins: markers or mediators of cardiovascular disease? J Lipid Res 2005; 46:389–403.
128. Saxena U, Kulkarni NM, Ferguson E, Newton RS. Lipoprotein lipase-mediated lipolysis of very low density lipoproteins increases monocyte adhesion to aortic endothelial cells. Biochem Biophys Res Commun 1992; 189:1653–1658.
129. Goldberg IJ. Lipoprotein lipase and lipolysis: central roles in lipoprotein metabolism and atherogenesis. J Lipid Res 1996; 37:693–707.
130. Khalil MF, Wagner WD, Goldberg IJ. Molecular interactions leading to lipoprotein retention and the initiation of atherosclerosis. Arterioscler Thromb Vasc Biol 2004; 24:2211–2218.
131. Ancsin JB, Kisilevsky R. The heparin/heparan sulfate-binding site on aposerum amyloid A. Implications for the therapeutic intervention of amyloidosis. J Biol Chem 1999; 274:7172–7181.
132. O'Brien KD, McDonald TO, Kunjathoor V, Eng K, Knopp EA, Lewis K, Lopez R, Kirk EA, Chait A, Wight TN, deBeer FC, LeBoeuf RC. Serum amyloid A and lipoprotein retention in murine models of atherosclerosis. Arterioscler Thromb Vasc Biol 2005; 25:785–790.
133. Steel DM, Whitehead AS. The major acute phase reactants: C-reactive protein, serum amyloid P component and serum amyloid A protein. Immunol Today 1994; 15:81–88.
134. Malle E, De Beer FC. Human serum amyloid A (SAA) protein: a prominent acute-phase reactant for clinical practice. Eur J Clin Invest 1996; 26:427–435.
135. Chang MY, Olin KL, Tsoi C, Wight TN, Chait A. Human monocyte-derived macrophages secrete two forms of proteoglycan-macrophage

colony-stimulating factor that differ in their ability to bind low density lipoproteins. J Biol Chem 1998; 273:15985–15992.
136. Makatsori E, Lamari FN, Theocharis AD, Anagnostides S, Hjerpe A, Tsegenidis T, Karamanos NK. Large matrix proteoglycans, versican and perlecan, are expressed and secreted by human leukemic monocytes. Anticancer Res 2003; 23:3303–3309.
137. Kuschert GS, Coulin F, Power CA, Proudfoot AE, Hubbard RE, Hoogewerf AJ, Wells TN. Glycosaminoglycans interact selectively with chemokines and modulate receptor binding and cellular responses. Biochemistry 1999; 38:12959–12968.
138. Frevert CW, Kinsella MG, Vathanaprida C, Goodman RB, Baskin DG, Proudfoot A, Wells TN, Wight TN, Martin TR. Binding of interleukin-8 to heparan sulfate and chondroitin sulfate in lung tissue. Am J Respir Cell Mol Biol 2003; 28:464–472.
139. Wrenshall LE, Platt JL, Stevens ET, Wight TN, Miller JD. Propagation and control of T cell responses by heparan sulfate-bound IL-2. J Immunol 2003; 170:5470–5474.
140. Wrenshall L. Role of the microenvironment in immune responses to transplantation. Springer Semin Immunopathol 2003; 25:199–213.
141. Giuffre L, Cordey AS, Monai N, Tardy Y, Schapira M, Spertini O. Monocyte adhesion to activated aortic endothelium: role of L-selectin and heparan sulfate proteoglycans. J Cell Biol 1997; 136:945–956.
142. Koenig A, Norgard-Sumnicht K, Linhardt R, Varki A. Differential interactions of heparin and heparan sulfate glycosaminoglycans with the selectins. Implications for the use of unfractionated and low molecular weight heparins as therapeutic agents. J Clin Invest 1998; 101:877–889.
143. Sivaram P, Obunike JC, Goldberg IJ. Lysolecithin-induced alteration of subendothelial heparan sulfate proteoglycans increases monocyte binding to matrix. J Biol Chem 1995; 270:29760–29765.
144. Vogl-Willis CA, Edwards IJ. High glucose-induced alterations in subendothelial matrix perlecan leads to increased monocyte binding. Arterioscler Thromb Vasc Biol 2004; 24:858–863.
145. Vilar RE, Ghael D, Li M, Bhagat DD, Arrigo LM, Cowman MK, Dweck HS, Rosenfeld L. Nitric oxide degradation of heparin and heparan sulphate. Biochem J 1997; 324 (Part 2):473–479.
146. Kjellen L. Glucosaminyl *N*-deacetylase/*N*-sulphotransferases in heparan sulphate biosynthesis and biology. Biochem Soc Trans 2003; 31:340–342.
147. Bingley JA, Hayward IP, Girjes AA, Campbell GR, Humphries DE, Stow JL, Campbell JH. Expression of heparan sulphate *N*-deacetylase/*N*-sulphotransferase by vascular smooth muscle cells. Histochem J 2002; 34:131–137.
148. Carter NM, Ali S, Kirby JA. Endothelial inflammation: the role of differential expression of *N*-deacetylase/*N*-sulphotransferase enzymes in alteration of the immunological properties of heparan sulphate. J Cell Sci 2003; 116:3591–3600.
149. Aviezer D, Iozzo RV, Noonan DM, Yayon A. Suppression of autocrine and paracrine functions of basic fibroblast growth factor by stable expression of perlecan antisense cDNA. Mol Cell Biol 1997; 17:1938–1946.

150. Adatia R, Albini A, Carlone S, Giunciuglio D, Benelli R, Santi L, Noonan DM. Suppression of invasive behavior of melanoma cells by stable expression of antisense perlecan cDNA. Annals Onc 1997; 8:1257–1261.
151. Sharma B, Handler M, Eichstetter I, Whitelock JM, Nugent MA, Iozzo RV. Antisense targeting of perlecan blocks tumor growth and angiogenesis in vivo. J Clin Invest 1998; 102:1599–1608.
152. Marchisone C, Del Grosso F, Masiello L, Prat M, Santi L, Noonan DM. Phenotypic alterations in Kaposi's sarcoma cells by antisense reduction of perlecan. Pathol Oncol Res 2000; 6:10–17.
153. Zhou Z, Wang J, Cao R, Morita H, Soininen R, Chan KM, Liu B, Cao Y, Tryggvason K. Impaired angiogenesis, delayed wound healing and retarded tumor growth in perlecan heparan sulfate-deficient mice. Cancer Res 2004; 64:4699–4702.
154. Jiang X, Couchman JR. Perlecan and tumor angiogenesis. J Histochem Cytochem 2003; 51:1393–1410.
155. Segev A, Nili N, Strauss BH. The role of perlecan in arterial injury and angiogenesis. Cardiovasc Res 2004; 63:603–610.
156. Knox S, Merry C, Stringer S, Melrose J, Whitelock J. Not all perlecans are created equal: interactions with fibroblast growth factor (FGF) 2 and FGF receptors. J Biol Chem 2002; 277:14657–14665.
157. Fukuda K, Inui Y, Kawata S, Higashiyama S, Matsuda Y, Maeda Y, Igura T, Yoshida S, Taniguchi N, Matsuzawa Y. Increased mitogenic response to heparin-binding epidermal growth factor-like growth factor in vascular smooth muscle cells of diabetic rats. Arterioscler Thromb Vasc Biol 1995; 15:1680–1687.
158. Fukuda K, Kawata S, Inui Y, Higashiyama S, Matsuda Y, Igura T, Tamura S, Taniguchi N, Matsuzawa Y. High concentration of glucose increases mitogenic responsiveness to heparin-binding epidermal growth factor-like growth factor in rat vascular smooth muscle cells. Arterioscler Thromb Vasc Biol 1997; 17:1962–1968.
159. Ghiselli G, Lindahl U, Salmivirta M. Foam cell conversion of macrophages alters the biosynthesis of heparan sulfate. Biochem Biophys Res Commun 1998; 247:790–795.
160. Houck KA, Leung DW, Rowland AM, Winer J, Ferrara N. Dual regulation of vascular endothelial growth factor bioavailability by genetic and proteolytic mechanisms. J Biol Chem 1992; 267:26031–26037.
161. Saksela O, Rifkin DB. Release of basic fibroblast growth factor-heparan sulfate complexes from endothelial cells by plasminogen activator-mediated proteolytic activity. J Cell Biol 1990; 110:767–775.
162. Whitelock JM, Murdoch AD, Iozzo RV, Underwood PA. The degradation of human endothelial cell-derived perlecan and release of bound basic fibroblast growth factor by stromelysin, collagenase, plasmin, and heparanases. J Biol Chem 1996; 271:10079–10086.
163. Garcia-Touchard A, Henry TD, Sangiorgi G, Spagnoli LG, Mauriello A, Conover C, Schwartz RS. Extracellular proteases in atherosclerosis and restenosis. Arterioscler Thromb Vasc Biol 2005; 25:1119–1127.
164. Lijnen HR. Extracellular proteolysis in the development and progression of atherosclerosis. Biochem Soc Trans 2002; 30:163–167.

165. Klebanoff SJ, Kinsella MG, Wight TN. Degradation of endothelial cell matrix heparan sulfate proteoglycan by elastase and the myeloperoxidase-H_2O_2-chloride system. Am J Pathol 1993; 143:907–917.
166. Fukuda S, Fini CA, Mabuchi T, Koziol JA, Eggleston Jr LL, del Zoppo GJ. Focal cerebral ischemia induces active proteases that degrade microvascular matrix. Stroke 2004; 35:998–1004.
167. Vlodavsky I, Goldshmidt O, Zcharia E, Atzmon R, Rangini-Guatta Z, Elkin M, Peretz T, Friedmann Y. Mammalian heparanase: involvement in cancer metastasis, angiogenesis and normal development. Semin Cancer Biol 2002; 12:121–129.
168. Reiland J, Sanderson RD, Waguespack M, Barker SA, Long R, Carson DD, Marchetti D. Heparanase degrades syndecan-1 and perlecan heparan sulfate: functional implications for tumor cell invasion. J Biol Chem 2004; 279: 8047–8055.
169. Chen G, Wang D, Vikramadithyan R, Yagyu H, Saxena U, Pillarisetti S, Goldberg IJ. Inflammatory cytokines and fatty acids regulate endothelial cell heparanase expression. Biochemistry 2004; 43:4971–4977.
170. Bix G, Iozzo RV. Matrix revolutions: "tails" of basement-membrane components with angiostatic functions. Trends Cell Biol 2005; 15:52–60.
171. Chang Z, Choon A, Friedl A. Endostatin binds to blood vessels in situ independent of heparan sulfate and does not compete for fibroblast growth factor-2 binding. Am J Pathol 1999; 155:71–76.
172. Javaherian K, Park SY, Pickl WF, LaMontagne KR, Sjin RT, Gillies S, Lo KM. Laminin modulates morphogenic properties of the collagen XVIII endostatin domain. J Biol Chem 2002; 277:45211–45218.
173. Kreuger J, Matsumoto T, Vanwildemeersch M, Sasaki T, Timpl R, Claesson-Welsh L, Spillmann D, Lindahl U. Role of heparan sulfate domain organization in endostatin inhibition of endothelial cell function. EMBO J 2002; 21:6303–6311.
174. Mongiat M, Sweeney SM, San Antonio JD, Fu J, Iozzo RV. Endorepellin, a novel inhibitor of angiogenesis derived from the C terminus of perlecan. J Biol Chem 2003; 278:4238–4249.
175. Gonzalez EM, Reed CC, Bix G, Fu J, Zhang Y, Gopalakrishnan B, Greenspan DS, Iozzo RV. BMP-1/Tolloid-like metalloproteases process endorepellin, the angiostatic C-terminal fragment of perlecan. J Biol Chem 2005; 280:7080–7087.
176. Bix G, Fu J, Gonzalez EM, Macro L, Barker A, Campbell S, Zutter MM, Santoro SA, Kim JK, Hook M, Reed CC, Iozzo RV. Endorepellin causes endothelial cell disassembly of actin cytoskeleton and focal adhesions through alpha2beta1 integrin. J Cell Biol 2004; 166:97–109.
177. Raymond MA, Desormeaux A, Laplante P, Vigneault N, Filep JG, Landry K, Pshezhetsky AV, Hebert MJ. Apoptosis of endothelial cells triggers a caspase-dependent anti-apoptotic paracrine loop active on VSMC. FASEB J 2004; 18:705–707.

Chemistry and Biology of Heparin and Heparan Sulfate
H.G. Garg, R.J. Linhardt and C.A. Hales (Editors)

Chapter 23

Heparin and Low Molecular Weight Heparins in Clinical Cardiology

MEHMET E. KORKMAZ

Department of Cardiology, Güven Hospital, Ankara, Turkey

I. Introduction

Thrombi are composed of fibrin and blood cells and may form in any part of the circulation. Arterial thrombi of coronary arteries cause significant disorders called acute coronary syndromes. Venous thrombi usually occur in the lower limbs and can produce acute symptoms due to inflammation of the vessel wall, obstruction of flow, or embolism in the pulmonary circulation. Intracardiac thrombi, especially in the setting of atrial fibrillation, may produce complications due to embolism in the cerebral or systemic circulation. Anticoagulants are effective for the prevention and treatment of these disorders. This chapter presents the basic pharmacology and use of heparin and low-molecular-weight heparins in clinical cardiology.

II. Overview Of Pharmacology

A. Mechanism of Action

Unfractionated heparin (UH) is the traditional anticoagulant agent used in various conditions, such as deep vein thrombosis and ACS. UH is heterogeneous with respect to molecular size, anticoagulant activity, and pharmacokinetic properties. Its molecular weight ranges from 3000 to 30,000 Da with a mean molecular weight of 15,000 Da (1). UH exerts its effects by binding to antithrombin (AT). A specific pentasaccharide sequence in UH accounts for its ability to bind with high affinity

to lysine sites on AT. In the absence of UH, AT binds to and neutralizes thrombin and other activated clotting factors slowly; however, UH-bound AT undergoes a conformational change that dramatically accelerates its ability to bind to and neutralize these factors. UH then dissociates from these complexes and can be reused to bind to other AT molecules. UH thus acts as a true catalyst in accelerating the neutralization of thrombin and other activated clotting factors by AT (2). Fibrin-bound thrombin is relatively protected from inactivation by the UH/AT complex. Only one-third of an administered dose of UH binds to AT and thus exerts its anticoagulant activity. The chain length of the molecules influences the anticoagulant profile and clearance of UH, with the higher-molecular weight species cleared from the circulation more rapidly than the lower-molecular-weight species. This differential clearance causes a heterogeneous anticoagulant activity (1). The complex pharmacokinetics of UH are due to its nonspecific binding to many plasma proteins and to vascular and blood cells. UH is poorly absorbed from the gastrointestinal tract and therefore must be administered parenterally (1,2).

Low-molecular-weight heparins (LMWHs) are produced through depolymerization of UH and consist of polysaccharide chains with an average molecular weight of about 4–5 kD. LMWHs inhibit the coagulation system as does UH, by catalyzing the AT-dependent activation of coagulation enzymes. The primary anticoagulant effect is mediated via a conformational interaction with AT III which, in turn, inactivates procoagulatory serine proteases (e.g., factors IIa or thrombin, IXa, and Xa). Thus, the indirect consequence of LMWH is inhibition of the conversion of prothrombin to thrombin, which reduces the thrombin-mediated conversion of fibrinogen to fibrin and prevents the formation of clots (3). Their interaction with AT is mediated by a unique pentasaccharide sequence found on less than one-third of LMWH molecules. Because a minimum chain length of 18 saccharides is required for ternary complex formation, only the 25–50% of LMWH species that are above this critical chain length are able to inactivate thrombin. In contrast, all LMWH chains that contain the high affinity pentasaccharide catalyze the inactivation of factor Xa. Consequently, LMWHs have an anti-factor Xa-to-anti-factor IIa ratio of 2:1 to 4:1 (depending on the preparation), while UH has a ratio of 1:1(4) (Table 1).

B. Effects on Tissue Factor Pathway Inhibitor

LMWHs also raise the levels of tissue factor pathway inhibitor (TFPI). TFPI is a modulator of the coagulation process, which binds to factor Xa. The resulting

Table 1 Comparison of the Low Molecular Weight Heparins

Preparation	Anti-Xa: anti-IIa ratio	Mean molecular weight	Plasma half-life (min)
Enoxaparin	2.7:1	4500	120–180
Dalteparin	2.0:1	5000	120–140
Nadroparin	3.2:1	4500	132–162
Reviparin	4.4:1	4400	162–258

complex binds to the factor VIIa–tissue factor complex and inactivates the extrinsic coagulation process. Preclinical and clinical studies have shown that reviparin, like other LMWHs and UH, stimulates the release of TFPI from endothelial cells, thereby increasing the rate of inactivation of factor Xa and the thromboplastin-factor VIIa complex (5).

C. Effects on von Willebrand Factor (vWF)

In a large cohort of patient with acute coronary syndromes (ACS) it was demonstrated that the early rise of vWF was an independent predictor of adverse clinical outcome at 14 days and at 30 days and enoxaparin provided protection, as evidenced by the reduced release of vWF (6). In a recent study the same group tested the hypothesis that different anticoagulant treatments may produce different platelet effects and vWF release in UA (7). A total of 54 patients with UA or NSTEMI were treated during at least 48 h by either intravenous UH, one of two different LMWHs (enoxaparin or dalteparin) or the direct thrombin inhibitor PEG-hirudin. All patients received aspirin but no IIb-IIIa inhibitors. The release of vWF over the first 48 h did not relate to the baseline characteristics. At 30 days of follow-up, delta vWF was 7-fold higher in patients with an endpoint than in patients free of events ($p = 0.004$). The same trend was present for each component of the composite endpoint with the highest levels for 1-month mortality ($+87 \pm 32\%$ *vs* $+26 \pm 8\%$, $p = 0.09$). The vWF values did not increase over 48 h in patients receiving either enoxaparin or PEG-hirudin. A serious rise of vWF was measured in UH-treated patients ($+87 \pm 11\%$), which differed significantly from the enoxaparin group ($p = 0.0006$) and PEG-hirudin group ($p < 0.0001$). In dalteparin-treated patients, delta vWF was elevated ($+48 \pm 8\%$) and did not differ significantly from the UH group. This finding may partly explain the different levels of benefit seen in clinical trials discussed in this article.

D. Limitations of Unfractionated Heparin

UH has some important pharmacokinetic, biophysical, and biological limitations. LMWHs overcome the pharmacokinetic and some of the biological limitations of UF, but they share the same biophysical limitations (8). The main pharmacokinetic limitation of UH is caused by its nonspecific binding to proteins and cells (9). Because UH is negatively charged, it binds in pentasaccharide-independent fashion to a variety of plasma proteins (including histidine-rich glycoprotein, vitronectin, lipoproteins, fibronectin, and fibrinogen) and to proteins secreted by platelets [platelet factor 4 (PF4) and high molecular weight vWF] (9). This nonspecific binding of UH to plasma proteins most likely contributes to the variable anti-IIa response to UH in patients with thromboembolic disease (10). In contrast, reduced nonspecific binding to plasma proteins of LMWHs leads to a more predictable response (10,11). Also the reduced binding of LMWHs to macrophages and endothelial cells compared to UH causes an increase in their plasma half-lives. This also improves the predictability of their dose–response relationship (10–12). It has been shown that clot-bound thrombin is relatively protected from inhibition by UH,

possibly because the UH binding site on thrombin is inaccessible when the enzyme is bound to fibrin, and clot-bound thrombin is susceptible to inactivation by AT III-independent inhibitors because the sites of their interaction are not masked by thrombin binding to fibrin. For these reasons, AT III-independent inhibitors may be more effective than UH in certain clinical settings (13).

Both UH and LMWHs have the potential complication of bleeding. However, UH can produce thrombocytopenia and osteoporosis in long-term use. UH binds to platelets, causing activation and release of PF4 (14). UH and other large, highly sulfated polysaccharides bind to PF4 to form a reactive antigen on the platelet surface. Heparin-induced thrombocytopenia (HIT) IgG then binds to this complex with activation of platelets through the platelet Fc receptors (15). This causes HIT (16). The incidence of HIT varies widely, but in a large randomized trial, it was three (17). Thrombocytopenia usually begins between 5 and 15 days after UH is begun but can occur within hours in patients who have previously been exposed to UH (9). Reduced binding of LMWHs to platelets and PF4 may give rise to the lower incidence of HIT, compared to UH (17). Patients with HIT may cross-react with LMWH. Fondaparinux is an acceptable LMWH. This confirms the biological advantage of LMWHs in regard to the development of HIT (18).

The second important biological limitation of UH is the development of osteoporosis. Osteoporosis is a well-recognized complication of long-term UH treatment (19,20). Available data suggest that 2–3% of patients receiving UH for >3 months develop symptomatic bone fractures and that a third have had a reduction in bone density (19–22). Possibly, LMWHs' lower binding to osteoblasts and the resulting lesser activation of osteoclasts lead to a lesser effect on bone loss (19–23). UH is usually administered via a continuous IV infusion and its effect should be monitored by frequent measurements of aPTT. LMWHs have advantages in terms of ease of administration, and do not require daily monitoring. LMWHs are cleared principally by the renal route and their biological half-life is increased in patients with renal failure. The advantages of LMWHs over UH are given in Table 2.

These data led to a shift away from UH toward LMWH. The interest in LMWH has caused a large amount of research in a variety of indications that, in the near future, may change clinical practice. This chapter summarizes the clinical

Table 2 Advantages of Low-Molecular-Weight Heparins over Unfractionated Heparin

Reduced binding to	Clinical relevance
Macrophages, endothelial cells	Longer half-life; can be given by once- or twice-daily subcutaneous injection
Plasma proteins	Predictable anticoagulant response; avoids need for laboratory monitoring in most patients
Platelets/platelet factor-4	Lower incidence of immune heparin-induced thrombocytopenia
Osteoblasts	Lower risk of osteoporosis

use of UH and LMWH in venous thromboembolism, in coronary and peripheral artery diseases, atrial fibrillation, in pregnant patients, and for perioperative anticoagulation.

III. Clinical Experience

A. Venous Thromboembolic Disease

Venous thromboembolism (VTE) is a common complication in patients undergoing surgery and remains a major cause of morbidity and mortality in hospitalized medical patients. VTE is a prevalent disorder that is projected to increase; it is a cause of mortality in the short-term and morbidity over the long-term. In the United States and Europe, VTE commonly occurs and is associated with a high risk of death. It has been estimated that almost 300,000 cases of VTE occur each year in the United States, corresponding to an incidence of 1 per 1000 (24). The early mortality rate can be as high as 3.8% in patients with deep vein thrombosis (DVT) and 38.9% in those with pulmonary embolism (PE) (25). The development of noninvasive reliable methods for the diagnosis of DVT and PE has facilitated recognition of VTE. Nevertheless, fatal PE can be the first manifestation of the disease. Furthermore, because older age is a major risk factor for VTE and its secondary complications, the increased proportion of elderly people in the population is likely to contribute to high morbidity and mortality in the future (25). Besides age, population studies have identified other major risk factors for VTE; these include obesity, chronic heart failure, chronic lung disease, malignancy, ischemic stroke, birth control pills, and postmenopausal hormone replacement therapy (24,25).

Anticoagulation is the main therapy for acute DVT of the leg. The objectives of anticoagulant therapy in the initial treatment of this disease are to prevent thrombus extension and early and late recurrences of DVT and PE. The evidence for the need for anticoagulation in patients with DVT has long been known. Many uncontrolled studies confirmed that mortality was reduced when heparin was used to treat VTE, and reported a high mortality when patients did not receive anticoagulant therapy. Patients with DVT should be treated with anticoagulants as soon as the diagnosis is confirmed by objective testing. If the clinical suspicion is high and there is a delay before diagnosis can be confirmed by objective tests, then treatment should be started while awaiting confirmation.

1. Initial Treatment of Deep Vein Thrombosis

a. Unfractionated Heparin

Until recently, IV UH has been the preferred initial treatment of DVT. UH has an unpredictable dose–response and a narrow therapeutic window, thereby making monitoring essential to ensure optimal efficacy and safety. The most widely used test for monitoring heparin therapy is the activated partial thromboplastin time (aPTT), which is a global coagulation test that not always correlates reliably with

plasma heparin levels or with the antithrombotic activity of heparin. In patients requiring large daily doses of UH without achieving a therapeutic aPTT, the so-called heparin-resistant patients, the dose of heparin should be adjusted by measuring the anti-Xa level because of a dissociation between the aPTT and heparin concentration.

The starting dose of UH for the treatment of DVT is either a bolus dose of 5000 U, followed by a continuous infusion of at least 30,000 U for the first 24 h or a weight-adjusted regimen of 80 U/kg bolus, followed by 18 U/kg/h. Subsequent doses should be adjusted according to aPTT levels (26). Intermittent IV injections of UH are associated with a higher risk of bleeding than IV infusion and are not recommended (27). As an alternative to IV administration, UH can be administered SC twice daily. The relative value of the IV and SC administration of UH has been evaluated in eight clinical studies and reviewed in a meta-analysis (28). SC UH administered twice daily appeared to be more effective and at least as safe as IV UH. The usual regimen includes an initial IV bolus of 5000 U followed by a SC dose of 17,500 U bid on the first day. When patients are receiving SC heparin, the aPTT should be drawn at 6 h after the morning administration and the dose of UH adjusted to achieve a 1.5–2.5 prolongation.

b. Low-Molecular-Weight Heparins

LMWH can be administered SC once or twice daily without laboratory monitoring in the majority of patients. However, in certain clinical situations, such as severe renal failure or pregnancy, dose adjustment might be required, and if so, can be achieved by monitoring plasma anti-Xa level. The most reasonable time to perform the anti-Xa assay is 4 h after the SC administration of a weight-adjusted dose of LMWH.

The initial studies reported fewer recurrent events and less bleeding with LMWH, while the most recent studies showed comparable outcomes. Consequently, the meta-analysis that only included the early studies reported that LMWH treatment results in fewer episodes of recurrence and bleeding than UH (29). The most recent meta-analysis included 13 randomized studies comparing IV heparin and LMWH for the initial treatment of acute DVT (30). There was no statistically significant difference in risk between LMWH and UH for recurrent VTE (RR in favor of LMWH, 0.85; 95% CI, 0.65–1.12), PE (RR, 1.02; 95% CI, 0.87–1.61), and major bleeding (RR, 0.63; 95% CI, 0.37–1.05). A statistically significant difference for risk of total mortality was observed in favor of LMWH (RR, 0.76; 95% CI, 0.59–0.90). The survival benefit was essentially accounted for by patients with malignancy. No apparent differences were observed in efficacy and safety among the different LMWHs.

Evidence indicates that outpatient treatment of DVT with LMWH is efficacious, safe, and cost-effective (31). Treatment at home leads to cost savings and improved quality of life. In addition, selected patients can be discharged from hospital early with a component of LMWH treatment at home. The large majority of the studies comparing LMWH treatment and UH in the initial treatment of DVT evaluated a twice-daily weight-adjusted regimen. However, once-daily administration is as effective and safe as twice-daily dosing. Subgroup analysis

suggested that the twice-daily dosing regimen might be more effective in patients with cancer (32). Treatment with a vitamin K antagonist is the preferred approach for long-term treatment in most patients with DVT. However, treatment with adjusted doses of UH or therapeutic doses of LMWH is indicated for selected patients in whom VKA are contraindicated (e.g., pregnancy) or impractical, or in patients with concurrent cancer, for whom LMWH regimens have been shown to be more effective and safer (30).

2. *Prevention of Venous Thromboembolism in Surgical and Medical Patients*

VTE is a common complication of surgical procedures. Prophylaxis with mechanical and pharmacological methods has been shown to be effective and safe in most types of surgery and should be routinely implemented. For patients undergoing general, gynecologic, vascular, and major urologic surgery, low-dose unfractionated heparin or LMWHs are the options of choice (33).

Thromboprophylaxis is not widely practiced in acutely ill medical patients, due in part to the heterogeneity of this group and the perceived difficulty in assessing those who would most benefit from treatment. Nevertheless, the results of recent well-conducted clinical trials support the evidence-based recommendations for more widespread systematic use of LMWH or UH in this population. The meta-analysis of all studies comparing UH and LMWH included nine trials for a total of 4669 patients (34). There was a trend in favor of LMWH for the reduction of DVT (relative risk 0.83, 95% CI 0.56–1.24) and of pulmonary embolism (relative risk 0.74, 95% CI 0.29–1.80). Major bleeding was marginally less frequent in the LMWH group (relative risk 0.48, 95% CI 0.23–1.0; $p = 0.049$).

B. Acute Coronary Syndromes

ACS are common causes of emergency hospital admission and a major cause of morbidity and mortality worldwide (35,36). There are two categories of patients with ACS:

1. Patients with ongoing chest discomfort and persistent ST-segment elevation. Persistent ST-segment elevation generally reflects acute total coronary occlusion. This situation is known as ST-segment elevation MI (STEMI). The therapeutic objective is rapid, complete, and sustained recanalization by fibrinolytic treatment or primary angioplasty.
2. Patients who present without ST-segment elevation are experiencing either unstable angina or non-STEMI (NSTEMI). The distinction between these two diagnoses is ultimately made by the measurements of markers of myocardial necrosis. The strategy in these cases is to alleviate ischemia and symptoms, and to initiate appropriate therapy if the diagnosis is confirmed (37).

In the USA, more than 12 million people have coronary heart disease and more than 1 million experience an acute MI or fatal coronary heart disease each

year, resulting in over 466,000 deaths attributed to coronary heart disease (38). A European survey yielded that the in-hospital mortality of patients with ST elevation ACS was 7.0%, for non-ST elevation ACS was 2.4%, and for undetermined electrocardiogram ACS was 11.8%. At 30 days, mortality was 8.4%, 3.5%, and 13.3%, respectively (39). Long-term mortality is also considerably higher. The Fragmin and Fast Revascularization During Instability in Coronary Artery Disease II Trial (FRISC II) has shown that the composite endpoint of death and MI was 10.4% and 14.1% for invasive and conservative strategies, respectively (40).

Following the rupture of an atheromatous plaque, collagen is exposed to the circulating blood. Platelets rapidly adhere to the area and became activated. In the activated platelets GP IIb-IIIa receptors become available for fibrinogen binding, and thus cross-linking and thrombus formation. Aspirin indirectly inhibits this process through its inhibition of thromboxane A2. Thromboxane A2 is involved in the processes of both platelet aggregation and vasoconstriction. On the other hand, glycoprotein IIb-IIIa antagonists, by directly binding to GP IIb-IIIa receptors and denying circulating fibrinogen the site of action on platelets, offer a more potent antiaggregating effect. Thrombin activates in a series of amplified steps. Thrombin promotes the conversion of soluble fibrinogen to insoluble fibrin, which forms a cross-linked mesh for the thrombus. There are also a number of antithrombotic factors, such as antithrombin. Antithrombin (AT) inhibits factor Xa and thrombin among some other coagulation factors. The activity of AT is potentiated some 1000-fold when it binds to UH or LMWH.

The current recommendations for medical treatment of ACS are very similar in both European and American guidelines (37,41). Antiplatelet therapy with aspirin and antithrombotic therapy with UH are well-established measures in ACSs. The prompt initiation of aspirin, or a thienopyridine if aspirin is not tolerated, is recommended. In the mentioned guidelines the choice between UH and LMWHs is left to the physician's discretion. The consistent benefit seen with glycoprotein IIb-IIIa antagonists – the most potent antiplatelet drugs available – led to recommendations for their use, in addition to standard treatment (aspirin and UH or LMWH) for patients with high-risk features such as increased troponin concentrations, ST-segment changes, or recurrent ischemia. Small molecules, such as tirofiban and eptifibatide, have been approved for this indication, whereas the evidence for abciximab is limited to patients scheduled for, or undergoing, percutaneous coronary interventions (PCI).

1. *Unstable Angina and Non-ST-Elevation Myocardial Infarction*

a. Unfractionated Heparin

Heparin has been evaluated in a number of randomized double-blind, placebo-controlled trials for the short-term treatment of ACS. The first trial compared aspirin (325 mg bid), UH (5000-U bolus, 1000 U/h IV), their combination, and placebo in 479 patients. It is the only study to compare UH (alone) and aspirin (alone) as well as combination therapy (42). Refractory angina occurred in 8.5%, 16.5%, and 10.7% of patients, respectively (0.47 RR for UH compared with aspirin;

95% CI, 0.21–1.05; $p = 0.06$). MI occurred in 0.9%, 3.3%, and 1.6% of patients, respectively (RR, 0.25; 95% CI, 0.03–2.27; $p = 0.18$) while any event was observed in 9.3%, 16.5%, and 11.5% of patients, respectively (RR, 0.52; 95% CI, 0.24–1.14; $p = 0.10$). The authors concluded that in the acute phase of unstable angina, either aspirin or heparin treatment is associated with a reduced incidence of myocardial infarction, and there is a trend favoring heparin over aspirin. Heparin treatment is also associated with a reduced incidence of refractory angina.

In contrast, the Research Group in Instability in Coronary Artery Disease (RISC) investigators did not show that heparin was more effective than aspirin (43). They compared low-dose aspirin (75 mg/day) with intermittent IV heparin (10,000 U bolus every 6 h during the initial 24 h followed by 7500 U every 6 h for 5 days) in 796 men with unstable angina or non-Q-wave MI. Patients were randomized on the basis of a factorial design to treatment with heparin, aspirin, heparin plus aspirin, or placebo. The main outcome was a composite of MI or death evaluated 5 days after enrollment. The rate of this endpoint was 6.0% in the placebo group, 5.6% in the heparin group, 3.7% in the aspirin group, and 1.4% in the combined treatment group and was significantly reduced only with the combination ($p = 0.027$). At 30 and 90 days, both the aspirin and aspirin plus heparin groups showed significantly better results than the placebo group, but the outcome with heparin alone was no better than with placebo.

A pooled analysis of the Antithrombotic Therapy in Acute Coronary Syndromes study (44), RISC (43) and Théroux et al. (42) studies yield an RR of 0.44 (95% CI, 0.21–0.93) for death/MI with combination aspirin and UH therapy compared with aspirin alone (45). The remaining trials investigated potential advantages of combination therapy (UH plus aspirin) over aspirin monotherapy. Although not statistically different, consistent trends across each study favored combined pharmacotherapy and its ability to reduce death or MI (combined endpoint).

The optimal level of anticoagulation in ACS is not well defined. The reason likely relates to inherent complexities in the pharmacokinetics and pharmacodynamics of UH, the dynamic nature of coronary arterial thrombosis, and the use of coagulation tests designed primarily to assess hemostatic potential. The activated partial thromboplastin time (aPTT), used widely to monitor UH, provides a general assessment of coagulation potential; however, it is most sensitive to factor IIa activity. The "therapeutic" level of anticoagulation with UH may vary with disease state. In venous thromboembolism, heparin levels >0.2 U/mL (protamine titration method) accompanied by aPTT values >1.5 times the upper limit of control appear to reduce the recurrence of thromboembolism (46). A similar aPTT range may be sufficient in the context of left ventricular mural thrombus prophylaxis (47). Becker et al. evaluated the relationship between levels of systemic anticoagulation and clinical events among 1473 patients with NSTE ACS (48). Although heparin levels and aPTT values did not differ significantly between patients experiencing *vs* those free of clinical events, a trend favored heparin levels >0.2 U/mL and aPTTs in the 45–60-s range as being protective. In addition, high levels of anticoagulation (aPTT >80 s) were not beneficial. The GUSTO-IIB study included 5861 patients with NSTE ACS who received UH for 72 h. A dose of 60 U/kg bolus and 12 U/kg/h

infusion resulted in the highest proportion of aPTT values within the prespecified target range of 50–70 s (49). After adjustment for baseline variables, a higher 12-h aPTT was associated with death or reinfarction at 30 days. A prolonged aPTT at 6 h increased the risk of moderate or severe bleeding. An aPTT of 50–60 s at 12 h was associated with the lowest risk of hemorrhagic complications.

The available evidence supports a weight-adjusted dosing regimen with UH as a means of providing a more predictable and constant level of systemic anticoagulation. An initial bolus of 60–70 U/kg (maximum, 5000 U) and initial infusion of 12–15 U/kg/h (maximum, 1000 U/h) titrated to a target aPTT of 50–75 s is recommended (50,51).

b. Low-Molecular-Weight Heparins

The first study of LMWH in UA was a single blind randomized trial that compared twice-daily treatment with weight-adjusted nadroparin (214 UIC/kg anti-Xa) and aspirin (200 mg/day), intravenous standard UH (adjusted for the activated partial thromboplastin time) and aspirin, or aspirin alone (52) (Table 3). This was a small study of 219 patients with UA. After 5–7 days, when the antithrombotic treatment was discontinued, there was a reduction greater than 50% in the rate of recurrent angina, as well as a significant decrease in the rates of silent ischemia and the need for revascularization in the group receiving nadroparin, as compared with the other two groups. In this study, treatment with aspirin plus a high dose of LMWH during the acute phase of UA was significantly better than treatment with aspirin alone or aspirin plus regular UH (52).

The second LMWH to be tested in this setting was dalteparin. The Fragmin During Instability in Coronary Artery Disease (FRISC) study (57) (Table 3) was the first large randomized, double blind, placebo-controlled trial of 1506 patients with UA or NSTEMI performed by the FRISC study group. Patients were randomly assigned either to dalteparin (120 IU/kg, maximum 10,000 IU) SC twice daily for 6 days then 7500 IU daily for 35–46 days, or placebo injections; all patients received aspirin. The primary endpoints were rate of death and MI in the first 6 days. Secondary endpoints were rates of death and new MI after 40 and 150 days, the frequency of revascularization, and the need for UH infusion. LMWH was shown to reduce the risk of death or MI by >60% at 6 days. Thus, of the 741 patients allocated to receive LMWH, 13 (1.8%) died or developed MI compared with 36 of 758 (4.7%) of those who received placebo. The composite endpoint of death, MI, and need for revascularization also showed a significant difference in favor of LMWH (5.4% *vs* 10.3%). At 40 days, the difference in rates of death and MI and of the composite endpoint persisted. However, there was a cluster of events in the patients assigned LMWH after the high initial dose was replaced by the lower maintenance dose, suggesting that a dose of 7500 anti-Xa units of dalteparin once daily produces inadequate protection even after a 6-day course of high-dose LMWH. At 40 days, the benefits persisted only in the nonsmokers (89% of the patients). At 4–5 months of follow-up, the significant difference between the two groups in the rates of death, MI, or revascularization was no longer evident. The rates for death or MI in the control and experimental groups were 15.3%

Table 3 Clinical Experience with Low-Molecular-Weight Heparins in Patients with ACS

Study	Patients	Treatment	Outcome
Comparisons with UH			
Gurfinkel(52)	219 patients with UA	Weight-adjusted nadroparin (214 UIC/kg anti-Xa) and aspirin (200 mg/day), intravenous UH (adjusted for the aPTT) and aspirin, or aspirin alone	Treatment with aspirin plus nadroparin during the acute phase of UA was significantly better than treatment with aspirin alone or aspirin plus UH
FRAXIS(53)	3468 patients with UA/NSTEMI	UH (adjusted for the aPTT), or Nadroparin 86 anti-Xa IU/kg, followed by twice daily 6 $\pm$ 2 or 14 days	No significant difference between the groups in incidence of death, MI, refractory angina, or recurrence of UA
FRIC(54)	1482 patients with UA/NSTEMI	Open phase: dalteparin, 120 IU/kg twice daily, or UH for 6 days	During the first 6 days, no difference between dalteparin and UH in risk of death, MI, and/or recurrent angina (9.3% *vs* 7.6%, respectively). At day 45, the rate of death, MI, or recurrent angina was 12.3% in both groups.
		Double blind phase: dalteparin, 7500 IU once daily or placebo	
ESSENCE(55)	3171 patients with UA/NSTEMI	1 mg/kg SC (100 anti-factor Xa U) of enoxaparin every 12 h or UH, as an IV bolus followed by infusion, for 2–8 days	17% risk reduction in the primary endpoint of death, MI, or recurrent angina at 14 days with LMWH ($p = 0.019$) and 15% risk reduction at 30 days ($p = 0.016$). Lower revascularization at 1 year

(*Continued*)

Table 3 *Cont'd*

Study	Patients	Treatment	Outcome
TIMI 11B(56)	3171 patients with UA/NSTEMI	Acute phase: enoxaparin, 30 mg bolus followed by 1 mg/kg twice daily, or UH (adjusted for the aPTT) for 28 days Outpatient phase: enoxaparin, 60 mg twice daily (40 mg twice daily for patients <65 kg) or placebo (in patients originally assigned to UH) until day 43	17% Reduction ($p = 0.048$) in death, MI, or urgent revascularization at day 8, 15% reduction ($p = 0.048$) at day 43
Placebo-controlled trials			
FRISC(57)	1506 patients with UA/NSTEMI	Placebo or dalteparin, 120 IU/kg twice daily, for 6 day, then 7500 IU once daily for 35–45 days	63% Reduction in risk of death or MI during the first 6 days ($p = 0.001$); 25% reduction (not significant) at day 40
FRISC II(58)	2267 patients with ischemic symptoms	Open-label phase: dalteparin, 120 IU/kg twice daily for at least 5 days Double-blind phase: placebo or dalteparin, 7500 IU twice daily (5000 IU in men <70 kg or women <80 kg) for 3 months	At 3 months a non-significant decrease in the endpoint of death or MI of 6.7% and 8.0% in the dalteparin and placebo groups, respectively (risk ratio 0.81, $p = 0.17$). At 30 days, this decrease was significant (3.1% *vs* 5.9%, 0.53, $p = 0.002$)

FRAXIS indicates FRAXiparine in ischemic syndrome; FRIC, Fragmin in Unstable Coronary Artery disease; ESSENCE, Efficacy and Safety of Subcutaneous Enoxaparin in Non-Q-wave Coronary Events; TIMI 11B, thrombolysis in myocardial infarction 11B; FRISC, Fragmin and Fast Revascularization During Instability in Coronary Artery Disease; UA, unstable angina; NSTEMI, non-ST-elevation myocardial infarction SC, Subcutaneous, aPTT, activated partial thromboplastin time; UH, unfractionated heparin

and 14.0%, respectively ($p = 0.41$) for death, MI, or revascularization, 43.6% and 42.7% ($p = 0.18$), respectively. This trial was designed to assess if dalteparin was more effective than placebo in the acute phase, and to identify if a subsequent lower dose of LMWH for 5–6 weeks would reduce the reactivation of disease seen with UH (59). The results of this study established the short-term value of LMWH (dalteparin) for the treatment of UA but suggested that protection with high-dose treatment is required for >6 days. Although all patients received aspirin, the control group did not receive UH, which is the standard treatment in most countries. Subgroup analysis of the FRISC data has produced interesting results (60). Toss et al. reported that minor bleeding was more frequent in women compared with men: RR 2.88 during the weight-adjusted and 2.36 during the fixed-dose treatment. The anti-Xa activity determined in samples obtained during the acute phase treatment was higher in women compared with men ($p < 0.001$) and in nonsmokers compared with smokers (<0.001) in multiple regression analysis. These results suggest that, it might be important to consider the influence of sex and smoking habits in order to improve future LMWH dosing regimens (60).

The Fragmin In Unstable Coronary Artery Disease (FRIC) study (54) (Table 3) used an open, randomized design; dalteparin (120 U/kg subcutaneously 12 hourly) was compared with UH (5000-U bolus followed by 1000-U/h continuous infusion for 6 days) in 1492 patients with UA or non-Q-wave infarction. In the double blind second phase (days 6–45), patients were randomized to either dalteparin (7500 U subcutaneously daily) or placebo. All patients received aspirin. Both treatment regimens were equivalent in terms of efficacy and safety. During the first 6 days, there was no statistical difference between dalteparin and UH in terms of probability of the composite endpoint of death, MI, and/or recurrent angina (9.3% *vs* 7.6%, respectively). The corresponding rates of composite of death or MI were 3.6% and 3.9%, respectively. Interestingly, there was a statistically significant increased incidence of death in the dalteparin group (LMWH 1.5% *vs* UH 0.5%, $p = 0.05$, CI 1.01–11.24). Death on its own was not a primary endpoint, and this may have been a consequence of more high-risk patients recruited in the LMWH group. Between days 6 and 45, the rate of death, MI, or recurrent angina was 12.3% in both groups. The authors concluded that twice-daily administration of subcutaneous dalteparin may be an effective and safe alternative to UH during the acute phase of unstable coronary artery disease and prolonged treatment with dalteparin at a lower once-daily dose did not confer any additional benefit over aspirin (75–165 mg) alone.

The Efficacy and Safety of Subcutaneous Enoxaparin in Non-Q-wave Coronary Events (ESSENCE) trial is the first of two studies that compared enoxaparin with UH (55) (Table 3). Patients ($n = 3171$) with UA or non-Q-wave MI were randomized in a double blind fashion to 1 mg/kg SC (100 anti-factor Xa U) of enoxaparin every 12 h or UH, administered as an IV bolus followed by a continuous infusion, for 2–8 days; the median duration of treatment in both groups was 2.6 days (Table 4). There was a significant 17% risk reduction in the primary endpoint of death, MI, or recurrent angina at 14 days with LMWH ($p = 0.019$) and 15% risk reduction at 30 days ($p = 0.016$). This difference was accounted for mainly by a lower incidence of recurrent angina in patients assigned to LMWH. There was no

Table 4 ICH Rates with Tissue Plasminogen Inhibitor Plus Heparin in Thrombolytic Trials

Study	*N*	Mean age (year)	Mean SBP (mmHg)	Heparin dosage (bolus plus infusion)	Target aPTT (s)	ICH rate (%)
International study(62)	5170			12,500 U SC bid		0.40
GUSTO-I(63)	10,268	62	130	5000 U plus 1000 U/h (1200 U/h if >80 kg)	60–85	0.72
GUSTO-IIA(64)	436	64	134	5000 U plus 1000 U/h (1300 U/h if >80 kg)	60–90	0.90
TIMI-9B(65)	1456	60		5000 U plus 1000 U/h	5–85	0.90
GUSTO-IIB (66)	1163	65	135	5000 U plus 1000 U/h	60–85	0.77
GUSTO-III (67)	4921	63	135	5000 U plus 1000 U/h (800 U/h if <80 kg)	50–70	0.87
ASSENT-II(68)	8488	61	133	>67 kg: 5000 U plus 1000 U/h <67 kg: 4000 U plus 800 U/h	50–75	0.94
InTIME-II(69)	5022	61	139	70 U/kg B (max 4000 U) plus 15 U/kg (maximum 1000 U/h) with adjustment based on aPTT at 3 h	50–70	0.62

ICH = intracranial hemorrhage, *N* = no. of patients, SBP = systolic blood pressure (mmHg).

difference in the incidence of major bleeding at 30 days (6.5% with LMWH *vs* 7.0% with UH), but total bleeding was more frequent with the LMWH group (18.4% *vs* 14.2%), primarily because of bruising at injection sites. The incidence of the composite triple endpoint at 1 year was lower among patients receiving enoxaparin as compared with those receiving UH (32.0% *vs* 35.7%, $p = 0.022$), with a trend toward a lower incidence of the secondary composite endpoint of death or MI (11.5% *vs* 13.5%, $p = 0.082$). At 1 year, the need for diagnostic catheterization and coronary revascularization was lower in the enoxaparin group (55.8% *vs* 59.4%, $p = 0.036$ and 35.9% *vs* 41.2%, $p = 0.002$, respectively) (61). These data imply that in patients with UA or non-Q-wave MI, enoxaparin therapy significantly reduced the rates of recurrent ischemic events and invasive diagnostic and therapeutic procedures in the short term. The benefit was sustained at 1 year (61).

Thrombolysis in myocardial infarction 11B (TIMI 11B) is the second large enoxaparin trial (56) (Table 3). The TIMI 11B study compared the effects of an extended course of enoxaparin with UH for the prevention of death and cardiac ischemic events in patients with ACS. The TIMI 11A study was a dose-ranging trial, which showed that an initial 30 mg intravenous bolus followed by subcutaneous injections of 1 mg/kg enoxaparin every 12 h was associated with a lower risk of major hemorrhage than higher dosages (1.25 mg/kg) without apparent loss of efficacy (70). The TIMI 11B study comprised acute and outpatient phases. During the acute phase, patients were randomized to treatment with UH (intravenous bolus of 70 IU/kg and an initial infusion of 15 IU/kg/h) or enoxaparin (intravenous bolus of 30 mg followed by subcutaneous injections of 1 mg/kg every 12 h) for between

3 and 8 days. The median duration of acute phase therapy was 3.0 days in patients receiving UH and 4.6 days in patients receiving enoxaparin (56). At day 8 the incidence of the primary endpoint was significantly lower in patients receiving enoxaparin than in those receiving UH. When the components of the triple endpoint were considered individually, the rates of MI at day 8 were significantly lower in the enoxaparin treatment group; however, death, urgent revascularization and the composite double endpoint of death/MI did not differ between treatment groups at day 8.

Patients who completed the acute phase (up to day 8) and who were eligible, enrolled in the outpatient phase in which patients were followed for a further 35 days after hospital discharge. Those patients receiving enoxaparin during the acute phase received 40 mg enoxaparin SC every 12 h (60 mg if bodyweight was >65 kg) throughout the outpatient phase. The patients assigned to UH in the acute phase received placebo subcutaneous injections twice daily during the outpatient phase. Incremental benefit during the outpatient phase was assessed at day 43 and additional a priori-specified times for comparison of treatments were at 48 h and day 14. Similar numbers of patients from each treatment group progressed to the outpatient phase of the study (enoxaparin $n = 1179$, 60.4%; UH $n = 1185$, 60.6%). The significant difference in the primary endpoint between the treatment groups seen at day 8 was maintained at day 1. At day 43 the incidence of the primary endpoint was 17.3% in patients receiving enoxaparin and 19.7% in patients randomized to UH. These differences also remained apparent 1 year after treatment (71).

Another large-scale trial evaluated the long-term administration of LMWH compared with placebo. Fragmin and Fast Revascularization During Instability in Coronary Artery Disease (FRISC II) was a randomized, placebo-controlled study trial of 2267 patients with UA/non-Q-wave MI (58) (Table 3). This study specifically addressed the question on the benefits of the long-term treatment, evaluating dalteparin in patients with unstable coronary disease. In a complex, randomized factorial trial design, the efficacy of prolonged (90 day) treatment with dalteparin was compared with that of short-term (5 day) treatment. During the first 5–7 days of this double blind randomized trial, all 2267 patients received 120 U/kg/12 h of dalteparin. During the prolonged double blind phase, 2105 patients were randomized to treatment with either subcutaneous dalteparin, at a dose of 5000 or 7500 U twice daily or placebo. Males >70 kg and females >80 kg were given the 7500 U dose twice daily, whereas 5000 U twice daily were given to those with lower body weights. The composite primary endpoint was death or MI. Analysis was by intention to treat. During the 3 months of double blind treatment, there was a nonsignificant decrease in the composite endpoint of death or MI of 6.7% and 8.0% in the dalteparin and placebo groups, respectively [risk ratio 0.81 (95% CI 0.60–1.10), $p = 0.17$]. At 30 days, this decrease was significant [3.1% *vs* 5.9%, 0.53 (0.35–0.80); $p = 0.002$]. In the total cohort there was at 3 months a decrease in death, MI, or revascularization [29.1 *vs* 33.4%, 0.87 (0.77–0.99); $p = 0.031$]. The initial benefits were not sustained at 6-month follow-up. These results were interpreted as long-term dalteparin lowers the risk of death, MI, and revascularization in UA disease at least during the first month of therapy (58).

Nadroparin was evaluated in the FRAXiparine in Ischemic Syndrome (FRAXIS) trial (53). This trial assessed the benefit of the short-term use of the

LMWH nadroparin compared with UH in UA or non-Q-wave MI patients and determined whether a longer, 2-week LMWH regimen would offer additional clinical benefit. This was a multicenter, prospective, randomized, double blind study in three parallel groups, involving 3468 patients. Patients received one of three treatment regimens: the UH group received an intravenous bolus of UH 5000 IU, followed by an activated partial thromboplastin time adjusted infusion of UH for 6 ± 2 days; the nadroparin 6 group received an intravenous bolus of nadroparin 86 anti-Xa IU/kg, followed by twice daily subcutaneous injections of nadroparin 86 anti-Xa IU/kg for 6 ± 2 days, and the nadroparin 14 group received an intravenous bolus of nadroparin 86 anti-Xa IU/kg, followed by twice daily subcutaneous injections of nadroparin 86 anti-Xa IU/kg for 14 days. No statistically significant differences were observed between the three treatment regimens with respect to the primary outcome The absolute differences between the groups in the incidence of the primary outcome were: −0.3% ($p = 0.85$) for the nadroparin 6 group *vs* the UH group and +1.9% ($p = 0.24$) for the nadroparin 14 group *vs* the UH group. Furthermore, there were no significant intergroup differences regarding any of the secondary efficacy outcomes. However, there was an increased risk of major hemorrhages in the nadroparin 14 group compared with UH (3.5% *vs* 1.6%, $p = 0.0035$) (53). Treatment with nadroparin for 6 ± 2 days provides similar efficacy and safety to treatment with UH; a prolonged regimen of 14 days did not provide any additional clinical benefit.

c. Efficacy of Low-Molecular-Weight Heparins in Acute Coronary Syndromes

As summarized above, there seems to be a variation in efficacy of LMWHs. The FRAXIS trial aimed to assess the benefit of the short-term use of the LMWH nadroparin compared with UH in UA or non-Q-wave MI patients and to determine whether a longer, 2-week LMWH regimen would offer additional benefit. In this trial nadroparin therapy failed to show any advantage (53). In the FRIC trial, although twice-daily administration of SC dalteparin may be an effective and safe alternative to UH during the acute phase of UA, prolonged treatment at a lower once-daily dose did not confer any additional benefit over aspirin (75–165 mg) alone (54). Enoxaparin was found to offer superior protection when compared with UH in the ESSENCE trial (55), a finding that was confirmed in the TIMI 11B trial (56), while a meta-analysis of these two studies showed that enoxaparin was associated with a 20% reduction in death and serious cardiac ischemic events that appeared within the first few days of treatment, and this benefit was sustained through 43 days (72). In the ESSENCE study the "hard" composite endpoint of death and MI was statistically significantly lower with enoxaparin at 43 days [6.2% enoxaparin, UH 8.2%, odds ratio (OR) 0.73; 95% confidence interval (CI) 0.56–0.96] (72). The FRISC II study permitted an evaluation of the long-term benefits of dalteparin among noninvasively managed patients with UA/NSTEMI (40). The composite endpoint of death or MI was 47% lower among dalteparin-treated patients at 30 days, but this benefit was not sustained at 3 months.

Heparins appear to vary in efficacy in the treatment of patients with UA/NSTEMI. Superior efficacy to UH has been shown for enoxaparin, but this has not been demonstrated for the other LMWHS. This difference may arise from the

variations in study design and/or study populations. The definitive answer to this question will arise from a large head-to-head comparison of LMWHs in ACS.

However, one must also consider the possibility that there is a real biochemical basis for product differences. There are marked variations in the anti-Xa activities and anti-Xa:anti-IIa ratios of the LMWHs used in different trials. A number of the effects of LMWHs are mediated via mechanisms that are independent of AT binding and anti-Xa activity. The release of TFPI may also contribute to the prolonged antithrombotic effect seen after subcutaneous administration of LMWHs (5). In a recent study, the UH-induced increase of circulating total and free TFPI antigen and the aXa- and aIIa activity after subcutaneous injection of 9000 aXa-U of 4 different heparins was measured (73). It was shown that enoxaparin was the most potent molecule, which caused the highest TFPI release (73). It was demonstrated that the early rise of vWF was an independent predictor of adverse clinical outcome (6). In a recent study that explored the effects of different heparins on vWF release, it was found that the vWF values did not increase over 48 h in patients receiving either enoxaparin or PEG-hirudin. A significant rise of vWF was measured in UH-treated patients ($+87 \pm 11\%$), which differed significantly from the enoxaparin group ($p < 0.0006$) and PEG-hirudin group ($p < 0.0001$). In dalteparin-treated patients, delta vWF was elevated ($+48 \pm 8\%$) and did not differ significantly from the UH group (7). Therefore, the differing action of UH and LMWH on TFPI and vWF release could be a potential biochemical basis for the different clinical benefits of these compounds.

The available evidence favors an early invasive strategy for patients with NSTE ACS. Although prolonged LMWH administration provides an element of protection for high-risk patients, those individuals should be treated aggressively (and early) whenever possible. If coronary angiography and intervention are planned but delayed, continued therapy as a "bridge" to revascularization should be considered.

d. Platelet GP IIb/IIIa Inhibitors and Low-Molecular-Weight Heparins Combination Therapy

The contribution of platelets and coagulation proteins to coronary arterial thrombosis supports combination pharmacotherapy in NSTE ACS. In the Anti Thrombotic Therapy Combination Using Tirofiban and Enoxaparin II study (74), 525 patients with NSTE ACS were treated with tirofiban plus aspirin and randomized to receive either UH (5000-U bolus, 1000 U/h adjusted to an aPTT of 1.5–2.5 times control) or enoxaparin (1.0 mg/kg SC q12h). In-hospital death or MI occurred in 9.0% and 9.2% of patients, respectively; however, refractory ischemia because of UA occurred more frequently in the UH group [4.3% *vs* 0.6%; risk ratio, 0.72 ($p = 0.01$); and 7.1% *vs* 1.6%; risk ratio, 0.44 ($p = 0.002$), respectively]. TIMI major bleeding occurred in 1.0% and 0.3% of patients, respectively (74).

In a GUSTO IV substudy, (75) 646 patients received dalteparin (120 IU/kg SC every 12 h), aspirin, and either 24 or 48 h of abciximab administered as an initial bolus followed by a continuous infusion. Death or MI at 30 days occurred in 9.6% of dalteparin-treated patients and 8.5% of UH-treated patients. The rates of major non-CABG bleeding were 1.2% and 0.7%, respectively (75).

The integrilin and enoxaparin randomized assessment of acute coronary syndrome treatment *study* (61) randomized 746 patients with NSTE ACS to open-label enoxaparin (1 mg/kg SC bid) or UH (70 U/kg bolus, 15 U/kg/h to a target aPTT of 1.5–2.0 times control) for 48 h. All patients received aspirin and eptifibatide (180 μg/kg bolus, 2 μg/kg/min infusion). Major bleeding at 96 h was significantly lower among enoxaparin-treated patients than those receiving UH (1.8% *vs* 4.6%, $p = 0.03$). Patients receiving enoxaparin were less likely to experience ischemia during the initial (14.3% *vs* 25.4%, $p = 0.002$) and subsequent (12.7% *vs* 25.9%, $p < 0.0001$) 48-h monitoring periods. Combined death or MI at 30 days was also lower in enoxaparin-treated patients (5% *vs* 9%, $p = 0.03$) (61).

In PARAGON B, (76) 5225 patients with NSTEMI received either lamifiban or placebo in combination with aspirin and heparin, 805 patients received a LMWH preparation, while the remainder received UH. The incidence of death, MI, or severe recurrent ischemia was 12.2% for the overall cohort and lowest in the lamifiban-plus-LMWH group (10.2%). The incidence of death or MI was 11.0% and 9.0%, respectively. The benefit for those receiving lamifiban plus LMWH was sustained at 6 months with lower revascularization rates (42.8% *vs* 51.5%) and a lower composite of death or MI (11.9% *vs* 13.8%). After correcting for baseline differences, there was a significantly lower revascularization rate at 30 days with use of LMWH ($p = 0.001$) (76).

e. Anticoagulation Monitoring with Low-Molecular-Weight Heparins

Anti-Xa activity can be measured by chromogenic and chronometric assays. As with other coagulation tests, variability does exist. A majority of clinical trials, whether based on deep vein thrombosis prophylaxis, venous thromboembolism treatment, or ACS, have not required drug titration according to anti-Xa monitoring; however, an ability to define safe and effective levels of anticoagulation is important for clinical reasons. Defining a target level of factor Xa inhibition is also important in patients with altered drug clearance such as renal insufficiency (particularly with LMWH preparations characterized by a high anti-Xa:anti-IIa ratio). Lastly, monitoring capabilities may be useful when drug reversal is required because of the possibility of hemorrhagic complications during invasive procedures with inherent bleeding risks. The optimal level of factor Xa inhibition has not been determined for patients with ACS receiving LMWH. The available information derived from nonrandomized clinical studies of PCI suggests that anti-Xa activity >0.5 IU/mL is associated with a low incidence of ischemic/thrombotic and hemorrhagic events (77).

2. ST Elevation Myocardial Infarction

Acute ST-segment elevation myocardial infarction is caused by coronary plaque rupture/erosion and resultant thrombosis leading to an occluded epicardial infarct-related artery. Timely fibrinolytic therapy can reestablish coronary flow and salvage jeopardized myocardium. Large randomized clinical trials have definitely demonstrated a significant mortality benefit with thrombolytic therapy.

a. Unfractionated Heparin

The theoretical rationale for adjunctive heparin in the setting of concomitant administration of aspirin is not strongly supported by clinical data. Patients receiving streptokinase, anistreplase, or alteplase in the ISIS-3 and GISSI-2 trials received adjunctive subcutaneous heparin treatment or no heparin at all (78,79). Treatment with SC heparin, 12,500 IU, was initiated late after clinical presentation (12 h in GISSI-2 and 4 h in ISIS-3). In ISIS-3, an initial reduction in mortality was observed during the period of treatment but the benefit was no longer evident at 1 month. This benefit was further tempered by an observed increase in hemorrhagic stroke (one to two per 1000 treated) and excess bleeding (three to five per 1000 treated). Patients receiving IV UH with streptokinase in the GUSTO-I trial had similar clinical outcomes of death and reinfarction as the group receiving SC heparin with streptokinase (63). A tendency to increased rates of bleeding and hemorrhagic stroke with IV UH were reported (63). Two large trials, the International Study Group (62) and the ISIS-3150 (International Study of Infarct Survival) (79), assessed the value of adjunctive heparin in patients receiving thrombolytic therapy and aspirin. In both, heparin was given (12,500 U SC every 12 h). In the International Study Group trial, heparin was begun 12 h after randomization to fibrinolytic therapy; in the ISIS-3 trial, heparin began 4 h after randomization. The International Study Group study of 20,891 patients reported no difference in mortality between the heparin (8.5%) and no-heparin (8.9%) groups, whereas the risk of major bleeding was significantly increased by 0.5% in the heparin-treated group. The ISIS-3 study of 41,299 patients reported a vascular mortality rate of 10.3% in the heparin group and 10.0% in the no-heparin control group at 35 days. During the 7-day treatment period, mortality was 7.4% in the heparin group and 7.9% in the control group ($p = 0.06$). In-hospital rates of reinfarction with heparin were 3.2% compared with 3.5% in the no-heparin group ($p = 0.09$); stroke rates were not different. Major bleeding requiring transfusion was slightly more frequent in the heparin group (1.0% *vs* 0.8%, p, 0.01). In both studies, moderate doses of heparin produced marginal benefits at the cost of increased bleeding (62,79).

The evidence for the use of heparin with tPA is stronger. Higher rates of angiographic patency were observed in several series, and a direct relationship between measured aPTT and infarct artery patency was observed with tPa (80–82). The superiority of front-loaded tPA with UH over streptokinase in the GUSTO-I trial led to widespread clinical use of the tPA/UH. The addition of IV heparin to tPA resulted in five fewer deaths, three fewer reinfarctions, and one less pulmonary embolism per 1000 subjects treated (83).

However, adjunctive heparin use in the setting of fibrinolytic agents appears to have a narrow therapeutic window. Table 4 shows the risk of intracranial hemorrhage (ICH) for patients receiving fibrin-specific agents in major thrombolytic trials. There appears to be a consistent association between heparin dosing and risk of ICH. The observed rates of ICH for patients receiving SC heparin with tPA in the International Study was 0.4% (62). In the GUSTO-I trial (63), IV heparin was used in combination with tPA, and an ICH incidence of 0.72% was observed. Higher rates of heparin infusion as well as a higher target aPTT resulted

in a prohibitive increase in ICH. This increase was even more striking with streptokinase, which was associated with a 3% ICH rate. Heparin dosages were subsequently decreased in the TIMI-9B and GUSTO-II B trials. Heparin utilization in recent trials has been guided by a weight-adjusted bolus with a target aPTT of 50–70 s. The use of an early 3-h aPTT in the InTIME-II (69) trial resulted in an observed ICH rate of 0.62%. A 60 U/kg bolus (with a maximum dose of 4000 U) followed by a maintenance infusion of 12 U/kg/h (maximum of 1000 U/h) is adequate with fibrin-specific agents (84).

In the light of these data, for patients receiving streptokinase, either IV UH, 5000-U bolus, followed by 1000 U/h for patients >80 kg, 800 U/h for <80 kg with a target aPTT of 50–75 s, or SC UH (12,500 U/12 h for 48 h) and for patients receiving alteplase, tenecteplase, or reteplase, weight-adjusted heparin (60 U/kg bolus for a maximum of 4000 U) followed by 12 U/kg/h (1000 U/h maximum) adjusted to maintain an aPTT of 50–75 s for 48 h is recommended.

b. Low-Molecular-Weight Heparins

Experience with LMWHs in patients with STEMI is encouraging. The first randomized, placebo-controlled study is the Fragmin in Acute Myocardial Infarction (FRAMI) study (85). A total of 776 patients received subcutaneous dalteparin (150 IU/kg body weight every 12 h during the hospital period) or placebo. Thrombolytic therapy and aspirin were administered in 91.5% and 97.6% of patients, respectively. The primary study endpoint was the composite of thrombus formation diagnosed by echocardiography and arterial embolism on day 9 $\pm$ 2. Thrombus formation or embolism, or both, was found in 59 (21.9%) of 270 patients in the placebo group and 35 (14.2%) of 247 patients in the dalteparin group ($p = 0.03$). The risk reduction of thrombus formation associated with dalteparin treatment was 0.63 (95% confidence interval 0.43–0.92, $p = 0.02$). Analyses of all randomized patients revealed no significant difference between the placebo and dalteparin groups with respect to arterial embolism, reinfarction and mortality rates. Dalteparin treatment significantly reduces left ventricular thrombus formation in acute anterior MI but is associated with increased hemorrhagic risk (85).

Frostfeldt et al. in a randomized, double blind, placebo-controlled pilot trial evaluated the effect of dalteparin as an adjuvant to thrombolysis in patients with acute MI regarding early reperfusion, recurrent ischemia and patency at 24 h. In 101 patients dalteparin/placebo 100 IU/kg was given just before streptokinase and a second injection 120 IU/kg after 12 h. Dalteparin added to streptokinase tended to provide a higher rate of TIMI grade 3 flow in infarct-related artery compared to placebo; 68% *vs* 51% ($p = 0.10$). Dalteparin had no effects on noninvasive signs of early reperfusion. In patients with signs of early reperfusion, there seemed to be a higher rate of TIMI grade 3 flow, 74% *vs* 46% (myoglobin) ($p = 0.04$) and 73% *vs* 52% (vector-ECG) ($p = 0.11$). Ischemic episodes 6–24 h after start of treatment were fewer in the dalteparin group: 16% *vs* 38% ($p = 0.04$) (86).

LMWH as an adjunct to tissue-plasminogen activator (tPA) has been evaluated in the second trial of Heparin and Aspirin Reperfusion Therapy (HART II) (87). Four hundred patients undergoing reperfusion therapy with an accelerated

recombinant tPA regimen and aspirin for AMI were randomly assigned to receive adjunctive therapy for at least 3 days with either enoxaparin or UH. The study was designed to show noninferiority of enoxaparin *vs* UH with regard to infarct-related artery patency. Ninety minutes after starting therapy, patency rates [thrombolysis in MI (TIMI) flow grade 2 or 3] were 80.1% and 75.1% in the enoxaparin and UH groups, respectively. Reocclusion at 5–7 days from TIMI grade 2 or 3 to TIMI 0 or 1 flow and TIMI grade 3 to TIMI 0 or 1 flow, respectively, occurred in 5.9% and 3.1% of the enoxaparin group *vs* 9.8% and 9.1% in the UH group. Adverse events occurred with similar frequency in both treatment groups. It was concluded that enoxaparin was at least as effective as UH as an adjunct to thrombolysis, with a trend toward higher recanalization rates and less reocclusion at 5–7 days (87).

A recent meta-analysis examined the randomized studies of enoxaparin as adjunctive therapy to fibrinolysis in patients with an ST-segment AMI. The analysis included a total of 6069 patients, 1108 of them treated with SK, 400 with t-PA, and 4561 with tenecteplase. The rates of AMI, recurrent ischemia, death or AMI, and AMI or recurrent ischemia were all significantly reduced, and there was a trend toward a 14% decrease in mortality. The results were very consistent across all trials, with no heterogeneity found; the results were of similar magnitude with SK and with t-PA or tenecteplase. However, there was excess bleeding with enoxaparin (88).

3. *Percutaneous Coronary Interventions*

a. *Unfractionated Heparin*

UH is the most commonly used anticoagulant during PCI. UH therapy requires dose–response monitoring. In the cardiac catheterization laboratory, the activated clotting time (ACT) measurement is the most widely used parameter for this purpose. A large retrospective analysis of data from 5216 patients receiving heparin, without adjunctive GP IIbIIIa inhibitors, during PCI suggested that ischemic complications at 7 days were 34% lower with an ACT in the range of 350–375 s than they were with an ACT between 171 and 295 s ($p = 0.001$) (89). Similarly, two randomized trials have shown comparable results with both empiric and weight-adjusted heparin dosing regimens (90,91). Based on these data, heparin administered in doses of 60–100 IU/kg and a target ACT between 250 and 350 s are advocated in the absence of adjunctive GP IIbIIIa inhibition. In contrast, a target ACT of 200 s is advocated when heparin is administered in conjunction with a GP IIbIIIa inhibitor. Removal of the femoral sheath should be delayed until the ACT is between 150 and 180 s (92).

Routine use of IV heparin after PCI is no longer used because several randomized studies have shown that prolonged heparin infusions do not reduce ischemic complications, and are associated with a higher rate of bleeding at the catheter insertion site (93,94). Heparin does not reduce the risk of restenosis after balloon angioplasty. IV heparin administered for 24 h after successful coronary angioplasty failed to reduce angiographic restenosis in a randomized clinical trial

comparing heparin with dextrose (41.2% and 36.7%, respectively; p = NS) (93). Another study randomized 339 patients to no heparin or to twice-daily subcutaneous (SC) heparin (12,500 IU) for 4 months after successful angioplasty. No differences in angiographic or clinical indexes of restenosis were identified between the two groups (95).

Patients receiving a GP IIbIIIa inhibitor, a heparin bolus of 50–70 IU/kg to achieve a target ACT > 200 s is recommended. In patients not receiving a GP IIbIIIa inhibitor, heparin must be administered in doses sufficient to produce an ACT of 250–350 s. There is no need for routine postprocedural infusion of heparin (92).

b. Low-Molecular-Weight Heparins

The success of LMWHs in the medical management of patients with ACS has extended their use as an adjunct during PCI. Currently there is considerable evidence to support the administration of LMWHs in patients with ACS who undergo PCI (96–99). Increasingly, LMWH is replacing heparin for the treatment of patients with NSTEMI/UA, many of whom undergo PCI (Table 5). Because of the difficulties of monitoring levels of anticoagulation with LMWH during PCI, empiric dosing algorithms have been developed (97). Enoxaparin is the most commonly used LMWH in this setting. Thus, if the last dose of enoxaparin is administered <8 h before PCI, no additional enoxaparin is used. When the last dose of enoxaparin is administered between 8 and 12 h before PCI, a 0.3 mg/kg bolus of IV enoxaparin is advocated at the time of PCI; whereas if the last enoxaparin dose is administered >12 h before PCI, conventional anticoagulation therapy is advocated during PCI.

The potential for combining LMWHs with GPIIB-IIIa inhibitors has been investigated. Dalteparin 60 IU/kg IV appears to be safe and effective when administered in conjunction with abciximab for PCI (100). Enoxaparin appears to be safe when used in combination with tirofiban or eptifibatide during PCI (74,101).

Short-term administration of LMWH after PCI does not significantly reduce the occurrence of early ischemic events. In the Antiplatelet Therapy alone *vs* Lovenox plus Antiplatelet therapy in patients at increased risk of Stent Thrombosis trial, 1102 patients at increased risk of stent thrombosis (STEMI within 48 h, diffuse distal disease, large thrombus volume, acute closure, or residual dissection) were randomly assigned to receive either enoxaparin (40 or 60 mg SC q12h for 14 days based on patient weight <60 kg or >60 kg) or placebo; all patients received aspirin (325 mg/day) and ticlopidine (250 mg bid) for 14 days. The primary endpoint, a 30-day composite of death, nonfatal MI, and urgent revascularization, occurred in 1.8% of patients receiving enoxaparin and in 2.7% of those receiving placebo (p = 0.295) (74,102). LMWH treatment has no effect on restenosis.

In patients who have received LMWH prior to PCI, it is recommended that administration of additional anticoagulant therapy is dependent on the timing of the last dose of LMWH. If the last dose of enoxaparin is administered = 8 h prior to PCI, no additional anticoagulant therapy is needed. If the last dose of enoxaparin is administered between 8 and 12 h before PCI, a 0.3 mg/kg bolus of IV enoxaparin at

Table 5 Low-Molecular-Weight Heparins During Percutaneous Coronary Interventions

Study	*N*	Setting	Agent	Dose	GP IIb-IIIa use	30-day ischemic events	Major bleeding
Kereiakes et al. (99)	828	Elective or urgent	Enoxaparin IV	1.0 mg/kg	No	7.7	1.1
Ferguson et al. (98)	671	ACS	Enoxaparin SQ	1.0 mg/kg †	Abciximab, eptifibatide, or tirofiban	7.4%	1.4
Kereiakes et al. (99)	818	Elective	Enoxaparin IV	0.75 mg/kg	Abciximab	0.2	0.4
Preisack et a.l (96)	306	Elective or ACS	Reviparin IV	10,500	No	3.9 ‡	2.3
	306		UH IV	24,000	No	8.2	2.6

*ACS = acute coronary syndrome. *N* = number of patients, GPIIb-IIIa = glycoprotein IIb-IIA inhibitor †Enoxaparin, 0.1 mg/kg SQ initiated on admission. No further enoxaparin was given if PCI was performed within 8 h of last SQ injection. If PCI was performed between 8 and 12 h after PCI, an additional 0.3 mg/kg IV was given. ‡$p < 0.05$. Restenosis defined as >50% follow-up diameter stenosis unless indicated otherwise.

the time of PCI is suitable. If the last enoxaparin dose is administered >12 h before PCI, conventional anticoagulation therapy during PCI is needed (92).

C. Peripheral Arterial Occlusive Disease

The effects of LMWH, UHF, and vitamin K antagonists have been assessed in patients with intermittent claudication (103). Endpoints included walking capacity (pain-free walking distance or absolute walking distance), mortality, cardiovascular events, ankle/brachial pressure index, progression to surgery, amputation-free survival, and side effects. No significant difference was observed between UH treatment and control groups for pain-free walking distance or maximum walking distance at the end of treatment. The review found no data to indicate that LMWHs benefit walking distance. No study reported a significant effect on overall mortality or cardiovascular events, and the pooled odds ratios were not significant for these outcomes. Major and minor bleeding events were significantly more frequent in patients treated with vitamin K antagonists compared to control, with a nonsignificant increase in fatal bleeding events. This Cochrane review concluded that the use of anticoagulants for intermittent claudication cannot be recommended (103).

Patients presenting with acute limb ischemia secondary to thromboembolic arterial occlusion usually receive prompt anticoagulation with therapeutic dosages of UH in order to prevent clot propagation and to obviate further embolism. IV UH is also traditionally administered for intraoperative anticoagulation during

vascular reconstructions. The goals are to prevent stasis thrombosis in the often-diseased proximal and distal vessels, and to avoid the accumulation of thrombi at anastomoses and other sites of vascular injury. A rational UH regimen is to administer 100–150 U/kg IV before application of cross-clamps, and to supplement this every 45–50 min with 50 U/kg until cross-clamps are removed and circulation is reestablished. The timing of the supplemental doses is based on the half-life of UH (50–80 min) (104).

D. Atrial Fibrillation

The multicenter, randomized, double-blind Heparin in acute embolic stroke trial (HAEST) found no evidence that LMWH is superior to aspirin for treatment of acute ischemic stroke in patients with atrial fibrillation (105). In HAEST, either the LMWH, dalteparin (100 U/kg SC twice daily), or aspirin (160 mg/day) was started within 30 h of stroke onset in 449 patients with atrial fibrillation (AF) and acute ischemic stroke. The frequency of recurrent ischemic stroke during the first 14 days was 8.5% in dalteparin-allocated patients *vs* 7.5% in aspirin-allocated patients (OR 1.13, 95% CI 0.57–2.24). There was no benefit of dalteparin compared with aspirin in reducing cerebral hemorrhage (12% *vs* 14%), progression of symptoms within the first 48 h (11% *vs* 8%), or death (9% *vs* 7%, all P5NS) or functional outcome at 14 days or 3 months.

LMWH has also been used in patients with AF as an adjunct to the strategy of transesophageal echocardiography-guided cardioversion. In one observational series, 242 patients referred for cardioversion of AF or flutter without prior anticoagulation were examined by transesophageal echocardiography. Dalteparin was administered together with warfarin before early cardioversion of these low-risk patients and continued until the international normalized ratio reached the therapeutic range (106). No ischemic events were observed; however, more studies are needed before LMWH can be routinely advocated before cardioversion.

E. Perioperative Anticoagulation in Patients on Chronic Warfarin Therapy

Oral anticoagulation therapy with warfarin is used as treatment or prophylaxis for thromboembolism. Accepted protocols have been to stop warfarin therapy at some point prior to the procedure and initiate intravenous UH therapy in the hospital, titrated to an appropriate level of anticoagulation during the time surrounding a procedure. Following the procedure, oral warfarin and intravenous UH are reinitiated concomitantly. Intravenous heparin is continued until the target INR level is achieved. However, drawbacks include the inconvenience of intravenous heparin therapy, the need to monitor coagulation parameters, and the costs associated with prolonged hospital stays.

A prospective multicenter study evaluated a standardized approach to perioperative anticoagulation bridging therapy using dalteparin in patients with

prosthetic heart valves or atrial fibrillation without a prosthetic heart valve (107). Oral anticoagulants were stopped 5 days before the procedure, and patients received SC dalteparin 200 U/kg on days −3 and −2 and 100 U/kg on day −1. No dalteparin was given on the day of the procedure. On day +1, or when hemostasis was achieved, patients at low risk for bleeding were given dalteparin 200 U/kg subcutaneously for at least 4 days or when their INR was >1.9; patients at high risk for bleeding were given 5000 U daily. Oral anticoagulants were reinitiated at twice the normal dose on the night of the procedure and given at the usual dose once daily thereafter. There was no significant difference regarding the outcomes. The researchers concluded that, although anticoagulation bridge therapy with dalteparin was feasible, randomized controlled trials were necessary to develop optimal regimens (107).

Safety and efficacy should be the ultimate determinants of the agent(s) used for perioperative anticoagulation bridge therapy. Until double-blind, randomized trials have been performed, questions will remain regarding the best method and agent to use for perioperative anticoagulation in this diverse group of patients.

F. Anticoagulation Therapy During Pregnancy

1. Venous Thromboembolism During Pregnancy

The true incidence of VTE during pregnancy is unknown, but there is a strong clinical impression that the risk is increased compared with nonpregnant individuals. Fatal PE remains a common cause of maternal mortality. The anticoagulants currently available for the prevention and treatment of VTE and arterial thromboembolism include UH, LMWH, coumarin derivatives, as well as aspirin. The "direct" thrombin inhibitors, such as hirudin, cross the placenta and have not yet been evaluated during pregnancy.

Based on the results of large clinical trials in nonpregnant patients, LMWH and heparinoids (danaparoid sodium) are at least as effective and safe as UH for the treatment of patients with acute proximal DVT (108) and for the prevention of DVT in patients who undergo surgery (109). LMWHs have the advantage of a longer plasma half-life and a more predictable dose–response than UH. There is also evidence that LMWH (and heparinoids) do not cross the placenta, and a recent overview concluded that LMWH was safe for the fetus (110). These agents have potential advantages over UH during pregnancy because they cause less HIT, have the potential for once-daily administration, and probably result in a lower risk of heparin-induced osteoporosis.

Because LMWHs are safe for the fetus and because of the evidence of their efficacy in nonpregnant patients, they are suitable for routine clinical use in pregnant patients who require anticoagulant therapy. If one of these agents is used for acute treatment of VTE, a weight-adjusted dose regimen (as per the recommendations of the manufacturer) should be used. As the pregnancy progresses (and most women gain weight), the volume of distribution for LMWH changes. Therefore, two options are available. The first is to simply change the dose in proportion to the weight change. The second is to perform weekly anti-factor Xa levels 4 h

after the morning dose and adjust the dose of LMWH to achieve an anti-Xa level of approximately 0.5–1.2 U/mL. SC dalteparin, 5000 U q24h; enoxaparin, 40 mg q24h; and dose-adjusted LMWH to achieve a peak anti-Xa level of 0.2–0.6 U/mL (111).

2. *Management of Pregnant Women with Prosthetic Valves*

Chan et al. performed a systematic review of the literature examining fetal and maternal outcomes of pregnant women with prosthetic heart valves (112). Since no randomized trials were identified, the overview consisted of prospective and retrospective cohort studies. Pooled estimates of maternal and fetal risks associated with the following three commonly used approaches were determined: (1) oral anticoagulants throughout pregnancy; (2) replacing oral anticoagulants with UH from 6 to 12 weeks; and (3) UH use throughout pregnancy. In both warfarin-containing regimens, heparin was usually used close to term in order to avoid delivery of an anticoagulated fetus. Outcomes included pregnancy loss and fetopathic effects, as well as maternal bleeding, thromboembolic complications, and death.

The use of oral anticoagulants throughout pregnancy was associated with warfarin embryopathy in 6.4% of live births. The substitution of heparin at or prior to 6 weeks eliminated this risk. Overall, the rates of fetal wastage (spontaneous loss, stillbirths, and neonatal deaths) were similar in the three groups. The overall pooled maternal mortality rate was 2.9%. Major bleeding occurred in 2.5% of all pregnancies, mostly at the time of delivery. The regimen associated with the lowest risk of valve thrombosis/systemic embolism (3.9%) was the use of oral anticoagulants throughout; using UH only between 6 and 12 weeks gestation was associated with an increased risk of valve thrombosis (9.2%).

This analysis suggests that oral anticoagulants are more efficacious than UH for thromboembolic prophylaxis of women with mechanical heart valves in pregnancy; however, coumarins increase the risk of embryopathy. Substituting oral anticoagulants with heparin between 6 and 12 weeks reduces the risk of fetopathic effects, but possibly subjects the woman to an increased risk of thromboembolic complications. If used, s/c UH therapy should be initiated in high doses (17,500–20,000 U q12h) and adjusted to prolong a 6-h postinjection APTT into the therapeutic range; strong efforts should be made to ensure an adequate anticoagulant effect, since inadequate doses of heparin are ineffective. LMWH is probably a reasonable substitute for UH because it seems to reduce the risk of bleeding and osteoporosis and does not cross the placenta, but further information is required about dosing for this indication (113).

IV. Conclusions

LMWH and UF have been used for various thrombotic disorders. LMWHs have a greater bioavailability, are conveniently administered by SC injection, exhibit a more predictable dose–response, cause less activation of platelets, and are less

likely to be associated with thrombocytopenia or osteoporosis. For both ACS and VTE LMWHs demonstrated superior efficacy to that of UH. More data are needed for LMWH use before cardioversion in patients with atrial fibrillation. UF is still the standard care for perioperative anticoagulation. In pregnant patients with mechanical valves we need further information.

References

1. Hirsh J, Anand SS, Halperin JL, Fuster V. Guide to anticoagulant therapy: heparin : a statement for healthcare professionals from the American Heart Association. Circulation 2001; 103:2994–3018.
2. Hirsh J, Anand SS, Halperin JL, Fuster V. Mechanism of action and pharmacology of unfractionated heparin. Arterioscler Thromb Vasc Biol 2001; 21:1094–1096.
3. Haines ST, Bussey HI. Thrombosis and the pharmacology of antithrombotic agents. Ann Pharmacother 1995; 29:892–905.
4. Holmer E, Soderberg K, Bergqvist D, Lindahl U. Heparin and its low molecular weight derivatives: anticoagulant and antithrombotic properties. Haemostasis 1986; 16 (Suppl 2):1–7.
5. Broze Jr GJ. Tissue factor pathway inhibitor. Thromb Haemost 1995; 74: 90–93.
6. Montalescot G, Philippe F, Ankri A, Vicaut E, Bearez E, Poulard JE, Carrie D, Flammang D, Dutoit A, Carayon A, Jardel C, Chevrot M, Bastard JP, Bigonzi F, Thomas D. Early increase of von Willebrand factor predicts adverse outcome in unstable coronary artery disease: beneficial effects of enoxaparin. French Investigators of the ESSENCE Trial. Circulation 1998; 98:294–299.
7. Montalescot G, Collet JP, Lison L, Choussat R, Ankri A, Vicaut E, Perlemuter K, Philippe F, Drobinski G, Thomas D. Effects of various anticoagulant treatments on von Willebrand factor release in unstable angina. J Am Coll Cardiol 2000; 36:110–114.
8. Hirsh J. Low-molecular-weight heparin: a review of the results of recent studies of the treatment of venous thromboembolism and unstable angina. Circulation 1998; 98:1575–1582.
9. Hirsh J, Warkentin TE, Raschke R, Granger C, Ohman EM, Dalen JE. Heparin and low-molecular-weight heparin: Mechanisms of action, pharmacokinetics, dosing considerations, monitoring, efficacy, and safety. Chest 1998; 114:489S–510S.
10. Cosmi B, Fredenburgh JC, Rischke J, Hirsh J, Young E, Weitz JI. Effect of nonspecific binding to plasma proteins on the antithrombin activities of unfractionated heparin, low-molecular-weight heparin, and dermatan sulfate. Circulation 1997; 95:118–124.
11. Young E, Prins M, Levine MN, Hirsh J. Heparin binding to plasma proteins, an important mechanism for heparin resistance. Thromb Haemost 1992; 67:639–643.
12. Young E, Cosmi B, Weitz J, Hirsh J. Comparison of the nonspecific binding of unfractionated heparin and low molecular weight heparin (enoxaparin) to plasma proteins. Thromb Haemost 1993; 70:625–630.

13. Weitz JI, Hudoba M, Massel D, Maraganore J, Hirsh J. Clot-bound thrombin is protected from inhibition by heparin-antithrombin III but is susceptible to inactivation by antithrombin III-independent inhibitors. J Clin Invest 1990; 86:385–391.
14. Salzman EW, Rosenberg RD, Smith MH, Lindon JN, Favreau L. Effect of heparin and heparin fractions on platelet aggregation. J Clin Invest 1980; 65:64–73.
15. Kelton JG, Smith JW, Warkentin TE, Hayward CP, Denomme GA, Horsewood P. Immunoglobulin G from patients with heparin-induced thrombocytopenia binds to a complex of heparin and platelet factor 4. Blood 1994; 83: 3232–3239.
16. Amiral J. Antigens involved in heparin-induced thrombocytopenia. Semin Hematol 1999; 36:7–11.
17. Warkentin TE, Levine MN, Hirsh J, Horsewood P, Roberts RS, Gent M, Kelton JG. Heparin-induced thrombocytopenia in patients treated with low-molecular-weight heparin or unfractionated heparin. N Engl J Med 1995; 332:1330–1335.
18. Vitoux JF, Mathieu JF, Roncato M, Fiessinger JN, Aiach M. Heparin-associated thrombocytopenia treatment with low molecular weight heparin. Thromb Haemost 1986; 55:37–39.
19. Monreal M, Olive A, Lafoz E, del Rio L. Heparins, coumarin, and bone density. Lancet 1991; 338:706.
20. Wawrzynska L, Przedlacki J, Hajduk B, Bielska FH, Tomkowski W, Torbicki A. Low-molecular-weight heparins, acenocoumarol and bone density. Haemostasis 2001; 31:69–70.
21. Schulman S Hellgren-Wangdahl M. Pregnancy, heparin and osteoporosis. Thromb Haemost 2002; 87:180–181.
22. Ginsberg JS, Kowalchuk G, Hirsh J, Brill-Edwards P, Burrows R, Coates G, Webber C. Heparin effect on bone density. Thromb Haemost 1990; 64: 286–289.
23. Monreal M, Vinas L, Monreal L, Lavin S, Lafoz E, Angles AM. Heparin-related osteoporosis in rats. A comparative study between unfractioned heparin and a low-molecular-weight heparin. Haemostasis 1990; 20:204–207.
24. Heit JA, Silverstein MD, Mohr DN, Petterson TM, Lohse CM, O'Fallon WM, Melton LJ, III. The epidemiology of venous thromboembolism in the community. Thromb Haemost 2001; 86:452–463.
25. Bosson JL, Labarere J, Sevestre MA, Belmin J, Beyssier L, Elias A, Franco A, Le RP. Deep vein thrombosis in elderly patients hospitalized in subacute care facilities: a multicenter cross-sectional study of risk factors, prophylaxis, and prevalence. Arch Intern Med 2003; 163:2613–2618.
26. Anand SS, Bates S, Ginsberg JS, Levine M, Buller H, Prins M, Haley S, Kearon C, Hirsh J, Gent M. Recurrent venous thrombosis and heparin therapy: an evaluation of the importance of early activated partial thromboplastin times. Arch Intern Med 1999; 159:2029–2032.
27. Levine MN, Raskob G, Landefeld S, Kearon C. Hemorrhagic complications of anticoagulant treatment. Chest 2001; 119:108S–121S.
28. Hommes DW, Bura A, Mazzolai L, Buller HR, ten Cate JW. Subcutaneous heparin compared with continuous intravenous heparin administration in the

initial treatment of deep vein thrombosis. A meta-analysis. Ann Intern Med 1992; 116:279–284.
29. Lensing AW, Prins MH, Davidson BL, Hirsh J. Treatment of deep venous thrombosis with low-molecular-weight heparins. A meta-analysis. Arch Intern Med 1995; 155:601–607.
30. Dolovich LR, Ginsberg JS, Douketis JD, Holbrook AM, Cheah G. A meta-analysis comparing low-molecular-weight heparins with unfractionated heparin in the treatment of venous thromboembolism: examining some unanswered questions regarding location of treatment, product type, and dosing frequency. Arch Intern Med 2000; 160:181–188.
31. Segal JB, Bolger DT, Jenckes MW, Krishnan JA, Streiff MB, Eng J, Tamariz LJ, Bass EB. Outpatient therapy with low molecular weight heparin for the treatment of venous thromboembolism: a review of efficacy, safety, and costs. Am J Med 2003; 115:298–308.
32. Charbonnier BA, Fiessinger JN, Banga JD, Wenzel E, d'Azemar P, Sagnard L. Comparison of a once daily with a twice daily subcutaneous low molecular weight heparin regimen in the treatment of deep vein thrombosis. FRAXODI group. Thromb Haemost 1998; 79:897–901.
33. Agnelli G. Prevention of venous thromboembolism in surgical patients. Circulation 2004; 110:IV4–12.
34. Mismetti P, Laporte-Simitsidis S, Tardy B, Cucherat M, Buchmuller A, Juillard-Delsart D, Decousus H. Prevention of venous thromboembolism in internal medicine with unfractionated or low-molecular-weight heparins: a meta-analysis of randomised clinical trials. Thromb Haemost 2000; 83:14–19.
35. Grace Investigators Rationale and design of the GRACE (Global Registry of Acute Coronary Events) Project: a multinational registry of patients hospitalized with acute coronary syndromes. Am Heart J 2001; 141:190–199.
36. Fox KA, Goodman SG, Klein W, Brieger D, Steg PG, Dabbous O, Avezum A. Management of acute coronary syndromes. Variations in practice and outcome; findings from the Global Registry of Acute Coronary Events (GRACE). Eur Heart J 2002; 23:1177–1189.
37. Bertrand ME, Simoons ML, Fox KA, Wallentin LC, Hamm CW, McFadden E, de Feyter PJ, Specchia G, Ruzyllo W. Management of acute coronary syndromes: acute coronary syndromes without persistent ST segment elevation; recommendations of the task force of the European Society of Cardiology. Eur Heart J 2000; 21:1406–1432.
38. American Heart Association. 2000 Heart and Stoke Statistical Update. Dallas, Texas American Heart Association, 1999.
39. Hasdai D, Behar S, Wallentin L, Danchin N, Gitt AK, Boersma E, Fioretti PM, Simoons ML, Battler A. A prospective survey of the characteristics, treatments and outcomes of patients with acute coronary syndromes in Europe and the mediterranean basin; the Euro heart survey of acute coronary syndromes (Euro heart survey ACS). Eur Heart J 2002; 23:1190–1201.
40. Wallentin L, Lagerqvist B, Husted S, Kontny F, Stahle E, Swahn E. Outcome at 1 year after an invasive compared with a noninvasive strategy in unstable coronary-artery disease: the FRISC II invasive randomised trial. FRISC II Investigators. Fast Revascularisation during instability in coronary artery disease. Lancet 2000; 356:9–16.

41. Braunwald E, Antman EM, Beasley JW, Califf RM, Cheitlin MD, Hochman JS, Jones RH, Kereiakes D, Kupersmith J, Levin TN, Pepine CJ, Schaeffer JW, Smith EE, III, Steward DE, Theroux P, Gibbons RJ, Alpert JS, Eagle KA, Faxon DP, Fuster V, Gardner TJ, Gregoratos G, Russell RO, Smith Jr SC. ACC/AHA guidelines for the management of patients with unstable angina and non-ST-segment elevation myocardial infarction: executive summary and recommendations. A report of the American College of Cardiology/American Heart Association task force on practice guidelines (committee on the management of patients with unstable angina). Circulation 2000; 102:1193–1209.
42. Theroux P, Ouimet H, McCans J, Latour JG, Joly P, Levy G, Pelletier E, Juneau M, Stasiak J, deGuise P, Guy B, Pelletier GB, Ringzler D, Waters DD. Aspirin, heparin, or both to treat acute unstable angina. N Engl J Med 1988; 319:1105–1111.
43. Risk of myocardial infarction and death during treatment with low dose aspirin and intravenous heparin in men with unstable coronary artery disease. The RISC Group. Lancet 1990; 336:827–830.
44. Cohen M, Adams PC, Parry G, Xiong J, Chamberlain D, Wieczorek I, Fox KA, Chesebro JH, Strain J, Keller C, Kelly A, Lancaster G, Ali J, Kronmel R, Fuster V. Combination antithrombotic therapy in unstable rest angina and non-Q-wave infarction in nonprior aspirin users. Primary end points analysis from the ATACS trial. Antithrombotic therapy in acute coronary syndromes research group. Circulation 1994; 89:81–88.
45. Oler A, Whooley MA, Oler J, Grady D. Adding heparin to aspirin reduces the incidence of myocardial infarction and death in patients with unstable angina. A meta-analysis. JAMA 1996; 276:811–815.
46. Basu D, Gallus A, Hirsh J, Cade J. A prospective study of the value of monitoring heparin treatment with the activated partial thromboplastin time. N Engl J Med 1972; 287:324–327.
47. Turpie AG, Robinson JG, Doyle DJ, Mulji AS, Mishkel GJ, Sealey BJ, Cairns JA, Skingley L, Hirsh J, Gent M. Comparison of high-dose with low-dose subcutaneous heparin to prevent left ventricular mural thrombosis in patients with acute transmural anterior myocardial infarction. N Engl J Med 1989; 320:352–357.
48. Becker RC, Cannon CP, Tracy RP, Thompson B, Bovill EG, svigne-Nickens P, Randall AM, Knatternud G, Braunwald E. Relation between systemic anticoagulation as determined by activated partial thromboplastin time and heparin measurements and in-hospital clinical events in unstable angina and non-Q wave myocardial infarction. Thrombolysis in myocardial ischemia III B investigators. Am Heart J 1996; 131:421–433.
49. Lee MS, Wali AU, Menon V, Berkowitz SD, Thompson TD, Califf RM, Topol EJ, Granger CB, Hochman JS. The determinants of activated partial thromboplastin time, relation of activated partial thromboplastin time to clinical outcomes, and optimal dosing regimens for heparin treated patients with acute coronary syndromes: a review of GUSTO-IIb. J Thromb Thrombolysis 2002; 14:91–101.
50. Becker RC, Ball SP, Eisenberg P, Borzak S, Held AC, Spencer F, Voyce SJ, Jesse R, Hendel R, Ma Y, Hurley T, Hebert J. A randomized, multicenter trial of weight-adjusted intravenous heparin dose titration and point-of-care coagulation monitoring in hospitalized patients with active thromboembolic

disease. Antithrombotic therapy consortium investigators. Am Heart J 1999; 137:59–71.
51. Hochman JS, Wali AU, Gavrila D, Sim MJ, Malhotra S, Palazzo AM, De La FB. A new regimen for heparin use in acute coronary syndromes. Am Heart J 1999; 138:313–318.
52. Gurfinkel EP, Manos EJ, Mejail RI, Cerda MA, Duronto EA, Garcia CN, Daroca AM, Mautner B. Low molecular weight heparin versus regular heparin or aspirin in the treatment of unstable angina and silent ischemia. J Am Coll Cardiol 1995; 26:313–318.
53. Comparison of two treatment durations (6 days and 14 days) of a low molecular weight heparin with a 6-day treatment of unfractionated heparin in the initial management of unstable angina or non-Q-wave myocardial infarction: FRAX.I.S. (FRAxiparine in Ischaemic syndrome). Eur Heart J 1999; 20: 1553–1562.
54. Klein W, Buchwald A, Hillis WS, Monrad S, Sanz G, Turpie AG, van der MJ, Olaisson E, Undeland S, Ludwig K. Fragmin in unstable angina pectoris or in non-Q-wave acute myocardial infarction (the FRIC study). Fragmin in Unstable Coronary Artery Disease. Am J Cardiol 1997; 80:30E–34E.
55. Cohen M, Demers C, Gurfinkel EP, Turpie AG, Fromell GJ, Goodman S, Langer A, Califf RM, Fox KA, Premmereur J, Bigonzi F. A comparison of low-molecular-weight heparin with unfractionated heparin for unstable coronary artery disease. efficacy and safety of subcutaneous enoxaparin in non-Q-wave coronary events study group. N Engl J Med 1997; 337:447–452.
56. Antman EM, McCabe CH, Gurfinkel EP, Turpie AG, Bernink PJ, Salein D, Bayes DL, Fox K, Lablanche JM, Radley D, Premmereur J, Braunwald E. Enoxaparin prevents death and cardiac ischemic events in unstable angina/non-Q-wave myocardial infarction. Results of the thrombolysis in myocardial infarction (TIMI) 11B trial. Circulation 1999; 100:1593–1601.
57. Low-molecular-weight heparin during instability in coronary artery disease, Fragmin during instability in coronary artery disease (FRISC) study group. Lancet 1996; 347:561–568.
58. Long-term low-molecular-mass heparin in unstable coronary-artery disease: FRISC II prospective randomised multicentre study. Fragmin and fast revascularisation during instability in coronary artery disease. Investigators. Lancet 1999; 354:701–707.
59. Theroux P, Waters D, Lam J, Juneau M, McCans J. Reactivation of unstable angina after the discontinuation of heparin. N Engl J Med 1992; 327:141–145.
60. Toss H, Wallentin L, Siegbahn A. Influences of sex and smoking habits on anticoagulant activity in low-molecular-weight heparin treatment of unstable coronary artery disease. Am Heart J 1999; 137:72–78.
61. Goodman SG, Cohen M, Bigonzi F, Gurfinkel EP, Radley DR, Le IV, Fromell GJ, Demers C, Turpie AG, Califf RM, Fox KA, Langer A. Randomized trial of low molecular weight heparin (enoxaparin) versus unfractionated heparin for unstable coronary artery disease: one-year results of the ESSENCE study. Efficacy and safety of subcutaneous enoxaparin in non-Q wave coronary events. J Am Coll Cardiol 2000; 36:693–698.
62. In-hospital mortality and clinical course of 20,891 patients with suspected acute myocardial infarction randomised between alteplase and streptokinase

with or without heparin. The International study group. Lancet 1990; 336: 71–75.
63. An international randomized trial comparing four thrombolytic strategies for acute myocardial infarction. The GUSTO investigators. N Engl J Med 1993; 329:673–682.
64. Randomized trial of intravenous heparin versus recombinant hirudin for acute coronary syndromes. the global use of strategies to open occluded coronary arteries (GUSTO) IIa Investigators. Circulation 1994; 90:1631–1637.
65. Antman EM. Hirudin in acute myocardial infarction. Thrombolysis and Thrombin Inhibition in Myocardial Infarction (TIMI) 9B trial. Circulation 1996; 94:911–921.
66. Metz BK, White HD, Granger CB, Simes RJ, Armstrong PW, Hirsh J, Fuster V, MacAulay CM, Califf RM, Topol EJ. Randomized comparison of direct thrombin inhibition versus heparin in conjunction with fibrinolytic therapy for acute myocardial infarction: results from the GUSTO-IIb Trial. Global use of strategies to open occluded coronary arteries in acute coronary syndromes (GUSTO-IIb) Investigators. J Am Coll Cardiol 1998; 31:1493–1498.
67. A comparison of reteplase with alteplase for acute myocardial infarction. The Global Use of Strategies to Open Occluded Coronary Arteries (GUSTO III) Investigators. N Engl J Med 1997; 337:1118–1123.
68. Single-bolus tenecteplase compared with front-loaded alteplase in acute myocardial infarction: the ASSENT-2 double-blind randomised trial. Assessment of the Safety and Efficacy of a New Thrombolytic Investigators. Lancet 1999; 354:716–722.
69. Intravenous NPA for the treatment of infarcting myocardium early; InTIME-II, a double-blind comparison of single-bolus lanoteplase vs accelerated alteplase for the treatment of patients with acute myocardial infarction. Eur Heart J 2000; 21:2005–2013.
70. Dose-ranging trial of enoxaparin for unstable angina: results of TIMI 11A. The Thrombolysis in Myocardial Infarction (TIMI) 11A Trial Investigators. J Am Coll Cardiol 1997; 29:1474–1482.
71. Antman EM, Cohen M, McCabe C, Goodman SG, Murphy SA, Braunwald E. Enoxaparin is superior to unfractionated heparin for preventing clinical events at 1-year follow-up of TIMI 11B and ESSENCE. Eur Heart J 2002; 23:308–314.
72. Antman EM, Cohen M, Radley D, McCabe C, Rush J, Premmereur J, Braunwald E. Assessment of the treatment effect of enoxaparin for unstable angina/non-Q-wave myocardial infarction. TIMI 11B-ESSENCE meta-analysis. Circulation 1999; 100:1602–1608.
73. Alban S, Gastpar R. Plasma levels of total and free tissue factor pathway inhibitor (TFPI) as individual pharmacological parameters of various heparins. Thromb Haemost 2001; 85:824–829.
74. Cohen M, Theroux P, Borzak S, Frey MJ, White HD, Van Mieghem W, Senatore F, Lis J, Mukherjee R, Harris K, Bigonzi F. Randomized double-blind safety study of enoxaparin versus unfractionated heparin in patients with non-ST-segment elevation acute coronary syndromes treated with tirofiban and aspirin: the ACUTE II study. The Antithrombotic combination using Tirofiban and Enoxaparin. Am Heart J 2002; 144:470–477.

75. James S, Armstrong P, Califf R, Husted S, Kontny F, Niemminen M, Pfisterer M, Simoons M, Wallentin L. Safety and efficacy of abciximab combined with dalteparin in treatment of acute coronary syndromes. Eur Heart J 2002; 23 (19):1538–1545.
76. Mukherjee D, Mahaffey KW, Moliterno DJ, Harrington RA, Yadav JS, Pieper KS, Gallup D, Dyke C, Roe MT, Berdan L, Lauer MS, Manttari M, White HD, Califf RM, Topol EJ. Promise of combined low-molecular-weight heparin and platelet glycoprotein IIb/IIIa inhibition: results from Platelet IIb/IIIa antagonist for the reduction of acute coronary syndrome events in a global organization network B (PARAGON B). Am Heart J 2002; 144: 995–1002.
77. Choussat R, Montalescot G, Collet JP, Vicaut E, Ankri A, Gallois V, Drobinski G, Sotirov I, Thomas D. A unique, low dose of intravenous enoxaparin in elective percutaneous coronary intervention. J Am Coll Cardiol 2002; 40:1943–1950.
78. Six-month survival in 20,891 patients with acute myocardial infarction randomized between alteplase and streptokinase with or without heparin. GISSI-2 and International Study Group. Gruppo Italiano per lo Studio della Sopravvivenza nell'Infarto. Eur Heart J 1992; 13:1692–1697.
79. ISIS-3: a randomised comparison of streptokinase vs tissue plasminogen activator vs anistreplase and of aspirin plus heparin vs aspirin alone among 41,299 cases of suspected acute myocardial infarction. ISIS-3 (Third International Study of Infarct Survival) Collaborative Group. Lancet 1992; 339:753–770.
80. Bleich SD, Nichols TC, Schumacher RR, Cooke DH, Tate DA, Teichman SL. Effect of heparin on coronary arterial patency after thrombolysis with tissue plasminogen activator in acute myocardial infarction. Am J Cardiol 1990; 66:1412–1417.
81. Hsia J, Hamilton WP, Kleiman N, Roberts R, Chaitman BR, Ross AM. A comparison between heparin and low-dose aspirin as adjunctive therapy with tissue plasminogen activator for acute myocardial infarction. Heparin-Aspirin Reperfusion Trial (HART) Investigators. N Engl J Med 1990; 323:1433–1437.
82. de Bono DP, Simoons ML, Tijssen J, Arnold AE, Betriu A, Burgersdijk C, Lopez BL, Mueller E, Pfisterer M, Van de WF, Zulstra F, Verstraete M. Effect of early intravenous heparin on coronary patency, infarct size, and bleeding complications after alteplase thrombolysis: results of a randomised double blind European cooperative study group trial. Br Heart J 1992; 67:122–128.
83. Menon V, Harrington RA, Hochman JS, Cannon CP, Goodman SD, Wilcox RG, Schunemann HJ, Ohman EM. Thrombolysis and adjunctive therapy in acute myocardial infarction: the seventh ACCP conference on Antithrombotic and Thrombolytic therapy. Chest 2004; 126:549S–575S.
84. Ryan TJ, Antman EM, Brooks NH, Califf RM, Hillis LD, Hiratzka LF, Rapaport E, Riegel B, Russell RO, Smith EE III, Weaver WD, Gibbons RJ, Alpert JS, Eagle KA, Gardner TJ, Garson Jr A. Gregoratos G, Smith Jr SC. 1999 update: ACC/AHA guidelines for the management of patients with acute myocardial infarction: Executive summary and recommendations: A report of the American College of Cardiology/American Heart Association task force on practice guidelines (committee on management of acute myocardial infarction). Circulation 1999; 100:1016–1030.

85. Kontny F, Dale J, Abildgaard U, Pedersen TR. Randomized trial of low molecular weight heparin (dalteparin) in prevention of left ventricular thrombus formation and arterial embolism after acute anterior myocardial infarction: The Fragmin in Acute Myocardial Infarction (FRAMI) Study. J Am Coll Cardiol 1997; 30:962–969.
86. Frostfeldt G, Ahlberg G, Gustafsson G, Helmius G, Lindahl B, Nygren A, Siegbahn A, Swahn E, Venge P, Wallentin L. Low molecular weight heparin (dalteparin) as adjuvant treatment of thrombolysis in acute myocardial infarction—a pilot study: biochemical markers in acute coronary syndromes (BIOMACS II). J Am Coll Cardiol 1999; 33:627–633.
87. Ross AM, Molhoek P, Lundergan C, Knudtson M, Draoui Y, Regalado L, Le LV, Bigonzi F, Schwartz W, de Jong E, Coyne K. Randomized comparison of enoxaparin, a low-molecular-weight heparin, with unfractionated heparin adjunctive to recombinant tissue plasminogen activator thrombolysis and aspirin: second trial of heparin and aspirin reperfusion therapy (HART II). Circulation 2001; 104:648–652.
88. Theroux P, Welsh RC. Meta-analysis of randomized trials comparing enoxaparin versus unfractionated heparin as adjunctive therapy to fibrinolysis in ST-elevation acute myocardial infarction. Am J Cardiol 2003; 91:860–864.
89. Chew DP, Bhatt DL, Lincoff AM, Moliterno DJ, Brener SJ, Wolski KE, Topol EJ. Defining the optimal activated clotting time during percutaneous coronary intervention: aggregate results from 6 randomized, controlled trials. Circulation 2001; 103:961–966.
90. Boccara A, Benamer H, Juliard JM, Aubry P, Goy P, Himbert D, Karrillon GJ, Steg PG. A randomized trial of a fixed high dose vs a weight-adjusted low dose of intravenous heparin during coronary angioplasty. Eur Heart J 1997; 18:631–635.
91. Koch KT, Piek JJ, de Winter RJ, Mulder K, David GK, Lie KI. Early ambulation after coronary angioplasty and stenting with six French guiding catheters and low-dose heparin. Am J Cardiol 1997; 80:1084–1086.
92. Popma JJ, Berger P, Ohman EM, Harrington RA, Grines C, Weitz JI. Antithrombotic therapy during percutaneous coronary intervention: the seventh ACCP conference on Antithrombotic and Thrombolytic therapy. Chest 2004; 126:576S–599S.
93. Ellis SG, Roubin GS, Wilentz J, Douglas Jr JS. King SB, III. Effect of 18- to 24-hour heparin administration for prevention of restenosis after uncomplicated coronary angioplasty. Am Heart J 1989; 117:777–782.
94. Friedman HZ, Cragg DR, Glazier SM, Gangadharan V, Marsalese DL, Schreiber TL, O'Neill WW. Randomized prospective evaluation of prolonged versus abbreviated intravenous heparin therapy after coronary angioplasty. J Am Coll Cardiol 1994; 24:1214–1219.
95. Brack MJ, Ray S, Chauhan A, Fox J, Hubner PJ, Schofield P, Harley A, Gershlick AH. The subcutaneous heparin and angioplasty restenosis prevention (SHARP) trial. Results of a multicenter randomized trial investigating the effects of high dose unfractionated heparin on angiographic restenosis and clinical outcome. J Am Coll Cardiol 1995; 26:947–954.
96. Preisack MB, Bonan R, Meisner C, Eschenfelder V, Karsch KR. Incidence, outcome and prediction of early clinical events following percutaneous transluminal coronary angioplasty. A comparison between treatment with

reviparin and unfractionated heparin/placebo (results of a substudy of the REDUCE trial). Eur Heart J 1998; 19:1232–1238.
97. Miller L, Gupta A, Bertolet BD. Use of clopidogrel loading, enoxaparin, and double-bolus eptifibatide in the setting of early percutaneous coronary intervention for acute coronary syndromes. J Invasive Cardiol 2002; 14:247–250.
98. Ferguson JJ, Antman EM, Bates ER, Cohen M, Every NR, Harrington RA, Pepine CJ, Theroux P. Combining enoxaparin and glycoprotein IIb/IIIa antagonists for the treatment of acute coronary syndromes: final results of the National Investigators Collaborating on Enoxaparin-3 (NICE-3) study. Am Heart J 2003; 146:628–634.
99. Kereiakes DJ, Grines C, Fry E, Esente P, Hoppensteadt D, Midei M, Barr L, Matthai W, Todd M, Broderick T, Rubinstein R, Fareed J, Santoian E, Neiderman A, Brodie B, Zidar J, Ferguson JJ, Cohen M. Enoxaparin and abciximab adjunctive pharmacotherapy during percutaneous coronary intervention. J Invasive Cardiol 2001; 13:272–278.
100. Kereiakes DJ, Kleiman NS, Fry E, Mwawasi G, Lengerich R, Maresh K, Burkert ML, Aquilina JW, DeLoof M, Broderick TM, Shimshak TM. Dalteparin in combination with abciximab during percutaneous coronary intervention. Am Heart J 2001; 141:348–352.
101. Bhatt DL, Lee BI, Casterella PJ, Pulsipher M, Rogers M, Cohen M, Corrigan VE, Ryan Jr TJ, Breall JA, Moses JW, Eaton GM, Sklar MA, Lincoff AM. Safety of concomitant therapy with eptifibatide and enoxaparin in patients undergoing percutaneous coronary intervention: results of the coronary revascularization using integrilin and single bolus enoxaparin study. J Am Coll Cardiol 2003; 41:20–25.
102. Berger PB, Mahaffey KW, Meier SJ, Buller CE, Batchelor W, Fry ET, Zidar JP. Safety and efficacy of only 2 weeks of ticlopidine therapy in patients at increased risk of coronary stent thrombosis: results from the antiplatelet therapy alone versus Lovenox plus antiplatelet therapy in patients at increased risk of Stent Thrombosis (ATLAST) trial. Am Heart J 2002; 143:841–846.
103. Cosmi B, Conti E, Coccheri S. Anticoagulants (heparin, low molecular weight heparin and oral anticoagulants) for intermittent claudication. Cochrane Database Syst Rev 2001; CD001999.
104. Clagett GP, Sobel M, Jackson MR, Lip GY, Tangelder M, Verhaeghe R. Antithrombotic therapy in peripheral arterial occlusive disease: The seventh ACCP conference on Antithrombotic and Thrombolytic therapy. Chest 2004; 126:609S–626S.
105. Berge E, Abdelnoor M, Nakstad PH, Sandset PM. Low molecular-weight heparin versus aspirin in patients with acute ischaemic stroke and atrial fibrillation: a double-blind randomised study. HAEST study group. Heparin in acute embolic stroke trial. Lancet 2000; 355:1205–1210.
106. Roijer A, Eskilsson J, Olsson B. Transoesophageal echocardiography-guided cardioversion of atrial fibrillation or flutter. Selection of a low-risk group for immediate cardioversion. Eur Heart J 2000; 21:837–847.
107. Kovacs MJ, Kearon C, Rodger M, Anderson DR, Turpie AG, Bates SM, Desjardins L, Douketis J, Kahn SR, Solymoss S, Wells PS. Single-arm study of bridging therapy with low-molecular-weight heparin for patients at risk of

arterial embolism who require temporary interruption of warfarin. Circulation 2004; 110:1658–1663.
108. Gould MK, Dembitzer AD, Doyle RL, Hastie TJ, Garber AM. Low-molecular-weight heparins compared with unfractionated heparin for treatment of acute deep venous thrombosis. A meta-analysis of randomized, controlled trials. Ann Intern Med 1999; 130:800–809.
109. Sanson BJ, Lensing AW, Prins MH, Ginsberg JS, Barkagan ZS, Lavenne-Pardonge E, Brenner B, Dulitzky M, Nielsen JD, Boda Z, Turi S, Mac Gillavry MR, Hamulyak K, Theunissen IM, Hunt BJ, Buller HR. Safety of low-molecular-weight heparin in pregnancy: a systematic review. Thromb Haemost 1999; 81:668–672.
110. Nurmohamed MT, Rosendaal FR, Buller HR, Dekker E, Hommes DW, Vandenbroucke JP, Briet E. Low-molecular-weight heparin versus standard heparin in general and orthopaedic surgery: A meta-analysis. Lancet 1992; 340:152–156.
111. Blomback M, Bremme K, Hellgren M, Siegbahn A, Lindberg H. Thromboprophylaxis with low molecular mass heparin, 'Fragmin' (dalteparin), during pregnancy – a longitudinal safety study. Blood Coagul Fibrinolysis 1998; 9: 1–9.
112. Chan WS, Anand S, Ginsberg JS. Anticoagulation of pregnant women with mechanical heart valves: a systematic review of the literature. Arch Intern Med 2000; 160:191–196.
113. Bates SM, Greer IA, Hirsh J, Ginsberg JS. Use of antithrombotic agents during pregnancy: the seventh ACCP conference on Antithrombotic and Thrombolytic therapy. Chest 2004; 126:627S–644S.

Chemistry and Biology of Heparin and Heparan Sulfate
H.G. Garg, R.J. Linhardt and C.A. Hales (Editors)

Chapter 24

Heparin-Induced Thrombocytopenia

THEODORE E. WARKENTIN

McMaster University, Hamilton, ON, Canada
and
WILLIAM E. DAGER

University of California Davis, Sacramento, CA, USA

I. Introduction

Heparin-induced thrombocytopenia (HIT) is an unusual immune-mediated adverse drug reaction with the central paradox being its strong association with thrombosis, despite the role of an anticoagulant (heparin) in causing a fall in platelet count (thrombocytopenia). HIT results from an interaction between (negatively charged) heparin and a (positively charged) protein, platelet factor 4 (PF4), leading to neoepitope formation on PF4. HIT can be defined as any clinical event – most often thrombocytopenia, with or without thrombosis – in which pathogenic heparin-dependent antibodies can be implicated (1). Such a "clinicopathologic" framework requires an understanding of the clinical events associated with HIT, together with an appreciation of the strengths and limitations of different laboratory tests used to detect the HIT antibodies.

II. Pathogenesis

Figure 1 summarizes the pathogenesis of HIT (2). The central concept is heparin-induced generation of pathogenic IgG antibodies that recognize multimolecular complexes of PF4 and heparin on platelet surfaces, leading to platelet activation *in vivo* and associated thrombin generation. There is evidence suggesting that endothelial cells and leukocytes (neutrophils, monocytes) can also be activated by HIT antibodies.

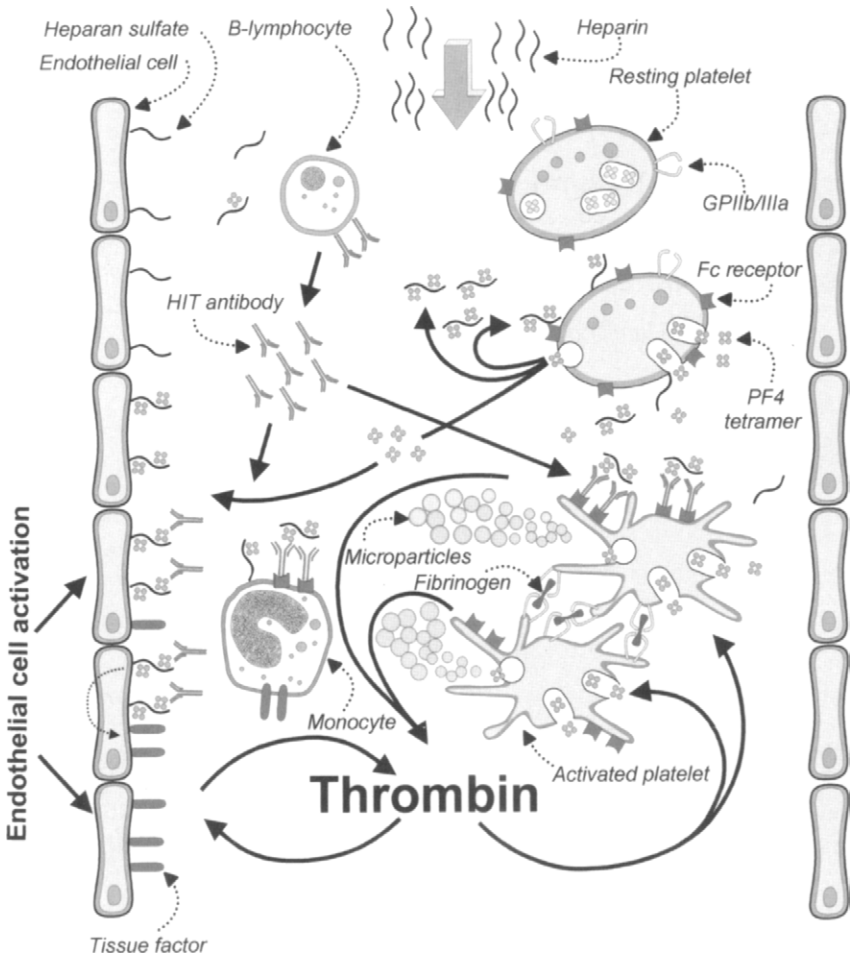

Figure 1 Pathogenesis of HIT: a central role for thrombin generation. HIT-IgG antibodies bind to several identical epitopes on the same antigen complex, thus forming immune complexes that become localized to the platelet surface. The IgG immune complexes can cross-link the platelet FcγRIIa receptors, resulting in FcγRIIa-dependent platelet activation. The GPIIb/IIIa complex is not required for platelet activation. The activated platelets trigger a cascade of events, leading ultimately to activation of the coagulation pathways, resulting in thrombin generation. Activated platelets release their α granule proteins, including PF4, leading to formation of more multimolecular PF4/heparin complexes, setting up a vicious cycle of platelet activation triggering even more platelet activation. The activated platelets bind fibrinogen, recruit other platelets, and start to form a primary clot. During shape change, procoagulant, platelet-derived microparticles are released, providing a phospholipid surface for amplifying thrombin generation. The released PF4 also binds to endothelial cell heparan sulfate, forming local antigen complexes to which HIT antibodies bind. Tissue factor expression on activated endothelial cells further enhances thrombin generation. Reprinted, with permission (2).

A. Platelet Factor 4/Heparin Interactions

The antigen(s) recognized by HIT antibodies are not located on heparin, but rather on PF4 that are formed when PF4 binds to heparin or certain other polyanions (3). PF4 is a 70-amino acid (7780 Da), platelet-specific member of the C-X-C subfamily of chemokines. Four PF4 molecules self-associate to form compact tetramers of globular structure (~31,000 Da). PF4 is rich in the basic amino acids, lysine and arginine (32 and 12 residues per tetramer, respectively), which form a "ring of positive charge" providing the interface between the PF4 tetramer and heparin.

PF4 is stored in platelet α-granules, where it is bound to chondroitin sulfate. Under normal conditions, only trace levels of PF4 (~3 ng/mL) are found in human plasma. However, heparin infusion increases PF4 levels up to 30-fold for several hours, by displacing PF4 from endothelial cell surfaces.

Unfractionated heparin (UFH) and low molecular weight heparin (LMWH) preparations are highly sulfated glycosaminoglycans (GAGs), with a mean of 2.0–2.5 sulfates per disaccharide unit (4). Their mean chain lengths (UFH, ~45 saccharide units; LMWH, ~15 saccharide units) (5) exceed the minimum (10–12 saccharide units) (6) for optimal binding to PF4 required to form the neoepitope(s) on PF4. Binding of PF4 to heparin is independent of its antithrombin-catalyzing pentasaccharide region.

Nonspecific charge interactions account for heparin-PF4 binding and formation of the HIT antigen(s). This is illustrated by the identification of numerous non-heparin polyanions that also can form antigens on PF4 recognized by HIT antibodies (Table 1) (4,6–19). In contrast, certain other polyanions, such as polystyrene sulfonate and the anticoagulant preparation, danaparoid, interact with PF4 in such a way that only a minority of HIT antibodies recognize them, and then only weakly (6).

PF4/heparin complexes are multimolecular (20), with ultralarge complexes formed between UFH and PF4 (21). Potentially, the importance of multimolecular complexes could reside in the need for at least two PF4 tetramers to be bound close together by heparin, which acts to charge-neutralize PF4 molecules that would otherwise be expected to charge-repel each other in the absence of heparin.

B. Heparin-Induced Thrombocytopenia Antibody-Induced Platelet Activation

Only anti-PF4/heparin antibodies of IgG class have the potential to activate platelets (22,23). This is because platelet activation occurs when the platelet FcγIIa receptors are occupied by IgG antibodies that recognize PF4/heparin complexes formed *in situ* on platelet surfaces (24). Although an Fc receptor-blocking monoclonal antibody will prevent platelet activation by HIT-IgG antibodies, it will not prevent binding of antibodies to platelets. Platelet activation also proceeds even if heparin is somewhat in molar excess to PF4 (compared with optimal ratios in the immunoassay), suggesting that the platelet surface microenvironment achieves the necessary PF4:heparin stoichiometric ratio as PF4 is increasingly released during platelet activation.

Table 1 Polyanions Interacting with PF4: Implications for HIT

Immunogenicity and cross-reactivity profile	Polyanion	References
Immunogenic and cross-reactive *in vivo* (i.e., can cause HIT or HIT-mimicking syndrome)	UFH, LMHW, pentosan polysulfate, hypersulfated chondroitin sulfate, PI-88 (anti-angiogenic compound)	7–12
Immunogenic but not significantly cross-reactive *in vivo*	Fondaparinux, danaparoid*	13–16
Cross-reactive *in vitro* (without clinical implications)	Various glucan sulfate polysaccharides, with cross-reactivity depending on sulfation grade, chain length, and degree of branching; highly sulfated 17-mer (SR121903); highly sulfated pentasaccharide (Org 32701)**; polyvinyl (PV) sulfonate***, PV sulfate, PV phosphate, PV phosphonate, polystyrene sulfonate (weak)	4,6,17–19

Abbreviations: HIT, heparin-induced thrombocytopenia; LMWH, low molecular weight heparin; PV, polyvinyl; UFH, unfractionated heparin.

*Immunogenicity is unknown (may be immunogenic, as it contains small amounts of high-sulfated heparan sulfate); weakly cross-reactive with 10–40% of HIT sera.

**Whereas the sulfated pentasaccharide, fondaparinux, is not significantly cross-reactive against HIT antibodies, a pentasaccharide with higher sulfation (Org 32701) is cross-reactive.

***Used in commercial immunoassay for HIT antibodies.

C. Coagulation Activation

A consequence of platelet activation in HIT is the formation of procoagulant, platelet-derived microparticles (25,26). Indeed, HIT antibodies and other platelet IgG agonists (heat-aggregated IgG, platelet-activating monoclonal IgG) cause an even greater platelet procoagulant response than physiologic platelet agonists such as collagen and thrombin (27). Evidence that platelet activation occurs *in vivo* in patients with HIT includes elevated P-selectin on circulating platelets (28) and increased numbers of platelet-derived microparticles (25).

D. Multicellular Activation

PF4 bound to endothelial surface heparan sulfate can be recognized by HIT antibodies, potentially causing endothelial cell activation, with procoagulant consequences (20,29,30). HIT-IgG can also activate monocytes in the presence of PF4, leading to expression of tissue factor (31,32). Heparin is not required for PF4 binding to monocytes, which is mediated by surface proteoglycans such as chondroitin sulfate. It is possible that HIT-IgG do not activate endothelium and leukocytes directly, but perhaps indirectly via activated platelets or platelet-derived

products, e.g., microparticles. There is evidence platelet–leukocyte complexes are formed in HIT (33,34).

III. Clinical Picture

Typically, there is a minimum of five days before clinically significant levels of anti-PF4/heparin antibodies can be generated in patients who receive heparin (35,36). In addition, most immunizing heparin exposures appear to occur in association with surgery, which could increase PF4 levels (from platelet activation) or other immune-stimulating, pro-inflammatory processes. Thus, the typical clinical profile of HIT is otherwise unexplained thrombocytopenia that begins about a week after beginning heparin.

A. Thrombocytopenia

Thrombocytopenia is the central clinical feature of HIT, and occurs in at least 85–90% of patients, if thrombocytopenia is defined as a platelet count fall to less than $150 \times 10^9\,L^{-1}$ (1). In the remaining patients, HIT is recognized either because of a substantial fall in the platelet count (e.g., 30–50% or more) that does not fall to less than $150 \times 10^9\,L^{-1}$ (8), or because of clinical events such as thrombosis or skin lesions at heparin injection sites that draw attention to the possibility of HIT despite less substantial platelet count declines (37,38). The median platelet count nadir in large patients series is about $60 \times 10^9\,L^{-1}$. It is unusual for the platelet count to be less than $10 \times 10^9\,L^{-1}$ in HIT.

B. Timing

In about two-thirds of patients, HIT is recognized because of a platelet count fall that begins 5–10 days after starting a course of heparin (*typical-onset HIT*), although thrombocytopenic levels may not be reached until days 7–14 (35,36). It is relatively uncommon for the platelet count fall of HIT to begin more than 10 days after beginning heparin.

In about a third of patients, HIT is recognized because of an abrupt drop in platelet count upon administering heparin (*rapid-onset HIT*). These patients have typically received heparin within the past 100 days, and so the thrombocytopenia is explained by heparin being given to a patient who already has clinically significant levels of HIT antibodies (35). Sometimes, the previous heparin exposure may have been minor or even unrecorded in the medical record, e.g., intraoperative heparin "flushes" (39).

In recent years it has been recognized that HIT can begin several days after the patient last received heparin (*delayed-onset HIT*) (40–42). These patients typically present with thrombosis, and are recognized as having HIT when laboratory testing shows unexpected thrombocytopenia. Serological features include strong positive results of *in vitro* testing for HIT antibodies, including the ability of the patient serum to activate platelet *in vitro* even in the absence of heparin.

C. Thrombosis

HIT is strongly associated with thrombosis: the odds ratio varies from about 20–40 (7,8,43,44). In some patient series, about half of all patients with HIT are recognized only after developing HIT-associated thrombosis (45).

Venous thrombosis complicates HIT more often than does arterial thrombosis (45,46). Indeed, pulmonary embolism is more common than all arterial thrombotic events combined. Arterial thrombosis most often involves large lower-limb arteries, with thrombotic stroke and myocardial infarction diagnosed less frequently. Rare but well-described thrombotic sequelae include cerebral venous thrombosis (presenting as severe headache and progressive neurologic deficits), adrenal vein thrombosis (presenting as unilateral or bilateral adrenal hemorrhagic infarction) (47). Localizing factors, such as atherosclerosis or vascular injury from catheters, influence site of thrombosis (43).

D. Miscellaneous Clinical Sequelae

Heparin-induced skin lesions occur at heparin injection sites in about 10% of patients forming anti-PF4/heparin antibodies. These range from erythematous plaques to skin necrosis. For unknown reasons, only a minority of patients with heparin-induced skin lesions develop thrombocytopenia, even though HIT antibodies are readily detected (37).

About one-quarter of patients who receive an intravenous heparin bolus at a time that they have circulating HIT antibodies develop acute symptoms or signs such as fever, chills, respiratory distress, hypertension, or even transient global amnesia (47–49). Sometimes, cardiac or respiratory arrest results. These acute systemic reactions characteristically begin 5–30 min following the intravenous heparin bolus, and are accompanied by abrupt platelet count fall.

Decompensated disseminated intravascular coagulation (DIC), defined as abnormally low fibrinogen or otherwise unexplained increase in the international normalized ratio (INR), occurs in only 5–15% of patients (47).

E. Differential Diagnosis

Thrombocytopenia is common in hospitalized patients, and thrombocytopenia that occurs in a patient receiving heparin has numerous potential explanations besides HIT. Indeed, certain disorders strongly resemble HIT on clinical grounds. Two examples include cancer-associated DIC with thrombosis, and pulmonary embolism with DIC-associated thrombocytopenia (50,51). The high negative predictive value of sensitive assays for HIT antibodies permits HIT to be ruled out in these pseudo-HIT disorders.

Evaluation of four clinical parameters may be useful in estimating the pretest probability of HIT (1,47,52). Even without thrombosis, a high pretest probability is suggested when the timing of onset of thrombocytopenia is consistent with heparin-induced immunization in the absence of another explanation. Very severe

thrombocytopenia (platelet count $< 10 \times 10^9\,L^{-1}$) with bleeding suggests a non-HIT diagnosis such as posttransfusion purpura (50,53).

IV. Laboratory Testing for Heparin-Induced Thrombocytopenia Antibodies

Only a minority of patients who form HIT antibodies develop thrombocytopenia, thrombosis, or other sequelae of HIT (22). This means that laboratory assays with greater sensitivity for detecting anti-PF4/heparin antibodies are less specific for clinical HIT, even if they have high specificity for detecting antibodies.

A. Platelet Activation Assays

Platelet activation assays detect HIT antibodies based upon their potent platelet-activating properties. HIT antibodies produce a characteristic reaction profile: maximal activation at 0.1–0.3 IU/mL heparin that exceeds the buffer control; minimal activation at 100 U/mL heparin; and inhibition by Fc receptor-blocking monoclonal antibody (54). Assays that use "washed" platelets from platelet donors selected for their responsiveness to HIT antibodies have the best operating characteristics (sensitivity-specificity trade-off) (22,55,56). Platelet activation endpoints vary widely, and include detection of radioactive serotonin release, formation of platelet-derived microparticles (57), and platelet aggregation (58). However, washed platelet assays are technically demanding, and performance varies widely among the laboratories that offer these assays (59). Formerly, platelet aggregation assays using conventional aggregometry were used widely for diagnosis of HIT, but lower sensitivity (60) and specificity for clinical HIT (61) compared with the washed platelet assays has limited their use in recent years.

B. Immunoassays

Two commercially available solid phase enzyme-immunoassays (EIAs) detect antibodies based upon their binding to PF4 in the presence of heparin (Asserachrom, Stago, France) (62) or the polyanion, polyvinyl sulfonate (GTI, Brookfield, WI) (6). These assays detect all three of the major immunoglobulin classes (IgG, IgM, IgA), which, unfortunately, worsens operating characteristics in comparison with in-house (noncommercially available) EIAs that only detect IgG class antibodies (56,63). A fluid-phase EIA developed by Newman et al. (16) allows binding of antibodies to PF4/heparin in solution, followed by IgG "capturing" using sepharose. This assay also avoids the problems of detecting nonpathogenic IgM and IgA antibodies, and is especially useful in assessing for *in vitro* cross-reactivity of HIT-IgG against polyanions other than heparin.

A rapid antigen assay (64) that detects anti-PF4/heparin antibodies of all immunoglobulin classes appears to have operating characteristics (sensitivity–specificity trade-offs) intermediate between the commercial EIAs and a washed platelet activation assay (65). Another rapid bedside assay that also detects anti-PF4/

heparin antibodies of all three antibody classes is about to be marketed in the US; the operating characteristics of this assay are unknown.

C. Diagnostic Interpretation

Washed platelet activation assays and PF4/polyanion EIAs have similar high sensitivity for diagnosis of HIT. Indeed, negative testing by these two assays essentially rules out HIT (61). Diagnostic specificity is greater with the washed platelet activation assays, compared with EIAs, as the latter are more likely to detect clinically insignificant antibodies (22,56). It is important to interpret the laboratory assay in the context of "pretest probability" for HIT, based upon clinical considerations. The reason is that nonpathogenic anti-PF4/heparin antibodies are generated in 15–70% of postoperative patients receiving UFH, and so a positive test does not necessarily confirm HIT, particularly when the test result is "weak" and the patient has strong evidence for an alternate diagnosis. The magnitude of a positive test result is useful in estimating the "likelihood ratio" that determines "posttest probability" of HIT, in a Bayesian model (52). For example, a strong-positive washed platelet activation assay is associated with a much higher likelihood ratio for HIT than a weak-positive EIA (about 20–50 *vs* 2–3). Strongly positive test results are a characteristic feature of delayed-onset HIT (40,42).

D. Iceberg Model

Figure 2 depicts the "iceberg model" of HIT, which illustrates the relationship between different laboratory assays for HIT, thrombocytopenia, and thrombosis (66,67). This model indicates: (a) only a subset of anti-PF4/heparin antibodies of IgG class have platelet-activating properties (22,68); (b) washed platelet activation assays have greater diagnostic specificity for clinical HIT than EIAs; and (c) thrombosis is not associated with antibody formation in the absence of thrombocytopenia (7,8).

E. Frequency of Heparin-Induced Thrombocytopenia

The frequency of HIT cannot be stated as a single precise value because its magnitude varies widely in different clinical situations and with different heparin preparations (Table 2) (7,8,22,66,69). For example, a high-risk situation (3–7%) is a female postoperative orthopedic surgery patient who receives prophylactic-dose UFH for 14 days beginning after surgery. A low-to-moderate risk situation (0.2–0.5%) is a male patient receiving intravenous therapeutic-dose UFH for acute coronary syndrome for 7 days. The risk of HIT is negligible (<0.1%) in a pregnant woman receiving LMWH.

V. Treatment

If HIT is strongly suspected, all exposure to heparin, including "flush" solutions and heparin-coated catheters should be immediately discontinued, if possible. However, simply stopping heparin will not reduce (and theoretically may even

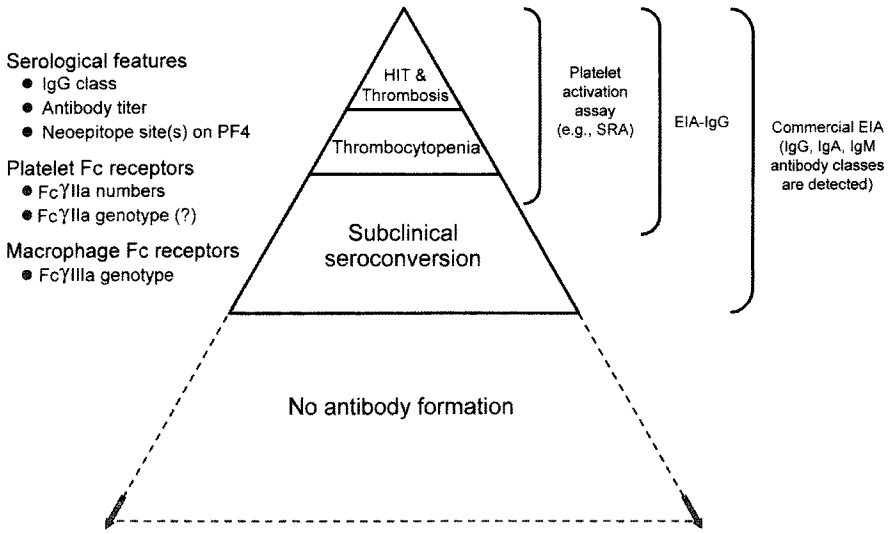

Figure 2 Iceberg model of HIT. This model depicts several features of HIT, including the hierarchy of sensitivity and specificity of three different types of laboratory assays used to detect HIT antibodies: (a) platelet activation assay that utilizes washed platelets, e.g., platelet serotonin release assay (SRA); (b) PF4/heparin enzyme-immunoassay that detects IgG class antibodies (EIA-IgG); and (c) commercial EIA that detects antibodies of IgG, IgM, and/or IgA class. Clinical HIT indicates either of the top two levels of the iceberg (HIT and thrombosis; thrombocytopenia). Subclinical seroconversion indicates formation of antibodies in the absence of developing clinical HIT. The relative proportion of patients who form antibodies *vs* those who do not form antibodies differs in various clinical situations. Various serological, platelet, and macrophage characteristics that determine the pathogenicity of PF4/heparin-reactive antibodies are shown on the left. Reprinted, with permission (67).

increase) the potential for HIT-related thrombosis (45,46). Thus, in most situations in which HIT is strongly suspected, heparin cessation should be accompanied by substitution of an alternative, non-heparin anticoagulant with rapid onset of action (2,70). Table 3 lists various options, including direct thrombin inhibitors (DTIs) such as lepirudin, argatroban, and bivalirudin, or a mixture of anticoagulant GAGs known as danaparoid.

DTIs block the catalytic site of thrombin, whether thrombin is soluble or clot-bound, thus inhibiting its ability to convert fibrinogen to fibrin, or to activate platelets or coagulation factors. Their designation as *direct* thrombin inhibitors reflects their inhibitory effect with requirement for antithrombin or heparin cofactor II (cf. heparin) (71). DTIs are univalent or divalent, depending on whether they interact with thrombin only at the active catalytic site (argatroban) or additionally bind to thrombin's fibrin(ogen) recognition site (lepirudin, bivalirudin) (72).

Table 2 Risk Factors for HIT

Factor	Importance	Hierarchy
Type of heparin	Major	UFH > LMWH > fondaparinux
Duration of heparin	Major	11–14 days* > 5–10 days > 4 (or fewer) days
Type of patient	Moderate	Postsurgery > medical > pregnancy or neonate
Dose of heparin	Moderate	Prophylaxis ≥ therapeutic > "flushes"
Gender of patient	Minor	Female > male

*Minimal additional risk if heparin continued beyond 14 days.
Interpretation of symbols: >, greater than; ≥, greater than or equal to.

Differences among DTIs include binding affinity for thrombin's active site, route of elimination, duration of effect, immunogenicity, and sensitivity to clot-based assays.

The duration of anticoagulation therapy primarily depends on the presence of any thrombosis. Vitamin K antagonists (VKAs) such as warfarin are currently the most common used agents for prolonged anticoagulation, targeting an INR value around 2.0–3.0. Caution should be used when initiating a VKA for HIT, waiting until treatment with a DTI is established, and substantial platelet count recovery ($> 150\times10^9\ L^{-1}$) has occurred (70). The DTI infusion should be continued until the platelet count has recovered and the patient is successfully anticoagulated with the VKA. LMWH has a high potential to cross-react fully with HIT antibodies, and is thus contraindicated for use in HIT (70).

A. Lepirudin

Hirudin is a naturally occurring and extremely potent anticoagulant 65-amino acid polypeptide (MW, ~7000 Da) derived from the salivary glands of the leech, *Hirudo medicinalis* (72–75). The recombinant hirudin (r-hirudin), lepirudin, is formed by the removal of a sulfate group and addition of NH_2 leucine residue in place of isoleucine, reducing its inhibition for thrombin somewhat (K_i, 6×10^{-14} M). Several open-label trials consisting of multicenter comparison to historical controls in patients with antibody-confirmed HIT or post-marketing assessments have demonstrated lepirudin to be effective in reducing the incidence of a composite endpoint (thrombosis, death, or loss of limbs) (76–81). For non-renally impaired patients who have HIT with thrombosis, lepirudin is typically started with a bolus dose (0.4 mg/kg) followed by an infusion of 0.15 mg/kg/h, aiming for a target aPTT (activated partial thromboplastin time) of 1.5–2.5× baseline (monitoring every 4 h until steady state aPTT is reached, then once daily). In the absence of thrombosis, 0.1 mg/kg/h without initial bolus is suggested (72–75). A substantially lower dose is required in the presence of even minor renal impairment, as lepirudin is almost completely renally eliminated. This agent has a limited effect on prolonging the INR, potentially making it easier to transition patients to warfarin. Besides reducing risk of accumulation, the potential for lepirudin bolus-associated anaphylaxis (82,83) is another reason to avoid the initial lepirudin bolus in most clinical situations.

Table 3 Anticoagulant Agents that have been used in the Treatment of HIT

Agent	Chemistry	Route of elimination	Half-life*	Assay (usual target range)**	Comments
Argatroban	DTI: L- arginine derivative	Hepato-biliary	40–50 min	aPTT: 1.5–3.0× baseline	FDA-approved for HIT prophylaxis or treatment, including PCI; prolongs INR
Lepirudin	DTI: 65-aa peptide derived from leech anticoagulant (hirudin)	Renal	≥80 min	aPTT: 1.5–2.5× baseline	FDA-approved for HIT complicated by thrombosis; immunogenic; iv or sc
Bivalirudin	DTI: 20-aa hirudin analogue	Enzymic (80%); renal (20%)	25 min	aPTT: 1.5–2.5× baseline	Not approved for HIT
Danaparoid	Mixture of GAGs with predominant anti-Xa activity	Renal; other	25 h	Anti-Xa activity (0.5–0.8 U/mL)	Not marketed in US (approved for HIT in EU, Canada); no effect on INR; iv or sc
Fondaparinux	Sulfated penta-saccharide with anti-Xa activity	Renal; other	17 h	NA	Not approved for HIT
Warfarin	Vitamin K antagonist	Hepatic	35–45 h	INR, 2.0–3.0	Potential for inducing microvascular thrombosis when given during acute HIT

Abbreviations: aa, amino acid; anti-Xa, anti-factor Xa; aPTT, activated partial thromboplastin time; DTI, direct thrombin inhibitor; EU, European Union; FDA, US Food and Drug Administration; INR, international normalized ratio; iv, intravenous; sc, subcutaneous; NA, not applicable.

*Half-life determined in normal subjects, and may be longer in many patients with HIT.

**Baseline is the patient's baseline aPTT off heparin, or the laboratory mean if the patient's baseline value is notably elevated.

B. Argatroban

Argatroban is a small synthetic DTI (MW, 526 Da) derived from L-arginine with a lower affinity (K_i 3.9×10^{-8} M) for thrombin but with a higher degree of clot-bound thrombin inhibition, compared with r-hirudin (84–86). Trials comparing argatroban to historical controls in suspected HIT (with or without thrombosis) have shown argatroban to be effective in reducing the composite endpoint of thrombosis, death or limb amputation (87,88). The typical starting dose is 2 μg/kg/min (mean rate about 1.6 μg/kg/min), targeting the aPTT at 1.5–3.0× baseline (89). Argatroban is hepatically eliminated, with limited data suggesting 75% dose reduction in the presence of impaired liver function (90–92). Newer observations also suggest reduced dosing is appropriate in patients with impaired renal function (93). Argatroban prolongs the INR considerably in many patients, which has the potential to complicate transition to warfarin (72).

C. Treatment Outcomes of Direct Thrombin Inhibitor Therapy

Table 4 summarizes treatment outcomes of thrombosis complicating HIT in the lepirudin and argatroban prospective cohort studies. The rates of new thrombosis following institution of DTI therapy ranged from 5–20%, which represented a relative risk reduction (compared with historical controls) as high as about 0.60–0.80. Mortality and limb amputation usually depend on comorbid illness and severity of limb ischemia at time of initiating HIT treatment.

D. Danaparoid

Danaparoid is a mixture of three depolymerized GAGs (84% heparan sulfate, 12% dermatan sulfate, 4% chondroitin sulfate) extracted from porcine gut mucosa

Table 4 Prospective Cohort Studies (with Historical Controls) of Lepirudin or Argatroban for Treatment of HIT Complicated by Thrombosis (Adapted, with Permission, from 44)

Trial (n = number of patients receiving DTI indicated)	%HIT antibody positive	Duration of DTI therapy (days)	% Thrombosis (% of controls)	RRR	% Major bleeding (% of controls)
Lepirudin					
HAT-1,2 (n = 113) (76)	100	13.3	10.1 (27.2)	0.63	18.8 (7.1)
HAT-3 (n = 98) (77)	100	14.0	6.1	0.78	20.4
Post-marketing (n = 496) (78)	77	12.1	5.2	0.81	5.4
Argatroban					
Arg-911 (n = 144) (87)	65	5.9	19.4 (34.8)	0.44	11.1 (2.2)
Arg-915 (n = 229) (88)	N.A.	7.1	13.1	0.62	6.1

Abbreviations: Arg, argatroban trial; DTI, direct thrombin inhibitor; HAT, heparin-associated thrombocytopenia trial; RRR, relative risk reduction.
Note: The RRR calculations shown for HAT-3/post-marketing studies, and for Arg-915, were based upon the historical control data reported for HAT-1,2 and Arg-911, respectively.

(94,95). Termed a heparinoid, it acts predominantly by inhibiting factor Xa, and can be given either by intravenous infusion or by subcutaneous injection. Although there is a low incidence of weak immunological cross-reactivity with HIT antibodies, it has been used successfully in many patients with HIT, including most with positive *in vitro* cross-reactivity (96–99). No comparative prospective trials with DTI therapy are available, although a retrospective study suggested that therapeutic-dose danaparoid and lepirudin have similar efficacy in HIT, but less bleeding with danaparoid (98). Therapeutic dosing for an average-size adult is 2250 U bolus, followed by intravenous infusion at 400 U/h for 4 h, then 300 U/h for 4 h, then continuing at 200 U/h, with anticoagulant monitoring by anti-Xa levels, if available. The dose should be reduced by about one-third in the presence of renal impairment. Danaparoid is not marketed in the US.

E. Fondaparinux, Bivalirudin, Melagatran

The antithrombin-binding pentasaccharide, fondaparinux, does not significantly cross-react with HIT antibodies (13,14,100), and may therefore have potential utility in treating patients with acute or previous HIT (101–103). Bivalirudin is a 20-amino acid bivalent DTI with certain structural similarities with lepirudin (K_i, 1.9×10^{-9} M). It has the shortest elimination half-life of the DTIs (about 25 min), and becomes inactivated by thrombin; this may reduce its dependence on either renal or hepatic function on elimination and dosing compared to other anticoagulants. Minimal clinical experience in patients with HIT is reported (104–106). The orally administered prodrug, ximelagatran, is metabolized following ingestion to the DTI, melagatran (K_i, 2×10^{-9} M). It may have potential as an alternative to warfarin or even to intravenous DTIs in treating HIT. Currently, however, no experience in HIT is available with melagatran (107).

F. Warfarin

Oral VKAs such as warfarin have long been the mainstay for providing long-term anticoagulation. Although most patients enrolled in the lepirudin and argatroban trials were transitioned to VKA, no information on its impact on preventing thrombosis is available. Indeed, there is evidence that warfarin use in acute HIT sometimes leads to tissue necrosis (skin necrosis and venous limb gangrene syndromes), which results from severe protein C depletion in conjunction with HIT-related hypercoagulability and persisting thrombin generation. This is typically observed in patients who attain excessive INR levels (usually >3.5) while receiving warfarin alone (108,109) or in whom the DTI is discontinued prior to platelet count recovery during DTI–warfarin overlap (110,111). Currently, it is recommended (70,112) that warfarin therapy be delayed until substantial platelet count recovery has occurred, and then begun in low initial doses (e.g., 5 mg or less), with a minimum 5-day overlap with DTI therapy.

G. Clot-Based Assays in the Presence of Heparin-Induced Thrombocytopenia Treatment

Measuring the intensity of anticoagulation during the administration of a DTI or warfarin is not a simple process, as the aPTT or INR values depend on factors besides the anticoagulant effect. Indeed, only danaparoid can have its anticoagulant level directly measured, although many laboratories do not routinely perform the requisite assay (anti-factor Xa activity). For DTIs, monitoring by the aPTT is recommended, targeting a ratio of 1.5–2.5 (lepirudin) or 1.5–3.0 (argatroban) times the patient's baseline value (or mean of the laboratory normal range). However, variability exists among available aPTT methods in sensitivity to DTI effects, and so different institutions effectively give different DTI dosing regimens (113). The laboratory's aPTT therapeutic range for UFH might not necessarily correspond to the aPTT therapeutic range for a DTI. Further, concomitant clinical factors such as HIT-associated DIC, liver dysfunction, or warfarin administration prolong the aPTT independently of the effect of the DTI. Some experts recommend calibrating the sensitivity of a particular aPTT reagent with a standard curve of "DTI-spiked" pooled plasma, so as to determine whether the aPTT–DTI relationship has sufficient upward slope (particularly at high-therapeutic DTI concentrations) to permit distinction between normal and supratherapeutic levels (74,75). Attaining steady state may be delayed beyond 4–6 h in the presence of reduced drug clearance (e.g., renal dysfunction and lepirudin), and so repeated aPTT monitoring until steady state is reached is now recommended (81). In situations in which higher DTI dosing is required [e.g., percutaneous coronary interventions (PCI), on-pump cardiac surgery], the aPTT may not be the best choice to monitor anticoagulation intensity compared to other methods [activated clotting time, ecarin clotting time (ECT)] (75,114). Even for standard dosing situations, the ECT provides a more linear dose–response relationship than aPTT measurements, but target ranges and recommendations on dosing adjustments with outcomes are currently not available (72,113).

DTIs can prolong the prothrombin time (INR), which complicates the transition to warfarin therapy. The intensity of the INR-prolonging effect differs among DTIs, and is greatest with argatroban, intermediate with bivalirudin, and least with lepirudin (72,115,116). Thromboplastin reagents with a higher international sensitivity index (ISI) tend to give higher INR values in the presence of the DTI. It is important for the clinician to take into account DTI-associated INR changes in decision-making regarding anticoagulant dosing, e.g., not to conclude prematurely that the patient has achieved the therapeutic range early during warfarin overlap, or that the patient has developed liver dysfunction.

The effects of DTIs on other clot-based assay have been examined (117). No effects on antithrombin, plasminogen, chromogenic protein C, von Willebrand factor, or fibrin D-dimer were observed. However, apparent decreases in fibrinogen, and increases in protein C and protein S levels, occurred with all three DTIs evaluated. For all DTIs, Russell viper venom times were elevated, and factor IX activity falsely decreased.

Few data exist on longer term anticoagulation of the patient recovering from acute HIT. For patients without thrombosis, practice ranges from treating with a DTI or danaparoid until the platelet count has fully recovered to administering VKAs for several weeks. For patients with thrombosis, eventual transition from the initial parenteral anticoagulant to a long-term anticoagulant such as VKA is usually performed. In some circumstances, subcutaneous danaparoid, lepirudin, or fondaparinux may be appropriate. Anticoagulation is usually given for a minimum of 3–6 months, although the transient nature of HIT means that long-term anticoagulant decisions are usually based on other factors such as the nature of the thrombotic event(s) and other risk factors, if any.

H. Pregnancy or Pediatrics

Although data are limited, the incidence of HIT appears to be low in children (118–121) and pregnant women (122). Most pediatric cases have been associated with the use of UFH (123). Accordingly, experience with DTI therapy in these settings is limited. Management of HIT in pregnancy is complicated by the limited data of DTI use in this setting. Beyond the initial parenteral management, options used include subcutaneous lepirudin, danaparoid, or possibly fondaparinux. Dosing revisions may be needed as pregnancy advances. Warfarin is not appropriate during the first trimester because of teratogenicity. Data on the teratogenic effects of the other agents are limited, but their "B" risk rating suggests a low perceived risk (112).

I. Cardiac Procedures

Despite recent inroads by bivalirudin (124), UFH remains the most common anticoagulant for PCI, and remains virtually the sole anticoagulant for cardiac surgery, both "off-pump" and "on-pump". When UFH is contraindicated because of acute or recent HIT, PCI can be performed using argatroban (FDA-approved) (125) or bivalirudin (not approved for HIT) (106). Numerous options have been reported for non-UFH anticoagulation during cardiac surgery, which are reviewed elsewhere (114). The unusual transience of the immune response in HIT (35) means that in a patient with previous HIT in whom HIT antibodies are no longer detectable, it is acceptable to use UFH for the cardiac surgery (70,114), although preoperative and postoperative anticoagulation are usually given with non-heparin anticoagulants to reduce the risk of restimulating the immune system. Lower infusion rates may be required in the postoperative period, especially if surgery-related hypoperfusion has resulted in renal or hepatic dysfunction. The need to stop anticoagulants for removal of pacer wires or chest tubes provides a rationale that favors agents with a shorter half-life.

J. Renal or Liver Failure

Selection of a suitable therapeutic agent to treat HIT often depends on the coexisting hepatic or renal impairment. Lepirudin is renally eliminated, and its elimination

half-life increases as renal function declines, necessitating large decreases in dosing (126,127). In the initial HAT-1 trial, the significance of adjusting the dose of lepirudin for renal function was not appreciated. Subsequent analysis of stored blood samples identified a significant increase in bleeding complications in patients with reduced renal function without reduction in the dose. The incidence of bleeding in later lepirudin trials is reduced as dosing is adjusted for renal function. With careful dosing and monitoring, lepirudin can be been used successfully even in situations such as anticoagulation during hemodialysis, either by intermittent bolus dosing, or by low-dose constant infusion. Argatroban (hepatically eliminated) is preferred in patients with reduced renal function, although recent observations suggest that many patients with renal compromise require lower doses of argatroban to achieve a therapeutic aPTT (92,93,128). Argatroban does not appear to be removed by the hemodialysis circuit (91,129). In patients whose hepatic and renal functions are both compromised, the DTI, bivalirudin, which undergoes substantial enzymic metabolism, may offer advantages (104).

K. Reversal

No specific antidotes exist for DTIs, danaparoid, or fondaparinux. Fresh frozen plasma and vitamin K offer no benefit to a bleeding patient with elevated aPTT or INRs during DTI therapy (91). Preliminary data also suggests that the panhemostatic agent, recombinant factor VIIa, may not reverse anticoagulant effects of DTIs (130,131). The efficacy and safety of prothrombin complex concentrates in this clinical situation is unclear (132,133). Hemodialysis does not clear argatroban, but may remove bivalirudin and, to a lesser extent, lepirudin (91,134,135).

Acknowledgments

Some of the studies cited (7, 8, 13, 22, 25–27, 35, 37–40, 42–45, 49, 52, 55–57, 67, 69, 108–110,116) were funded by the Heart and Stroke Foundation of Ontario (operating grants, A2449, T2967, B3763, T4502, T4502) (T.E.W.). Thanks are due to Dr Karen Dager for her constant support and review of the manuscript, and to my colleagues who continue to present interesting HIT treatment challenges to resolve (W.E.D.).

References

1. Warkentin TE. Heparin-induced thrombocytopenia: pathogenesis and management. Br J Haematol 2003; 121:535–555.
2. Greinacher A, Warkentin TE. Treatment of heparin-induced thrombocytopenia. In: Warkentin TE, Greinacher A, eds. Heparin-Induced Thrombocytopenia, 3rd ed. New York: Marcel-Dekker, 2004; 335–370.
3. Li ZQ, Liu W, Park KS, Sachais BS, Arepally GM, Cines DB, Poncz M. Defining a second epitope for heparin-induced thrombocytopenia/thrombosis antibodies

using KKO, a murine HIT-like monoclonal antibody. Blood 2002; 99: 1230–1236.
4. Alban S, Greinacher A. Role of sulfated polysaccharides in the pathogenesis of heparin-induced thrombocytopenia. In: Warkentin TE, Greinacher A, eds. Heparin-Induced Thrombocytopenia, 3rd ed. New York: Marcel-Dekker, 2004; 197–221.
5. Hirsh J, Raschke R. Heparin and low-molecular-weight heparin. The Seventh ACCP Conference on Antithrombotic and Thrombolytic Therapy. Chest 2004; 126 (Suppl):188S–203S.
6. Visentin GP, Moghaddam M, Beery SE, McFarland JG, Aster RH. Heparin is not required for detection of antibodies associated with heparin-induced thrombocytopenia/thrombosis. J Lab Clin Med 2001; 138:22–31.
7. Warkentin TE, Levine MN, Hirsh J, Horsewood P, Roberts RS, Gent M, Kelton JG. Heparin-induced thrombocytopenia in patients treated with low-molecular-weight heparin or unfractionated heparin. N Engl J Med 1995; 332:1330–1335.
8. Warkentin TE, Roberts RS, Hirsh J, Kelton JG. An improved definition of immune heparin-induced thrombocytopenia in postoperative orthopedic patients. Arch Intern Med 2003; 163:2518–2524.
9. Goad KE, Horne III MK, Gralnick HR. Pentosan-induced thrombocytopenia: support for an immune complex mechanism. Br J Haematol 1994; 88:803–808.
10. Rice L, Kennedy D, Veach A. Pentosan induced cerebral sagittal sinus thrombosis: a variant of heparin induced thrombocytopenia. J Urol 2004; 160:2148.
11. Greinacher A, Michels I, Schafer M, Kiefel V, Mueller-Eckhardt C. Heparin-associated thrombocytopenia in a patient treated with polysulphated chondroitin sulphate: evidence for immunological cross-reactivity between heparin and polysulphated glycosaminoglycan. Br J Haematol 1992; 81:252–254.
12. Rosenthal MA, Rischin D, McArthur G, Ribbons K, Chong B, Fareed J, Toner G, Green MD, Basser RL. Treatment with the novel anti-angiogenic agent PI-88 is associated with immune-mediated thrombocytopenia. Ann Oncol 2002; 13:770–776.
13. Warkentin TE, Cook RJ, Marder VJ, Sheppard JI, Moore JC, Eriksson BI, Greinacher A, Kelton JG. Antiplatelet factor 4/heparin antibodies in orthopedic surgery patients receiving antithrombotic prophylaxis with fondaparinux or enoxaparin. Blood 2005; 106 in press.
14. Savi P, Chong BH, Greinacher A, Gruel Y, Kelton JG, Warkentin TE, Eicheler P, Meuleman D, Petitou M, Herault JP, Cariou R, Herbert JM. Effect of fondaparinux on platelet activation in the presence of heparin-dependent antibodies. A blinded comparative multicenter study with infractionated heparin. Blood 2005; 105:139–144.
15. Greinacher A, Michels I, Mueller-Eckhardt C. Heparin-associated thrombocytopenia: the antibody is not heparin specific. Thromb Haemost 1992; 67:545–549.
16. Newman PM, Swanson RL, Chong BH. Heparin-induced thrombocytopenia: IgG binding to PF4-heparin complexes in the fluid phase and cross-reactivity with low molecular weight heparin and heparinoid. Thromb Haemost 1998; 80:292–297.

17. Greinacher A, Alban S, Dummel V, Franz G, Mueller-Eckhardt C. Characterization of the structural requirements for a carbohydrate based anticoagulant with a reduced risk of inducing the immunological type of heparin-associated thrombocytopenia. Thromb Haemost 1995; 74:886–892.
18. Petitou M, Herault JP, Bernat A, Driguez PA, Duchaussoy P, Lormeau JC, Herbert JM. Synthesis of thrombin-inhibiting heparin mimetics without side effects. Nature 1999; 398:417–422.
19. Savi P, Pflieger AM, Hérault JP, Michaux C, Duchaussoy P, Petitou M, Herbert JM. Comparative effects of two synthetic oligosaccharides on platelet activation induced by plasma from HIT patients. J Thromb Haemost 2003; 1:2008–2013.
20. Greinacher A, Pöetzsch B, Amiral J, Dummel V, Eichner A, Mueller-Eckhardt C. Heparin-associated thrombocytopenia: isolation of the antibody and characterization of a multimolecular PF4-heparin complex as the major antigen. Thromb Haemost 1994; 71:247–251.
21. Rauova L, Poncz M, McKenzie SE, Reilly MP, Arepally G, Weisel JW, Nagaswami C, Cines DB, Sachais BS. Ultralarge complexes of PF4 and heparin are central to the pathogenesis of heparin-induced thrombocytopenia. Blood 2005; 105:131–138.
22. Warkentin TE, Sheppard JI, Horsewood P, Simpson PJ, Moore JC, Kelton JG. Impact of the patient population on the risk for heparin-induced thrombocytopenia. Blood 2000; 96:1703–1708.
23. Denomme GA. The platelet Fc receptor in heparin-induced thrombocytopenia. In: Warkentin TE, Greinacher A, eds. Heparin-Induced Thrombocytopenia, 3rd ed. New York: Marcel-Dekker, 2004; 223–251.
24. Newman PM, Chong BH. Heparin-induced thrombocytopenia: new evidence for the dynamic binding of purified anti-PF4-heparin antibodies to platelets and the resultant platelet activation. Blood 2000; 96:182–187.
25. Warkentin TE, Hayward CPM, Boshkov LK, Santos AV, Sheppard JI, Bode AP, Kelton JG. Sera from patients with heparin-induced thrombocytopenia generate platelet-derived microparticles with procoagulant activity: an explanation for the thrombotic complications of heparin-induced thrombocytopenia. Blood 1994; 84:3691–3699.
26. Hughes M, Hayward CPM, Warkentin TE, Horsewood P, Chorneyko KA, Kelton JG. Morphological analysis of microparticle generation in heparin-induced thrombocytopenia. Blood 2000; 96:188–194.
27. Warkentin TE, Sheppard JI. Generation of platelet-derived microparticles and procoagulant activity by heparin-induced thrombocytopenia IgG/serum and other IgG platelet agonists: a comparison with standard platelet agonists. Platelets 1999; 10:319–326.
28. Chong BH, Murray B, Berndt MC, Dunlop LC, Brighton T, Chesterman CN. Plasma P-selectin is increased in thrombotic consumptive platelet disorders. Blood 1994; 83:1535–1541.
29. Warkentin TE. An overview of the heparin-induced thrombocytopenia syndrome. Semin Thromb Hemost 2004; 30:273–283.
30. Visentin GP, Ford SE, Scott JP, Aster RH. Antibodies from patients with heparin-induced thrombocytopenia/thrombosis are specific for platelet factor 4 complexed with heparin or bound to endothelial cells. J Clin Invest 1994; 93:81–88.

31. Pouplard C, Iochmann S, Renard B, Herault O, Colombat P, Amiral J, Gruel Y. Induction of monocyte tissue factor expression by antibodies to heparin-platelet factor 4 complexes developed in heparin-induced thrombocytopenia. Blood 2001; 97:3300–3302.
32. Arepally GM, Mayer IM. Antibodies from patients with heparin-induced thrombocytopenia stimulate monocytic cells to express cells to express tissue factor and secrete interleukin-8. Blood 2001; 98:1252–1254.
33. Khairy M, Lasne D, Brohard-Bohn B, Aiach M, Rendu F, Bachelot-Loza C. A new approach in the study of the molecular and cellular events implicated in heparin-induced thrombocytopenia. Thromb Haemost 2001; 85:1090–1096.
34. Khairy M, Lasne D, Amelot A, Crespin M, Rendu F, Aiach M, Bachelot-Loza C. Polymorphonuclear leukocyte and monocyte activation induced by plasma from patients with heparin-induced thrombocytopenia in whole blood. Thromb Haemost 2004; 92:1411–1419.
35. Warkentin TE, Kelton JG. Temporal aspects of heparin-induced thrombocytopenia. N Engl J Med 2001; 344:1286–1292.
36. Lubenow N, Kempf R, Eichner A, Eichler P, Carlsson LE, Greinacher A. Heparin-induced thrombocytopenia: temporal pattern of thrombocytopenia in relation to initial use or reexposure to heparin. Chest 2002; 122:37–42.
37. Warkentin TE. Heparin-induced skin lesions. Br J Haematol 1996; 92: 494–497.
38. Warkentin TE, Roberts RS, Hirsh J, Kelton JG. Heparin-induced skin lesions and other unusual sequelae of the heparin-induced thrombocytopenia syndrome: a nested cohort study. Chest; 2005; 127: 1857–1861.
39. Ling E, Warkentin TE. Intraoperative heparin flushes and subsequent acute heparin-induced thrombocytopenia. Anesthesiology 1998; 89:1567–1569.
40. Warkentin TE, Kelton JG. Delayed-onset heparin-induced thrombocytopenia and thrombosis. Ann Intern Med 2001; 135:502–506.
41. Rice L, Attisha WK, Drexler A, Francis JL. Delayed-onset heparin-induced thrombocytopenia. Ann Intern Med 2002; 136:210–215.
42. Warkentin TE, Bernstein RA. Delayed-onset heparin-induced thrombocytopenia and cerebral thrombosis after a single administration of unfractionated heparin. N Engl J Med 2003; 348:1067–1069.
43. Hong AP, Cook DJ, Sigouin CS, Warkentin TE. Central venous catheters and upper-extremity deep-vein thrombosis complicating immune heparin-induced thrombocytopenia. Blood 2003; 101:3049–3051.
44. Warkentin TE. Management of heparin-induced thrombocytopenia: a critical comparison of lepirudin and argatroban. Thromb Res 2003; 110:73–82.
45. Warkentin TE, Kelton JG. A 14-year study of heparin-induced thrombocytopenia. Am J Med 1996; 101:502–507.
46. Wallis DE, Workman DL, Lewis BE, Steen L, Pifarre R, Moran JF. Failure of early heparin cessation as treatment for heparin-induced thrombocytopenia. Am J Med 1999; 106:629–635.
47. Warkentin TE. Clinical picture of heparin-induced thrombocytopenia. In: Warkentin TE, Greinacher A, eds. Heparin-Induced Thrombocytopenia, 3rd ed. New York: Marcel-Dekker, 2004; 53–106.
48. Popov D, Zarrabi MH, Foda H, Graber M. Pseudopulmonary embolism: acute respiratory distress in the syndrome of heparin-induced thrombocytopenia. Am J Kidney Dis 1997; 29:449–452.

49. Warkentin TE, Hirte HW, Anderson DR, Wilson WEC, O'Connell GJ, Lo RC. Transient global amnesia associated with acute heparin-induced thrombocytopenia. Am J Med 1994; 97:489–491.
50. Warkentin TE. Pseudo-heparin-induced thrombocytopenia. In: Warkentin TE, Greinacher A, eds. Heparin-Induced Thrombocytopenia, 3rd ed. New York: Marcel-Dekker, 2004; 313–334.
51. Kitchens CS. Thrombocytopenia due to acute venous thromboembolism and its role in expanding the differential diagnosis of heparin-induced thrombocytopenia. Am J Hematol 2004; 76:69–73.
52. Warkentin TE, Heddle NM. Laboratory diagnosis of immune heparin-induced thrombocytopenia. Curr Hematol Rep 2003; 2:148–157.
53. Lubenow N, Eichler P, Albrecht D, Carlsson LE, Kothmann J, Rossocha WR, Hahn M, Quitman H, Greinacher A. Very low platelet counts in post-transfusion purpura falsely diagnosed as heparin-induced thrombocytopenia. Report of four cases and review of literature. Thromb Res 2000; 100:115–125.
54. Kelton JG, Sheridan D, Santos A, Smith J, Steeves K, Smith C, Brown C, Murphy WG. Heparin-induced thrombocytopenia: laboratory studies. Blood 1988; 72:925–930.
55. Warkentin TE, Hayward CPM, Smith CA, Kelly PM, Kelton JG. Determinants of donor platelet variability when testing for heparin-induced thrombocytopenia. J Lab Clin Med 1992; 120:371–379.
56. Warkentin TE, Sheppard JI, Moore JC, Moore KM, Sigouin CS, Kelton JG. Laboratory testing for the antibodies that cause heparin induced thrombocytopenia: how much class do we need? J Lab Clin Med 2005; in press.
57. Lee DH, Warkentin TE, Denomme GA, Hayward CPM, Kelton JG. A diagnostic test for heparin-induced thrombocytopenia: detection of platelet microparticles using flow cytometry. Br J Haematol 1996; 95:724–731.
58. Greinacher A, Michels I, Kiefel V, Mueller-Eckhardt C. A rapid and sensitive test for diagnosing heparin-associated thrombocytopenia. Thromb Haemost 1991; 66:734–736.
59. Eichler P, Budde U, Haas S, Kroll H, Loreth RM, Meyer O, Pachmann U, Pötzsch B, Schabel A, Albrecht D, Greinacher A. First Workshop for detection of heparin-induced antibodies: validation of the heparin-induced platelet activation (HIPA) test in comparison with a PF4/heparin ELISA. Thromb Haemost 1999; 81:625–629.
60. Greinacher A, Amiral J, Dummel V, Vissac A, Kiefel V, Mueller-Eckhardt C. Laboratory diagnosis of heparin-associated thrombocytopenia and comparison of platelet aggregation test, heparin-induced platelet activation test, and platelet factor 4/heparin enzyme-linked immunosorbent assay. Transfusion 1994; 34:381–385.
61. Warkentin TE, Greinacher A. Laboratory testing for heparin-induced thrombocytopenia. In: Warkentin TE, Greinacher A, eds. Heparin-Induced Thrombocytopenia, 3rd ed. New York: Marcel-Dekker, 2004; 271–311.
62. Amiral J, Bridey F, Dreyfus M, Vissac AM, Fressinaud E, Wolf M, Meyer D. Platelet factor 4 complexed to heparin is the target for antibodies generated in heparin-induced thrombocytopenia. Thromb Haemost 1992; 68:95–96.
63. Lindhoff-Last E, Gerdsen F, Ackermann H, Bauersachs R. Determination of heparin-platelet factor 4-IgG antibodies improves diagnosis of heparin-induced thrombocytopenia. Br J Haematol 2001; 113:886–890.

64. Meyer O, Salama A, Pittet N, Schwind P. Rapid detection of heparin-induced platelet antibodies with particle gel immunoassay (ID-HPF4). Lancet 1999; 354:1525–1526.
65. Eichler P, Raschke R, Lubenow N, Meyer O, Schwind P, Greinacher A. The new ID-heparin/PF4 antibody test for rapid detection of heparin-induced antibodies in comparison with functional and antigenic assays. Br J Haematol 2002; 116:887–891.
66. Lee DH, Warkentin TE. Frequency of heparin-induced thrombocytopenia. In: Warkentin TE, Greinacher A, eds. Heparin-Induced Thrombocytopenia, 3rd ed. New York: Marcel-Dekker, 2004; 107–148.
67. Warkentin TE, Cook DJ. Heparin, Low molecular weight heparin, and heparin-induced thrombocytopenia in the ICU. Crit Care Clin; 2005; 21:513–529.
68. Amiral J, Pouplard C, Vissac AM, Walenga JM, Jeske W, Gruel Y. Affinity purification of heparin-dependent antibodies to platelet factor 4 developed in heparin-induced thrombocytopenia: biological characteristics and effects on platelet activation. Br J Haematol 2000; 109:336–341.
69. Warkentin TE, Sigouin CS. Gender and risk of immune heparin-induced thrombocytopenia. Blood 2002; 100 (Suppl):17a [abstract].
70. Warkentin TE, Greinacher A. Heparin-induced thrombocytopenia: recognition, treatment, and prevention. The Seventh ACCP Conference on Antithrombotic and Thrombolytic Therapy. Chest 2004; 126 (Suppl):311S–337S.
71. Kaplan KL. Direct thrombin inhibitors. Expert Opin Pharmacother 2003; 4:653–666.
72. Warkentin TE. Bivalent direct thrombin inhibitors: hirudin and bivalirudin. Best Pract Res Clin Haematol 2004; 17:105–125.
73. Greinacher A. Lepirudin: a bivalent direct thrombin inhibitor for anticoagulation therapy. Exp Rev Cardiovasc Ther 2004; 2:339–357.
74. Greinacher A. Treatment options for heparin-induced thrombocytopenia. Am J Health Syst Pharm 2003; 60 (Suppl 5):S12–S18.
75. Greinacher A. Lepirudin for the treatment of heparin-induced thrombocytopenia. In: Warkentin TE, Greinacher A, eds. Heparin-Induced Thrombocytopenia, 3rd ed. New York: Marcel-Dekker, 2004; 397–436.
76. Greinacher A, Völpel H, Janssens U, Hach-Wunderle V, Kemkes-Matthes B, Eichler P, Mueller-Velten HG, Pötzsch B. Recombinant hirudin (lepirudin) provides safe and effective anticoagulation in patients with heparin-induced thrombocytopenia: a prospective study. Circulation 1999; 99:73–80.
77. Greinacher A, Janssens U, Berg G, Böck M, Kwasny H, Kemkes-Matthes B, Eichler P, Völpel H, Pötzsch B, Luz M. Lepirudin (recombinant hirudin) for parenteral anticoagulation in patients with heparin-induced thrombocytopenia. Circulation 1999; 100:587–593.
78. Greinacher A, Eichler P, Lubenow N, Kwasny H, Luz M. Heparin-induced thrombocytopenia with thromboembolic complications: meta-analysis of 2 prospective trials to assess the value of parenteral treatment with lepirudin and its therapeutic aPTT range. Blood 2000; 96:846–851.
79. Eichler P, Lubenow N, Greinacher A. Results of the third prospective study of treatment with lepirudin in patients with heparin-induced thrombocytopenia (HIT). Blood 2002; 100 (Suppl):704a [abstract].

80. Lubenow N, Eicher P, Greinacher A. Results of a large drug-monitoring program confirm the safety and efficacy of lepirudin in patients with immune-mediated heparin-induced thrombocytopenia (HIT). Blood 2002; 100 (Suppl):502a.
81. Lubenow N, Eichler P, Leitz T, Farner B, Greinacher A. Lepirudin for prophylaxis of thrombosis in patients with acute isolated heparin-induced thrombocytopenia: an analysis of 3 prospective studies. Blood 2004; 104:3072–3077.
82. Greinacher A, Lubenow N, Eichler P. Anaphylactic and anaphylactoid reactions associated with lepirudin in patients with heparin-induced thrombocytopenia. Circulation 2003; 108:2062–2065.
83. Badger NO, Butler K, Hallman LC. Excessive anticoagulation and anaphylactic reaction after rechallange with lepirudin in a patient with heparin-induced thrombocytopenia. Pharmacotherapy 2004; 24:1800–1803.
84. Kikumoto R, Tamao Y, Tezeka T, Tonomura S, Hara H, Ninomiya K, Hijikata A, Okamoto S. Selective inhibition of thrombin by (2R,4R)-4-methyl-1-[N^2-[(3-methyl-1,2,3,4-tetrahydro-8-quinolinyl)sulfonyl]-L-arginyl)]-2-piperidinecar boxylic acid. Biochemistry 1984; 23:85–90.
85. Berry CN, Girardot C, Lecoffre C, Lunven C. Effects of the synthetic thrombin inhibitor argatroban on fibrin- or clot-incorporated thrombin: comparison with heparin and recombinant hirudin. Thromb Heamost 1994; 72:381–386.
86. Lewis BE, Hursting MJ. Argatroban therapy in heparin-induced thrombocytopenia. In: Warkentin TE, Greinacher A, eds. Heparin-Induced Thrombocytopenia, 3rd ed. New York: Marcel-Dekker, 2004; 437–474.
87. Lewis BE, Walis DE, Berkowitz SD, Matthai WH, Fareed J, Walenga JM, Bartholomew J, Sham R, Lerner RG, Zeigler ZR, Rustagi PK, Jang IK, Rifkin SD, Moran J, Hursting MJ, Kelton JG, for the ARG-911 Study Investigators. Argatroban anticoagulant therapy in patients with heparin-induced thrombocytopenia. Circulation 2001; 103:1838–1843.
88. Lewis BE, Wallis DE, Leya F, Hursting MJ, Kelton JG. Argatroban anticoagulant in patients with heparin-induced thrombocytopenia. Arch Intern Med 2003; 163:1849–1856.
89. Verme-Gibboney CN, Hursting MJ. Argatroban dosing in patients with heparin-induced thrombocytopenia. Ann Pharmacother 2003; 37:970–975.
90. Swan SK, Hursting MJ. The pharmacokinetics and pharmacodynamics of argatroban: effects of age, gender, and hepatic or renal dysfunction. Pharmacotherapy 2000; 20:318–329.
91. Dager WE, White RH. Argatroban for heparin-induced thrombocytopenia in hepato-renal failure and CVVHD. Ann Pharmacother 2003; 37:1232–1236.
92. Williamson DR, Boulanger I, Tardif M, Albert M, Gregoire G. Argatroban dosing in intensive care patients with acute renal failure and liver dysfunction. Pharmacotherapy 2004; 24:409–414.
93. Arpino PA, Hallisey RK. Effect of renal function on the pharmacodynamics of argatroban. Ann Pharmacother 2004; 38:25–29.
94. Chong BH, Magnani HN. Danaparoid for the treatment of heparin-induced thrombocytopenia. In: Warkentin TE, Greinacher A, eds. Heparin-Induced Thrombocytopenia, 3rd ed. New York: Marcel-Dekker, 2004; 371–396.
95. Warkentin TE, Barkin RL. Newer strategies for the treatment of heparin-induced thrombocytopenia. Pharmacotherapy 1999; 19:181–195.

96. Magnani HN. Orgaran (danaparoid sodium) use in the syndrome of heparin-induced-thrombocytopenia. Platelets 1997; 8:74–81.
97. Chong BH, Gallus AS, Cade JF, Magnani H, Manoharan A, Oldmeadow M, Arthur C, Rickard K, Gallo J, Lloyd J, Seshadri P, Chesterman CN, Australian HIT Study Group. Prospective randomized open-label comparison of danaparoid with dextran 70 in the treatment of heparin-induced thrombocytopaenia with thrombosis: a clinical outcome study. Thromb Haemost 2001; 86:1170–1175.
98. Farner B, Eichler P, Kroll H, Greinacher A. A comparison of danaparoid and lepirudin in heparin-induced thrombocytopenia. Thromb Haemost 2001; 85:950–957.
99. Warkentin TE. Danaparoid (Orgaran) for the treatment of heparin-induced thrombocytopenia (HIT) and thrombosis: effects on in vivo thrombin and cross-linked fibrin generation, and evaluation of the clinical significance of in vitro cross-reactivity of danaparoid for HIT-IgG. Blood 1996; 88:626a [abstract].
100. Dager WE, Andersen J, Nutescu E. Special considerations with fondaparinux therapy: heparin-induced thrombocytopenia and wound healing. Pharmacotherapy 2004; 24:88S–94S.
101. Harenberg J, Jorg I, Fenyvesi T. Treatment of heparin-induced thrombocytopenia with fondaparinux. Hematologica 2004; 89:1017–1018.
102. Bradner J, Hallisey RK, Kuter DJ. Fondaparinux in the treatment of heparin-induced thrombocytopenia. Blood 2004; 104 (Suppl):492a [abstract].
103. Kuo KHM, Kovacs MJ. Successful treatment of heparin induced thrombocytopenia (HIT) with fondaparinux. Blood 2003; 102 (Suppl):319a [abstract].
104. Berilgen JE, Nguyen PH, Baker KR, Rice L. Bivalirudin treatment of heparin-induced thrombocytopenia. Blood 2003; 102 (Suppl):537a [abstract].
105. Francis JL, Drexler A, Gwyn G, Moroose R. Successful use of bivalirudin in the treatment of patients suspected, or at risk of, heparin-induced thrombocytopenia. Blood 2004; 104 (Suppl):105b [abstract].
106. Mahaffey KW, Lewis BE, Wildermann NM, Berkowitz SD, Oliverio RM, Turco MA, Shalev Y, Ver Lee P, Traverse JH, Rodriguez AR, Ohman EM, Harrington RA, Califf RM, for the ATBAT Investigators. The anticoagulant therapy with bivalurudin to assist in the performance of percutaneous coronary intervention in patients with heparin-induced thrombocytopenia (ATBAT) study: main results. J Invasive Cardiol 2003; 15:611–616.
107. Dager WE, Vondracek TG, McIntosh BA, Nutescu EA. Ximelagatran: an oral direct thrombin inhibitor. Ann Pharmacother 2004; 38:1881–1897.
108. Warkentin TE. Venous limb gangrene during warfarin treatment of cancer associated deep vein thrombosis. Ann Intern Med 2001; 135:589–593.
109. Warkentin TE, Sikov WM, Lillicrap DP. Multicentric warfarin-induced skin necrosis complicating heparin-induced thrombocytopenia. Am J Hematol 1999; 62:44–48.
110. Smythe MA, Warkentin TE, Stephens JL, Zakalik D, Mattson JC. Venous limb gangrene during overlapping therapy with warfarin and a direct thrombin inhibitor for immune heparin-induced thrombocytopenia. Am J Haematol 2002; 71:50–52.
111. Srinivasan AF, Rice L, Bartholomew JR, Rangaswamy C, La Perna L, Thompson JE, Murphy S, Baker KR. Warfarin-induced skin necrosis and

venous limb gangrene in the setting of heparin-induced thrombocytopenia. Arch Intern Med 2004; 164:66–70.
112. Dager WE, White RH. Pharmacotherapy of heparin-induced thrombocytopenia. Expert Opin Pharmacother 2003; 4:919–940.
113. Gosselin RC, King JH, Janatpour KA, Dager WE, Larkin EC, Owings JT. Comparing direct thrombin inhibitors using aPTT, ecarin clotting times, and thrombin inhibitor management testing. Ann Pharmacother 2004; 38: 1383–1388.
114. Warkentin TE, Greinacher A. Heparin-induced thrombocytopenia and cardiac surgery. Ann Thorac Surg 2003; 76:2121–2131.
115. Gosselin RC, Dager WE, King JH, Janatpour KA, Mahackian KA, Larkin EC, Owings JT. Effect of direct-thrombin-inhibitors: bivalirudin, lepirudin, and argatroban, on prothrombin time and INR measurements. Am J Clin Path 2004; 121:593–599.
116. Warkentin TE, Greinacher A, Craven S, Dewar L, Sheppard JI, Ofosn FA. Differences in the clinically effective molar concentrations of four direct thrombin inhibitors explain their variable prothrombin time prolongation. Thromp Haemost 2005; in press.
117. Gosselin RC, King JH, Janatpour KA, Dager WH, Larkin EC, Owings JT. Effects of pentasaccharide (fondaparinux) and direct thrombin inhibitors on coagulation testing. Arch Pathol Lab Med 2004; 128:1142–1145.
118. Newall F, Barnes C, Ignjatovic V, Monagle P. Heparin-induced thrombocytopenia in children. J Paediatr Child Health 2003; 39:289–292.
119. Risch L, Fischer JE, Herklotz R, Huber AR. Heparin-induced thrombocytopenia in paediatrics: clinical characteristics, therapy and outcomes. Intensive Care Med 2004; 30:1615–1624.
120. Klenner AF, Fusch C, Rakow A, Kadow I, Beyersdorff E, Eichler P, Wander K, Lietz T, Greinacher A. Benefit and risk of heparin for maintaining peripheral venous catheters in neonates: a placebo-controlled trial. J Pediatr 2003; 143:741–745.
121. Klenner AF, Greinacher A. Heparin-induced thrombocytopenia in children. In: Warkentin TE, Greinacher A, eds. Heparin-Induced Thrombocytopenia, 3rd ed. New York: Marcel-Dekker, 2004; 553–571.
122. Lindhoff-Last E, Bauersachs R. Heparin-induced thrombocytopenia – alternative anticoagulation in pregnancy and lactation. Semin Thromb Hemost 2002; 28:439–446.
123. Dager WE, White RH. Low-molecular-weight heparin-induced thrombocytopenia in a child. Ann Pharmacother 2004; 38:247–250.
124. Lincoff AM, Kleiman NS, Kereiakes DJ, Feit F, Bittl JA, Jackman JD, Sarembock IJ, Cohen DJ, Spriggs D, Ebrahimi R, Keren G, Carr J, Cohen EA, Betriu A, Desmet W, Rutsch W, Wilcox RG, de Feyter PJ, Vahanian A, Topol EJ, REPLACE-2 investigators. Long-term efficacy of bivalirudin and provisional glycoprotein IIb/IIIa blockade vs heparin and planned glycoprotein IIb/IIIa blockade during percutaneous coronary revascularization: REPLACE-2 randomized trial. JAMA 2004; 292:696–703.
125. Lewis B, Matthai WH, Cohen M, Moses JW, Hursting MJ, Leya F, for the ARG-216/310/311 investigators. Argatroban anticoagulation during percutaneous coronary intervention in patients with heparin-induced thrombocytopenia. Catheter Cardiovasc Interv 2002; 57:177–184.

126. Fischer KG. Hirudin in renal insufficiency. Semin Thromb Hemost 2002; 28:467–482.
127. Fischer KG. Hemodialysis in heparin-induced thrombocytopenia. In: Warkentin TE, Greinacher A, eds. Heparin-Induced Thrombocytopenia, 3rd ed. New York: Marcel-Dekker, 2004; 509–530.
128. Reichert MG, Macgregor DA, Kincaid EH, Dolinski SY. Excessive argatroban anticoagulation for heparin-induced thrombocytopenia. Ann Pharmacother 2003; 37:652–654.
129. Tang IY, Cox DS, Patel K, Reddy BV, Nahlik L, Trevino S, Murray PT. Argatroban and renal replacement therapy in patients with heparin-induced thrombocytopenia. Ann Pharmacother 2005; 39:231–236.
130. Wolzt M, Levi M, Sarich TC, Bostrom SL, Eriksson UG, Eriksson-Lepkowska M, Svensson M, Weitz JI, Elg M, Wahlander K. Effect of recombinant factor VIIa on melagatran-induced inhibition of thrombin generation and platelet activation in healthy volunteers. Thromb Haemost 2004; 91:1090–1096.
131. Malherbe S, Tsui BCH, Stobart K, Koller J. Argatroban as anticoagulant in cardiopulmonary bypass in an infant and attempted reversal with recombinant activated factor VII. Anesthesiology 2004; 100:443–445.
132. Elg M, Carlsson S, Gustafsson D. Effect of activated prothrombin complex concentrate or recombinant factor VIIa on the bleeding time and thrombus formation during anticoagulation with a direct thrombin inhibitor. Thromb Res 2001; 101:145–157.
133. Ulvinge JC, Berntsson P, Bostrom SL. Melagatran-induced inhibition of thrombin generation is reversed by FEIBA. Blood 2000; 96 (Suppl):103b [abstract].
134. Willey ML, de Denus S, Spinler SA. Removal of lepirudin, a recombinant hirudin, by hemodialysis, hemofiltration, or plasmapheresis. Pharmacotherapy 2002; 22:492–499.
135. Stratmann G, deSilva AM, Tseng EE, Hambleton J, Balea M, Romo AJ, Mann MJ, Achorn NL, Moskalik WF, Hoopes CW. Reversal of direct thrombin inhibition after cardiopulmonary bypass in a patients with heparin-induced thrombocytopenia. Anesth Analg 2004; 98:1635–1639.

Chemistry and Biology of Heparin and Heparan Sulfate
H.G. Garg, R.J. Linhardt and C.A. Hales (Editors)

Chapter 25

Role of Heparan Sulfate in Cancer

DONGFANG LIU

AstraZeneca Oncology Research and Development, Waltham, MA, USA

and

RAM SASISEKHARAN

Biological Engineering Division, Massachusetts Institute of Technology, Cambridge, MA, USA

I. Introduction

Glycosaminoglycans (GAGs) include heparin (HP), heparan sulfate (HS), dermatan sulfate (DS), chondroitin sulfate (CS), keratan sulfate (KS), and hyaluronic acid (HA), which are polymers of a disaccharide repeat unit, comprising a uronic acid and a hexosamine (1). Glycosaminoglycans are synthesized as homopolymers that may subsequently be modified by *N*-deacetylation and *N*-sulfation, eventually followed by C5-epimerization to iduronic acid (I) and 2-*O*-sulfation of the uronic acid, and 6-*O*-and 3-*O*-sulfation of the hexosamine (2–5). The position and number of sulfate groups attached to the component sugar residues, as well as kind of sugar residues provide an enormous number of structural variations to each glycosaminoglycan with the exception of hyaluronic acid that lacks the modifications. Heparan sulfate-like GAGs (HSGAGs) include heparins and heparan sulfates, which are the structurally most diverse GAGs. The disaccharide repeat consists of a glucosamine and uronic acid linked by two 1,4-glycosidic bonds. All chemical modifications possible for GAGs have been found for HSGAGs.

II. Structural Features of Glycosaminoglycans

A. Heparan Sulfate Glycosaminoglycans

Despite many shared structural features, heparin and heparan sulfate have distinct features. Several criteria have been proposed to distinguish heparin from heparan sulfate. Some researchers recommended that the term heparin be restricted to

HSGAGs in which more than 80% of the GlcN residues are *N*-sulfated and the number of *O*-sulfates is greater than the number of *N*-sulfates; all other related HSGAGs would be referred to as heparan sulfate (6). Gallagher and Walker (7) have stated that all heparan sulfates have about 50% of their GlcN residues *N*-sulfated and have ratios of *O*-sulfates to *N*-sulfates of 1 or less. Heparins are composed largely of I_{2S}-$H_{NS,6S}$ and G-$H_{NS,6S}$, whereas heparan sulfate contain only a few percentage of the I_{2S}-$H_{NS,6S}$ disaccharide, but contain a much more complex mixture of less highly sulfated disaccharides than heparin (6–8). Heparin is synthesized exclusively on the serglycin core protein, and is found stored in intracellular vesicles in mast cells. Heparan sulfate proteoglycans are ubiquitously present on cell surfaces. Cell surface proteoglycans typically have 4–6 heparan sulfate chains of 14–20 kDa, while in basement membranes as many as 12 heparan sulfate chains varying from 25–70 kDa can be attached to a single protein anchor (6–8).

B. Chondroitin and Dermatan Sulfate

Chondroitin and dermatan sulfates arise from a single homogeneous precursor, chondroitin, with the disaccharide repeat unit: [Gal_{NAc}-(β1, 4)-G(β1, 3)-] (1). Subsequent modification involves C5-epimerization of glucuronic acid to iduronic acid, and/or *O*-sulfation at C2 of uronic acids and C4 or C6 of galactosamine, which results in complex primary structures of dermatan and chondroitin sulfates, much like for heparin and heparan sulfate (9). The fraction of uronic acids in dermatan sulfate that are isomerized to iduronic acids varies widely, whereas all the uronic acids of chondroitin sulfate are glucuronic acid (9). Dermatan sulfate occurs predominantly in small proteoglycans, each containing 2–8-DS chains of 15–55 kDa, while chondroitin sulfates more often are found in large aggregating proteoglycans with 20–100-CS chains of 15–70 kDa (1).

C. Keratan Sulfate

Keratan sulfate is the only GAG that does not contain uronic acid; therefore, it is not cleavable by the eliminative enzymatic cleavage. Almost all glucosamines and some of galactose units are 6-sulfated in keratan sulfate (10). The chains contain a few nonsulfated residues at the reducing end adjacent to the linkage region, followed by a monosulfated region of about 10–12 disaccharides, and a disulfated region of 7–34 disaccharides. These suggest that the enzymes that generated sulfation of keratan sulfate are specific for different sections of chain (1).

The branched region and the presence of fucose and sialic acid are characteristics of keratan sulfate, which are also found in the oligosaccharide chains of many glycoproteins (11), but not among the other GAGs. In other glycoconjugates, fucose and sialic acid often lead to highly specific binding to proteins (11), however, specific binding of keratan sulfate has not been found to bind specifically to any protein of known biological function.

D. Hyaluronic Acid

The disaccharide repeat of hyaluronic acid is [H_{NAc}-(β1, 4)-G-(β1, 3)-]. Therefore, the monosaccharides are the same as in unmodified heparan; however, the glycosidic linkage is similar to those of chondroitin sulfate (1). The disaccharide repeat is not modified further, and consequently, hyaluronic acid is homogenous in its primary structure, and does not contain sulfates. Hyaluronic acid chains are considerably larger than those of other GAGs, and can contain up to several thousand disaccharides corresponding to molecular weights of 100–1000 kDa (12–15). As opposed to the other GAGs, hyaluronic acid is not synthesized in the Golgi from a core protein, but rather by an integral plasma membrane synthase, which secretes the nascent chain immediately (12–15). Large amount of hyaluronic acid is found in cartilage tissue.

E. Proteoglycans

Proteoglycans are heavily glycosylated proteins, generally consisting of a core protein with one or more covalently linked GAG chains that constitute most of the mass of the proteoglycan (16–21). Because of the presence of the oligosaccharide chains, the molecular mass of proteoglycans is routinely over 100 kDa and can reach 1000 kDa.

The oligosaccharide chains associated with the core proteins of proteoglycans are generally of the GAG family. The GAG chains attached to proteoglycans typically comprise 20–100 disaccharide repeat units. Most proteoglycans also contain *O*- and *N*-glycans typically found on glycoproteins. The GAG chains are much larger than these other types of glycans. Proteoglycans are either secreted into the ECM or linked to the cell surface in the form of syndecans and glypicans, thereby providing the cells with a GAG "sugar coat". Because of chemical modifications, it appears that there is a signature associated with the GAG sugar coat worn by divergent cell types such that each cell type responds to the repertoire of signaling molecules in different, sometimes dramatic, ways. Therefore, the appreciation of the nature of a cell's GAG sugar coat requires an understanding of the molecular structure of the oligosaccharide chains.

Two gene families, syndecans and glypicans, account for most cell surface HSPGs, both consist of discrete core proteins covalently attached with several GAG chains. The syndecan family was first discovered, which in mammals contains four gene products with distinctive extracellular domains (ectodomains) and highly conserved short cytoplasmic domains. The glypican family, in contrast to syndecan family, contains six gene products that are covalently linked to plasma membrane lipid by glycosylphosphatidylinositol (GPI) anchor (22–24).

The ECM proteoglycans include small interstitial proteoglycans (decorin, biglycan, and fibromodulin), a proteoglycan form of type IX collagen, and one or more members of the aggrecan family of proteolycans. The matrix proteoglycans typically contain the CS or DS, but HS proteoglycans perlecan and agrin are major species found in basement membranes (25).

III. Biosynthesis and Degradation of Heparan Sulfate Glycosaminoglycans

A. Biosynthesis

Most biosynthetic enzymes for HSGAGs have been identified and their characterization has improved the understanding of the basis for HSGAG chain structure complexity and function diversity (3–5,13). Heparan sulfate/heparin is synthesized by: (a) formation of a region linking the heparan sulfate/heparin chain to protein, (b) generation of the polysaccharide chain, and (c) enzymatic modification of the chain to yield the specific saccharide sequences and structural organization that are responsible for protein binding. Chondroitin sulfate, dermatan sulfate, heparan sulfate, and heparin chains, except keratan sulfate, share the linkage region to the core protein with a common structure, GlcA-(β1, 3)-Gal-(β1, 3)-Gal-(β1, 4)-Xyl-β1-*O*-protein.

Biosynthesis of these GAGs is initiated by the transfer of Xyl from UDP-Xyl to a hydroxide group of specific Ser residues in core protein (3–5,13). The transfer of Xyl to core protein is essentially different from that of either GlcNAc or GalNAc to GlcA residue at the nonreducing terminal. The former is a reaction to determine the number of GAG chains in the proteoglycan, and the later determines the species of GAG (4,5,22). A distinct transferase then adds a single GlcNAc residue to the nonreducing end of the linkage region. This enzyme distinguishes between sites on the core protein intended for glycosylation with HS chains, initiated with GlcNAc, from those sites to be glycosylated with CS chains.

Alternate addition of GlcA and GlcNAc from their respective UDP-sugar nucleotide precursors forms the repeating 1,4-linked disaccharide HS chain (4,5,26). Polymerization is catalyzed by one or more members of the EXT gene family. Genetic studies in fruit fly and mice indicate both EXT-1 and EXT-2 participate in HS synthesis in a synergistic manner. EXTs contain two catalytic domains, independently responsible for GlcNAc transferase or GlcA transferase activity (26). The length of the HS chains can vary over 10-fold with cell type and core protein, but the chain termination mechanisms are mostly unknown. Once the HS chain is assembled, generally 50–150 disaccharides, the individual saccharide units are subjected to a series of sequential enzymatic modification reactions in which the products of one reaction are substrate for the next. These reactions apparently do not convert all of the available substrate, resulting in substantial sequence diversity in the final chain. The initial modification enzyme is the *N*-deacetylase/*N*-sulfotransferase (NDST) that replaces the *N*-acetyl group of GlcNAc residues, leaving regions of the chain unmodified. The extent of this modification varies among the distinct *N*-deacetylase/*N*-sulfotransferase enzymes from rat liver, mouse mastocytoma, and trachea. Then D-glucuronic acid residues adjacent to $GlcNSO_3$ residues are epimerized to L-iduronic acid units by glucuronyl C5- epimerase.

These modified disaccharides will receive the bulk of the subsequent *O*-sulfations. An iduronosyl 2-*O*-sulfotransferase (2-ST) acts, then a glucosaminyl 6-*O*-sulfotransferase (6-ST) acts, and the modification reactions are completed with modification of a few residues by glucosaminyl 3-*O*-sulfotransferase (3-ST). The sulfotransferase use 3′-phosphoadenosine 5′-phosphosulfate (PAPS) as a sulfate

donor. The PAPS is synthesized from ATP and SO_3 via a single enzyme having both ATP sulfurylase and adenosine 5′-phosphosulfate (APS) kinase activities (4,5,26). Each of these sulfotransferases has multiple isoforms, some of which are tissue specific, share distinct substrate specificities, or both.

Biosynthesis of HSGAGs is a concerted process. Cells produce HSGAGs in the lumen of the endoplasmic reticulum (ER), Golgi apparatus, and trans Golgi network (26). The NDST, the C-5 epimerase, the 2-ST, and 6-ST enzymes all appear to be type II membrane-bound proteins, while 3-STs lack a hydrophobic sequence of sufficient length.

Other factors that are potentially important include the availability of the sulfate donor, PAPS. The sulfation patterns may change because of modulations of the intra-Golgi PAPS concentration as determined by the K_m of the various sulfotransferases. However, the overall kinetics of HS assembly, as determined by the membrane-bound state of the biosynthetic machinery, remains poorly understood (27).

B. Degradation

Up to date, at least six nonmammalian HSGAG degrading enzymes have been isolated from bacteria (1,28,29). Two mammalian heparan sulfate degradation enzymes, heparanase I and II, have also been cloned and characterized (30–33).

Heparinases I, II, and III, HSGAG degrading enzymes derived from *Flavobacterium heparinum*, have been well characterized (29,34–36). Each of these heparinases is specific for a different combination of modifications of the trisaccharide sequence containing the scissile glucosamine–uronic acid linkage: heparinase I cleaves $H_{NS,\,6X}$-I_{2S}/G_{2S}-$H_{NS,\,6S}$ sequences, which are primarily found in the NS regions, while heparinase III cleaves $H_{NY,\,6X}$-I/G-$H_{NY,\,6X}$ sequences, which are principal components of NAc-regions of HSGAGs (1). Interestingly heparinase II displays unusual enzymatic activity as it is capable of cleaving glycosidic linkages containing either a glucuronic or an iduronic acid residue with no specific substitution requirements (i.e., $H_{NY,\,6X}$-I_{2X}/G_{2X}-$H_{NY,\,6X}$) as a result that it cleaves both regions of HSGAGs.

Heparanase cleaves glycosidic bonds via a hydrolase mechanism, and is thus distinct from heparinases, which depolymerize HSGAGs by eliminative cleavage. It appears that the highly sulfated structure is important for heparanase substrate recognition and the GlcN(2-*N*-sulfate) structure on the reducing side and the GlcN(6-*O*-sulfate) structure on the nonreducing side of the cleavage site are important for substrate recognition by heparanase (37,38).

IV. Biological Functions of Heparan Sulfate Glycosaminoglycans

A. Heparan Sulfate Glycosaminoglycans Are Information Rich Biopolymers

Of all members of the GAG family, HSGAGs are best understood. Theoretically, there are 48 possible disaccharide units for HSGAGs based on our current

understanding of HSGAG structure (39). Thus, HSGAGs have the potential to encode more information than any other biopolymers, including either DNA (made up of four bases) or proteins (made up of 20 amino acids). Consider, for instance, a simple polymer of each kind made of four units. For DNA, there are 4^4 or 256 possible sequences for this 4-mer. In contrast, for a tetrapeptide, there are many more possibilities, 20^4 or 160,000 permutations. However, for HSGAGs, a polymer made of four disaccharide units could have a total of over 5 million possible sequences, a staggering degree of variation, over 30 times as much as for polypeptides and 10,000 times that of DNA.

There is increasing evidence that HSGAGs interact, in a sequence-specific manner, with numerous signaling molecules and regulate their biological activities. These signaling molecules range from growth factors, morphogens, cytokines, chemokines, and adhesion molecules to structural proteins. Thus, HSGAGs modulate a wide spectrum of biological processes, ranging from homeostasis, development, and angiogenesis to tumorigenesis (4,22,40–43). The broad range of activities contained by HSGAGs can be categorized as follows.

B. Heparan Sulfate Glycosaminoglycans in the Extracellular Matrix Can Act as a Reservoir, Binding, and Storing Signaling Molecules

The storage function of HSGAGs is exemplified by the heparin found in the granules of mast cells, where these highly sulfated polysaccharides bind to specific granule proteases and store them in an inactive form (22,39,44). Similarly, HSGAGs in the ECM bind to many signaling molecules, such as FGFs, HGFs and regulate their biological activities (Fig. 1). Specifically, the binding of these

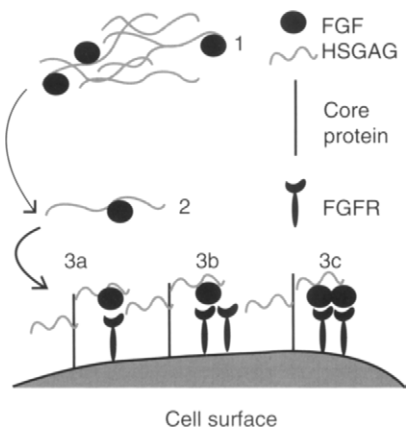

Figure 1 HSGAGs have multiple effects on signaling molecules. HSGAGs regulate signaling molecules, for example, FGF signaling by (1) sequestering FGF in ECM (step 1), (2) transporting FGF to its target receptors (step 2), and (3) being directly involved in the formation of a ternary signaling complex (steps 3a, 3b, and 3c).

protein-signaling molecules to HSGAGs protects them against proteolytic degradation and allows their rapid release upon introduction of a stimulus.

C. Heparan Sulfate Glycosaminoglycans Influence Diffusion of Signaling Molecules

Genetic studies in Drosophila and mice have convincingly demonstrated the critical roles of HSGAGs in signaling events controlled by wingless (Wg), FGF, Decapentaplegic (Dpp), and Hedgehogs (Hh) (45–56). Heparan sulfate-like GAGs regulate diffusion of these potent mitogens and control both the time of transit and how steep a concentration gradient is formed (46,51,53,57–60). This process is closely regulated by HSGAGs in a sequence-specific manner. For instance, while complete loss of HS is embryonic lethal in mouse, animals with defective 2-ST survive into the neonatal stage with discrete morphological defects including renal agenesis (26). In addition, at the cell surface, binding of growth factors to HSGAGs can serve to localize signaling molecules to the cell surface, increasing their effective concentration and promoting binding to their cognate protein receptors (61).

D. Mechanism of Heparan Sulfate Glycosaminoglycan Action

Heparan sulfate-like GAGs at the cell surface act as receptors and regulate the signaling of HSGAG binding proteins in a number of ways (Fig. 1) (22,26,62–64). (1) Protein binding to HSGAGs can induce a conformational change in the ligand, converting it from an inactive form into an active form. For instance, HSGAGs bind to antithrombin III and convert it into an active inhibitor of thrombin and factor Xa, serine proteases involved in the coagulation cascade. In this way, HSGAGs play an intimate role in regulating homeostasis. (2) Heparan sulfate-like GAGs can act as a template or platform for dimerization of the ligand leading to receptor oligomerization and phosphorylation and concomitant signaling. This is the probable role that HSGAGs play in modulating the activity of a number of growth factors. (3) Heparan sulfate-like GAGs can stabilize an active ligand–receptor complex through the formation of a ternary complex, thereby mediating ligand–receptor specificity (Fig. 1) (65–68). It has been shown that cell surface HSGAGs modulate the specificities of FGFRs by bridging the receptor to the FGF ligand (65). (4) Heparan sulfate-like GAGs are known to participate in the cell–cell and cell–ECM adhesion processes by acting as the ligands or coreceptors for protein adhesion molecules such as integrins and selectins. For instance, cell surface syndecans have been shown to facilitate integrin-mediated cell adhesion by binding to the heparin-binding domain of the fibronectin (69–77). In addition, cell surface HSGAGs can act as the ligands for selectin-mediated cell adhesion (Figs. 3, 4) (78–89).

E. Sequence-Specific Modulation of Protein Functions

The breathtaking multitude of functions regulated by HSGAGs raises the question of exactly how these complex polysaccharides are involved in such divergent processes. The exquisite specificity of HSGAG–protein interactions takes place at

several levels. The general observation is that most proteins that recognize HSGAG oligosaccharides bind tightly to a tetrasaccharide or a hexasaccharide. This "minimal-binding size" of HSGAGs is observed in crystal structures of several protein–HSGAG complexes (26,90–95). In several cases, within the tetrasaccharide or hexasaccharide sequence, there are rare modifications, for instance, 3- *O*-sulfation, the presence of an unsubstituted glucosamine (formed by deacetylation of *N*-acetylglucosamine), or 2-*O*-sulfation of a glucuronic acid. One or more of these might be recognized by a protein within a given sequence context and be required for high-affinity binding. The involvement of a rare modification is conceptually attractive because it provides a ready basis for selection. Indeed, this has proved to be the case for some proteins, such as antithrombin, and has facilitated identification of its HSGAG-binding sequence, but it is certainly not true of many protein systems.

Specificity might also arise from spacing of binding sites (96,97). This level of specificity is most readily envisioned when one appreciates that many proteins that bind to HSGAGs are not monomeric units but rather form oligomers. For instance, hepatocyte growth factor has been postulated to form a dimer upon binding to an HSGAG oligosaccharide, as has FGF. In this case, selectivity does not arise from unusual modifications within the tetrasaccharide to hexasaccharide sequence recognized by the monomer; rather, specificity arises from the *spacing* of these units. The sequences that are spaced for optimal formation of the dimer (or higher oligomer) bind with tight affinity in a cooperative manner, and those sequences that do not have optimal spacing bind with lower affinity.

V. Heparan Sulfate Glycosaminoglycans in Cancer

A. Heparan Sulfate Glycosaminoglycans Are Implicated in Cancer Progression

Tumor progression requires sequential steps involving proper coordination of cell proliferation, survival, adhesion, migration, and angiogenesis (Figs. 2–4) (19,39,62). The strategic placement of HSGAGs at the interface between the cell and its surrounding ECM environment suggests that HSGAGs might be critical modulators of cancer onset and progression (62). In fact, numerous studies have clarified particular roles for HSGAGs as modulators in each step of the tumorigenic process (19,20,98–101). Thus, the picture that is emerging is one where HSGAGs, depending on sequence and location, play different, sometimes opposing, roles in tumor initiation, progression, and metastasis.

B. Heparan Sulfate Glycosaminoglycans Are Involved in the Transformation Process

Heparan sulfate-like GAGs have been shown to be involved in tumor initiation. Germline mutations in the Exostoses-1 (EXT-1) and EXT-2 are found in hereditary multiple exostoses (HME) syndrome, which is characterized by the formation

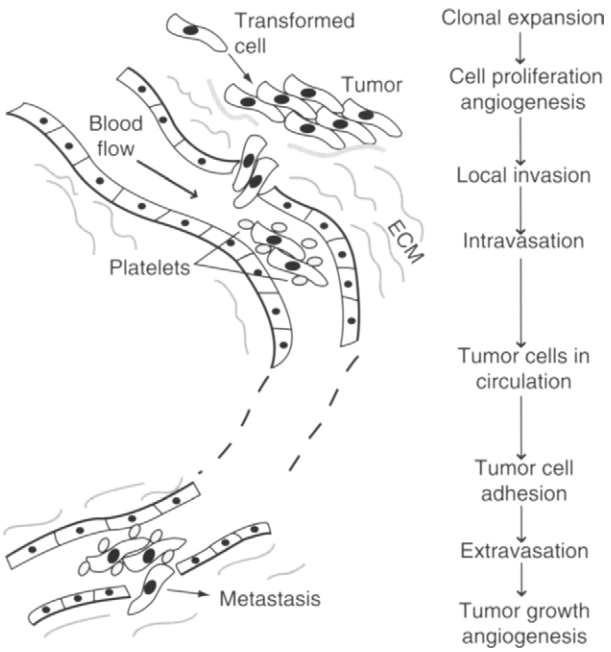

Figure 2 Sequential steps involved in malignant tumor growth and metastasis (39).

of osteochondromas and an increased risk of chondrosarcomas and osteosarcomas (47,99,102,103). Epigenetic inactivation of EXT-1 by promoter hypermethylation abrogated EXT-1 function that led to a loss of HS synthesis in a number of sporadic human malignancies including acute promyelocytic leukemia (APL), acute lymphoblastic leukemia (ALL), and non-melanoma skin cancer (NMSC) (104). Importantly, reintroduction of EXT-1 into cancer cell lines displaying methylation-dependent silencing of EXT-1 induces tumor-suppressor-like features (e.g., reduced colony formation density and tumor growth in nude mouse xenograft models) (104). Thus, EXT-1 and EXT-2 possess tumor suppressor functions.

Changes in both the expression level and the structural characteristics of cell surface HSGAGs have been discovered to correlate with transformation in certain cell types (105–112). For example, the proper expression of syndecan (a particular HSGAG proteoglycan) has been shown to be essential in maintaining the differentiated morphology and localization of epithelial cells; down-regulation of syndecan was found to correlate strongly with transformation to a tumorigenic phenotype (19). Indeed, mice deficient in syndecan-1 are resistant to Wnt-1 induced mammary tumorigenesis (113).

In addition to cell surface HSGAGs, HSGAG proteoglycans in the ECM are known to be intricately involved in transformation and progression of tumors. It has been shown that blocking of perlecan synthesis or its glycosylation with HS chains in experimental systems results in a reduced tumorigenic phenotype as well as decreased tumor angiogenesis (114–116).

C. Heparan Sulfate Glycosaminoglycans in Angiogenesis

In addition to the *direct* roles played by HSGAGs located on the tumor cell surface and in the ECM, HSGAGs are important modulators of the angiogenic process (Fig. 3) (43,82,90,115,117–123), which is critical for tumor progression beyond a size of 1–2 mm. The anticoagulant activity of certain HSGAG sequences inhibits the formation of blood vessels. In addition, many of the potent angiogenic growth factors involved in autocrine signaling loops, such as FGFs and VEGFs, are known HSGAG binding proteins; specific HSGAGs can serve to either inhibit or promote neovascularization by mediating the signaling processes of FGFs and VEGFs in a sequence-specific manner (124–126). To make the situation more complex, HSGAGs on endothelial cells serve as a binding site for the potent anti-angiogenic factor endostatin (90,127). It has been shown that specific sequences on glypicans are required for the specificity of endostatin binding as well as its pronounced effects on endothelial cells. Significantly, several studies have indicated that the HSGAG binding site for endostatin is distinct from that of proangiogenic factors such as FGF (126,128). This raises the possibility that endothelial cells can potentially modulate their HSGAG cell surface profile to become either more or less sensitive to angiogenic signals from the growing tumor.

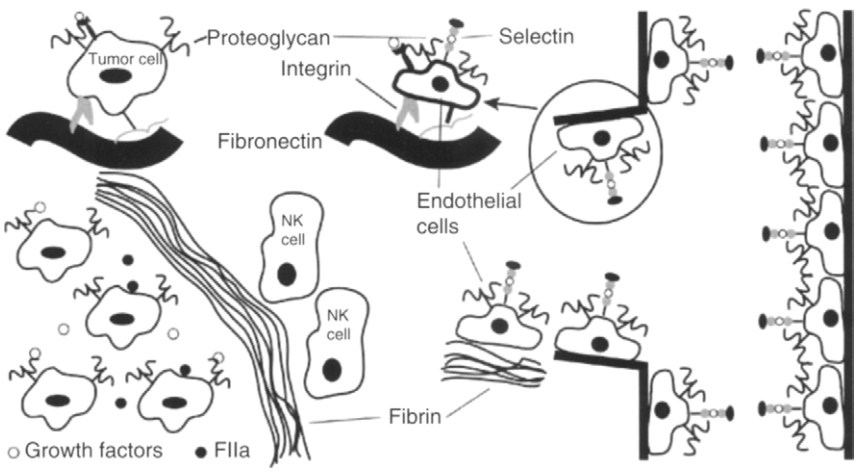

Figure 3 HSGAGs regulate primary tumor growth. HSGAGs at the cell surface and in the extracellular matrix (ECM) serve as: (1) co-receptors for HSGAG-binding growth factors; (2) transporters for protein molecules; and (3) storage sites for HSGAG binding growth factors, proteases, and other HSGAG binding proteins. HSGAGs at the tumor and endothelial cell surface participate in cell proliferation and adhesion by acting as co-receptors for growth factors and integrins. In addition, HSGAGs regulate tumor-induced thrombosis or coagulation by regulating the activities of antithrombin (AT) and other components of the coagulation cascade. The tumor-induced fibrin serves to protect tumor cells from host defenses such as natural killer (NK) cells, and provides the substrate and extracellular environment for cell adhesion and growth factor binding that is required for tumor growth and angiogenesis (39).

D. Heparan Sulfate Glycosaminoglycans as Barriers to Tumor Invasion and Metastasis

Along with structural proteins, such as collagen and laminin, HSGAG proteoglycans are part of a physical barrier to tumor metastasis. During tumor invasion and metastasis, tumor cells must secrete enzymes to degrade both the protein and polysaccharide component of the basement membrane barrier. Indeed, the cloning of mammalian heparanase genes reveals a direct link between the production of heparanases and the invasiveness of tumor cells (33,37,129–132). The transfection of the heparanase cDNA into a non-metastatic cell type results in a greatly enhanced metastatic potential (33,129). It is believed that heparanases can also promote tumor growth by releasing growth factors sequestered by HSGAG proteoglycans in the ECM (33,129).

E. Heparan Sulfate Glycosaminoglycans Are Important for Cell–Cell and Cell–Extracellular Matrix Adhesions

In addition to their passive role in tumor invasion and metastasis, HSGAGs are found to regulate tumor growth and metastasis by actively participating in cell–cell and cell–ECM adhesion processes mediated by integrins and selectins (19,39,75). In this manner, specific HSGAG sequences can act as important signals to elicit organ-specific metastasis. For instance, the sequences contained in the HSGAG proteoglycan of the liver sinusoidal membrane and blood vessels are responsible for the selective metastasis to the liver by murine 3LL-HH tumor cells (133). On the other hand, HSGAGs can also inhibit the tumor metastasis by interfering with cell adhesion processes (19,79,82,83,118,134,135).

F. Tumor Cell Surface Heparan Sulfate Glycosaminoglycans as Cryptic Modulators of Tumor Growth and Metastasis

More recent studies have provided direct evidence that tumor cell surface HSGAGs contain "cryptic" sequences that are activatory and inhibitory toward tumor growth and metastasis (62). A set of HSGAG fragments, released from the cell surface of B16 melanoma cells by heparinase III treatment, potently inhibited primary tumor growth, as well as secondary metastasis to the lung. Conversely, heparinase I-derived HSGAG fragments showed the opposite effect. Immunohistochemistry of the tumor samples revealed changes in both tumor cell kinetics and neovascularization. Decreased cell proliferation, neovascularization, and increased cell apoptosis were observed in the tumor samples treated with heparinase III-derived HSGAG fragments. The opposite changes were observed for heparinase I-treated tumors. This study further identified FGF-2 signaling pathways as the primary target of bioactive HSGAG fragments. This observation was further confirmed by an *in vivo* corneal angiogenesis assay in which heparinase III-derived fragments inhibited FGF-2-induced angiogenesis and heparinase I-derived fragments promoted the process. Therefore, like the proteolytically cleaved collagen

fragment endostatin, distinct HSGAG oligosaccharides, upon release by enzymatic cleavage from the tumor cell surface, can serve as potent inhibitors of tumor progression (62).

G. Heparan Sulfate Glycosaminoglycans Modulate Growth Factor Signaling in Cancer

As described in detail in the previous section, HSGAGs elicit their effects through binding growth factors, cytokines, and structural proteins. Thus, these molecules are intimately involved in modulating autocrine and paracrine signaling loops that are critical for tumor growth. The diverse structural characteristics of HSGAGs allow them to act either as inhibitors or potentiators of such signaling loops, depending on sequence context. Tumor cell surface HSGAGs can act as co-receptors for many HSGAG-binding growth factors, promoting growth factor signaling and facilitating an increase in tumor cell kinetics. The co-receptor role of HSGAGs in growth factor signaling is best studied in FGF-2 signaling, where specific cell surface HSGAG sequences are believed to bind specifically to both FGF-2 and its transmembrane receptor, promoting the formation of a signaling complex at the cell surface (65,91,92,95,126,128,136,137). Conversely, specific sequences of HSGAGs can also act as inhibitors of FGF signaling by competing with "co-receptor" HSGAGs for FGF binding, thus sequestering FGFs (68,126,138,139). Many other signaling molecules important for tumor growth, including epidermal growth factor (EGF), hepatocyte growth factor (HGF), VEGF, and transforming growth factor β (TGF-β), also bind to HSGAG proteoglycans, and their activity is modulated by HSGAG binding (140–146).

In a recent study, loss of hSulf1 (HS 6-*O*-sulfatase) expression was observed in 29% of human hepatocellular carcinoma (HCC) samples and 82% of HCC cell lines (141). LOH at the hSulf1 locus was observed in 42% of HCCs. Treatment with 5-aza-deoxycytidine reactivated hSulf1 expression in hSulf1-negative cell lines. Low hSulf1-expressing cell lines also showed increased sulfation of cell surface HSPGs, enhanced FGF and HGF-mediated signaling, and increased HCC cell growth. Conversely, forced expression of hSulf1 decreased sulfation of cell surface HSPGs and abrogated growth factor signaling. Additionally, HCC cells with high-level hSulf1 expression were sensitive to staurosporine- or cisplatin-induced apoptosis, whereas low expressing cells were resistant. Transfection of hSulf1 into hSulf-1 negative cells restored staurosporine and cisplatin sensitivity (141). Thus, 6-*O*-sulfation of HSGAGs is necessary for HSGAGs' co-receptor function for HSGAG binding growth factors such as FGF and HGF.

Consistent with this notion, using phenotypic screens, several HSGAG based therapeutics displaying antagonistic activities against discrete cancer phenotypes have been described (67,125,147–150). For instance, neoglycans, derived from chemical modification of GAG chains, reduced the viability of several human cancer cell lines both *in vitro* and *in vivo* (149).

H. Heparan Sulfate Glycosaminoglycans in Coagulation and Cancer

Heparan sulfate-like GAGs are known to regulate hemeostasis through interaction with the key components of the coagulation cascade. Heparin, both unfractionated heparin (UFH) and newer low-molecular-weight heparins (LMWHs) are used clinically to inhibit the coagulation by inactivating several proteases of the coagulation cascade, most notably factor Xa and factor IIa (thrombin), the ultimate effector enzyme of the coagulation cascade.

Hypercoagulable state with concurrent increase in thrombin activity is closely linked to human cancer and correlates with poor prognosis (151–154). The elevated thrombosis risk – known as cancer coagulopathy – appears to be tumor-type dependent and is particularly pronounced in glioblastoma, ovarian cancer, melanoma, and pancreatic cancer (155).

Thrombin promotes tumor metastasis primarily through fibrinogen and protease activated receptor-1 (PAR-1, thrombin receptor) dependent mechanisms (Fig. 4). *In vitro*, thrombin binds to tumor cells, making them 2–3-fold more adhesive to

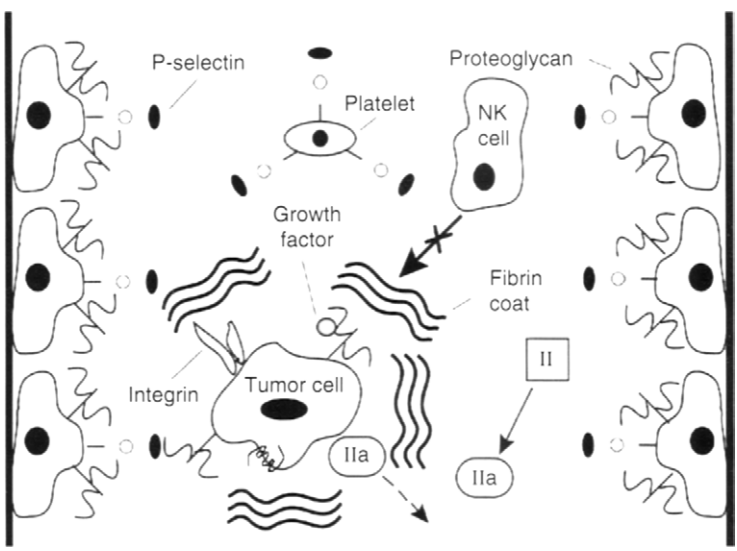

Figure 4 Diverse activities of HSGAGs during tumor metastasis. HSGAGs at the tumor cell surface play multiple roles during metastasis. First, tumor cell surface HSGAGs can act as ligands for P-selectin-mediated adhesion to either platelets or the endothelium lining the capillary system, which promotes tumor adhesion and metastasis. Second, tumor cell surface HSGAGs can act as co-receptors for integrin-mediated cell adhesion, which is known to be important for tumor cell adhesion and extravasation. Finally, HSGAGs at the tumor cell surface can also modulate proliferation and migration of tumor cells by binding and regulating the activities of HSGAG binding proteins. Tumor cell surface HSGAGs in addition contain sequences that can regulate the tumor cell-induced coagulation, which results in the formation of a protective layer of fibrin around the tumor cells and the generation of thrombin that in turn activates PAR-1 at tumor (shown as a 7-transmembrane protein receptor) and endothelial cell surface that promotes proliferation, adhesion, and survival phenotypes (39).

platelets, fibronectin, and Von Willebrand Factor (156,157), as well as microvascular endothelium (158). Thrombin promotes tumor cell survival and adhesion to endothelium of the host organ by forming a protective layer of fibrin around the tumor cells (82,159–161). The experimental metastasis of murine cancer cell lines was diminished in the fibrinogen-deficient transgenic mice compared with wild-type mice, and tumor fate studies showed greatly reduced tumor cell adhesion and survival within the lung of fibrinogen deficient mice (159–162), thereby corroborating the earlier studies.

Protease activated receptor-1 mediated thrombin signaling has recently been shown to promote tumor metastasis (163–165). Introduction of PAR-1 anti-sense cDNA considerably inhibited the invasion of the metastatic breast carcinoma cells in culture (164,166,167). Monoclonal antibodies specific to human PAR-1 inhibited thrombin enhanced chemotactic cell migration *in vitro*, and significantly reduced experimental metastasis of human melanoma cells (M24met) *in vivo* (165). Similar inhibition of metastasis was observed with a small molecule PAR-1 antagonist. Furthermore, the number of B16F10 lung metastases was significantly reduced in PAR-1 deficient mice compared with the PAR-1 wild-type littermates, suggesting that both host and tumor cell PAR-1 facilitate tumor metastasis (165).

In human cancers, thrombin and PAR-1 expression correlates with the invasiveness and metastasis in multiple independent studies (165,167–172). Thrombin expression was detected at the invasion front of solid tumors by immunostaining; over-expression of PAR-1 was documented in several major cancers including breast, pancreas, prostate, and head and neck carcinoma.

In addition, thrombin is a well-established mitogen for a number of tumor cell lines (173,174). Thrombin-treated tumor cells have approximately 2-fold increased growth *in vitro* (173,174). *In vivo*, thrombin-treated tumor cells enhance subcutaneous tumor cell growth 18-fold and experimental pulmonary metastasis (tumor volume) 10–156-fold following ligation of their PAR-1 after 17–21 days of implantation, respectively (157,164).

Thrombin's role in angiogenesis is well documented. During angiogenesis, tissue factor is up-regulated in endothelium, which binds to FVIIa to initiate production of FXa and thrombin (166,175–177). Protease activated receptor-1 cleavage by thrombin triggers the expression of a host of angiogenic factors and receptors among endothelial cells and surrounding smooth muscle cells (178), and activates platelets that led to release of multiple angiogenic growth factors including VEGF. The concerted actions of these factors promote endothelial cell proliferation, migration, and smooth muscle cell recruitment, proliferation and differentiation that are key events in the formation of functional blood vessels. *In vivo*, both thrombin and peptide ligands induce angiogenesis through PAR-1 activation in chorioallantoic membrane (CAM) and matrigel models independent of blood coagulation (175). Protease activated receptor-1 is also essential in blood vessel maturation. Fifty percent of PAR-1 knockout mice die of fatal bleeding at midgestation (E9.5) (175,179–181). The bleeding is caused by fragile, leaky blood vessels due to PAR-1 deficiency in endothelial cells.

Consistent with the diverse roles played by thrombin in promoting tumor progression, pharmacological inhibition of thrombin's activity in various *in vitro*

and *in vivo* model systems has consistently suppressed thrombin dependent proliferation, angiogenesis, invasion, and metastasis phenotypes (135,157,160,182,183). Thus, it is clear that coagulation cascade in general and thrombin in particular plays an important role in cancer progression.

Clinically, anti-coagulation treatment with heparin, particularly LMWHs, and warfarin in clinical trials have revealed survival benefit in a number of human solid malignancies. Warfarin, a coumarin homologue, was the first anticoagulant evaluated in a cancer setting. In 1984, it was reported to promote a doubling of survival time in a group of SCLC patients (328 patients) in combination with chemotherapy (50 weeks for the warfarin group *vs* 24 weeks for the control group) and a significant increase in over all response rate in the warfarin group compared to chemotherapy alone (184). In a separate study with 281 evaluable SCLC patients, a short heparin treatment after chemotherapy increased median survival from 261 days (chemotherapy alone) to 317 days (heparin plus chemotherapy) (185). In a recent trial with 84 patients, Dalteparin (a LMWH) in combination with chemotherapy showed an overall median survival of 13 months compared with 8 months in the chemotherapy group (186). In separate clinical studies, LMWHs also improved survival rate in malignant melanoma (187), ovarian and uterine cancers (188). Thus, the anti-coagulation activities are likely to be important for the observed antitumor effects of LMWHs.

However, the diverse biological activities of HSGAGs arising from its chemical complexity and heterogeneity strongly suggest that HSGAGs can exert antitumor activities via coagulation-independent mechanisms (Fig. 4). For instance, substantial evidence indicates selectin-mediated tumor cell–platelet and tumor cell–endothelial cell adhesions are important for tumor metastasis and invasion: more importantly, HSGAGs such as heparin were shown to interrupt selectin-mediated adhesions and diminish tumor metastasis in animal models (78,79,84,87). Additionally, heparin was shown to boost host immune response by stimulating natural killer (NK)-cell activity to exert its anti-metastatic activities (189,190). Specifically, NK-cell activity was shown to be reduced in lung cancer patients and anticoagulants such as heparin restore NK-cell's activity both *in vitro* and *in vivo*.

In light of increased thrombosis risk associated chemotherapy and anti-angiogenesis therapies (191–196), anticoagulants such as LMWHs may synergize with standard therapies in improving efficacy, while reducing thrombosis risk. Due to the heterogeneity of the heparin structure and function, it is also likely that different heparin preparations will yield different outcomes in cancer trials. Further understanding of the mechanisms of HSGAGs' biological activities should lead to development of next generation of HSGAGs that exhibit improved potency against cancer progression, while minimize side effects associated with existing heparin based therapies.

References

1. Ernst S. PhD thesis. Massachusetts Institute of Technology, 1998.
2. Balduini C, De Luca, Castellani, AA. Biosynthesis of skeletal and corneal keratan sulphate. In: Keratan Sulphate—Chemistry, Biology, Clinical Pathology. London: The Biochemical Society, 1989; 53–65.

3. Lindahl U, Kusche, M, Lidholt K, Oscarsson LG. Biosynthesis of heparin and heparan sulfate. Ann NY Acad Sci 1989; 556:36–50.
4. Sasisekharan R, Venkataraman G. Heparin and heparan sulfate: biosynthesis, structure and function. Curr Opin Chem Biol 2000; 4:626–631.
5. Sugahara K, Kitagawa H. Heparin and heparan sulfate biosynthesis. IUBMB Life 2002; 54:163–175.
6. Conrad H. Heparin-Binding Proteins. San Diego: Academic Press, 1998; 1–348.
7. Gallagher JT, Walker A. Molecular distinctions between heparan sulphate and heparin. Analysis of sulphation patterns indicates that heparan sulphate and heparin are separate families of *N*-sulphated polysaccharides. Biochem J 1985; 230:665–674.
8. Nader HB, Chavante SF, dos-Santos EA, Oliveira TW, de-Paiva JF, Jeronimo SM, Medeiros, GF, de-Abreu LR, Leite EL, de-Sousa-Filho JF, Castro RA, Toma L, Tersariol IL, Porcionatto MA, Dietrich CP. Heparan sulfates and heparins: similar compounds performing the same functions in vertebrates and invertebrates? Braz J Med Biol Res 1999; 32:529–538.
9. Conrad HE. Structure of heparan sulfate and dermatan sulfate. Ann NY Acad Sci 1989; 556:18–28.
10. Stuhlsatz H, Keller R. Structure of keratan sulphate proteoglycans: core proteins, linkage regions, carbohydrate chains. In: Keratan Sulphate—Chemistry, Biology, Clinical Pathology. London: The Biochemical Society, 1989; 1–11.
11. Varki A. Biological roles of oligosaccharides: all of the theories are correct. Glycobiology 1993; 3:97–130.
12. Toole BP. Hyaluronan: from extracellular glue to pericellular cue. Nat Rev Cancer 2004; 4:528–539.
13. Fraser JR, Laurent TC, Laurent UB. Hyaluronan: its nature, distribution, functions and turnover. J Intern Med 1997; 242:27–33.
14. Laurent TC, Laurent UB, Fraser JR. The structure and function of hyaluronan: an overview. Immunol Cell Biol 1996; 74:A1–A7.
15. Laurent TC, Fraser JR. Hyaluronan. FASEB J 1992; 6:2397–2404.
16. Blackhall FH, Merry CL, Davies EJ, Jayson GC. Heparan sulfate proteoglycans and cancer. Br J Cancer 2001; 85:1094–1098.
17. Filmus J, Selleck SB. Glypicans: proteoglycans with a surprise. J Clin Invest 2001; 108:497–501.
18. Iozzo RV, San Antonio JD. Heparan sulfate proteoglycans: heavy hitters in the angiogenesis arena. J Clin Invest 2001; 108:349–355.
19. Sanderson RD. Heparan sulfate proteoglycans in invasion and metastasis. Semin Cell Dev Biol 2001; 12:89–98.
20. Sasisekharan R, Shriver Z, Venkataraman G, Narayanasami U. Roles of heparan-sulphate glycosaminoglycans in cancer. Nat Rev Cancer 2002; 2:521–528.
21. Tumova S, Woods A, Couchman JR. Heparan sulfate proteoglycans on the cell surface: versatile coordinators of cellular functions. Int J Biochem Cell Biol 2000; 32:269–288.
22. Bernfield M, Gotte M, Park PW, Reizes O, Fitzgerald ML, Lincecum J, Zako M. Functions of cell surface heparan sulfate proteoglycans. Annu Rev Biochem 1999; 68:729–777.

23. Park PW, Reizes O, Bernfield M. Cell surface heparan sulfate proteoglycans: selective regulators of ligand-receptor encounters. J Biol Chem 2000; 275:29923–29926.
24. Zimmermann P, David G. The syndecans, tuners of transmembrane signaling. FASEB J 1999; 13 (Suppl):S91–S100.
25. Esko J. Proteoglycans and glycosaminoglycans. In: Varki AC, Cummings RR, Esko J, Freeze H, Hart G, Marth J, eds. Essentials of Glycobiology. New York: Cold Spring Harbor Laboratory Press, 1999; 145–160.
26. Esko JD, Selleck SB. Order out of chaos: assembly of ligand binding sites in heparan sulfate. Annu Rev Biochem 2002; 71:435–471.
27. Lindahl U, Kusche-Gullberg M, Kjellen L. Regulated diversity of heparan sulfate. J Biol Chem 1998; 273:24979–24982.
28. Desai UR, Wang HM, Linhardt RJ. Specificity studies on the heparin lyases from *Flavobacterium heparinum*. Biochemistry 1993; 32:8140–8145.
29. Linhardt RJ, Turnbull JE, Wang HM, Loganathan D, Gallagher JT. Examination of the substrate specificity of heparin and heparan sulfate lyases. Biochemistry 1990; 29:2611–2617.
30. McKenzie E, Tyson K, Stamps A, Smith P, Turner P, Barry R, Hircock M, Patel S, Barry E, Stubberfield C, Terrett J, Page M. Cloning and expression profiling of Hpa2, a novel mammalian heparanase family member. Biochem Biophys Res Commun 2000; 276:1170–1177.
31. Kussie PH, Hulmes JD, Ludwig DL, Patel S, Navarro EC, Seddon AP, Giorgio NA, Bohlen P. Cloning and functional expression of a human heparanase gene. Biochem Biophys Res Commun 1999; 261:183–187.
32. Hulett MD, Freeman C, Hamdorf BJ, Baker RT, Harris MJ, Parish CR. Cloning of mammalian heparanase, an important enzyme in tumor invasion and metastasis. Nat Med 1999; 5:803–809.
33. Vlodavsky I, Friedmann Y, Elkin M, Aingorn H, Atzmon R, Ishai-Michaeli R, Bitan M, Pappo O, Peretz T, Michal I, Spector L, Pecker I. Mammalian heparanase: gene cloning, expression and function in tumor progression and metastasis. Nat Med 1999; 5:793–802.
34. Ernst S, Langer R, Cooney CL, Sasisekharan R. Enzymatic degradation of glycosaminoglycans. Crit Rev Biochem Mol Biol 1995; 30:387–444.
35. Shriver Z, Hu Y, Sasisekharan R. Heparinase II from *Flavobacterium heparinum*. Role of histidine residues in enzymatic activity as probed by chemical modification and site-directed mutagenesis. J Biol Chem 1998; 273: 10160–10167.
36. Sasisekharan R, Leckband D, Godavarti R, Venkataraman G, Cooney CL, Langer R. Heparinase I from *Flavobacterium heparinum*: the role of the cysteine residue in catalysis as probed by chemical modification and site-directed mutagenesis. Biochemistry 1995; 34:14441–14448.
37. Ishida K, Hirai G, Murakami K, Teruya T, Simizu S, Sodeoka M, Osada H. Structure-based design of a selective heparanase inhibitor as an antimetastatic agent. Mol Cancer Ther 2004; 3:1069–1077.
38. Ishida K, Wierzba MK, Teruya T, Simizu S, Osada H. Novel heparan sulfate mimetic compounds as antitumor agents. Chem Biol 2004; 11:367–377.
39. Liu D, Shriver Z, Qi Y, Venkataraman G, Sasisekharan R. Dynamic regulation of tumor growth and metastasis by heparan sulfate glycosaminoglycans. Semin Thromb Hemost 2002; 28:67–78.

40. Lin X, Perrimon N. Role of heparan sulfate proteoglycans in cell–cell signaling in Drosophila. Matrix Biol 2000; 19:303–307.
41. Lin X, Buff EM, Perrimon N, Michelson AM. Heparan sulfate proteoglycans are essential for FGF receptor signaling during Drosophila embryonic development. Development 1999; 126:3715–3723.
42. Lin X, Perrimon N. Dally cooperates with Drosophila Frizzled 2 to transduce Wingless signalling. Nature 1999; 400:281–284.
43. Sasisekharan R, Moses MA, Nugent MA, Cooney CL, Langer R. Heparinase inhibits neovascularization. Proc Natl Acad Sci USA 1994; 91:1524–1528.
44. Humphries DE, Wong GW, Friend DS, Gurish MF, Qiu WT, Huang C, Sharpe AH, Stevens RL. Heparin is essential for the storage of specific granule proteases in mast cells. Nature 1999; 400:769–772.
45. Bornemann DJ, Duncan JE, Staatz W, Selleck S, Warrior R. Abrogation of heparan sulfate synthesis in Drosophila disrupts the Wingless, Hedgehog and Decapentaplegic signaling pathways. Development 2004; 131:1927–1938.
46. Han C, Belenkaya TY, Khodoun M, Tauchi M, Lin X. Distinct and collaborative roles of Drosophila EXT family proteins in morphogen signalling and gradient formation. Development 2004; 131:1563–1575.
47. Jones KB, Morcuende JA. Of hedgehogs and hereditary bone tumors: reexamination of the pathogenesis of osteochondromas. Iowa Orthop J 2003; 23:87–95.
48. Sedita J, Izvolsky K, Cardoso WV. Differential expression of heparan sulfate 6-*O*-sulfotransferase isoforms in the mouse embryo suggests distinctive roles during organogenesis. Dev Dyn 2004; 231:782–794.
49. Shimo T, Gentili C, Iwamoto M, Wu C, Koyama E, Pacifici M. Indian hedgehog and syndecans-3 coregulate chondrocyte proliferation and function during chick limb skeletogenesis. Dev Dyn 2004; 229:607–617.
50. Perrimon N, Hacker U. Wingless, hedgehog and heparan sulfate proteoglycans. Development 2004; 131:2509–2511; author reply 11–13.
51. Cadigan KM. Regulating morphogen gradients in the Drosophila wing. Semin Cell Dev Biol 2002; 13:83–90.
52. Park Y, Rangel C, Reynolds MM, Caldwell MC, Johns M, Nayak M, Welsh CJ, McDermott S, Datta S. Drosophila perlecan modulates FGF and hedgehog signals to activate neural stem cell division. Dev Biol 2003; 253:247–257.
53. Lin X, Perrimon N. Developmental roles of heparan sulfate proteoglycans in Drosophila. Glycoconj J 2002; 19:363–368.
54. The I, Bellaiche Y, Perrimon N. Hedgehog movement is regulated through tout velu-dependent synthesis of a heparan sulfate proteoglycan. Mol Cell 1999; 4:633–639.
55. Baeg GH, Perrimon N. Functional binding of secreted molecules to heparan sulfate proteoglycans in Drosophila. Curr Opin Cell Biol 2000; 12:575–580.
56. Koziel L, Kunath M, Kelly OG, Vortkamp A. Ext1-dependent heparan sulfate regulates the range of Ihh signaling during endochondral ossification. Dev Cell 2004; 6:801–813.
57. Fujise M, Takeo S, Kamimura K, Matsuo T, Aigaki T, Izumi S, Nakato H. Dally regulates Dpp morphogen gradient formation in the Drosophila wing. Development 2003; 130:1515–1522.

58. Turnbull JE, Gallagher JT. Sequence analysis of heparan sulphate indicates defined location of *N*-sulphated glucosamine and iduronate 2-sulphate residues proximal to the protein-linkage region. Biochem J 1991; 277:297–303.
59. Takei Y, Ozawa Y, Sato M, Watanabe A, Tabata T. Three Drosophila EXT genes shape morphogen gradients through synthesis of heparan sulfate proteoglycans. Development 2004; 131:73–82.
60. Nybakken K, Perrimon N. Heparan sulfate proteoglycan modulation of developmental signaling in Drosophila. Biochim Biophys Acta 2002; 1573: 280–291.
61. Perrimon N, Bernfield M. Specificities of heparan sulphate proteoglycans in developmental processes. Nature 2000; 404:725–728.
62. Liu D, Shriver Z, Venkataraman G, El Shabrawi Y, Sasisekharan R. Tumor cell surface heparan sulfate as cryptic promoters or inhibitors of tumor growth and metastasis. Proc Natl Acad Sci USA 2002; 99:568–573.
63. Shriver Z, Raguram S, Sasisekharan R. Glycomics: a pathway to a class of new and improved therapeutics. Nat Rev Drug Discov 2004; 3:863–873.
64. Shriver Z, Raman R, Venkataraman G, Drummond K, Turnbull J, Toida T, Linhardt R, Biemann K, Sasisekharan R. Sequencing of 3-*O*-sulfate containing heparin decasaccharides with a partial antithrombin III binding site. Proc Natl Acad Sci USA 2000; 97:10359–10364.
65. Guimond SE, Turnbull JE. Fibroblast growth factor receptor signalling is dictated by specific heparan sulphate saccharides. Curr Biol 1999; 9:1343–1346.
66. Powell AK, Fernig DG, Turnbull JE. Fibroblast growth factor receptors 1 and 2 interact differently with heparin/heparan sulfate. Implications for dynamic assembly of a ternary signaling complex. J Biol Chem 2002; 277:28554–28563.
67. Ostrovsky O, Berman B, Gallagher J, Mulloy B, Fernig DG, Delehedde M, Ron D. Differential effects of heparin saccharides on the formation of specific fibroblast growth factor (FGF) and FGF receptor complexes. J Biol Chem 2002; 277:2444–2453.
68. Pye DA, Vives RR, Hyde P, Gallagher JT. Regulation of FGF-1 mitogenic activity by heparan sulfate oligosaccharides is dependent on specific structural features: differential requirements for the modulation of FGF-1 and FGF-2. Glycobiology 2000; 10:1183–1192.
69. Woods A, Couchman JR. Integrin modulation by lateral association. J Biol Chem 2000; 275:24233–24236.
70. Couchman JR, Chen L, Woods A. Syndecans and cell adhesion. Int Rev Cytol 2001; 207:113–150.
71. Woods A, Couchman JR. Syndecan-4 and focal adhesion function. Curr Opin Cell Biol 2001; 13:578–583.
72. Mostafavi-Pour Z, Askari JA, Parkinson SJ, Parker PJ, Ng TT, Humphries MJ. Integrin-specific signaling pathways controlling focal adhesion formation and cell migration. J Cell Biol 2003; 161:155–167.
73. Yoneda A, Couchman JR. Regulation of cytoskeletal organization by syndecan transmembrane proteoglycans. Matrix Biol 2003; 22:25–33.
74. Beauvais DM, Burbach BJ, Rapraeger AC. The syndecan-1 ectodomain regulates alphavbeta3 integrin activity in human mammary carcinoma cells. J Cell Biol 2004; 167:171–181.
75. Woods A, Couchman JR. Syndecans: synergistic activators of cell adhesion. Trends Cell Biol 1998; 8:189–192.

76. Saoncella S, Echtermeyer F, Denhez F, Nowlen JK, Mosher DF, Robinson SD, Hynes RO, Goetinck PF. Syndecan-4 signals cooperatively with integrins in a Rho-dependent manner in the assembly of focal adhesions and actin stress fibers. Proc Natl Acad Sci USA 1999; 96:2805–2810.
77. Couchman JR, Woods A. Syndecan-4 and integrins: combinatorial signaling in cell adhesion. J Cell Sci 1999; 112:3415–3420.
78. Wei M, Tai G, Gao Y, Li N, Huang B, Zhou Y, Hao S, Zeng X. Modified heparin inhibits P-selectin-mediated cell adhesion of human colon carcinoma cells to immobilized platelets under dynamic flow conditions. J Biol Chem 2004; 279:29202–29210.
79. Borsig L. Selectins facilitate carcinoma metastasis and heparin can prevent them. News Physiol Sci 2004; 19:16–21.
80. Wahrenbrock M, Borsig L, Le D, Varki N, Varki A. Selectin-mucin interactions as a probable molecular explanation for the association of Trousseau syndrome with mucinous adenocarcinomas. J Clin Invest 2003; 112:853–862.
81. Wang JG, Geng JG. Affinity and kinetics of P-selectin binding to heparin. Thromb Haemost 2003; 90:309–316.
82. Zacharski LR, Loynes JT. The heparins and cancer. Curr Opin Pulm Med 2002; 8:379–382.
83. Varki NM, Varki A. Heparin inhibition of selectin-mediated interactions during the hematogenous phase of carcinoma metastasis: rationale for clinical studies in humans. Semin Thromb Hemost 2002; 28:53–66.
84. Varki A, Varki NM. P-selectin, carcinoma metastasis and heparin: novel mechanistic connections with therapeutic implications. Braz J Med Biol Res 2001; 34:711–717.
85. Ma YQ, Geng JG. Heparan sulfate-like proteoglycans mediate adhesion of human malignant melanoma A375 cells to P-selectin under flow. J Immunol 2000; 165:558–565.
86. Wang L, Brown JR, Varki A, Esko JD. Heparin's anti-inflammatory effects require glucosamine 6-*O*-sulfation and are mediated by blockade of L- and P-selectins. J Clin Invest 2002; 110:127–136.
87. Borsig L, Wong R, Feramisco J, Nadeau DR, Varki NM, Varki A. Heparin and cancer revisited: mechanistic connections involving platelets, P-selectin, carcinoma mucins, and tumor metastasis. Proc Natl Acad Sci USA 2001; 98:3352–3357.
88. Koenig A, Norgard-Sumnicht K, Linhardt R, Varki A. Differential interactions of heparin and heparan sulfate glycosaminoglycans with the selectins. Implications for the use of unfractionated and low molecular weight heparins as therapeutic agents. J Clin Invest 1998; 101:877–889.
89. Luo J, Kato M, Wang H, Bernfield M, Bischoff J. Heparan sulfate and chondroitin sulfate proteoglycans inhibit E-selectin binding to endothelial cells. J Cell Biochem 2001; 80:522–523.
90. Sasaki T, Larsson H, Kreuger J, Salmivirta M, Claesson-Welsh L, Lindahl U, Hohenester E, Timpl R. Structural basis and potential role of heparin/heparan sulfate binding to the angiogenesis inhibitor endostatin. EMBO J 1999; 18:6240–6248.
91. Pellegrini L, Burke DF, von Delft F, Mulloy B, Blundell TL. Crystal structure of fibroblast growth factor receptor ectodomain bound to ligand and heparin. Nature 2000; 407:1029–1034.

92. Schlessinger J, Plotnikov AN, Ibrahimi OA, Eliseenkova AV, Yeh BK, Yayon A, Linhardt RJ, Mohammadi M. Crystal structure of a ternary FGF–FGFR–heparin complex reveals a dual role for heparin in FGFR binding and dimerization. Mol Cell 2000; 6:743–750.
93. Faham S, Hileman RE, Fromm JR, Linhardt RJ, Rees DC. Heparin structure and interactions with basic fibroblast growth factor. Science 1996; 271:1116–1120.
94. Ernst S, Venkataraman G, Winkler S, Godavarti R, Langer R, Cooney CL, Sasisekharan R. Expression in *Escherichia coli*, purification and characterization of heparinase I from *Flavobacterium heparinum*. Biochem J 1996; 315:589–597.
95. Guimond S, Maccarana M, Olwin BB, Lindahl U, Rapraeger AC. Activating and inhibitory heparin sequences for FGF-2 (basic FGF). Distinct requirements for FGF-1, FGF-2, and FGF-4. J Biol Chem 1993; 268:23906–23914.
96. Hileman RE, Fromm JR, Weiler JM, Linhardt RJ. Glycosaminoglycan–protein interactions: definition of consensus sites in glycosaminoglycan binding proteins. Bioessays 1998; 20:156–167.
97. Caldwell EE, Nadkarni VD, Fromm JR, Linhardt RJ, Weiler JM. Importance of specific amino acids in protein binding sites for heparin and heparan sulfate. Int J Biochem Cell Biol 1996; 28:203–216.
98. Pilia G, Hughes-Benzie RM, MacKenzie A, Baybayan P, Chen EY, Huber R, Neri G, Cao A, Forabosco A, Schlessinger D. Mutations in GPC3, a glypican gene, cause the Simpson–Golabi–Behmel overgrowth syndrome. Nat Genet 1996; 12:241–247.
99. McCormick C, Duncan G, Tufaro F. Herpes simplex virus: discovering the link between heparan sulphate and hereditary bone tumours. Rev Med Virol 2000; 10:373–384.
100. Sanderson RD, Yang Y, Suva LJ, Kelly T. Heparan sulfate proteoglycans and heparanase–partners in osteolytic tumor growth and metastasis. Matrix Biol 2004; 23:341–352.
101. Safaiyan F, Lindahl U, Salmivirta M. Selective reduction of 6-*O*-sulfation in heparan sulfate from transformed mammary epithelial cells. Eur J Biochem 1998; 252:576–582.
102. Lind T, Tufaro F, McCormick C, Lindahl U, Lidholt K. The putative tumor suppressors EXT1 and EXT2 are glycosyltransferases required for the biosynthesis of heparan sulfate. J Biol Chem 1998; 273:26265–26268.
103. Senay C, Lind T, Muguruma K, Tone Y, Kitagawa H, Sugahara K, Lidholt K, Lindahl U, Kusche-Gullberg M. The EXT1/EXT2 tumor suppressors: catalytic activities and role in heparan sulfate biosynthesis. EMBO Rep 2000; 1:282–286.
104. Ropero S, Setien F, Espada J, Fraga MF, Herranz M, Asp J, Benassi MS, Franchi A, Patino A, Ward LS, Bovee J, Cigudosa JC, Wim W, Esteller M. Epigenetic loss of the familial tumor-suppressor gene exostosin-1 (EXT1) disrupts heparan sulfate synthesis in cancer cells. Hum Mol Genet 2004; 13:2753–2765.
105. Emoto N, Shimizu K, Onose H, Ishii S, Sugihara H, Wakabayashi I. A subpopulation of fibroblast growth factor-2-binding heparan sulfate is lost in human papillary thyroid carcinomas. Thyroid 2000; 10:843–849.

106. Birch MA, Skerry TM. Differential regulation of syndecan expression by osteosarcoma cell lines in response to cytokines but not osteotropic hormones. Bone 1999; 24:571–578.
107. Salmivirta M, Safaiyan F, Prydz K, Andresen MS, Aryan M, Kolset SO. Differentiation-associated modulation of heparan sulfate structure and function in CaCo-2 colon carcinoma cells. Glycobiology 1998; 8:1029–1036.
108. Nackaerts K, Verbeken E, Deneffe G, Vanderschueren B, Demedts M, David G. Heparan sulfate proteoglycan expression in human lung-cancer cells. Int J Cancer 1997; 74:335–345.
109. Iida S, Suzuki K, Matsuoka K, Takazono I, Shimada A, Inoue M, Yahara J, Noda S. Analysis of glycosaminoglycans in human prostate by high-performance liquid chromatography. Br J Urol 1997; 79:763–769.
110. Ida M, Kamada A. Changes in glycosaminoglycan characteristics during progression of a human gingival carcinoma xenograft line in nude mice. J Osaka Dent Univ 1995; 29:39–50.
111. Cohen IR, Murdoch AD, Naso MF, Marchetti D, Berd D, Iozzo RV. Abnormal expression of perlecan proteoglycan in metastatic melanomas. Cancer Res 1994; 54:5771–5774.
112. Lelongt B, Piedagnel R, Chatelet F, Baudouin B, Brenchley PE, Verroust PJ, Cassingena R, Vandewalle A, Ronco PM. Dramatic changes of sulfated proteoglycans composition in a tumorigenic SV-40-transformed renal proximal-tubule cell line. J Biol Chem 1992; 267:23815–23822.
113. Alexander CM, Reichsman F, Hinkes MT, Lincecum J, Becker KA, Cumberledge S, Bernfield M. Syndecan-1 is required for Wnt-1-induced mammary tumorigenesis in mice. Nat Genet 2000; 25:329–332.
114. Jiang X, Couchman JR. Perlecan and tumor angiogenesis. J Histochem Cytochem 2003; 51:1393–1410.
115. Jiang X, Multhaupt H, Chan E, Schaefer L, Schaefer RM, Couchman JR. Essential contribution of tumor-derived perlecan to epidermal tumor growth and angiogenesis. J Histochem Cytochem 2004; 52:1575–1590.
116. Zhou Z, Wang J, Cao R, Morita H, Soininen R, Chan KM, Liu B, Cao Y, Tryggvason K. Impaired angiogenesis, delayed wound healing and retarded tumor growth in perlecan heparan sulfate-deficient mice. Cancer Res 2004; 64:4699–4702.
117. Bierhaus A, Nawroth PP. Antiangiogenic properties of low molecular weight heparin – does tissue factor provide the answer? Thromb Haemost 2004; 92:438–439.
118. Mousa SA. Low-molecular-weight heparins in thrombosis and cancer: emerging links. Cardiovasc Drug Rev 2004; 22:121–134.
119. Rak J, Weitz JI. Heparin and angiogenesis: size matters! Arterioscler Thromb Vasc Biol 2003; 23:1954–1955.
120. Presta M, Leali D, Stabile H, Ronca R, Camozzi M, Coco L, Moroni E, Liekens S, Rusnati M. Heparin derivatives as angiogenesis inhibitors. Curr Pharm Des 2003; 9:553–566.
121. Casu B, Guerrini M, Guglieri S, Naggi A, Perez M, Torri G, Cassinelli G, Ribatti D, Carminati P, Giannini G, Penco S, Pisano C, Belleri M, Rusnati M, Presta M. Undersulfated and glycol-split heparins endowed with antiangiogenic activity. J Med Chem 2004; 47:838–848.

122. Natke B, Venkataraman G, Nugent MA, Sasisekharan R. Heparinase treatment of bovine smooth muscle cells inhibits fibroblast growth factor-2 binding to fibroblast growth factor receptor but not FGF-2 mediated cellular proliferation. Angiogenesis 1999; 3:249–257.
123. Smorenburg SM. Inhibition of angiogenesis with heparin? Haemostasis 2001; 31 (Suppl 1):25–29.
124. Brickman YG, Nurcombe V, Ford MD, Gallagher JT, Bartlett PF, Turnbull JE. Structural comparison of fibroblast growth factor-specific heparan sulfates derived from a growing or differentiating neuroepithelial cell line. Glycobiology 1998; 8:463–471.
125. Jayson GC, Gallagher JT. Heparin oligosaccharides: inhibitors of the biological activity of bFGF on Caco-2 cells. Br J Cancer 1997; 75:9–16.
126. Gallagher JT. Structure–activity relationship of heparan sulphate. Biochem Soc Trans 1997; 25:1206–1209.
127. Karumanchi SA, Jha V, Ramchandran R, Karihaloo A, Tsiokas L, Chan B, Dhanabal M, Hanai JI, Venkataraman G, Shriver Z, Keiser N, Kalluri R, Zeng H, Mukhopadhyay D, Chen RL, Lander AD, Hagihara K, Yamaguchi Y, Sasisekharan R, Cantley L, Sukhatme VP. Cell surface glypicans are low-affinity endostatin receptors. Mol Cell 2001; 7:811–822.
128. Turnbull JE, Fernig DG, Ke Y, Wilkinson MC, Gallagher JT. Identification of the basic fibroblast growth factor binding sequence in fibroblast heparan sulfate. J Biol Chem 1992; 267:10337–10341.
129. Vlodavsky I, Elkin M, Pappo O, Aingorn H, Atzmon R, Ishai-Michaeli R, Peretz T, Friedmann Y. Mammalian heparanase as mediator of tumor metastasis and angiogenesis. Isr Med Assoc J 2000; 2 (Suppl):37–45.
130. Edovitsky E, Elkin M, Zcharia E, Peretz T, Vlodavsky I. Heparanase gene silencing, tumor invasiveness, angiogenesis, and metastasis. J Natl Cancer Inst 2004; 96:1219–1230.
131. Boyd DD, Nakajima M. Involvement of heparanase in tumor metastases: a new target in cancer therapy? J Natl Cancer Inst 2004; 96:1194–1195.
132. Ferro V, Hammond E, Fairweather JK. The development of inhibitors of heparanase, a key enzyme involved in tumour metastasis, angiogenesis and inflammation. Mini Rev Med Chem 2004; 4:693–702.
133. Tovari J, Paku S, Raso E, Pogany G, Kovalszky I, Ladanyi A, Lapis K, Timar J. Role of sinusoidal heparan sulfate proteoglycan in liver metastasis formation. Int J Cancer 1997; 71:825–831.
134. Borsig L. Non-anticoagulant effects of heparin in carcinoma metastasis and Trousseau's syndrome. Pathophysiol Haemost Thromb 2003; 33 (Suppl 1):64–66.
135. Amirkhosravi A, Mousa SA, Amaya M, Francis JL. Antimetastatic effect of tinzaparin, a low-molecular-weight heparin. J Thromb Haemost 2003; 1:1972–1976.
136. Venkataraman G, Shriver Z, Davis JC, Sasisekharan R. Fibroblast growth factors 1 and 2 are distinct in oligomerization in the presence of heparin-like glycosaminoglycans. Proc Natl Acad Sci USA 1999; 96:1892–1897.
137. Belting M, Borsig L, Fuster MM, Brown JR, Persson L, Fransson LA, Esko JD. Tumor attenuation by combined heparan sulfate and polyamine depletion. Proc Natl Acad Sci USA 2002; 99:371–376.

138. Fannon M, Forsten KE, Nugent MA. Potentiation and inhibition of bFGF binding by heparin: a model for regulation of cellular response. Biochemistry 2000; 39:1434–1445.
139. Pye DA, Vives RR, Turnbull JE, Hyde P, Gallagher JT. Heparan sulfate oligosaccharides require 6-*O*-sulfation for promotion of basic fibroblast growth factor mitogenic activity. J Biol Chem 1998; 273:22936–22942.
140. Li J, Kleeff J, Kayed H, Felix K, Penzel R, Buchler MW, Korc M, Friess H. Glypican-1 antisense transfection modulates TGF-beta-dependent signaling in Colo-357 pancreatic cancer cells. Biochem Biophys Res Commun 2004; 320:1148–1155.
141. Lai JP, Chien JR, Moser DR, Staub JK, Aderca I, Montoya DP, Matthews TA, Nagorney DM, Cunningham JM, Smith DI, Greene EL, Shridhar V, Roberts LR. hSulf1 sulfatase promotes apoptosis of hepatocellular cancer cells by decreasing heparin-binding growth factor signaling. Gastroenterology 2004; 126:231–248.
142. Karihaloo A, Kale S, Rosenblum ND, Cantley LG. Hepatocyte growth factor-mediated renal epithelial branching morphogenesis is regulated by glypican-4 expression. Mol Cell Biol 2004; 24:8745–8752.
143. Delehedde M, Lyon M, Vidyasagar R, McDonnell TJ, Fernig DG. Hepatocyte growth factor/scatter factor binds to small heparin-derived oligosaccharides and stimulates the proliferation of human HaCaT keratinocytes. J Biol Chem 2002; 277:12456–12462.
144. Fairbrother WJ, Champe MA, Christinger HW, Keyt BA, Starovasnik MA. Solution structure of the heparin-binding domain of vascular endothelial growth factor. Structure 1998; 6:637–648.
145. Gengrinovitch S, Berman B, David G, Witte L, Neufeld G, Ron D. Glypican-1 is a VEGF165 binding proteoglycan that acts as an extracellular chaperone for VEGF165. J Biol Chem 1999; 274:10816–10822.
146. Ito N, Claesson-Welsh L. Dual effects of heparin on VEGF binding to VEGF receptor-1 and transduction of biological responses. Angiogenesis 1999; 3:159–166.
147. Humphries MJ, Matsumoto K, White SL, Olden K. Oligosaccharide modification by swainsonine treatment inhibits pulmonary colonization by B16-F10 murine melanoma cells. Proc Natl Acad Sci USA 1986; 83:1752–1756.
148. Freeman C, Liu L, Banwell MG, Brown KJ, Bezos A, Ferro V, Parish CR. Use of sulfated linked cyclitols as heparan sulfate mimetics to probe the heparin/heparan sulfate binding specificity of proteins. J Biol Chem 2005; 280:8842–8849.
149. Pumphrey CY, Theus AM, Li S, Parrish RS, Sanderson RD. Neoglycans, carbodiimide-modified glycosaminoglycans: a new class of anticancer agents that inhibit cancer cell proliferation and induce apoptosis. Cancer Res 2002; 62:3722–3728.
150. Naggi A, Casu B, Perez M, Torri G, Cassinelli G, Penco S, Pisano C, Giannini G, Ishai-Michaeli R, Vlodavsky I. Modulation of the heparanase-inhibiting activity of heparin through selective desulfation, graded *N*-acetylation, and glycol-splitting. J Biol Chem 2005; 280:12103–12113.
151. Francis JL, Biggerstaff J, Amirkhosravi A. Hemostasis and malignancy. Semin Thromb Hemost 1998; 24:93–109.

152. Rickles FR, Levine M, Edwards RL. Hemostatic alterations in cancer patients. Cancer Metastasis Rev 1992; 11:237–248.
153. Costantini V, Zacharski LR. The role of fibrin in tumor metastasis. Cancer Metastasis Rev 1992; 11:283–290.
154. Wojtukiewicz MZ, Zacharski LR, Memoli VA, Kisiel W, Kudryk BJ, Rousseau SM, Stump DC. Abnormal regulation of coagulation/fibrinolysis in small cell carcinoma of the lung. Cancer 1990; 65:481–485.
155. Levitan N, Dowlati A, Remick SC, Tahsildar HI, Sivinski LD, Beyth R, Rimm AA. Rates of initial and recurrent thromboembolic disease among patients with malignancy versus those without malignancy. Risk analysis using Medicare claims data. Medicine (Baltimore) 1999; 78:285–291.
156. Nierodzik ML, Kajumo F, Karpatkin S. Effect of thrombin treatment of tumor cells on adhesion of tumor cells to platelets *in vitro* and tumor metastasis *in vivo*. Cancer Res 1992; 52:3267–3272.
157. Nierodzik ML, Plotkin A, Kajumo F, Karpatkin S. Thrombin stimulates tumor-platelet adhesion *in vitro* and metastasis *in vivo*. J Clin Invest 1991; 87:229–236.
158. Klepfish A, Greco MA, Karpatkin S. Thrombin stimulates melanoma tumor-cell binding to endothelial cells and subendothelial matrix. Int J Cancer 1993; 53:978–982.
159. Palumbo JS, Potter JM, Kaplan LS, Talmage K, Jackson DG, Degen JL. Spontaneous hematogenous and lymphatic metastasis, but not primary tumor growth or angiogenesis, is diminished in fibrinogen-deficient mice. Cancer Res 2002; 62:6966–6972.
160. Palumbo JS, Degen JL. Fibrinogen and tumor cell metastasis. Haemostasis 2001; 31 (Suppl 1):11–15.
161. Palumbo JS, Kombrinck KW, Drew AF, Grimes TS, Kiser JH, Degen JL, Bugge TH. Fibrinogen is an important determinant of the metastatic potential of circulating tumor cells. Blood 2000; 96:3302–3309.
162. Palumbo JS, Talmage KE, Massari JV, La Jeunesse CM, Flick MJ, Kombrinck KW, Jirouskova M, Degen JL. Platelets and fibrinogen increase metastatic potential by impeding natural killer cell-mediated elimination of tumor cells. Blood 2005; 105:178–185.
163. Rudroff C, Striegler S, Schilli M, Scheele J. Thrombin enhances adhesion in pancreatic cancer *in vitro* through the activation of the thrombin receptor PAR 1. Eur J Sur Oncol 2001; 27:472–476.
164. Nierodzik ML, Chen K, Takeshita K, Li JJ, Huang YQ, Feng XS, D'Andrea MR, Andrade-Gordon P, Karpatkin S. Protease-activated receptor 1 (PAR-1) is required and rate-limiting for thrombin-enhanced experimental pulmonary metastasis. Blood 1998; 92:3694–3700.
165. Shi X, Gangadharan B, Brass LF, Andrade-Gordon P, Ruf W, Mueller BM. Host and tumor cell PAR1 contribute to hematogenous metastasis. In: AACR. Toronto, Canada, 2003.
166. Yin YJ, Salah Z, Grisaru-Granovsky S, Cohen I, Even-Ram SC, Maoz M, Uziely B, Peretz T, Bar-Shavit R. Human protease-activated receptor 1 expression in malignant epithelia: a role in invasiveness. Arterioscler Thromb Vasc Biol 2003; 23:940–944.

167. Even-Ram S, Uziely B, Cohen P, Grisaru-Granovsky S, Maoz M, Ginzburg Y, Reich R, Vlodavsky I, Bar-Shavit R. Thrombin receptor overexpression in malignant and physiological invasion processes. Nat Med 1998; 4:909–914.
168. D'Andrea MR, Derian CK, Santulli RJ, Andrade-Gordon P. Differential expression of protease-activated receptors-1 and -2 in stromal fibroblasts of normal, benign, and malignant human tissues. Am J Pathol 2001; 158: 2031–2041.
169. Wojtukiewicz MZ, Tang DG, Ben-Josef E, Renaud C, Walz DA, Honn KV. Solid tumor cells express functional "tethered ligand" thrombin receptor. Cancer Res 1995; 55:698–704.
170. Wojtukiewicz MZ, Tang DG, Ciarelli JJ, Nelson KK, Walz DA, Diglio CA, Mammen EF, Honn KV. Thrombin increases the metastatic potential of tumor cells. Int J Cancer. 1993; 54:793–806.
171. Henrikson KP, Salazar SL, Fenton 2nd JW, Pentecost BT. Role of thrombin receptor in breast cancer invasiveness. Br J Cancer 1999; 79:401–406.
172. Schiller H, Bartscht T, Arlt A, Zahn MO, Seifert A, Bruhn T, Bruhn HD, Gieseler F. Thrombin as a survival factor for cancer cells: thrombin activation in malignant effusions *in vivo* and inhibition of idarubicin-induced cell death *in vitro*. Int J Clin Pharmacol Ther 2002; 40:329–335.
173. Zain J, Huang YQ, Feng X, Nierodzik ML, Li JJ, Karpatkin S. Concentration-dependent dual effect of thrombin on impaired growth/apoptosis or mitogenesis in tumor cells. Blood 2000; 95:3133–3138.
174. Darmoul D, Gratio V, Devaud H, Lehy T, Laburthe M. Aberrant expression and activation of the thrombin receptor protease-activated receptor-1 induces cell proliferation and motility in human colon cancer cells. Am J Pathol 2003; 162:1503–1513.
175. Maragoudakis ME, Tsopanoglou NE, Andriopoulou P. Andriopoulou P. Mechanism of thrombin-induced angiogenesis. Biochem Soc Trans 2002; 30:173–177.
176. Stenina OI. Regulation of gene expression in vascular cells by coagulation proteins. Curr Drug Targets 2003; 4:143–158.
177. Yin YJ, Salah Z, Maoz M, Ram SC, Ochayon S, Neufeld G, Katzav S, Bar-Shavit R. Oncogenic transformation induces tumor angiogenesis: a role for PAR-1 activation. FASEB J 2003; 17:163–174.
178. Carmeliet P. Biomedicine. Clotting factors build blood vessels. Science 2001; 293:1602–1604.
179. Coughlin SR. Thrombin signalling and protease-activated receptors. Nature 2000; 407:258–264.
180. Coughlin SR. Protease-activated receptors in vascular biology. Thromb Haemost 2001; 86:298–307.
181. Camerer E, Kataoka H, Kahn M, Lease K, Coughlin SR. Genetic evidence that protease-activated receptors mediate factor Xa signaling in endothelial cells. J Biol Chem 2002; 277:16081–16087.
182. Esumi N, Fan D, Fidler IJ. Inhibition of murine melanoma experimental metastasis by recombinant desulfatohirudin, a highly specific thrombin inhibitor. Cancer Res 1991; 51:4549–4556.
183. Zacharski LR. Anticoagulants in cancer treatment: malignancy as a solid phase coagulopathy. Cancer Lett 2002; 186:1–9.
184. Zacharski LR, Henderson WG, Rickles FR, Forman WB, Cornell Jr CJ, Forcier RJ, Edwards RL, Headley E, Kim SH, O'Donnell JF. Effect of warfarin anticoagulation on survival in carcinoma of the lung, colon, head

and neck, and prostate. Final report of VA Cooperative Study No. 75. Cancer 1984; 53:2046–2052.
185. Lebeau B, Chastang C, Brechot JM, Capron F, Dautzenberg B, Delaisements C, Mornet M, Brun J, Hurdebourcq JP, Lemarie E. Subcutaneous heparin treatment increases survival in small cell lung cancer. "Petites Cellules" Group Cancer 1994; 74:38–45.
186. Altinbas M, Coskun HS, Er O, Ozkan M, Eser B, Unal A, Cetin M, Soyuer S. A randomized clinical trial of combination chemotherapy with and without low-molecular-weight heparin in small cell lung cancer. J Thromb Haemost 2004; 2:1266–1271.
187. Wojtukiewicz MZ, Kozlowski L, Ostrowska K, Dmitruk A, Zacharski LR. Low molecular weight heparin treatment for malignant melanoma: a pilot clinical trial. Thromb Haemost 2003; 89:405–407.
188. von Tempelhoff GF, Harenberg J, Niemann F, Hommel G, Kirkpatrick CJ, Heilmann L. Effect of low molecular weight heparin (Certoparin) versus unfractionated heparin on cancer survival following breast and pelvic cancer surgery: a prospective randomized double-blind trial. Int J Oncol 2000; 16:815–824.
189. Bobek V, Boubelik M, Fiserova A, L'Uptovcova M, Vannucci L, Kacprzak G, Kolodzej J, Majewski AM, Hoffman RM. Anticoagulant drugs increase natural killer cell activity in lung cancer. Lung Cancer 2005; 47:215–223.
190. Gorelik E, Bere WW, Herberman RB. Role of NK cells in the antimetastatic effect of anticoagulant drugs. Int J Cancer 1984; 33:87–94.
191. Zangari M, Anaissie E, Barlogie B, Badros A, Desikan R, Gopal AV, Morris C, Toor A, Siegel E, Fink L, Tricot G. Increased risk of deep-vein thrombosis in patients with multiple myeloma receiving thalidomide and chemotherapy. Blood 2001; 98:1614–1615.
192. Kaushal V, Kohli M, Zangari M, Fink L, Mehta P. Endothelial dysfunction in antiangiogenesis-associated thrombosis. J Clin Oncol 2002; 20:3042.
193. Kuenen BC. Analysis of prothrombotic mechanisms and endothelial perturbation during treatment with angiogenesis inhibitors. Pathophysiol Haemost Thromb 2003; 33 (Suppl 1):13–14.
194. Kuenen BC, Tabernero J, Baselga J, Cavalli F, Pfanner E, Conte PF, Seeber S, Madhusudan S, Deplanque G, Huisman H, Scigalla P, Hoekman K, Harris AL. Efficacy and toxicity of the angiogenesis inhibitor SU5416 as a single agent in patients with advanced renal cell carcinoma, melanoma, and soft tissue sarcoma. Clin Cancer Res 2003; 9:1648–1655.
195. Kuenen BC, Levi M, Meijers JC, van Hinsbergh VW, Berkhof J, Kakkar AK, Hoekman K, Pinedo HM. Potential role of platelets in endothelial damage observed during treatment with cisplatin, gemcitabine, and the angiogenesis inhibitor SU5416. J Clin Oncol 2003; 21:2192–2198.
196. Kuenen BC, Levi M, Meijers JC, Kakkar AK, van Hinsbergh VW, Kostense PJ, Pinedo HM, Hoekman K. Analysis of coagulation cascade and endothelial cell activation during inhibition of vascular endothelial growth factor/vascular endothelial growth factor receptor pathway in cancer patients. Arterioscler Thromb Vasc Biol 2002; 22:1500–1505.

Chemistry and Biology of Heparin and Heparan Sulfate
H.G. Garg, R.J. Linhardt and C.A. Hales (Editors)

Chapter 26

Use of Heparin Preparations in Older Patients

ANTONELLA TUFANO and MATTEO NICOLA DARIO DI MINNO

Reference Centre of Coagulation Disorders,
Department of Clinical and Experimental Medicine, Naples, Italy

I. Introduction

Advanced age is associated with a dramatic increase in the rate of venous and arterial thrombosis; a shift to a pro-coagulant state occurs with aging, and aging itself is a risk factor for arterial and venous thrombosis (1–4). Moreover, there is an increased incidence of comorbid conditions with increasing age, which *per se* enhances the risk of developing thrombosis. On the other hand, age-related bleeding complications, changes in the coagulation system with aging, comorbidities, and poly-pharmacy may complicate anticoagulant treatment in the elderly (Table 1). In this chapter, the clinical use of heparins with emphasis on the limitations of their use in the elderly is examined, and perspectives in the area are presented.

Strategies to improve the safety of heparins in the elderly include: reducing dosages in older patients regardless of kidney function; using monitored unfractionated heparin therapy rather than subcutaneous low molecular weight heparins (LMWHs) in cases of severe renal insufficiency; monitoring anti-Xa activity of LMWHs in older individuals with renal failure; and replacing LMWHs with the theoretically safer direct Xa-inhibitor fondaparinux (5). Although suggestive, these possibilities deserve to be properly investigated. In this respect, it is worth stressing that older individuals have often been excluded from clinical trials devoted to prevention and treatment of arterial and venous thrombosis. Greater representation by geriatric patients in future studies with such agents would help address major unsolved issues and hopefully define newer strategies against thrombosis in the elderly.

II. Aging and the Haemostatic System

Thrombotic events are a major cause of morbidity in the elderly and are a growing concern in the medical community as the population ages. A shift to a pro-coagulant state occurs with aging and aging itself is a risk factor for arterial and venous thrombosis (Table 1); 80% of all deaths due to myocardial infarction (MI) occur in patients over the age of 65 years, 60% of them in patients aged 75, or older (1–4).

The abnormally high incidence of arterial and venous thrombosis in the elderly has prompted investigations of age-related changes in the haemostatic system (1–4; 6–10). Some broad conclusions are largely supported by the latest evidence:

- An increased responsiveness to various aggregating stimuli, elevated levels of β-thromboglobulin and an increased production of thromboxane A2 have been reported in the platelets of older individuals (reviewed in Ref. 1). Moreover, a decrease in the number of platelet prostacyclin and thromboxane A2 receptors has been observed with aging. These biochemical abnormalities are associated with changes in platelet membrane lipid composition (increase in the cholesterol/phospholipid ratio and decrease in linoleic acid) that in turn lead to changes in membrane fluidity.
- Fibrinolysis is impaired in the elderly, probably due to the abnormally high circulating levels of plasminogen activator inhibitor 1 (PAI 1) (1).
- Plasma concentrations of pro-coagulant factors increase in healthy adults, in parallel with the physiologic aging process. Aging is associated with raised plasma levels of factors VII, VIII, and IX, and fibrinogen, i.e., of factors predisposing to thrombosis (1–4; 6–10).
- Raised plasma concentrations of some coagulation factors (fibrinogen, factors VII, VIII, and IX), as well as abnormalities in plasma coagulation factors and inhibitors are associated with the development and progression of ischemic heart disease and stroke (11–22).
- Indices (markers) of coagulation activation, including prothrombin fragment 1 + 2 (F 1 + 2), thrombin–antithrombin complex (TAT), and D-dimer (DD), are positively correlated with age and are independent

Table 1 Older Individuals: High Risk Setting for Thrombosis/Bleeding

Thrombosis	Factors predisposing to bleeding	Both
Hypercoagulability*	Vascular fragility	Hypertension
Diabetes, obesity	Psychiatric disorders	Drug metabolism
Dyslipidemia	Falls, traumas, dementia	Stroke history
Immobility		Liver disease

*High levels of plasma fibrinogen, factors VII and VIII, fibrinopeptide A, PAI-1, and/or increased platelet activation.

of sex. Mean plasma levels of (F 1 + 2), TAT, and DD are 2- to 3-fold higher in individuals $\geq$ 60 years of age than in younger individuals (19).

- In community-dwelling elderly persons, each decade of age is associated with a 25.9% elevation in DD, or a 1.8 increased odds of having a DD > 600 μg/L (21). In patients, > 70 years of age undergoing major abdominal surgery, baseline F 1 + 2, TAT, and DD levels are higher than in those < 60 years of age (22).
- With increasing age, there is an increased incidence of comorbid conditions (prolonged bed rest, heart failure, previous thromboembolic events, cancer, and arterial hypertension), which *per se* are associated with an increased risk of thrombosis (2,3).

III. Unfractionated Heparin, Low Molecular Weight Heparins, and Fondaparinux: Pharmacological Properties

At present, unfractionated heparin (UFH) and LMWHs are the strategies of choice for the prevention and treatment of acute venous thromboembolism (VTE) [deep vein thrombosis (DVT) and pulmonary embolism (PE)], and for the early treatment of acute coronary syndromes (ACS) and myocardial infarction (MI) (23–25). Heparins have also been evaluated in the secondary prevention of VTE as an alternative to oral anticoagulation (OAC) (23–25). A short description of the pharmacological properties of heparins and fondaparinux will help clarify efficacy and safety issues related to their use.

A. Unfractionated Heparin

UFH is a heterogeneous mixture of glycosaminoglycans that binds to antithrombin via a pentasaccharide, and catalyzes the inactivation of thrombin and of other clotting factors (23). Its molecular weight ranges from 3000 to 30,000 Da, with a mean molecular weight of 15,000 Da. Binding to entities other than antithrombin (endothelial cells, platelet factor 4, blood platelets, and macrophages), leads to rather unpredictable pharmacokinetic and pharmacodynamic properties. UFH is cleared through a rapid saturable mechanism (binding to endothelial cell receptors and macrophages, where it is depolymerized), and a slower nonsaturable mechanism (renal clearance) (23). At therapeutic doses, a considerable proportion of heparin is cleared through the rapid, saturable mechanism. These kinetics make the anticoagulant response to heparin rather unpredictable at therapeutic doses, and explain the very high heparin requirement of some patients ("heparin resistance") (23). UFH also has biological [heparin-induced thrombocytopenia (HIT) and osteoporosis] and biophysical limitations (the heparin-antithrombin complex is unable to inactivate thrombin bound to fibrin and factor Xa bound to phospholipid surfaces within the prothrombinase complex). This may explain why heparin is of limited efficacy in the presence of thrombi, such as in unstable angina, in high-risk coronary angioplasty, and in coronary thrombolysis (23).

B. Low Molecular Weight Heparins

LMWHs have a mean molecular weight of 4000–5000 Da, with a range of 2000–9000 Da (23). They are derived from UFH by chemical or enzymatic depolymerization. Because of the different methods of depolymerization, LMWHs differ in pharmacokinetic properties and anticoagulant profiles, and may not be clinically interchangeable (23–25). The depolymerization of heparin yields fragments with decreased propensity to bind proteins and cells (endothelial cells and macrophages). As a result, LMWHs have a rather predictable pharmacokinetics. In particular, the reduced binding to plasma proteins leads to an almost linear dose–response relationship (23), while the lower binding to macrophages and endothelial cells prolongs their plasma half-life (23). Moreover, compared with UFH, LMWHs have a lower binding to platelet factor 4 (PF4), which implies a lower incidence of heparin-induced thrombocytopenia and to osteoblasts (lower levels of bone loss) (23). However, LMWHs have the same biophysical limitation of UFH (i.e., they are unable to inactivate thrombin bound to fibrin and factor Xa bound to phospholipid surfaces within the prothrombinase complex) (23–25). Nevertheless, LMWHs have almost replaced UFH for most clinical indications because of: the quicker onset of anticoagulant activity; the longer half-life that allows for twice-daily, or once-daily dosing; the possibility to be administered as subcutaneous (s.c.) injections, which allows for out-of-hospital administration and, in turn, to the reduction of costs (home therapy or early hospital discharge); and the evidence from clinical trials that LMWHs are as least as effective and as safe as UFH.

Because of their predictable dose–response, LMWHs are administered in fixed doses for thromboprophylaxis, and in total body weight-adjusted doses for therapy; no laboratory monitoring is needed in either instance (23). In spite of this general rule, dose-finding trials in special populations (e.g., patients with renal failure, obese patients) are not available, suggesting the need for laboratory monitoring (antifactor Xa activity: "aXa") in these settings (23). At variance with UFH, LMWHs are mainly excreted through the kidney. Thus, repeated administration of therapeutic doses of LMWHs may lead to overdosage and/or an accumulation effect especially in patients with renal impairment, such as older individuals with a creatinine clearance (CrCl) = 30 mL/min. The clearance of the antifactor Xa effect of LMWHs is strongly correlated with CrCl, and there are differences among different LMWH preparations as to dependence on renal clearance (different pharmacokinetics). However, there is no CrCl cutoff value that correlates with an increased risk of bleeding complications for all LMWH preparations (23). Moreover, the doses currently used in prophylaxis have not been reported to require adjustment, or laboratory monitoring in the elderly or in patients with renal failure (23).

C. Fondaparinux

Fondaparinux is a small, synthetic molecule that selectively inhibits factor Xa (5) without significant effects on usual coagulation tests (aPTT and PT). In contrast to UFH and LMWH, fondaparinux does not bind to other purified plasma proteins

commonly involved in drug binding, including albumin and α_1-acid glycoprotein (5). Interestingly enough, fondaparinux does not interact with protamine sulfate, the antidote for UFH and some LMWH, it neither cross-reacts with heparin-platelet factor 4 antibodies, nor affects platelet aggregation and adhesion (5). This limited ability to interact with entities other than factor Xa predicts its reliable dose–responsiveness, and its low inter- and intra-individual variability (5). Pharmacokinetic studies in healthy volunteers indicate similar profiles in both young and older individuals (5). However, being excreted in the urine, dose adjustments are needed in renal insufficiency, and fondaparinux should not be used in patients with renal failure.

IV. Unfractionated Heparin, Low Molecular Weight Heparins, and Fondaparinux: Clinical Use in the Elderly

A. Unfractionated Heparin, Low Molecular Weight Heparins

1. VTE is a serious and potentially fatal complication associated with surgical trauma, particularly in elderly patients undergoing joint replacement and hip-fracture surgery (Table 2) (24). Because of prolonged immobility in bed after the operation, older patients with hip fractures undergoing major *orthopedic operations* are highly susceptible to fatal PE. Without prophylaxis, the risk of DVT in patients undergoing hip or knee replacement, or hip-fracture surgery ranges 41–85% (Table 2). Hip fracture surgery is primarily performed in very old individuals (>75 years), more so than hip and knee arthroplasty (65–69 years) (24). Fatal PE occurs in ≈1 out of 500 patients undergoing elective hip replacement (23,24). Randomized studies have documented the finding that LMWHs are safer and better than UFH in reducing the risk of VTE and PE in such patients (24).
2. *Acute medical illnesses* (acute infectious diseases, heart failure, acute respiratory failure, inflammatory bowel disease, acute ischemic stroke, acute MI, and cancer) are risk factors for VTE (24,26). Findings from a recent study evaluating the prevalence of asymptomatic DVT in older patients on admission to hospital for medical illnesses indicate a prevalence of silent DVT that increases from 4% in those 70–80 years, to almost 18% in those older than 80 years (26). In the MEDENOX trial, a population of acutely ill medical patients, more than half of

Table 2 VTE Prevalence After Major Orthopedic Surgery (Phlebography), in the Absence of Thromboprophylaxis

	DVT		PE	
	Total (%)	Proximal (%)	Total (%)	Fatal (%)
Hip arthroplasty	42–57	18–36	0.9–28	0.1–2.0
Knee arthroplasty	41–85	5–22	1.5–10	0.1–1.7
Hip fracture surgery*	46–60	23–30	3–11	2.5–7.5

* Hip fracture surgery is primarily performed in very old individuals (≥75 years).

whom were 75 years and older (mean age $\approx 73 \pm 10$ years) were randomized to receive 20- or 40-mg doses of enoxaparin or placebo for the prevention of VTE (27). Fourteen days after the randomization, the incidence of VTE was 14.9 and 15.0% in the group receiving placebo and the 20-mg dose of enoxaparin, respectively, and 5.5% in the group receiving the 40-mg dose of enoxaparin (significant reduction of VTE events with thromboprophylaxis with enoxaparin 40 mg; $P = 0.0002$). Major bleeding occurred in 1.7% of patients receiving the 40-mg dose, in 0.3% of patients receiving the 20-mg dose of enoxaparin, and in 1.1% of patients receiving placebo. Injection site hematomas were more frequent in patients on enoxaparin (27).

3. As in younger settings, i.v. UFH or s.c. LMWHs are the preferred *initial treatment of acute DVT and/or PE* in the elderly (28). Randomized trials have documented the equivalence of i.v. heparin and s.c. LMWHs in this setting. However, the inherent advantages (s.c. administration, home therapy, or early hospital discharge) argue for the use of LMWHs (28). Compared with younger patients, older patients require lower doses of i.v. UFH to maintain therapeutic aPTT levels. Treatment with i.v. UFH or s.c. LMWHs is recommended for at least 5 days (28). The administration of OAC is recommended in combination with heparins during the initial treatment with heparin, heparin withdrawal being recommended when the international normalized ratio (INR) of the PT value is consistently >2.0 (28).

4. Secondary treatment of VTE with vitamin K antagonists to prevent VTE recurrence is particularly challenging in the elderly because of this population's sensitivity to OAC-related bleeding (2,3). In the search for suitable alternatives to OAC-based therapy with vitamin K antagonists (VKA), heparins have been studied in the *secondary prevention of VTE*. This strategy turned out to be as effective as OAC in older patients and to exert a limited bleeding tendency. In this respect, enoxaparin (40 mg s.c. once-daily) has been compared with OAC (INR 2.0–3.0) for long-term (3-month) treatment (following standard 10-day UFH, i.v.) of confirmed symptomatic proximal DVT in a population with a mean age of 80 years (29). Recurrent DVT rates during the 3-month treatment period were 4% with enoxaparin and 2% with OAC, but during the total 1-year follow-up and surveillance period, these figures rose to 16 and 12%, respectively. Bleeding complications during the treatment period were 2% with enoxaparin, all minor bleedings, and 4% major and 8% minor bleedings with OAC. Major osteoporotic complications (4%) and unexplained back pain (4%) were both restricted to the enoxaparin arm of this study (29). The latter complications raise concerns about long-term treatment with heparins in the elderly. The reported 15% incidence of vertebral fractures in a subgroup of elderly patients undergoing long-term treatment for VTE with subcutaneous UFH (30) is of interest in this regard. In the study by Wawrzynska et al. (31), patients receiving LMWH or acenocoumarol for 3–24 months were studied with densitometry to assess their bone mineral density (BMD) at the beginning of the treatment, and after 1- and 2-years of follow-up. This study confirmed that the long-term exposure to drugs commonly used for the secondary prophylaxis of VTE causes a limited although progressive decrease in BMD, more evident with LMWHs than with acenocoumarol (31).

5. UFH and LMWHs have also been demonstrated to be effective in the *prevention of ischemic complications of unstable angina and non-Q-wave MI*, when concurrently administered with aspirin. The American College of Chest Physicians (ACCP) recommends UFH treatment in addition to antiplatelet therapy after fibrinolytic therapy (with either streptokinase or tPA) (32,33), or after percutaneous coronary angioplasty (PCI) (34).

Two studies have shown that antithrombotic therapy with enoxaparin was more effective than i.v. UFH in reducing the incidence of ischemic events in patients with unstable angina, or in the early phase of non-Q-wave MI [Efficacy Safety Subcutaneous Enoxaparin in Non-Q-wave Coronary Events (ESSENCE) and Thrombolysis in Myocardial Infarction 11B trials (TIMI 11B)] (35–37). However, the results of other studies in which different LMWHs have been employed (dalteparin and nadroparin) have been inconclusive with respect to the issue (38).

B. Fondaparinux

When compared with enoxaparin, fondaparinux, administered for 7 days, significantly reduced the risk of VTE in patients undergoing major orthopedic surgery (i.e., surgery for hip fracture) (5). Subpopulation analysis of the data showed that fondaparinux is equally effective in younger and older individuals (5,24). Additional data suggest that fondaparinux is beneficial also in treating acute DVT and possibly in preventing arterial thrombosis (5,24).

1. In clinical trials of *VTE prevention in patients undergoing hip replacement surgery*, fondaparinux reduced the risk of VTE by 55.9% when compared with enoxaparin (39,40), the risk reduction of VTE being 55.2% in patients undergoing *knee replacement surgery* ($P < 0.001$) (41). Importantly, this benefit was independent of patient age (42). In patients undergoing surgery for *hip fracture repair*, fondaparinux reduced the risk of VTE by 56.4% compared with enoxaparin (42). A pooled analysis of four phase III multicenter, randomized, double-blind trials in major orthopedic surgery (elective hip replacement, elective major knee surgery, and surgery for hip fracture) in 7344 patients (mean ages >65 years), led to the conclusion that fondaparinux was significantly more effective than enoxaparin for the prevention of VTE following major orthopedic surgery (6.8% *vs* 13.7%), with a common odds reduction of 55.2% ($P < 0.001$), the benefit was independent of patient's age. Major bleedings were more frequent in fondaparinux-treated patients ($P = 0.008$), but the incidence of hemorrhages leading to death or reoperation, or occurring in a critical organ, did not differ between the groups (43). It is possible that the increase in major bleeding with fondaparinux relative to enoxaparin reflects the fact that fondaparinux prophylaxis was started 6 h after surgery, whereas enoxaparin prophylaxis was started 12–24 h after surgery. Whether, and the extent to which, this asymmetry also accounts for the superior efficacy of fondaparinux relative to enoxaparin in the incidence of VTE is unclear as yet, and deserves to be absolutely clarified.

In the Penthifra Plus trial, extended prophylaxis with fondaparinux was evaluated in an elderly study population (median age, 79 years; range 23–96 years) undergoing surgery for hip fracture (44). Fondaparinux (2.5 mg once daily) was administered for an initial period of 7 ± 1 days to all patients, followed by randomization to the same fondaparinux dose, or to placebo for an additional 21 ± 2 days. Extended prophylaxis with fondaparinux reduced the incidence of *phlebographic VTE* [1.4% (3/208) *vs* 35.0% (77/220) in the placebo group], corresponding to a relative risk reduction of 96% ($P < 0.001$), and reduced the incidence of *symptomatic VTE* accordingly [0.3% (1/326) *vs* 2.7% (9/330)], corresponding to a relative risk reduction of 89% ($P = 0.02$) (44). A subanalysis of the Penthifra Plus data demonstrated that even in those defined as high-risk individuals (i.e., advanced age, female sex, and impaired renal function), extended prophylaxis for up to 31 days postsurgery was highly effective in reducing the risk of VTE without any increase in clinically relevant bleeding (44).

2. Fondaparinux has been evaluated in the *initial treatment of VTE* in two phase III trials (54,55). In the MATISSE DVT trial (45) and in the MATISSE PE trial (46), it was at least as effective and as safe as LMWHs or UFH for the initial treatment of DVT and PE (45,46).
3. Finally, fondaparinux has been evaluated in *percutaneous transluminal coronary angioplasty* (PTCA) (47), in patients with *ST-elevation acute MI* (333 patients, mean age 55–61 years) (PENTALYSE study) (48) and in *Unstable Angina* (PENTUA study) (reported in abstract 49).

V. Heparin and Low Molecular Weight Heparins: Risk of Bleeding in the Elderly

Different factors affect drug levels and drug sensitivity in the elderly (50–53). Alteration in drug kinetics and toxicity, coagulation factors, and changes in body composition and weight due to aging can affect anticoagulant therapy (53). In the Italian Study on Complications of Oral Anticoagulant Therapy (ISCOAT), the rate of bleeding complications during OAC was 10.5% per year in subjects 70 years or older, and 6.0% per year in those younger than 70 years (54). In 2376 patients followed in six anticoagulation clinics, patients older than 80 years had a relative risk (RR) of 4.5 for life threatening or fatal bleeding complications compared with patients younger than 50 years (55). In 565 warfarin-treated outpatients, a RR of 3.2 for major bleeding in patients 65 years and older was found with respect to younger patients (56).

UFH, like warfarin, is associated with an increased risk of bleeding in the elderly (53). This is associated with changes in coagulation factors and in body composition and weight, and to age-related changes in the quantity or quality of drug-binding proteins (i.e., albumin) (53). Renal function, in particular glomerular filtration rate, is reduced with aging, and this may contribute to the heparin response in these patients (53): older patients have higher than normal aPTTs

during UFH therapy for acute VTE or MI, and they require lower doses (800 IU/h rather than 1000–1200 IU/h) of i.v. UFH to maintain therapeutic aPTT levels (53). The risk of heparin-associated bleeding is increased not only by dose, but also by age, and by concomitant thrombolytic or antiplatelet therapy (23). In 11 studies that have examined age as a risk factor for heparin-related bleeding, eight (3662 patients) have reported a higher rate of bleeding among older patients, four demonstrating a RR of 2.9–4.2 for those older than 60 years, as compared with those younger than 60 years (57). Comorbid conditions, particularly recent surgery or trauma, are important cofactors for heparin-induced bleeding. The risk of bleeding is also increased by hemostatic defects, such as those occurring in subjects treated with antiplatelet and/or nonsteroidal antiinflammatory drugs (NSAID) (23,58). In keeping with this, other reports document that age >70 years is associated with a clinically relevant increased risk of major bleedings (58): poly-pharmacy is very common in subjects >70 years of age.

The risk of bleeding by LMWHs has been correlated with older age and impaired renal function (58). In this respect, a systematic case note review, from July 2002 to March 2003, has been carried out by the Department of Renal Medicine, the Hope Hospital, Salford, UK. Ten patients experienced an adverse incident on LMWH therapy. Five patients were on maintenance hemodialysis therapy; one patient was on continuous ambulatory peritoneal dialysis therapy; three patients had calculated CrCl of 5, 11, and 33 mL/min (0.08, 0.18, and 0.55 mL/s), and one patient had an estimated glomerular filtration rate of 12 mL/min. Age range was 45–89 years (59). Indications for anticoagulation were: suspected PE (1 patient), ACS (7 patients), severe nephrotic syndrome (1 patient), and prevention of postoperative VTE (1 patient). Three patients were also receiving aspirin; one, clopidogrel; and three were on aspirin + clopidogrel. The LMWHs used were enoxaparin (six patients), tinzaparin (three patients), and dalteparin sodium (one patient). Bleeding sources were retroperitoneal (one patient), soft tissues (three patients), gastrointestinal (two patients), sites of dialysis catheter and cannula (two patients), pericardium (one patient), and intracranial (one patient). Activated partial thromboplastin time was prolonged in 7 out of 10 patients, all other parameters were normal. Three patients died despite aggressive resuscitation. In all cases, LMWHs had been administered at fixed-weight doses without monitoring (59).

A careful evaluation of renal function and of poly-pharmacotherapy appears to be mandatory before therapy with LMWH is started in older patients. Because of the risk of accumulation and of increased anticoagulant effect, it has been suggested that patients with a CrCl of 30 mL/min, or less be excluded from treatment with LMWHs, or have aXa heparin level monitoring performed.

A systemic review of prospective papers comparing differences in pharmacokinetics of LMWH in nondialyzed patients with varying degrees of renal dysfunction, has evaluated three single-dose pharmacokinetic trials (in studies devoted to DVT prophylaxis) and two multiple-dose trials (DVT treatment) (60). The data from these studies argue against the use of a 30-mL/min (0.50-mL/s) cutoff of CrCl to identify individuals at risk of accumulation of LMWH. In contrast, four out of

the five trials argue for a cumulative effect of the antifactor Xa activity of only some LMWH preparations. For instance, tinzaparin sodium, a LMWH with a higher-than-average molecular weight distribution, does not exhibit accumulation in patients with CrCl as low as 20 mL/min (0.33 mL/s). (60). Thus, pharmacokinetic studies document that the response to impaired renal function, especially the risk of accumulation, may differ among different LMWH preparations (23). Other authors claim that maintaining the anti-Xa activity in its therapeutic range would minimize enoxaparin-associated hemorrhagic complications, particularly in high-risk patients. However, LMWHs-associated bleeding complications has been described in patients whose anti-Xa activity was within therapeutic ranges (23).

A retrospective analysis of antithrombotic effects on obese patients and on patients with severe renal impairment has been performed by the ESSENCE and by TIMI 11B trials, in which patients (mean ages >60 years) were treated with enoxaparin or UFH (61). The primary composite end point was death, MI, and urgent revascularization (UR), secondary end points being major and any bleeding. When compared to UFH, enoxaparin reduced the rate of the primary end point in obese subjects (14.3% *vs* 18.0%, $P = 0.05$), in subjects with normal body mass index (16.1% *vs* 19.2%, $P < 0.01$), and in those with normal renal function (15.7% *vs* 18.4%, $P < 0.01$). There was no significant difference between enoxaparin and UFH in the four subgroups, with respect to both primary end point (17.6% *vs* 16.2%, $P = 0.39$), and major and any bleeding (1.3% *vs* 0.8%, $P = 0.12$). This was true in obese patients and in those with normal body mass index, and both for UFH and enoxaparin. Patients with severe renal impairment tended to have a higher rate of the composite end point of death, MI, and urgent revascularization (25.9% *vs* 17%, $P = 0.09$) and experienced a higher number of major bleedings (6.6% *vs* 1.1%, $P < 0.0001$). Thus, in the combined analysis of ESSENCE and TIMI 11B trials, obesity did not impact clinical outcomes, while severe renal impairment did, the abnormally high risk of clinical events and of major bleedings being similar in subjects receiving UFH and in those on enoxaparin, in the latter setting (61).

There are reports implicating enoxaparin as a predisposing factor for *retroperitoneal hematoma* in older patients (62–64). Two cases of retroperitoneal hematoma in older patients receiving enoxaparin have been reported: two white men, aged 70 and 71 years, received enoxaparin 80 mg s.c. twice daily for 8 and 4 days, respectively (62). Baseline hemoglobin and hematocrit values were 9.5 g/dL and 28.9% and 11.2 g/dL and 32.8%, respectively. In both cases, after the hemoglobin and hematocrit values had decreased to 6.6 g/dL and 20.4%, and 5.1 g/dL and 15.2%, respectively, a computed tomography scan revealed a retroperitoneal hematoma. In addition to advanced age, both patients had mild renal impairment: one was receiving aspirin concomitantly; the other had received aspirin 4 days prior and warfarin 1 day prior to bleeding (62).

Although recent studies support the use of enoxaparin in the management of ACS, it is noteworthy that these studies excluded patients with CrCl less than 30 mL/min. Recent studies showed that using 65% of the recommended enoxaparin dose minimizes life-threatening bleeding complications in those with ACS and severe renal impairment (CrCl < 30 mL/min) (23). Vadnekar et al. (64)

reported two cases of old patients with impaired CrCl who spontaneously developed retroperitoneal hematomas while receiving enoxaparin therapy for ACS. An 86-year-old woman (weight 70 kg) being treated for acute pyelonephritis, developed a non-ST-elevation MI (NSTEMI) on the second day of her hospital stay. Her treatment regimen included enoxaparin, 70 mg every 12 h s.c., metoprolol, captopril, aspirin, and nitroglycerin. Her serum creatinine was 1.9 mg/dL with an estimated CrCl of 23 mL/min. On day 4, she complained of left hip pain, unresponsive to analgesics. She subsequently became hypotensive and tachycardic, and her hemoglobin decreased by 2 g/dL from the admission value. Abdominal computed tomography scan revealed a large left retroperitoneal hematoma. A 76-year-old woman (weight 73 kg) was admitted for new-onset atrial fibrillation. She was treated with enoxaparin 70 mg every 12 h s.c., metoprolol, digoxin, aspirin, and nitroglycerin. Her serum creatinine was 1.5 mg/dL with an estimated CrCl of 35 mL/min. On Day 5, the patient complained of severe right-sided flank pain. Examination showed ecchymoses of the right abdominal wall, and a significant drop (3.5 g/dL) in her hemoglobin value. Abdominal computed tomography scan showed a large right retroperitoneal hematoma. Platelet count, Pt INR, activated partial thromboplastin time were all within normal ranges, in both cases. Both patients were resuscitated with packed red blood cells and fresh frozen plasma with subsequent clinical improvement, although both needed prolonged hospitalization for rehabilitation (64). The patients were receiving conventional doses (1 mg/kg every 12 h) of enoxaparin. Based on these data, the authors suggest that although no definite guidelines are available for dosage adjustment of enoxaparin therapy in patients with impaired renal function, caution is needed in treating these subjects. They also suggest that, when treating geriatric patients with severe renal impairment (patients with ClCr = 30 mL/min have a 65% increase in their anti-Xa activity), the therapeutic dose of enoxaparin should be reduced to 65% of its recommended dose to minimize life-threatening bleeding complications. As to patients with mild (CrCl: 50–80 mL/min), or moderate (CrCl = 30–50 mL/min) renal dysfunction who are receiving enoxaparin, the authors suggest careful monitoring, while waiting for evidence-based information, which would define appropriate dose adjustments in these patients (64).

VI. Conclusions and Perspectives

UFH and LMWH are at least as effective in older individuals as in younger ones to prevent and treat thrombosis. However, they are associated with a higher risk of bleeding in older individuals, especially in those with kidney insufficiency. Comorbidities and poly-pharmacy, as well as changes in the coagulation system with aging emphasize such risk. To minimize the risk, thus improving the risk/benefit ratio of LMWHs in this setting, several approaches (65,66) are theoretically conceivable:

- *Replacing LMWHs with monitored UFH in cases of severe renal insufficiency.* No definitive report is available in this area. Comparative studies are needed to clarify whether UFH is really safer in this setting.

- *Using initial reduced dosages in older patients with or without renal failure.* Such a strategy has to be validated in controlled trials for each individual LMWH.
- *Monitoring anti-Xa activity before the next dose of LMWH in cases of renal impairment.* To document whether or not LMWH is accumulating in the blood, anti-Xa should be determined on two or three occasions. The reliability and cost-effectiveness of such monitoring is unclear so far.
- *Employing newer agents, such as factor Xa inhibitors,* to allow for higher selectivity and better control of anticoagulation than that presently achieved with UFH or LMWH. Whether the increase in major bleeding observed with fondaparinux relative to enoxaparin is only the result of different dose schedulings deserves to be further clarified.

Since older patients, especially those with renal failure, have been excluded from the large majority of the trials concerning anticoagulation in the elderly, and since the concepts stressed above imply the need for effective anticoagulation in such setting, *ad hoc* studies with clear-cut endpoints, and greater representation by geriatric patients in clinical trials of thromboembolism is mandatory. In addition to their obvious pathophysiological and clinical relevance as to efficacy and safety issues, we believe that this strategy will help define tailored interventions against thrombosis in older individuals.

References

1. Abbate R, Prisco D, Rostagno C, Boddi M, Gensini GF. Age-related changes in the hemostatic system. Int J Clin Lab Res 1993; 23:1–3.
2. Tufano A, Cerbone AM, Di Minno G. The use of antithrombotic drugs in older people. Minerva Med 2002; 93:13–26.
3. Di Minno G, Tufano A. Challenges in the prevention of venous thromboembolism in the elderly. J Thromb Haemost 2004; 2:1292–1298.
4. Di Minno G, Mannucci PM, Tufano A *et al.* The first ambulatory screening on thromboembolism a multicentre, cross-sectional, observational study on risk factors for venous thromboembdism. J Thromb Haemost 2005; 3:1459–1466.
5. Weitz JI, Hirsh J, Samama MM. New anticoagulant drugs. The Seventh ACCP Conference on Antithrombotic and Thrombolytic Therapy. Chest 2004; 126:265S–286S.
6. Cadroy Y, Pierrejean D, Fontan B, Sié P, Boneu B. Influence of aging on the activity of the hemostatic system: prothrombin fragment 1+2, thrombin-antithrombin III complexes and D-dimers in 80 healthy subjects with age ranging from 20 to 94 years. Nouv Rev Fr Hematol 1992; 34:43–46.
7. Mari D, Mannucci PM, Coppola R, Bottasso B, Bauer KA, Rosenberg RD. Hypercoagulability in centenarians: the paradox of successful aging. Blood 1995; 85:3144–3149.
8. Bauer KA, Weiss LM, Sparrow D, Vokonas PS, Rosenberg RD. Aging-associated changes in indices of thrombin generation and protein C activation in humans. Normative Aging Study. J Clin Invest 1987; 80:1527–1534.

9. Javorschi S, Richard-Harston S, Labrouche S, Manciet G, Freyburger G. Relative influence of age and thrombotic history on hemostatic parameters. Thromb Res 1998; 91:241–248.
10. Sagripanti A, Carpi A. Natural anticoagulants, aging, and thromboembolism. Exp Gerontol 1998; 33:891–896.
11. Meade TW. Fibrinogen and cardiovascular disease. J Clin Pathol 1997; 50: 13–15.
12. Balleisen L, Bailey J, Epping P-H, Schulte H, van de LJ. Epidemiological study on factor VII, factor VIII and fibrinogen in an industrial population: I. Baseline data on the relation to age, gender, body-weight, smoking, alcohol, pill-using, and menopause. Thromb Haemost 1985; 54:475–479.
13. Baker IA, Eastham R, Elwood PC, Etherington M, O'Brien JR, Sweetnam PM. Haemostatic factors associated with ischaemic heart disease in men aged 45 to 64 years. The Speedwell study. Br Heart J 1982; 47:490–494.
14. Kannel WB, Wolf PA, Castelli WP, D'Agostino RB. Fibrinogen and risk of cardiovascular disease. The Framingham Study. JAMA 1987; 258:1183–1186.
15. Meade TW, Mellows S, Brozovic M, Miller GJ, Chakrabarti RR, North WR, Haines AP, Stirling Y, Imeson JD, Thompson SG. Haemostatic function and ischaemic heart disease: principal results of the Northwick Park Heart Study. Lancet 1986; 2:533–537.
16. Woodward M, Lowe GD, Rumley A, Tunstall-Pedoe H, Philippou H, Lane DA, Morrison CE. Epidemiology of coagulation factors, inhibitors and activation markers: the Third Glasgow MONICA Survey. II. Relationships to cardiovascular risk factors and prevalent cardiovascular disease. Br J Haematol 1997; 97:785–797.
17. Conlan MG, Folsom AR, Finch A, Davis CE, Sorlie P, Marcucci G, Wu KK. Associations of factor VIII and von Willebrand factor with age, race, sex, and risk factors for atherosclerosis. The Atherosclerosis Risk in Communities (ARIC) Study. Thromb Haemost 1993; 70:380–385.
18. Conlan MG, Folsom AR, Finch A, Davis CE, Marcucci G, Sorlie P, Wu KK. Antithrombin III: associations with age, race, sex and cardiovascular disease risk factors. The Atherosclerosis Risk in Communities (ARIC) Study Investigators. Thromb Haemost 1994; 72:551–556.
19. Lowe GD, Rumley A, Woodward M, Morrison CE, Philippou H, Lane DA, Tunstall-Pedoe H. Epidemiology of coagulation factors, inhibitors and activation markers: the Third Glasgow MONICA Survey. I. Illustrative reference ranges by age, sex and hormone use. Br J Haematol 1997; 97:775–784.
20. Cadroy Y, Pierrejean D, Fontan B, Sie P, Boneu B. Influence of aging on the activity of the hemostatic system: prothrombin fragment 1+2, thrombin-antithrombin III complexes and D-dimers in 80 healthy subjects with age ranging from 20 to 94 years. Nouv Rev Fr Hematol 1992; 34:43–46.
21. Pieper CF, Rao KM, Currie MS, Harris TB, Chen HJ. Age, functional status, and racial differences in plasma D-dimer levels in community-dwelling elderly persons. J Gerontol A Biol Sci Med Sci 2000; 55:M649–M657.
22. Boldt J, Huttner I, Suttner S, Kumle B, Piper SN, Berchthold G. Changes of haemostasis in patients undergoing major abdominal surgery is there a difference between elderly and younger patients? Br J Anaesth 2001; 87:435–440.

23. Hirsh J, Raschke R. Heparin and low-molecular-weight heparin. The Seventh ACCP Conference on Antithrombotic and Thrombolytic Therapy. Chest. 2004; 126:188S–203S.
24. Geerts WH, Pineo GF, Heit JA, Bergqvist D, Lassen MR, Colwell CW, Ray JG. Prevention of venous thromboembolism. The Seventh ACCP Conference on Antithrombotic and Thrombolytic Therapy. Chest 2004; 126:338S–400S.
25. Hirsh J. Low-molecular weight heparin. A review of the results of recent studies of the treatment of venous thromboembolism and unstable angina. Circulation 1998; 98:1575–1582.
26. Oger E, Bressollette L, Nonent M, Lacut K, Guias B, Couturaud F, Leroyer C, Mottier D. High prevalence of asymptomatic deep vein thrombosis on admission in a medical unit among elderly patients. Thromb Haemost 2002; 88: 592–597.
27. Samama MM, Cohen AT, Darmon J-Y, Desjardins L, Eldor A, Janbon C, Leizorovicz A, Nguyen H, Olsson C-G, Turpie AG, Weisslinger N, for the Prophylaxis in Medical Patients with Enoxaparin Study Group. A comparison of enoxaparin with placebo for the prevention of venous thromboembolism in acutely ill medical patients. N Engl J Med 1999; 341:793–800.
28. Buller HR, Agnelli G, Hull RH, Hyers TM, Prins MH, Raskob GE. Antithrombotic therapy for venous thromboembolic disease. The Seventh ACCP Conference on Antithrombotic and Thrombolytic Therapy. Chest 2004; 126:401S–428S.
29. Veiga F, Escribá A, Maluenda MP, López Rubio M, Margalet I, Lezana A, Gallego J, Ribera JM. Low molecular weight heparin (enoxaparin) versus oral anticoagulant therapy (acenocoumarol) in the long-term treatment of deep venous thrombosis in the elderly: a randomized trial. Thromb Haemost 2000; 84:559–564.
30. Monreal M, Lafoz E, Olive A, del Rio L, Vedia C. Comparison of subcutaneous unfractionated heparin with a low molecular weight heparin (Fragmin) in patients with venous thromboembolism and contraindications to coumarin. Thromb Haemost 1994; 71:7–11.
31. Wawrzynska L, Tomkowski WZ, Przedlacki J, Hajduk B, Torbicki A. Changes in bone density during long-term administration of low-molecular weight heparins or acenocoumarol for secondary prophylaxis of venous thromboembolism. Pathophysiol Haemost Thromb 2003; 33:64–67.
32. Harrington RA, Becker RC, Ezekowitz M, Meade TW, O'Connor CM, Volchheimer DA, Guyatt GH. Antithrombotic therapy for coronary artery disease. The Seventh ACCP Conference on Antithrombotic and Thrombolytic Therapy. Chest 2004; 126:513S–548S.
33. Menon V, Harrington RA, Hochman JS, Cannon CP, Goodman SD, Wilcox RG, Schunemann HJ, Ohman EM. Thrombolysis and adjunctive therapy in acute myocardial infarction. The Seventh ACCP Conference on Antithrombotic and Thrombolytic Therapy. Chest 2004; 126:549S–575S.
34. Popma JJ, Berger P, Ohman EM, Harrington RA, Grines C, Weitz JI. Antithrombotic Therapy during Percutaneous Coronary Intervention. The Seventh ACCP Conference on Antithrombotic and Thrombolytic Therapy. Chest 2004; 126:576S–599S.

35. Cohen M, Demers C, Gurfinkel EP, Turpie AG, Fromell GJ, Goodman S, Langer A, Califf RM, Fox KA, Premmereur J, Bigonzi F. A comparison of low-molecular-weight heparin with unfractionated heparin for unstable coronary artery disease. Efficacy and Safety of Subcutaneous Enoxaparin in Non-Q-Wave Coronary Events Study Group. N Engl J Med 1997; 337:447–452.
36. Antman EM, McCabe CH, Gurfinkel EP, Turpie AG, Bernink PJ, Salein D, Bayes De Luna A, Fox K, Lablanche JM, Radley D, Premmereur J, Braunwald E. Enoxaparin prevents death and cardiac ischemic events in unstable angina/non-Q-wave myocardial infarction. Results of the Thrombolysis in Myocardial Infarction (TIMI) 11B trial. Circulation 1999; 100:1593–1601.
37. Antman EM, Cohen M, Radley D, Mc Cabe C, Rush J, Premmereur J, Antman EM, Cohen M, Radley D, McCabe C, Rush J, Premmereur J, Braunwald E. Assessment of the treatment effect of enoxaparin for unstable angina/non-Q-wave myocardial infarction. TIMI11B-ESSENCE meta-analysis. Circulation 1999; 100:1602–1608.
38. Turpie AG, Antman EM. Low-molecular-weight heparins in the treatment of acute coronary syndromes. Arch Intern Med 2001; 161:1484–1490.
39. Lassen MR, Bauer KA, Eriksson BI, Turpie AGG, for the European Pentasaccharide Hip Elective Surgery Study (EPHESUS) Steering Committee. Postoperative fondaparinux versus preoperative enoxaparin for prevention of venous thromboembolism in elective hip-replacement surgery: a randomised double-blind comparison. Lancet 2002; 359:1715–1720.
40. Turpie AGG, Bauer KA, Eriksson BI, Lassen MR, for the PENTATHLON 2000 Study Steering Committee. Postoperative fondaparinux versus postoperative enoxaparin for prevention of venous thromboembolism after elective hip-replacement surgery: a randomised double-blind trial. Lancet 2002; 359:1721–1726.
41. Bauer KA, Eriksson BI, Lassen MR, Turpie AGG, for the Steering Committee of the Pentasaccharide in Major Knee Surgery Study. Fondaparinux compared with enoxaparin for the prevention of venous thromboembolism after elective major knee surgery. N Engl J Med 2001; 345:1305–1310.
42. Eriksson BI, Bauer KA, Lassen MR, Turpie AGG, for the Steering Committee of the Pentasaccharide in Hip-Fracture Surgery Study. Fondaparinux compared with enoxaparin for the prevention of venous thromboembolism after hip-fracture surgery. N Engl J Med 2001; 345:1298–1304.
43. Turpie AGG, Bauer KA, Eriksson BI, Lassen MR, for the Steering Committees of the Pentasaccharide Orthopedic Prophylaxis Studies. Fondaparinux vs enoxaparin for the prevention of venous thromboembolism in major orthopedic surgery: a meta-analysis of 4 randomized double-blind studies. Arch Intern Med 2002; 162:1833–1840.
44. Eriksson BI, Lassen MR, for the PENTasaccharide in Hip-FRActure Surgery Plus (PENTHIFRA Plus) Investigators. Duration of prophylaxis against venous thromboembolism with fondaparinux after hip fracture surgery. Arch Intern Med 2003; 163:1337–1342.
45. Buller HR, Davidson BL, Decousus H, Gallus A, Gent M, Piovella F, Prins MH, Raskob G, Segers AE, Cariou R, Leeuwenkamp O, Lensing AW; Matisse Investigators. Fondaparinux or enoxaparin for the initial treatment of

symptomatic deep venous thrombosis: a randomized trial. Ann Intern Med 2004; 140:867–873.
46. The MATISSE Investigators. Subcutaneous fondaparinux versus intravenous unfractionated heparin in the initial treatment of pulmonary embolism. N Engl J Med 2003; 349:1695–1702.
47. Vuillemenot A, Schiele F, Meneveau N, Claudel S, Donat F, Fontecave S, Cariou R, Samama MM, Bassand JP. Efficacy of a synthetic pentasaccharide, a pure factor Xa inhibitor, as an antithrombotic agent—a pilot study in the setting of coronary angioplasty. Thromb Haemost 1999; 81:214–220.
48. Coussement PK, Bassand JP, Convens C, Vrolix M, Boland J, Grollier G, Michels R, Vahanian A, Vanderheyden M, Rupprecht H-J, Van de Werf F, for the PENTALYSE investigators. A synthetic factor-Xa inhibitor (ORG31540/SR9017A) as an adjunct to fibrinolysis in acute myocardial infarction. The PENTALYSE study. Eur Heart J 2001; 22:1716–1724.
49. Ferguson JJ. Meeting highlights: American Heart Association scientific sessions 2001. Circulation 2002; 105:e37–e41.
50. Gurwitz JH, Avorn J. The ambigous relation between ageing and adverse reactions. Ann Intern Med 1991; 114:956–966.
51. Montamat SC, Cusack BJ, Vestal RE. Management of drug therapy in the elderly. N Engl J Med 1989; 321:303–309.
52. Everitt DE, Avorn J. Drug prescribing for the elderly. Arch Intern Med 1986; 146:2393–2396.
53. Campbell NRC, Hull RD, Brant R, Hogan DB, Pineo GF, Raskob GE. Aging and heparin-related bleeding. Arch Intern Med 1996; 156:857–860.
54. Palareti G, Leali N, Coccheri S, Poggi M, Manotti C, D'Angelo A, Pengo V, Erba N, Moia M, Ciavarella N, Devoto G, Berrettini M, Musolesi S, on behalf of the Italian Study on Complications of Oral Anticoagulant Therapy. Bleeding complications of oral anticoagulant treatment: an inception-cohort, prospective collaborative study (ISCOAT). Lancet 1996; 348:423–428.
55. Fihn SD, Callahan CM, Martin DC, McDonell MB, Henikoff JG, White RH, for the National Consortium of Anticoagulation Clinics. The risk for and severity of bleeding complications in elderly patients treated with warfarin. Ann Intern Med 1996; 124:970–979.
56. Landefeld CS, Goldman L. Major bleeding in outpatients treated with warfarin: incidence and prediction by factors known at the start of outpatient therapy. Am J Med 1989; 87:144–152.
57. Beyth RJ, Landefeld CS. Anticoagulants in older patients: a safety perspective. Drugs Aging 1995; 6:45–54.
58. Levine MN, Raskob G, Beyth RJ, Kearon C, Schulman S. Hemorrhagic Complications of Anticoagulant Treatment. The Seventh ACCP Conference on Antithrombotic and Thrombolytic Therapy. Chest 2004; 126:287S–310S.
59. Farooq V, Hegarty J, Chandrasekar T, Lamerton EH, Mitra S, Houghton JB, Kalra PA, Waldek S, O'Donoghue DJ, Wood GN. Serious adverse incidents with the usage of low molecular weight heparins in patients with chronic kidney disease. Am J Kidney Dis 2004; 43:531–537.
60. Nagge J, Crowther M, Hirsh J. Is impaired renal function a contraindication to the use of low-molecular-weight heparin? Arch Intern Med 2002; 162: 2605–2609.

61. Spinler SA, Inverso SM, Cohen M, Goodman SG, Stringer KA, Antman EM; ESSENCE and TIMI 11B Investigators. Safety and efficacy of unfractionated heparin versus enoxaparin in patients who are obese and patients with severe renal impairment: analysis from the ESSENCE and TIMI 11B studies. Am Heart J 2003; 146:33–41.
62. Melde SL. Enoxaparin-induced retroperitoneal hematoma. Ann Pharmacother 2003; 37:822–824.
63. Vadnerkar A, Brensilver JM. Enoxaparin-associated spontaneous retroperitoneal hematoma in elderly patients with impaired creatinine clearance: a report of two cases. J Am Geriatr Soc 2004; 52:477–479.
64. Montoya JP, Polaka N, Melde SL. Retroperitoneal hematoma and enoxaparin. Ann Intern Med 1999; 131:796–797.
65. Siguret VA, Pautas EB, Gouin IA. Low molecular weight heparin treatment in elderly subjects with or without renal insufficiency: new insights between June 2002 and March 2004. Curr Opin Vasc Med 2004; 10:366–370.
66. Shojania AM. More on: laboratory monitoring of low molecular weight heparin necessary? J Thromb Haemost 2004; 2:2276–2277.

Chemistry and Biology of Heparin and Heparan Sulfate
H.G. Garg, R.J. Linhardt and C.A. Hales (Editors)

Chapter 27

Advances in Low Molecular Weight Heparin Use in Pregnancy

ANDREW J. THOMSON

Department of Obstetrics and Gynaecology,
Royal Alexandra Hospital, Paisley, Scotland, UK

and

IAN A. GREER

Regius Professor of Obstetrics and Gynaecology,
Reproductive and Maternal Medicine, University of Glasgow,
Glasgow, Scotland, UK

I. Introduction

Antithrombotic therapy is commonly employed in pregnancy for prophylaxis and treatment of venous thromboembolism (VTE). In these situations, low molecular weight heparin (LMWH) is preferred to either unfractionated heparin or oral anticoagulants. Compared with unfractionated heparin, LMWH has a better safety profile, is easier to administer, and at least in the non-pregnant patient, is as effective for prophylaxis and treatment of VTE. This chapter focuses on the pharmacology of LMWH in pregnancy, outlines the indications for heparin treatment in pregnancy and reviews the evidence for the safety of LMWH use in pregnancy.

II. Pharmacology and Pharmacokinetics of Low Molecular Weight Heparin in Pregnancy

LMWHs are polysulphated glycosaminoglycans with a mean molecular weight of 4000–5000 Da (range 2000–9000 Da). They are derived from unfractionated heparin by chemical or enzymatic depolymerisation. Since the LMWHs in clinical use are produced by different methods of depolarisation, their pharmacokinetic properties differ to some extent and they are not clinically interchangeable. Furthermore,

depolymerisation results in low-molecular-weight fragments with reduced binding to proteins or cells. Many of the pharmacokinetic and biological differences between LMWH and unfractionated heparin can be explained by the lower binding properties of LMWHs (1). Reduced binding to plasma proteins is responsible for the more predictable dose–response relationship of LMWHs (2), and a reduced binding to macrophages and endothelial cells increases the plasma half-life of LMWHs compared with unfractionated heparin (3). The lower binding properties of LMWHs compared with unfractionated heparin may also explain the better side-effect profile of LMWHs (see following text). For example, reduced binding of LMWHs to platelets and platelet factor 4 may explain the lower incidence of heparin-induced thrombocytopenia (4), whilst reduced binding to osteoclasts result in a lower incidence of activation of osteoclasts and less bone loss (5,6). Early studies in non-pregnant subjects indicated that LMWHs had superior pharmacokinetic properties than unfractionated heparins.

In summary, LMWHs were found to have a subcutaneous bioavailability approaching 100% at low doses, whilst peak activity (determined by anti-factor Xa activity) occurred 3–5 h after subcutaneous injection, with a more predictable dose response (7). LMWHs are cleared principally by the renal route, and compared with unfractionated heparin, their elimination half-life is longer.

The physiological adaptations of pregnancy can alter the pharmacokinetics of LMWH (8,9). In normal pregnancy, the plasma volume increases progressively and by 34 weeks' gestation, it increases by about 50%. The renal plasma flow rises very early in pregnancy and increases by 60–80% by the second trimester whilst the glomerular filtration rate also increases significantly and creatinine clearance rises by about 50%.

Studies have reported on the pharmacokinetics of various LMWH preparations administered in pregnancy, including enoxaparin sodium (10,11), dalteparin (12–14), reviparin (15), and tinzaparin (16).

A. Pharmacokinetics of Enoxaparin in Pregnancy

Casele et al. (11) investigated the pharmacokinetics of enoxaparin in pregnancy by determining the anti-factor Xa activity following the administration of 40 mg of the drug in 13 pregnant women in early pregnancy, late pregnancy, and in the non-pregnant state. They demonstrated that during early and late pregnancy, maximum concentration and the last measurable anti-factor Xa activity level were significantly lower than in the non-pregnant state. The authors conclude that these differences arise because of increased renal clearance of enoxaparin during pregnancy and that they may have implications for appropriate dosing of enoxaparin in pregnancy.

B. Pharmacokinetics of Dalteparin in Pregnancy

The pharmacokinetics of dalteparin has been investigated by several groups (12–14). Sephton et al. (13) undertook a longitudinal prospective, observational study in 24 women with antiphospholipid syndrome who self-administered 5000 IU

of dalteparin once daily throughout pregnancy. Plasma anti-factor Xa activity was determined at 12, 24, and 36 weeks' gestation and at 6 weeks' postpartum. This group demonstrated that mean peak anti-factor Xa activities were significantly less in each trimester than in the non-pregnant state, and that the lowest dose–response curve was at 36 weeks' gestation. The authors concluded that it would be inappropriate to extrapolate dosing and lack of dose monitoring in pregnant women, using data derived from the non-pregnant.

In a similar study performed to investigate the administration of dalteparin and unfractionated heparin, before, and in each of the trimesters of pregnancy in women with antiphospholipid syndrome, Ensom and Stephenson (14) demonstrated differences in the pharmacokinetics of dalteparin, but not unfractionated heparin, during pregnancy. For dalteparin, significant differences were detected (using area under the curve) between: (1) pre-pregnancy levels *vs* third trimester, (2) first *vs* second trimester, (3) first *vs* third trimester, and (4) second *vs* third trimester. The authors conclude that the dose of dalteparin should be increased in pregnancy and that dosing adjustments guided by selective anti-factor Xa activity may be warranted.

C. Pharmacokinetics of Reviparin in Pregnancy

Crowther et al. (15) determined the pharmacokinetics of the LMWH reviparin in 42 women who were participating in a pilot project to investigate the use of LMWH in high-risk pregnancies. The authors found that the initial degree of anticoagulation (measured by the anti-factors Xa activity) is dependent on the patient's weight, and that the achieved degree of anticoagulation falls throughout pregnancy as the patient's weight increases. These results suggest that, at least for reviparin, dose adjustment will be required during pregnancy to reflect changes in patient's weight.

D. Pharmacokinetics of Tinzaparin in Pregnancy

Tinzaparin has been investigated during pregnancy in pharmacokinetic studies performed to determine the appropriate dosage required for both prevention and treatment of VTE (16,17). In total, 54 pregnant women were investigated – 12 received treatment doses of tinzaparin to manage acute VTE (175 IU/kg/day), whilst another 42 received thromboprophylaxis. Women receiving thromboprophylaxis were allocated to one of four doses of tinzaparin: 50, 75, 100, or 175 IU/kg depending on the perceived clinical risk. Peak anti-Xa levels (4 h after subcutaneous injection) were determined in each trimester of pregnancy. Further, 24-h anti-Xa profiles were measured at 28 and 36 weeks' gestation. The dose of tinzaparin was increased when peak anti-Xa levels were less than 0.1 IU/ml.

The authors concluded that the pharmacokinetics of tinzaparin was affected by pregnancy. Twenty per cent of women receiving 50 IU/kg of tinzaparin per day required a dose increase and a small but significant reduction in anti-Xa levels was observed in the high risk/treatment group (175 IU/kg) with advancing gestation.

In summary, these studies indicate that the pharmacokinetics of LMWHs is altered in pregnancy probably secondary to an increase in the plasma volume and an increased renal excretion. These findings may have implications for the dosing and monitoring of LMWH treatment in pregnancy.

III. Indications for the Use of Low Molecular Weight Heparin in Pregnancy

National clinical guidelines have recommended the use of anticoagulant therapy with LMWH in several situations in pregnancy, including: (1) the management of VTE (18,19), (2) prophylaxis against arterial or venous thrombosis (19–21), (3) the prevention of thrombosis in women with mechanical heart valves (19), and (4) the management of recurrent miscarriage associated with antiphospholipid syndrome (19,22). Antithrombotic therapy with LMWH has also been recommended in the management of women with congenital or acquired thrombophilia and a history of adverse pregnancy outcome (recurrent miscarriage, prior severe or recurrent pre-eclampsia, placental abruption, or unexplained foetal death) (19,23).

A. Management of Venous Thromboembolism in Pregnancy

Venous thromboembolism remains a major cause of maternal death in the developed world. When VTE is suspected during pregnancy, treatment with LWMH (or, unfractionated heparin) should be given until the diagnosis is confirmed or refuted by objective testing, unless such treatment is contraindicated. In non-pregnant patients, many well-conducted randomised trials and meta-analyses have compared intravenous unfractionated heparin and subcutaneous LMWH for the treatment of acute DVT and PTE (24,25). These studies show that LMWH is at least as safe and effective as unfractionated heparin in the non-pregnant, but LMWH is preferable during pregnancy in terms of ease of administration and safety (see later).

Other studies in non-pregnant patients have shown that long-term LMWH (and unfractionated heparin) is as effective and safe as warfarin for the prevention of recurrent VTE (26–28). In light of these data, guideline documents have proposed that in the pregnant patient with acute VTE, two alternative approaches are acceptable:

1. intravenous unfractionated heparin followed by at least 3 months of subcutaneous LMWH in therapeutic doses or adjusted-dose subcutaneous unfractionated heparin, or
2. adjusted-dose subcutaneous unfractionated heparin or therapeutic doses of LMWH can be used both for initial and long-term treatment.

Unfractionated heparin is monitored using the mid-interval activated partial thromboplastin time (APTT). The dose of unfractionated heparin will need to be adjusted so that the APTT ratio falls into the therapeutic target range (usually 1.5–2.5 times the average laboratory control value). The use of the APTT to monitor treatment with unfractionated heparin is problematic in pregnancy.

Clinical audits have shown that APTT testing is often poorly performed and is technically problematic, especially in late pregnancy when an apparent heparin resistance occurs owing to increased levels of fibrinogen and factor VIII. These difficulties can lead to unnecessarily high doses of heparin being administered, with subsequent haemorrhagic complications.

LMWHs have clear advantages over unfractionated heparin. They have a better bioavailabilty, a better safety profile compared to unfractionated heparin, and are more convenient for the patient to use and more convenient for the clinician to monitor. Treatment with LMWHs is monitored by measuring peak anti-Xa activity (3 h post-injection) using a chromogenic substrate assay. In this situation, a target therapeutic range of approximately 0.5–1.2 U/ml for anti-Xa should be used (18,29).

In non-pregnant patients, different therapeutic doses of LMWHs are recommended by different manufacturers (enoxaparin 1.5 mg/kg once daily; dalteparin 10,000–18,000 units once daily depending on body weight; tinzaparin 175 U/kg once daily). In view of recognised alterations in the pharmacokinetics of dalteparin and enoxaparin during pregnancy (see section above on pharmacokinetics of LMWHs in pregnancy), a twice daily dosage regimen is recommended for these LMWHs in the treatment of VTE in pregnancy (30) (enoxaparin 1 mg/kg twice daily; dalteparin 100 U/kg twice daily up to a maximum of 18,000 units per 24 h. These doses are also used to treat VTE without pregnancy). Preliminary data suggest that once daily administration of tinzaparin (175 IU/kg) may be appropriate in the treatment of VTE in pregnancy (17).

Since most women gain weight as pregnancy progresses, there is the potential for a change in the LMWH's volume of distribution, and some authors have proposed that the dose of LMWH should be increased as pregnancy advances (13,15). Our experience of the LMWH, enoxaparin administered in a dose of 1 mg/kg 12 hourly (Table 1) suggests that dose adjustments are rarely required and monitoring is not necessary (using the therapeutic range of approximately 0.5–1.2 U/ml for anti-Xa), or need only be done infrequently (29), or in unusual situations such as extremes of body weight.

1. Maintenance Treatment

Following initial heparinisation, maintenance of anticoagulation with warfarin is recommended in non-pregnant patients with VTE. In view of the foetal complica-

Table 1 Initial Dose of the LMWH Enoxaparin for Acute Treatment of VTE in Pregnancy

Early pregnancy weight (kg)	Initial dose of enoxaparin (mg twice daily)
<50	40
50–69	60
70–89	80
≥90	100

tions of warfarin administration during pregnancy (discussed below), adjusted-dose subcutaneous, unfractionated heparin, or subcutaneous LMWH in therapeutic doses are employed for maintenance treatment in pregnancy (19). Guideline documents recommend that therapeutic levels of anticoagulation should be continued throughout pregnancy because of the ongoing prothrombotic changes in the coagulation system and venous flow, and the risk of recurrent venous thromboembolism during this time (18). However, in certain clinical situations, notably patients with contraindications to warfarin (31) and patients with malignant disease (32), the dose of heparin has been successfully reduced to an intermediate dose after initial full-dose anticoagulation in an attempt to reduce the risks of anticoagulant-related bleeding and heparin-induced osteoporosis. This type of modified dosing regimen may be useful in pregnant women who require prolonged periods of anticoagulation with heparin although there have been no comparative studies investigating these strategies in pregnancy. Further, a high recurrence rate of VTE was reported (47%) in a trial of non-pregnant patients when thromboprophylactic doses of unfractionated heparin were employed after initial management with intravenous unfractionated heparin (33).

2. *Labour and Delivery*

In an attempt to minimise bleeding complications at the time of delivery (including epidural haematoma formation during neuraxial anaesthesia), heparin treatment should be discontinued 24 h prior to elective induction of labour or delivery by Caesarean section. If spontaneous labour occurs, the woman should be advised that she should not inject any further heparin until she has been clinically assessed. If the woman is in labour and she has been administering unfractionated heparin, then monitoring of the APTT should be performed and protamine sulphate may be given to reverse the heparin's anticoagulant effect, if required. A similar strategy has been proposed for the management of LMWH therapy during labour and delivery (i.e., discontinuing the LMWH 24 h prior to elective induction of labour or Caesarean section). Bleeding complications in pregnancy associated with LMWH do not appear to be a problem. However, the anticoagulant effects of LMWH are not fully reversed with protamine sulphate (34). For this reason, if this is considered to be a high risk of haemorrhage in a woman requiring anticoagulation, intravenous unfractionated heparin should be employed (as with cessation of the heparin infusion, the anticoagulant effects reverse promptly). Similarly, if the woman is deemed to have a very high risk of recurrent VTE (for example, a VTE diagnosed near term), then therapeutic intravenous unfractionated heparin can be initiated and discontinued 4–6 h prior to the expected time of delivery in order to limit the duration of time without therapeutic anticoagulation. These are essentially the only situations, where UFH may be preferred over LMWH in pregnancy. Some clinicians have proposed that in this situation, consideration should be given to the insertion of a temporary IVC filter and a planned induction of labour after reversal of anticoagulation (19,35).

The risk of epidural or spinal haematoma formation during neuraxial instrumentation in pregnant patients receiving LMWH has not been clearly quantified (36). In summary, guideline documents suggest that regional techniques should not be used until at least 12 h after the previous prophylactic dose of LMWH. When a woman presents on a therapeutic regimen of LMWH (for example enoxaparin 1 mg/kg, 12 hourly), then regional techniques should not be employed for at least 24 h after the last dose of LMWH. LMWH should not be given for at least 4 h after the epidural catheter has been removed and the cannula should not be removed within 10–12 h of the most recent injection (18).

Postpartum anticoagulants (either heparin or warfarin) should be given for at least six weeks, or until at least three months of anticoagulant therapy has been completed. Both heparin (unfractionated and LMWH) and warfarin can be used safely during breastfeeding.

B. Prophylaxis Against Thrombosis in Pregnancy

Controversy has surrounded the management of women with a single previous VTE. This has resulted from a wide variation in the risk of recurrent thrombosis that has been reported (1–13%) (19,37–40), and concerns about the hazards of long-term unfractionated heparin therapy that is discussed above. The higher estimate of risk led many clinicians to employ pharmacological prophylaxis with heparin, or low molecular weight heparin during pregnancy and the puerperium. However, these estimates of risk have significant limitations. For example, objective testing was not used in all cases; some of the studies were retrospective and the prospective studies had relatively small sample sizes. Brill-Edwards and Ginsberg (41) reported a prospective study of 125 pregnant women with a single previous objectively diagnosed VTE. No heparin was given antenatally but anticoagulants, usually coumarin following an initial short course of heparin or LMWH, was given for 4–6 weeks postpartum. The overall rate for recurrent antenatal VTE was 2.4% (95% CI 0.2–6.9). However, none of the 44 women (95% CI 0.0–8.0), who did not have an underlying thrombophilia and whose previous VTE had been associated with a temporary risk factor, developed a VTE, while 5.9% (95% CI 1.2–16%) of the women who were found to have an underlying thrombophilia, or whose previous VTE had been idiopathic, had a recurrent event. As pregnancy is associated with hyper-estrogenism, this should probably be considered a recurrent risk factor in women with a previous VTE on the combined oral contraceptive pill, or in pregnancy.

Thus, in the woman with a previous VTE that was not pregnancy-related, associated with a risk factor that is no longer present and with no additional risk factor, or underlying thrombophilia (Table 2), antenatal LMWH should not be routinely prescribed. This strategy must be discussed with the woman and her views taken into account, especially in view of the wide confidence intervals reported by Brill-Edwards and Ginsberg (41) (95% CI 0–8.0%). Graduated elastic compression stockings and/or low dose aspirin can be employed antenatally in these women. Postpartum, she should receive anticoagulant therapy for at least six

Table 2 Common Risk Factors for VTE in Pregnancy

Patient factors
Age over 35 years
Obesity (BMI $>29\,kg/M^2$) in early pregnancy
Thrombophilia
Past history of VTE (especially if idiopathic or thrombophilia associated)
Gross varicose veins
Significant current medical problem (e.g., nephrotic syndrome)
Current infection or inflammatory process (e.g., active inflammatory bowel disease or urinary tract infection)
Immobility (e.g., bed rest or lower limb fracture)
Paraplegia
Recent long distance air plane travel
Dehydration
Intravenous drug abuse
Ovarian hyperstimulation
Pregnancy/obstetric factors
Caesarean section particularly as an emergency in labour
Operative vaginal delivery
Major obstetric haemorrhage
Hyperemesis gravidarum
Pre-eclampsia
Caesarean section particularly as an emergency in labour

weeks (e.g., 40 mg enoxaparin or 5000 IU dalteparin daily or warfarin (target INR 2–3) with LMWH overlap until the INR is >2.0) ± graduated elastic compression stockings (Table 3).

In those women with a single previous VTE and an underlying thrombophilia, or where the VTE was idiopathic or pregnancy-related, or associated with use of the combined oral contraceptive pill, or where there are additional risk factors, such as obesity or nephrotic syndrome, there is a stronger case for LMWH prophylaxis. Antenatally, these women should be considered for prophylactic doses of LMWH (e.g., 40 mg enoxaparin or 5000 IU dalteparin daily) ± graduated elastic compression stockings. This should be started as soon as possible following the diagnosis of pregnancy. More intense LMWH therapy in the presence of antithrombin deficiency is usually prescribed (e.g., enoxaparin 0.5–1 mg/kg 12 hourly or dalteparin 50–100 IU/kg 12 hourly), although many women with previous VTE and antithrombin deficiency will be on long-term anticoagulant therapy (see later). Postpartum anticoagulant therapy for at least 6 weeks [e.g., 40 mg enoxaparin or 5000 IU dalteparin daily or warfarin (target INR 2–3) with LMWH overlap until the INR is >2.0] ± graduated elastic compression stockings is recommended (Table 3).

In a woman with multiple previous episodes of VTE and no identifiable thrombophilia, and who is not on long-term anticoagulant therapy, there is consensus that she should receive antenatal LMWH thromboprophylaxis (e.g., 40 mg enoxaparin or 5000 IU dalteparin daily), and graduated elastic compression stockings. This should be started as soon as possible following the diagnosis of

Table 3 Suggested Thromboprophylactic Strategies in Pregnancy (It is Recommended that Specialist Advice for Individualised Management of Patients is Advisable in Many of These Situations)

Clinical situation	Suggested thromboprophylaxis strategy
Single previous VTE (not pregnancy or "pill" related) associated with a transient risk factor and no additional current risk factors, such as obesity	*Antenatal*: Surveillance *or* prophylactic doses of LMWH (e.g., 40 mg enoxaparin or 5000 IU dalteparin daily), ± graduated elastic compression stockings Discuss decision regarding antenatal LMWH with the woman *Postpartum*: Anticoagulant therapy for at least six weeks (e.g., 40 mg enoxaparin or 5000 IU dalteparin daily or warfarin (target INR 2–3) with LMWH overlap until the INR is ≥2.0) ± graduated elastic compression stockings
Single previous *idiopathic* VTE or single previous VTE with underlying thrombophilia and not on long-term anticoagulant therapy, or single previous VTE and additional current risk factor(s) (e.g., morbid obesity, nephrotic syndrome)	*Antenatal*: Prophylactic doses of LMWH (e.g., 40 mg enoxaparin or 5000 IU dalteparin daily) ± graduated elastic compression stockings. NB: There is a strong case for more intense LMWH therapy in antithrombin deficiency (e.g., enoxaparin 0.5–1 mg/kg 12 hourly or dalteparin 50–100 IU/kg 12 hourly) *Postpartum*: Anticoagulant therapy for at least six weeks (e.g., 40 mg enoxaparin or 5000 IU dalteparin daily or warfarin (target INR 2–3) with LMWH overlap until the INR is ≥2.0) ± graduated elastic compression stockings
More than one previous episode of VTE, with no thrombophilia and not on long-term anticoagulant therapy	*Antenatal*: Prophylactic doses of LMWH (e.g., 40 mg enoxaparin or 5000 IU dalteparin daily) + graduated elastic compression stockings *Postpartum*: Anticoagulant therapy for at least six weeks (e.g., 40 mg enoxaparin or 5000 IU dalteparin daily or warfarin (target INR 2–3) with LMWH overlap until the INR is ≥2.0) + graduated elastic compression stockings
Previous episode(s) of VTE in women receiving long-term anticoagulants (e.g., with underlying thrombophilia)	*Antenatal*: Switch from oral anticoagulants to LMWH therapy (e.g., enoxaparin 0.5–1 mg/kg 12 hourly or dalteparin 50–100 IU/kg 12 hourly) by six weeks gestation + graduated elastic compression stockings *Postpartum*: Resume long-term anticoagulants with LMWH overlap until INR in pre-pregnancy therapeutic range + graduated elastic compression stockings

(*Continued*)

Table 3 *Cont'd*

Clinical situation	Suggested thromboprophylaxis strategy
Thrombophilia (confirmed laboratory abnormality) but no prior VTE	*Antenatal*: Surveillance *or* prophylactic LMWH ± graduated elastic compression stockings. The indication for pharmacological prophylaxis in the antenatal period is stronger in AT deficient women and compound hereozygotes than the other thrombophilias, in symptomatic kindred compared to asymptomatic kindred and also where additional risk factors are present *Postpartum*: Anticoagulant therapy for at least six weeks (e.g., 40 mg enoxaparin or 5000 IU dalteparin daily or warfarin (target INR 2–3) with LMWH overlap until the INR is ≥2.0) ± graduated elastic compression stockings
Following Caesarean section or vaginal delivery	Carry out risk assessment for VTE. If additional risk factors such as emergency section in labour, age over 35 years, high BMI, etc., present then consider LMWH thromboprophylaxis (e.g., 40 mg enoxaparin or 5000 IU dalteparin) ± graduated elastic compression stockings

pregnancy. Postpartum, she should receive at least six weeks pharmacological prophylaxis, either with low molecular weight heparin, or warfarin. If she is switched to warfarin postpartum, the target INR is 2–3 and LMWH should be continued until the INR is two. A longer duration of postpartum prophylaxis may be required for women with additional risk factors (Table 3).

When prophylactic doses of LMWH are used, the dose may require being adjusted in women with very low or very high body weight. At low body weight (<50 kg or BMI less than 20 kg/M^2), lower doses of LMWH may be required (e.g., 20 mg enoxaparin daily or 2500 IU dalteparin daily), while in obese patients (e.g., BMI >30 in early pregnancy), higher doses of LMWH may be required.

The woman with previous episode(s) of VTE receiving long-term anticoagulants (e.g., with underlying thrombophilia) should switch from oral anticoagulants to LMWH by six weeks' gestation, and be fitted with graduated elastic compression stockings. These women should be considered at very high risk of antenatal VTE and should receive anticoagulant prophylaxis throughout pregnancy. They should be advised, ideally, pre-pregnancy, of the need to switch from warfarin to LMWH as soon as pregnancy is confirmed. The dose of heparin given should be closer to that used for the treatment of VTE rather than that used for prophylaxis (e.g., enoxaparin 0.5–1 mg/kg 12 hourly or dalteparin 50–100 IU/kg 12 hourly. Furthermore, 12 hourly injections may be preferable to once daily injections in view of the

altered pharmacokinetics of LMWH in pregnancy), based on the early pregnancy weight (42). Postpartum, she should resume long-term anticoagulants with LMWH overlap until INR is in the pre-pregnancy therapeutic range, plus graduated elastic compression stockings.

When a woman has thrombophilia confirmed on laboratory testing, but no prior VTE, surveillance *or* prophylactic LMWH ± graduated elastic compression stockings can be used antenatally. The indication for pharmacological prophylaxis in the antenatal period is stronger in antithrombin deficient women (where the doses of LMWH of enoxaparin 0.5–1 mg/kg 12 hourly or dalteparin 50–100 IU/kg 12 hourly are usually employed), and in compound heterozygotes such as those women with both factor V Leiden and prothrombin G20210A, than the other thrombophilias and also in symptomatic kindred compared to asymptomatic kindred. The presence of additional risk factors (e.g., obesity or immobility) may also merit consideration for antenatal thromboprophylaxis with LMWH. Postpartum, these women should receive anticoagulant therapy for at least six weeks [e.g., 40 mg enoxaparin or 5000 IU dalteparin daily or warfarin (target INR 2–3) with LMWH overlap until the INR is >2.0] ± graduated elastic compression stockings. These women usually require individual advice from clinicians with expertise in the area.

Women undergoing Caesarean section and vaginal delivery should also have a risk assessment for VTE (19–21,43). In a patient undergoing Caesarean section, thromboprophylaxis (e.g., 40 mg enoxaparin or 5000 IU dalteparin) should be prescribed if she has one or more additional risk factors, such as emergency section in labour, age over 35 years, and high BMI. In patients at high risk, graduated elastic compression stockings should be used. These can also be employed if heparin is contraindicated. In women undergoing vaginal delivery, a similar strategy can be used with LMWH being prescribed if there are two or more additional minor risk factors, or one major risk factor (e.g., morbid obesity) (21,44).

C. The Prevention of Thrombosis in Women with Mechanical Heart Valves

The use of antithrombotic therapy in pregnant women with prosthetic heart valves is especially problematic. Treatment options include oral anticoagulants (coumarin therapy), unfractionated heparin, and LMWH. The three main approaches are: (1) the use of vitamin K antagonists throughout pregnancy; (2) replacement of vitamin K antagonists with unfractionated heparin or LMWH from 6 to 12 weeks' gestation (a strategy employed to minimise the teratogenic effects of warfarin); and (3) the use of unfractionated heparin or LMWH throughout pregnancy. With regard to LMWH use in this situation there are now reports and case-series describing the use of LMWH in this situation (45–53).

At present, there is no consensus on the safest and most effective anticoagulation regimen since: (1) there is a lack of data on the efficacy or appropriate doses of LMWH and unfractionated heparin in preventing thrombotic complications; and (2) oral anticoagulant therapy is associated with risks of teratogenesis, neurodevelopmental problems, and maternal and foetal bleeding.

Chan et al. (54) in a systematic review of foetal and maternal outcomes in pregnant women with prosthetic heart valves concluded that the use of vitamin K antagonists throughout pregnancy was associated with the lowest risk of thromboembolic complications (3.9%). When warfarin was replaced by unfractionated heparin between 6 and 12 weeks' gestation, the risk of valve thrombosis increased to 9.2%. The use of unfractionated heparin throughout pregnancy was associated with an increased rate of valve thrombosis – 25% with adjusted doses of unfractionated heparin and 60% with low doses. There is a lack of data regarding the risk of thrombotic complications when LMWH is used in pregnancy. LMWHs are not licensed for use with prosthetic valves outside of pregnancy and their use in pregnant women with prosthetic heart valves has been discouraged [for discussion see (55)]. There are reports of valve thrombosis and stroke when LMWH have been employed in this situation (49–53), although in some of these cases the dose of LMWH employed would be regarded as sub-therapeutic [e.g., enoxaparin 20 mg once daily (56) and enoxaparin sodium 40 mg 12 hourly (52)]. In a review of the literature (1989–2004) regarding the use of LMWH in women with mechanical heart valves during pregnancy, Oran et al. (57) found that amongst 81 pregnancies in 75 women, the rate of valve thrombosis was 8.64% (7/81; 95% CI, 2.52–14.76%). The risk of thrombotic complication was much less (1 patient in 51 pregnancies), when anti-factor Xa levels were monitored and the dose of LMWH adjusted to maintain the peak anti-factor Xa level at a minimum of 1.0 U/ml.

Ginsberg et al. (58) have summarised many of the controversies and issues surrounding the anticoagulation of pregnant women with mechanical heart valves. They conclude that there should be a consensus conference among experts to systematically gather the best evidence, identify key unresolved issues, and devise appropriate studies to address these issues.

Whilst it appears that vitamin K antagonists are more efficacious than unfractionated heparin in preventing maternal thromboembolic complications, these apparent benefits need to be balanced against their potential adverse effects on the foetus. Unlike unfractionated heparin and LMWH, coumarin derivatives, such as warfarin, cross the placenta and are associated with congenital malformations and foetal and neonatal haemorrhage (59,60). In the first trimester of pregnancy, warfarin can cause an embryopathy (Table 4) if taken between 6 and 12 weeks of gestation. In their systematic review, Chan et al. (54) found that the use of warfarin throughout pregnancy was associated with warfarin embryopathy in 6.4% of live births. It is probable that the risk can be eliminated by avoiding warfarin between 6 and 12 weeks of gestation, and the risk may be higher when the dose of warfarin is greater than 5 mg/day (61).

In addition to embryopathy, warfarin is associated with foetal and neonatal haemorrhage. As the foetal liver is immature and levels of vitamin-K dependent clotting factors are low (factors II, VII, IX, and X), maternal warfarin therapy maintained in the therapeutic range (INR of 2–3), will be associated with excessive anticoagulation in the foetus. This can lead to haemorrhagic complications in the foetus and is a concern, particularly at the time of delivery, when the combination of the anticoagulant effect and trauma of delivery can lead to bleeding in the neonate.

Table 4 The Features of Warfarin Embryopathy

Mid-facial, particularly nasal, hypoplasia
Stippled chondral calcification
Short proximal limbs
Short phalanges
Scoliosis

Further, the administration of warfarin during the second and third trimesters of pregnancy may lead to neurodevelopmental problems in childhood (62).

There is, therefore, insufficient data to make evidence-based recommendations about optimal antithrombotic strategies in pregnant women with mechanical heart valves. Recent guidelines from the American College of Chest Physicians (19), suggest one of three regimens:

1. Adjusted dose LMWH administered twice daily throughout pregnancy maintaining the peak (4 h post-injection) anti-Xa level at 1.0–1.2 U/ml.
2. Aggressive adjusted-dose unfractionated heparin throughout pregnancy (administered subcutaneously every 12 h) maintaining the mid-interval activated partial thromboplastin time (APTT) at least twice control.
3. Unfractionated heparin or LMWH until the 13th week of pregnancy, change to warfarin until the middle of the third trimester, and then recommence unfractionated heparin or LMWH until delivery.

With each of these suggested regimens, the authors suggested the addition of low dose aspirin (80–150 mg/day) in women with prosthetic valves at high risk.

D. Management of Recurrent Miscarriage in Thrombophilic Women

Recurrent miscarriage – the occurrence of three or more miscarriages – is estimated to occur in 0.5–1% of all couples trying to conceive (63). Recurrent miscarriage may be a feature of the antiphospholipid syndrome (APLS), an acquired hypercoagulable state induced by the presence of a lupus anticoagulant or anticardiolipin antibodies (64). In women with APLS, adverse pregnancy outcomes may be the result of poor placental perfusion due to localised thrombosis and it is attractive to hypothesise that antithrombotic therapy would have a beneficial effect in this situation. Antiphospholipid antibody may also interefere with trophoblast invasion, and at least *in vitro*, the use of heparin has been shown to ameliorate this effect (65,66).

Clinical guidelines in the United Kingdom (22) and in North America (19) recommend the use of low dose aspirin and heparin (unfractionated or LMWH) in women with a history of recurrent miscarriage and antiphospholipid antibodies. The original studies on which these recommendations are based are limited since they do not include a control group in which neither aspirin nor heparin was administered (67–72).

Sanson et al. (73) were the first group to demonstrate an association between hereditary thrombophilias (deficiencies of antithrombin, protein C, and protein S)

and an increased risk of pregnancy loss compared to their female family members without such defects. Since then, other inherited and acquired thrombophilic disorders have also been linked to recurrent pregnancy loss [see Kujovich (2004), for review (74)]. These include heterozygosity for factor V Leiden and the prothrombin (G20210A) gene mutation. Observational studies have suggested a role for thromboprophylaxis in women with recurrent miscarriage and inherited thrombophilia (75–77). These data suggest that a prothrombotic phenotype (regardless of the specific underlying thrombophilia) is a risk factor for first trimester loss. Further this raises the question as to whether antithrombotic therapy should be used more widely in women with recurrent miscarriage (78,79). Randomised trials of adequate power are required to address these issues.

E. Management of Thrombophilic Women with a History of Adverse Pregnancy Outcome (Prior Severe or Recurrent Pre-Eclampsia, Placental Abruption, or Unexplained Foetal Death)

Evidence is accumulating that inherited and acquired thrombophilias are associated with a proportion of cases of placental dysfunction in later pregnancy, manifesting as intrauterine growth restriction, pre-eclampsia, placental abruption, and intrauterine foetal death (74,80–84). These pregnancy complications may be associated with reduced placental perfusion and fibrin deposition and thrombus formation at the uterine vessels and intervillous spaces. In histological studies, placental infarcts were identified in 72–89% of placentae from thrombophilic women with serious pregnancy complications, compared with 28–39% of non-thrombophilic women (81,85). In contrast, other studies have shown that placental thrombotic lesions were equally frequent in women without thrombophilia who suffered an adverse pregnancy outcome (86–88).

In view of the data suggesting an association between maternal thrombophilia and placental dysfunction, guideline documents recommend screening for underlying congenital thrombophilia in women with recurrent pregnancy loss, second trimester miscarriage, or a history of intrauterine death, or severe or recurrent pre-eclampsia (19). At present there are no conclusive data from randomised controlled trials (that have included a "no treatment" group), to indicate whether antithrombotic therapy is beneficial in women with previous placental dysfunction and inherited thrombophilia. Several observational studies have indicated a benefit of LMWH in this situation (75,89,90). A randomised study comparing the effects of the LMWH enoxaparin (40 mg/day) and low dose aspirin (100 mg/day) administered during pregnancy to women with a history of second or third trimester foetal loss, concluded that enoxaparin was associated with a significantly higher birth rate (91). More recently, Brenner and colleagues have reported a randomised trial where they compared two doses of enoxaparin (40 mg and 80 mg) in women with thrombophilia and a heterogeneous history of pregnancy loss (23). Whilst the authors conclude that enoxaparin, in either dose, results in a favourable outcome in the majority of women, this study has been criticised for its design and in particular, because it lacked a group of women who received no treatment (92).

IV. Safety of Low Molecular Weight Heparin in Pregnancy

Pregnancy is one of the few situations in modern therapeutics where heparin is employed and recommended for use over a prolonged period. LMWH is preferred to unfractionated heparin in this situation for several reasons, including a better safety profile, though when LMWH was introduced to clinical practice, there were concerns about its safety in pregnancy. These concerns were based on the assumption that LMWH would have the same side effects as those encountered with prolonged use of unfractionated heparin, namely osteoporosis, heparin-induced thrombocytopenia, and allergy (93–98). Accumulating evidence over the last decade indicates that LMWHs are safer than unfractionated heparin in pregnancy [for systematic reviews, see (99,100)].

A. Foetal Complications of Low Molecular Weight Heparin

Neither LMWH nor unfractionated heparin cross the placenta (101–103). As a result, neither agent is able to cause teratogenicity or foetal bleeding.

B. Maternal Complications of Low Molecular Weight Heparin

1. Haemorrhage

One of the advantages of LMWH over unfractionated heparin is an enhanced anti-Xa (antithrombotic): anti IIa (anticoagulant) ratio, which presumably should be responsible for a reduced risk of bleeding. Ginsberg et al. (104) in a cohort study reported a 2% rate of major bleeding in pregnant women treated with unfractionated heparin. A recent systematic review of 2777 pregnancies managed with either therapeutic or thromboprophylactic doses of LMWH (100), reported that significant bleeding occurred in 1.98% (95% confidence intervals 1.50–2.57). In most cases of postpartum haemorrhage, the bleeding was associated with primary obstetric cause, such as uterine atony, or vaginal lacerations although the authors conclude that the blood loss may have been increased by the concomitant use of LMWH.

2. Heparin-Induced Thrombocytopenia

An early onset thrombocytopenia can occur after initiation of unfractionated heparin treatment (see Chapter 24).

Guideline documents recommend that routine platelet count monitoring is not required in obstetric patients who have received only LMWH (105). If unfractionated heparin is employed, or if the obstetric patient is receiving LMWH after first receiving unfractionated heparin, the platelet count should be monitored every 2–3 days from day 4 to day 14, or until heparin is stopped.

3. Allergic Skin Reactions with Low Molecular Weight Heparin

Allergic reactions to heparins (both unfractionated and LMWH) usually take the form of itchy, erythematous raised plaque-like lesions at the injection sites. Changing heparin preparations, or switching from a LMWH to unfractionated heparin may be helpful, although a degree of cross-reactivity can occur (106). Sanson et al. (99) reported a rate of allergic skin reactions of 0.6% in a study of 486 pregnant patients managed with LMWH in pregnancy. A higher rate (1.8%) was reported in a more recent systematic review (100).

4. Heparin-Induced Osteoporosis

Unfractionated heparin has been demonstrated in animal experiments to cause a dose-dependent loss of cancellous bone through decreased rates of bone formation and increased bone resorption (107). Long-term heparin therapy has, in turn, been found to induce osteoporosis in both laboratory animals and humans (93,96,108,109). The incidence of symptomatic vertebral fractures when heparin is administered for prolonged periods (more than one month) is 2–3% of the patient population and significant reductions in bone density have been reported in up to 30% of patients receiving long-term unfractionated heparin (93,96).

In recent years, animal studies, observational studies, and randomised trials have indicated that LMWHs have a lower risk of osteoporosis than unfractionated heparin. Studies in rats have demonstrated that unfractionated heparin decreases cancellous bone volume both by decreasing the rate of bone formation and increasing the rate of bone resorption. LMWH caused less osteopenia than unfractionated heparin because it only decreases the rate of bone formation (108–110).

Observational studies in women are compatible with these animal data and indicate that LMWH has less effect on bone density than unfractionated heparin (97,111–113). Indeed, Carlin et al. (113) conclude that bone loss associated with the long-term use of LMWH (5000 U/day) was not significantly different from physiological losses during pregnancy.

Pettila et al. (114) assessed bone mineral density using dual X-ray absorptiometry in 44 pregnant women with confirmed previous or current VTE, who were randomised to receive either LMWH (dalteparin) or unfractionated heparin. They found that mean bone mineral density of the lumbar spine was significantly lower in the unfractionated heparin group compared with the dalteparin group. Bone mineral density in the dalteparin-treated group did not differ from that of healthy postpartum women. In a study by Monreal et al. (31), dalteparin (5000 IU anti-Xa s/c bid) was compared with unfractionated heparin (10,000 IU s/c bid) in 80 patients with DVT. Both treatments were administered for a period of 3–6 months. Six of the 40 (15%; 95% CI, 6–30%) patients who received UFH developed spinal fractures compared with only one of 40 (3%; 95% CI, 0–11%) receiving dalteparin.

More recently, a systematic review (100) concluded that the risk of osteoporotic fracture associated with LMWH use in pregnancy is 0.04% (95% CI < 0.01–0.20). This review examined studies that were published up to December 2003. Since then,

one unit has reported three cases of osteoporotic fractures in association with tinzaparin use in pregnancy (115). These three cases were complex and each had other risk factors for osteoporosis.

V. Conclusions

LMWH is now established in current obstetric practice for the treatment and prevention of thrombotic complications – although it is recognised that there is a lack of controlled trials to evaluate outcomes such as adverse effects, venous thrombosis, and other vascular complications. When LMWHs are administered in pregnancy, it is not appropriate to extrapolate drug doses from studies in the non-pregnant, since their pharmacokinetics are altered secondary to the physiological changes of pregnancy. Preliminary data suggest a role for LMWHs in the management of women with thrombophilia and placental vascular complications. Before this practice becomes established, it would seem prudent to investigate this further in adequately powered, randomised studies.

References

1. Hirsh J, Raschke R. Heparin and low-molecular-weight heparin. The Seventh ACCP Conference on Antithrombotic and Thrombolytic Therapy. Chest 2004; 126:188S–203S.
2. Hirsh J, Levine MN. Low molecular weight heparin. Blood 1992; 79:1–17.
3. Weitz JI. Low-molecular-weight heparins. N Engl J Med 1997; 337:688–698.
4. Warkentin TE, Levine MN, Hirsh J, Horsewood P, Roberts RS, Gent M, Kelton JG. Heparin-induced thrombocytopenia in patients treated with low-molecular-weight heparin or unfractionated heparin. N Engl J Med 1995; 332:1330–1335.
5. Shaughnessy SG, Young E, Deschamps P, Hirsh J. The effects of low molecular weight and standard heparin on calcium loss from the foetal rat calvaria. Blood 1995; 86:1368–1373.
6. Castellot JJ, Favreau LV, Karnovsky MJ, Rosenberg RD. Inhibition of vascular smooth muscle cell growth by endothelial cell-derived heparin: possible role of a platelet endoglycosidase. J Biol Chem 1982; 257:11256–11260.
7. Handeland GF, Abidgaard GF, Holm U, Arnesen KE. Dose adjusted heparin treatment of deep venous thrombosis: a comparison of unfractionated and low molecular weight heparin. Eur J Clin Pharmacol 1990; 39:107–112.
8. Duplaga BA, Rivers CW, Nutescu E. Dosing and monitoring of low-molecular-weight heparins in special populations. Pharmacotherapy 2001; 21:218–234.
9. Ensom MHH, Stevenson MD. Low-molecular-weight heparins in pregnancy. Pharmacotherapy 1999; 19:1013–1025.
10. Brennand JE, Walker ID, Greer IA. Anti-activated factor X profiles in pregnant women receiving antenatal thromboprophylaxis with enoxaparin. Acta Haematol 1999; 101:53–55.

11. Casele HL, Laifer SA, Woelkers DA, Venkataramanan R. Changes in the pharmacokinetics of the low-molecular-weight heparin enoxaparin sodium during pregnancy. Am J Obstet Gynecol 1999; 181:1113–1117.
12. Blomback M, Bremme K, Hellgren M, Lindberg H. A pharmacokinetic study of dalteparin (Fragmin) during late pregnancy. Blood Coagul Fibrinolysis 1998; 9:343–350.
13. Sephton V, Farquharson RG, Topping J, Quenby SM, Cowan C, Back DJ, Toh CH. A longitudinal study of maternal dose response to low molecular weight heparin in pregnancy. Obstet Gynecol 2003; 101:1307–1311.
14. Ensom MHH, Stephenson MD. Pharmacokinetics of low molecular weight heparin and unfractionated heparin in pregnancy. J Soc Gynecol Investig 2004; 11:377–383.
15. Crowther MA, Spitzer K, Julian J, Ginsberg J, Johnston M, Crowther R, Laskin C. Pharmacokinetic profile of a low-molecular weight heparin (Reviparin) in pregnant patients: a prospective cohort study. Thromb Res 2000; 98:133–138.
16. Norris LA, Bonnar J, Smith MP, Steer PJ, Savidge G. Low molecular weight heparin (tinzaparin) therapy for moderate risk thromboprophylaxis during pregnancy. A pharmacokinetic study. Thromb Haemost 2004; 92:791–796.
17. Smith MP, Norris LA, Steer PJ, Savidge GF, Bonnar J. Tinzaparin sodium for thrombosis treatment and prevention during pregnancy. Am J Obstet Gynecol 2004; 190:495–501.
18. Thomson AJ, Greer IA. Thromboembolic Disease in Pregnancy and the Puerperium: Acute Management. RCOG Guideline Number 28. London: RCOG Press, 2001.
19. Bates SM, Greer IA, Hirsh J, Ginsberg JS. Use of antithrombotic agents during pregnancy. The Seventh ACCP Conference on Antithrombotic and Thrombolytic Therapy. Chest 2004; 163:627S–644S.
20. Royal College of Obstetricians and Gynaecologists. Report of the RCOG Working Party on Prophylaxis Against Thromboembolism in Gynaecology and Obstetrics. London: RCOG Press, 1995.
21. Nelson-Piercy C. Thromboprophylaxis During Pregnancy Labour and After Vaginal Delivery. RCOG Guideline Number 37. London: RCOG Press, 2004.
22. Regan L, Backos MJ, Rai R. The Investigation and Management of Couples with Recurrent Miscarriage. RCOG Guideline Number 17. London: RCOG Press, 2003.
23. Brenner B, Hoffman R, Carp H, Dulitsky M, Younis J. Efficacy and safety of two doses of enoxaparin in women with thrombophilia and recurrent pregnancy loss: the LIVE-ENOX study. J Thromb Haemost 2005; 3:227–229.
24. Dolovich L, Ginsberg JS, Douketis JD, Holbrook AM, Cheah G. A meta-analysis comparing low molecular weight heparins to unfractionated heparin in the treatment of venous thromboembolism: examining some unanswered questions regarding location of treatment, product type, and dosing frequency. Arch Intern Med 2000; 160:181–188.
25. Gould MK, Dembitzer AD, Doyle RL, Hastie TJ, Garber AM. Low-molecular-weight heparins compared with unfractionated heparin for treatment of acute deep venous thrombosis. A meta-analysis of randomized, controlled trials. Ann Intern Med 1999; 130:800–809.

26. Lopaciuk S, Bilska-Falda H, Noszczyk W, Bielawiec M, Witkiewicz W, Filipecki S, Michalek J, Ciesielski L, Mackiewicz Z, Czestochowska E, Zawilska K, Cencora A. Low-molecular-weight heparin versus acenocoumarol in the secondary prophylaxis of deep vein thrombosis. Thromb Haemost 1999; 81:26–31.
27. Pini M, Aiello S, Manotti C, Pattacini C, Quintavalla R, Poli T, Tagliaferri A, Detorri AG. Low-molecular-weight heparin versus warfarin in the prevention of recurrences after deep vein thrombosis. Thromb Haemost 1994; 72:191–197.
28. van der Heijden JF, Hutten BA, Buller HR, Prins MH. Vitamin K antagonists or low-molecular-weight heparin for the long term treatment of symptomatic venous thromboembolism. Cochrane Database Syst Rev 2000; 4:CD002001.
29. Rodie VA, Thomson AJ, Stewart FM, Quinn AJ, Walker ID, Greer IA. Low molecular weight heparin for the treatment of venous thromboembolism in pregnancy – case series. Br J Obstet Gynaecol 2002; 109:1020–1024.
30. Thomson AJ, Walker ID, Greer IA. Low molecular weight heparin for the immediate management of thromboembolic disease in pregnancy. Lancet 1998; 352:1904.
31. Monreal M, Lafoz E, Olive A, del Rio L, Vedia C. Comparison of subcutaneous unfractionated heparin with a low molecular weight heparin (Fragmin) in patients with venous thromboembolism and contraindications for coumarin. Thromb Haemost 1994; 71:7–11.
32. Lee AY, Levine MN, Baker RI, Bowden C, Kakkar AK, Prins M, Rickles FR, Julian JA, Haley S, Kovacs MJ, Gent M. Randomized comparison of low-molecular-weight heparin versus oral anticoagulant therapy for the prevention of recurrent venous thromboembolism in patients with cancer (CLOT) investigators. Low-molecular-weight heparin versus a coumarin for the prevention of recurrent venous thromboembolism in patients with cancer. N Engl J Med. 2003; 349:146–153.
33. Hull RD, Delmore T, Carter C, Hirsh J, Genton E, Gent M, Turpie G, McLaughlin D. Adjusted subcutaneous heparin versus warfarin sodium in the long-term treatment of venous thrombosis. N Engl J Med 1982; 306:1676–1681.
34. Crowther MA, Berry LR, Monagle PT, Chan AK. Mechanisms responsible for the failure of protamine to inactivate low-molecular-weight heparin. Br J Haematol 2002; 116:178–186.
35. Rodger MA, Walker M, Wells PS. Diagnosis and treatment of venous thromboembolism in pregnancy. Best Practice Research Clin Haematol 2003; 16:279–296.
36. Abramovitz S, Beilin Y. Thrombocytopenia, low molecular weight heparin, and obstetric anesthesia. Anesthesiol Clin North Am 2003; 21:99–109.
37. De Swiet M, Floyd E, Letsky E. Low risk of recurrent thromboembolism in pregnancy. Br J Hospital Med 1987; 38:264 [letter].
38. Howell R, Fidler J, Letsky E, de Swiet M. The risk of antenatal subcutaneous heparin prophylaxis: a controlled trial. Br J Obstet Gynaecol 1983; 90: 1124–1128.
39. Badaracco MA, Vessey M. Recurrent venous thromboembolic disease and use of oral contraceptives. BMJ 1974; 1:215–217.
40. Tengborn L. Recurrent thromboembolism in pregnancy and puerperium: is there a need for thromboprophylaxis? Am J Obstet Gynecol 1989; 160:90–94.

41. Brill-Edwards P, Ginsberg JS, for the Recurrence of Clot in this Pregnancy (ROCIT) Study Group. Safety of withholding antepartum heparin in women with a previous episode of venous thromboembolism. N Eng J Med 2000; 343:1439–1444.
42. Scottish Intercollegiate Guidelines Network. Prophylaxis of Venous Thromboembolism. A National Clinical Guideline. SIGN: Edinburgh, 2002; ISBN 1 899893 03 2.
43. Greer IA. Epidemiology, risk factors and prophylaxis of venous thromboembolism in obstetrics and gynaecology. In: Greer IA, ed. Bailliere's Clinical Obstetrics and Gynaecology – Thromboembolic Disease in Obstetrics and Gynaecology. London: Bailliere Tindall, 1997; 403–30.
44. The National Institute for Clinical Excellence, Scottish Executive Health Department and Department of Health, Social Services and Public Safety: Northern Ireland. Confidential Enquiries into Maternal Deaths in the United Kingdom 1997–1999. London: TSO, 2001.
45. Arnaout MS, Kazma H, Khalil A, Shasha N, Nasrallah A, Karam K, Alam SE. Is there a safe anticoagulation protocol for pregnant women with prosthetic valves? Clin Exp Obstet Gynecol 1998; 25:101–104.
46. Lee LH, Liauw PC, Ng AS. Low molecular weight heparin for thromboprophylaxis during pregnancy in 2 patients with mechanical mitral valve replacement. Thromb Hemost 1996; 76:628–630 [letter].
47. Ellison J, Thomson AJ, Walker ID, Greer IA. Use of enoxaparin in a pregnant woman with a mechanical heart valve prosthesis. Br J Obstet Gynaecol 2001; 108:757–759.
48. Rowan JA, McCowan LM, Raudkivi PJ, North RA. Enoxaparin treatment in women with mechanical heart valves during pregnancy. Am J Obstet Gynecol 2001; 185:633–637.
49. Roberts N, Ross D, Flint SK, Arya R, Blott M. Thromboembolism in pregnant women with mechanical prosthetic heart valves anticoagulated with low molecular weight heparin. Br J Obstet Gynaecol 2001; 108:327–329.
50. Leyh RG, Fischer S, Ruhparwar A, Haverich A. Anticoagulation for prosthetic heart valves during pregnancy: is low-molecular-weight heparin an alternative. Eur J Cardiothorac Surg 2002; 21:577–579.
51. Mahesh B, Evans S, Bryan AJ. Failure of low molecular-weight heparin in the prevention of prosthetic mitral valve thrombosis during pregnancy: case report and review of options for anticoagulation. J Heart Valve Dis 2002; 11:745–750.
52. Lev-Ran O, Kramer A, Gurevitch J, Shapira I, Mohr R. Low-molecular-weight heparin for prosthetic heart valves: treatment failure. Ann Thorac Surg 2000; 69:264–265.
53. Nassar AH, Hobeika EM, Abd Essamad HM, Taher A, Khalil AM, Usta IM. Pregnancy outcome in women with prosthetic heart valves. Am J Obstet Gynecol 2004; 191:1009–1013.
54. Chan WS, Anand S, Ginsberg JS. Anticoagulation of pregnant women with mechanical heart valves: a systematic review of the literature. Arch Intern Med 2000; 160:191–196.
55. Greer I, Hunt BJ. Low molecular weight heparin in pregnancy: current issues. Br J Haematol 2004; 128:593–601.

56. Berndt N, Khan I, Gallo R. A complication in anticoagulation using low-molecular weight heparin in a patient with a mechanical valve prosthesis. A case report. J Heart Valve Dis 2000; 9:844–846.
57. Oran B, Lee-Parritz A, Ansell J. Low molecular weight heparin for the prophylaxis of thromboembolism in women with prosthetic mechanical heart valves during pregnancy. Thromb Haemost 2004; 92 (4):747–751.
58. Ginsberg JS, Chan WS, Bates SM, Kaatz S. Anticoagulation of pregnant women with mechanical heart valves. Arch Intern Med 2003; 163:694–698.
59. Hall JAG, Paul RM, Wilson KM. Maternal and foetal sequelae of anticoagulation during pregnancy. Am J Med 1980; 68:122–140.
60. Ginsberg JS, Hirsh J, Turner CD, Levine MN, Burrows R. Risks to the fetus of anticoagulant therapy during pregnancy. Thromb Haemost 1989; 61:197–203.
61. Vitale N, De Feo M, De Santo LS, Pollice A, Tedesco N, Contrufo M. Dose-dependent foetal complications of warfarin in pregnant women with mechanical heart valves. J Am Coll Cardiol 1999; 33:1642–1645.
62. Wesseling J, van Driel D, Heymans HAS, Rosendaal FR, Geven-Boere LM, Smrkovsky M, Touwen BC, Sauer PJ, van der Veer E. Coumarins during pregnancy: long term effects on growth and development in school age children. Thromb Haemostas 2001; 85:609–613.
63. Regan L, Rai R. Epidemiology and the medical causes of miscarriage. Baillieres Best Pract Res Clin Obstet Gynaecol 2000; 14:839–854.
64. Derksen RHWM, Khamashta MA, Branch DW. Management of the obstetric antiphospholipid syndrome. Arthritis Rheum 2004; 50:1028–1039.
65. Chamley LW, Duncalf AM, Mitchell MD, Johnson PN. Action of anticardiolipin and antibodies to beta-2-glycoprotein-1 on trophoblast proliferation as a mechanism for foetal death. Lancet 1998; 352:1037–1038.
66. Di Simone N, Caliandro C, Castellain R, Ferrazzani S, De Carolis S, Caruso A. Low-molecular weight heparin restores in-vitro trophoblast invasiveness and differentiation in presence of immunoglobulin G fractions obtained from patients with antiphospholipid syndrome. Hum Reprod 1999; 14:489–495.
67. Cohen H. Randomized trial of aspirin versus aspirin and heparin in pregnant women with the antiphospholipid syndrome. Ann Med Interne 1996; 147:144.
68. Farquharson RG, Quenby S, Greaves M. Antiphospholipid syndrome in pregnancy: a randomised, controlled trial of treatment. Obstet Gynecol 2002; 100:408–413.
69. Kutteh WH. Antiphospholipid antibody-associated recurrent pregnancy loss: treatment with heparin and low-dose aspirin is superior to low-dose aspirin alone. Am J Obstet Gynecol 1996; 174:1584–1589.
70. Kutteh WH, Ermel LD. A clinical trial for the treatment of antiphospholipid antibody-associated recurrent pregnancy loss with lower dose heparin and aspirin. Am J Reprod Immunol 1996; 35:402–407.
71. Rai R, Cohen H, Dave M, Regan L. Randomised controlled trial of aspirin and aspirin plus heparin in pregnant women with recurrent miscarriage associated with phospholipid antibodies (or antiphospholipid antibodies). BMJ 1997; 314:253–257.
72. Pattison NS, Chamley LW, Birdsall M, Zanderigo AM, Lideell HS, McDougall J. Does aspirin have a role in improving pregnancy outcome for women with the antiphospholipid syndrome? A randomised controlled trial. Am J Obstet Gynecol 2000; 183:1008–1012.

73. Sanson BJ, Friederich PW, Simioni P, Zanardi S, Huisman MV, Girolami A, ten Cate JW, Prins MH. The risk of abortion and stillbirth in antithrombin-, protein C- and protein S-deficient women. Thromb Haemost 1996; 75: 387–388.
74. Kujovich JL. Thrombophilia and pregnancy complications. Am J Obstet Gynecol 2004; 191:412–424.
75. Brenner B, Hoffman R, Blumenfeld Z, Weiner Z, Younis JS. Gestational outcome in thrombophilic women with recurrent pregnancy loss treated by enoxaparin. Thromb Haemost 2000; 83:693–697.
76. Tzafettas J, Mamopoulos A, Anapliotis A, loufopoulos A, Psarra A, Klearchou N, Mamopoulos M. Thromboprophylaxis throughout pregnancy in women with previous history of recurrent miscarriage of unknown aetiology. Clin Exp Obstet Gynecol 2002; 29:267–270.
77. Carp H, Dolitzky M, Inbal A. Thromboprophylaxis improves the live birth rate in women with consecutive recurrent miscarriages and hereditary thrombophilia. J Thromb Haemost 2003; 1:433–438.
78. Brenner B. Antithrombotic prophylaxis for women with thrombophilia and pregnancy complications – Yes. J Thromb Haemost 2004; 1:2070–2072.
79. Middeldorp S. Antithrombotic prophylaxis for women with thrombophilia and pregnancy complications – No. J Thromb Haemost 2004; 1:2073–2074.
80. Preston FE, Rosendaal FR, Walker ID, Briet E, Berntorp E, Conrad J, Fontcuberta J, Makris M, Mariani G, Noteboom W, Pabinger legnani C, Scharrer I, Schulam, van der Meer FJ. Increased foetal loss in women with heritable thrombophilia. Lancet 1996; 348:913–916.
81. Gris JC, Quere I, Monperyroux F, Mercier E, Ripart-Neveu S, Taillar ML, Hoffet M, Beraln J, Daures JP, Mares P. Case–control study of the frequency of thrombophilic disorders in couples with late foetal loss and no thrombotic antecedent – the Nimes Obstetricians and Haematologists study5 (NOHA5). Thromb Haemost 1999; 81:891–899.
82. Kupferminc MJ, Eldor A, Steinman N, Many A, Bar-Am A, Jaffa A, Lessing JB. Increased frequency of genetic thrombophilia in women with complications in pregnancy. N Eng J Med 1999; 340:50–52.
83. Brenner B. Clinical manifestation of thrombophilia-related placental vascular complication. Blood 2004; 103:4003–4009.
84. Vossen CY, Preston FE, Conrad J, Fontcuberta J, Makris M, van der Meer GJ, Pabinger I, Palareti G, Scharrer I, Souto JC, Svensson P, Walker ID, Rodsendaal FR. Hereditary thrombophilia and foetal loss: a prospective follow up study. J Thromb Haemost 2004; 2:592–596.
85. Many A, Schreiber L, Rosner S, Lessing JB, Eldor A, Kupferminc MJ. Pathologic features of the placenta in women with severe pregnancy complications and thrombophilia. Obstet Gynecol 2001; 98:1041–1044.
86. Mousa HA, Alfirevic Z. Do placental lesions reflect thrombophilia state in women with adverse pregnancy outcome? Hum Reprod 2000; 15:1830–1833.
87. Morssink LP, Santema JG, Willemse F. Thrombophilia is not associated with an increase in placental abnormalities in women with intrauterine foetal death. Acta Obstet Gynaecol Scand 2004; 83:348–350.
88. Mooney E, Vaughan J, Ryan F, et al. Placental thrombotic vasculopathy is not associated with thrombophilic mutations. Lab Invest 2003; 83:303A [abstract].

89. Grandone E, Brancaccio V, Colaizzo D, Scianname N, Pavone G, Di Manno G, Margaglione M. Preventing adverse obstetric outcomes in women with genetic thrombophilia. Fertil Steril 2002; 78:371–375.
90. Younis JS, Ohel G, Brenner B, Haddad S, Lanir N, Ben-Ami M. The effect of thromboprophylaxis on pregnancy outcome in patients with recurrent pregnancy loss associated with factor V Leiden mutation. Br J Obstet Gynaecol 2000; 107:415–419.
91. Gris JC, Mercier E, Quere I, Lavigne-Lissalde G, Cochery-Nouveellot Hoffet M, Ripart-Neveu S, Tailland ML, Dauzat M, Mares P. Low-molecular-weight heparin versus low-dose aspirin in women with one foetal loss and a constitutional thrombophilic disorder. Blood 2004; 103:3695–3699.
92. Middeldorp S. The use of LMWH in pregnancies at risk: new evidence or perception? J Thromb Haemost; doi: 10.1111/j.1538–7836.2005.01288.x.
93. Dahlman TC. Osteoporotic fractures and the recurrence of thromboembolism during pregnancy and the puerperium in 184 women undergoing thromboprophylaxis with heparin. Am J Obstet Gynecol 1993; 168:1265–1270.
94. Barbour LA, Kick SD, Steiner JF, LoVerde ME, Heddleston LN, Lear JL, Baron AE, Barton PL. A prospective study of heparin-induced osteoporosis in pregnancy using bone densitometry. Am J Obstet Gynecol 1994; 170: 862–869.
95. Dahlman TC, Sjoberg HE, Ringertz H. Bone-mineral density during long-term prophylaxis with heparin in pregnancy. Am J Obstet Gynecol 1994; 170:1315–1320.
96. Douketis JD, Ginsberg JS, Burrows RF, Duku EK, Webber CE, Brill-Edwards P. The effects of long-term heparin therapy during pregnancy on bone density. A prospective matched cohort study. Thromb Haemost 1996; 75:254–257.
97. Shefras J, Farquharson RG. Bone density studies in pregnant women receiving heparin. Eur J Obstet Gynecol Reprod Biol 1996; 65:171–174.
98. Backos M, Rai R, Baxter N, Chilcott IT, Cohen H, Regan L. Pregnancy complications in women with recurrent miscarriage associated with antiphospholipid antibodies treated with low dose aspirin and heparin. Br J Obstet Gynaecol 1999; 106:102–107.
99. Sanson B, Lensing AWA, Prins MH, Ginsberg JS, Barkagan ZS, Lavenne-Pardonge E, Brenner B, Dulitzky M, Nielsen JD, Boda Z, Turi S, Mac Gillavry MR, Theunissen IM, Hunt BJ, Büller HR. Safety of low-molecular-weight heparin in pregnancy: a systematic review. Thromb Haemost 1999; 81:668–672.
100. Greer IA, Nelson-Piercy C. Low-molecular weight heparins for thromboprophylaxis and treatment of venous thromboembolism in pregnancy: a systematic review of safety and efficacy. Blood 2005; 106:401–407.
101. Flessa HC, Klapstrom AB, Glueck MJ, Will JJ. Placental transport of heparin. Am J Obstet Gynecol 1965; 93:570–573.
102. Forestier F, Daffos F, Capella-Pavlovsky M. Low molecular weight heparin (PK 10169) does not cross the placenta during the second trimester of pregnancy: study by direct foetal blood sampling under ultrasound. Thromb Res 1984; 34:557–560.

103. Forestier F, Daffos F, Rainaut M, Toulemonde F. Low molecular weight heparin (CY 216) does not cross the placenta during the third trimester of pregnancy. Thromb Haemost 1987; 57:234.
104. Ginsberg JS, Kowalchuk G, Hirsh J, Brill-Edwards P, Burrows R. Heparin therapy during pregnancy: risks to the fetus and mother. Arch Intern Med 1989; 149:2233–2236.
105. Warkentin TE, Greinacher A. Heparin-induced thrombocytopenia: recognition, treatment and prevention. The Seventh ACCP Conference on Antithrombotic and Thrombolytic Therapy. Chest 2004; 126:311S–337S.
106. Mora A, Belchi J, Contreras L, Rubio G. Delayed-type hypersensitivity skin reactions to low molecular weight heparins in a pregnant woman. Contact Dermatitis 2002; 47:177–178.
107. Shaughnessy SG, Hirsh J, Bhandari M, Muir JM, Young E, Weitz JI. Histomorphometric evaluation of heparin-induced bone loss after discontinuation of heparin treatment in rats. Blood 1999; 93:1231–1236.
108. Muir J, Andrew M, Hirsh J, Weitz JI, Young E, Deschamps P, Shaughnessy SG. Histomorphometric analysis of the effects of standard heparin on trabecular bone *in vivo*. Blood 1996; 88:1314–1320.
109. Muir JM, Hirsh J, Weitz JI, Andrew M, Young E, Shaughnessy SG. A histomorphometric comparison of the effects of heparin and low-molecular-weight heparin on cancellous bone in rats. Blood 1997; 89:3236–3242.
110. Nishiyama M, Itoh F, Ujiie A. Low-molecular-weight heparin (dalteparin) demonstrated a weaker effect on rat bone metabolism compared with heparin. Jpn J Pharmacol 1997; 74:59–68.
111. Casele HL, Laifer SA. Prospective evaluation of bone density in pregnant women receiving the low molecular weight heparin enoxaparin sodium. J Matern Fetal Med 2000; 9:122–125.
112. Schulman S, Hellgren-Wangdahl M. Pregnancy, heparin and osteoporosis. Thromb Haemost 2002; 87:180–181.
113. Carlin AJ, Farquharson RG, Quenby SM, Topping J, Fraser WD. Prospective observational study of bone mineral density during pregnancy: low molecular weight heparin versus control. Hum Reprod 2004; 19:1211–1214.
114. Pettila V, Leinonen P, Markkola A, Hiilesmaa V, Kaaja R. Postpartum bone mineral density in women treated for thromboprophylaxis with unfractionated heparin or LMW heparin. Thromb Haemost 2002; 87:182–186.
115. Byrd LM, Johnston TA, Shiach C, Hay CRM. Osteoporotic fracture and low molecular weight heparin. J Obstet Gynaecol 2004; 24 (Suppl 1):S11.

Subject index

Page numbers followed by *t* and *f* indicates tables and figures, respectively.

D

E

F

T

U

V

W

X